Distribution Agreement

In presenting this thesis or dissertation as a partial fulfillment of the requirements for an advanced degree from Emory University, I hereby grant to Emory University and its agents the non-exclusive license to archive, make accessible, and display my thesis or dissertation in whole or in part in all forms of media, now or hereafter known, including display on the world wide web. I understand that I may select some access restrictions as part of the online submission of this thesis or dissertation. I retain all ownership rights to the copyright of the thesis or dissertation. I also retain the right to use in future works (such as articles or books) all or part of this thesis or dissertation.

Signature:

_____ _____

William Francis Tracy Date

Leveraging Catalysis to Enable the Asymmetric Synthesis of Novel Cereblon E3 Ligase Modulatory Drug Cores

By

William F. Tracy
Doctor of Philosophy

Chemistry

_____

Huw M. L. Davies, Ph.D.

Advisor

_____

Frank E. McDonald, Ph.D.

Committee Member

_____

William M. Wuest, Ph.D.

Committee Member

Accepted:

_____

Kimberly Jacob Arriola, Ph.D, MPH

Dean of the James T. Laney School of Graduate Studies

_____

Date

Leveraging Catalysis to Enable the Asymmetric Synthesis of Novel Cereblon E3 Ligase Modulatory Drug Cores

By

William F. Tracy

B.A., University of North Carolina at Chapel Hill, 2020

Advisor: Huw M. L. Davies, Ph.D.

An abstract of

A dissertation submitted to the Faculty of the James T. Laney School of Graduate Studies of Emory University in partial fulfillment of the requirements for the degree of Doctor of Philosophy in Chemistry, 2025

Leveraging Catalysis to Enable the Asymmetric Synthesis of Novel Cereblon E3 Ligase Modulatory Drug Cores

By

William F. Tracy

Glutarimide-containing compounds, particularly immunomodulatory imide drugs (IMiDs), are an exceptional class of compounds that can degrade previously "undruggable" proteins of interest. The glutarimides ubiquitous in the class modulate Cereblon (CRBN), an E3 ubquitin ligase receptor. The synthetic challenges surrounding these structures such as hydrolytic instability, sensitive stereochemical elements, and insolubility make the development and adaptation of new methods for their preparation of high value. Rhodium carbene chemistry, catalyzed by chiral dirhodium complexes, is a powerful method for use in medicinally relevant contexts. Herein, we develop a new adaptation of the Suzuki-Miyaura cross-coupling to enable the synthesis of diverse and stereodefined IMiDs via asymmetric rhodium cyclopropanation and cyclopropenation. These novel and bioactive IMiDs comprise a study demonstrating the subtle interplay of regiochemistry and stereochemistry in neosubstrate degradation. Further exploration of the impact of rhodium carbenes on the study of IMiDs lead to the development of carbene precursors containing CBRN-modulatory cores, which are capable of not only effective cycloaddition chemistry but also selective C–H functionalization, for the creation of stereodefined molecular glue-like compounds and bioactive bifunctional degrader compounds. This work expands the current understanding of how catalysis—especially rhodium catalysis—can impact drug discovery efforts via the facile generation of different kinds of structural complexity, enhance the tools available to medicinal chemists, and by doing so develop further knowledge of the subtleties of rhodium carbene chemistry.

Chapter 1: This chapter will discuss the challenges associated with derivatizing IMiD cores via Suzuki-Miyaura cross-couplings, and the discovery of highly effective reaction conditions for introducing alkene-type trifluoroborates in an enantioretentive manner. This reaction also seems to proceed by a mechanism distinct from that of typical Suzuki-Miyaura reactions, and a computational investigation of the mechanism will be discussed briefly.
Chapter 2: This section will explore the effectiveness of dirhodium-catalyzed asymmetric cyclopropanation and cyclopropenation of alkene- and alkyne-derivatized IMiD cores. The resulting stereoenriched derivatives have distinct biological properties based on both stereochemical and regiochemical factors.
Chapter 3: The final chapter will discuss the development of IMiD-like cores as aryldiazoacetate carbene precursors for rhodium carbene-mediated transformations. These aryldiazoacetates, in combination with chiral catalysts, enable high-yielding and highly diastereoselective C-H functionalization and cyclopropanation reactions for the creation of bioactive bifunctional protein-degrading compounds and complex structures with potentially cereblon-modulating cores.

Leveraging Catalysis to Enable the Asymmetric Synthesis of Novel Cereblon E3 Ligase Modulatory Drug Cores

By

William F. Tracy

B.A., University of North Carolina at Chapel Hill, 2020

Advisor: Huw M. L. Davies, Ph.D.

A dissertation submitted to the Faculty of the James T. Laney School of Graduate Studies of Emory University in partial fulfillment of the requirements for the degree of Doctor of Philosophy in Chemistry, 2025

Acknowledgements

Huw, thank you for all of your support over the past few years. Starting a PhD program during a pandemic wasn't easy. Even though we had to do our rotations on Zoom I had a feeling that I would find a good place in the Davies lab, and that feeling was confirmed time and again during my PhD. Thank you for your kindness and support all the way through, and the opportunities you gave me to grow as a scientist.

Frank and **Bill**, thank you for your support and encouragement over the years. I valued the helpful discussions that we had during my yearly milestones.

Jack, your mentorship and friendship carried me through the first three years of graduate school. I'm sure I annoyed you with countless questions about anything and everything in lab, but I learned so much from you as a chemist. You helped to set me on a trajectory that ended up being a major reason for my success at Emory, and I can't thank you enough.

Robert, your mentorship when I was just starting in the Davies group was invaluable. The way you do chemistry heavily influenced how I approached the rest of my PhD work.

Brock and Josh, thank you for being great officemates and friends. You guys always cheered me up.

Geraint, **Emily**, and **Jesus**, you were such great collaborators and mentors. I grew a lot working with you over 2+ years, and our work together, as you will see, makes up the core and substance of my PhD work. It wouldn't have been possible without your help.

Andrew, you're the chemist that got me fascinated by synthesis in the first place. I spent a lot of grad school asking myself, "what would Andrew Perkowski do?" Your habits and attitude in the lab made a major contribution to how I do and think about chemistry. **Jeff**, thank you for giving a junior transfer student a chance to do chemistry in your lab at UNC. I wouldn't be here without that chance.

To **my family**—thank you for your support and encouragement all the way through.

To **Megan**, my wife, I wouldn't have made it through grad school without you. I've been complaining to you about everything from my second-year exam onward, and you were there every day to support me and listen to me. Love you.

Table of Contents

List of Abbreviations

IMiDs: Immunomodulatory imide drugs

TPD: Targeted protein degradation

PROTAC®: Proteolysis action targeting chimera

LDD: Ligand directed degrader

CRBN: Cereblon

CELMoD: Cereblon E3 Ligase Modulator

$CRL4^{CRBN}$: CUL4–RBX1–DDB1–CRBN

CUL4: Cullin-4 protein

RBX1: RING-box protein 1

DDB1: Damage-Specific DNA Binding Protein 1

API: Active pharmaceutical ingredient

HFIP: 1,1,1,3,3,3-hexafluoroisopropanol

SFC: Supercritical Fluid Chromatograph, Supercritical Fluid Chromatography

DFT: Density Functional Theory

SAR: Structure-and-reactivity

UMAP: Uniform Manifold Approximation and Projection

IKZF3: Ikaros family zinc finger protein 3

CK1α: Casein Kinase 1 alpha

GSPT1: G1 to S phase transition 1

SALL4: Spalt-like Transcription Factor 4

DoE: Design of Experiment

ECFP4: Extended Connectivity Fingerprints, Radius = 2

UMAP: Uniform Manifold Approximation and Projection

PMI: Principal Moments of Inertia

HTRF: Homogenous Time-Resolved Fluorescence

IC_{50}: Half-maximal Inhibitory Concentration

EC_{50}: Half-maximal Effective Concentration

PDB: Protein Database

SP: Standard Precision

MOE: Molecular Operating Environment

BRD4: Bromodomain 4

Table of Figures

Table of Schemes

Introduction

Thalidomide (**Figure I-1**, **I.1**) was a morning sickness drug approved in Germany in the 1950s that gained infamy after physicians began noting severe teratogenic effects.[1] Following discovery of its activity against erythema nodosum leprosum in 1965, researchers discovered the utility of thalidomide in the treatment of a panoply of oncological and autoimmune diseases and disorders in the following decades.[2] Intensive study of the properties of thalidomide along with efforts to reduce its side effects in oncological contexts led to the discovery and eventual clinical approval of two important and far more potent derivatives, lenalidomide (**I.2**) and pomalidomide (**I.3**) (**Figure I-1**).[3] These drugs are exceptionally valuable in the clinic, especially for the treatment of myelomas.[4]

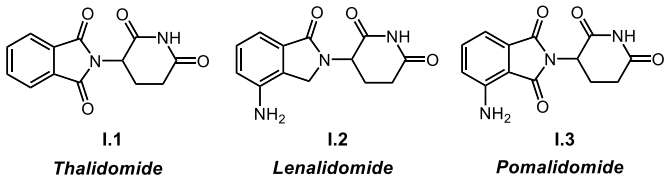

Figure I-1: Archetypal CELMoDs used in the clinic today

The activity of thalidomide and its related compounds, described as immunomodulatory imide drugs or IMiDs, have only been linked more recently to their ability to induce degradation of proteins within the body. This degradation of proteins—often highly specific—is termed targeted protein degradation (TPD), and novel IMiDs are highly sought after for their capability to degrade previously "undruggable" proteins implicated in disease.[2, 4-5] While not limited to one cellular degradation pathway, TPD was first conceptualized in the context of ubiquitin ligases, which tag proteins, or neosubstrates, with ubiquitin. This tag signals for destruction of the associated neosubstrate by the proteasome.[6] The initial iteration of TPD utilized larger molecules

containing a ligand for ubiquitin ligase linked to a ligand selective for the desired protein (**Figure I-2A**). These bifunctional or bivalent degraders are commonly called PROTACs® (proteolysis action targeting chimeras) or LDDs (ligand directed degraders). One current example is bavdegalutamide(**I.4**),[7] which contains a thalidomide-like core with a disubstituted arene (pink, ubiquitin ligase ligand), linked to an androgen receptor ligand (blue) via a linker (black). LDDs are distinct from IMiDs. IMiDs are monovalent molecules that stabilize the protein-protein interactions between ubiquitin ligases and neosubstrates instead of relying on separate moieties to induce proximity between neosubstrate and ligase (**Figure I-2B**). For example, in the case of golcadomide (**I.5**)[8] the molecule has no native affinity for the zinc-finger family proteins which it degrades; instead, the only initial affinity is that which exists between golcadomide and the ubiquitin ligase. IMiDs and many LDDs interact with an E3 ubiquitin ligase adapter called Cereblon (CRBN), which is the substrate receptor for an endogenous enzyme known as CUL4–RBX1–DDB1–CRBN, or CRL4^{CRBN} (depicted in **Figure I-2**).[9]

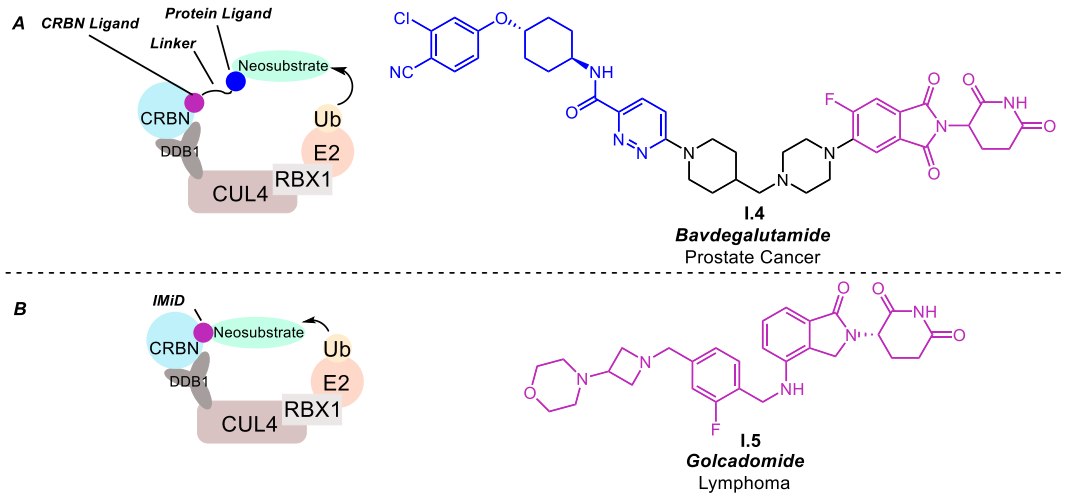

Figure I-2: A. General mechanism of TPD via LDDs featuring an LDD in the clinic. B. General mechanism of TPD via IMiDs featuring an IMiD in the clinic.

The general mechanism of degradation by IMiDs was discovered retroactively, using a combination of proteomics and crystal structures of IMiDs bound to $CUL4^{CRBN}$.[5b, 10] The CRBN-binding portion of IMiDs is the glutarimide portion of the core structure.[10b, 11] Interestingly, the degradation efficacy of IMIDs is not linked to the affinity of the glutarimide-containing compound for CRBN.[10b] Instead, effects on protein degradation are due to the aforementioned stabilization of proximity-inducing protein-protein interactions caused by the binding of an IMiD to CRBN. In the case of lenalidomide-mediated degradation of CK1α, a protein indicated in mechanisms of myelodysplastic syndromes,[12] structural changes induced by the binding of lenalidomide to CRBN lead to interaction between CK1α and CRBN, which is underpinned by lenalidomide–CK1α van der Waals interactions.[13] This induced proximity of the E2–ubiquitin portion of $CRL4^{CRBN}$ to CK1α is followed by ubiquitination and subsequent degradation by the proteasome.[13] The structural origins of IMiD activity vary between neosubstrates even when the same IMiD is used, highlighting the complexity of IMiD–$CUL4^{CRBN}$-mediated TPD.[5b]

In 2022, Woo and coworkers published a seminal study linking the affinity of CRBN for the glutarimides in IMiDs to endogenous processes.[11] Native asparagine and glutamine residues undergo post-translational modifications (e.g. deamidation),[14] which in the case of glutamine produces the glutarimide. CRBN recognizes the glutarimide, initiating ubiquitination of the associated protein.[11] This mechanism is hypothesized to facilitate protein clearance during the ageing process,[11, 15] and without an ubiquitin ligase, the accumulation of post-translationally modified proteins and their hydrolysis products is associated with several degenerative diseases.[16] Glutarimides undergo rapid hydrolysis and racemization under physiological conditions,[17] although Woo provides evidence that endogenous hydrolysis is slow enough in some cases to allow CRBN recognition.[11]

This inherent instability makes IMiDs difficult to modify without ring-opening of the glutarimide. In even slightly basic solutions the glutarimide in thalidomide ring-opens to multiple products (**Figure I-3A**).[17c] Contributing to the synthetic difficulty of working with glutarimide-containing compounds like thalidomide is the facile racemization of the glutarimide stereogenic center both in solution and in vitro,[17d, 18] and the acidity of the imide N-H.[19] Glutarimides readily form hydrogen-bonding dimers (**Figure I-3B**), exacerbating insolubility in the case of racemic thalidomide and perhaps contributing to the notable insolubility of thalidomide-like compounds in common organic solvents.[20]

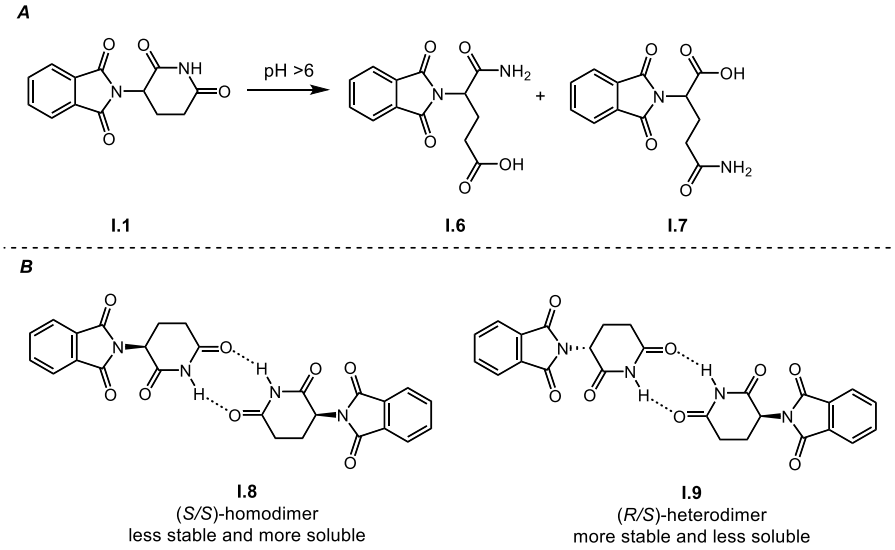

Figure I-3: A. Hydrolysis products of thalidomide. B. Hydrogen-bonding dimers of the enantiomers of thalidomide.

As a result of the synthetic challenges surrounding IMiDs, clinically successful compounds often share disconnections derived from simple transformations; benzylic substitutions and reductive aminations dominate structures found in IMiDs currently in clinical development (**Scheme I-1A**).[21] A cavalcade of further derivatives and intermediates in the academic literature have been developed beyond benzylic substitutions and reductive aminations based around chemistries that make connections to IMiD cores containing an anilinic (as in **I.5**) or phenolic (as in **I.10**) element

or to form a C-heteroatom bond (**Scheme I-1B**).[19, 22] Beyond these, only a handful of examples demonstrate the formation of carbon-carbon bonds between IMiD cores and substituents,

Scheme I-1. A. Examples of IMiDs Currently in Clinical Development. B. Examples of Methods Used to Prepare IMiD Intermediates.

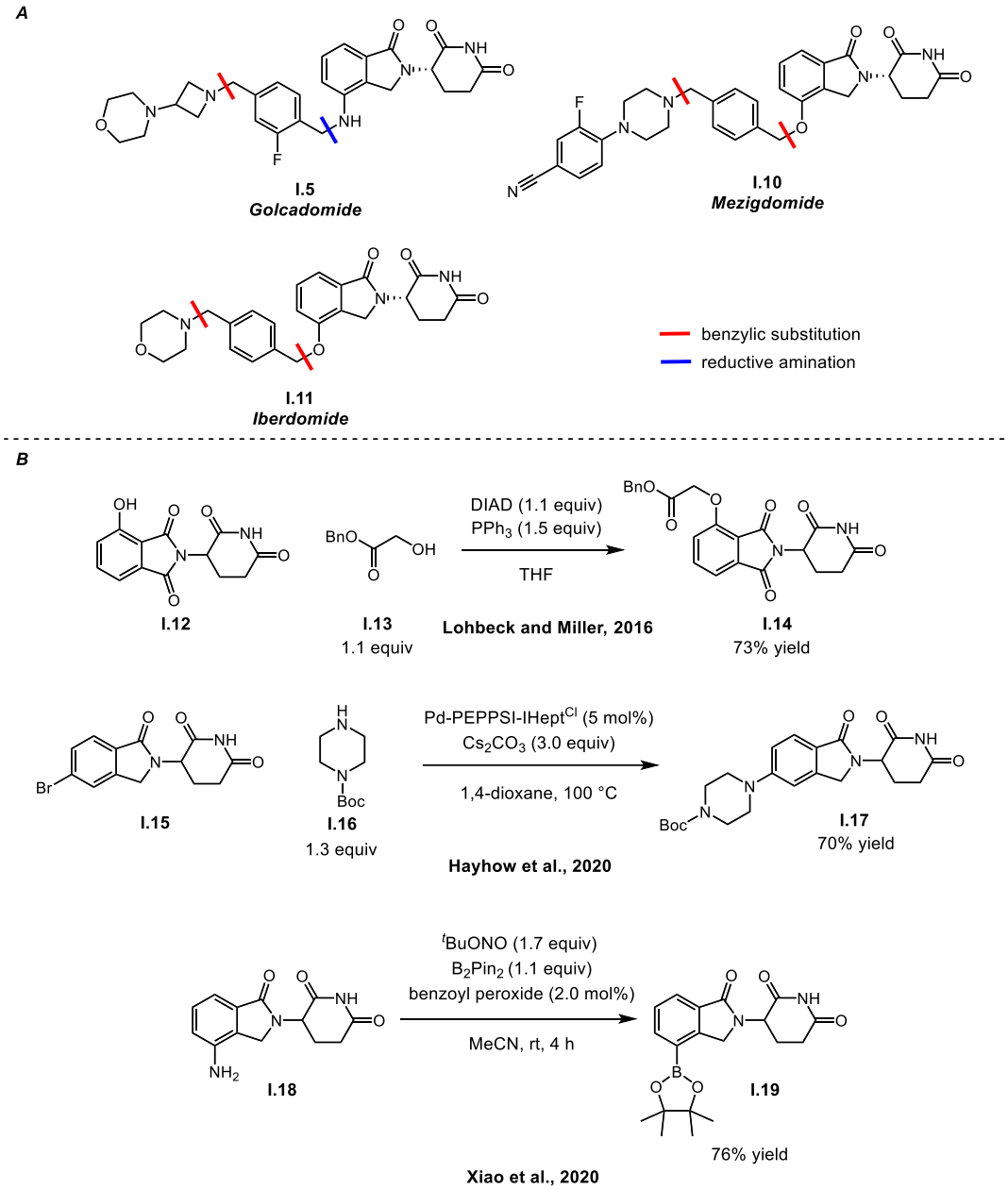

including the Sonogashira, Heck, and Suzuki-Miyaura couplings of halogenated cores,[23] although isolated examples of novel methods used to prepare IMiD derivatives such as decarbonylative cross-electrophile coupling exist (**Scheme I-2**).[24]

Scheme I-2. Examples of C-C bond-forming transformations used for IMiD synthesis.

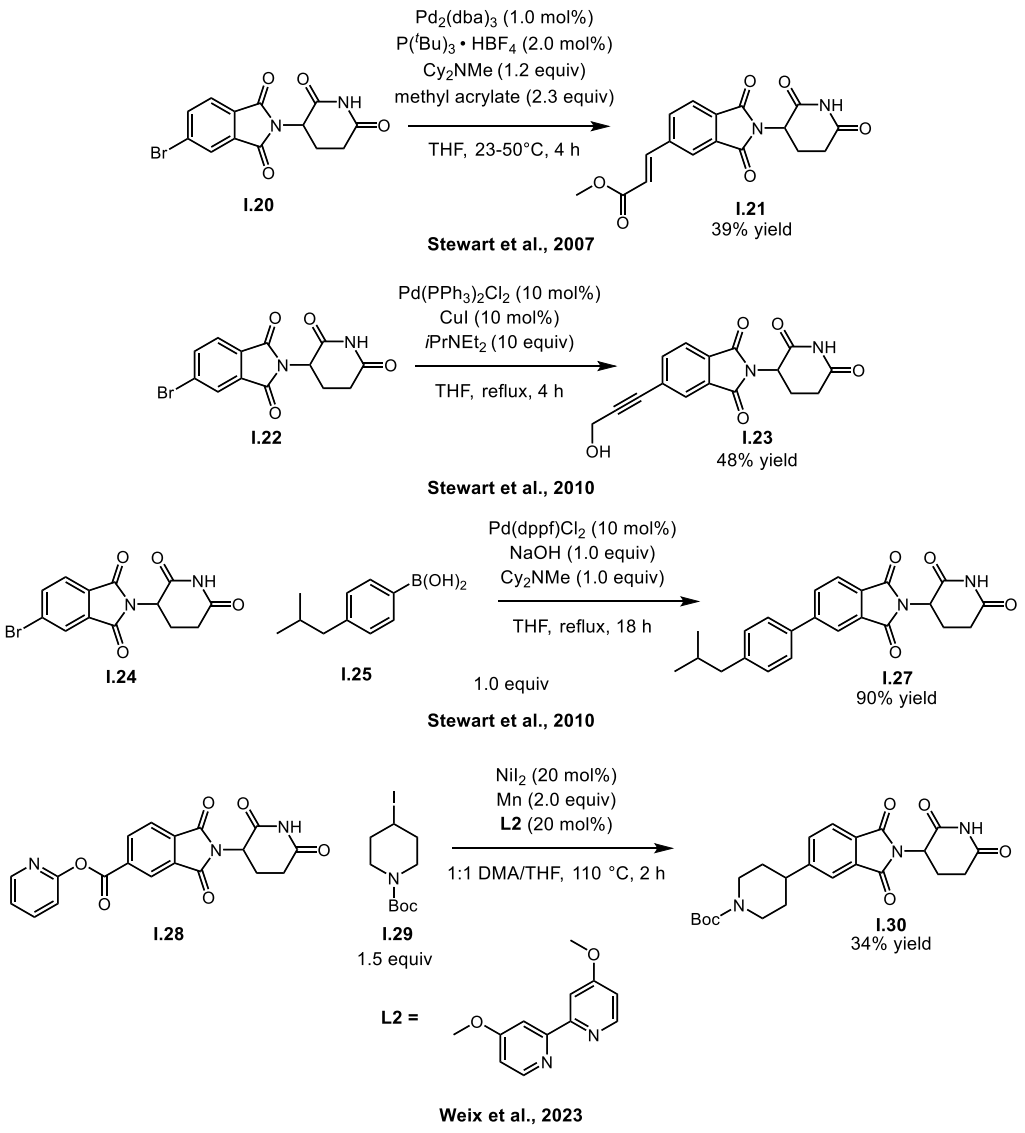

None of these existing methods are particularly amenable to producing stereochemically enriched structures distal to the IMiD core, and as a result publicly available IMiD structures are almost entirely either achiral or contain chiral elements introduced to the core rather than chiral

elements generated because of an enantioselective reaction with the IMiD core. Overall, the challenges of working with glutarimides have produced a space in which only a limited number of methods are available for preparing novel IMiDs, especially those with stereochemically enriched distal functionality.

One final complication with the synthesis of IMiDs exists; that is, the preparation of derivatives with an enantioenriched glutarimide stereogenic center. Many synthetic methods only address the synthesis of derivatives of IMiDs with undefined (i.e., racemic) stereocenters (see **Scheme I-1B**, **Scheme I-2**). Very few methods exist to create or preserve this stereocenter; one recent example by Reisman and coworkers is an enantioselective reductive arylation of glutarimides (**Scheme I-3A**). The reason for this is, as mentioned previously, the proton at the glutarimide stereogenic center is highly labile and therefore unlikely to retain its enantioenrichment in many synthetic methods.[17d, 18] Despite this, study of enantioenriched derivatives is valuable due to the differential effects of the glutarimide enantiomers in biological systems.[20a, 21b, 25] Often, these enantiomeric derivatives are isolated by chiral separation, or by preparing the molecule with any complex functionality prior to installation of the glutarimide.[19, 21b, 26] One increasingly common method of preserving both the glutarimide and its stereocenter through a synthesis is by carrying the enantioenriched glutarimide as a ring-opened *tert*-butyl ester, which is subjected to an acid-mediated ring-closure only at the end of the synthetic sequence (**Scheme I-3B**).[27] The drawback to this method is that the ring-closure reaction must be carefully monitored to prevent racemization.[27b] Other available methods used for the late-stage unveiling of glutarimides are insufficient as they do not provide any level of stereocontrol (**Scheme I-3C**).[28] The development of methods designed to address these challenges is highly significant. We propose that the full adaptation of novel synthetic technologies—not merely as

an afterthought or an application, but with full modification to the difficulties of working with glutarimides—would allow impactful expansion of the knowledge of how novel and biologically effective IMiDs can be developed.

Scheme I-3. A. Rare Example of Method for Preparing Enantioenriched Glutarimides. B. Late-Stage Technique for Unveiling an Enantioenriched Glutarimide. C. Alternative Glutarimide "Deprotection" Technique

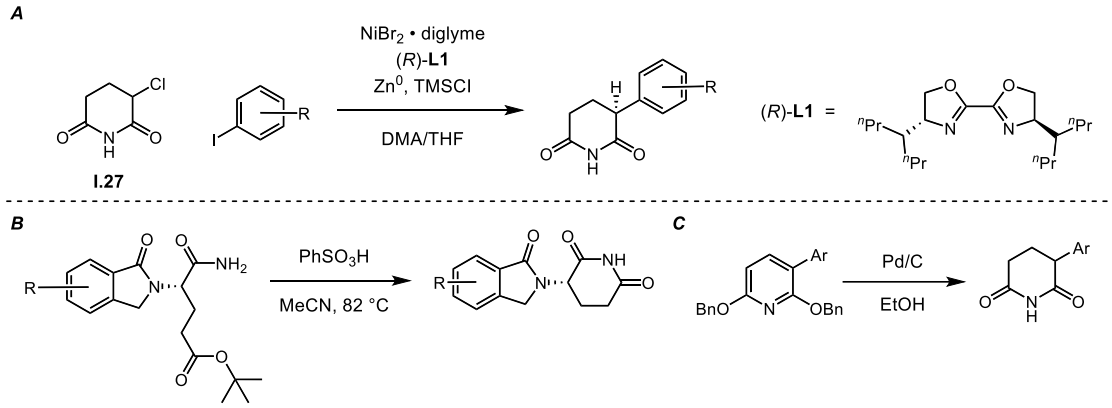

One of the synthetic technologies with potential for impact on the development of IMiDs is dirhodium–catalyzed carbene chemistry. Rhodium carbene chemistry—especially its asymmetric variant—is a powerful technique for the rapid introduction of chemical and special complexity, and with the right components is highly chemo, regio, and stereoselective. The primary components of a successful dirhodium-catalyzed carbene reaction are twofold: a carbene precursor with the right balance of selectivity and reactivity, and a chiral dirhodium catalyst. The most prevalent carbene precursor useful for formation of a metal-carbene bond is the diazo compound, which can take several forms. An electron-withdrawing group attached to a diazomethyl core will make the ensuing carbene more highly electron-deficient and thus more reactive, while an electron-donating substituent will decrease the electrophilicity and thus make the carbene more difficult to react with (**Figure I-4A**). Donor/acceptor carbenes balance these trends by including both kinds of groups to make a carbene that is both reactive and selective, as in compounds **I.28** and **I.30**, which have been used by the Davies group as highly selective

carbene precursors in an array of contexts.[29] Donor/acceptor diazo compounds can be induced to form carbenes by different methods; when exposed to light, a donor/acceptor carbene like **I.28** extrudes nitrogen, releasing a free carbene **I.29** (**Figure I-4B**).[30] In the presence of a dirhodium catalyst, this nitrogen extrusion is mediated by rhodium, producing a rhodium-carbene intermediate (**I.31**, **Figure I-4B**).[31]

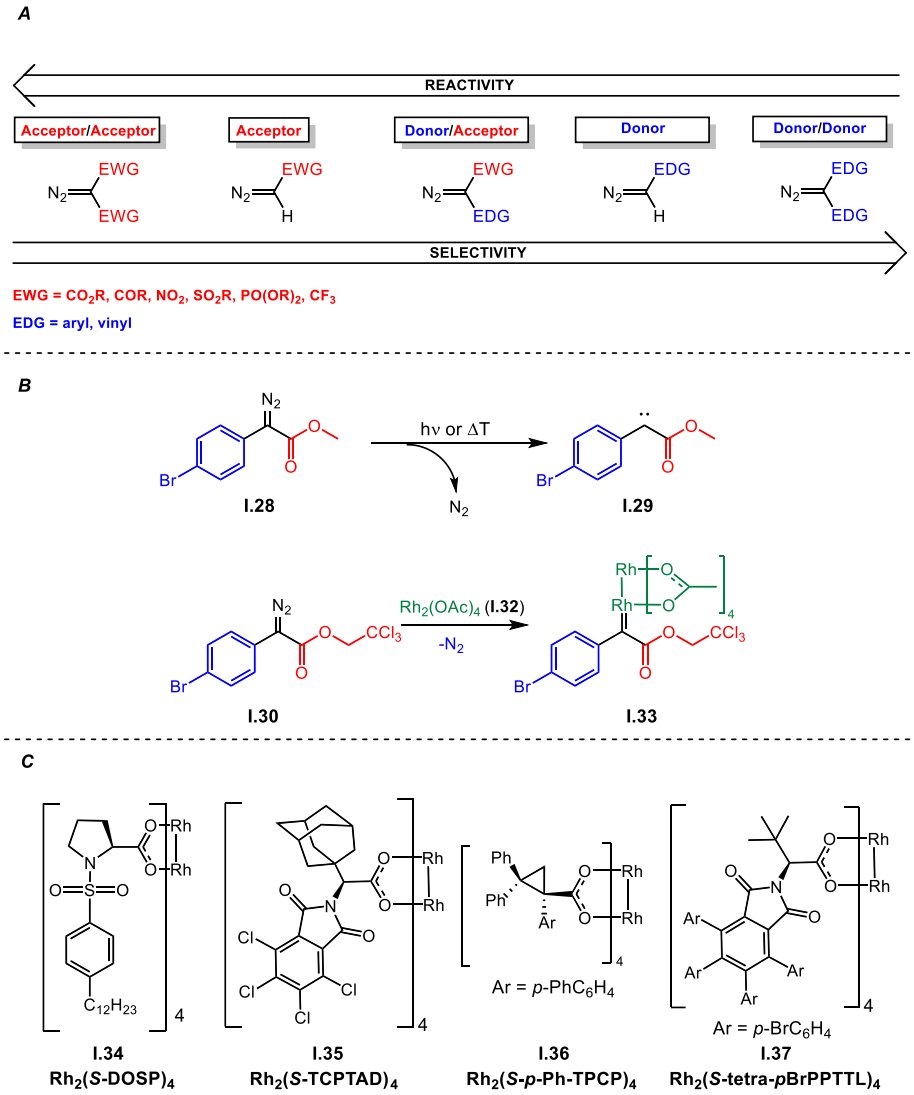

Figure I-4: A. Spectrum of reactivity and selectivity in diazo compounds. B. Examples of production of carbenes via diazo compounds. C. Representative examples of dirhodium catalysts used.

The rhodium catalyst mediates the reactions of the carbene, and in the case of chiral dirhodium catalysts (**Figure I-4C**), the resulting reaction is highly enantio-, regio-, and diastereoselective depending on the nature of catalyst and substrate. While the scope of transformations available to rhodium carbenes is quite large, two classes of reaction have been greatly improved by donor/acceptor rhodium carbenes and have been the subject of much research by the Davies group: C–H functionalization reactions and [2+1] cycloadditions (**Scheme I-4**).[32] Whether via [2+1] cycloaddition with an alkene or alkyne in cyclopropanation or cyclopropenation, or insertion into a C–H bond, the general mechanisms of these transformations follow the same general mechanism depicted in **Scheme I-5**.

Scheme I-4. Primary Rhodium Carbene Reactions Explored by the Davies Group

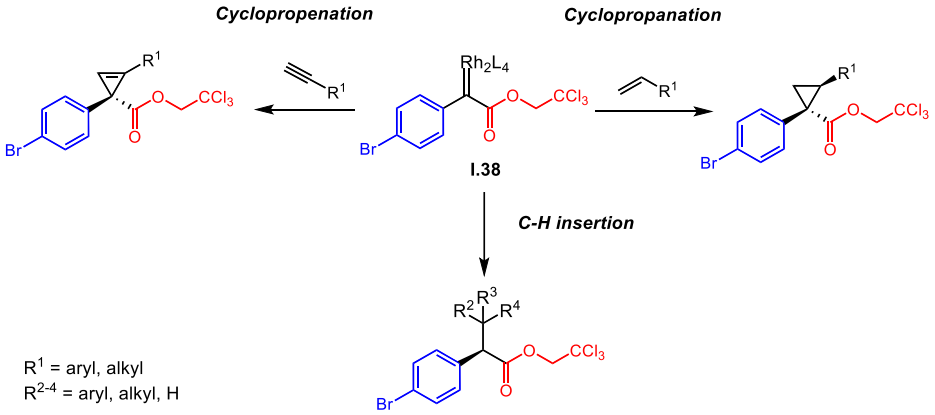

Scheme I-5. Generalized Mechanism of Dirhodium Carbene Reactions

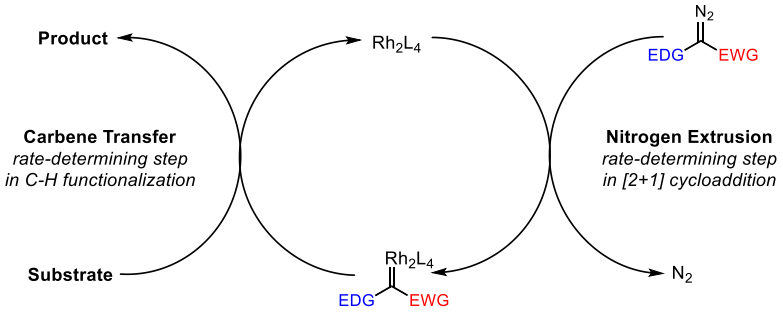

In [2+1] cycloadditions, the decomposition of the diazo compound into a rhodium-bound carbene is the rate-determining step,[33] while in C–H functionalization, the C–H insertion step is rate-determining.[34]

Both C–H functionalization and cyclopropanation have been applied in biologically relevant contexts such as the total synthesis of natural products.[32b, 35] Cyclopropanation has been an exceptional tool for rhodium catalysis as applied to medicinal chemistry contexts (**Scheme I-6**). Although formally a [4+3] cycloaddition, one of the Davies group's first forays into medicinal chemistry was the tandem cyclopropanation/Cope rearrangement reaction of rhodium vinyl carbenoids with pyrroles to produce novel tropane derivatives like **I.42** (**Scheme I-6A**).[36] These were used as a tool to probe biological systems for the mechanisms of cocaine addiction.[37] A 2013 collaboration between the Davies and Spring groups generated an array of cyclopropanation and cyclopropenation products, among others, which were then subjected to further derivatization in a diversity-oriented synthesis program to help identify cellular mitosis modulators (**Scheme I-6B**).[38] Somewhat more recently, Bristol Myers Squibb applied a large-scale cyclopropanation of a styrene derivative (**1.47**) with Rh_2(*S*-DOSP)$_4$ (**I.49**) to produce a key intermediate in the process synthesis of beclabuvir (**I.51**, **Scheme I-6C**).[39] A collaboration between the Davies group and Abbvie found that 2-chloropyridine could significantly enhance the enantioselectivity of cyclopropanations with *ortho*-substituted aryldiazoacetates,[40] which enabled the development of a flow process to produce **I.55** as an intermediate in the synthesis of an API (active pharmaceutical ingredient) (**Scheme I-6D**).[41]

Scheme I-6. A. Synthesis of Novel Tropane Derivatives Using Formal [4+3] Cycloadditions. B. Cycloadditions Used for Diversity-Oriented Synthesis. C. Application of Cyclopropanation in the Synthesis of Beclabuvir. D. Additives Enable Cyclopropanation for the Generation of Valuable API.

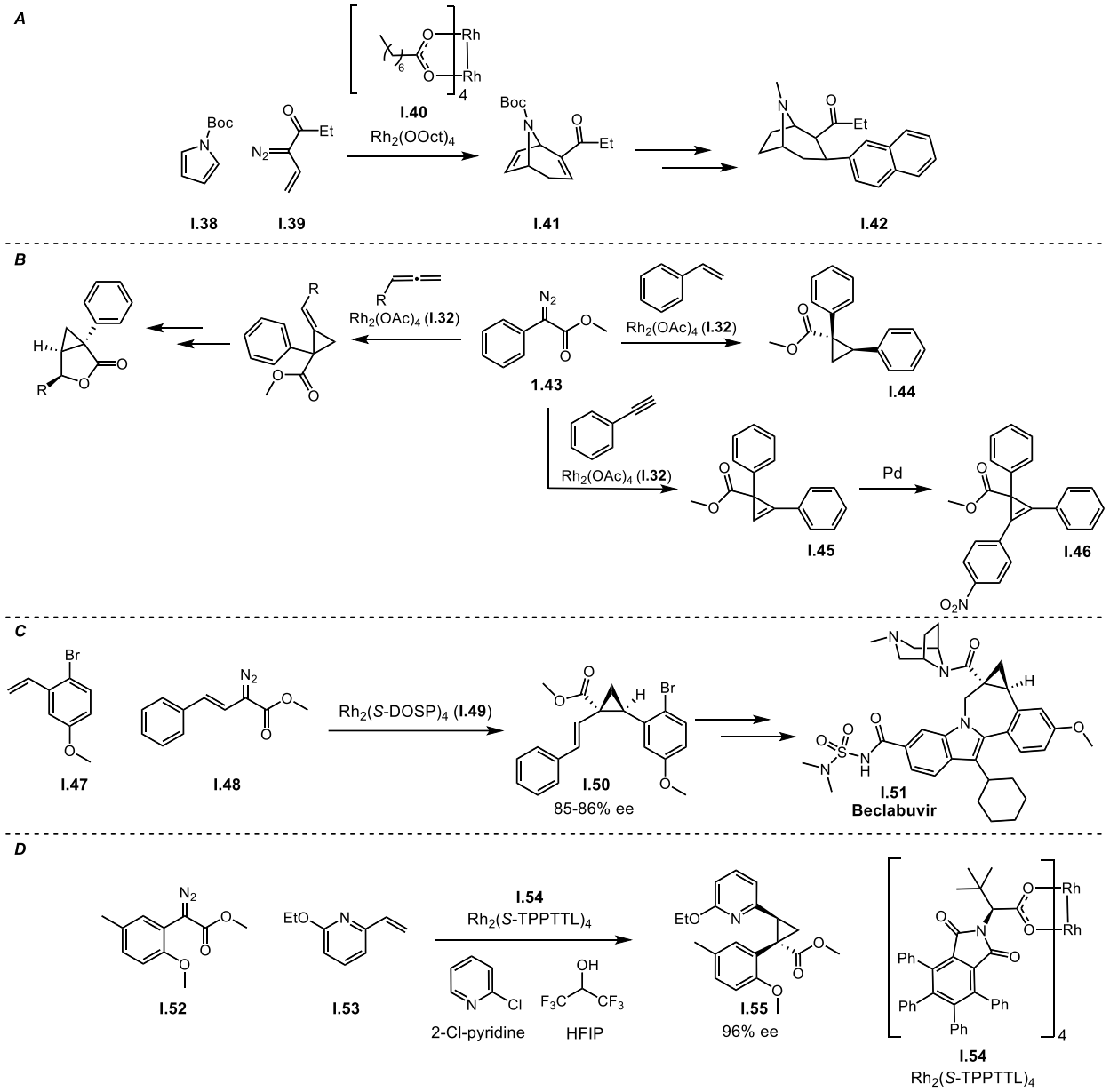

The use of 1,1,1,3,3,3-hexafluoroisopropanol (HFIP) as a water-sequestration additive in the flow process led to an important discovery that varying amounts of HFIP in a cyclopropanation reaction can rescue both the yield and enantioselectivity of the reaction in the presence of nucleophilic components that poison the rhodium catalyst (**Scheme I-7**).[42]

Scheme I-7. HFIP Enables Cyclopropanation Despite the Presence of Nucleophilic Catalyst Poisons

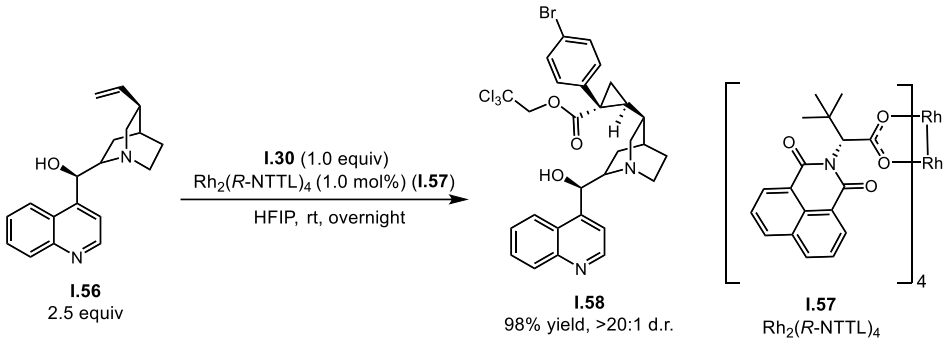

While C–H functionalization has yet to see the same scope of application in medicinal chemistry as cyclopropanation, it has been applied in contexts relevant to medicinal chemistry such as the C–H functionalization of bicyclo[1.1.1]pentanes[43] and the synthesis of methylphenidate (i.e., Ritalin®) analogues (**Scheme I-8**).[44]

Scheme I-8. Selected Applications of Rhodium-Catalyzed C-H Functionalization in Medicinal Contexts

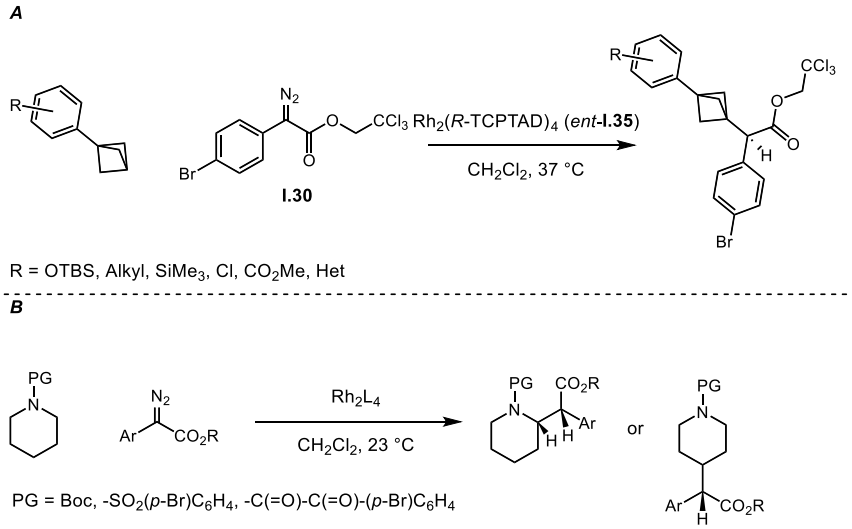

Rhodium catalysis, whether centered around cyclopropanation or C–H functionalization, has had a significant impact on changing the way chemists think about preparing complex, medicinally relevant products. Cyclopropanes are key motifs in many medicinally relevant compounds and introduce potentially valuable Csp^3-rich elements, as do C–H functionalization

products.[39, 45] The introduction of increasingly complex and challenging contexts has had the effect of generating valuable advances in how rhodium-catalyzed reactions are designed and conducted,[35, 40-42, 46] generating valuable and medicinally applicable molecules as a result.[37b, 39]

Questions in this space remain in terms of how these methods can be more directly applied to medicinally relevant scaffolds, rather than just as methods to generate intermediates, and how recent advances in the use of additives like HFIP can be used to enable these applications. One of these potentially productive applications—leveraging rhodium catalysis to enable the synthesis of novel IMiD drugs—is the primary focus of this work (**Chapters 2-3**). We hypothesized that rhodium catalysis could enable (1) the systematic biological study of IMiDs, (2) the synthesis of novel, stereochemically enriched IMiDs and IMiD cores while being mild enough to maintain the sensitive glutarimide stereogenic center, and (3) provide potentially valuable Csp^3-rich and diverse motifs to an important class of drug compounds.[45b, 47] To enable this exploration, we also developed an adaptation of the Suzuki-Miyaura cross-coupling, which expands the synthetic methods available for work on IMiDs and highlights the impact of transition-metal catalysis in general in a valuable medicinal chemistry context (**Chapter 1**).

References

(1) (a) Lenz, W., Thalidomide and congenital abnormalities. *Lancet* **1961,** *1*, 45; (b) McBride, W. G., Thalidomide and congenital abnormalities. *Lancet* **1961,** *2*, 1358.

(2) Bartlett, J. B.; Dredge, K.; Dalgleish, A. G., The evolution of thalidomide and its IMiD derivatives as anticancer agents. *Nat. Rev. Cancer* **2004,** *4*, 314-322.

(3) Hernandez-Ilizaliturri, F. J.; Reddy, N.; Holkova, B.; Ottman, E.; Czuczman, M. S., Immunomodulatory Drug CC-5013 or CC-4047 and Rituximab Enhance Antitumor Activity in a Severe Combined Immunodeficient Mouse Lymphoma Model. *Clin. Cancer Res.* **2005,** *11*, 5984-5992.

(4) Fuchs, O., Targeting cereblon in hematologic malignancies. *Blood Rev.* **2023,** *57*, 100994.

(5) (a) Chirnomas, D.; Hornberger, K. R.; Crews, C. M., Protein degraders enter the clinic — a new approach to cancer therapy. *Nat. Rev. Clin. Oncol.* **2023,** *20*, 265-278; (b) Tsai, J. M.; Nowak, R. P.; Ebert, B. L.; Fischer, E. S., Targeted protein degradation: from mechanisms to clinic. *Nat. Rev. Mol. Cell Biol.* **2024,** *25*, 740-757.

(6) Sakamoto, K. M.; Kim, K. B.; Kumagai, A.; Mercurio, F.; Crews, C. M.; Deshaies, R. J., Protacs: Chimeric molecules that target proteins to the Skp1–Cullin–F box complex for ubiquitination and degradation. *Proc. Natl. Acad. Sci.* **2001,** *98*, 8554-8559.

(7) (a) Snyder, L. B.; Neklesa, T. K.; Willard, R. R.; Gordon, D. A.; Pizzano, J.; Vitale, N.; Robling, K.; Dorso, M. A.; Moghrabi, W.; Landrette, S.; Gedrich, R.; Lee, S. H.; Taylor, I. C. A.; Houston, J. G., Preclinical Evaluation of Bavdegalutamide (ARV-110), a Novel PROteolysis TArgeting Chimera Androgen Receptor Degrader. *Mol. Cancer Ther.* **2024**; (b) Shore, N. D.; Shen, J.; Devitt, M. E.; Lu, H.; Alicea, J.; Parameswaran, J.; Chirnomas, D.; Gao, X.; McKean, M., Phase 1b study of bavdegalutamide, an androgen receptor PROTAC degrader, combined with abiraterone in patients with metastatic prostate cancer. *J. Clin. Oncol.* **2022,** *40*, TPS5106-TPS5106.

(8) Hsu, C.-C.; Zhao, J.; Polonskaia, A.; Bjorklund, C. C.; Ortiz Estevez, M.; Gandhi, A. K.; Hagner, P. R., Golcadomide-Mediated Degradation of Aiolos/Ikaros Synergizes with BET Inhibitors through Bidirectional Restructuring of the Directly Regulated Epigenetic Environment in DLBCL. *Blood* **2024,** *144*, 2739-2739.

(9) Ito, T.; Ando, H.; Suzuki, T.; Ogura, T.; Hotta, K.; Imamura, Y.; Yamaguchi, Y.; Handa, H., Identification of a Primary Target of Thalidomide Teratogenicity. *Science* **2010,** *327*, 1345-1350.

(10) (a) Fischer, E. S.; Böhm, K.; Lydeard, J. R.; Yang, H.; Stadler, M. B.; Cavadini, S.; Nagel, J.; Serluca, F.; Acker, V.; Lingaraju, G. M.; Tichkule, R. B.; Schebesta, M.; Forrester, W. C.; Schirle, M.; Hassiepen, U.; Ottl, J.; Hild, M.; Beckwith, R. E. J.; Harper, J. W.; Jenkins, J. L.; Thomä, N. H., Structure of the DDB1–CRBN E3 ubiquitin ligase in complex with thalidomide. *Nature* **2014,** *512*, 49-53; (b) Chamberlain, P. P.; Lopez-Girona, A.; Miller, K.; Carmel, G.; Pagarigan, B.; Chie-Leon, B.; Rychak, E.; Corral, L. G.; Ren, Y. J.; Wang, M.; Riley, M.; Delker, S. L.; Ito, T.; Ando, H.; Mori, T.; Hirano, Y.; Handa, H.; Hakoshima, T.; Daniel, T. O.; Cathers, B. E., Structure of the human Cereblon–DDB1–lenalidomide complex

reveals basis for responsiveness to thalidomide analogs. *Nat. Struct. Mol. Biol.* **2014,** *21*, 803-809.

(11) Ichikawa, S.; Flaxman, H. A.; Xu, W.; Vallavoju, N.; Lloyd, H. C.; Wang, B.; Shen, D.; Pratt, M. R.; Woo, C. M., The E3 ligase adapter cereblon targets the C-terminal cyclic imide degron. *Nature* **2022,** *610*, 775-782.

(12) Jiang, S.; Zhang, M.; Sun, J.; Yang, X., Casein kinase 1α: biological mechanisms and theranostic potential. *Cell Commun. Signal* **2018,** *16*, 23.

(13) Petzold, G.; Fischer, E. S.; Thomä, N. H., Structural basis of lenalidomide-induced CK1α degradation by the CRL4CRBN ubiquitin ligase. *Nature* **2016,** *532*, 127-130.

(14) Serra, A.; Gallart-Palau, X.; Wei, J.; Sze, S. K., Characterization of Glutamine Deamidation by Long-Length Electrostatic Repulsion-Hydrophilic Interaction Chromatography-Tandem Mass Spectrometry (LERLIC-MS/MS) in Shotgun Proteomics. *Anal. Chem.* **2016,** *88*, 10573-10582.

(15) Takata, T.; Oxford, J. T.; Demeler, B.; Lampi, K. J., Deamidation destabilizes and triggers aggregation of a lens protein, βA3-crystallin. *Protein Sci.* **2008,** *17*, 1565-1575.

(16) (a) Li, M.; Ogilvie, H.; Ochala, J.; Artemenko, K.; Iwamoto, H.; Yagi, N.; Bergquist, J.; Larsson, L., Aberrant post-translational modifications compromise human myosin motor function in old age. *Aging Cell* **2015,** *14*, 228-235; (b) Sadakane, Y.; Kawahara, M., Implications of Metal Binding and Asparagine Deamidation for Amyloid Formation. *Int J Mol Sci* **2018,** *19*; (c) Gallart-Palau, X.; Serra, A.; Sze, S. K., Chapter Four - Uncovering Neurodegenerative Protein Modifications via Proteomic Profiling. In *Int. Rev. Neurobiol.*, Hurley, M. J., Ed. Academic Press: 2015; Vol. 121, pp 87-116.

(17) (a) Schumacher, H.; Smith, R. L.; Williams, R. T., The Metabolism of Thalidomide: The Fate of Thalidomide and Some of its Hydrolysis Products in Various Species. *Br. J. Pharmacol.* **1965,** *25*, 338-351; (b) Schumacher, H.; Smith, R. L.; Williams, R. T., The Metabolism of Thalidomide: The Spontaneous Hydrolysis of Thalidomide in Solution. *Br. J. Pharmacol.* **1965,** *25*, 324-337; (c) Reist, M.; Carrupt, P.-A.; Francotte, E.; Testa, B., Chiral Inversion and Hydrolysis of Thalidomide: Mechanisms and Catalysis by Bases and Serum Albumin, and Chiral Stability of Teratogenic Metabolites. *Chem. Res. Toxicol.* **1998,** *11*, 1521-1528; (d) Knoche, B.; Blaschke, G., Investigations on the in vitro racemization of thalidomide by high-performance liquid chromatography. *J. Chromatogr. A* **1994,** *666*, 235-240.

(18) (a) Wnendt, S.; Finkam, M.; Winter, W.; Ossig, J.; Raabe, G.; Zwingenberger, K., Enantioselective inhibition of TNF-α release by thalidomide and thalidomide-analogues. *Chirality* **1996,** *8*, 390-396; (b) Nishimura, K.; Hashimoto, Y.; Iwasaki, S., (*S*)-form of α-methyl-N(α)-phthalimidoglutarimide, but not its (*R*)-form, enhanced phorbol ester-induced tumor necrosis factor-α production by human leukemia cell HL-60: implication of optical resolution of thalidomidal effects. *Chem. Pharm. Bull.* **1994,** *42*, 1157-1159.

(19) Sosič, I.; Bricelj, A.; Steinebach, C., E3 ligase ligand chemistries: from building blocks to protein degraders. *Chem. Soc. Rev.* **2022,** *51*, 3487-3534.

(20) (a) Tokunaga, E.; Yamamoto, T.; Ito, E.; Shibata, N., Understanding the Thalidomide Chirality in Biological Processes by the Self-disproportionation of Enantiomers. *Sci. Rep.* **2018,** *8*, 17131; (b) Thalidomide. In *The Merck Index Online*, The Merck Index Online database, 2013.

(21) (a) Matyskiela, M. E.; Zhang, W.; Man, H.-W.; Muller, G.; Khambatta, G.; Baculi, F.; Hickman, M.; LeBrun, L.; Pagarigan, B.; Carmel, G.; Lu, C.-C.; Lu, G.; Riley, M.; Satoh, Y.; Schafer, P.; Daniel, T. O.; Carmichael, J.; Cathers, B. E.; Chamberlain, P. P., A Cereblon Modulator (CC-220) with Improved Degradation of Ikaros and Aiolos. *J. Med. Chem.* **2018,** *61*, 535-542; (b) Hansen, J. D.; Correa, M.; Nagy, M. A.; Alexander, M.; Plantevin, V.; Grant, V.; Whitefield, B.; Huang, D.; Kercher, T.; Harris, R.; Narla, R. K.; Leisten, J.; Tang, Y.; Moghaddam, M.; Ebinger, K.; Piccotti, J.; Havens, C. G.; Cathers, B.; Carmichael, J.; Daniel, T.; Vessey, R.; Hamann, L. G.; Leftheris, K.; Mendy, D.; Baculi, F.; LeBrun, L. A.; Khambatta, G.; Lopez-Girona, A., Discovery of CRBN E3 Ligase Modulator CC-92480 for the Treatment of Relapsed and Refractory Multiple Myeloma. *J. Med. Chem.* **2020,** *63*, 6648-6676; (c) Anton, M. S. C.; Buchholz, T. J.; Lopez-Girona, A.; Narla, R. K.; Pourdehnad, M. Methods of treating non-hodgkin lymphoma using 2-(2,6-dioxopiperidin-3-yl)-4-((2-fluoro-4-((3-morpholinoazetidin-1-yl)methyl)benzyl)amino)isoindoline-1,3-dione. US20220324855A1, 2024.

(22) (a) Xiao, D.; Wang, Y.-j.; Wang, H.-l.; Zhou, Y.-b.; Li, J.; Lu, W.; Jin, J., Design and synthesis of new lenalidomide analogs via Suzuki cross-coupling reaction. *Arch. Pharm.* **2020,** *353*, 1900376; (b) Hayhow, T. G.; Borrows, R. E. A.; Diène, C. R.; Fairley, G.; Fallan, C.; Fillery, S. M.; Scott, J. S.; Watson, D. W., A Buchwald–Hartwig Protocol to Enable Rapid Linker Exploration of Cereblon E3-Ligase PROTACs. *Chem. Eur. J.* **2020,** *26*, 16818-16823; (c) Lohbeck, J.; Miller, A. K., Practical synthesis of a phthalimide-based Cereblon ligand to enable PROTAC development. *Bioorg. Med. Chem. Lett.* **2016,** *26*, 5260-5262.

(23) (a) Stewart, S. G.; Braun, C. J.; Ng, S.-L.; Polomska, M. E.; Karimi, M.; Abraham, L. J., New thalidomide analogues derived through Sonogashira or Suzuki reactions and their TNF expression inhibition profiles. *Bioorg. Med. Chem. Lett.* **2010,** *18*, 650-662; (b) Stewart, S. G.; Spagnolo, D.; Polomska, M. E.; Sin, M.; Karimi, M.; Abraham, L. J., Synthesis and TNF expression inhibitory properties of new thalidomide analogues derived via Heck cross coupling. *Bioorg. Med. Chem. Lett.* **2007,** *17*, 5819-5824.

(24) Wang, J.; Ehehalt, L. E.; Huang, Z.; Beleh, O. M.; Guzei, I. A.; Weix, D. J., Formation of C(sp^2)–C(sp^3) Bonds Instead of Amide C–N Bonds from Carboxylic Acid and Amine Substrate Pools by Decarbonylative Cross-Electrophile Coupling. *J. Am. Chem. Soc.* **2023,** *145*, 9951-9958.

(25) (a) Yamamoto, T.; Tokunaga, E.; Nakamura, S.; Shibata, N.; Toru, T., Synthesis and Configurational Stability of (*S*)- and (*R*)-Deuteriothalidomides. *Chem. Pharm. Bull.* **2010,** *58*, 110-112; (b) Mori, T.; Ito, T.; Liu, S.; Ando, H.; Sakamoto, S.; Yamaguchi, Y.; Tokunaga, E.; Shibata, N.; Handa, H.; Hakoshima, T., Structural basis of thalidomide enantiomer binding to cereblon. *Sci. Rep.* **2018,** *8*, 1294.

(26) Qian, Y.; Crew, A.; Crews, C.; Dong, H.; Hornberger, K. R.; Wang, J. Modulators of Estrogen Receptor Proteolysis and Associated Methods of Use. US 237418 A1, 2018.

(27) (a) Zacuto, M. J.; Traverse, J. F.; Bostwick, K. F.; Geherty, M. E.; Primer, D. N.; Zhang, W.; Zhang, C.; Janes, R. D.; Marton, C., Process Development and Kilogram-Scale Manufacture of Key Intermediates toward Single-Enantiomer CELMoDs: Synthesis of Iberdomide·BSA, Part 1. *Org. Process Res. Dev.* **2024,** *28*, 46-56; (b) Zacuto, M. J.; Traverse, J. F.; Geherty, M. E.; Bostwick, K. F.; Jordan, C.; Zhang, C., Chirality Control in the Kilogram-Scale Manufacture of Single-Enantiomer CELMoDs: Synthesis of Iberdomide·BSA, Part 2. *Org. Process Res. Dev.* **2024,** *28*, 57-66.

(28) Min, J.; Mayasundari, A.; Keramatnia, F.; Jonchere, B.; Yang, S. W.; Jarusiewicz, J.; Actis, M.; Das, S.; Young, B.; Slavish, J.; Yang, L.; Li, Y.; Fu, X.; Garrett, S. H.; Yun, M.-K.; Li, Z.; Nithianantham, S.; Chai, S.; Chen, T.; Shelat, A.; Lee, R. E.; Nishiguchi, G.; White, S. W.; Roussel, M. F.; Potts, P. R.; Fischer, M.; Rankovic, Z., Phenyl-Glutarimides: Alternative Cereblon Binders for the Design of PROTACs. *Angew. Chem. Int. Ed.* **2021,** *60*, 26663-26670.

(29) (a) Guptill, D. M.; Davies, H. M. L., 2,2,2-Trichloroethyl Aryldiazoacetates as Robust Reagents for the Enantioselective C–H Functionalization of Methyl Ethers. *J. Am. Chem. Soc.* **2014,** *136*, 17718-17721; (b) Davies, H. M. L., Finding Opportunities from Surprises and Failures. Development of Rhodium-Stabilized Donor/Acceptor Carbenes and Their Application to Catalyst-Controlled C–H Functionalization. *J. Org. Chem.* **2019,** *84*, 12722-12745.

(30) Jurberg, I. D.; Davies, H. M. L., Blue light-promoted photolysis of aryldiazoacetates. *Chem. Sci.* **2018,** *9*, 5112-5118.

(31) Ren, Z.; Musaev, D. G.; Davies, H. M. L., Key Selectivity Controlling Elements in Rhodium-Catalyzed C–H Functionalization with Donor/Acceptor Carbenes. *ACS Catal.* **2022,** *12*, 13446-13456.

(32) (a) Lebel, H.; Marcoux, J.-F.; Molinaro, C.; Charette, A. B., Stereoselective Cyclopropanation Reactions. *Chem. Rev.* **2003,** *103*, 977-1050; (b) Davies, H. M. L.; Denton, J. R., Application of donor/acceptor-carbenoids to the synthesis of natural products. *Chem. Soc. Rev.* **2009,** *38*, 3061-3071; (c) Davies, H.; Morton, D., Recent Advances in C–H Functionalization. *J. Org. Chem.* **2016,** *81*, 343-350; (d) Davies, H. M. L.; Lian, Y., The Combined C–H Functionalization/Cope Rearrangement: Discovery and Applications in Organic Synthesis. *Acc. Chem. Res.* **2012,** *45*, 923-935; (e) Briones, J. F.; Hansen, J.; Hardcastle, K. I.; Autschbach, J.; Davies, H. M. L., Highly Enantioselective Rh_2(*S*-DOSP)$_4$-Catalyzed Cyclopropenation of Alkynes with Styryldiazoacetates. *J. Am. Chem. Soc.* **2010,** *132*, 17211-17215; (f) Briones, J. F.; Davies, H. M. L., Rh_2(*S*-PTAD)$_4$-catalyzed asymmetric cyclopropenation of aryl alkynes. *Tetrahedron* **2011,** *67*, 4313-4317.

(33) Wei, B.; Sharland, J. C.; Lin, P.; Wilkerson-Hill, S. M.; Fullilove, F. A.; McKinnon, S.; Blackmond, D. G.; Davies, H. M. L., In Situ Kinetic Studies of Rh(II)-Catalyzed Asymmetric Cyclopropanation with Low Catalyst Loadings. *ACS Catal.* **2020,** *10*, 1161-1170.

(34) Wei, B.; Sharland, J. C.; Blackmond, D. G.; Musaev, D. G.; Davies, H. M. L., In Situ Kinetic Studies of Rh(II)-Catalyzed C–H Functionalization to Achieve High Catalyst Turnover Numbers. *ACS Catal.* **2022,** *12*, 13400-13410.

(35) Bosse, A. T.; Hunt, L. R.; Suarez, C. A.; Casselman, T. D.; Goldstein, E. L.; Wright, A. C.; Park, H.; Virgil, S. C.; Yu, J.-Q.; Stoltz, B. M.; Davies, H. M. L., Total synthesis of (−)-cylindrocyclophane A facilitated by C−H functionalization. *Science* **2024,** *386*, 641-646.

(36) Davies, H. M. L.; Young, W. B.; Smith, H. D., Novel entry to the tropane system by reaction of rhodium(II) acetate stabilized vinylcarbenoids with pyrroles. *Tet. Lett.* **1989,** *30*, 4653-4656.

(37) (a) Davies, H. M. L.; Gilliatt, V.; Kuhn, L. A.; Saikali, E.; Ren, P.; Hammond, P. S.; Sexton, T.; Childers, S. R., Synthesis of 2β-Acyl-3β-(substituted naphthyl)-8-azabicyclo[3.2.1]octanes and Their Binding Affinities at Dopamine and Serotonin Transport Sites. *J. Med. Chem.* **2001,** *44*, 1509-1515; (b) Davies, H. M. L.; Kuhn, L. A.; Thornley, C.; Matasi, J. J.; Sexton, T.; Childers, S. R., Synthesis of 3β-Aryl-8-azabicyclo[3.2.1]octanes with High Binding Affinities and Selectivities for the Serotonin Transporter Site. *J. Med. Chem.* **1996,** *39*, 2554-2558.

(38) Ibbeson, B. M.; Laraia, L.; Alza, E.; O' Connor, C. J.; Tan, Y. S.; Davies, H. M. L.; McKenzie, G.; Venkitaraman, A. R.; Spring, D. R., Diversity-oriented synthesis as a tool for identifying new modulators of mitosis. *Nat. Commun.* **2014,** *5*, 3155.

(39) Bien, J.; Davulcu, A.; DelMonte, A. J.; Fraunhoffer, K. J.; Gao, Z.; Hang, C.; Hsiao, Y.; Hu, W.; Katipally, K.; Littke, A.; Pedro, A.; Qiu, Y.; Sandoval, M.; Schild, R.; Soltani, M.; Tedesco, A.; Vanyo, D.; Vemishetti, P.; Waltermire, R. E., The First Kilogram Synthesis of Beclabuvir, an HCV NS5B Polymerase Inhibitor. *Org. Process Res. Dev.* **2018,** *22*, 1393-1408.

(40) Sharland, J. C.; Wei, B.; Hardee, D. J.; Hodges, T. R.; Gong, W.; Voight, E. A.; Davies, H. M. L., Asymmetric synthesis of pharmaceutically relevant 1-aryl-2-heteroaryl- and 1,2-diheteroarylcyclopropane-1-carboxylates. *Chem. Sci.* **2021,** *12*, 11181-11190.

(41) Lathrop, S. P.; Mlinar, L. B.; Manjrekar, O. N.; Zhou, Y.; Harper, K. C.; Sacia, E. R.; Higgins, M.; Bogdan, A. R.; Wang, Z.; Richter, S. M.; Gong, W.; Voight, E. A.; Henle, J.; Diwan, M.; Kallemeyn, J. M.; Sharland, J. C.; Wei, B.; Davies, H. M. L., Continuous Process to Safely Manufacture an Aryldiazoacetate and Its Direct Use in a Dirhodium-Catalyzed Enantioselective Cyclopropanation. *Org. Process Res. Dev.* **2023,** *27*, 90-104.

(42) Sharland, J. C.; Dunstan, D.; Majumdar, D.; Gao, J.; Tan, K.; Malik, H. A.; Davies, H. M. L., Hexafluoroisopropanol for the Selective Deactivation of Poisonous Nucleophiles Enabling Catalytic Asymmetric Cyclopropanation of Complex Molecules. *ACS Catal.* **2022,** *12*, 12530-12542.

(43) Garlets, Z. J.; Sanders, J. N.; Malik, H.; Gampe, C.; Houk, K. N.; Davies, H. M. L., Enantioselective C–H functionalization of bicyclo[1.1.1]pentanes. *Nat. Catal.* **2020,** *3*, 351-357.

(44) Liu, W.; Babl, T.; Röther, A.; Reiser, O.; Davies, H. M. L., Functionalization of Piperidine Derivatives for the Site-Selective and Stereoselective Synthesis of Positional Analogues of Methylphenidate. *Chem. Eur. J.* **2020,** *26*, 4236-4241.

(45) (a) Martin, S. F.; Dorsey, G. O.; Gane, T.; Hillier, M. C.; Kessler, H.; Baur, M.; Mathä, B.; Erickson, J. W.; Bhat, T. N.; Munshi, S.; Gulnik, S. V.; Topol, I. A., Cyclopropane-Derived Peptidomimetics. Design, Synthesis, Evaluation, and Structure of Novel HIV-1 Protease Inhibitors. *J. Med. Chem.* **1998,** *41*, 1581-1597; (b) Lovering, F.; Bikker, J.; Humblet, C., Escape from Flatland: Increasing Saturation as an Approach to Improving Clinical Success. *J. Med. Chem.* **2009,** *52*, 6752-6756.

(46) Garlets, Z. J.; Boni, Y. T.; Sharland, J. C.; Kirby, R. P.; Fu, J.; Bacsa, J.; Davies, H. M. L., Design, Synthesis, and Evaluation of Extended C4–Symmetric Dirhodium Tetracarboxylate Catalysts. *ACS Catal.* **2022,** *12*, 10841-10848.

(47) Szewczyk, S. M.; Verma, I.; Edwards, J. T.; Weiss, D. R.; Chekler, E. L. P., Trends in Neosubstrate Degradation by Cereblon-Based Molecular Glues and the Development of Novel Multiparameter Optimization Scores. *J. Med. Chem.* **2024,** *67*, 1327-1335.

Chapter 1: Development of an Anhydrous and Stereoretentive Fluoride-Enhanced Suzuki-Miyaura Reaction for the Synthesis of Derivatized Cereblon E3 ligase Modulatory Drug Cores.

Introduction

At the outset of the project, we wanted to investigate the cyclopropanation of vinyl thalidomide derivatives as a set of proof-of-concept reactions (**Scheme 1-1**). This would allow us to investigate the viability of the project vis-à-vis the compatibility of rhodium carbene chemistry with glutarimide-containing compounds.

Scheme 1-1. The Starting Material Problem

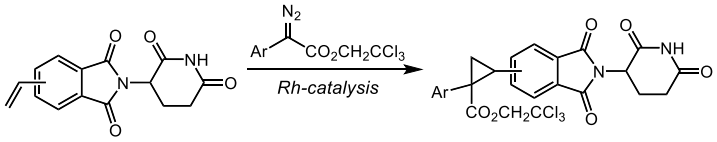

We considered several different methods of preparing a model 5-vinyl thalidomide derivative **1.4**, depicted in **Scheme 1-2**. Examples of Wittig olefination from **1.1** were unprecedented in the literature and we considered the stronger bases typically used in the reaction to be a potential

Scheme 1-2. Potential Routes Towards a Vinylated Thalidomide Derivative.

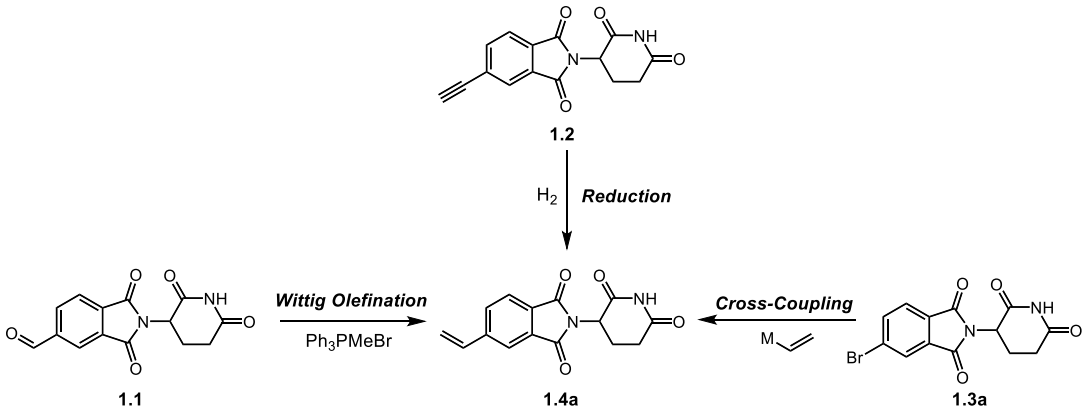

liability. Preliminary studies of semi-reduction from **1.2** were ineffective, and since the aryl bromide **1.3** is widely commercially available, we elected to explore the cross-coupling approach to **1.4**.

While the vinylation of aryl halides is a well-researched reaction class,[1] examples of vinylation of glutarimide-containing compounds generally only exist in the patent literature.[2] As mentioned previously, there are only a few examples in the academic literature of any Suzuki-Miyaura cross-coupling with thalidomide-like compounds.[3] We considered that the dearth of precedent for the preparation of these derivatives might be because of the synthetic problems surrounding IMiDs (vide supra). This can be brought further into perspective by considering the prototypical Suzuki-Miyaura reaction: a palladium catalyst, an organoboron nucleophile, and a solvent system that generally must include water and a base. This basic system is incompatible with glutarimide-containing compounds due to the degradation of either the glutarimide, or even cleavage of the core in phthalimide-containing variants.[4] Other researchers have begun to address the issue of conducting Suzuki-Miyaura reactions with base-sensitive elements present. However, many of these solutions rely on stoichiometric reagents and additives that are not commercially available, such as neopentyl boronates in the case of Denamark's work,[5] or a zinc-based Lewis acid in the case of Niwa and coworkers' research.[6] Methods developed for base-sensitive substrates also rely on a single or small subset of usable solvents.[6-7] In the course of finding a productive route for synthesizing **1.4a**, we developed a Suzuki-Miyaura coupling of potassium trifluoroborates that was effective for all regioisomers of the desired vinyl IMiD derivatives. These conditions utilize inorganic fluoride as an additive to enable a mild, anhydrous, and high-yielding reaction. We found that vinyl trifluoroborates were unusually

competent in the reaction when compared to other trifluoroborates, which effected a computation study of the role of inorganic fluoride in the reaction.

Results and Discussion

We began our efforts towards the synthesis of **1.4a** (**Scheme 1-3**) by assessing Suzuki-Miyaura conditions previously developed for use on thalidomide-like structures,[3] as well as more general vinylation conditions (See the supporting information for Chapter 1 for more details).[7-8] However, we found these to be generally ineffective. We had some success with conditions from the patent literature (entry 2),[2a] which gave **1.4a** in 33% yield under anhydrous conditions, using cesium carbonate as a base. We did not know what the role of cesium carbonate would be in the reaction without water present, as hydroxide formation is understood to be key in the accepted mechanism of the Suzuki-Miyaura reaction under the most common conditions.[9] Additionally, we were concerned that the cesium carbonate along with any adventitious water might be degrading the glutarimide.

We hypothesized that substituting cesium carbonate for a milder base might be more compatible with **1.3a** and substituted potassium fluoride, which gave an improved 44% yield. We were curious about the effects of fluoride in the reaction and screened several inorganic fluoride sources (entries 2-6). Regardless of the metal counterion, the enhancement effect remained and yields only slightly fluctuated. Silver fluoride and sodium fluoride seemed to perform slightly better than the others, and we elected to optimize further with sodium fluoride to eliminate any potential oxidative activity caused by the presence of a silver salt in the reaction.[6] We next investigated the effects of different phosphine ligands in the reaction—both monodentate and bidentate (entries 7-9). The bulky, electron rich ligand $P(^tBu)_3$, used in Pd(0) form as $Pd(P(^tBu)_3)_2$, gave a large increase in yield (82%, entry 9). Owing to the instability of

Pd(0) sources on the bench,[10] we elected to attempt using P(^{t}Bu)$_3$ Pd G4 as an alternative source of Pd-P(^{t}Bu)$_3$.[11] Using a small amount of diisopropylamine to activate the precatalyst (entry 10), this source gave a decreased yield of 70%. The yield increased slightly to 74% using triethylamine in place of diisopropylamine (entry 11). An alternative precursor, P(^{t}Bu)$_3$Pd(crotyl)Cl, performed similarly. Noticing that the reaction quickly generated palladium

Scheme 1-3. Optimization of Reaction Conditions

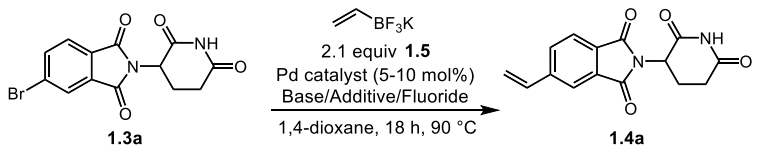

Entry	Catalyst	Fluoride Source	Base/Additive	Yield 1.4a (%)
1[a,b]	$PdCl_2$(dppf) (10 mol%)	—	Cs_2CO_3 (2 equiv)	33
2	$PdCl_2$(dppf) (10 mol%)	KF (3 equiv)	—	44
3	$PdCl_2$(dppf) (10 mol%)	CsF (3 equiv)	—	45
4	$PdCl_2$(dppf) (10 mol%)	LiF (3 equiv)	—	41
5	$PdCl_2$(dppf) (10 mol%)	AgF (3 equiv)	—	50
6	$PdCl_2$(dppf) (10 mol%)	NaF (3 equiv)	—	53
7	Pd(amphos)$_2$Cl$_2$ (10 mol%)	NaF (3 equiv)	—	55
8	dppf Pd G$_4$ (10 mol%)	NaF (3 equiv)	—	19
9	Pd(P^{t}Bu$_3$)$_2$ (10 mol%)	NaF (3 equiv)	—	82
10	P(^{t}Bu)$_3$ Pd G4 (5 mol%)	NaF (3 equiv)	^{i}Pr$_2$NH (10 mol%)	70
11	P(^{t}Bu)$_3$ Pd G4 (5 mol%)	NaF (3 equiv)	Et$_3$N (10 mol%)	74
12	P(^{t}Bu)$_3$Pd(crotyl)Cl (5 mol%)	NaF (3 equiv)	Et$_3$N (10 mol%)	78
13	P(^{t}Bu)$_3$ Pd G4 (5 mol%)	NaF (3 equiv)	Et$_3$N (15 mol%) P^{t}Bu$_3$ • HBF$_4$ (5 mol%)	80 (56)[c]
14	Pd(P(^{t}Bu)$_3$)$_2$ (5 mol%)	NaF (3 equiv)	Et$_3$N (15 mol%) P^{t}Bu$_3$ • HBF$_4$ (5 mol%)	81 (60)[c]
15	(P(^{t}Bu)$_3$)Pd(4-CF$_3$-C$_6$H$_4$)(Br) (5 mol%)	NaF (3 equiv)	Et$_3$N (15 mol%) P^{t}Bu$_3$ • HBF$_4$ (5 mol%)	84 (60)[c]
16[e]	Pd(amphos)$_2$Cl$_2$ (2 mol%)	—	[(tmeda)Zn(OH)(OTf)]$_3$	85
17[d]	**P(^{t}Bu)$_3$Pd(crotyl)Cl (5 mol%)**	NaF (3 equiv)	Et$_3$N (15 mol%) P^{t}Bu$_3$ • HBF$_4$ (5 mol%)	**93 (56)**[c]

Isolated yields reported. [a] 3.0 equiv **1.5** used [b] 10 mol% catalyst used. [c] Isolated reaction yield without added fluoride. [d] A reaction run in a PTFE-lined vessel gave **1.4a** in 78% yield. [e] Reaction conducted using 2 mol% catalyst, 2.34 equiv [(tmeda)Zn(OH)(OTf)]$_3$, 1.1 equiv **1.5**, in THF.

black, we wondered if using an excess of ligand in the reaction might protect the catalyst from potential degradation pathways. Using an equimolar amount of ligand as the phosphonium

tetrafluoroborate salt gave an increased yield using $P(^tBu)_3$ Pd G4 (entry 13); however, this result was outperformed significantly when we swapped the G4 for $P(^tBu)_3Pd(crotyl)Cl$ (entry 17, 93% yield).

The notable success of a one precatalyst over another, even with a common phosphine ligand between them, taken along with the effects of fluoride led us to ask whether the relationship between precatalyst and fluoride was important. We ran four reactions with and without added fluoride (entries 13-15, 17) and found that fluoride is responsible for a significant increase in yield, irrespective of the catalyst precursor used. Yields without fluoride show little variation between the four precatalysts used. We also wondered whether the fluoride was interacting with the glassware used for the reaction and ran the reaction in a PTFE tube.[12] Interestingly, we observed a slight decrease in yield (78%), but we hypothesize that a decrease in yield of this size may be due to differences in reaction setup.

In the course of investigating the fluoride-enhanced conditions, we also attempted to use Niwa's zinc-mediated Suzuki-Miyaura coupling, which gave an 85% yield of **1.4a** (entry 16).[6] However, when we attempted the same conditions to other IMiDs (vide infra), we found that the conditions gave only partial conversion. Compounds **1.3b**-**1.3e** were only sparingly soluble in the ethereal solvents required for the conditions, which we presume contributed to the poor conversion observed.[6]

We briefly investigated the generality of the conditions to alternative aryl halides (**Scheme 1-4**) and found that the conditions were agnostic as to the identity of the aryl halide, giving **1.4a** from the chloride and iodide in similar yields compared to the bromide. To successfully investigate the scope and biological activity of rhodium-catalyzed cyclopropanation on these vinyl IMiD derivatives, we deemed it important to prepare all the possible regioisomers. This

includes both the thalidomide-like regioisomers (phthalimide core, 4- and 5-substitutions) and the lenalidomide-like regioisomers (isoindolinone core, 4-7 substitution possible). When extending the conditions, we found that switching the solvent from 1,4-dioxane to DMSO boosted the solubility of the aryl bromides and gave an equivalent yield (in the case of **1.4a**) to 1,4-dioxane. Additionally, we found that the reactions were completed in only 1 hour. Compound **1.4b** required an increase in catalyst loading (to 10% catalyst) to give a yield comparable to the others.

Scheme 1-4. Scope of IMiD-Type Compounds

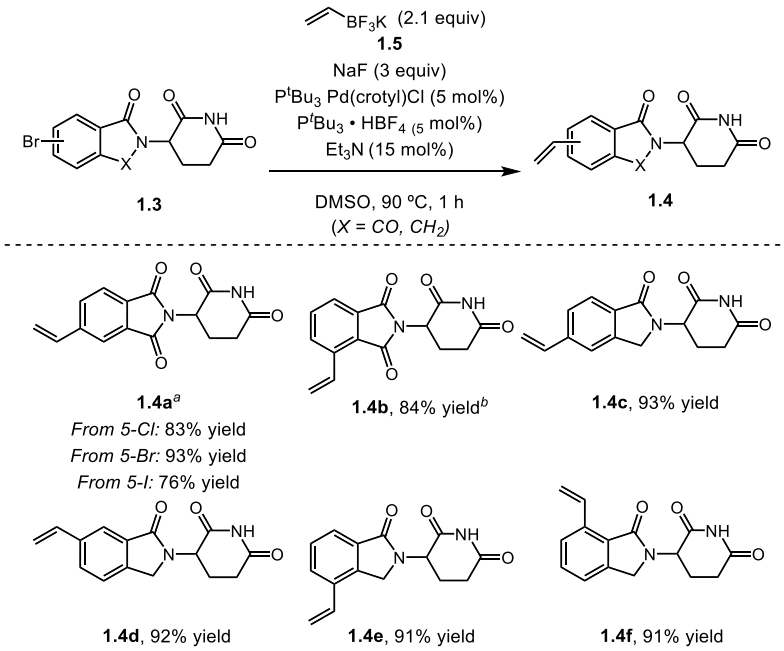

Isolated yields reported. [a] Reaction run using 1,4-dioxane as solvent. [b] Reaction conducted using 10 mol% catalyst, 30 mol% Et_3N, 10 mol% ligand.

Since study of enantioenriched IMiD derivatives is valuable and often requires preparative chiral HPLC or SFC separation,[2a, 13] we investigated the viability of conducting a vinylation on enantioenriched starting material. Using the optimal conditions listed in **Scheme 1-4**, we were immediately beset by degradation of the enantioenrichment of the glutarimide stereogenic center (**Scheme 1-5**). **(*S*)-1.3c**, enriched to 99% ee, gave **(*S*)-1.4c** in 82% ee under the standard

conditions. We initially hypothesized that the presence of amine base in the reaction was leading to the racemization, and conducted the reaction with no added ligand or amine base, using an oxidative addition complex as the Pd(0) source.[14] This had the opposite of the intended effect, giving **(*S*)-1.4c** in 69% ee (entry 2). Efforts to eliminate the workup as a potential contributing factor led us to attempt an acidic workup (entry 3), which resulted in less racemization (90% ee). Running the reaction at a lowered temperature (entry 4) gave a slight increase in the enantioenrichment of **(*S*)-1.4c** (92% ee). We ran the reaction again at 90 °C, taking samples from the reaction every five min to run on a chiral SFC, and found that if the reaction is run for only

Scheme 1-5. Optimization of an Enantioretentive Reaction.

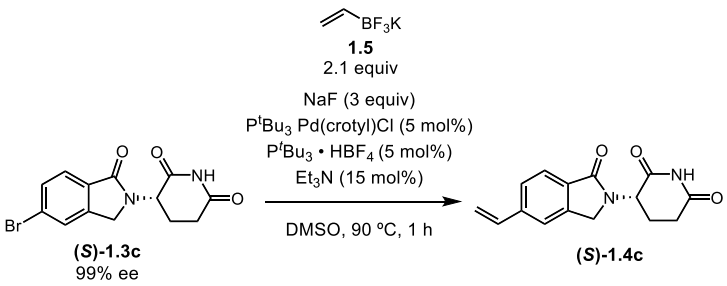

Entry	Variation	% ee 1.4c[a]
1[b]	None	82
2[b]	5 mol% (P(^{t}Bu)$_3$)Pd(4-CF$_3$-C$_6$H$_4$)(Br), no added ligand/Et$_3$N	69
3[b]	1M citric acid workup	90
4[b]	1M citric acid workup, 70 °C reaction	92
5[c]	1M citric acid workup, 90 °C reaction, 0.17 h reaction time	99

[a] % ee measured by chiral SFC [b] An isolated yield was not acquired for these reactions. [c] Reaction gave an 88% isolated yield

10 minutes, **(*S*)-1.4c** can be isolated in an 88% yield without racemization (99% ee). As a comparison, we ran the reaction using conditions from the patent literature,[15] and observed complete racemization of the starting material **(*S*)-1.3c**.

We returned to our investigation of the generality of the reaction conditions by conducting the reaction with aryl halides other than IMiD derivatives. We were inspired by Buchwald and

workers' research on C–N couplings of base-sensitive 5-membered heterocycles with aliphatic amines,[16] and subjected a subset of these substrates (**Scheme 1-6**, **1.8a-h**) to the vinylation conditions. To avoid issues with volatility, we used potassium 4-methyl-ß-styryltrifluoroborate (**1.7e**) in place of potassium (vinyl)trifluoroborate. Excluding isothiazole (**1.8b**) and 1,2,4-triazole (**1.8e**), all heteroaryl bromides gave modest to excellent yields. We also tested the reaction of a pyridyl substrate with potassium (vinyl)trifluoroborate to ensure relevance to six-membered heterocycles, and this substrate gave an excellent 87% yield (**1.8h**).

Scheme 1-6. Scope of Heteroaryl Bromides

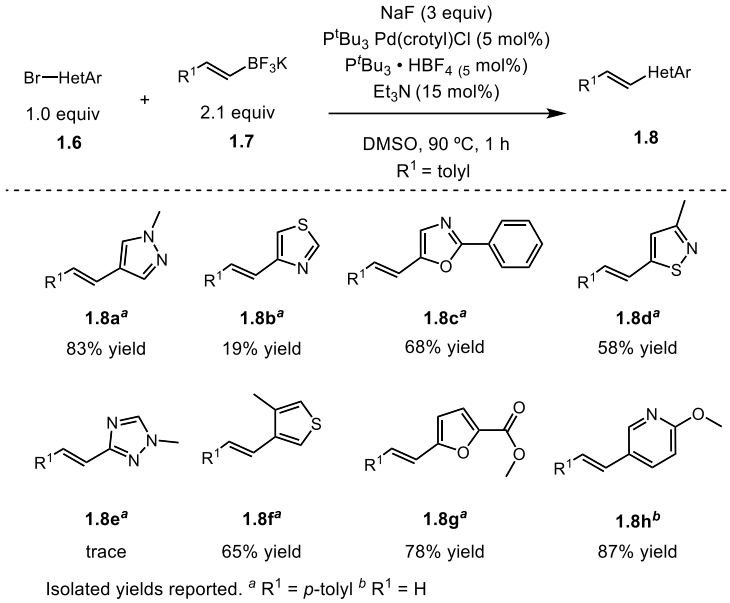

We next explored the scope of trifluoroborates under the reaction conditions with aryl bromide **1.3a**. Simple allyl and vinyl trifluoroborates performed very well (**1.9a-1.9c**, **Scheme 1-7**), but these presented an additional intrigue. In the case of **1.9a** and **1.9b**, the reaction had to be stopped after 10 minutes, as additional reaction time produced rearrangement products of the substrate alkene. These presumably result from off-cycle palladium species generated during the reaction. Both **1.9a** and **1.9c** rearrange to the more thermodynamically stable product **1.9b**. Other simple trifluoroborates give excellent performance in the reaction (**1.9d-e**). Aryl trifluoroborates

do not perform as well; for example, phenyl trifluoroborate only gives a 26% yield of **1.9f**. When the reaction is conducted for 10 minutes with vinyl trifluoroborate, a 75% yield of **1.9** is produced. However, when the reaction is conducted for 10 minutes with phenyl trifluoroborate, the reaction gives a 7% yield of **1.9f**. Interestingly, heteroaryl trifluoroborates give high yields all around (**1.9h-l**). We attempted to extend the scope of trifluoroborates to alkyl trifluoroborates, but we recovered the starting aryl bromide and the trifluoroborate in most of these cases (See the

Scheme 1-7. Scope of Potassium Trifluoroborates

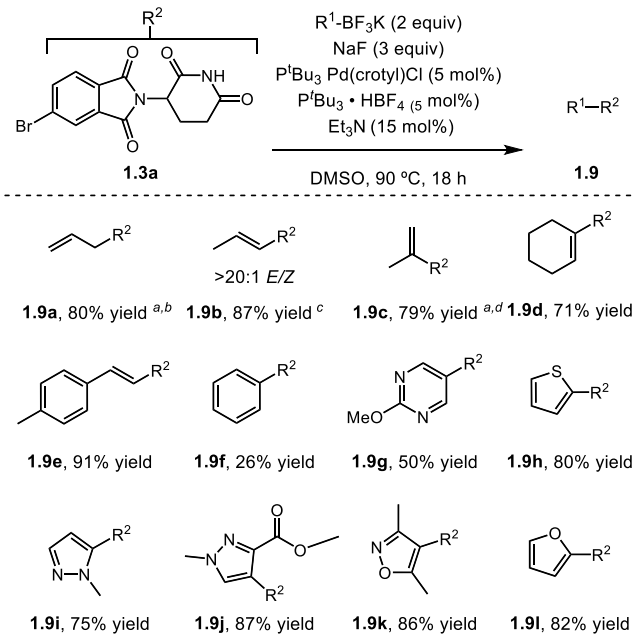

Isolated yields reported. [a] Reaction run with for 0.17 h using 10 mol% P^tBu_3 Pd(crotyl)Cl, 10 mol% $P^tBu_3 \cdot HBF_4$, 30 mol% TEA
[b] 18:1 ratio of terminal to internal (i.e., Pd-isomerized, i.e, **1.9a** to **1.9b**) alkene.
[c] >20:1 ratio **1.9b**:**1.9a**
[d] 7.5:1 ratio **1.9c**:**1.9b**; standard conditions gave a 1:2 ratio of **1.9c**:**1.9b**

Supporting Information for **Chapter 1** for more information).

With the exception of a few special cases, trifluoroborates are slow to react under anhydrous conditions due to the strength of the B–F bonds and their weak nucleophilicity.[6, 17] The standard reaction pathway of a trifluoroborate in fact requires water, which under basic conditions will convert the trifluoroborate to a boronic acid in situ.[12b, 17c] One special case relies on an

electrophilic acyl halide coupling partner and a key potassium-mediated interaction to transmetalate from an alkyl trifluoroborate, which releases BF_3 and KCl in the process (**Figure 1-1A**).[17a] Another known pathway involves transmetallation from trifluoroborate encouraged by a palladium center with either a partially positive[6] or fully positive charge[17b] generated via abstraction of the halide with a Lewis acid. This pathway, as exemplified by Niwa's proposed

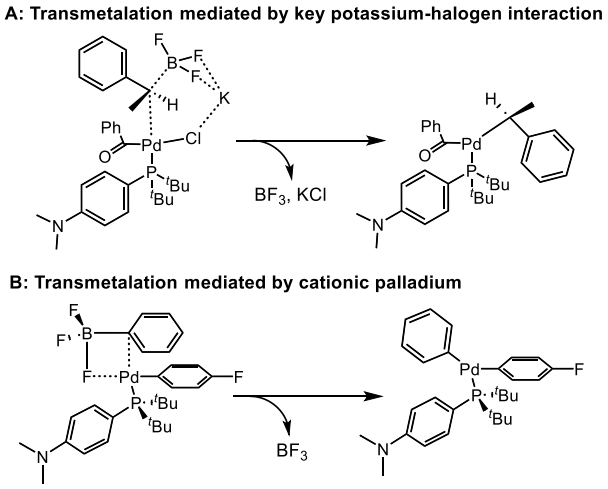

Figure 1-1. Mechanistic Examples of Transmetalation of Trifluoroborates Under Anhydrous Conditions

mechanism in **Figure 1-1B**, involves a four-center transition state in which BF_3 is released as the Pd–C bond with the substrate forms. In light of these known mechanisms, the ease of the cross-coupling of the vinyl trifluoroborate under our conditions was intriguing and prompted us to investigate the mechanism further.

We elected to probe the mechanism with DFT calculations, using the M06/6-31G* level of theory. These calculations were conducted by Lauren Grant from Bristol Myers Squibb. We first computed a proposed "association complex," (**I**, **Figure 1-2**) where the fluoride of the trifluoroborate coordinates with the palladium center. Due to the excess of fluoride in the system, we also proposed this complex with a fluoride in place of the vestigial bromide derived from oxidative addition into **1.3a**. We calculated the stability of the possible isomeric arrangements

for this structure. The most stable features the trifluoroborate *trans* to the phosphine ligand and *cis* to the phenyl ring. We then proposed a rearrangement coordinating the π-system of the vinyl group to palladium to prepare for transmetallation. This is a favorable rearrangement in terms of ΔG, as demonstrated by the 9.8 kcal/mol exotherm leading to the rearranged structure **II**. A $\Delta G^{\ddagger}$ of 17.3 kcal/mol leads to a proposed structure **III** in which the B–C bonds begin to weaken.

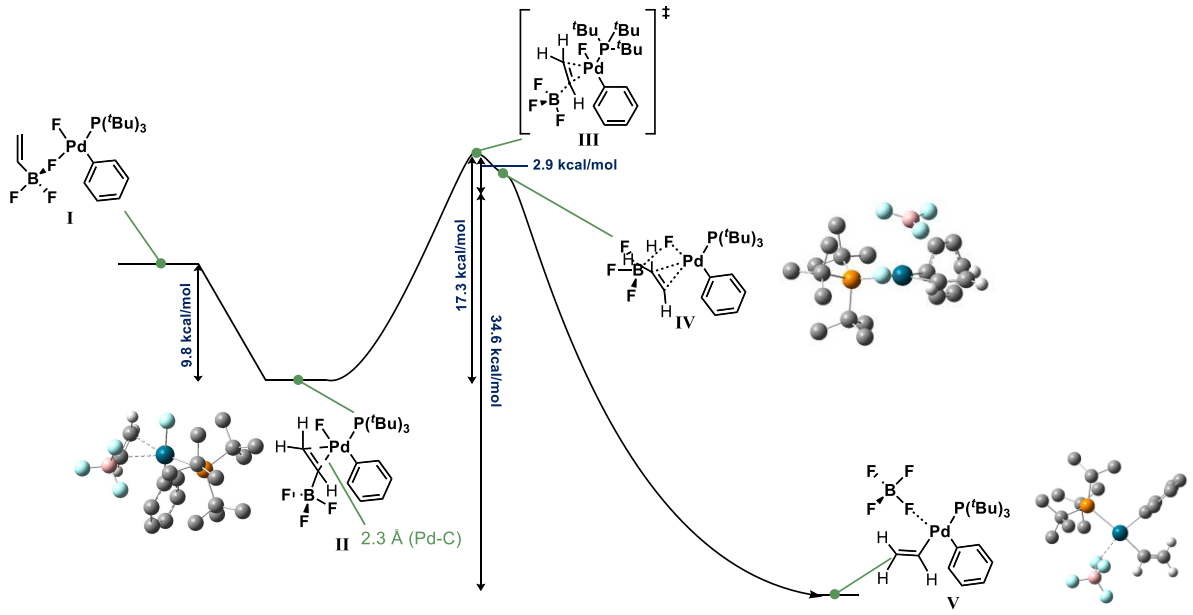

Figure 1-2. Computed structures of association and rearrangement complexes of the trifluoroborate. ΔG demonstrates the favorability of this transformation for potassium vinyltrifluoroborate salts.

A slight (2.9 kcal/mol) depression in energy shows **IV**, in which a bond begins to form between the borate center and the palladium-ligated fluoride, and near-complete breakage of the B–C bond. Relative to the rearrangement complex, this leads to an exotherm of 20.2 kcal/mol and complex **V**, primed for reductive elimination. Interestingly, this proposed mechanism does not exactly model the mechanisms proposed in **Figure 1-1**.

Based on these findings, we conducted a study on the reaction with phenyl trifluoroborate to investigate reasons why the reaction proceeds more poorly than with the vinyl trifluoroborate (**Figure 1-3**). Phenyl trifluoroborate is clearly less favorable as a transmetalation partner: in the

stage of pre-transmetalation analogous to that from **I** to **II** in **Figure 1-1**, **VII** is produced by an exothermic rearrangement (1.7 kcal/mol). Significantly, efforts to find other analogous transition states were unsuccessful. This suggests either that the process is far less favorable or that the transmetalation proceeds by a mechanism not considered here. We considered a potential role for potassium in calculations, but the ground state trend in free energy was upheld in this case.

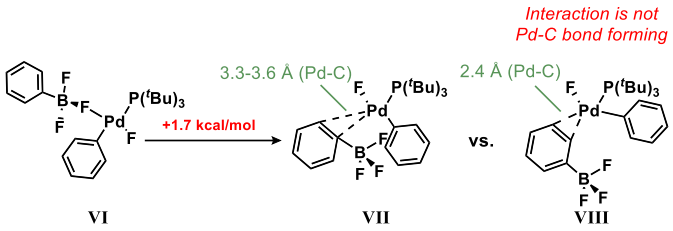

Figure 1-3. Computed structures of productive and non-productive association and rearrangement complexes of phenylborate. ΔG as well elongated π -bonding interactions demonstrate that this transformation for phenylborate salts is less favorable.

One illuminating factor is that the π-interaction between the phenyl ring and the palladium is weaker than that of the vinyl group. The calculated distance between the ring and the metal center is elongated at 3.3–3.6 Å versus the vinyl group and the metal center (2.3 Å). We did identify an instance in which the bond length was shortened (**VIII**, **Figure 1-3**), but in this case it is not a productive interaction as the interaction is not with the π-system immediately adjacent to the borate. We hypothesize that steric effects play a role in modulating these distances, when comparing the phenyl trifluoroborate to the vinyl trifluoroborate. Additionally, the ability of the vinyl π-system to donate electron density is better than that of the aromatic phenyl π-system. One additional argument for this point is that in the calculated association complexes **XI** and **X** for heterocyclic trifluoroborates, which are less aromatic systems than the phenyl, the bond distances are similar to that of the vinyl trifluoroborate (**Figure 1-4**). This is corroborated by the isolated yields of **1.9k** and **1.9l** (**Scheme 1-7**), which are 82 and 86%, respectively.

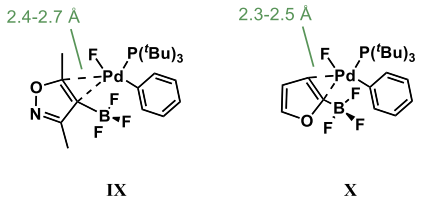

Figure 1-4. Computed structures of association for a more hindered isoxazoleborate and furanborate reveal the ability to form vinyl-like association complexes despite aromaticity or increased steric demand.

To round out our investigations, we next conducted a screen of alternative organoboron nucleophiles as the vinyl source for the reaction (**Scheme I-8**). We did not screen vinylboronic acid due to the impracticality of its use.[1] The MIDA-protected boronate ester (entry 2) only gave trace amounts of product. The pinacol ester (entry 3) gave a 28% yield. Overall, these results indicate that the role of the trifluoroborate as a vinyl source under these conditions may be somewhat unique.

Scheme 1-8. Investigation of Alternative Nucleophiles

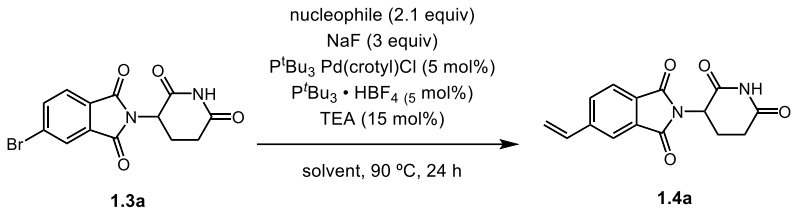

Entry	Nucleophile	Solvent	% Yield 1.4a [1]
1	potassium vinyltrifluoroborate	1,4-dioxane	93
2	vinylboronic acid MIDA ester	"	trace
3	vinylboronic acid pinacol ester	"	28

[1] Isolated yield of purified product

We were left with questions about the role of fluoride. The role of fluoride is understood due to the work of Fu, Le Duc, and others, but only under hydrolytic conditions.[11-12, 18] In one 2000 study by Fu, potassium fluoride is utilized as a base in a Suzuki-Miyaura coupling with boronic acids under anhydrous conditions, and a trifluoroborate is proposed as an intermediate. However, they go on to demonstrate that a potassium *o*-tolyl trifluoroborate cannot couple with an aryl

chloride under their conditions.[19] We hypothesize that fluoride might serve to make the pre-transmetalation palladium complex more electrophilic and therefore more prone to transmetalation compared to a palladium-bromide complex, contributing to the success of the reaction along with the uniquely suitable alkene-type trifluoroborates. While we demonstrate the impact of inorganic fluoride independent of precatalyst (vide supra), we were curious whether other Lewis-basic additives or even halide scavengers would influence the reaction similarly (**Scheme 1-9**).

Scheme 1-9. Investigation of Alternative Additives

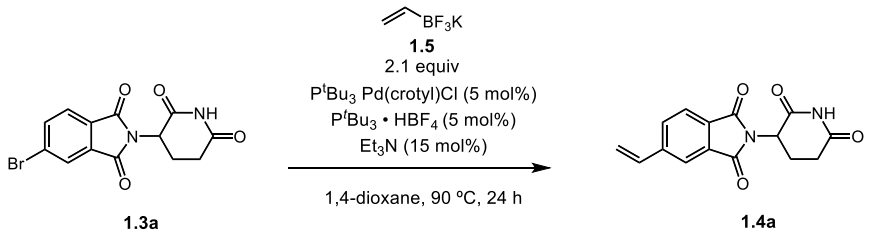

Entry	Base	% Yield 1.4a [1]	Entry	Base	% Yield 1.4a [1]
1	NaF	93	**7**	NaOH	49
2	Cs_2CO_3	22	**8**	$NaHCO_3$	47
3[2]	TBAF	39	**9**	NaOAc	63
4	K_3PO_4	63	**10**	NaOTf	65
5	TMSOK	n.d.	**11**	NaTFA	74
6	^{t}BuOK	n.d.			

[1] Isolated yield of purified product [2] Commerical TBAF (Millipore Sigma, 1.0 M in THF, 216143) contains ca. 5 wt% H_2O

We tested inorganic bases under the conditions (entries 2, 4, 7, 8), which when compared to reaction outcome without fluoride gave equivalent or diminished yield. An alternative source of fluoride (TBAF, entry 3) gave a diminished yield, which we contribute to the introduction of water into the reaction. Suzuki-Miyaura additives successful in other contexts (entry 5)[9] eliminated reaction product entirely. Interestingly, mild bases like sodium triflate and sodium trifluoroacetate increased the reaction yield slightly, relative to a reaction with no fluoride (entries 9-11). We hypothesize a possible halide scavenging effect of these ligands in the reaction, but this cannot be fully deconvoluted from other potential effects.[20]

Conclusions

During our efforts to prepare substrates for modification by rhodium carbene chemistry, we discovered generally applicable Suzuki-Miyaura conditions effective for the cross-coupling of glutarimide-containing compounds with alkene-type potassium trifluoroborates. We found that fluoride played an essential role in ensuring high reaction yields, and that the reaction conditions were mild enough to ensure enantiofidelity at the sensitive and important stereogenic center found in thalidomide-like compounds. Upon computational investigation, we found that a π-complex potentially formed during the pre-transmetalation process illuminated an experimental preference for alkene-type trifluoroborates and some heterocyclic trifluoroborates over arene-type trifluoroborates. This study represents a significant addition to the methods available to medicinal chemists in the preparation of important IMiD-type compounds.

The research contained in this chapter was published in the *Journal of Organic Chemistry* in 2024:

Tracy, W. F.; Davies, G. H. M.; Grant, L. N.; Ganley, J. M.; Moreno, J.; Cherney, E. C.; Davies, H. M. L., Anhydrous and Stereoretentive Fluoride-Enhanced Suzuki–Miyaura Coupling of Immunomodulatory Imide Drug Derivatives. *J. Org. Chem.* **2024,** *89*, 4595-4606.

This work was a collaborative project with Bristol Myers Squibb. W.F. Tracy conducted all of the experimental work. L.N. Grant provided the computational analysis. G.H.M. Davies provided valuable optimization advice that led to further exploration of the fluoride effects and helped to provide substrates for the project. J.M. Ganley provided valuable mechanistic insights and analysis. E.C. Cherney and J. Moreno provided valuable support, ideas, and analysis.

References

(1) Denmark, S. E.; Butler, C. R., Palladium- (and nickel-) catalyzed vinylation of aryl halides. *Chem. Commun.* **2009**, 20-33.

(2) (a) Qian, Y.; Crew, A.; Crews, C.; Dong, H.; Hornberger, K. R.; Wang, J. Modulators of Estrogen Receptor Proteolysis and Associated Methods of Use. US 237418 A1, 2018; (b) Beckwith, J. E. R.; Bonazzi, S.; Cernijenko, A. Heteroaryl substituted 3-(1-oxoisoindolin-2-yl)piperidine-2,6-dione derivatives and uses thereof. US 0271940 A1, 2021.

(3) Stewart, S. G.; Braun, C. J.; Ng, S.-L.; Polomska, M. E.; Karimi, M.; Abraham, L. J., New thalidomide analogues derived through Sonogashira or Suzuki reactions and their TNF expression inhibition profiles. *Bioorg. Med. Chem. Lett.* **2010,** *18*, 650-662.

(4) Reist, M.; Carrupt, P.-A.; Francotte, E.; Testa, B., Chiral Inversion and Hydrolysis of Thalidomide: Mechanisms and Catalysis by Bases and Serum Albumin, and Chiral Stability of Teratogenic Metabolites. *Chem. Res. Toxicol.* **1998,** *11*, 1521-1528.

(5) Kassel, V. M.; Hanneman, C. M.; Delaney, C. P.; Denmark, S. E., Heteroaryl–Heteroaryl, Suzuki–Miyaura, Anhydrous Cross-Coupling Reactions Enabled by Trimethyl Borate. *J. Am. Chem. Soc.* **2021,** *143*, 13845-13853.

(6) Niwa, T.; Uetake, Y.; Isoda, M.; Takimoto, T.; Nakaoka, M.; Hashizume, D.; Sakurai, H.; Hosoya, T., Lewis acid-mediated Suzuki–Miyaura cross-coupling reaction. *Nat. Catal.* **2021,** *4*, 1080-1088.

(7) Su, M.; Huang, X.; Lei, C.; Jin, J., Nickel-Catalyzed Reductive Cross-Coupling of Aryl Bromides with Vinyl Acetate in Dimethyl Isosorbide as a Sustainable Solvent. *Org. Lett.* **2022,** *24*, 354-358.

(8) Sharland, J. C.; Wei, B.; Hardee, D. J.; Hodges, T. R.; Gong, W.; Voight, E. A.; Davies, H. M. L., Asymmetric synthesis of pharmaceutically relevant 1-aryl-2-heteroaryl- and 1,2-diheteroarylcyclopropane-1-carboxylates. *Chem. Sci.* **2021,** *12*, 11181-11190.

(9) Delaney, C. P.; Marron, D. P.; Shved, A. S.; Zare, R. N.; Waymouth, R. M.; Denmark, S. E., Potassium Trimethylsilanolate-Promoted, Anhydrous Suzuki–Miyaura Cross-Coupling Reaction Proceeds via the "Boronate Mechanism": Evidence for the Alternative Fork in the Trail. *J. Am. Chem. Soc.* **2022,** *144*, 4345-4364.

(10) Colacot, T. J.; Shea, H. A., $Cp_2Fe(PR_2)_2PdCl_2$ (R = *i*-Pr, *t*-Bu) Complexes as Air-Stable Catalysts for Challenging Suzuki Coupling Reactions. *Org. Lett.* **2004,** *6*, 3731-3734.

(11) Firsan, S. J.; Sivakumar, V.; Colacot, T. J., Emerging Trends in Cross-Coupling: Twelve-Electron-Based L1Pd(0) Catalysts, Their Mechanism of Action, and Selected Applications. *Chem. Rev.* **2022,** *122*, 16983-17027.

(12) (a) Butters, M.; Harvey, J. N.; Jover, J.; Lennox, A. J. J.; Lloyd-Jones, G. C.; Murray, P. M., Aryl Trifluoroborates in Suzuki–Miyaura Coupling: The Roles of Endogenous Aryl Boronic Acid and Fluoride. *Angew. Chem. Int. Ed.* **2010,** *49*, 5156-5160; (b) Lennox, A. J. J.; Lloyd-Jones, G. C., Organotrifluoroborate Hydrolysis: Boronic Acid Release Mechanism and an Acid–Base Paradox in Cross-Coupling. *J. Am. Chem. Soc.* **2012,** *134*, 7431-7441.

(13) (a) Sosič, I.; Bricelj, A.; Steinebach, C., E3 ligase ligand chemistries: from building blocks to protein degraders. *Chem. Soc. Rev.* **2022,** *51*, 3487-3534; (b) Hansen, J. D.; Correa, M.; Nagy, M. A.; Alexander, M.; Plantevin, V.; Grant, V.; Whitefield, B.; Huang, D.; Kercher, T.; Harris, R.; Narla, R. K.; Leisten, J.; Tang, Y.; Moghaddam, M.; Ebinger, K.; Piccotti, J.; Havens, C. G.; Cathers, B.; Carmichael, J.; Daniel, T.; Vessey, R.; Hamann, L. G.; Leftheris, K.; Mendy, D.; Baculi, F.; LeBrun, L. A.; Khambatta, G.; Lopez-Girona, A., Discovery of CRBN E3 Ligase Modulator CC-92480 for the Treatment of Relapsed and Refractory Multiple Myeloma. *J. Med. Chem.* **2020,** *63*, 6648-6676; (c) Yamamoto, T.; Tokunaga, E.; Nakamura, S.; Shibata, N.; Toru, T., Synthesis and Configurational Stability of (*S*)- and (*R*)-Deuteriothalidomides. *Chem. Pharm. Bull.* **2010,** *58*, 110-112; (d) Tokunaga, E.; Yamamoto, T.; Ito, E.; Shibata, N., Understanding the Thalidomide Chirality in Biological Processes by the Self-disproportionation of Enantiomers. *Sci. Rep.* **2018,** *8*, 17131; (e) Mori, T.; Ito, T.; Liu, S.; Ando, H.; Sakamoto, S.; Yamaguchi, Y.; Tokunaga, E.; Shibata, N.; Handa, H.; Hakoshima, T., Structural basis of thalidomide enantiomer binding to cereblon. *Sci. Rep.* **2018,** *8*, 1294.

(14) Timsina, Y. N.; Xu, G.; Colacot, T. J., It Is Not All about the Ligands: Exploring the Hidden Potentials of tBu3P through Its Oxidative Addition Complex as the Precatalyst. *ACS Catal.* **2023,** *13*, 8106-8118.

(15) Lu, L.; Combs, A.; Basch, C.; Shetty, R.; Dai, C.; Bersch, K.; Rose, J. A.; Beam, D. J.; Mei, S. BRM Targeting Compounds and Associated Methods of Use. US 0083376 A1, 2021.

(16) Reichert, E. C.; Feng, K.; Sather, A. C.; Buchwald, S. L., Pd-Catalyzed Amination of Base-Sensitive Five-Membered Heteroaryl Halides with Aliphatic Amines. *J. Am. Chem. Soc.* **2023,** *145*, 3323-3329.

(17) (a) Roh, B.; Farah, A. O.; Kim, B.; Feoktistova, T.; Moeller, F.; Kim, K. D.; Cheong, P. H.-Y.; Lee, H. G., Stereospecific Acylative Suzuki–Miyaura Cross-Coupling: General Access to Optically Active α-Aryl Carbonyl Compounds. *J. Am. Chem. Soc.* **2023,** *145*, 7075-7083; (b) Bardin, V. V.; Shabalin, A. Y.; Adonin, N. Y., Weakly nucleophilic potassium aryltrifluoroborates in palladium-catalyzed Suzuki–Miyaura reactions: relative reactivity of K[4-RC6F4BF3] and the role of silver-assistance in acceleration of transmetallation. *Beilstein J. Org. Chem.* **2015,** *11*, 608-616; (c) Molander, G. A.; Biolatto, B., Palladium-Catalyzed Suzuki−Miyaura Cross-Coupling Reactions of Potassium Aryl- and Heteroaryltrifluoroborates. *J. Org. Chem.* **2003,** *68*, 4302-4314.

(18) (a) Ichikawa, J.; Hamada, S.; Sonoda, T.; Kobayashi, H., A one-pot synthesis of 2,2-difluorovinyl carbonyl compounds from 2,2,2,-trifluoroethyl p-toluenesulfonate via 2,2-difluorovinylboranes. *Tet. Lett.* **1992,** *33*, 337-340; (b) Wright, S. W.; Hageman, D. L.; McClure, L. D., Fluoride-Mediated Boronic Acid Coupling Reactions. *J. Org. Chem.* **1994,** *59*, 6095-6097; (c) Fagnou, K.; Lautens, M., Halide Effects in Transition Metal Catalysis. *Angew. Chem. Int. Ed.* **2002,** *41*, 26-47; (d) Amatore, C.; Jutand, A.; Le Duc, G., The Triple Role of Fluoride Ions in Palladium-Catalyzed Suzuki–Miyaura Reactions: Unprecedented Transmetalation from [ArPdFL2] Complexes. *Angew. Chem. Int. Ed.* **2012,** *51*, 1379-1382.

(19) Littke, A. F.; Dai, C.; Fu, G. C., Versatile Catalysts for the Suzuki Cross-Coupling of Arylboronic Acids with Aryl and Vinyl Halides and Triflates under Mild Conditions. *J. Am. Chem. Soc.* **2000,** *122*, 4020-4028.

(20) Mondal, A.; van Gemmeren, M., Silver-Free C−H Activation: Strategic Approaches towards Realizing the Full Potential of C−H Activation in Sustainable Organic Synthesis. *Angew. Chem. Int. Ed.* **2022,** *61*, e202210825.

Chapter 2: Asymmetric Dirhodium-Catalyzed Cyclopropanation and Cyclopropenation of Cereblon E3 Ligase Modulatory Drug Cores and their Biological Evaluation.

Introduction

Despite the value of IMiDs as a drug class, many challenges remain on the path to full understanding of how to design clinically effective IMiDs. Several decades ago, IMiDs were evaluated and classified according to phenotypic observations (i.e., their function in biological systems).[1] Advances in the field led to target elucidation, such as discovery of the targeting of proteins implicated in the metabolisms of multiple myeloma by lenalidomide.[2] More recently, medicinal chemists have been guided by structural biology and computational work solving ternary complexes of CRBN with IMiDs and multiple neosubstrates.[3] This has also led to identification of common themes in neosubstrates targeted by IMiDs like the G-motif or G-loop, an eight-amino-acid stretch comtaining glycine in the primary classes of successfully targeted neosubstrates.[4]

Because of this work, researchers now have deeper understanding of the teratogenicity of IMiDs, target elucidation and off-target effects, and the beginnings of how to design selective IMiDs. However, what remains out of reach is a more *a priori* design approach. Designing protein degradation efficacy and selectivity for a single neosubstrate into an IMiD is semi-empirical, even among the now well-studied protein classes like zinc finger family proteins. Some efforts towards *a priori* design of IMiDs are underway: systemic neosubstrate selectivity correlations are becoming less rare in the literature.[3c, 4-5] There are two primary factors limiting further understanding of IMiDs: Systematic structure-and-reactivity (SAR) correlations for distal

modifications to IMiDs across a range of neosubstrates, of which reports are rare,[5a] and the limitations of structure-based modelling, especially in computation.[6]

SAR correlations have arguably been hampered by the lack of development in synthetic approaches to IMiDs. As discussed in the introduction to this work, there is pressure in the field to (1) demonstrate compatibility between known methods and glutarimide-containing compounds, (2) re-optimize known methods for compatibility and (3) develop new, glutarimide-compatible methods. We aimed to adapt rhodium-catalyzed [2+1] cycloadditions to the modification of glutarimides (**Figure 2-1**) as this will enable facile introduction of stereochemically defined and complex functionality to IMiDs, which is currently lacking in the space. We propose that the introduction of stereochemically defined and Csp^3-rich content may be a valuable strategy to avoid off-target neosubstrate degradation.[7] In the previous chapter, we developed an anhydrous, stereoretentive Suzuki-Miyaura coupling to gain access to the vinyl derivatives required to begin our planned campaign.

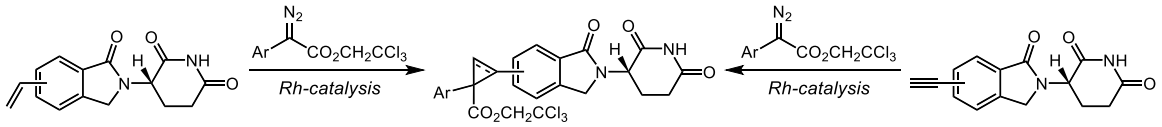

Figure 2-1. Conception of the project: Adapt rhodium-catalyzed [2+1] cycloadditions to prepare regio- and stereochemically diverse IMiD derivatives.

In this chapter, we show the highly effective and highly asymmetric cyclopropanation of these derivatives. The cyclopropanations are mild enough to be fully stereoretentive in reactions with enantioenriched starting material. We also demonstrate the successful cyclopropenation of IMiD derivatives with terminal alkynes. These reactions enabled systematic SAR studies across several neosubstrates (IKZF3 or Aiolos, CK1α, GSPT1, and SALL4) of how stereochemical and regiochemical changes distal to the IMiD cores (both phtalimide and isoindolinone) affect

degradation selectivity and activity, which is to our knowledge one of the first studies of its kind. We evaluate the products resulting from the adapted rhodium-catalyzed methods using cheminformatic approaches and find that they provide highly divergent structures in terms of both chemical space and moments of inertia (compound shape). Finally, we take advantage of the highly diversifiable ester groups introduced by 2,2,2-trichloroethyl 2-(4-bromophenyl)-2-diazoacetate in the reactions to demonstrate possible routes of further modifications.

Results and Discussion

The primary goal of the project was singular: demonstrate enantioselective cyclopropanation of vinyl IMiD derivatives with both pthalimide (thalidomide-like) and isoindolinone (lenalidomide-like) cores, across the range of possible vinyl substitutions. As a secondary goal, we desired to conduct an analogous campaign of cyclopropenation of ethynyl IMiD derivatives. Going into the project, we did not know whether the vinyl IMiD derivatives we synthesized would work in the reactions, given that we found them to be mostly insoluble in the dichloromethane ubiquitous in our cycloaddition chemistry. We also wondered whether the glutarimide N–H would interfere with the reaction by poisoning the catalyst or inserting into the carbene generated from the diazoacetate. We selected 2,2,2-trichloroethyl 2-(4-bromophenyl)-2-diazoacetate as the carbene precursor or the reactions, due to its precedented robust asymmetric induction and the highly diversifiable functional groups contained within (i.e., the ester and aryl bromide functionalities).[8]

The starting vinyl glutarimides we selected for the initial studies are racemates. In a cyclopropanation, two new stereocenters are formed. We report two diastereomeric ratios (**Scheme 2-1**); the first is for the relative configuration of the two new stereogenic centers formed during the cyclopropanation, and the second is for the level of asymmetric induction achieved by the chiral catalyst. Starting with the 5-substituted vinyl thalidomide, we conducted a

brief screen of chiral catalysts (**Scheme 2-1**). Although other catalysts (entries 1-3) gave slightly higher yields, Rh_2(*S*-*p*-Ph-TPCP)$_4$ (**Figure 2-2**), an effective chiral catalyst developed by our group,[9] gave the highest level of asymmetric induction (entry 4), with a ratio of greater than 20:1 between relative configurations of the newly formed cyclopropane, and a d.r. of 99:1 for the asymmetric induction achieved by the catalyst.

Scheme 2-1. Finding the Best Chiral Catalyst for Cyclopropanation.

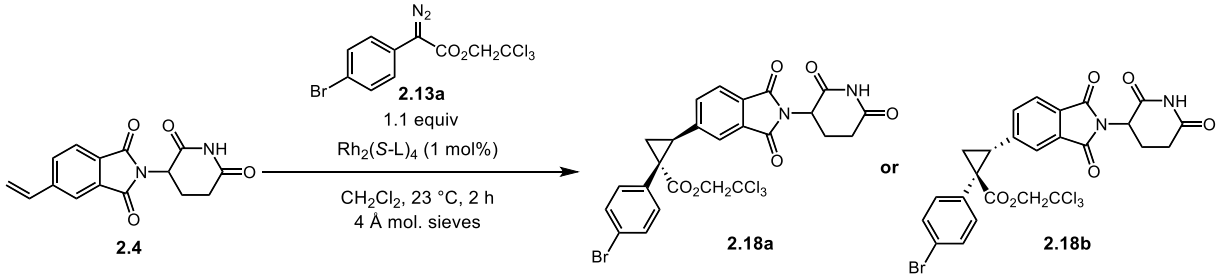

Entry	L	% yield	d.r.[a]	d.r.[b] (2.18a or 2.18b)
1	TPPTTL	77	>20:1	73:27 (2.18b)
2	PTAD	80	>20:1	87:13 (2.18a)
3[c]	NTTL	82	>20:1	95:5 (2.18b)
4	*p*-Ph-TPCP	72	>20:1	99:1 (2.18a)

Reactions conducted on material in which the glutarimide stereocenter is racemic. Entries 1 and 3 gave the stereoisomers of product **2.18b**, equivalent to those produced from the reaction with Rh_2(*R*-p-Ph-TPCP)$_4$. [a] Diastereomeric ratio for the relative configuration of the two new stereogenic centers, determined by ^{1}H NMR analysis. [b] Asymmetric induction arising from formation of the major relative diastereomer, determined by SFC analysis. [c] Reaction run with HFIP as solvent instead of CH_2Cl_2.

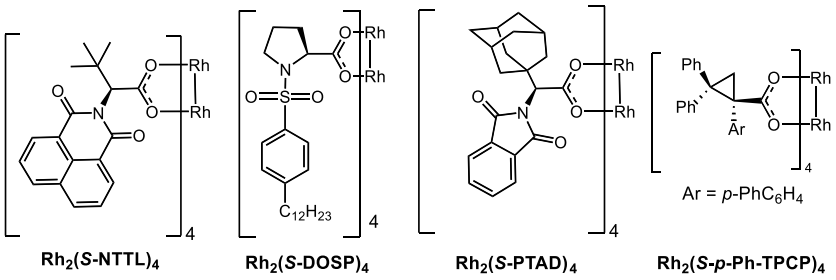

Figure 2-2. Catalysts Used in the Optimization Study

Because we were particularly interested in the differential biological effects of different cyclopropane stereroisomers, we elected to use both enantiomers of the chiral catalyst in our reactions with the different vinyl-IMiD regioisomers. In **Scheme 2-2**, the "**a**" series are products

Scheme 2-2. Cyclopropanation of Vinyl IMiD Derivatives

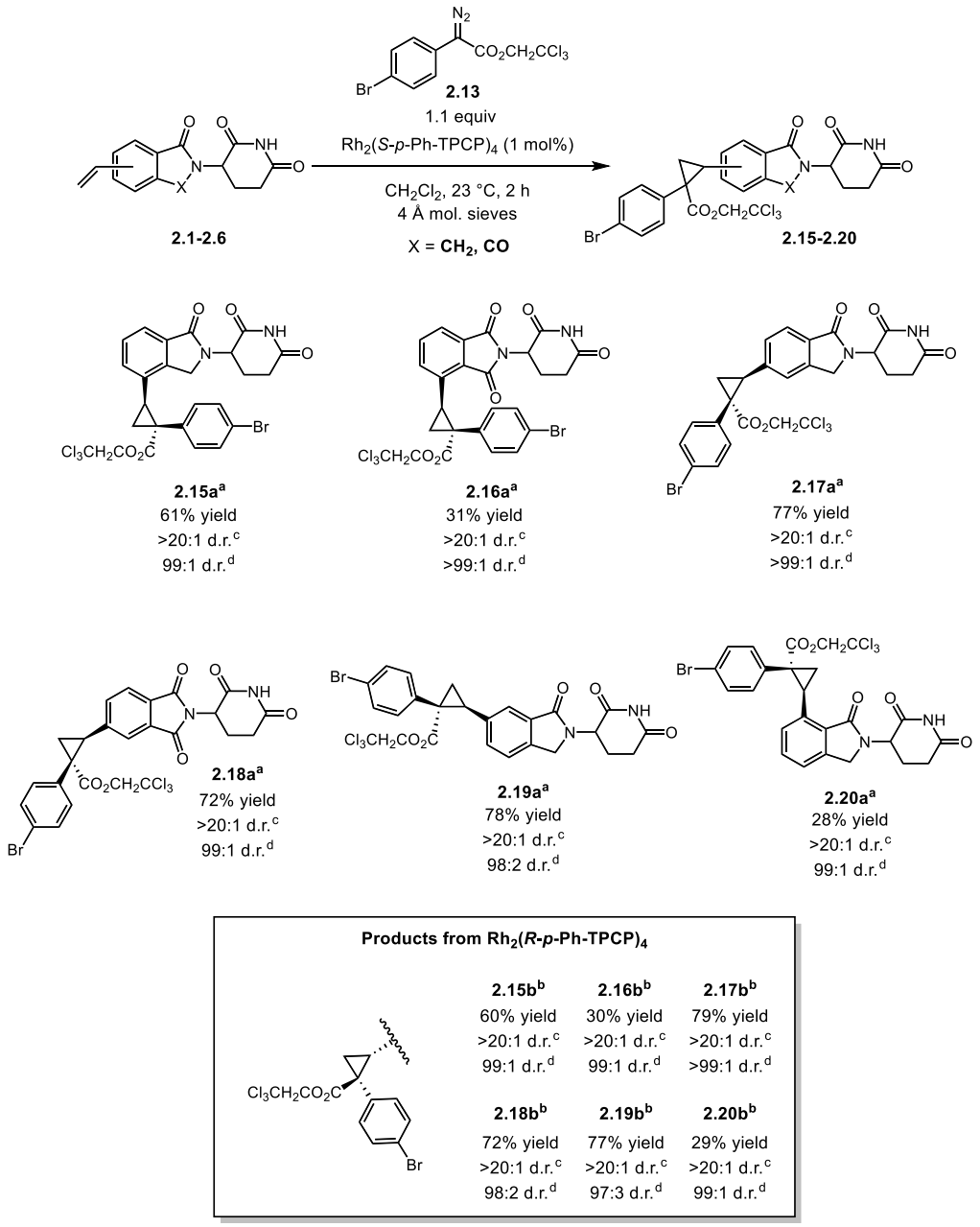

All reactions were performed on racemic glutarimide intermediates. Yields are reported as isolated yields of purified product. [a] Product arising from reaction with Rh_2(*S*-p-Ph-TPCP)$_4$ [b] Product arising from reaction with Rh_2(*R*-p-Ph-TPCP)$_4$ [c] Diastereomeric ratio for the relative configuration of the two new stereogenic centers, determined by ^{1}H NMR analysis. [d] Asymmetric induction arising from formation of the major relative diastereomer, determined by SFC analysis.

derived from reactions catalyzed by Rh_2(*S*-*p*-Ph-TPCP)$_4$ and the "**b**" series are products derived from reactions catalyzed by Rh_2(*R*-*p*-Ph-TPCP)$_4$. The absolute stereochemistry of the products were determined in reference to the X-ray crystallographic structure of compound **2.17a** acquired by John Bacsa and Mackenzie Young. The reactions proceed in good yields, with the exception of compounds in which the vinyl group is adjacent to the carbonyl group (**2.16a,b** and **2.20a,b**). The reactions proceeded with high levels of asymmetric induction and diastereoselectivity.

An analogous series of aryl alkynes were subjected to cyclopropenation reactions (**Scheme 2-3**) using the same diazoacetate (**2.13**). All reactions proceeded in good yield, irrespective of the position of the alkyne to the carbonyl. The reactions generate the cyclopropene products in high (up to >99:1) d.r., except when the alkyne is immediately adjacent to the carbonyl (**2.22a,b** and **2.26a,b**), which give poor diastereomeric ratios. Since the analogous cyclopropanation products (for example, **2.16a,b**) are produced in comparatively high d.r., we hypothesize that these differential effects may be due to the "end-on" approach of these substrates to the carbene. This places the site of reaction closer to the adjacent carbonyl in cyclopropenation than in cyclopropanation.[10] Alternatively, some difference in how the substrate approach is affected by the chiral catalyst used may cause the difference in reactivities and selectivities.

Since the conditions of rhodium-catalyzed cyclopropanation are quite mild, we wondered whether the reaction would preserve the sensitive glutarimide stereocenter. We prepared **(*S*)-2.3** and **(*R*)-2.3** from the enantiopure aryl bromides as discussed in Chapter 1 and subjected them to the reaction conditions (**Scheme 2-4**). The cyclopropanations proceed with full retention of stereochemistry at the glutarimide stereogenic center.

Scheme 2-3. Cyclopropenation of Ethynyl IMiD Derivatives

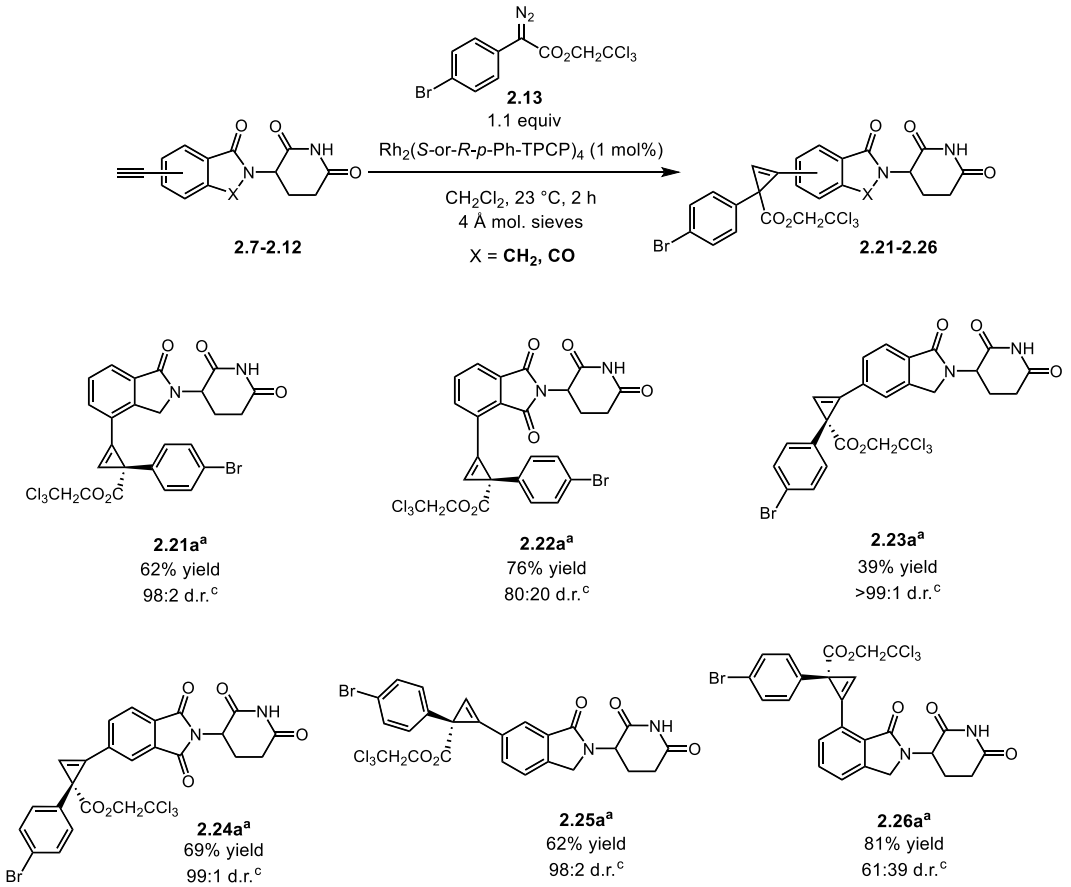

Products from Rh_2(*R*-*p*-Ph-TPCP)$_4$

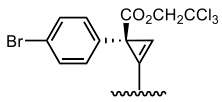

2.21b[b] 64% yield 98:2 d.r.[c]	**2.22b**[b] 79% yield 81:19 d.r.[c]	**2.23b**[b] 37% yield 99:1 d.r.[c]
2.24b[b] 70% yield 98:2 d.r.[c]	**2.25b**[b] 63% yield 98:2 d.r.[c]	**2.26b**[b] 79% yield 60:40 d.r.[c]

All reactions were performed on racemic glutarimide intermediates. Yields are reported as isolated yields of purified product. [a] Product arising from reaction with Rh_2(*S*-p-Ph-TPCP)$_4$ [b] Product arising from reaction with Rh_2(*R*-p-Ph-TPCP)$_4$. [c] Asymmetric induction arising from formation of the major relative diastereomer, determined by SFC analysis.

Scheme 2-4. Stereoretentive cyclopropanation of (S)- and (R)-3-(1-oxo-5-vinylisoindolin-2-yl)piperidine-2,6-dione

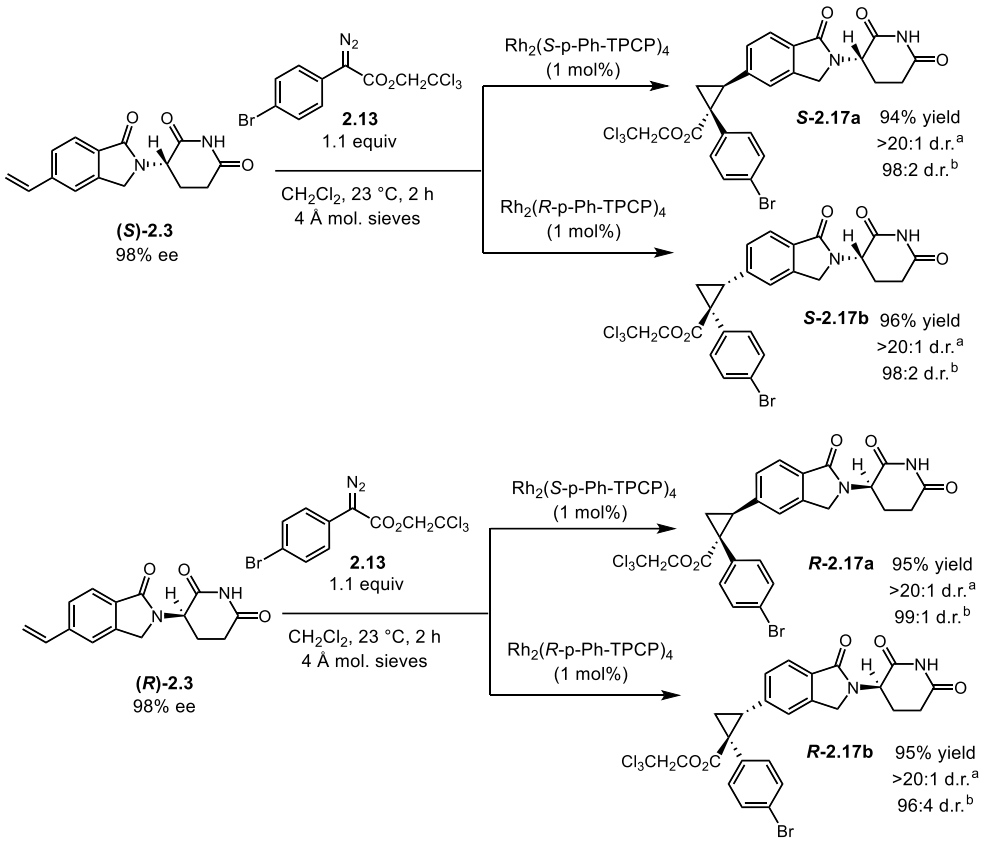

This retention is well-illustrated by the corresponding SFC traces of compounds **(*S*)-** and **(*R*)-2.17a** and **b** (**Figure 2-3**). With a racemic trace at the top for reference, the traces demonstrate how the Suzuki-Miyaura conditions developed in Chapter 1 combined with rhodium-catalyzed cyclopropanation enable the preparation of four individual stereoisomers.

Aryldiazoacetates in themselves contain useful synthetic potential beyond that of any carbene chemistry. The arene portion can be modified to contain valuable motifs and introduced to the substrate of interest to provide a rapid expansion of chemical complexity. In the context of the project, we were interested in how a more drug-like arene portion—potentially even one with a nucleophilic site that might react with the carbene—could be introduced to a vinyl-thalidomide core. We prepared a trichloroethyl diazoacetate with a benzyl morpholine moiety (**2.14**),

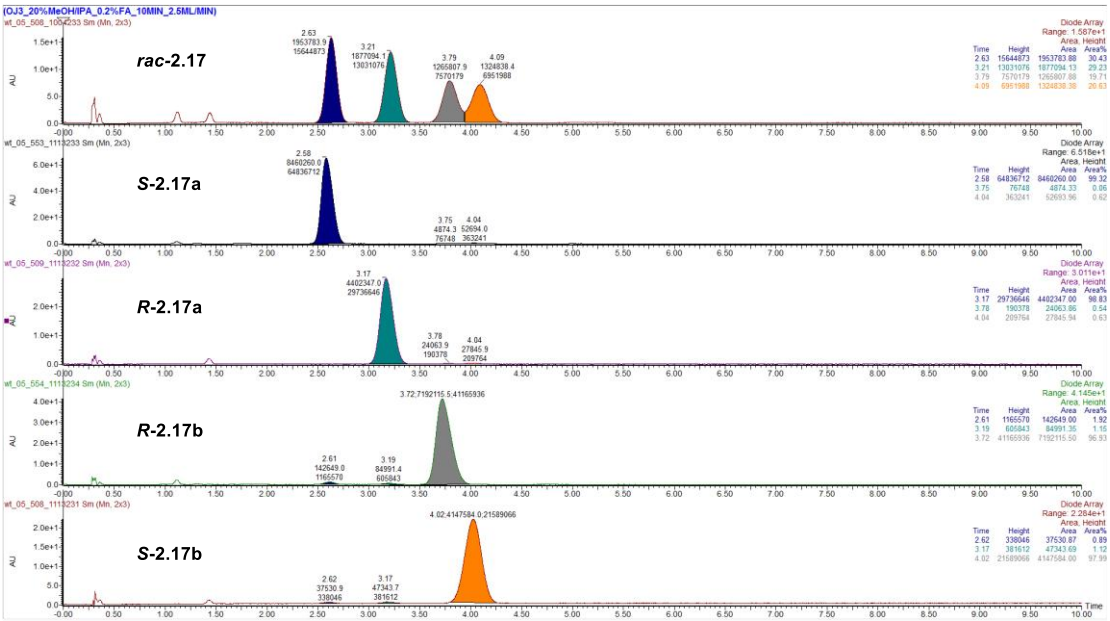

Figure 2-3. SFC trace showing retention of stereochemistry in the cyclopropanation of enantionriched vinyl IMiDs

reminiscent of that in iberdomide (**Scheme 2-5**). Under the standard conditions for cyclopropanation (**Scheme 2-2**), no reaction is observed. However, using Rh_2(*tetra-p*-Br-PPTTL)$_4$ in conjunction with 10 equivalents of HFIP, the cyclopropanation of the 4-vinyl isoindolinone core (**2.27a,b**) proceeds with modest asymmetric induction and good yield using both enantiomers of the chiral catalyst.

The trichloroethyl ester portion of the diazo can also be leveraged as a handle for diversification (**Scheme 2-6**). Typically the ester is modified by first converting it to the acid under reductive conditions (zinc dust in acetic acid)—conditions which have rarely needed modification in our hands.[11] However, with the cyclopropane products we wished to modify (**2.17a,b**), we saw low conversion and degradation of the starting material. Inspired by the work of Just and Grozinger supporting that the success and rate of hydrolysis can be pH-dependent,[12] we conducted a 16-experiment Design of Experiment (DoE) study using an adaptation of their system evaluating the effects of the ratio of THF and aqueous buffer in the solvent system, and the concentration, pH, and amount of buffer. We identified conditions that successfully cleaved

Scheme 2-5. Introduction of Further Complexity via the Arene Portion of the Diazo

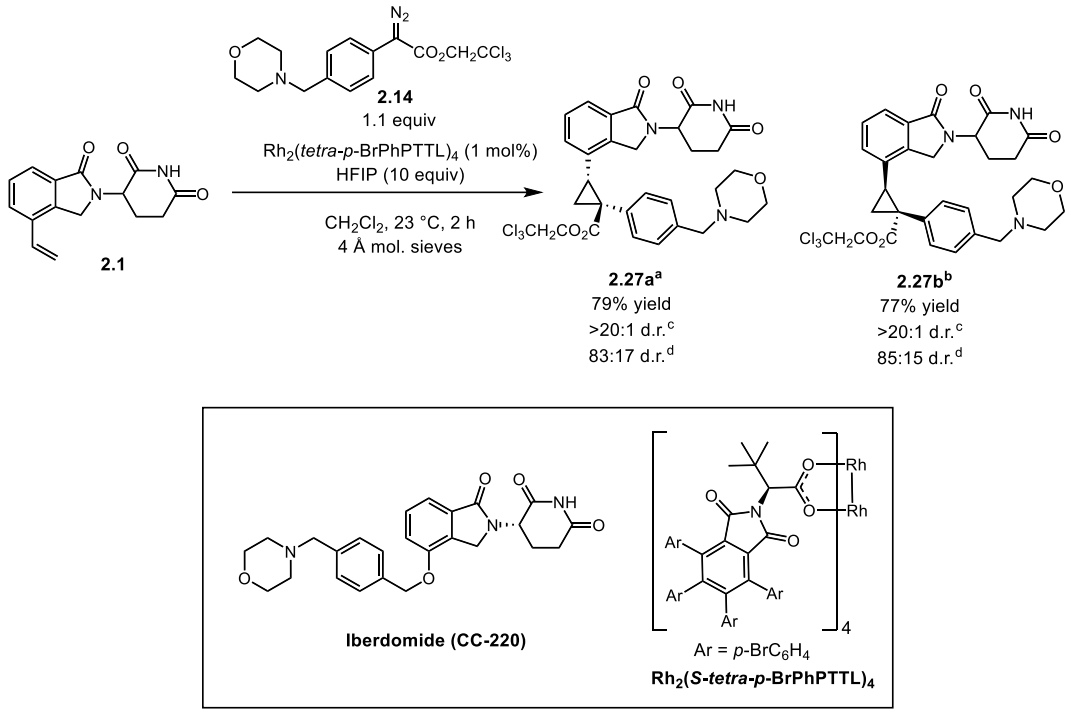

All reactions were performed on racemic glutarimide intermediates. Yields are reported as isolated yields of purified product. [a] Product arising from reaction with Rh_2(*tetra-p*-BrPhPTTL)$_4$ [b] Product arising from reaction with Rh_2(*tetra-p*-BrPhPTTL)$_4$ [c] Diastereomeric ratio for the relative configuration of the two new stereogenic centers, determined by ^{1}H NMR analysis. [d] Asymmetric induction arising from formation of the major relative diastereomer, determined by SFC analysis

Scheme 2-6. Introduction of Further Complexity via the Ester Portion of the Diazo

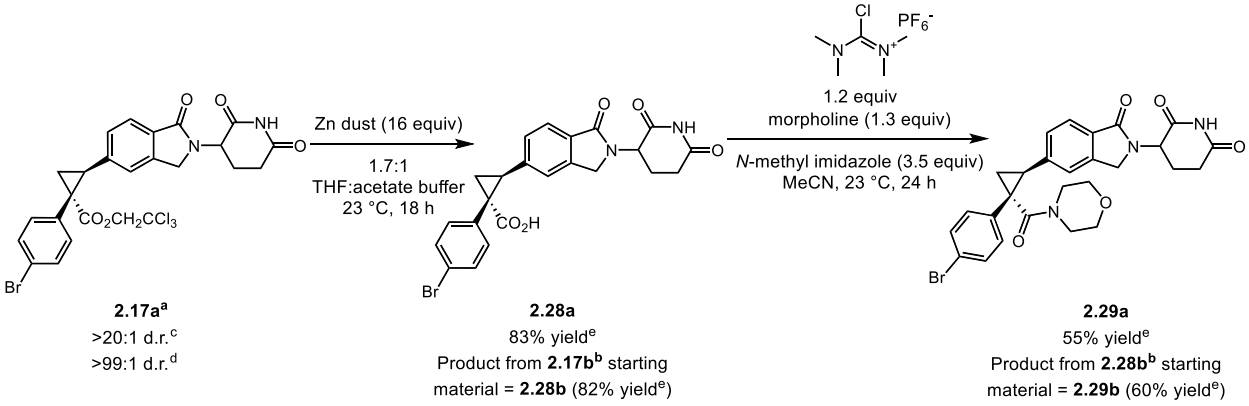

All reactions were performed on racemic glutarimide intermediates. Yields are reported as isolated yields of purified product. [a] Product arising from reaction with Rh_2(*S*-p-Ph-TPCP)$_4$ [b] Product arising from reaction with Rh_2(*R*-p-Ph-TPCP)$_4$ [c] Diastereomeric ratio for the relative configuration of the two new stereogenic centers, determined by ^{1}H NMR analysis [d] Asymmetric induction arising from formation of the major relative diastereomer, determined by SFC analysis [e] Stereochemical information from the starting material was retained, as determined by ^{1}H NMR and SFC analysis. 1.2 M acetate buffer: calc'd pH = 3.7.

the trichloroethyl ester of **2.17a** and **b** in high yield (**Scheme 2-6**). This acid can be converted

into an amide (**2.29a,b**) with complete retention of the stereochemistry induced by cyclopropanation, highlighting another way to generate complexity.

We next set out to evaluate how the novel IMiD structures synthesized compared to IMiDs in the public domain. This cheminformatics analysis was conducted by Lei Jia and Ethan Evans from Bristol Myers Squibb. The molecular features were captured using 2048 bit extended-connectivity fingerprints with a radius of 2 (ECFP4), along with the features of 18,175 public-domain compounds.[13, 14] These fingerprints were then embedded into a two-component Uniform Manifold Approximation and Projection (UMAP) algorithm to visualize the data (**Figure 2-4a**).[15] While our compounds (orange) cluster together due to their similarity, they occupy a part of chemical space relatively unoccupied by known compounds (blue). We also set out with a

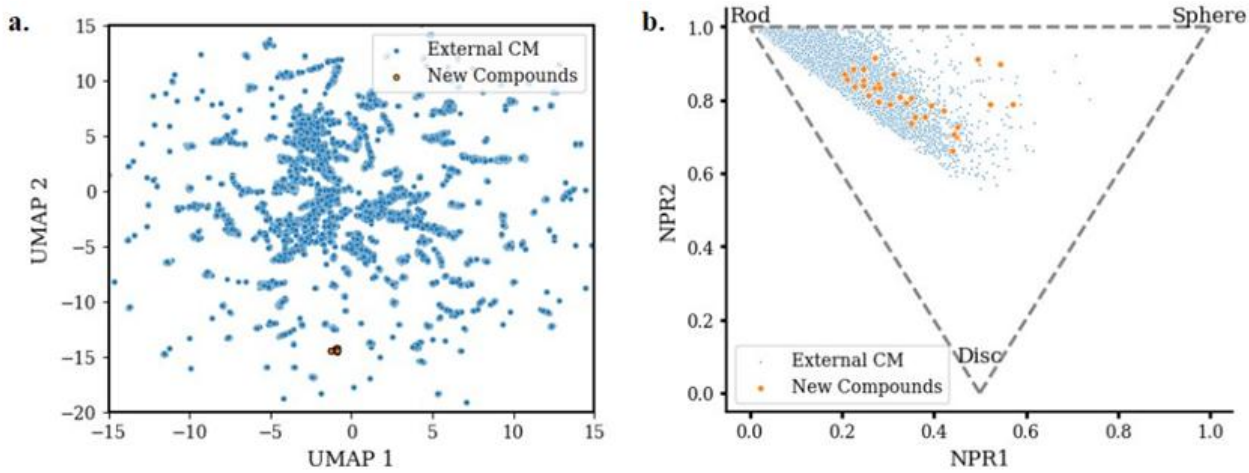

Figure 2-4. Representation of chemical and structural space accessed by the novel IMiDs relative to literature precedence (18,175 compounds). (A) 2-dimensional UMAP projection from 2048 bit ECFP4 fingerprints. (B) Principal moments of inertia analysis. Both plots depict the new IMiDs shown in orange relative to existing compounds shown in blue. Data prepared by Lei Jia and Ethan Evans of BMS.

hypothesis that cyclopropanation and cyclopropenation would increase the structural complexity and diversity of known IMiDs. We modeled the 3-D shape of our compounds and visualized this using a principal moments of inertia (PMI) plot (**Figure 2-4b**).[16] The PMI plot describes whether the compounds are more rod-shaped (upper left), disk-shaped (bottom), sphere-shaped (upper

right), and combinations of the three. Relative to the external collection (blue), our compounds (orange) take on a more spherical shape, but in general occupy a broad swath, suggesting diversity despite a smaller sample size. Going in line with the accepted notion that structural and chemical diversity increases the likelihood of interaction with a broader range of biological targets, these analyses demonstrate the effectiveness of our methods.

We evaluated the biological effectiveness of the core series of cyclopropane (**2.15a,b-2.20a,b**) and cyclopropene (**21a,b-26a,b**) by evaluating their function in assays with four important G-motif-containing substrates: IKZF3, CK1α, GSPT1, and SALL4.[4] Both the compounds' binding to CRBN and their degradation activity were evaluated. The biological studies were conducted by Zhenghang Sun, Jennifer Buenviaje, Gody Khambatta, Shan Yu, and Lihong Shi from Bristol Myers Squibb. **Figure 2-5a** correlates CRBN binding ability (HTRF IC_{50}) to neosubstrate degradation (Y_{min} indicates depth of degradation where 100% represents no degradation and 0% represents complete neosubstrate degradation). There was no correlation between CRBN binding and neosubstrates, which is expected and reflects the importance of forming a productive ternary complex between CRBN and a neosubstrate (versus simply binding to CRBN).[6, 17] **Figure 2-5b** depicts trends in neosubstrate activity with EC_{50} (half-maximal concentration required to reach 50% degradation effect). The boxes are colored to represent the Y_{min} of the compounds, with red showing very little degradation (i.e., closer to 100%) and green showing more degradation (i.e., closer to 0% protein remaining). Most of the compounds tested showed measurable CRBN binding; only a small fraction (4 out of 24) showing a CRBN IC_{50} >10 μM (see supporting information for CRBN data). Matched pairs of of the isoindolinone (abbreviated as "Len") and phthalimide (abbreviated as "Thal") cores (**2.15a,b** vs **2.16a,b**,

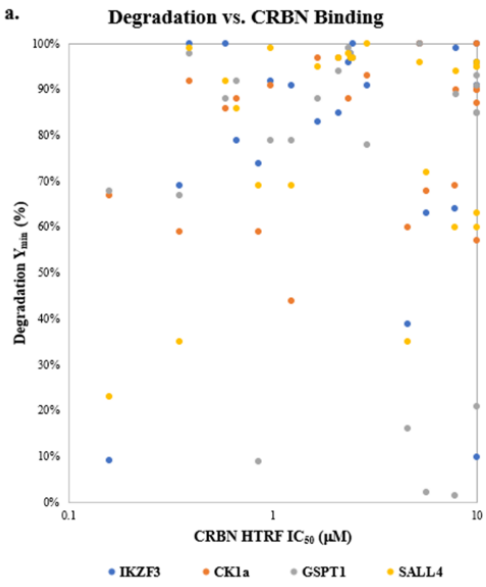

b.

		4-Len	4-Thal	5-Len	5-Thal	6-Len	7-Len
S-catalyst cyclopropanes	**Cmpd**	**2.15a**	**2.16a**	**2.17a**	**2.18a**	**2.19a**	**2.20a**
	IKZF3	>10	>10	>10	>10	>10	>10
	CK1α	>10	>10	>10	>10	>10	>10
	GSPT1	>10	>10	>10	>10	>10	>10
	SALL4	>10	>10	>10	>10	>10	>10
R-catalyst cyclopropanes	**Cmpd**	**2.15b**	**2.16b**	**2.17b**	**2.18b**	**2.19b**	**2.20b**
	IKZF3	>10	>10	>10	>10	>10	>10
	CK1α	>10	>10	0.22	>10	>10	>10
	GSPT1	>10	>10	>10	>10	>10	>10
	SALL4	>10	>10	0.16	0.41	>10	>10
S-catalyst cyclopropenes	**Cmpd**	**2.21a**	**2.22a**	**2.23a**	**2.24a**	**2.25a**	**2.26a**
	IKZF3	0.012	0.90	>10	1.3	>10	>10
	CK1α	0.17	1.5	>10	1.2	>10	>10
	GSPT1	0.17	4.3	>10	1.1	>10	>10
	SALL4	0.019	0.56	>10	3.6	>10	>10
R-catalyst cyclopropenes	**Cmpd**	**2.21b**	**2.22b**	**2.23b**	**2.24b**	**2.25b**	**2.26b**
	IKZF3	0.11	3.7	4.8	0.31	>10	>10
	CK1α	1.5	2.1	0.25	1.6	>10	>10
	GSPT1	0.55	5.1	3.3	1.4	>10	>10
	SALL4	0.17	2.8	0.075	2.4	>10	>10

Numerical values refer to degradation EC_{50} (μM)
Colors refer to degradation Y_{min} (%)
Y_{min} 0% 100%

Figure 2-5. Biological activity and trends. (A) Correlation of CRBN binding (HTRF IC_{50}) to neosubstrate degradation (Y_{min}). (B) Trends in neosubstrate activity with EC_{50} (concentration required to achieve 50% of total degradation effect) reported in μM and boxes colored by Y_{min} (with red showing weak depth of degradation and green showing strong depth of degradation); data reported as an average of $N \geq 3$ test occasions. Data prepared by Lei Jia, Ethan Evans, Jesus Moreno, and Emily Cherney of BMS.

2.17a,b vs **2.18a,b**, **2.19a,b** vs **2.20a,b**, **2.21a,b** vs **2.22a,b**, **2.23a,b** vs **2.24a,b**, and **2.25a,b** vs **2.26a,b**) generally show similar trends. A few matched pairs show inactivity across neosubstrates (**2.15a,b** vs **2.16a,b**, **2.17a** vs **2.18a**, **2.19a,b** vs **2.20a,b, 2.25a,b** vs **2.26a,b**) all show inactivity across substrates in matched pairs. On the other hand, others (**2.21a,b** vs **2.22a,b** and **2.23a,b** vs **2.24a,b**) show some level of activity across neosubstrates. Two pairs exhibited exceptions to this trend. The first was **2.17b** and **2.18b**, where **2.17b** showed more activity than **2.18b** against CK1α. This may be due to the carbonyl in the phthalimide core of **2.18b** interfering with ternary complex formation (the lack of a carbonyl in the isoindolinone core as in **2.17b** is hypothesized to allow better complex formation).[3a] Interestingly, the carbonyl is better tolerated for CK1α recruitment and degradation in phthalimide cores that contain cyclopropenes

rather than cyclopropanes (**22a,b** and **24a,b**). In the other exception, **2.23a** was inactive across neosubstrates, while **2.24a** showed activity across neosubstrates.

Trends in regiochemistry of the substitution patterns (4- vs 5- vs 6- vs 7- position) were the most universal with 6- and 7-substituted isoindolinone cores being generally inactive. However, these compounds maintain binding to CRBN. This suggests that the lack of degradation is due to inability to form a productive ternary complex between CRBN and the neosubstrates investigated, all of which contain G-motifs. This lack of an ability to form productive complexes may be advantageous in some scenarios in which degradation selectivity for G-motif-containing substrates (e.g., GSPT1) is undesired.[18]

The general preference in degradation for cyclopropenes over cyclopropanes was not anticipated a priori. Excluding the inactivity of the 6- and 7-substituted isoindolinone cores discussed previously, the trend for the cyclopropanes to be less active holds true for 4- and 5-substituted cyclopropanated cores (compounds **2.15-2.18**) regardless of stereochemistry. One exception is compound **2.17b**, where (compared to **2.17a**) stereochemical effects on neosubstrate degradation are observed (vide infra). The trend becomes more striking when comparing the degradation of a singular neosubstrate for matched pairs, such as the difference in IKZF3 degradation between **2.16b** (EC_{50} >10 μM, 99% Y_{min}) and **2.22b** (EC_{50} = 3.67 μM, 10% Y_{min}) or **2.15a** (EC_{50} = 1.86 μM, 79% Y_{min}) and **2.21a** (EC_{50} = 0.012 μM, 9.2% Y_{min}). Two examples highlighting GSPT1 selectivity are **2.18a** (EC_{50} >10 μM, 100% Ymin) vs. **2.24a** (EC_{50} 1.4 μM, 2.3% Y_{min}) and **2.18b** (EC_{50} = 3.1 μM, 85% Y_{min}) vs. **2.24b** (EC_{50} = 1.4 □M, 1.4% Y_{min}). The only outlier of the cyclopropenes is compound **2.23a**, which is the only 4- or 5-substituted cyclopropene that does not significantly degrade any of the neosubstrates tested.

Finally, distal stereochemistry effects on neosubstrate degradation were analyzed. Strikingly, while subtle in terms of structural change, these changes lead to significant changes in neosubstrate selectivity. For instance, cyclopropene compound **2.21a**, generated from Rh_2(*S*-*p*-Ph-TPCP)$_4$ is a significantly deeper degrader of IKZF3 (9.2% Y_{min}) than its counterpart **2.21b** (69% Y_{min}), generated from Rh_2(*R*-*p*-Ph-TPCP)$_4$. (**2.23a** vs **2.23b**). Perhaps the most conspicuous stereochemical pair is **2.23a** and **2.23b** for which one is universally less active than the other. While the SAR arising from distal changes in stereochemistry may be more nuanced, the demonstration of the ability of distal stereochemistry alone to strongly impact neosubstrate selectivity is significant. This finding highlights the importance of enabling enantioselective methodologies, like asymmetric rhodium catalysis, on glutarimide-containing molecules to help medicinal chemists fine-tune neosubstrate selectivity.

We were interested in rationalizing the observed binding and degradation data using computational modeling and attempted to rationalize the observed binding and degradation data using molecular docking methods. We used publicly available structures of the neosubstrates in complex with CRBN (PDB IDS: 5FQD for CK1α, 6XK9 for GSPT1, and 8U15 for SALL4). We had to use the structure of IKZF1 (8D7Z), which has an identical G-motif sequence to IKZF3, as a replacement as the structure of IKZF3 was not available. We attempted docking our compounds using both Glide (SP and induced fit) and MOE-based induced fit docking. For all neosubstrates and methods there was no trend between docking success or score with binding affinity or Y_{min} values. The small molecule focused docking scores likely do not fully capture the intricacies of the ternary complex in which water and protein-protein interactions play a key role as recently suggested, highlighting the need for more sophisticated modelling approaches.[19]

Conclusions

We have demonstrated rhodium-catalyzed cyclopropanations and cyclopropenations to be effective and useful methods for the creation of chemically and structurally distinct IMiDs. Due to the mild nature of the reactions, we were able to generate IMiDs with a high degree of asymmetric induction, without interfering with the sensitive functionality in IMiDs. This method enables highly convergent synthesis and provides opportunities for further diversification. We demonstrated that the compounds degrade common G-motif-containing neosubstrates with measurable CRBN-binding activity. SAR analysis revealed the subtle interplay of distal stereochemistry and regiochemistry on neosubstrate degradation activity, which can significantly influence future efforts to design new prospective IMiD-class durgs. Our work highlights the effectiveness of rhodium-carbene chemistry as a tool for the diversification of important drug classes—even those in which diversification is a synthetic challenge.

This work was published in *ACS Medicinal Chemistry Letters* in 2024:
Tracy, W. F.; Davies, G. H. M.; Jia, L.; Evans, E. D.; Sun, Z.; Buenviaje, J.; Khambatta, G.; Yu, S.; Shi, L.; Shanmugasundaram, V.; Moreno, J.; Cherney, E. C.; Davies, H. M. L., Asymmetric Dirhodium-Catalyzed Modification of Immunomodulatory Imide Drugs and Their Biological Assessment. *ACS Med. Chem. Lett.* **2024,** *15*, 1575-1583.
W.F. Tracy conducted all of the synthetic work. G.H.M. Davies led the project with H.M.L. Davies in its early stages and provided valuable guidance on project direction. E.D. Evans and L. Jia conducted the cheminformatics analysis. Z. Sun, J. Buenviaje, G. Khambatta, S. Yu, and L. Shi conducted the biological studies. J. Moreno, E.C. Cherney, and V. Shanmugasundaram provided valuable support, guidance, and analysis. Chuong-Thu Thai and Blayne Lenoir assisted with analytical chemistry, structural validation, and compound management. Zia Lozewski,

Carolindah Ntimi, Kaitlyn Wieler, Ishani Patel, Giselles Perez, Gabe Mintier, John Feder, Derek Mendy, and Lynda Groocock assisted with cell line development. John Bacsa and Mackenzie Young were responsible for the X-ray crystallographic data.

Reference

(1) (a) D'Amato, R. J.; Loughnan, M. S.; Flynn, E.; Folkman, J., Thalidomide is an inhibitor of angiogenesis. *Proc. Natl. Acad. Sci.* **1994,** *91*, 4082-4085; (b) Sampaio, E. P.; Sarno, E. N.; Galilly, R.; Cohn, Z. A.; Kaplan, G., Thalidomide selectively inhibits tumor necrosis factor alpha production by stimulated human monocytes. *J. Exp. Med.* **1991,** *173*, 699-703.

(2) (a) Krönke, J.; Udeshi, N. D.; Narla, A.; Grauman, P.; Hurst, S. N.; McConkey, M.; Svinkina, T.; Heckl, D.; Comer, E.; Li, X.; Ciarlo, C.; Hartman, E.; Munshi, N.; Schenone, M.; Schreiber, S. L.; Carr, S. A.; Ebert, B. L., Lenalidomide Causes Selective Degradation of IKZF1 and IKZF3 in Multiple Myeloma Cells. *Science* **2014,** *343*, 301-305; (b) Lu, G.; Middleton, R. E.; Sun, H.; Naniong, M.; Ott, C. J.; Mitsiades, C. S.; Wong, K.-K.; Bradner, J. E.; Kaelin, W. G., The Myeloma Drug Lenalidomide Promotes the Cereblon-Dependent Destruction of Ikaros Proteins. *Science* **2014,** *343*, 305-309.

(3) (a) Petzold, G.; Fischer, E. S.; Thomä, N. H., Structural basis of lenalidomide-induced CK1α degradation by the CRL4CRBN ubiquitin ligase. *Nature* **2016,** *532*, 127-130; (b) Matyskiela, M. E.; Lu, G.; Ito, T.; Pagarigan, B.; Lu, C.-C.; Miller, K.; Fang, W.; Wang, N.-Y.; Nguyen, D.; Houston, J.; Carmel, G.; Tran, T.; Riley, M.; Nosaka, L. A.; Lander, G. C.; Gaidarova, S.; Xu, S.; Ruchelman, A. L.; Handa, H.; Carmichael, J.; Daniel, T. O.; Cathers, B. E.; Lopez-Girona, A.; Chamberlain, P. P., A novel cereblon modulator recruits GSPT1 to the CRL4CRBN ubiquitin ligase. *Nature* **2016,** *535*, 252-257; (c) Sievers, Q. L.; Petzold, G.; Bunker, R. D.; Renneville, A.; Słabicki, M.; Liddicoat, B. J.; Abdulrahman, W.; Mikkelsen, T.; Ebert, B. L.; Thomä, N. H., Defining the human C2H2 zinc finger degrome targeted by thalidomide analogs through CRBN. *Science* **2018,** *362*, eaat0572; (d) Matyskiela, M. E.; Clayton, T.; Zheng, X.; Mayne, C.; Tran, E.; Carpenter, A.; Pagarigan, B.; McDonald, J.; Rolfe, M.; Hamann, L. G.; Lu, G.; Chamberlain, P. P., Crystal structure of the SALL4–pomalidomide–cereblon–DDB1 complex. *Nat. Struct. Mol. Biol.* **2020,** *27*, 319-322; (e) Wang,

E. S.; Verano, A. L.; Nowak, R. P.; Yuan, J. C.; Donovan, K. A.; Eleuteri, N. A.; Yue, H.; Ngo, K. H.; Lizotte, P. H.; Gokhale, P. C.; Gray, N. S.; Fischer, E. S., Acute pharmacological degradation of Helios destabilizes regulatory T cells. *Nat. Chem. Biol.* **2021,** *17*, 711-717; (f) Watson, E. R.; Novick, S.; Matyskiela, M. E.; Chamberlain, P. P.; H. de la Peña, A.; Zhu, J.; Tran, E.; Griffin, P. R.; Wertz, I. E.; Lander, G. C., Molecular glue CELMoD compounds are regulators of cereblon conformation. *Science* **2022,** *378*, 549-553; (g) Bonazzi, S.; d'Hennezel, E.; Beckwith, R. E. J.; Xu, L.; Fazal, A.; Magracheva, A.; Ramesh, R.; Cernijenko, A.; Antonakos, B.; Bhang, H.-e. C.; Caro, R. G.; Cobb, J. S.; Ornelas, E.; Ma, X.; Wartchow, C. A.; Clifton, M. C.; Forseth, R. R.; Fortnam, B. H.; Lu, H.; Csibi, A.; Tullai, J.; Carbonneau, S.; Thomsen, N. M.; Larrow, J.; Chie-Leon, B.; Hainzl, D.; Gu, Y.; Lu, D.; Meyer, M. J.; Alexander, D.; Kinyamu-Akunda, J.; Sabatos-Peyton, C. A.; Dales, N. A.; Zécri, F. J.; Jain, R. K.; Shulok, J.; Wang, Y. K.; Briner, K.; Porter, J. A.; Tallarico, J. A.; Engelman, J. A.; Dranoff, G.; Bradner, J. E.; Visser, M.; Solomon, J. M., Discovery and characterization of a selective IKZF2 glue degrader for cancer immunotherapy. *Cell Chem. Biol.* **2023,** *30*, 235-247.e12.

(4) Oleinikovas, V.; Gainza, P.; Ryckmans, T.; Fasching, B.; Thomä, N. H., From Thalidomide to Rational Molecular Glue Design for Targeted Protein Degradation. *Annu. Rev. Pharmacool. Toxicol.* **2024,** *64*, 291-312.

(5) (a) Yamanaka, S.; Furihata, H.; Yanagihara, Y.; Taya, A.; Nagasaka, T.; Usui, M.; Nagaoka, K.; Shoya, Y.; Nishino, K.; Yoshida, S.; Kosako, H.; Tanokura, M.; Miyakawa, T.; Imai, Y.; Shibata, N.; Sawasaki, T., Lenalidomide derivatives and proteolysis-targeting chimeras for controlling neosubstrate degradation. *Nat. Commun.* **2023,** *14*, 4683; (b) Nowak, R. P.; Che, J.; Ferrao, S.; Kong, N. R.; Liu, H.; Zerfas, B. L.; Jones, L. H., Structural rationalization of GSPT1 and IKZF1 degradation by thalidomide molecular glue derivatives. *RSC Med. Chem.* **2023,** *14*, 501-506.

(6) Weiss, D. R.; Bortolato, A.; Sun, Y.; Cai, X.; Lai, C.; Guo, S.; Shi, L.; Shanmugasundaram, V., On Ternary Complex Stability in Protein Degradation: In Silico Molecular Glue Binding Affinity Calculations. *J. Chem. Inf. Model.* **2023,** *63*, 2382-2392.

(7) Szewczyk, S. M.; Verma, I.; Edwards, J. T.; Weiss, D. R.; Chekler, E. L. P., Trends in Neosubstrate Degradation by Cereblon-Based Molecular Glues and the Development of Novel Multiparameter Optimization Scores. *J. Med. Chem.* **2024,** *67*, 1327-1335.

(8) Guptill, D. M.; Davies, H. M. L., 2,2,2-Trichloroethyl Aryldiazoacetates as Robust Reagents for the Enantioselective C–H Functionalization of Methyl Ethers. *J. Am. Chem. Soc.* **2014,** *136*, 17718-17721.

(9) Liao, K.; Liu, W.; Niemeyer, Z. L.; Ren, Z.; Bacsa, J.; Musaev, D. G.; Sigman, M. S.; Davies, H. M. L., Site-Selective Carbene-Induced C–H Functionalization Catalyzed by Dirhodium Tetrakis(triarylcyclopropanecarboxylate) Complexes. *ACS Catal.* **2018,** *8*, 678-682.

(10) Davies, H. M. L.; Lee, G. H., Dirhodium(II) Tetra(N-(dodecylbenzenesulfonyl)prolinate) Catalyzed Enantioselective Cyclopropenation of Alkynes. *Org. Lett.* **2004,** *6*, 1233-1236.

(11) (a) Woodward, R. B.; Heusler, K.; Gosteli, J.; Naegeli, P.; Oppolzer, W.; Ramage, R.; Ranganathan, S.; Vorbrüggen, H., The Total Synthesis of Cephalosporin C1. *J. Am. Chem. Soc.* **1966,** *88*, 852-853; (b) Negretti, S.; Cohen, C. M.; Chang, J. J.; Guptill, D. M.; Davies, H. M. L., Enantioselective dirhodium(II)-catalyzed cyclopropanations with trimethylsilylethyl and trichloroethyl aryldiazoacetates. *Tetrahedron* **2015,** *71*, 7415-7420.

(12) Just, G.; Grozinger, K., A Selective, Mild Clevage of Trichloroethyl Esters, Carbamates, and Carbonates to Carboxylic Acids, Amines, and Phenols using Zinc/Tetrahydrofuran/pH 4.2-7.2 Buffer. *Synthesis* **1976,** *1976*, 457-458.

(13) (a) Axen, S. D.; Huang, X.-P.; Cáceres, E. L.; Gendelev, L.; Roth, B. L.; Keiser, M. J., A Simple Representation of Three-Dimensional Molecular Structure. *J. Med. Chem.* **2017,** *60*, 7393-7409; (b) Rogers, D.; Hahn, M., Extended-Connectivity Fingerprints. *J. Chem. Inf. Model.* **2010,** *50*, 742-754.

(14) The compound database was an internally curated list from Bristol Myers Squibb of non-BMS compounds, mostly scraping patent literature and publications.

(15) McInnes, L.; Healy, J.; Melville, J., UMAP: Uniform Manifold Approximation and Projection for Dimension Reduction. *arXiv* **2020**.

(16) Sauer, W. H. B.; Schwarz, M. K., Molecular Shape Diversity of Combinatorial Libraries: A Prerequisite for Broad Bioactivity. *J. Chem. Inf. Comput.* **2003,** *43*, 987-1003.

(17) Chamberlain, P. P.; Lopez-Girona, A.; Miller, K.; Carmel, G.; Pagarigan, B.; Chie-Leon, B.; Rychak, E.; Corral, L. G.; Ren, Y. J.; Wang, M.; Riley, M.; Delker, S. L.; Ito, T.; Ando, H.; Mori, T.; Hirano, Y.; Handa, H.; Hakoshima, T.; Daniel, T. O.; Cathers, B. E.,

Structure of the human Cereblon–DDB1–lenalidomide complex reveals basis for responsiveness to thalidomide analogs. *Nat. Struct. Mol. Biol.* **2014,** *21*, 803-809.

(18) Vetma, V.; Casarez-Perez, L.; Eliaš, J.; Stingu, A.; Kombara, A.; Gmaschitz, T.; Braun, N.; Ciftci, T.; Dahmann, G.; Diers, E.; Gerstberger, T.; Greb, P.; Kidd, G.; Kofink, C.; Puoti, I.; Spiteri, V.; Trainor, N.; Westermaier, Y.; Whitworth, C.; Ciulli, A.; Farnaby, W.; McAulay, K.; Frost, A. B.; Chessum, N.; Koegl, M., Confounding factors in targeted degradation of short-lived proteins. *bioRxiv* **2024**, 2024.02.19.581012.

(19) Miñarro-Lleonar, M.; Bertran-Mostazo, A.; Duro, J.; Barril, X.; Juárez-Jiménez, J., Lenalidomide Stabilizes Protein–Protein Complexes by Turning Labile Intermolecular H-Bonds into Robust Interactions. *J. Med. Chem.* **2023,** *66*, 6037-6046.

Chapter 3: Adapting Cereblon E3 Ligase Modulatory Drug Cores as Rhodium Carbene Precursors for C-H Functionalization and Cyclopropanation.

Introduction

In Chapter 2, we expanded into new chemical space by adapting dirhodium-catalyzed asymmetric cyclopropanation and cyclopropenation to vinyl and ethynyl IMiD cores. This work was enabled largely by enabled largely by the anhydrous, fluoride-enhanced and stereoretentive Suzuki-Miyaura coupling discussed in Chapter 1. This allowed the synthesis of stereodefined, CRBN-modulating structures with a highly convergent, rapid introduction of diversity in a single step from vinyl and ethynyl CELMoD derivatives. We demonstrated how this diversity can be extended even further by modifying the aryldiazoacetate used in cyclopropanation (**Scheme 2-5**), or by hydrolysis of the trichloroethyl ester and subsequent amide coupling (**Scheme 2-6**).

However, these routes are only a partial display of how rhodium carbene reactions and their products can be used to create novel IMiDs.

The Davies laboratory has a long history of developing rhodium-carbene mediated C–H functionalization reactions.[1] The key components of C–H functionalization—a chiral dirhodium catalyst and the appropriate aryldiazoacetate— are capable of performing highly stereo- and regioselective functionalization of a range of C–H bonds, both in activated and activated systems.[1-2] As discussed in the introduction, relative to cyclopropanation and related reactions, C–H functionalization has been underutilized in medicinal contexts outside of total synthesis. Utilization of IMiD cores in a C–H functionalization context would not only further increase the power of synthetic methods to create chemical diversity and convergent syntheses in IMiDs, but also explore the limits of how C–H functionalization can be applied in a challenging context. C–H functionalization presents an additional challenge over cycloaddition reactions as the substrates are often less reactive. For example, holding the diazoacetate and catalyst the same, styrene is 24,000 times more reactive than cyclohexane.[3] Some substrates can be even more strikingly less reactive; for example, 2,2-dimethylbutane is roughly 307,000 times less reactive than styrene.[3] Therefore, when considering the challenges presented by IMiD-like structures, features like the glutarimide N-H bond and insolubility become even more intimidating. However, the benefits make C–H functionalization with IMiDs a worthy challenge; the rapid introduction of high-sp^3, stereodefined context in a highly convergent manner would greatly improve the synthetic possibilities available to medicinal chemists. In the following, we show that IMiD cores can be modified to become aryldiazoacetates and become highly effective precursors for the C–H functionalization of both activated and unactivated hydrocarbons. Cyclopropanation also proceeds well using these IMiD–diazo compounds. We also take

advantage of the cyclopropanation reactions and further diversification to create stereodefined LDDs. HFIP, which we have previously shown to be a nucleophilicity-moderating[4] and occasional enantioselectivity-enhancing[5] agent plays a key role in these cyclopropanation and C–H functionalization reactions. This work adds to what is only a small collection of known stereoselective transformations on glutarimide-containing compounds.[6]

Results and Discussion

The initial iteration of C–H functionalization in an IMiD context began as an extension of the work discussed in Chapter 2. We envisioned using the same aryldiazoacetate, but with 5-methyl substituent in place of the 5-vinyl group used for cyclopropanation (**Scheme 3-1**). However, we were unable to observe any of the intended C–H functionalization product **3.3**. Instead, the diazo (**3.2**) preferentially inserted into the N–H bond of the substrate (**3.1**) to generate a 35% yield of **3.4**, with the rest of the mass balance being carbene dimerization byproducts. Any attempt to rescue the reaction by the addition of HFIP was unsuccessful and generated complex mixtures.

Scheme 3-1. Unsuccessful C–H Functionalization of 5-Methylthalidomide

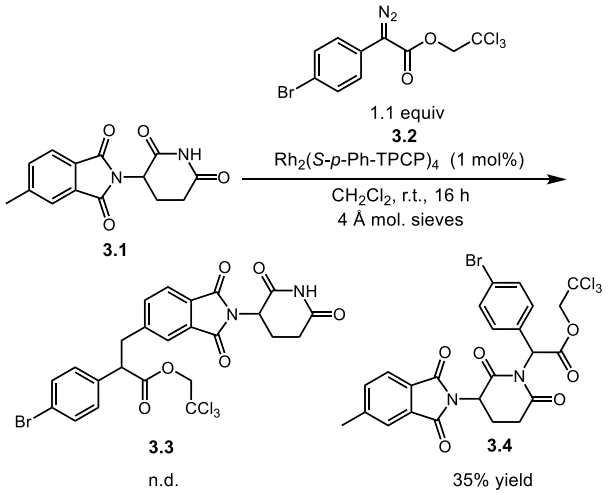

At this point, we elected to change strategies. Instead of using an IMiD-like core as a substrate, the IMiD-like core could be incorporated as the donor portion of a donor/acceptor

carbene precursor like a 2,2,2-trichloroethyl aryldiazoacetate. An effective acceptor portion would be the 2,2,2-trichloroethyl ester as it historically enhances both reactivity and stereoselectivity in C–H functionalization reactions with our chiral catalysts.[7] We opted to use a cross-coupling approach based on some of our previous work to access the planned diazo compounds as the starting aryl iodide was commercially available, as opposed to the phenylacetate required for the typical diazo transfer reaction with a sulfonyl azide.[8] The solubility of the iodo- derivatives of thalidomide-like and lenalidomide-like structures is very poor, and were found to be only sparingly soluble in toluene, the typical solvent for cross-coupling.[8a] We also experienced problems with palladium black formation. We hypothesize that the the presence of a silver compound (silver carbonate is included in the reaction) capable of oxidation and a glutarimide-containing substrate work in tandem to encourage the formation of off-cycle palladium species. One of our industrial collaborators on the project, Jake Ganley, conducted a high-throughput screen with a simpler model substrate (5-bromo-2-methylisoindolin-1-one) to explore whether reaction without silver and with a more optimal aryl bromide was possible (See supporting information for details). However, this screen produced no promising results, indicating that either silver carbonate or an aryl iodide are necessary for reaction, or both. Turning back to the original conditions,[8a] Jack Sharland, who conducted some of the early explorations into adapting the cross-coupling, found that toluene could be exchanged for *N*,*N*-dimethylformamide to successfully produce the intended 5-substituted precursor **3.6a** from **3.5a**. Along with an increase in the amount of acceptor-only diazo used compared to the literature conditions, aryldiazoacetate **3.6a** can be produced in a modest 40% yield (**Scheme 3-2**). The synthesis of the 5-substituted isoindolinone analog required more forcing conditions to produce **3.6b** in useful yield (28%). The 4-substituted aryl iodides **3.5c** and **3.5d** provided more

Scheme 3-2. Synthesis of Carbene Precursors 3.6

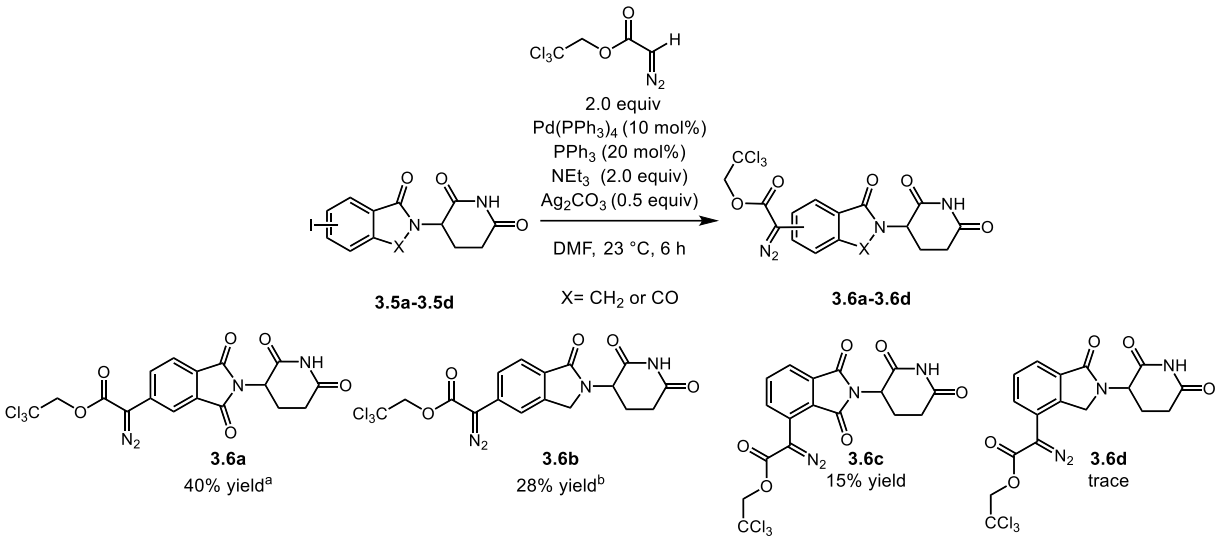

[a] When conducted in toluene, no product was observed. [b] Reaction conducted with 6 equiv diazo, 30 mol% $Pd(PPh_3)_4$, 60 mol% PPh_3, 6 equiv Et_3N, and 1 equiv Ag_2CO_3 in DMSO (0.20 M) for 16 h.

of a challenge. *Ortho*-substituted substrates are difficult substrates for this class of cross-coupling;[8b] we previously reported that *ortho*-substituted aryl iodides were completely unsuccessful under our conditions.[8a] We were pleased to find that the conditions produced aryldiazoacetate **3.6c**, despite the lowered yield of the reaction. Unfortunately, the 4-substituted isoindoline core **3.5d** resisted our efforts, possibly due to the lack of an adjacent carbonyl, which in **3.5c** makes the aryl iodide more amenable to oxidative addition by making the site more electron-deficient.

Industrial chemists have used the ring-opened form of glutarimides to circumvent any synthetic problems associated with the ring-closed glutarimide, and to allow preparation of enantioenriched IMiDs.[9] Another advantage offered by use of ring-opened glutarimides is that they are known to be less neuro- and embryotoxic, relative to thalidomide.[10] Despite the utility and clinical value of IMiDs, the toxicity of thalidomide derivatives is of constant concern to chemists.[11] We considered that the safety and synthetic advantages conferred by the use of ring-opened derivatives might be useful. The ring-opened aryl iodide cores **3.7a** and **3.7b** were much

Scheme 3-3. Synthesis of Carbene Precursors 3.7

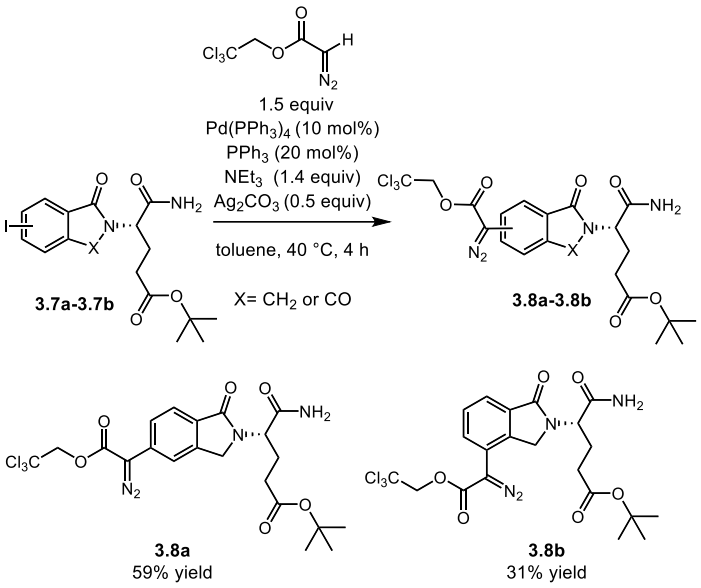

more soluble than the ring-closed variants, allowing the cross-couplings to be run in toluene (**Scheme 3-3**). The ring-opened diazo compounds **3.8a** and **3.8b** formed in modest yields under the reaction conditions. The formation of the 4-substituted isoindolinone **3.8b** is noteworthy as the efforts to prepare the corresponding ring-closed variant **3.6d** were unsuccessful.

We selected **3.6a** as a model carbene precursor for optimization in C–H functionalization reactions with cyclohexane as a susbtrate. Rh_2(*p*-PhTPCP)$_4$ (**Figure 3-1**), when added as a solution to a suspension of the diazo compound in neat cyclohexane, does not react (entry 1, **Scheme 3-4**). Instead, the diazo remains in suspension. Hypothesizing that HFIP might assist in compound solubility, when HFIP (10 equiv) is added to the reaction vessel before addition of the

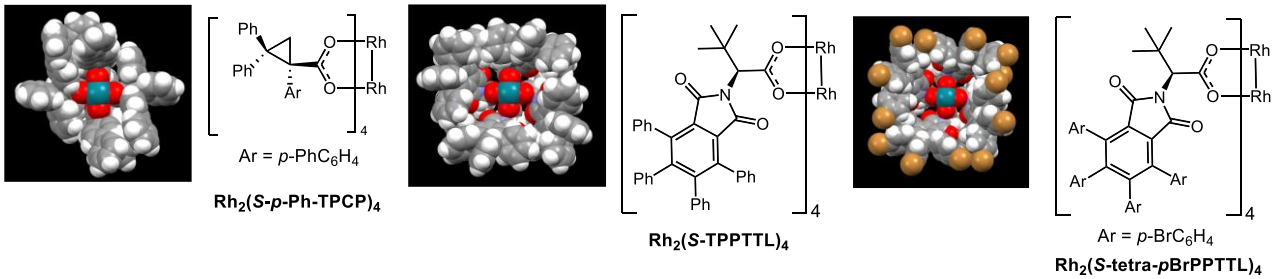

Figure 3-1. Chiral Catalysts Used in this Study

Rh_2(*p*-PhTPCP)$_4$ solution, the C–H functionalized product **3.9a** is produced in 54% yield (entry 2). However, **3.9a** is produced in modest asymmetric induction (76:24 d.r.), which stands in contrast to the high stereoinduction conferred by Rh_2(*p*-PhTPCP)$_4$ in the cycloaddition reactions in Chapter 2. The reported d.r. values represent the asymmetric induction generated at the carbene site by the chiral catalyst. Compounds **3.6a-c** are racemic, and both enantiomers of **3.6a-c** react at essentially the same rate in the presence of the chiral catalyst. The resulting diastereomeric products **3.9a** are formed with essentially the same levels of asymmetric induction. The absolute configuration at the newly formed stereogenic center in **3.9a** is tentatively assigned as *R* by analogy to the assignments made in a related C–H functionalization with the same catalyst.[12]

Scheme 3-4. Optimization of the C–H Functionalization Reaction with Ring-Closed Diazo

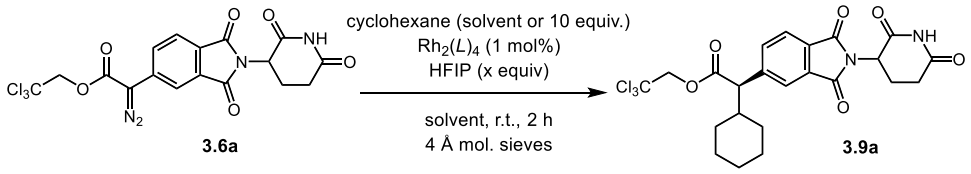

Entry	*L* =	Solvent	Cyclohexane (equiv)	HFIP (equiv)	Yield 3.9a (%)	d.r.
1	*S*-*p*-Ph-TPCP	cyclohexane	solvent	None	n.r.	N/A
2	*S*-*p*-Ph-TPCP	cyclohexane	solvent	10	54	76:24
3	*S*-TPPTTL	cyclohexane	solvent	10	77	82:18
4	*S*-tetra-*p*BrPPTTL	cyclohexane	solvent	10	81	98:2
5	*S*-tetra-*p*BrPPTTL	1:1 CH_2Cl_2:cyclohexane	solvent	None	64	99:1
6	*S*-tetra-*p*BrPPTTL	1:1 CH_2Cl_2:cyclohexane	solvent	10	89	99:1
7	*S*-tetra-*p*BrPPTTL	CH_2Cl_2	10	10	89	99:1

Reactions were conducted on 0.1 mmol scale. Yields reported as isolated yields of purified material. Asymmetric induction determined by SFC analysis. See SI for details.

The C_4-symmetric bowl-shaped catalyst Rh_2(*S*-TPPTTL)$_4$ formed **3.9a** in improved yield (77%) and asymmetric induction (82:18 d.r.) (entry 3). A more recently developed derivative of the TPPTTL scaffold, Rh_2(*S*-tetra-*p*BrPPTTL)$_4$[12] gave even better results, forming **3.9a** in excellent yield (81%) and with high levels of asymmetric induction (98:2 d.r.) (entry 4). Rh_2(*S*-tetra-*p*BrPPTTL)$_4$ has also previously been successful when used in conjunction with non-

solvent amounts of HFIP in our previous studies (also see Chapter 2, **Scheme 2-5**).[4] We conducted further optimization studies with Rh_2(*S*-tetra-*p*BrPPTTL)$_4$ to further gauge the nature of the system. Interestingly, when the reaction is conducted in a 1:1 mixture of cyclohexane and dichloromethane, the reaction proceeds in the absence of HFIP (64% yield, entry 5). The lowered yield is the result of more carbene dimerization byproducts; interestingly, no N-H insertion is observed in the crude ^{1}H NMR spectra. Addition of HFIP (10 equiv, entry 6) increases the yield to 89%. When the amount of cyclohexane used is lowered to 10 equiv, the reaction is equally effective. Instead of adding a catalyst solution to a stirred suspension of diazo in neat substrate, the diazo is dissolved in dichloromethane with the aid of HFIP (10 equiv), and the solution is added slowly, over 1 h, to a solution of catalyst (1 mol%) and cyclohexane (10 equiv) in dichloromethane.

Optimization studies were also carried out with the ring opened derivative **3.8a** (**Scheme 3-5**). As with the aryl iodides **3.7a** and **3.7b**, the ring-opened diazo compounds like **3.8a** are far more soluble than the ring-closed variants in relatively nonpolar solvents. Thus, the diazo can be dissolved in dichloromethane without the use of HFIP. However, without HFIP **(*S*,*R*)-3.10a** is formed in only 13% yield (entry 1). In this reaction, we observed carbene dimerization as the major byproduct. The addition of HFIP (10 equiv) to the reaction vessel prior to diazo addition allows a 60% yield of **(*S*,*R*)-3.10a**, with a high level of asymmetric induction at the site of reaction (98:2 d.r., entry 2). Reaction under the same conditions with the enantiomer of the catalyst, Rh_2(*R*-tetra-*p*BrPPTTL)$_4$, preferentially generates the other diastereomer of the product in only 16% yield (entry 3). An improved yield (70%) of **(*S*,*R*)-3.10a** can be achieved in the Rh_2(*S*-tetra-*p*BrPPTTL)$_4$-catalyzed reaction by using cyclohexane as solvent (entry 4).

Scheme 3-5. Optimization of the C–H Functionalization Reaction with Ring-Opened Diazo

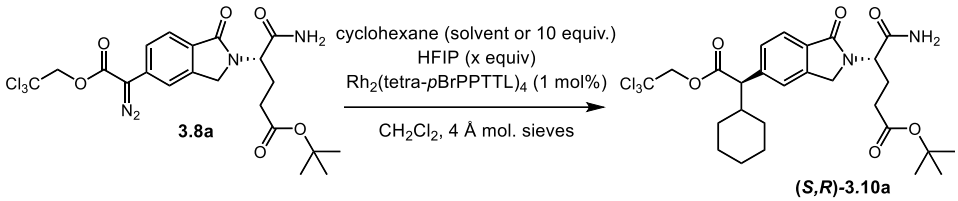

Entry	Solvent	Catalyst Enantiomer	cyclohexane (equiv)	HFIP (equiv)	yield 3.10a (%)	d.r.
1	CH_2Cl_2	*S*	10	0	13	99:1
2	CH_2Cl_2	*S*	10	10	60	98:2
3[a]	CH_2Cl_2	*R*	10	10	16	7:93
4	cyclohexane	*S*	solvent	10	71	98:2

Reactions were conducted on 0.1 mmol scale. Yields reported as isolated yields of purified material. Asymmetric induction determined by SFC analysis. See SI for details. [a] Reaction with the *R* catalyst produced (*S*,*S*)-3.10a as the major diastereomer.

We found the reaction with the opposite catalyst enantiomer (entry 3) to be one of the more intriguing features of these transformations from a catalyst design perspective. Even though the stereocenter in **3.8a** is far removed from the diazoacetate, the C–H functionalization reaction experiences significant matched/mis-matched conditions (i.e., reactivity dependent on the enantiomer of the chiral catalyst used). The reaction with Rh_2(*S*-tetra-*p*BrPPTTL)$_4$ forms **3.10a** in higher yield (60%) than the reaction with Rh_2(*R*-tetra-*p*BrPPTTL)$_4$ (16%), but both enantiomers of the catalyst produce the same high (and opposite) asymmetric induction. We have observed the effects of distal functionality in substrates in the past, arising from secondary interactions between the catalyst wall and the approaching substrate.[13] The influence of the stereochemistry of the catalyst on yield, by our reckoning, is due to the bowl-shape of the catalyst, which is the major contributing factor in our past studies.[13] In this case, the bowl-shaped catalyst might favor differing orientations of **3.8a** within the catalyst based on catalyst enantiomer. To further explore this hypothesis, we conducted density functional theory (DFT) calculations to model the relative stability of the rhodium carbene intermediates of **3.8a** in Rh_2(*S*-tetra-*p*BrPPTTL)$_4$ versus Rh_2(*R*-tetra-*p*BrPPTTL)$_4$ (**Figure 3-2**). Duc Ly conducted the

calculations, and Djamaladdin Musaev assisted with and checked the calculations. Calculations were initially difficult due to the large size of the catalyst-carbene system (up to 400 atoms). To work around this we used the two-layer ONIOM (B3LYP:UFF) approach, which uses the more powerful but more intensive quantum mechanics-based approach to model the carbene system and the core of the catalyst, and a less demanding molecular mechanics (which is an adapted method relying on classical mechanics) approach to model the more peripheral atoms (See SI for details). We found that the rhodium-carbene intermediate **A** resulting from Rh_2(*S-tetra-p*BrPPTTL)$_4$ is thermodynamically more stable than **B (**Rh_2(*R*-tetra-*p*BrPPTTL)$_4$) by 1.7 kcal/mol (**Figure 3-2**). Structural analysis reveals that the ring-opened side chain of the carbene fragment and the trichloroethyl acetate are arranged differently in **A** versus **B**. On the *Si* face of the carbene, where the reaction with the substrate and Rh_2(*R-tetra*-BrTPPTTL)$_4$ occurs, the ring-opened side chain in **B** folds towards the trichloroethyl acetate group. In **A**, this side chain fold

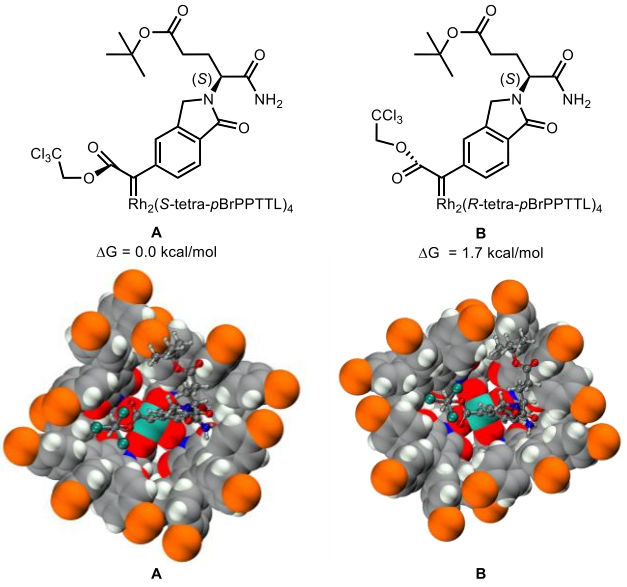

Figure 3-2. DFT-optimized structures of ***8a*** *as a carbene complex with* Rh_2*(S-tetra-pBrPPTTL)*$_4$ *(A) and* Rh_2*(R-tetra-pBrPPTTL)*$_4$ *(B).*

towards the opposite side of the trichloroethyl acetate group. This differential folding makes the open face of **A** less sterically demanding than in **B**, which allows better reactivity. These insights gleaned from computational analysis illustrate the subtle but impactful effects of secondary interactions between substrates and bowl-shaped catalysts like Rh_2(*tetra*-BrTPPTTL)$_4$

With good conditions in hand for both the ring-closed and ring-opened diazo compounds, we tested the other carbene precursors (**3.6b**, **3.6c**, **3.8b**) in the C–H functionalization of cyclohexane using Rh_2(*S*-tetra-*p*BrPPTTL)$_4$ (**Scheme 3-6**). The optimized conditions are well-suited to all analogs, generating compounds **3.9a-c** and **3.10a-b** in high yields. We conducted the reactions using 10 equiv cyclohexane and a slow addition of diazo, as well as using catalyst addition to a stirred solution of diazo in neat cyclohexane. The latter "catalyst addition" method is superior in terms of yield and generates far less carbene dimerization byproducts. All C–H

Scheme 3-6. Scope of the C–H Functionalization of Cyclohexane

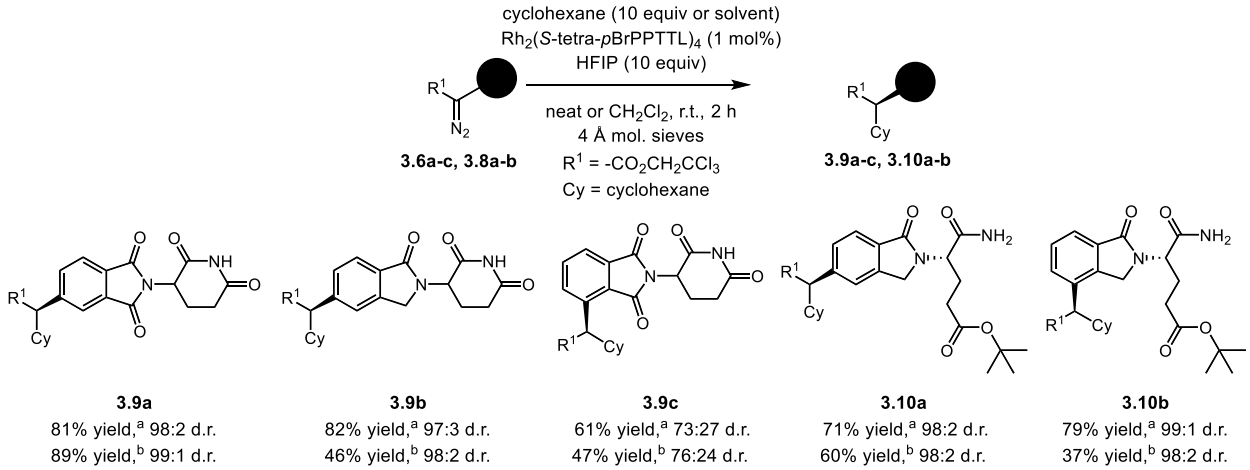

Reactions conducted on 0.1 mmol scale. Yields reported as isolated yields of purified material. Diastereomeric ratio (d.r.) represents asymmetric induction by catalysts. See SI for details. [a] cyclohexane as solvent. [b] cyclohexane (10 equiv) as trap.

functionalization products were produced with high levels of asymmetric induction, except for **3.9c**, which we hypothesized is due to interference from the proximal carbonyl oxygen.

Both the ring-closed and ring-opened carbene precursors are competent in the cyclopropanation reactions as illustrated in the Rh_2(*S*-tetra-*p*BrPPTTL)$_4$ catalyzed reactions with

Scheme 3-7. Scope of the Cyclopropanation of Styrene

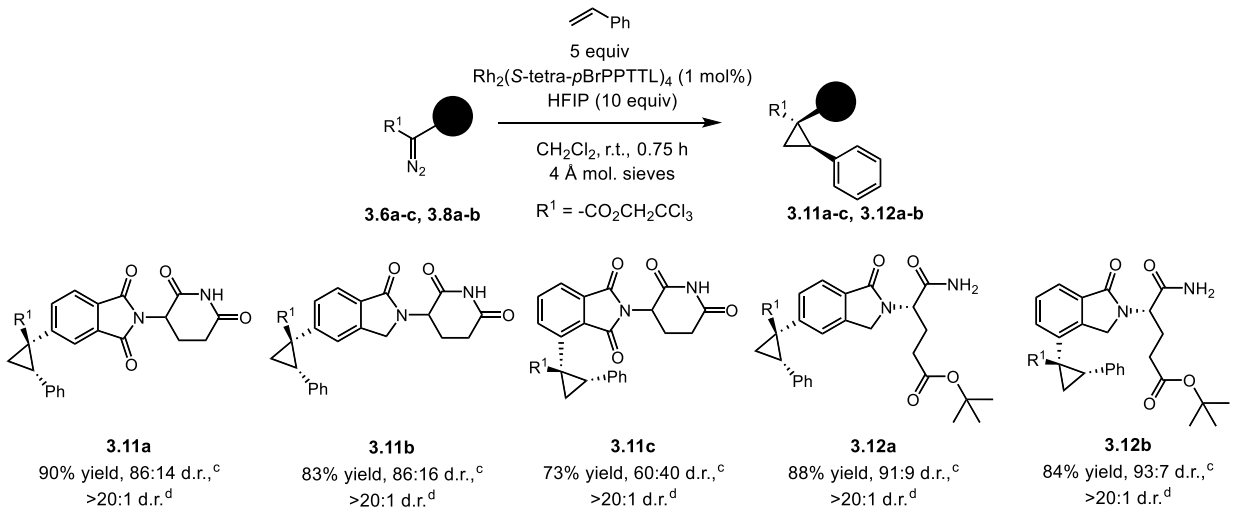

Reactions conducted on 0.1 mmol scale. Yields reported as isolated yields of purified material. Diastereomeric ratio (d.r.) represents asymmetric induction by catalysts. See SI for details. [a] cyclohexane as solvent. [b] cyclohexane (10 equiv) as trap. [c] d.r. for asymmetric induction by catalyst [d] d.r. for ratio of two newly formed stereogenic centers

styrene (**Scheme 3-7**). Just 5 equiv of styrene is necessary for a good reaction, as cyclopropanation is in general a more favorable reaction than C–H functionalization.[3] The desired products **3.11a-c**, **3.12a**, and **3.12b** were produced in excellent yield, although these products displayed lower levels of asymmetric induction. The absolute configuration of these products is tentatively assigned as 1*R*, 2*S* by analogy to assignments made previously from X-ray crystal structures of similar products formed from the reaction of aryldiazoacetates with Rh_2(*S*-tetra-*p*BrPPTTL)$_4$.[4]

The ring-opened products such as **3.10a,b** and **3.12a,b** can be subjected to acid-mediated ring closure with retention of stereochemistry both at the site of carbene reaction and at the glutarimide stereogenic center.[9b] In **Scheme 3-8** we show the conversion of **3.10b** to **3.13** (also see compounds **SI2-SI4** in the supporting information). This example gives an enantioenriched product which could not be reached by direct synthesis of the diazo compound (**3.6d**, **Scheme 2**).

*Scheme 3-8. Stereoretentive Ring-Closure of **3.10b***

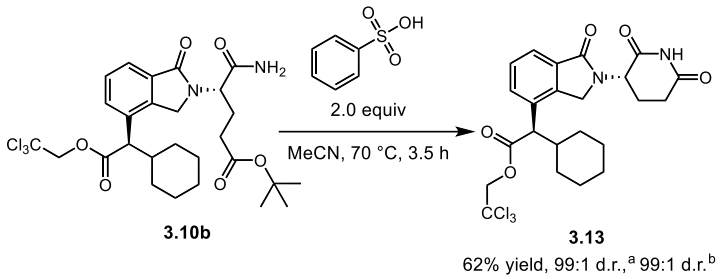

[a] d.r. for retained asymmetric induction from catalyst [b] d.r. for glutarimide stereogenic center

In Chapter 2, we observed during analysis of the biological studies that often the 5-substituted derivatives (see **Figure 2-5**) were more biologically active than others, so we selected carbene precursor **3.6a** to probe the scope of potential C–H functionalization products (**Scheme 3-9**). Addition of solution of catalyst into a solution of diazo and neat substrate with HFIP (10 equiv) allowed for the generation of secondary C–H functionalization products **3.14**-**3.16** in excellent asymmetric induction and yield. Of note is product **3.14** which showed an exquisite selectivity for C2 over other sites (>30:1 r.r.). Slow addition of **3.6a** in dichloromethane and HFIP into a solution of catalyst and 10 equiv substrate allowed the generation of compound **3.17**-**3.21**. The mildly electron-withdrawing bromide of compound **3.18** causes a slightly lower yield (35%), although it offers the potential for further functionalization. The system favors benzylic tertiary sites over benzylic primary sites for C–H functionalization, as we observed in the formation of compound **3.19**. The yield of compound **3.19** can be increased to near-quantitative levels using the substrate (*p*-cymene) as solvent, compared to using 10 equiv of *p*-cymene (53% yield). Interestingly there is a variation in selectivity observed between the set of conditions; compound **3.19** is produced with enhanced regioselectivity but decreased asymmetric induction when *p*-cymene is used as solvent. Other tertiary-site functionalizations perform well as with the reaction of 1-(4-(*tert*-butyl)phenyl)bicyclo[1.1.1]pentane and compound **3.6a**, which form **3.20**

*Scheme 3-9. Scope of C-H Functionalization with **3.6a***

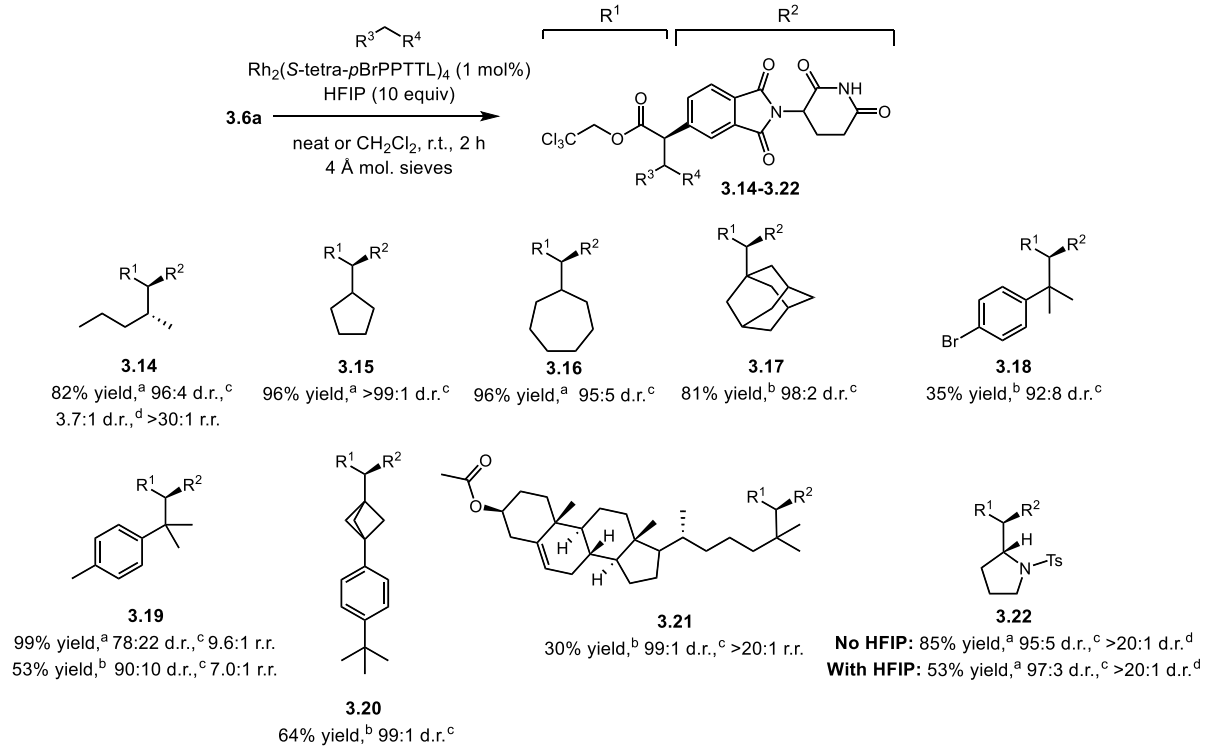

Reactions conducted on 0.1 mmol scale. Yields reported as isolated yields of purified material. See SI for details. [a] Substrate used as solvent. [b] 10 equiv substrate used. [c] d.r. for asymmetric induction by the catalyst [d] d.r. for ratio of two newly formed stereogenic centers

in modest yield and asymmetric induction while preserving the strained carbocycle of the substrate. The reaction of compound **3.6a** and cholesteryl acetate with high diastereoselectivity, with only one observed regioisomer (**3.21**) present (>30:1 r.r.). We also tested compound **3.6a** in the C–H functionalization of *N*-tosyl pyrrolidine, which is produced in excellent d.r. and 53% yield. We hypothesized that the slightly decreased yield be due to HFIP hydrogen-bonding to the nitrogen of the substrate, thereby making the α-proton less hydridic. Removal of HFIP from the conditions by adding a solution of catalyst to a reaction containing diazo, only 10 equiv substrate, and catalyst in dichloromethane produces the product **3.22** in appreciably higher yield (85%) with good d.r. (95:5).

These IMiD-core diazo compounds are demonstrably effective at creating them in a stereodefined manner. While the primary focus of our work so far has been on IMiDs, we proposed that our method might also be effective in creating novel bifunctional LDDs, as many LDDs rely on glutarimide-containing and thalidomide-like compounds.[14] The product of a reaction between a "linker" and a diazo compound like **3.6a** could then be appended to a bioactive ligand. Our particular approach was to prepare a protected piperazine with a 6-carbon chain terminated by an alkene, and perform a cyclopropanation using diazo **3.6a** (**Scheme 3-10**).

Scheme 3-10. Synthesis of LDDs with Stereodefined Cereblon Modulating Components

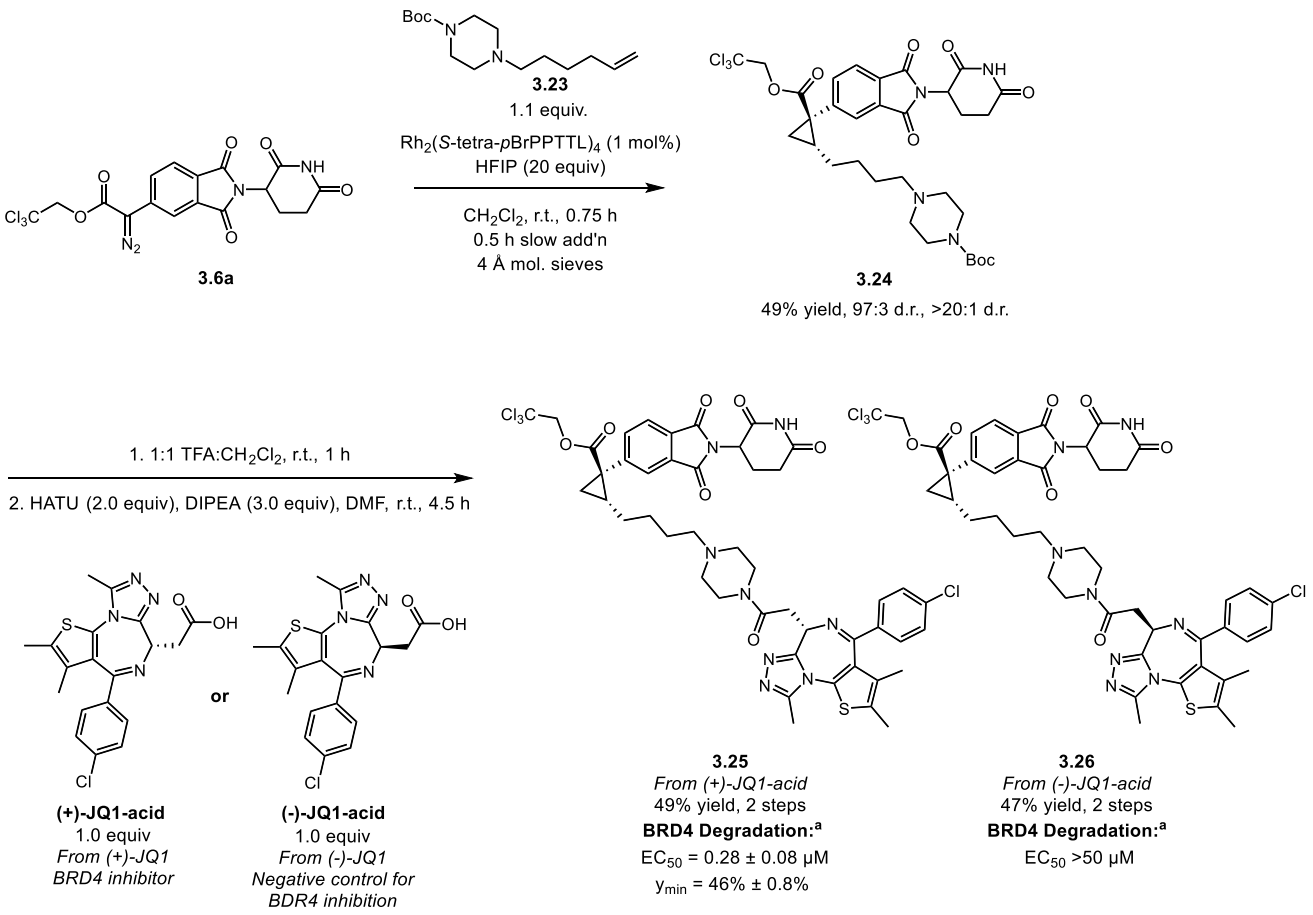

[a] EC_{50} indicates the concentration required to achieve 50% of total degradation effect and Y_{min} indicates depth of degradation with 100% representing no reduction in protein level and 0% representing complete degradation; data reported as an average of N = 3 test occasions.

Using only 1.1 equiv of the trap **3.23**, the reaction forms the cyclopropanation product **3.24** in 49% yield with excellent relative and absolute stereochemical control. We then performed a boc-deprotection with trifluoroacetic acid and immediately subjected this intermediate to amide coupling with a potent bromodomain 4 (BRD4) inhibitor, (+)-JQ1 to form LDD **3.25**.[15] We also performed the same amide coupling with the inactive enantiomeric partner (-)-JQ1 to form compound **3.26** (**Scheme 3-10**). The ability of **25** and **26** to degrade BRD4 was assessed in a HiBiT (a tagging system for endogenous proteins)[16] assay in A549 cells (a line derived from human adenocarcinoma).[17] Hua Fang of Bristol Myers Squibb conducted the biological study. Compound **3.25** displayed modest BRD4 degradation, with an EC_{50} of 0.28 mM and partial level of degradation (46% Y_{max}). The negative control (**3.26**) containing (-)-JQ1 did not significantly degrade BRD4, at concentrations up to 50 mM. The degradation effects of compound **3.25** highlight the potential of our method to applied towards the generation of biologically effective compounds.

Conclusions

Aryldiazoacetates with IMiD-like cores are exceptionally useful dirhodium carbene precursors for C–H functionalization and cyclopropanation. The reaction conditions remain mild but can produce stereodefined structures with high diastereoselectivity, regioselectivity, and yields. HFIP acts as a solubilizing agent and a nucleophile-deactivating agent in the carbene reactions, enabling the synthesis of diverse IMiD-like compounds as well as bioactive, stereodefined LDDs. This work reinforces the synthetic utility of rhodium carbene chemistry in medicinally relevant contexts.

We proposed that asymmetric rhodium catalysis could influence the study of immunomodulatory imide drugs by introducing mild yet effective methods of synthesizing

novel, diverse, and stereodefined IMiDs and IMiD-like structures. Dirhodium-catalyzed cycloadditions (Chapter 2), enabled by the development of an anhydrous, stereoretentive, and fluoride-enhanced Suzuki-Miyaura reaction (Chapter 1), allowed both this kind of synthesis and a seminal SAR study of how stereochemistry affects neosubstrate degradation. Overcoming obstacles with expanding the scope of reactions to C–H functionalization produced the development of rhodium carbene precursors based on IMiDs, which enabled the highly convergent creation of novel IMiD-like structures and LDDs (Chapter 3). The challenge of adapting rhodium carbene chemistry to the IMiD space expanded the knowledge of how both cyclopropanation and C–H functionalization (a heretofore underutilized method relative to cyclopropanation) can potentially revolutionize how medicinal chemists approach the preparation of synthetically challenging yet valuable drug classes.

The work in Chapter 3 was submitted for publication in 2025:

Tracy, W.F.; Sharland, J.C.; Ly, D.; Davies, G.H.M.; Musaev, D.G.; Fang, H.; Moreno, J.; Cherney, E.C.; Davies, H.M.L. Diversity Synthesis Using CELMoD Cores as Rhodium Carbene Precursors in Enantioselective C–H Functionalization and Cyclopropanation. *Manuscript Submitted*.

J.C. Sharland performed the initial exploration into diazo synthesis. W.F. Tracy conducted the rest of the synthetic work. D. Ly performed the computational work, and D.G. Musaev provided advice, support, and validation for the computational work. Hua Fang performed the biological studies. G.H.M Davies, J. Moreno, and E.C. Cherney provided valuable support and advice.

References

(1) Davies, H. M. L., Finding Opportunities from Surprises and Failures. Development of Rhodium-Stabilized Donor/Acceptor Carbenes and Their Application to Catalyst-Controlled C–H Functionalization. *J. Org. Chem.* **2019,** *84*, 12722-12745.

(2) Davies, H. M. L.; Liao, K., Dirhodium tetracarboxylates as catalysts for selective intermolecular C–H functionalization. *Nat. Rev. Chem.* **2019,** *3*, 347-360.

(3) Davies, H. M. L.; Hansen, T.; Churchill, M. R., Catalytic Asymmetric C−H Activation of Alkanes and Tetrahydrofuran. *J. Am. Chem. Soc.* **2000,** *122*, 3063-3070.

(4) Sharland, J. C.; Dunstan, D.; Majumdar, D.; Gao, J.; Tan, K.; Malik, H. A.; Davies, H. M. L., Hexafluoroisopropanol for the Selective Deactivation of Poisonous Nucleophiles Enabling Catalytic Asymmetric Cyclopropanation of Complex Molecules. *ACS Catal.* **2022,** *12*, 12530-12542.

(5) (a) Vaitla, J.; Boni, Y. T.; Davies, H. M. L., Distal Allylic/Benzylic C−H Functionalization of Silyl Ethers Using Donor/Acceptor Rhodium(II) Carbenes. *Angew. Chem. Int. Ed.* **2020,** *59*, 7397-7402; (b) Boni, Y. T.; Vaitla, J.; Davies, H. M. L., Catalyst Controlled Site- and Stereoselective Rhodium(II) Carbene C(sp^3)–H Functionalization of Allyl Boronates. *Org. Lett.* **2023,** *25*, 5-10.

(6) Chen, L.-M.; Shin, C.; DeLano, T. J.; Carretero-Cerdán, A.; Gheibi, G.; Reisman, S. E., Ni-Catalyzed Asymmetric Reductive Arylation of α-Substituted Imides. *J. Am. Chem. Soc.* **2024**.

(7) Guptill, D. M.; Davies, H. M. L., 2,2,2-Trichloroethyl Aryldiazoacetates as Robust Reagents for the Enantioselective C–H Functionalization of Methyl Ethers. *J. Am. Chem. Soc.* **2014,** *136*, 17718-17721.

(8) (a) Fu, L.; Mighion, J. D.; Voight, E. A.; Davies, H. M. L., Synthesis of 2,2,2,-Trichloroethyl Aryl- and Vinyldiazoacetates by Palladium-Catalyzed Cross-Coupling. *Chem. Eur. J.* **2017,** *23*, 3272-3275; (b) Ye, F.; Qu, S.; Zhou, L.; Peng, C.; Wang, C.; Cheng, J.; Hossain, M. L.; Liu, Y.; Zhang, Y.; Wang, Z.-X.; Wang, J., Palladium-Catalyzed C–H Functionalization of Acyldiazomethane and Tandem Cross-Coupling Reactions. *J. Am. Chem. Soc.* **2015,** *137*, 4435-4444; (c) Tortoreto, C.; Rackl, D.; Davies, H. M. L., Metal-Free C–H Functionalization of Alkanes by Aryldiazoacetates. *Org. Lett.* **2017,** *19*, 770-773.

(9) (a) Zacuto, M. J.; Traverse, J. F.; Bostwick, K. F.; Geherty, M. E.; Primer, D. N.; Zhang, W.; Zhang, C.; Janes, R. D.; Marton, C., Process Development and Kilogram-Scale Manufacture of Key Intermediates toward Single-Enantiomer CELMoDs: Synthesis of Iberdomide·BSA, Part 1. *Org. Process Res. Dev.* **2024,** *28*, 46-56; (b) Zacuto, M. J.; Traverse, J. F.; Geherty, M. E.; Bostwick, K. F.; Jordan, C.; Zhang, C., Chirality Control in the Kilogram-Scale Manufacture of Single-Enantiomer CELMoDs: Synthesis of Iberdomide·BSA, Part 2. *Org. Process Res. Dev.* **2024,** *28*, 57-66.

(10) Fabro, S.; Schumacher, H.; Smith, R. L.; Stagg, R. B. L.; Williams, R. T., The metabolism of thalidomide: Some biological effects of thalidomide and its metabolites. *Br. J. Pharmacol.* **1965,** *25*, 352-362.

(11) From private communications with process and medicinal chemists from Pfizer, Bristol Myers Squibb, and Adesis.

(12) Garlets, Z. J.; Boni, Y. T.; Sharland, J. C.; Kirby, R. P.; Fu, J.; Bacsa, J.; Davies, H. M. L., Design, Synthesis, and Evaluation of Extended C4–Symmetric Dirhodium Tetracarboxylate Catalysts. *ACS Catal.* **2022,** *12*, 10841-10848.

(13) Fu, J.; Ren, Z.; Bacsa, J.; Musaev, D. G.; Davies, H. M. L., Desymmetrization of cyclohexanes by site- and stereoselective C–H functionalization. *Nature* **2018,** *564*, 395-399.

(14) Sosič, I.; Bricelj, A.; Steinebach, C., E3 ligase ligand chemistries: from building blocks to protein degraders. *Chem. Soc. Rev.* **2022,** *51*, 3487-3534.

(15) Pérez-Salvia, M.; Simó-Riudalbas, L.; Llinàs-Arias, P.; Roa, L.; Setien, F.; Soler, M.; Castro de Moura, M.; Bradner, J. E.; Gonzalez-Suarez, E.; Moutinho, C.; Esteller, M., Bromodomain inhibition shows antitumoral activity in mice and human luminal breast cancer. *Oncotarget* **2017,** *8*.

(16) Schwinn, M. K.; Machleidt, T.; Zimmerman, K.; Eggers, C. T.; Dixon, A. S.; Hurst, R.; Hall, M. P.; Encell, L. P.; Binkowski, B. F.; Wood, K. V., CRISPR-Mediated Tagging of Endogenous Proteins with a Luminescent Peptide. *ACS Chem. Biol.* **2018,** *13*, 467-474.

(17) (a) Lieber, M.; Todaro, G.; Smith, B.; Szakal, A.; Nelson-Rees, W., A continuous tumor-cell line from a human lung carcinoma with properties of type II alveolar epithelial cells. *Int. J. Cancer* **1976,** *17*, 62-70; (b) Riching, K. M.; Mahan, S.; Corona, C. R.; McDougall, M.; Vasta, J. D.; Robers, M. B.; Urh, M.; Daniels, D. L., Quantitative Live-Cell Kinetic

Degradation and Mechanistic Profiling of PROTAC Mode of Action. *ACS Chem. Biol.* **2018,** *13*, 2758-2770.

Appendix A: Supporting Information for Chapter 1

Section 1: Supplemental Figures

Scheme S2-1: Attempts at generation of 1.4a and 1.4c using literature and patent conditions

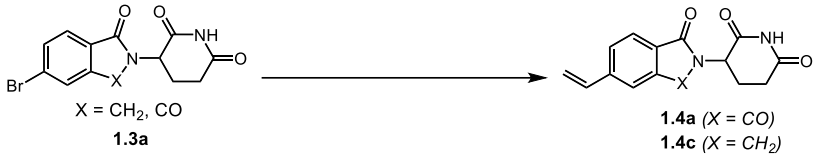

Entry	Conditions	Vinyl source	Result	Reference
1	$PdCl_2$(dppf) (10 mol%), Cs_2CO_3 (2 equiv), 1,4-dioxane, 90 °C, 18 h	BF_3K 3.0 equiv	33% yield **1.4a**	Lu, L., et al. US 0083376 A1, **2021**.
2	$PdCl_2$(dppf) (10 mol%), NaOH (1 equiv), *N*-cyclohexyl-*N*-methylcyclohexanamine (1 equiv), THF, 67 °C, 18 h	BPin 1.2 equiv	trace **1.4a**	Stewart, S.G., et al. *Biorg. Med. Chem.* **2010**, 18, 650-662
3	$Pd_2(dba)_3$ (0.5 mol%), PAPh (1.5 mol%), K_2CO_3 (2.5 equiv), 1,4-dioxane:H_2O (4:1), 80 °C, 18h	BPin 1.5 equiv	11% yield **1.4a**	Sharland, J. C., et al. . *Chem. Sci.* **2021**, 12, 11181-11190.
4	$NiCl_2$(dppp) (10 mol%), LiI (3.5 equiv), Zn (2 equiv), dimethyl isosorbide, 65 °C, 8 h	2 equiv	trace **1.4a**	Su, M., et al. *Org. Lett.* **2022**, 24, 354-358.
5	$PdCl_2(amphos)_2$ (2 mol%), 2.34 equiv $[(tmeda)Zn(OH)(OTf)]_3$, 1,4-dioxane, 80 °C, 3 h	BF_3K 1.1 equiv	85% yield **1.4a** 42% yield **1.4c**	Niwa, T., et al. *Nature Catalysis* **2021**, 4, 1080-1088
6	This Work	BF_3K 2.1 equiv	High yield for all derivatives	

Scheme S2-2: Limitations of the substrate scope

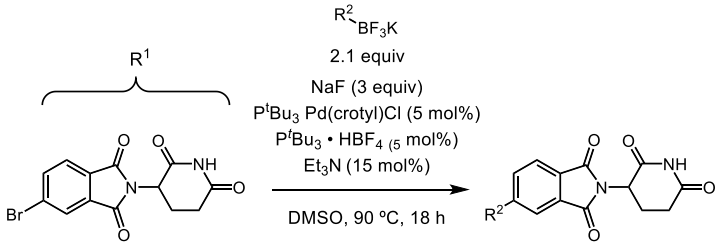

Recovered ArBr

Modification	Yield
None	n.d.
120 °C	n.d.

Modification	Yield
None	n.d.
120 °C	n.d.

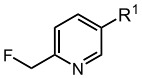

trace

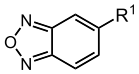

trace

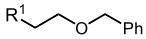

n.d.

Modification	Yield
None	n.d.
$Pd(OAc)_2/P(^tBu)_3$	n.d.
$Pd(OAc)_2/^tBuXPhos$	n.d.
$Pd(OAc)_2$/RuPhos	n.d.
$Pd(OAc)_2$/SPhos	n.d.
$Pd(OAc)_2$/PAPH	n.d.

PAPH =

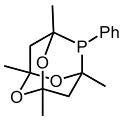

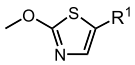

trace

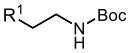

Modification	Yield
None	n.d.
Catacxium A G3	n.d.

Protodehalogenation as major product

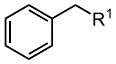

n.d.

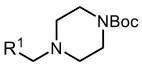

n.d.

Complex mixture

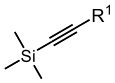

n.d.

Section 2: General Information

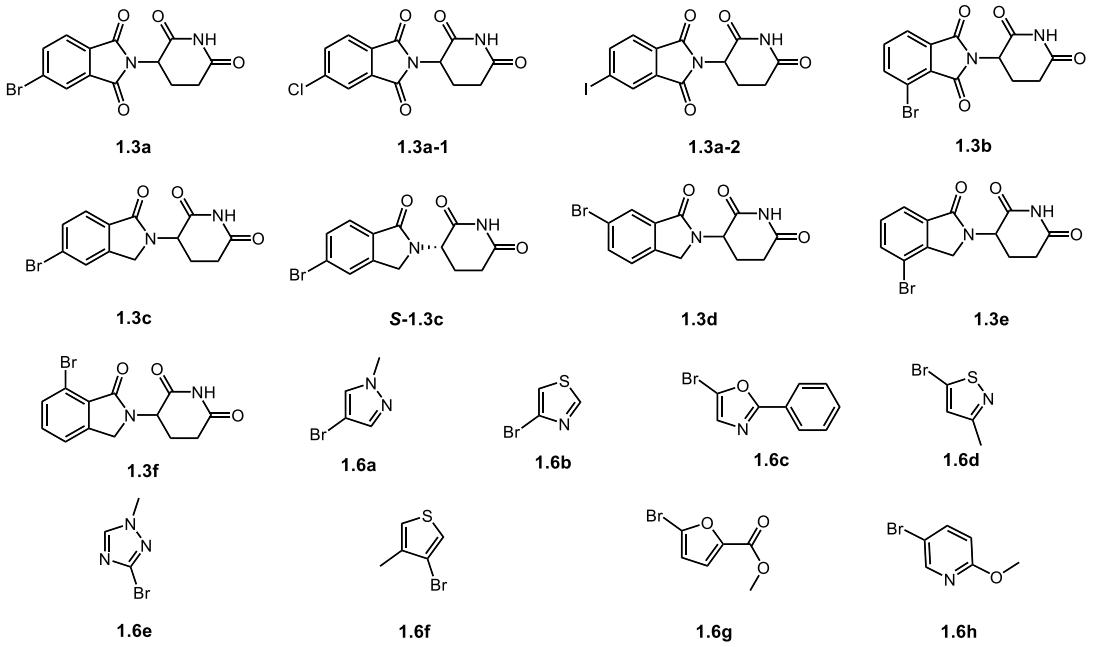

Figure S2-1: Aryl halides used in this study

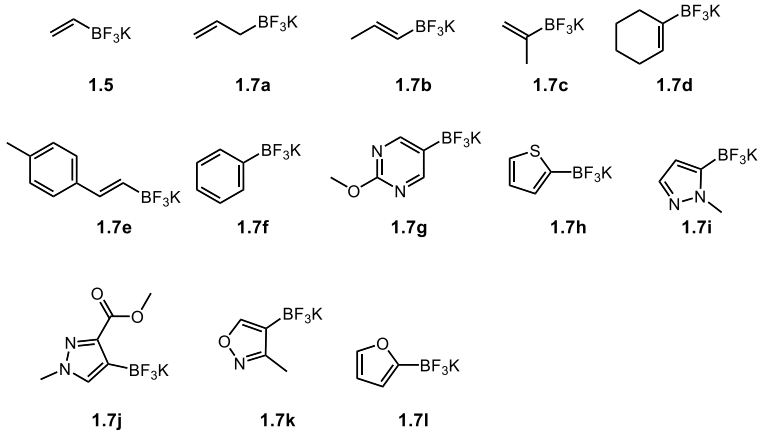

Figure S2-2: Aryl halides used in this study

Section 3: Synthetic Procedures and Compound Characterization

General Synthetic and Characterization Information

All reactions were conducted in flame-dried glassware under an inert atmosphere of dry nitrogen or argon, unless otherwise noted. All reagents were purchased from Oakwood, Combi-Blocks, Millipore Sigma, Strem, or Ambeed, and used as received. Anhydrous dimethylsulfoxide (DMSO), 1,4-dioxane, and all other solvents were purchased from Fisher Scientific and used as received. Proton (^{1}H) NMR spectra were recorded at 400 MHz on Varian and Bruker spectrometers, 500 MHz on an Inova-500 spectrometer, or 600 MHz on an Inova-600

spectrometer. Carbon-13 ($^{13}C\{^{1}H\}$) NMR spectra were recorded at 100 MHz on Varian and Bruker spectrometers or 151 MHz on an Inova-600 spectrometer. NMR spectra were recorded in deuterated solvents and were referenced to tetramethylsilane (in the case of $CDCl_3$) or the respective residual solvent signal. NMR chemical shifts were reported in parts per million (ppm). Abbreviations for signal couplings are as follows: s, singlet; d, doublet; t, triplet; q, quartet; quin, quintet; sex, sextet; sep, septet; and m, multiplet. Coupling constants were taken from the spectra directly and are uncorrected. Fourier Transform Infrared (FTIR) Spectra were collected on a Nicolet Impact Series 10 FT-IR equipped with an attenuated total reflection (ATR) apparatus. Mass spectrometric determinations were carried out on a Thermo Finnigan LTQ-FTMS spectrometer with atmospheric pressure chemical ionization (APCI), using a Fourier transform ion cyclotron resonance (FT-ICR) mass analyzer. Optical rotations were measured on a Rudolph Research Analytical Automatic Polarimeter APIV-1W. Analytical thin layer chromatography (TLC) was performed on silica gel plates using ultraviolet (UV) light to visualize analytes. Normal phase column chromatography was performed with SiliCycle silica gel 60 Å (50 µm) hand-packed in Biotage Sfär columns, on Biotage Isolera Four chromatographs, with Celite® as a dry-loading absorbent. Reverse phase chromatography was conducted using Teledyne ISCO RediSep Gold 18 reverse-phase columns using Teledyne ISCO CombiFlash or Biotage Isolera chromatographs. Supercritical fluid chromatography (SFC) analysis was performed on a Water Acquity UPC2 instrument. Melting points were measured on an Electrothermal IA6304 melting point apparatus.

Caution! Glutarimide-containing compounds such as thalidomide are known reproductive, neurological, and hematological toxins. Care must be exercised to avoid direct contact with glutarimide-containing material; any glassware used with glutarimide-containing material should be treated with a 2 M aqueous solution of strong base such as sodium hydroxide to destroy the material.

General procedure A for reaction optimization.

A septum-cap vial was equipped with a PTFE magnetic stir bar and flame dried under vacuum, then allowed to cool under N_2 atmosphere. The vial was charged with 5-bromo-2-(2,6-dioxopiperidin-3-yl)isoindoline-1,3-dione (169 mg, 1.0 equiv, 0.50 mmol), sodium fluoride (63 mg, 3 Eq, 1.50 mmol), chloro(crotyl)(tri-*tert*-butylphosphine)palladium(II) (10 mg, 5 mol%, 25.0 µmol), tri-*tert*-butylphosphoniumtetrafluoroborate (7 mg, 5 mol%, 25.0 µmol), and potassium trifluoro(vinyl)borate (142 mg, 2.12 equiv, 1.06 mmol) under backflow of nitrogen. Dry 1,4-dioxane (1.71 mL) and triethylamine (10.5 µL, 15 mol%, 75.0 µmol) were charged by syringe, and the vial was equipped with an argon-filled balloon. The vial was placed in an aluminum heating block preheated to 90 °C, and was stirred at this temperature for 24 hours. The reaction was concentrated in vacuuo onto Celite® and purified by flash column chromatography (20-50% EtOAc/hexanes). The product-containing fractions were aggregated and concentrated in vacuuo, affording 2-(2,6-dioxopiperidin-3-yl)-5-vinylisoindoline-1,3-dione as an amorphous tan to off-white solid.

General procedure B-1 for the cross-coupling of potassium trifluoro(vinyl)borates and aryl halides.

A septum-cap vial was equipped with a PTFE magnetic stir bar and flame dried under vacuum, then allowed to cool under N_2 atmosphere. The vial was charged with aryl halide (1.0 equiv, 0.50 mmol), sodium fluoride (63 mg, 3 Eq, 1.50 mmol), chloro(crotyl)(tri-*tert*-butylphosphine)palladium(II) (10 mg, 5 mol%, 25.0 µmol), tri-*tert*-butylphosphoniumtetrafluoroborate (7 mg, 5 mol%, 25.0 µmol), and potassium

trifluoro(vinyl)borate (142 mg, 2.12 equiv, 1.06 mmol) under backflow of nitrogen. Dry DMSO (0.70 mL) and triethylamine (10.5 µL, 15 mol%, 75.0 µmol) were charged by syringe, and the vial was equipped with an argon-filled balloon. The vial was placed in an aluminum heating block preheated to 90 °C, and was stirred at this temperature for one hour. The reaction was partitioned between ethyl acetate (25 mL) and water (50 mL). The aqueous layer was extracted thrice with 25 mL portions of ethyl acetate, after which the combined organic layers were washed with a 10% w/w aqueous solution of lithium chloride. The organic layers were dried over magnesium sulfate, then filtered and concentrated in vacuuo. The material was purified via reverse phase chromatography (C_{18}, 10-100% MeCN/H_2O, 0.1% v/v TFA) and/or normal phase column chromatography with an appropriate mixture of solvents (SiO_2).

General procedure B-2 for the cross-coupling of potassium trifluoroborates and aryl bromides.

A septum-cap vial was equipped with a PTFE magnetic stir bar and flame dried under vacuum, then allowed to cool under N_2 atmosphere. The vial was charged aryl halide (1.0 equiv, 0.50 mmol), sodium fluoride (63 mg, 3 Eq, 1.50 mmol), chloro(crotyl)(tri-*tert*-butylphosphine)palladium(II) (10 mg, 5 mol%, 25.0 µmol), tri-*tert*-butylphosphoniumtetrafluoroborate (7 mg, 5 mol%, 25.0 µmol), and potassium trifluoro(vinyl)borate (142 mg, 2.12 equiv, 1.06 mmol) under backflow of nitrogen. Dry DMSO (0.70 mL) and triethylamine (10.5 µL, 15 mol%, 75.0 µmol) were charged by syringe, and the vial was equipped with an argon-filled balloon. The vial was placed in an aluminum heating block preheated to 90 °C, and was stirred at this temperature for 18 hours. The reaction was partitioned between ethyl acetate (25 mL) and water (50 mL). The aqueous layer was extracted thrice with 25 mL portions of ethyl acetate, after which the combined organic layers were washed with a 10% w/w aqueous solution of lithium chloride. The organic layers were dried over magnesium sulfate, then filtered and concentrated in vacuuo. The material was purified via reverse phase chromatography (C_{18}, 10-100% MeCN/H_2O, 0.1% v/v TFA) and/or normal phase column chromatography with an appropriate mixture of solvents (SiO_2).

General Procedure B-3 for the 1 mmol-scale cross-coupling of potassium trifluoro(vinyl)borate and 5-bromo-2-(2,6-dioxopiperidin-3-yl)isoindoline-1,3-dione.

A septum-cap vial was equipped with a PTFE magnetic stir bar and flame dried under vacuum, then allowed to cool under N_2 atmosphere. The vial was charged with 5-bromo-2-(2,6-dioxopiperidin-3-yl)isoindoline-1,3-dione (337 mg, 1.0 equiv, 1.00 mmol), sodium fluoride (126 mg, 3.0 equiv, 3.00 mmol), chloro(crotyl)(tri-*tert*-butylphosphine)palladium(II) (21 mg, 5 mol%, 50.0 µmol), tri-*tert*-butylphosphoniumtetrafluoroborate (15 mg, 5 mol%, 50.0 µmol), and potassium trifluoro(vinyl)borate (284 mg, 2.12 equiv, 2.12 mmol) under backflow of nitrogen. Dry DMSO (1.71 mL) and triethylamine (10.5 µL, 15 mol%, 75.0 µmol) were charged by syringe, and the vial was equipped with an argon-filled balloon. The vial was placed in an aluminum heating block preheated to 90 °C, and was stirred at this temperature for 24 hours. The reaction was partitioned between ethyl acetate (25 mL) and water (50 mL). The aqueous layer was extracted thrice with 25 mL portions of ethyl acetate, after which the combined organic layers were washed with a 10% w/w aqueous solution of lithium chloride. The organic layers were dried over magnesium sulfate, then filtered and concentrated in vacuuo. The material was concentrated in vacuuo onto Celite® and purified by flash column chromatography (20-50% EtOAc/hexanes). The product-containing fractions were aggregated and concentrated in vacuuo, affording 2-(2,6-dioxopiperidin-3-yl)-5-vinylisoindoline-1,3-dione (261 mg, 0.92 mmol, 92% yield) as a fine, amorphous tan solid.

General Procedure C for the stereoretentive cross-coupling of potassium trifluoroborates and thalidomide derivatives.

A septum-cap vial was equipped with PTFE magnetic stir bar and flame dried under vacuum, then allowed to cool under N_2 atmosphere. The vial was charged with thalidomide derivative (81 mg, 1.0 equiv, 0.25 mmol), sodium fluoride (32 mg, 3.0 equiv, 0.75 mmol), potassium trifluoro(vinyl)borate (71 mg, 2.12 equiv, 0.53 µmol), chloro(crotyl)(tri-*tert*-butylphosphine)palladium(II) (5 mg, 5 mol% 13 µmol), and tri-*tert*-butylphosphonium tetrafluoroborate (4 mg, 5 mol%, 13 µmol) under backflow of nitrogen. Dry DMSO (0.9 mL,) and triethylamine (5.2 µL, 15 mol%, 38 µmol) were charged by syringe. The vial was placed in an aluminum heating block preheated to 90 °C, and was stirred at this temperature for 10 minutes. The reaction was partitioned between 20 mL 1 M aqueous citric acid solution and 10 mL ethyl acetate. The aqueous layer was extracted thrice with 10 mL portions of ethyl acetate, which was dried over magnesium sulfate and evaporated in vacuuo. The material was purified by reverse phase chromatography (10-100% MeCN/H_2O, 0.1% v/v TFA).

Compound Synthesis and Characterization

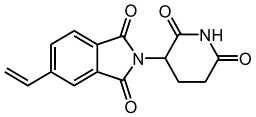

1.4a

2-(2,6-dioxopiperidin-3-yl)-5-vinylisoindoline-1,3-dione (1.4a). Compound **1.4a** was prepared via General Procedure **A**, using **1.3a**, (169 mg, 1.0 equiv, 0.50 mmol), sodium fluoride (63 mg, 3 equiv, 1.50 mmol), chloro(crotyl)(tri-*tert*-butylphosphine)palladium(II) (10 mg, 5 mol%, 25.0 µmol), tri-*tert*-butylphosphoniumtetrafluoroborate (7 mg, 5 mol%, 25.0 µmol), **1.5** (142 mg, 2.12 equiv, 1.06 mmol), dry 1,4-dioxane (1.71 mL), and triethylamine (10.5 µL, 15 mol%, 75.0 µmol). The material was purified by flash column chromatography (SiO_2, 20-50% EtOAc/hexanes). The product-containing fractions were aggregated and concentrated in vacuuo, affording **1.4a** (132 mg, 0.46 mmol, 93% yield) as a fine amorphous tan solid.

HRMS (APCI) *m/z*: $[M+H]^+$ calcd for $C_{15}H_{13}O_4N_2$ 285.0870; Found 285.0868.

^{1}H NMR (500 MHz, DMSO-d_6): δ 11.15 (s, 1H), 8.06 (s, 1H), 7.95 (d, J = 7.6 Hz, 1H), 7.89 (d, J = 7.6 Hz, 1H), 6.95 (dd, J = 17.6, 11.0 Hz, 1H), 6.20 (d, J = 17.6 Hz, 1H), 5.54 (d, J = 11.0 Hz, 1H), 5.16 (dd, J = 12.7, 5.2 Hz, 1H), 2.93 – 2.86 (m, 1H), 2.62 – 2.50 (m, 2H, partially obscured by solvent signal), 2.08-2.05 (m, 1H).

^{13}C{^{1}H} NMR (101 MHz, DMSO-d_6): δ 172.8, 169.9, 167.1, 166.9, 143.8, 135.2, 132.4, 132.1, 130.1, 123.9, 120.7, 119.1, 49.1, 31.0, 22.0.

FTIR (neat): ν_{max}/cm^{-1} 3468, 3202, 3101, 2990, 2904, 1773, 1695, 1616.

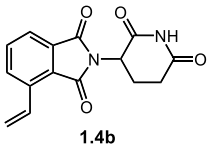

1.4b

2-(2,6-dioxopiperidin-3-yl)-4-vinylisoindoline-1,3-dione (1.4b). Compound **1.4b** was prepared via a modification of General Procedure **B-1**, using **1.3b** (169 mg, 1.0 equiv, 0.50 mmol), sodium fluoride (63 mg, 3 equiv, 1.50 mmol), chloro(crotyl)(tri-*tert*-butylphosphine)palladium(II) (21

mg, 10 mol%, 50.0 μmol), tri-*tert*-butylphosphoniumtetrafluoroborate (15 mg, 10 mol%, 10.0 μmol), **1.5** (142 mg, 2.12 equiv, 1.06 mmol), dry DMSO (1.71 mL), and triethylamine (21 μL, 30 mol%, 0.15 mmol). The material was purified by flash column chromatography (SiO_2, 0-10% MeOH/CH_2Cl_2), affording **1.4b** (120 mg, 0.42 mmol, 84% yield) as a fine, amorphous tan solid.

HRMS (APCI) *m/z*: $[M+H]^+$ calcd for $C_{15}H_{13}O_4N_2$ 285.0870; Found 285.0868.

^{1}H NMR (500 MHz, DMSO-d_6): δ 11.13 (s, 1H), 8.21 – 8.14 (m, 1H), 7.87 – 7.78 (m, 1H), 7.66 (dd, J = 17.8, 11.1 Hz, 1H), 6.23 (dd, J = 17.8, 0.9 Hz, 1H), 5.66 (dd, J = 11.1, 0.9 Hz, 1H), 5.15 (dd, J = 12.8, 5.4 Hz, 11H), 2.89 (ddd, J = 16.9, 13.9, 5.4 Hz, 1H), 2.66 – 2.50 (m, 2H, partially obscured by solvent signal), 2.13 – 1.97 (m, 1H).

^{13}C{^{1}H} NMR (101 MHz, DMSO-d_6): δ 172.8, 169.9, 167.6, 166.8, 135.7, 134.7, 131.8, 130.6, 129.8, 125.9, 122.7, 120.6, 48.9, 30.9, 21.9.

FTIR (neat): ν_{max}/cm^{-1} 3202, 3097, 2920, 1774, 1698, 1391, 1370, 1262, 1201.

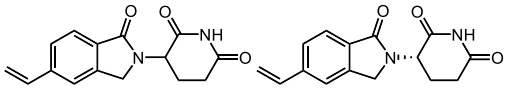

1.4c **(*S*)-1.4c**

3-(1-oxo-5-vinylisoindolin-2-yl)piperidine-2,6-dione (1.4c, racemic material), (*S*)-3-(1-oxo-5-vinylisoindolin-2-yl)piperidine-2,6-dione ((*S*)-1.4c, enantioenriched material).

Compound **1.4c** was prepared via General Procedure **B-1**, using **1.3c**, (162 mg, 1.0 equiv, 0.50 mmol), sodium fluoride (63 mg, 3 equiv, 1.50 mmol), chloro(crotyl)(tri-*tert*-butylphosphine)palladium(II) (10 mg, 5 mol%, 25.0 μmol), tri-*tert*-butylphosphoniumtetrafluoroborate (7 mg, 5 mol%, 25.0 μmol), **1.5** (142 mg, 2.12 equiv, 1.06 mmol), dry DMSO (1.71 mL), and triethylamine (10.5 μL, 15 mol%, 75.0 μmol). The material was purified by flash column chromatography (SiO_2, 0-3% MeOH/CH_2Cl_2), affording **1.4c** (126 mg, 0.47 mmol, 93% yield) as a fine, amorphous tan solid.

Compound (***S***)**-1.4c** was prepared via General Procedure **C**, using (***S***)**-1.3c** (99% ee by SFC) (81 mg, 1.0 equiv, 0.25 mmol), sodium fluoride (32 mg, 3.0 equiv, 0.75 mmol), **1.5**(71 mg, 2.12 equiv, 0.53 μmol), chloro(crotyl)(tri-*tert*-butylphosphine)palladium(II) (5 mg, 5 mol% 13 μmol), and tri-*tert*-butylphosphonium tetrafluoroborate (4 mg, 5 mol%, 13 μmol), dry DMSO (0.9 mL,) and triethylamine (5.2 μL, 15 mol%, 38 μmol). The material was purified by reverse phase chromatography (C_{18}, 10-100% MeCN/H_2O, 0.1% v/v TFA), giving (***S***)**-1.4c** as a fine, amorphous light-gray solid in 99% ee (59 mg, 0.22 mmol, 88% yield). The same reaction run at 70 °C for 0.5 h gave an 80% yield and 99% ee (54 mg, 0.20 mmol).

HRMS (APCI) *m/z*: $[M+H]^+$ calcd for $C_{15}H_{15}O_3N_2$ 271.1077; Found 271.1076.

^{1}H NMR (400 MHz, DMSO-d_6): δ 11.00 (s, 1H), 7.96 – 7.65 (m, 2H), 7.62 (dd, J = 7.9, 1.4 Hz, 1H), 6.87 (dd, J = 17.6, 11.0 Hz, 1H), 6.00 (d, J = 17.7 Hz, 1H), 5.41 (d, J = 11.0 Hz, 1H), 5.12 (dd, J = 13.3, 5.1 Hz, 1H), 4.46 (d, J = 17.3 Hz, 1H), 4.33 (d, J = 17.2 Hz, 1H), 2.92 (ddd, J = 17.3, 13.6, 5.4 Hz, 1H), 2.65 – 2.56 (m, 1H), 2.40 (qd, J = 13.2, 4.4 Hz, 1H), 2.01 (ddq, J = 10.3, 5.3, 2.5 Hz, 1H).

^{13}C{^{1}H} NMR (101 MHz, DMSO-d_6): δ 172.9, 171.0, 167.8, 142.7, 140.6, 136.2, 131.1, 126.2, 123.2, 121.0, 116.7, 51.6, 47.1, 31.2, 22.5.

FTIR (neat): ν_{max}/cm^{-1} 3079, 2854, 1712, 1677, 1619, 1349, 1198.

For **(*S*)-1.4c**:

Specific rotation: $[\alpha]_D^{23}$ −42.0° (c 0.57, DMSO).

SFC analysis: major enantiomer (Chiralcel OJ-3, 20% 1:1 MeOH:^{i}PrOH in CO_2, 2.5 mL/min, 254 nm) indicated 99% ee: t_R (major enantiomer) = 1.43 min, t_R (minor enantiomer) = 1.12 min.

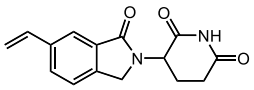

1.4d

3-(1-oxo-6-vinylisoindolin-2-yl)piperidine-2,6-dione (1.4d). Compound **1.4d** was prepared via General Procedure **B-1**, using **1.3d** (162 mg, 1.0 equiv, 0.50 mmol), sodium fluoride (63 mg, 3 equiv, 1.50 mmol), chloro(crotyl)(tri-*tert*-butylphosphine)palladium(II) (10 mg, 5 mol%, 25.0 µmol), tri-*tert*-butylphosphoniumtetrafluoroborate (7 mg, 5 mol%, 25.0 µmol), **1.5** (142 mg, 2.12 equiv, 1.06 mmol), dry DMSO (1.71 mL), and triethylamine (10.5 µL, 15 mol%, 75.0 µmol). The material was purified by flash column chromatography (SiO_2, 0-10% MeOH/CH_2Cl_2), affording **2d** (126 mg, 0.47 mmol, 92% yield) as a fine, amorphous tan solid.

HRMS (APCI) *m/z*: $[M+H]^+$ calcd for $C_{15}H_{15}O_3N_2$ 271.1077; Found 271.1076.

^{1}H NMR (600 MHz, DMSO-d_6): δ 10.99 (s, 1H), 7.82 (d, J = 1.5 Hz, 1H), 7.75 (d, J = 1.6 Hz, 1H), 7.59 (d, J = 7.9 Hz, 1H), 6.87 (dd, J = 17.7, 11.0 Hz, 1H), 5.98 (d, J = 18.1 Hz, 1H), 5.34 (d, J = 11.0 Hz, 1H), 5.13 (dd, J = 13.3, 5.1 Hz, 1H), 4.46 (d, J = 17.4 Hz, 1H), 4.33 (d, J = 17.4 Hz, 1H), 2.91 (ddd, J = 17.3, 13.7, 5.4 Hz, 1H), 2.64 – 2.56 (m, 1H), 2.40 (qd, J = 13.3, 4.4 Hz, 1H), 2.01 (dtd, J = 12.7, 5.3, 2.3 Hz, 1H).

^{13}C{^{1}H} NMR (151 MHz, DMSO-d_6): δ 172.9, 171.0, 167.9, 141.6, 137.2, 136.0, 132.2, 129.6, 123.8, 120.3, 115.4, 51.6, 47.1, 31.2, 22.4.

FTIR (neat) ν_{max}/cm^{-1} 2967, 2365, 1739, 1664, 1371, 1271.

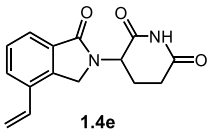

1.4e

3-(1-oxo-4-vinylisoindolin-2-yl)piperidine-2,6-dione (1.4e). Compound **1.4e** was prepared via General Procedure **B-1**, using **1.3e** (162 mg, 1.0 equiv, 0.50 mmol), sodium fluoride (63 mg, 3 equiv, 1.50 mmol), chloro(crotyl)(tri-*tert*-butylphosphine)palladium(II) (10 mg, 5 mol%, 25.0 µmol), tri-*tert*-butylphosphoniumtetrafluoroborate (7 mg, 5 mol%, 25.0 µmol), **1.5** (142 mg, 2.12 equiv, 1.06 mmol), dry DMSO (1.71 mL), and triethylamine (10.5 µL, 15 mol%, 75.0 µmol). The material was purified by flash column chromatography (SiO_2, 0-10% MeOH/CH_2Cl_2), affording **1.4e** (126 mg, 0.47 mmol, 91% yield) as a fine, amorphous tan solid.

HRMS (APCI) *m/z*: $[M+H]^+$ calcd for $C_{15}H_{15}O_3N_2$ 271.1077; Found 271.1075.

^{1}H NMR (400 MHz, DMSO-d_6): δ 11.03 (s, 1H), 7.80 (d, J = 7.6 Hz, 1H), 7.66 (d, J = 7.4 Hz, 1H), 7.54 (t, J = 7.6 Hz, 1H), 6.83 (dd, J = 17.8, 11.3 Hz, 1H), 5.90 (d, J = 17.7 Hz, 1H), 5.50 (d, J = 11.3 Hz, 1H), 5.15 (dd, J = 13.3, 5.1 Hz, 1H), 4.57 (d, J = 17.5 Hz, 1H), 4.41 (d, J = 17.6 Hz, 1H), 2.93 (ddd, J = 17.2, 13.7, 5.4 Hz, 1H), 2.74 – 2.56 (m, 1H), 2.46 – 2.27 (m, 1H, partially obscured by solvent signal at 2.50 ppm), 2.11 – 1.72 (m, 1H).

^{13}C{1H} NMR (101 MHz, DMSO-d_6): δ 172.9, 171.0, 167.9, 139.3, 132.8, 132.4, 132.1, 129.1, 128.5, 122.5, 117.9, 51.6, 47.0, 31.2, 22.5.

FTIR (neat): ν_{max}/cm^{-1} 3712, 3083, 3016, 2914, 1706, 1660, 1628.

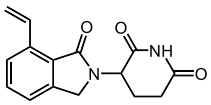

1.4f

3-(1-oxo-7-vinylisoindolin-2-yl)piperidine-2,6-dione (1.4f). Compound **1.4f** was prepared via General Procedure **B-1**, using **1.3f** (50 mg, 1.0 equiv, 0.16 mmol), sodium fluoride (20 mg, 3 equiv, 0.46 mmol), chloro(crotyl)(tri-*tert*-butylphosphine)palladium(II) (3.2 mg, 5 mol%, 7.7µmol), tri-*tert*-butylphosphoniumtetrafluoroborate (2.2 mg, 5 mol%, 7.7 µmol), **1.5** (44 mg, 2.12 equiv, 0.33 mmol), dry DMSO (0.53 mL), and triethylamine (3.2 µL, 15 mol%, 23 µmol). The material was purified by flash column chromatography (C_{18}, 10-100% MeCN/H_2O, 0.1% v/v TFA), followed by a second purification (SiO_2, 0-10% MeOH/CH_2Cl_2), affording **1.4f** (38 mg, 0.14 mmol, 91% yield) as an amorphous solid.

HRMS (APCI) *m/z*: $[M+H]^+$ calcd for $C_{15}H_{15}O_3N_2$ 271.1077; Found 271.1076.

^{1}H NMR (500 MHz, DMSO-d_6): δ 11.00 (s, 1H), 7.99 (dd, *J* = 17.9, 11.1 Hz, 1H), 7.79 (dt, *J* = 7.8, 0.7 Hz, 1H), 7.59 (td, *J* = 7.6, 0.7 Hz, 1H), 7.50 (dd, *J* = 7.5, 0.9 Hz, 1H), 6.02 (dd, *J* = 17.9, 1.2 Hz, 1H), 5.44 (dd, *J* = 11.1, 1.2 Hz, 1H), 5.10 (dd, *J* = 13.3, 5.1 Hz, 1H), 4.42 (d, *J* = 17.2 Hz, 1H), 4.29 (d, *J* = 17.2 Hz, 1H), 2.91 (ddd, *J* = 17.4, 13.7, 5.4 Hz, 1H), 2.60 (dddd, *J* = 17.4, 4.5, 2.3, 1.0 Hz, 1H), 2.39 (qd, *J* = 13.6, 4.5 Hz, 1H), 2.00 (dtd, *J* = 12.7, 5.4, 2.3 Hz, 1H).
^{13}C{^{1}H} NMR (101 MHz, DMSO-d_6): δ 173.0, 171.1, 168.5, 142.7, 135.3, 131.6, 130.9, 127.0, 123.5, 122.8, 117.0, 51.5, 46.6, 31.3, 22.4.

FTIR (neat): ν_{max}/cm^{-1} 3195, 3099, 2979, 2193, 1732, 0693, 1590, 1454, 1411, 1484, 1226, 1198, 1179, 1042, 1004, 949, 931, 860, 800.

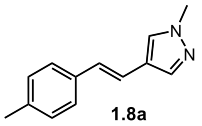

1.8a

(*E*)-1-methyl-4-(4-methylstyryl)-1H-pyrazole (1.8a). Compound **1.8a** was prepared via General Procedure **B-1**, using **1.6a** (51.7 µL, 1.0 equiv, 0.50 mmol), sodium fluoride (63 mg, 3 equiv, 1.50 mmol), chloro(crotyl)(tri-*tert*-butylphosphine)palladium(II) (10 mg, 5 mol%, 25.0 µmol), tri-*tert*-butylphosphoniumtetrafluoroborate (7 mg, 5 mol%, 25.0 µmol), **1.7e** (142 mg, 2.12 equiv, 1.06 mmol), dry DMSO (1.71 mL), and triethylamine (10.5 µL, 15 mol%, 75.0 µmol). The material was purified by flash column chromatography (SiO_2, 20-30% EtOAc/hexanes). The product-containing fractions were aggregated and concentrated in vacuuo, affording **1.8a** (82 mg, 0.41 mmol, 83% yield) as a crystalline tan solid. ^{1}H NMR indicated a >20:1 *E*:*Z* ratio of the alkene.

HRMS (APCI) *m/z*: $[M+H]^+$, calcd for $C_{13}H_{15}N_2$ 199.1230; Found 199.1228.

^{1}H NMR (400 MHz, $CDCl_3$): δ 7.66 (s, 1H), 7.44 (s, 1H), 7.33 (d, *J* = 8.1 Hz, 2H), 7.14 (d, *J* = 7.8 Hz, 2H), 6.88 (d, *J* = 16.4 Hz, 1H), 6.79 (d, *J* = 16.4 Hz, 1H), 3.90 (s, 3H), 2.34 (s, 3H).
^{13}C{^{1}H} NMR (101 MHz, $CDCl_3$): δ 137.3, 137.0, 134.9, 129.4, 127.8, 126.9, 125.9, 121.2, 117.7, 39.1, 21.3.

FTIR: (film) ν_{max}/cm^{-1} 2915, 1738, 1638, 1510, 1407, 967, 624.

Melting point: 129-131 °C

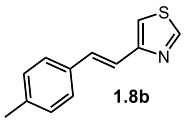

(*E*)-4-(4-methylstyryl)thiazole (1.8b). Compound **1.8b** was prepared via General Procedure **B-1**, using **1.6b** (17.8 µL, 1.0 equiv, 0.20 mmol), sodium fluoride (25 mg, 3.0 equiv, 0.60 mmol), chloro(crotyl)(tri-*tert*-butylphosphine)palladium(II) (4 mg, 5 mol%, 10.0 µmol), tri-*tert*-butylphosphoniumtetrafluoroborate (3 mg, 5 mol%, 10.0 µmol), **1.7e** (142 mg, 2.12 equiv, 0.42 mmol), dry DMSO (0.70 mL) and triethylamine (4.2 µL, 15 mol%, 30.0 µmol). The material was purified by flash column chromatography (SiO_2, 0-40% EtOAc/hexanes). The product-containing fractions were aggregated and concentrated in vacuuo, affording **1.8b** as an amorphous white solid (7 mg, 0.03 mmol, 19% yield).

^{1}H NMR indicated a >20:1 *E*:*Z* of the alkene.

HRMS (APCI) *m/z*: $[M+H]^+$ calcd for $C_{12}H_{12}N^{32}S$ 202.0685; Found 202.0684.

^{1}H NMR (600 MHz, $CDCl_3$): δ 8.82 (d, *J* = 2.0 Hz, 1H), 7.49 (d, *J* = 16.0 Hz, 1H), 7.43 (d, *J* = 8.1 Hz, 2H), 7.19 (d, *J* = 2.0 Hz, 1H), 7.17 (d, *J* = 7.9 Hz, 2H), 7.12 (d, *J* = 15.9 Hz, 1H), 2.36 (s, 3H).

^{13}C NMR{^{1}H} (101 MHz, $CDCl_3$): δ 155.3, 153.1, 138.1, 134.2, 131.8, 129.6, 126.8, 120.1, 114.4, 21.4.

FTIR (neat): ν_{max}/cm^{-1} 3107, 3031, 2920, 2854, 1737, 1680, 1606, 1514, 973, 819, 808.

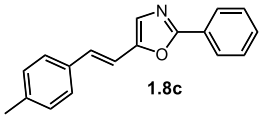

(*E*)-5-(4-methylstyryl)-2-phenyloxazole (1.8c). Compound **1.8c** was prepared via General Procedure **B-1**, using **1.6c** (45 mg, 1.0 equiv, 0.20 mmol), sodium fluoride (25 mg, 3.0 equiv, 0.60 mmol), chloro(crotyl)(tri-*tert*-butylphosphine)palladium(II) (4 mg, 5 mol%, 10.0 µmol), tri-*tert*-butylphosphoniumtetrafluoroborate (3 mg, 5 mol%, 10.0 µmol), **1.7e** (142 mg, 2.12 equiv, 0.42 mmol), dry DMSO (0.70 mL) and triethylamine (4.2 µL, 15 mol%, 30.0 µmol). The material was purified by flash column chromatography (SiO_2, 0-10% EtOAc/hexanes). The product-containing fractions were aggregated and concentrated in vacuuo, affording **1.8c** as an amorphous white solid (35 mg, 0.14 mmol, 68% yield). ^{1}H NMR indicated a >20:1 *E*:*Z* of the alkene.

HRMS (APCI) *m/z*: $[M+H]^+$ calcd for $C_{18}H_{16}ON$ 262.1226; Found 262.1225.

^{1}H NMR (400 MHz, $CDCl_3$): δ 8.16 – 7.88 (m, 2H), 7.52 – 7.44 (m, 3H), 7.41 (d, *J* = 8.1 Hz, 2H), 7.21 – 7.10 (m, 4H), 6.89 (d, *J* = 16.3 Hz, 1H), 2.37 (s, 3H).

^{13}C{^{1}H} NMR (101 MHz, $CDCl_3$): δ 161.0, 150.7, 138.4, 133.7, 130.5, 129.7, 129.6, 128.9, 127.5, 126.6, 126.5, 126.2, 112.3, 21.5.

FTIR (film): ν_{max}/cm^{-1} 3202, 2920, 1607, 1535, 1508, 1483, 1449.

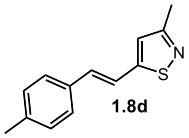

1.8d

(*E*)-3-methyl-5-(4-methylstyryl)isothiazole (1.8d). Compound **1.8d** was prepared via General Procedure **B-1**, using **1.6d** (20.9 µL, 1.0 equiv, 0.20 mmol), sodium fluoride (25 mg, 3.0 equiv, 0.60 mmol), chloro(crotyl)(tri-*tert*-butylphosphine)palladium(II) (4 mg, 5 mol%, 10.0 µmol), tri-*tert*-butylphosphoniumtetrafluoroborate (3 mg, 5 mol%, 10.0 µmol), **1.7e** (142 mg, 2.12 equiv, 0.42 mmol), dry DMSO (0.70 mL) and triethylamine (4.2 µL, 15 mol%, 30.0 µmol). The material was purified by flash column chromatography (SiO_2, 0-10% EtOAc/hexanes). The product-containing fractions were aggregated and concentrated in vacuuo, affording **1.8d** as an amorphous white solid (25 mg, 0.12 mmol, 58% yield). ^{1}H NMR indicated a >20:1 *E*:*Z* of the alkene.

HRMS (APCI) *m/z*: $[M+H]^+$ calcd for $C_{13}H_{14}N^{32}S$ 216.0842; Found 216.0841.

^{1}H NMR (400 MHz, $CDCl_3$): δ 7.38 (d, *J* = 8.0 Hz, 2H), 7.18 (d, *J* = 7.9 Hz, 2H), 7.13 (d, *J* = 16.2 Hz, 1H), 7.02 (d, *J* = 16.2 Hz, 1H), 6.95 (s, 1H), 2.48 (s, 3H), 2.37 (s, 3H).

^{13}C{^{1}H} NMR (101 MHz, $CDCl_3$): δ 167.6, 165.1, 139.0, 133.8, 133.2, 129.7, 126.9, 121.7, 116.7, 21.5, 19.1.

FTIR (film): ν_{max}/cm^{-1} 3028, 2921, 2360, 1739, 1523, 961, 826, 802.

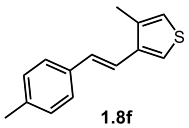

1.8f

(*E*)-3-methyl-4-(4-methylstyryl)thiophene (1.8f). Compound **1.8f** was prepared via General Procedure **B-1**, using **1.6f** (22.3 µL, 1.0 equiv, 0.20 mmol), sodium fluoride (25 mg, 3.0 equiv, 0.60 mmol), chloro(crotyl)(tri-*tert*-butylphosphine)palladium(II) (4 mg, 5 mol%, 10.0 µmol), tri-*tert*-butylphosphoniumtetrafluoroborate (3 mg, 5 mol%, 10.0 µmol), **1.7e** (142 mg, 2.12 equiv, 0.42 mmol), dry DMSO (0.70 mL) and triethylamine (4.2 µL, 15 mol%, 30.0 µmol). The material was purified by flash column chromatography (SiO_2, 0-1% EtOAc/hexanes). The product-containing fractions were aggregated and concentrated in vacuuo, affording **1.8f** as an amorphous white solid (28 mg, 0.13 mmol, 65% yield). ^{1}H NMR indicated a >20:1 *E*:*Z* of the alkene.

HRMS (APCI) *m/z*: $[M+H]^+$ calcd for $C_{14}H_{15}{}^{32}S$ 215.0889; Found 215.0888.

^{1}H NMR (400 MHz, $CDCl_3$): δ 7.41 (d, *J* = 8.0 Hz, 2H), 7.37 (d, *J* = 3.2 Hz, 1H), 7.18 (d, *J* = 7.9 Hz, 2H), 7.06 – 6.91 (m, 3H), 2.38 (s, 3H), 2.35 (s, 3H).

^{13}C NMR{^{1}H} (101 MHz, $CDCl_3$): δ 139.3, 137.5, 136.6, 134.9, 129.5, 129.5, 126.4, 121.7, 121.0, 120.4, 21.4, 15.2.

FTIR (film): ν_{max}/cm^{-1}3025, 2919, 2862, 1511, 1448, 959, 801, 780, 510.

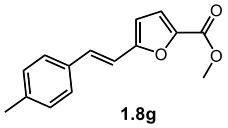

1.8g

Methyl (*E*)-5-(4-methylstyryl)furan-2-carboxylate (1.8g).

Compound **1.8g** was prepared via General Procedure **B-1**, using **1.6g** (41, 1.0 equiv, 0.20 mmol), sodium fluoride (25 mg, 3.0 equiv, 0.60 mmol), chloro(crotyl)(tri-*tert*-butylphosphine)palladium(II) (4 mg, 5 mol%, 10.0 µmol), tri-*tert*-butylphosphoniumtetrafluoroborate (3 mg, 5 mol%, 10.0 µmol), **1.7e** (142 mg, 2.12 equiv, 0.42 mmol), dry DMSO (0.70 mL) and triethylamine (4.2 µL, 15 mol%, 30.0 µmol). The material was purified by flash column chromatography (SiO_2, 0-20% EtOAc/hexanes). The product-containing fractions were aggregated and concentrated in vacuuo, affording **1.8g** as an amorphous white solid (38 mg, 0.16 mmol, 78% yield). ^{1}H NMR indicated a >20:1 *E*:*Z* of the alkene.

HRMS (APCI) *m/z*: $[M+H]^+$ calcd for $C_{15}H_{15}O_3$ 243.1016; Found 243.1015.

^{1}H NMR (400 MHz, $CDCl_3$): δ 7.39 (d, *J* = 8.1 Hz, 2H), 7.26 (d, *J* = 16.3 Hz, 1H), 7.20 – 7.13 (m, 3H), 6.86 (d, *J* = 16.4 Hz, 1H), 6.42 (d, *J* = 3.6 Hz, 1H), 3.91 (s, 3H), 2.36 (s, 3H).

^{13}C{^{1}H} NMR (101 MHz, $CDCl_3$): δ 159.3, 157.3, 143.3, 138.8, 133.5, 131.6, 129.7, 126.9, 120.2, 114.7, 109.5, 52.0, 21.5.

FTIR (film): ν_{max}/cm^{-1} 3018, 2590, 1716, 1517, 1496, 1300, 994, 1136, 808.

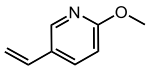

1.8h

2-methoxy-5-vinylpyridine (1.8h). Compound **1.8h** was prepared via General Procedure **B-1**, using **1.6h** (129 µL, 1.0 equiv, 0.50 mmol), sodium fluoride (63 mg, 3 equiv, 1.50 mmol), chloro(crotyl)(tri-*tert*-butylphosphine)palladium(II) (10 mg, 5 mol%, 25.0 µmol), tri-*tert*-butylphosphoniumtetrafluoroborate (7 mg, 5 mol%, 25.0 µmol), **1.5** (142 mg, 2.12 equiv, 1.06 mmol), dry DMSO (1.71 mL), and triethylamine (10.5 µL, 15 mol%, 75.0 µmol). The material was purified by flash column chromatography (SiO2, 0-7% pentane/ether,). The product-containing fractions were aggregated and concentrated in vacuuo, affording **1.8h** (117 mg, 0.87 mmol, 87% yield) as a translucent yellow liquid.

^{1}H NMR (600 MHz, $CDCl_3$): δ 8.12 (d, *J* = 2.4 Hz, 1H), 7.69 (dd, *J* = 8.6, 2.5 Hz, 1H), 6.72 (d, *J* = 8.6 Hz, 1H), 6.65 (dd, *J* = 17.6, 10.9 Hz, 1H), 5.64 (d, *J* = 18.4 Hz, 1H), 5.21 (d, *J* = 11.0 Hz, 1H), 3.94 (s, 3H). Spectral data were consistent with the literature.[1]

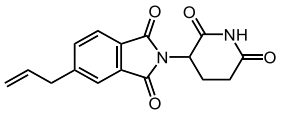

1.9a

5-allyl-2-(2,6-dioxopiperidin-3-yl)isoindoline-1,3-dione (1.9a). A septum-cap vial was equipped with a PTFE magnetic stir bar and flame dried under vacuum, then allowed to cool under N_2 atmosphere. The vial was charged with **1.3a** (337 mg, 1.0 equiv, 1.000 mmol), sodium fluoride (126 mg, 3.0 equiv, 3.0 mmol), **1.7a** (314 mg, 2.12 equiv, 2.12 mmol), chloro(crotyl)(tri-

tert-butylphosphine)palladium(II) (42 mg, 10 mol%, 0.10 mmol), and tri-*tert*-butylphosphonium tetrafluoroborate (29 mg, 10 mol%, 0.10 mmol) under backflow of nitrogen. Dry DMSO (1.71 mL) and triethylamine (42 µL, 30 mol%, 0.30 mmol) were charged by syringe, and the vial was equipped with an argon-filled balloon. The vial was placed in an aluminum heating block preheated to 90 °C, and was stirred at this temperature for 10 minutes. The reaction was partitioned between ethyl acetate (25 mL) and water (50 mL). The aqueous layer was extracted thrice with 25 mL portions of ethyl acetate, after which the combined organic layers were washed with a 10% w/w aqueous solution of lithium chloride. The organic layers were dried over magnesium sulfate, then filtered and concentrated in vacuuo. The material was concentrated in vacuuo onto Celite® and purified by flash column chromatography (SiO_2, 30-50% EtOAc/hexanes). The product-containing fractions were aggregated and concentrated in vacuuo, affording **1.9a** (239 mg, 0.80 mmol, 80% yield) as a fine, amorphous white solid. Crude ^{1}H NMR indicated a 20:1 ratio of **1.9a** to the internal alkene product **1.9b**. ^{1}H NMR of the purified product indicated a >20:1 ratio of **1.9a** to **1.9b**.

HRMS (APCI) *m/z*: $[M+H]^+$ calcd for $C_{16}H_{15}O_4N_2$ 299.1026; Found 299.10255.

^{1}H NMR (600 MHz, $CDCl_3$): δ 7.92 (s, 1H), 7.79 (d, *J* = 7.6 Hz, 1H), 7.73 – 7.66 (m, 1H), 7.63 – 7.46 (m, 1H), 5.93 (ddt, *J* = 16.8, 10.1, 6.7 Hz, 1H), 5.24 – 5.05 (m, 2H), 4.96 (dd, *J* = 12.7, 5.4 Hz, 1H), 3.53 (d, *J* = 6.7 Hz, 2H), 2.95 – 2.68 (m, 3H), 2.14 (ddtd, *J* = 12.5, 6.2, 3.0, 1.7 Hz, 1H).

^{13}C{^{1}H} NMR (101 MHz, $CDCl_3$): δ 171.4, 168.4, 167.5, 167.4, 148.1, 135.5, 134.8, 132.3, 129.8, 124.1, 124.0, 117.8, 49.4, 40.4, 31.5, 22.7.

FTIR (neat): ν_{max}/cm^{-1} 3024, 2361, 1735, 1365, 1217.

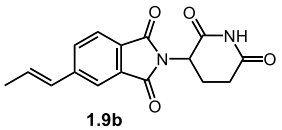

1.9b

(*E*)-2-(2,6-dioxopiperidin-3-yl)-5-(prop-1-en-1-yl)isoindoline-1,3-dione (1.9b). Compound **1.9b** was prepared via General Procedure **B-2**, using **1.3a**, (169 mg, 1.0 equiv, 0.50 mmol), sodium fluoride (63 mg, 3 equiv, 1.50 mmol), chloro(crotyl)(tri-*tert*-butylphosphine)palladium(II) (10 mg, 5 mol%, 25.0 µmol), tri-*tert*-butylphosphoniumtetrafluoroborate (7 mg, 5 mol%, 25.0 µmol), **1.7b** (157 mg, 2.12 equiv, 1.06 mmol), dry DMSO (1.71 mL), and triethylamine (10.5 µL, 15 mol%, 75.0 µmol). The material was purified by flash column chromatography (C_{18}, 10-100% MeCN/H_2O, 0.1% v/v TFA), followed by a second column purification (SiO_2, 30-50% EtOAc/hexanes), which afforded **1.9b** (128 mg, 0.43 mmol, 87% yield) as a fine, amorphous white solid. Crude ^{1}H NMR indicated a >20:1 ratio of **1.9b** to the terminal alkene product **1.9a**. ^{1}H NMR of the purified product indicated a >20:1 ratio of **1.9b** to **1.9a**. ^{1}H NMR indicated a >20:1 *E*:*Z* of the alkene.

HRMS (APCI) *m/z*: $[M+H]^+$ calcd for $C_{16}H_{15}O_4N_2$ 299.1026**;** Found 299.1029.

^{1}H NMR (400 MHz, DMSO-d_6): δ 11.14 (s, 1H), 7.94 (s, 1H), 7.84 (d, *J* = 0.9 Hz, 2H), 6.75 – 6.58 (m, 2H), 5.14 (dd, *J* = 12.9, 5.4 Hz, 1H), 2.89 (ddd, *J* = 17.3, 14.1, 5.4 Hz, 1H), 2.64 – 2.52 (m, 2H), 2.06 (dtd, *J* = 12.7, 6.0, 2.9 Hz, 1H), 1.90 (d, *J* = 5.3 Hz, 3H).

^{13}C{^{1}H} NMR (101 MHz, DMSO-d_6): δ 173.5, 170.6, 167.6, 144.9, 132.8, 132.4, 131.8, 130.2, 129.6, 124.5, 120.8, 49.6, 31.6, 22.7, 19.3.

FTIR (neat): ν_{max}/cm^{-1} 3219, 1774, 1616, 1387, 1261, 1199, 1134, 743.

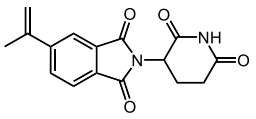

1.9c

2-(2,6-dioxopiperidin-3-yl)-5-(prop-1-en-2-yl)isoindoline-1,3-dione (1.9c). A septum-cap vial was equipped with a PTFE magnetic stir bar and flame dried under vacuum, then allowed to cool under N_2 atmosphere. The vial was charged with **1.3a** (67 mg, 1.0 equiv, 0.20 mmol), sodium fluoride (25 mg, 3.0 equiv, 0.60 mmol), **1.7c** (63 mg, 2.12 equiv, 0.42 mmol), chloro(crotyl)(tri-*tert*-butylphosphine)palladium(II) (8.3 mg, 10 mol%, 0.02 mmol), and tri-*tert*-butylphosphonium tetrafluoroborate (6 mg, 10 mol%, 0.02 mmol) under backflow of nitrogen. Dry DMSO (1.71 mL) and triethylamine (8.4 µL, 30 mol%, 0.06 mmol) were charged by syringe, and the vial was equipped with an argon-filled balloon. The vial was placed in an aluminum heating block preheated to 90 °C, and was stirred at this temperature for 10 minutes. The reaction was partitioned between ethyl acetate (10 mL) and water (20 mL). The aqueous layer was extracted thrice with 20 mL portions of ethyl acetate, after which the combined organic layers were washed with a 10% w/w aqueous solution of lithium chloride. The organic layers were dried over magnesium sulfate, then filtered and concentrated in vacuuo. The material was concentrated in vacuuo onto Celite® and purified by flash column chromatography (C_{18}, 10-100% MeCN/H_2O, 0.1% v/v TFA), followed by a second column purification (SiO_2, 40% EtOAc/hexanes), which afforded **1.9c** (47 mg, 0.16 mmol, 79% yield) as a fine, amorphous white solid. ^{1}H NMR of the crude reaction mixture showed a 7.5:1 ratio of the isoprenyl product **1.9c** to the rearranged product (**1.9b**). ^{1}H NMR of the purified reaction mixture showed a 6:1 ratio to **1.9c** to **1.9b**.

HRMS (APCI) *m/z*: $[M+H]^+$ calcd for $C_{16}H_{15}O_4N_2$ 299.1026; Found 299.1026.

^{1}H NMR (400 MHz, DMSO-d_6): δ 11.44 (s, 1H), 8.35 – 8.06 (m, 3H), 6.03 (s, 1H), 5.66 (s, 1H), 5.47 (dd, J = 13.0, 5.3 Hz, 1H), 3.20 (ddd, J = 17.3, 14.0, 5.4 Hz, 1H), 2.95 – 2.82 (m, 2H), 2.37 (ddd, J = 10.8, 5.6, 3.2 Hz, 1H).

^{13}C{^{1}H} NMR (101 MHz, DMSO-d_6): δ 172.8, 169.8, 167.1, 166.9, 147.0, 141.3, 131.8, 131.5, 129.9, 123.6, 120.1, 116.7, 49.0, 30.9, 22.0, 21.3.

FTIR (neat): ν_{max}/cm^{-1} 3214, 3100, 2914, 1772, 1694, 1615, 1375, 1193, 1110.

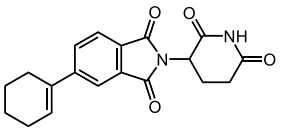

1.9d

5-(cyclohex-1-en-1-yl)-2-(2,6-dioxopiperidin-3-yl)isoindoline-1,3-dione (1.9d). Compound **1.9d** was prepared via General Procedure **B-2**, using **1.3a** (67 mg, 1.0 equiv, 0.20 mmol), sodium fluoride (25 mg, 3.0 equiv, 0.60 mmol), chloro(crotyl)(tri-*tert*-butylphosphine)palladium(II) (4 mg, 5 mol%, 10.0 µmol), tri-*tert*-butylphosphoniumtetrafluoroborate (3 mg, 5 mol%, 10.0 µmol), **1.7d** (80 mg, 2.12 equiv, 0.42 mmol), dry DMSO (0.70 mL) and triethylamine (4.2 µL, 15 mol%, 30.0 µmol). The material was purified by flash column chromatography (C_{18}, 10-100% MeCN/H_2O, 0.1% v/v TFA). The product-containing fractions were aggregated and concentrated in vacuuo, affording **6d** as a fine, amorphous tan solid (48 mg, 0.14 mmol, 71% yield).

HRMS (APCI) *m/z*: $[M+H]^+$ calcd for $C_{19}H_{19}O_4N_2$ 339.1339; Found 339.1338.

^{1}H NMR (600 MHz, $CDCl_3$): δ 8.14 (s, 1H), 7.87 (d, *J* = 1.2 Hz, 1H), 7.79 (d, *J* = 7.9 Hz, 1H), 7.72 (dd, *J* = 7.9, 1.5 Hz, 1H), 6.35 (tt, *J* = 4.0, 1.7 Hz, 1H), 4.98 (dd, *J* = 12.6, 5.4 Hz, 1H), 2.93 – 2.88 (m, 1H), 2.84 (qd, *J* = 12.6, 3.9 Hz, 2H), 2.75 (ddd, *J* = 16.8, 13.5, 5.0 Hz, 2H), 2.43 (tt, *J* = 4.0, 1.9 Hz, 2H), 2.27 (tt, *J* = 6.3, 3.1 Hz, 2H), 2.15 (dtd, *J* = 12.5, 4.9, 2.3 Hz, 2H), 1.81 (ddd, *J* = 12.0, 5.8, 3.1 Hz, 2H), 1.69 (ddd, *J* = 12.1, 6.3, 2.9 Hz, 2H).

^{13}C{^{1}H} NMR (101 MHz, $CDCl_3$): δ 171.3, 168.3, 167.7, 167.4, 149.6, 135.4, 132.2, 130.6, 129.5, 129.3, 123.9, 120.3, 49.4, 31.5, 27.4, 26.2, 22.8, 22.8, 21.8.

FTIR (neat): ν_{max}/cm^{-1} 3467, 3207, 3090, 2918, 1772, 1699, 1604.

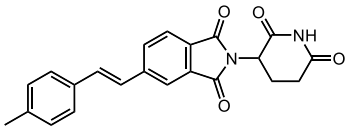

1.9e

(*E*)-2-(2,6-dioxopiperidin-3-yl)-5-(4-methylstyryl)isoindoline-1,3-dione (1.9e). Compound **1.9e** was prepared via General Procedure **B-2**, using **1.3a** (67 mg, 1.0 equiv, 0.20 mmol), sodium fluoride (25 mg, 3.0 equiv, 0.60 mmol), chloro(crotyl)(tri-*tert*-butylphosphine)palladium(II) (4 mg, 5 mol%, 10.0 µmol), tri-*tert*-butylphosphoniumtetrafluoroborate (3 mg, 5 mol%, 10.0 µmol), **1.7e** (94 mg, 2.12 equiv, 0.42 mmol), dry DMSO (0.70 mL) and triethylamine (4.2 µL, 15 mol%, 30.0 µmol). The material was purified by flash column chromatography (C_{18}, 10-100% MeCN/H_2O, 0.1% v/v TFA), followed by a second column purification (SiO_2, 40% EtOAc/hexanes). The product-containing fractions were aggregated and concentrated in vacuuo, affording **1.9e** as a fine, amorphous yellow solid (68 mg, 0.18 mmol, 91% yield). ^{1}H NMR indicated a >20:1 *E*:*Z* of the alkene.

HRMS (APCI) *m/z*: $[M+H]^+$ calcd for $C_{22}H_{19}O_4N_2$, 375.1339); Found 375.1336

^{1}H NMR (600 MHz, $CDCl_3$): δ 8.12 (s, 1H), 8.02 (s, 1H), 7.84 (d, *J* = 7.9 Hz, *1H*), 7.79 (dd, *J* = 7.8, 1.5 Hz, 1H), 7.45 (d, *J* = 8.1 Hz, 2H), 7.29 (d, *J* = 16.3 Hz, 1H), 7.21 (d, *J* = 7.8 Hz, 2H), 7.13 (d, *J* = 16.2 Hz, 1H), 5.00 (dd, *J* = 12.5, 5.4 Hz, 1H), 3.01 – 2.80 (m, 3H), 2.80 – 2.68 (m, 1H), 2.38 (s, 3H), 2.17 (dtd, *J* = 12.6, 5.0, 2.2 Hz, 1H).

^{13}C{^{1}H} NMR (101 MHz, $CDCl_3$): δ 171.0, 168.1, 167.4, 167.2, 144.6, 139.3, 133.4, 132.7, 132.4, 129.8, 129.6, 127.1, 125.5, 124.4, 120.9, 49.5, 31.6, 22.8, 21.5.

FTIR (neat): ν_{max}/cm^{-1} 3467, 3207, 3090, 2918, 1772, 1699, 1604.

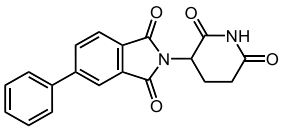

1.9f

2-(2,6-dioxopiperidin-3-yl)-5-phenylisoindoline-1,3-dione (1.9f). Compound **1.9f** was prepared via General Procedure **B-2**, using **1.3a** (67 mg, 1.0 equiv, 0.20 mmol), sodium fluoride (25 mg, 3.0 equiv, 0.60 mmol), chloro(crotyl)(tri-*tert*-butylphosphine)palladium(II) (4 mg, 5 mol%, 10.0 µmol), tri-*tert*-butylphosphoniumtetrafluoroborate (3 mg, 5 mol%, 10.0 µmol), **1.7f** (94 mg, 2.12 equiv, 0.42 mmol), dry DMSO (0.70 mL) and triethylamine (4.2 µL, 15 mol%, 30.0 µmol). The material was purified by flash column chromatography (C_{18}, 10-100% MeCN/H_2O,

0.1% v/v TFA), followed by a second column purification (SiO_2, 40% EtOAc/hexanes). The product-containing fractions were aggregated and concentrated in vacuuo, affording **1.9f** as a fine, amorphous yellow solid (17 mg, 0.05 mmol, 26% yield).

^{1}H NMR (600 MHz, DMSO-d_6): δ 11.16 (s, 1H), 8.21 – 8.14 (m, 2H), 8.01 (d, J = 8.2 Hz, 1H), 7.85 (d, J = 7.3 Hz, 2H), 7.54 (t, J = 7.5 Hz, 2H), 7.49 (t, J = 7.3 Hz, 1H), 5.19 (dd, J = 12.8, 5.5 Hz, 1H), 2.91 (ddd, J = 16.7, 13.8, 5.4 Hz, 1H), 2.68 – 2.54 (m, 2H), 2.13 – 2.00 (m, 1H). Spectral data were consistent with the literature.[2]

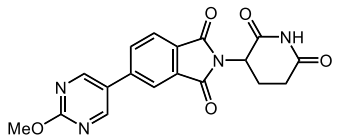

1.9g

2-(2,6-dioxopiperidin-3-yl)-5-(2-methoxypyrimidin-5-yl)isoindoline-1,3-dione (1.9g).

Compound **1.9g** was prepared via General Procedure **B-2**, using **1.3a** (67 mg, 1.0 equiv, 0.20 mmol), sodium fluoride (25 mg, 3.0 equiv, 0.60 mmol), chloro(crotyl)(tri-tert-butylphosphine)palladium(II) (4 mg, 5 mol%, 10.0 µmol), tri-tert-butylphosphoniumtetrafluoroborate (3 mg, 5 mol%, 10.0 µmol), **1.7g** (91 mg, 2.12 equiv, 0.42 mmol), dry DMSO (0.70 mL) and triethylamine (4.2 µL, 15 mol%, 30.0 µmol). The material was purified by flash column chromatography (C_{18}, 10-100% MeCN/H_2O, 0.1% v/v TFA), followed by a second column purification (SiO_2, 70-100% EtOAc/hexanes). The product-containing fractions were aggregated and concentrated in vacuuo, affording **1.9g** as a fine, amorphous white solid (37 mg, 0.10 mmol, 50% yield).

HRMS (APCI) *m/z*: $[M+H]^+$ calcd for $C_{18}H_{15}O_5N_4$ 367.1037; Found 367.1035.

^{1}H NMR (600 MHz, DMSO-d_6): δ 11.16 (s, 1H), 9.12 (s, 2H), 8.33 (d, J = 1.6 Hz, 1H), 8.25 (dd, J = 7.8, 1.5 Hz, 1H), 8.03 (d, J = 7.8 Hz, 1H), 5.20 (dd, J = 12.8, 5.4 Hz, 1H), 3.99 (s, 3H), 2.91 (ddd, J = 16.9, 13.7, 5.4 Hz, 1H), 2.66 – 2.54 (m, 2H), 2.14 – 2.04 (m, 1H).

^{13}C{^{1}H} NMR (101 MHz, DMSO-d_6): δ 172.8, 169.8, 166.9, 166.8, 165.2, 158.2, 140.6, 132.5, 132.4, 130.3, 125.7, 124.1, 121.3, 55.0, 49.1, 31.0, 22.0.

FTIR (neat): ν_{max}/cm^{-1} 3468, 3233, 2918, 1775, 1702, 1595, 1471, 1411, 1393, 1327, 1116, 1028, 910, 730, 610.

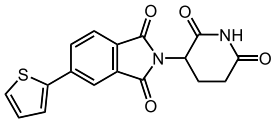

1.9h

2-(2,6-dioxopiperidin-3-yl)-5-(thiophen-2-yl)isoindoline-1,3-dione (1.9h). Compound **1.9h** was prepared via General Procedure **B-2**, using **1.3a**, (169 mg, 1.0 equiv, 0.50 mmol), sodium fluoride (63 mg, 3 equiv, 1.50 mmol), chloro(crotyl)(tri-*tert*-butylphosphine)palladium(II) (10 mg, 5 mol%, 25.0 µmol), tri-*tert*-butylphosphoniumtetrafluoroborate (7 mg, 5 mol%, 25.0 µmol), **1.7h** (201 mg, 2.12 equiv, 1.06 mmol), dry DMSO (1.71 mL), and triethylamine (10.5 µL, 15 mol%, 75.0 µmol). The material was purified by flash column chromatography (40-70% EtOAc/hexanes, SiO_2), followed by a second column purification (10-100% MeCN/H_2O, 0.1%

v/v TFA, C_{18}), which afforded **1.9h** (137 mg, 0.40 mmol, 80% yield) as a fine, amorphous yellow solid.

HRMS (APCI) *m/z*: $[M+H]^+$ calcd for $C_{17}H_{14}O_4N_2{}^{32}S$ 341.0591; Found 341.0591.

^{1}H NMR (600 MHz, DMSO-d_6): δ 11.13 (s, 1H), 8.16 (s, 1H), 8.10 (d, J = 7.9 Hz, 1H), 7.91 (d, J = 7.8 Hz, 1H), 7.89 (d, J = 3.8 Hz, 1H), 7.73 (d, J = 5.1 Hz, 1H), 7.22 – 7.15 (m, 1H), 5.15 (dd, J = 12.9, 5.5 Hz, 1H), 2.87 (ddd, J = 18.1, 13.7, 5.5 Hz, 1H), 2.61 – 2.48 (m, 2H), 2.10 – 1.95 (m, 1H).

^{13}C{^{1}H} NMR (101 MHz, DMSO-d_6): δ 174.1, 171.1, 168.1, 168.0, 142.3, 141.2, 133.9, 132.2, 130.5, 130.4, 129.8, 128.2, 125.7, 120.8, 50.3, 32.2, 23.3.

FTIR (neat): ν_{max}/cm^{-1} 3470, 3191, 3088, 2896, 1770, 1703, 1616.

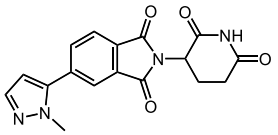

1.9i

2-(2,6-dioxopiperidin-3-yl)-5-(1-methyl-1H-pyrazol-5-yl)isoindoline-1,3-dione (1.9i).
Compound **1.9i** was prepared via General Procedure **B-2**, using **1.3a**, (169 mg, 1.0 equiv, 0.50 mmol), sodium fluoride (63 mg, 3 equiv, 1.50 mmol), chloro(crotyl)(tri-*tert*-butylphosphine)palladium(II) (10 mg, 5 mol%, 25.0 µmol), tri-*tert*-butylphosphoniumtetrafluoroborate (7 mg, 5 mol%, 25.0 µmol), **1.7i** (199 mg, 2.12 equiv, 1.06 mmol), dry DMSO (1.71 mL), and triethylamine (10.5 µL, 15 mol%, 75.0 µmol). The material was purified by flash column chromatography (50-100% EtOAc/hexanes, SiO_2). The product-containing fractions were aggregated and concentrated in vacuuo, affording **1.9i** (127 mg, 0.38 mmol, 82% yield) as a fine amorphous yellow solid.

HRMS (APCI) *m/z*: $[M+H]^+$ calcd for $C_{17}H_{15}O_4N_4$ 339.1088; Found 339.1086.

^{1}H NMR (400 MHz, DMSO-d_6): δ 11.16 (s, 1H), 8.16 – 7.87 (m, 3H), 7.55 (d, J = 1.9 Hz, 1H), 6.66 (d, J = 1.9 Hz, 1H), 5.20 (dd, J = 13.0, 5.3 Hz, 1H), 3.94 (s, 3H), 2.91 (ddd, J = 17.4, 14.0, 5.4 Hz, 1H), 2.66 – 2.53 (m, 2H), 2.14 – 2.02 (m, 1H).

^{13}C{^{1}H} NMR (101 MHz, DMSO-d_6): δ 172.8, 169.8, 166.7, 166.7, 140.9, 138.2, 136.3, 134.5, 132.0, 130.4, 123.9, 122.9, 107.3, 49.1, 37.9, 30.9, 22.0.

FTIR (neat): ν_{max}/cm^{-1} 3076, 1712, 1379, 1202.

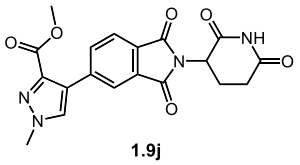

1.9j

Methyl 4-(2-(2,6-dioxopiperidin-3-yl)-1,3-dioxoisoindolin-5-yl)-1-methyl-1H-pyrazole-3-carboxylate (1.9j).

Compound **1.9j** was prepared via General Procedure **B-2**, using **1.3a**, (169 mg, 1.0 equiv, 0.50 mmol), sodium fluoride (63 mg, 3 equiv, 1.50 mmol), chloro(crotyl)(tri-*tert*-butylphosphine)palladium(II) (10 mg, 5 mol%, 25.0 µmol), tri-*tert*-butylphosphoniumtetrafluoroborate (7 mg, 5 mol%, 25.0 µmol), **1.7j** (261 mg, 2.12 equiv, 1.06

mmol), dry DMSO (1.71 mL), and triethylamine (10.5 µL, 15 mol%, 75.0 µmol). The material was purified by flash column chromatography (SiO_2, 50-100% EtOAc/hexanes to 5% EtOH/EtOAC). The product-containing fractions were aggregated and concentrated in vacuuo, affording **1.9j** (172 mg, 0.43 mmol, 87% yield) as a fine amorphous yellow solid.

HRMS (APCI) *m/z*: $[M+H]^+$ calcd for $C_{19}H_{17}O_6N_4$ 397.1143; Found 397.1142.

^{1}H NMR (600 MHz, DMSO-d_6): δ 11.15 (s, 1H), 8.29 (s, 1H), 8.03 (s, 1H), 7.98 – 7.82 (m, 2H), 5.17 (dd, J = 12.9, 5.4 Hz, 1H), 3.97 (s, 3H), 3.77 (s, 3H), 2.91 (ddd, J = 17.3, 14.0, 5.5 Hz, 1H), 2.67 – 2.53 (m, 2H), 2.16 – 2.04 (m, 1H).

^{13}C{^{1}H} NMR (101 MHz, DMSO-*d*6): δ 172.8, 169.9, 167.1, 166.9, 162.4, 138.4, 138.2, 134.8, 133.2, 131.4, 129.4, 123.5, 123.2, 123.0, 51.6, 49.1, 31.0, 22.0.

FTIR (neat): ν_{max}/cm^{-1} 3195, 2957, 1774, 1698, 1620, 1557, 1698, 1411, 1198, 1377, 639.

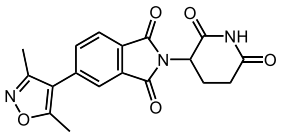

1.9k

5-(3,5-dimethylisoxazol-4-yl)-2-(2,6-dioxopiperidin-3-yl)isoindoline-1,3-dione (1.9k). Compound **1.9k** was prepared via General Procedure **B-2**, using **1.3a**, (169 mg, 1.0 equiv, 0.50 mmol), sodium fluoride (63 mg, 3 equiv, 1.50 mmol), chloro(crotyl)(tri-*tert*-butylphosphine)palladium(II) (10 mg, 5 mol%, 25.0 µmol), tri-*tert*-butylphosphoniumtetrafluoroborate (7 mg, 5 mol%, 25.0 µmol), **1.7k** (215 mg, 2.12 equiv, 1.06 mmol), dry DMSO (1.71 mL), and triethylamine (10.5 µL, 15 mol%, 75.0 µmol). The material was purified by flash column chromatography (C_{18}, 10-100% MeCN/H_2O, 0.1% v/v TFA), followed by a second column purification (SiO_2, 50-100% EtOAc/hexanes). The product-containing fractions were aggregated and concentrated in vacuuo, affording **1.9k** (151 mg, 0.43 mmol, 86% yield) as a fine amorphous yellow solid.

HRMS (APCI) *m/z*: $[M+H]^+$ calcd for $C_{18}H_{16}O_5N_3$ 354.1085; Found 354.1084**.**

^{1}H NMR (600 MHz, DMSO-d_6): δ 11.16 (s, 1H), 8.02 (d, J = 7.7 Hz, 1H), 7.96 (s, 1H), 7.90 (dd, J = 7.7, 1.5 Hz, 1H), 5.19 (dd, J = 12.9, 5.4 Hz, 1H), 2.91 (ddd, J = 16.9, 13.9, 5.4 Hz, 1H), 2.67 – 2.53 (m, 2H), 2.46 (s, 3H), 2.28 (s, 3H), 2.15 – 2.01 (m, 1H).

^{13}C{^{1}H} NMR (101 MHz, DMSO-d_6): δ 172.9, 169.9, 166.9, 166.9, 166.6, 158.1, 136.8, 135.2, 132.2, 130.0, 124.0, 123.6, 115.0, 49.1, 31.0, 22.0, 11.5, 10.4.

FTIR (neat): ν_{max}/cm^{-1} 3213, 3109, 2917, 1776, 1708, 1626, 1380, 1260, 1195.

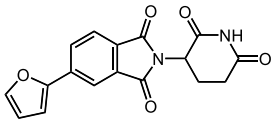

1.9l

2-(2,6-dioxopiperidin-3-yl)-5-(furan-2-yl)isoindoline-1,3-dione (1.9l). Compound **1.9l** was prepared via General Procedure **B-2**, using **1.3a** (67 mg, 1.0 equiv, 0.20 mmol), sodium fluoride (25 mg, 3.0 equiv, 0.60 mmol), chloro(crotyl)(tri-*tert*-butylphosphine)palladium(II) (4 mg, 5 mol%, 10.0 µmol), tri-*tert*-butylphosphoniumtetrafluoroborate (3 mg, 5 mol%, 10.0 µmol), **1.7l** (74 mg, 2.12 equiv, 0.42 mmol), dry DMSO (0.70 mL) and triethylamine (4.2 µL, 15 mol%, 30.0

μmol). The material was purified by flash column chromatography (C_{18}, 10-100% MeCN/H_2O, 0.1% v/v TFA), The product-containing fractions were aggregated and concentrated in vacuuo, affording **1.9l** as a fine, amorphous tan solid (53 mg, 0.16 mmol, 82% yield).

HRMS (APCI) *m/z*: $[M+H]^+$ calcd for $C_{17}H_{13}O_5N_2$ 325.0819; Found 325.0816.

^{1}H NMR (600 MHz, DMSO-d_6): δ 11.15 (s, 1H), 8.21 (s, 1H), 8.16 (dd, J = 7.8, 1.5 Hz, 1H), 7.97 (d, J = 7.9 Hz, 1H), 7.92 (d, J = 1.6 Hz, 1H), 7.44 (d, J = 1.4 Hz, 1H), 6.72 (dd, J = 3.4, 1.7 Hz, 1H), 5.18 (dd, J = 12.9, 5.4 Hz, 1H), 2.90 (ddd, J = 17.1, 14.2, 5.4 Hz, 1H), 2.65 – 2.52 (m, 2H), 2.13 – 2.03 (m, 1H).

^{13}C{^{1}H} NMR (101 MHz, DMSO-d_6): δ 172.8, 169.9, 166.8, 166.8, 151.2, 145.0, 136.0, 132.5, 129.0, 128.6, 124.3, 117.8, 112.9, 110.1, 49.1, 30.9, 22.0.

FTIR (neat): ν_{max}/cm^{-1} 3469, 3211, 3143, 3110, 3043, 2858, 1776, 1706, 1619.

Section 4: Computation Details

The data in this section were generated by Lauren Grant.

All DFT geometry optimization and frequency calculations were conducted with Gaussian 16, revision C.01.[1] Geometry optimizations were performed in the gas phase with the M06 functional and 6-311G++(d,p) basis sets for all atoms, excluding Pd and Br. Pd was computed with a Stuttgart 1997 (with ECP) basis set and LANL2DZ (with ECP for Br). All stationary points were characterized by frequency calculations to confirm local minima for ground state optimizations (zero imaginary frequencies). All energy values are reported in Hartrees and are the sum of electronic and thermal free energies as computed by Gaussian16.

Potassium (vinyl)trifluoroborate Association Complexes

Three fluoride associated complexes were considered in this study (**S1**, **S2** and **I**). Structure **I** was found to be the most stable and the further calculations began from that structure.:

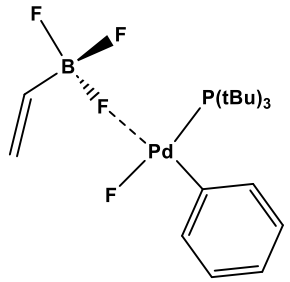

Isomer **S1** arrangement:
Borate and phenyl are transoid
Fluoride and phosphine are transoid

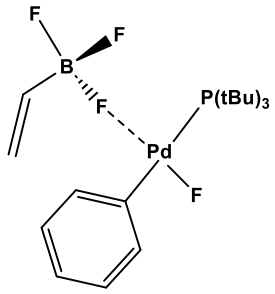

Isomer **S2** arrangement:
Borate and phenyl are cisoid
Phenyl and phosphine are transoid

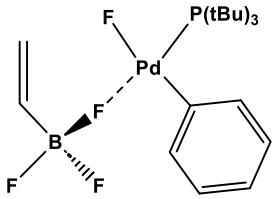

Isomer **I** arrangement:
Borate and phenyl are transoid
Borate and phosphine are transoid

Cartesian Coordinates:

$((tBu)_3P)Pd(Ph)(F)(BF_3(CH{=}CH_2))$ association anion isomer **I**

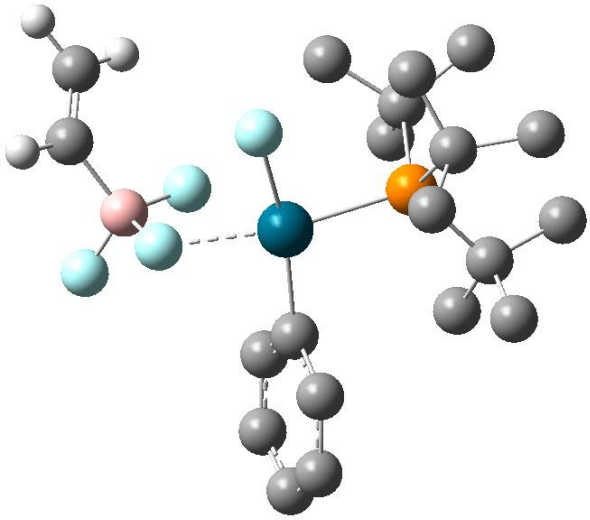

Cartesian coordinates for association anion isomer **I**

Sum of electronic and thermal free energies: -1675.663058

Pd	-0.59213100	-0.15188900	-0.74325200
F	-2.76256200	-0.39422500	-1.01893300
B	-3.45091700	-0.95243900	0.17145600
F	-4.45365600	-0.05164400	0.49386100
F	-2.48961100	-0.98135500	1.21051000
C	-3.98692700	-2.41703700	-0.18735100
C	-3.70076500	-3.52155000	0.50293400
C	-1.00385200	1.73833800	-0.27781800
C	-0.64547000	2.74756800	-1.17886100
C	-1.05884400	4.06661600	-0.98202300
C	-1.84687100	4.39292700	0.11717400
C	-2.24139200	3.38589700	0.99714800
C	-1.83079700	2.06990200	0.80115800
P	1.55400000	-0.21499700	0.10836100
C	2.40853100	1.37317700	0.82467800
C	3.64962500	1.08635700	1.67908400
C	1.44852900	2.20106600	1.69377600
C	2.80903000	2.30878100	-0.32194300
C	2.72568100	-0.89751700	-1.27103600
C	2.42066500	-2.37343500	-1.55685300
C	4.22948700	-0.78505500	-1.00770800
C	2.37011900	-0.13797400	-2.55715600
C	1.45641200	-1.50708500	1.53593600
C	2.79677000	-2.14156100	1.91842200
C	0.47328000	-2.62092500	1.14492100
C	0.85413500	-0.85039600	2.78185500
H	-4.64998900	-2.52904300	-1.05452000
H	-4.08365000	-4.51276000	0.24331100

H	-3.04243700	-3.48154400	1.37399600
H	-0.03670000	2.50326700	-2.05377800
H	-0.76393700	4.83942100	-1.69422000
H	-2.16761200	5.42255000	0.27837600
H	-2.88758400	3.62534700	1.84290100
H	-2.17267500	1.28256900	1.47266700
H	4.38892000	0.44187200	1.19374000
H	4.14540500	2.04577900	1.89846100
H	3.38548200	0.63935300	2.64550900
H	0.69964200	2.71810600	1.08981200
H	2.04671300	2.96621400	2.21518000
H	0.91633200	1.62436000	2.45350400
H	3.62849000	1.92792300	-0.94086500
H	1.95210900	2.54086900	-0.96639600
H	3.14941100	3.26006700	0.11756300
H	2.76752900	-3.04106900	-0.75835400
H	1.34429600	-2.51792200	-1.72819500
H	2.97263000	-2.65444000	-2.46898100
H	4.59598100	0.24494000	-0.92911100
H	4.75554700	-1.24694700	-1.85854600
H	4.53851300	-1.33186300	-0.10679600
H	1.32024300	-0.31470900	-2.82619100
H	2.53146500	0.94378900	-2.48793400
H	3.00351900	-0.51660500	-3.37580000
H	3.55218500	-1.41498200	2.23835000
H	2.62405700	-2.82441000	2.76561500
H	3.22212200	-2.74294200	1.10682500
H	-0.55170200	-2.23929700	1.05929900
H	0.49374100	-3.37381800	1.95041900
H	0.70521500	-3.11412000	0.19940000
H	1.53316500	-0.14416600	3.27646600
H	-0.09601000	-0.34877600	2.55322800
H	0.63030100	-1.64680200	3.50851300
F	-0.43108100	-1.99107800	-1.62595000

$((tBu)_3P)Pd(Ph)(F)(BF_3(CH{=}CH_2))$ association anion isomer **S2**

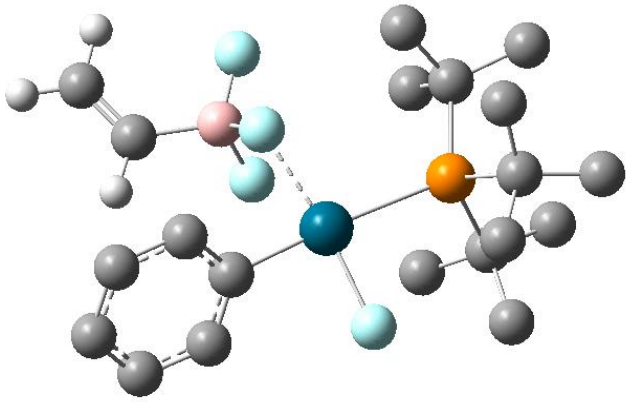

Cartesian coordinates for association anion isomer **S2**

Sum of electronic and thermal free energies: -1675.665091

Pd	0.59642600	-0.64176100	-0.16066600
F	1.31645500	1.28015400	-0.78337500
B	1.81471800	2.22924900	0.28880500
F	1.33008600	1.68775900	1.48596700
F	1.19062500	3.43361500	0.01241400
C	3.40744100	2.27775200	0.21986600
C	4.10331000	3.37613400	-0.07654700
C	2.50883500	-1.19968100	-0.17459600
C	3.32089500	-0.89719900	-1.26706400
C	4.67465600	-1.23347700	-1.24868200
C	5.22721100	-1.85491900	-0.13224900
C	4.41589700	-2.15300900	0.96048300
C	3.05789000	-1.83961400	0.93525300
P	-1.86194500	-0.06777500	-0.06100300
C	-2.45854600	-0.63031600	1.68248100
C	-3.81285100	-0.09247300	2.14491300
C	-1.36940500	-0.20005400	2.67736200
C	-2.49912800	-2.16159800	1.75739100
C	-2.83710100	-1.07536900	-1.37889700
C	-2.67832700	-0.41237200	-2.75034000
C	-4.33115700	-1.26307900	-1.11131000
C	-2.16916500	-2.44968600	-1.51674300
C	-2.33903800	1.78748500	-0.27633200
C	-3.82545100	2.08948800	-0.47451500
C	-1.56412300	2.35393300	-1.47512000
C	-1.83862100	2.56799800	0.94520800
H	3.96646000	1.35803500	0.43464200
H	5.19569200	3.40663600	-0.11509900
H	3.59282400	4.31645600	-0.29764200
H	2.90384900	-0.37285600	-2.12768800
H	5.30315800	-0.99133900	-2.10718300
H	6.28860300	-2.10460000	-0.11218500

H	4.84260300	-2.63837700	1.83998200
H	2.41782200	-2.09007800	1.78130400
H	-4.63082400	-0.37010400	1.46663300
H	-4.04488300	-0.52854300	3.13075800
H	-3.82422200	0.99724800	2.26701000
H	-0.40340700	-0.65836700	2.42460000
H	-1.65987900	-0.54476100	3.68370000
H	-1.21298300	0.88110900	2.72577200
H	-3.33599500	-2.59753600	1.19655700
H	-1.55203400	-2.59247900	1.40643200
H	-2.64334400	-2.44390200	2.81333400
H	-3.26109200	0.51046000	-2.85516800
H	-1.62555600	-0.19249500	-2.97624800
H	-3.04188900	-1.11360300	-3.51871500
H	-4.52487800	-1.85521200	-0.20909200
H	-4.78041900	-1.80953800	-1.95756900
H	-4.86863600	-0.31147400	-1.01448700
H	-1.12174700	-2.34894400	-1.82778000
H	-2.16185200	-3.03444900	-0.59523200
H	-2.71229500	-3.02196800	-2.28772400
H	-4.45676100	1.71646500	0.34130300
H	-3.95668400	3.18339000	-0.51764300
H	-4.21443000	1.68606500	-1.41850200
H	-0.48925000	2.17260700	-1.38260600
H	-1.71036900	3.44568200	-1.49391600
H	-1.91083500	1.96504200	-2.43700600
H	-2.42984100	2.37119700	1.84787800
H	-0.77919800	2.37814400	1.15723300
H	-1.93000400	3.64340600	0.72639600
F	0.18871600	-2.50814800	0.42124400

$((tBu)_3P)Pd(Ph)(F)(BF_3(CH{=}CH_2))$ association anion isomer **S1**

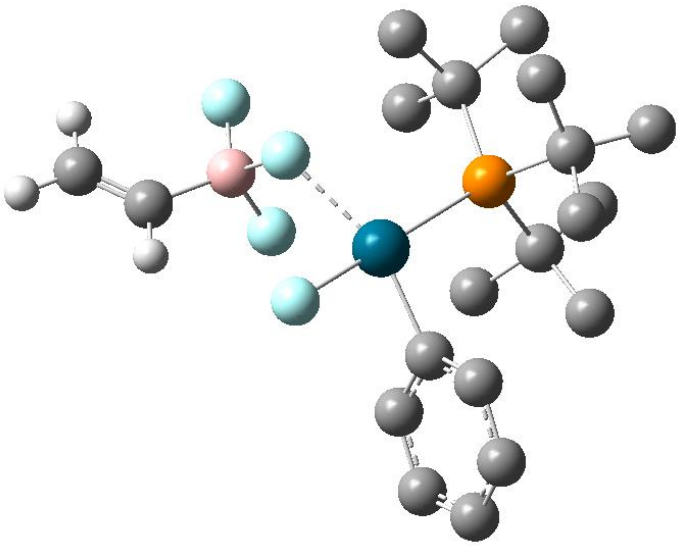

Cartesian coordinates for association anion isomer **S1**

Sum of electronic and thermal free energies: -1675.655906

Pd	-0.41710300	0.80715700	-0.61554400
F	-2.47078700	-0.05299300	-0.92032800
B	-3.35443900	0.15031700	0.25804400
F	-2.48078100	0.50668300	1.31334500
F	-3.92117800	-1.08984300	0.53047400
C	-4.40357600	1.30068100	-0.08190600
C	-5.72735800	1.15402200	-0.01475800
C	0.97933600	2.15761400	-0.17624100
C	2.01990500	2.60134900	-0.99263600
C	2.84742500	3.65114100	-0.58937400
C	2.63248300	4.29575500	0.62343700
C	1.54857300	3.91042000	1.40920600
C	0.72010600	2.86795900	1.00347400
P	0.76438500	-1.19195000	0.00431600
C	1.78866400	-0.96717400	1.63173400
C	2.27063200	-2.24975100	2.31612300
C	0.92017600	-0.19588900	2.63325400
C	3.02296900	-0.09273200	1.37514200
C	2.00686800	-1.72331900	-1.37643700
C	1.23791100	-2.31953600	-2.55939000
C	3.09299300	-2.71904200	-0.96250200
C	2.68165800	-0.46932300	-1.93264500
C	-0.39966300	-2.72177900	0.28719700
C	0.29432000	-4.08509200	0.38137400
C	-1.43382800	-2.83247400	-0.84270700
C	-1.19555800	-2.48667200	1.57678100
H	-3.99747700	2.26958900	-0.39291500
H	-6.43803600	1.95252500	-0.24825800

H	-6.16837300	0.19910600	0.28285500
H	2.19725700	2.14063900	-1.96195000
H	3.66301000	3.96936700	-1.24098000
H	3.28425000	5.11007600	0.94050000
H	1.33135800	4.43763400	2.33924200
H	-0.16137600	2.61678700	1.59587300
H	2.87925000	-2.88914000	1.66546400
H	2.90185200	-1.96350500	3.17291900
H	1.44543200	-2.84847700	2.71856100
H	0.66289100	0.79705100	2.25537100
H	1.49859800	-0.06303800	3.56219600
H	-0.01265600	-0.70300600	2.88932300
H	3.79818700	-0.60251700	0.78971700
H	2.77374400	0.85487100	0.88378300
H	3.47044000	0.15480800	2.35085900
H	0.88716200	-3.34002600	-2.37088200
H	0.37866500	-1.69734900	-2.84554600
H	1.91741100	-2.36624700	-3.42540700
H	3.80127900	-2.29475800	-0.24102300
H	3.67472200	-2.99350900	-1.85787800
H	2.69028800	-3.64630000	-0.54002000
H	1.93388500	0.18275600	-2.40064500
H	3.21648100	0.11973600	-1.18194100
H	3.40693100	-0.77123100	-2.70616200
H	1.07026000	-4.14670900	1.15095100
H	-0.47498200	-4.83186500	0.63558100
H	0.73157100	-4.39969400	-0.57500400
H	-1.99105500	-1.90603700	-0.99001800
H	-2.16199000	-3.60480000	-0.54982900
H	-0.99976600	-3.14845200	-1.79517900
H	-0.58590300	-2.63056400	2.47785800
H	-1.66710100	-1.49649100	1.60525900
H	-2.01167900	-3.22345100	1.61771300
F	-1.33565700	2.44767700	-1.24627900

Potassium (vinyl)trifluoroborate π-Association Complexes

(**Structure II**)

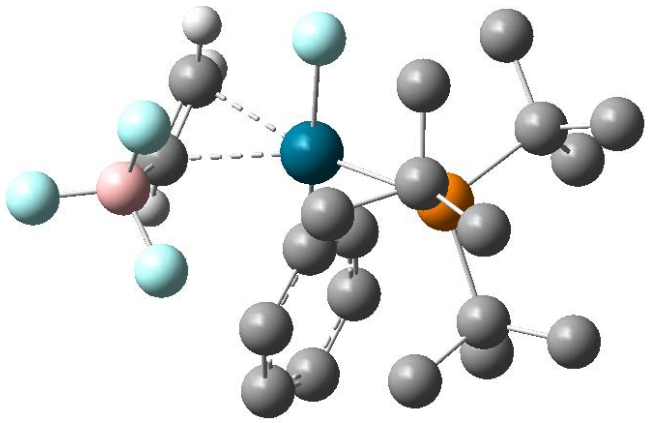

Cartesian coordinates for **Structure II**

Sum of electronic and thermal free energies: -1675.678683

Pd	0.74733400	-0.28870000	-0.80233400
C	2.64418700	-0.82708100	-1.88653200
C	3.04702700	-0.69786000	-0.57895100
F	4.40566300	-2.08378000	0.91901600
F	2.48379600	-1.16945600	1.78393700
B	3.06959400	-1.78510500	0.64334500
F	2.35797800	-2.94215000	0.32753000
C	1.36672000	1.54683700	-0.27741000
C	1.19798800	2.56616100	-1.22233400
C	1.59603100	3.87627700	-0.95058500
C	2.18821100	4.18859600	0.26931300
C	2.40050000	3.17333800	1.20157400
C	2.00184000	1.86597300	0.93152500
P	-1.51169900	-0.08147900	0.11097300
C	-2.75490500	0.22018500	-1.32682400
C	-4.20181300	-0.19212800	-1.04526900
C	-2.25386800	-0.53178500	-2.56513600
C	-2.75422300	1.70281500	-1.71069000
C	-1.89107400	1.24691600	1.47339700
C	-1.10843500	0.86677400	2.73664700
C	-3.37369100	1.41752900	1.82673800
C	-1.37661800	2.64343300	1.09251500
C	-1.89372200	-1.80901700	0.90836500
C	-3.09040000	-1.85668400	1.86251400
C	-0.62833300	-2.24748800	1.66075000
C	-2.13204700	-2.87295600	-0.16996500
H	2.84848900	-0.04205900	-2.62309900
H	2.25777400	-1.77223600	-2.26883300
H	0.73923000	2.33671400	-2.18850200
H	1.44210200	4.65547600	-1.69926000

H	2.49851200	5.21103400	0.48616000
H	2.88873400	3.40003300	2.15083200
H	2.20523900	1.06618100	1.64637100
H	-4.63207400	0.31921200	-0.17627500
H	-4.81883200	0.07413600	-1.91942000
H	-4.30937200	-1.27173500	-0.89382100
H	-1.27150900	-0.15840100	-2.88250700
H	-2.97561300	-0.36414700	-3.38225300
H	-2.13014600	-1.60546800	-2.41358000
H	-3.28584700	2.33341400	-0.98761700
H	-1.73583800	2.09539600	-1.83907700
H	-3.27498400	1.80967000	-2.67575000
H	-0.04642800	0.69057600	2.51797500
H	-1.16443100	1.70835700	3.44545000
H	-1.50584100	-0.01568900	3.24899800
H	-3.92603600	1.92605900	1.02533100
H	-3.44326600	2.06419000	2.71676000
H	-3.89404000	0.48506300	2.06097200
H	-0.28770700	2.67641500	1.03593400
H	-1.77698700	3.03235800	0.15371700
H	-1.68835900	3.33682200	1.89075200
H	-4.03319000	-1.56453000	1.37998300
H	-3.20948800	-2.90086500	2.19264800
H	-2.96080300	-1.25360000	2.76878100
H	0.22897100	-2.39913300	0.99250300
H	-0.84249500	-3.21420500	2.14538100
H	-0.31135600	-1.55293300	2.44429800
H	-3.09236900	-2.75436500	-0.68868600
H	-1.30509700	-2.87516000	-0.89075000
H	-2.16272300	-3.85063100	0.33726400
H	3.53136200	0.25731700	-0.34678200
F	0.14082200	-2.04176500	-1.71000400

$((tBu)_3P)Pd(Ph)(F)(BF_3(CH{=}CH_2))$ rearrangement π-complex **S3**

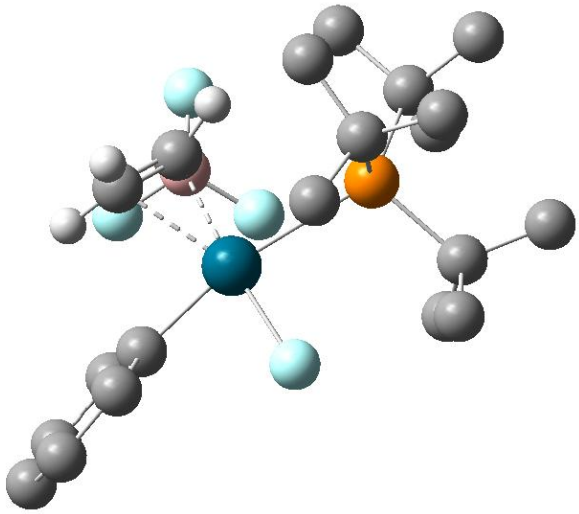

Cartesian coordinates for π-complex **S3**

Sum of electronic and thermal free energies: -1675.670679

Pd	-0.92412700	-0.26311300	0.17628500
C	-1.72995800	1.03644200	1.81468700
C	-0.79417000	1.75943900	1.10756800
F	-0.42638600	4.03339300	0.24483900
F	-0.56553800	2.36276600	-1.31685700
B	-1.08621700	2.83909800	-0.08730500
F	-2.45992000	3.05443600	-0.22371000
C	-2.90070500	-0.62451500	0.07072300
C	-3.39684900	-1.80588500	0.61832300
C	-4.73277900	-2.15334000	0.42709000
C	-5.57238200	-1.32982900	-0.31950900
C	-5.06980900	-0.15103700	-0.86275400
C	-3.73764300	0.21399100	-0.66143800
P	1.73757900	-0.27535300	-0.02147400
C	2.29390100	-1.22009800	1.56448900
C	3.66276100	-1.90199600	1.52439300
C	1.22307300	-2.27801600	1.86719500
C	2.28396900	-0.25670200	2.75518400
C	2.85761900	1.31494100	-0.16867500
C	2.66315500	1.92164300	-1.56470200
C	4.34941000	1.07963200	0.09511100
C	2.42185600	2.43897200	0.78586200
C	2.20436000	-1.37239900	-1.55293500
C	3.66647700	-1.34981700	-2.00567600
C	1.29531800	-0.89350900	-2.69665000
C	1.84477000	-2.84648000	-1.32179200
H	-1.48313200	0.50343800	2.73974100
H	-2.79376600	1.18280300	1.63889000
H	-2.73018000	-2.46789400	1.17271000
H	-5.11602700	-3.08066200	0.85657000

H	-6.61622700	-1.60525400	-0.47394500
H	-5.72104200	0.50397200	-1.44353200
H	-3.36016700	1.16279300	-1.04372500
H	4.48440000	-1.19561400	1.35972000
H	3.84483600	-2.39496200	2.49422300
H	3.72427300	-2.67823100	0.75364100
H	0.22738400	-1.82232000	1.97771700
H	1.48240100	-2.78191500	2.81338300
H	1.13450100	-3.04074100	1.08912200
H	3.11210900	0.46212200	2.72930000
H	1.33937500	0.30117400	2.82876400
H	2.39218100	-0.84237900	3.68253900
H	1.59958200	2.11369600	-1.75973800
H	3.18001400	2.89462400	-1.58606600
H	3.08119200	1.31867100	-2.37746300
H	4.55060100	0.91333900	1.16225300
H	4.90002700	1.99131200	-0.18982900
H	4.78412100	0.24799100	-0.46623200
H	1.47799700	2.90582900	0.48736000
H	2.35252900	2.13716000	1.83583400
H	3.19038100	3.22764500	0.73316800
H	4.35264400	-1.72029900	-1.23128500
H	3.76161400	-2.02862300	-2.86885600
H	4.01820300	-0.36683400	-2.33649500
H	0.25092600	-1.11729100	-2.44854000
H	1.56314700	-1.44596900	-3.61282900
H	1.38136400	0.17567600	-2.91399300
H	2.51495100	-3.34883700	-0.61248700
H	0.79918900	-2.94343000	-1.01112600
H	1.95963800	-3.36696800	-2.28714000
H	0.20309400	1.74522800	1.55026800
F	-0.87694700	-2.00502400	-0.86553000

$((tBu)_3P)Pd(Ph)(F)(BF_3(CH{=}CH_2))$ rearrangement isomer **S4**

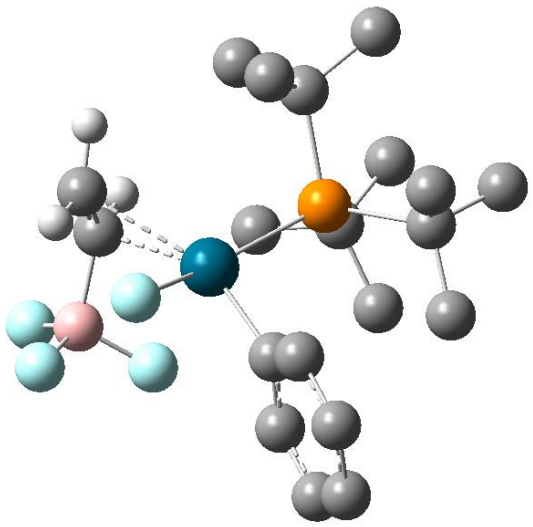

Cartesian coordinates for rearrangement isomer **S4**

Sum of electronic and thermal free energies: -1675.649115

Pd	-0.88050600	0.09648900	0.73314900
C	-1.50381000	2.27439600	1.75889800
C	-1.49278700	2.51368300	0.42418400
F	-2.97022200	3.43188800	-1.29901900
F	-2.13642500	1.33342300	-1.69299100
B	-2.66152500	2.21263700	-0.68594000
F	-3.77899800	1.63367800	-0.11315200
C	-1.25166800	-1.77163200	0.15302300
C	-1.22545500	-2.86139200	1.02145500
C	-1.63268000	-4.11782900	0.57695400
C	-2.09783400	-4.28573400	-0.72616500
C	-2.18370300	-3.18105900	-1.56980600
C	-1.76916000	-1.92241400	-1.13317400
P	1.39518600	0.12904600	-0.08986500
C	2.33280900	1.09729100	1.31771500
C	3.85535100	0.94755100	1.38680200
C	1.75480900	0.66006000	2.67289600
C	2.04669400	2.59695300	1.18319400
C	1.77989600	1.02788300	-1.76486500
C	1.39178100	0.09121500	-2.91360100
C	3.22443000	1.49018800	-1.97585400
C	0.87376900	2.25270800	-1.91956000
C	2.30030000	-1.59642500	-0.20926400
C	3.72615800	-1.54960900	-0.77436000
C	1.53125400	-2.61295900	-1.07255000
C	2.35655100	-2.22162800	1.18905000
H	-0.72751600	2.65710200	2.43195200
H	-2.33918900	1.75672900	2.22927800
H	-0.90684900	-2.72090200	2.05491500

H	-1.59805300	-4.96953000	1.25857500
H	-2.41704400	-5.26896100	-1.07307000
H	-2.58599600	-3.29387900	-2.57771900
H	-1.87457800	-1.04844300	-1.77829300
H	4.35882300	1.24551800	0.45883300
H	4.22761700	1.61201100	2.18360900
H	4.17889100	-0.06654500	1.64735700
H	0.66143300	0.75725900	2.70843600
H	2.18421300	1.30211500	3.45932300
H	1.99871800	-0.37590200	2.92751300
H	2.57466600	3.05517000	0.33830100
H	0.97925600	2.81314500	1.08461400
H	2.40401000	3.10021400	2.09563700
H	0.37643100	-0.30955200	-2.78516200
H	1.39505200	0.67200400	-3.84884300
H	2.09295000	-0.74079900	-3.04864400
H	3.51616600	2.28033500	-1.27296100
H	3.29949600	1.92443200	-2.98604400
H	3.96512900	0.68689400	-1.91418900
H	-0.18942500	1.98788300	-1.87535900
H	1.07781200	3.03488100	-1.18195800
H	1.06926100	2.69147000	-2.91140500
H	4.37786400	-0.80867500	-0.30330500
H	4.18791200	-2.53748500	-0.61460000
H	3.73068400	-1.37393100	-1.85749200
H	0.65320200	-3.00233600	-0.55580200
H	2.20814900	-3.46207100	-1.26223100
H	1.20146600	-2.23430200	-2.04179800
H	3.09469600	-1.74847200	1.84704200
H	1.37567200	-2.20330300	1.68117900
H	2.64977500	-3.27824600	1.08305200
H	-0.64507200	3.10312800	0.05491700
F	-2.42243900	-0.36141100	1.95486700

Transmetalation structures III-V

Structure **III**

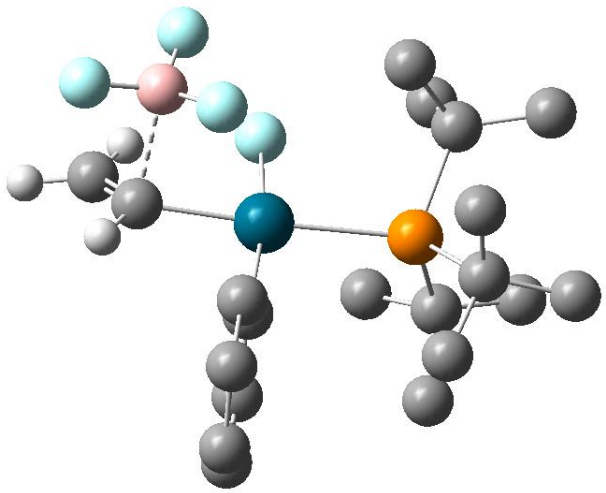

Cartesian coordinates for Structure III

Sum of electronic and thermal free energies: -1675.651047

Pd	0.79572400	-0.32407800	-0.53135300
C	3.05715600	-1.55743900	-1.93477300
C	2.80180800	-0.63653600	-0.98687800
F	4.41931300	-1.73419100	0.75730400
F	2.54144900	-1.01549100	1.80500000
B	3.07079300	-1.77010500	0.81163800
F	2.49099000	-2.95900800	0.61284900
C	1.41774000	1.55721800	-0.20171500
C	1.23795300	2.51852600	-1.21033800
C	1.63523100	3.84449800	-1.04308500
C	2.25006900	4.24966900	0.13913100
C	2.48498800	3.30202500	1.13292100
C	2.08439900	1.97763600	0.96039300
P	-1.58066000	-0.07512000	0.07083100
C	-2.62937600	0.30883500	-1.49414600
C	-4.12173400	-0.01960500	-1.42070300
C	-1.99053700	-0.46360800	-2.65549000
C	-2.49997500	1.79259100	-1.85053700
C	-2.05305100	1.23890600	1.41376200
C	-1.42593100	0.79284200	2.74009600
C	-3.54985200	1.49650800	1.61404300
C	-1.40924100	2.60014600	1.11318100
C	-2.16357800	-1.79259600	0.76489600
C	-3.45483200	-1.79880300	1.58536400
C	-1.00284700	-2.33356000	1.61587600
C	-2.33974400	-2.81575900	-0.36551200
H	4.00410300	-1.60010100	-2.48707900
H	2.31063000	-2.32515000	-2.14996000
H	0.77109100	2.22285700	-2.15422100
H	1.46546900	4.56610500	-1.84503900

H	2.55794100	5.28680900	0.27695300
H	2.98803000	3.59625800	2.05646800
H	2.29134300	1.24817100	1.74360000
H	-4.63396500	0.52241800	-0.61595300
H	-4.59821600	0.27869200	-2.36989000
H	-4.31735500	-1.08908100	-1.28649700
H	-0.93095600	-0.19515100	-2.77243300
H	-2.52704800	-0.20969000	-3.58533600
H	-2.02101900	-1.54818900	-2.52542000
H	-3.09423900	2.43952900	-1.19280200
H	-1.45694800	2.13649200	-1.83074700
H	-2.88076100	1.93910300	-2.87443300
H	-0.35327700	0.58289900	2.62113400
H	-1.52439900	1.61355300	3.46879200
H	-1.90457100	-0.08955200	3.17885300
H	-3.98859800	2.01979700	0.75372900
H	-3.67833700	2.15985300	2.48568700
H	-4.14068900	0.59498500	1.80002100
H	-0.31788000	2.54271300	1.09758400
H	-1.73450100	3.05001400	0.17165200
H	-1.69895900	3.29194000	1.92147600
H	-4.32023600	-1.43196100	1.01589900
H	-3.67317600	-2.84228900	1.86547400
H	-3.38907900	-1.22922200	2.51996500
H	-0.13530000	-2.53308800	0.97381800
H	-1.32209100	-3.28485200	2.07395800
H	-0.69105400	-1.66479900	2.42540800
H	-3.22327300	-2.63033700	-0.98898500
H	-1.42672200	-2.85753900	-0.97290000
H	-2.48655700	-3.80209300	0.10540300
H	3.56404700	0.13789500	-0.82656000
F	0.35906100	-2.24475900	-1.20347800

Structure **IV**

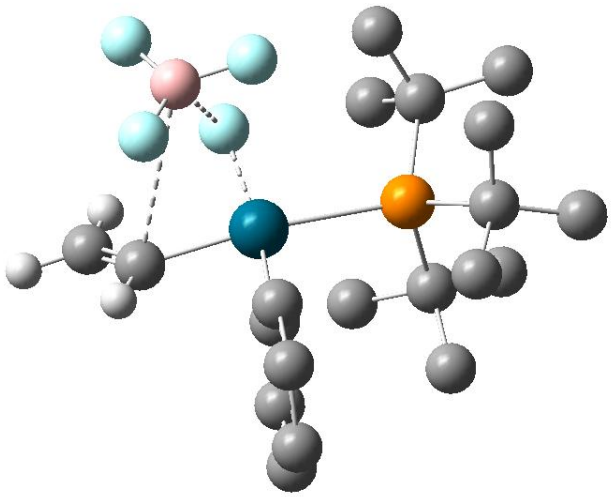

Cartesian coordinates for Structure **IV**

Sum of electronic and thermal free energies: -1675.655691

Pd	0.91598300	-0.36937300	-0.53224600
C	2.80719600	-1.56305000	-2.44547800
C	2.69313600	-0.67917800	-1.44960200
F	3.26545300	-1.81167400	1.22767000
F	1.17452600	-2.30619700	1.95667100
B	2.18256800	-2.56607000	1.13752500
F	2.26698300	-3.73609200	0.54784100
C	1.74982900	1.41090100	-0.09459500
C	1.81746400	2.49478800	-0.98475200
C	2.39385000	3.71360000	-0.62639700
C	2.96002300	3.88106300	0.63430400
C	2.96017300	2.80300000	1.51741500
C	2.37454900	1.59201700	1.15267400
P	-1.52580100	0.11245200	0.05552900
C	-2.18692100	1.09411400	-1.47302400
C	-3.70018300	1.08145000	-1.69918600
C	-1.48863400	0.51868200	-2.71463300
C	-1.75097900	2.55996400	-1.38810600
C	-1.96469200	1.15636100	1.62294300
C	-1.76686500	0.26956700	2.85692500
C	-3.36366800	1.77401300	1.67987700
C	-0.94048200	2.28674300	1.77947000
C	-2.58386500	-1.50809000	0.16375600
C	-4.02351300	-1.36412200	0.66096200
C	-1.83627500	-2.49557900	1.07107100
C	-2.60588800	-2.19289600	-1.20958400
H	3.75009900	-1.71202400	-2.98580600
H	1.97061300	-2.19988300	-2.73641100

H	1.41287300	2.38252200	-1.99442600
H	2.40985800	4.53631600	-1.34471900
H	3.41211600	4.83212800	0.91839500
H	3.42270900	2.90529300	2.50147000
H	2.38818900	0.76155300	1.86413500
H	-4.25750800	1.49628500	-0.84933800
H	-3.93175600	1.70746500	-2.57750100
H	-4.09312300	0.08005100	-1.90747900
H	-0.39468900	0.58782100	-2.62466100
H	-1.80613600	1.09622500	-3.59922500
H	-1.72302500	-0.53381000	-2.89782000
H	-2.31690900	3.13138800	-0.64153600
H	-0.68041300	2.66547200	-1.17327800
H	-1.94142300	3.03426200	-2.36503700
H	-0.79145200	-0.23810200	2.83451200
H	-1.79046400	0.90709000	3.75570900
H	-2.55079100	-0.48739800	2.97565600
H	-3.50479600	2.55042300	0.91717600
H	-3.49528300	2.26385100	2.65961400
H	-4.16998700	1.04073900	1.57089100
H	0.07758400	1.89645700	1.87808300
H	-0.93070900	3.00254500	0.95274300
H	-1.18199900	2.84710400	2.69822800
H	-4.62313600	-0.65910000	0.07121400
H	-4.51276100	-2.34956600	0.58581300
H	-4.08184800	-1.06555000	1.71575800
H	-0.85833700	-2.71318000	0.62639500
H	-2.42297400	-3.42887200	1.11651500
H	-1.69986100	-2.14613100	2.09858600
H	-3.20903300	-1.66479100	-1.95781100
H	-1.57768400	-2.34046300	-1.56680000
H	-3.06148600	-3.18860000	-1.07931600
H	3.57152100	-0.08557500	-1.16634900
F	0.37808800	-2.34351400	-0.91383500

Structure **V**

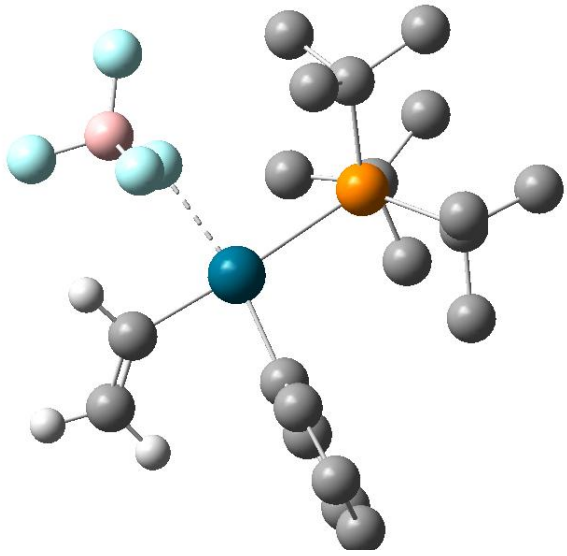

Cartesian coordinates for Structure **V**

Sum of electronic and thermal free energies: 1675.710866

Pd	0.49256600	1.01039000	0.20786300
C	2.42440400	3.20089300	1.23702900
C	1.30978800	2.80899700	0.61761000
F	-1.27604400	2.79932500	-1.56386000
F	-3.33454500	2.75743500	-0.57379200
B	-1.99240900	3.02489900	-0.39126500
F	-1.76441800	4.28631700	0.10458900
C	2.38362800	0.46829600	-0.11883200
C	3.21969800	-0.01845700	0.89577400
C	4.50742200	-0.47546900	0.62081000
C	5.00692400	-0.43374700	-0.67862200
C	4.20671100	0.08787400	-1.69271700
C	2.91656700	0.53747200	-1.41464600
P	-0.71063200	-1.25100200	0.02744200
C	-0.93654600	-1.80880600	1.86002800
C	-1.99978500	-2.87341200	2.13557200
C	-1.25912100	-0.55140500	2.67962800
C	0.39717300	-2.32940000	2.40375100
C	0.15791400	-2.71285700	-0.90336500
C	0.06949700	-2.44444000	-2.40982400
C	-0.37954300	-4.11669200	-0.61199000
C	1.66146400	-2.72769700	-0.59866000
C	-2.48069900	-1.09622100	-0.74872600
C	-3.18832900	-2.40123000	-1.12182900
C	-2.34682400	-0.22842700	-2.00845300
C	-3.41705200	-0.33404500	0.19709500
H	2.60064000	4.25531200	1.47703300
H	3.21785000	2.51115900	1.53327800
H	2.85702300	-0.03700300	1.92683800
H	5.12744700	-0.86415000	1.43105600

H	6.01430700	-0.78983900	-0.89597900
H	4.59158800	0.15040600	-2.71231000
H	2.30707200	0.95022700	-2.22056200
H	-1.81250400	-3.81029400	1.59678300
H	-1.99425400	-3.10971300	3.21283700
H	-3.01248700	-2.53625900	1.88810400
H	-0.47012900	0.20816000	2.56994000
H	-1.32289000	-0.83106400	3.74437100
H	-2.20452400	-0.07836500	2.40105500
H	0.65790800	-3.32210000	2.01612100
H	1.22522300	-1.63974800	2.19168200
H	0.31418700	-2.42273400	3.49868600
H	0.40427300	-1.42639400	-2.65550600
H	0.74072000	-3.14632500	-2.93015600
H	-0.93444000	-2.59103400	-2.82312200
H	-0.14230600	-4.43985100	0.41007400
H	0.11451200	-4.83073600	-1.29195500
H	-1.45938000	-4.21884200	-0.75902900
H	2.15328200	-1.81566500	-0.94876900
H	1.90438600	-2.84832300	0.45993000
H	2.10721700	-3.58036600	-1.13716300
H	-3.32090900	-3.07499300	-0.26475000
H	-4.19437700	-2.14973100	-1.49520200
H	-2.68501000	-2.95653500	-1.92232800
H	-1.90919300	0.75437600	-1.79767600
H	-3.35501500	-0.05087300	-2.41597600
H	-1.75542100	-0.70366500	-2.79806100
H	-3.72220900	-0.93034500	1.06574700
H	-2.99328800	0.61573100	0.53008100
H	-4.33253800	-0.08649100	-0.36222100
H	0.56948100	3.57125700	0.34007200
F	-1.49638400	2.06026100	0.59776200

Potassium (phenyl)trifluoroborate Association Complexes

Structure **VI**

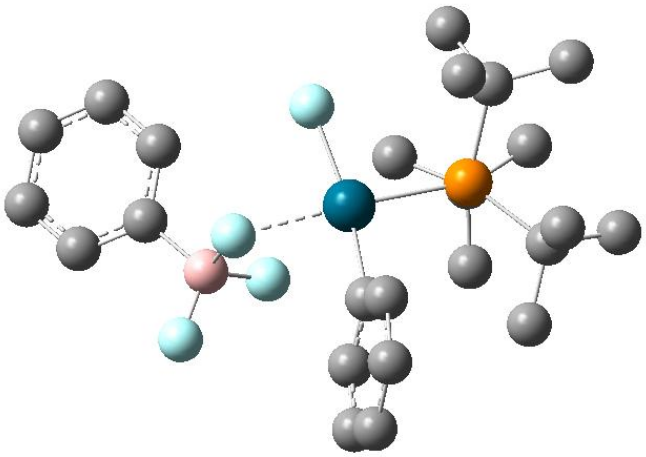

Cartesian coordinates for Structure **VI**

Sum of electronic and thermal free energies: -1829.165213

Pd	-0.06870800	0.18198300	-0.62196500
F	-2.11504500	0.96627200	-0.87878400
B	-2.92726100	0.91360800	0.35654200
F	-3.31601000	2.20667100	0.65595200
F	-2.04454000	0.43895600	1.36081200
C	0.45468700	2.08035500	-0.35919800
C	1.12761400	2.75457700	-1.38343100
C	1.36121300	4.12873100	-1.30228800
C	0.91395200	4.84810000	-0.19843600
C	0.20504100	4.18931500	0.80507300
C	-0.02921900	2.81914100	0.72517300
P	1.90179300	-0.77239000	0.12431800
C	3.44965000	0.30950800	0.57383400
C	4.51904700	-0.43288600	1.38558200
C	3.06707000	1.56022400	1.38139500
C	4.09512400	0.84923600	-0.70768500
C	2.48431700	-2.03748900	-1.21905800
C	1.52772400	-3.23445100	-1.29400700
C	3.89952900	-2.59805800	-1.05672300
C	2.36650400	-1.31885700	-2.57108800
C	1.39647100	-1.73666300	1.71348400
C	2.34104800	-2.87781700	2.10116900
C	-0.01789700	-2.30488400	1.52840000
C	1.29495600	-0.76557000	2.89369300
H	1.47150300	2.20331800	-2.26269800
H	1.89267200	4.63663000	-2.10890600

H	1.09889300	5.92032200	-0.12892200
H	-0.18188400	4.75076400	1.65648100
H	-0.61906600	2.31756400	1.49199200
H	4.83653200	-1.38408800	0.94783100
H	5.41069900	0.21149300	1.44809400
H	4.19288800	-0.62025700	2.41616500
H	2.56055800	2.30366200	0.76216000
H	4.00039700	2.01330900	1.75357200
H	2.43040700	1.36242500	2.24656000
H	4.58162500	0.08078100	-1.31768000
H	3.36750300	1.38902600	-1.32620000
H	4.87285200	1.57386400	-0.41808100
H	1.62803700	-3.91265700	-0.43748000
H	0.48693700	-2.89521800	-1.38573800
H	1.79569900	-3.81487900	-2.19203900
H	4.69244600	-1.84565900	-1.13634800
H	4.06809000	-3.32603500	-1.86626000
H	4.02833500	-3.13838300	-0.10934700
H	1.32487600	-1.02597100	-2.75846400
H	2.99546200	-0.42489200	-2.65100600
H	2.67609300	-2.01498700	-3.36734200
H	3.37432000	-2.55488900	2.27046400
H	1.97957900	-3.31731600	3.04448400
H	2.35081800	-3.68403400	1.35890900
H	-0.76433200	-1.50518000	1.44891500
H	-0.25199800	-2.90668000	2.42184000
H	-0.13409000	-2.93281000	0.64411400
H	2.26881300	-0.41258800	3.25550400
H	0.65928200	0.09752900	2.65330600
H	0.81285000	-1.29743400	3.72844400
F	-0.86032800	-1.60772300	-1.25749700
C	-4.15671600	-0.09219000	0.12622200
C	-5.46238900	0.25219600	0.48578300
C	-3.94482600	-1.36953200	-0.41239100
C	-6.52489200	-0.63502700	0.32381300
H	-5.64535700	1.24554600	0.89953700
C	-5.00039200	-2.26242000	-0.57829200
H	-2.93155100	-1.64597400	-0.72050100
C	-6.29497100	-1.90008200	-0.20922300
H	-7.53601600	-0.33930400	0.61137700
H	-4.81443200	-3.25037800	-1.00402900
H	-7.12201000	-2.60035400	-0.34093500

$((tBu)_3P)Pd(Ph)(F)(BF_3(Ph))$ association anion **S5**

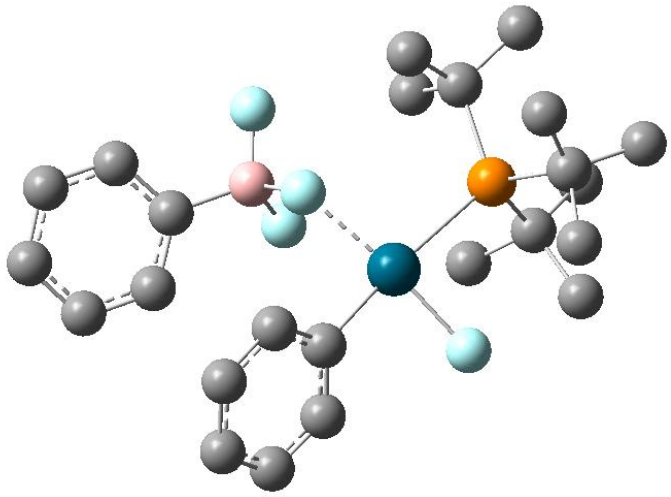

Cartesian coordinates for association anion isomer **S5**

Sum of electronic and thermal free energies: -1829.160612

Pd	-0.05916500	-0.86761200	-0.19349600
F	1.06400700	0.89407000	-0.73781100
B	1.68408100	1.75207700	0.33890200
F	1.18978100	1.23094400	1.53441600
F	1.18955500	3.02725800	0.10754300
C	1.67708300	-1.85182600	-0.24829900
C	2.59914300	-1.60651200	-1.26490000
C	3.82346200	-2.27505100	-1.27612300
C	4.14123900	-3.17537500	-0.26369100
C	3.22119500	-3.41707600	0.75427900
C	1.98653700	-2.76994400	0.75512600
P	-2.36486900	0.18148700	-0.05523600
C	-3.07160300	-0.32589500	1.66492000
C	-4.29345200	0.45178500	2.15524100
C	-1.92518500	-0.16502600	2.67504900
C	-3.42247300	-1.81881700	1.67355600
C	-3.51507600	-0.55529400	-1.41099200
C	-3.21873000	0.12167900	-2.75252300
C	-5.01762500	-0.44736500	-1.14609900
C	-3.14123300	-2.02959300	-1.61239700
C	-2.46239700	2.10037000	-0.18952400
C	-3.85444200	2.70924400	-0.36631000
C	-1.58761600	2.54525100	-1.37133900
C	-1.82228300	2.70531400	1.06597500
H	2.37970100	-0.86974800	-2.03781200
H	4.54293500	-2.06721100	-2.06934300
H	5.10534300	-3.68514700	-0.26546200
H	3.46186000	-4.12274200	1.55142600
H	1.25215500	-2.98289200	1.53106100

H	-5.14786800	0.37172000	1.46990700
H	-4.61169100	0.02919100	3.12267300
H	-4.08860700	1.51566200	2.32436800
H	-1.05589900	-0.77186200	2.38602900
H	-2.27535700	-0.51398800	3.66056300
H	-1.57916000	0.86603000	2.79009000
H	-4.32462500	-2.05050600	1.09295500
H	-2.58001800	-2.41791300	1.30446800
H	-3.63243700	-2.11008400	2.71588200
H	-3.60800000	1.14470700	-2.81528600
H	-2.14190100	0.13971600	-2.97105400
H	-3.70825600	-0.45981400	-3.55023300
H	-5.33307000	-1.03037600	-0.27273300
H	-5.56353000	-0.85005900	-2.01578000
H	-5.35137600	0.58775400	-1.00178400
H	-2.09383200	-2.13237300	-1.92199300
H	-3.26175400	-2.64502400	-0.71905100
H	-3.78517400	-2.44190000	-2.40747000
H	-4.54949500	2.44606600	0.44060900
H	-3.75627100	3.80745700	-0.37002000
H	-4.31788000	2.42908000	-1.32123600
H	-0.58703600	2.10572400	-1.32589700
H	-1.46226300	3.63805200	-1.31730200
H	-2.03504600	2.31815700	-2.34359300
H	-2.45771300	2.60415500	1.95424200
H	-0.83337900	2.28287400	1.27911200
H	-1.67341600	3.78244800	0.89373400
F	-0.87086200	-2.62058000	0.30399200
C	3.28101700	1.67050600	0.22269400
C	4.00978300	2.67129800	-0.42844600
C	4.00345700	0.60102900	0.76477500
C	5.39632600	2.61054300	-0.54580500
H	3.46970500	3.52265000	-0.84558800
C	5.38883600	0.52577100	0.65275900
H	3.46307500	-0.19707700	1.27748200
C	6.09169100	1.53238700	-0.00478100
H	5.93814700	3.40704700	-1.05908000
H	5.92048400	-0.32882100	1.07390000
H	7.17764900	1.47683800	-0.09505600

$((tBu)_3P)Pd(Ph)(F)(BF_3(Ph))$ association anion isomer **S6**

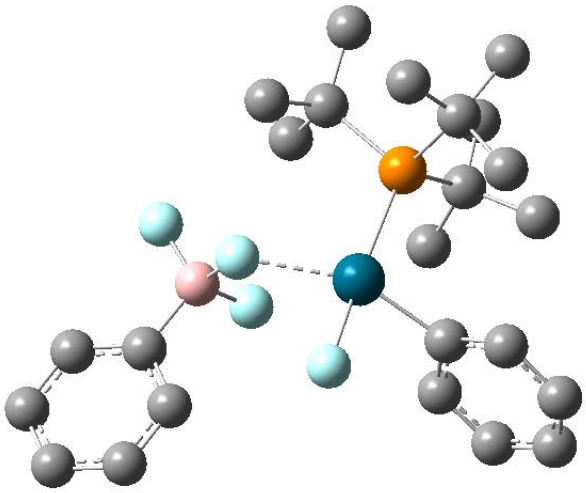

Cartesian coordinates for association anion isomer **S6**

Sum of electronic and thermal free energies: -1829.155054

Pd	-0.08145400	0.57931500	-0.61811800
F	-1.78858200	-0.91449100	-0.90416600
B	-2.58328000	-1.13663400	0.31937200
F	-1.88436200	-0.45139400	1.34141800
F	-2.54666400	-2.50567700	0.57820000
C	0.72932100	2.32203100	-0.10301200
C	1.54605100	3.15018900	-0.87162800
C	1.91712200	4.41299200	-0.40511900
C	1.45529900	4.87906000	0.82050000
C	0.57823600	4.08696500	1.55776400
C	0.20322600	2.82998800	1.09110500
P	1.73447300	-0.86970000	-0.01405400
C	2.65430200	-0.32964500	1.60004700
C	3.57937600	-1.37553200	2.22889100
C	1.59520600	0.05816900	2.64007500
C	3.49159700	0.93178400	1.35441900
C	3.04124100	-0.89233500	-1.43650600
C	2.49536400	-1.69346000	-2.62274600
C	4.42225300	-1.44763800	-1.07977800
C	3.21421800	0.53273900	-1.96311200
C	1.19483100	-2.71605000	0.24515500
C	2.32561500	-3.75010200	0.27729900
C	0.22932700	-3.14904200	-0.86738300
C	0.41508900	-2.80821400	1.56257000
H	1.89949100	2.82860300	-1.84876100
H	2.56838800	5.03829700	-1.01803000
H	1.75181200	5.86262100	1.18503800

H	0.16420500	4.45563700	2.49708400
H	-0.53007300	2.24326600	1.64716300
H	4.35388600	-1.73903500	1.54282600
H	4.09490700	-0.90717100	3.08279800
H	3.03265800	-2.23876500	2.62461300
H	1.01251300	0.92210100	2.30882400
H	2.11253000	0.34002500	3.57173200
H	0.89187600	-0.74362100	2.87650400
H	4.38388600	0.74416900	0.74445400
H	2.91190700	1.74085800	0.89566700
H	3.84442100	1.29786000	2.33165700
H	2.53410200	-2.77651700	-2.46240600
H	1.46333400	-1.40910600	-2.87024700
H	3.11974700	-1.47550400	-3.50382100
H	4.95828400	-0.81530600	-0.36202500
H	5.03319700	-1.47696200	-1.99692700
H	4.39025000	-2.46712600	-0.67955800
H	2.26855000	0.89616400	-2.38457700
H	3.54220900	1.24912800	-1.20407400
H	3.96856600	0.52305700	-2.76688800
H	3.09592600	-3.55475500	1.03073900
H	1.87512000	-4.72631500	0.51843900
H	2.81719300	-3.86489900	-0.69713500
H	-0.60460900	-2.45696300	-0.99470500
H	-0.20329900	-4.11817900	-0.57548700
H	0.72565400	-3.29663100	-1.83045400
H	1.06981600	-2.74941000	2.44110900
H	-0.37372100	-2.05064900	1.63889100
H	-0.08789400	-3.78580000	1.59785300
F	-1.46339700	1.82199600	-1.33524800
C	-4.06910000	-0.57245800	0.11463100
C	-4.28242700	0.70447500	-0.42306300
C	-5.19119300	-1.31344900	0.49598400
C	-5.56948500	1.21664000	-0.56435600
H	-3.41366900	1.28686100	-0.74403400
C	-6.48285600	-0.80848100	0.35867300
H	-5.04309200	-2.31319900	0.90846700
C	-6.67515200	0.46360600	-0.17246700
H	-5.71348500	2.21246100	-0.98736800
H	-7.34243300	-1.40852400	0.66452400
H	-7.68368500	0.86623800	-0.28399600

Potassium (phenyl)trifluoroborate π-Association Complexes

Structure **VIII**

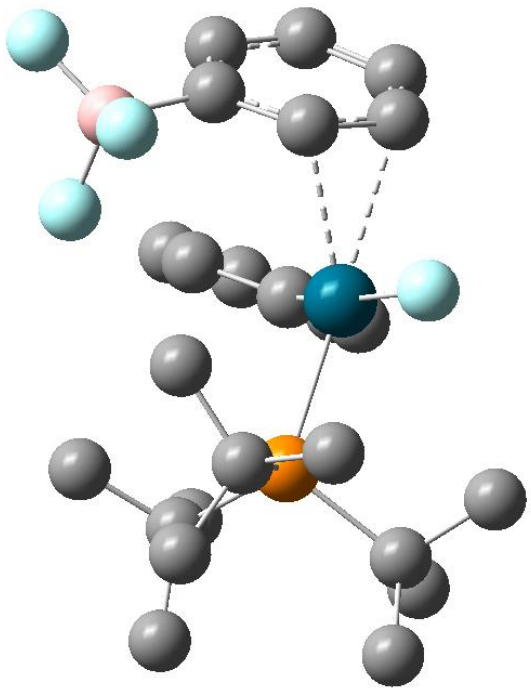

Cartesian coordinates for Structure **VIII**

Sum of electronic and thermal free energies: -1829.165066
*note that the C atoms are not those involved in C-C bond formation (not interacting with borate)

Pd	-0.21581200	0.04850800	1.00569400
F	-4.03004000	-2.45200100	-1.72893800
F	-1.91340600	-1.59495900	-1.96037000
B	-2.84761700	-2.18256300	-1.04112300
F	-2.27458400	-3.35380500	-0.53300500
C	-0.89928500	1.57346300	-0.08105900
C	-0.68528100	2.83800200	0.48003400
C	-1.24246300	3.97989200	-0.09463300
C	-2.01448100	3.87310500	-1.24878700
C	-2.22799000	2.61801900	-1.81291600
C	-1.67539200	1.47275300	-1.23883900
P	1.86613500	-0.08458400	-0.12478300
C	3.22585200	0.73633700	0.95911900
C	4.64747500	0.21560500	0.73379800
C	2.84214500	0.53514000	2.42946000
C	3.23696400	2.25042600	0.73035800
C	2.06169900	0.59806900	-1.92629500
C	1.17503000	-0.23993900	-2.85697300
C	3.50535600	0.58077300	-2.44706500
C	1.57379100	2.04729500	-2.08026100

C	2.19595500	-1.99495400	-0.21026900
C	3.30033900	-2.43833600	-1.17376800
C	0.87465000	-2.66929000	-0.60978200
C	2.55384700	-2.54984600	1.17423400
H	-0.09093900	2.93533300	1.39345900
H	-1.07240700	4.95562500	0.36370000
H	-2.44852900	4.76375400	-1.70409100
H	-2.83496100	2.52103400	-2.71444500
H	-1.86058300	0.49558000	-1.68669900
H	4.98905500	0.33897900	-0.30062000
H	5.33610100	0.78946900	1.37547100
H	4.75887900	-0.83935100	1.00679300
H	1.89424800	1.03986600	2.66040700
H	3.63468600	0.97505600	3.05744700
H	2.70347700	-0.50978400	2.71410600
H	3.68902300	2.53537700	-0.22748800
H	2.22953100	2.68555900	0.78715700
H	3.84389500	2.71365500	1.52465300
H	0.14665900	-0.34594500	-2.48675600
H	1.12497200	0.27001000	-3.83198300
H	1.57039900	-1.24499300	-3.04033400
H	4.11934800	1.35750900	-1.97164600
H	3.48151000	0.81194700	-3.52413200
H	4.01752900	-0.37797000	-2.33308600
H	0.49127100	2.13245300	-1.97463000
H	2.03893300	2.75597900	-1.39108300
H	1.83267200	2.36896800	-3.10206000
H	4.27764200	-1.99581900	-0.93733900
H	3.40914300	-3.52933100	-1.07050400
H	3.07167700	-2.24404400	-2.22761400
H	0.11391900	-2.56679700	0.17173700
H	1.06476800	-3.74683400	-0.73784500
H	0.41913900	-2.30131000	-1.53255700
H	3.56077200	-2.26577800	1.50713400
H	1.80603500	-2.25188100	1.92052400
H	2.54393800	-3.64868500	1.09450400
F	0.34445200	-1.23995000	2.53608700
C	-3.10461500	-1.10843500	0.15532300
C	-2.32002300	-1.12787300	1.32726900
C	-4.00787200	-0.05795200	0.03153400
C	-2.37896000	-0.09446000	2.28422600
H	-1.71250000	-2.00789900	1.53755200
C	-4.10611800	0.96426600	0.98603500
H	-4.64518900	-0.02489100	-0.85507400
C	-3.28350200	0.96496400	2.09883700
H	-1.79778600	-0.18158900	3.20242700

H	-4.81546100	1.78009400	0.83606000
H	-3.33797100	1.77114400	2.83084300

$((tBu)_3P)Pd(Ph)(F)(BF_3(Ph))$ rearrangement π-complex **S7**

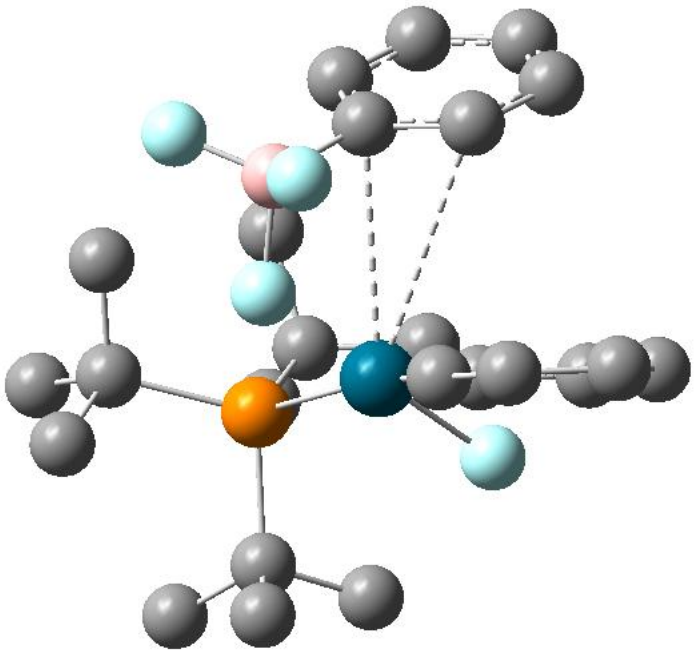

Cartesian coordinates for π-complex **S7**
Sum of electronic and thermal free energies: -1829.157902

Pd	-0.42986000	-0.74199700	-0.01346400
F	-1.23512000	2.62550000	-2.44978700
F	-0.93968600	0.46171400	-1.72740100
B	-1.88666600	1.66589200	-1.69228400
F	-3.04953600	1.23516400	-2.29039400
C	-2.28494200	-1.49997500	-0.01548400
C	-2.88537500	-1.88832300	1.18232700
C	-4.19820600	-2.35386300	1.18507900
C	-4.90992400	-2.46255700	-0.00843000
C	-4.29874700	-2.10247400	-1.20534800
C	-2.98935800	-1.61881100	-1.21280400
P	2.05852300	-0.17555300	-0.00178500
C	2.64577000	0.72385300	1.59364000
C	4.12276600	0.55762500	1.95504000
C	1.76542700	0.22520200	2.74725700
C	2.35799900	2.22382800	1.48637600
C	2.72392400	0.82305500	-1.50921400
C	2.52210100	-0.02031100	-2.77309100
C	4.18182300	1.28146600	-1.44292600
C	1.84271600	2.06221800	-1.70967300
C	2.91268300	-1.91311400	-0.04388900

C	4.38371700	-1.93984300	-0.46107600
C	2.10384400	-2.79320400	-1.01021500
C	2.79185000	-2.59817400	1.32333800
H	-2.31503100	-1.81921100	2.10716300
H	-4.66796500	-2.63858400	2.12849200
H	-5.93794000	-2.82712600	-0.00457000
H	-4.84669700	-2.18028800	-2.14558300
H	-2.54129500	-1.29183700	-2.14892600
H	4.79407600	0.91431400	1.16314000
H	4.33566600	1.15496100	2.85726500
H	4.39250000	-0.47873100	2.18682500
H	0.71231700	0.47972200	2.56762500
H	2.09058200	0.72721600	3.67386100
H	1.80565100	-0.85455800	2.90522200
H	3.04623200	2.74886900	0.81267600
H	1.32436300	2.41911700	1.17136100
H	2.48240100	2.66880800	2.48709300
H	1.48544900	-0.37460100	-2.85733200
H	2.72176700	0.61416300	-3.65093200
H	3.19990500	-0.87971800	-2.83601500
H	4.34764000	2.01458700	-0.64297200
H	4.43621500	1.78348500	-2.39120600
H	4.89521500	0.46125000	-1.30527900
H	0.78497600	1.80446100	-1.80857200
H	1.94731800	2.80392300	-0.91320800
H	2.14799000	2.55433800	-2.64733100
H	5.02048000	-1.32618600	0.18974100
H	4.74847700	-2.97781200	-0.38792800
H	4.54318700	-1.61897800	-1.49799100
H	1.05955100	-2.88347600	-0.68106900
H	2.54699000	-3.80277800	-1.01762700
H	2.10195600	-2.42795200	-2.04194900
H	3.43593100	-2.15009700	2.08949900
H	1.74979600	-2.59338700	1.66630200
H	3.11833000	-3.64475100	1.20638000
F	-0.10543100	-1.91662800	1.56689200
C	-2.06344400	2.09377700	-0.15555600
C	-3.08453500	1.56495200	0.64253200
C	-1.17430600	2.98606400	0.45398200
C	-3.18892500	1.87472300	1.99513000
H	-3.80013800	0.87611300	0.19090600
C	-1.26800000	3.30930500	1.80622800
H	-0.39135100	3.44043300	-0.15809300
C	-2.27405900	2.74348000	2.58553600
H	-3.98358100	1.42689400	2.59366700
H	-0.55279000	4.00242400	2.25416500

H	-2.34998000	2.98554500	3.64636700

Structure **VII**

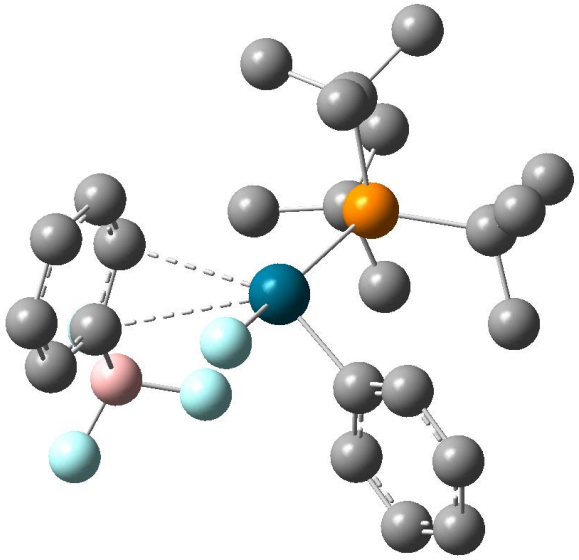

Cartesian coordinates for Structure **VII**

Sum of electronic and thermal free energies: -1829.138831

Pd	-0.44816300	0.39896200	-0.62853400
F	-2.85245400	-1.86120600	2.44566900
F	-1.76979600	0.12923300	2.14207000
B	-2.98746400	-0.58677100	1.86749200
F	-4.04973800	0.10465100	2.44103500
C	0.08892800	2.25099400	-0.18543100
C	0.60151700	3.12128900	-1.14354600
C	0.87724000	4.44307300	-0.79609200
C	0.60672000	4.90132900	0.49159400
C	0.03246400	4.03778100	1.42166500
C	-0.23806600	2.71021800	1.08833100
P	1.58193400	-0.69364200	0.05136000
C	1.87089400	-1.92050300	-1.42970200
C	3.28127200	-2.49303600	-1.59362300
C	1.48411900	-1.20180800	-2.73203100
C	0.92001900	-3.11534500	-1.30678700
C	1.56542900	-1.74096800	1.67619000
C	1.68967400	-0.78739300	2.86905200
C	2.62976600	-2.83461900	1.79738400
C	0.19112400	-2.39418300	1.83630000
C	3.18249200	0.40839100	0.14030800
C	4.43784800	-0.30816700	0.65250100
C	2.97111600	1.63524300	1.04500600
C	3.49267500	0.98205300	-1.24651200
H	0.76496800	2.77194800	-2.16350900

H	1.29170700	5.12187700	-1.54310200
H	0.82046900	5.93575400	0.76161000
H	-0.21782000	4.39887700	2.42002600
H	-0.71630500	2.03713600	1.80102900
H	3.62928700	-3.02888200	-0.70194200
H	3.26509800	-3.21972300	-2.42225000
H	4.02810500	-1.73452000	-1.85370700
H	0.44138000	-0.85259900	-2.71647500
H	1.59506400	-1.91087400	-3.56898600
H	2.11230400	-0.33247700	-2.95079500
H	1.20687000	-3.80968900	-0.50865000
H	-0.11821300	-2.80938600	-1.14402000
H	0.95082600	-3.67979300	-2.25252400
H	0.94225100	0.01646000	2.81651300
H	1.48012300	-1.35818400	3.78655100
H	2.69050400	-0.35332000	2.97940500
H	2.49436600	-3.63278700	1.05662600
H	2.52305400	-3.30473100	2.78817300
H	3.65918100	-2.46939100	1.72179100
H	-0.60945100	-1.65012000	1.87206400
H	-0.03579500	-3.13683000	1.06487400
H	0.17258400	-2.92414200	2.80155500
H	4.66595900	-1.24267800	0.13090100
H	5.29865800	0.36448900	0.50728700
H	4.38105400	-0.51834600	1.72753000
H	2.36008200	2.39569500	0.55553100
H	3.95997300	2.07984100	1.24320000
H	2.50900700	1.41535700	2.00984100
H	3.88737500	0.23938200	-1.94942300
H	2.61428000	1.46541600	-1.69151400
H	4.26594400	1.75836400	-1.13035600
F	-1.74992200	1.40495700	-1.75507000
C	-3.18642700	-0.73394200	0.25944200
C	-4.20953900	-0.07423600	-0.42285900
C	-2.35638400	-1.56947400	-0.51369000
C	-4.39726800	-0.22551500	-1.79400700
H	-4.87546300	0.57301000	0.14795300
C	-2.53654900	-1.73188400	-1.89227300
H	-1.63347800	-2.19486900	0.01057800
C	-3.56217800	-1.05272600	-2.53814600
H	-5.20533300	0.31170700	-2.29336600
H	-1.89072700	-2.40975300	-2.45680600
H	-3.70822700	-1.16410400	-3.61271100

Heterocyclic trifluoroborate π-complexes

Structure **IX**

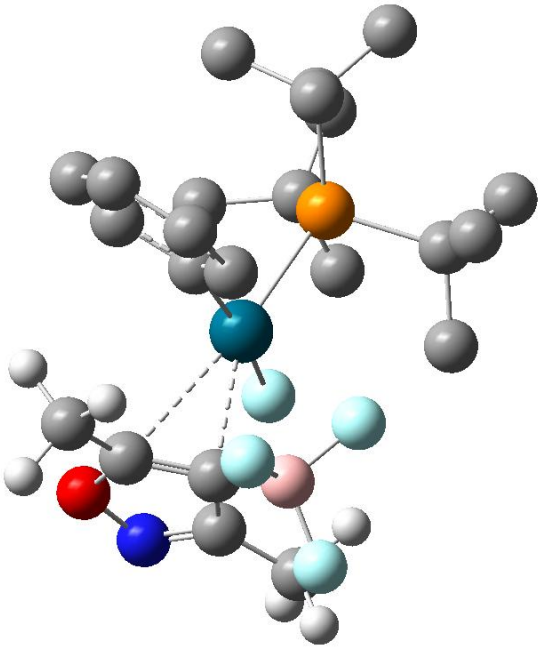

Cartesian coordinates for structure **IX**

Sum of electronic and thermal free energies: -1921.566936

Pd	-0.40517700	-0.20265000	-0.38872700
C	-2.72452700	-0.72710900	-0.04158000
C	-3.05856300	0.01989400	-1.15939300
C	-0.61008000	1.77364400	-0.17933600
C	-1.02952300	2.40661900	0.99529600
C	-1.24424600	3.78300200	1.01968900
C	-1.03688200	4.55732900	-0.12115700
C	-0.62078800	3.93921800	-1.29709500
C	-0.41211300	2.55946000	-1.32250900
P	1.95522800	-0.23241300	0.04129700
C	2.13635500	-1.18216300	1.70604800
C	3.51846400	-1.79256300	1.95409400
C	1.08075200	-2.29578900	1.75970300
C	1.80419200	-0.24841400	2.87400400
C	2.98211200	1.41175800	0.20116200
C	3.12291100	2.06288700	-1.18049400
C	4.37694800	1.23552500	0.81588700
C	2.26127500	2.46553700	1.05715900
C	2.81812500	-1.26552500	-1.35891200
C	4.34204700	-1.14466500	-1.45305300
C	2.17744600	-0.80171800	-2.67502100
C	2.51133100	-2.76516000	-1.24308300
H	-1.22055300	1.81084500	1.88535500

H	-1.58523800	4.25477000	1.94228900
H	-1.20449500	5.63435200	-0.09463400
H	-0.46188400	4.52945300	-2.20134200
H	-0.10740500	2.08168700	-2.25900400
H	4.32680700	-1.05361800	1.95795600
H	3.51008600	-2.26964900	2.94721300
H	3.77271300	-2.57266500	1.22819800
H	0.07042700	-1.87099100	1.81311000
H	1.25522300	-2.87494700	2.68149400
H	1.10672000	-2.97692900	0.90669800
H	2.57941400	0.50516500	3.06162500
H	0.83186800	0.24331600	2.73659900
H	1.72404000	-0.86274500	3.78440200
H	2.14284200	2.21435900	-1.65046700
H	3.57149300	3.05989800	-1.04304900
H	3.76687500	1.51179100	-1.87335000
H	4.32035500	1.03995400	1.89419000
H	4.92658400	2.18320600	0.69549000
H	4.98149300	0.44893500	0.35606600
H	1.42011700	2.91226200	0.52524300
H	1.88613000	2.09418600	2.01343300
H	2.98404500	3.26925400	1.27315900
H	4.84409300	-1.50140800	-0.54347700
H	4.67720500	-1.79419500	-2.27742900
H	4.70697900	-0.13684900	-1.67734600
H	1.10338100	-1.02879800	-2.67086600
H	2.64282100	-1.35218500	-3.50882200
H	2.30763700	0.26898900	-2.87246200
H	3.02418200	-3.24378100	-0.40000400
H	1.43085000	-2.93013000	-1.17491200
H	2.88926000	-3.24778000	-2.15937800
F	-0.25530500	-2.18085000	-0.92907600
B	-2.90789300	-0.37501300	1.55870200
F	-3.44304700	0.90938200	1.70619600
F	-3.77518700	-1.32148200	2.10595800
F	-1.67126900	-0.44213700	2.25954900
C	-3.45942200	1.43571700	-1.34999400
H	-4.51104700	1.45843900	-1.66845400
H	-3.35984700	1.98169500	-0.40893900
H	-2.86120500	1.93331900	-2.12324700
O	-3.26966800	-0.76502200	-2.23146000
N	-3.14253100	-2.10990700	-1.84014500
C	-2.82354800	-2.07368000	-0.57774100
C	-2.66590900	-3.33577800	0.18683400
H	-1.72081700	-3.31213100	0.73986500
H	-3.48065000	-3.43269900	0.91351600

H	-2.66114500	-4.19406400	-0.49422800

Structure **X**

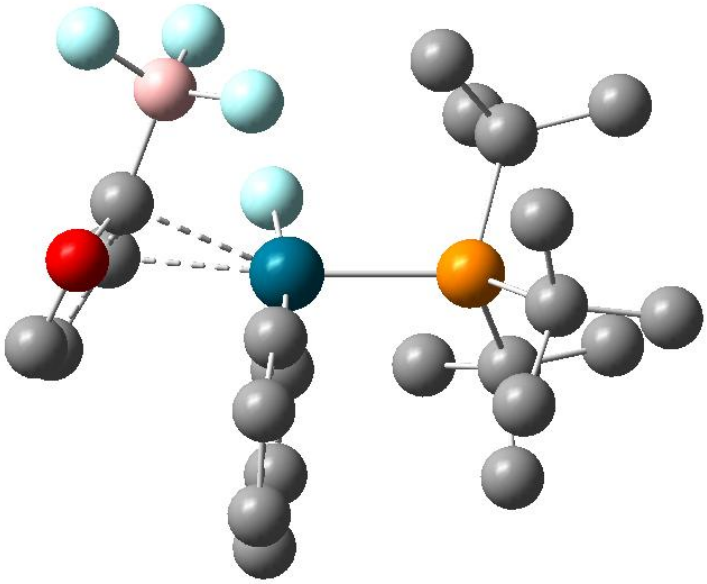

Cartesian coordinates for Structure **X**

Sum of electronic and thermal free energies: -1827.018056

Pd	-0.46783000	-0.29516200	0.68011000
C	-2.52581500	-0.91962400	1.58621800
C	-2.87597000	-1.01677100	0.23660000
F	-3.80208200	-2.54022500	-1.46247300
F	-1.88976200	-1.41180700	-2.02465800
B	-2.58317100	-2.07536900	-0.98406700
F	-1.80164600	-3.11970700	-0.49115500
C	-1.12344000	1.45559500	-0.02632800
C	-1.04773000	2.55269100	0.84108000
C	-1.56709600	3.79567000	0.48092200
C	-2.18204800	3.96194500	-0.75711300
C	-2.28356100	2.87106900	-1.61846200
C	-1.75896200	1.62952900	-1.26128600
P	1.80208600	-0.00898500	-0.05108800
C	2.86658500	0.57591300	1.44093100
C	4.35967000	0.24959500	1.35528700
C	2.28273000	-0.05909000	2.70848400
C	2.73176300	2.09009700	1.62590600
C	2.20720300	1.16786500	-1.53899400
C	1.57959400	0.56657500	-2.80262600
C	3.70293600	1.41234300	-1.77672100
C	1.56646900	2.55699400	-1.39654500
C	2.39672700	-1.78303800	-0.57242200

C	3.68691800	-1.84306000	-1.39484700
C	1.25746800	-2.42571700	-1.37612300
C	2.59984800	-2.67862300	0.65675700
H	-1.95863800	-1.67470100	2.12531400
H	-0.58807000	2.43295900	1.82637400
H	-1.49318600	4.63602800	1.17362900
H	-2.58891300	4.93199700	-1.04455700
H	-2.78078700	2.98391800	-2.58322300
H	-1.87187900	0.77291300	-1.92590000
H	4.84234200	0.68815200	0.47381900
H	4.86106100	0.66826100	2.24351200
H	4.55825100	-0.82731900	1.35269000
H	1.25407500	0.28496200	2.88181200
H	2.90469700	0.24524500	3.56692200
H	2.23091800	-1.14926400	2.67482500
H	3.29501300	2.66455300	0.87996200
H	1.68417400	2.41928800	1.60466400
H	3.14294400	2.35377500	2.61360500
H	0.52089300	0.31514700	-2.65079400
H	1.63038700	1.31853000	-3.60602500
H	2.09762300	-0.32833900	-3.16361400
H	4.13412500	2.06416100	-1.00525100
H	3.81592200	1.94226900	-2.73652500
H	4.30887700	0.50460400	-1.83387100
H	0.47820700	2.51540100	-1.46544500
H	1.82675500	3.08292200	-0.47547000
H	1.92994200	3.17109700	-2.23671800
H	4.54906000	-1.40671400	-0.87234900
H	3.92015200	-2.90586600	-1.56623600
H	3.60407000	-1.37689900	-2.38355400
H	0.34794200	-2.56276100	-0.77865300
H	1.59458300	-3.42471500	-1.69782600
H	0.97714100	-1.87077300	-2.27582700
H	3.48344700	-2.40865200	1.24938500
H	1.69950800	-2.67586400	1.28462800
H	2.76634500	-3.70328900	0.28730200
F	0.06722400	-1.95785400	1.80301500
C	-3.29503300	0.16537000	2.14393600
H	-3.27717000	0.52555000	3.16598000
O	-3.78723400	-0.03426300	-0.02406800
C	-4.02128100	0.66201900	1.11944100
H	-4.70265100	1.49886000	1.02442200

Section 5: Spectroscopic Data

^{1}H NMR Spectra

^{1}H NMR (500 MHz) spectrum for 1.4a

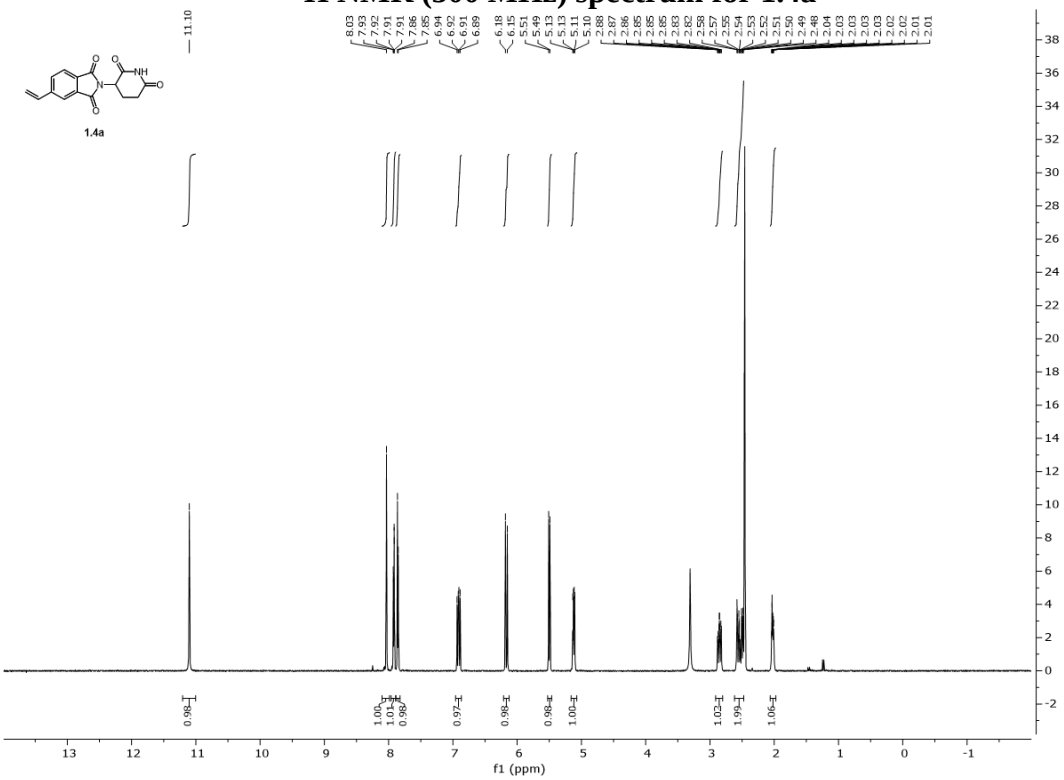

^{1}H NMR (500 MHz) spectrum for 1.4b

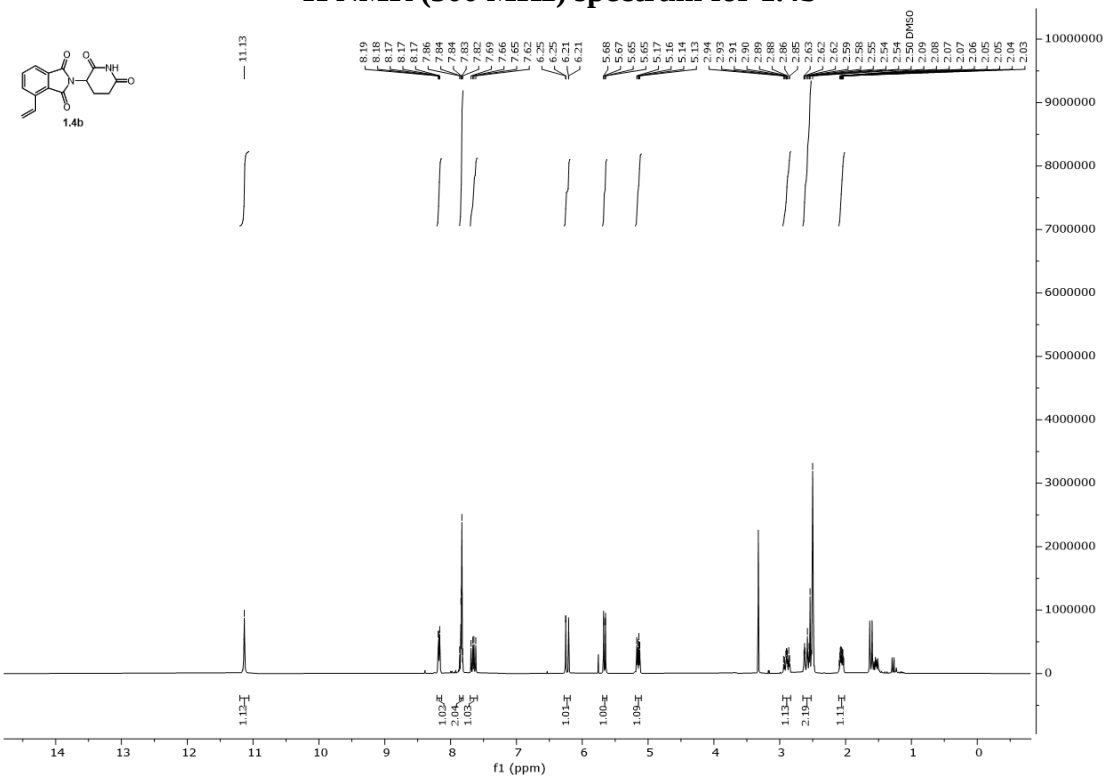

^{1}H NMR (400 MHz) spectrum for 1.4c

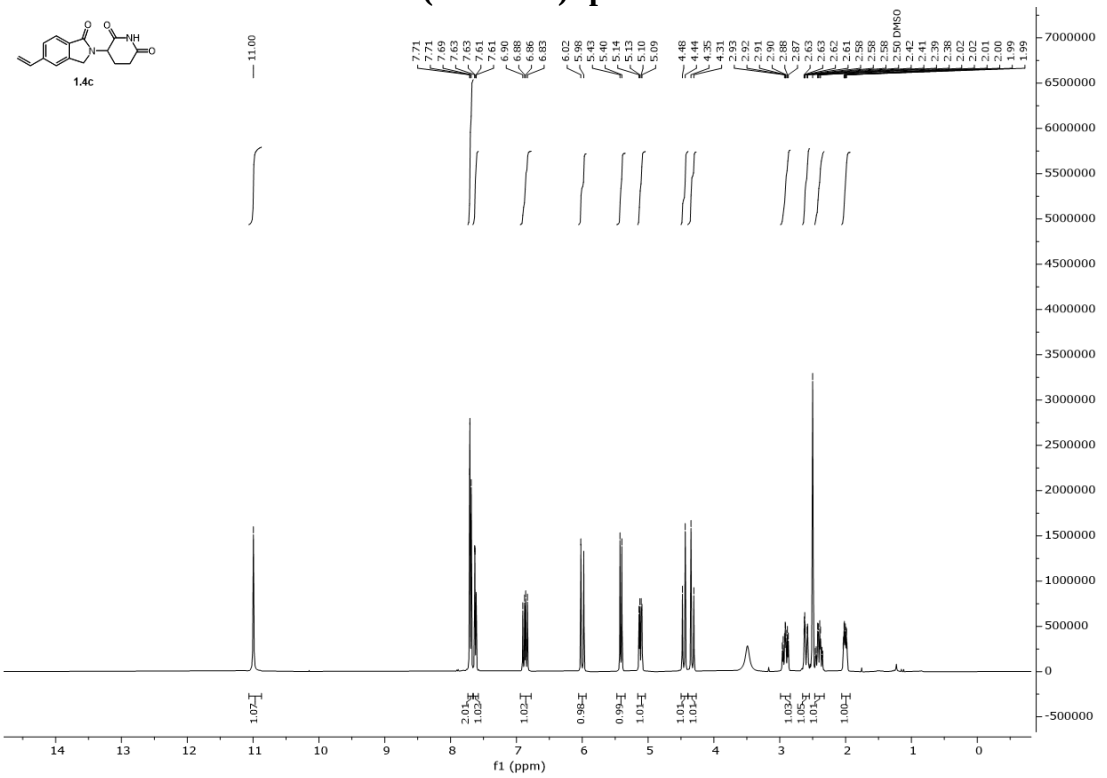

^{1}H NMR (600 MHz) spectrum for 1.4d

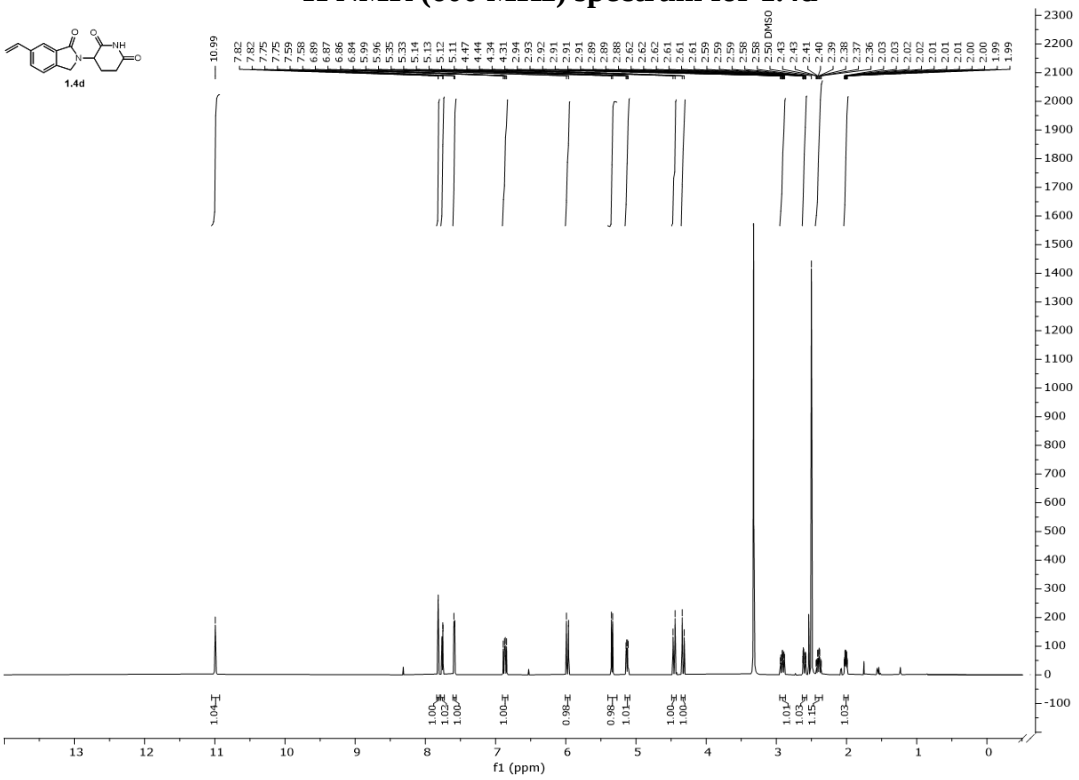

^{1}H NMR (400 MHz) spectrum for 1.4e

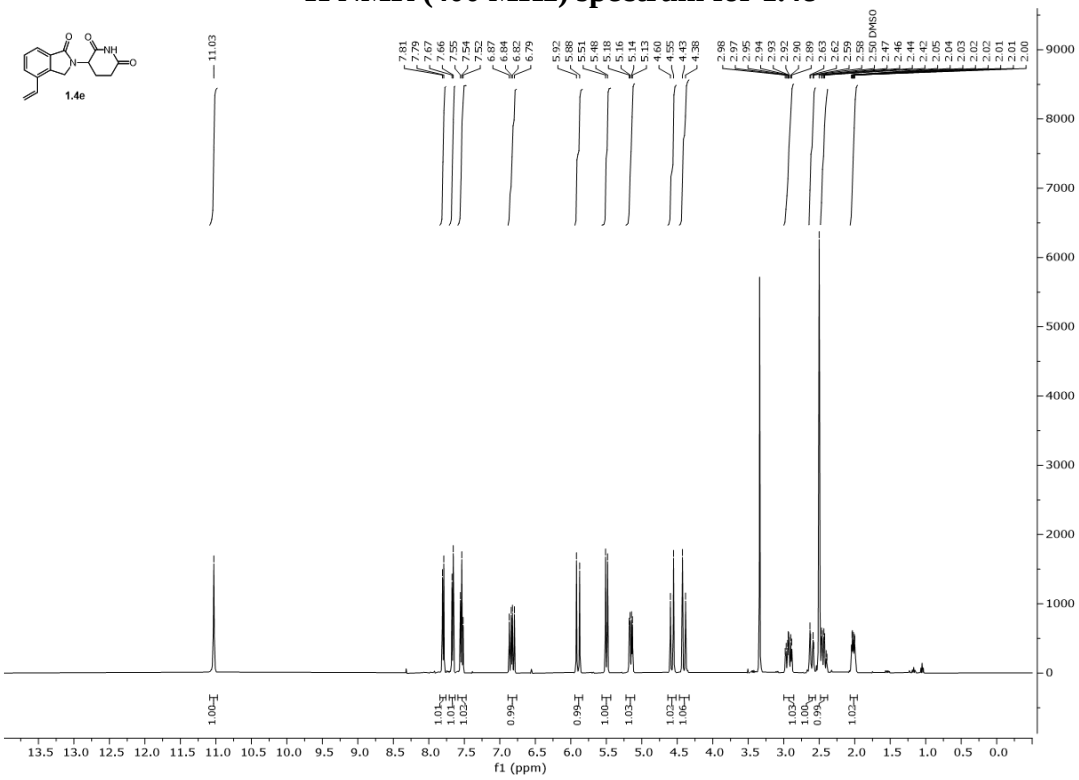

^{1}H NMR (500 MHz) spectrum for 1.4f

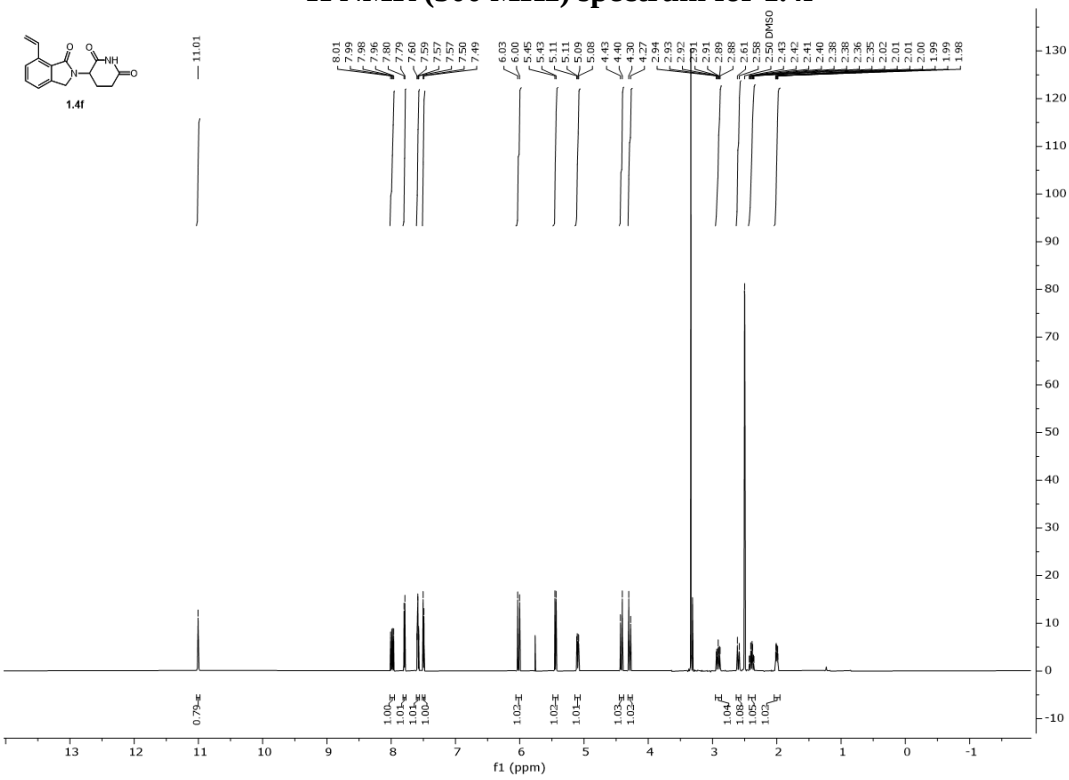

^{1}H NMR (400 MHz) spectrum for 1.8a

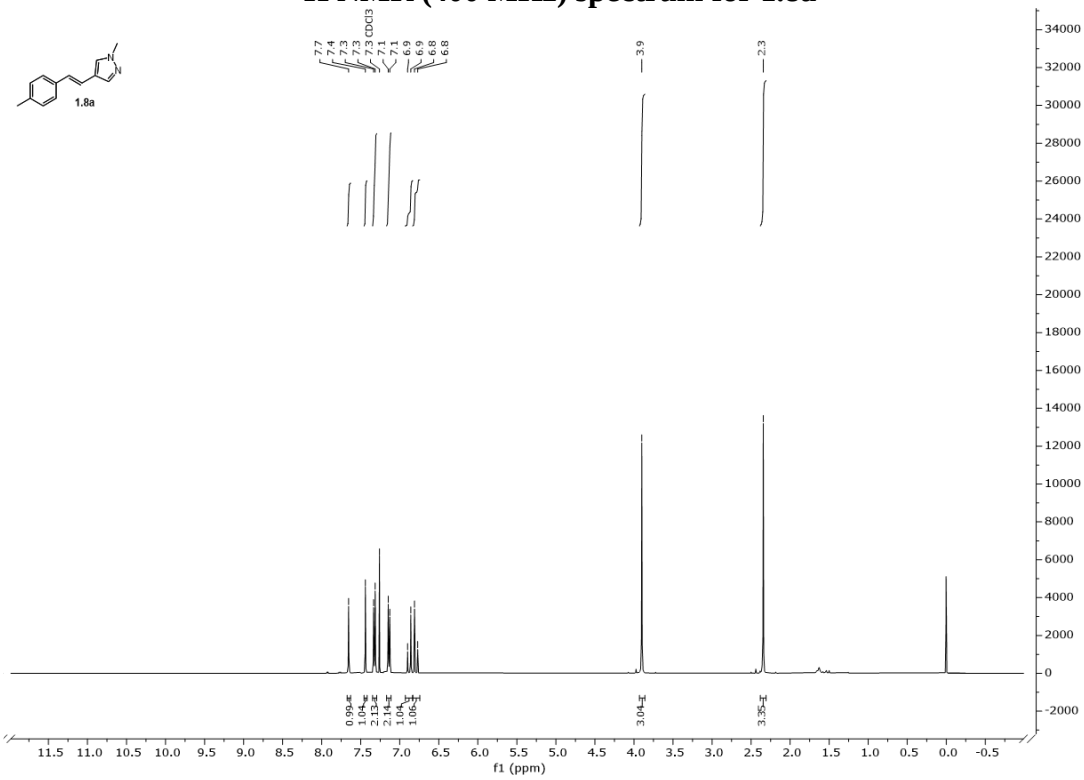

^{1}H NMR (600 MHz) spectrum for 1.8b

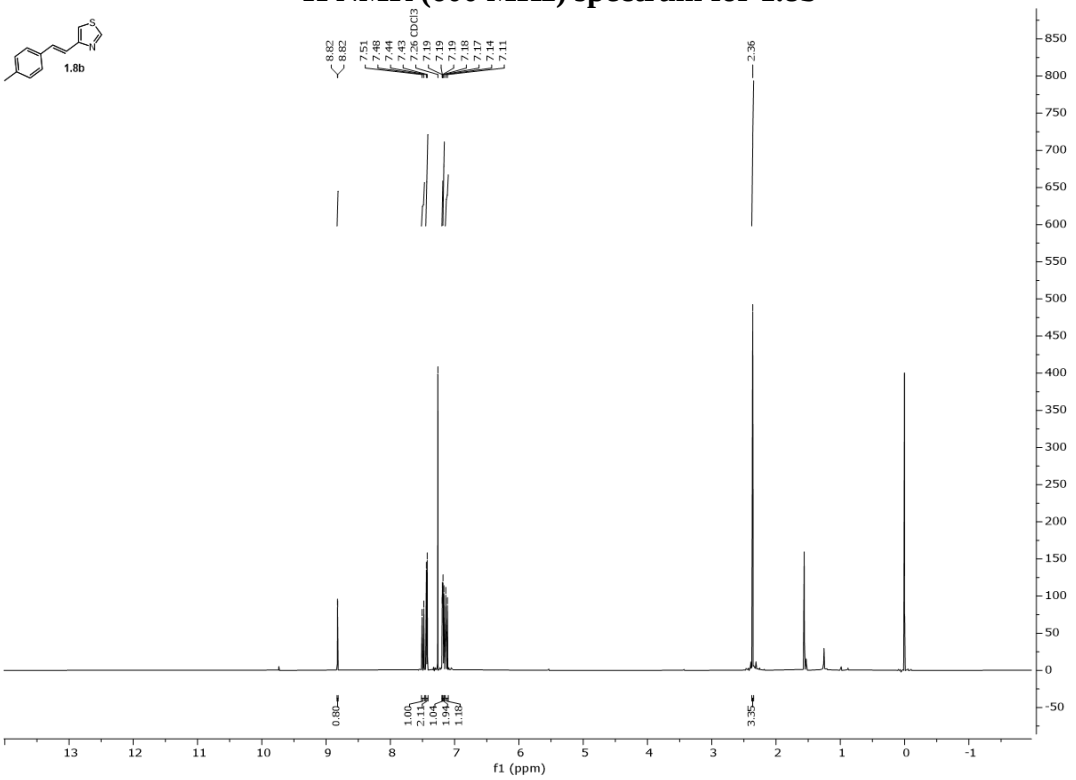

^{1}H NMR (400 MHz) spectrum for 1.8c

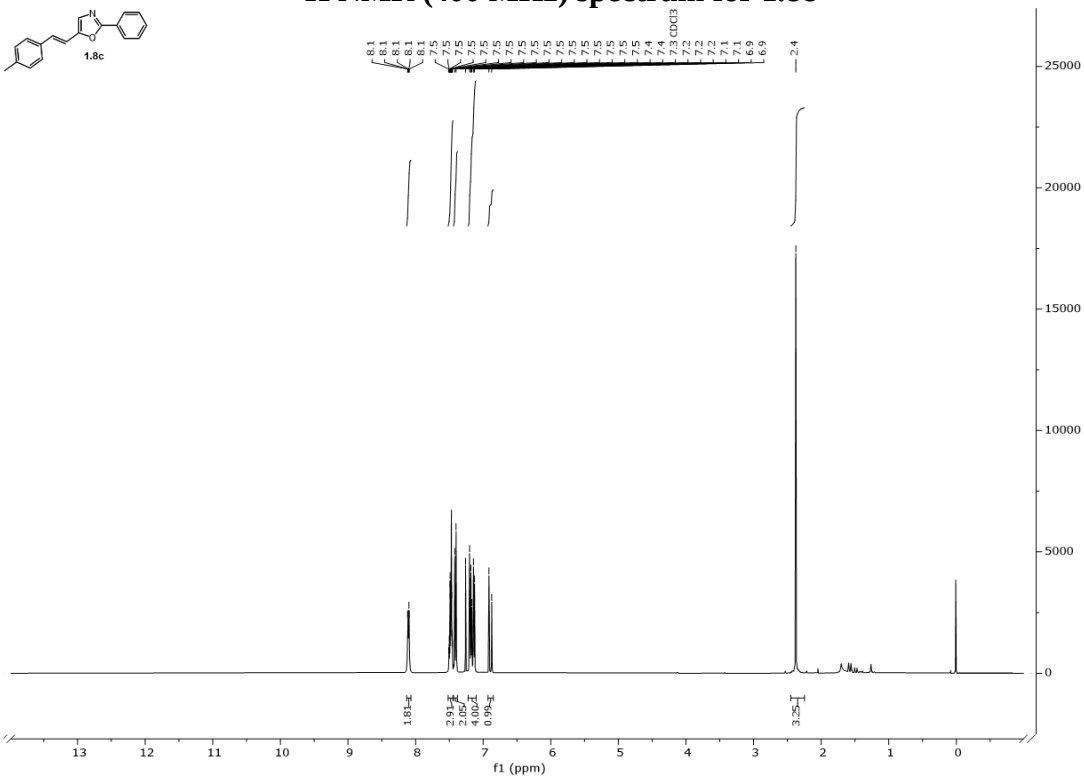

^{1}H NMR (400 MHz) spectrum for 1.8d

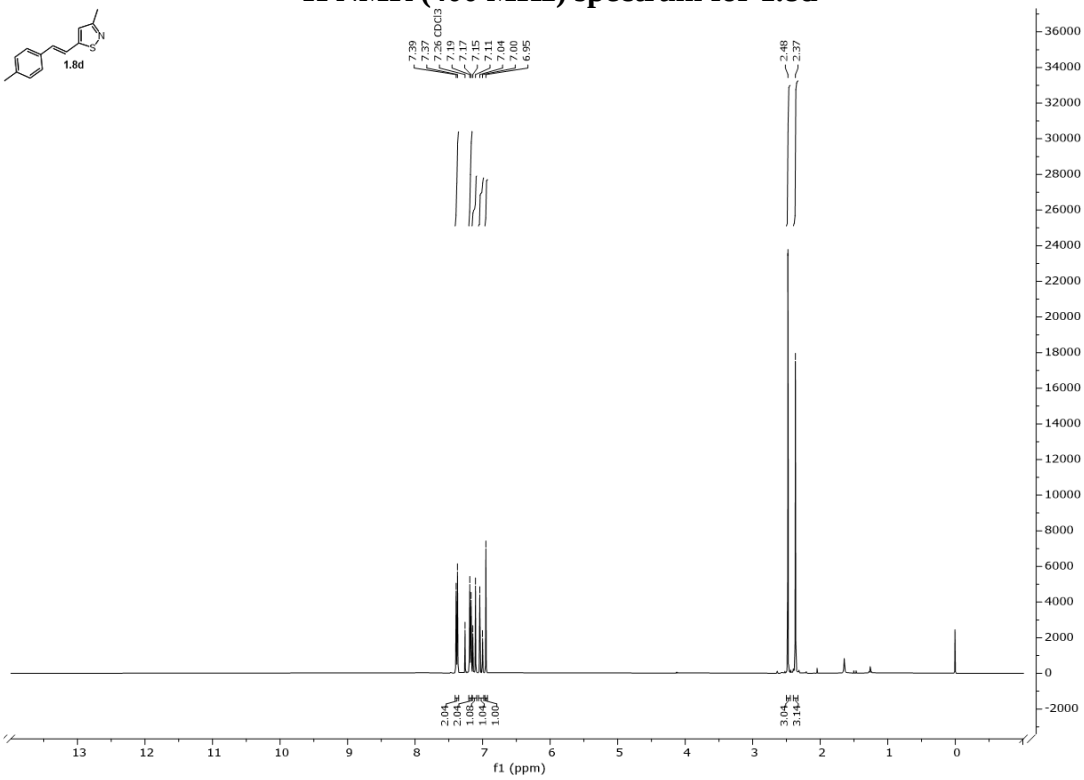

^{1}H NMR (400 MHz) spectrum for 1.8f

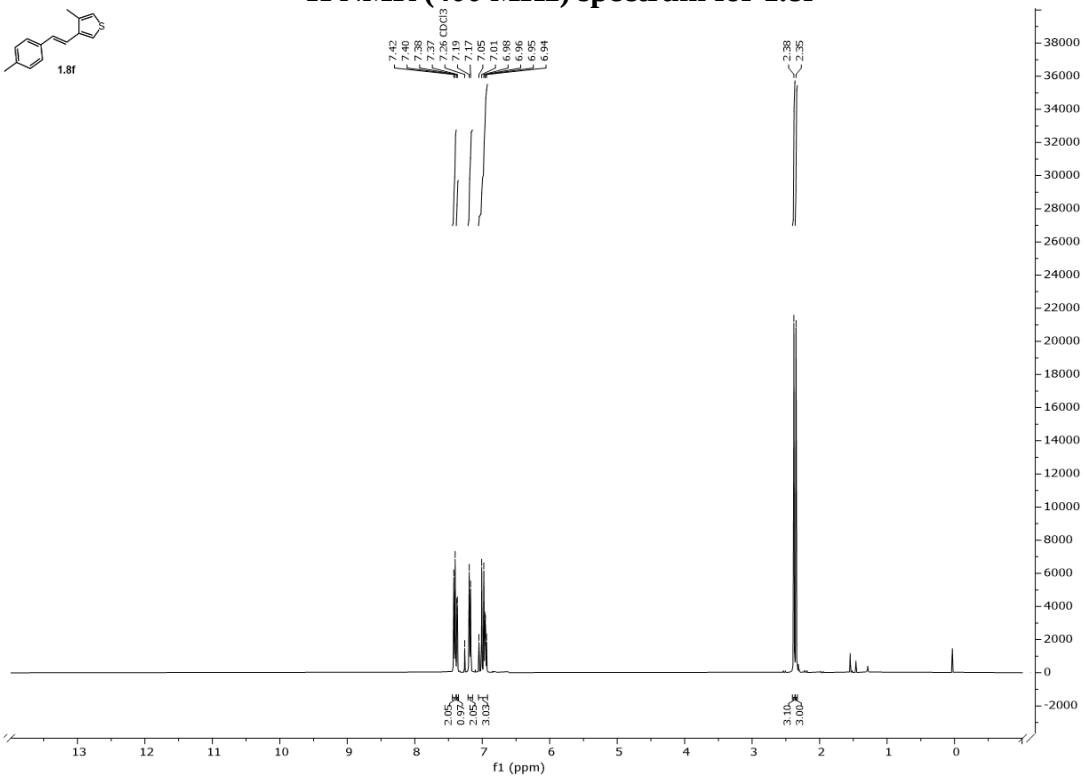

^{1}H NMR (400 MHz) spectrum for 1.8g

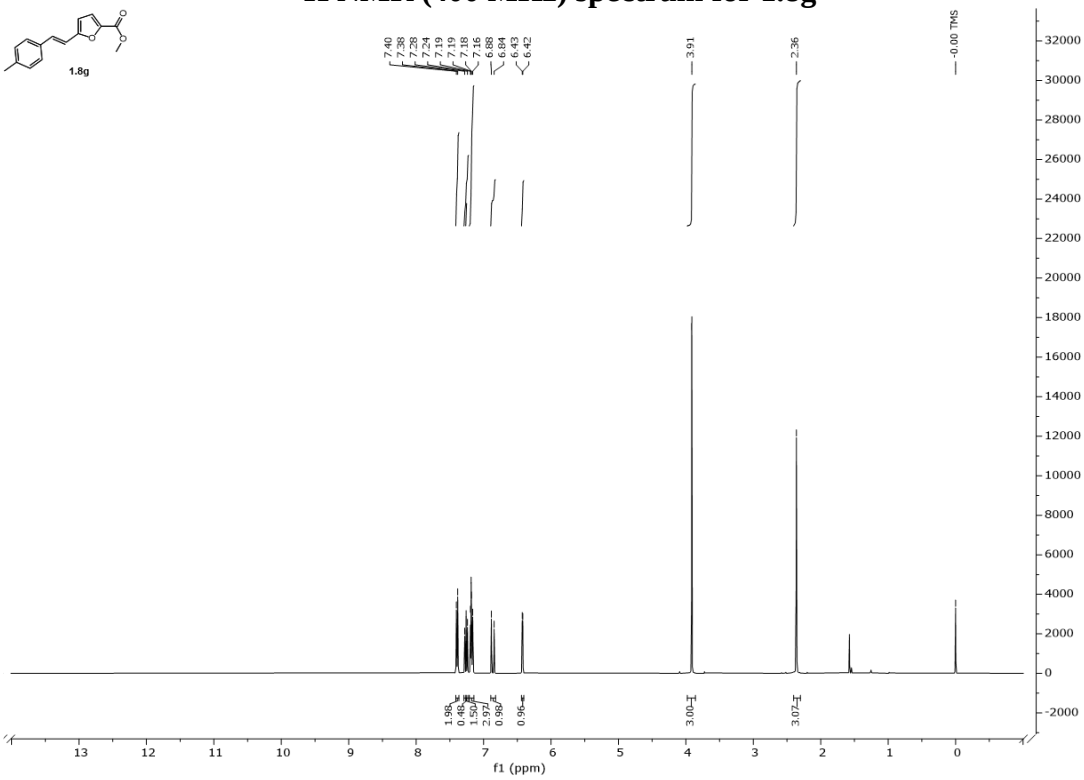

^{1}H NMR (600 MHz) spectrum for 1.8h

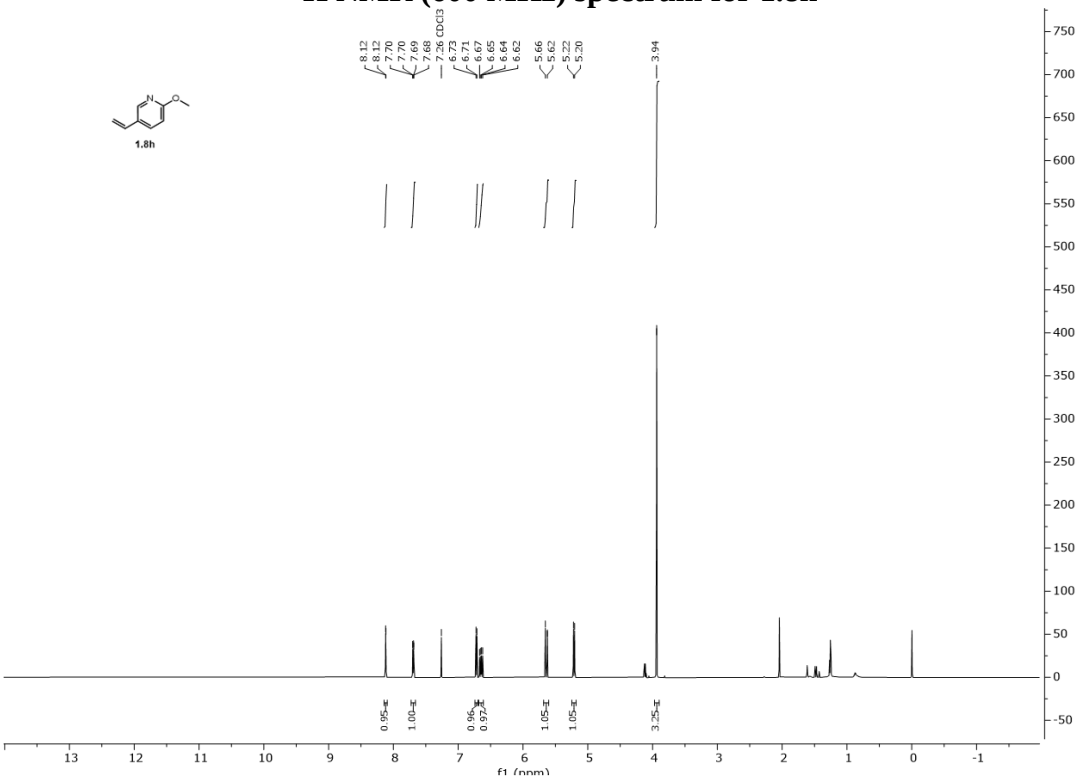

^{1}H NMR (600 MHz) spectrum for 1.9a

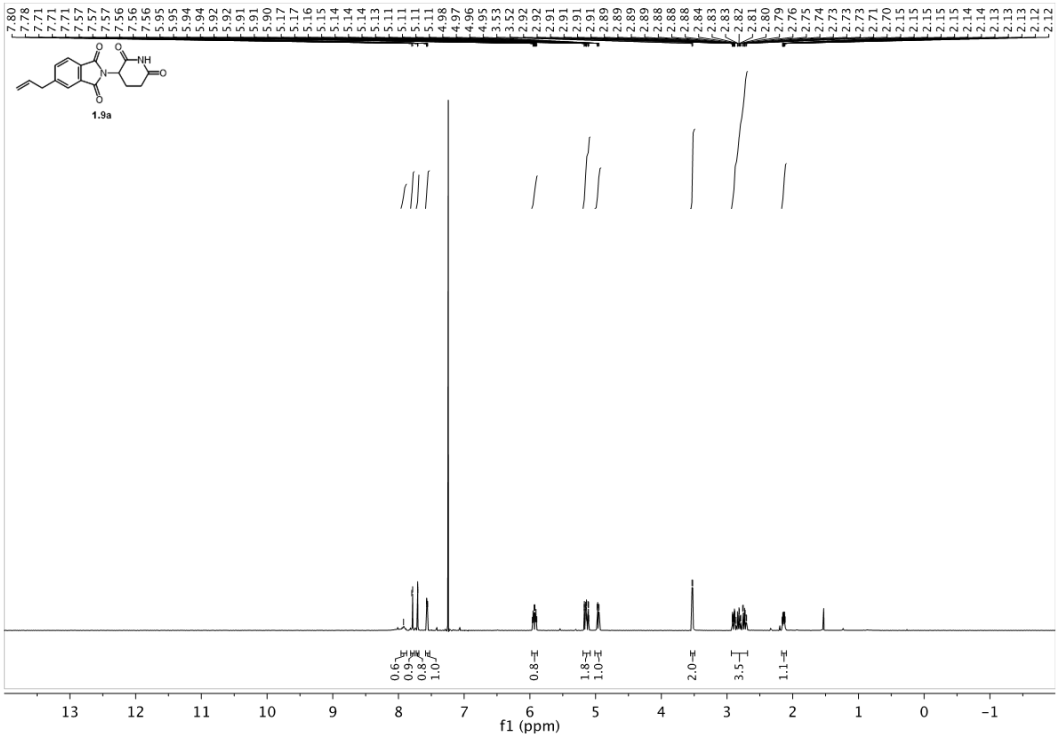

^{1}H NMR (400 MHz) spectrum for 1.9b

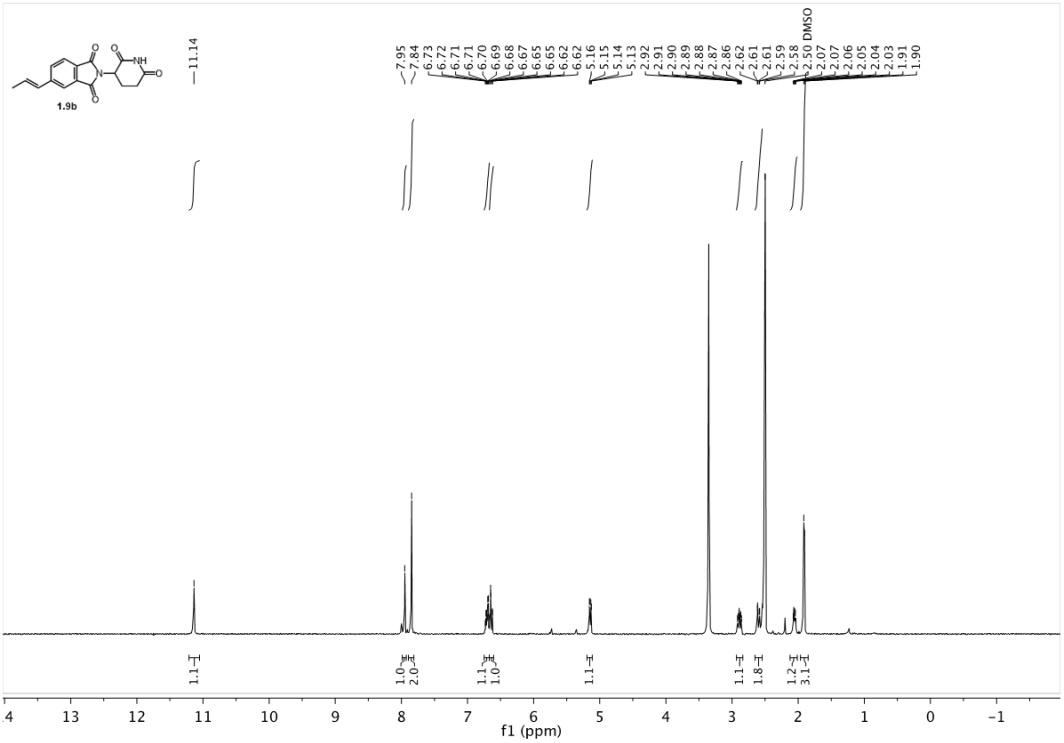

^{1}H NMR (400 MHz) spectrum for 1.9c

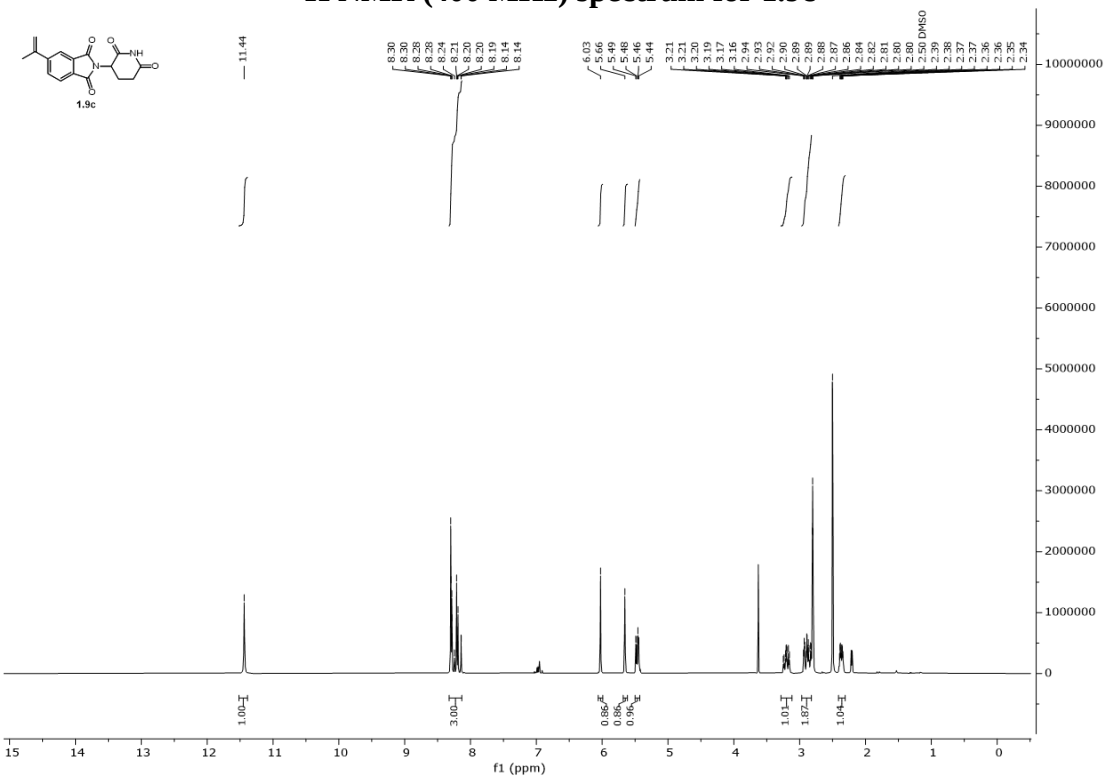

^{1}H NMR (600 MHz) spectrum for 1.9d

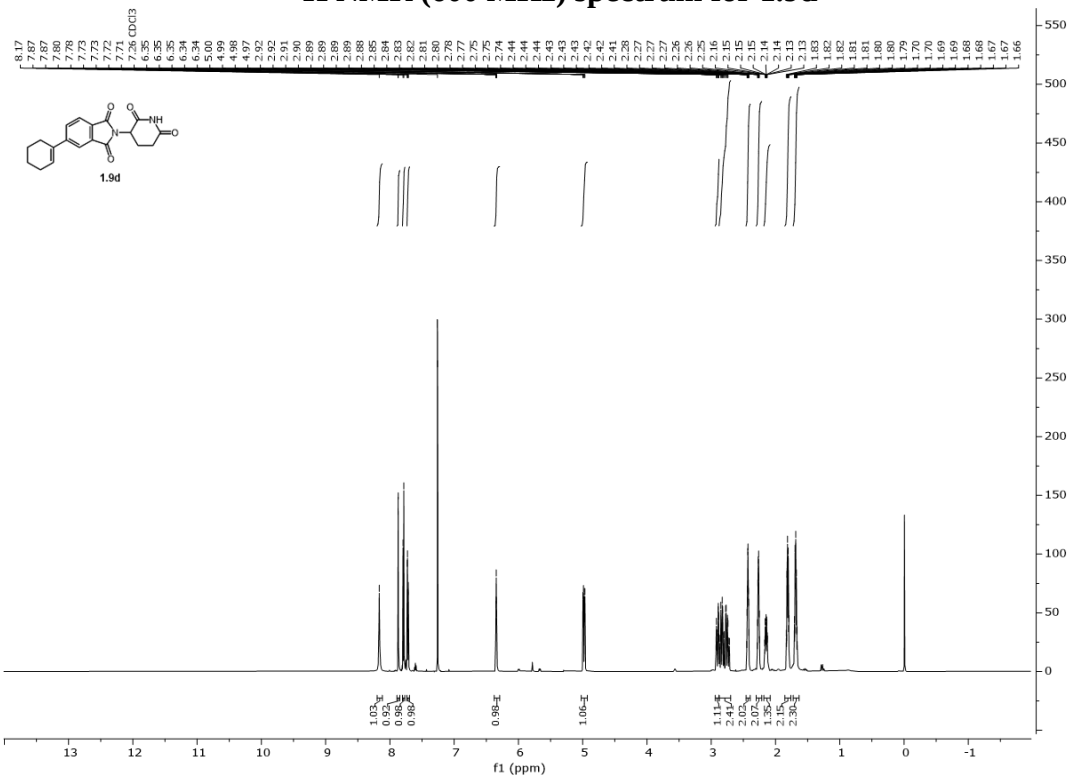

^{1}H NMR (600 MHz) spectrum for 1.9e

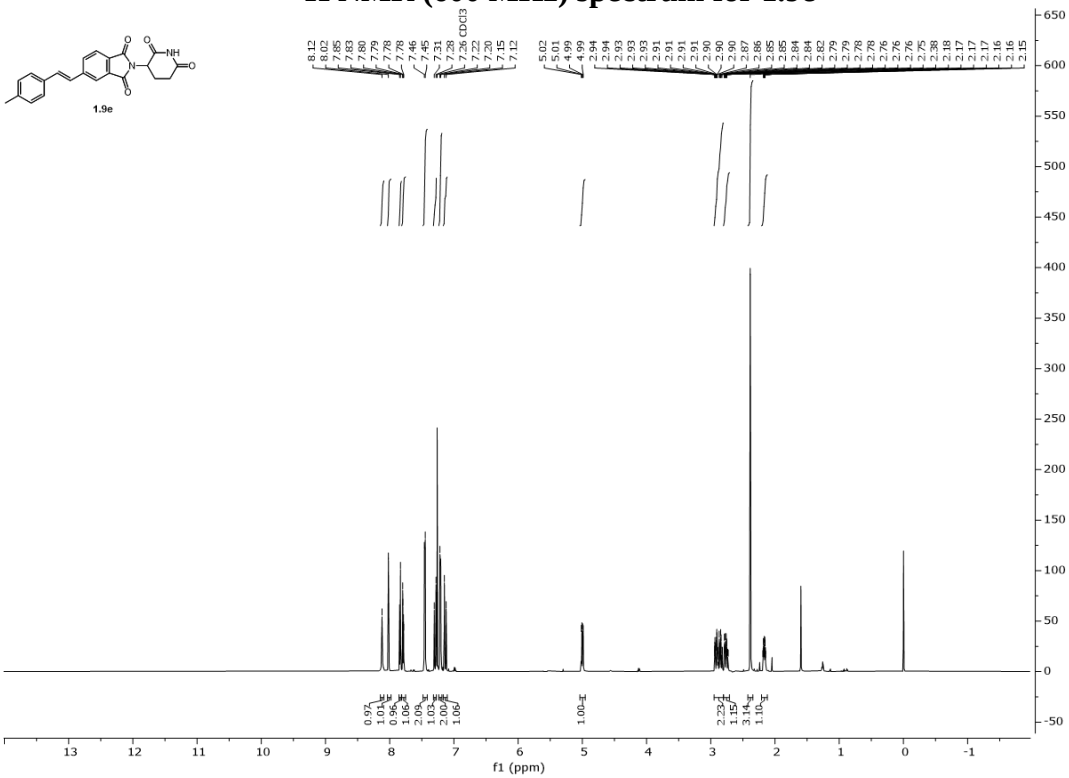

^{1}H NMR (600 MHz) spectrum for 1.9f

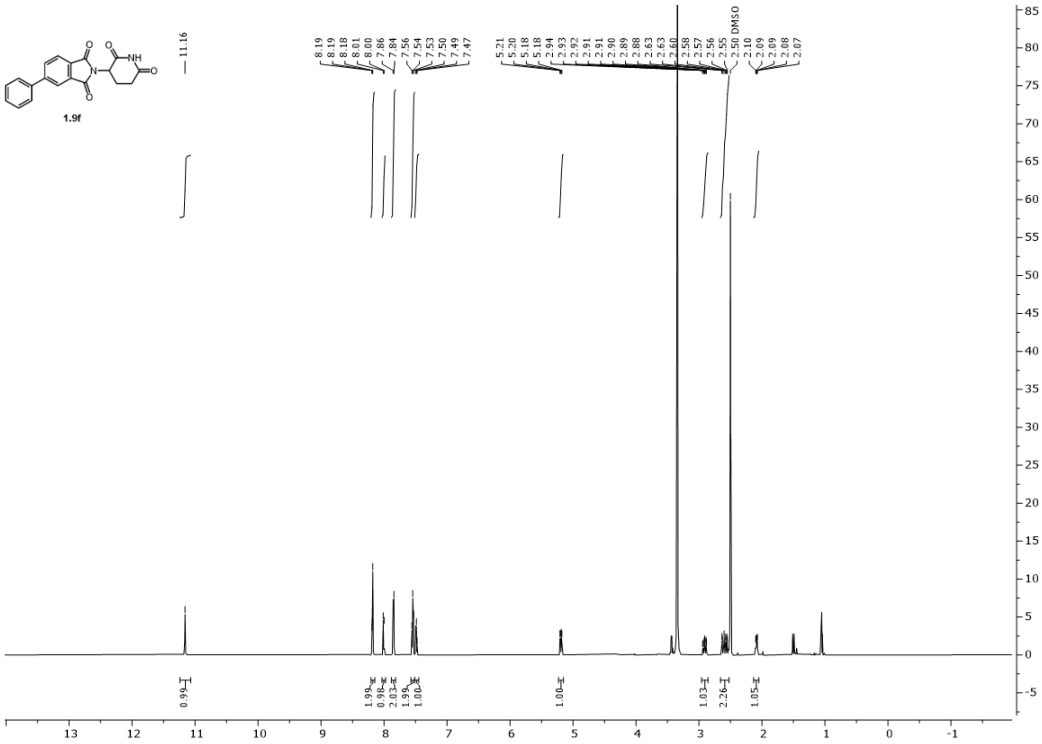

^{1}H NMR (600 MHz) spectrum for 1.9g

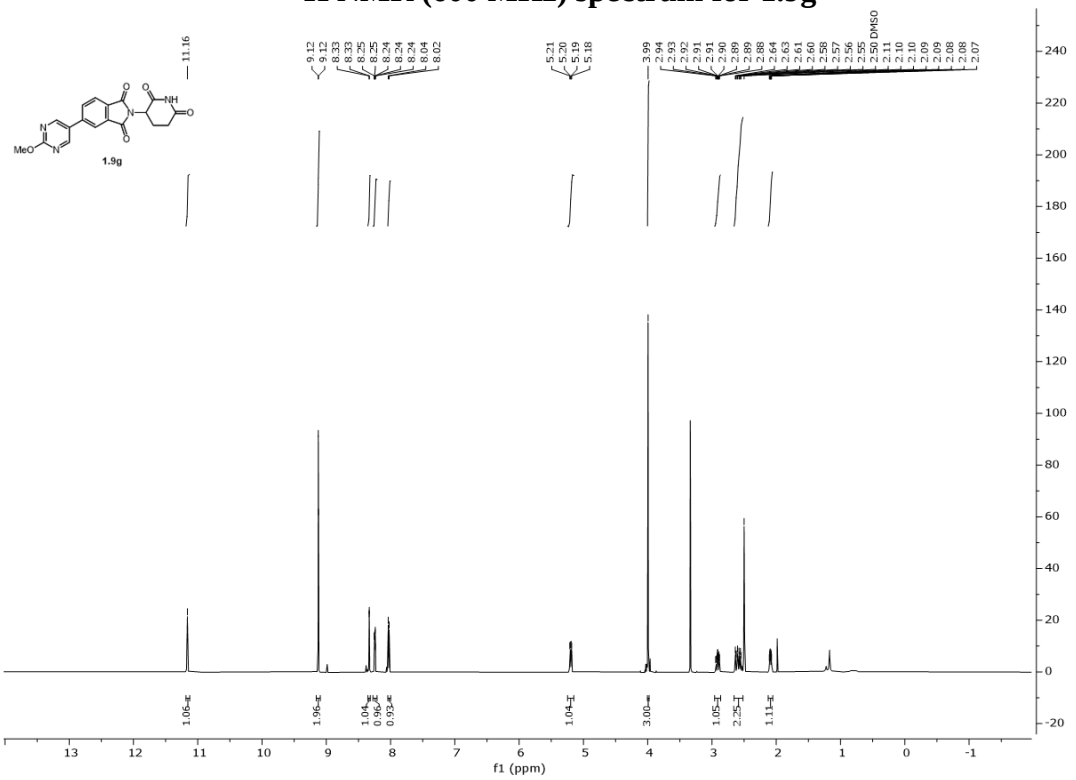

^{1}H NMR (600 MHz) spectrum for 1.9h

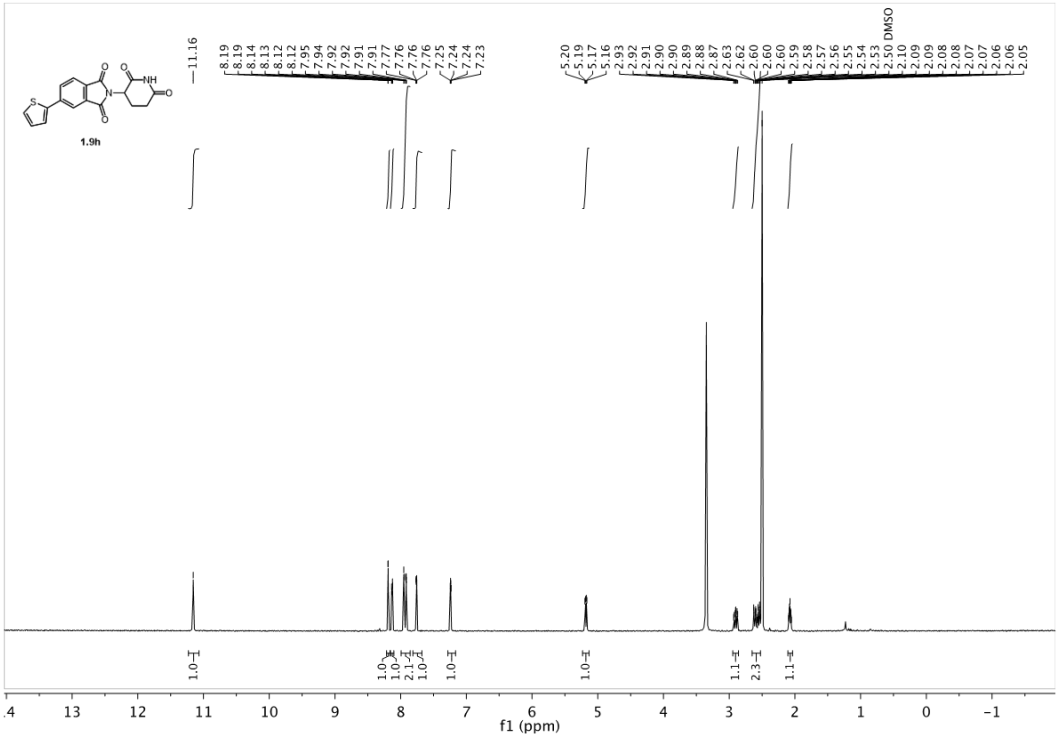

^{1}H NMR (400 MHz) spectrum for 1.9i

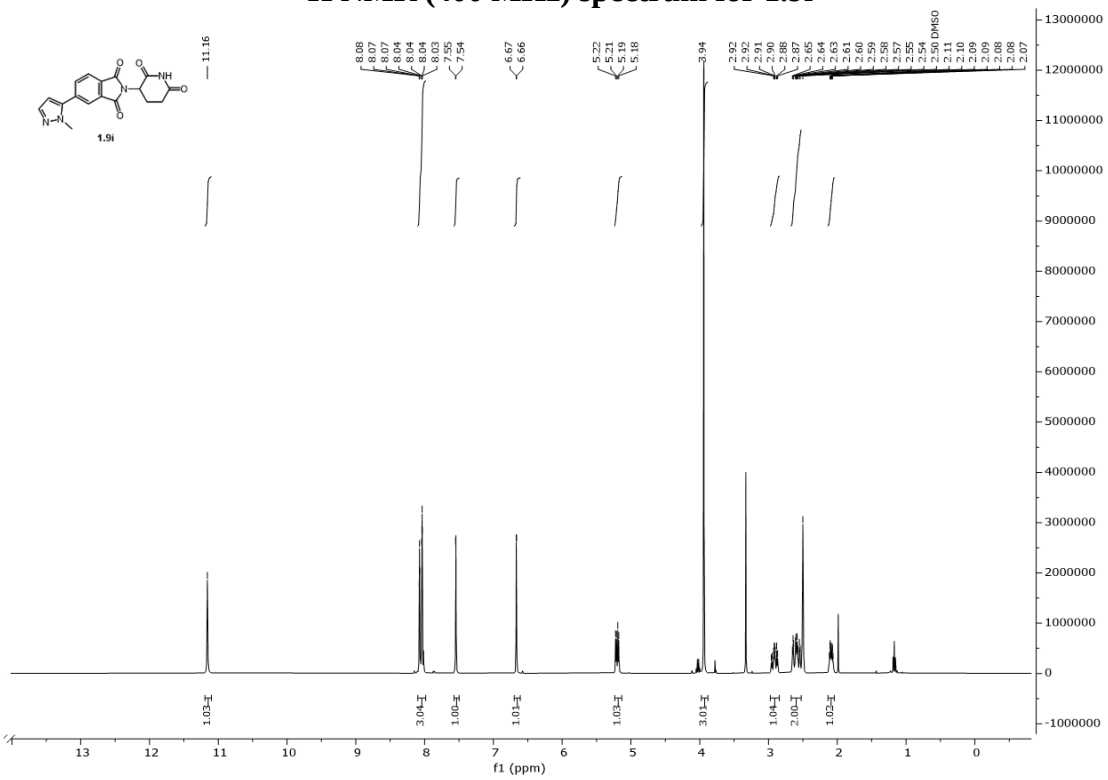

^{1}H NMR (600 MHz) spectrum for 1.9j

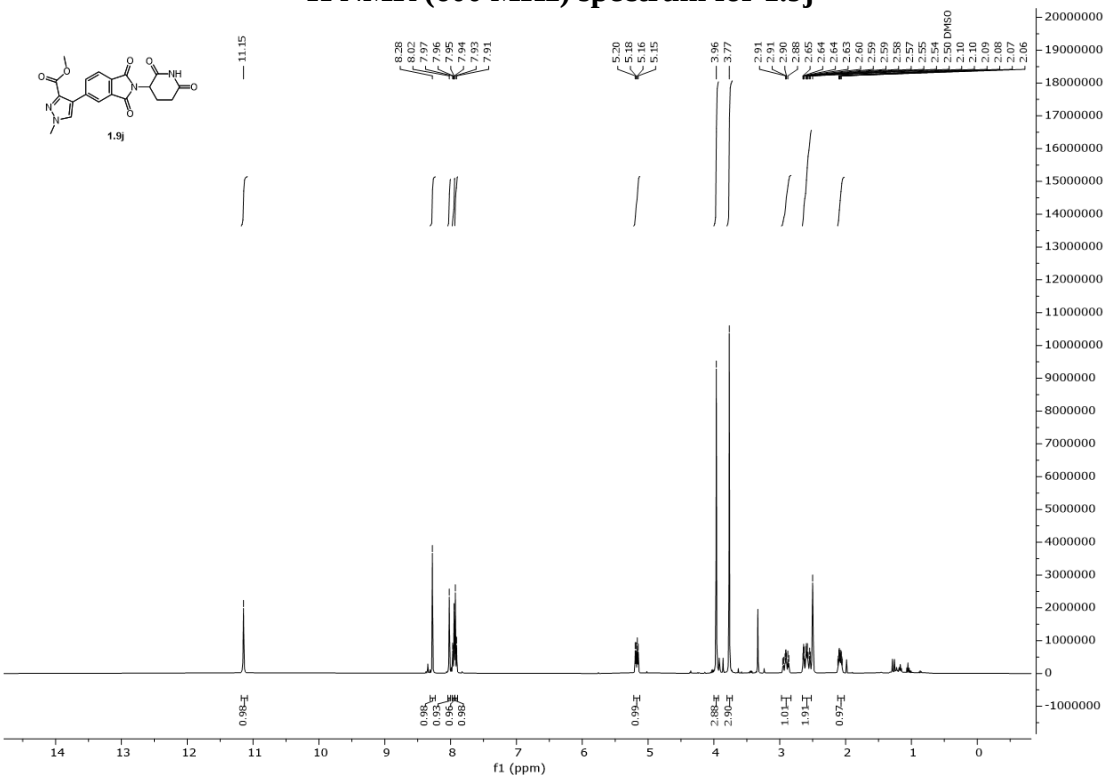

^{1}H NMR (600 MHz) spectrum for 1.9k

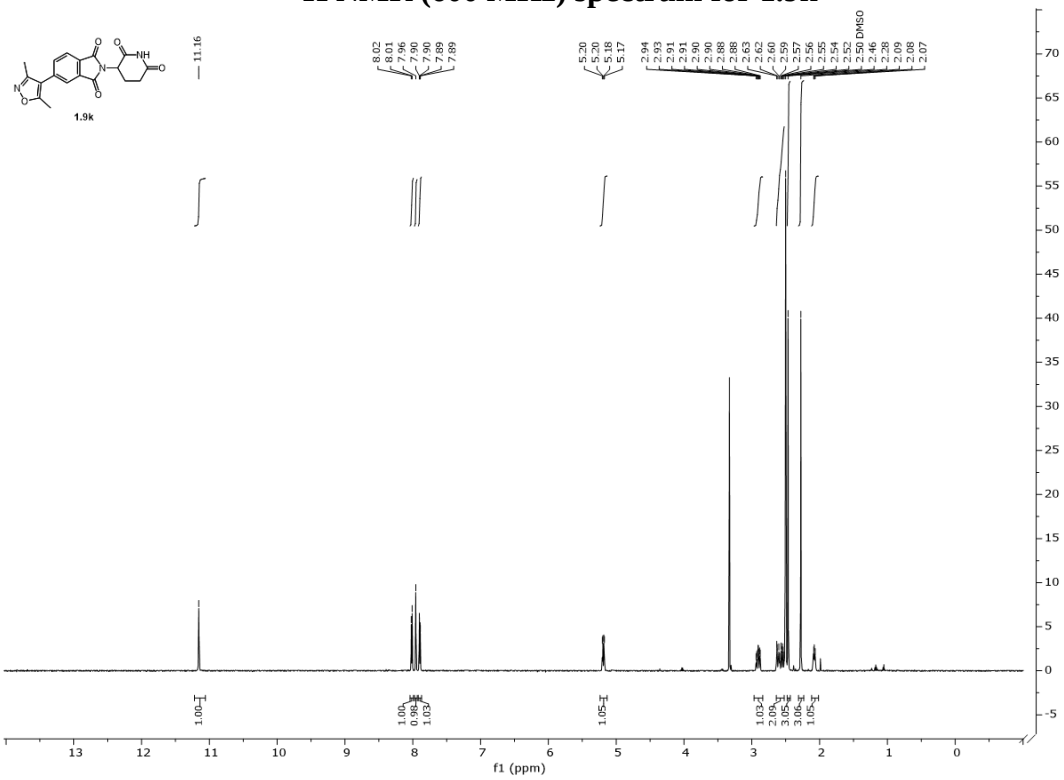

^{1}H NMR (600 MHz) spectrum for 1.9l

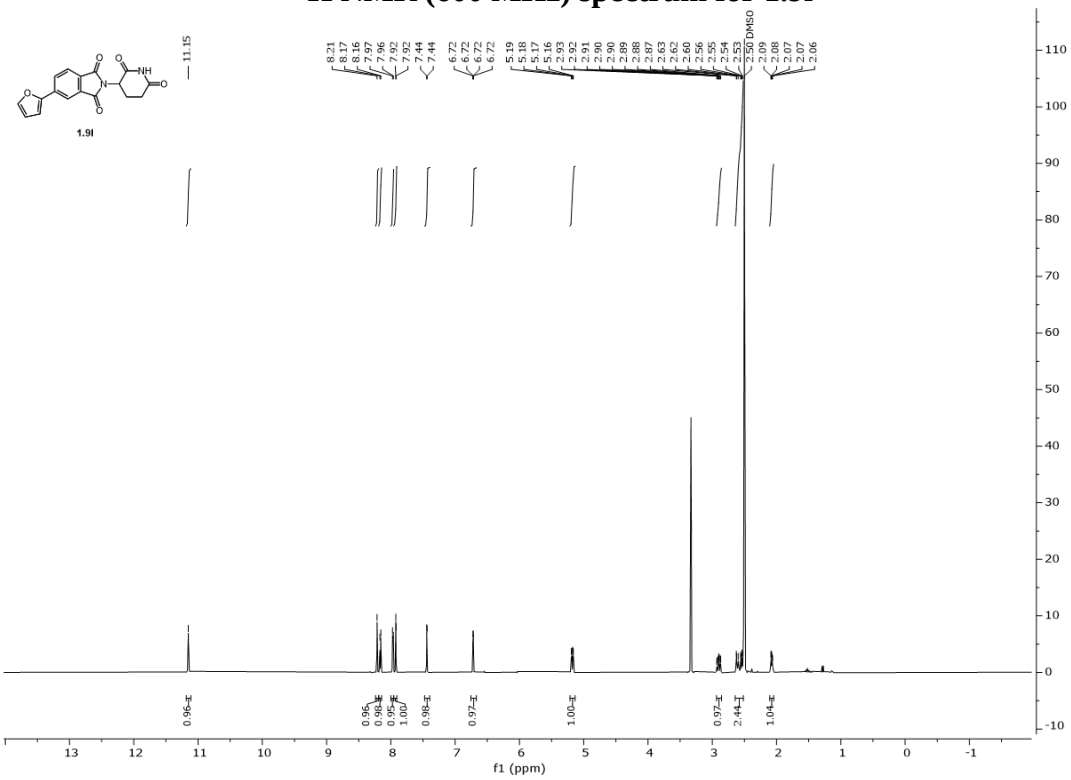

^{13}C NMR Spectra

^{13}C{^{1}H} NMR (101 MHz) spectrum for 1.4a

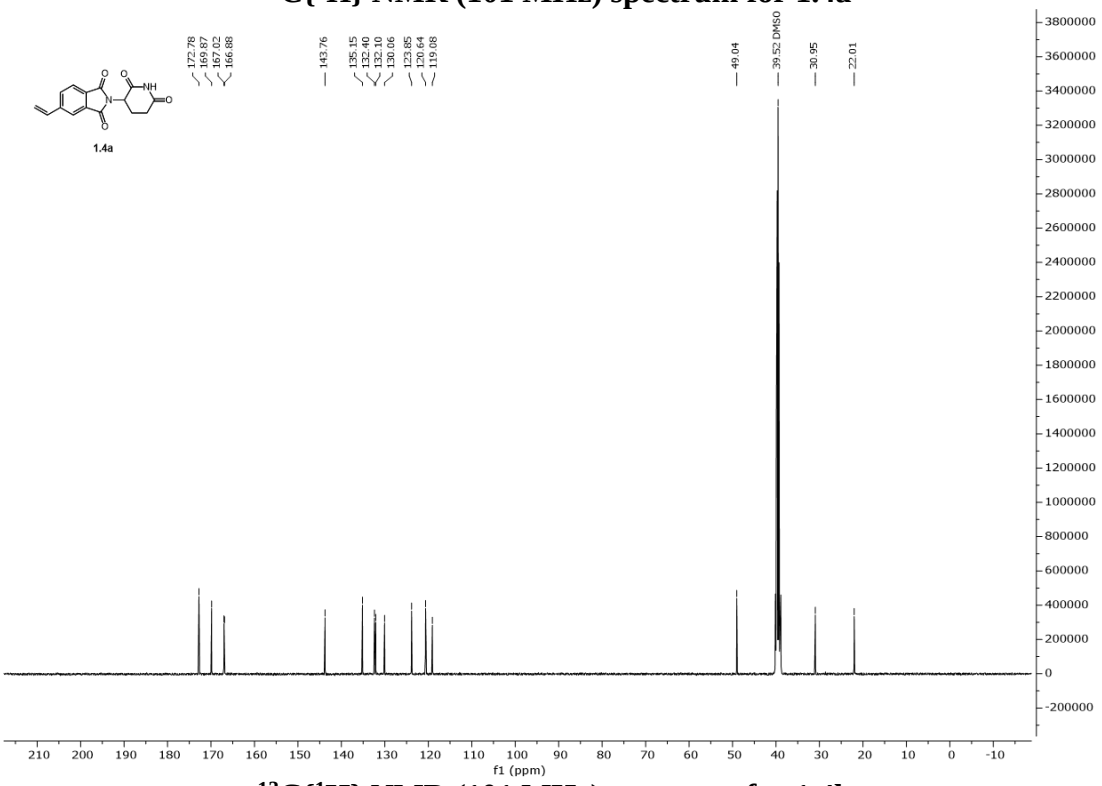

^{13}C{^{1}H} NMR (101 MHz) spectrum for 1.4b

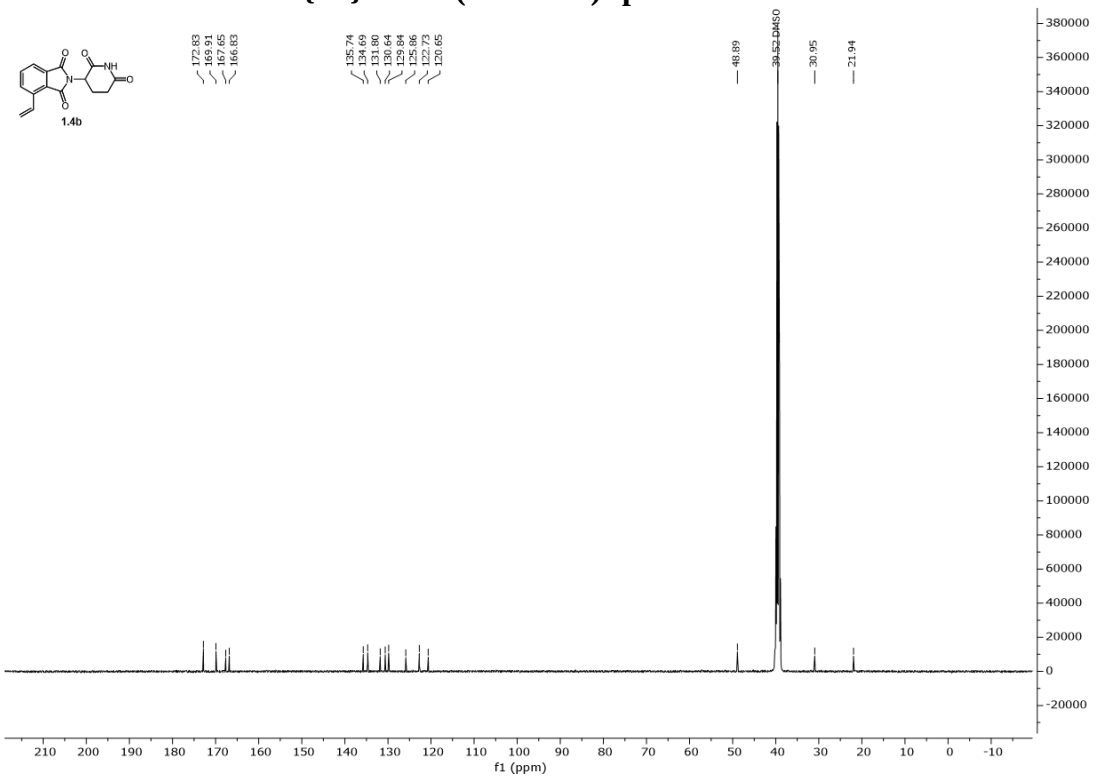

$^{13}C\{^{1}H\}$ NMR (101 MHz) spectrum for 1.4c

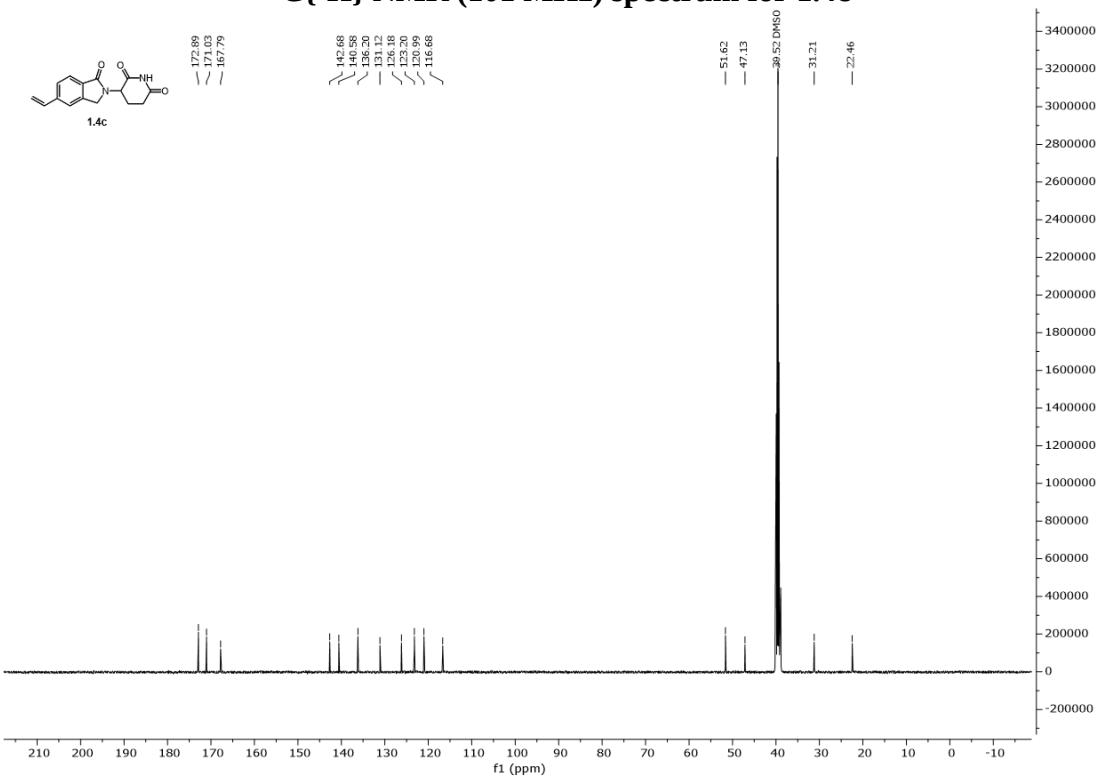

$^{13}C\{^{1}H\}$ NMR (151 MHz) spectrum for 1.4d

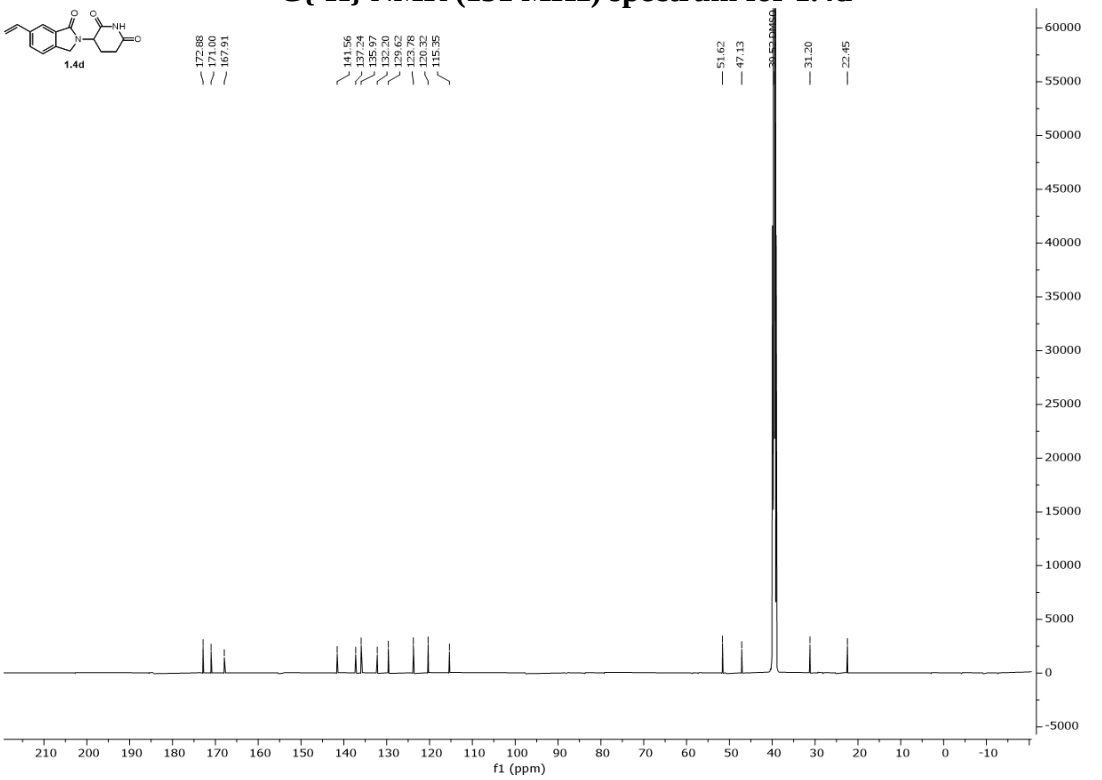

$^{13}C\{^{1}H\}$ NMR (101 MHz) spectrum for 1.4e

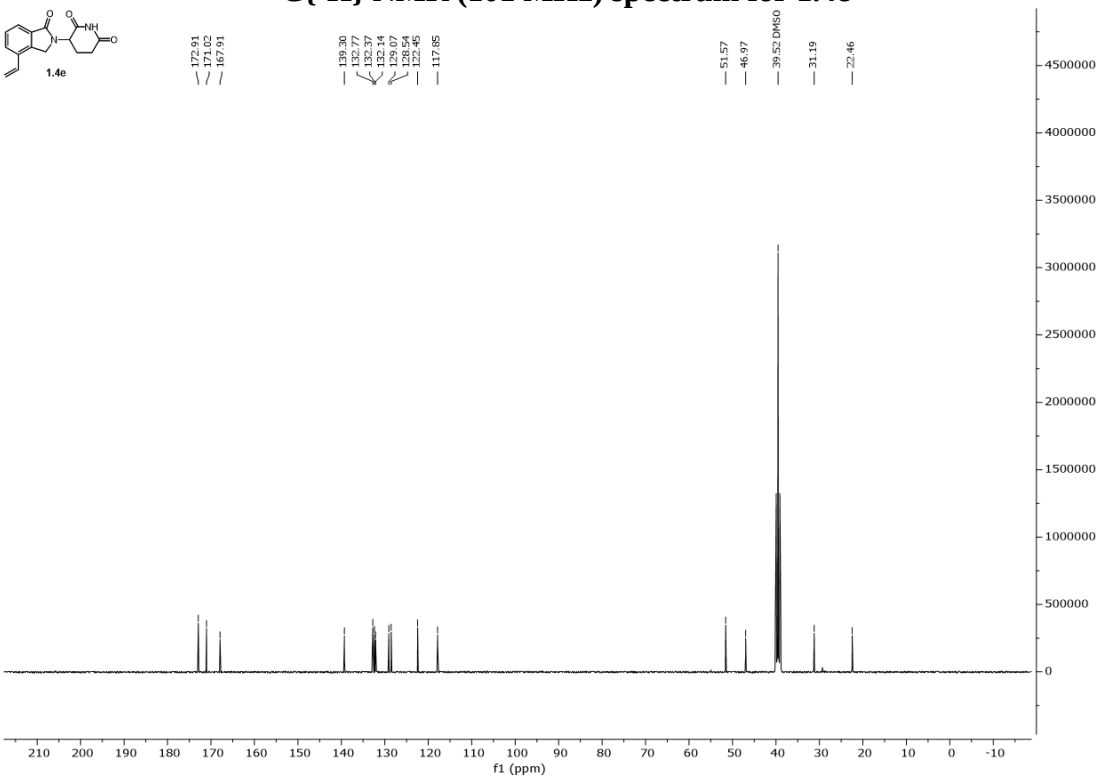

$^{13}C\{^{1}H\}$ NMR (101 MHz) spectrum for 1.4f

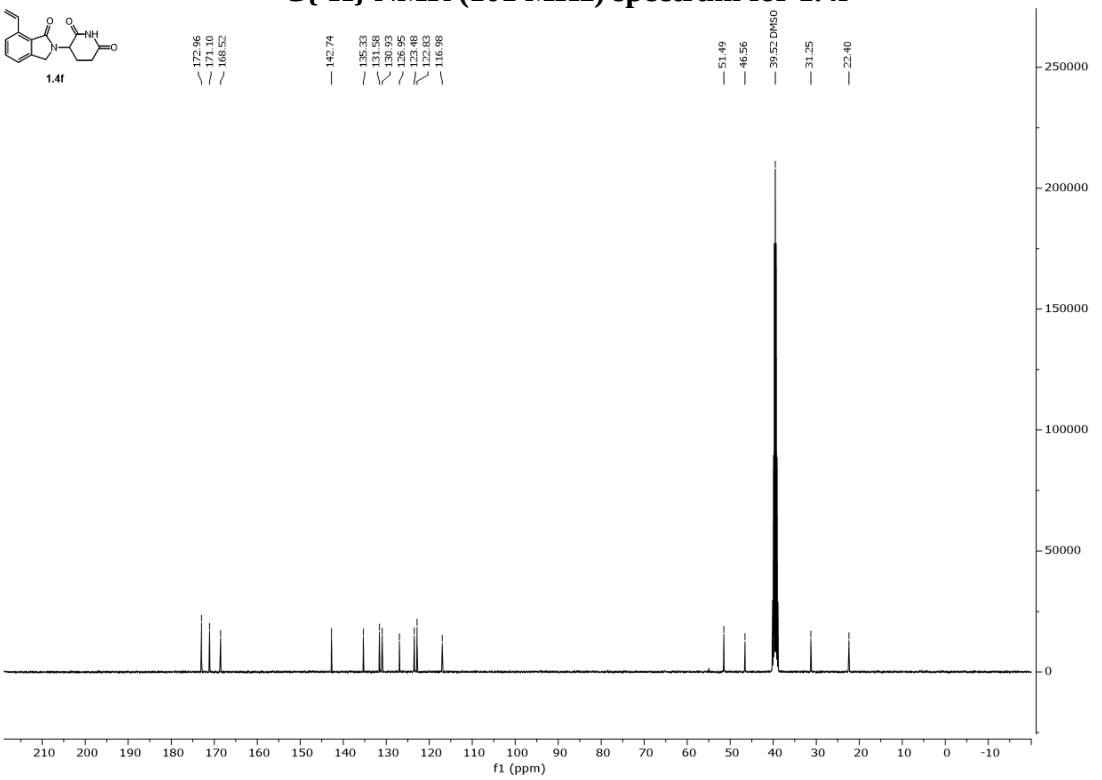

$^{13}C\{^{1}H\}$ NMR (101 MHz) spectrum for 1.8a

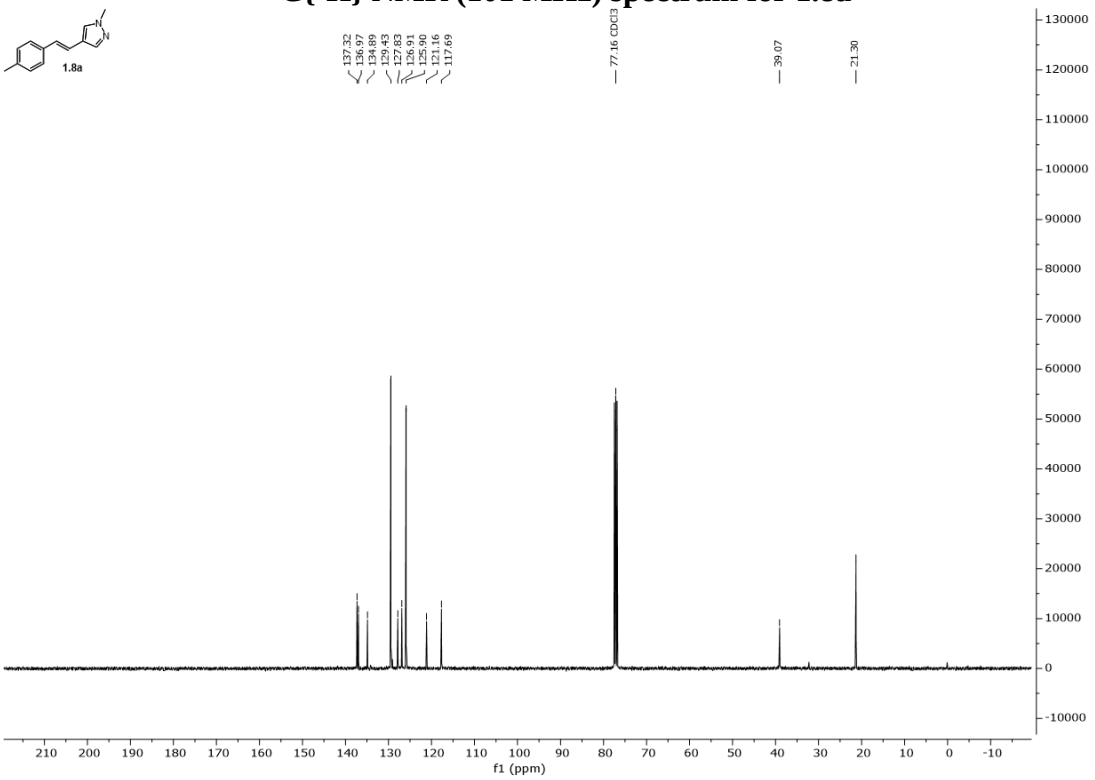

$^{13}C\{^{1}H\}$ NMR (101 MHz) spectrum for 1.8b

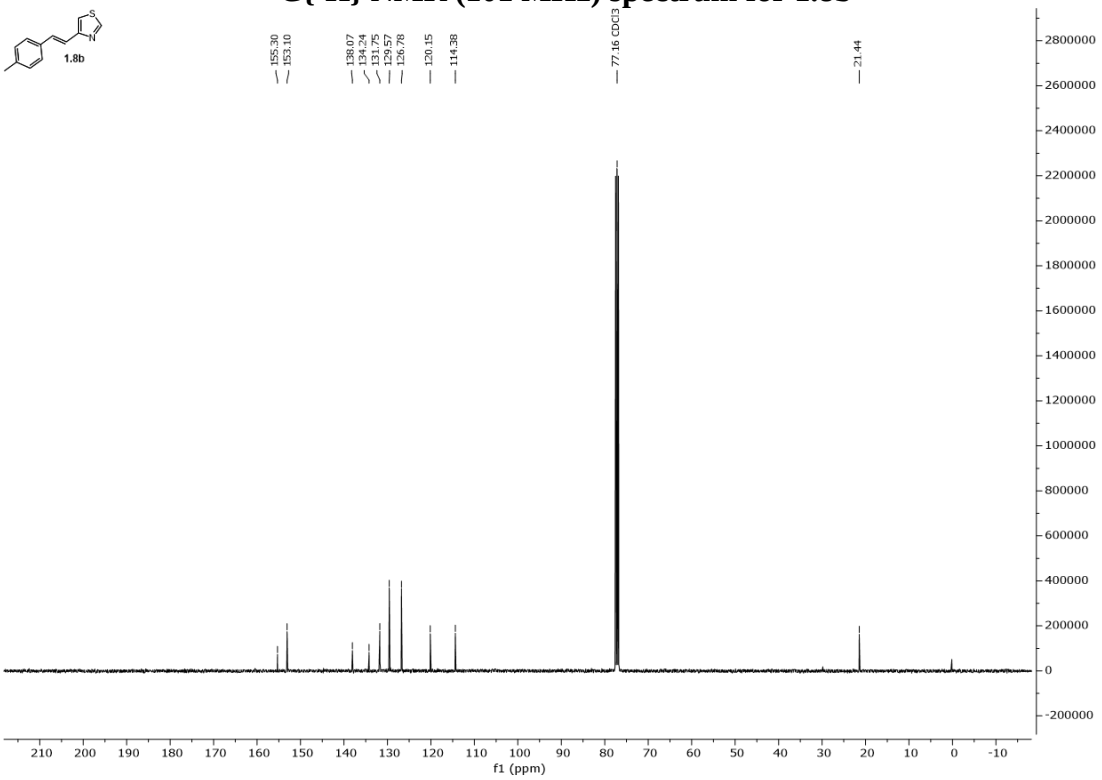

$^{13}C\{^{1}H\}$ NMR (101 MHz) spectrum for 1.8c

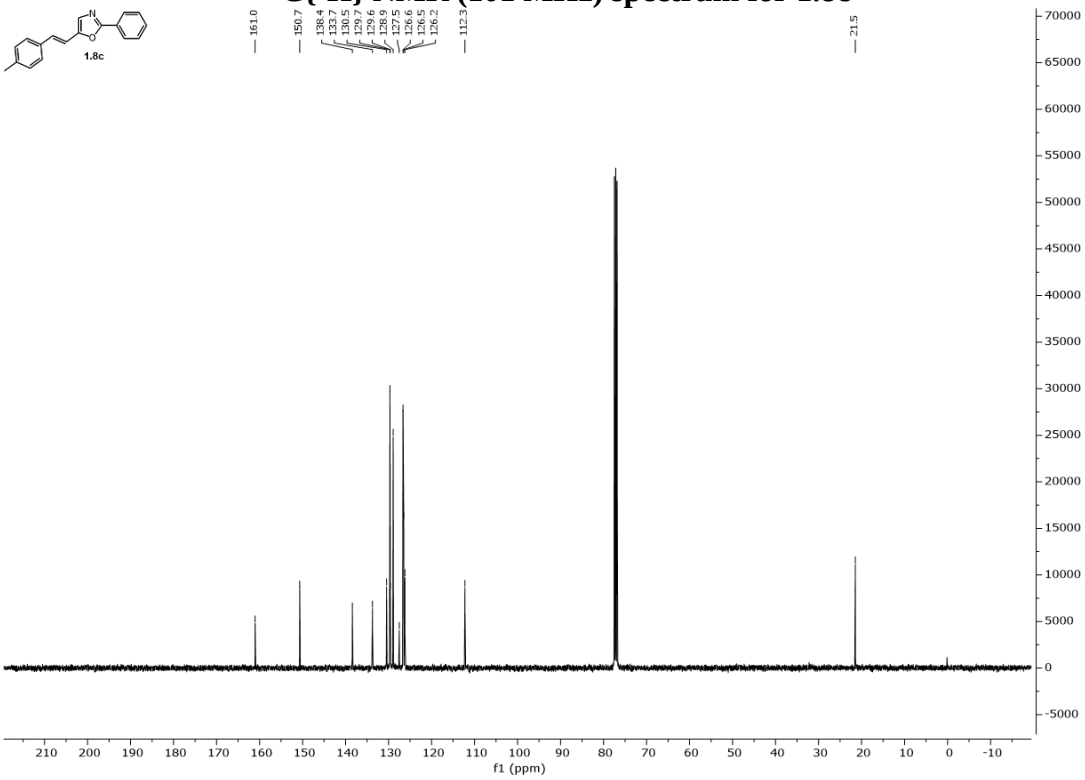

$^{13}C\{^{1}H\}$ NMR (101 MHz) spectrum for 1.8d

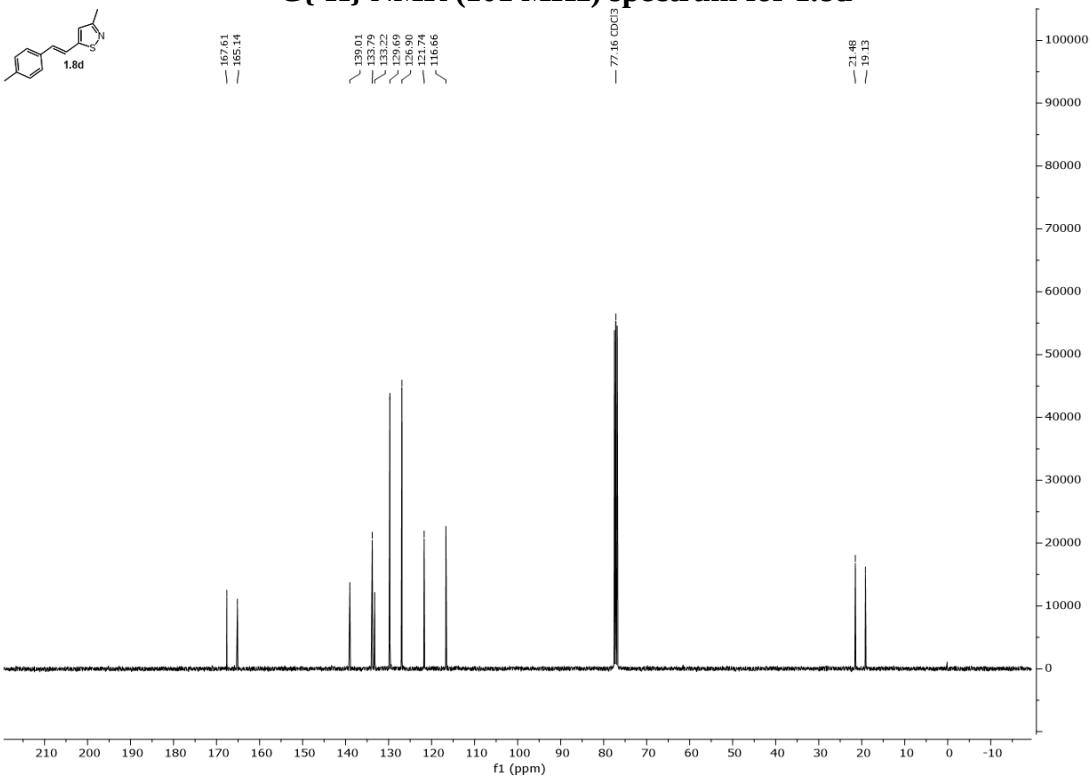

$^{13}C\{^{1}H\}$ NMR (101 MHz) spectrum for 1.8f

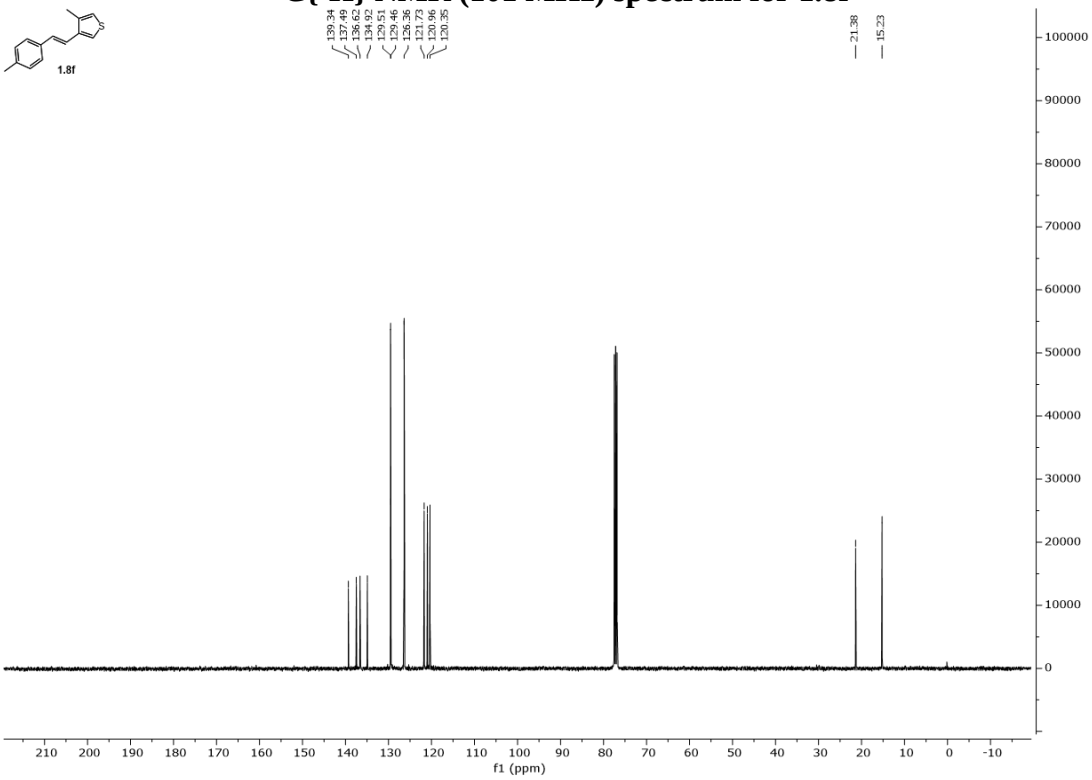

$^{13}C\{^{1}H\}$ NMR (101 MHz) spectrum for 1.8g

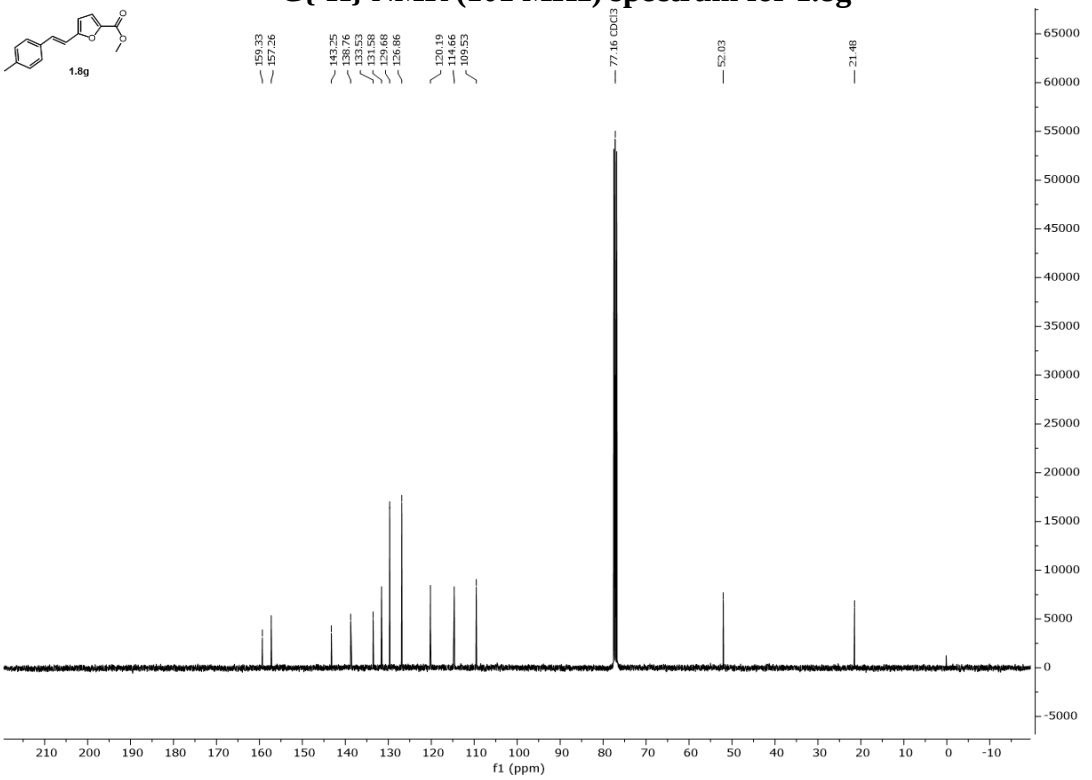

$^{13}C\{^{1}H\}$ NMR (101 MHz) spectrum for 1.9a

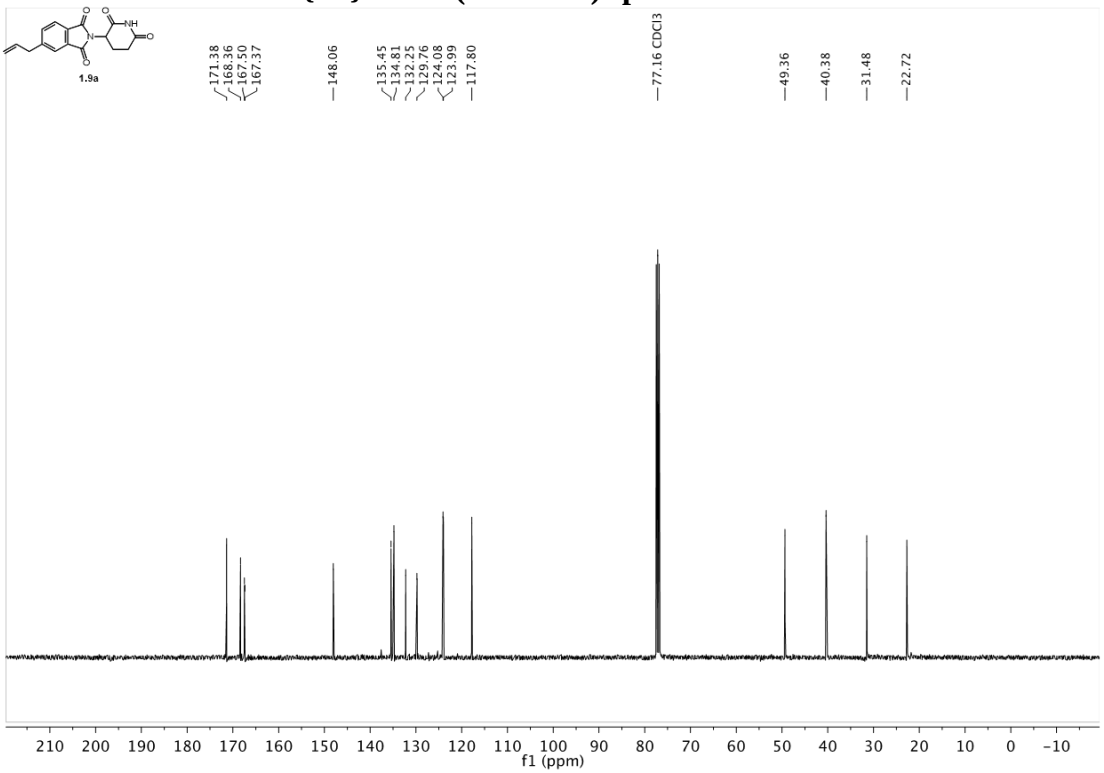

$^{13}C\{^{1}H\}$ NMR (101 MHz) spectrum for 1.9b

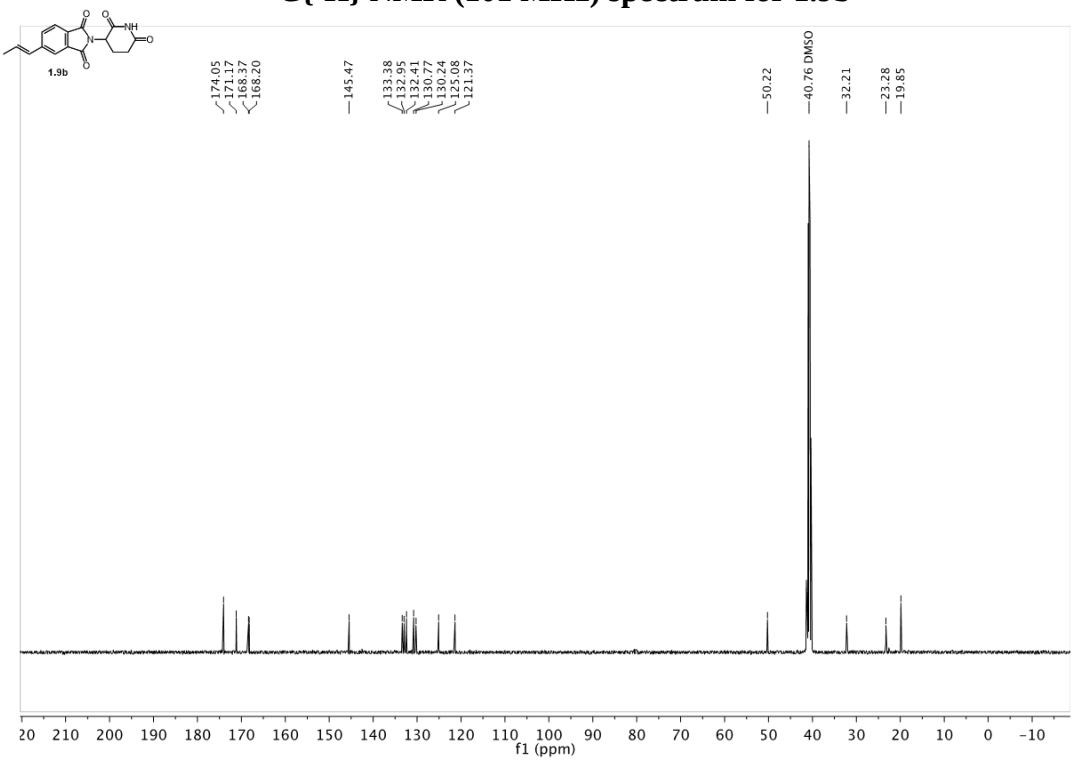

$^{13}C\{^{1}H\}$ NMR (101 MHz) spectrum for 1.9c

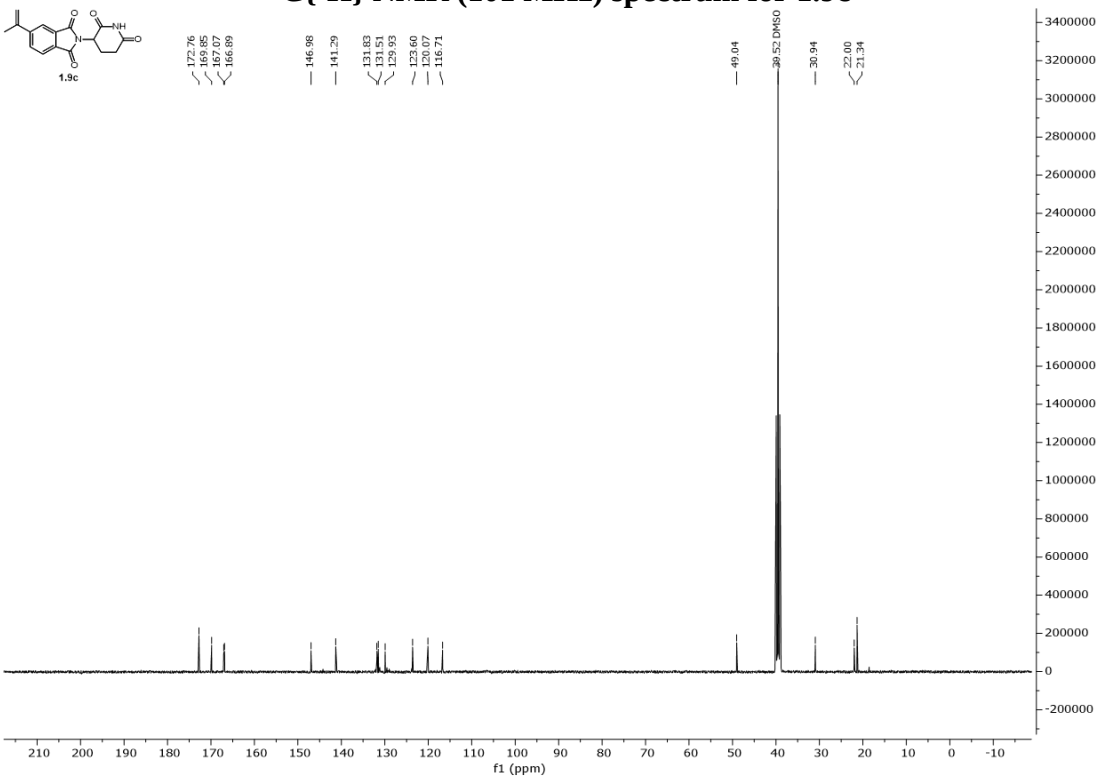

$^{13}C\{^{1}H\}$ NMR (101 MHz) spectrum for 1.9d

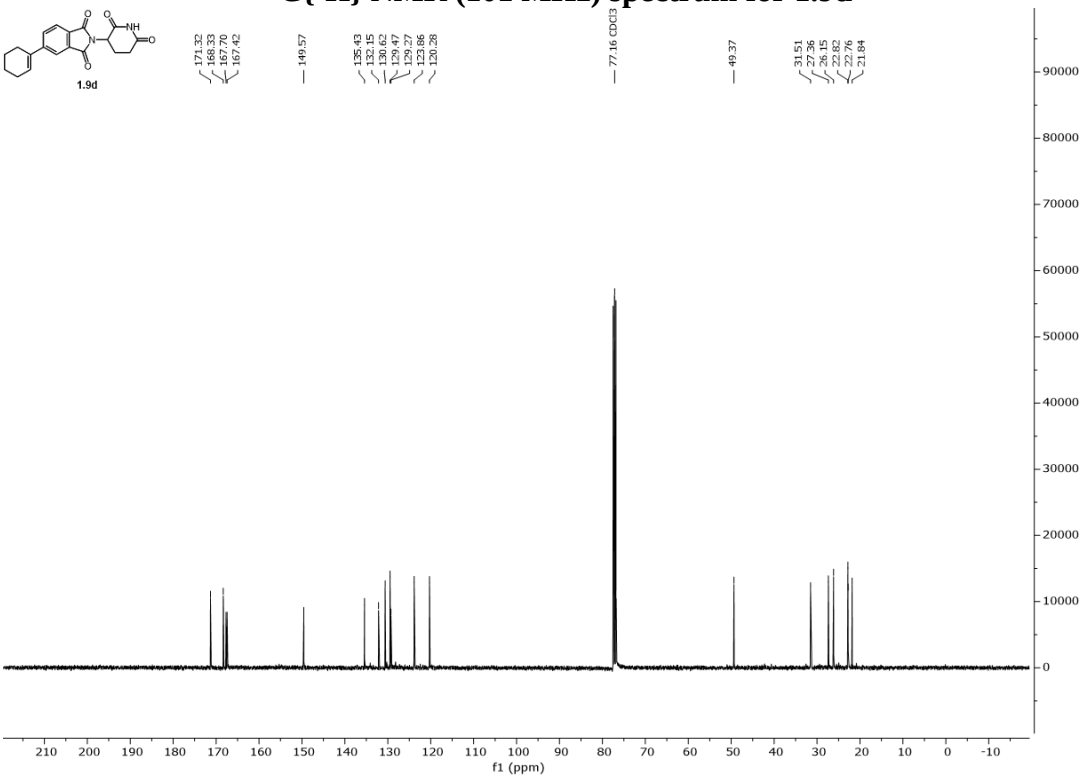

$^{13}C\{^{1}H\}$ NMR (101 MHz) spectrum for 1.9e

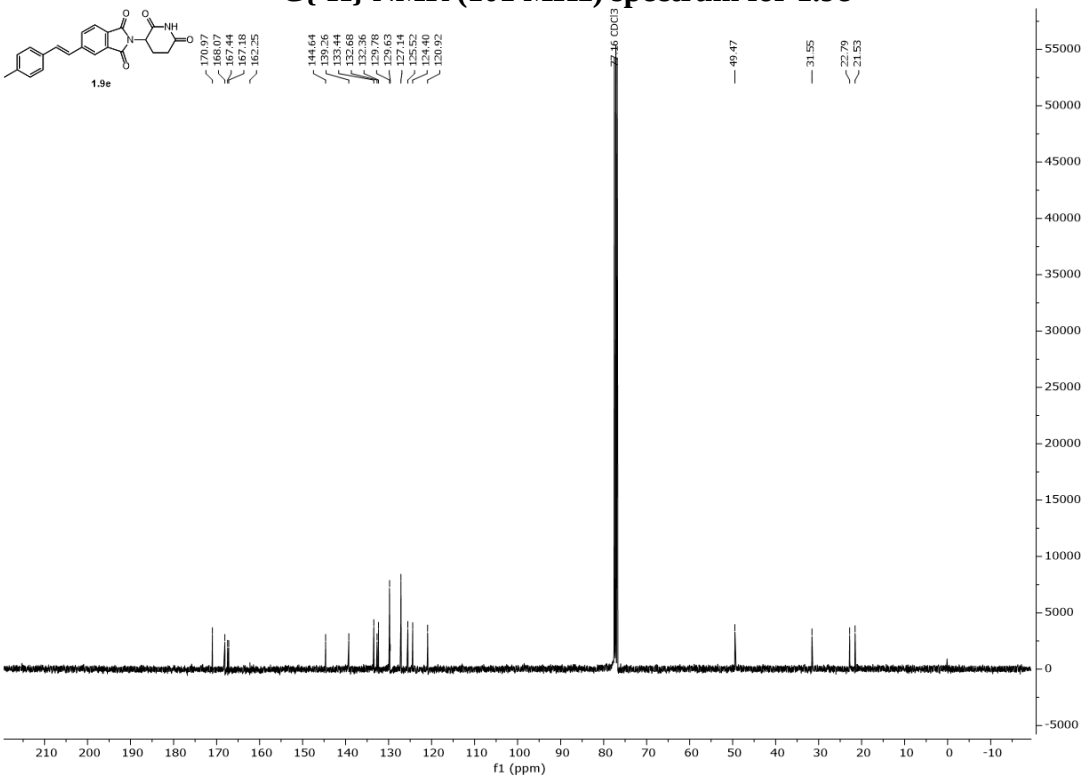

$^{13}C\{^{1}H\}$ NMR (101 MHz) spectrum for 1.9g

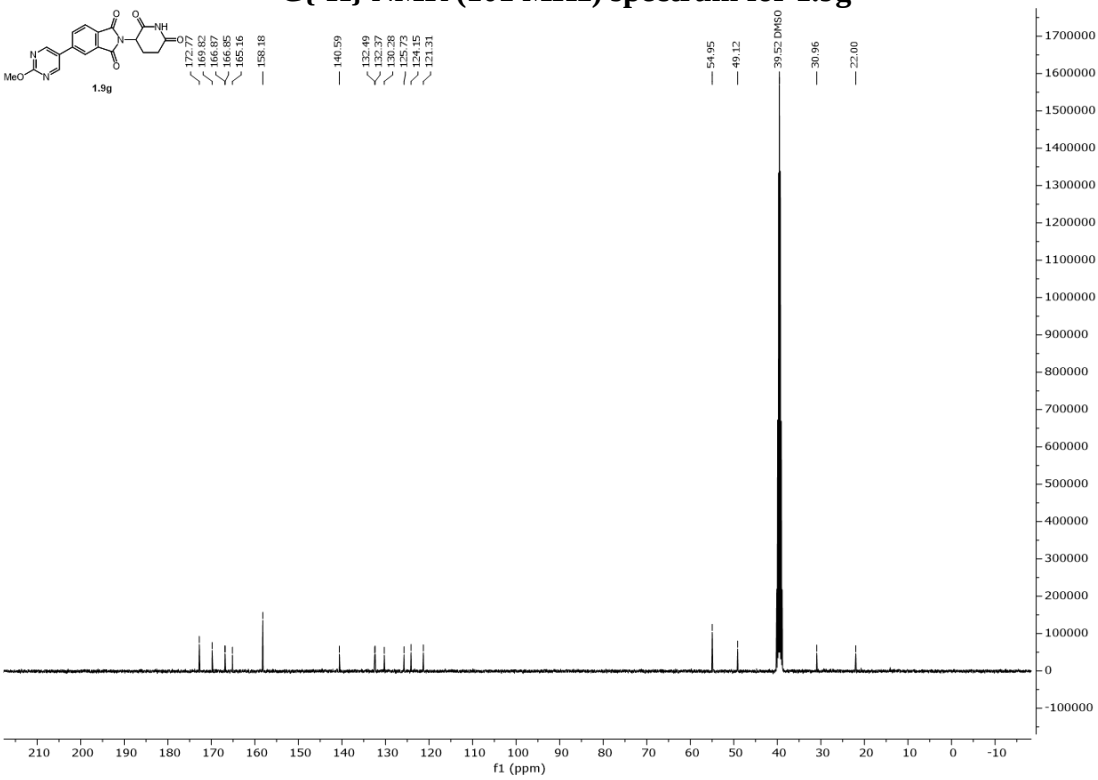

$^{13}C\{^{1}H\}$ NMR (101 MHz) spectrum for 1.9h

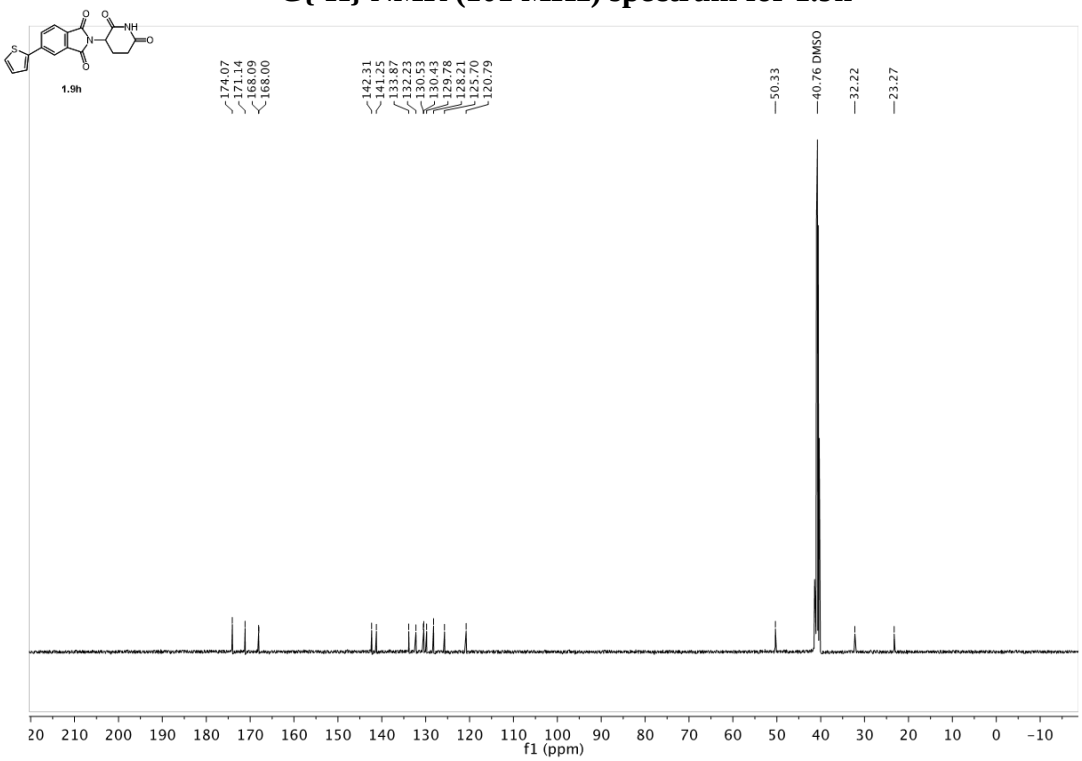

$^{13}C\{^{1}H\}$ NMR (101 MHz) spectrum for 1.9i

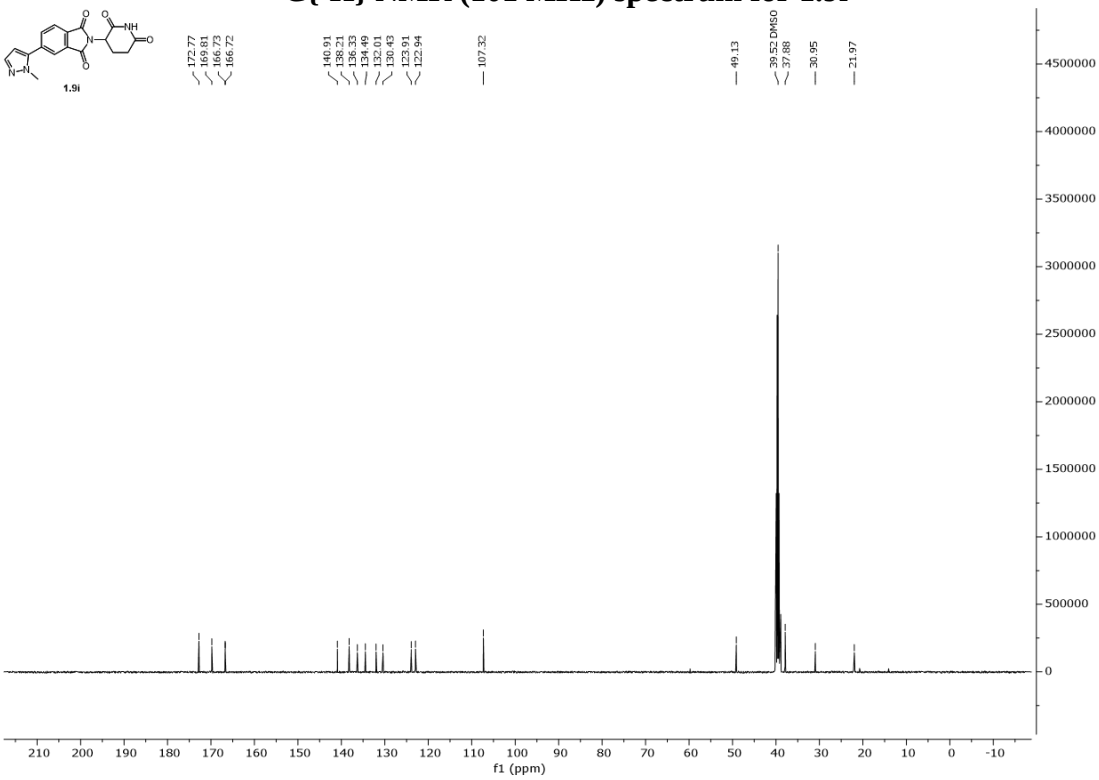

$^{13}C\{^{1}H\}$ NMR (101 MHz) spectrum for 1.9j

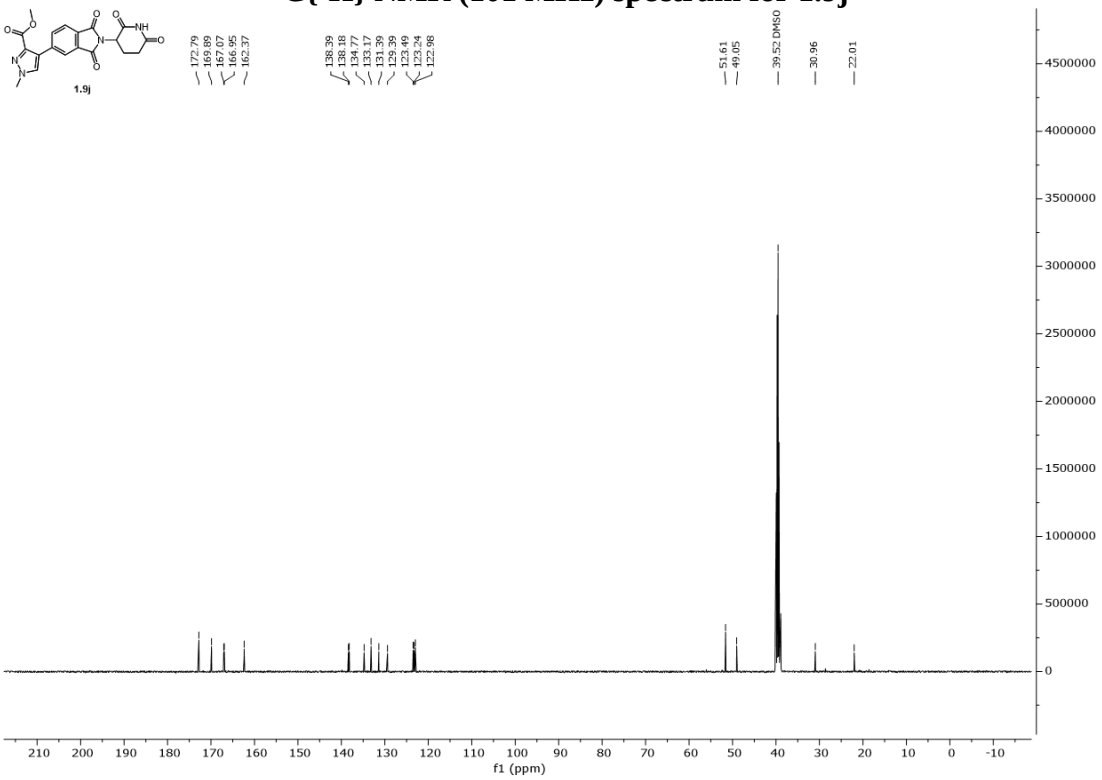

$^{13}C\{^{1}H\}$ NMR (101 MHz) spectrum for 1.9k

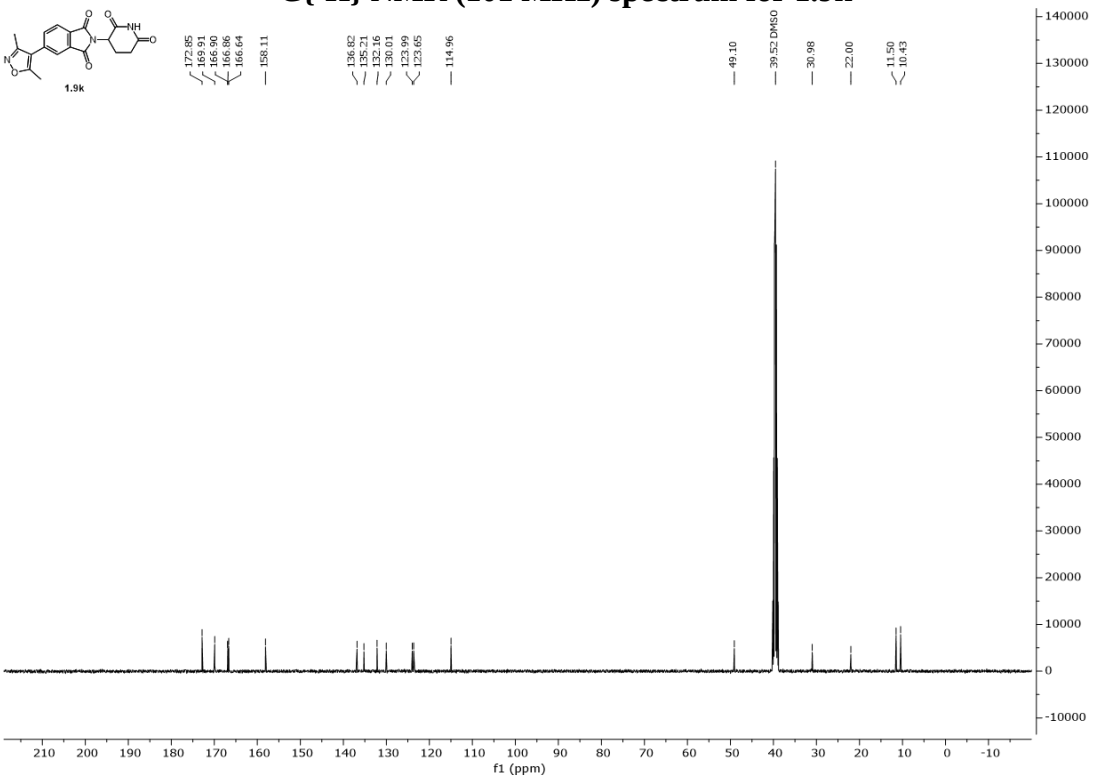

$^{13}C\{^{1}H\}$ NMR (101 MHz) spectrum for 1.9l

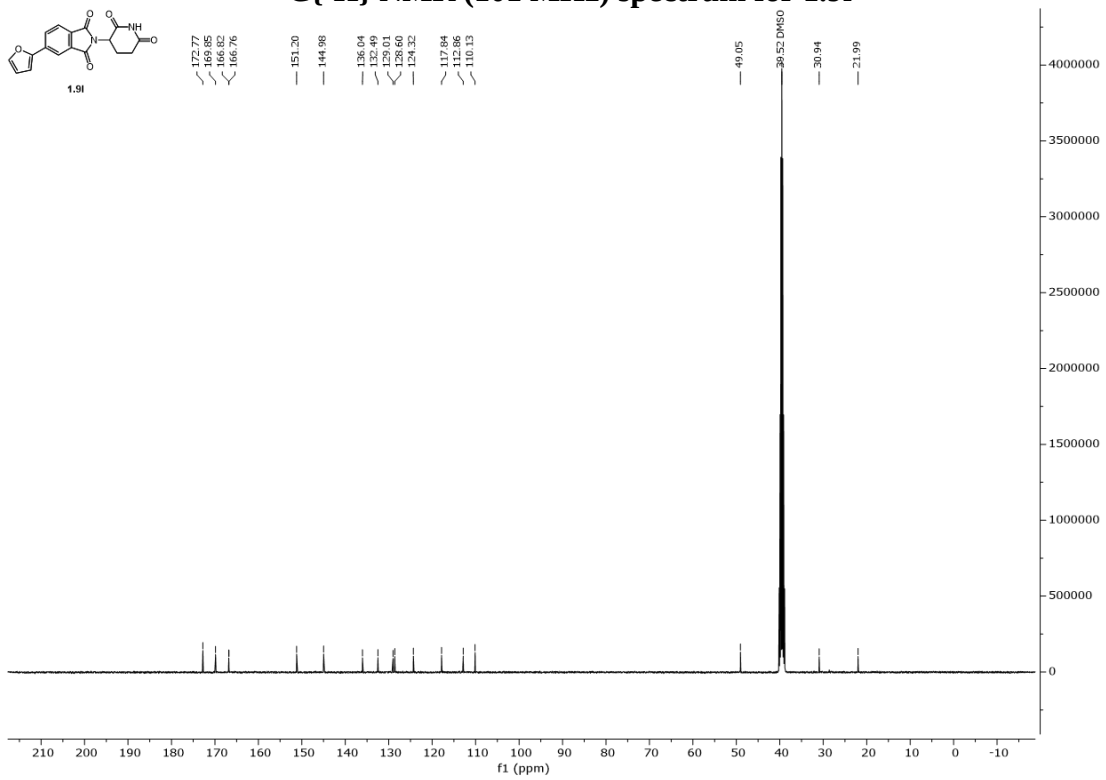

Section 6: Chromatographic Data

Racemic SFC Chromatogram, 1.3c

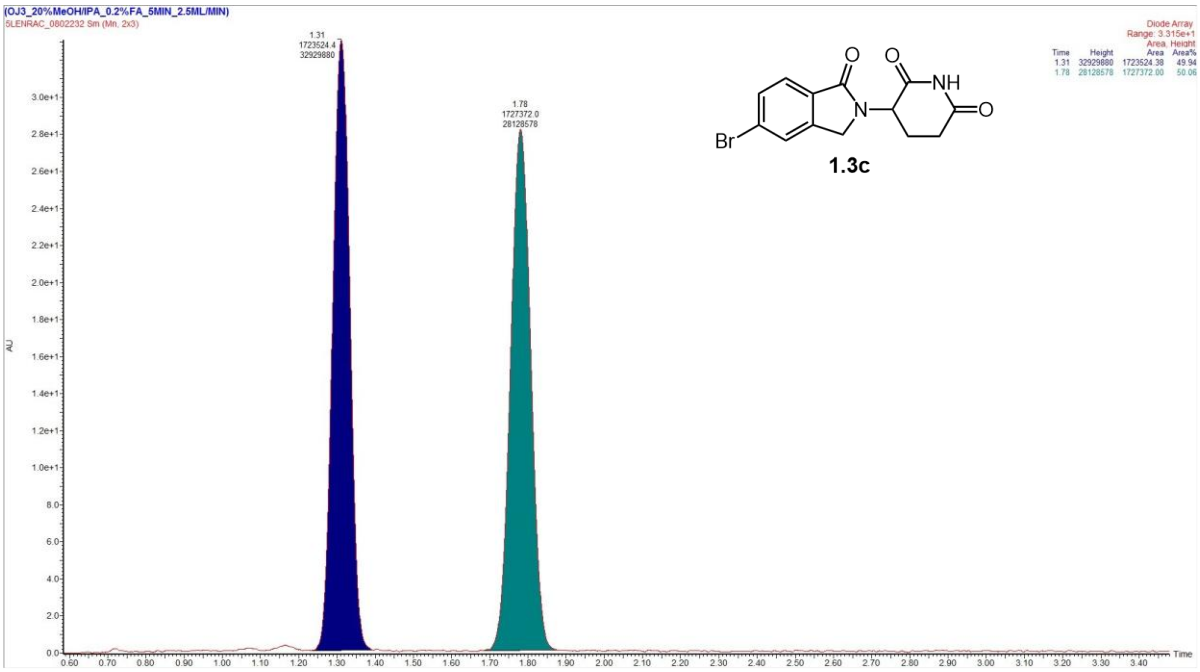

SFC Chromatogram, (*S*)-1.3c

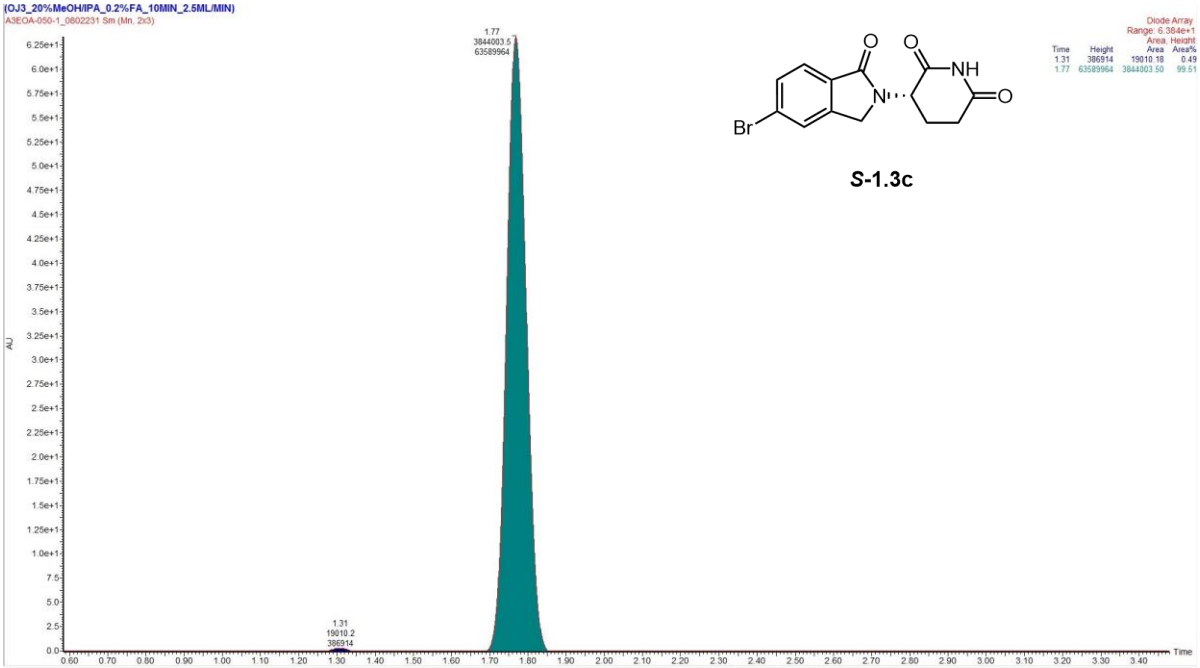

Racemic SFC Chromatogram, 1.4c

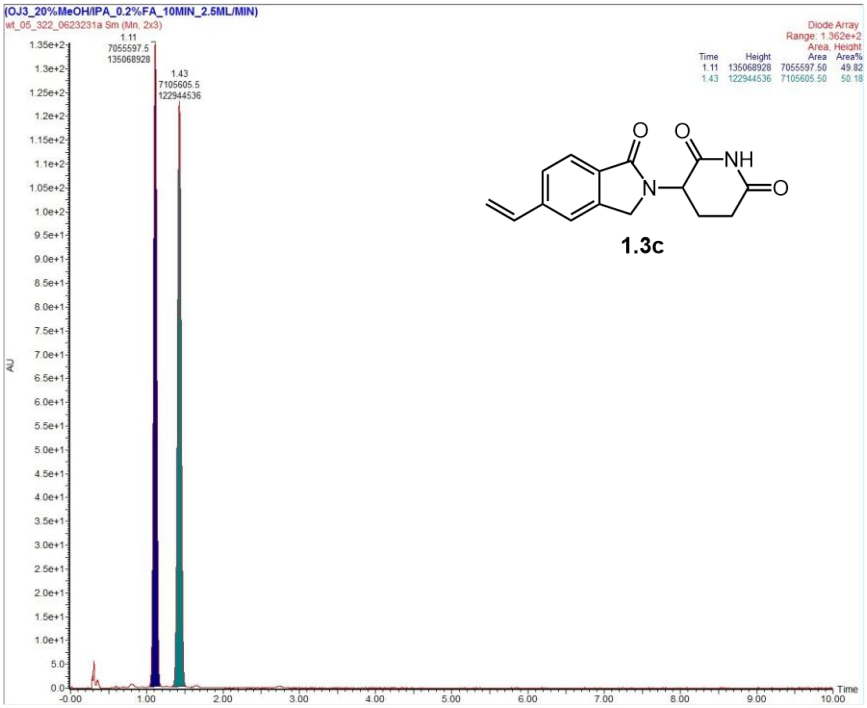

SFC Chromatogram, (*S*)-1.4c

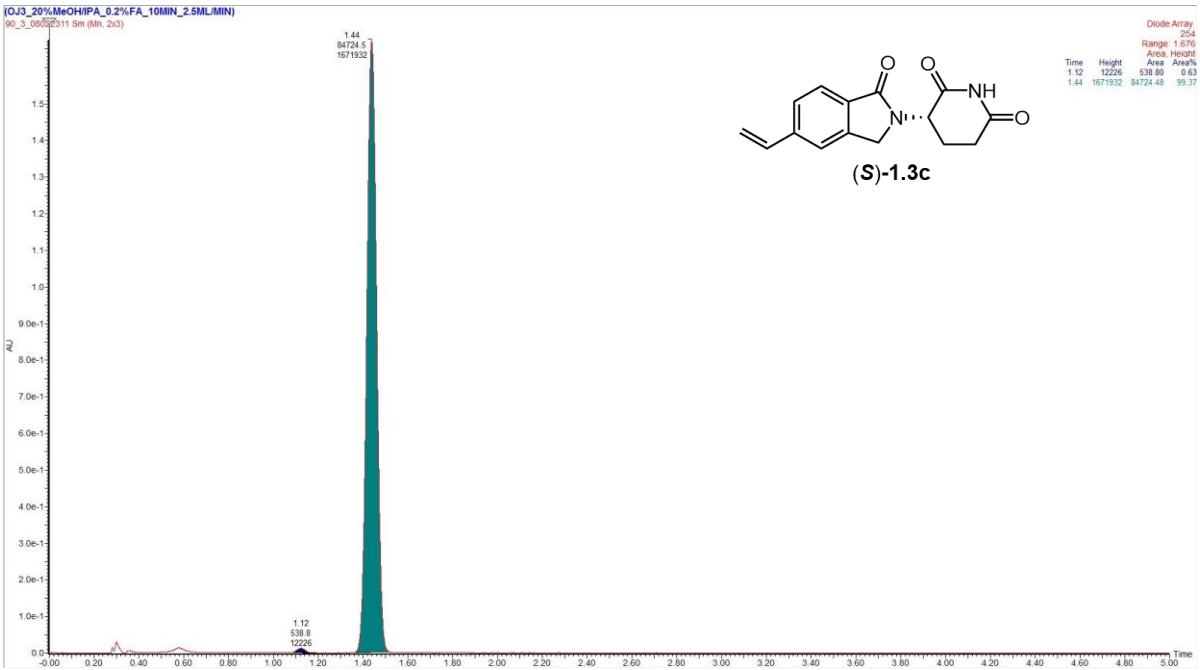

Section 7: References

(1) Yamamoto, T.; Yamakawa, T., Nickel-Catalyzed Vinylation of Aryl Chlorides and Bromides with Vinyl ZnBr·MgBrCl. *J. Org. Chem.* **2009,** *74*, 3603-3605.

(2) Stewart, S. G.; Braun, C. J.; Ng, S.-L.; Polomska, M. E.; Karimi, M.; Abraham, L. J., New thalidomide analogues derived through Sonogashira or Suzuki reactions and their TNF expression inhibition profiles. *Bioorg. Med. Chem. Lett.* **2010,** *18*, 650-662.

Appendix B: Supporting Information for Chapter 2

Section 1: DoE Study Details

The DoE study was designed using StatEase® software. Parameters selected for testing in the study were as follows: volume of tetrahydrofuran (high value, 200 μL, low value, 75 μL), volume of buffer (high value, 240 μL, low value, 30 μL), buffer concentration (high value, 2 M, low value, 1 M), and buffer pH (high value, 4.2, low value, 3.6). The parameters were arranged by StatEase® into 16 experiments. The procedure for the experiments was as follows:
Under ambient conditions, a 16-well plate containing glass reaction tubes equipped with PTFE-coated magnetic stir bars was charged 17 mg zinc powder (0.26 mmol, 16 equiv) and **2.17a** (10 mg, 16 μmol, 1.0 equiv) for each reaction. The corresponding amounts of tetrahydrofuran and buffer (see **Table S2-1**) were charged via adjustable automatic micropipette. The reactions were stirred for 16 h, after which they were filtered through a Celite® plug and concentrated by streams of compressed air. The yields of the reactions were assessed by quantitative ^{1}H NMR in DMSO-d_6 using 1,3,5-trimethoxybenzene as an internal standard. Yields are listed in **Table S2-1**. The reaction yields were assessed using the StatEase® software. The buffers were prepared beforehand using a mixture of sodium acetate and acetic acid in water, using https://www.liverpool.ac.uk/pfg//Tools/BuffferCalc/Buffer.html to calculate the requisite reagent amounts.

Figure S2-1 shows the variables which were assessed by the software as having the most impact. Three relationships were evaluated to be above the requisite t-value limit (statistically significant): The relationship between the amount of buffer and the buffer pH, the ratio between THF and buffer, and the relationship between the ratio of THF, water, and the buffer pH. The most important relationship was the amount of buffer and the buffer pH used, as this correlation was above the Bonferroni limit (statistically significant and unlikely to be a false positive.

The StatEase® software also calculated the theoretical "best conditions" for future runs of the reaction (**Figure S2-2**). These were the final conditions used for the hydrolysis of **2.17a** and **2.17b**. The theoretical yield for these conditions was 137%, indicating some possible sources of error in the statistical analysis. However, these conditions worked well for the reaction. The predicted "best conditions" were reproduced using the same procedure with 33 μmol **2.17a** before running a full-scale reaction. The calculated conditions gave an isolated 92% yield of **2.28a**.

Table S2-1: DoE Reaction Parameters and Yields

Std	Run	Factor 1: THF volume (mL)	Factor 2: Buffer volume (mL)	Factor 3: Buffer molarity (M)	Factor 4: Buffer pH	Yield (%)
14	1	0.2	0.03	2	4.2	63
15	2	0.075	0.24	2	4.2	21
13	3	0.075	0.03	2	4.2	30
7	4	0.075	0.24	2	3.6	30
16	5	0.2	0.24	2	4.2	0
5	6	0.075	0.03	2	3.6	57
9	7	0.075	0.03	1	4.2	72
2	8	0.2	0.03	1	3.6	0
6	9	0.2	0.03	2	3.6	0
4	10	0.2	0.24	1	3.6	33
12	11	0.2	0.24	1	4.2	0
10	12	0.2	0.03	1	4.2	93
1	13	0.075	0.03	1	3.6	63
3	14	0.075	0.24	1	3.6	3
11	15	0.075	0.24	1	4.2	39
8	16	0.2	0.24	2	3.6	33

Figure S2-1: DoE Reaction Analysis—Pareto Chart

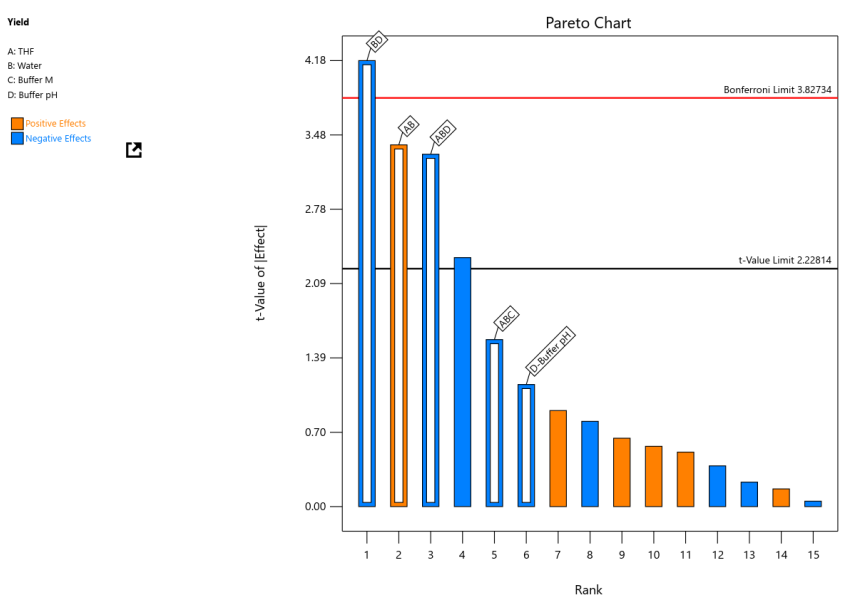

Figure S2-2: DoE Reaction Analysis—Calculated Best Conditions

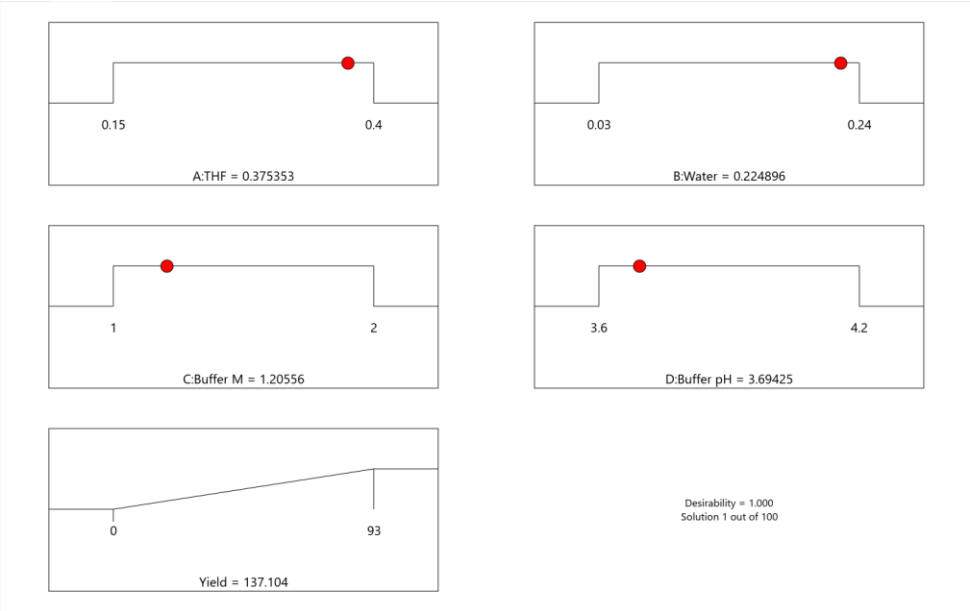

Section 2: General Information

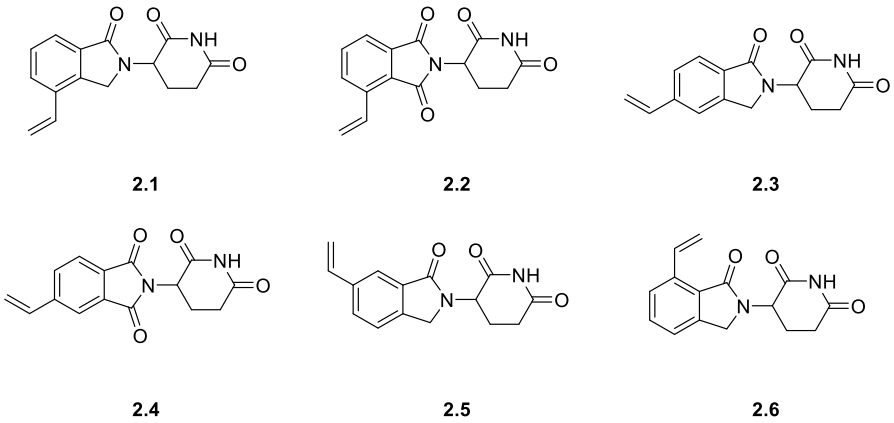

Figure S2-3. Aryl alkenes used in this study

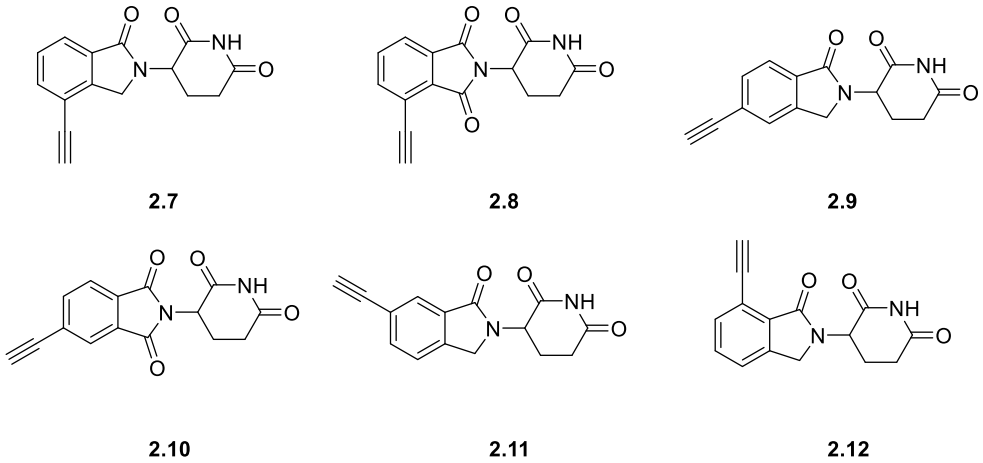

Figure S2-4. Aryl alkynes used in this study

Section 3: Synthetic Procedures and Compound Characterization

General Synthetic and Characterization Information

All reactions were conducted in flame-dried glassware under an inert atmosphere of dry nitrogen or argon, unless otherwise noted. All reagents were purchased, unless otherwise noted, from Oakwood, CombiBlocks, Millipore Sigma, Ambeed, and WuXi and used as received. Anhydrous dichloromethane was obtained from a Grubbs-type solvent purification system and further dried under an argon atmosphere for 24 hours over 4 Å molecular sieves. Molecular sieves were activated by heating under vacuum (<1 torr) for three hours at 300 °C.

Proton (^{1}H) NMR spectra were recorded at 400 MHz on Varian and Bruker spectrometers, 500 MHz on an Inova-500 spectrometer, or 600 MHz on an Inova-600 spectrometer. Proton-decoupled carbon (^{13}C{^{1}H}) NMR spectra were recorded at 100 MHz on Varian and Bruker spectrometers or 151 MHz on an Inova-600 spectrometer. NMR spectra were recorded in deuterated solvents and were referenced to tetramethylsilane (in the case of $CDCl_3$) or the respective residual solvent signal. NMR chemical shifts were reported in parts per million (ppm). Abbreviations for signal couplings are as follows: s, singlet; d, doublet; t, triplet; q, quartet; quin, quintet; sex, sextet; sep, septet; and m, multiplet. The coupling constants were taken from the spectra directly and are uncorrected.

Mass spectrometric determinations were carried out on a Thermo Finnigan LTQ-FTMS spectrometer with atmospheric pressure chemical ionization (APCI), using a Fourier transform ion cyclotron resonance mass analyzer. Optical rotations were measured on a Rudolph Research Analytical Automatic Polarimeter, APIV-1W. Analytical thin layer chromatography was performed on silica gel plates using ultraviolet light to visualize analytes. Normal phase column chromatography was performed with SiliCycle silica gel 60 Å (50 µm) hand-packed in Biotage Sfär columns on Biotage Isolera Four chromatographs, with SiliCycle silica gel 60 Å or Celite® as a dry-loading absorbent. Reverse phase chromatography was conducted using Teledyne ISCO RediSep Gold 18 reverse-phase columns using Teledyne ISCO CombiFlash or Biotage Isolera chromatographs. Supercritical fluid chromatography (SFC) analysis was performed on a Waters Acquity UPC2 instrument.

Purity of key compounds was assessed using SFC analysis (Waters Acquity UPC2 instrument), high-performance liquid chromatography analysis (HPLC) on an Agilent 1260 Infinity HPLC, or Waters AutoPurification System. All key compounds were ≥95% pure by HPLC or SFC analysis.

Dirhodium catalysts Rh_2(*S*-p-Ph-TPCP)$_4$,[1] Rh_2(*R*-p-Ph-TPCP)$_4$,[1] Rh_2(*S-tetra*-p-Br-PPTL)$_4$,[2] and Rh_2(*R-tetra*-p-Br-PPTL)$_4$[2] were prepared according to their respective literature procedures. Racemic standards were prepared by using a 1:1 mixture of *R* and *S* catalyst under the same reaction conditions used to prepare enantioenriched compounds.

Aryl alkenes **2.1-2.6** were prepared following the procedure outline in the supporting information for Chapter 1 in 84-93% yield.

Caution! Glutarimide-containing compounds such as thalidomide are known reproductive, neurological, and hematological toxins. Care must be exercised to avoid direct contact with glutarimide-containing material; any glassware used with glutarimide-containing material should be treated with a 2 M aqueous solution of a strong base such as sodium hydroxide to destroy the material.

Compound Synthesis and Characterization
Synthesis of Starting Materials

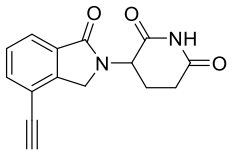

2.7

3-(4-ethynyl-1-oxoisoindolin-2-yl)piperidine-2,6-dione (2.7)

3-(4-bromo-1-oxoisoindolin-2-yl)piperidine-2,6-dione (1.00 g, 1.0 equiv, 3.1 mmol) and $Pd(PPh_3)_2Cl_2$ (217 mg, 10 mol%, 0.30 mmol) were added to a flame-dried round-bottom flask under inert atmosphere. Dry *N*,*N*-dimethylformamide (14.6 mL) was added via syringe, and the mixture was degassed with N_2 for 30 min. Diisopropylethylamine (1.77 mL, 3.2 equiv, 9.9 mmol) and ethynyltrimethylsilane (2.2 mL, 5.0 equiv, 15.5 mmol) were charged via syringe, and finally CuI (59 mg, 10 mol%, 0.30 mmol) was charged. The reaction was heated to 65 ºC in an oil bath overnight, after which it was cooled to room temperature. The reaction was filtered through Celite® and poured into ethyl acetate. The solution was washed with water and thrice with saturated aqueous sodium chloride solution, then dried over magnesium sulfate. The solution was filtered and concentrated in vacuuo onto silica gel, then purified by flash column chromatography (SiO_2 0-40% acetone in CH_2Cl_2). The residue from the concentrated fractions were taken up in CH_2Cl_2, precipitated with hexanes, and the solid was collected by vacuum filtration. The material was carried forward to the next step without further purification.

3-(1-oxo-4-((trimethylsilyl)ethynyl)isoindolin-2-yl)piperidine-2,6-dione (650 mg, 1.0 equiv, 1.9 mmol) was added to a flame-dried flask under inert atmosphere. Dry THF (7.0 mL) was added via syringe, and the mixture was cooled to 0 ºC. TBAF (2.3 mL, 1.0 molar in THF, 1.2 equiv, 2.3 mmol) was added dropwise to the cooled reaction over 30 min by syringe pump. The reaction was quenched with 40 mL 0.1 M citric acid after addition of the THF solution, then diluted with CH_2Cl_2. The organic layer was separated and concentrated in vacuuo. The residue was suspended in CH_2Cl_2

and thrice the volume of hexanes was added. The solid was isolated via vacuum filtration, giving **2.7** (496 mg, 1.85 mmol, 60% overall yield) as a light brown amorphous solid.

HRMS (APCI) *m/z*: $[M+H]^+$ calcd for $C_{15}H_{13}O_3N_2$ 269.0921; Found 269.0923

^{1}H NMR (500 MHz, DMSO-d_6): δ 11.01 (s, 1H), 7.78 (dd, J = 7.6, 1.0 Hz, 1H), 7.74 (dd, J = 7.7, 1.0 Hz, 1H), 7.56 (t, J = 7.6 Hz, 1H), 4.62 (s, 1H), 4.50 (d, J = 17.8 Hz, 1H), 4.34 (d, J = 17.8 Hz, 1H), 2.92 (ddd, J = 17.3, 13.6, 5.4 Hz, 1H), 2.59 (ddt, J = 17.2, 4.4, 2.1 Hz, 1H), 2.53 – 2.40 (m, 1H, partially obscured by solvent signal at 2.50), 2.01 (dtd, J = 12.6, 5.2, 2.1 Hz, 1H).

^{13}C{^{1}H} NMR (151 MHz, DMSO-d_6): δ 172.9, 170.9, 167.5, 144.4, 134.6, 132.1, 128.7, 123.7, 117.3, 86.1, 79.3, 51.7, 46.9, 31.2, 22.3.

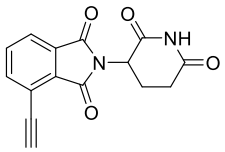

2.8

2-(2,6-dioxopiperidin-3-yl)-4-ethynylisoindoline-1,3-dione (2.8)

4-bromo-2-(2,6-dioxopiperidin-3-yl)isoindoline-1,3-dione (1.0 g, 1.0 equiv, 2.97 mmol) and $Pd(PPh_3)_2Cl_2$ (208 mg, 10 mol%, 0.30 mmol) were added to a flame-dried round-bottom flask under inert atmosphere, and diisopropylethylamine (1.7 mL, 3.2 equiv, 9.5 mmol) was added via syringe along with dry *N*,*N*-dimethylformamide (30 mL). This mixture was degassed with N_2 for thirty minutes, and ethynyltrimethylsilane (2.1 mL, 5.0 equiv, 15 mmol) was added by syringe. CuI (57 mg, 10 mol%, 0.30 mmol) was then added and the reaction was heated to 65 ºC in an aluminum heating block for two days. The reaction was cooled to room temperature and poured into ethyl acetate. The solution was washed with water and saturated aqueous sodium chloride solution. The organic layer was dried over magnesium sulfate and filtered, then concentrated. The reaction was dry-mounted onto silica gel and purified via flash column chromatography (SiO_2, 30-100% ethyl acetate in hexanes). The material from the isolated column fractions was then suspended in methanol and isolated via vacuum filtration, giving 2-(2,6-dioxopiperidin-3-yl)-4-((trimethylsilyl)ethynyl)isoindoline-1,3-dione, which was carried to the next step without further purification.

(2,6-dioxopiperidin-3-yl)-4-((trimethylsilyl)ethynyl)isoindoline-1,3-dione (600 mg, 1.0 equiv, 1.69 mmol) was added to a flame-dried round-bottom flask under inert atmosphere. Dry tetrahydrofuran (6.2 mL) was added via syringe, and the reaction was cooled to 0 ºC in an ice bath. TBAF (2.03 mL, 1.0 molar in THF, 1.2 equiv, 2.03 mmol) was added over 30 min via syringe pump to the cooled reaction. After addition of the TBAF solution, 30 mL 0.1 M aqueous citric acid solution was added. 50 mL ethyl acetate was added to form an organic layer and the aqueous layer was separated. The organic layer was concentrated in vacuuo, and the resulting residue was suspended in methanol. The solid was isolated by vacuum filtration, giving **2.8** (429 mg, 1.52 mmol, 51% overall yield) as a tan amorphous solid.

HRMS (APCI) *m/z*: $[M+H]^+$ calcd for $C_{15}H_{11}O_4N_2$ 283.0713; Found 283.0716

^{1}H NMR (500 MHz, DMSO-d_6): δ 11.16 (s, 1H), 7.98 – 7.91 (m, 2H), 7.90 – 7.83 (m, 1H), 5.15 (dd, J = 12.9, 5.4 Hz, 1H), 4.77 (s, 1H), 2.89 (ddd, J = 17.1, 13.9, 5.4 Hz, 1H), 2.60 (dt, J = 16.9, 3.0 Hz, 1H), 2.57 – 2.44 (m, 1H, partially obscured by solvent signal at 2.50), 2.06 (dtd, J = 9.8, 5.0, 2.3 Hz, 1H).

$^{13}C\{^1H\}$ NMR (151 MHz, DMSO): δ 172.8, 169.8, 166.2, 165.5, 138.8, 134.8, 132.1, 130.9, 123.7, 118.3, 88.2, 78.5, 49.0, 30.9, 21.9.

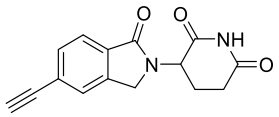

2.9

3-(5-ethynyl-1-oxoisoindolin-2-yl)piperidine-2,6-dione (2.9)

Compounds **2.9** was prepared via an adaptation of a literature procedure.[3] 3-(5-iodo-1-oxoisoindolin-2-yl)piperidine-2,6-dione (553 mg, 1.0 equiv, 1.50 mmol), $Pd(PhCN)_2Cl_2$ (17 mg, 3 mol%, 45 µmol), tri-*tert*-butylphosphoniumtetrafluoroborate (28 mg, 6.5 mol%, 97 µmol) were added to a flame-dried flask under inert atmosphere. Ethynyltrimethylsilane (0.25 mL, 1.2 equiv, 1.8 mmol), dry 1,4-dioxane (3.1 mL), and diisopropylamine (0.25 mL, 1.2 equiv, 1.8 mmol) were added by syringe. The reaction was degassed with argon under sonication for 15 min, after which CuI (5.7 mg, 2 mol%, 30 µmol) was charged. The reaction was stirred at room temperature for 18 h, after which the reaction mixture was poured into ethyl acetate and filtered through Celite®. The reaction was partitioned between ethyl acetate and water, then extracted thrice into ethyl acetate. The combined organic layers were washed with saturated aqueous sodium chloride solution, and were then dried over magnesium sulfate, filtered, and concentrated in vacuuo. The material was dry-mounted onto silica gel and purified by flash column chromatography (SiO_2, 0-5% methanol in CH_2Cl_2. The material was then carried forward to the next reaction without further purification.

3-(1-oxo-5-((trimethylsilyl)ethynyl)isoindolin-2-yl)piperidine-2,6-dione (200 mg, 1.0 equiv, 0.59 mmol) was added to a flame-dried round-bottom flask under inert atmosphere. Dry tetrahydrofuran (4.8 mL) was added via syringe, and the reaction was cooled to 0 ºC in an ice bath. TBAF (0.68 mL, 1.0 molar in THF, 1.2 equiv, 0.68 mmol) was added over 30 min via syringe pump to the cooled reaction. After addition of the TBAF solution, 30 mL 0.1 M aqueous citric acid solution was added. 50 mL ethyl acetate was added to form an organic layer and the aqueous layer was separated. The organic layer was concentrated in vacuuo, and the resulting residue was suspended in methanol. The solid was isolated by vacuum filtration, giving **2.9** (131 mg, 0.49 mmol, 33% overall yield) as a tan amorphous solid.

HRMS (APCI) *m/z*: $[M+H]^+$ calcd for $C_{15}H_{13}O_3N_2$ 269.0921; Found 269.0923

^1H NMR (400 MHz, DMSO-d_6): δ 11.01 (s, 1H), 7.76 – 7.69 (m, 2H), 7.64 – 7.57 (m, 1H), 5.12 (dd, J = 13.3, 5.1 Hz, 1H), 4.47 (d, J = 17.5 Hz, 1H), 4.43 (s, 1H), 4.34 (d, J = 17.5 Hz, 1H), 2.91 (ddd, J = 17.2, 13.6, 5.4 Hz, 1H), 2.60 (d, J = 17.1 Hz, 1H), 2.39 (qd, J = 13.3, 4.5 Hz, 1H), 2.01 (ddd, J = 10.5, 5.0, 2.8 Hz, 1H).

$^{13}C\{^1H\}$ NMR (151 MHz, DMSO): δ 172.9, 170.9, 167.3, 142.4, 131.9, 131.6, 126.9, 124.9, 123.3, 83.0, 82.9, 51.7, 47.1, 31.2, 22.4.

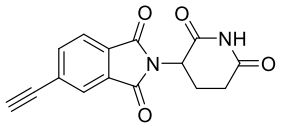

2.10

2-(2,6-dioxopiperidin-3-yl)-5-ethynylisoindoline-1,3-dione (2.10)

5-bromo-2-(2,6-dioxopiperidin-3-yl)isoindoline-1,3-dione (3.0 g, 1.0 equiv, 8.9 mmol) and $Pd(PPh_3)_2Cl_2$ (625 mg, 10 mol%, 0.89 mmol) were added to a flame-dried round-bottom flask under inert atmosphere, and diisopropylethylamine (5.1 mL, 3.2 equiv, 9.5 mmol) was added via syringe along with dry *N*,*N*-dimethylformamide (42 mL). This mixture was degassed with N_2 for thirty minutes, and ethynyltrimethylsilane (2.1 mL, 5.0 equiv, 15 mmol) was added by syringe. CuI (169 mg, 10 mol%, 0.89 mmol) was then added and the reaction was heated to 65 ºC in an aluminum heating block for two days. The reaction was cooled to room temperature and poured into ethyl acetate. The solution was washed with water and saturated aqueous sodium chloride solution. The organic layer was dried over magnesium sulfate and filtered, then concentrated. The reaction was dry-mounted onto silica gel and purified via flash column chromatography (SiO_2, 30-100% ethyl acetate in hexanes). The material from the isolated column fractions was then suspended in methanol and isolated via vacuum filtration, which was carried to the next step without further purification.

2-(2,6-dioxopiperidin-3-yl)-5-((trimethylsilyl)ethynyl)isoindoline-1,3-dione (1.65 g, 1.0 equiv, 4.7 mmol) was added to a flame-dried round-bottom flask under inert atmosphere. Dry tetrahydrofuran (16.4 mL) was added via syringe, and the reaction was cooled to 0 ºC in an ice bath. TBAF (5.4 mL, 1.0 molar in THF, 1.2 equiv, 5.4 mmol) was added over 30 min via syringe pump to the cooled reaction. After addition of the TBAF solution, 50 mL 0.1 M aqueous citric acid solution was added. 50 mL ethyl acetate was added to form an organic layer and the aqueous layer was separated. The organic layer was concentrated in vacuuo, and the resulting residue was suspended in methanol. The solid was isolated by vacuum filtration, giving **2.10** (494 mg, 1.75 mmol, 20% overall yield) as a tan amorphous solid.

HRMS (APCI) *m/z*: $[M+H]^+$ calcd for $C_{15}H_{11}O_4N_2$ 283.0713; Found 283.0713

^{1}H NMR (400 MHz, DMSO-d_6): δ 11.16 (s, 1H), 8.10 – 7.73 (m, 3H), 5.17 (dd, J = 12.8, 5.4 Hz, 1H), 4.68 (s, 1H), 2.89 (ddd, J = 16.9, 13.8, 5.4 Hz, 1H), 2.69 – 2.48 (m, 2H, partially obscured by solvent signal at 2.50), 2.06 (ddd, J = 10.4, 5.5, 3.2 Hz, 1H).

^{13}C{^{1}H} NMR (151 MHz, DMSO-d_6)**:** δ 173.2, 170.2, 166.9, 166.8, 138.5, 132.2, 131.3, 128.5, 126.6, 124.3, 85.9, 82.4, 49.6, 31.4, 22.4.

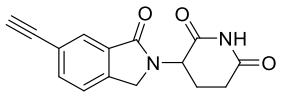

2.11

3-(6-ethynyl-1-oxoisoindolin-2-yl)piperidine-2,6-dione (2.11)

3-(6-bromo-1-oxoisoindolin-2-yl)piperidine-2,6-dione (713 mg, 1.0 equiv, 2.2 mmol) and $Pd(PPh_3)_2Cl_2$ (155 mg, 10 mol%, 0.22 mmol) were added to a flame-dried round-bottom flask under inert atmosphere, and diisopropylethylamine (1.3 mL, 3.2 equiv, 7.1 mmol) was added via syringe along with dry *N*,*N*-dimethylformamide (10.4 mL). This mixture was degassed with N_2 for thirty

minutes, and ethynyltrimethylsilane (1.6 mL, 5.0 equiv, 11 mmol) was added by syringe. CuI (42 mg, 10 mol%, 0.22 mmol) was then added and the reaction was heated to 65 ºC in an aluminum heating block for two days. The reaction was cooled to room temperature and poured into ethyl acetate. The solution was washed with water and saturated aqueous sodium chloride solution. The organic layer was dried over magnesium sulfate and filtered, then concentrated. The reaction was dry-mounted onto silica gel and purified via flash column chromatography (SiO_2, 30-100% ethyl acetate in hexanes). The material from the isolated column fractions was then suspended in methanol and isolated via vacuum filtration, which was carried to the next step without further purification.

3-(1-oxo-6-((trimethylsilyl)ethynyl)isoindolin-2-yl)piperidine-2,6-dione (280 mg, 1.0 equiv, 0.82 mmol) was added to a flame-dried round-bottom flask under inert atmosphere. Dry tetrahydrofuran (2.9 mL) was added via syringe, and the reaction was cooled to 0 ºC in an ice bath. TBAF (0.95 mL, 1.0 molar in THF, 1.2 equiv, 0.95 mmol) was added over 30 min via syringe pump to the cooled reaction. After addition of the TBAF solution, 30 mL 0.1 M aqueous citric acid solution was added. 50 mL ethyl acetate was added to form an organic layer and the aqueous layer was separated. The organic layer was concentrated in vacuuo, and the resulting residue was suspended in methanol. The solid was isolated by vacuum filtration, giving **2.11** (175 mg, 0.65 mmol, 30% overall yield) as a tan amorphous solid.

HRMS (APCI) *m/z*: $[M+H]^+$ calcd for $C_{15}H_{13}O_3N_2$ 269.0921; Found 269.0919

^{1}H NMR (500 MHz, DMSO-d_6): δ 11.02 (s, 1H), 7.76 (dd, J = 1.5, 0.8 Hz, 1H), 7.74 (dd, J = 7.8, 1.6 Hz, 1H), 7.65 (dd, J = 7.8, 0.9 Hz, 1H), 5.12 (dd, J = 13.3, 5.1 Hz, 1H), 4.50 (d, J = 17.9 Hz, 1H), 4.36 (d, J = 17.8 Hz, 1H), 4.31 (s, 1H), 2.91 (ddd, J = 17.3, 13.7, 5.4 Hz, 1H), 2.66 – 2.55 (m, 1H), 2.39 (qd, J = 13.3, 4.5 Hz, 1H), 2.01 (dtd, J = 11.5, 4.7, 1.7 Hz, 1H).

^{13}C{^{1}H} NMR (151 MHz, DMSO-d_6): δ 172.9, 170.9, 167.1, 142.6, 135.0, 132.1, 125.9, 124.2, 121.5, 82.7, 81.5, 51.7, 47.3, 31.2, 22.4.

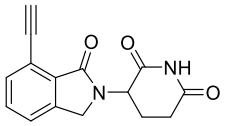

2.12

3-(7-ethynyl-1-oxoisoindolin-2-yl)piperidine-2,6-dione (2.12)

3-(7-bromo-1-oxoisoindolin-2-yl)piperidine-2,6-dione (1.0 g, 1.0 equiv, 3.1 mmol) and $Pd(PPh_3)_2Cl_2$ (217 mg, 10 mol%, 0.31 mmol) were added to a flame-dried round-bottom flask under inert atmosphere, and diisopropylethylamine (1.8 mL, 3.2 equiv, 9.9 mmol) was added via syringe along with dry *N*,*N*-dimethylformamide (14.6 mL). This mixture was degassed with N_2 for thirty minutes, and ethynyltrimethylsilane (2.2 mL, 5.0 equiv, 16 mmol) was added by syringe. CuI (59 mg, 10 mol%, 0.31 mmol) was then added and the reaction was heated to 65 ºC in an aluminum heating block for two days. The reaction was cooled to room temperature and poured into ethyl acetate. The solution was washed with water and saturated aqueous sodium chloride solution. The organic layer was dried over magnesium sulfate and filtered, then concentrated. The reaction was dry-mounted onto silica gel and purified via flash column chromatography (SiO_2, 0-5% methanol in CH_2Cl_2). The material from the isolated column fractions was then suspended in methanol and isolated via vacuum filtration, which was carried to the next step without further purification.

Under inert atmosphere, a flask was charged with 3-(1-oxo-7-((trimethylsilyl)ethynyl)isoindolin-2-yl)piperidine-2,6-dione (540 mg, 1.0 equiv, 1.6 mmol), followed by tetrahydrofuran (5.8 mL). The reaction was cooled to 0 ºC in the ice bath. TBAF (1.9 mL, 1.0 molar in THF, 1.2 equiv, 1.9 mmol) in THF was added over 30 min to the cooled reaction. Following this, the reaction was quenched with 30 mL 0.1 M citric acid solution. The reaction was diluted with THF and saturated aqueous sodium chloride. The THF layer was washed with saturated aqueous sodium chloride, then concentrated. The material was purified by flash column chromatography (SiO_2, 0-10% methanol in CH_2Cl_2) , the concentrated fractions of which were washed with 1:1 CH_2Cl_2:hexanes, affording **2.12** (176 mg, 0.66 mmol, 21% overall yield) as an amorphous tan solid.

HRMS (APCI) *m/z*: $[M+H]^+$ calcd for $C_{15}H_{13}O_3N_2$ 269.0921; Found 269.0923

^{1}H NMR (500 MHz, DMSO-d_6): δ 11.01 (s, 1H), 7.80 – 7.50 (m, 3H), 5.07 (dd, J = 13.2, 5.1 Hz, 1H), 4.48 (s, 1H), 4.43 (d, J = 17.5 Hz, 1H), 4.30 (d, J = 17.5 Hz, 1H), 2.91 (ddd, J = 17.3, 13.7, 5.4 Hz, 1H), 2.60 (d, J = 17.8 Hz, 1H), 2.40 (qd, J = 13.2, 4.4 Hz, 1H), 2.01 (ddd, J = 9.8, 5.4, 2.7 Hz, 1H).

^{13}C{^{1}H} NMR (151 MHz, DMSO): δ 172.9, 171.0, 166.4, 143.2, 133.0, 131.5, 131.4, 124.1, 118.0, 86.4, 79.9, 51.6, 46.7, 31.2, 22.3.

Preparation of Aryldiazoacetatess.

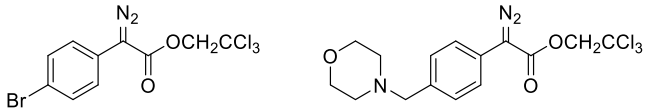

2.13 **2.14**

Figure S2-5. Aryldiazoacetatess used in this study

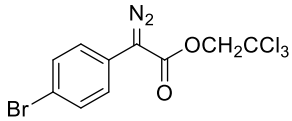

2.13

2,2,2-trichloroethyl 2-(4-bromophenyl)-2-diazoacetate (**2.13**) was prepared via the literature procedure, in 90% yield.[4]

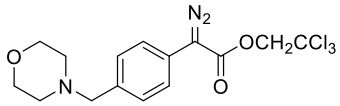

2.14

2,2,2-trichloroethyl 2-diazo-2-(4-(morpholinomethyl)phenyl)acetate (**2.14**) was prepared from 2-(4-(bromomethyl)phenyl)acetic acid in three steps. Following an adaptation of the literature procedure,[4] 2-(4-(bromomethyl)phenyl)acetic acid (1.0 g, 1.0 equiv, 4.4 mmol), 2,2,2-trichloroethanol (0.51 mL, 1.2 equiv, 5.2 mmol), and 4-(dimethylamino)pyridine (53 mg, 10 mol%, 0.44 mmol) were dissolved in dry CH_2Cl_2 (10 mL), and cooled to 0 °C. A solution of dicyclohexylcarbodiimide (1.0 g, 4.8 mmol, 1.1 equiv) in CH_2Cl_2 (5.7 mL) was added dropwise to the cooled reaction, which was allowed

to stir and come to room temperature overnight. The reaction was filtered through Celite® to remove the white precipitate that had formed, rinsing with diethyl ether, and the filtrate was concentrated in vacuuo. The material was filtered through a short plug of silica gel with diethyl ether, and concentrated in vacuuo. The product obtained was used in the next step without further purification.

Following a procedure from the literature,[5] potassium carbonate (359 mg, 1.3 equiv, 2.6 mmol), morpholine (0.17 mL, 1.0 equiv, 2.0 mmol), and 2,2,2-trichloroethyl 2-(4-(bromomethyl)phenyl)acetate (793 mg, 1.1 equiv, 2.2 mmol) were combined in a flame-dried vial under inert atmosphere, dissolved in dry acetonitrile (6.7 mL), and stirred at room temperature overnight. The acetonitrile was removed in vacuuo and the residue was partitioned between water and ethyl acetate. The aqueous layer was extracted thrice with ethyl acetate, after which the organic layers were washed with brine, dried over magnesium sulfate, and concentrated in vacuuo. The material was filtered through a silica plug with diethyl ether. The product obtained was used in the next step without further purification.

Following the literature procedure,[4] 2,2,2-trichloroethyl 2-(4-(morpholinomethyl)phenyl)acetate (475 mg, 1 equiv, 1.3 mmol) and 2-nitrobenzenesulfonyl azide (443 mg, 1.5 equiv, 1.9 mmol) were taken up in dry acetonitrile (7.2 mL) and cooled to 0 °C. 2,3,4,6,7,8,9,10-octahydropyrimido[1,2-a]azepine (0.43 mL, 2.2 equiv, 2.9 mmol) was added dropwise to the cooled reaction. The reaction was allowed to stir for three hours at 0 °C, after which the reaction was quenched with a saturated solution of ammonium chloride in water. The reaction was extracted with three portions of diethyl ether. The combined organic layers were washed with brine, dried over magnesium sulfate, and concentrated in vacuuo. The crude residue was purified via flash column chromatography (SiO_2, 10-30% EtOAc in hexanes), which gave 2,2,2-trichloroethyl 2-diazo-2-(4-(morpholinomethyl)phenyl)acetate (345 mg, 0.88 mmol, 68% yield) as a yellow-orange amorphous solid.

HRMS (APCI) *m/z*: $[M+H]^+$ calcd for $C_{15}H_{17}O_3N_3{}^{35}Cl_3$ 392.0330; Found 392.0336

^{1}H NMR (400 MHz, $CDCl_3$): δ 7.45 (d, *J* = 8.4 Hz, 1H), 7.38 (d, *J* = 8.3 Hz, 1H), 4.92 (s, 1H), 3.71 (t, *J* = 4.7 Hz, 3H), 3.49 (s, 1H), 2.44 (t, *J* = 4.7 Hz, 2H).

^{13}C{^{1}H} NMR (151 MHz, $CDCl_3$): δ 163.5, 136.3, 130.0, 124.2, 123.5, 95.2, 74.0, 67.1, 63.0, 53.7.

Note: We did not observe the resonance associated with the diazo carbon.

FTIR (film): ν_{max}/cm^{-1} *inter alia* 2089 (N=N), 1709 (C=O).

Synthesis of Final Compounds

General Cyclopropanation Procedure (GP 1)

A 10 mL round-bottom flask was charged with a PTFE magnetic stir bar and ca. 200% w/w 4 Å molecular sieves, then flame dried under vacuum. The flask was then backfilled with dry nitrogen. Rh_2(*S*-p-Ph-TPCP)$_4$ (1 mol%) and the aryl alkene (1.0 equiv) were charged to the flask, and the flask was evacuated and backfilled with nitrogen. The flask was equipped with an argon balloon and rubber septum, and dry CH_2Cl_2 (0.2 M) was charged via syringe. A solution of 2,2,2-trichloroethyl 2-(4-bromophenyl)-2-diazoacetate (1.1 equiv) in dry CH_2Cl_2 (0.2 M, prepared in the same manner under inert atmosphere) was added dropwise to the stirred reaction at room temperature. The reaction was allowed to stir for two hours, after which the reaction was filtered through Celite, rinsing the filter pad with CH_2Cl_2. The crude residue was dry-mounted onto silica gel and was purified by flash column chromatography (SiO_2).

General Cyclopropenation Procedure (GP 2)

A 10 mL round-bottom flask was charged with a PTFE magnetic stir bar and ca. 200% w/w 4 Å molecular sieves, then flame dried under vacuum. The flask was then backfilled with dry nitrogen. Rh_2(*S*-p-Ph-TPCP)$_4$ (1 mol%) and the aryl alkyne (1.0 equiv) were charged to the flask, and the flask was evacuated and backfilled with nitrogen. The flask was equipped with an argon balloon and rubber septum, and dry CH_2Cl_2 (0.2 M) was charged via syringe. A solution of 2,2,2-trichloroethyl 2-(4-bromophenyl)-2-diazoacetate (1.1 equiv) in dry CH_2Cl_2 (0.2 M, prepared in the same manner under inert atmosphere) was added over 15 minutes to the stirred reaction at room temperature, via syringe pump. The reaction was allowed to stir for two hours, after which the reaction was filtered through Celite, rinsing the filter pad with CH_2Cl_2. The crude residue was dry-mounted onto silica gel and was purified by flash column chromatography (SiO_2).

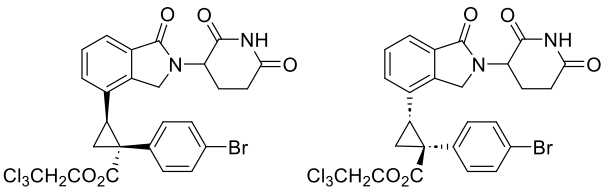

2.15a **2.15b**

2,2,2-trichloroethyl (1*R*,2*S*)-1-(4-bromophenyl)-2-(2-(2,6-dioxopiperidin-3-yl)-1-oxoisoindolin-4-yl)cyclopropane-1-carboxylate (2.15a).

2,2,2-trichloroethyl (1*S*,2*R*)-1-(4-bromophenyl)-2-(2-(2,6-dioxopiperidin-3-yl)-1-oxoisoindolin-4-yl)cyclopropane-1-carboxylate (2.15b).

Compound **2.15a** was prepared following **GP 1**, using Rh_2(*S*-p-Ph-TPCP)$_4$ (3.5 mg, 1 mol%, 2.0 µmol), 3-(1-oxo-4-vinylisoindolin-2-yl)piperidine-2,6-dione (54 mg, 1.0 equiv, 0.20 mmol), 2,2,2-trichloroethyl 2-(4-bromophenyl)-2-diazoacetate (82 mg, 1.1 equiv, 0.22 mmol), and CH_2Cl_2 (2 mL) at room temperature for two hours. Purification via flash column chromatography (SiO_2, gradient of 40% to 100% EtOAc in hexanes) afforded 2,2,2-trichloroethyl (1*R*,2*S*)-1-(4-bromophenyl)-2-(2-(2,6-dioxopiperidin-3-yl)-1-oxoisoindolin-4-yl)cyclopropane-1-carboxylate as an amorphous white solid. (78 mg, 0.12 mmol, 62% yield).

Compound **2.15b** was prepared in the same manner using Rh_2(*R*-p-Ph-TPCP)$_4$, which afforded 2,2,2-trichloroethyl (1*S*,2*R*)-1-(4-bromophenyl)-2-(2-(2,6-dioxopiperidin-3-yl)-1-oxoisoindolin-4-yl)cyclopropane-1-carboxylate as an amorphous white solid. (77 mg, 0.12 mmol, 61% yield).

HRMS (APCI) *m/z*: $[M+H]^+$ calcd for $C_{25}H_{20}{}^{79}Br^{35}Cl_3N_2O_5$ 612.9694; Found 612.9702

^{1}H NMR (600 MHz, $CDCl_3$, reported as a mixture of diastereomers): δ 8.26 and 8.25 (s, 1H), 7.655 and 7.652 (d, *J* = 7.6 Hz, 1H), 7.28 and 7.26 (d, *J* = 8.5 Hz, 2H, partially obscured by solvent signal), 7.16-7.10 (m, 1H), 6.89 and 6.86 (d, *J* = 8.5 Hz, 2H), 6.49 and 6.43 (d, *J* = 7.7 Hz, 1H), 5.29 and 5.26 (dd, *J* = 13.2, 5.2 Hz, 1H), 4.88 and 4.87 (d, *J* = 12.0 Hz, 1H), 4.66 and 4.65 (d, *J* = 12.0 Hz, 1H), 4.59 and 4.54 (d, *J* = 16.0 Hz, 1H), 4.39 and 4.37 (d, *J* = 16.0 Hz, 1H), 3.07 (dd, *J* = 9.3, 7.3 Hz, 1H), 2.98-2.81 (m, 2H), 2.40-2.20 (m, 3H), 2.12-2.06 (m, 1H).

^{13}C{^{1}H} NMR (126 MHz, $CDCl_3$, reported as a mixture of diastereomers): δ 171.4, 171.1, 169.63, 169.59, 169.42, 169.37, 141.6, 133.3, 133.2, 132.3, 131.5, 131.4, 130.7, 129.0, 128.9, 128.4, 122.93, 122.91, 122.2, 74.4, 74.3, 52.1, 52.0, 46.4, 36.8, 36.7, 31.7, 29.9, 29.7, 23.7, 23.6, 19.8, 19.7.

SFC analysis: **2.15a** (Trefoil® AMY1, 25% 1:1 MeOH:^{i}PrOH with 0.2% formic acid in CO_2, 2.5 mL/min, diode array) indicated 99:1 d.r.: t_R (major diastereomers) = 2.89 and 4.82 min, t_R (minor diastereomers) = 3.24 and 3.96 min. **2.15b** indicated the opposite diastereomers in 99:1 d.r.

Purity (SFC): **2.15a** – 99%; **2.15b** – 99%

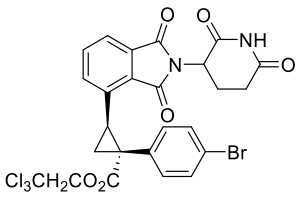

2.16a

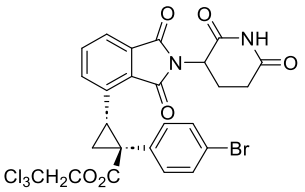

2.16b

2,2,2-trichloroethyl (1*R*,2*S*)-1-(4-bromophenyl)-2-(2-(2,6-dioxopiperidin-3-yl)-1,3-dioxoisoindolin-4-yl)cyclopropane-1-carboxylate (2.16a).

2,2,2-trichloroethyl (1*S*,2*R*)-1-(4-bromophenyl)-2-(2-(2,6-dioxopiperidin-3-yl)-1,3-dioxoisoindolin-4-yl)cyclopropane-1-carboxylate (2.16b).

Compound **2.16a** was prepared following **GP 1**, using Rh_2(*S*-p-Ph-TPCP)$_4$ (3.5 mg, 1 mol%, 2.0 µmol), 2-(2,6-dioxopiperidin-3-yl)-4-vinylisoindoline-1,3-dione (57 mg, 1.0 equiv, 0.20 mmol), 2,2,2-trichloroethyl 2-(4-bromophenyl)-2-diazoacetate (82 mg, 1.1 equiv, 0.22 mmol), and CH_2Cl_2 (2 mL) at room temperature for two hours. Purification via flash column chromatography (SiO_2, gradient of 40% to 100% EtOAc in hexanes) afforded 2,2,2-trichloroethyl (1*R*,2*S*)-1-(4-bromophenyl)-2-(2-(2,6-dioxopiperidin-3-yl)-1,3-dioxoisoindolin-4-yl)cyclopropane-1-carboxylate as an amorphous white solid. (40 mg, 62 µmol, 31% yield).
Compound **2.16b** was prepared in the same manner using Rh_2(*R*-p-Ph-TPCP)$_4$, which afforded 2,2,2-trichloroethyl (1*S*,2*R*)-1-(4-bromophenyl)-2-(2-(2,6-dioxopiperidin-3-yl)-1,3-dioxoisoindolin-4-yl)cyclopropane-1-carboxylate as an amorphous white solid. (38 mg, 59 µmol, 30% yield).

HRMS (APCI) *m/z*: $[M]^+$ calcd for $C_{25}H_{18}BrCl_3N_2O_6$ 625.9422; Found 625.9417
^{1}H NMR (500 MHz, $CDCl_3$, reported as a mixture of diastereomers): δ 8.22 and 8.21 (s, 1H), 7.624 and 7.617 (dd, *J* = 7.40, 0.70 Hz, 1H), 7.38-7.33 (m, 1H), 7.27 (d, *J* =7.9 Hz, 2H, partially obscured by solvent signal), 6.95 (t, *J*=8.2 Hz, 2H), 6.77 and 6.68 (d, *J* =8.0 Hz, 1H), 5.00 (dt, *J* = 12.4, 6.1 Hz, 1H), 4.95 and 4.93 (d, J =11.9 Hz, 1H), 4.64 and 4.61 (d, *J* =11.2 Hz, 1H), 4.21-4.09 (m, 1H) 2.95-2.72 (m, 3H), 2.39 and 2.35 (dd, *J* = 9.1, 5.4 Hz, 1H), 2.20-2.13 (m, 2H).
^{13}C{^{1}H} NMR (101 MHz, $CDCl_3$, reported as a mixture of diastereomers): δ 171.1, 171.0, 170.9, 168.1, 168.0, 167.9, 166.95, 166.93, 136.3, 136.1, 134.0, 133.9, 133.2, 133.1, 132.4, 132.37, 132.32, 132.19, 132.17, 131.40, 131.37, 130.0, 129.8, 122.4, 122.3, 122.1, 122.0, 94.8, 74.81, 74.76, 49.5, 37.1, 36.8, 31.5, 29.5, 29.0, 22.8, 22.7, 19.7, 19.3.
SFC analysis: 2.16a (Chiralcel® OX-3, 35% 1:1 MeOH:^{i}PrOH with 0.2% formic acid in CO_2, 2.5 mL/min, diode array) indicated >99:1 d.r.: t_R (major diastereomers) = 2.16 and 2.36 min, t_R (minor diastereomers) = 4.09 and 7.32 min. **2.16b** indicated the opposite diastereomers in 99:1 d.r.
Purity (SFC): **2.16a** – 99%; **2.16b** – 96%

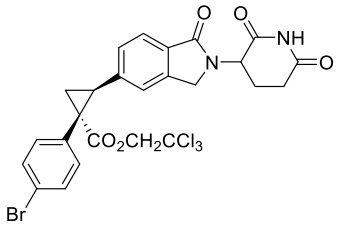

2.17a

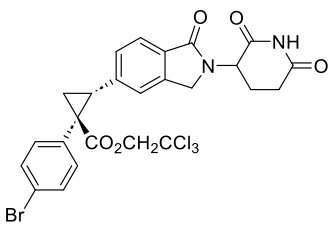

2.17b

2,2,2-trichloroethyl (1*R*,2*S*)-1-(4-bromophenyl)-2-(2-(2,6-dioxopiperidin-3-yl)-1-oxoisoindolin-5-yl)cyclopropane-1-carboxylate (2.17a).

2,2,2-trichloroethyl (1*S*,2*R*)-1-(4-bromophenyl)-2-(2-(2,6-dioxopiperidin-3-yl)-1-oxoisoindolin-5-yl)cyclopropane-1-carboxylate (2.17b).

Compound **2.17a** was prepared following **GP 1**, using Rh_2(*S*-p-Ph-TPCP)$_4$ (3.5 mg, 1 mol%, 2.0 µmol), 3-(1-oxo-5-vinylisoindolin-2-yl)piperidine-2,6-dione (54 mg, 1.0 equiv, 0.20 mmol), 2,2,2-trichloroethyl 2-(4-bromophenyl)-2-diazoacetate (82 mg, 1.1 equiv, 0.22 mmol), and CH_2Cl_2 (2 mL) at room temperature for two hours. Purification via flash column chromatography (SiO_2, gradient of 25% to 75% EtOAc in hexanes) afforded 2,2,2-trichloroethyl (1*R*,2*S*)-1-(4-bromophenyl)-2-(2-(2,6-dioxopiperidin-3-yl)-1-oxoisoindolin-5-yl)cyclopropane-1-carboxylate as an amorphous white solid. (95 mg, 0.16 mmol, 77% yield).
Compound **2.17b** was prepared in the same manner using Rh_2(*R*-p-Ph-TPCP)$_4$, which afforded 2,2,2-trichloroethyl (1*S*,2*R*)-1-(4-bromophenyl)-2-(2-(2,6-dioxopiperidin-3-yl)-1-oxoisoindolin-5-yl)cyclopropane-1-carboxylate as an amorphous white solid. (97 mg, 0.16 mmol, 79% yield).

HRMS (APCI) *m/z*: $[M+H]^+$ calcd for $C_{25}H_{20}BrCl_3N_2O_5$ 612.9686; Found 612.9702
^{1}H NMR (500 MHz, $CDCl_3$, reported as a mixture of diastereomers): 8.42 (s, 1H), 7.60 (12.0, 8.0 Hz, 1H), 7.28 and 7.27 (d, *J* = 8.5 Hz, 2H), 6.96-6.93 (m, 3H), 6.86-6.85 (m, 1H), 5.16 (ddd, *J* = 18.0, 13.3, 5.2 Hz), 4.83 and 4.81 (d, *J* = 2.8 Hz, 1H), 4.66 and 4.64 (d, *J* = 3.2 Hz, 1H), 4.34 and 4.31 (d, *J* = 16.0 Hz, 1H), 4.21 and 4.10 (d, 16.0 Hz, 1H), 3.29 (dd, *J* = 9.4, 7.2 Hz, 1H), 2.89-2.76 (m, 2H), 2.36-2.23 (m, 2H), 2.23-2.18 (m, 1H), 2.03-2.00 (m, 1H).
^{13}C{^{1}H} NMR (101 MHz, $CDCl_3$, reported as a mixture of diastereomers): δ 171.33, 171.30, 171.3, 169.72, 169.66, 169.0, 141.50, 141.48, 140.4, 133.7, 133.6, 132.5, 132.4, 131.46, 131.38, 130.33, 130.27, 128.7, 128.3, 123.8, 122.9, 122.4, 122.1, 122.0, 94.9, 74.6, 52.0, 51.8, 47.0, 46.8, 37.4, 37.3, 33.9, 33.8, 31.6, 23.54, 23.47, 20.91, 20.86.
SFC analysis: 2.17a (Chiralcel® OJ-3, 30% 1:1 MeOH:^{i}PrOH with 0.2% formic acid in CO_2, 2.5 mL/min, diode array) indicated >99:1 d.r.: t_R (major diastereomers) = 2.72 and 4.60 min, t_R (minor diastereomers) = 3.38 and 3.98 min. **2.17b** indicated the opposite diastereomers in >99:1 d.r.
Purity (SFC): **2.17a** – 99%; **2.17b** – 99%

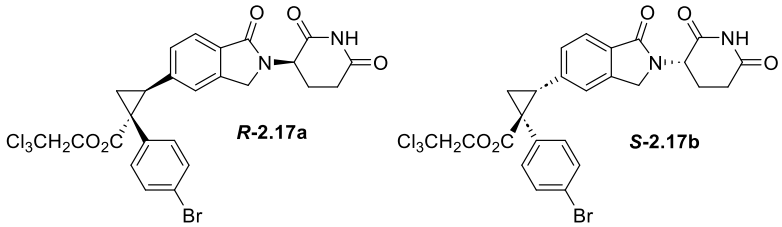

2,2,2-trichloroethyl (1*R*,2*S*)-1-(4-bromophenyl)-2-(2-((*R*)-2,6-dioxopiperidin-3-yl)-1-oxoisoindolin-5-yl)cyclopropane-1-carboxylate (*R*-2.17a).

2,2,2-trichloroethyl (1*S*,2*R*)-1-(4-bromophenyl)-2-(2-((*S*)-2,6-dioxopiperidin-3-yl)-1-oxoisoindolin-5-yl)cyclopropane-1-carboxylate (*S*-2.17b).

Compound ***S*-2.17a** was prepared following **GP 1**, using Rh_2(*S*-p-Ph-TPCP)$_4$ (3.5 mg, 1 mol%, 2.0 µmol), (*S*)-3-(1-oxo-5-vinylisoindolin-2-yl)piperidine-2,6-dione (54 mg, 1.0 equiv, 0.20 mmol), 2,2,2-trichloroethyl 2-(4-bromophenyl)-2-diazoacetate (82 mg, 1.1 equiv, 0.22 mmol), and CH_2Cl_2 (2 mL) at room temperature for two hours. Purification via flash column chromatography (SiO_2, gradient of 25% to 75% EtOAc in hexanes) afforded 2,2,2-trichloroethyl (1*R*,2*S*)-1-(4-bromophenyl)-2-(2-((*S*)-2,6-dioxopiperidin-3-yl)-1-oxoisoindolin-5-yl)cyclopropane-1-carboxylate as an amorphous white solid. (115 mg, 0.19 mmol, 94% yield).
Compound ***R*-2.17b** was prepared in the same manner using (*R*)-3-(1-oxo-5-vinylisoindolin-2-yl)piperidine-2,6-dione and Rh_2(*R*-p-Ph-TPCP)$_4$, which afforded 2,2,2-trichloroethyl (1*S*,2*R*)-1-(4-bromophenyl)-2-(2-((*R*)-2,6-dioxopiperidin-3-yl)-1-oxoisoindolin-5-yl)cyclopropane-1-carboxylate as an amorphous white solid. (117 mg, 0.19 mmol, 95% yield).

^{1}H NMR (400 MHz, $CDCl_3$): δ 8.00 (s, 1H), 7.61 (d, *J* = 7.9 Hz, 1H), 7.29 (d, *J* = 8.5 Hz, 2H), 7.00 – 6.91 (m, 3H), 6.87 (dd, *J* = 7.9, 1.5 Hz, 1H), 5.15 (dd, *J* = 13.2, 5.2 Hz, 1H), 4.83 (d, *J* = 11.9 Hz, 1H), 4.65 (d, *J* = 11.9 Hz, 1H), 4.32 (d, *J* = 16.0 Hz, 1H), 4.22 (d, *J* = 16.0 Hz, 1H), 3.30 (dd, *J* = 9.3, 7.4 Hz, 1H), 2.94 – 2.87 (m, 1H), 2.87-2.73 (m, 1H), 2.41 – 2.26 (m, 2H), 2.25-2.13 (m, 1H), 2.06 – 1.95 (m, 1H).

^{13}C{^{1}H} NMR (101 MHz, $CDCl_3$): δ 171.5, 171.3, 169.8, 168.9, 141.5, 140.4, 133.6, 132.3, 131.3, 130.3, 128.2, 123.7, 122.9, 122.0, 94.9, 74.5, 51.9, 47.0, 37.3, 33.8, 31.6, 23.4, 20.9.

SFC analysis: *S*-2.17a (Chiralcel® OJ-3, 30% 1:1 MeOH:^{i}PrOH with 0.2% formic acid in CO_2, 2.5 mL/min, diode array) indicated 98:2 d.r.: t_R (major diastereomers) = 4.08 min (peak representing minor enantiomer of ***S*-2.17a** n.d.), t_R (minor diastereomers) = 2.64 and 3.22 min. ***R*-2.17b** indicated the opposite diastereomers in 96:4 d.r.
Specific rotation: *S*-2.17a [α]D^{22} 12.7 (c 1, $CHCl_3$) ***R*-2.17b** [α]D^{22} -17.6 (c 1.9, $CHCl_3$)
Purity (SFC): ***S*-2.17a** – 97%; ***R*-2.17b** – 98%

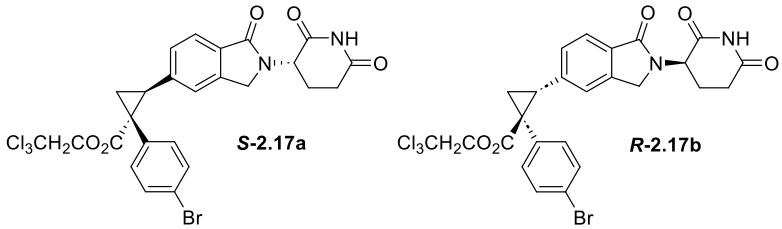

2,2,2-trichloroethyl (1*R*,2*S*)-1-(4-bromophenyl)-2-(2-((*S*)-2,6-dioxopiperidin-3-yl)-1-oxoisoindolin-5-yl)cyclopropane-1-carboxylate (*S*-2.17a).

2,2,2-trichloroethyl (1*S*,2*R*)-1-(4-bromophenyl)-2-(2-((*R*)-2,6-dioxopiperidin-3-yl)-1-oxoisoindolin-5-yl)cyclopropane-1-carboxylate (*R*-2.17b).

Compound ***R*-2.17a** was prepared following **GP 1**, using Rh_2(*S*-p-Ph-TPCP)$_4$ (3.5 mg, 1 mol%, 2.0 µmol), (*R*)-3-(1-oxo-5-vinylisoindolin-2-yl)piperidine-2,6-dione (54 mg, 1.0 equiv, 0.20 mmol), 2,2,2-trichloroethyl 2-(4-bromophenyl)-2-diazoacetate (82 mg, 1.1 equiv, 0.22 mmol), and CH_2Cl_2 (2 mL) at room temperature for two hours. Purification via flash column chromatography (SiO_2, gradient of 25% to 75% EtOAc in hexanes) afforded 2,2,2-trichloroethyl (1*R*,2*S*)-1-(4-bromophenyl)-2-(2-((*S*)-2,6-dioxopiperidin-3-yl)-1-oxoisoindolin-5-yl)cyclopropane-1-carboxylate as an amorphous white solid. (118 mg, 0.19 mmol, 96% yield).
Compound ***S*-2.17b** was prepared in the same manner using (*S*)-3-(1-oxo-5-vinylisoindolin-2-yl)piperidine-2,6-dione and Rh_2(*R*-p-Ph-TPCP)$_4$, which afforded 2,2,2-trichloroethyl (1*S*,2*R*)-1-(4-bromophenyl)-2-(2-((*S*)-2,6-dioxopiperidin-3-yl)-1-oxoisoindolin-5-yl)cyclopropane-1-carboxylate as an amorphous white solid. (117 mg, 0.19 mmol, 95% yield).

^{1}H NMR (400 MHz, $CDCl_3$): δ 7.97 (s, 1H), 7.63 (d, *J* = 7.9 Hz, 1H), 7.29 (d, *J* = 8.5 Hz, 2H), 6.98 – 6.93 (m, 3H), 6.86 (s, 1H), 5.19 (dd, *J* = 13.2, 5.3 Hz, 1H), 4.83 (d, *J* = 11.9 Hz, 1H), 4.66 (d, *J* = 11.9 Hz, 1H), 4.36 (d, *J* = 16.0 Hz, 1H), 4.12 (d, *J* = 16.1 Hz, 1H), 3.30 (dd, *J* = 9.3, 7.4 Hz, 1H), 2.97-2.87, (m, 1H), 2.87-2.72 (m, 1H), 2.41 – 2.27 (m, 2H), 2.27 – 2.15 (m, 1H), 2.08 – 1.94 (m, 1H).
^{13}C NMR (101 MHz, $CDCl_3$): δ 171.5, 171.3, 169.8, 169.0, 141.5, 140.4, 133.6, 132.4, 131.3, 130.2, 128.6, 123.7, 122.4, 121.9, 94.9, 74.6, 51.8, 46.8, 37.4, 33.8, 31.6, 23.5, 20.8.
SFC analysis: *R*-2.17a (Chiralcel® OJ-3, 30% 1:1 MeOH:^{i}PrOH with 0.2% formic acid in CO_2, 2.5 mL/min, diode array) indicated 99:1 d.r.: t_R (major diastereomers) = 2.53 min (peak representing minor enantiomer of ***R*-2.17a** n.d.), t_R (minor diastereomers) = 3.71 and 3.98 min. ***S*-15b** indicated the opposite diastereomers in 98:2 d.r.
Specific rotation: *R*-2.17a $[\alpha]D^{22}$ -4.8 (c 1, $CHCl_3$) ***S*-2.17b** $[\alpha]D^{22}$ 5.5 (c 1.9, $CHCl_3$)
Purity (SFC): ***R*-2.17a** – 96%; ***S*-2.17b** – 97%

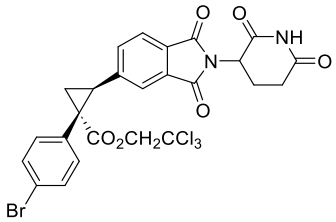

2.18a

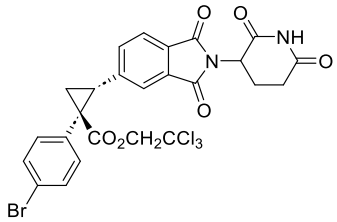

2.18b

2,2,2-trichloroethyl (1*R*,2*S*)-1-(4-bromophenyl)-2-(2-(2,6-dioxopiperidin-3-yl)-1,3-dioxoisoindolin-5-yl)cyclopropane-1-carboxylate (2.18a).

2,2,2-trichloroethyl (1*S*,2*R*)-1-(4-bromophenyl)-2-(2-(2,6-dioxopiperidin-3-yl)-1,3-dioxoisoindolin-5-yl)cyclopropane-1-carboxylate (2.18b).

Compound **2.18a** was prepared following **GP 1**, using Rh_2(*S*-p-Ph-TPCP)$_4$ (3.5 mg, 1 mol%, 2.0 µmol), 2-(2,6-dioxopiperidin-3-yl)-5-vinylisoindoline-1,3-dione (57 mg, 1.0 equiv, 0.20 mmol), 2,2,2-trichloroethyl 2-(4-bromophenyl)-2-diazoacetate (82 mg, 1.1 equiv, 0.22 mmol), and CH_2Cl_2 (2 mL) at room temperature for two hours. Purification via flash column chromatography (SiO_2, gradient of 20% to 60% EtOAc in hexanes) afforded 2,2,2-trichloroethyl (1*R*,2*S*)-1-(4-bromophenyl)-2-(2-(2,6-dioxopiperidin-3-yl)-1,3-dioxoisoindolin-5-yl)cyclopropane-1-carboxylate as an amorphous white solid. (90 mg, 0.14 mmol, 72% yield).
Compound **2.18b** was prepared in the same manner using Rh_2(*R*-p-Ph-TPCP)$_4$, which afforded 2,2,2-trichloroethyl (1*S*,2*R*)-1-(4-bromophenyl)-2-(2-(2,6-dioxopiperidin-3-yl)-1,3-dioxoisoindolin-5-yl)cyclopropane-1-carboxylate as an amorphous white solid. (90 mg, 0.14 mmol, 72% yield).

HRMS (APCI) *m/z*: $[M+H]^+$ calcd for $C_{25}H_{18}{}^{79}Br^{35}Cl_3N_2O_6$ 625.9487; Found 626.9492
^{1}H NMR (500 MHz, $CDCl_3$, reported as a mixture of diastereomers): 8.49 (s, 1H), 7.59 and 7.58 (d, *J*=2.0 Hz, 1H), 7.40 (d, 10.2 Hz, 1H), 7.29 (d, 8.0 Hz, 2H), 7.12-7.10 (m, 1H), 6.95 (d, *J*=8.0 Hz, 2H), 4.93 (dd, *J*=12.2, 5.3 Hz, 1H), 4.83 (d, 12.0 Hz, 1H), 4.65 (d, 12.0 Hz, 1H), 3.37-3.33 (m, 1H), 2.88-2.71 (m, 3H), 2.37 (dd, 9.2, 5.5 Hz, 1H), 2.13-2.08 (m, 2H).
^{13}C{^{1}H} NMR (126 MHz, $CDCl_3$, reported as a mixture of diastereomers): δ 171.2, 170.9, 168.2, 167.04, 167.02, 166.90, 166.88, 143.72, 143.70, 133.91, 133.88, 133.47, 133.46, 131.9, 131.8, 131.6, 130.1, 129.1, 128.3, 125.4, 123.4, 123.47, 123.44, 122.3, 94.8, 74.7, 49.42, 49.39, 37.76, 37.74, 33.4, 31.42, 31.40, 22.69, 22.64, 20.68, 20.64.
SFC analysis: 2.18a (Trefoil® CEL1, 20% 1:1 MeOH:^{i}PrOH with 0.2% formic acid in CO_2, 2.5 mL/min, diode array) indicated 99:1 d.r.: t_R (major diastereomers) = 5.17 and 5.62 min, t_R (minor diastereomers) = 4.31 and 4.92 min. **2.18b** indicated the opposite diastereomers in 98:2 d.r.
Purity (SFC): **2.18a** – 98%; **2.18b** – 96%

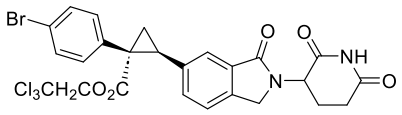

2.19a

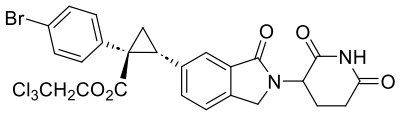

2.19b

2,2,2-trichloroethyl (1*R*,2*S*)-1-(4-bromophenyl)-2-(2-(2,6-dioxopiperidin-3-yl)-3-oxoisoindolin-5-yl)cyclopropane-1-carboxylate (2.19a).

2,2,2-trichloroethyl (1*S*,2*R*)-1-(4-bromophenyl)-2-(2-(2,6-dioxopiperidin-3-yl)-3-oxoisoindolin-5-yl)cyclopropane-1-carboxylate (2.19b).

Compound **2.19a** was prepared following **GP 1** using Rh_2(*S*-p-Ph-TPCP)$_4$ (3.5 mg, 1 mol%, 2.0 µmol), 3-(1-oxo-6-vinylisoindolin-2-yl)piperidine-2,6-dione (54 mg, 1.0 equiv, 0.20 mmol), 2,2,2-trichloroethyl 2-(4-bromophenyl)-2-diazoacetate (82 mg, 1.1 equiv, 0.22 mmol), and CH_2Cl_2 (2 mL)

at room temperature for two hours. Purification via flash column chromatography (SiO_2, gradient of 20% to 75% EtOAc in hexanes) afforded 2,2,2-trichloroethyl (1*R*,2*S*)-1-(4-bromophenyl)-2-(2-(2,6-dioxopiperidin-3-yl)-3-oxoisoindolin-5-yl)cyclopropane-1-carboxylate as an amorphous white solid. (96 mg, 0.16 mmol, 78% yield).
Compound **2.19b** was prepared in the same manner using Rh_2(*R*-p-Ph-TPCP)$_4$, which afforded 2,2,2-trichloroethyl (1*S*,2*R*)-1-(4-bromophenyl)-2-(2-(2,6-dioxopiperidin-3-yl)-3-oxoisoindolin-5-yl)cyclopropane-1-carboxylate as an amorphous white solid. (95 mg, 0.15 mmol, 77% yield).
HRMS (APCI) *m/z*: $[M+H]^+$ calcd for $C_{25}H_{21}O_5N_2{}^{79}Br^{35}Cl_3$ 612.9694; Found 612.9698
^{1}H NMR (600 MHz, $CDCl_3$, reported as a mixture of diastereomers): δ 7.94 (s, 1H), 7.53 and 7.43 (s, 1H), 7.26 (d, *J* = 8.6 Hz, 2H, partially obscured by solvent signal), 7.21 and 7.19 (d, *J* = 7.9 Hz, 1H), 7.02 and 6.92 (dd, *J* = 8.0, 1.7 Hz, 1H), 6.96 (d, *J* = 8.6 Hz, 2H), 5.20 and 5.17 (dd, *J* = 15.6, 5.0 Hz, 1H), 4.843 and 4.841 (d, *J* = 12.0 Hz, 1H), 4.65 and 4.648 (d, *J* = 11.9 Hz, 1H), 4.41 and 4.39 (d, *J* = 16.0 Hz, 1H), 4.25 and 4.24 (d, *J* = 15.9 Hz, 0H), 3.34 (t, *J* = 8.3 Hz, 1H), 2.97 – 2.88 (m, 1H), 2.86 – 2.77 (m, 1H), 2.45 – 2.26 (m, 2H), 2.24-2.18 (m, 1H), 2.10 – 1.97 (m, 1H).
^{13}C{^{1}H} NMR (101 MHz, $CDCl_3$, reported as a mixture of diastereomers): δ 171.4, 171.3, 169.72, 169.69, 169.1, 140.20, 140.18, 136.23, 136.21, 133.7, 133.6, 132.5, 132.2, 131.62, 131.58, 131.28, 131.26, 124.4, 123.7, 122.7, 121.9, 121.8, 95.0, 74.6, 51.98, 51.85, 47.0, 46.8, 36.94,36.87, 33.57, 31.64, 31.62, 23.5, 20.1, 20.0.
SFC analysis: 2.19a (Trefoil® CEL1, 25% 1:1 EtOH:^{i}PrOH with 0.2% formic acid in CO_2, 2.0 mL/min, diode array) indicated 98:2 d.r.: t_R (major diastereomers) = 4.85 and 5.60 min, t_R (minor diastereomers) = 4.34 and 4.72min. **2.19b** indicated the opposite diastereomers in 97:3 d.r.
Purity (SFC): **2.19a** – 99%; **2.19b** – 95%

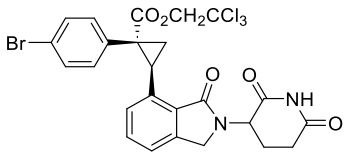

2.20a

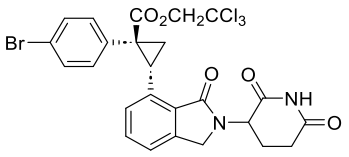

2.20b

2,2,2-trichloroethyl (1*R*,2*S*)-1-(4-bromophenyl)-2-(2-(2,6-dioxopiperidin-3-yl)-3-oxoisoindolin-4-yl)cyclopropane-1-carboxylate (2.20a).

2,2,2-trichloroethyl (1*S*,2*R*)-1-(4-bromophenyl)-2-(2-(2,6-dioxopiperidin-3-yl)-3-oxoisoindolin-4-yl)cyclopropane-1-carboxylate (2.20b).

Compound **2.20a** was prepared following **GP 1**, using Rh_2(*S*-p-Ph-TPCP)$_4$ (3.5 mg, 1 mol%, 2.0 μmol), 3-(1-oxo-7-vinylisoindolin-2-yl)piperidine-2,6-dione (54 mg, 1.0 equiv, 0.20 mmol), 2,2,2-trichloroethyl 2-(4-bromophenyl)-2-diazoacetate (82 mg, 1.1 equiv, 0.22 mmol), and CH_2Cl_2 (2 mL) at room temperature for two hours. Purification via flash column chromatography (SiO_2, gradient of 50% to 60% EtOAc in hexanes) afforded 2,2,2-trichloroethyl (1*R*,2*S*)-1-(4-bromophenyl)-2-(2-(2,6-dioxopiperidin-3-yl)-3-oxoisoindolin-4-yl)cyclopropane-1-carboxylate as an amorphous white solid. (35 mg, 56 μmol, 28% yield).
Compound **2.20b** was prepared in the same manner using Rh_2(*R*-p-Ph-TPCP)$_4$, which afforded 2,2,2-trichloroethyl (1*S*,2*R*)-1-(4-bromophenyl)-2-(2-(2,6-dioxopiperidin-3-yl)-3-oxoisoindolin-4-yl)cyclopropane-1-carboxylate as an amorphous white solid. (36 mg, 57 μmol, 29% yield).

HRMS (APCI) *m/z*: $[M+H]^+$ calcd for $C_{25}H_{21}O_5N_2{}^{79}Br^{35}Cl_3$ 612.9694; Found 612.9698
^{1}H NMR (400 MHz, $CDCl_3$, reported as a mixture of diastereomers): δ 8.30 and 8.23 (s, 1H), 7.24 – 7.14 (m, 4H), 7.00 and 6.97 (d, *J* = 8.5 Hz, 2H), 6.60-6.52 and 6.52-6.45 (m, 1H), 5.27 and 5.19 (dd, *J* = 13.3, 5.1 Hz, 1H), 4.91 and 4.89, (d, *J* = 11.9 Hz, 1H), 4.67 and 4.65 (d, *J* = 11.9 Hz, 1H), 4.47-4.22 (m, 3H), 3.00 – 2.75 (m, 2H), 2.50 – 2.18 (m, 3H), 2.15-2.10 (m, 1H).

$^{13}C\{^1H\}$ NMR (101 MHz, $CDCl_3$, reported as a mixture of diastereomers): δ 171.5 and 171.4, 171.34 and 171.30, 170.0 and 169.73, 169.72 and 169.61, 142.14 and 142.12, 135.47 and 135.45, 133.45 and 133.28. 133.42 and 133.38, 131.6 and 131.5, 131.0 and 130.9, 130.1 and 129.9, 126.1 and 126.0, 121.7 and 121.6, 121.49, 121.46, 95.1, 74.8 and 74.7, 52.1 and 51.9, 46.9 and 46.6, 36.8 and 36.5, 31.8 and 31.7, 29.6 and 29.3, 23.6 and 23.4, 19.2 and 19.0.
SFC analysis: 2.20a (Trefoil® AMY1, 30% 1:1 MeOH:^{i}PrOH with 0.2% formic acid in CO_2, 2.5 mL/min, diode array) indicated 99:1 d.r.: t_R (major diastereomers) = 3.65 and 5.13 min, t_R (minor diastereomers) = 3.17 and 4.24 min. **2.20b** indicated the opposite diastereomers in 99:1 d.r.
Purity (SFC): **2.20a** – 98%; **2.20b** – 99%

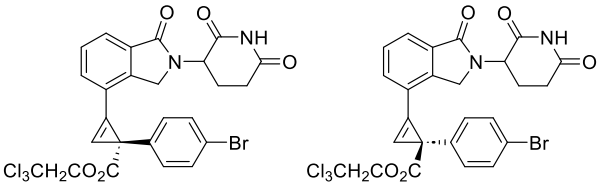

2.21a **2.21b**

2,2,2-trichloroethyl (1*S*)-1-(4-bromophenyl)-2-(2-(2,6-dioxopiperidin-3-yl)-1-oxoisoindolin-4-yl)cycloprop-2-ene-1-carboxylate (2.21a).

2,2,2-trichloroethyl (1*R*)-1-(4-bromophenyl)-2-(2-(2,6-dioxopiperidin-3-yl)-1-oxoisoindolin-4-yl)cycloprop-2-ene-1-carboxylate (2.21b).

Compound **2.21a** was prepared following **GP 2**, using Rh_2(*S*-p-Ph-TPCP)$_4$ (3.5 mg, 1 mol%, 2.0 µmol), 3-(4-ethynyl-1-oxoisoindolin-2-yl)piperidine-2,6-dione (54 mg, 1.0 equiv, 0.20 mmol), 2,2,2-trichloroethyl 2-(4-bromophenyl)-2-diazoacetate (82 mg, 1.1 equiv, 0.22 mmol), and CH_2Cl_2 (2 mL) at room temperature for two hours. Purification via flash column chromatography (SiO_2, gradient of 30% to 90% EtOAc in hexanes) afforded 2,2,2-trichloroethyl (1*S*)-1-(4-bromophenyl)-2-(2-(2,6-dioxopiperidin-3-yl)-1-oxoisoindolin-4-yl)cycloprop-2-ene-1-carboxylate as an amorphous white solid. (76 mg, 0.12 mmol, 62% yield).
Compound **2.21b** was prepared in the same manner using Rh_2(*R*-p-Ph-TPCP)$_4$, which afforded 2,2,2-trichloroethyl (1*R*)-1-(4-bromophenyl)-2-(2-(2,6-dioxopiperidin-3-yl)-1-oxoisoindolin-4-yl)cycloprop-2-ene-1-carboxylate as an amorphous white solid. (79 mg, 0.13 mmol, 64% yield).

HRMS (APCI) *m/z*: $[M+H]^+$ calcd for $C_{25}H_{19}O_5N_2{}^{79}Br^{35}Cl_3$ 610.9537; Found 610.9536
^1H NMR (600 MHz, $CDCl_3$, reported as a mixture of diastereomers): δ 8.27 (s, 1H), 7.96 (d, *J* = 7.6 Hz, 1H), 7.74 (t, *J* = 7.5 Hz, 1H), 7.58 (td, *J* = 7.6, 2.7 Hz, 1H), 7.444 and 7.437 (d, *J* = 8.5 Hz, 2H), 7.39 and 7.38 (s, 1H), 7.29 and 7.28 (d, *J* = 8.5 Hz, 2H), 5.25 and 5.22 (dd, *J* = 13.4, 5.2 Hz, 1H), 4.81 and 4.80 (d, *J* = 12 Hz, 1H), 4.762 and 4.760 (d, *J* = 12 Hz, 1H), 4.60 and 4.58 (d, *J* = 15.7 Hz, 1H), 4.43 and 4.40 (d, 16.5 Hz, 1H), 2.95-2.89 (m, 1H), 2.88-2.81 (m, 1H), 2.40-2.30 (m, 1H), 2.26 – 2.18 (m, 1H).
$^{13}C\{^1H\}$ NMR (101 MHz, $CDCl_3$, reported as a mixture of diastereomers): δ 171.92, 171.90, 171.0, 169.5, 169.4, 168.60, 168.58, 142.41, 142.40, 138.6, 138.5, 133.02, 133.97, 132.60, 132.57, 131.6, 129.9, 129.32, 126.29, 121.3, 120.32, 120.29, 113.7, 113.3, 102.41, 102.37, 95.0, 74.5, 74.4, 52.1, 52.0, 46.8, 46.7, 32.5, 32.4, 31.6, 23.6.
SFC analysis: 2.21a (Trefoil® AMY1, 30% 1:1 MeOH:^{i}PrOH with 0.2% formic acid in CO_2, 2.5 mL/min, diode array) indicated 98:2 d.r.: t_R (major diastereomers) = 3.00 and 3.55 min, t_R (minor diastereomers) = 4.41 and 5.81 min. **19b** indicated the opposite diastereomers in 98:2 d.r.
Purity (SFC): **2.21a** – 98%; **2.21b** – 95%

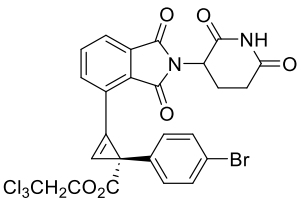

2.22a

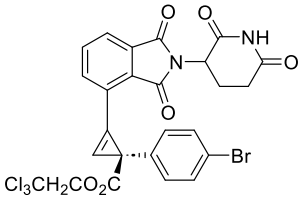

2.22b

2,2,2-trichloroethyl (1*S*)-1-(4-bromophenyl)-2-(2-(2,6-dioxopiperidin-3-yl)-1,3-dioxoisoindolin-4-yl)cycloprop-2-ene-1-carboxylate (2.22a).

2,2,2-trichloroethyl (1*R*)-1-(4-bromophenyl)-2-(2-(2,6-dioxopiperidin-3-yl)-1,3-dioxoisoindolin-4-yl)cycloprop-2-ene-1-carboxylate (2.22b).

Compound **2.22a** was prepared following **GP 2**, using Rh_2(*S*-p-Ph-TPCP)$_4$ (3.5 mg, 1 mol%, 2.0 µmol), 2-(2,6-dioxopiperidin-3-yl)-4-ethynylisoindoline-1,3-dione (56 mg, 1.0 equiv, 0.20 mmol), 2,2,2-trichloroethyl 2-(4-bromophenyl)-2-diazoacetate (82 mg, 1.1 equiv, 0.22 mmol), and CH_2Cl_2 (2 mL) at room temperature for two hours. Purification via flash column chromatography (SiO_2, gradient of 30% to 55% EtOAc in hexanes) afforded 2,2,2-trichloroethyl (1*S*)-1-(4-bromophenyl)-2-(2-(2,6-dioxopiperidin-3-yl)-1,3-dioxoisoindolin-4-yl)cycloprop-2-ene-1-carboxylate as an amorphous white solid. (93 mg, 0.15 mmol, 76% yield).
Compound **2.22b** was prepared in the same manner using Rh_2(*R*-p-Ph-TPCP)$_4$, which afforded 2,2,2-trichloroethyl (1*R*)-1-(4-bromophenyl)-2-(2-(2,6-dioxopiperidin-3-yl)-1,3-dioxoisoindolin-4-yl)cycloprop-2-ene-1-carboxylate as an amorphous white solid. (99 mg, 0.16 mmol, 79% yield).

HRMS (APCI) *m/z*: $[M+H]^+$ calcd for $C_{25}H_{17}O_6N_2{}^{79}Br^{35}Cl_3$ 624.9330; Found 624.9330
^{1}H NMR (600 MHz, $CDCl_3$, reported as a mixture of diastereomers): δ 8.29 (s, 1H), 7.95 (d, *J* = 7.7 Hz, 1H), 7.74 (t, *J* = 7.6 Hz, 1H), 7.584 and 7.58 (t, *J* = 7.7 Hz, 1H), 7.443 and 7.436 (d, *J* = 8.6 Hz, 2H), 7.39 and 7.38 (s, 1H), 7.29 and 7.28 (d, *J* = 8.6 Hz, 2H), 5.26 and 5.22 (dd, *J* = 13.4, 5.0 Hz, 1H), 4.81 and 4.79 (d, *J* = 12.0 Hz, 1H), 4.761 and 4.760 (d, *J* = 11.9 Hz, 1H), 4.61 and 4.56 (d, *J* = 16.6 Hz, 1H), 4.43 and 4.40 (d, *J* = 16.5 Hz, 1H), 2.97-2.87 (m, 1H), 2.87-2.79 (m, 1H), 2.41-2.29 (m, 1H), 2.27 – 2.11 (m, 1H).
^{13}C{^{1}H} NMR (101 MHz, $CDCl_3$, reported as a mixture of diastereomers): δ 171.8, 170.9, 168.0, 166.59, 166.57, 166.24, 166.22, 138.3, 138.2, 135.8, 135.7, 134.9, 133.1, 131.5, 130.1, 129.91, 129.86, 125.2, 122.70, 122.68, 121.2, 112.48, 112.45, 108.11, 108.06, 95.11, 95.08, 74.49, 74.47, 49.6, 33.92, 33.91, 31.5, 22.7.
SFC analysis: 2.22a (Chiralcel® OX-3, 30% 1:1 MeOH:^{i}PrOH with 0.2% formic acid in CO_2, 2.5 mL/min, diode array) indicated 80:20 d.r.: t_R (major diastereomers) = 6.92 and 12.88 min, t_R (minor diastereomers) = 4.57 and 4.97 min. **2.22b** indicated the opposite diastereomers in 81:19 d.r.
Purity (SFC): **2.22a** – 99%; **20b** – 98%

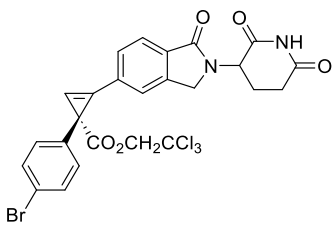

2.23a

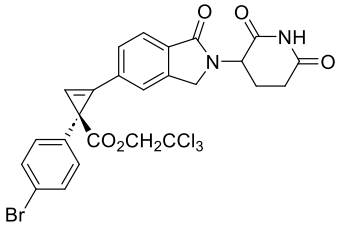

2.23b

2,2,2-trichloroethyl (1*S*)-1-(4-bromophenyl)-2-(2-(2,6-dioxopiperidin-3-yl)-1-oxoisoindolin-5-yl)cycloprop-2-ene-1-carboxylate (2.23a).

2,2,2-trichloroethyl (1*R*)-1-(4-bromophenyl)-2-(2-(2,6-dioxopiperidin-3-yl)-1-oxoisoindolin-5-yl)cycloprop-2-ene-1-carboxylate (2.23b).

Compound **2.23a** was prepared following **GP 2**, using Rh_2(*S*-p-Ph-TPCP)$_4$ (3.5 mg, 1 mol%, 2.0 µmol), 3-(5-ethynyl-1-oxoisoindolin-2-yl)piperidine-2,6-dione (54 mg, 1.0 equiv, 0.20 mmol), 2,2,2-trichloroethyl 2-(4-bromophenyl)-2-diazoacetate (82 mg, 1.1 equiv, 0.22 mmol), and CH_2Cl_2 (2 mL) at room temperature for two hours. Purification via flash column chromatography (SiO_2, gradient of 35% to 55% EtOAc in hexanes) afforded 2,2,2-trichloroethyl (*S*)-1-(4-bromophenyl)-2-(2-(2,6-dioxopiperidin-3-yl)-1-oxoisoindolin-5-yl)cycloprop-2-ene-1-carboxylate as an amorphous white solid. (48 mg, 78 µmol, 39% yield).
Compound **2.23b** was prepared in the same manner using Rh_2(*R*-p-Ph-TPCP)$_4$, which afforded 2,2,2-trichloroethyl (1*R*)-1-(4-bromophenyl)-2-(2-(2,6-dioxopiperidin-3-yl)-1-oxoisoindolin-5-yl)cycloprop-2-ene-1-carboxylate as an amorphous white solid. (46 mg, 74 µmol, 37% yield).

HRMS (APCI) *m/z*: $[M+H]^+$ calcd for $C_{25}H_{19}O_5N_2{}^{79}Br^{35}Cl_3$ 610.9537; Found 610.9536
^{1}H NMR (400 MHz, $CDCl_3$, reported as a mixture of diastereomers): δ 8.27 (s, 1H), 7.952 and 7.950 (d, *J* = 7.9 Hz, 1H), 7.79 – 7.71 (m, 1H), 7.69 – 7.64 (m, 1H), 7.43 (d, *J* = 8.5 Hz, 2H), 7.39 (s, 1H), 7.29 (d, *J* = 8.6 Hz, 2H), 5.23 (dd, *J* = 13.3, 5.2 Hz, 1H), 4.823 and 4.816 (d, *J* = 12.0 Hz, 1H), 4.764 and 4.760 (d, *J* = 12.0 Hz, 1H), 4.52 and 4.51 (d, *J* = 16.3 Hz, 1H), 4.37 and 4.35 (d, *J* = 16.3 Hz, 1H), 2.98 – 2.88 (m, 2H), 2.88 – 2.76 (m, 1H), 2.35 (qd, *J* = 13.1, 5.1 Hz, 1H), 2.26 – 2.15 (m, 1H).
^{13}C{^{1}H} NMR (101 MHz, $CDCl_3$, reported as a mixture of diastereomers): δ ^{13}C NMR (101 MHz, $CDCl_3$) δ 172.08, 172.06, 171.1, 169.5, 168.5, 142.1, 138.5, 133.17, 133.15, 131.50, 131.48, 130.32, 130.30, 129.95, 128.4, 125.0, 124.5, 121.13, 121.10, 116.2, 102.2, 102.1, 95.1, 74.42, 74.39, 52.1, 47.1, 33.3, 31.6, 23.5.
SFC analysis: 2.23a (Chiralpak® AS3, 20% 1:1:1 EtOH:^{i}PrOH:MeCN with 20 mM NH_4HCO_2 in CO_2, 2.5 mL/min, diode array) indicated >99:1 d.r.: t_R (major diastereomers) = 3.94 and 6.41 min, t_R (minor diastereomers) = 3.41 and 4.88 min. **2.23b** indicated the opposite diastereomers in 99:1 d.r.
Purity (SFC): 2.23a – 97%; **2.23b** – 95%

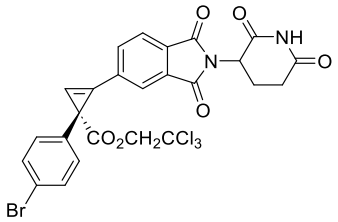

2.24a

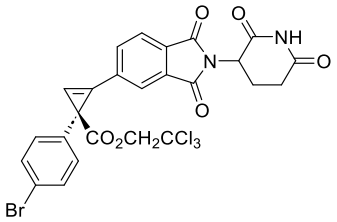

2.24b

2,2,2-trichloroethyl (1*S*)-1-(4-bromophenyl)-2-(2-(2,6-dioxopiperidin-3-yl)-1,3-dioxoisoindolin-5-yl)cycloprop-2-ene-1-carboxylate (2.24a).

2,2,2-trichloroethyl (1*R*)-1-(4-bromophenyl)-2-(2-(2,6-dioxopiperidin-3-yl)-1,3-dioxoisoindolin-5-yl)cycloprop-2-ene-1-carboxylate (2.24b).

Compound **2.24a** was prepared following **GP 2**, using Rh_2(*S*-p-Ph-TPCP)$_4$ (3.5 mg, 1 mol%, 2.0 µmol), 2-(2,6-dioxopiperidin-3-yl)-5-ethynylisoindoline-1,3-dione (56 mg, 1.0 equiv, 0.20 mmol), 2,2,2-trichloroethyl 2-(4-bromophenyl)-2-diazoacetate (82 mg, 1.1 equiv, 0.22 mmol), and CH_2Cl_2 (2 mL) at room temperature for two hours. Purification via flash column chromatography (SiO_2, gradient of 20% to 50% EtOAc in hexanes) afforded 2,2,2-trichloroethyl (1*S*)-1-(4-bromophenyl)-2-(2-(2,6-dioxopiperidin-3-yl)-1,3-dioxoisoindolin-5-yl)cycloprop-2-ene-1-carboxylate as an amorphous white solid. (87 mg, 0.14 mmol, 69% yield).
Compound **2.24b** was prepared in the same manner using Rh_2(*R*-p-Ph-TPCP)$_4$, which afforded 2,2,2-trichloroethyl (1*R*)-1-(4-bromophenyl)-2-(2-(2,6-dioxopiperidin-3-yl)-1,3-dioxoisoindolin-5-yl)cycloprop-2-ene-1-carboxylate as an amorphous white solid. (88 mg, 0.14 mmol, 70% yield).

HRMS (APCI) *m/z*: $[M+H]^+$ calcd for $C_{25}H_{16}{}^{79}Br_{35}Cl_3N_2O_6$ 624.9344; Found 624.9341
^{1}H NMR (500 MHz, $CDCl_3$, reported as a mixture of diastereomers): δ 8.26 (s, 1H), 8.11-8.10 (m, 1H), 7.98-7.94 (m, 2H), 7.54 (s, 1H), 7.45 (d, *J*=8.5 Hz, 2H), 7.28 (d, *J*=8.5 Hz, 2H), 5.01 (dd, *J*=12.5, 5.1 Hz, 1H), 4.84 and 4.83 (d, *J*=12.0 Hz, 1H), 4.76 (d, *J*=12.0 Hz, 1H), 2.94-2.72 (m, 3H), 2.19-2.14 (m, 1H).
^{13}C{^{1}H} NMR (126 MHz, $CDCl_3$, reported as a mixture of diastereomers): δ 171.5, 171.0, 167.9, 166.5, 166.4, 137.9, 135.7, 132.7, 132.6, 131.6, 131.2, 129.90, 129.89, 124.89, 124.88, 124.6, 121.4, 116.1, 116.0, 104.5, 95.0, 74.5, 60.5, 49.7, 33.7, 31.48, 31.46, 22.7, 22.6, 14.3.
SFC analysis: 2.24a (Chiralcel® OJ-3, 20% 1:1 MeOH:^{i}PrOH with 0.2% formic acid in CO_2, 2.5 mL/min, diode array) indicated 98:2 d.r.: t_R (major diastereomers) = 7.10 and 8.24 min, t_R (minor diastereomers) = 9.20 and 11.52 min. **2.24b** indicated the opposite diastereomers in 99:1 d.r.
Purity (SFC): 2.24a – 98%; **2.24b** – 95%

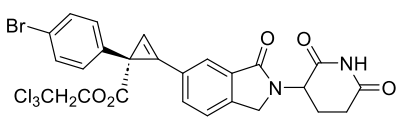

2.25a

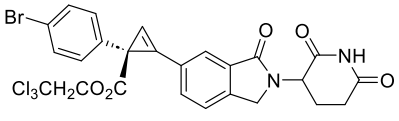

2.25b

2,2,2-trichloroethyl (1*S*)-1-(4-bromophenyl)-2-(2-(2,6-dioxopiperidin-3-yl)-3-oxoisoindolin-5-yl)cycloprop-2-ene-1-carboxylate (2.25a).

2,2,2-trichloroethyl (1*R*)-1-(4-bromophenyl)-2-(2-(2,6-dioxopiperidin-3-yl)-3-oxoisoindolin-5-yl)cycloprop-2-ene-1-carboxylate (2.25b).

Compound **2.25a** was prepared following **GP 2**, using Rh_2(*S*-p-Ph-TPCP)$_4$ (3.5 mg, 1 mol%, 2.0 µmol), 3-(6-ethynyl-1-oxoisoindolin-2-yl)piperidine-2,6-dione (54 mg, 1.0 equiv, 0.20 mmol), 2,2,2-trichloroethyl 2-(4-bromophenyl)-2-diazoacetate (82 mg, 1.1 equiv, 0.22 mmol), and CH_2Cl_2 (2 mL) at room temperature for two hours. Purification via flash column chromatography (SiO_2,

gradient of 60% to 75% EtOAc in hexanes) afforded 2,2,2-trichloroethyl (1*S*)-1-(4-bromophenyl)-2-(2-(2,6-dioxopiperidin-3-yl)-3-oxoisoindolin-5-yl)cycloprop-2-ene-1-carboxylate as an amorphous white solid. (76 mg, 12 mmol, 62% yield).
Compound **2.25b** was prepared in the same manner using Rh_2(*R*-p-Ph-TPCP)$_4$, which afforded 2,2,2-trichloroethyl (1*R*)-1-(4-bromophenyl)-2-(2-(2,6-dioxopiperidin-3-yl)-3-oxoisoindolin-5-yl)cycloprop-2-ene-1-carboxylate as an amorphous white solid. (77 mg, 0.13 mmol, 63% yield).

HRMS (APCI) *m/z*: $[M+H]^+$ calc'd for $C_{25}H_{19}O_5N_2{}^{79}Br^{35}Cl_3$ 610.9537; Found 610.9540
^{1}H NMR (600 MHz, $CDCl_3$, reported as a mixture of diastereomers): δ 8.17 (s, 1H), 8.13 (d, *J* = 6.2 Hz, 1H), 7.81 (t, *J* = 7.9 Hz, 1H), 7.54 (d, *J* = 7.9 Hz, 1H), 7.42 (d, *J* = 8.6 Hz, 2H), 7.32 (s, 1H), 7.31 (d, *J* = 8.4 Hz, 2H), 5.29 – 5.17 (m, 1H), 4.82 and 4.81 (d, *J* = 11.9 Hz, 1H), 4.76 and 4.75 Hz (d, *J* = 11.9 Hz, 1H), 4.54 (d, *J* = 16.7 Hz, 1H), 4.39 (d, *J* = 16.5 Hz, 1H), 2.97 – 2.90 (m, 1H), 2.88 – 2.77 (m, 1H), 2.41 – 2.30 (m, 1H), 2.25 – 2.18 (m, 1H).
^{13}C{^{1}H} NMR (101 MHz, $CDCl_3$, reported as a mixture of diastereomers): δ 172.2, 169.5, 171.3, 168.5, 143.3, 138.6, 133.61, 133.57, 132.54, 132.52, 131.4, 130.1, 125.65, 125.61, 125.4, 123.9, 121.02, 121.00, 116.3, 116.2, 100.7, 95.1, 74.4, 52.03, 52.00, 47.3, 33.3, 31.6, 23.5.
SFC analysis: 2.25a (Chiralcel® OJ-3, 30% 1:1 MeOH:^{i}PrOH with 0.2% formic acid in CO_2, 2.5 mL/min, diode array) indicated 98:2 d.r.: t_R (major diastereomers) = 1.81 and 2.40 min, t_R (minor diastereomers) = 2.12 and 3.16 min. **2.25b** indicated the opposite diastereomers in 98:2 d.r.
Purity (SFC): **2.25a** – 99%; **2.25b** – 99%

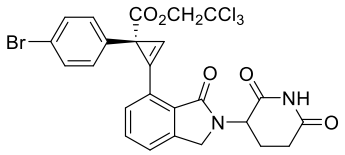

2.26a

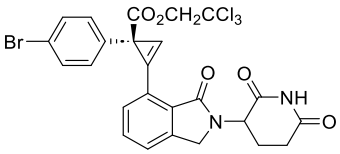

2.26b

2,2,2-trichloroethyl (1*S*)-1-(4-bromophenyl)-2-(2-(2,6-dioxopiperidin-3-yl)-3-oxoisoindolin-4-yl)cycloprop-2-ene-1-carboxylate (2.26a).

2,2,2-trichloroethyl (1*R*)-1-(4-bromophenyl)-2-(2-(2,6-dioxopiperidin-3-yl)-3-oxoisoindolin-4-yl)cycloprop-2-ene-1-carboxylate (2.26b).

Compound **2.26a** was prepared following **GP 2**, using Rh_2(*S*-p-Ph-TPCP)$_4$ (3.5 mg, 1 mol%, 2.0 µmol), 3-(7-ethynyl-1-oxoisoindolin-2-yl)piperidine-2,6-dione (54 mg, 1.0 equiv, 0.20 mmol), 2,2,2-trichloroethyl 2-(4-bromophenyl)-2-diazoacetate (82 mg, 1.1 equiv, 0.22 mmol), and CH_2Cl_2 (2 mL) at room temperature for two hours. Purification via flash column chromatography (SiO_2, gradient of 45% to 70% EtOAc in hexanes) afforded 2,2,2-trichloroethyl (1*S*)-1-(4-bromophenyl)-2-(2-(2,6-dioxopiperidin-3-yl)-3-oxoisoindolin-4-yl)cycloprop-2-ene-1-carboxylate as an amorphous white solid. (99 mg, 0.16 mmol, 81% yield).
Compound **2.26b** was prepared in the same manner using Rh_2(*R*-p-Ph-TPCP)$_4$, which afforded 2,2,2-trichloroethyl (1*R*)-1-(4-bromophenyl)-2-(2-(2,6-dioxopiperidin-3-yl)-3-oxoisoindolin-4-yl)cycloprop-2-ene-1-carboxylate as an amorphous white solid. (97 mg, 0.16 mmol, 79% yield).

HRMS (APCI) *m/z*: $[M+H]^+$ calcd for $C_{25}H_{19}O_5N_2{}^{79}Br^{35}Cl_3$ 610.9537; Found 610.9545
^{1}H NMR (600 MHz, $CDCl_3$, reported as a mixture of diastereomers): δ 8.17 (s, 1H), 7.66 (d, *J* = 3.6 Hz, 1H), 7.63 – 7.54 (m, 2H), 7.51 and 7.50 (s, 1H), 7.41 and 7.40 (d, *J* = 8.6 Hz, 2H), 7.34 and 7.33 (d, *J* = 8.6 Hz, 2H), 5.25 and 5.23 (dd, *J* = 13.0, 5.1 Hz, 1H), 4.85 and 4.83 (d, *J* = 11.9 Hz, 1H),

4.74 and 4.73 (d, J = 12.0 Hz, 1H), 2.95-2.89 (m, 1H), 2.89-2.84 (m, 1H), 2.43-2.33 (m, 1H), 2.29-2.14 (m, 1H).

^{13}C{^{1}H} NMR (101 MHz, $CDCl_3$, reported as a mixture of diastereomers): δ 172.5, 172.4, 171.3, 169.7, 168.4, 143.1, 139.1, 139.0, 132.2, 131.29, 131.28, 130.45, 130.43, 130.37, 130.26, 130.24, 124.8, 122.5, 120.80, 120.77, 112.7, 112.5, 106.0, 105.9, 95.3, 74.4,74.3, 52.1, 52.0, 47.1, 47.0, 33.27, 33.26, 31.7, 23.5.

SFC analysis: 2.26a (Chiralpak® AS3, 20% 1:1 MeOH:^{i}PrOH with 0.2% formic acid in CO_2, 2.5 mL/min, diode array) indicated 61:39 d.r.: t_R (major diastereomers) = 4.05 and 5.21 min, t_R (minor diastereomers) = 4.49 and 7.67 min. **2.26b** indicated the opposite diastereomers in 60:40 d.r.

Purity (SFC): 2.26a – 95%; **2.26b** – 95%

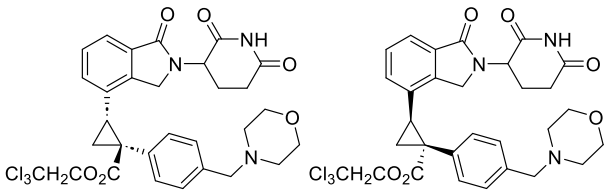

2.27a **2.27b**

2,2,2-trichloroethyl (1*S*,2*R*)-2-(2-(2,6-dioxopiperidin-3-yl)-1-oxoisoindolin-4-yl)-1-(4-(morpholinomethyl)phenyl)cyclopropane-1-carboxylate (2.27a).

2,2,2-trichloroethyl (1*R*,2*S*)-2-(2-(2,6-dioxopiperidin-3-yl)-1-oxoisoindolin-4-yl)-1-(4-(morpholinomethyl)phenyl)cyclopropane-1-carboxylate (2.27b).

A 10 mL round-bottom flask was charged with a PTFE magnetic stir bar and ca. 200% w/w 4 Å molecular sieves, then flame dried under vacuum. The flask was then backfilled with dry nitrogen. Rh_2(*S-tetra-p*-BrPPTTL)$_4$ (3.7 mg, 1 mol%, 1.0 μmol) and 3-(1-oxo-4-vinylisoindolin-2-yl)piperidine-2,6-dione (27 mg, 1.0 equiv, 0.10 mmol) were charged to the flask, and the flask was evacuated and backfilled with nitrogen. The flask was equipped with an argon balloon and rubber septum, and dry CH_2Cl_2 (0.5 mL) along with 0.10 mL 1,1,1,3,3,3-hexafluoroisopropanol (10 equiv, 1.0 mmol) were charged via syringe. A solution of 2,2,2-trichloroethyl 2-diazo-2-(4-(morpholinomethyl)phenyl)acetate (43 mg, 1.1 equiv, 0.11 mmol) in dry CH_2Cl_2 (0.5 mL, prepared in the same manner under inert atmosphere) was added dropwise to the stirred reaction at room temperature. The reaction was allowed to stir for two hours, after which the reaction was filtered through Celite®, rinsing the filter pad with CH_2Cl_2. The crude residue was dry-mounted onto silica gel and was purified by flash column chromatography (SiO_2, 0-5% methanol in CH_2Cl_2), which afforded 2,2,2-trichloroethyl (1*S*,2*R*)-2-(2-(2,6-dioxopiperidin-3-yl)-1-oxoisoindolin-4-yl)-1-(4-(morpholinomethyl)phenyl)cyclopropane-1-carboxylate as an amorphous white solid (50 mg, 79 μmol, 79% yield).

Compound **2.27b** was prepared in the same manner using Rh_2(*R-tetra-p*-BrPPTTL)$_4$, which afforded 2,2,2-trichloroethyl (1*R*,2*S*)-2-(2-(2,6-dioxopiperidin-3-yl)-1-oxoisoindolin-4-yl)-1-(4-(morpholinomethyl)phenyl)cyclopropane-1-carboxylate as an amorphous white solid as an amorphous white solid. (49 mg, 77 μmol, 77% yield).

HRMS (APCI) *m/z*: $[M+H]^+$ calcd for $C_{30}H_{31}O_6N_3{}^{35}Cl_3$ 634.1273; Found 634.1279

^{1}H NMR (400 MHz, $CDCl_3$, reported as a mixture of diastereomers): δ 8.54 (s, 1H), 7.595 and 7.593 (d, J = 7.6 Hz, 1H), 7.10 – 7.00 (m, 3H), 6.96 and 6.93 (d, J = 12.3 Hz, 2H), 5.29 and 5.25 (dd, J = 9.6, 5.2 Hz, 1H), 4.86 and 4.85 (d, J = 12.0 Hz, 1H), 4.664 and 4.658 (d, J = 12.0 Hz, 1H), 4.58 and 4.56 (d, J = 16.0 Hz, 1H), 4.42 and 4.38 (d, J = 16.2 Hz, 1H), 3.69 – 3.58 (m, 4H), 3.43 – 3.36 (m,

2H), 3.07 (ddd, J = 9.4, 7.4, 2.1 Hz, 1H), 3.01 – 2.77 (m, 2H), 2.42 – 2.19 (m, 7H), 2.15 (ddd, J = 7.5, 5.3, 2.2 Hz, 1H).
^{13}C{^{1}H} NMR (101 MHz, $CDCl_3$, reported as a mixture of diastereomers): δ 171.9, 171.8, 171.29, 171.27, 169.7, 169.53, 169.48, 141.7, 141.6, 137.3, 137.2, 132.0, 131.9, 131.5, 131.4, 131.30, 131.27, 131.19, 131.18, 129.12, 129.06, 129.05, 128.0, 122.6, 95.3, 95.2, 74.4, 74.3, 67.0, 62.9, 53.50, 53.46, 52.03, 51.96, 46.61, 46.50, 37.1, 37.0, 31.7, 29.8, 29.7, 29.6, 23.63, 23.60, 19.7, 19.6.
SFC analysis: 2.27a (Trefoil® CEL2, 35% 1:1 MeOH:^{i}PrOH with 0.2% formic acid in CO_2, 2.5 mL/min, diode array) indicated 83:17 d.r.: t_R (major diastereomers) = 6.04 and 8.83 min, t_R (minor diastereomers) = 6.80 and 13.50 min. **2.27b** indicated the opposite diastereomers in 85:15 d.r.
Purity (SFC): 2.27a – 99%; **2.27b** – 99%

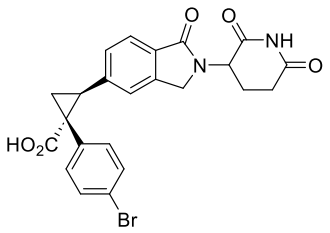

2.28a

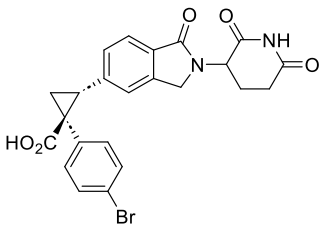

2.28b

(1*R*,2*S*)-1-(4-bromophenyl)-2-(2-(2,6-dioxopiperidin-3-yl)-1-oxoisoindolin-5-yl)cyclopropane-1-carboxylic acid (2.28a).

(1*S*,2*R*)-1-(4-bromophenyl)-2-(2-(2,6-dioxopiperidin-3-yl)-1-oxoisoindolin-5-yl)cyclopropane-1-carboxylic acid (2.28b).

A 100 mL round-bottom flask was charged with a PTFE magnetic stir bar and zinc dust (754 mg, 16 equiv, 11.5 mmol) under ambient conditions, followed by 2,2,2-trichloroethyl (1*S*,2*R*)-1-(4-bromophenyl)-2-(2-(2,6-dioxopiperidin-3-yl)-1-oxoisoindolin-5-yl)cyclopropane-1-carboxylate (443 mg, 1.0 equiv, 0.72 mmol). Tetrahydrofuran (16.6 mL) was charged via syringe followed by acetate buffer (10 mL, pH = 3.7, 1.2 M in H_2O, NaOAc/AcOH). The reaction was stirred at room temperature for 18 hours, after which the reaction was filtered through Celite®, rinsing with ethyl acetate. The aqueous layer was extracted thrice with 50 mL portions of ethyl acetate, after which the combined organics were washed with 150 mL brine. The combined organics were dried over magnesium sulfate, then filtered and concentrated in vacuuo. The crude material was purified via flash column chromatography (C18, 10-95% MeCN in H_2O, 0.1% trifluoroacetic acid buffer), which gave (1*R*,2*S*)-1-(4-bromophenyl)-2-(2-(2,6-dioxopiperidin-3-yl)-1-oxoisoindolin-5-yl)cyclopropane-1-carboxylic acid as an amorphous white solid (280 mg, 0.58 mmol, 83% yield).

Compound **2.28b** was prepared in the same manner using zinc dust (727 mg, 16 equiv, 11.1 mmol), 2,2,2-trichloroethyl (1*R*,2*S*)-1-(4-bromophenyl)-2-(2-(2,6-dioxopiperidin-3-yl)-1-oxoisoindolin-5-yl)cyclopropane-1-carboxylate (427 mg, 1.0 equiv, 0.70 mmol), tetrahydrofuran (16.0 mL), and acetate buffer (9.6 mL), which gave (1*S*,2*R*)-1-(4-bromophenyl)-2-(2-(2,6-dioxopiperidin-3-yl)-1-oxoisoindolin-5-yl)cyclopropane-1-carboxylic acid (286 mg, 0.59 mmol, 82% yield) as an amorphous white solid.

HRMS (APCI) *m/z*: $[M+H]^+$ calcd for $C_{23}H_{20}O_5N_2{}^{79}Br$ 483.0550; Found 483.0559
^{1}H NMR (600 MHz, CD_3OD, reported as a mixture of diastereomers): δ 7.55 – 7.42 (m, 1H), 7.26 (d, J = 8.1 Hz, 2H), 7.14 and 7.10 (s, 1H), 7.05-6.98 (m, 1H, partially obscured by signal at 7.00), 7.00 (d, J = 8.0 Hz, 3H), 5.10 and 5.07 (dd, J = 10.9, 5.2 Hz, 1H), 4.39 and 4.34 (d, J = 17.0 Hz, 1H), 4.27 and 4.26 (d, J = 17.0 Hz, 1H), 3.27 (t, J = 8.2 Hz, 1H), 2.87 (ddd, J = 18.5, 13.6, 5.4 Hz, 1H), 2.81 – 2.70 (m, 1H), 2.43 (pd, J = 13.5, 4.5 Hz, 1H), 2.17-2.08 (m, 3H).

$^{13}C\{^1H\}$ NMR (101 MHz, CD_3OD, reported as a mixture of diastereomers): δ 176.2, 174.7, 172.22, 172.20, 171.19, 171.17, 143.5, 143.01, 143.29, 135.7, 135.6, 135.0, 134.9, 131.9, 131.0, 130.9, 129.7, 129.3, 124.3, 124.0, 123.73, 123.71, 122.0, 53.6, 53.5, 38.6, 38.5, 34.0, 32.3, 24.0, 20.5, 20.4.

SFC analysis: 2.28a (Chiralpak® AS3, 20% 1:1 EtOH:^{i}PrOH with 0.2% formic acid in CO_2, 2.5 mL/min, diode array) indicated 99:1 d.r.: t_R (major diastereomers) = 4.56 and 6.30 min, t_R (minor diastereomers) = 5.73 and 8.81 min. **2.28b** indicated the opposite diastereomers in 99:1 d.r.
Purity (SFC): **2.28a** – 98%; **2.28b** – 98%

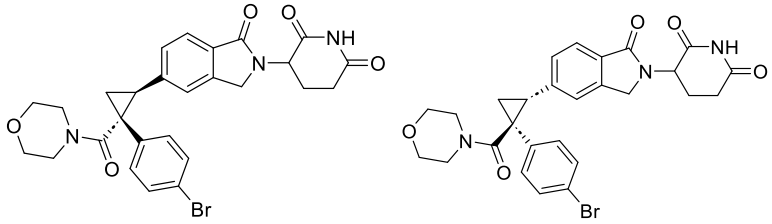

2.29a **2.29b**

3-(5-((1*S*,2*R*)-2-(4-bromophenyl)-2-(morpholine-4-carbonyl)cyclopropyl)-1-oxoisoindolin-2-yl)piperidine-2,6-dione (2.29a).

3-(5-((1*R*,2*S*)-2-(4-bromophenyl)-2-(morpholine-4-carbonyl)cyclopropyl)-1-oxoisoindolin-2-yl)piperidine-2,6-dione (2.29b).

A 4 mL scintillation vial equipped with a PTFE magnkjetic stir bar was flame-dried under vacuum and backfilled with dry nitrogen. The vial was charged with (1*S*,2*R*)-1-(4-bromophenyl)-2-(2-(2,6-dioxopiperidin-3-yl)-1-oxoisoindolin-5-yl)cyclopropane-1-carboxylic acid (50 mg, 1.0 equiv, 0.10 mmol) and N-(chloro(dimethylamino)methylene)-N-methylmethanaminium hexafluorophosphate(V) (34 mg, 1.2 equiv, 0.12 mmol). Morpholine (11 µL, 1.3 equiv, 0.13 mmol), 1-methyl-1H-imidazole (28 µL, 3.5 equiv, 0.35 mmol), and acetonitrile (0.25 mL) were charged successively by syringe, and the reaction was stirred at room temperature for 18 hours. The reaction was stirred at room temperature for 18 hours, after which the reaction was partitioned between water (50 mL) and ethyl acetate (50 mL). The aqueous layer was extracted thrice with 50 mL portions of ethyl acetate, after which the combined organics were washed with 150 mL of brine. The combined organics were dried over magnesium sulfate, then filtered and concentrated in vacuuo. The crude material was purified via flash column chromatography (SiO_2, 0-10% methanol in CH_2Cl_2), which gave 3-(5-((1*S*,2*R*)-2-(4-bromophenyl)-2-(morpholine-4-carbonyl)cyclopropyl)-1-oxoisoindolin-2-yl)piperidine-2,6-dione as an amorphous white solid (31 mg, 55 µmol, 55% yield).

Compound **2.29b** was prepared in the same manner from (1*S*,2*R*)-1-(4-bromophenyl)-2-(2-(2,6-dioxopiperidin-3-yl)-1-oxoisoindolin-5-yl)cyclopropane-1-carboxylic acid, which gave 3-(5-((1*R*,2*S*)-2-(4-bromophenyl)-2-(morpholine-4-carbonyl)cyclopropyl)-1-oxoisoindolin-2-yl)piperidine-2,6-dione as an amorphous white solid (34 mg, 60 µmol, 60% yield).

HRMS (APCI) *m/z*: $[M+H]^-$ calcd for $C_{27}H_{27}O_5N_3{}^{79}Br$ 552.1129; Found 552.1139
^1H NMR (600 MHz, $CDCl_3$, reported as a mixture of diastereomers): δ 7.99 and 7.98 (s, 1H), 7.60 (d, *J* and 7.58 (d, *J* = 5.9 Hz, 1H), 7.29 – 7.26 (m, 2H, partially obscured by solvent signal), 7.17 and 7.10 (s, 1H), 7.07 and 7.02 (dd, *J* = 7.9, 1.4 Hz, 1H), 6.99 – 6.92 (m, 2H), 5.160 and 5.156 (dd, *J* = 13.3, 5.1 Hz, 1H), 4.343 and 4.338 (d, *J* = 15.9 Hz, 1H), 4.17 and 4.16 (d, *J* = 15.9 Hz, 1H), 3.74 – 3.37 (m, 7H), 3.30 (dt, *J* = 9.2, 6.9 Hz, 1H), 3.18 (s, 1H), 2.92 – 2.87 (m, 1H), 2.80 (ddd, *J* = 18.1,

13.4, 5.4 Hz, 1H), 2.37 – 2.25 (m, 1H), 2.23 – 2.13 (m, 1H), 2.08 (ddd, *J* = 7.0, 5.8, 3.2 Hz, 1H), 1.68 (ddd, *J* = 9.1, 5.8, 4.5 Hz, 1H).
$^{13}C\{^1H\}$ NMR (101 MHz, $CDCl_3$, reported as a mixture of diastereomers): δ 171.74, 171.72, 170.27, 170.23, 170.0, 169.1, 141.4, 141.25, 141.21, 134.26, 134.21, 131.74, 131.71, 129.87,129.7, 128.6, 128.3, 123.8, 123.51, 123.48, 123.2, 121.2, 121.1, 66.4, 51.8, 51.7, 46.80, 46.76, 38.1, 37.9, 31.6, 30.2, 30.1, 23.4, 16.1, 16.0.
SFC analysis: 2.29a (Chiralcel® OJ-3, 20% 1:1 MeOH:^{i}PrOH with 0.2% formic acid in CO_2, 2.5 mL/min, diode array) indicated 99:1 d.r.: t_R (major diastereomers) = 2.80 and 3.65 min, t_R (minor diastereomers) = 3.21 and 4.77 min. **2.29b** indicated the opposite diastereomers in 99:1 d.r.
Purity (SFC): 2.29a – 98%; **2.29b** – 98%

Synthetic References

(1) Qin, C.; Davies, H. M. L., Role of Sterically Demanding Chiral Dirhodium Catalysts in Site-Selective C–H Functionalization of Activated Primary C–H Bonds. *J. Am. Chem. Soc.* **2014,** *136*, 9792-9796.

(2) Garlets, Z. J.; Boni, Y. T.; Sharland, J. C.; Kirby, R. P.; Fu, J.; Bacsa, J.; Davies, H. M. L., Design, Synthesis, and Evaluation of Extended C4–Symmetric Dirhodium Tetracarboxylate Catalysts. *ACS Catal.* **2022,** *12*, 10841-10848.

(3) Hundertmark, T.; Littke, A. F.; Buchwald, S. L.; Fu, G. C., Pd(PhCN)2Cl2/P(t-Bu)3: A Versatile Catalyst for Sonogashira Reactions of Aryl Bromides at Room Temperature. *Org. Lett.* **2000,** *2*, 1729-1731.

(4) Tortoreto, C.; Rackl, D.; Davies, H. M. L., Metal-Free C–H Functionalization of Alkanes by Aryldiazoacetates. *Org. Lett.* **2017,** *19*, 770-773.

(5) Tilden, J. A. R.; Lubben, A. T.; Reeksting, S. B.; Kociok-Köhn, G.; Frost, C. G., Pd(II)-Mediated C−H Activation for Cysteine Bioconjugation. *Chem. Eur. J.* **2022,** *28*, e202104385.

Section 4: Crystallographic Information

Submitted by: **William Tracy, Huw Davies Lab**
Solved by: **John Bacsa, Mackenzie Young**

R_1=5.45%

Crystal Data and Experimental

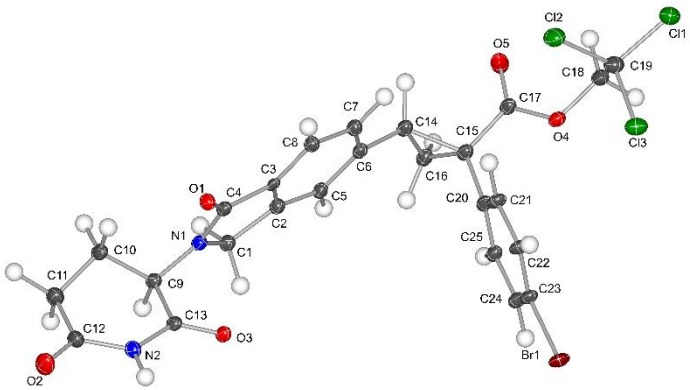

Figure S2-6 Crystal Structure of (*R*)-2.17a

Experimental. Single colourless plate-shaped crystals of WT-05-553 were crystallized from methanol by slow evaporation. A suitable crystal with dimensions 0.13 × 0.10 × 0.05 mm³ was selected and mounted on a loop with paratone on a XtaLAB Synergy, Dualflex, HyPix diffractometer. The crystal was kept at a steady T = 104(6) K during data collection. The structure was solved with the ShelXT (Sheldrick, 2015) solution program using dual methods and by using Olex2 1.5-alpha (Dolomanov et al., 2009) as the graphical interface. The model was refined with olex2.refine 1.5-alpha (Bourhis et al., 2015) using full matrix least squares minimisation on $\boldsymbol{F^2}$.

Crystal Data. $C_{25}H_{20}BrCl_3N_2O_5$, M_r = 614.709, monoclinic, $P2_1$ (No. 4), a = 6.1901(4) Å, b = 9.2069(6) Å, c = 22.1261(17) Å, β = 90.543(7)°, α = γ = 90°, V = 1260.94(16) Å³, T = 104(6) K, Z = 2, Z' = 1, μ(Mo K$_\alpha$) = 1.988, 15376 reflections measured, 5610 unique (R_{int} = 0.0782) which were used in all calculations. The final wR_2 was 0.1153 (all data) and R_1 was 0.0545 (I≥2 σ(I)).

Compound	WT-05-553
Formula	$C_{25}H_{20}BrCl_3N_2O_5$
$D_{calc.}$/ g cm^{-3}	1.619
μ/mm^{-1}	1.988
Formula Weight	614.709
Color	colorless
Shape	plate-shaped
Size/mm³	0.13×0.10×0.05
T/K	104(6)
Crystal System	monoclinic
Flack Parameter	-0.006(8)
Hooft Parameter	-0.006(8)
Space Group	$P2_1$
a/Å	6.1901(4)
b/Å	9.2069(6)
c/Å	22.1261(17)
α/°	90
β/°	90.543(7)
γ/°	90
V/Å³	1260.94(16)
Z	2
Z'	1
Wavelength/Å	0.71073
Radiation type	Mo K$_\alpha$
Θ_{min}/°	3.41
Θ_{max}/°	27.57
Measured Refl's.	15376
Indep't Refl's	5610
Refl's I≥2 σ(I)	4416
R_{int}	0.0782
Parameters	451
Restraints	823
Largest Peak	1.5961
Deepest Hole	-0.6735
GooF	1.0057
wR_2 (all data)	0.1153
wR_2	0.1076
R_1 (all data)	0.0786
R_1	0.0545

Structure Quality Indicators

Reflections:	d min (MoKα) 2Θ=55.1° 0.77	I/σ(I) 10.2	Rint m=2.69 7.82%	Full 50.5° 95.6	
Refinement:	Shift -0.001	Max Peak 1.6	Min Peak -0.7	GooF 1.006	Hooft -.006(8)

A colorless plate-shaped-shaped crystal with dimensions 0.13 × 0.10 × 0.05 mm^3 was mounted on a loop with paratone. Data were collected using a XtaLAB Synergy, Dualflex, HyPix diffractometer equipped with an Oxford Cryosystems low-temperature device operating at T = 104(6) K.

Data were measured using ω scans with Mo K_α radiation. The diffraction pattern was indexed and the total number of runs and images was based on the strategy calculation from the program CrysAlisPro system (CCD 43.92a 64-bit (release 05-10-2023)). The maximum resolution that was achieved was Θ = 27.57° (0.77 Å).

The unit cell was refined using CrysAlisPro 1.171.43.121a (Rigaku OD, 2024) on 3358 reflections, 22% of the observed reflections.

Data reduction, scaling and absorption corrections were performed using CrysAlisPro 1.171.43.121a (Rigaku OD, 2024). The final completeness is 98.65 % out to 27.57° in Θ. An analytical numeric absorption correction using a multifaceted crystal model based on expressions derived by R.C. Clark & J.S. Reid. (Clark, R. C. & Reid, J. S. (1995). Acta Cryst. A51, 887-897) was performed using CrysAlisPro 1.171.43.121a (Rigaku Oxford Diffraction, 2024). An empirical absorption correction using spherical harmonics, implemented in SCALE3 ABSPACK scaling algorithm was also applied. The absorption coefficient μ of this material is 1.988 mm^{-1} at this wavelength (λ = 0.71073Å) and the minimum and maximum transmissions are 0.821 and 0.924.

The structure was solved and the space group $P2_1$ (# 4) determined by the ShelXT (Sheldrick, 2015) structure solution program using using dual methods and refined by full matrix least squares minimisation on $\boldsymbol{F^2}$ using version of olex2.refine 1.5-alpha (Bourhis et al., 2015). All atoms, even hydrogen atoms, were refined anisotropically. Hydrogen atom positions were located from the electron densities and freely refined using Hirshfeld scattering factors. Refinement was by using NoSpherA2, an implementation of non-spherical atom-form-factors (F. Kleemiss, H. Puschmann, O. Dolomanov, S.Grabowsky - https://doi.org/10.1039/D0SC05526C – 2020). NoSpherA2 implementation of HAR makes use of tailor-made aspherical atomic form factors calculated from a Hirshfeld-partitioned electron density (ED) not from spherical-atom form factors. The ED was calculated from a Gaussian basis set single determinant SCF wavefunction from DFT using selected functionals for a fragment of this crystal. This fragment was embedded in an electrostatic crystal field by employing cluster charges. The following options were used: software: SOFTWARE: ORCA PARTITIONING: NoSpherA2 INT ACCURACY: Normal METHOD: PBE BASIS SET: x2c-SVP CHARGE: 0 MULTIPLICITY: 1 SOLVATION: Methanol RELATIVISTIC: DKH2 DATE: 2024-05-14_13-44-20

There is a single formula unit in the asymmetric unit, which is represented by the reported sum formula. In other words: Z is 2 and Z' is 1. The moiety formula is C25 H20 Br Cl3 N2 O5.

The Flack parameter was refined to -0.006(8). Determination of absolute structure using Bayesian statistics on Bijvoet differences using the Olex2 results in -0.006(8). The chiral atoms in this structure are: C9(R), C14(S), C15(R). Note: The Flack parameter is used to determine chirality of the crystal studied, the value should be near 0, a value of 1 means that the stereochemistry is wrong and the model should be inverted. A value of 0.5 means that the crystal consists of a racemic mixture of the two enantiomers.

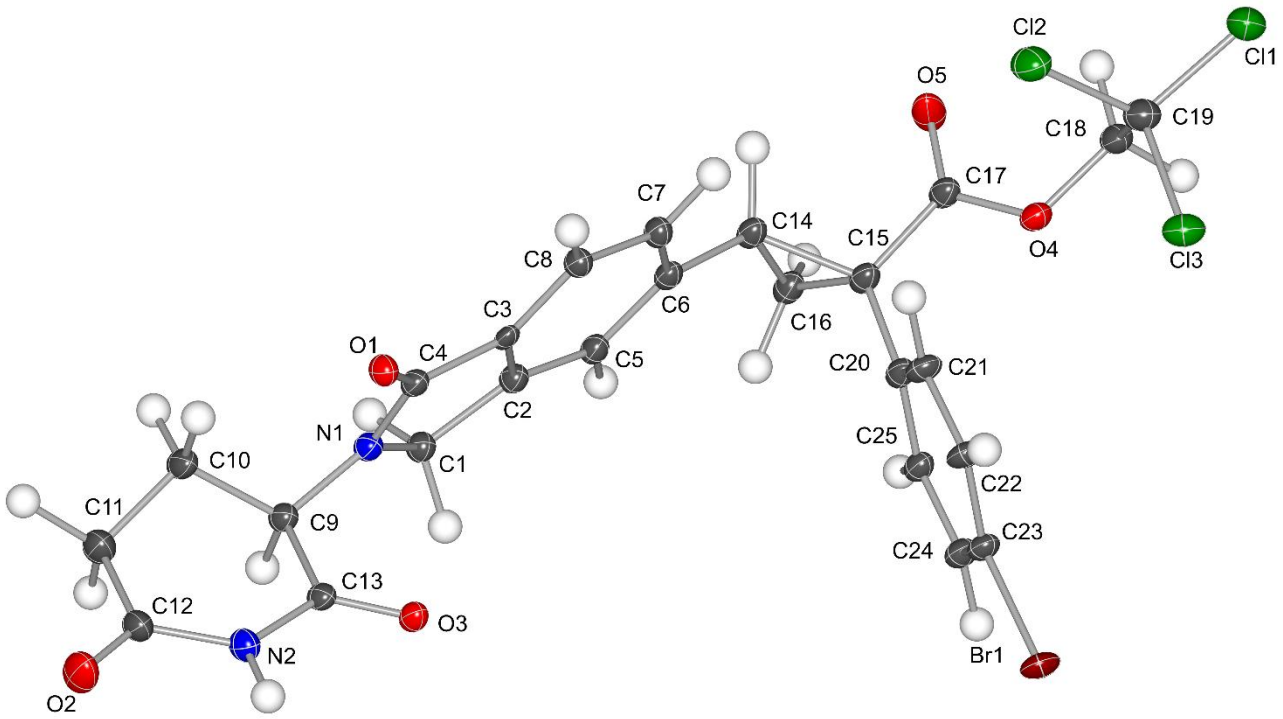

Figure S2-7. A thermal ellipsoidal representation of the asymmetric unit in the crystal structure (50% probability) which consists of one whole molecule. The chiral atoms in this structure are: C9(R), C14(S), and C15(R).

Figure S2-8: Diffraction Data

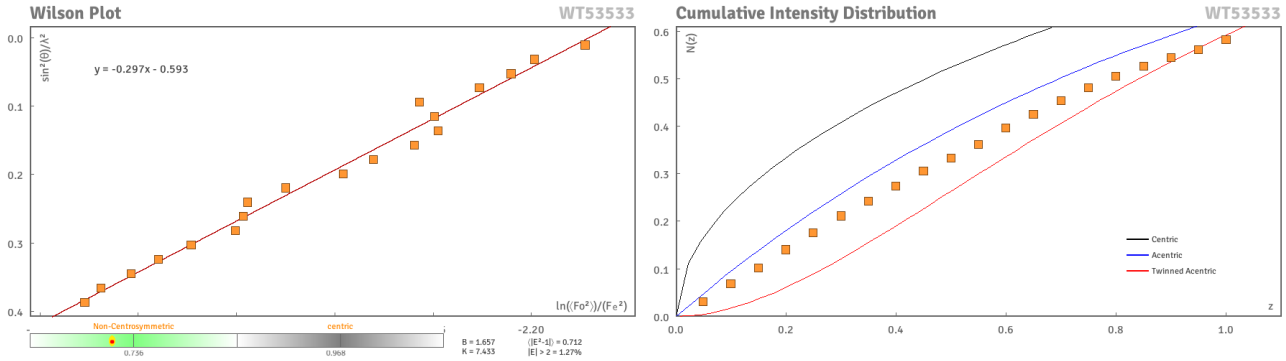

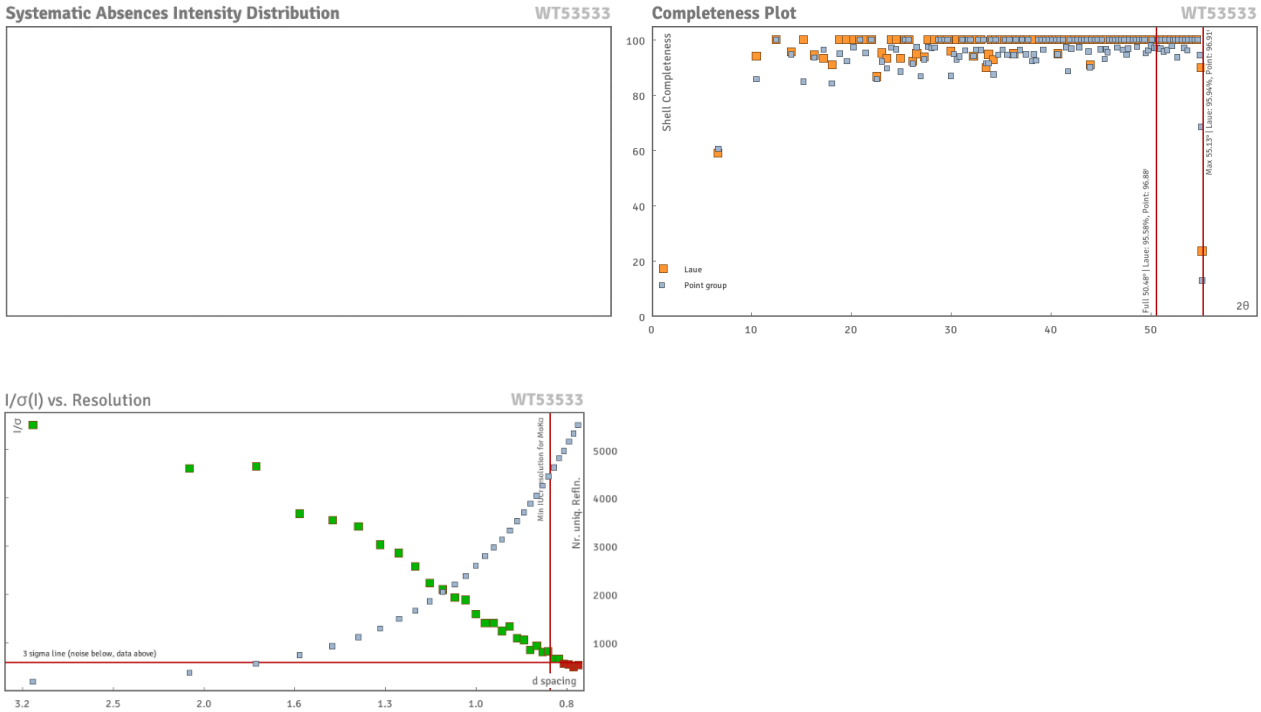

Figure S2-9: Refinement and Data

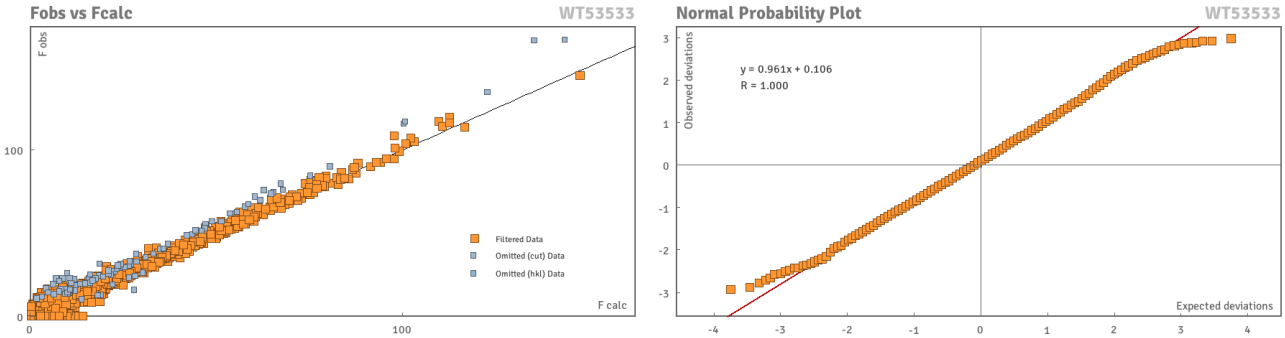

Reflection Statistics

Total reflections (after filtering)	15067	Unique reflections	5610
Completeness	0.969	Mean I/σ	9.61
hkl_{max} collected	(8, 11, 28)	hkl_{min} collected	(-8, -11, -28)
hkl_{max} used	(8, 11, 28)	hkl_{min} used	(-8, -11, 0)
Lim d_{max} collected	100.0	Lim d_{min} collected	0.36
d_{max} used	5.98	d_{min} used	0.77
Friedel pairs	3967	Friedel pairs merged	0
Inconsistent equivalents	5	R_{int}	0.079
R_{sigma}	0.0982	Intensity transformed	0
Omitted reflections	309	Omitted by user (OMIT hkl)	3
Multiplicity	(5283, 3149, 948, 182, 41, 3)	Maximum multiplicity	9
Removed systematic absences	0	Filtered off (Shel/OMIT)	0

Table S2-1: Fractional Atomic Coordinates (×10^4) and Equivalent Isotropic Displacement Parameters (Å^2×10^3) for WT-05-553. U_{eq} is defined as 1/3 of the trace of the orthogonalised U_{ij}.

Atom	x	y	z	U_{eq}
Br1	5371.5(7)	1137.5(3)	1682.0(2)	21.17(12)
Cl3	3100.3(17)	5997.6(11)	86.8(5)	26.1(3)
Cl1	761(2)	8186.8(11)	-588.1(6)	28.2(3)
Cl2	2633(2)	8864.4(11)	589.3(6)	29.2(3)
O1	7753(5)	8378(3)	4542.3(14)	17.2(6)
O2	10793(5)	6114(5)	6695.3(14)	32.8(8)
O3	7875(5)	4979(3)	4887.5(14)	17.5(7)
O4	-410(5)	6480(3)	1003.0(14)	19.3(5)
O5	-2542(6)	8132(4)	1452.0(16)	33.7(9)
N1	4848(6)	7116(4)	4900.2(18)	16.2(6)
N2	9217(6)	5538(4)	5810.9(18)	18.4(8)
C1	2699(7)	6635(5)	4700(2)	16.9(7)
C2	2630(7)	7101(4)	4056(2)	16.0(7)
C3	4518(7)	7884(4)	3935(2)	13.4(7)
C4	5927(7)	7865(4)	4472(2)	15.2(7)
C5	1035(7)	6939(4)	3619(2)	16.3(8)
C6	1334(7)	7600(5)	3054(2)	15.8(6)
C7	3204(7)	8426(4)	2945(2)	16.9(8)
C8	4842(7)	8574(4)	3376(2)	16.2(8)
C9	5785(7)	6673(4)	5473(2)	17.0(6)
C10	6482(8)	7933(5)	5882(2)	22.2(9)
C11	7441(9)	7325(5)	6465(2)	25.4(9)
C12	9287(7)	6297(5)	6349(2)	21.8(9)
C13	7694(7)	5653(4)	5353(2)	15.7(8)
C14	-410(8)	7585(5)	2582(2)	17.9(5)
C15	-528(7)	6447(4)	2067(2)	17.8(4)
C16	-2184(7)	6491(4)	2567(2)	19.1(5)
C17	-1285(7)	7124(5)	1485(2)	18.5(6)
C18	-833(8)	7092(5)	422(2)	21.0(5)
C19	1315(9)	7524(5)	144(2)	23.8(4)
C20	963(7)	5191(5)	2009(2)	16.9(5)
C21	3039(7)	5365(5)	1791(2)	18.8(8)
C22	4392(8)	4176(5)	1687(2)	20.1(9)
C23	3612(8)	2779(5)	1814(2)	17.2(8)
C24	1527(8)	2574(5)	2030(2)	18.4(8)
C25	228(8)	3780(5)	2133(2)	17.6(8)

Table S2-2: Anisotropic Displacement Parameters (×10^4) for WT-05-553. The anisotropic displacement factor exponent takes the form: $-2\pi^2[h^2a^{*2} \times U_{11} + \ldots + 2hka^* \times b^* \times U_{12}]$

Atom	U_{11}	U_{22}	U_{33}	U_{23}	U_{13}	U_{12}
Br1	22.6(2)	11.99(18)	28.9(3)	5.0(2)	1.08(16)	-0.4(2)
Cl3	27.2(5)	19.5(5)	31.5(6)	1.8(4)	0.1(4)	3.2(4)

Atom	U_{11}	U_{22}	U_{33}	U_{23}	U_{13}	U_{12}
Cl1	36.4(7)	22.4(6)	25.6(5)	4.3(4)	-3.2(3)	2.4(3)
Cl2	35.7(7)	20.7(5)	31.0(6)	-1.6(4)	-7.2(4)	0.8(3)
O1	18.1(8)	17.2(14)	16.3(12)	-0.9(5)	-4.0(5)	-0.6(7)
O2	38.0(15)	32.9(17)	27.2(15)	10.1(13)	-15.7(8)	-6.6(14)
O3	18.8(17)	16.0(14)	17.6(11)	1.9(11)	-5.1(8)	-2.3(7)
O4	23.5(11)	13.6(10)	20.9(6)	3.4(5)	-3.4(3)	-2.2(3)
O5	45.3(17)	33.9(13)	21.7(12)	25.3(8)	-7.5(6)	-4.9(5)
N1	17.9(8)	13.8(13)	16.9(7)	0.8(5)	-3.2(4)	-1.3(5)
N2	18.5(15)	19.0(16)	17.6(11)	-0.5(8)	-4.7(7)	-0.3(8)
H2	17(8)	10(20)	18(9)	-3(6)	-2(4)	3(6)
C1	18.1(8)	15.1(16)	17.3(7)	0.4(6)	-3.2(4)	-1.6(5)
H1a	19(5)	15(2)	17(5)	0.3(10)	-2.3(19)	-1.9(10)
H1b	18(3)	16(5)	19(4)	0.1(15)	-3.0(14)	-2.9(17)
C2	17.2(8)	13.7(16)	17.2(7)	1.2(6)	-3.0(4)	-2.1(5)
C3	15.8(8)	9.0(15)	15.4(7)	3.7(6)	-2.3(4)	-3.9(5)
C4	17.1(8)	12.2(16)	16.2(7)	1.3(6)	-3.3(4)	-2.0(5)
C5	17.0(9)	14.3(16)	17.5(7)	2.2(6)	-3.1(4)	-3.2(5)
H5	27(8)	50(30)	23(6)	-15(7)	-10(3)	9(5)
C6	16.4(9)	13.5(12)	17.5(7)	3.4(5)	-2.6(4)	-3.4(4)
C7	17.3(9)	16.6(17)	16.5(8)	1.7(6)	-3.6(4)	-2.1(5)
H7	26(7)	50(20)	23(4)	-16(6)	-12(3)	13(5)
C8	17.3(9)	14.9(16)	16.4(8)	1.2(6)	-3.4(4)	-1.3(5)
H8	26(7)	50(20)	23(4)	-16(6)	-12(3)	13(5)
C9	18.9(10)	14.7(12)	17.2(8)	0.8(6)	-3.6(4)	-0.9(4)
H9	19(4)	15(4)	18(4)	1.6(16)	-3.1(15)	-0.8(16)
C10	30(2)	15.6(12)	20.6(13)	0.5(7)	-8.2(8)	-1.9(6)
H10a	30(4)	18(4)	20(5)	-0.4(16)	-9.0(17)	-1.6(17)
H10b	31(4)	17(4)	22(5)	1.8(16)	-7.6(16)	-2.0(18)
C11	32.4(16)	23.4(17)	20.3(14)	6.0(10)	-6.7(7)	-1.1(7)
H11a	32(5)	24(4)	21(4)	5.9(17)	-7.4(18)	-2.1(16)
H11b	32(4)	24(5)	22(5)	6.0(18)	-6.3(16)	0.5(18)
C12	29.2(15)	18.6(17)	17.6(12)	2.2(10)	-6.6(7)	-0.1(8)
C13	17.5(12)	12.9(15)	16.7(11)	-0.7(7)	-3.7(5)	-0.7(7)
C14	18.1(8)	15.7(8)	19.7(7)	3.7(4)	-4.6(3)	-3.8(3)
H14	19(6)	16(2)	22(6)	3.7(11)	-6(2)	-3.5(11)
C15	18.1(8)	15.3(7)	20.0(6)	3.9(3)	-4.8(3)	-3.7(3)
C16	18.7(8)	17.3(11)	21.1(9)	2.8(4)	-4.0(4)	-4.8(4)
H16a	19(5)	19(5)	22(5)	2.6(17)	-4.1(18)	-4(2)
H16b	20(2)	22(6)	26(7)	3.9(12)	-4.4(11)	-3(2)
C17	19.1(12)	15.8(10)	20.5(6)	3.4(5)	-5.5(3)	-3.3(3)
C18	26.4(7)	15.2(11)	21.4(7)	1.6(4)	-4.5(3)	-1.2(4)
H18a	27(5)	16(3)	21(4)	1.2(15)	-4.2(16)	-1.1(15)
H18b	26(4)	16(3)	23(6)	1.6(15)	-4.7(17)	-1.0(15)
C19	26.9(7)	18.8(6)	25.5(6)	1.4(3)	-2.9(3)	1.4(3)
C20	17.7(8)	14.8(7)	18.3(12)	3.4(3)	-4.9(4)	-3.4(4)
C21	18.6(8)	12.3(6)	25(2)	4.2(3)	-2.4(6)	-2.1(4)
H21	30(5)	11(6)	100(30)	6.7(15)	28(6)	5(3)
C22	19.2(9)	12.0(6)	29(2)	4.1(3)	-0.4(6)	-1.3(4)
H22	30(5)	11(6)	100(30)	6.7(15)	28(6)	5(3)
C23	19.1(8)	11.8(5)	21(2)	3.7(3)	-3.2(6)	-2.0(4)
C24	19.2(8)	14.4(7)	22(2)	3.2(3)	-2.7(6)	-2.6(4)
H24	29(8)	15(2)	90(40)	4.1(14)	22(9)	1.6(19)
C25	18.7(8)	14.8(7)	19(2)	3.3(3)	-4.3(6)	-3.3(4)
H25	38(9)	17(6)	140(50)	7.1(16)	44(11)	7(3)

Table S2-3: Bond Lengths in Å for WT-05-553.

Atom	Atom	Length/Å
Br1	C23	1.887(4)
Cl3	C19	1.793(5)
Cl1	C19	1.762(5)
Cl2	C19	1.773(5)
O1	C4	1.234(5)
O2	C12	1.213(5)
O3	C13	1.208(5)
O4	C17	1.340(6)
O4	C18	1.426(6)
O5	C17	1.213(5)
N1	C1	1.467(5)
N1	C4	1.353(6)
N1	C9	1.447(6)
N2	H2	0.97(5)
N2	C12	1.381(6)
N2	C13	1.382(5)
C1	H1a	1.04(3)
C1	H1b	1.04(3)
C1	C2	1.489(6)
C2	C3	1.402(6)
C2	C5	1.383(6)
C3	C4	1.469(6)
C3	C8	1.405(6)
C5	H5	1.06(5)
C5	C6	1.405(6)
C6	C7	1.407(6)
C6	C14	1.494(6)
C7	H7	1.0780
C7	C8	1.393(6)
C8	H8	1.0780

Atom	Atom	Length/Å
C9	H9	1.17(5)
C9	C10	1.531(6)
C9	C13	1.534(6)
C10	H10a	1.08(3)
C10	H10b	1.08(3)
C10	C11	1.523(6)
C11	H11a	1.12(4)
C11	H11b	1.12(4)
C11	C12	1.508(7)
C14	H14	1.070(3)
C14	C15	1.550(6)
C14	C16	1.490(6)
C15	C16	1.516(7)
C15	C17	1.500(6)
C15	C20	1.486(6)
C16	H16a	1.0702(18)
C16	H16b	1.0702(18)
C18	H18a	1.098(9)
C18	H18b	1.097(9)
C18	C19	1.522(7)
C20	C21	1.386(6)
C20	C25	1.405(6)
C21	H21	1.0780
C21	C22	1.399(6)
C22	H22	1.0780
C22	C23	1.403(6)
C23	C24	1.394(7)
C24	H24	1.0780
C24	C25	1.391(6)
C25	H25	1.0780

Table S2-4: Bond Angles in ° for WT-05-553.

Atom	Atom	Atom	Angle/°
C18	O4	C17	118.1(3)
C4	N1	C1	113.3(4)
C9	N1	C1	122.3(4)
C9	N1	C4	124.1(4)
C12	N2	H2	117(3)
C13	N2	H2	115(3)
C13	N2	C12	127.5(4)
H1a	C1	N1	111.2(2)
H1b	C1	N1	111.2(2)
H1b	C1	H1a	109.1
C2	C1	N1	102.7(4)
C2	C1	H1a	111.2(2)
C2	C1	H1b	111.2(2)
C3	C2	C1	108.4(4)
C5	C2	C1	130.7(4)
C5	C2	C3	120.9(4)
C4	C3	C2	109.2(4)
C8	C3	C2	121.8(4)
C8	C3	C4	129.0(4)

Atom	Atom	Atom	Angle/°
N1	C4	O1	124.4(4)
C3	C4	O1	129.3(4)
C3	C4	N1	106.3(4)
H5	C5	C2	120.8(3)
C6	C5	C2	118.4(4)
C6	C5	H5	120.8(3)
C7	C6	C5	120.1(4)
C14	C6	C5	121.1(4)
C14	C6	C7	118.4(4)
H7	C7	C6	119.0(3)
C8	C7	C6	122.0(4)
C8	C7	H7	119.0(3)
C7	C8	C3	116.7(4)
H8	C8	C3	121.6(3)
H8	C8	C7	121.6(3)
H9	C9	N1	107.5(2)
C10	C9	N1	114.4(4)
C10	C9	H9	107.5(3)
C13	C9	N1	108.9(4)

Atom	Atom	Atom	Angle/°
C13	C9	H9	107.5(2)
C13	C9	C10	110.7(4)
H10a	C10	C9	109.8(3)
H10b	C10	C9	109.8(3)
H10b	C10	H10a	108.3
C11	C10	C9	109.2(4)
C11	C10	H10a	109.8(3)
C11	C10	H10b	109.8(3)
H11a	C11	C10	109.2(3)
H11b	C11	C10	109.2(3)
H11b	C11	H11a	107.892608686(15)
C12	C11	C10	112.1(4)
C12	C11	H11a	109.2(3)
C12	C11	H11b	109.2(3)
N2	C12	O2	119.5(4)
C11	C12	O2	124.0(4)
C11	C12	N2	116.6(4)
N2	C13	O3	121.1(4)
C9	C13	O3	122.7(4)
C9	C13	N2	116.2(4)
H14	C14	C6	115(2)
C15	C14	C6	123.3(4)
C15	C14	H14	111(2)
C16	C14	C6	123.4(4)
C16	C14	H14	114(2)
C16	C14	C15	59.8(3)
C16	C15	C14	58.2(3)
C17	C15	C14	111.3(3)
C17	C15	C16	114.0(4)
C20	C15	C14	124.4(4)
C20	C15	C16	120.6(4)
C20	C15	C17	116.0(4)
C15	C16	C14	62.1(3)
H16a	C16	C14	117.6(2)
H16a	C16	C15	117.6(2)
H16b	C16	C14	117.6(2)
H16b	C16	C15	117.6(2)
H16b	C16	H16a	114.7
O5	C17	O4	123.6(4)
C15	C17	O4	112.0(4)
C15	C17	O5	124.4(4)
H18a	C18	O4	105(2)
H18b	C18	O4	113(2)
H18b	C18	H18a	107.6(11)
C19	C18	O4	108.3(4)
C19	C18	H18a	111(2)
C19	C18	H18b	111(2)
Cl1	C19	Cl3	108.7(3)
Cl2	C19	Cl3	107.7(3)
Cl2	C19	Cl1	110.7(3)
C18	C19	Cl3	111.4(3)
C18	C19	Cl1	107.3(3)
C18	C19	Cl2	110.9(4)
C21	C20	C15	121.3(4)
C25	C20	C15	120.0(4)
C25	C20	C21	118.6(4)
H21	C21	C20	119.1(2)
C22	C21	C20	121.7(4)
C22	C21	H21	119.1(3)
H22	C22	C21	120.8(3)
C23	C22	C21	118.4(4)
C23	C22	H22	120.8(3)
C22	C23	Br1	120.2(4)
C24	C23	Br1	118.8(3)
C24	C23	C22	121.0(4)
H24	C24	C23	120.4(3)
C25	C24	C23	119.1(4)
C25	C24	H24	120.4(3)
C24	C25	C20	121.1(4)
H25	C25	C20	119.4(3)
H25	C25	C24	119.4(3)

Table S2-5: Torsion Angles in ° for WT-05-553.

Atom	Atom	Atom	Atom	Angle/°
Br1	C23	C22	C21	-179.9(3)
Br1	C23	C24	C25	179.5(3)
Cl3	C19	C18	O4	58.1(3)
Cl1	C19	C18	O4	177.0(3)
Cl2	C19	C18	O4	-61.9(3)
O1	C4	N1	C1	179.6(4)
O1	C4	N1	C9	-7.4(5)
O1	C4	C3	C2	177.0(5)
O1	C4	C3	C8	-4.6(6)
O2	C12	N2	C13	-176.8(4)
O2	C12	C11	C10	150.3(5)
O3	C13	N2	C12	176.1(4)
O3	C13	C9	N1	-22.4(5)
O3	C13	C9	C10	-148.9(5)
O4	C17	C15	C14	148.0(4)

Atom	Atom	Atom	Atom	Angle/°
O4	C17	C15	C16	-148.5(4)
O4	C17	C15	C20	-1.7(4)
O5	C17	C15	C14	-32.1(5)
O5	C17	C15	C16	31.4(5)
O5	C17	C15	C20	178.2(5)
N1	C1	C2	C3	-4.8(4)
N1	C1	C2	C5	179.0(3)
N1	C4	C3	C2	-1.5(4)
N1	C4	C3	C8	176.9(3)
N1	C9	C10	C11	-179.9(4)
N1	C9	C13	N2	157.8(3)
N2	C12	C11	C10	-29.4(5)
N2	C13	C9	C10	31.2(4)
C1	C2	C3	C4	4.0(4)
C1	C2	C3	C8	-174.5(3)
C1	C2	C5	C6	174.7(5)
C2	C3	C8	C7	-0.9(5)
C2	C5	C6	C7	-1.1(5)
C2	C5	C6	C14	-174.3(4)
C3	C8	C7	C6	-1.4(5)
C5	C6	C7	C8	2.4(5)
C5	C6	C14	C15	-95.8(4)
C5	C6	C14	C16	-22.6(5)
C6	C14	C15	C16	112.3(6)
C6	C14	C15	C17	-141.9(5)
C6	C14	C15	C20	4.8(6)
C6	C14	C16	C15	-112.2(6)
C9	C10	C11	C12	55.9(4)
C14	C15	C20	C21	-77.5(5)
C14	C15	C20	C25	107.2(5)
C14	C16	C15	C17	-101.0(3)
C14	C16	C15	C20	113.9(3)
C15	C20	C21	C22	-174.5(4)
C15	C20	C25	C24	174.1(4)
C20	C21	C22	C23	-0.6(5)
C20	C25	C24	C23	1.6(5)
C21	C22	C23	C24	0.9(5)
C22	C23	C24	C25	-1.4(5)

Table S2-6: Hydrogen Fractional Atomic Coordinates (×10^4) and Equivalent Isotropic Displacement Parameters (Å^2×10^3) for WT-05-553. U_{eq} is defined as 1/3 of the trace of the orthogonalised U_{ij}.

Atom	x	y	z	U_{eq}
H2	10440(80)	4920(60)	5720(20)	16(11)
H1a	2539(9)	5520(40)	4738(2)	17(3)
H1b	1490(40)	7135(16)	4947(8)	17(3)
H5	-380(60)	6330(30)	3709(5)	32(13)
H7	3374(7)	8960(4)	2514(2)	33(10)
H8	6286(7)	9189(4)	3287(2)	33(10)
H9	4480(50)	6010(30)	5731(10)	17(3)
H10a	7660(40)	8590(20)	5656(8)	23(3)
H10b	5110(50)	8610(20)	5982(4)	23(3)
H11a	8030(20)	8240(30)	6755(10)	26(3)
H11b	6150(40)	6738(19)	6720(9)	26(3)
H14	-890(70)	8640(20)	2420(20)	19(3)
H16a	-2135(7)	5640(5)	2896(2)	20(3)
H16b	-3773(8)	6866(4)	2452(2)	22(3)
H18a	-1610(50)	6220(30)	163(17)	22(3)
H18b	-1960(50)	8010(30)	430(20)	22(3)
H21	3626(7)	6444(5)	1700(2)	48(13)
H22	5997(8)	4329(5)	1513(2)	48(13)
H24	929(8)	1495(5)	2117(2)	45(17)
H25	-1371(8)	3629(5)	2312(2)	70(20)

Citations for crystallographic work

CrysAlisPro (ROD), Rigaku Oxford Diffraction, Poland (2019).

CrysAlisPro Software System, Rigaku Oxford Diffraction, (2024).

L.J. Bourhis and O.V. Dolomanov and R.J. Gildea and J.A.K. Howard and H. Puschmann, The Anatomy of a Comprehensive Constrained, Restrained, Refinement Program for the Modern Computing Environment - Olex2 Disected, *Acta Cryst. A*, (2015), **A71**, 59-71.

O.V. Dolomanov and L.J. Bourhis and R.J. Gildea and J.A.K. Howard and H. Puschmann, Olex2: A complete structure solution, refinement and analysis program, *J. Appl. Cryst.*, (2009), **42**, 339-341.

Sheldrick, G.M., ShelXT-Integrated space-group and crystal-structure determination, *Acta Cryst.*, (2015), **A71**, 3-8.

Section 5: Spectroscopic Data

^{1}H NMR Spectra

^{1}H NMR (500 MHz) Spectrum for Compound 2.7

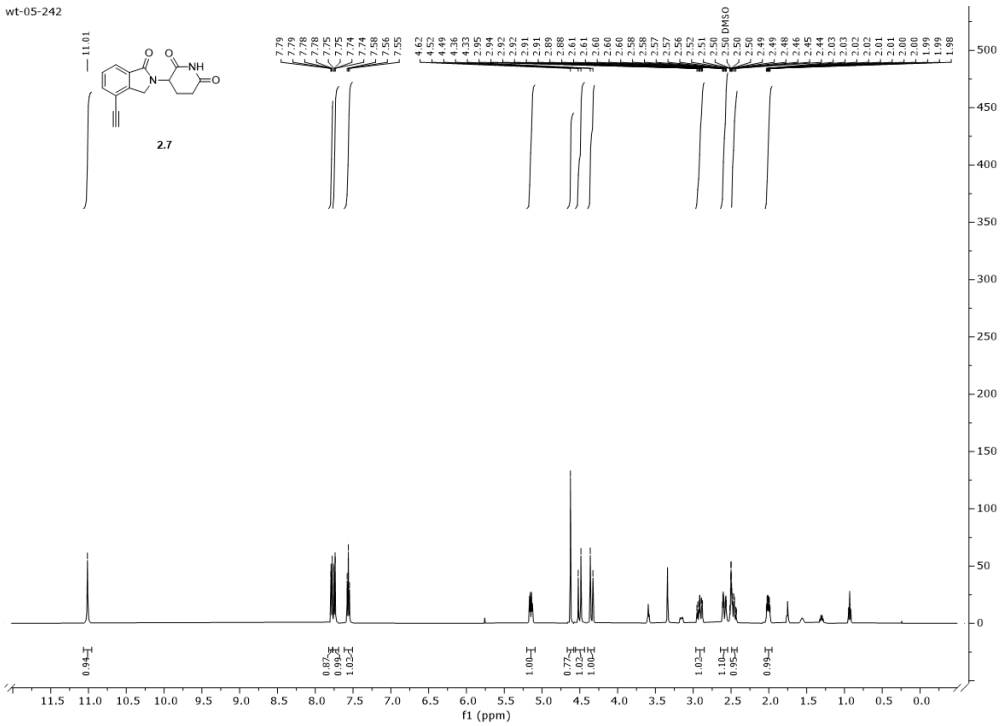

^{1}H NMR (500 MHz) Spectrum for Compound 2.8

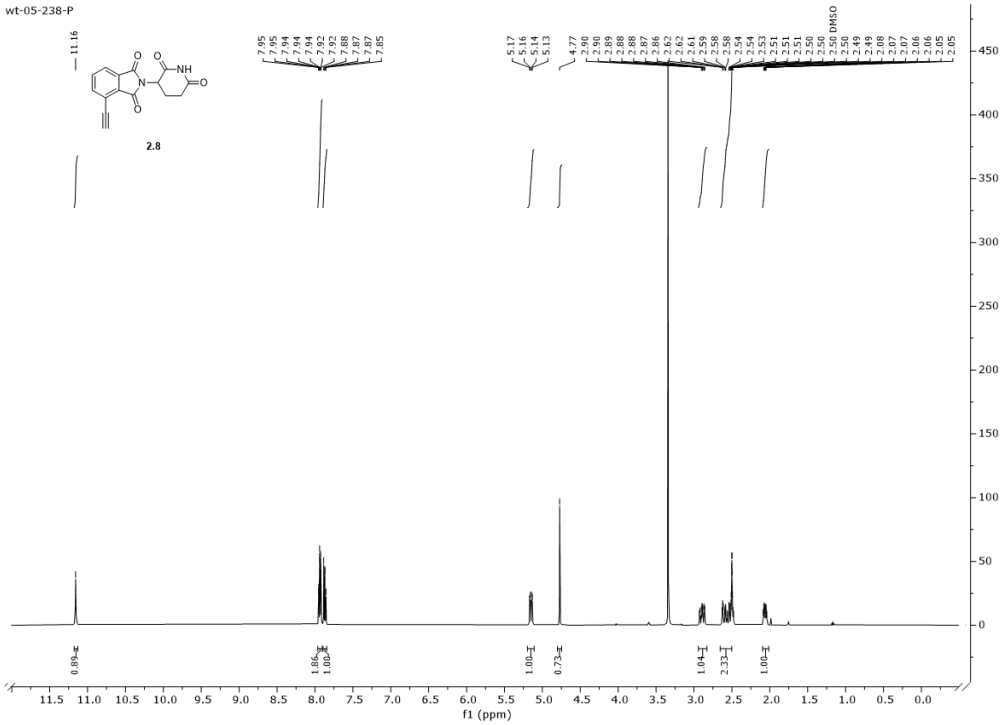

^{1}H NMR (400 MHz) Spectrum for Compound 2.9

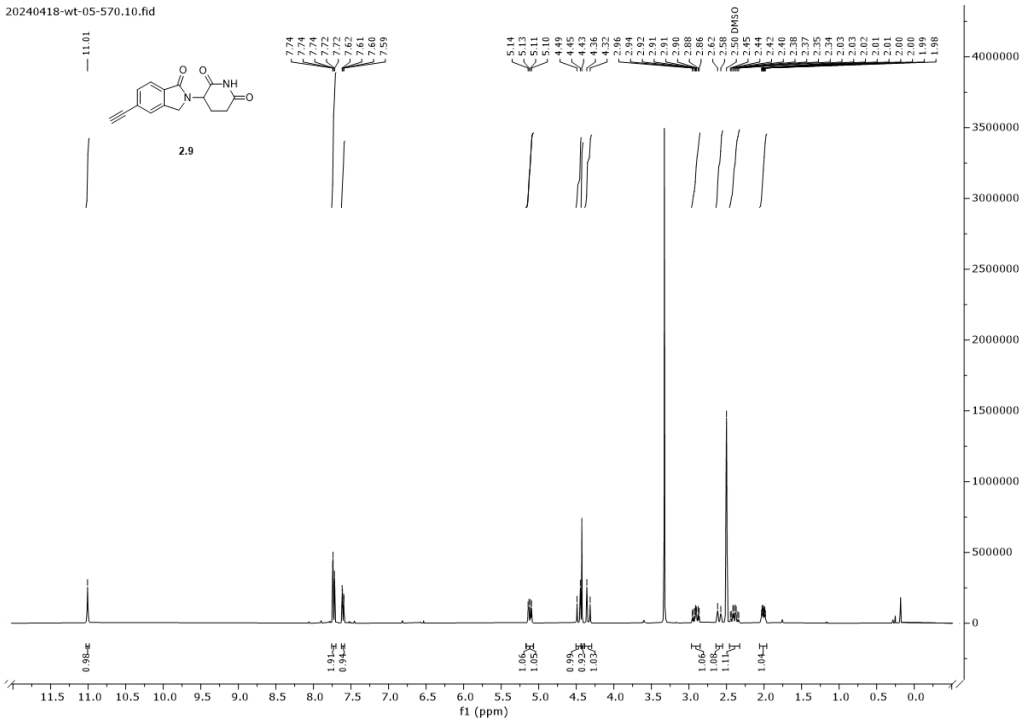

^{1}H NMR (400 MHz) Spectrum for Compound 2.10

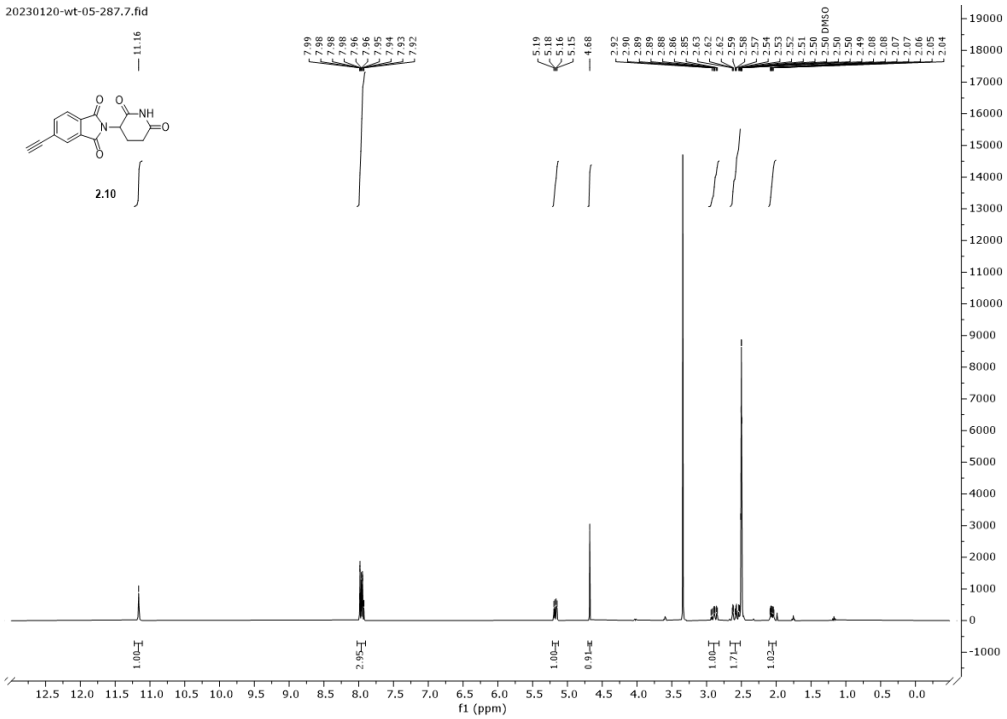

^{1}H NMR (500 MHz) Spectrum for Compound 2.11

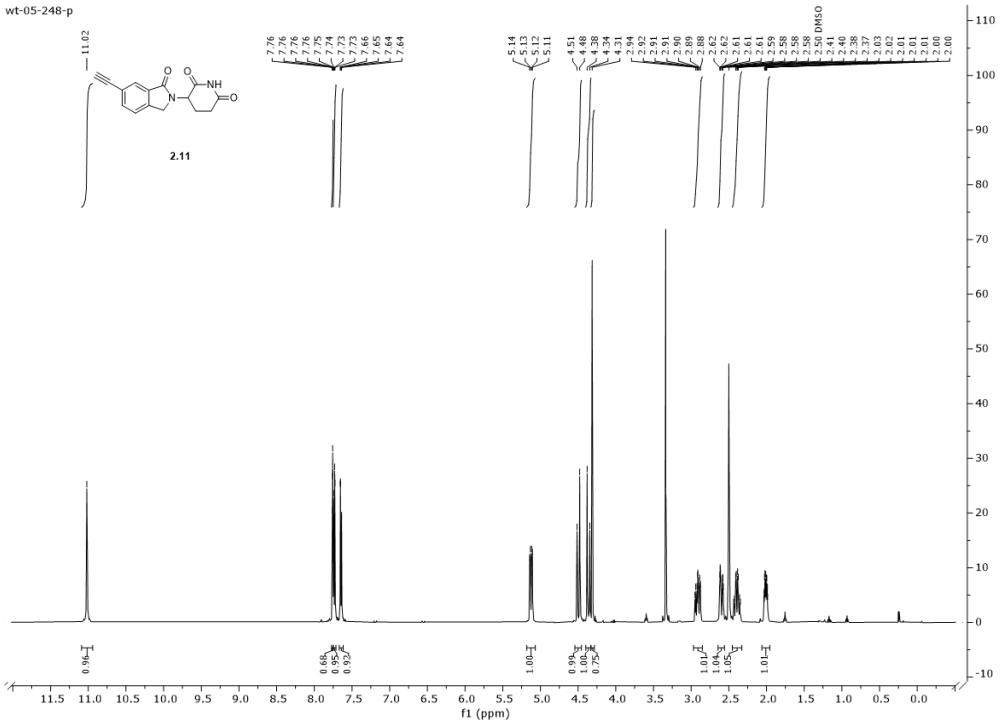

^{1}H NMR (500 MHz) Spectrum for Compound 2.12

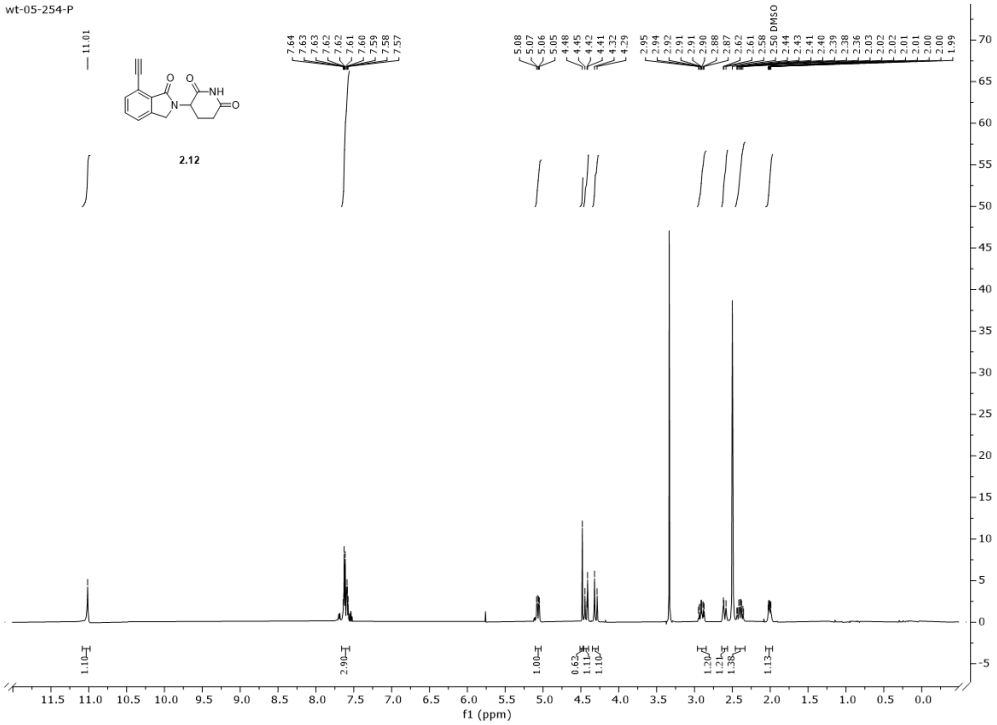

^{1}H NMR (400 MHz) Spectrum for Compound 2.14

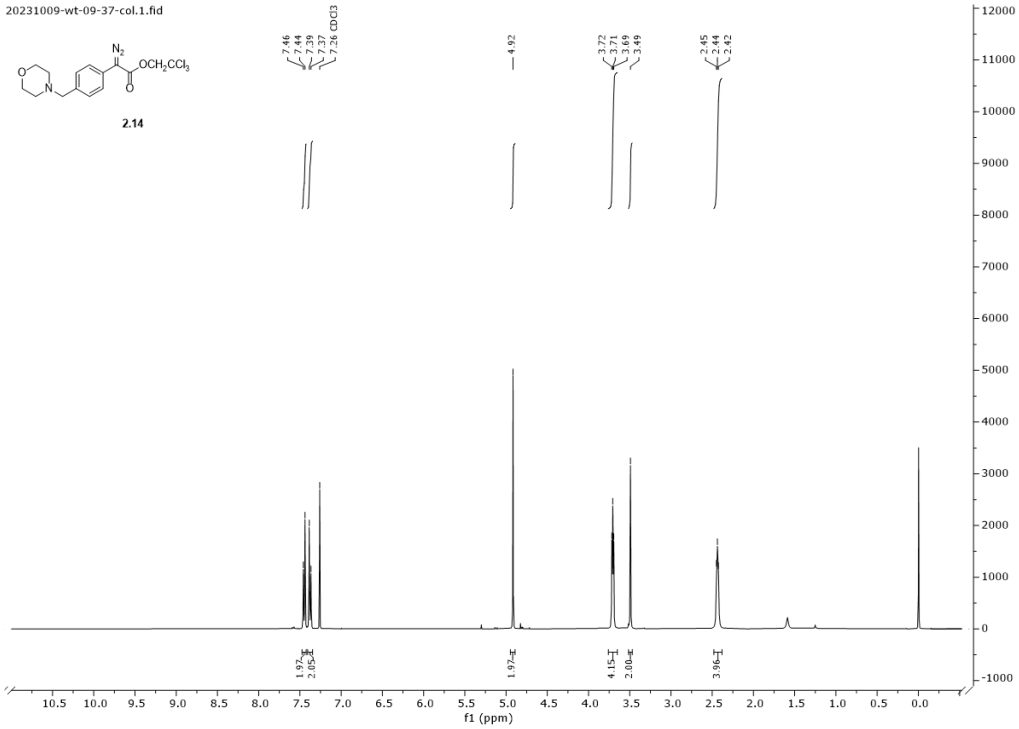

^{1}H NMR (600 MHz) Spectrum for Compounds 2.15a and 2.15b

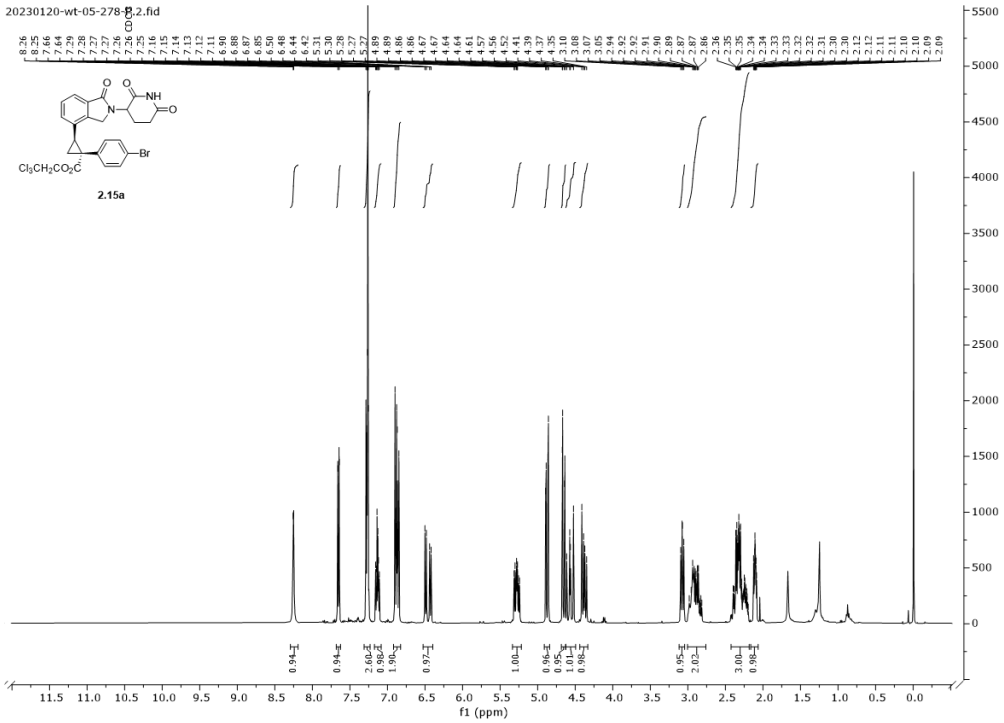

^{1}H NMR (500 MHz) Spectrum for Compounds 2.16a and 2.16b

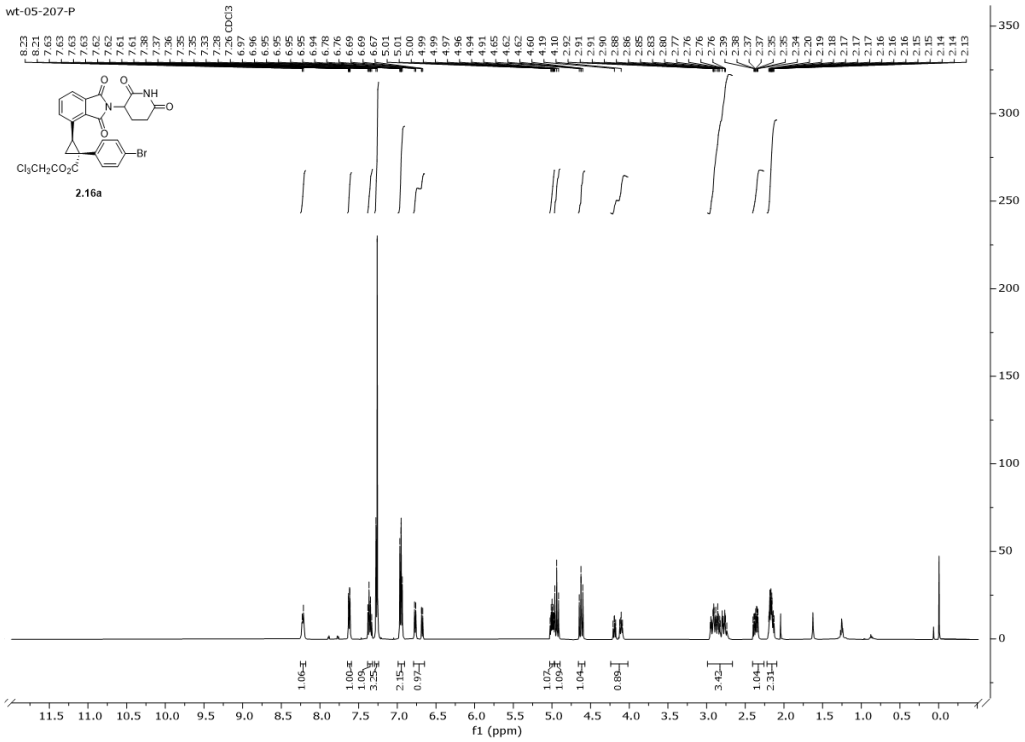

^{1}H NMR (500 MHz) Spectrum for Compounds 2.17a and 2.17b

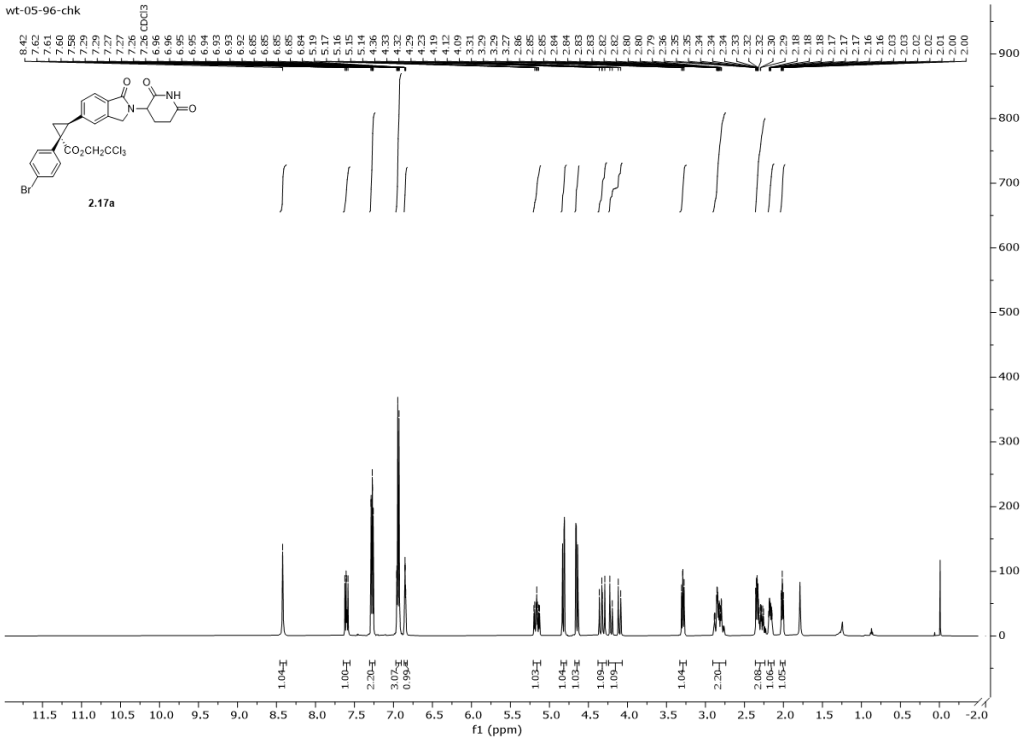

^{1}H NMR (400 MHz) Spectrum for Compounds *S*-2.17a and *R*-2.17b

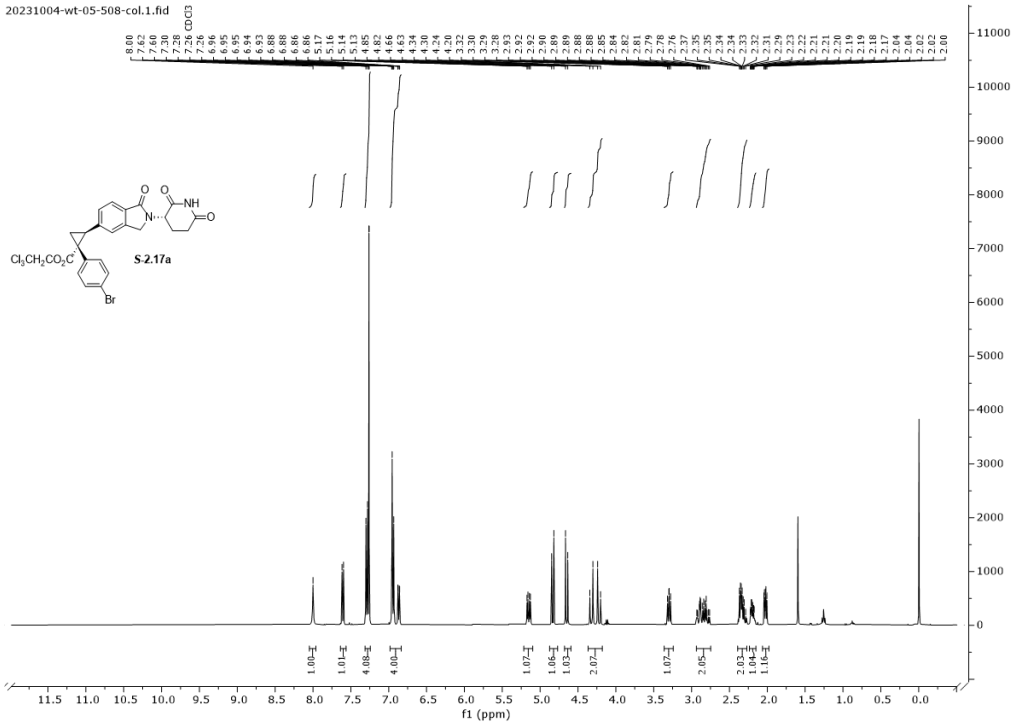

^{1}H NMR (400 MHz) Spectrum for Compounds *R*-2.17a and *S*-2.17b

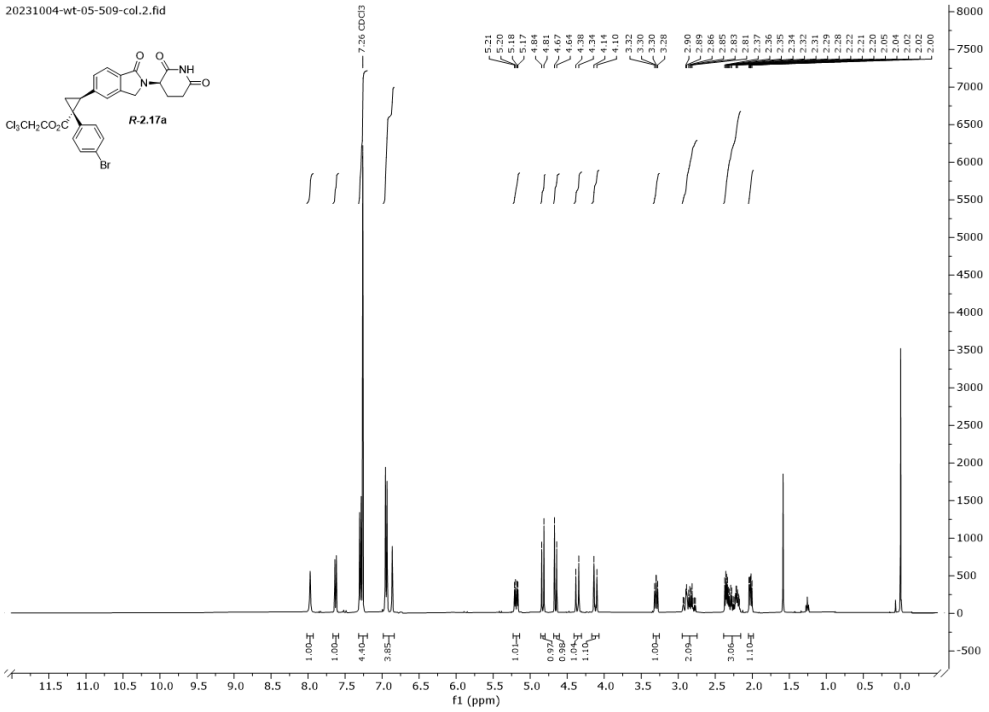

^{1}H NMR (500 MHz) Spectrum for Compounds 2.18a and 2.18b

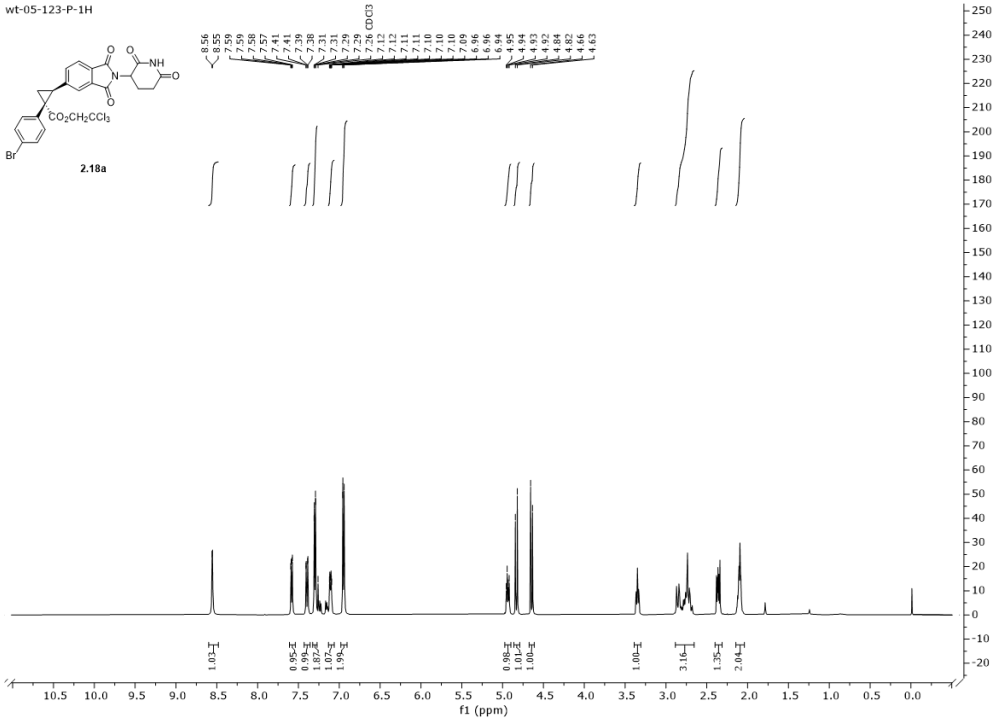

^{1}H NMR (600 MHz) Spectrum for Compounds 2.19a and 2.19b

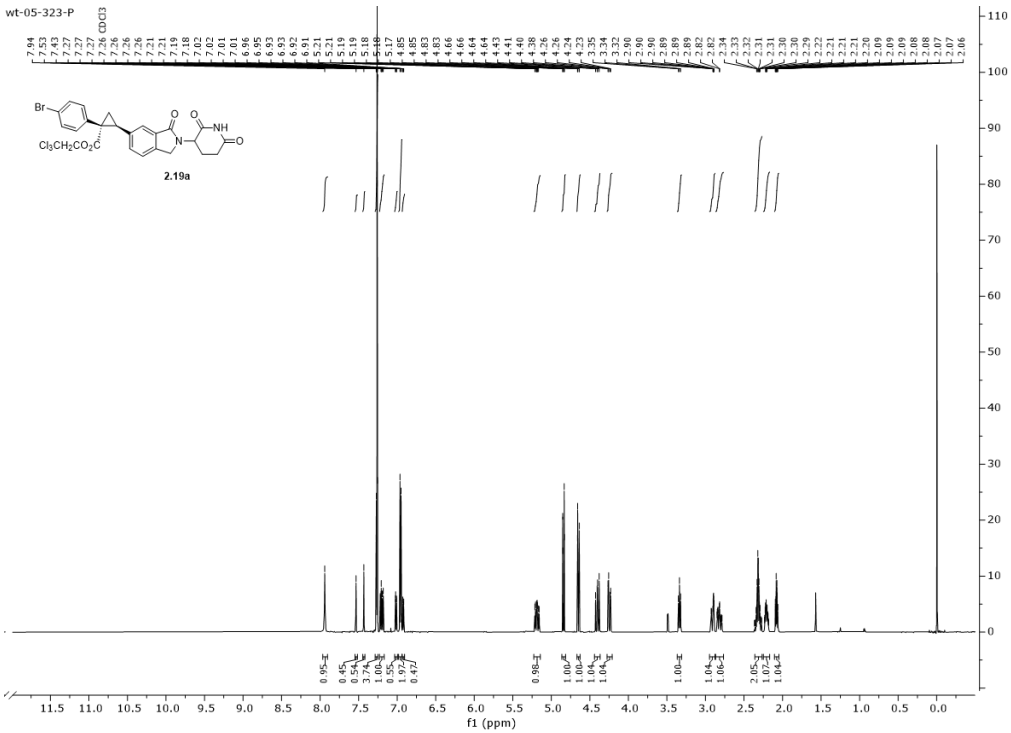

^{1}H NMR (400 MHz) Spectrum for Compounds 2.20a and 2.20b

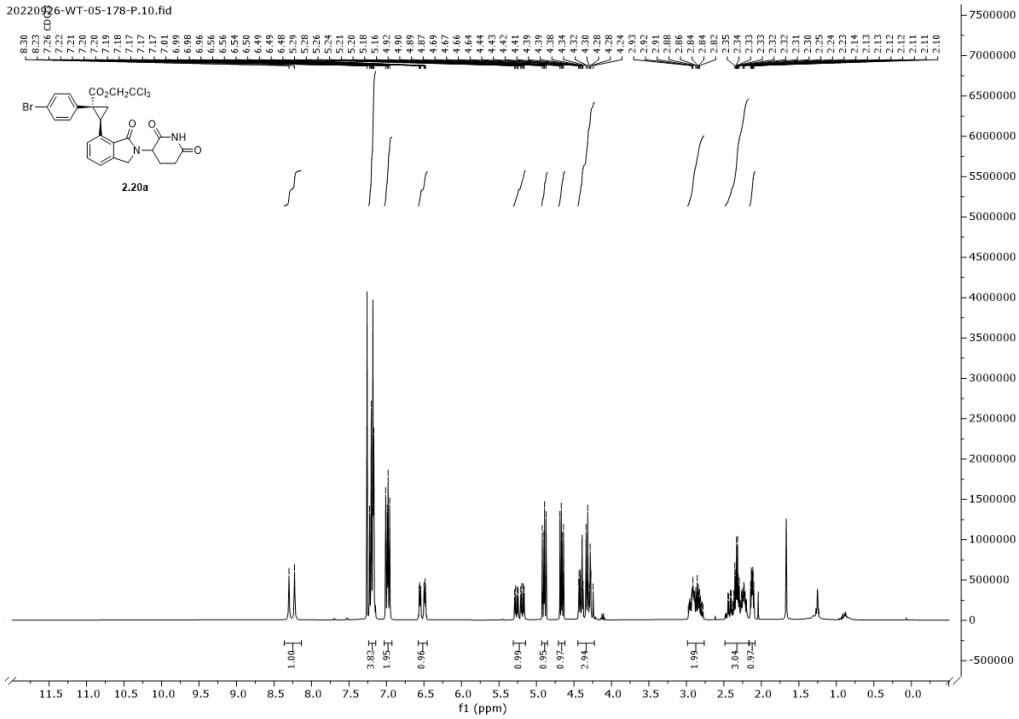

^{1}H NMR (600 MHz) Spectrum for Compounds 2.21a and 2.21b

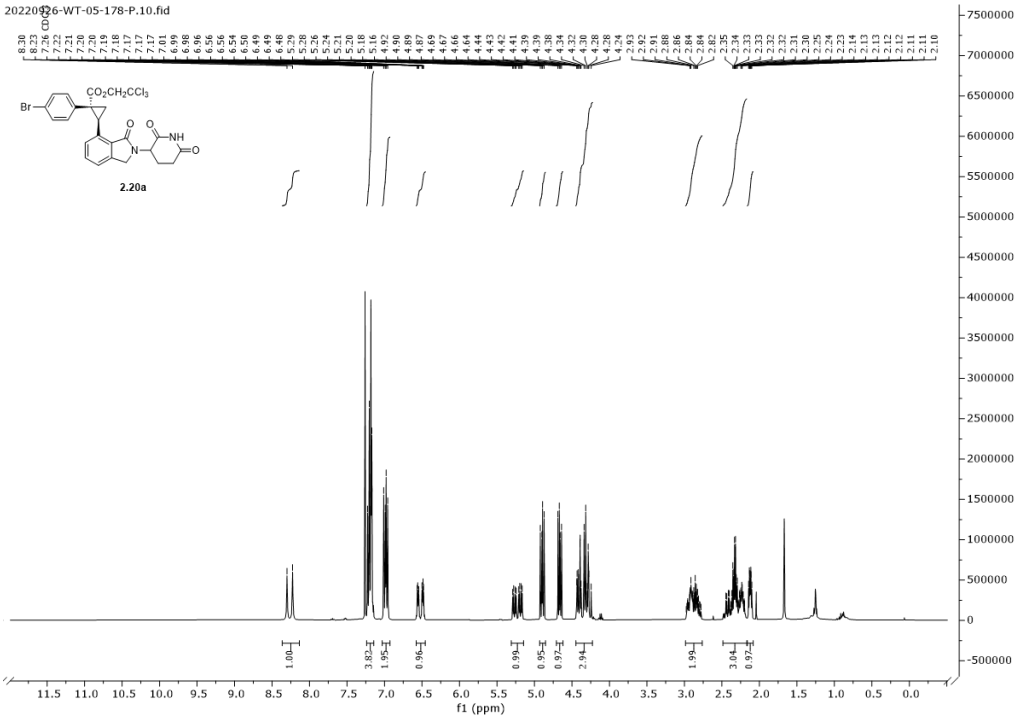

^{1}H NMR (600 MHz) Spectrum for Compounds 2.22a and 2.22b

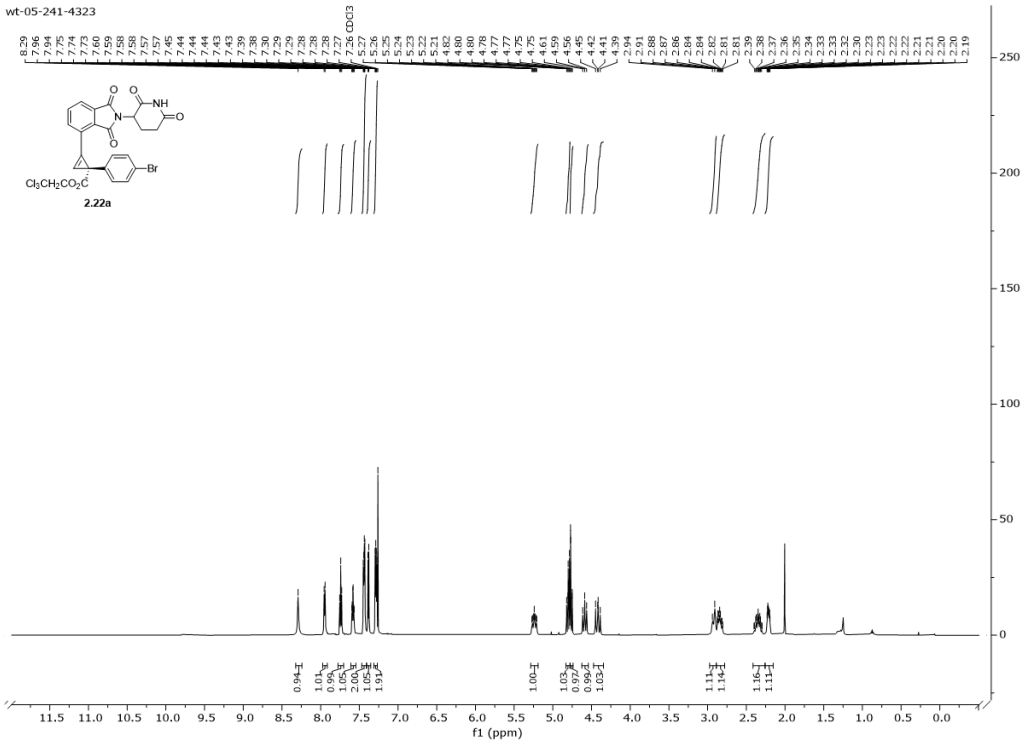

^{1}H NMR (400 MHz) Spectrum for Compounds 2.23a and 2.23b

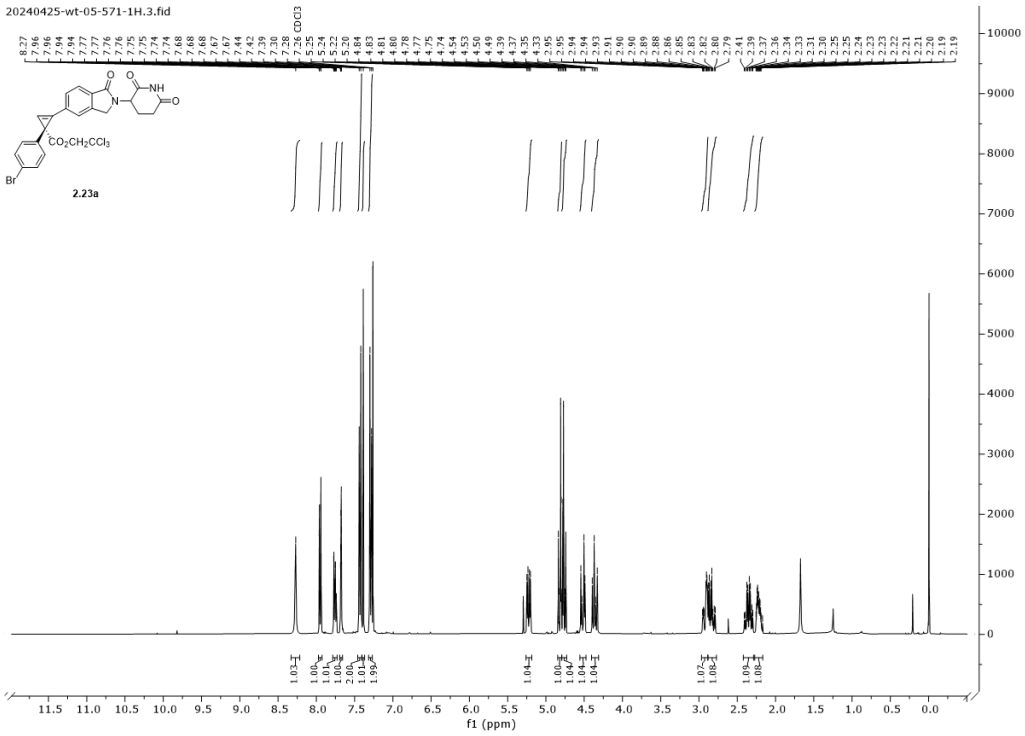

^{1}H NMR (500 MHz) Spectrum for Compounds 2.24a and 2.24b

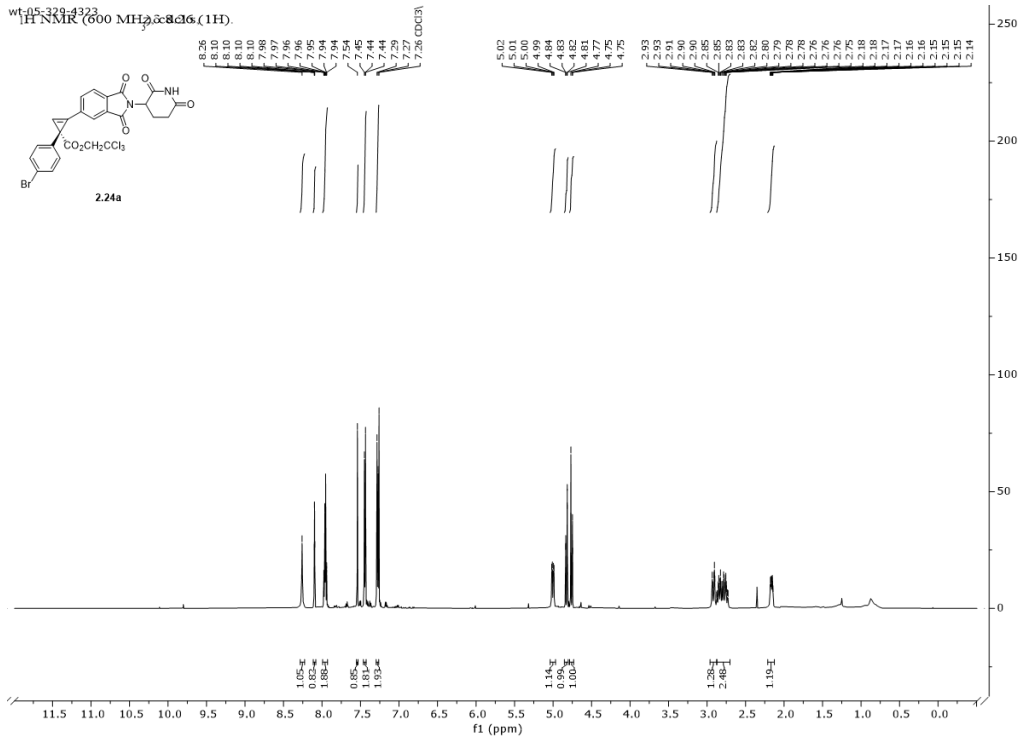

^{1}H NMR (600 MHz) Spectrum for Compounds 2.25a and 2.25b

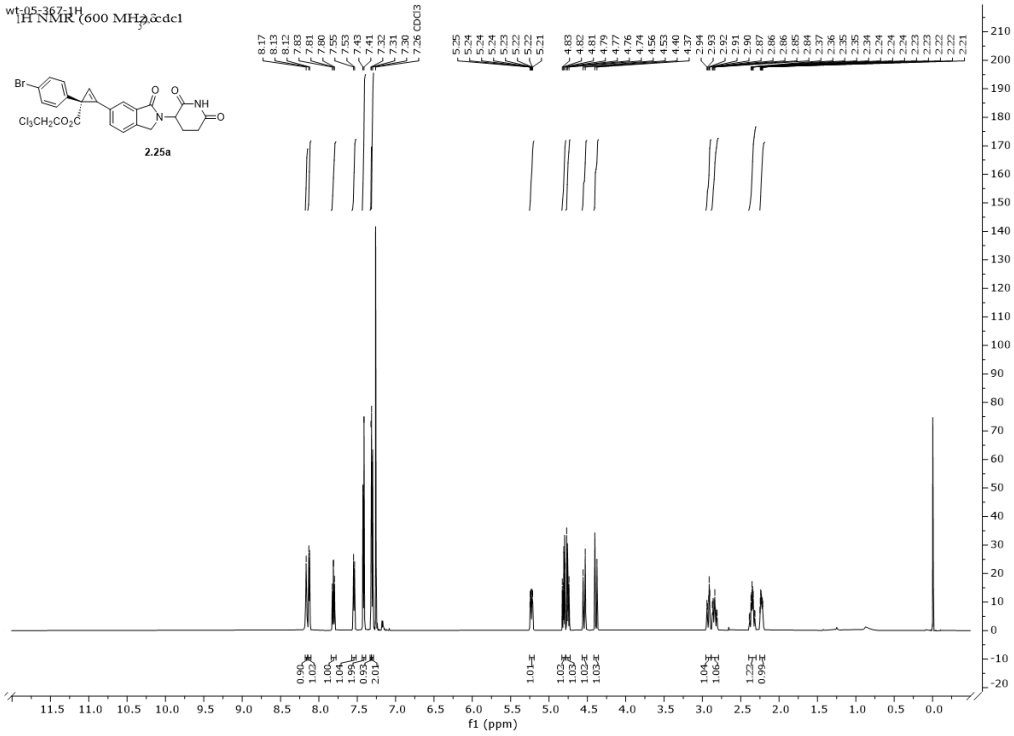

^{1}H NMR (600 MHz) Spectrum for Compounds 2.26a and 2.26b

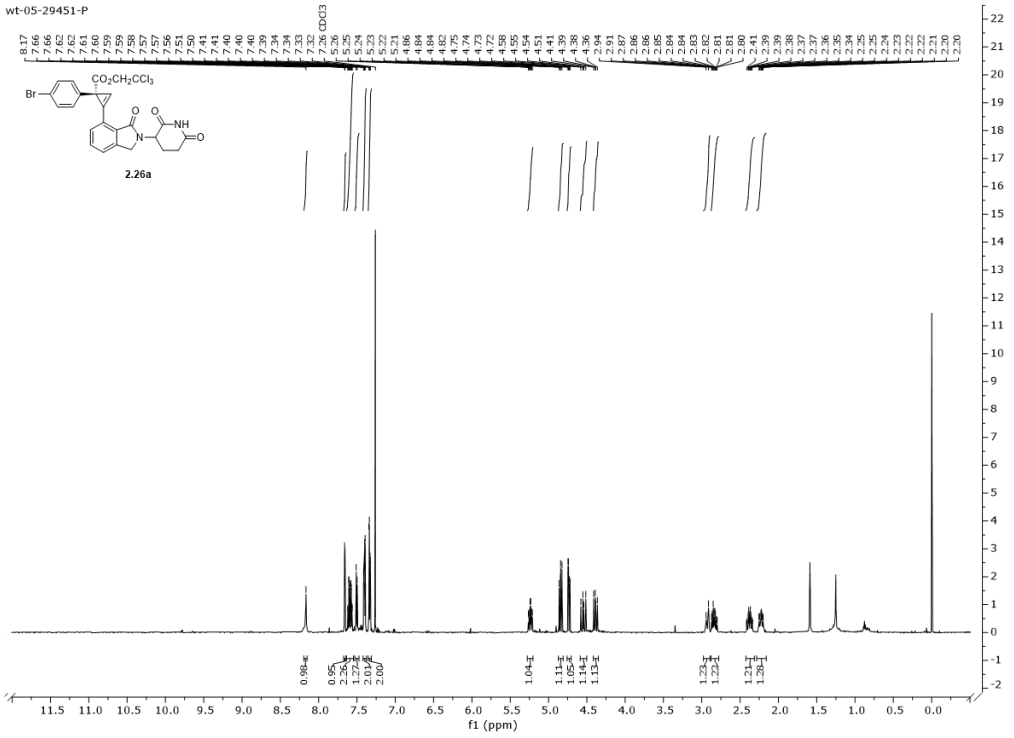

^{1}H NMR (400 MHz) Spectrum for Compounds 2.27a and 2.27b

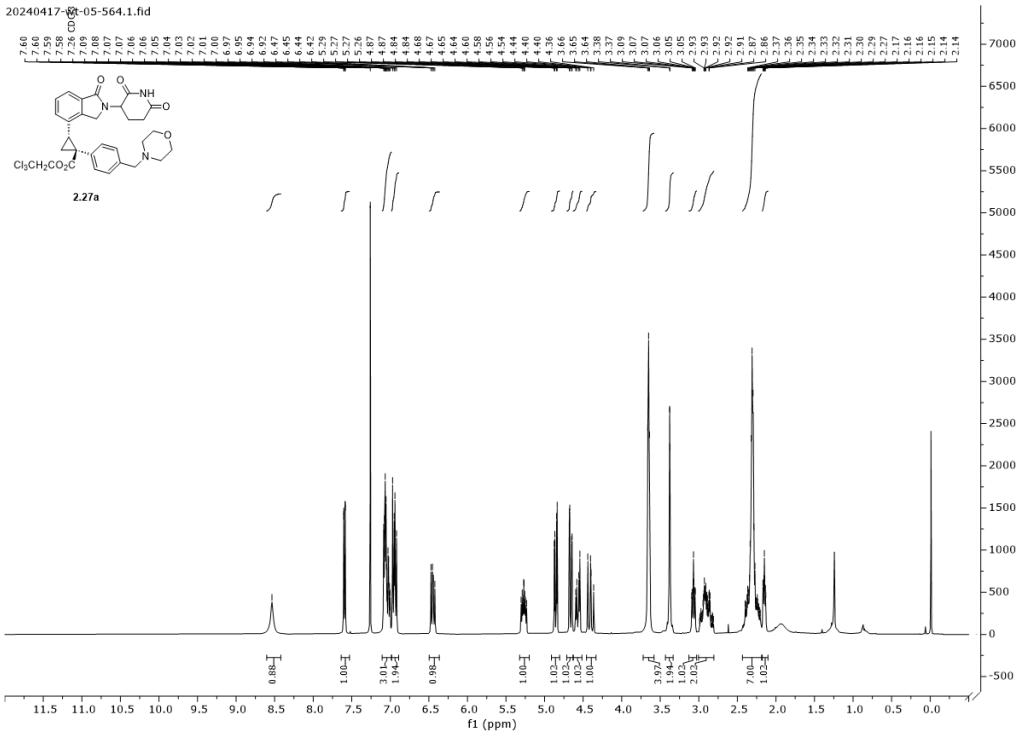

^{1}H NMR (600 MHz) Spectrum for Compounds 2.28a and 2.28b

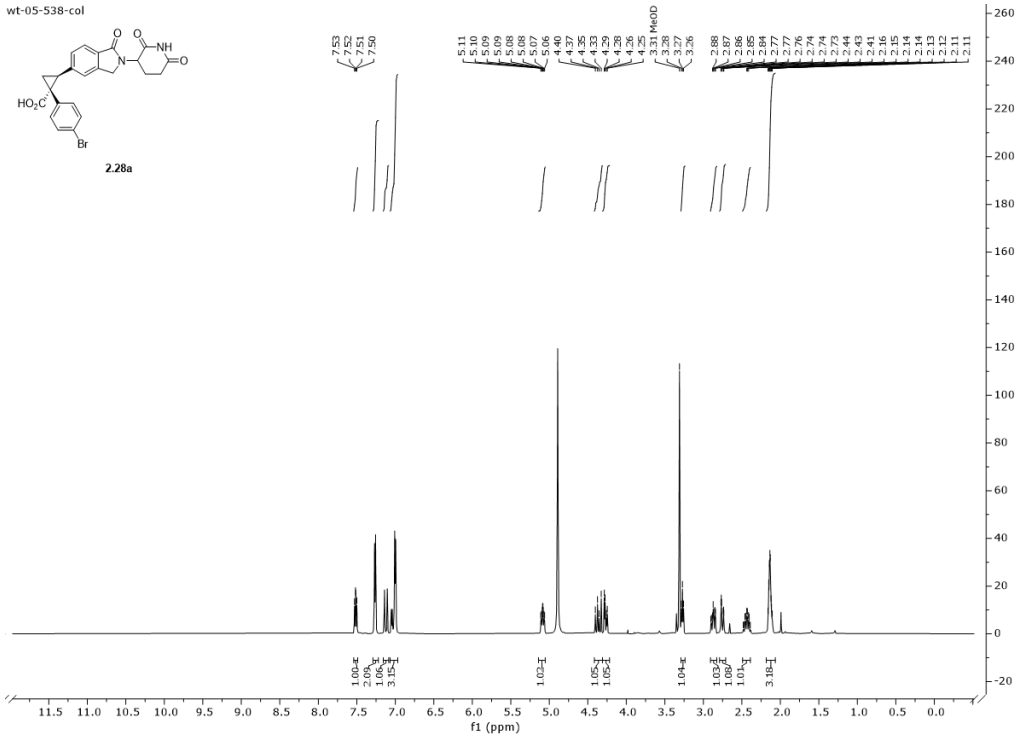

^{1}H NMR (600 MHz) Spectrum for Compounds 2.29a and 2.29b

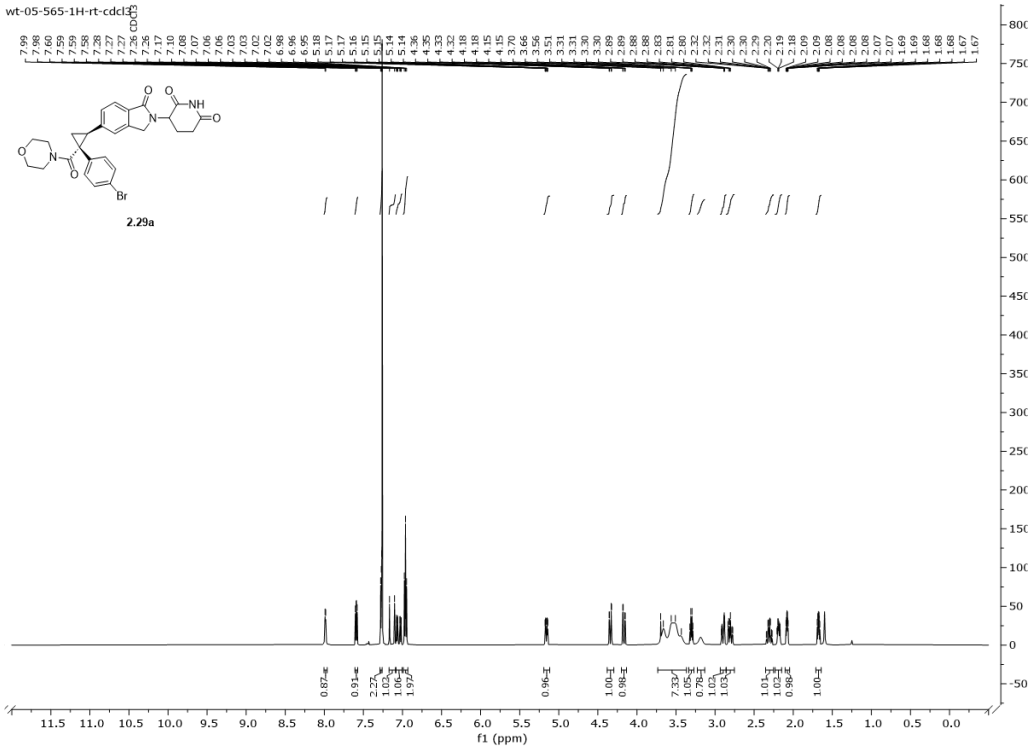

^{13}C NMR Spectra

^{13}C{^{1}H} (151 MHz) NMR Spectrum for Compound 2.7.

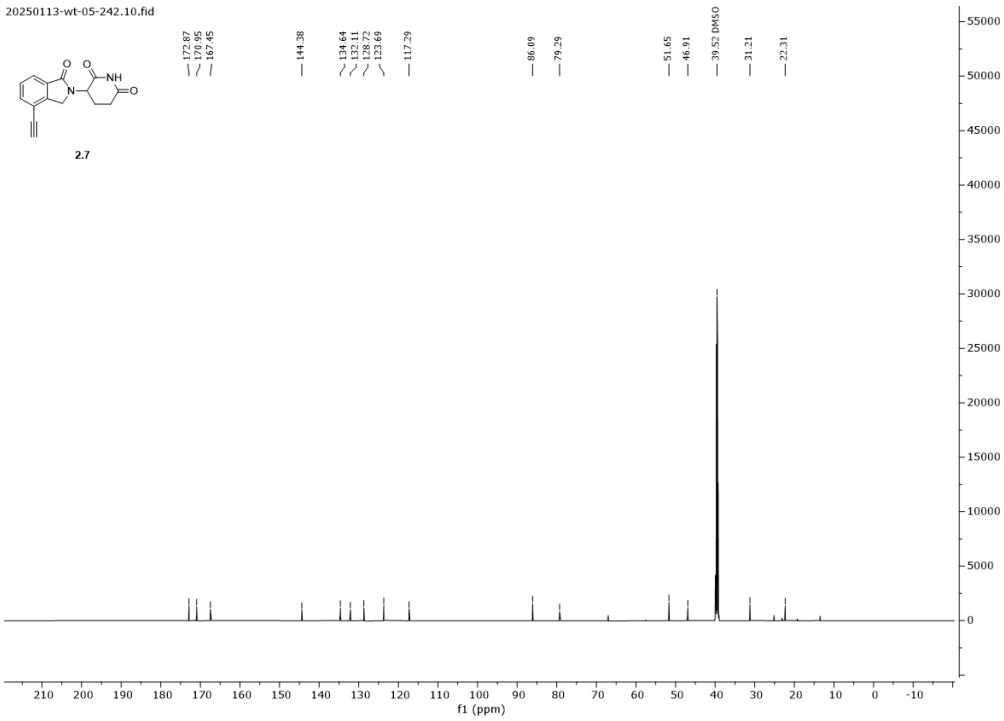

$^{13}C\{^1H\}$ (151 MHz) NMR Spectrum for Compound 2.8.

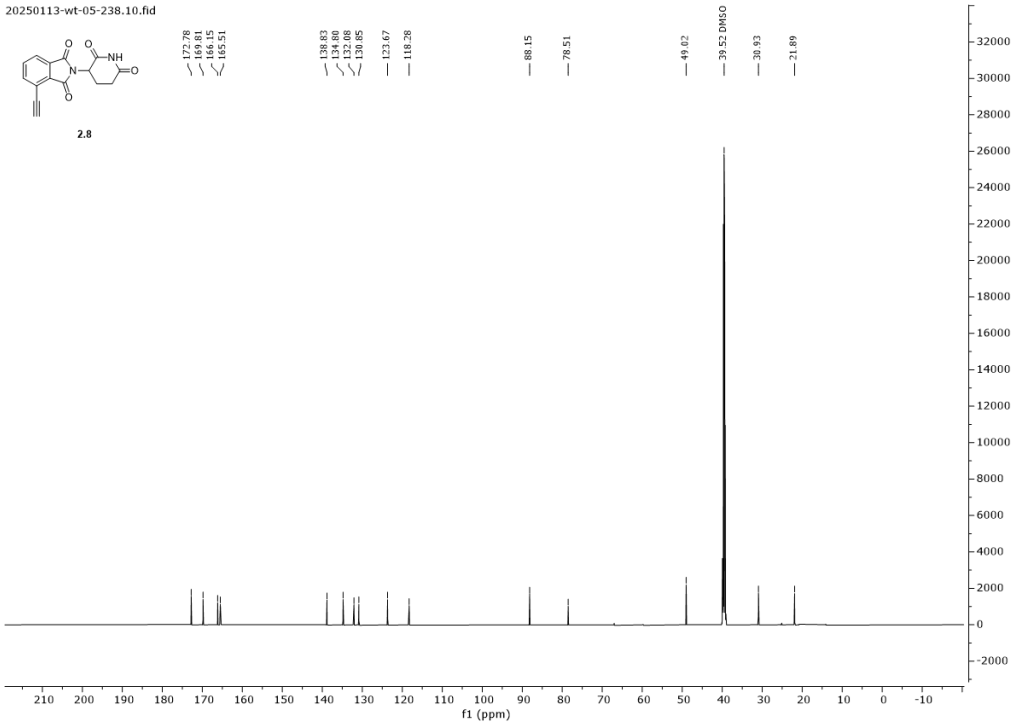

$^{13}C\{^1H\}$ (151 MHz) NMR Spectrum for Compound 2.9.

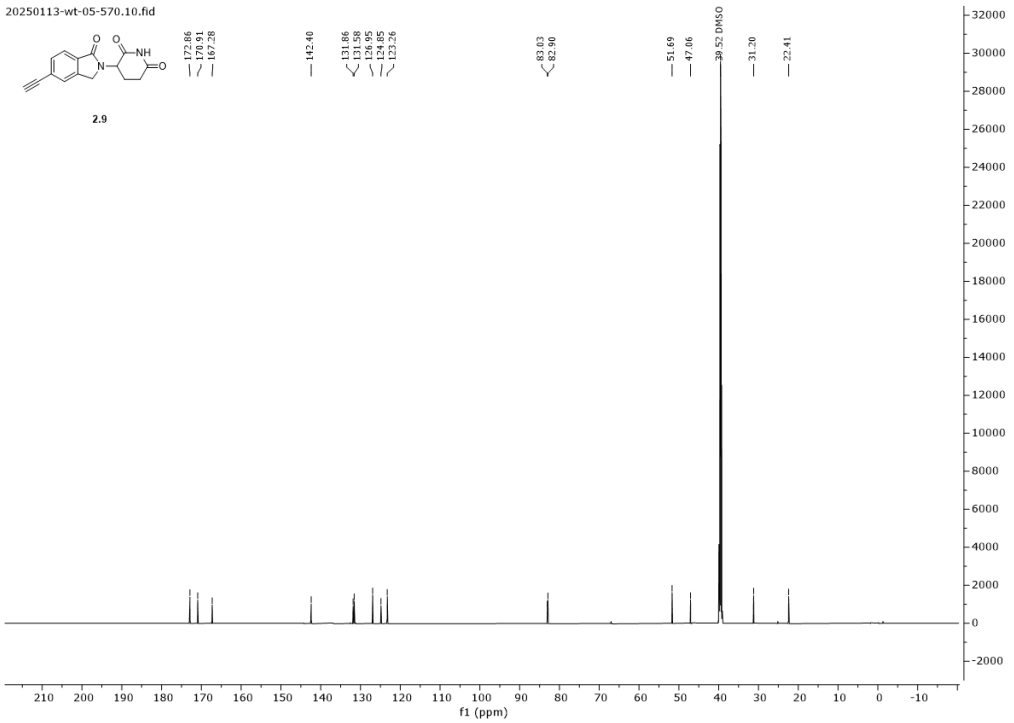

$^{13}C\{^{1}H\}$ NMR (151 MHz) Spectrum for Compound 2.10.

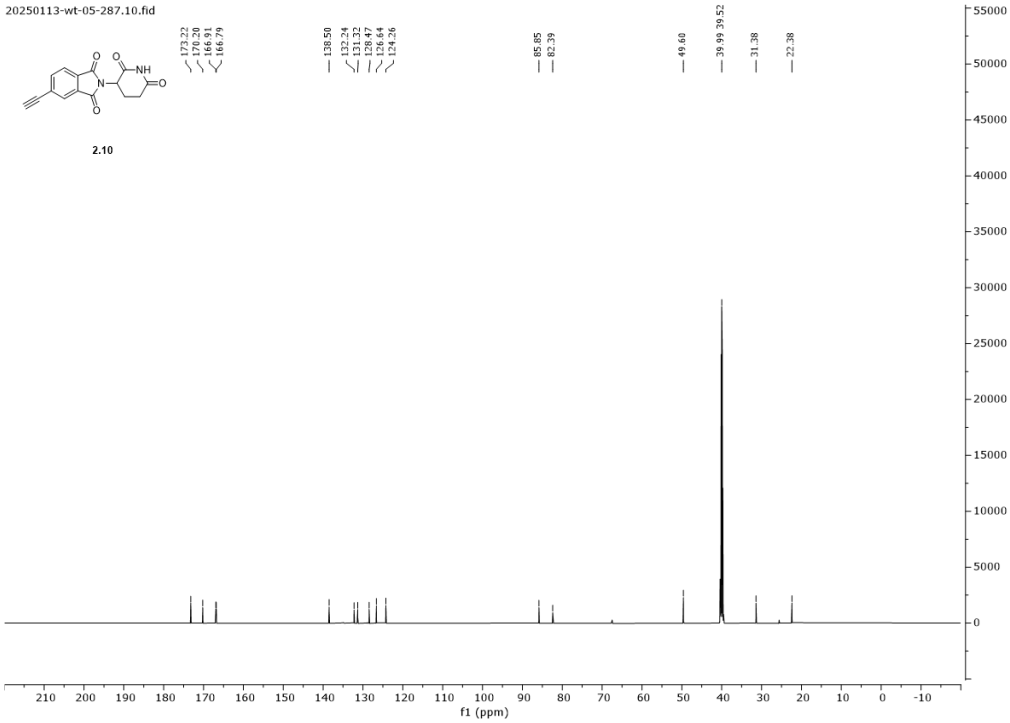

$^{13}C\{^{1}H\}$ NMR (151 MHz) Spectrum for Compound 2.11.

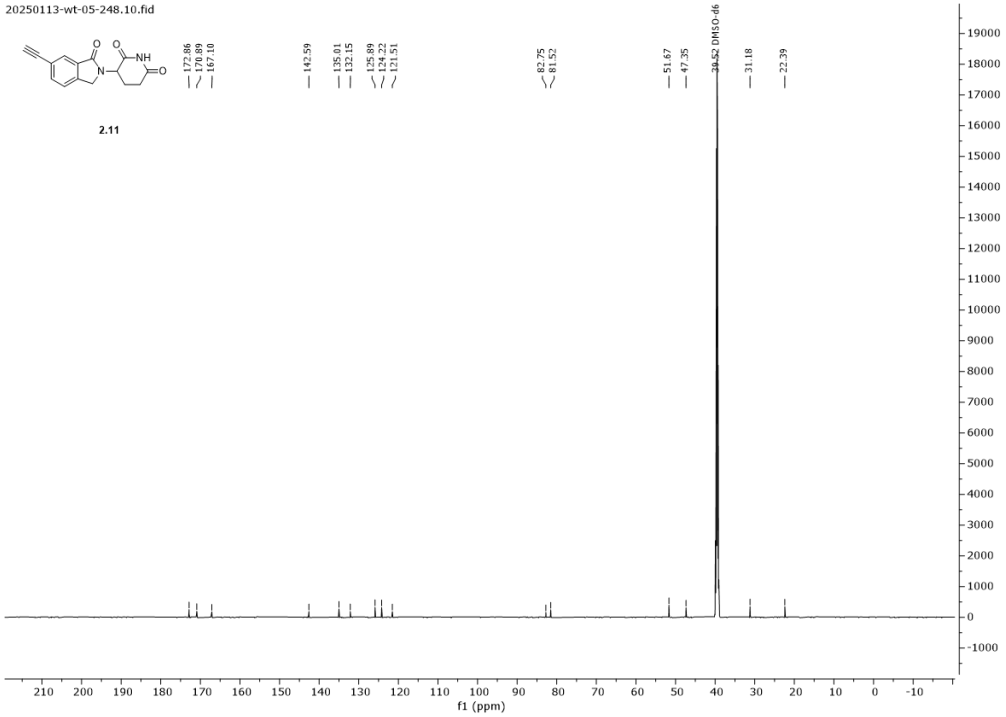

$^{13}C\{^{1}H\}$ (151 MHz) NMR Spectrum for Compound 2.12.

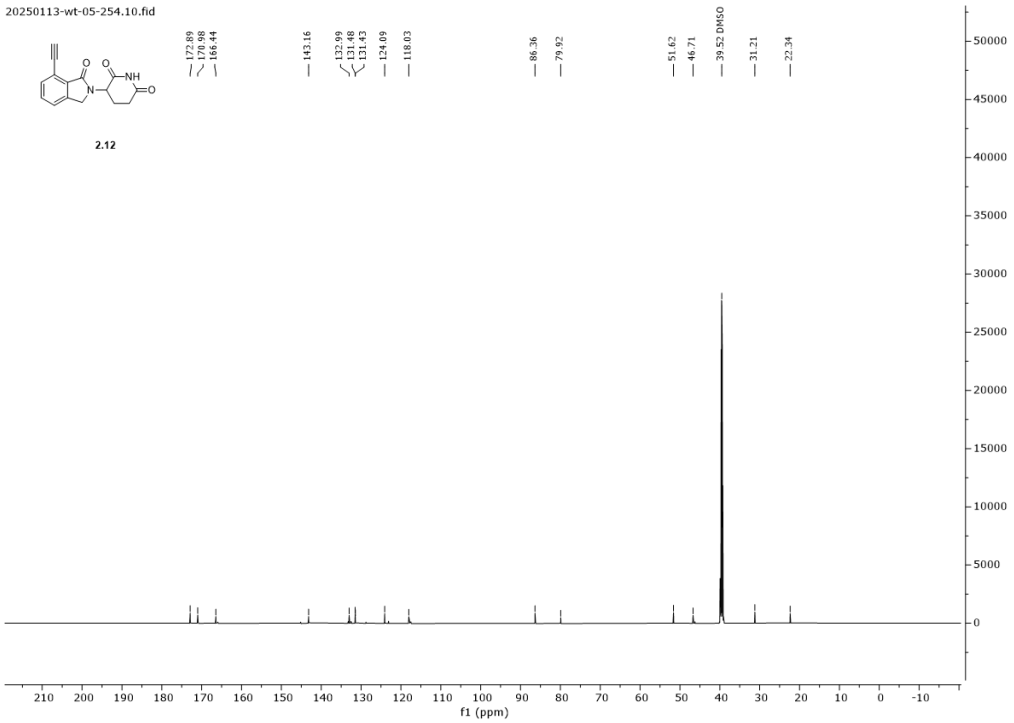

$^{13}C\{^{1}H\}$ NMR (151 MHz) Spectrum for Compound 2.14.

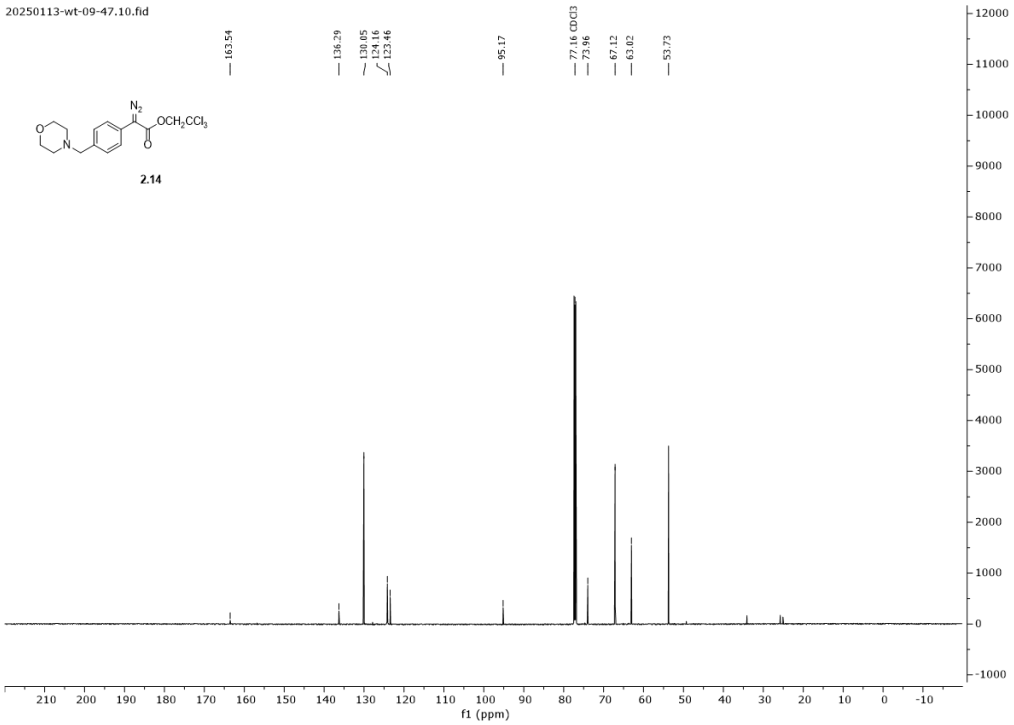

$^{13}C\{^1H\}$ NMR (126 MHz) Spectrum for Compounds 2.15a and 2.15b.

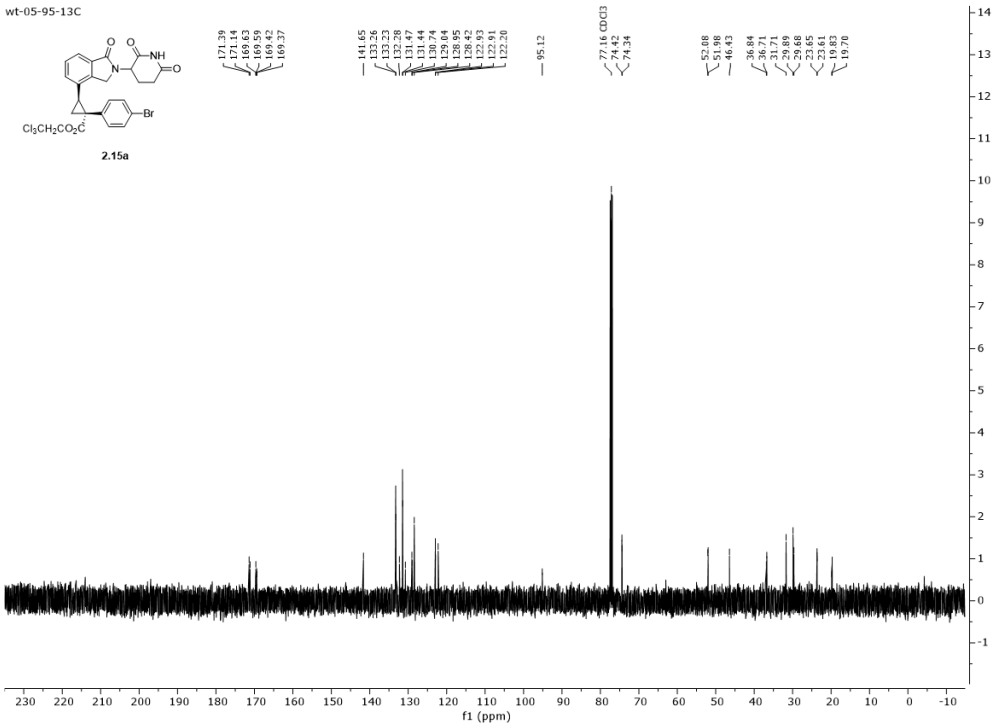

$^{13}C\{^1H\}$ NMR (101 MHz) Spectrum for Compounds 2.16a and 2.16b.

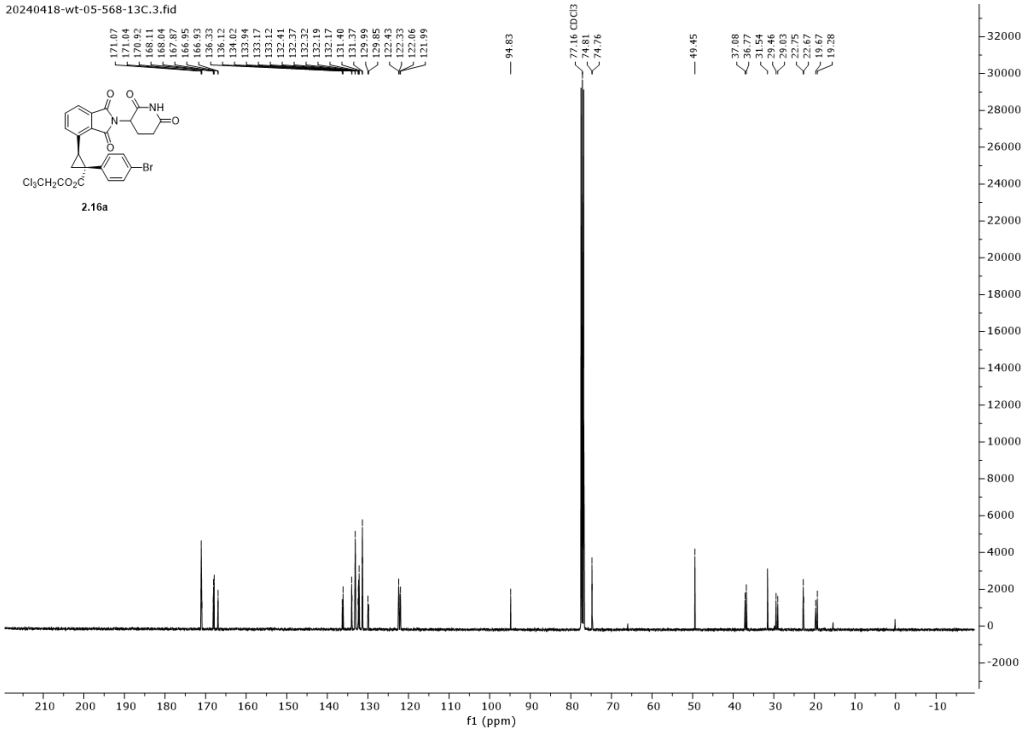

$^{13}C\{^{1}H\}$ NMR (101 MHz) Spectrum for Compounds 2.17a and 2.17b.

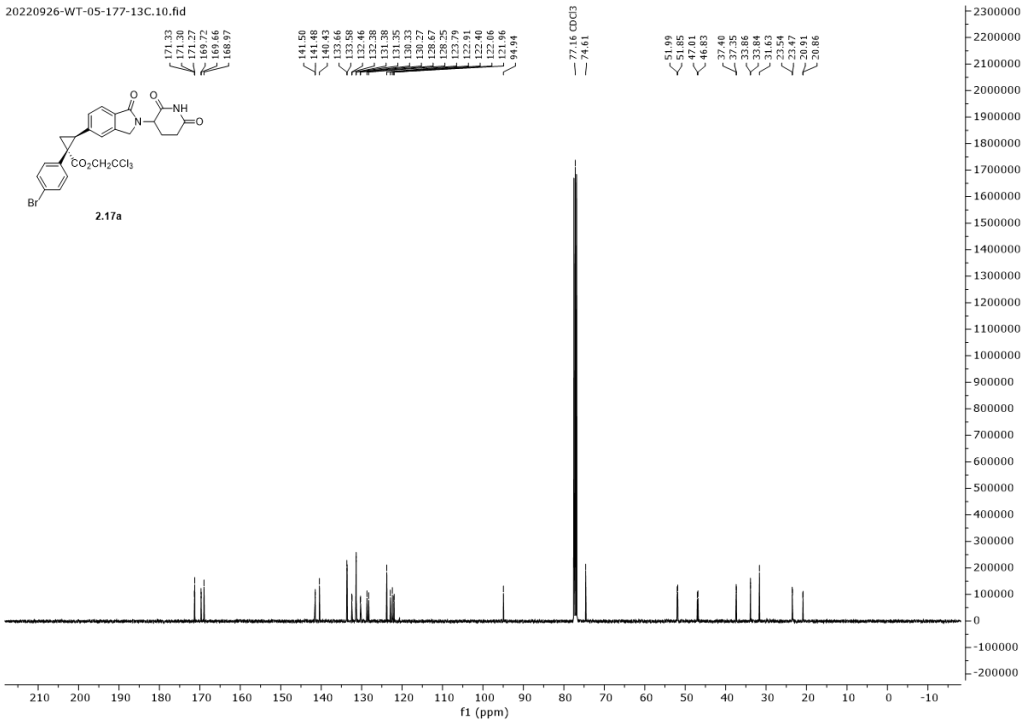

$^{13}C\{^{1}H\}$ NMR (101 MHz) Spectrum for Compounds *S*-2.17a and *R*-2.17b.

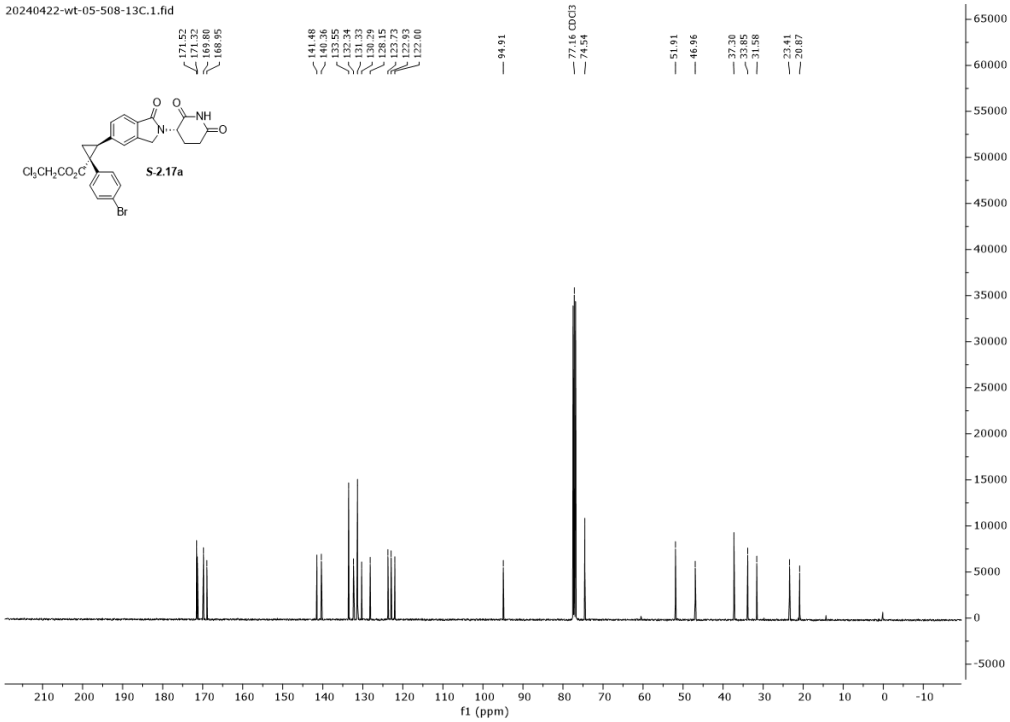

$^{13}C\{^1H\}$ NMR (101 MHz) Spectrum for Compounds *R*-2.17a and *S*-2.17b.

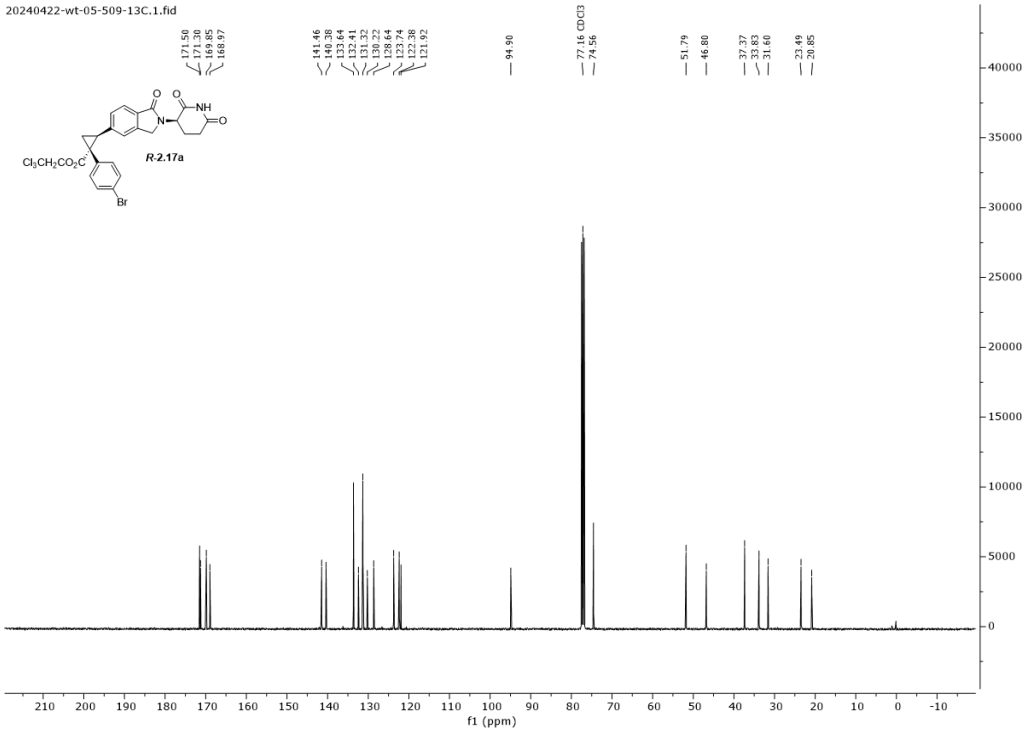

$^{13}C\{^1H\}$ NMR (126 MHz) Spectrum for Compounds 2.18a and 2.18b.

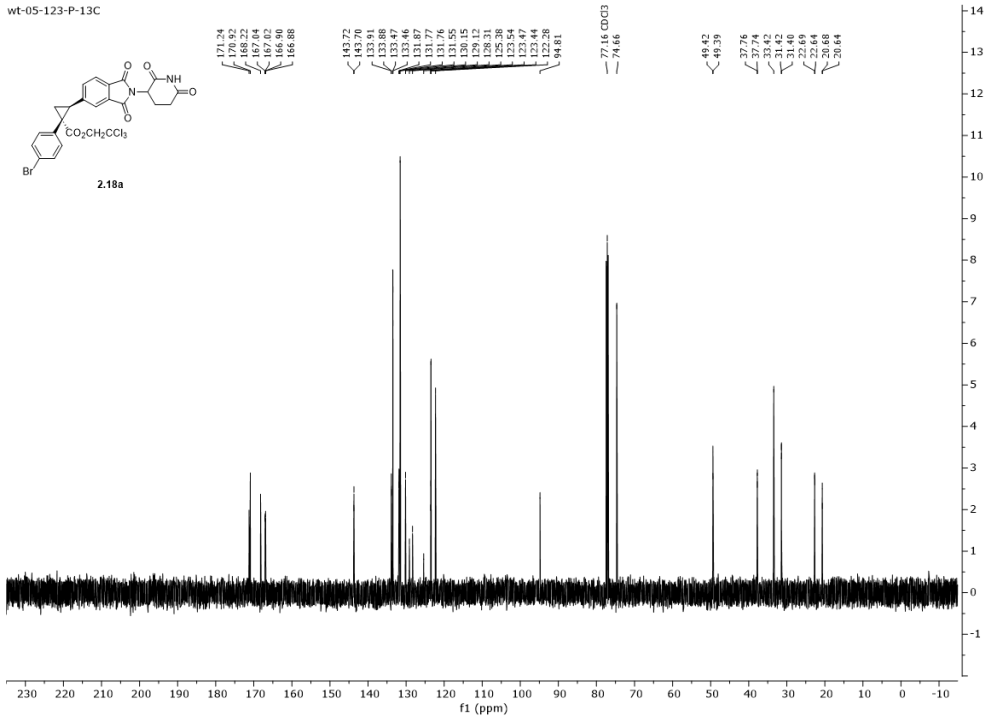

$^{13}C\{^{1}H\}$ NMR (101 MHz) Spectrum for Compounds 2.19a and 2.19b.

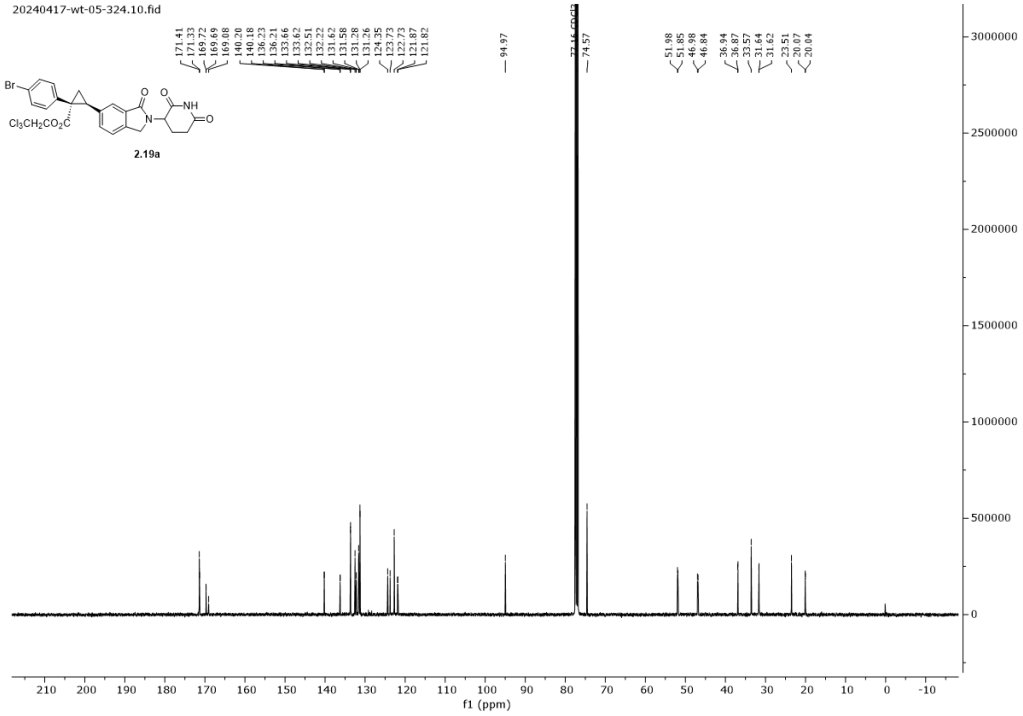

$^{13}C\{^{1}H\}$ NMR (101 MHz) Spectrum for Compounds 2.20a and 2.20b.

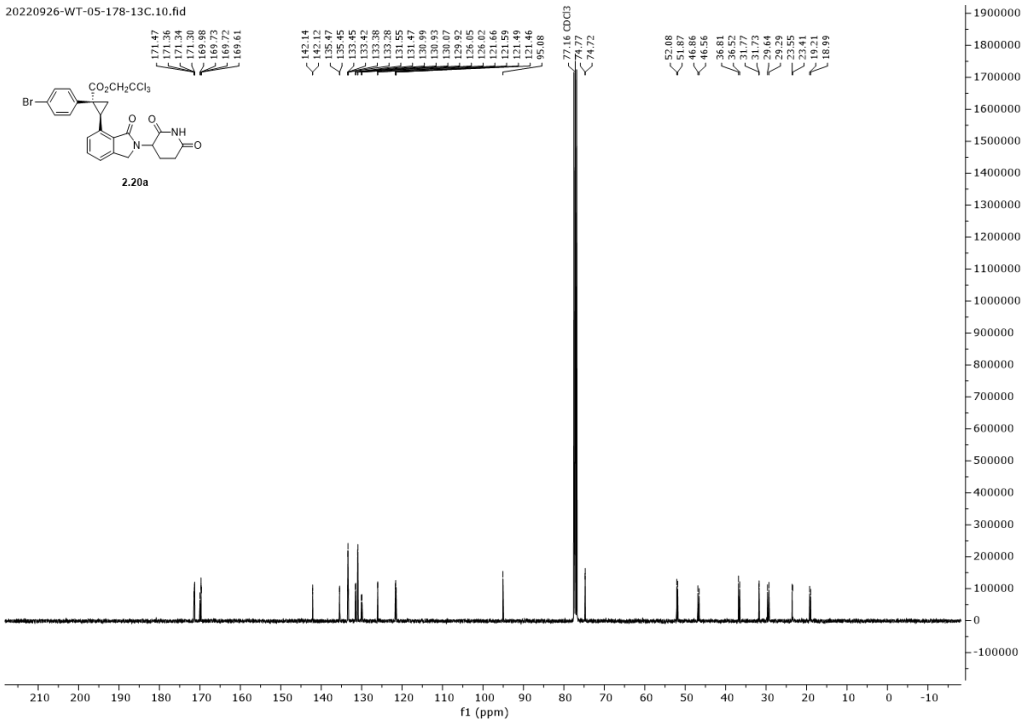

$^{13}C\{^{1}H\}$ NMR (101 MHz) Spectrum for Compounds 2.21a and 2.21b.

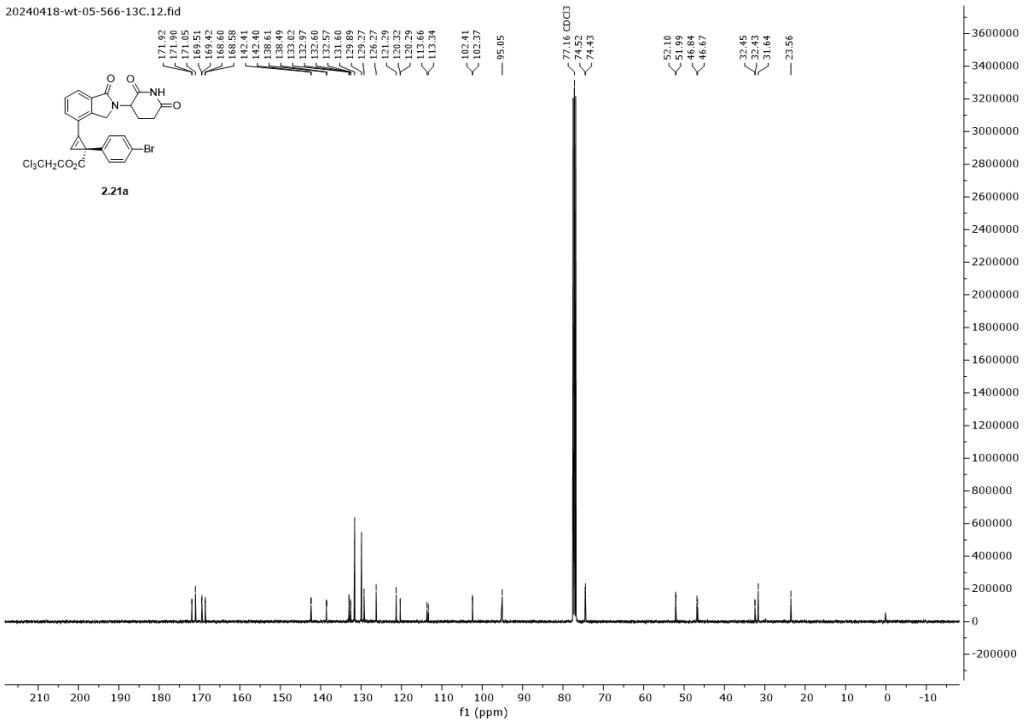

$^{13}C\{^{1}H\}$ NMR (101 MHz) Spectrum for Compounds 2.22a and 2.22b.

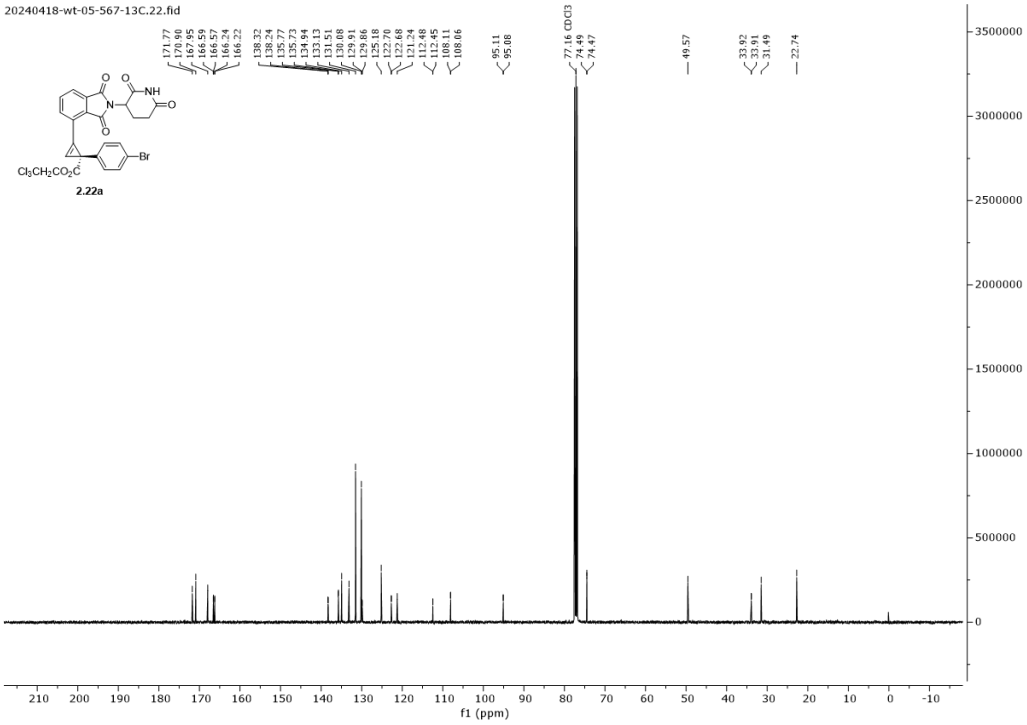

$^{13}C\{^{1}H\}$ NMR (101 MHz) Spectrum for Compounds 2.23a and 2.23b.

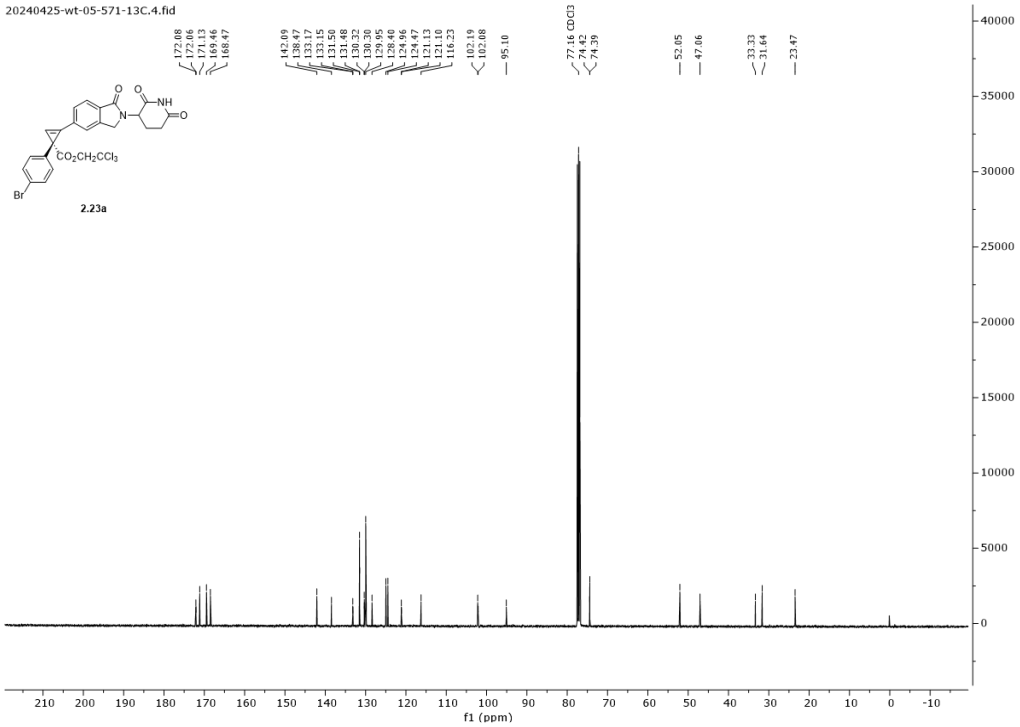

$^{13}C\{^{1}H\}$ NMR (126 MHz) Spectrum for Compounds 2.24a and 2.24b.

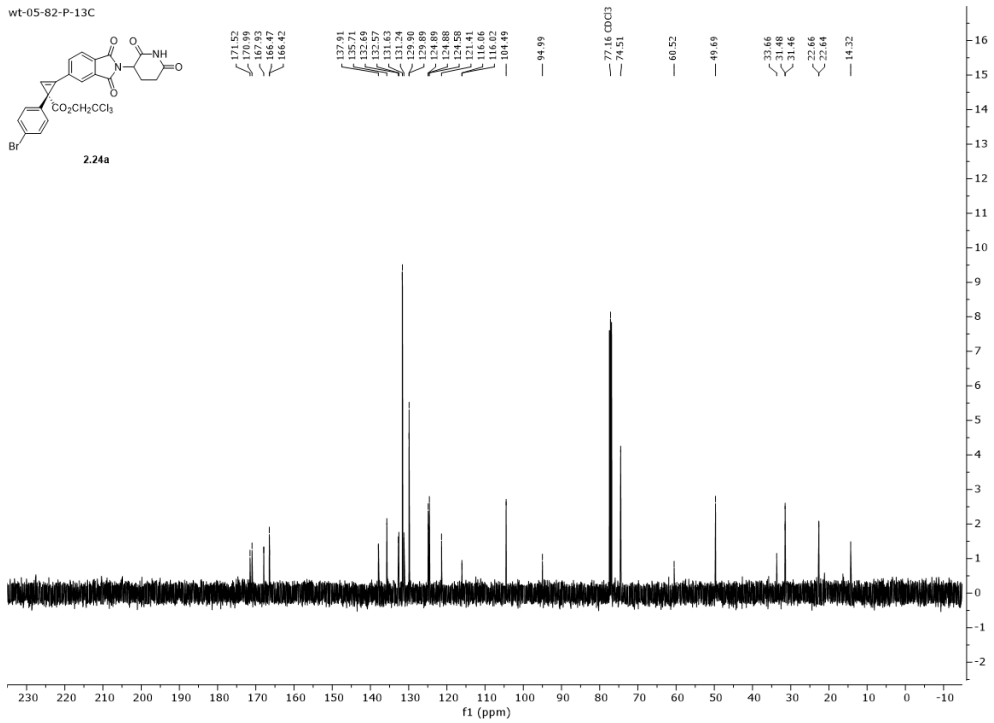

$^{13}C\{^{1}H\}$ NMR (101 MHz) Spectrum for Compounds 2.25a and 2.25b.

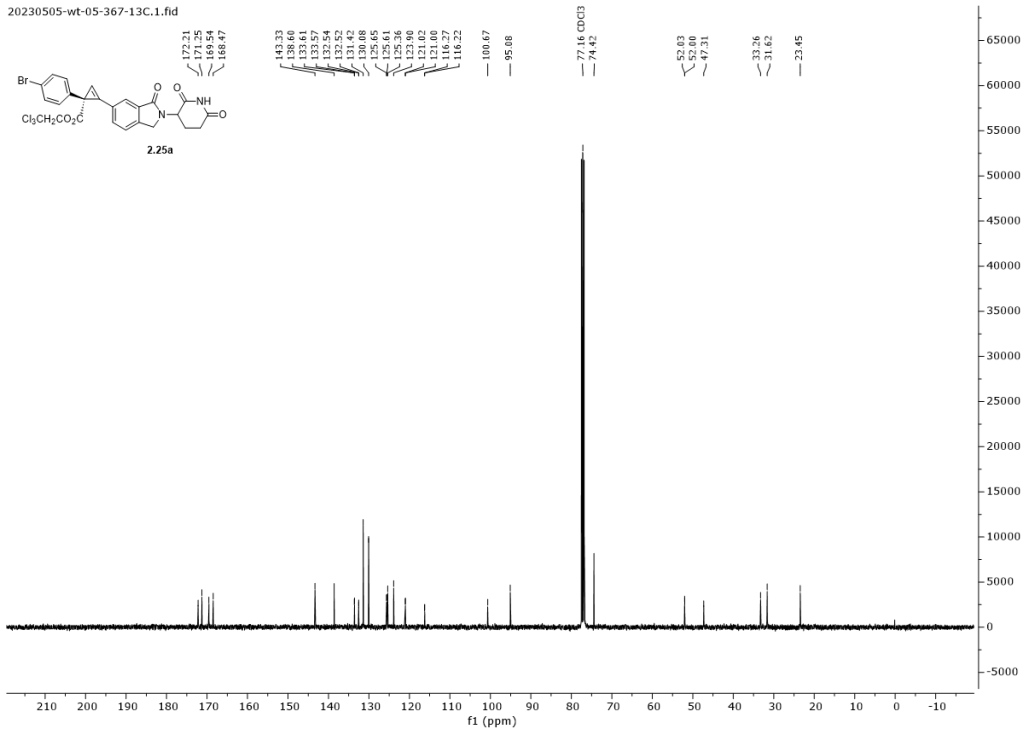

$^{13}C\{^{1}H\}$ NMR (101 MHz) Spectrum for Compounds 2.26a and 2.26b.

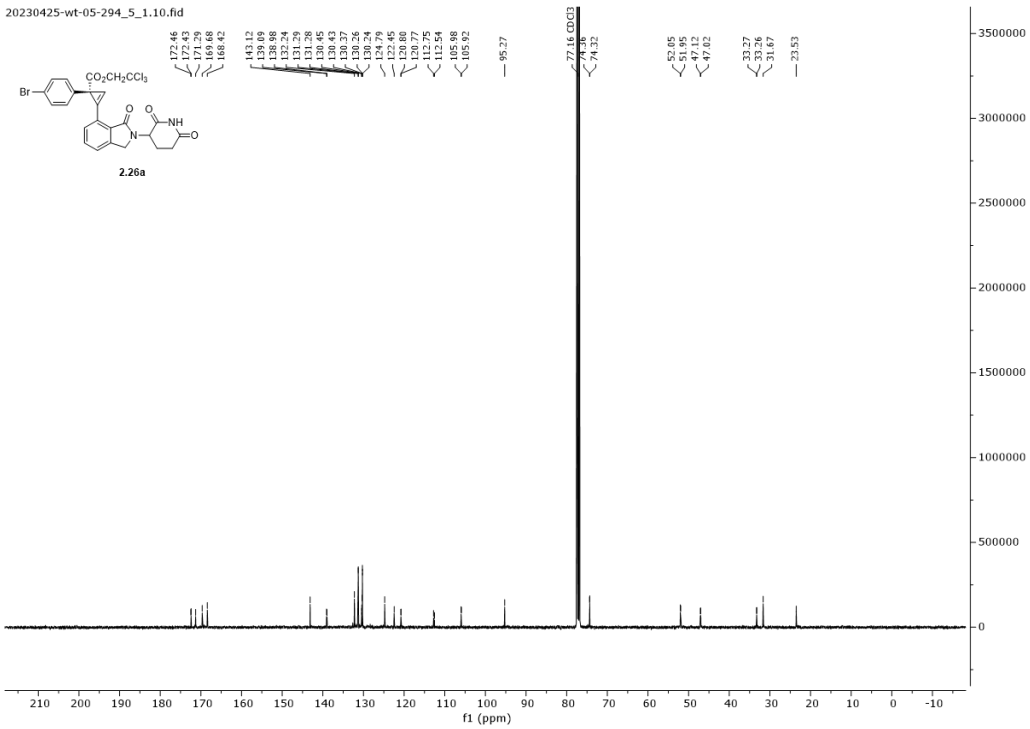

$^{13}C\{^{1}H\}$ NMR (101 MHz) Spectrum for Compounds 2.27a and 2.27b.

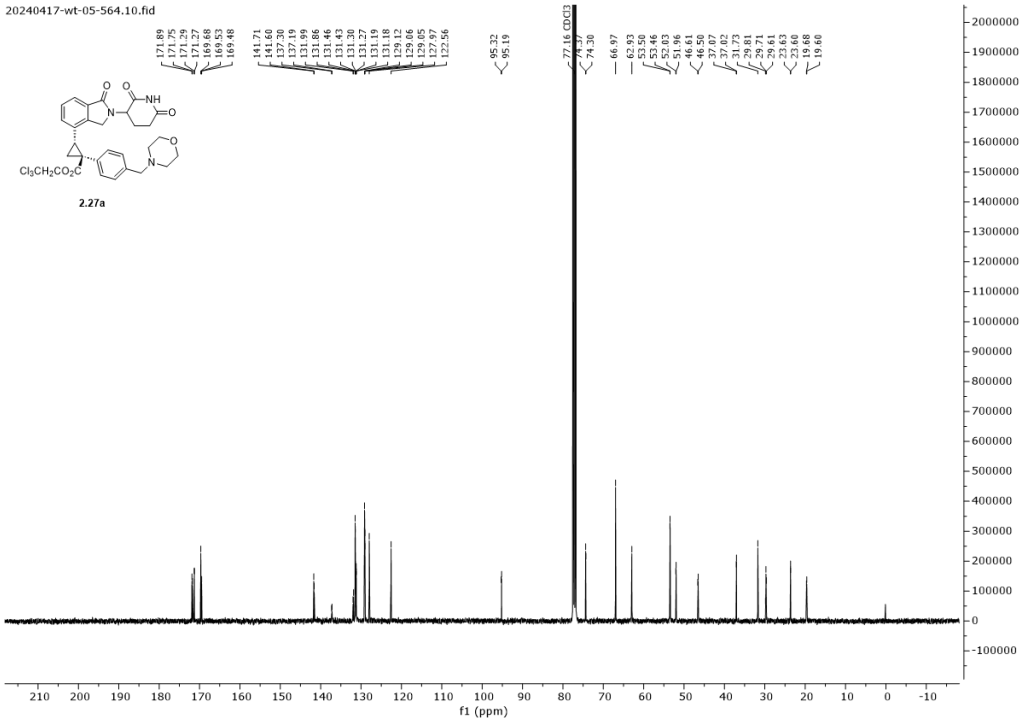

$^{13}C\{^{1}H\}$ NMR (101 MHz) Spectrum for Compounds 2.28a and 2.28b.

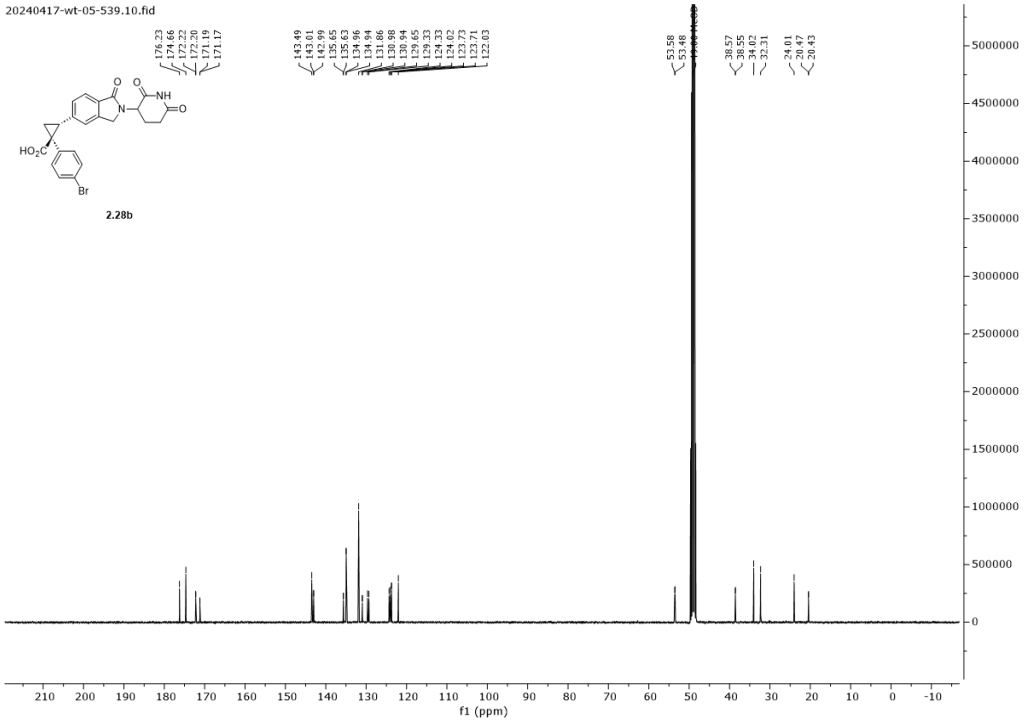

$^{13}C\{^{1}H\}$ NMR (101 MHz) Spectrum for Compounds 2.29a and 2.29b.

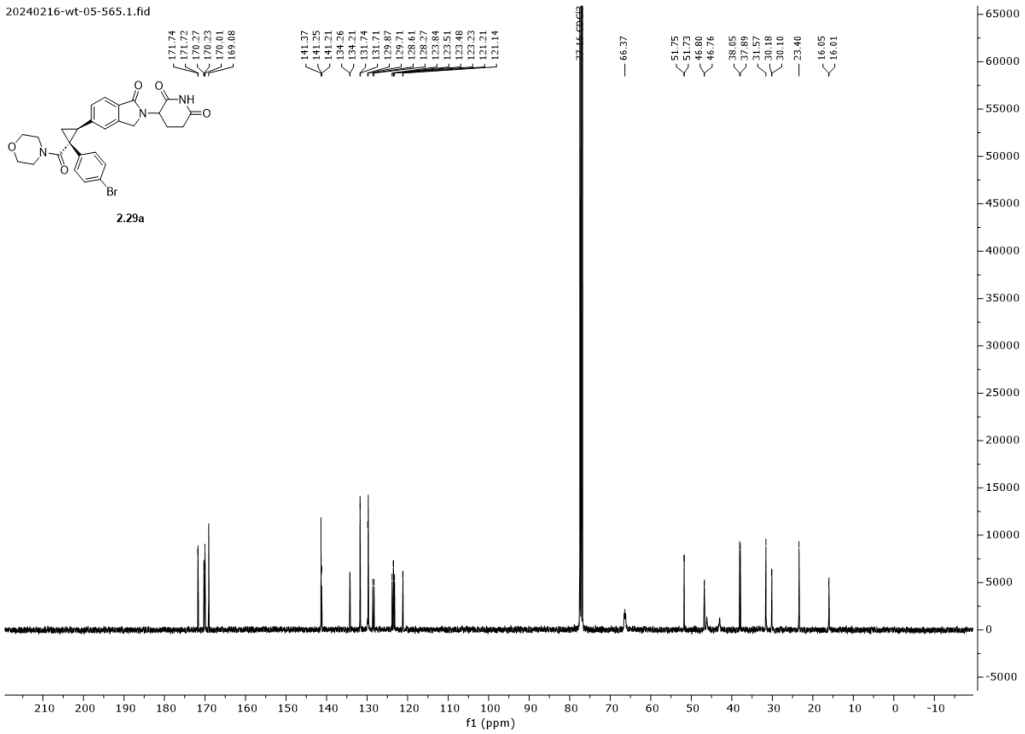

Section 6: Chromatographic Data

Chiral SFC Chromatograms
Racemic Chromatogram, 2.15

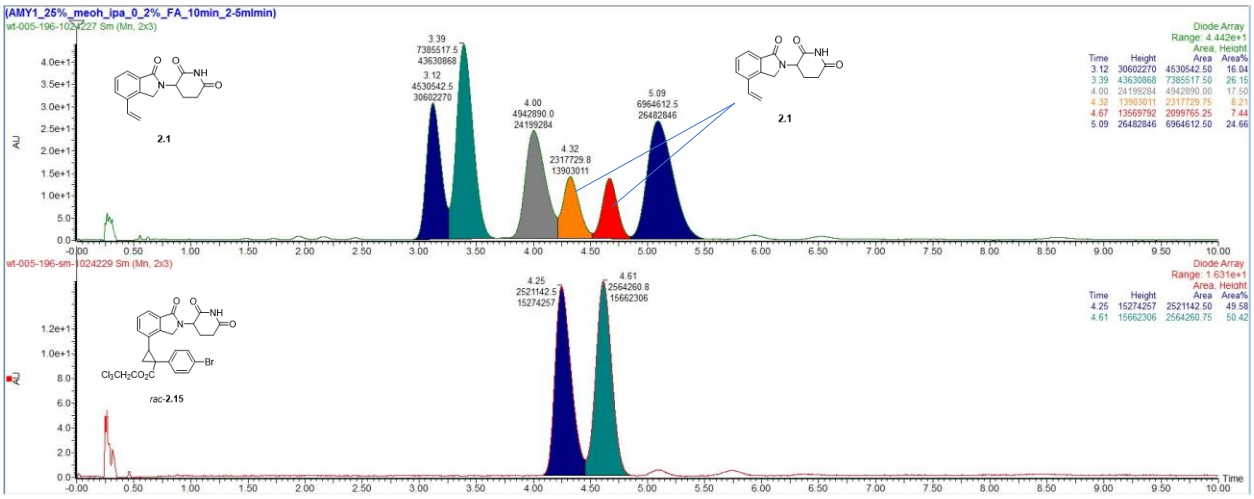

2.15a

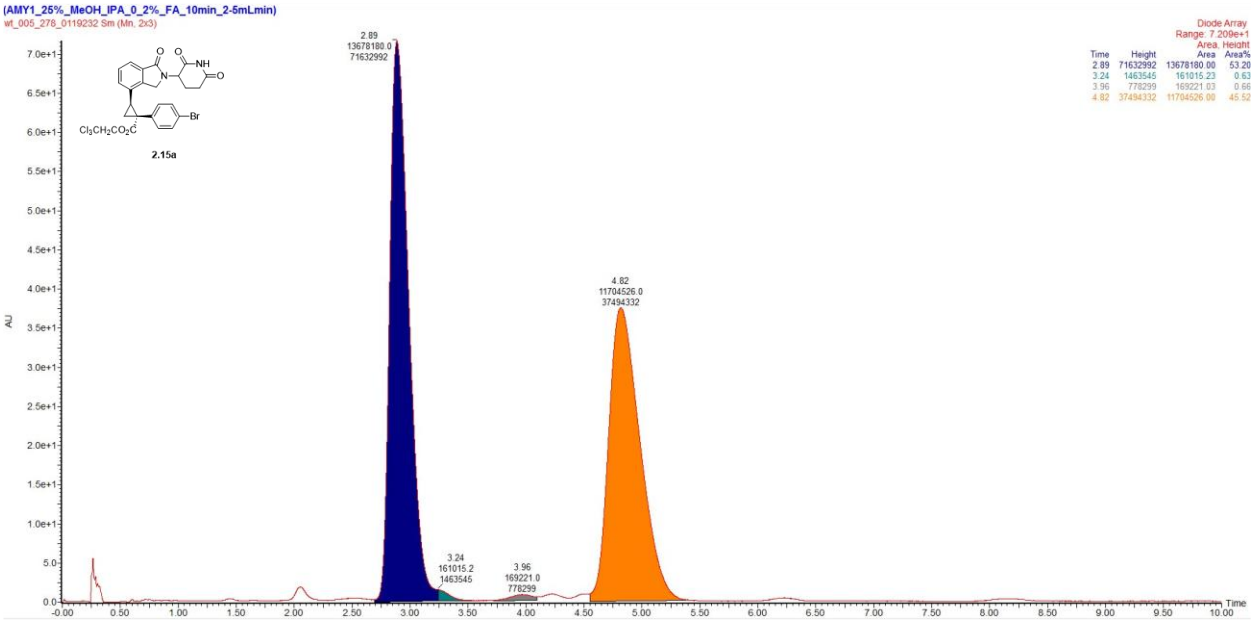

2.15b

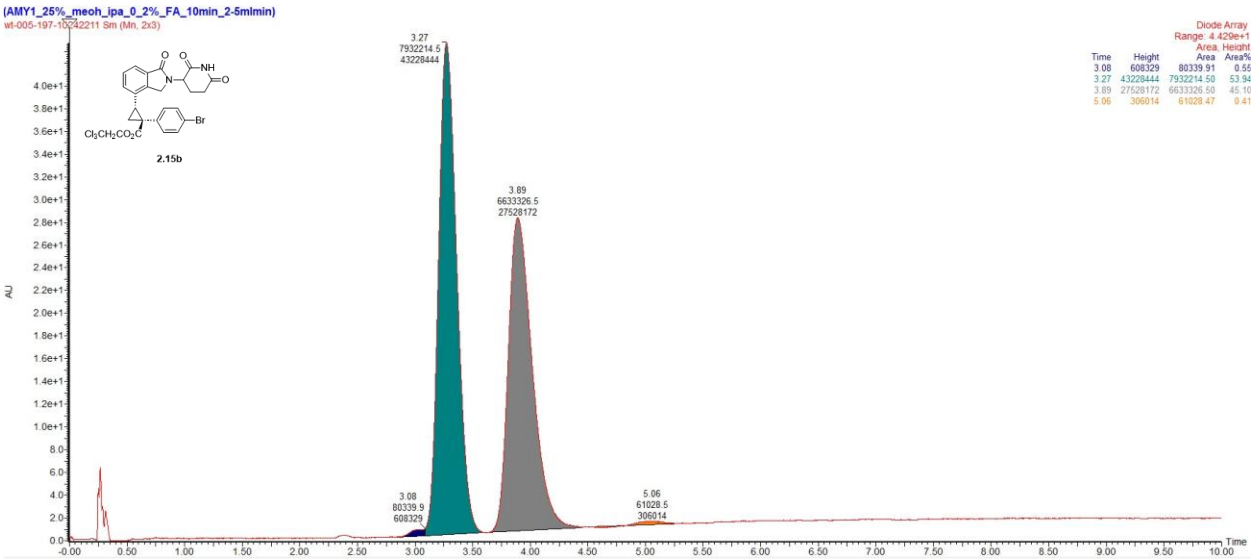

Racemic Chromatogram, 2.16

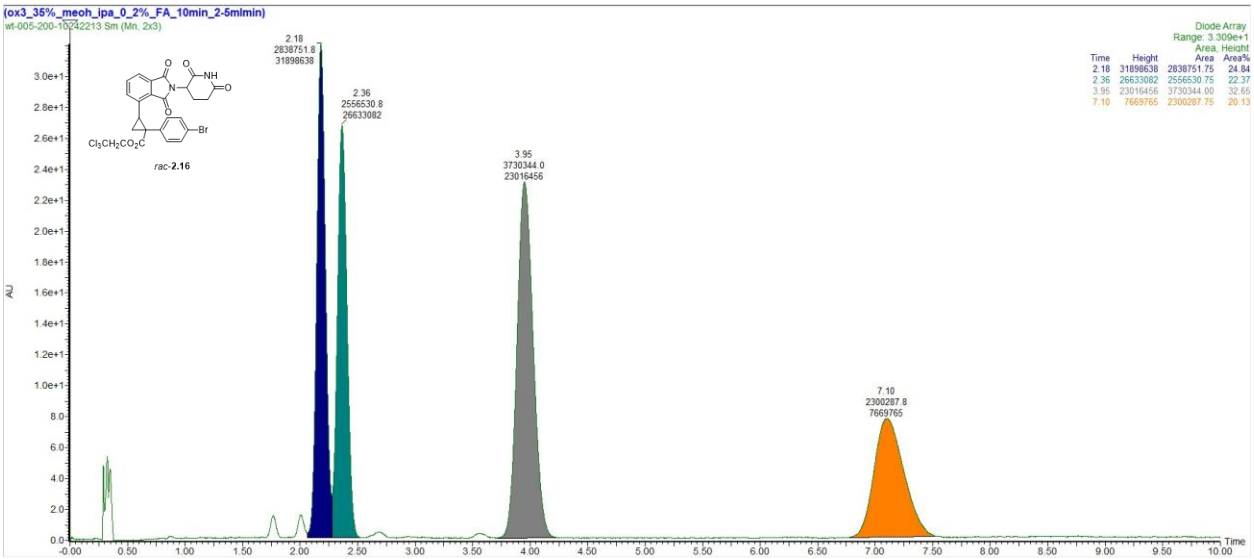

2.16a

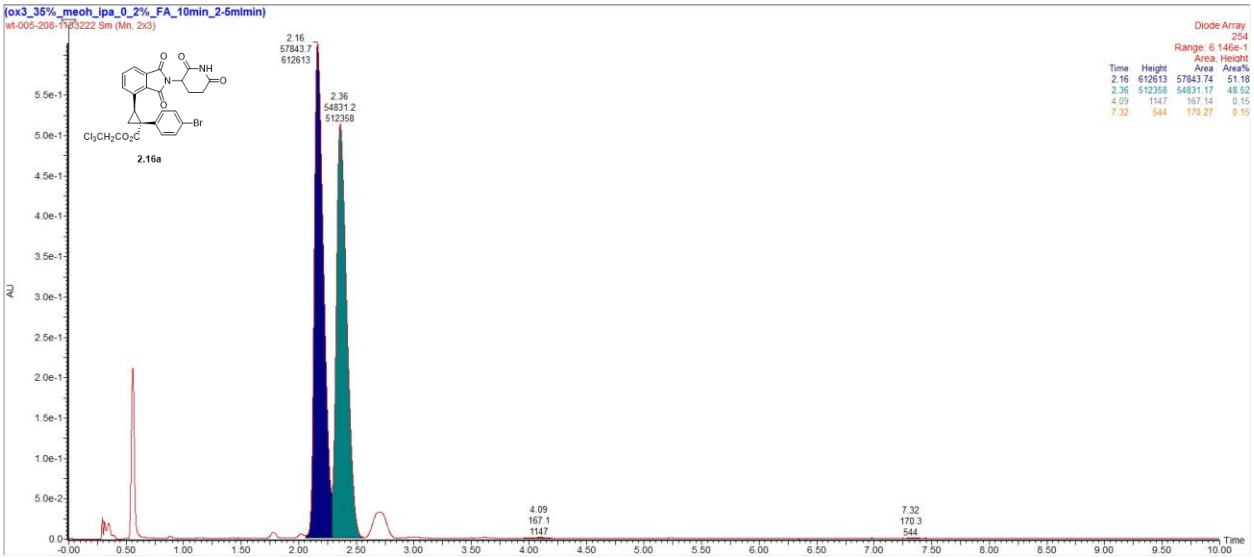
(ox3_35%_meoh_ipa_0_2%_FA_10min_2-5mlmin)
wt-005-208-1103222 Sm (Mn, 2x3)
2.16
57843.7
612613
2.36
54831.2
512358
4.09
167.1
1147
7.32
170.3
544
2.16a
Diode Array
254
Range: 6.146e-1
Time Height Area Area%
2.16 612613 57843.74 51.18
2.36 512358 54831.17 48.52
4.09 1147 167.14 0.15
7.32 544 170.27 0.15
AU
Time

2.16b

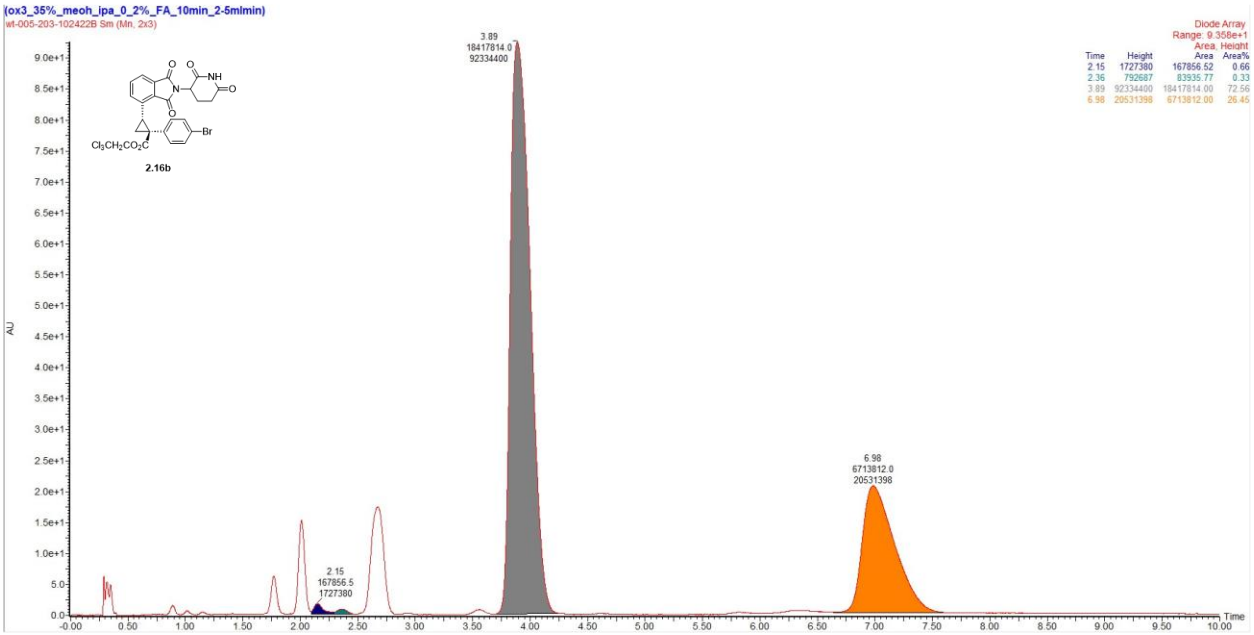
(ox3_35%_meoh_ipa_0_2%_FA_10min_2-5mlmin)
wt-005-203-102422B Sm (Mn, 2x3)
3.89
18417814.0
92334400
2.15
167856.5
1727380
6.98
6713812.0
20531398
2.16b
Diode Array
Range: 9.358e+1
Time Height Area Area%
2.15 1727380 167856.52 0.66
2.36 792687 83935.77 0.33
3.89 92334400 18417814.00 72.56
6.98 20531398 6713812.00 26.45
AU
Time

Racemic Chromatogram, 2.17

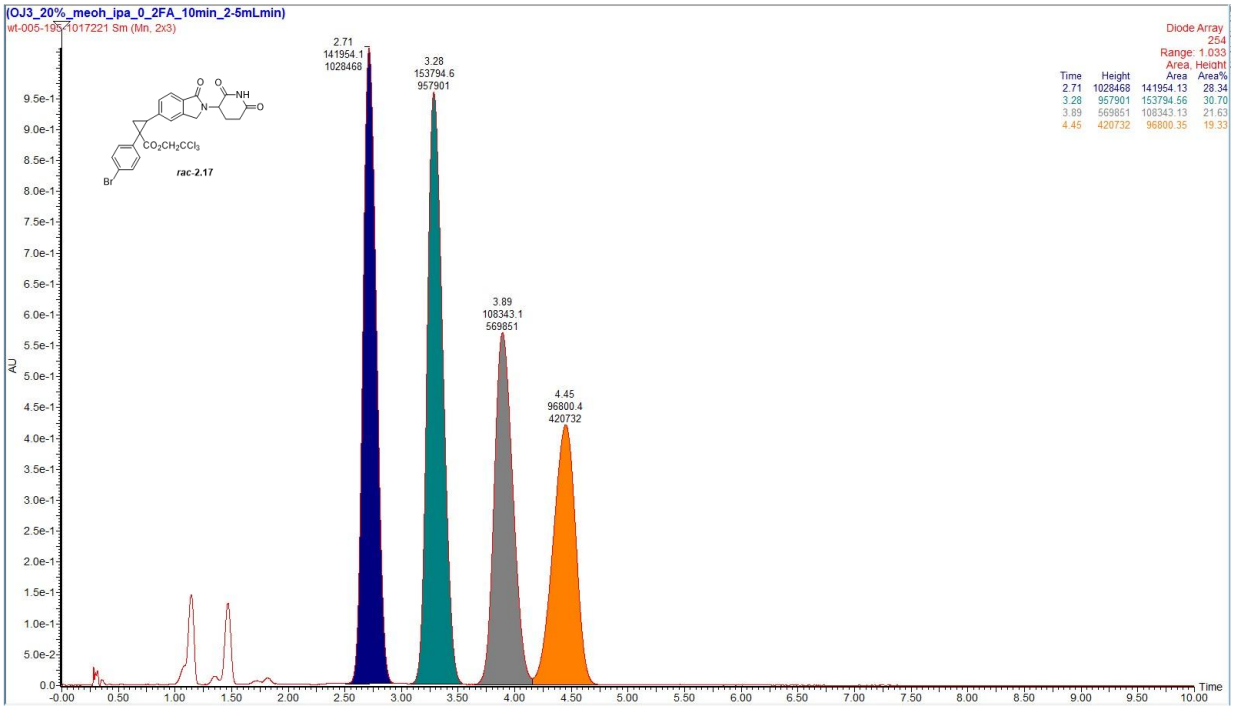

2.17a

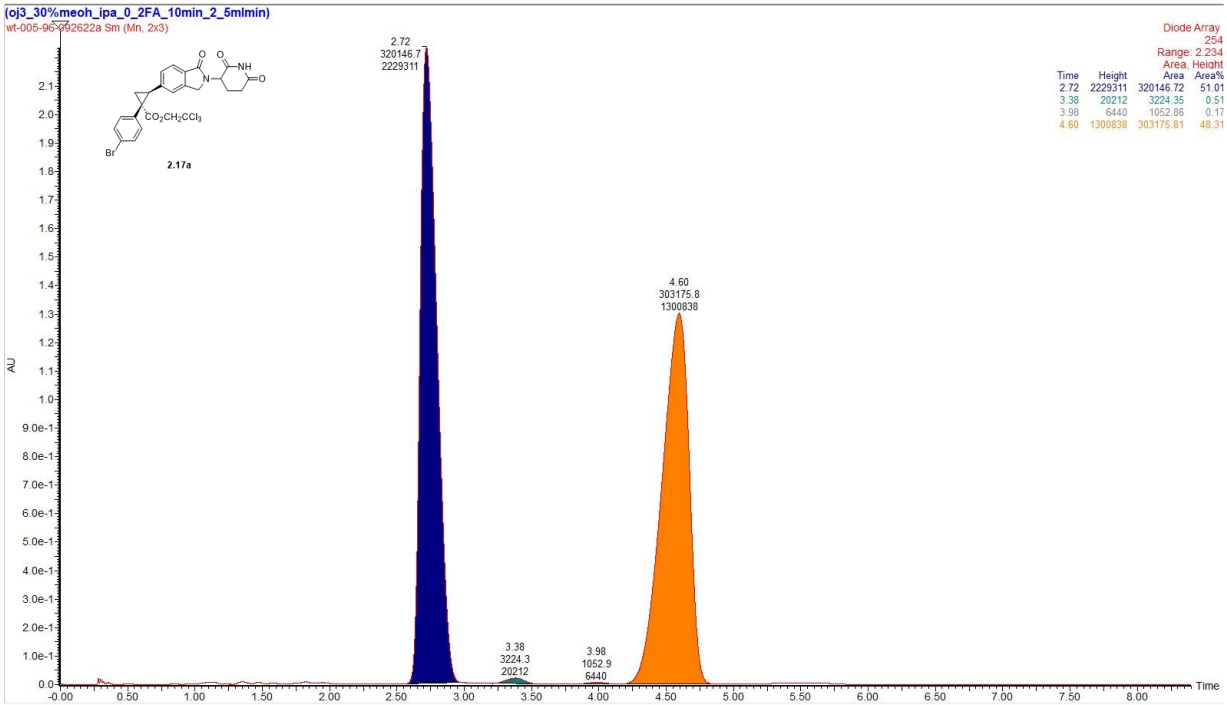

2.17b

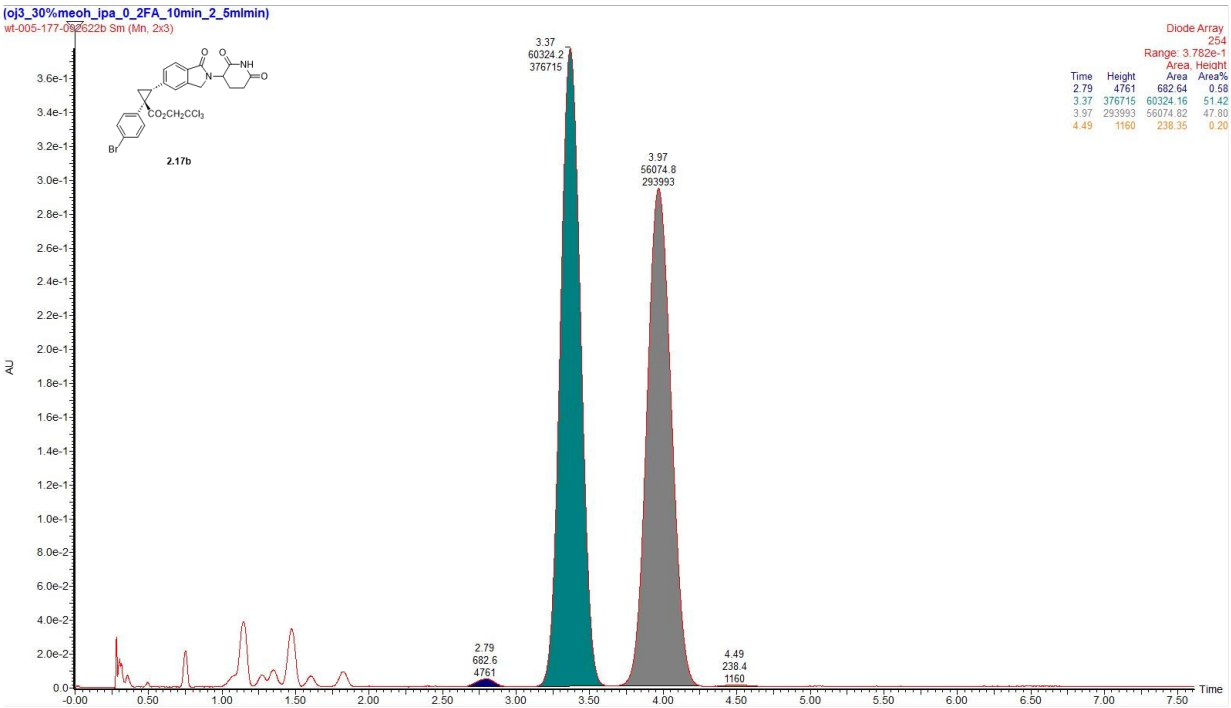
(oj3_30%meoh_ipa_0_2FA_10min_2_5mlmin)
wt-005-177-082622b Sm (Mn, 2x3)
2.17b
Diode Array
254
Range: 3.782e-1
Area, Height
Time Height Area Area%
2.79 4761 682.64 0.58
3.37 376715 60324.16 51.42
3.97 293993 56074.82 47.80
4.49 1160 238.35 0.20
3.37
60324.2
376715
3.97
56074.8
293993
2.79
682.6
4761
4.49
238.4
1160
AU
Time

***S*-2.17a**

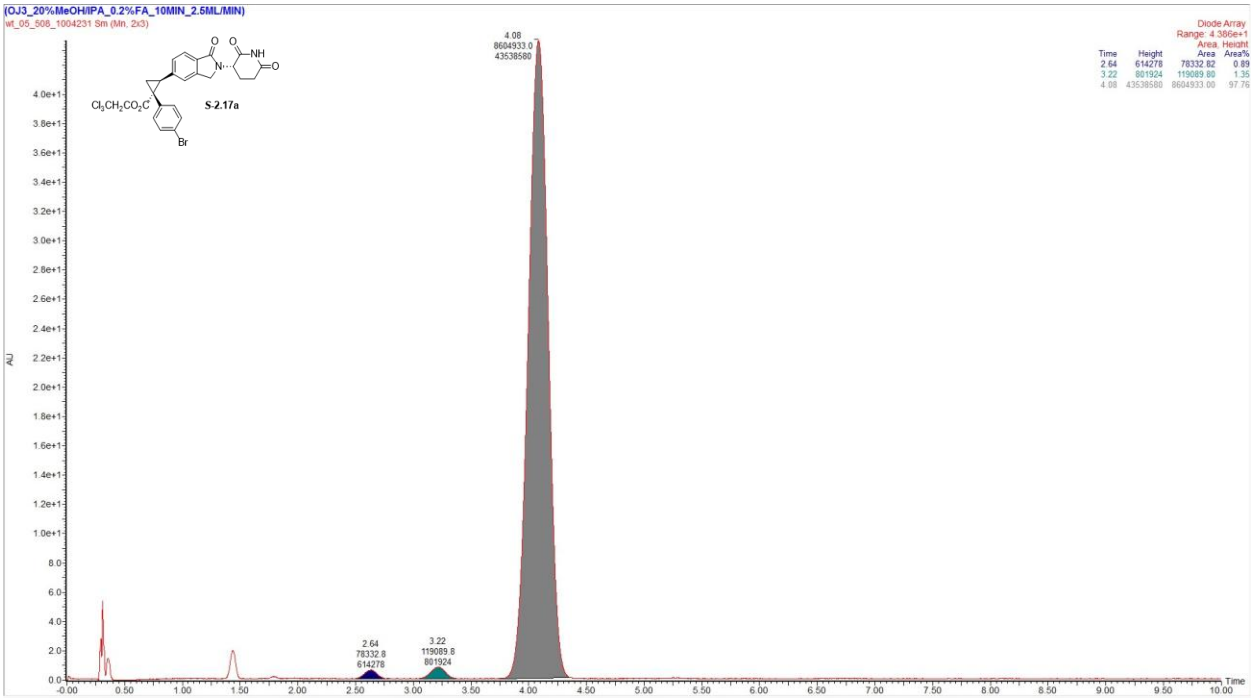
(OJ3_20%MeOH/IPA_0.2%FA_10MIN_2.5ML/MIN)
wt_05_508_1004231 Sm (Mn, 2x3)
S-2.17a
Diode Array
Range: 4.386e+1
Area, Height
Time Height Area Area%
2.64 614278 78332.82 0.89
3.22 801924 119089.80 1.35
4.08 43538580 8604933.00 97.76
4.08
8604933.0
43538580
2.64
78332.8
614278
3.22
119089.8
801924
AU
Time

S-2.17b

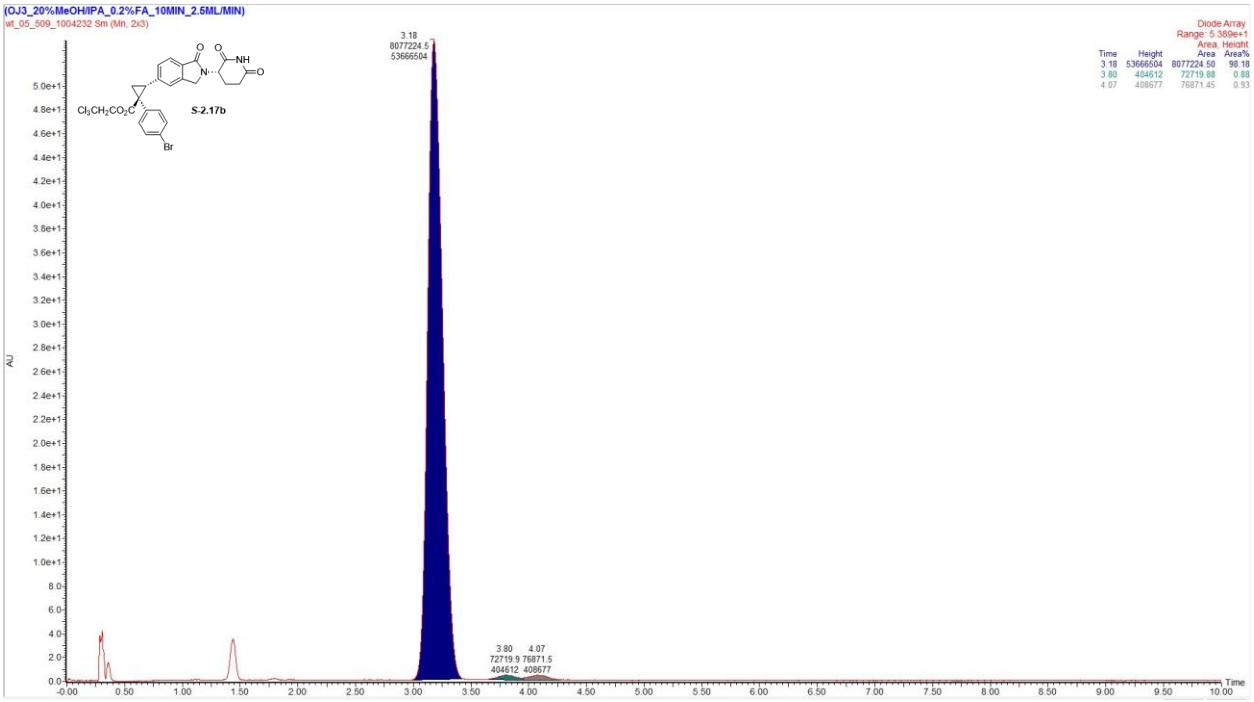
(OJ3_20%MeOH/IPA_0.2%FA_10MIN_2.5ML/MIN)
wt_05_509_1004232 Sm (Mn, 2x3)
S-2.17b
Diode Array
Range: 5.389e+1
Area, Height
Time Height Area Area%
3.18 53666504 8077224.50 98.18
3.80 404612 72719.88 0.88
4.07 408677 76871.45 0.93
3.18
8077224.5
53666504
3.80 4.07
72719.9 76871.5
404612 408677
AU
Time

R-2.17a

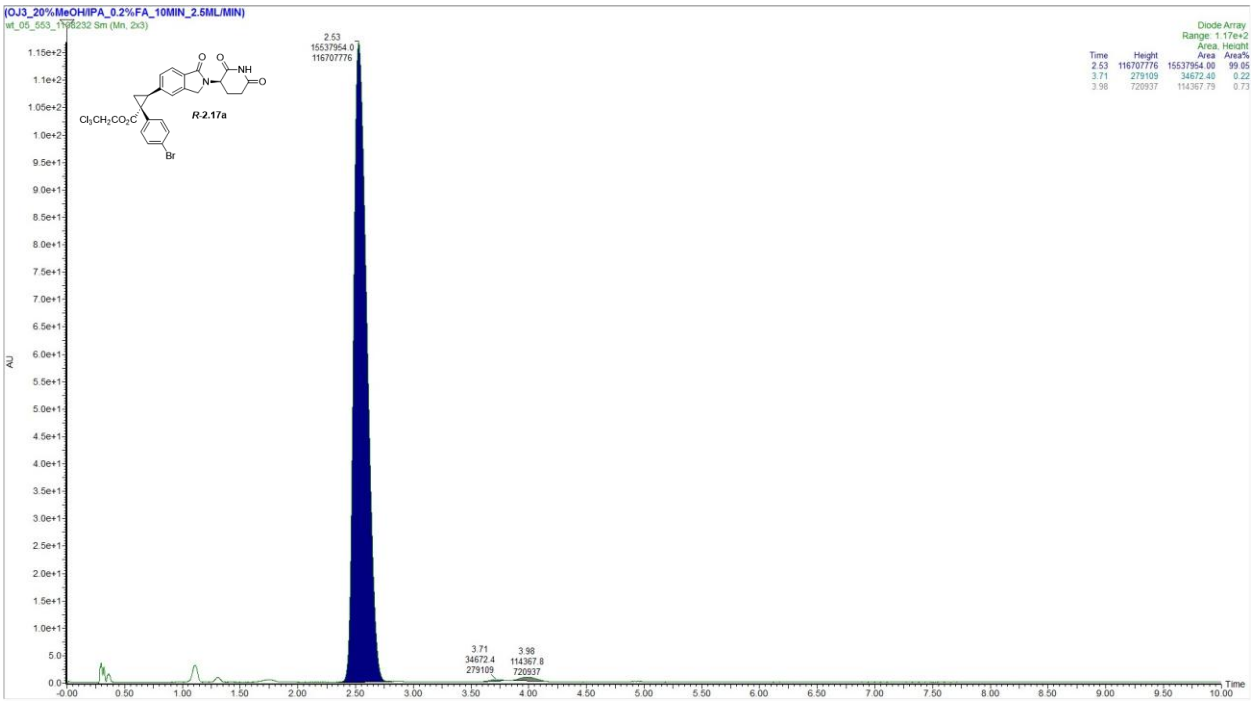
(OJ3_20%MeOH/IPA_0.2%FA_10MIN_2.5ML/MIN)
wt_05_553_1116232 Sm (Mn, 2x3)
R-2.17a
Diode Array
Range: 1.17e+2
Area, Height
Time Height Area Area%
2.53 116707776 15537954.00 99.05
3.71 279109 34672.40 0.22
3.98 720937 114367.79 0.73
2.53
15537954.0
116707776
3.71 3.98
34672.4 114367.8
279109 720937
AU
Time

R-2.17b

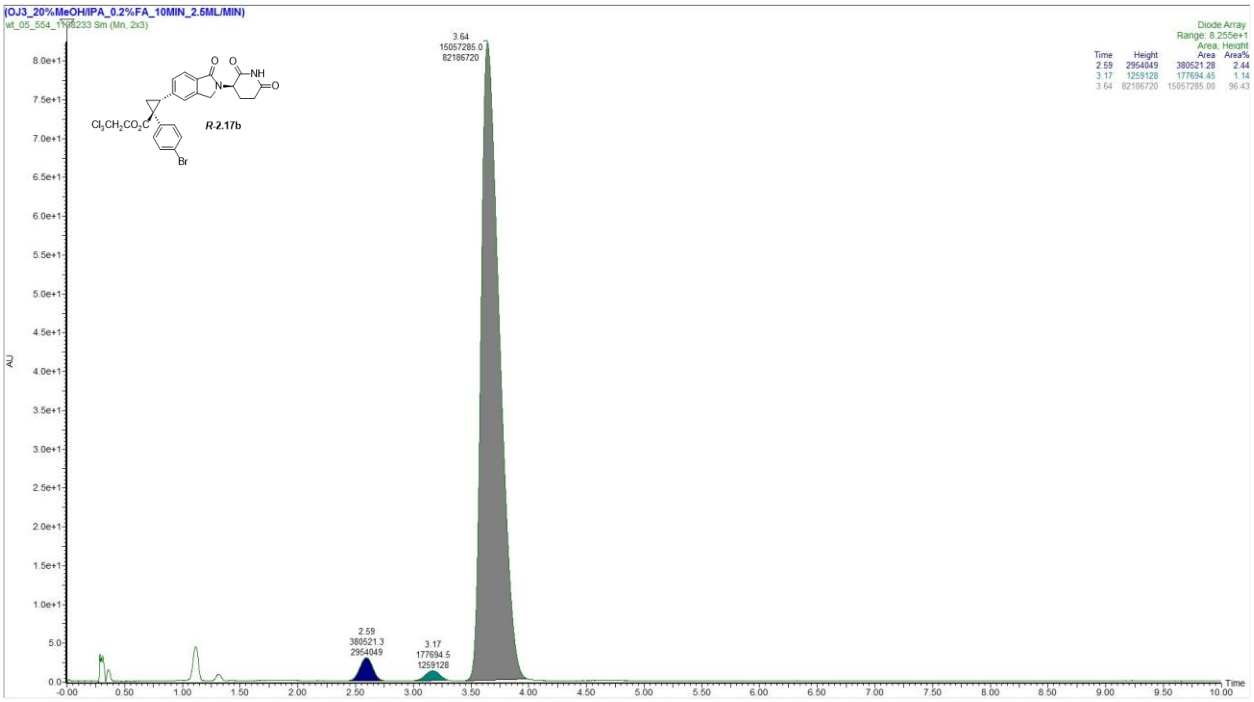

Racemic Chromatogram, 2.18

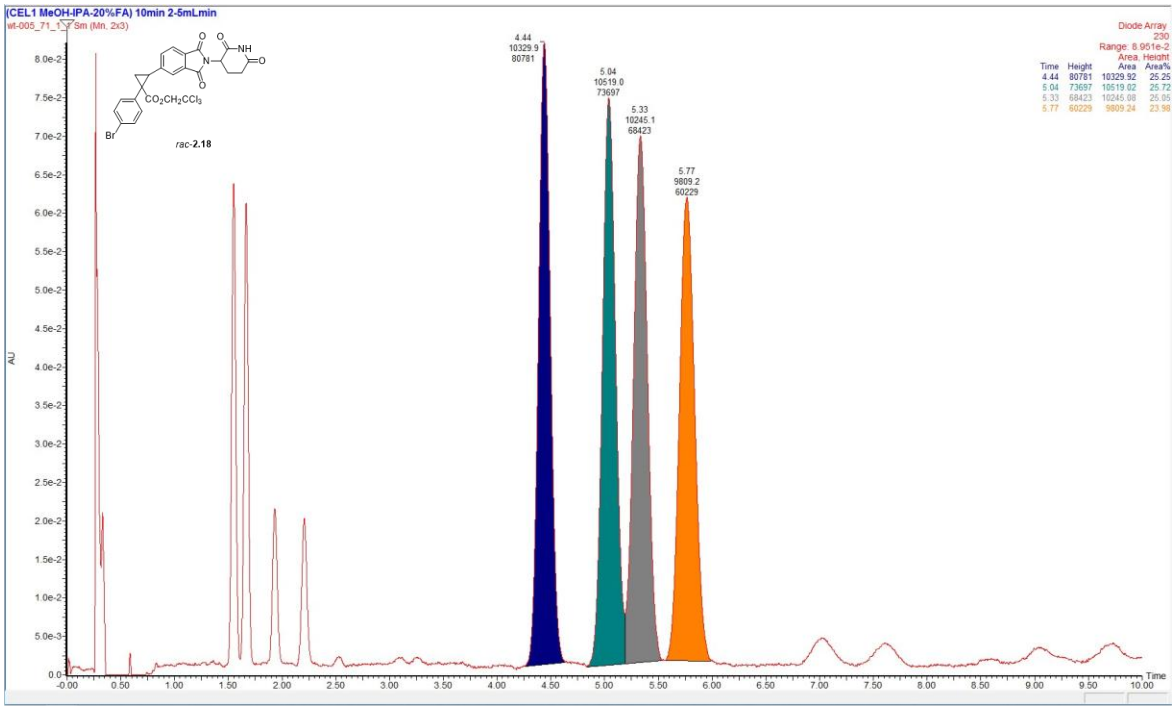

2.18a

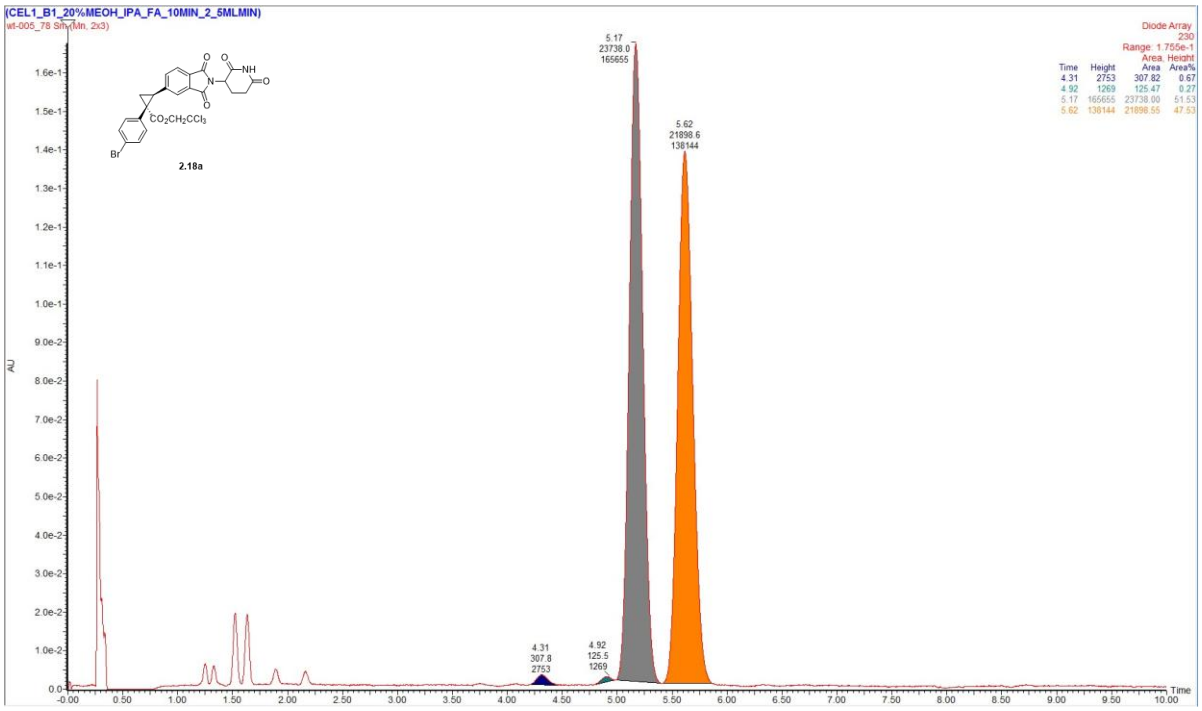
(CEL1_B1_20%MEOH_IPA_FA_10MIN_2_5MLMIN)
wt-005_78 Sm (Mn, 2x3)
Diode Array
230
Range: 1.755e-1
Time Height Area Area%
4.31 2753 307.82 0.67
4.92 1269 125.47 0.27
5.17 165655 23738.00 51.53
5.62 138144 21898.55 47.53
5.17
23738.0
165655
5.62
21898.6
138144
4.31
307.8
2753
4.92
125.5
1269
2.18a
AU
Time

2.18b

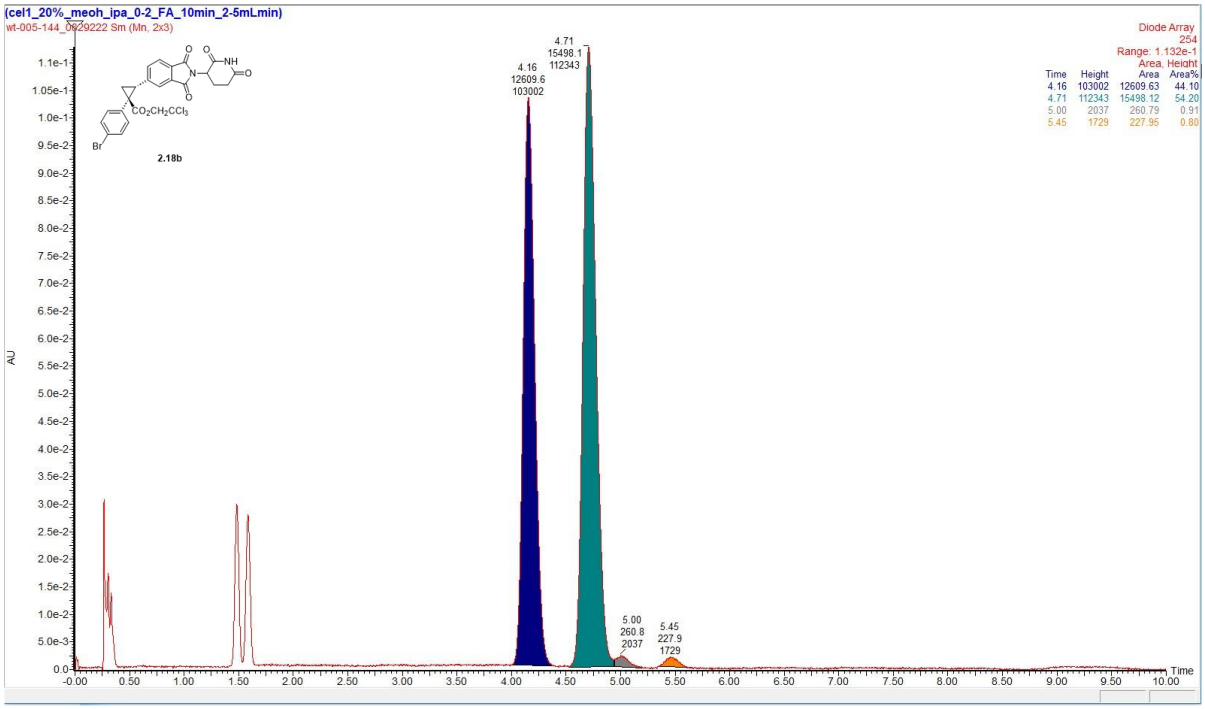
(cel1_20%_meoh_ipa_0-2_FA_10min_2-5mLmin)
wt-005-144_0629222 Sm (Mn, 2x3)
Diode Array
254
Range: 1.132e-1
Time Height Area Area%
4.16 103002 12609.63 44.10
4.71 112343 15498.12 54.20
5.00 2037 260.79 0.91
5.45 1729 227.95 0.80
4.16
12609.6
103002
4.71
15498.1
112343
5.00
260.8
2037
5.45
227.9
1729
2.18b
AU
Time

Racemic Chromatogram, 2.19

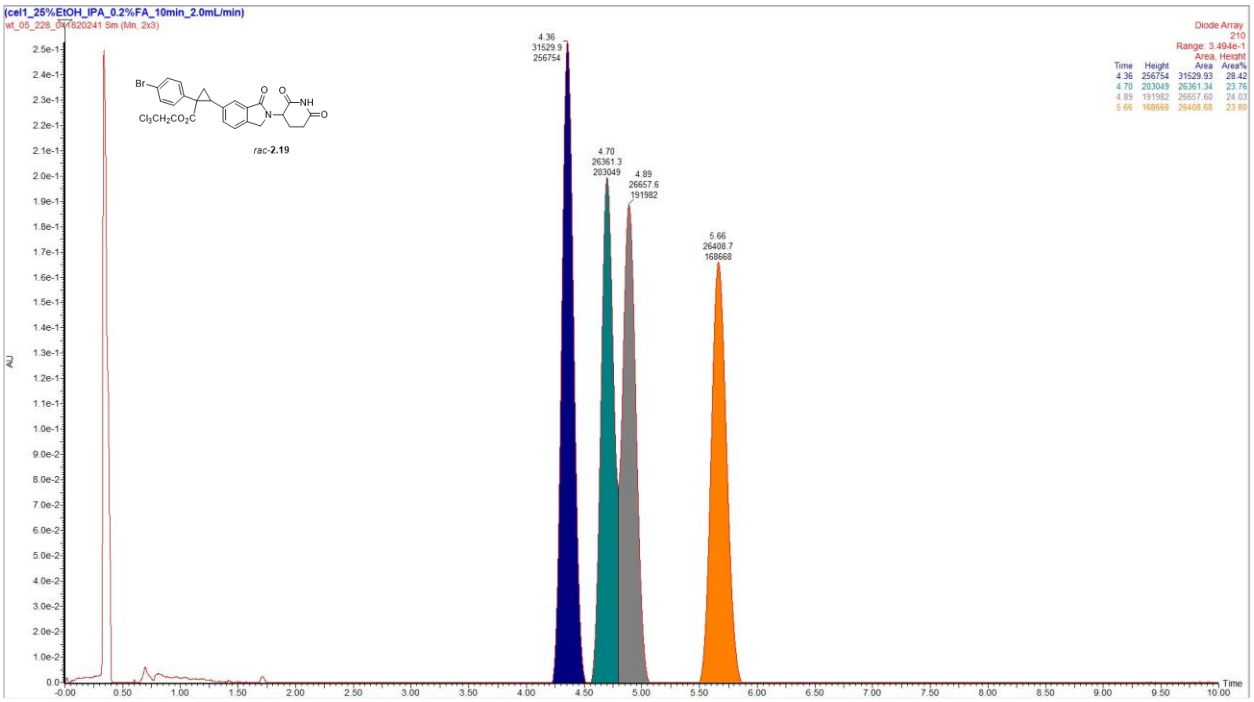

2.19a

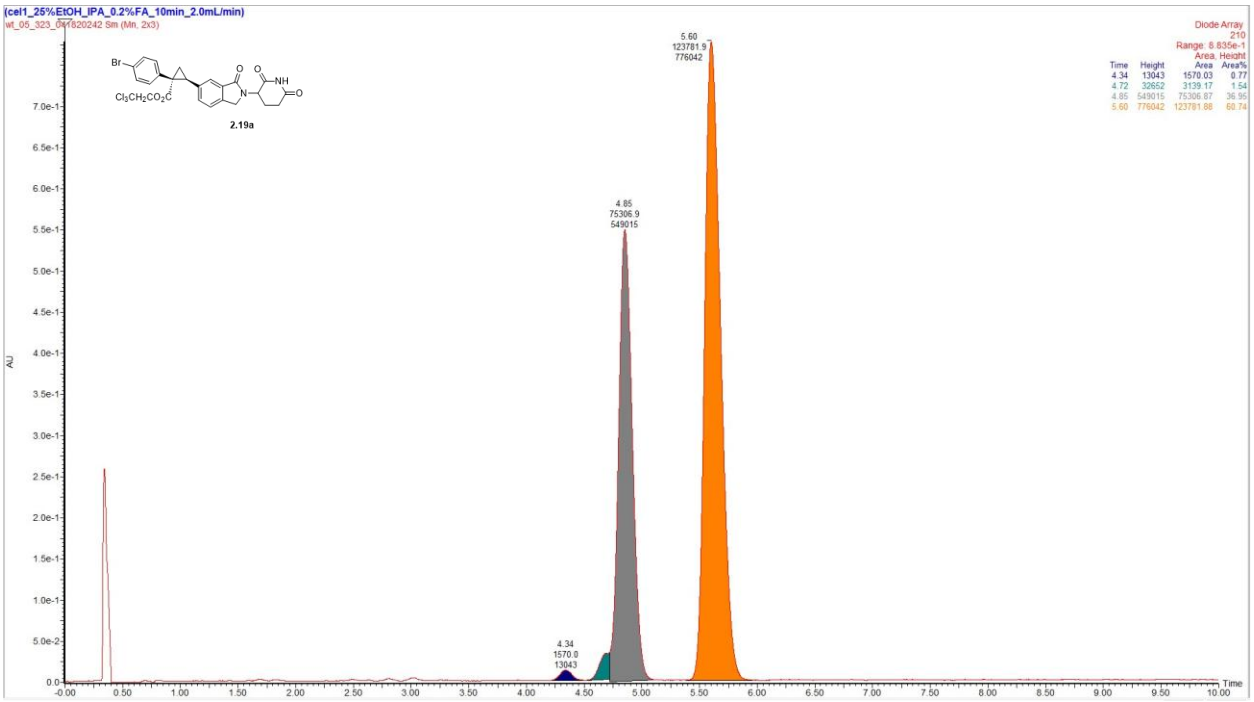

2.19b

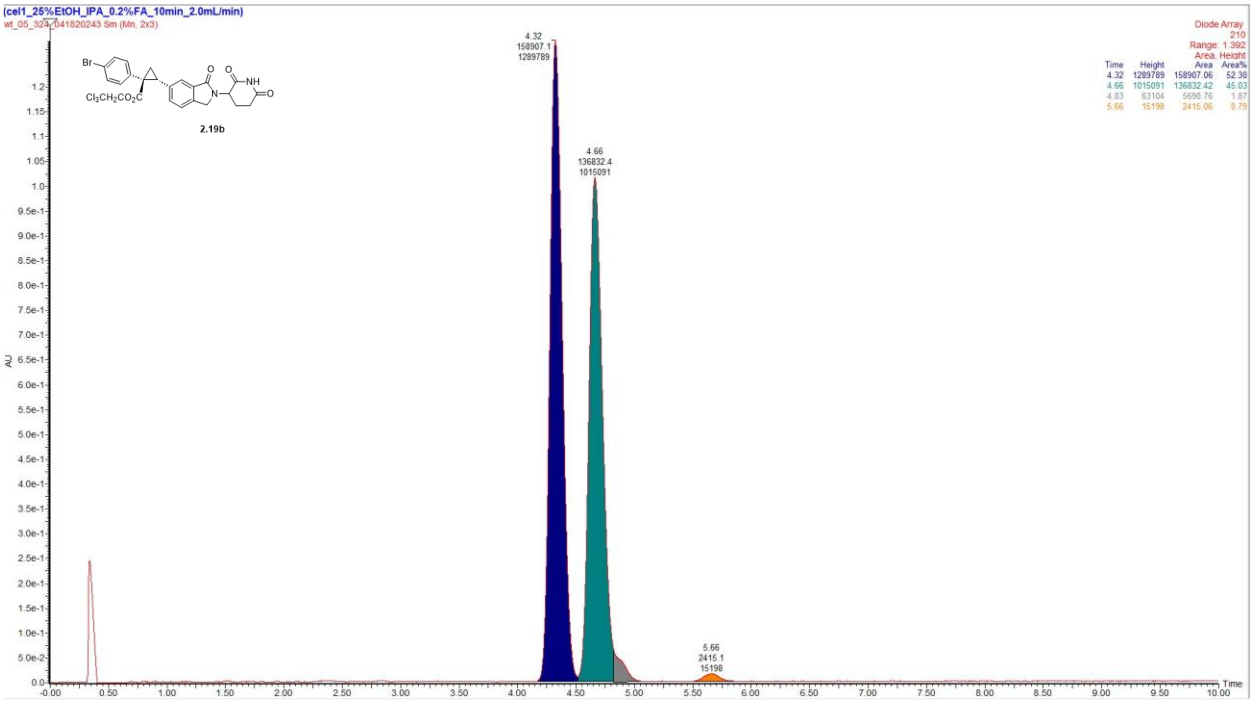

Racemic Chromatogram, 2.20

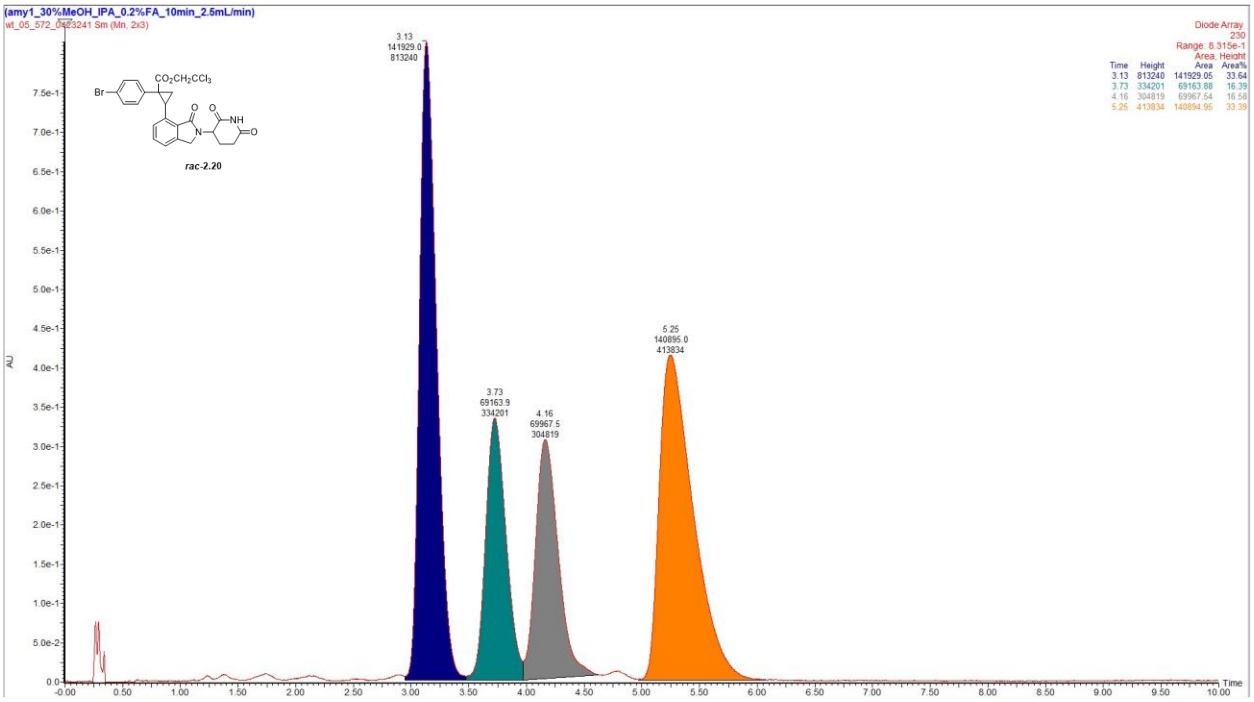

2.20a

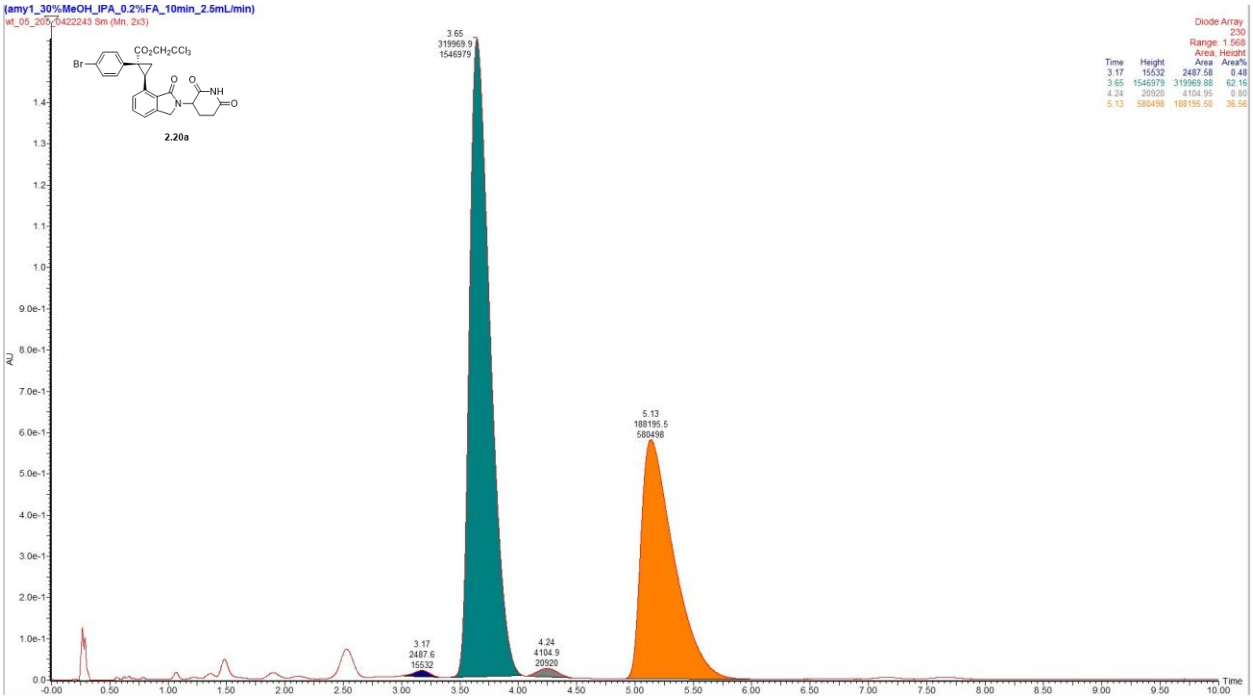
(amy1_30%MeOH_IPA_0.2%FA_10min_2.5mL/min)
wt_05_205_0422243 Sm (Mn, 2x3)
Diode Array
230
Range: 1.568
Time Height Area Area%
3.17 15532 2487.58 0.48
3.65 1546979 319969.88 62.16
4.24 20920 4104.95 0.80
5.13 580498 188195.50 36.56
3.65
319969.9
1546979
5.13
188195.5
580498
3.17
2487.6
15532
4.24
4.104.9
20920
AU
Time
2.20a

2.20b

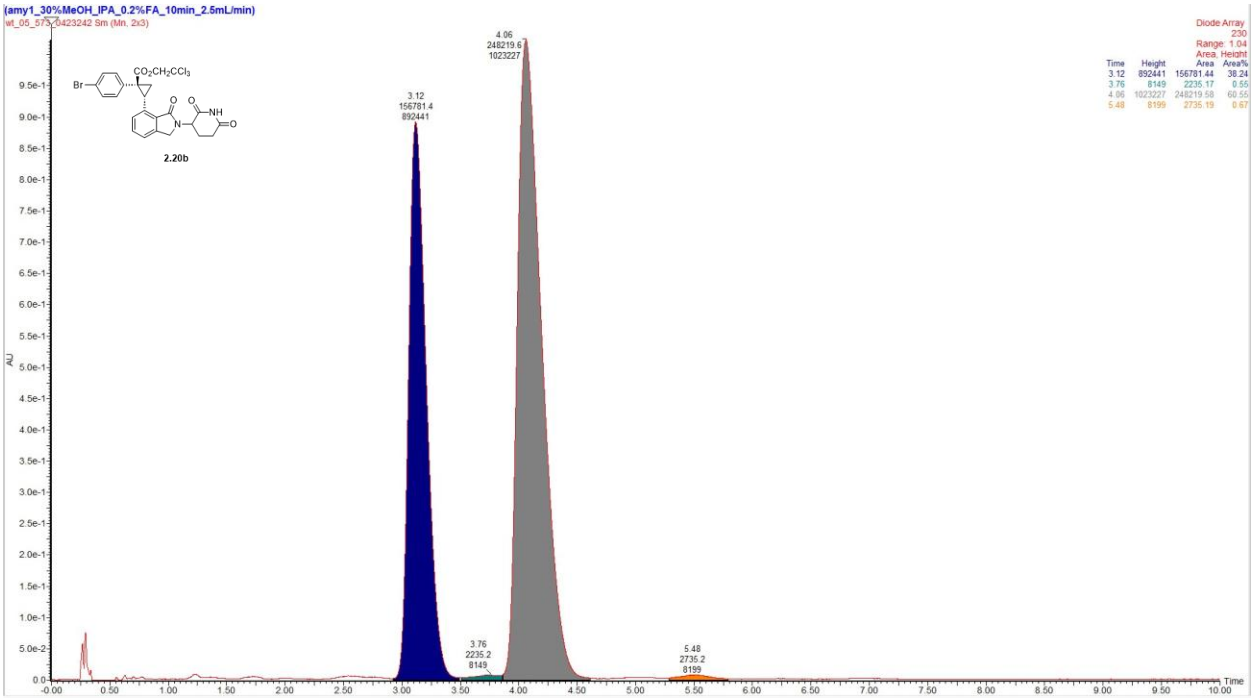
(amy1_30%MeOH_IPA_0.2%FA_10min_2.5mL/min)
wt_05_575_0423242 Sm (Mn, 2x3)
Diode Array
230
Range: 1.04
Time Height Area Area%
3.12 892441 156781.44 38.24
3.76 8149 2235.17 0.55
4.06 1023227 248219.58 60.55
5.48 8199 2735.19 0.67
4.06
248219.6
1023227
3.12
156781.4
892441
3.76
2235.2
8149
5.48
2735.2
8199
AU
Time
2.20b

Racemic Chromatogram, 2.21

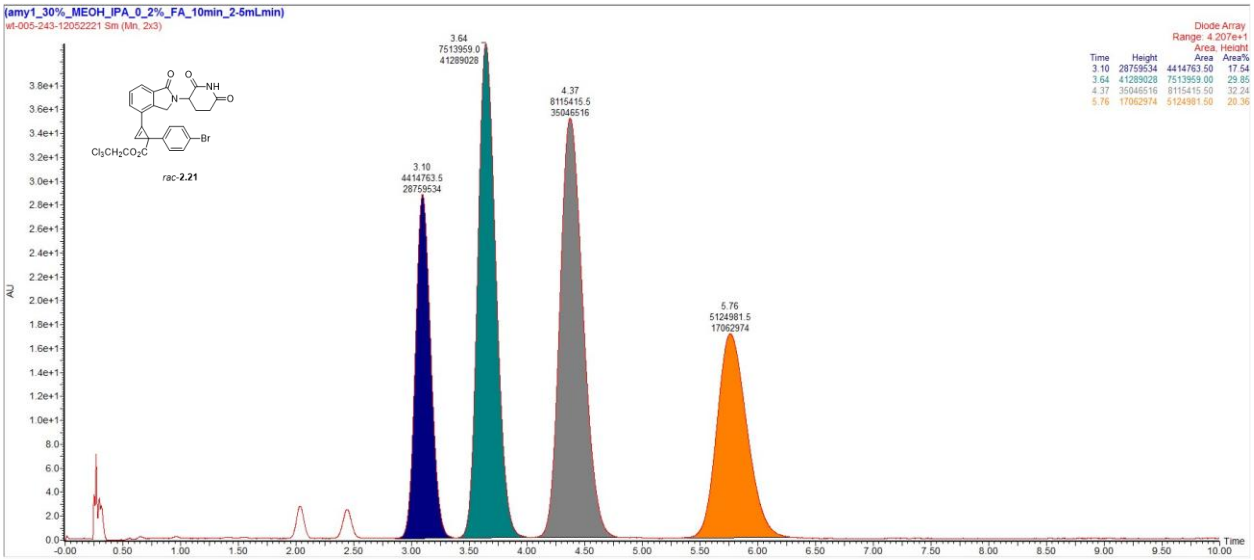

2.21a

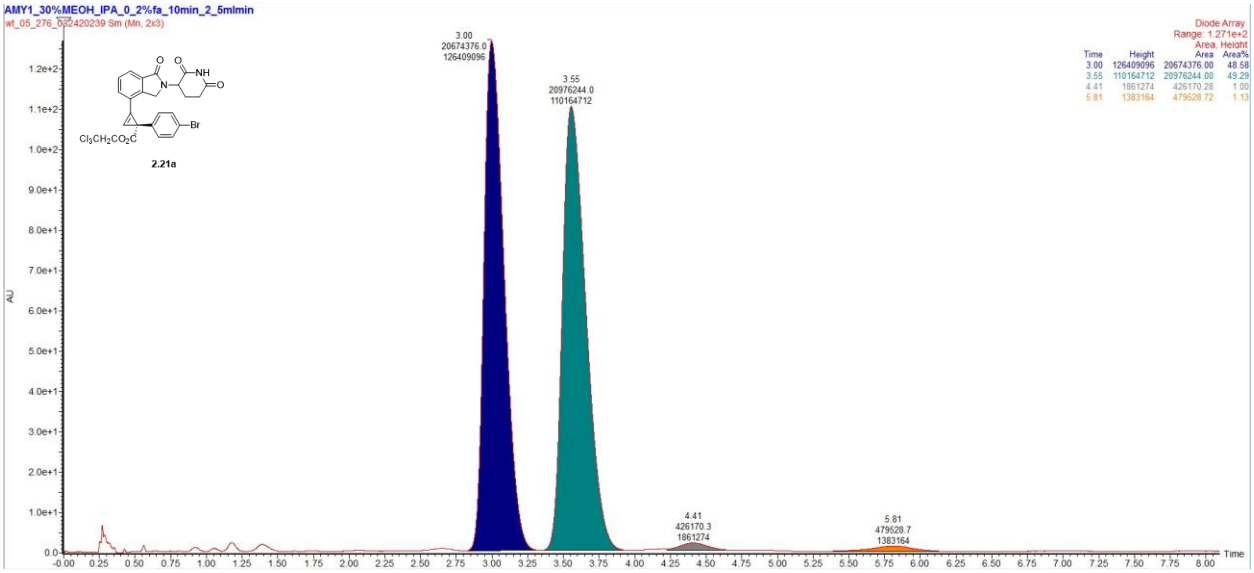

2.21b

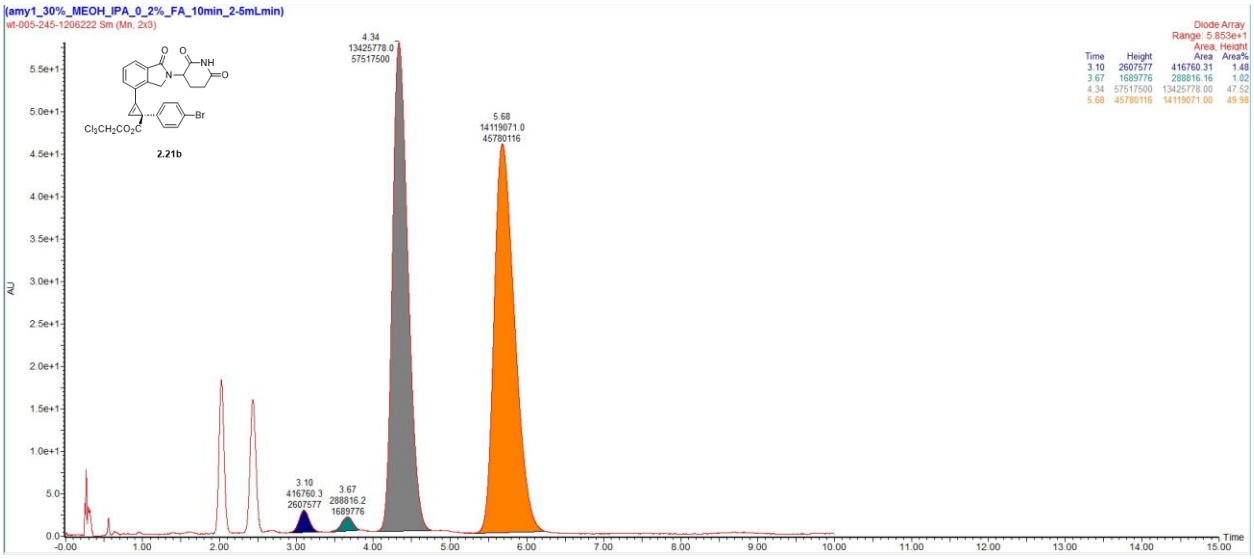

Racemic Chromatogram, 2.22

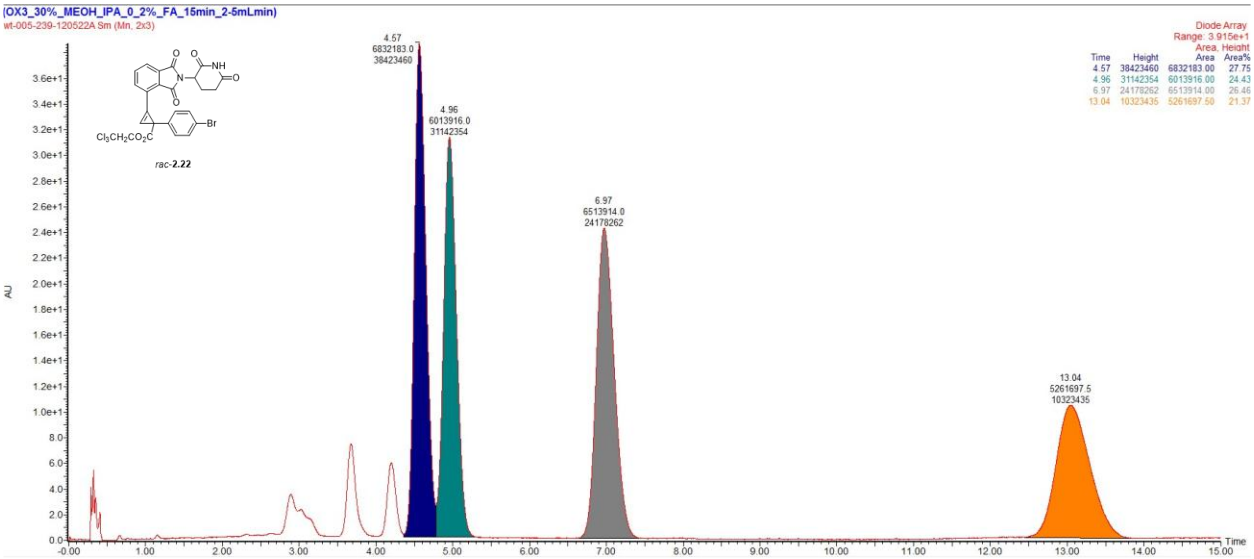

2.22a

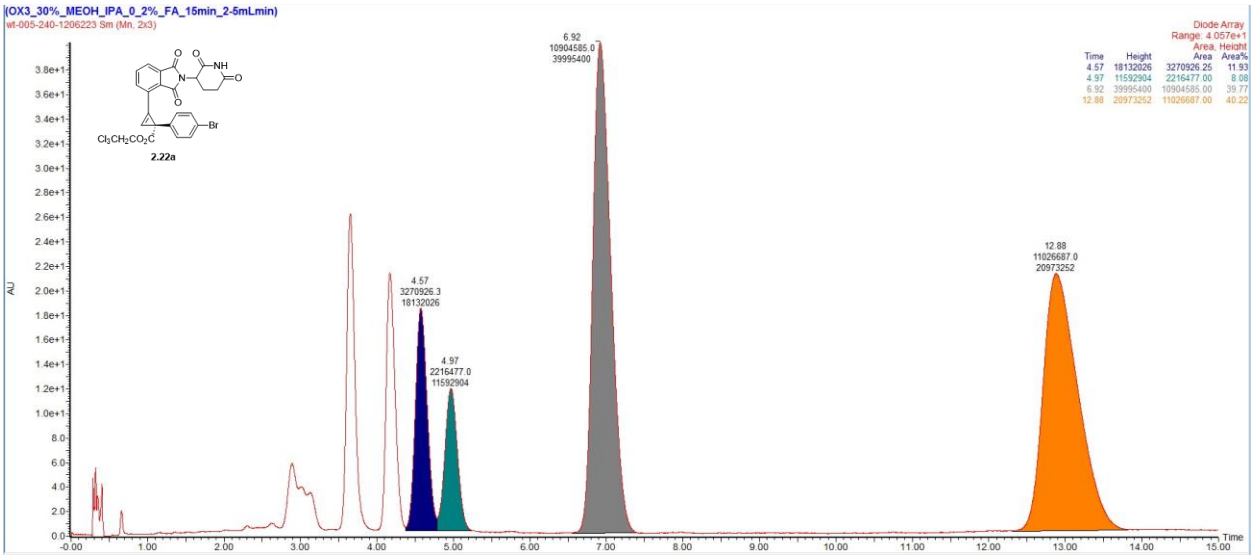
(OX3_30%_MEOH_IPA_0_2%_FA_15min_2-5mLmin)
wt-005-240-1206223 Sm (Mn, 2x3)
Diode Array
Range: 4.057e+1
Time Height Area Area%
4.57 18132026 3270926.25 11.93
4.97 11592904 2216477.00 8.08
6.92 39995400 10904585.00 39.77
12.88 20973252 11026687.00 40.22
4.57
3270926.3
18132026
4.97
2216477.0
11592904
6.92
10904585.0
39995400
12.88
11026687.0
20973252
AU
Time
2.22a

2.22b

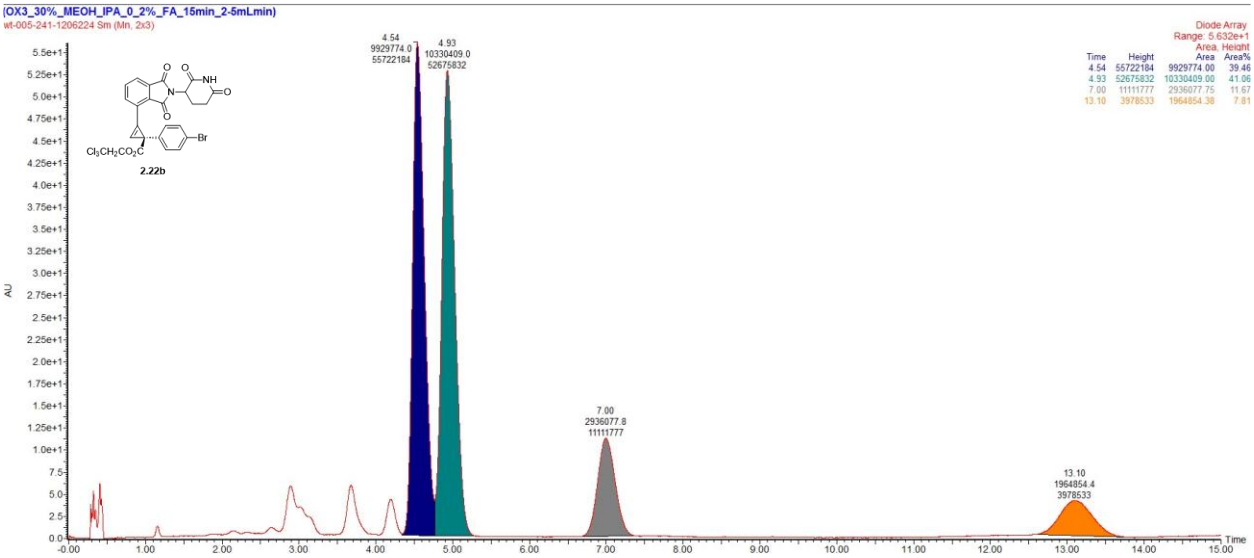
(OX3_30%_MEOH_IPA_0_2%_FA_15min_2-5mLmin)
wt-005-241-1206224 Sm (Mn, 2x3)
Diode Array
Range: 5.632e+1
Time Height Area Area%
4.54 55722184 9929774.00 39.46
4.93 52675832 10330409.00 41.06
7.00 11111777 2936077.75 11.67
13.10 3978533 1964854.38 7.81
4.54
9929774.0
55722184
4.93
10330409.0
52675832
7.00
2936077.8
11111777
13.10
1964854.4
3978533
AU
Time
2.22b

Racemic Chromatogram, 2.23

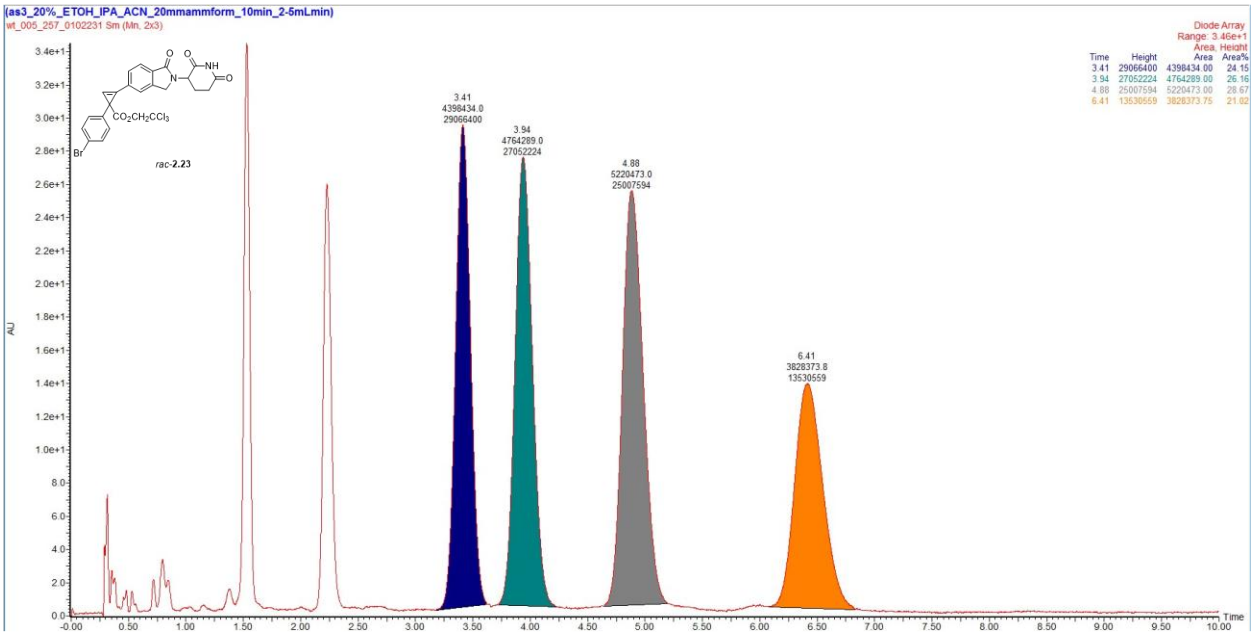

2.23a

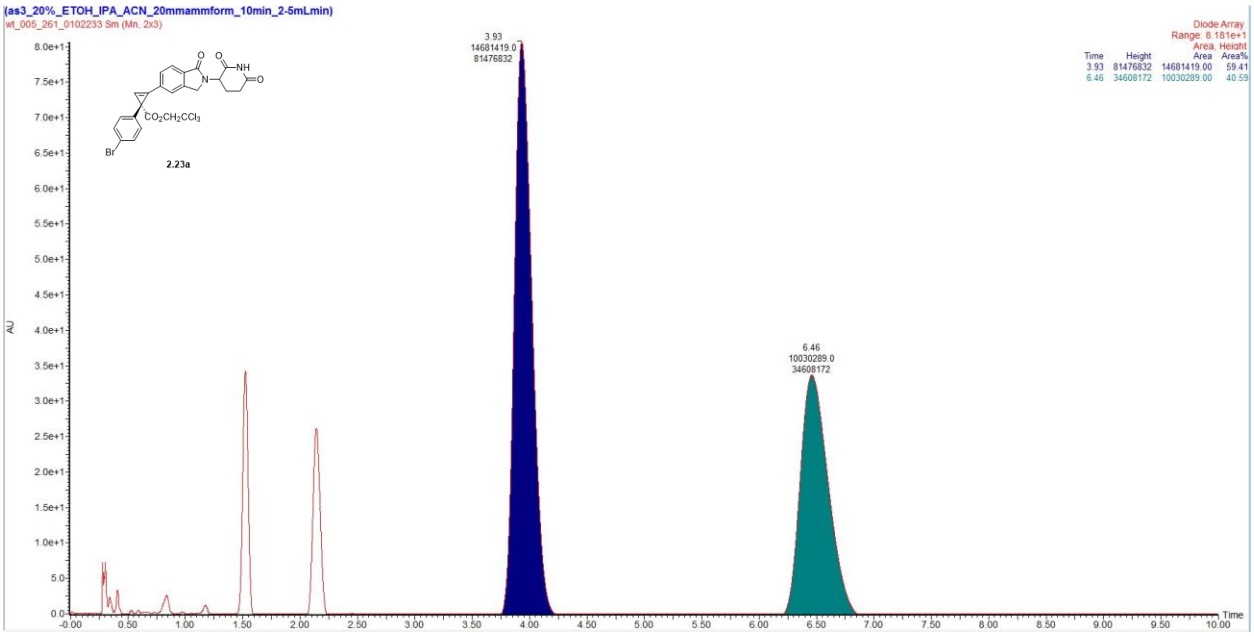

2.23b

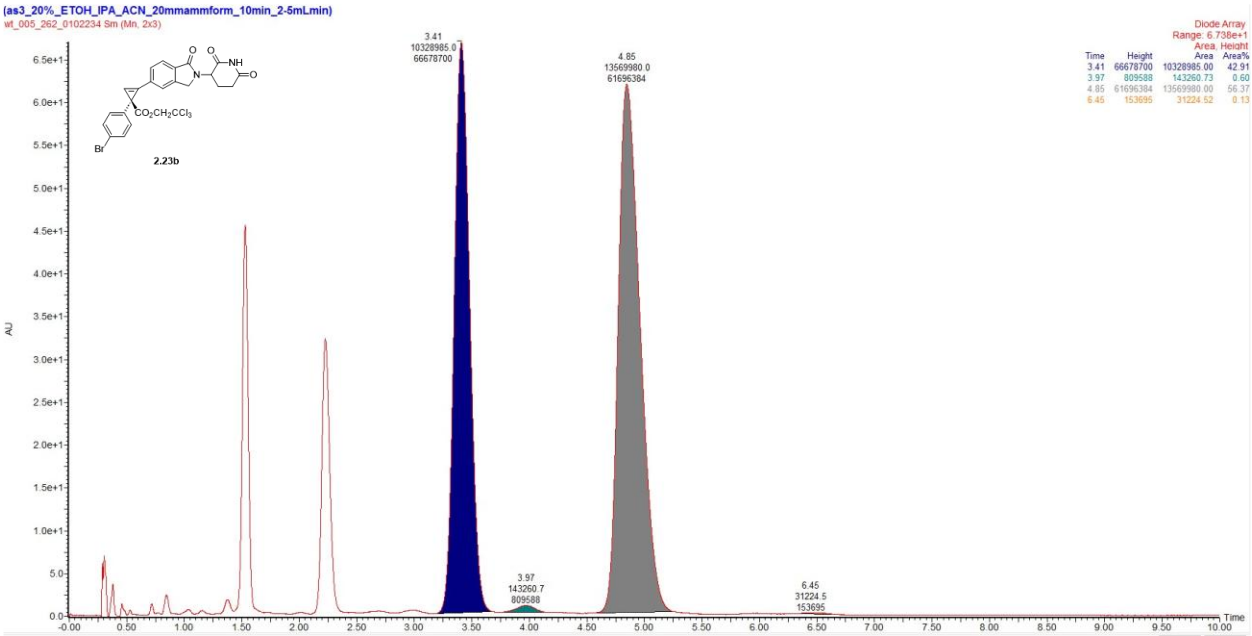

Racemic Chromatogram, 2.24

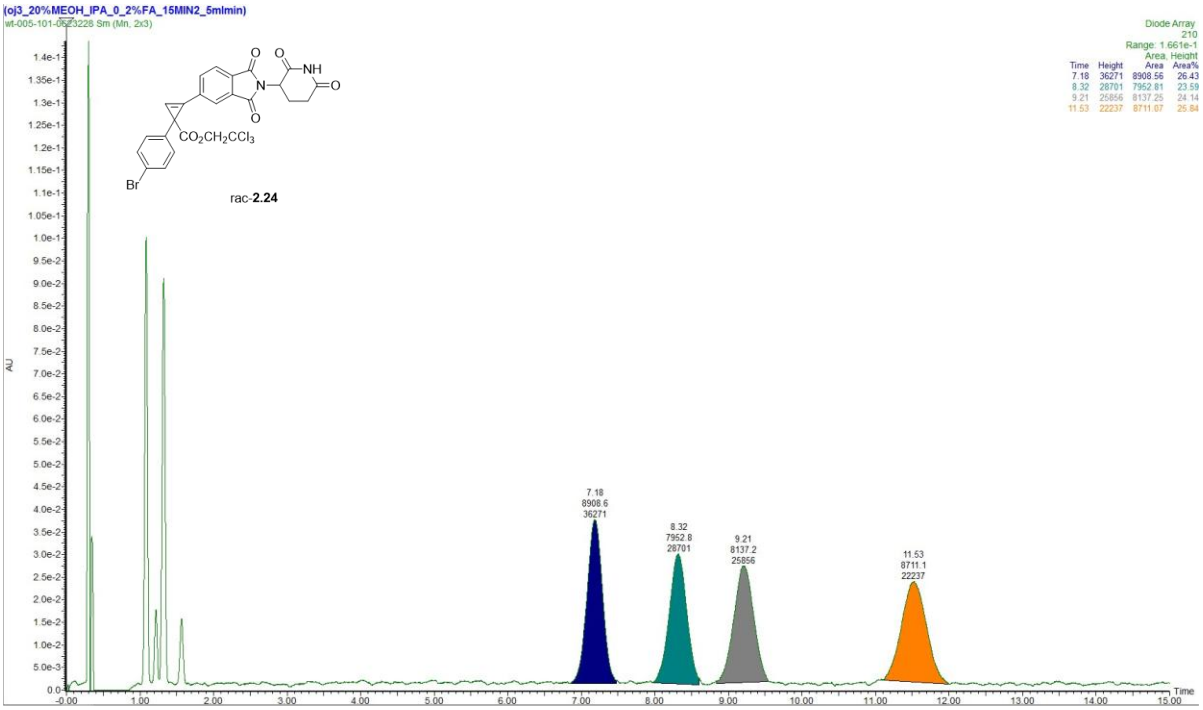

2.24a

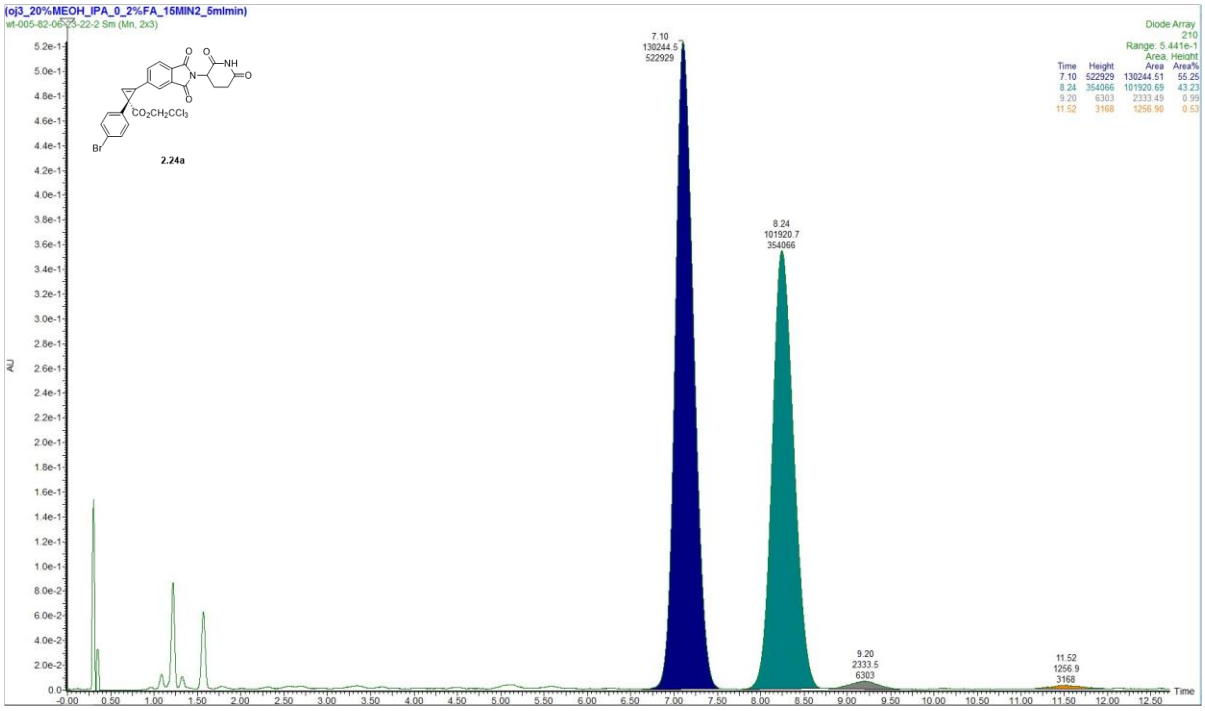
(oj3_20%MEOH_IPA_0_2%FA_15MIN2_5mlmin)
wt-005-82-06-23-22-2 Sm (Mn, 2x3)
Diode Array
210
Range: 5.441e-1
Area, Height
Time Height Area Area%
7.10 522929 130244.51 55.25
8.24 354066 101920.69 43.23
9.20 6303 2333.49 0.99
11.52 3168 1256.90 0.53
7.10
130244.5
522929
8.24
101920.7
354066
9.20
2333.5
6303
11.52
1256.9
3168
2.24a
AU
Time

2.24b

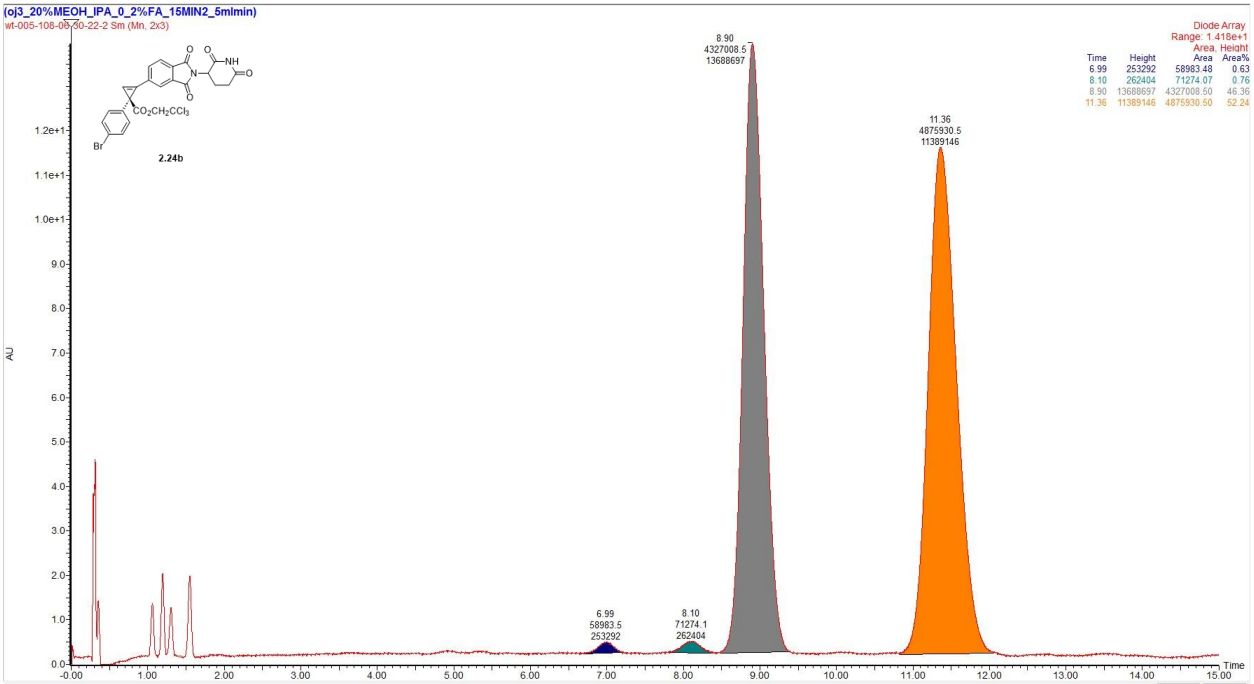
(oj3_20%MEOH_IPA_0_2%FA_15MIN2_5mlmin)
wt-005-108-08-30-22-2 Sm (Mn, 2x3)
Diode Array
Range: 1.418e+1
Area, Height
Time Height Area Area%
6.99 253292 58983.48 0.63
8.10 262404 71274.07 0.76
8.90 13688697 4327008.50 46.36
11.36 11389146 4875930.50 52.24
8.90
4327008.5
13688697
11.36
4875930.5
11389146
6.99
58983.5
253292
8.10
71274.1
262404
2.24b
AU
Time

Racemic Chromatogram, 2.25

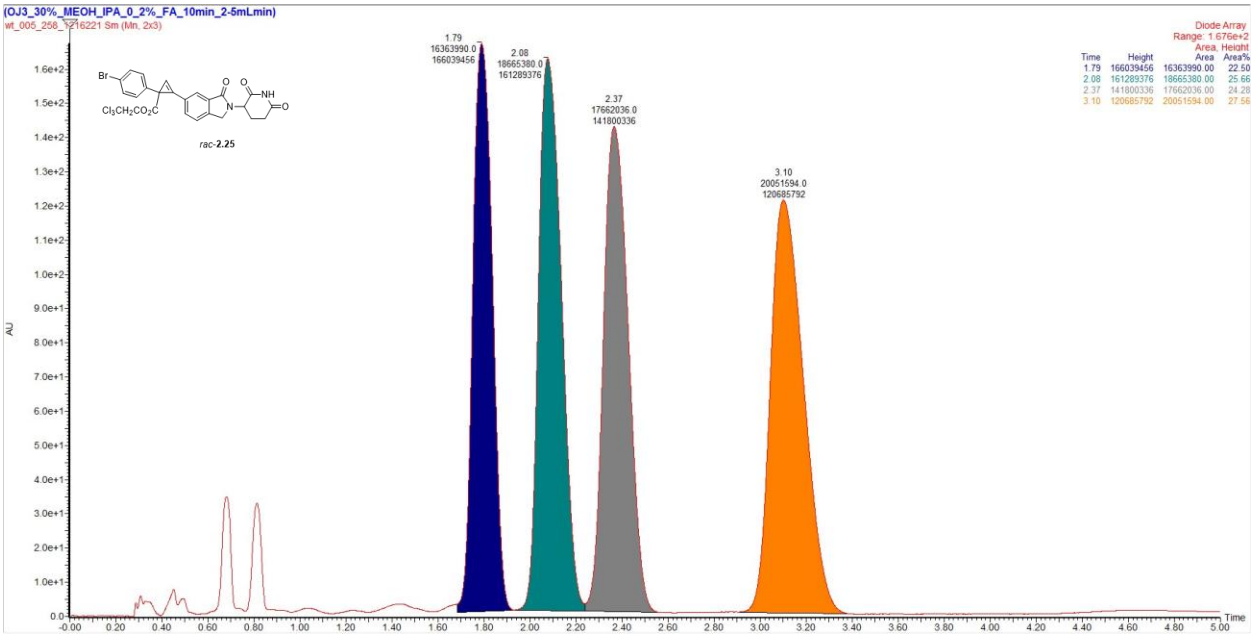

2.25a

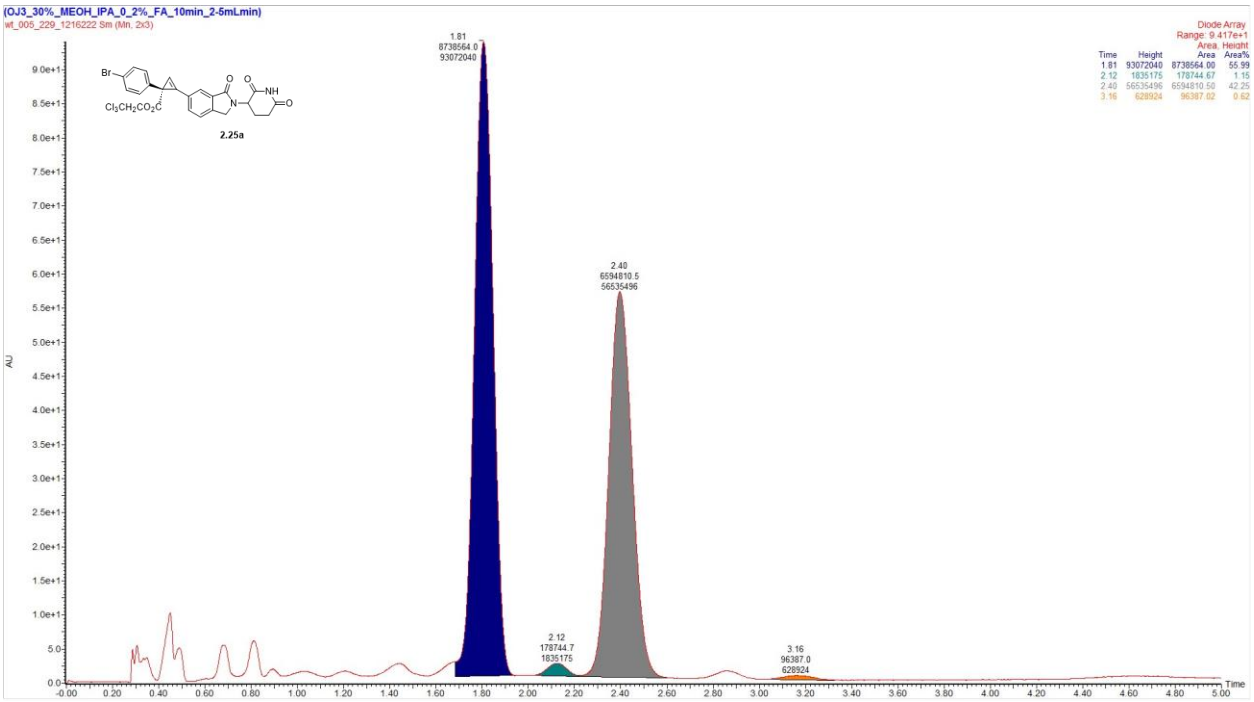

2.25b

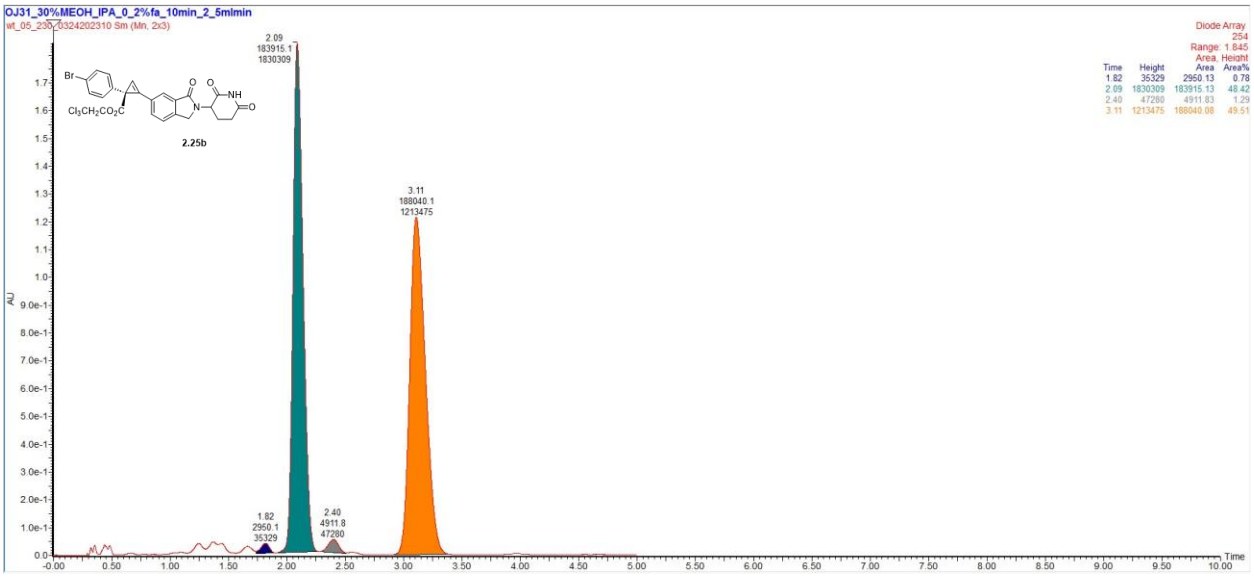

Racemic Chromatogram, 2.26

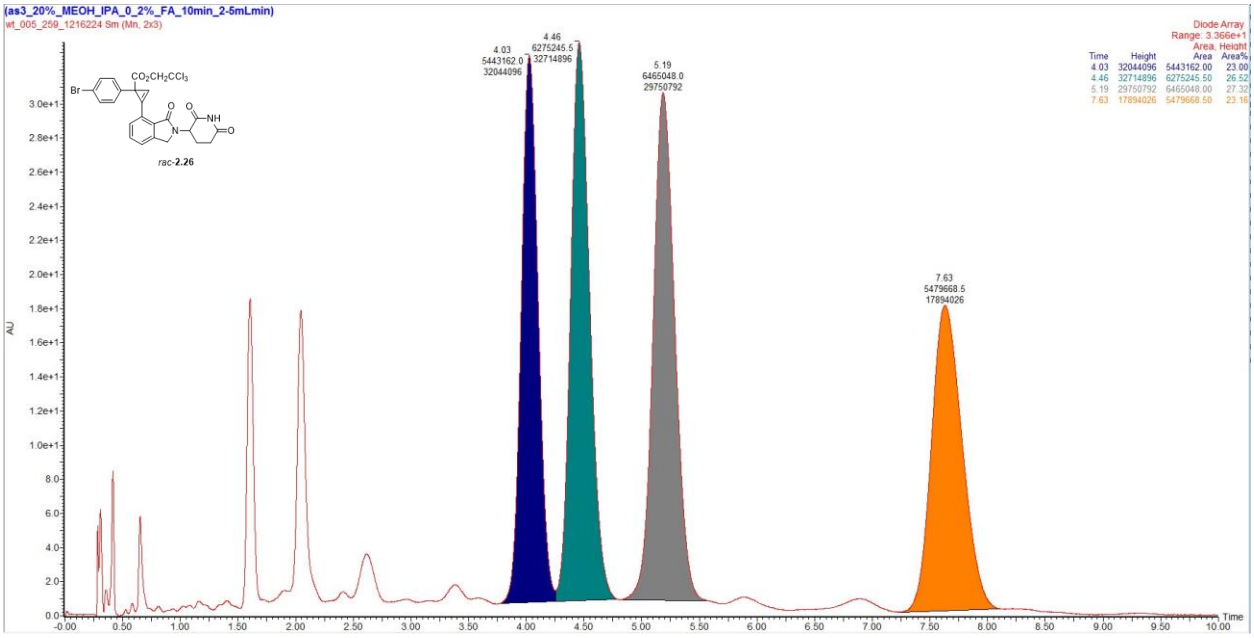

2.26a

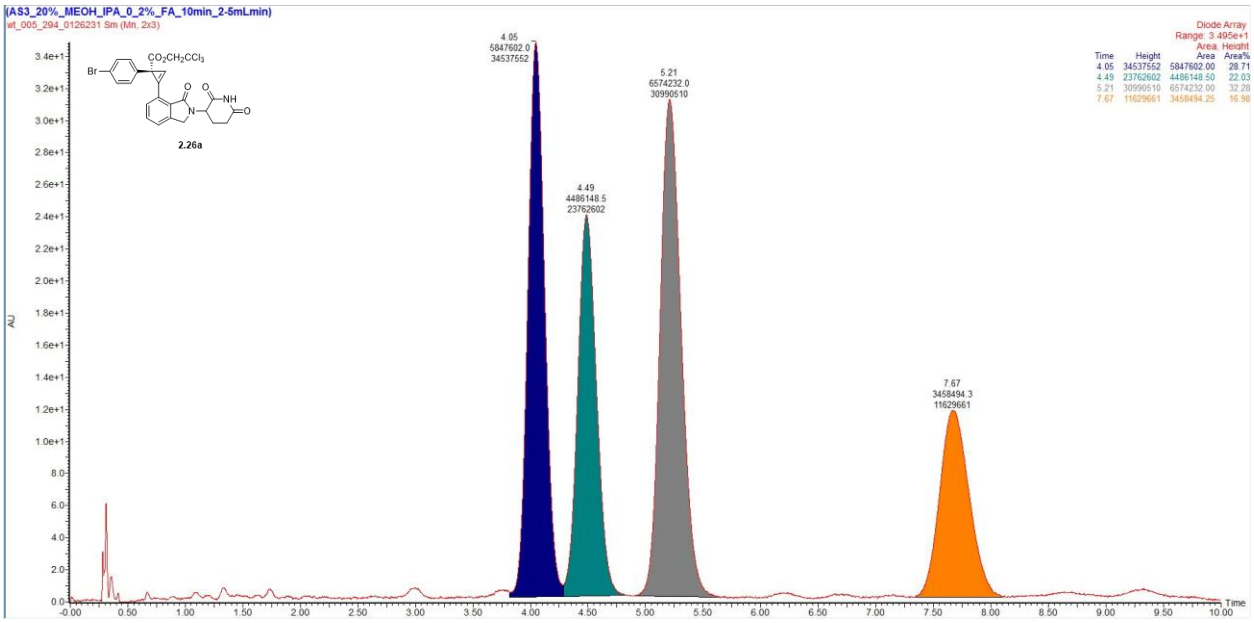
(AS3_20%_MEOH_IPA_0_2%_FA_10min_2-5mLmin)
wt_005_294_0126231 Sm (Mn, 2x3)
Diode Array
Range: 3.495e+1
Time Height Area Area%
4.05 34537552 5847602.00 28.71
4.49 23762602 4486148.50 22.03
5.21 30990510 6574232.00 32.28
7.67 11629661 3458494.25 16.98
4.05
5847602.0
34537552
4.49
4486148.5
23762602
5.21
6574232.0
30990510
7.67
3458494.3
11629661
2.26a
AU
Time

2.26b

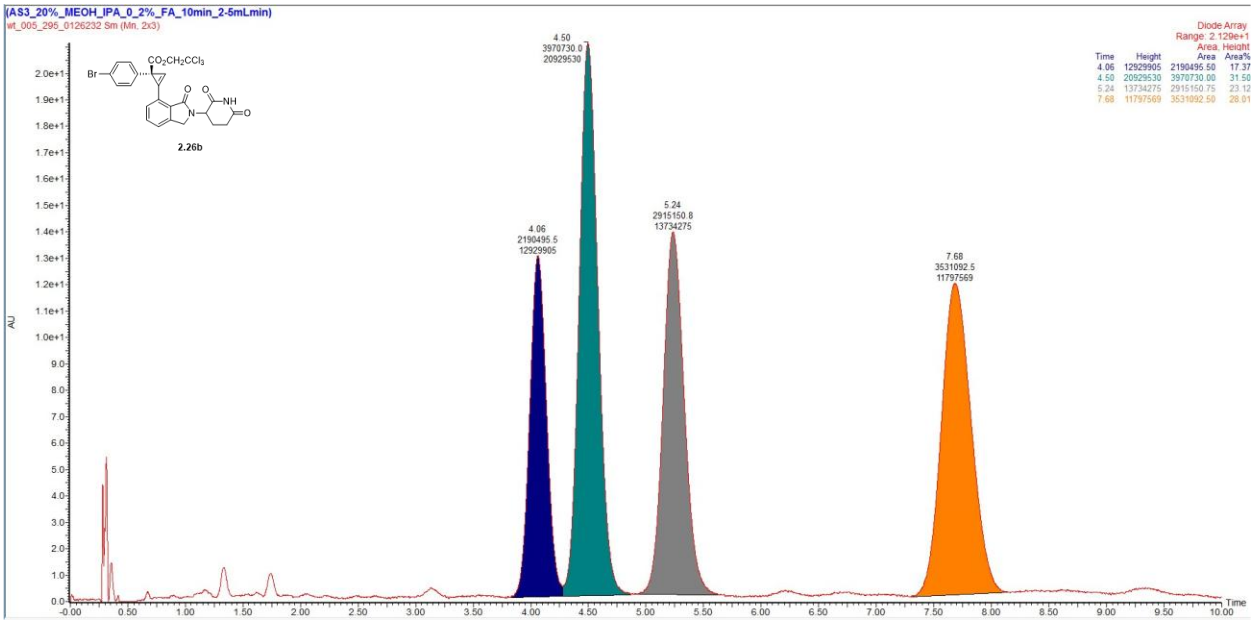
(AS3_20%_MEOH_IPA_0_2%_FA_10min_2-5mLmin)
wt_005_295_0126232 Sm (Mn, 2x3)
Diode Array
Range: 2.129e+1
Time Height Area Area%
4.06 12929905 2190495.50 17.37
4.50 20929530 3970730.00 31.50
5.24 13734275 2915150.75 23.12
7.68 11797569 3531092.50 28.01
4.06
2190495.5
12929905
4.50
3970730.0
20929530
5.24
2915150.8
13734275
7.68
3531092.5
11797569
2.26b
AU
Time

Racemic Chromatogram, 2.27

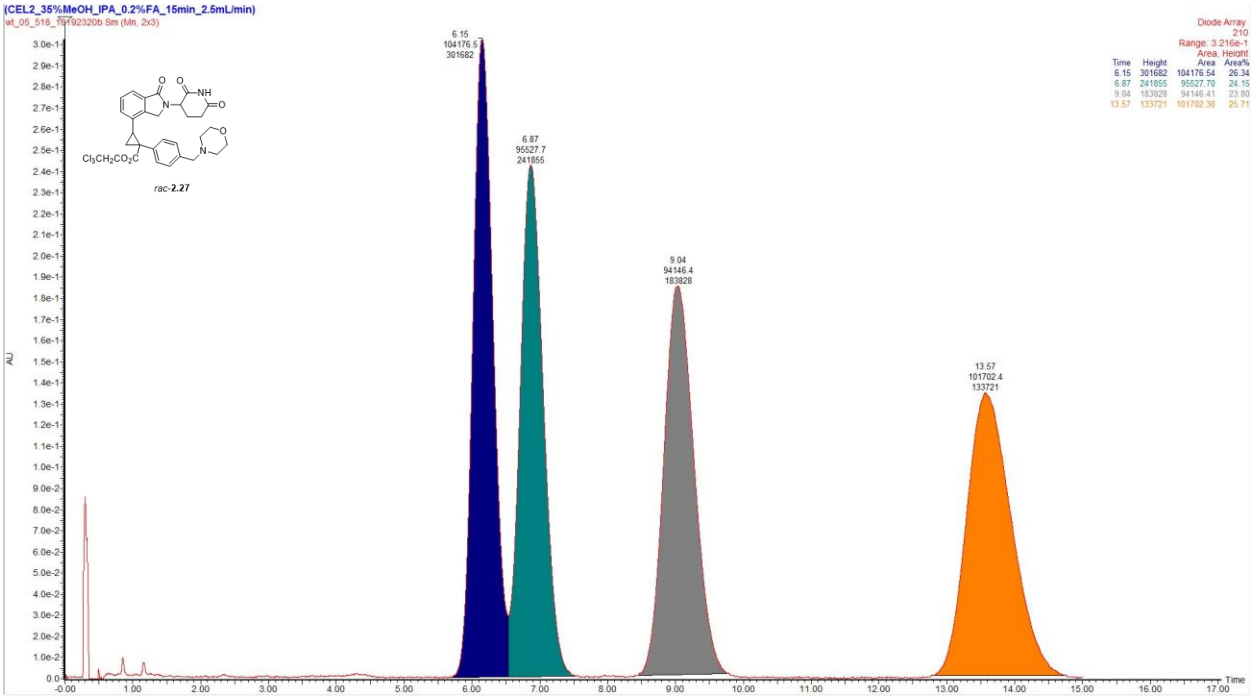

2.27a

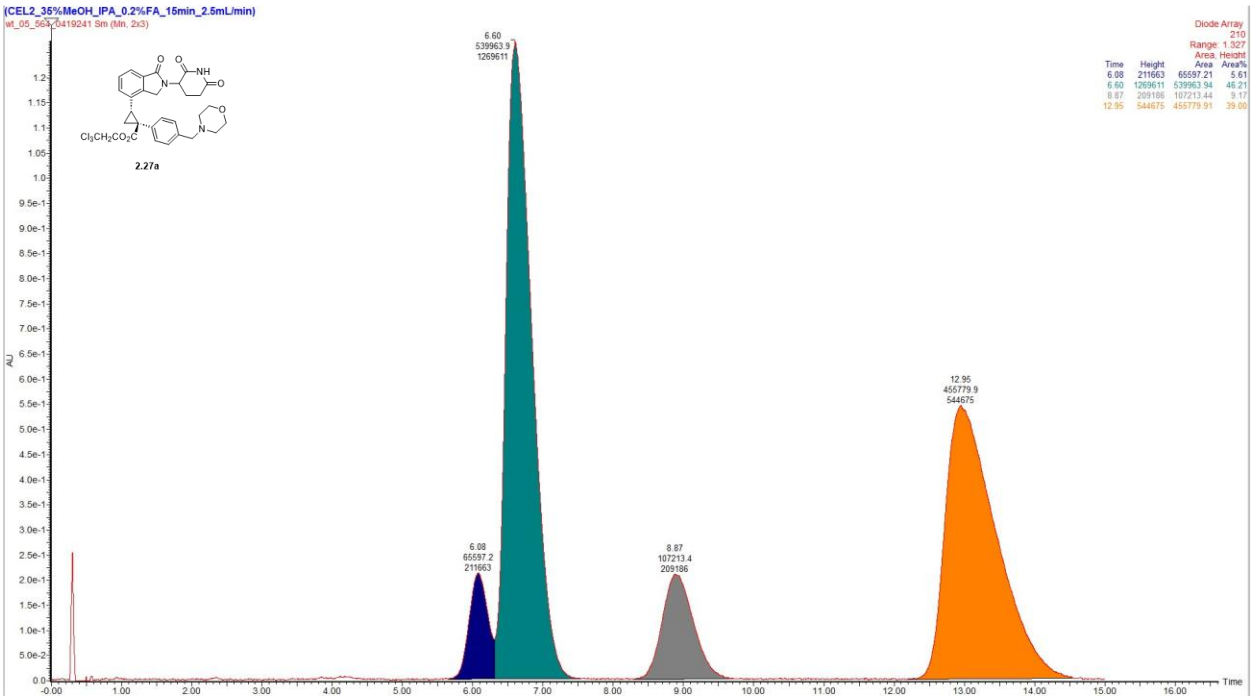

2.27b

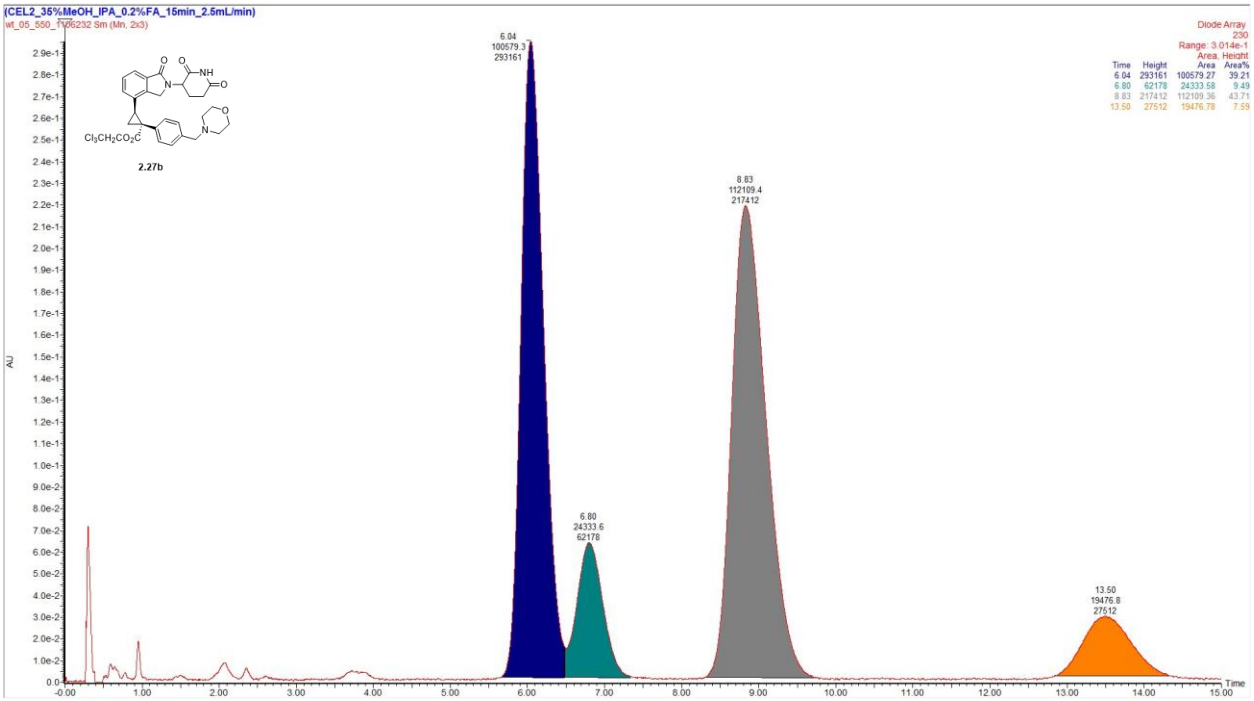

Racemic Chromatogram, 2.28

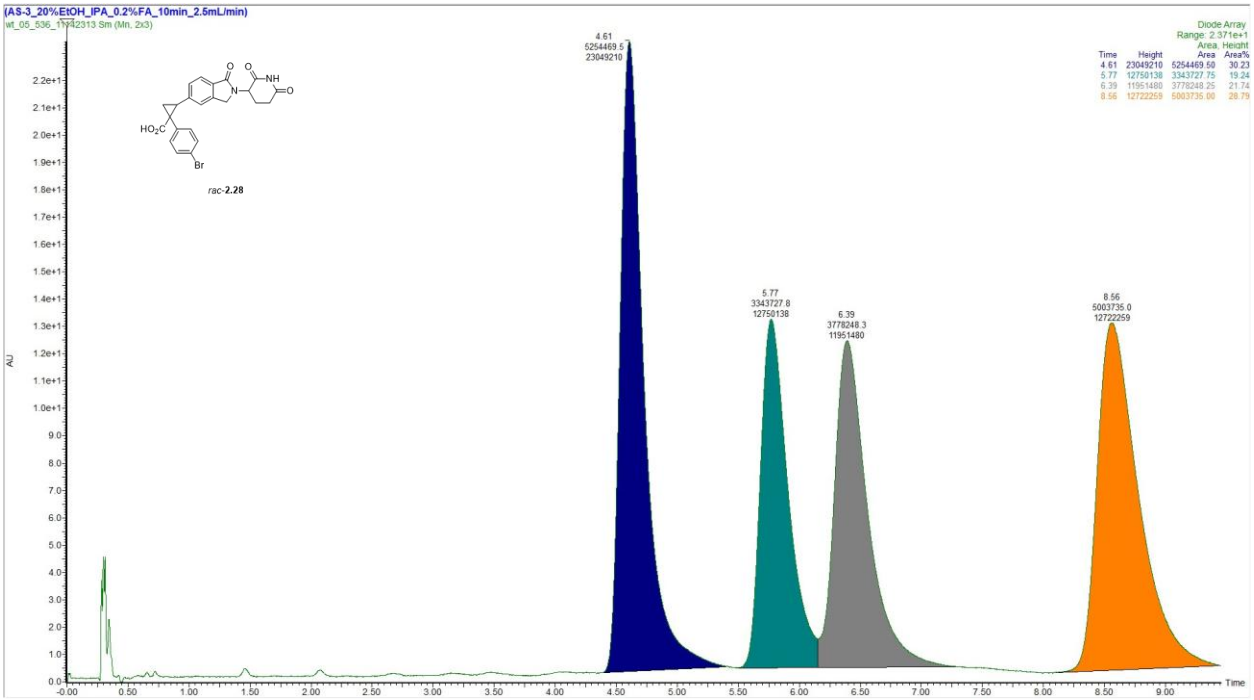

2.28a

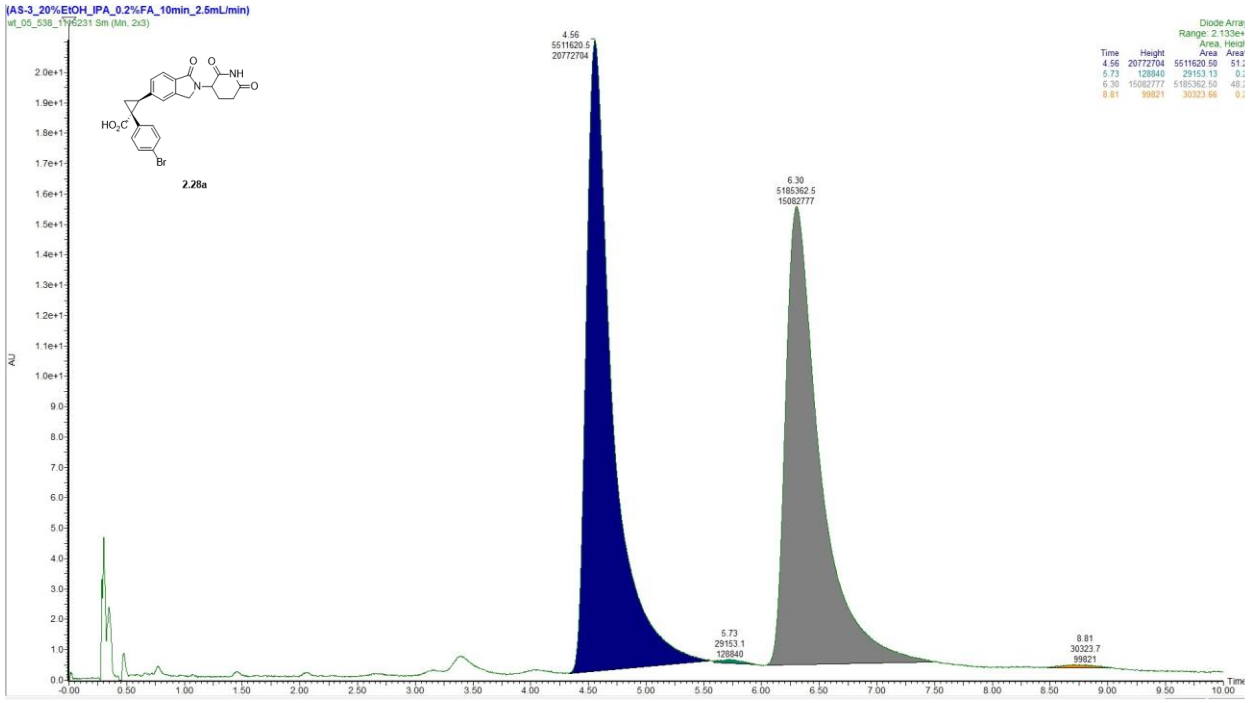
(AS-3_20%EtOH_IPA_0.2%FA_10min_2.5mL/min)
2.28a
4.56
5511620.5
20772704
5.73
29153.1
128840
6.30
5185362.5
15082777
8.81
30323.7
99821
AU
Time

2.28b

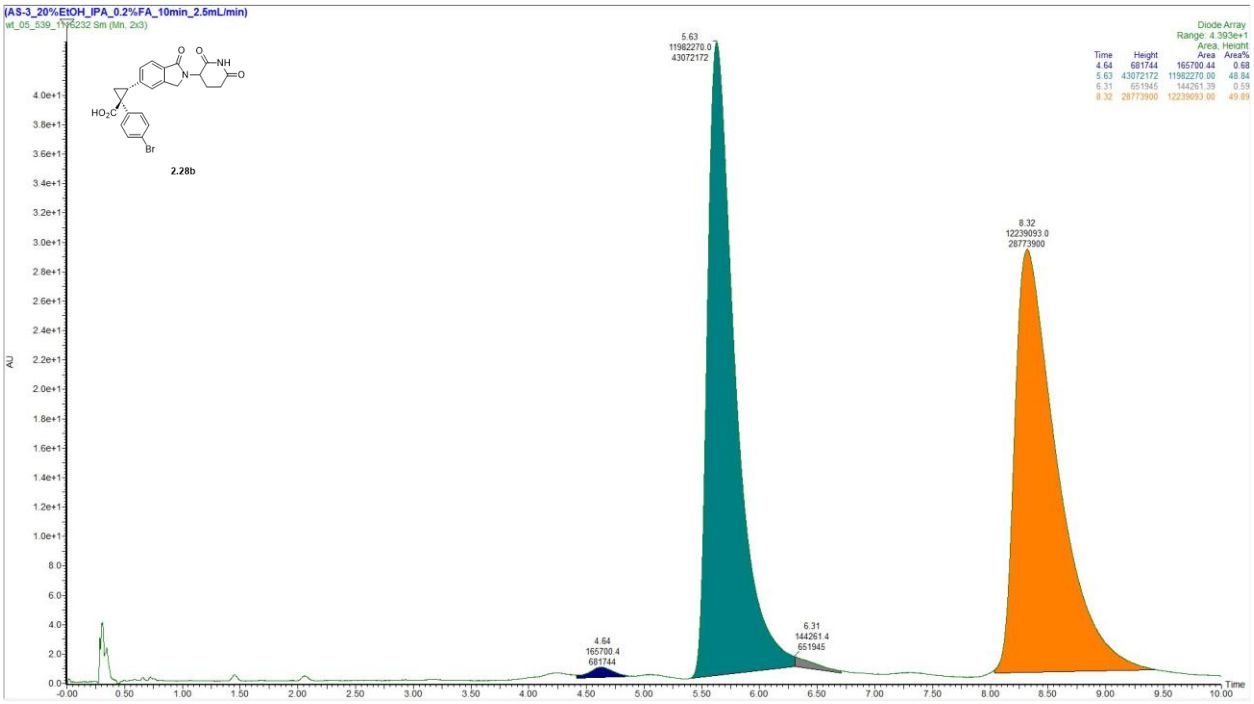
(AS-3_20%EtOH_IPA_0.2%FA_10min_2.5mL/min)
2.28b
4.64
165700.4
681744
5.63
11982270.0
43072172
6.31
144261.4
651945
8.32
12239093.0
28773900
AU
Time

Racemic Chromatogram, 2.29

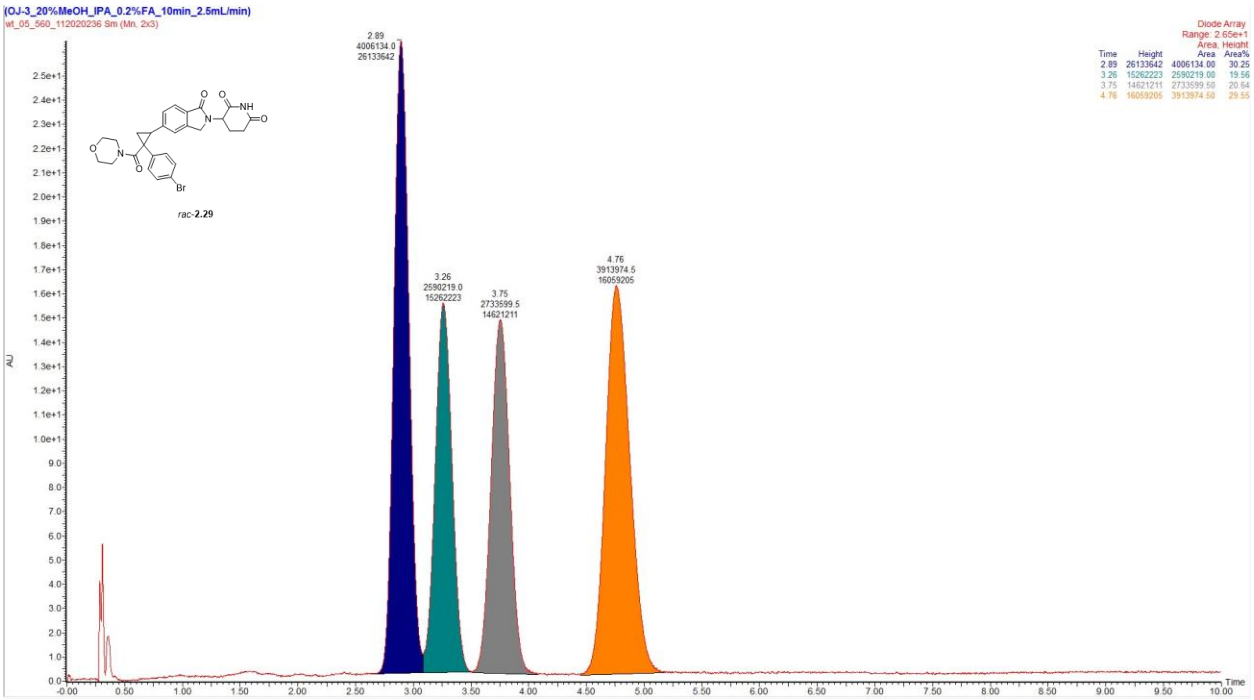

2.29a

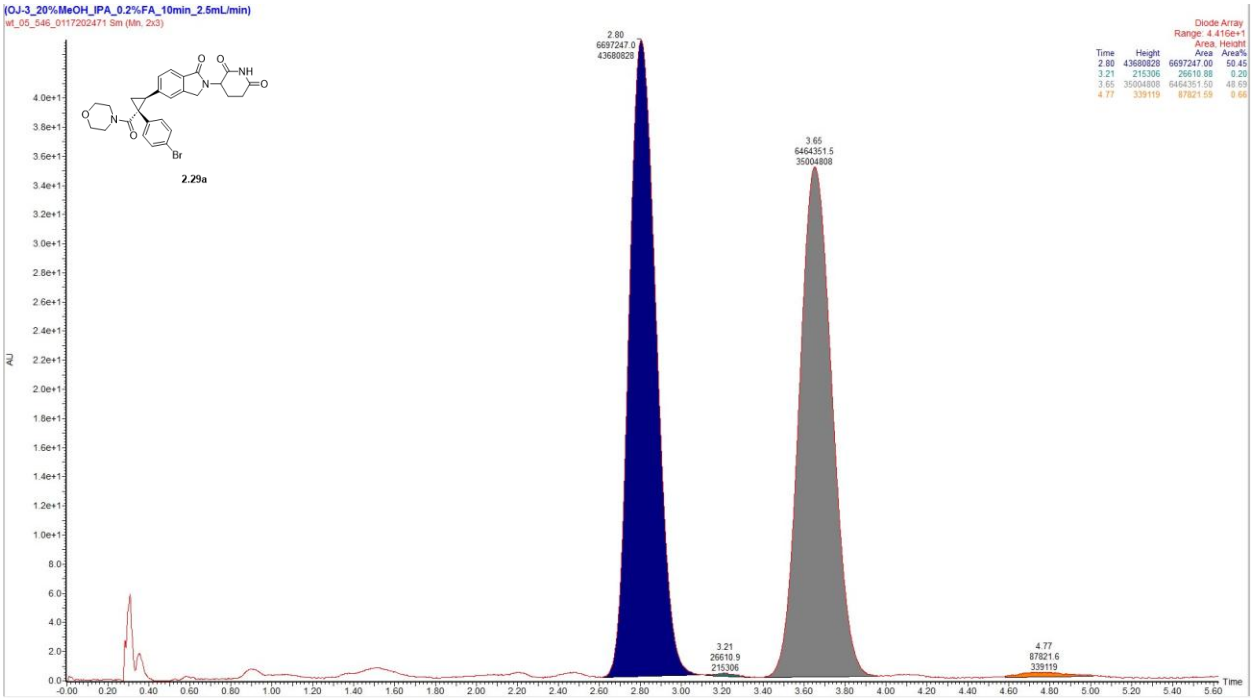

2.29b

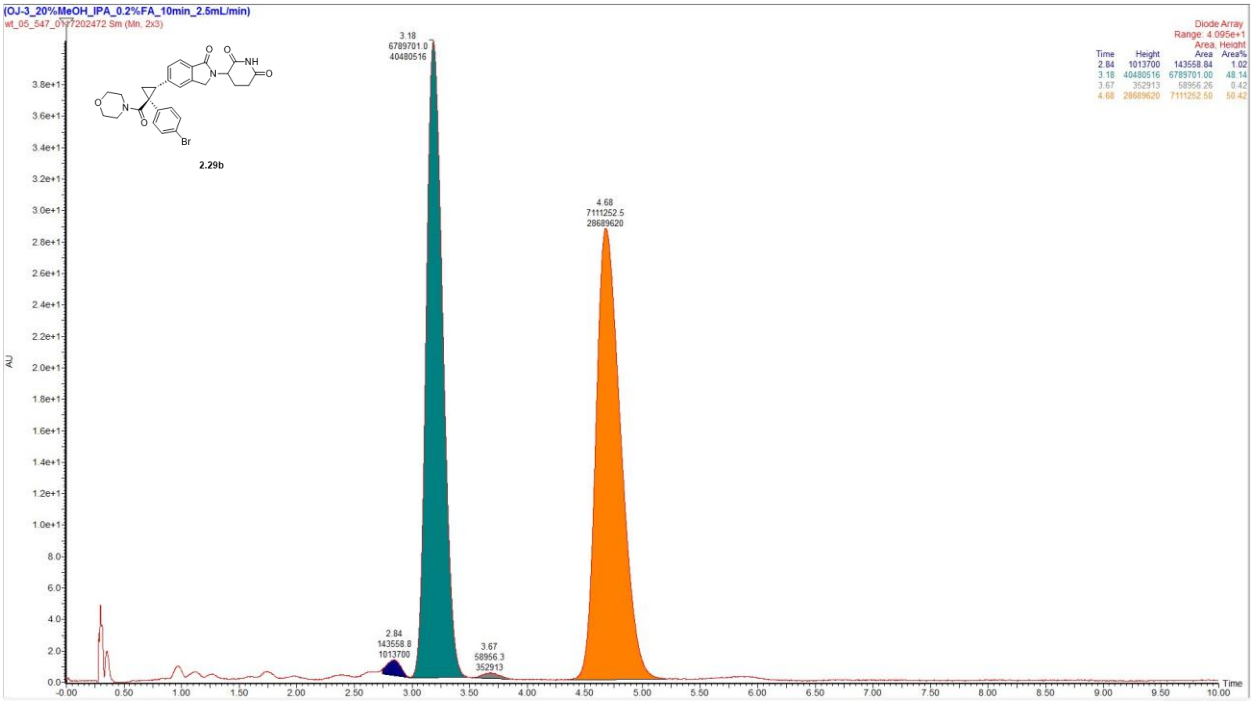

Purity Chromatograms

2.15a

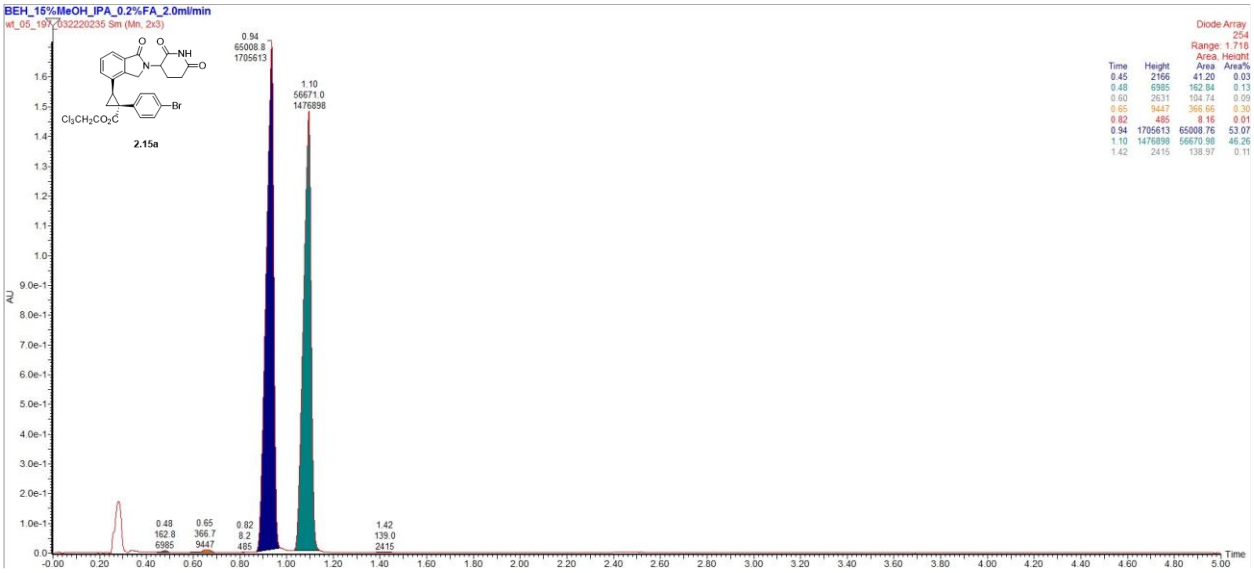

2.15b

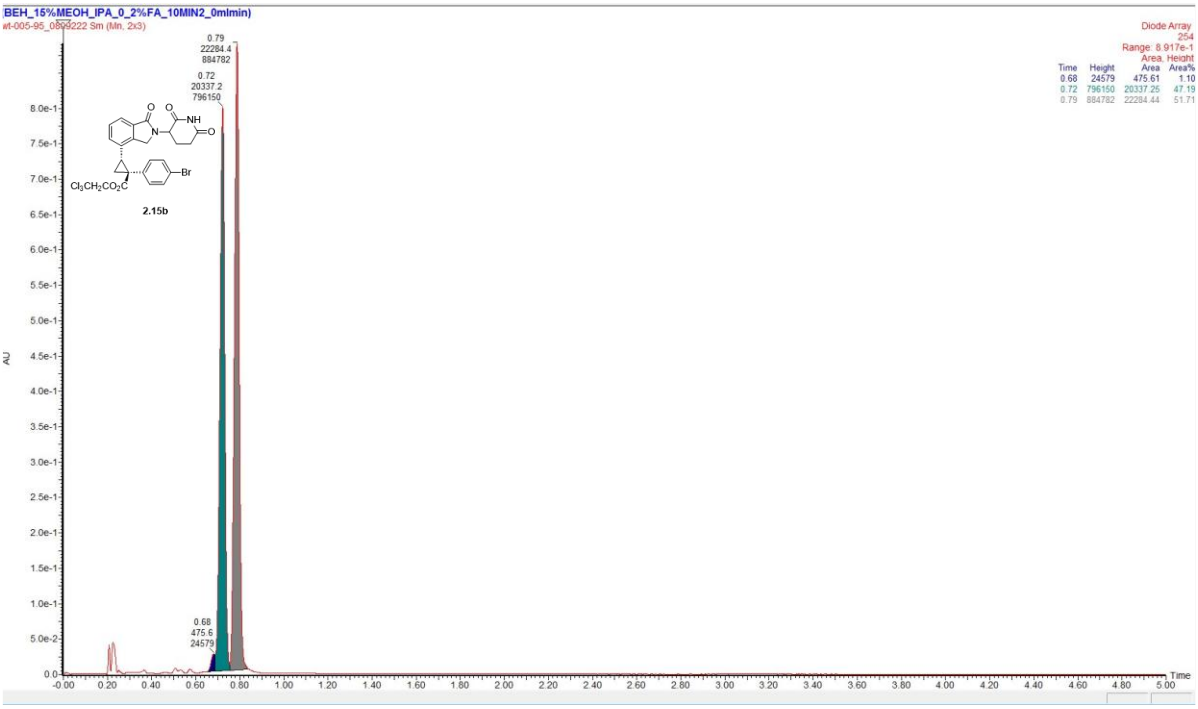
BEH_15%MEOH_IPA_0_2%FA_10MIN2_0mlmin)
wt-005-95_0806222 Sm (Mn, 2x3)
Diode Array
254
Range: 8.917e-1
Area, Height
Time Height Area Area%
0.68 24579 475.61 1.10
0.72 796150 20337.25 47.19
0.79 884782 22284.44 51.71
0.79
22284.4
884782
0.72
20337.2
796150
0.68
475.6
24579
2.15b
AU
Time

2.16a

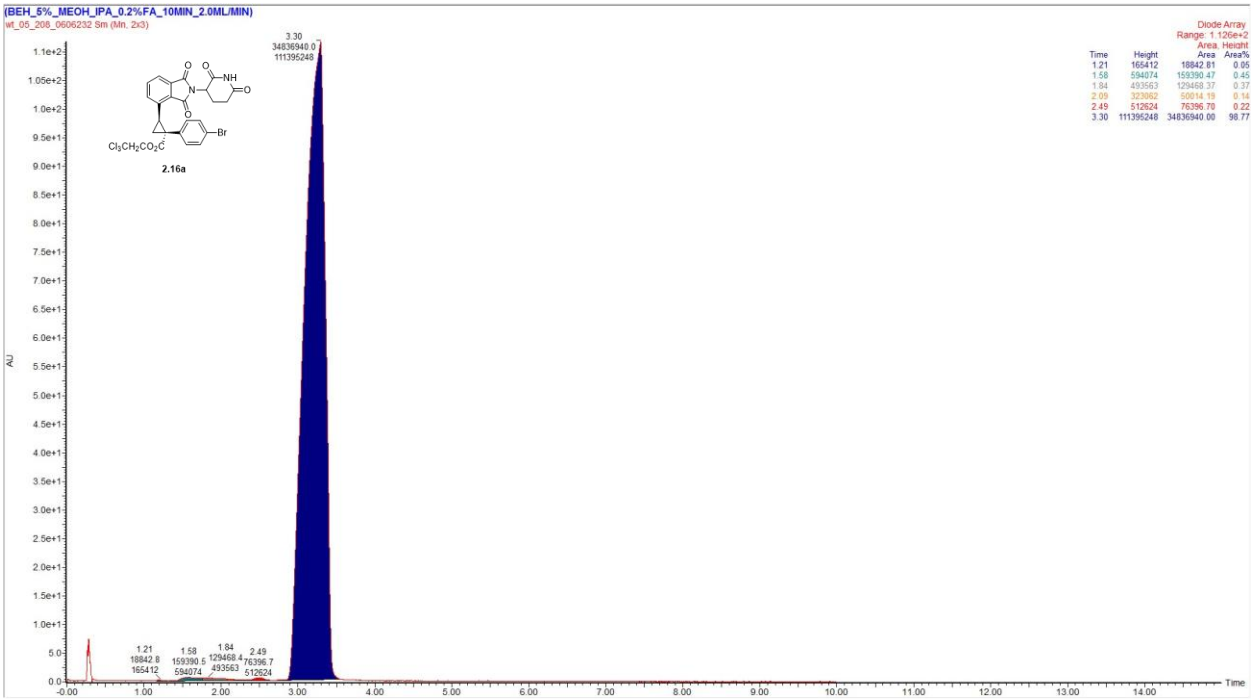
(BEH_5%_MEOH_IPA_0.2%FA_10MIN_2.0ML/MIN)
wt_05_206_0606232 Sm (Mn, 2x3)
Diode Array
Range: 1.126e+2
Area, Height
Time Height Area Area%
1.21 165412 18842.81 0.05
1.58 594074 159390.47 0.45
1.84 493563 129468.37 0.37
2.09 323062 50014.19 0.14
2.49 512624 76396.70 0.22
3.30 111395248 34836940.00 98.77
3.30
34836940.0
111395248
1.21
18842.8
165412
1.58
159390.5
594074
1.84
129468.4
493563
2.49
76396.7
512624
2.16a
AU
Time

2.16b

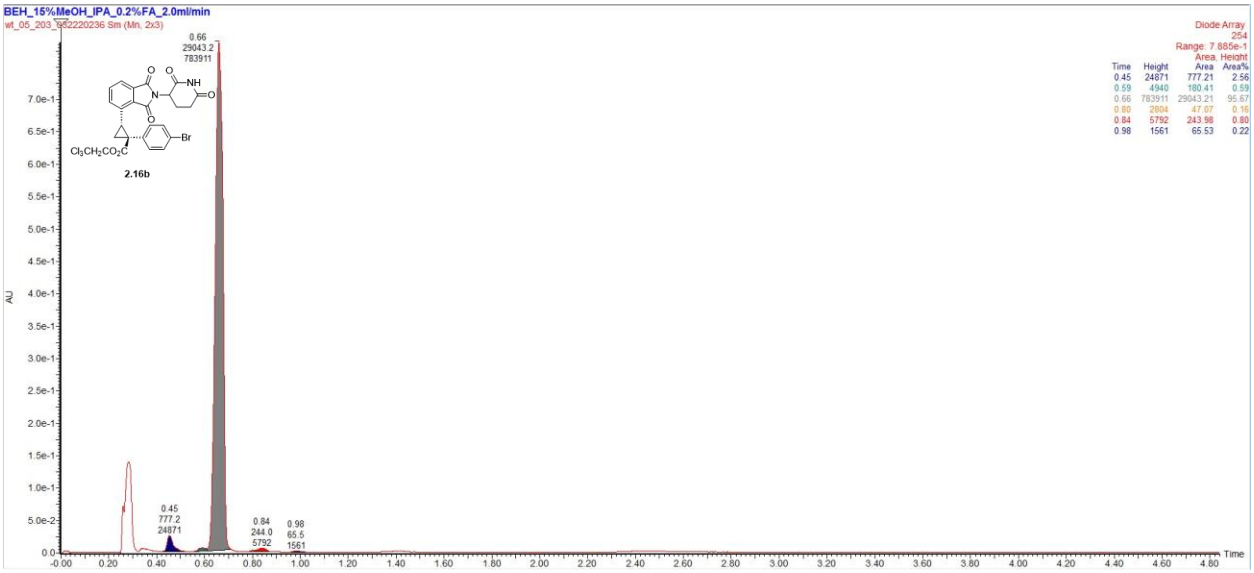
BEH_15%MeOH_IPA_0.2%FA_2.0ml/min
Diode Array
254
Range: 7.885e-1
Area, Height
Time Height Area Area%
0.45 24871 777.21 2.56
0.59 4940 180.41 0.59
0.66 783911 29043.21 95.67
0.80 2804 47.07 0.16
0.84 5792 243.98 0.80
0.98 1561 65.53 0.22
2.16b
AU
Time

2.17a

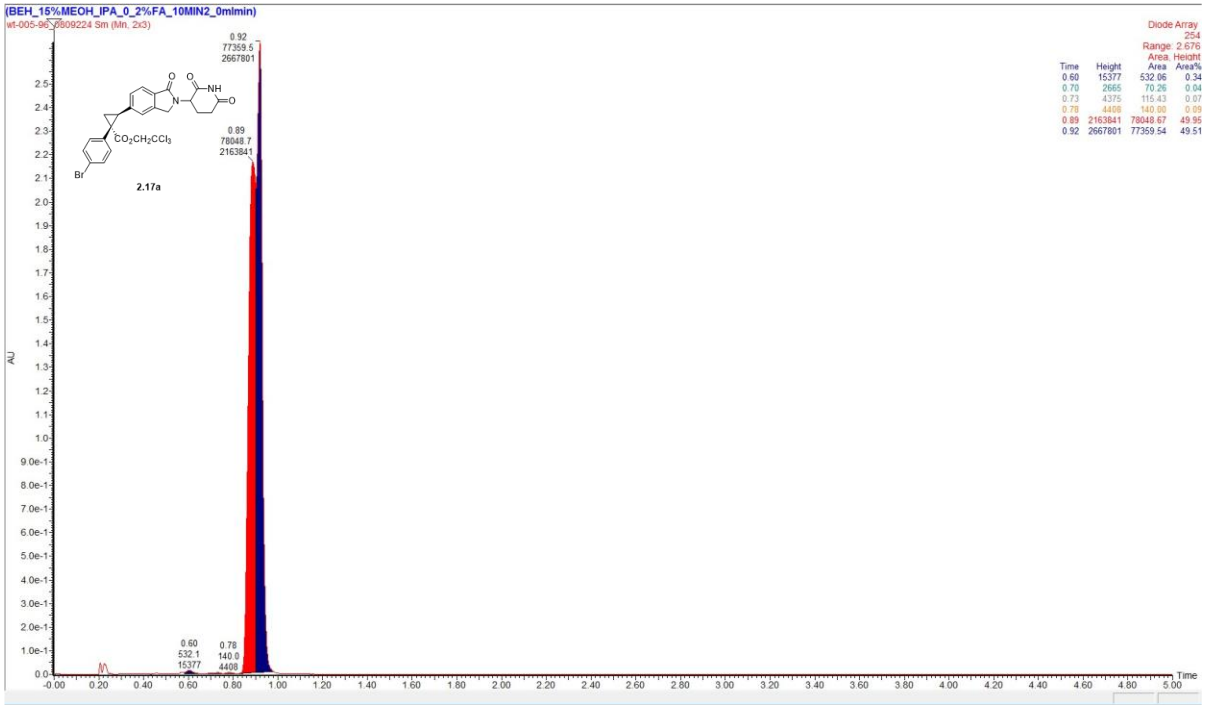
(BEH_15%MEOH_IPA_0_2%FA_10MIN2_0mlmin)
Diode Array
254
Range: 2.676
Area, Height
Time Height Area Area%
0.60 15377 532.06 0.34
0.70 2665 70.26 0.04
0.73 4375 116.43 0.07
0.78 4408 140.00 0.09
0.89 2163841 78048.67 49.95
0.92 2667801 77359.54 49.51
2.17a
AU
Time

2.17b

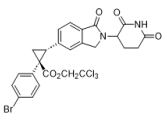

2.17b

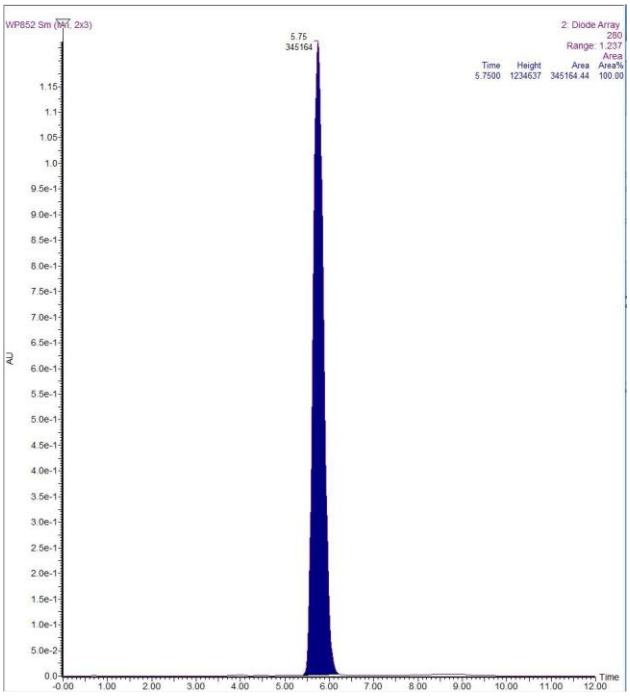

S-2.17a

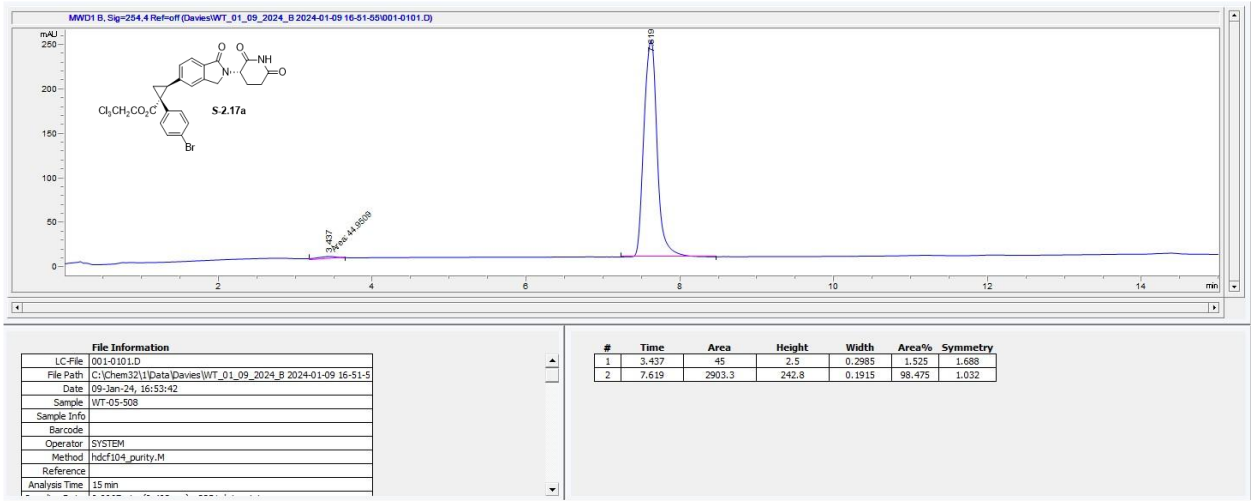

S-2.17b

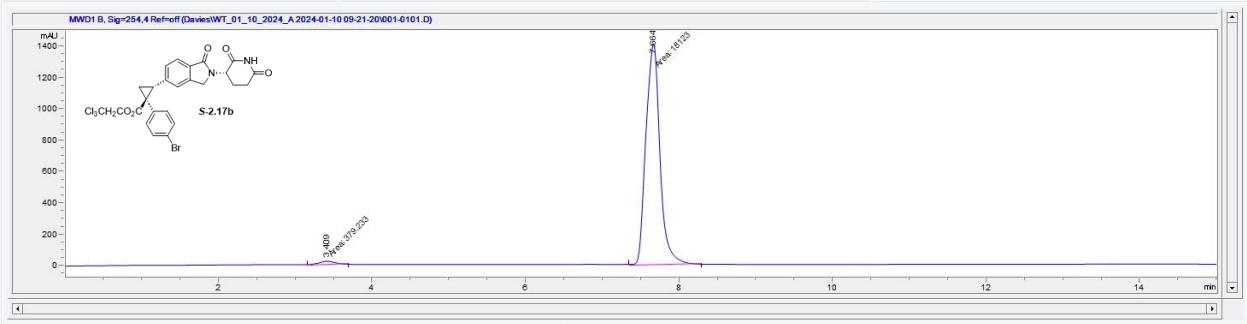

File Information

LC-File	001-0101.D
File Path	C:\Chem32\1\Data\Davies\WT_01_10_2024_A 2024-01-10 09-21-2
Date	10-Jan-24, 09:23:06
Sample	WT-05-509
Sample Info	
Barcode	
Operator	SYSTEM
Method	hdcf104_purity.M
Reference	
Analysis Time	15 min

#	Time	Area	Height	Width	Area%	Symmetry
1	3.409	379.2	23.8	0.265	2.050	0.986
2	7.664	18123	1418.4	0.213	97.950	1.084

R-2.17a

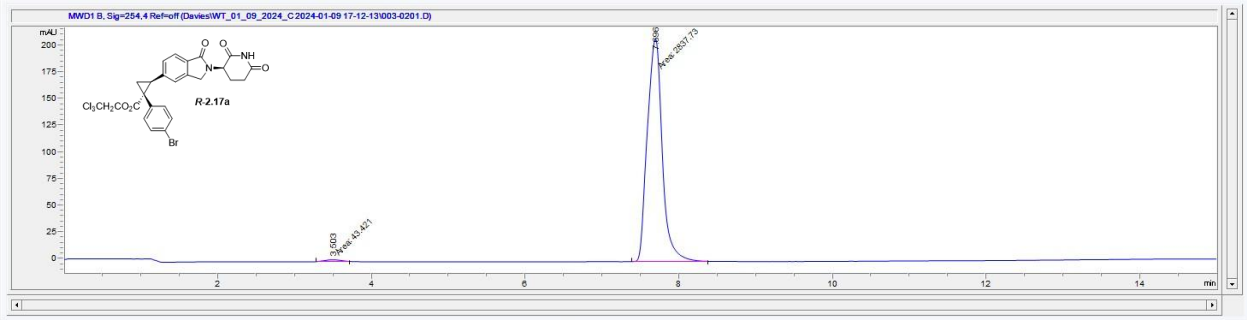

File Information

LC-File	003-0201.D
File Path	C:\Chem32\1\Data\Davies\WT_01_09_2024_C 2024-01-09 17-12-1
Date	09-Jan-24, 17:29:54
Sample	WT-05-553
Sample Info	
Barcode	
Operator	SYSTEM
Method	hdcf104_purity.M
Reference	
Analysis Time	14.993 min

#	Time	Area	Height	Width	Area%	Symmetry
1	3.503	43.4	2.4	0.3032	1.507	1.037
2	7.696	2837.7	209.1	0.2262	98.493	1.106

R-2.17b

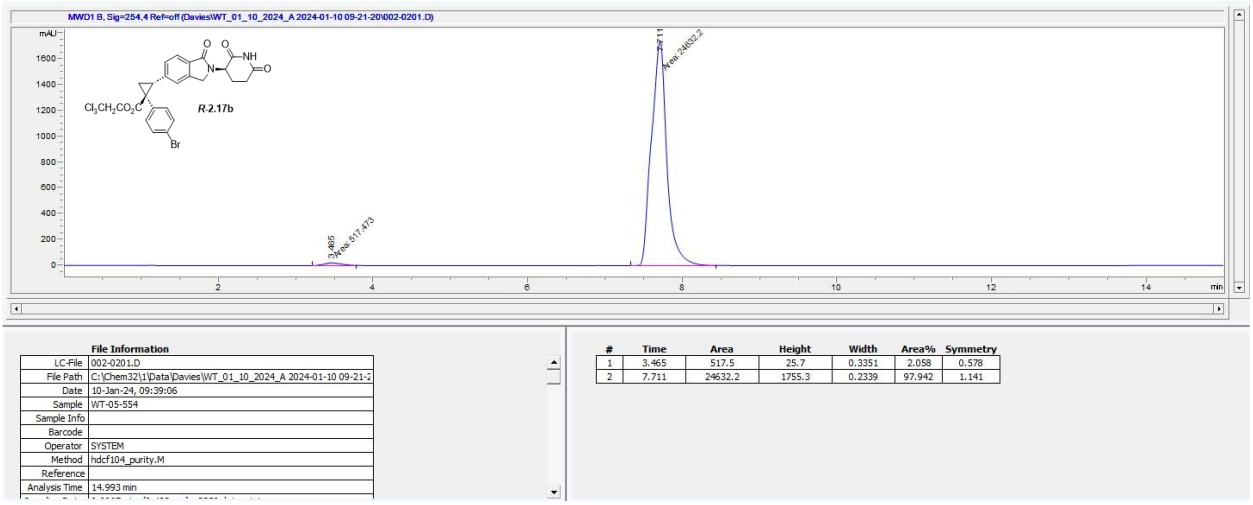
MWD1 B, Sig=254,4 Ref=off (Davies\WT_01_10_2024_A 2024-01-10 09-21-20\002-0201.D)
mAU
R-2.17b
Area: 24632.2
Area: 517.473
min
File Information
LC-File 002-0201.D
File Path C:\Chem32\1\Data\Davies\WT_01_10_2024_A 2024-01-10 09-21-2
Date 10-Jan-24, 09:39:06
Sample WT-05-554
Sample Info
Barcode
Operator SYSTEM
Method hdcf104_purity.M
Reference
Analysis Time 14.993 min
Time Area Height Width Area% Symmetry
1 3.465 517.5 25.7 0.3351 2.058 0.578
2 7.711 24632.2 1755.3 0.2339 97.942 1.141

2.18a

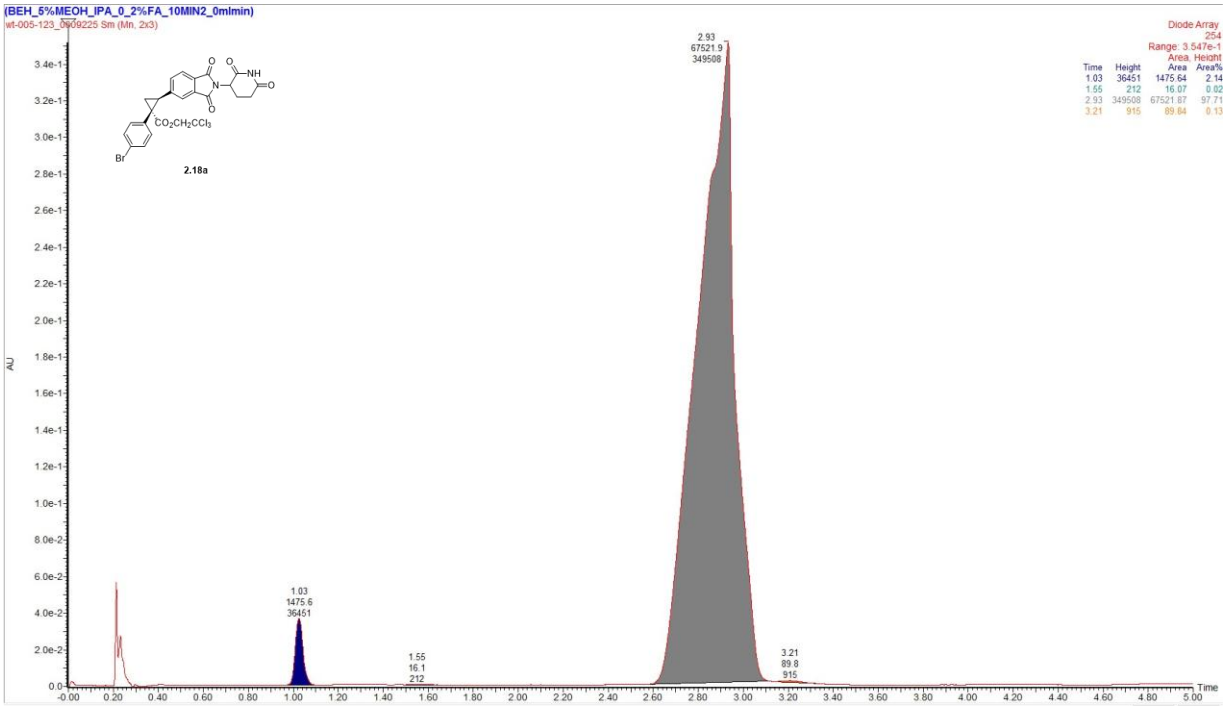
(BEH_5%MEOH_IPA_0_2%FA_10MIN2_0mlmin)
wt-005-123_0909225 Sm (Mn, 2x3)
2.18a
Diode Array
254
Range: 3.547e-1
Time Height Area Area%
1.03 36451 1475.64 2.14
1.55 212 16.07 0.02
2.93 349508 67521.87 97.71
3.21 915 89.84 0.13
2.93
67521.9
349508
1.03
1475.6
36451
1.55
16.1
212
3.21
89.8
915
AU
Time

2.18b

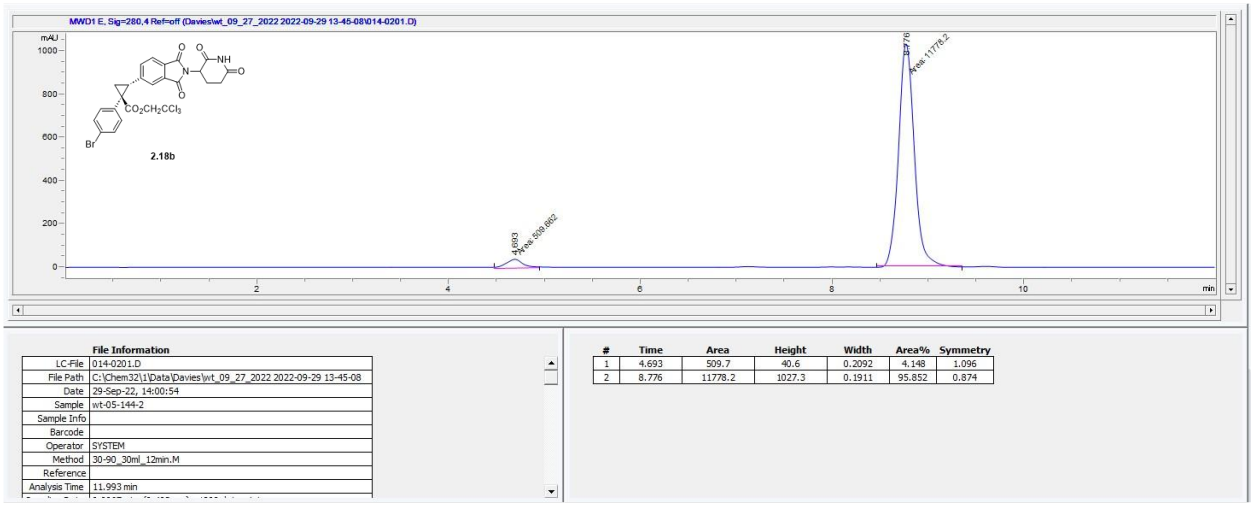
MWD1 E, Sig=280,4 Ref=off (Davies\wt_09_27_2022 2022-09-29 13-45-08\014-0201.D)
mAU
2.18b
4.693
Area: 509.862
8.776
Area: 11778.2
min
File Information
LC-File 014-0201.D
File Path C:\Chem32\1\Data\Davies\wt_09_27_2022 2022-09-29 13-45-08
Date 29-Sep-22, 14:00:54
Sample wt-05-144-2
Sample Info
Barcode
Operator SYSTEM
Method 30-90_30ml_12min.M
Reference
Analysis Time 11.993 min
Time Area Height Width Area% Symmetry
1 4.693 509.7 40.6 0.2092 4.148 1.096
2 8.776 11778.2 1027.3 0.1911 95.852 0.874

2.19a

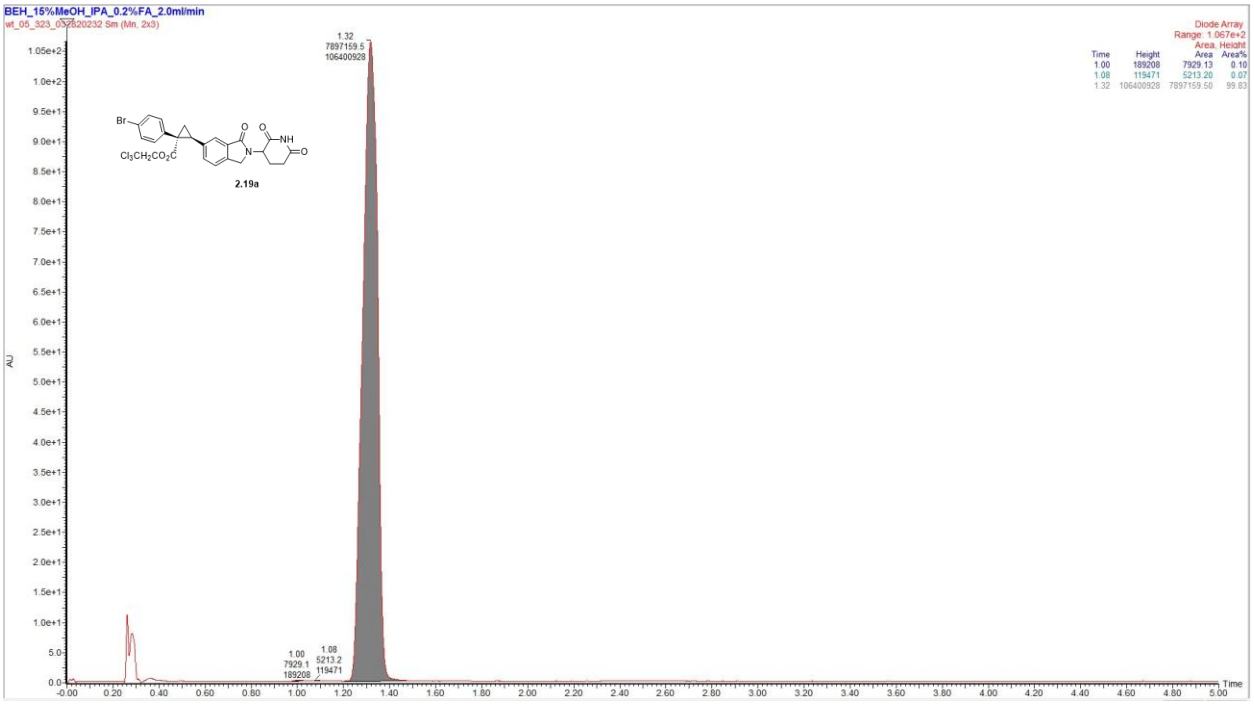
BEH_15%MeOH_IPA_0.2%FA_2.0ml/min
wt_05_323_05220232 Sm (Mn, 2x3)
2.19a
1.32
7897159.5
106400928
1.00
7929.1
189208
1.08
5213.2
119471
Diode Array
Range: 1.067e+2
Time Height Area Area%
1.00 189208 7929.13 0.10
1.08 119471 5213.20 0.07
1.32 106400928 7897159.50 99.83
AU
Time

2.19b

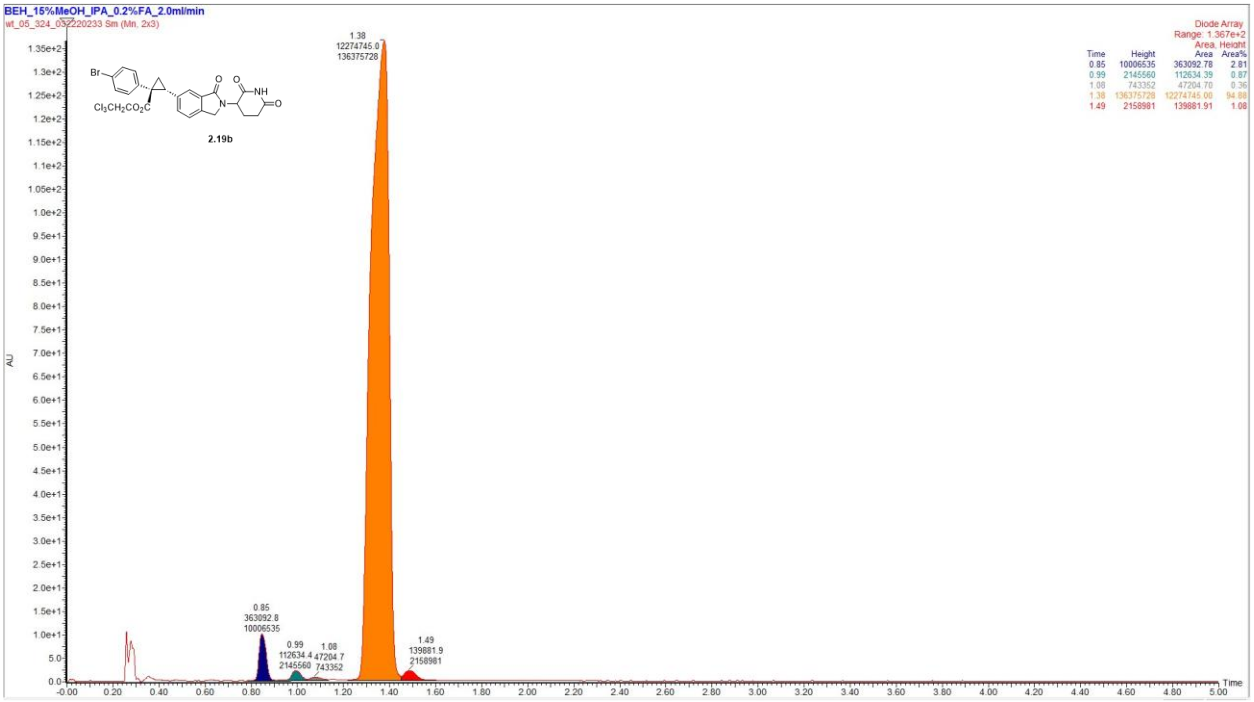
BEH_15%MeOH_IPA_0.2%FA_2.0ml/min
wt_05_324_0522220233 Sm (Mn, 2x3)
Diode Array
Range: 1.367e+2
Time Height Area Area%
0.85 10006535 363092.78 2.81
0.99 2145560 112634.39 0.87
1.08 743352 47204.70 0.36
1.38 136375726 12274745.00 94.88
1.49 2158981 139881.91 1.08
1.38
12274745.0
136375726
0.85
363092.8
10006535
0.99
112634.4
2145560
1.08
47204.7
743352
1.49
139881.9
2158981
AU
Time
2.19b

2.20a

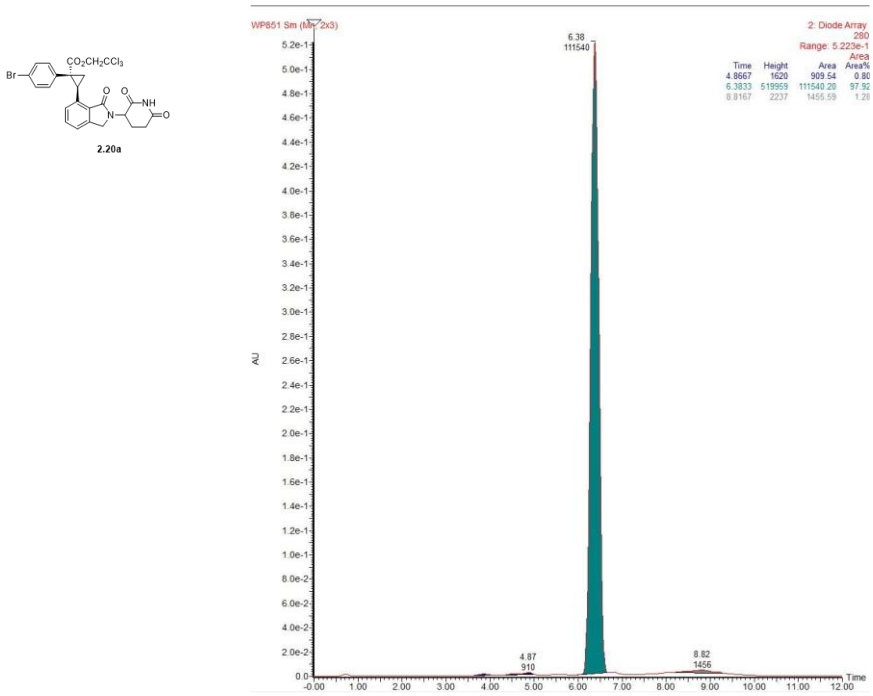
WP851 Sm (Mn, 2x3)
2: Diode Array
280
Range: 5.223e-1
Time Height Area Area%
4.8667 1620 909.54 0.80
6.3833 519959 111540.20 97.92
8.8167 2237 1455.59 1.28
6.38
111540
4.87
910
8.82
1456
AU
Time
2.20a

2.20b

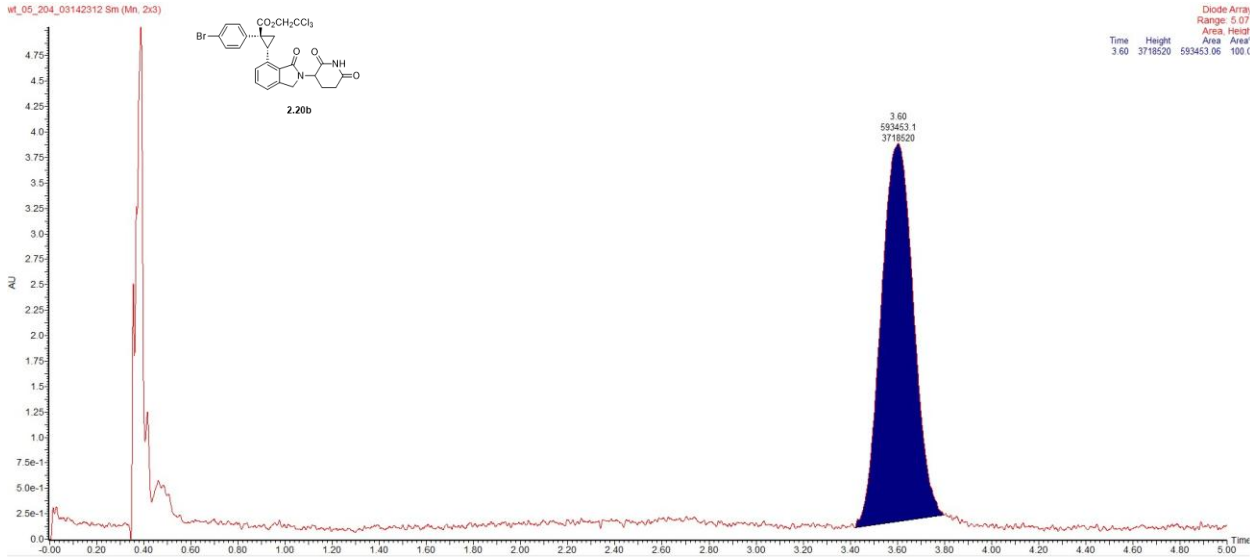
wt_05_204_03142312 Sm (Mn, 2x3)
2.20b
3.60
593453.1
3718520
Time
Height
Area
593453.06
AU
Time

2.21a

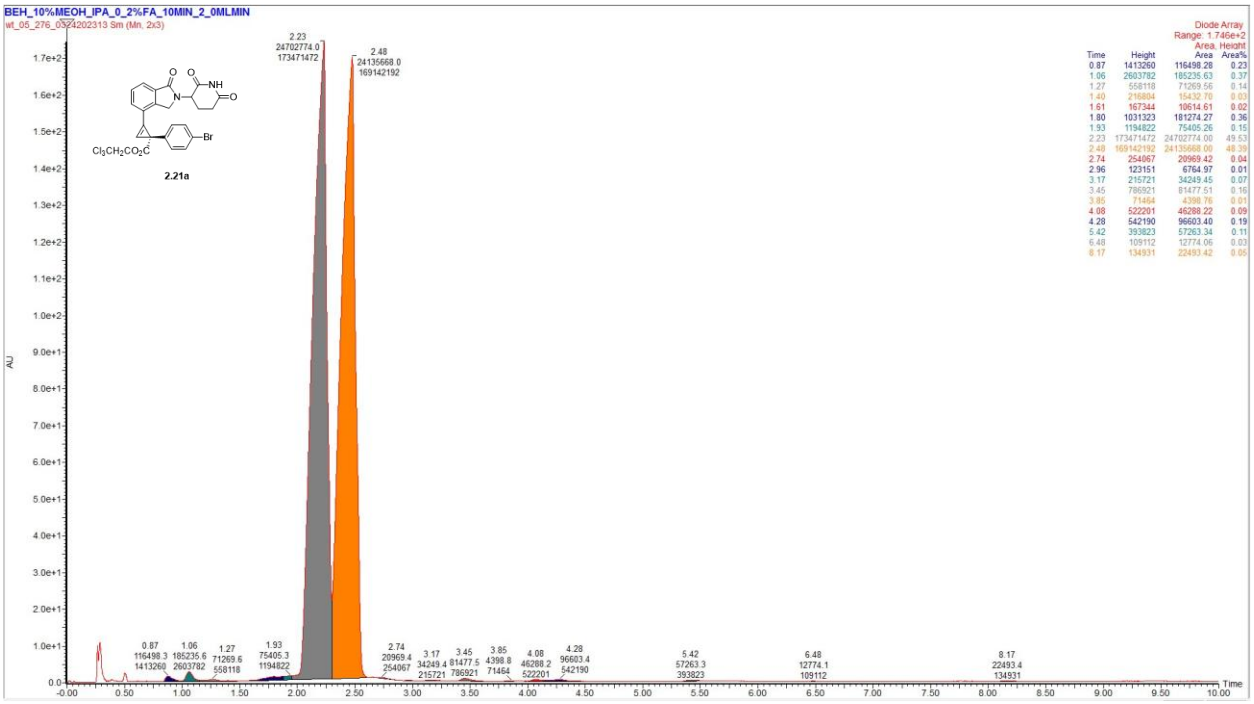
BEH_10%MEOH_IPA_0_2%FA_10MIN_2_0MLMIN
wt_05_276_03242023 13 Sm (Mn, 2x3)
2.21a
2.23
24702774.0
173471472
2.48
24135668.0
169142192
Time
Height
Area
AU
Time

2.21b

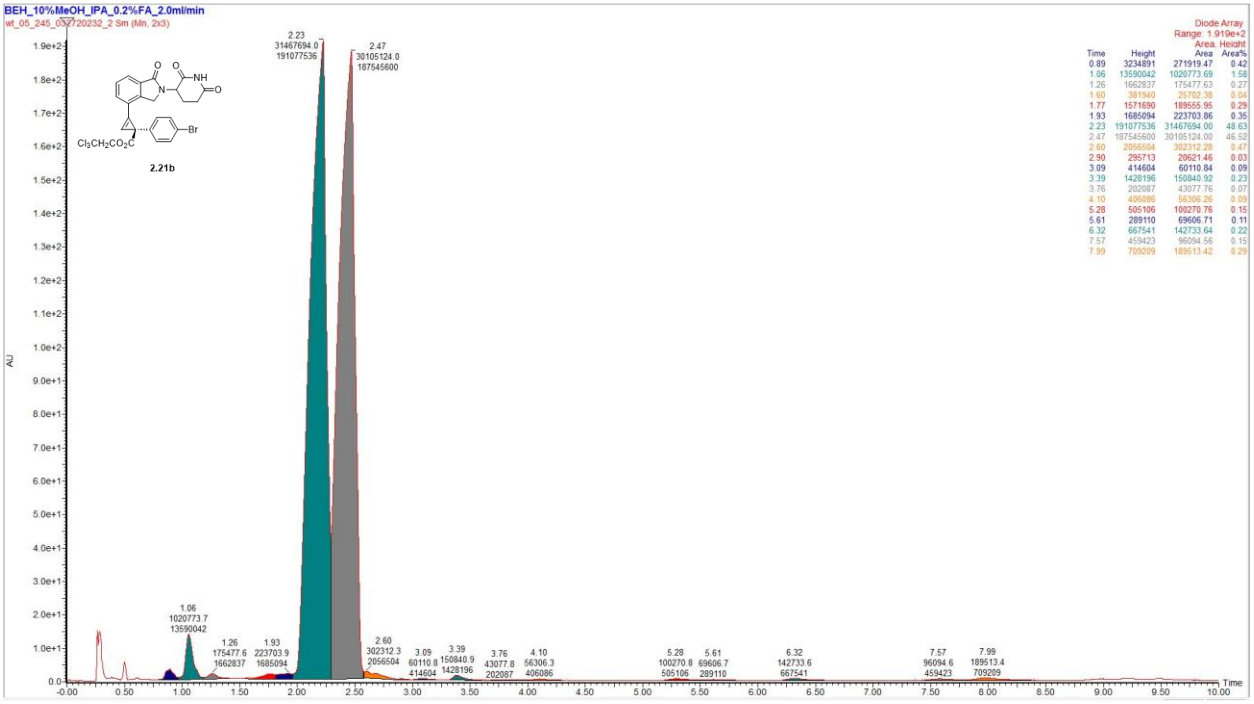
BEH_10%MeOH_IPA_0.2%FA_2.0ml/min
2.21b
Diode Array
Range: 1.910e+2
Time Height Area Area%
0.89 3234891 271919.47 0.42
1.06 13590042 1020773.69 1.58
1.26 1662837 175477.63 0.27
1.60 381940 25702.38 0.04
1.77 1571690 189555.95 0.29
1.93 1685094 223703.86 0.35
2.23 191077536 31467694.00 48.63
2.47 187545600 30105124.00 46.52
2.60 2056504 302312.28 0.47
2.90 295713 20621.46 0.03
3.09 414604 60110.84 0.09
3.39 1428196 150840.92 0.23
3.76 202087 43077.76 0.07
4.10 406086 56306.26 0.09
5.28 505106 100270.76 0.15
5.61 289110 69606.71 0.11
6.32 667541 142733.64 0.22
7.57 459423 96094.56 0.15
7.99 709209 189513.42 0.29

2.22a


BEH_10%MeOH_IPA_0.2%FA_2.0ml/min
2.22a
Diode Array
Range: 7.492
Time Height Area Area%
0.96 6818581 225261.16 99.90
1.04 29299 231.47 0.10

2.22b

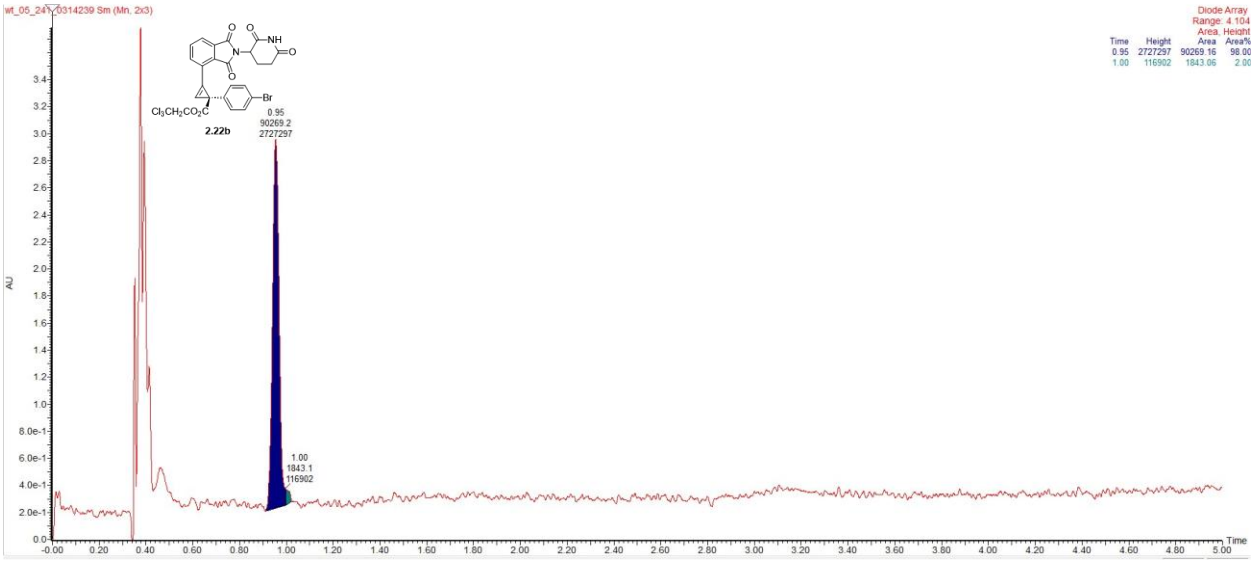
wt_05_241_0314239 Sm (Mn, 2x3)
Diode Array
Range: 4.104
Time Height Area Area%
0.95 2727297 90269.16 98.00
1.00 116902 1843.06 2.00
2.22b
0.95
90269.2
2727297
1.00
1843.1
116902
AU
Time

2.23a

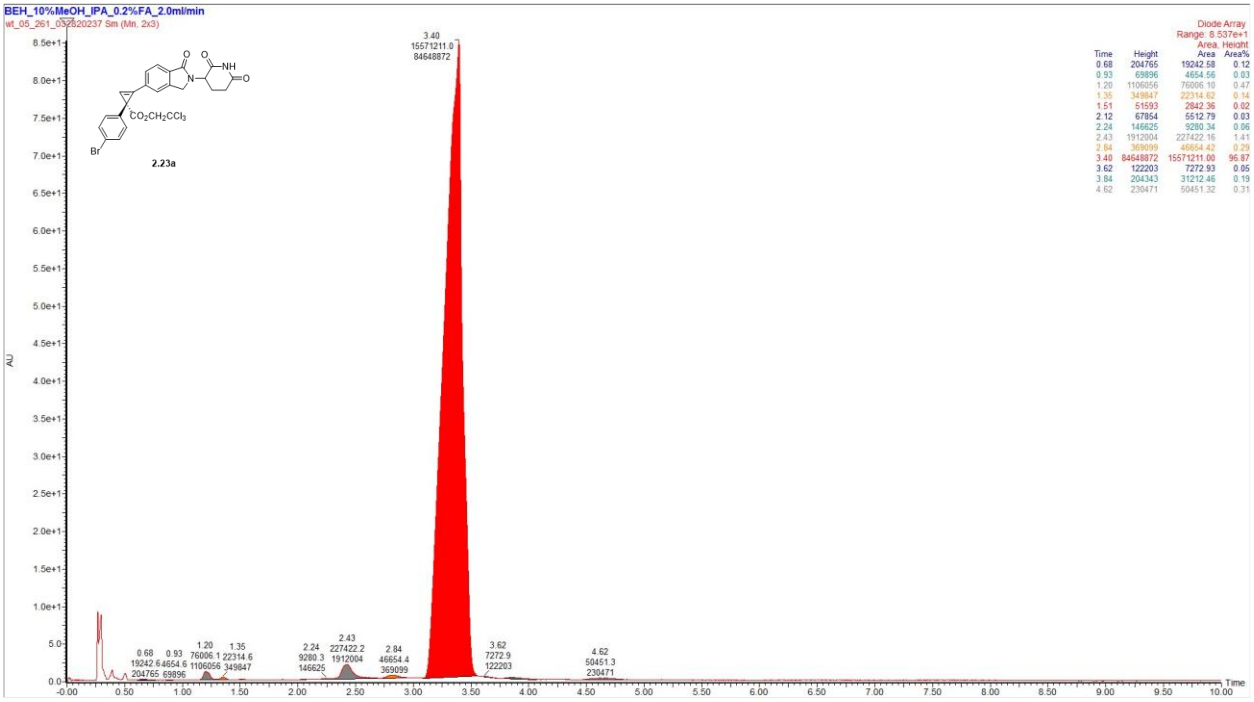
BEH_10%MeOH_IPA_0.2%FA_2.0ml/min
wt_05_261_0328020237 Sm (Mn, 2x3)
Diode Array
Range: 8.537e+1
Time Height Area Area%
0.68 204765 19242.58 0.12
0.93 69896 4654.56 0.03
1.20 1106056 76006.10 0.47
1.35 349847 22314.62 0.14
1.51 51593 2842.36 0.02
2.12 67854 5512.79 0.03
2.24 146625 9280.34 0.06
2.43 1912004 227422.16 1.41
2.84 369099 46654.42 0.29
3.40 84648872 15571211.00 96.87
3.62 122203 7272.93 0.05
3.84 204343 31212.46 0.19
4.62 230471 50451.32 0.31
2.23a
3.40
15571211.0
84648872
0.68
19242.6
204765
0.93
4654.6
69896
1.20
76006.1
1106056
1.35
22314.6
349847
2.24
9280.3
146625
2.43
227422.2
1912004
2.84
46654.4
369099
3.62
7272.9
122203
4.62
50451.3
230471
AU
Time

2.23b

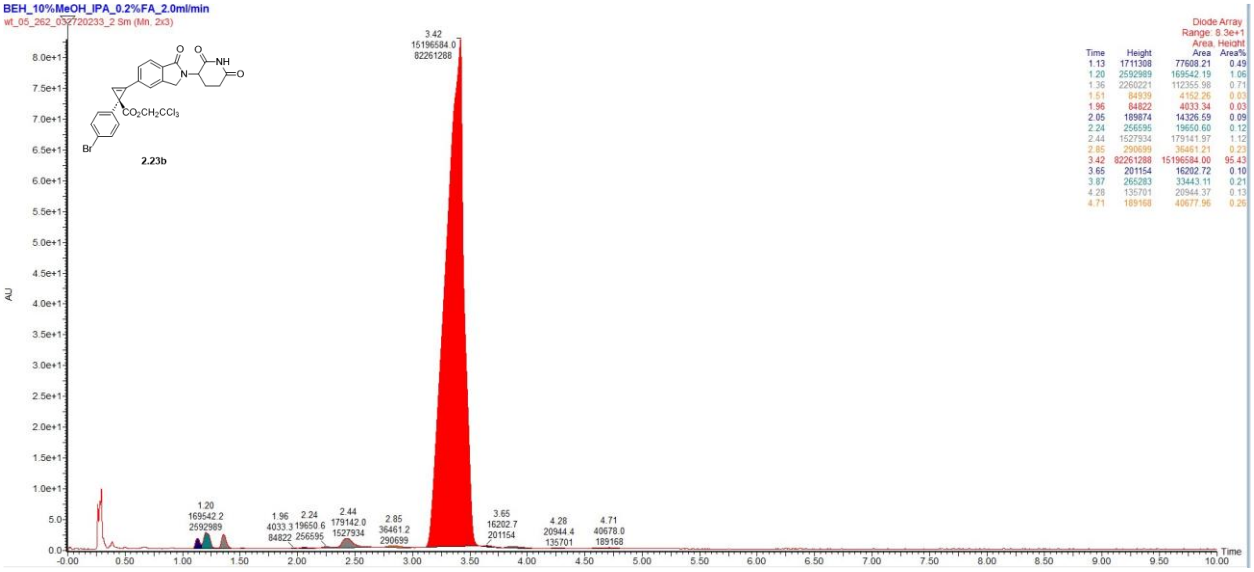
BEH_10%MeOH_IPA_0.2%FA_2.0ml/min
2.23b
Diode Array
Range: 6.3e+1
Time Height Area Area%
1.13 1711308 77608.21 0.49
1.20 2592989 169542.19 1.06
1.36 2260221 112355.98 0.71
1.51 84939 4152.26 0.03
1.96 84822 4033.34 0.03
2.05 189874 14326.59 0.09
2.24 256595 19650.60 0.12
2.44 1527934 179141.97 1.12
2.85 290699 36461.21 0.23
3.42 82261288 15196584.00 95.43
3.65 201154 16202.72 0.10
3.87 265283 33443.11 0.21
4.28 135701 20944.37 0.13
4.71 189168 40677.96 0.26

2.24a

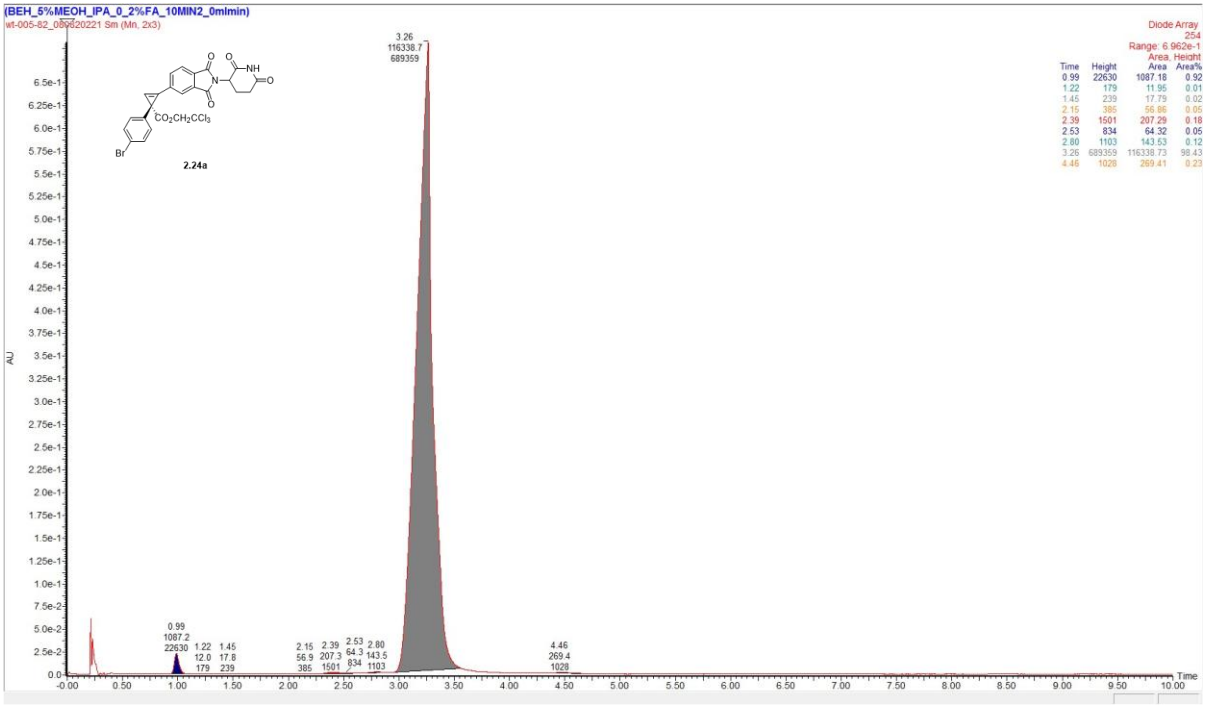
(BEH_5%MEOH_IPA_0_2%FA_10MIN2_0mlmin)
2.24a
Diode Array
254
Range: 6.962e-1
Time Height Area Area%
0.99 22630 1087.18 0.92
1.22 179 11.95 0.01
1.45 239 17.79 0.02
2.15 385 56.86 0.05
2.39 1501 207.29 0.18
2.53 834 64.32 0.05
2.80 1103 143.53 0.12
3.26 689359 116338.73 98.43
4.46 1028 269.41 0.23

2.24b

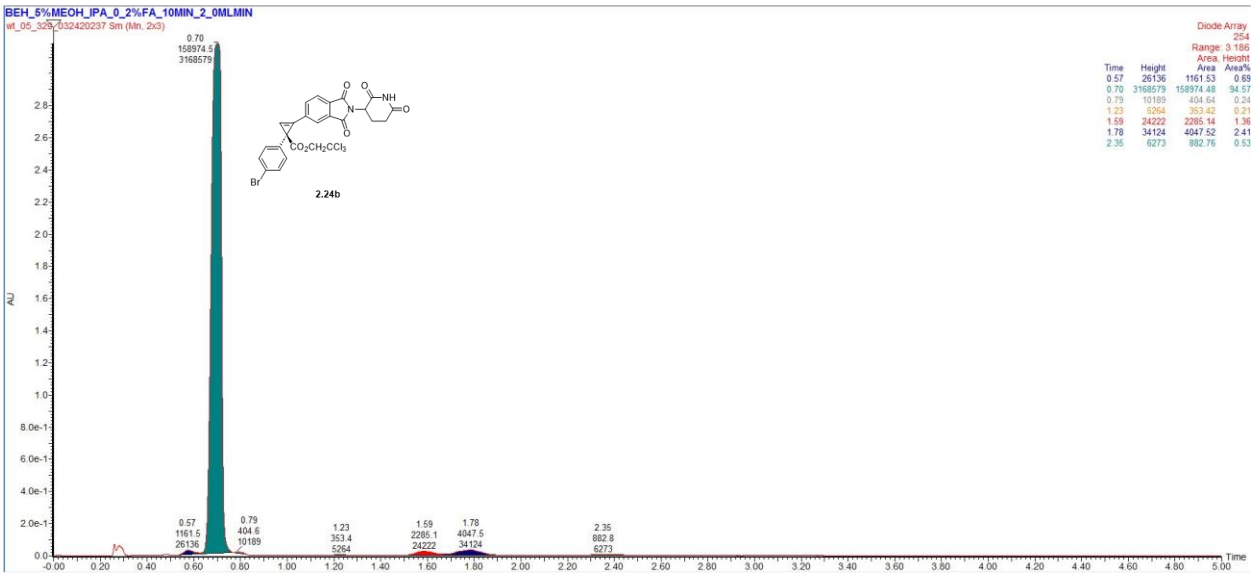
BEH_5%MEOH_IPA_0_2%FA_10MIN_2_0ML.MIN
Diode Array
254
Range: 3.186
Area, Height
Time Height Area Area%
0.57 26136 1161.53 0.69
0.70 3168579 158974.48 94.57
0.79 10189 404.64 0.24
1.23 5264 353.42 0.21
1.59 24222 2285.14 1.36
1.78 34124 4047.52 2.41
2.35 6273 882.76 0.53
0.70
158974.5
3168579
0.57
1161.5
26136
0.79
404.6
10189
1.23
353.4
5264
1.59
2285.1
24222
1.78
4047.5
34124
2.35
882.8
6273
2.24b
AU
Time

2.25a

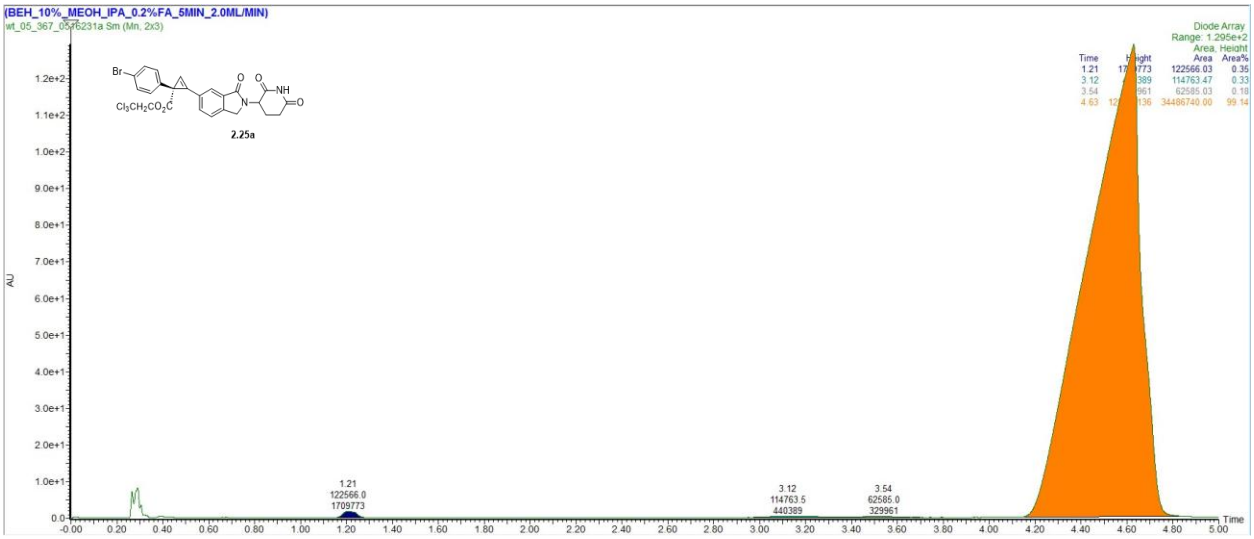
(BEH_10%_MEOH_IPA_0.2%FA_5MIN_2.0ML/MIN)
Diode Array
Range: 1.295e+2
Area, Height
Time Height Area Area%
1.21 122566.03 0.35
3.12 114763.47 0.33
3.54 62585.03 0.18
4.63 34486740.00 99.14
1.21
122566.0
1709773
3.12
114763.5
440389
3.54
62585.0
329961
2.25a
AU
Time

2.25b

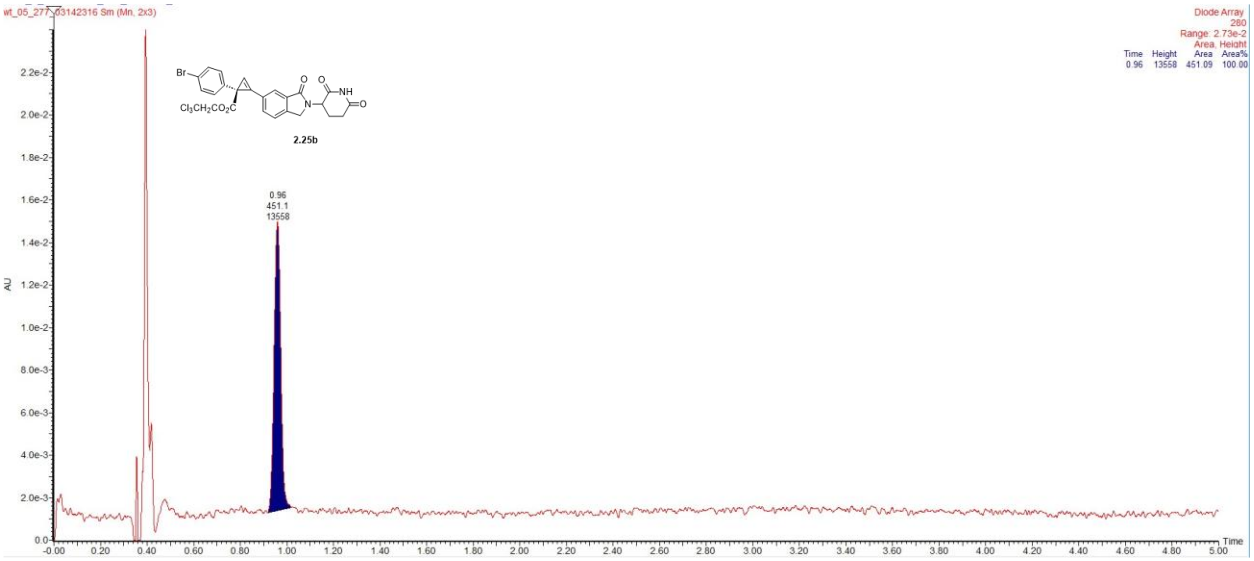
2.25b
0.96
451.1
13558
Diode Array
260
Range: 2.73e-2
Area, Height
Time Height Area Area%
0.96 13558 451.09 100.00
AU
Time

2.26a

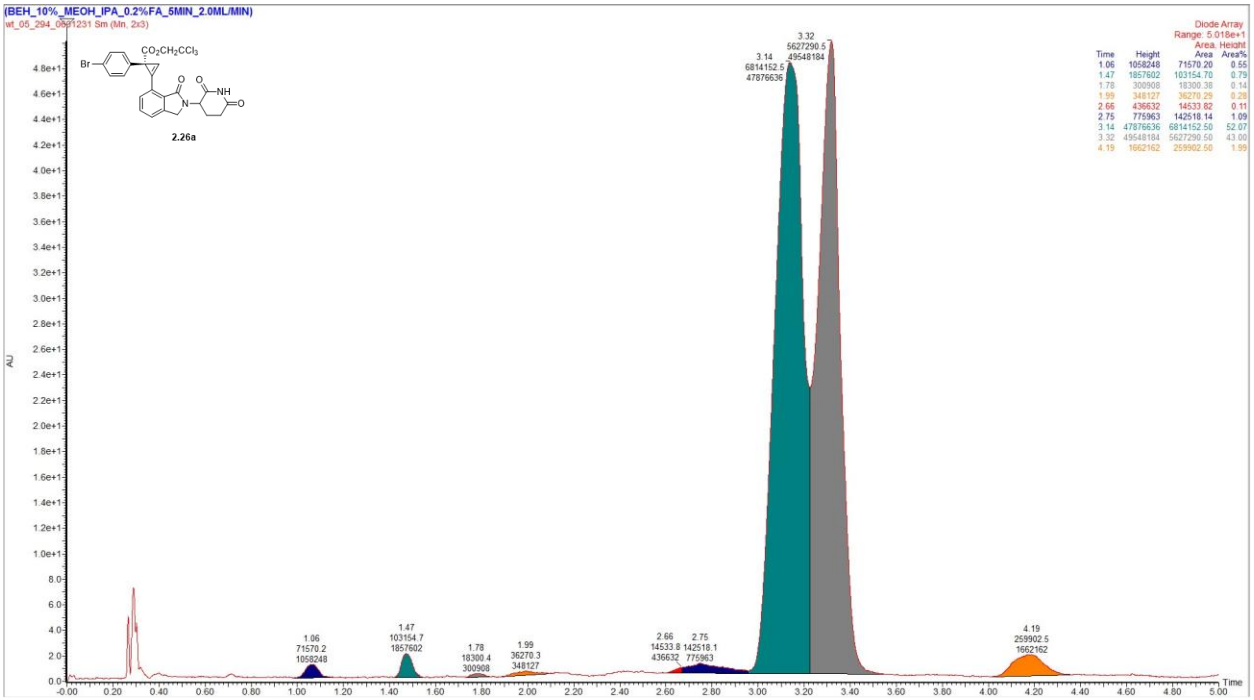
(BEH_10%_MEOH_IPA_0.2%FA_5MIN_2.0ML/MIN)
2.26a
Diode Array
Range: 5.018e+1
Area, Height
Time Height Area Area%
1.06 1058248 71570.20 0.55
1.47 1857602 103154.70 0.79
1.78 300908 18300.38 0.14
1.99 348127 36270.29 0.28
2.66 436632 14533.82 0.11
2.75 775963 142518.14 1.09
3.14 47876636 6814152.50 52.07
3.32 49548184 5627290.50 43.00
4.19 1662162 259902.50 1.99
AU
Time

2.26b

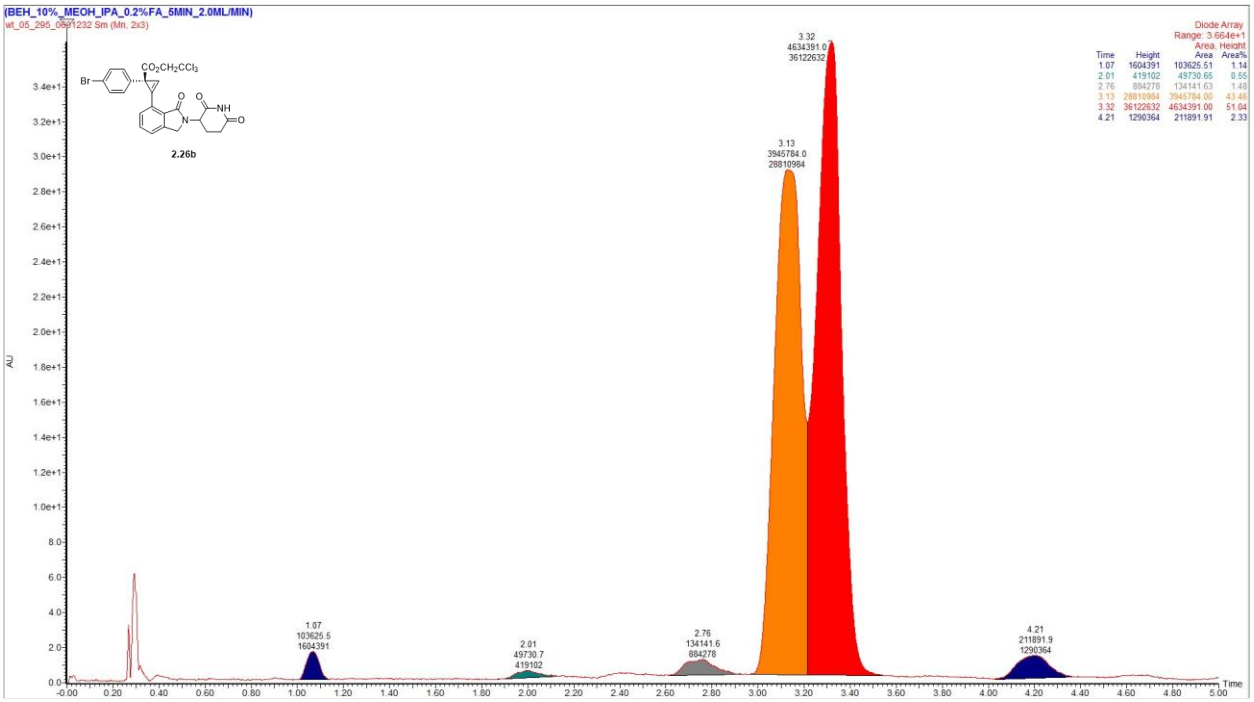

2.27a

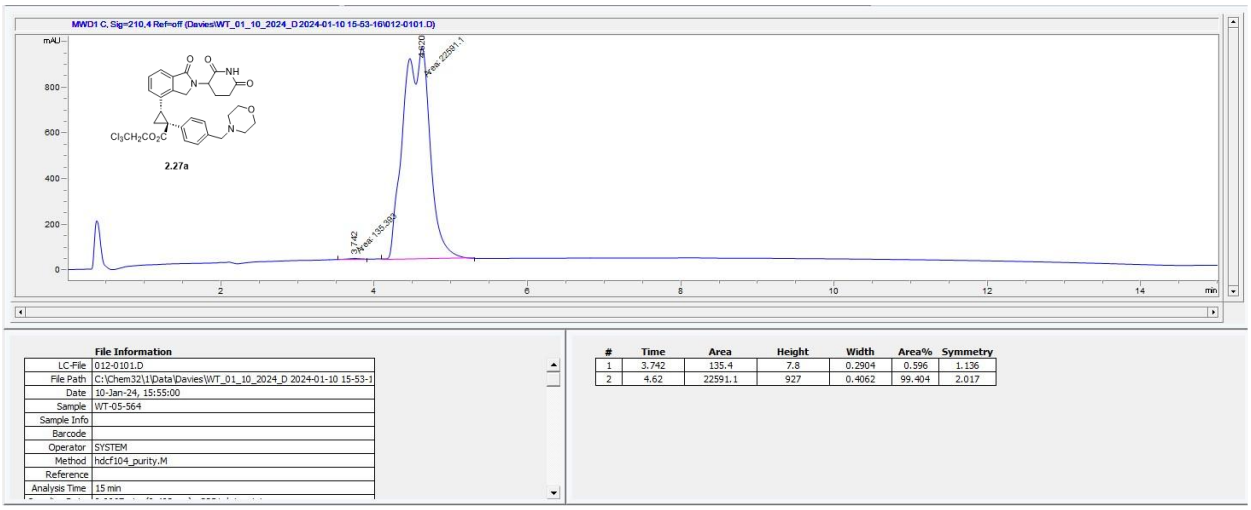

File Information	
LC-File	012-0101.D
File Path	C:\Chem32\1\Data\Davies\WT_01_10_2024_D 2024-01-10 15-53-1
Date	10-Jan-24, 15:55:00
Sample	WT-05-564
Sample Info	
Barcode	
Operator	SYSTEM
Method	hdcf104_purity.M
Reference	
Analysis Time	15 min

#	Time	Area	Height	Width	Area%	Symmetry
1	3.742	135.4	7.8	0.2904	0.596	1.136
2	4.62	22591.1	927	0.4062	99.404	2.017

2.27b

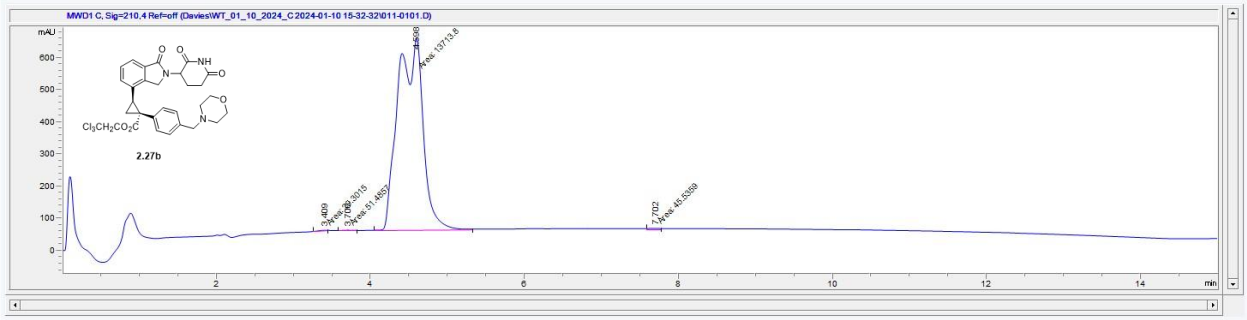

File Information	
LC-File	011-0101.D
File Path	C:\Chem32\1\Data\Davies\WT_01_10_2024_C 2024-01-10 15-32-3
Date	10-Jan-24, 15:34:17
Sample	WT-05-550
Sample Info	
Barcode	
Operator	SYSTEM
Method	hdcf104_purity.M
Reference	
Analysis Time	14.993 min

#	Time	Area	Height	Width	Area%	Symmetry
1	3.409	29.3	2.3	0.2082	0.212	5.947
2	3.706	51.5	3.8	0.2259	0.372	0.919
3	4.598	13713.8	597.3	0.3827	99.087	2.343
4	7.702	45.5	3.8	0.1992	0.329	1.331

2.28a

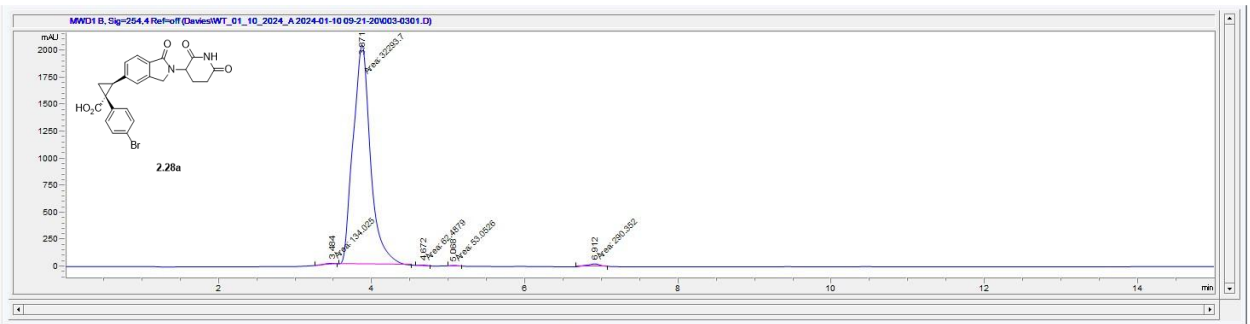

File Information	
LC-File	003-0301.D
File Path	C:\Chem32\1\Data\Davies\WT_01_10_2024_A 2024-01-10 09-21-2
Date	10-Jan-24, 09:55:04
Sample	WT-05-538
Sample Info	
Barcode	
Operator	SYSTEM
Method	hdcf104_purity.M
Reference	
Analysis Time	14.993 min

#	Time	Area	Height	Width	Area%	Symmetry
1	3.484	134	11.2	0.1992	0.408	3.036
2	3.871	32293.7	2039.6	0.2639	98.356	0.988
3	4.672	62.5	7.7	0.1349	0.190	0.645
4	5.068	53.1	7.1	0.1237	0.162	0.864
5	6.912	290.4	24.4	0.1982	0.884	1.496

2.28b

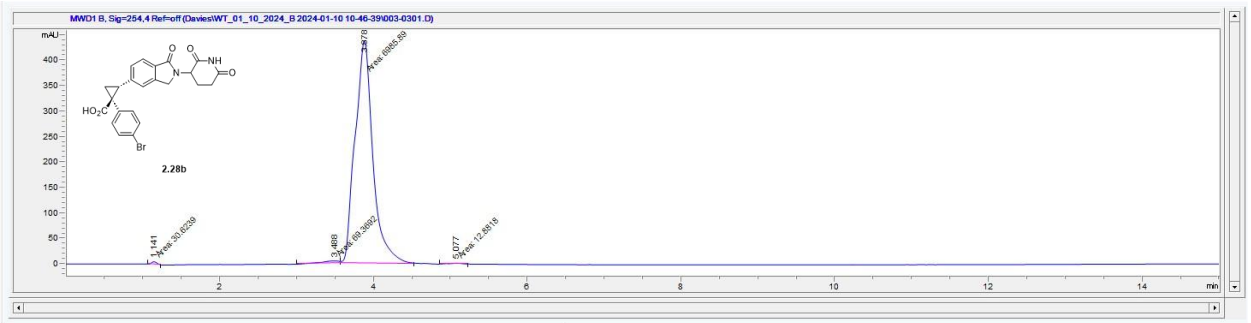

File Information

LC-File	003-0301.D
File Path	C:\Chem32\1\Data\Davies\WT_01_10_2024_B 2024-01-10 10-46-3
Date	10-Jan-24, 11:20:24
Sample	WT-05-539
Sample Info	
Barcode	
Operator	SYSTEM
Method	hdcf104_purity.M
Reference	
Analysis Time	15 min

#	Time	Area	Height	Width	Area%	Symmetry
1	1.141	30.6	5.7	0.0901	0.431	0.677
2	3.488	69.4	3.8	0.3047	0.977	3.234
3	3.878	6985.9	435	0.2677	98.410	1.015
4	5.077	12.9	1.1	0.1936	0.181	3.661

2.29a

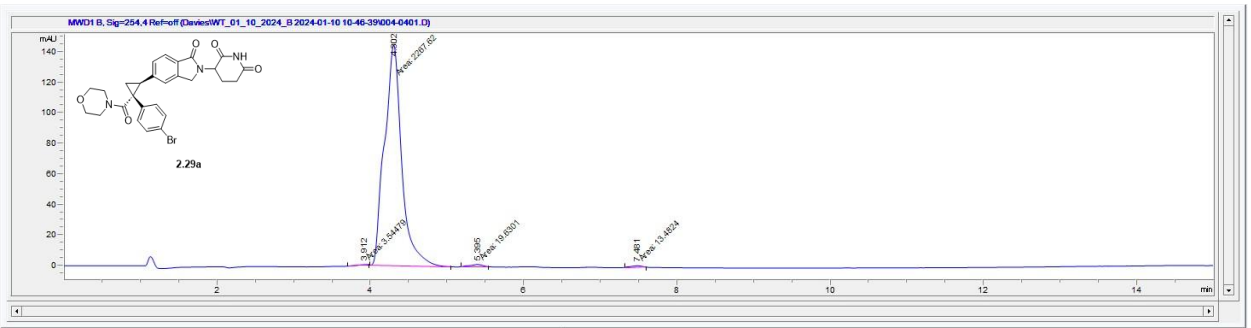

File Information

LC-File	004-0401.D
File Path	C:\Chem32\1\Data\Davies\WT_01_10_2024_B 2024-01-10 10-46-3
Date	10-Jan-24, 11:36:25
Sample	WT-05-546
Sample Info	
Barcode	
Operator	SYSTEM
Method	hdcf104_purity.M
Reference	
Analysis Time	14.993 min

#	Time	Area	Height	Width	Area%	Symmetry
1	3.912	3.5	4E-1	0.1495	0.154	2.991
2	4.302	2267.6	144.3	0.2618	98.409	1.057
3	5.395	19.6	1.6	0.2065	0.852	1.45
4	7.481	13.5	1.2	0.1889	0.585	1.71

2.29b

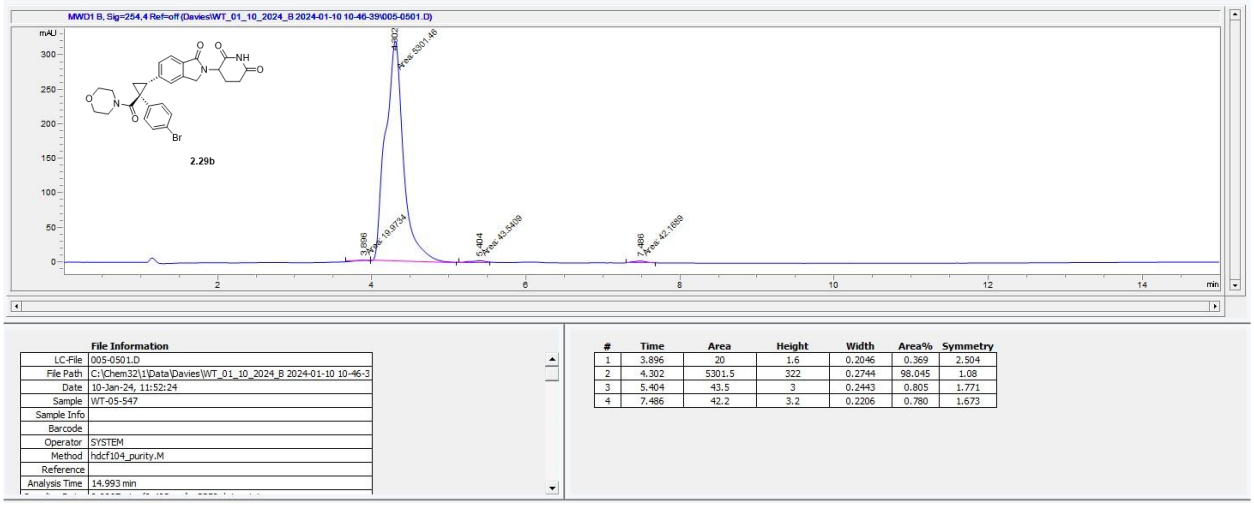

#	Time	Area	Height	Width	Area%	Symmetry
1	3.896	20	1.6	0.2046	0.369	2.504
2	4.302	5301.5	322	0.2744	98.045	1.08
3	5.404	43.5	3	0.2443	0.805	1.771
4	7.486	42.2	3.2	0.2206	0.780	1.673

Section 7: Assay Protocols

Fluorescence Resonance Energy Transfer-Based NSD@ PWWP Cereblon Binding Assay.

A solution containing 0.5 nM purified 6×His-CRBN_005-DDB1_026 (CRBN a.a. 1−442, DDB1 a.a. 1−1140, generated in-house) and 20 nM Tracer compound (CC0782985) was premixed in FRET-assay buffer (50 mM HEPES pH 7.3, 50 mM NaCl, 0.005% Brij35, 1mg/mL BSA and 0.5mM TCEP). Compounds for testing were spotted into a 1536 well plate (Greiner Cat#782075). CRBN and Tracer solution were incubated in compound wells for 20 minutes. Detection mix containing Anti6xHis Tb Crytate (CisBio Cat#61HI2TLF) was then added to assay wells for a final 0.5x assay concentration of detection antibody (stock is provided at 400x). Plates were incubated for 30 minutes before being read on Pherastar FSX plate reader using TR-FRET module (Excitation 340nM, Emssion 615/665nm).

ePL and HiBiT degradation assays

DF15 cells overexpressing ePL tagged GSPT1 (DF15/GSPT1 ePL OE) was used to monitor the degradation of GSPT1 induced by experimental compounds. MDS-L cells overexpressing ePL tagged CK1α and GSPT1^{G575N} (MDS-L/CK1α ePL OE_ GSPT1^{G575N} OE) was used to monitor the degradation of CK1α induced by experimental compounds. NCCIT cells with HiBiT tag knocked in at the c-terminus of *SALL4* (NCCIT/SALL4-HiBiT KI) was used to monitor the degradation of SALL4 induced by experimental compounds. DF15 cells with HiBiT tag knocked in at the n-terminus of *IKZF3* (DF15/HiBiT-IKZF3 KI) was used to monitor the degradation of AIOLOS (IKZF3) induced by experimental compounds.

The cell culture medium recipes, seeding densities and compound incubation time with cells are shown in the table below:

Table S2-7: Cell Cultures and Assay Details

Target	Cell line	Cell culture medium	Seeding density (cells/well)	Compound incubation time (hr)
GSPT1	DF15/GSPT1 ePL OE	RPMI 1640, 10% heat inactivated (HI) FBS, 1mM sodium pyruvate, 25mM Hepes, 0.1% pluronic acid, 1X NEAA	800	20
CK1α	MDS-L/CK1α ePL OE_ GSPT1^{G575N} OE	RPMI 1640, 20% HI FBS and 50 ng/mL of human recombinant IL3	1,000	4
SALL4	NCCIT/SALL4-HiBiT KI	RPMI 1640 and 10% HI FBS	800	2
IKZF3	DF15/HiBiT-IKZF3 KI	RPMI 1640, 10% HI FBS, 1mM sodium pyruvate, 25mM Hepes, 0.1% pluronic acid, 1X NEAA	800	4

For all degradation assays, compounds were pre-spotted in a 1536 well plate (Corning 3727) starting at 10uM with 3-fold serial dilution down 11 points in replicates using an Echo 650 series acoustic liquid handler. 5uL/well cells were seeded in the assay ready plate at the density and in the medium as indicated in the table. The final DMSO concentration in the cell culture was 0.25%. The plates were equilibrated at room temperature for 30 minutes before putting into a 37 °C CO_2 incubator. After appropriate incubation period, plates were retrieved from the incubator and set at room temperature to equilibrate for 30 minutes, before adding ePL or HiBiT detection reagent. For ePL detection, the pre-prepared mixture of EA reagent, lysis buffer, and substrate reagent at ratio 1:1:4 from the DiscoverX InCELL Detection Kit (Eurofins 96-0079L) according to the manufacturer's recommendation was added 3ul/well into the plate. Plates were incubated in the dark for 1hr at room temperature before reading using a BMG PheraStar luminescence reader. For HiBiT detection, Nano-Glo HiBiT Lytic Reagent (Promega, N3050) prepared according to the manufacturer's recommendation was added 3 uL/well into the plate. Plates were incubated 30 minutes at room temperature in the dark before reading using a BMG PheraStar luminescence reader.

To determine EC_{50} values for degradation, a four parameter logistic model (Sigmoidal Dose-Response Model) (FIT= (A+((B-A)/1+((C/x)^D)))) C is the inflection point (EC_{50}), D is the correlation coefficient , A and B are the low and high limits of the fit respectively) was used to determine the compound's EC_{50} value, which is the half maximum effective concentration. In the

degradation assays, the Y_{const} of each compound was calculated by normalizing the lowest point of the fitted curve to the media only control, which is 0%, and the cells treated with DMSO control, which is 100%. All degradation curves were processed and evaluated using Dotmatics.

Section 8: Biological Data Tables

The data in this section were generated by Zhenghang Sun, Jennifer Buenviaje, Gody Khambatta, Shan Yu, and Lihong Shi.

Table S2-8: Fluorescence Resonance Energy Transfer-Based Cereblon Binding Assay Data

Compound Number	CRBN HTRF IC_{50} (μM)
2.15a	0.66
2.15b	2.4
2.16a	>10
2.16b	7.9
2.17a	0.39
2.17b	1.3
2.18a	5.3
2.18b	>10
2.19a	2.1
2.19b	2.5
2.20a	>10
2.20b	>10
2.21a	0.16
2.21b	0.35
2.22a	4.6
2.22b	35
2.23a	0.59
2.23b	0.8
2.24a	5.7
2.24b	7.8
2.25a	0.98
2.25b	1.7
2.26a	2.4
2.26b	2.9

Table S2-9: Neosubstrate Degradation Assay Data*

Compound Number	IKZF3 EC_{50} (μM)	IKZF3 Y_{min} (%)	CK1a EC_{50} (μM)	CK1a Y_{min} (%)	GSPT1 EC_{50} (μM)	GSPT1 Y_{min} (%)	SALL4 EC_{50} (μM)	SALL4 Y_{min} (%)

2.15a	>10 ± 0.00	81 ± 3.3	>10 ± 0.00	87 ± 0.55	>10 ± 0.00	92 ± 7.8	>10 ± 0.00	85 ± 7.3
2.15b	>10 ± 0.00	97 ± 4.9	>10 ± 0.00	90 ± 7.1	>10 ± 0.00	99 ± 2.2	>10 ± 0.00	97 ± 3.1
2.16a	>10 ± 0.00	89 ± 3.2	>10 ± 0.00	92 ± 3.8	>10 ± 0.00	91 ± 16	>10 ± 0.00	91 ± 8.0
2.16b	>10 ± 0.00	95 ± 4.3	>10 ± 0.00	94 ± 5.1	>10 ± 0.00	87 ± 11	>10 ± 0.00	87 ± 13
2.17a	>10 ± 0.00	100 ± 4.6	>10 ± 0.00	89 ± 5.1	>10 ± 0.00	96 ± 7.8	>10 ± 0.00	99 ± 1.2
2.17b	>10 ± 0.00	89 ± 5.0	0.22 ± 0.089	47 ± 5.0	>10 ± 0.00	83 ± 7.0	0.16 ± 0.05	67 ± 5.4
2.18a	>10 ± 0.00	94 ± 8.3	>10 ± 0.00	94 ± 9.9	>10 ± 0.00	94 ± 11	>10 ± 0.00	92 ± 8.2
2.18b	>10 ± 0.00	97 ± 3.6	>10 ± 0.00	85 ± 4.1	>10 ± 0.00	86 ± 8.2	0.41 ± 0.16	60 ± 6.1
2.19a	>10 ± 0.00	95 ± 7.6	>10 ± 0.00	98 ± 12	>10 ± 0.00	95 ± 5.4	>10 ± 0.00	97 ± 2.2
2.19b	>10 ± 0.00	89 ± 6.5	>10 ± 0.00	96 ± 12	>10 ± 0.00	93 ± 5.8	>10 ± 0.00	96 ± 3.1
2.20a	>10 ± 0.00	91 ± 0.6	>10 ± 0.00	89 ± 1.7	>10 ± 0.00	87 ± 6.5	>10 ± 0.00	93 ± 3.8
2.20b	>10 ± 0.00	96 ± 5.7	>10 ± 0.00	91 ± 7.1	>10 ± 0.00	83 ± 15	>10 ± 0.00	96 ± 5.4
2.21a	0.012 ± 0.010	7.9 ± 1.8	0.17 ± 0.18	64 ± 4.3	0.17 ± 0.13	64 ± 8.7	0.019 ± 0.010	23 ± 4.5
2.21b	0.11 ± 0.05	69 ± 3.3	1.5 ± 1.1	60 ± 7.4	0.55 ± 0.47	66 ± 5.5	0.17 ± 0.06	35 ± 5.9
2.22a	0.90 ± 0.18	40 ± 2.2	1.5 ± 0.94	56 ± 14	4.3 ± 1.9	12 ± 13	0.56 ± 0.27	34 ± 7.4
2.22b	3.7 ± 0.62	10 ± 8.2	2.1 ± 1.3	54 ± 8.9	5.1 ± 1.4	17 ± 13	2.8 ± 1.6	57 ±7.7
2.23a	>10 ± 0.00	95 ± 7.6	>10 ± 0.00	89 ± 9.3	>10 ± 0.00	81 ± 17	>10 ± 0.00	89 ± 4.2
2.23b	4.8 ± 2.6	79 ± 6.4	0.25 ± 0.37	57 ± 8.0	3.3 ± 3.0	7.7 ± 4.7	0.075 ± 0.050	68 ± 2.1
2.24a	1.3 ± 2.1	73 ± 6.2	1.2 ± 1.2	60 ± 26	1.1 ± 0.69	2.7 ± 0.7	3.6 ± 0.74	67 ± 7.8
2.24b	0.31 ± 0.11	71 ± 9.7	1.6 ± 0.71	55 ± 39	1.4 ± 0.88	1.8 ± 0.86	2.4 ± 1.7	58 ± 3.2
2.25a	>10 ± 0.00	94 ± 2.3	>10 ± 0.00	93 ± 10	>10 ± 0.00	82 ± 7.1	>10 ± 0.00	95 ± 6.5
2.25b	>10 ± 0.00	81 ± 4.6	>10 ± 0.00	95 ± 6.0	>10 ± 0.00	88 ± 10	>10 ± 0.00	91 ± 10
2.26a	>10 ± 0.00	97 ± 0.58	>10 ± 0.00	96 ± 12	>10 ± 0.00	85 ± 24	>10 ± 0.00	95 ± 5.0
2.26b	>10 ± 0.00	93 ± 2.5	>10 ± 0.00	93 ± 6.8	>10 ± 0.00	80 ± 4.3	>10 ± 0.00	97 ± 5.2

* N ≥ 3 for all data

Appendix C: Supporting Information for Chapter 3.

Section 1: General Information

All reactions were conducted in flame-dried glassware under an inert atmosphere of dry nitrogen or argon, unless otherwise noted. All reagents were purchased from commercial suppliers and used as received, unless otherwise noted. Anhydrous dichloromethane was obtained from a Grubbs-type solvent purification system and further dried under an argon atmosphere for 24 hours over 4 Å molecular sieves. Anhydrous *N*,*N*-dimethylformamide, dimethyl sulfoxide, and toluene were obtained from DriSolv® Supelco® bottles. Molecular sieves were activated by heating under vacuum (<1 torr) for three hours at 300 °C. 1,1,1,3,3,3-hexafluoroisopropanol was obtained from Oakwood Chemical, distilled, and stored under inert atmosphere over 4 Å molecular sieves. Pentane, cyclopentane, cyclohexane, cycloheptane, *p*-bromo cumene, and *p*-cymene were stored over 4 Å molecular sieves for at least 24 hours prior to reaction.

Proton (^{1}H) NMR spectra were recorded at 400 MHz on Varian and Bruker spectrometers, 500 MHz on an Inova-500 spectrometer, 600 MHz on an Inova-600 spectrometer, or 800 MHz on a Bruker-800 spectrometer. Proton-decoupled carbon (^{13}C{^{1}H}) NMR spectra were recorded at 100 MHz on Varian and Bruker spectrometers, 151 MHz on an Inova-600 spectrometer, or 201 MHz on a Bruker-800 spectrometer. NMR spectra were recorded in deuterated solvents and were referenced to tetramethylsilane or the respective residual solvent signal. NMR chemical shifts were reported in parts per million (ppm). Abbreviations for signal couplings are as follows: s, singlet; d, doublet; t, triplet; q, quartet; quin, quintet; sex, sextet; sep, septet; m, multiplet; dd, doublet of doublets; dt, doublet of triplets; dtd, doublet of triplet of doublets; ddt, doublet of doublet of triplets; and dq, doublet of quartets. The coupling constants were taken from the spectra directly and are uncorrected.

Mass spectrometric determinations were carried out on a Thermo Finnigan LTQ-FTMS spectrometer with atmospheric pressure chemical ionization (APCI) or electrospray ionization (ESI) using a Fourier transform ion cyclotron resonance mass analyzer. Optical rotations were measured on a Rudolph Research Analytical Automatic Polarimeter, APIV-1W. Analytical thin layer chromatography was performed on silica gel plates using ultraviolet light, iodine vapor, or potassium permanganate stain to visualize analytes. Normal phase column chromatography was performed with SiliCycle silica gel 60 Å (50 µm) or neutral alumina hand-packed in Biotage Sfär columns on Biotage Isolera Four chromatographs or hand-packed glass columns, with SiliCycle silica gel 60 Å or Celite® as a dry-loading absorbent. Reverse phase chromatography was conducted using Teledyne ISCO RediSep Gold 18 reverse-phase columns using Teledyne ISCO CombiFlash or Biotage Isolera chromatographs. Supercritical fluid chromatography (SFC) analysis was performed on a Waters Acquity UPC2 instrument.

Purity of biologically tested compounds was tested by high-performance liquid chromatography analysis (HPLC) on an Agilent 1260 Infinity HPLC. All tested compounds were ≥95% pure by HPLC analysis.

1-(4-(tert-butyl)phenyl)bicyclo[1.1.1]pentane was prepared following the literature procedure.[1] 2,2,2-trichloroethyl 2-(4-bromophenyl)-2-diazoacetate (**3.2**) was prepared via the literature procedure.[2] 2,2,2-trichloroethyl 2-diazoacetate was also prepared following the literature procedure.[3] Dirhodium catalysts Rh_2(*S*-p-Ph-TPCP)$_4$,[4] Rh_2(*S*-*tetra*-p-Br-PPTTL)$_4$,[5] Rh_2(*R*-*tetra*-p-Br-PPTTL)$_4$,[5] and Rh_2(*S*-TPPTTL)$_4$[6] were prepared according to their respective literature procedures.

Racemic standards for the products of reactions with ring-closed diazo compounds were prepared by using a 1:1 mixture of *R* and *S* catalyst under the same reaction conditions used to prepare enantioenriched compounds. Racemic standards for the cyclopropanation of styrene with ring-opened diazo compounds were prepared using $Rh_2(esp)_2$ under the same reaction conditions used to prepare enantioenriched diazo compounds. Racemic standards for the C-H insertion of cyclohexane using ring-opened diazo compounds were prepared from the enantioenriched material by epimerization with 1,8-diazabicyclo[5.4.0]undec-7-ene in acetonitrile. Racemic standards for **3.13** and **SI-3** were prepared from the racemic standards for **3.11b** and **3.12b** using **GP 8** (detailed below) and the resulting glutarimide stereogenic centers were epimerized with 1,8-diazabicyclo[5.4.0]undec-7-ene in acetonitrile.

Caution! Glutarimide-containing compounds such as thalidomide are known reproductive, neurological, and hematological toxins. Care must be exercised to avoid direct contact with glutarimide-containing compounds. The neat compounds and their solutions must only be handled in a chemical fume hood. Any glassware used with glutarimide-containing material should be treated with a 2 M aqueous solution of a strong base such as sodium hydroxide to destroy the material. Caution! Diazo compounds are potentially energetic and must be handled carefully; initiation temperatures for similar compounds are often below 100 °C.[7] Off-gassing of nitrogen during rhodium-catalyzed reactions with diazo compounds must be accounted for in reaction setup.

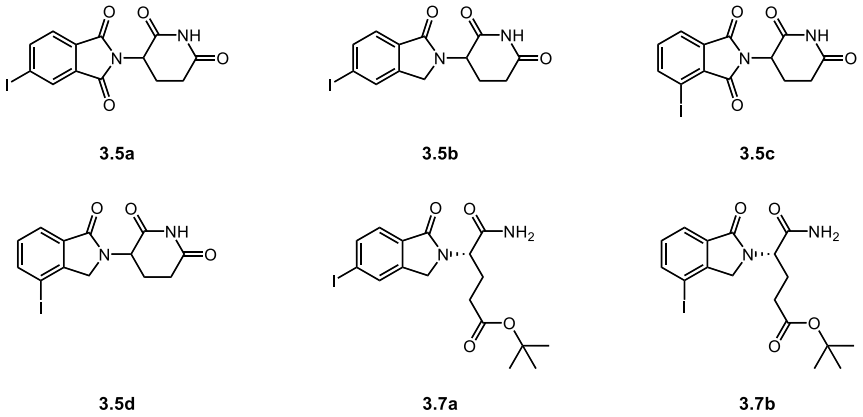

Figure S3-1. Aryl iodides used in this study

Section 2: Synthetic Procedures and Compound Characterization

Synthesis of Starting Materials

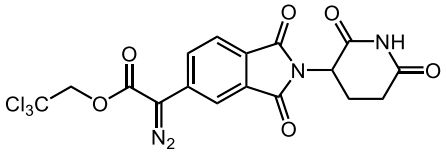

3.6a

2,2,2-trichloroethyl 2-diazo-2-(2-(2,6-dioxopiperidin-3-yl)-1,3-dioxoisoindolin-5-yl)acetate (3.6a).

Compound **3.6a** was produced following a modified literature procedure.[3] Under inert atmosphere, a flame-dried round-bottom flask equipped with PTFE magnetic stir bar was charged with 2-(2,6-dioxopiperidin-3-yl)-5-iodoisoindoline-1,3-dione (1.33 g, 1.0 equiv, 3.46 mmol) (**3.5a**), triphenylphosphine (182 mg, 20 mol%, 0.69 mmol), silver (I) carbonate (477 mg, 50 mol%, 1.7 mmol), and $Pd(PPh_3)_4$ (400 mg, 10 mol%, 0.35 mmol). 2,2,2-trichloroethyl 2-diazoacetate (1.51 g, 2.0 equiv, 6.9 mmol), triethylamine (0.97 mL, 2.0 equiv, 6.9 mmol) and 19 mL dry DMF were charged via syringe. The reaction was stirred vigorously at room temperature for six hours, after which it was poured into saturated aqueous sodium chloride solution and filtered through Celite® with 200 mL ethyl acetate. The organic phase was separated and washed thrice with saturated aqueous sodium chloride solution, then dried over sodium sulfate. The solution was filtered and concentrated onto Celite®. The residue was purified via flash column chromatography (SiO_2, gradient of 20% to 60% ethyl acetate in hexanes with 3% v/v triethylamine). The obtained material was dissolved in acetone, then concentrated in vacuuo until a viscous red liquid was obtained. The solution was placed in a -20 °C freezer overnight. The precipitated yellow solid was collected by vacuum filtration, washing with minimal -20 °C acetone, which gave 2,2,2-trichloroethyl 2-diazo-2-(2-(2,6-dioxopiperidin-3-yl)-1,3-dioxoisoindolin-5-yl)acetate **(3.6a)** as an amorphous light yellow solid (655 mg, 1.38 mmol, 40% yield).

HRMS (APCI) *m/z*: $[M+H]^+$ calcd for $C_{17}H_{12}O_6N_4{}^{35}Cl_3$ 472.9817; Found 472.9818

^{1}H NMR (400 MHz, Acetone-*d*6): δ 9.93 (s, 1H), 8.19 – 8.17 (m, 1H), 8.03 (dd, *J* = 8.1, 1.8 Hz, 1H), 7.94 (dd, *J* = 8.0, 0.7 Hz, 1H), 5.16 (dd, *J* = 12.7, 5.4 Hz, 1H), 5.12 (s, 2H), 3.09 – 2.88 (m, 1H), 2.86 – 2.68 (m, 2H, partially obscured by residual water peak at 2.82), 2.31 – 2.19 (m, 1H).
^{13}C{^{1}H} NMR (151 MHz, Acetone-*d*6): δ 172.6, 169.9, 167.7, 167.6, 163.1, 134.2, 133.8, 129.4, 129.3, 124.7, 118.8, 96.0, 74.6, 66.5, 50.4, 32.0, 23.3.
FT-IR (film): ν_{max}/cm^{-1} *inter alia* 2100 (N=N).

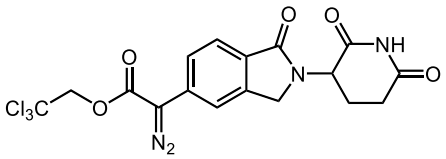

3.6b

2,2,2-trichloroethyl 2-diazo-2-(2-(2,6-dioxopiperidin-3-yl)-1-oxoisoindolin-5-yl)acetate (3.6b).
Under inert atmosphere, a flame-dried round-bottom flask was charged with a PTFE magnetic stir bar, Compound **3.6b** was produced following a modified literature procedure.[3] 5-iodo-1-oxoisoindolin-2-yl)piperidine-2,6-dione (370 mg, 1.0 equiv, 1.0 mmol) (**3.5b**), triphenylphosphine (71 mg, 10 mol%, 0.10 mmol), silver(I) carbonate (138 mg, 50 mol%, 0.50 mmol), and $Pd(PPh_3)_4$ (58 mg, 5.0 mol%, 0.05 mmol). 2,2,2-trichloroethyl 2-diazoacetate (261 mg, 1.2 equiv, 1.2 mmol), triethylamine (0.21 mL, 1.5 equiv, 1.5 mmol), and dry DMSO (5.6 mL) were charged via syringe. After two hours of stirring at room temperature, the reaction was recharged with $Pd(PPh_3)_4$ (58 mg, 5.0 mol%, 0.05 mmol) and triphenylphosphine (71 mg, 10 mol%, 0.10 mmol). After five hours of stirring at room temperature, the reaction was recharged with $Pd(PPh_3)_4$ (58 mg, 5.0 mol%, 0.05 mmol), triphenylphosphine (71 mg, 10 mol%, 0.10 mmol), and triethylamine (0.21 mL, 1.5 equiv, 1.5 mmol). The reaction was stirred for a further 12 hours at room temperature. The reaction was recharged with $Pd(PPh_3)_4$ (58 mg, 5.0 mol%, 0.05 mmol), triphenylphosphine (71 mg, 10 mol%, 0.10 mmol), triethylamine triethylamine (0.21 mL, 1.5 equiv, 1.5 mmol), silver(I) carbonate (138 mg, 50 mol%, 0.50 mmol) and 2,2,2-trichloroethyl 2-diazoacetate (261 mg, 1.2 equiv, 1.2 mmol), then stirred for a further two hours (total reaction time, 19 hours). The reaction was poured into 100 mL ethyl acetate with 1% v/v triethylamine and filtered through a layered plug of Celite®, silica gel, and neutral alumina. The solution was washed with 100 mL 10% w/w aqueous LiCl solution once, and twice with saturated aqueous NaCl solution. The organic layer was dried over sodium sulfate and filtered, then concentrated in vacuuo onto Celite®. The reaction was purified via flash column chromatography on neutral alumina using a gradient of 0-10% MeOH in CH_2Cl_2. The product-containing fractions were concentrated in vacuuo, and the obtained residue was sonicated with 4 mL acetone and stored in a -20 °C freezer overnight in the acetone. The yellow insoluble material was collected via vacuum filtration, rinsing with an additional 4 mL of acetone cooled to -20 °C, which gave 2,2,2-trichloroethyl 2-diazo-2-(2-(2,6-dioxopiperidin-3-yl)-1-oxoisoindolin-5-yl)acetate **(3.6b)** as a pale yellow amorphous solid (130 mg, 0.28 mmol, 28% yield).

HRMS (APCI) *m/z*: $[M+H]^+$ calcd for $C_{17}H_{14}O_5N_4{}^{35}Cl_3$, 459.0024; Found 459.0021

^{1}H NMR (600 MHz, DMSO-*d*6): δ 10.99 (s, 1H), 7.82 (dd, *J* = 1.7, 0.8 Hz, 1H), 7.78 (dd, *J* = 8.1, 0.7 Hz, 1H), 7.69 (dd, *J* = 8.1, 1.7 Hz, 1H), 5.11 (dd, *J* = 13.3, 5.2 Hz, 1H, partially obscured by signal at 5.10), 5.10 (s, 2H) 4.48 (d, *J* = 17.4 Hz, 1H), 4.35 (d, *J* = 17.3 Hz, 1H), 2.91 (ddd, *J* = 17.4, 13.7, 5.4 Hz, 1H), 2.60 (ddd, *J* = 17.2, 4.4, 2.4 Hz, 1H), 2.40 (qd, *J* = 12.6, 4.5 Hz, 1H), 2.01 (dtd, *J* = 12.4, 5.3, 2.4 Hz, 1H).
^{13}C{^{1}H} NMR (151 MHz, DMSO-*d*6): δ 172.9, 171.0, 167.6, 162.5, 143.0, 129.4, 128.8, 123.6, 123.3, 118.4, 95.3, 73.2, 51.6, 47.2, 31.2, 30.7, 22.5.
FT-IR (film): ν_{max}/cm^{-1} *inter alia* 2103 (N=N).

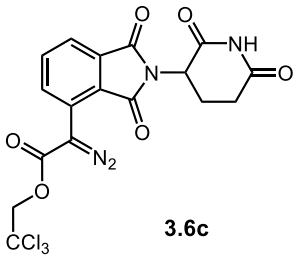

3.6c

2,2,2-trichloroethyl 2-diazo-2-(2-(2,6-dioxopiperidin-3-yl)-1,3-dioxoisoindolin-4-yl)acetate (3.6c).

Compound **3.6c** was produced following a modified literature procedure.[3] Under inert atmosphere, a flame-dried round-bottom flask equipped with PTFE magnetic stir bar was charged with 2-(2,6-dioxopiperidin-3-yl)-4-iodoisoindoline-1,3-dione (768 mg, 1.0 equiv, 2.0 mmol) (**3.5c**), triphenylphosphine (105 mg, 20 mol%, 0.4 mmol), silver (I) carbonate (276 mg, 50 mol%, 1.0 mmol), and $Pd(PPh_3)_4$ (231 mg, 10 mol%, 0.20 mmol). 2,2,2-trichloroethyl 2-diazoacetate (870 mg, 2.0 equiv, 4.0 mmol), triethylamine (0.56 mL, 2.0 equiv, 4.0 mmol) and 11 mL dry DMF were charged via syringe. The reaction was stirred vigorously at room temperature for six hours, after which it was poured into saturated aqueous sodium chloride solution and filtered through Celite® with 100 mL ethyl acetate. The organic phase was separated and washed thrice with saturated aqueous sodium chloride solution, then dried over sodium sulfate. The solution was filtered and concentrated onto Celite®. The residue was purified via flash column chromatography (SiO_2, gradient of 20% to 60% ethyl acetate in hexanes with 3% v/v triethylamine) and further purified via flash column chromatography (SiO_2, gradient of 0% to 5% acetone in CH_2Cl_2 with 3% v/v triethylamine). The obtained material was further purified via reverse phase flash column chromatography (C18, gradient of 20% to 90% EtOH in H_2O with 10 mM NH_4OAc buffer), which gave 2,2,2-trichloroethyl 2-diazo-2-(2-(2,6-dioxopiperidin-3-yl)-1,3-dioxoisoindolin-4-yl)acetate **(3.6c)** as an amorphous light yellow solid (145 mg, 0.30 mmol, 15% yield).

HRMS (ESI) *m/z*: $[M+Na]^+$ calcd for $C_{17}H_{11}O_6N_4{}^{35}Cl_3{}^{23}Na$ 494.9636; Found 494.9640

^{1}H NMR (400 MHz, Acetone-*d*6): δ 9.94 (s, 1H), 8.13 (dd, *J* = 8.0, 1.0 Hz, 1H), 7.94 (dd, *J* = 8.1, 7.3 Hz, 1H), 7.87 (dd, *J* = 7.4, 1.0 Hz, 1H), 5.19 (dd, *J* = 12.6, 5.4 Hz, 1H), 5.07 (s, 2H), 3.07 – 2.91 (m, 1H), 2.86 – 2.70 (m, 2H), 2.30 – 2.20 (m, 1H).

^{13}C{^{1}H} NMR (151 MHz, Acetone-*d*6): δ 206.1, 172.5, 169.8, 167.6, 167.4, 163.7, 135.9, 135.3, 133.7, 126.3, 125.3, 123.1, 96.1, 74.7, 50.4, 31.9, 23.2.

FT-IR (film): ν_{max}/cm^{-1} *inter alia* 2100 (N=N).

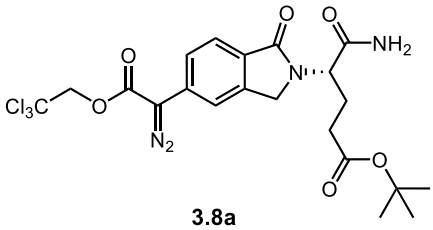

3.8a

***tert*-butyl (*S*)-5-amino-4-(5-(1-diazo-2-oxo-2-(2,2,2-trichloroethoxy)ethyl)-1-oxoisoindolin-2-yl)-5-oxopentanoate (3.8a).**

Compound **3.8a** was produced following a modified literature procedure.[3] Under inert atmosphere, a flame-dried 16 mL vial equipped with PTFE magnetic stir bar was charged with *tert*-butyl (*S*)-5-amino-4-(5-iodo-1-oxoisoindolin-2-yl)-5-oxopentanoate (**3.7a**) (89 mg, 1.0 equiv, 0.20 mmol), triphenylphosphine (28 mg, 20 mol%, 0.04 mmol), silver (I) carbonate (28 mg, 50 mol%, 0.10 mmol), and $Pd(PPh_3)_4$ (23 mg, 10 mol%, 0.02 mmol). 2,2,2-trichloroethyl 2-diazoacetate (65 mg, 1.5 equiv, 0.30 mmol), triethylamine (42 mL, 1.5 equiv, 0.30 mmol) and 4.0 mL dry toluene were charged via syringe. The reaction was placed in a preheated aluminum heating block (40 °C) and stirred vigorously at this temperature for four hours. The reaction was then cooled, rinsed through a silica plug with 20 mL ethyl acetate, and concentrated in vacuuo. The crude residue was mounted into Celite® and purified by flash column chromatography (SiO_2, gradient of 20% to 90% ethyl acetate in hexanes with 1% v/v triethylamine). The obtained material was further purified by reverse-phase flash column chromatography (C18, 20-90% acetonitrile in H_2O, with 10 mM NH_4OAc as buffer), which afforded *tert*-butyl (*S*)-5-amino-4-(5-(1-diazo-2-oxo-2-(2,2,2-trichloroethoxy)ethyl)-1-oxoisoindolin-2-yl)-5-oxopentanoate (**3.8a**) as an amorphous light yellow solid (63 mg, 0.12 mmol, 59% yield).

HRMS (APCI) *m/z*: $[M+H]^+$ calcd for $C_{21}H_{24}O_6N_4{}^{35}Cl_3$ 533.0756; Found 533.0759.

^{1}H NMR (400 MHz, $CDCl_3$): δ 7.86 (d, *J* = 8.0 Hz, 1H), 7.79 (d, *J* = 1.7 Hz, 1H), 7.48 (dd, *J* = 8.1, 1.7 Hz, 1H), 6.24 (s, 1H), 5.30 (s, 1H), 4.93 (s, 2H), 4.89 (dd, *J* = 8.7, 6.3 Hz, 1H), 4.55 (d, *J* = 17.2 Hz, 1H), 4.46 (d, *J* = 17.2 Hz, 1H), 2.50 – 2.08 (m, 4H), 1.42 (s, 9H).

^{13}C{^{1}H} NMR (101 MHz, $CDCl_3$): δ 171.8, 168.8, 142.9, 129.8, 129.4, 124.5, 123.1, 118.4, 94.9, 81.0, 74.1, 54.1, 47.3, 32.0, 28.2, 24.4.

FT-IR (film): ν_{max}/cm^{-1} *inter alia* 2099 (N=N).

Specific Rotation: $[\alpha]_D^{22}$ -55.2 (c 1.0, $CHCl_3$).

Note: *The degree of enantioenrichment of the stereogenic center was not measured by SFC analysis due to the instability of the compound under the conditions of analysis.*

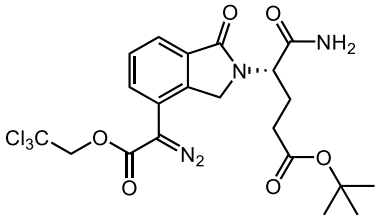

3.8b

***tert*-butyl (*S*)-5-amino-4-(4-(1-diazo-2-oxo-2-(2,2,2-trichloroethoxy)ethyl)-1-oxoisoindolin-2-yl)-5-oxopentanoate (3.8b).**

Compound **3.8b** was produced following a modified literature procedure.[3] Under inert atmosphere, a flame-dried 16 mL vial equipped with PTFE magnetic stir bar was charged with *tert*-butyl (*S*)-5-amino-4-(4-iodo-1-oxoisoindolin-2-yl)-5-oxopentanoate (**3.7b**) (89 mg, 1.0 equiv, 0.20 mmol), triphenylphosphine (28 mg, 20 mol%, 0.04 mmol), silver (I) carbonate (28 mg, 50 mol%, 0.10 mmol), and $Pd(PPh_3)_4$ (23 mg, 10 mol%, 0.02 mmol). 2,2,2-trichloroethyl 2-diazoacetate (65 mg, 1.5 equiv, 0.30 mmol), triethylamine (42 mL, 1.5 equiv, 0.30 mmol) and 4.0 mL dry toluene were charged via syringe. The reaction was placed in a preheated aluminum heating block (40 °C) and stirred vigorously at this temperature for four hours. The reaction was then cooled, rinsed through a silica plug with 20 mL ethyl acetate, and concentrated in vacuuo. The crude residue was mounted into Celite® and purified by flash column chromatography (SiO_2, gradient of 20% to 90% ethyl acetate in hexanes with 1% v/v triethylamine). The obtained material was further purified by reverse-phase flash column chromatography (C18, 20-90% acetonitrile in H_2O, with 10 mM NH_4OAc as buffer), which afforded *tert*-butyl (*S*)-5-amino-4-(4-(1-diazo-2-oxo-2-(2,2,2-trichloroethoxy)ethyl)-1-oxoisoindolin-2-yl)-5-oxopentanoate **(3.8b)** as an amorphous light yellow solid (33 mg, 0.06 mmol, 31% yield).

HRMS (ESI) *m/z*: $[M+H]^+$ calcd for $C_{21}H_{24}O_6N_4{}^{35}Cl_3$ 533.0763; Found 533.0756.

^{1}H NMR (400 MHz, $CDCl_3$): δ 7.83 (dd, *J* = 7.5, 1.2 Hz, 1H), 7.64 (dd, *J* = 7.8, 1.1 Hz, 1H), 7.57 (t, *J* = 7.6 Hz, 1H), 6.32 (s, 1H), 5.35 (s, 1H), 4.97 – 4.89 (m, 3H), 4.55 (d, *J* = 17.5 Hz, 1H), 4.45 (d, *J* = 17.5 Hz, 1H), 2.46 – 2.21 (m, 3H), 2.20 – 2.09 (m, 1H), 1.42 (s, 9H).

^{13}C{^{1}H} NMR: (151 MHz, $CDCl_3$): δ 171.9, 171.6, 168.7, 140.0, 133.3, 129.3, 123.9, 120.5, 95.0, 81.1, 74.3, 54.2, 47.0, 32.0, 28.2, 24.4.

FT-IR (film): ν_{max}/cm^{-1} *inter alia* 2099 (N=N).

Specific Rotation: $[\alpha]_D^{22}$ -43.2 (*c* 0.5, $CHCl_3$).

Note: *The degree of enantioenrichment of the stereogenic center was not measured by SFC analysis due to the instability of the compound under the conditions of analysis.*

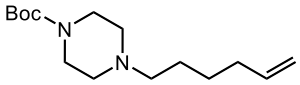

3.23

***tert*-butyl 4-(hex-5-en-1-yl)piperazine-1-carboxylate (3.23).**

Under inert atmosphere, a flame-dried round-bottom flask fitted with reflux condenser was charged with sodium iodide (75 mg, 10 mol%, 0.50 mmol), tert-butyl piperazine-1-carboxylate (0.93 g, 1.0 equiv, 5.0 mmol), and potassium carbonate (1.5 g, 2.2 equiv, 11 mmol). 6-

bromohex-1-ene (0.90 g, 1.1 equiv, 5.5 mmol) and 23 mL dry acetonitrile were charged by syringe. The reaction was stirred overnight at reflux then cooled, filtered through Celite® with CH_2Cl_2, and concentrated in vacuuo. The crude residue was purified via flash column chromatography (SiO_2, gradient of 0-10% methanol in CH_2Cl_2), which produced tert-butyl 4-(hex-5-en-1-yl)piperazine-1-carboxylate (**3.23**) (1.23 g, 92% yield, 4.6 mmol) as a translucent yellow oil.

HRMS (APCI) *m/z*: $[M+H]^+$ calcd for $C_{15}H_{29}O_2N$ 269.2224; Found 269.2223.
^{1}H NMR (400 MHz, $CDCl_3$): δ 5.79 (ddt, *J* = 16.9, 10.2, 6.7 Hz, 1H), 5.00 (dq, *J* = 17.1, 1.7 Hz, 1H), 4.94 (ddt, *J* = 10.2, 2.2, 1.2 Hz, 1H), 3.42 (t, *J* = 5.1 Hz, 4H), 2.47 – 2.27 (m, 6H), 2.06 (qt, *J* = 7.1, 1.4 Hz, 2H), 1.55 – 1.35 (m, 13H).
^{13}C{^{1}H} NMR (151 MHz, $CDCl_3$): δ 154.9, 138.8, 114.7, 79.7, 58.7, 53.2, 33.8, 28.6, 26.9, 26.4.

Synthesis of Final Compounds

General Procedure 1 (GP1)

A flame-dried 4 mL vial under inert atmosphere was equipped with ca. 200 wt% 4Å mol. sieves and a PTFE magnetic stir bar. The vial was charged with diazo (1.0 equiv, 0.10 mmol) and 1,1,1,3,3,3-hexafluoropropan-2-ol (0.10 mL, 10.0 equiv, 1.0 mmol). 1.0 mL substrate was charged via syringe, and a 20 mM solution of Rh_2(*S*-tetra-p-Br-TPPTTL)$_4$ (50 µL, 1 mol%, 1.0 µmol) in dry CH_2Cl_2 was charged via syringe at room temperature to the stirred reaction. The reaction was allowed to stir at r.t. for 0.5 h and was filtered through Celite®, then concentrated in vacuuo, removing excess substrate by Kugelrohr distillation if possible. The reaction was dry-mounted into Celite® and purified by flash column chromatography.

General Procedure 2 (GP2)

A flame-dried 4 mL vial under inert atmosphere was equipped with ca. 200 wt% 4Å mol. sieves and a PTFE magnetic stir bar. The vial was charged with diazo (1.0 equiv, 0.10 mmol) and 1,1,1,3,3,3-hexafluoropropan-2-ol (0.10 mL, 10.0 equiv, 1.0 mmol). 0.5 mL substrate and 0.5 mL CH_2Cl_2 were charged via syringe, and a 20 mM solution of Rh_2(*S*-tetra-p-Br-TPPTTL)$_4$ (50 µL, 1 mol%, 1.0 µmol) in dry CH_2Cl_2 was charged via syringe at room temperature to the stirred reaction. The reaction was allowed to stir at r.t. for 0.5 h and was filtered through Celite®, then concentrated in vacuuo, removing excess substrate by Kugelrohr distillation if possible. The reaction was dry-mounted into Celite® and purified by flash column chromatography.

General Procedure 3 (GP3)

A flame-dried 4 mL vial equipped with 200 w/w% 4 Å mol. sieves and PTFE magnetic stir bar was charged with Rh_2(*S-tetra*-p-Br-PPTTL)$_4$ (1 mol%, 1.0 µmol) and substrate (10.0 equiv, 1.0 mmol) under inert atmosphere. 0.5 mL dry CH_2Cl_2 was charged by syringe. A solution of diazo (1.0 equiv, 0.10 mmol) in 0.5 mL dry CH_2Cl_2 and 1,1,1,3,3,3-hexafluoropropan-2-ol (0.10 mL, 10.0 equiv, 1.0 mmol) was prepared under inert atmosphere in a flame-dried vial. The diazoacetate solution was added over the course of 1 hour using a syringe pump to the stirred reaction vial at room temperature. The reaction was stirred for 0.5 h further, after which the reaction was filtered through a pad of Celite®, rinsing with CH_2Cl_2. The solution was concentrated in vacuuo. If possible, remaining substrate was removed via Kugelrohr distillation. The crude residue was analyzed by ^{1}H NMR. The crude material was dry-mounted on Celite® and purified by flash column chromatography.

General Procedure 4 (GP4)

A flame-dried 4 mL vial equipped with 200 w/w% 4 Å mol. sieves and PTFE magnetic stir bar was charged with Rh_2(*S-tetra*-p-Br-PPTTL)$_4$ (1 mol%, 1.0 μmol) and substrate (10.0 equiv, 1.0 mmol) under inert atmosphere. 0.5 mL dry CH_2Cl_2 and 1,1,1,3,3,3-hexafluoropropan-2-ol (0.10 mL, 10.0 equiv, 1.0 mmol) were charged by syringe. A solution of diazo (1.0 equiv, 0.10 mmol) in 0.5 mL dry CH_2Cl_2 was prepared under inert atmosphere in a flame-dried vial. The diazoacetate solution was added over the course of 3 hours using a syringe pump to the stirred reaction vial at room temperature. The reaction was stirred for 0.5 h further, after which the reaction was filtered through a pad of Celite®, rinsing with CH_2Cl_2. The solution was concentrated in vacuuo. If possible, remaining substrate was removed via Kugelrohr distillation. The crude residue was analyzed by ^{1}H NMR. The crude material was dry-mounted on Celite® and purified by flash column chromatography.

General Procedure 5 (GP5)

A flame-dried 4 mL vial equipped with 200 w/w% 4 Å mol. sieves and PTFE magnetic stir bar was charged with Rh_2(*S-tetra*-p-Br-PPTTL)$_4$ (1 mol%, 1.0 μmol) and substrate (5.0 equiv, 0.5 mmol) under inert atmosphere. 0.5 mL dry CH_2Cl_2 was charged by syringe. A solution of diazo (1.0 equiv, 0.10 mmol) in 0.5 mL dry CH_2Cl_2 and 1,1,1,3,3,3-hexafluoropropan-2-ol (0.10 mL, 10.0 equiv, 1.0 mmol) was prepared under inert atmosphere in a flame-dried vial. The diazoacetate solution was added over the course of 0.25 h using a syringe pump to the stirred reaction vial at room temperature. The reaction was stirred for 0.5 h further, after which the reaction was filtered through a pad of Celite®, rinsing with CH_2Cl_2. The solution was concentrated in vacuuo. The crude residue was analyzed by ^{1}H NMR. The crude material was dry-mounted on Celite® and purified by flash column chromatography.

General Procedure 6 (GP6)

A flame-dried 4 mL vial equipped with 200 w/w% 4 Å mol. sieves and PTFE magnetic stir bar was charged with Rh_2(*S-tetra*-p-Br-PPTTL)$_4$ (1 mol%, 1.0 μmol) and substrate (5.0 equiv, 0.5 mmol) under inert atmosphere. 0.5 mL dry CH_2Cl_2 and 1,1,1,3,3,3-hexafluoropropan-2-ol (0.10 mL, 10.0 equiv, 1.0 mmol) were charged by syringe. A solution of diazo (1.0 equiv, 0.10 mmol) in 0.5 mL dry CH_2Cl_2 was prepared under inert atmosphere in a flame-dried vial. The diazoacetate solution was added over the course of 0.25 h using a syringe pump to the stirred reaction vial at room temperature. The reaction was stirred for 0.5 h further, after which the reaction was filtered through a pad of Celite®, rinsing with CH_2Cl_2. The solution was concentrated in vacuuo. The crude residue was analyzed by ^{1}H NMR. The crude material was dry-mounted on Celite® and purified by flash column chromatography.

General Procedure 7 (GP7)

Under inert atmosphere, a flame-dried vial equipped with PTFE magnetic stir bar was charged with ring-opened product (1.0 equiv). Dry acetonitrile (0.2 M) was charged via syringe. Benzenesulfonic acid (2.0 equiv) was added to the reaction mixture neat, and the reaction was placed in a preheated aluminum heating block (70 °C). The reaction was stirred at this temperature for 3.5 h, after which the reaction was allowed to cool, and was filtered through a short plug of silica with 4 mL ethyl acetate. The reaction was concentrated in vacuuo, dry mounted to Celite®, and purified via flash column chromatography (SiO_2) to afford the product. It is important to note that as per the publication of this method as adapted to similar substrates, the reaction must be run for no longer than ca. 3-3.5 h, as the risk of racemization at the

glutarimide stereogenic center increases with time.[8] These reactions were run with this parameter in mind, and no significant degradation of the stereocenter was noted.

General Procedure 8 (GP8)

A flame-dried 4 mL vial under inert atmosphere was equipped with ca. 200 wt% 4Å mol. sieves and a PTFE magnetic stir bar. The vial was charged with diazo (1.0 equiv, 0.10 mmol) and substrate (10.0 equiv, 1.0 mmol). 1.0 mL dry CH_2Cl_2 was charged via syringe, and a 20 mM solution of Rh_2(*S*-tetra-p-Br-TPPTTL)$_4$ (50 µL, 1 mol%, 1.0 µmol) in dry CH_2Cl_2 was charged via syringe at room temperature to the stirred reaction. The reaction was allowed to stir at r.t. for 0.5 h and was filtered through Celite®, then concentrated in vacuuo, removing excess substrate by Kugelrohr distillation if possible. The reaction was dry-mounted into Celite® and purified by flash column chromatography.

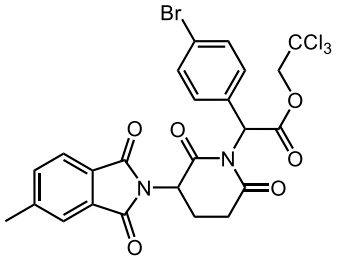

3.4

2,2,2-trichloroethyl 2-(4-bromophenyl)-2-(3-(5-methyl-1,3-dioxoisoindolin-2-yl)-2,6-dioxopiperidin-1-yl)acetate (3.4).

2-(2,6-dioxopiperidin-3-yl)-5-methylisoindoline-1,3-dione (54 mg, 1.0 equiv, 0.20 mmol) and Rh_2(*S*-p-Ph-TPCP)$_4$ (3.5 mg, 1 mol%, 2.0 µmol) were charged to an oven-dried vial under inert atmosphere along with ~200% w/w 4Å molecular sieves. The vial was charged with 1.0 mL dry CH_2Cl_2 via syringe. A solution of 2,2,2-trichloroethyl 2-(4-bromophenyl)-2-diazoacetate (82 mg, 1.1 Eq, 0.22 mmol) was prepared under inert atmosphere in 1.0 mL dry CH_2Cl_2 and added to the stirred reaction at room temperature over the course of thirty minutes, using a syringe pump. The reaction was allowed to stir for 17 hours following addition, after which the reaction was dry-mounted onto Celite® and purified by flash column chromatography (SiO_2, 1:1 ethyl acetate:hexanes), which produced 2,2,2-trichloroethyl 2-(4-bromophenyl)-2-(3-(5-methyl-1,3-dioxoisoindolin-2-yl)-2,6-dioxopiperidin-1-yl)acetate (**3.4**) as an amorphous white solid (43 mg, 70 µmol, 35% yield).

HRMS (APCI) *m/z*: $[M+H]^+$ calcd for $C_{24}H_{19}O_6N_2{}^{79}Br^{35}Cl_3$ 614.9487; Found 614.9488

^{1}H NMR (500 MHz, $CDCl_3$): 7.75 – 7.69 (m, 1H), 7.67 – 7.63 (m, 1H), 7.561 and 7.556 (d, *J* = 8.6 Hz, 1H), 7.53 – 7.50 (m, 2H), 7.431 and 7.427 (d, *J* = 8.6 Hz, 1H), 6.45 and 6.41 (s, 1H), 4.92 and 4.86 (dd, *J* = 13.3, 5.7 Hz, 1H, partially obscured by signals at 4.904 and 4.902), 4.904 and 4.902 (d, *J* = 11.9 Hz, 1H, partially obscured by signal at 4.92), 4.67 and 4.60 (d, *J* = 11.9 Hz), 3.09 – 2.72 (m, 3H), 2.51 (s, 3H), 2.27 – 2.13 (m, 1H).

^{13}C{^{1}H} NMR (151 MHz, $CDCl_3$): δ 179.2, 179.1, 175.6, 175.4, 167.9, 167.84, 167.75, 167.71, 166.5, 166.3, 145.7, 134.9, 132.4, 132.3, 132.3, 131.7, 131.5, 129.7, 129.6, 129.5, 124.29, 124.27, 123.7, 94.28, 94.26, 76.02, 76.98, 74.7, 74.6, 49.93, 49.85, 27.7, 27.6, 23.0, 22.9, 22.2.

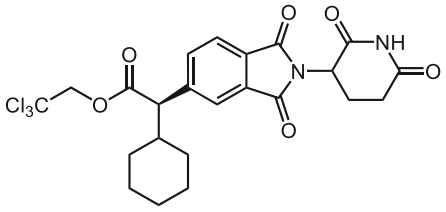

3.9a

2,2,2-trichloroethyl (2*R*)-2-cyclohexyl-2-(2-(2,6-dioxopiperidin-3-yl)-1,3-dioxoisoindolin-5-yl)acetate (3.9a).

Compound **3.9a** was produced via **GP1** using **3.6a** (47 mg, 1.0 equiv, 0.10 mmol), 1,1,1,3,3,3-hexafluoroisopropanol (0.11 mL, 10.0 equiv, 1.00 mmol), Rh_2(*S-tetra*-p-Br-PPTTL)$_4$ (20 mM in CH_2Cl_2, 50 µL, 1 mol%, 1.0 µmol), and cyclohexane (1.0 mL). Purification via flash column chromatography (SiO_2, 20% to 50% ethyl acetate in hexanes) produced 2,2,2-trichloroethyl (2*R*)-2-cyclohexyl-2-(2-(2,6-dioxopiperidin-3-yl)-1,3-dioxoisoindolin-5-yl)acetate **(9a)** as an amorphous white solid (47 mg, 89 µmol, 89% yield).

Compound **3.9a** was produced via **GP2** using **3.6a** (47 mg, 1.0 equiv, 0.10 mmol), 1,1,1,3,3,3-hexafluoroisopropanol (0.11 mL, 10.0 equiv, 1.00 mmol), Rh_2(*S-tetra*-p-Br-PPTTL)$_4$ (20 mM in CH_2Cl_2, 50 µL, 1 mol%, 1.0 µmol), CH_2Cl_2 (0.5 mL), and cyclohexane (0.5 mL). Purification via flash column chromatography (SiO_2, 20% to 50% ethyl acetate in hexanes) produced 2,2,2-trichloroethyl (2*R*)-2-cyclohexyl-2-(2-(2,6-dioxopiperidin-3-yl)-1,3-dioxoisoindolin-5-yl)acetate **(3.9a)** as an amorphous white solid (47 mg, 89 µmol, 89% yield).

Compound **3.9a** was prepared via **GP3** using **3.6a** (47 mg, 1.0 equiv, 0.10 mmol), Rh_2(*S-tetra*-p-Br-PPTTL)$_4$ (3.7 mg, 1 mol%, 1.0 µmol), 2,2,2-trichloroethyl 2-diazo-2-(2-(2,6-dioxopiperidin-3-yl)-1,3-dioxoisoindolin-5-yl)acetate (**1c**) (47 mg, 1.0 equiv, 0.10 mmol), 1,1,1,3,3,3-hexafluoropropan-2-ol (0.10 mL, 10.0 equiv, 1.0 mmol), and 1.0 mL CH_2Cl_2 at room temperature with a one hour slow addition of diazo and 0.5 h additional stirring. Purification via flash column chromatography (SiO_2, gradient of 20% to 50% EtOAc in hexanes) afforded 2,2,2-trichloroethyl (2*R*)-2-cyclohexyl-2-(2-(2,6-dioxopiperidin-3-yl)-1,3-dioxoisoindolin-5-yl)acetate **(3.9a)** as an amorphous white solid (47 mg, 89 µmol, 89% yield).

HRMS (APCI) *m/z*: $[M+H]^+$ calcd for $C_{23}H_{24}O_6N_2{}^{35}Cl_3$ 529.0695; Found 529.0697

^{1}H NMR (400 MHz, $CDCl_3$, reported as a mixture of diastereomers): δ 8.09 (s, 1H), 7.94 (d, *J* = 1.6 Hz, 1H), 7.84 (d, *J* = 7.7 Hz, 1H), 7.76 (dd, *J* = 7.8, 1.7 Hz, 1H), 4.99 (dd, *J* = 12.5, 5.3 Hz, 1H), 4.79 (d, *J* = 11.9 Hz, 1H), 4.65 (d, *J* = 12.0 Hz, 1H), 3.58 (d, *J* = 10.5 Hz, 1H), 3.01 – 2.87 (m, 1H), 2.87 – 2.68 (m, 2H), 2.26 – 2.09 (m, 2H), 1.99 – 1.83 (m, 1H), 1.82 – 1.73 (m, 1H), 1.69 – 1.61 (m, 2H), 1.41 – 1.29 (m, 2H), 1.22 – 1.08 (m, 3H), 0.94 – 0.75 (m, 1H).

^{13}C{^{1}H} NMR (151 MHz, $CDCl_3$, reported as a mixture of diastereomers): δ 171.2, 171.0, 168.2, 167.1, 167.0, 144.7, 135.2, 132.3, 131.0, 124.27, 124.25, 124.1, 94.7, 74.4, 58.9, 49.5, 41.4, 31.8, 31.5, 30.4, 26.1, 25.9, 25.8, 22.7.

SFC analysis: Using **GP1**, **3.9a** (Trefoil® AMY1, 30% 1:1 MeOH:^{i}PrOH with 0.2% formic acid in CO_2, 2.5 mL/min, 210 nm) indicated 98:2 d.r. for asymmetric induction observed at the newly

formed stereogenic center: t_R (major diastereomers) = 2.43 and 6.85 min., t_R (minor diastereomers) = 2.2 and 5.4 min. Using **GP2**, **3.9a** indicated 99:1 d.r. Using **GP3**, **3.9a** indicated 99:1 d.r.

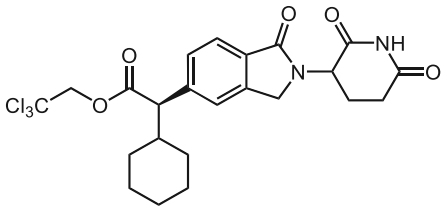

3.9b

2,2,2-trichloroethyl (2*R*)-2-cyclohexyl-2-(2-(2,6-dioxopiperidin-3-yl)-1-oxoisoindolin-5-yl)acetate (3.9b).

Compound **3.9b** was produced via **GP1** using **3.6b** (46 mg, 1.0 equiv, 0.10 mmol), 1,1,1,3,3,3-hexafluoroisopropanol (0.11 mL, 10.0 equiv, 1.00 mmol), Rh_2(*S*-*tetra*-p-Br-PPTTL)$_4$ (20 mM in CH_2Cl_2, 50 µL, 1 mol%, 1.0 µmol), and cyclohexane (1.0 mL). Purification via flash column chromatography (SiO_2, 40% to 100% ethyl acetate in hexanes) produced 2,2,2-trichloroethyl (2*R*)-2-cyclohexyl-2-(2-(2,6-dioxopiperidin-3-yl)-1-oxoisoindolin-5-yl)acetate **(3.9b)** as an amorphous white solid (42 mg, 82 µmol, 82% yield).

Compound **3.9b** was prepared via **GP3** using **3.6b** (46 mg, 1.0 equiv, 0.10 mmol), Rh_2(*S*-*tetra*-p-Br-PPTTL)$_4$ (3.7 mg, 1 mol%, µ.0 mmol), 1,1,1,3,3,3-hexafluoropropan-2-ol (0.10 mL, 10.0 equiv, 1.0 mmol), and 1.0 mL CH_2Cl_2 at room temperature with a one hour slow addition of diazo and 0.5 h additional stirring. Purification via flash column chromatography (SiO_2, gradient of 40% to 100% EtOAc in hexanes) afforded 2,2,2-trichloroethyl (2*R*)-2-cyclohexyl-2-(2-(2,6-dioxopiperidin-3-yl)-1-oxoisoindolin-5-yl)acetate **(3.9b)** as an amorphous white solid (24 mg, 46 µmol, 46% yield).

HRMS (APCI) *m/z*: $[M+H]^+$ calcd for $C_{23}H_{26}O_5N_2{}^{35}Cl_3$ 515.0902; Found 515.0902
^{1}H NMR (400 MHz, $CDCl_3$, reported as a mixture of diastereomers): δ 8.12 and 8.09 (s, 1H), 7.84 (d, *J* = 7.9 Hz, 1H), 7.53 and 7.50 (s, 1H), 7.47 (d, *J* = 8.6 Hz, 1H), 5.23 and 5.22 (dd, *J* = 13.4, 5.1 Hz, 1H), 4.799 and 4.796 (d, *J* = 12.0 Hz, 1H), 4.62 and 4.61 (d, *J* = 11.9 Hz, 1H), 4.50 and 4.48 (d, *J* = 16.1 Hz, 1H), 4.35 and 4.32 (d, *J* = 16.0 Hz, 1H), 3.51 and 3.50 (d, *J* = 10.6 Hz, 1H), 3.01 – 2.76 (m, 2H), 2.45 – 2.28 (m, 1H), 2.28 – 2.16 (m, 1H), 2.15 – 2.06 (m, 1H), 1.94 – 1.85 (m, 1H), 1.81 – 1.73 (m, 1H), 1.68 – 1.54 (m, 2H), 1.39 – 1.04 (m, 5H), 0.88 – 0.74 (m, 1H).
^{13}C{^{1}H} NMR (151 MHz, $CDCl_3$, reported as a mixture of diastereomers): δ 171.8, 171.7, 171.2, 169.69, 169.67, 169.1, 142.0, 141.7, 131.0, 129.5, 129.3, 124.40, 124.37, 123.3, 123.1, 94.8, 74.3, 59.0, 58.9, 52.0, 51.9, 47.09, 47.06, 32.0, 31.7, 30.5, 26.2, 26.0, 25.9, 23.56, 23.55.
SFC analysis: Using **GP1**, **3.9b** (CHIRALCEL® OZ-3, 20% 1:1 MeOH:^{i}PrOH with 0.2% formic acid in CO_2, 2.5 mL/min, 210 nm) indicated 97:3 d.r. for asymmetric induction observed at the newly formed stereogenic center: t_R (major diastereomers) = 6.7 and 15.8 min., t_R (minor diastereomers) = 7.2 and 15.0 min. Using **GP3**, **3.9a** indicated 98:2 d.r.

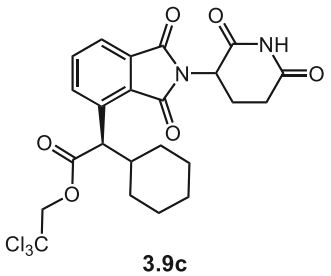

3.9c

2,2,2-trichloroethyl (2*R*)-2-cyclohexyl-2-(2-(2,6-dioxopiperidin-3-yl)-1,3-dioxoisoindolin-4-yl)acetate (3.9c).

Compound **3.9c** was produced via **GP1** using **3.6c** (47 mg, 1.0 equiv, 0.10 mmol), 1,1,1,3,3,3-hexafluoroisopropanol (0.11 mL, 10.0 equiv, 1.00 mmol), Rh_2(*S*-*tetra*-p-Br-PPTTL)$_4$ (20 mM in CH_2Cl_2, 50 µL, 1 mol%, 1.0 µmol), and cyclohexane (1.0 mL). Purification via flash column chromatography (SiO_2, gradient of 20% to 50% EtOAc in hexanes) afforded 2,2,2-trichloroethyl (2*R*)-2-cyclohexyl-2-(2-(2,6-dioxopiperidin-3-yl)-1,3-dioxoisoindolin-4-yl)acetate **(9c)** as an amorphous white solid (32 mg, 61 µmol, 61% yield).

Compound **3.9c** was prepared via **GP3** using cyclohexane (0.11 mL, 10.0 equiv, 1.0 mmol), Rh_2(*S*-*tetra*-p-Br-PPTTL)$_4$ (3.7 mg, 1 mol%, 1.0 µmol), **3.6c** (47 mg, 1.0 equiv, 0.10 mmol), 1,1,1,3,3,3-hexafluoropropan-2-ol (0.10 mL, 10.0 equiv, 1.0 mmol), and 1.0 mL CH_2Cl_2 at room temperature with a one hour slow addition of diazo and 0.5 h additional stirring. Purification via flash column chromatography (SiO_2, gradient of 20% to 50% EtOAc in hexanes) afforded 2,2,2-trichloroethyl (2*R*)-2-cyclohexyl-2-(2-(2,6-dioxopiperidin-3-yl)-1,3-dioxoisoindolin-4-yl)acetate **(9c)** as an amorphous white solid (25 mg, 47 µmol, 47% yield).

HRMS (APCI) *m/z*: $[M+H]^+$ calcd for $C_{23}H_{24}O_6N_2{}^{35}Cl_3$ 529.0695; Found 529.0700

^{1}H NMR (600 MHz, $CDCl_3$, reported as a mixture of diastereomers): δ 8.10 (s, 1H), 7.95 (d, *J* = 7.9 Hz, 1H), 7.80 (ddd, *J* = 7.4, 2.9, 1.0 Hz, 1H), 7.72 (ddd, *J* = 8.0, 7.3, 1.0 Hz, 1H), 5.00 (d, *J* = 10.2 Hz, 1H, overlapping with dd at 4.99), 4.99 (dd, *J* = 15.7, 4.8 Hz, 1H, overlapping with d at 5.00), 4.76 – 4.59 (m, 2H), 2.94 – 2.88 (m, 1H), 2.87 – 2.69 (m, 2H), 2.22 – 2.12 (m, 2H), 1.97 – 1.90 (m, 1H), 1.82 – 1.74 (m, 1H), 1.68 – 1.61 (m, 2H), 1.37 – 1.28 (m, 2H), 1.22 – 1.12 (m, 3H), 1.01 – 0.91 (m, 1H).

^{13}C{^{1}H} NMR (151 MHz, $CDCl_3$, reported as a mixture of diastereomers): δ 171.11, 171.08, 170.9, 167.93, 167.90, 167.8, 167.7, 166.8, 137.6, 134.8, 134.7, 134.59, 134.57, 132.1, 129.2, 129.1, 123.99, 123.97, 94.82, 94.81, 74.2, 50.4, 50.3, 49.41, 49.37, 41.3, 41.2, 31.68, 31.66, 31.51, 31.49, 30.1, 30.0, 26.1, 26.00, 25.98, 22.77, 22.76.

SFC analysis: Using **GP1**, **3.9c** (CHIRALPAK® AS-3, 15% 1:1 MeOH:^{i}PrOH with 0.2% formic acid in CO_2, 2.5 mL/min, 210 nm) indicated 73:27 d.r. for asymmetric induction observed at the newly formed stereogenic center: t_R (major diastereomers) = 2.5 and 3.1 min., t_R (minor diastereomers) = 1.6 and 1.8 min. Using **GP3**, **3.9c** indicated 76:24 d.r.

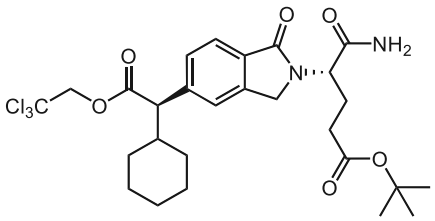

***(S,R)*-3.10a**

***tert*-butyl (*S*)-5-amino-4-(5-((*R*)-1-cyclohexyl-2-oxo-2-(2,2,2-trichloroethoxy)ethyl)-1-oxoisoindolin-2-yl)-5-oxopentanoate ((*S,R)*-3.10a).**

Compound **(*S,R)*-3.10a** was produced via **GP1** using **3.8a** (53 mg, 1.0 equiv, 0.10 mmol), 1,1,1,3,3,3-hexafluoroisopropanol (0.11 mL, 10.0 equiv, 1.00 mmol), Rh_2(*S-tetra*-p-Br-PPTTL)$_4$ (20 mM in CH_2Cl_2, 50 µL, 1 mol%, 1.0 µmol), and cyclohexane (1.0 mL). Purification via flash column chromatography (SiO_2, 40% to 100% ethyl acetate in hexanes) produced *tert*-butyl (*S*)-5-amino-4-(5-((*R*)-1-cyclohexyl-2-oxo-2-(2,2,2-trichloroethoxy)ethyl)-1-oxoisoindolin-2-yl)-5-oxopentanoate (**(*S,R)*-3.10a**) as an amorphous white solid (42 mg, 71 µmol, 71% yield).

Compound **(*S,R)*-3.10a** was prepared via **GP4** using **3.8a** (53 mg, 1.0 equiv, 0.10 mmol), Rh_2(*S-tetra*-p-Br-PPTTL)$_4$ (3.7 mg, 1 mol%, 1.0 µmol), 1,1,1,3,3,3-hexafluoropropan-2-ol (0.10 mL, 10.0 equiv, 1.0 mmol), and 1.0 mL CH_2Cl_2 at room temperature with a three hour slow addition of diazo and 0.5 h additional stirring.. Purification via flash column chromatography (SiO_2, gradient of 40% to 100% EtOAc in hexanes) afforded *tert*-butyl (*S*)-5-amino-4-(5-((*R*)-1-cyclohexyl-2-oxo-2-(2,2,2-trichloroethoxy)ethyl)-1-oxoisoindolin-2-yl)-5-oxopentanoate (**(*S,R)*-3.10a**) as an amorphous white solid (36 mg, 60 µmol, 60% yield).

HRMS (APCI) *m/z*: $[M+H]^+$ calcd for $C_{27}H_{36}O_6N_2{}^{35}Cl_3$ 589.1634; Found 589.1638
^{1}H NMR (600 MHz, $CDCl_3$): δ 7.78 (d, *J* = 7.9 Hz, 1H), 7.50 (s, 1H), 7.46 (dd, *J* = 7.9, 1.5 Hz, 1H), 6.34 (s, 1H), 5.46 (s, 1H), 4.90 (dd, *J* = 8.9, 6.3 Hz, 1H), 4.79 (d, *J* = 12.0 Hz, 1H), 4.61 (d, *J* = 12.0 Hz, 1H), 4.54 (d, *J* = 17.0 Hz, 1H), 4.43 (d, *J* = 17.0 Hz, 1H), 3.49 (d, *J* = 10.6 Hz, 1H), 2.42 – 2.29 (m, 2H), 2.28 – 2.19 (m, 1H), 2.19 – 2.07 (m, 2H), 1.92 – 1.85 (m, 1H), 1.79 – 1.74 (m, 1H), 1.68 – 1.60 (m, 2H), 1.41 (s, 9H), 1.36 – 1.27 (m, 2H), 1.21 – 1.09 (m, 3H), 0.80 (qd, *J* = 11.9, 3.6 Hz, 1H).
^{13}C{^{1}H} NMR (151 MHz, $CDCl_3$): δ 171.9, 171.8, 171.7, 169.1, 142.2, 141.6, 131.3, 129.3, 124.1, 123.3, 94.8, 81.0, 74.3, 59.0, 54.1, 47.3, 41.3, 32.02, 31.99, 30.5, 28.2, 26.2, 26.0, 25.9, 24.3.
SFC analysis: Using **GP1**, **(*S,R)*-3.10a** (CHIRALCEL® OJ-3, 5% 1:1 MeOH:^{i}PrOH with 0.2% formic acid in CO_2, 2.5 mL/min, 210 nm) indicated 98:2 d.r. for asymmetric induction observed at the newly formed stereogenic center: t_R (major diastereomer) = 7.2 min., t_R (minor diastereomer) = 5.6 min. Using **GP4**, **(*S,R)*-3.10a** indicated 98:2 d.r.
Specific Rotation: Specific Rotation: $[\alpha]_D^{22}$ -49.5 (*c* 1, $CHCl_3$)

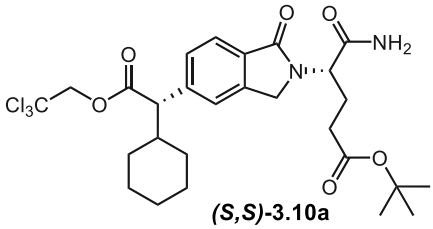

***(S,S)*-3.10a**

***tert*-butyl (*S*)-5-amino-4-(5-((*S*)-1-cyclohexyl-2-oxo-2-(2,2,2-trichloroethoxy)ethyl)-1-oxoisoindolin-2-yl)-5-oxopentanoate ((*S,S)*-3.10a)**

Compound **(*S,S)*-3.10a** was prepared via **GP4** using **3.8a** (53 mg, 1.0 equiv, 0.10 mmol), Rh_2(*R*-*tetra*-p-Br-PPTTL)$_4$ (3.7 mg, 1 mol%, 1.0 µmol), 1,1,1,3,3,3-hexafluoropropan-2-ol (0.10 mL, 10.0 equiv, 1.0 mmol), and 1.0 mL CH_2Cl_2 at room temperature with a three hour slow addition of diazo and 0.5 h additional stirring.. Purification via flash column chromatography (SiO_2, gradient of 40% to 100% EtOAc in hexanes) afforded *tert*-butyl (*S*)-5-amino-4-(5-((*S*)-1-cyclohexyl-2-oxo-2-(2,2,2-trichloroethoxy)ethyl)-1-oxoisoindolin-2-yl)-5-oxopentanoate **(*S,S)*-3.10a** as an amorphous white solid (9.3 mg, 16 µmol, 16% yield).

HRMS (APCI) *m/z*: $[M+H]^+$ calcd for $C_{27}H_{36}O_6N_2{}^{35}Cl_3$ 589.1634; Found 589.1633
^{1}H NMR (600 MHz, $CDCl_3$): δ 7.79 (d, *J* = 7.9 Hz, 1H), 7.51 (d, *J* = 1.4 Hz, 1H), 7.47 (dd, *J* = 7.9, 1.5 Hz, 1H), 6.25 (s, 1H), 5.35 (s, 1H), 4.89 (dd, *J* = 9.0, 6.3 Hz, 1H), 4.79 (d, *J* = 12.0 Hz, 1H), 4.62 (d, *J* = 12.0 Hz, 1H), 4.50 (d, *J* = 17.0 Hz, 1H), 4.45 (d, *J* = 17.0 Hz, 1H), 3.50 (d, *J* = 10.7 Hz, 1H), 2.42 – 2.30 (m, 2H), 2.29 – 2.21 (m, 1H), 2.20 – 2.10 (m, 2H), 1.93 – 1.86 (m, 1H), 1.80 – 1.72 (m, 1H), 1.67 – 1.63 (m, 2H), 1.41 (s, 9H), 1.35 – 1.27 (m, 2H), 1.22 – 1.04 (m, 3H), 0.84 – 0.74 (m, 1H).
^{13}C{^{1}H} NMR (151 MHz, $CDCl_3$): δ 171.9, 171.9, 171.8, 171.7, 169.1, 142.2, 141.5, 131.3, 129.2, 124.0, 123.4, 94.8, 81.0, 74.3, 59.0, 54.1, 47.3, 41.3, 32.0, 32.0, 30.5, 28.2, 26.2, 26.0, 25.9, 24.3.
SFC analysis: Using **GP4**, **(*S,S)*-3.10a** (CHIRALCEL® OJ-3, 5% 1:1 MeOH:^{i}PrOH with 0.2% formic acid in CO_2, 2.5 mL/min, 210 nm) indicated 93:7 d.r. for asymmetric induction observed at the newly formed stereogenic center: t_R (major diastereomer) = 5.6 min., t_R (minor diastereomer) = 7.2 min.

Specific Rotation: $[\alpha]_D^{22}$ -52.7 (*c* 0.5, $CHCl_3$).

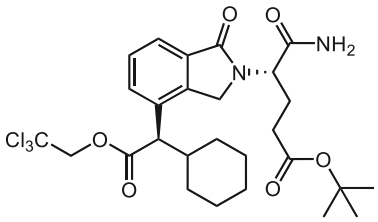

3.10b

***tert*-butyl (*S*)-5-amino-4-(4-((*R*)-1-cyclohexyl-2-oxo-2-(2,2,2-trichloroethoxy)ethyl)-1-oxoisoindolin-2-yl)-5-oxopentanoate (3.10b).**

Compound **3.10b** was produced via **GP1** using **3.8b** (53 mg, 1.0 equiv, 0.10 mmol), 1,1,1,3,3,3-hexafluoroisopropanol (0.11 mL, 10.0 equiv, 1.00 mmol), Rh_2(*S*-*tetra*-p-Br-PPTTL)$_4$ (20 mM in

CH_2Cl_2, 50 µL, 1 mol%, 1.0 µmol), and cyclohexane (1.0 mL). Purification via flash column chromatography (SiO_2, gradient of 20% to 100% EtOAc in hexanes) afforded *tert*-butyl (*S*)-5-amino-4-(4-((*R*)-1-cyclohexyl-2-oxo-2-(2,2,2-trichloroethoxy)ethyl)-1-oxoisoindolin-2-yl)-5-oxopentanoate **(3.10b)** as an amorphous white solid (47 mg, 79 µmol, 79% yield).

Compound **3.10b** was prepared via **GP4** using cyclohexane (0.10 mL, 10.0 equiv, 0.94 mmol), Rh_2(*S*-*tetra*-p-Br-PPTTL)$_4$ (3.5 mg, 1 mol%, 0.94 µmol), **3.8b** (50 mg, 1.0 equiv, 94 mmol), 1,1,1,3,3,3-hexafluoropropan-2-ol (99 µL, 10.0 equiv, 0.94 mmol), and 0.94 mL CH_2Cl_2 at room temperature with a three hour slow addition of diazo and 0.5 h additional stirring. Purification via flash column chromatography (SiO_2, gradient of 20% to 100% EtOAc in hexanes) afforded *tert*-butyl (*S*)-5-amino-4-(4-((*R*)-1-cyclohexyl-2-oxo-2-(2,2,2-trichloroethoxy)ethyl)-1-oxoisoindolin-2-yl)-5-oxopentanoate **(3.10b)** as an amorphous white solid (21 mg, 35 µmol, 37% yield).

HRMS (ESI) *m/z*: $[M+H]^+$ calcd for $C_{27}H_{36}O_6N_2{}^{35}Cl_3$ 589.1634, Found 589.1632
^{1}H NMR (400 MHz, $CDCl_3$): δ 7.76 (dd, *J* = 7.5, 1.0 Hz, 1H), 7.67 (dd, *J* = 7.8, 1.0 Hz, 1H), 7.48 (t, *J* = 7.6 Hz, 1H), 6.25 (s, 1H), 5.30 (s, 1H), 4.90 (dd, *J* = 8.2, 6.7 Hz, 1H), 4.70 (d, *J* = 11.9 Hz, 1H), 4.64 (d, *J* = 12.0 Hz, 1H), 4.50 (d, *J* = 16.9 Hz, 1H), 3.46 (d, *J* = 11.0 Hz, 1H), 2.48 – 2.33 (m, 2H), 2.32 – 2.10 (m, 3H), 1.99 – 1.88 (m, 1H), 1.85 – 1.75 (m, 1H), 1.72 – 1.52 (m, 3H), 1.41 (s, 9H), 1.23 – 1.12 (m, 4H), 0.92 – 0.62 (m, 1H).
^{13}C{^{1}H} NMR (151 MHz, $CDCl_3$): δ 171.9, 171.5, 171.1, 169.3, 141.4, 132.4, 132.2, 131.2, 129.1, 123.2, 94.7, 81.0, 74.2, 54.6, 54.2, 46.8, 39.9, 32.0, 30.3, 28.2, 26.2, 25.95, 25.92, 24.2.
SFC analysis: Using **GP1**, **3.10b** (Trefoil® AMY1, 20% 1:1 MeOH:^{i}PrOH with 0.2% formic acid in CO_2, 1.5 mL/min, 210 nm) indicated 99:1 d.r. for asymmetric induction observed at the newly formed stereogenic center: t_R (major diastereomer) = 2.7 min., t_R (minor diastereomer) = 1.2 min. Using **GP4**, **3.10b** indicated 98:2 d.r.
Specific Rotation: $[\alpha]_D^{24}$ -106.2 (c 0.25, $CHCl_3$).

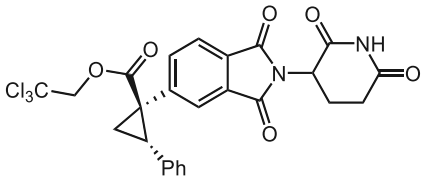

3.11a

2,2,2-trichloroethyl (1*R*,2*S*)-1-(2-(2,6-dioxopiperidin-3-yl)-1,3-dioxoisoindolin-5-yl)-2-phenylcyclopropane-1-carboxylate (3.11a).

Compound **3.11a** was prepared via **GP5** using styrene (57 µL, 5.0 equiv, 0.50 mmol), Rh_2(*S*-*tetra*-p-Br-PPTTL)$_4$ (3.7 mg, 1 mol%, 1.0 µmol), **3.6a** (47 mg, 1.0 equiv, 0.10 mmol), 1,1,1,3,3,3-hexafluoropropan-2-ol (0.10 mL, 10.0 equiv, 1.0 mmol), and 1.0 mL CH_2Cl_2 at room temperature with a 0.25 hour slow addition of diazo and 0.5 h additional stirring. Purification via flash column chromatography (SiO_2, gradient of 30% to 50% EtOAc in hexanes) afforded 2,2,2-trichloroethyl (1*R*,2*S*)-1-(2-(2,6-dioxopiperidin-3-yl)-1,3-dioxoisoindolin-5-yl)-2-phenylcyclopropane-1-carboxylate **(3.11a)** as an amorphous white solid (50 mg, 90 µmol, 90% yield).

HRMS (APCI) *m/z*: $[M+H]^+$ calcd for $C_{25}H_{20}O_6N_2{}^{35}Cl_3$ 549.0382; Found 549.0381

^{1}H NMR (400 MHz, $CDCl_3$, reported as a mixture of diastereomers): δ 8.15 (s, 1H), 7.74 – 7.67 (m, 1H), 7.59 (dd, *J* = 7.8, 2.4 Hz, 1H), 7.38 (dt, *J* = 7.8, 1.7 Hz, 1H), 7.17 – 7.07 (m, 3H), 6.92 – 6.80 (m, 2H), 4.94 and 4.93 (dd, *J* = 12.3, 5.4 Hz, 1H), 4.87 and 4.86 (d, *J* = 12.0 Hz, 1H), 4.64 (d, *J* = 11.9 Hz, 1H), 3.36 (dd, *J* = 9.4, 7.6 Hz, 1H), 2.94 – 2.85 (m, 1H), 2.84 – 2.64 (m, 2H), 2.39 (dd, *J* = 9.4, 5.5 Hz, 1H), 2.15-2.09 (m, 1H, obfuscated by dd at 2.13), 2.13 (dd, *J* = 7.8, 5.6 Hz, 1H, obfuscated by m from 2.15-2.09).

^{13}C{^{1}H} NMR (151 MHz, $CDCl_3$, reported as a mixture of diastereomers): δ 171.0, 170.8, 168.1, 167.09, 167.06, 167.02, 167.00, 141.9, 138.82, 138.76, 134.4, 131.6, 131.5, 130.7, 128.6, 128.2, 127.5, 127.1, 127.0, 123.2, 94.9, 74.6, 49.41, 49.39, 37.1, 34.7, 31.47, 31.45, 22.8, 22.7, 20.04, 20.03.

SFC analysis: Using **GP5**, **3.11a** (CHIRALCEL® OZ-3, 20% 1:1 MeOH:^{i}PrOH with 0.2% formic acid in CO_2, 2.5 mL/min, 210 nm) indicated 86:14 d.r. for asymmetric induction observed from formation of the major relative diasteromer: t_R (major diastereomers) = 7.3 and 8.8 min., t_R (minor diastereomers) = 6.1 and 6.8 min.

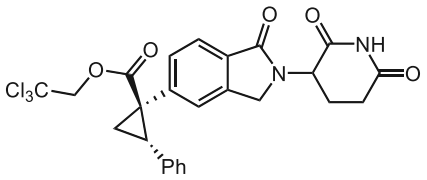

3.11b

2,2,2-trichloroethyl (1*R*,2*S*)-1-(2-(2,6-dioxopiperidin-3-yl)-1-oxoisoindolin-5-yl)-2-phenylcyclopropane-1-carboxylate (3.11b).

Compound **3.11b** was prepared via **GP5** using styrene (57 µL, 5.0 equiv, 0.50 mmol), Rh_2(*S*-*tetra*-p-Br-PPTTL)$_4$ (3.7 mg, 1 mol%, 1.0 µmol), **3.6b** (47 mg, 1.0 equiv, 0.10 mmol), 1,1,1,3,3,3-hexafluoropropan-2-ol (0.10 mL, 10.0 equiv, 1.0 mmol), and 1.0 mL CH_2Cl_2 at room temperature with a 0.25 hour slow addition of diazo and 0.5 h additional stirring. Purification via flash column chromatography (SiO_2, gradient of 40% to 100% EtOAc in hexanes) afforded 2,2,2-trichloroethyl (1*R*,2*S*)-1-(2-(2,6-dioxopiperidin-3-yl)-1-oxoisoindolin-5-yl)-2-phenylcyclopropane-1-carboxylate **(3.11b)** as an amorphous white solid (45 mg, 83 µmol, 83% yield).

HRMS (APCI) *m/z*: $[M+H]^+$ calcd for $C_{25}H_{22}O_5N_2{}^{35}Cl_3$ 535.0589; Found 535.0591

^{1}H NMR (600 MHz, $CDCl_3$, reported as a mixture of diastereomers): δ 8.01 and 8.00, (s, 1H), 7.66 and 7.63 (d, *J* = 7.9 Hz, 1H), 7.24 and 7.17 (d, *J* = 8.0 Hz, 1H), 7.21 and 7.15 (s, 1H), 7.12 – 7.05 (m, 3H), 6.89 – 6.76 (m, 2H), 5.17 and 5.16 (dd, *J* = 13.6, 5.0 Hz, 1H), 4.855 and 4.849 (d, *J* = 11.9 Hz, 1H), 4.64 (d, *J* = 11.9 Hz, 1H), 4.39 and 4.29 (d, *J* = 15.8 Hz, 1H), 4.21 and 4.14 (d, *J* = 15.9 Hz, 1H), 3.29 (t, *J* = 8.4 Hz, 1H), 2.95 – 2.86 (m, 1H), 2.85 – 2.74 (m, 1H), 2.41 – 2.33 (m, 1H), 2.33 – 2.25 (m, 1H), 2.21 – 2.12 (m, 1H), 2.10 – 2.03 (m, 1H).

$^{13}C\{^1H\}$ NMR (151 MHz, $CDCl_3$, reported as a mixture of diastereomers): δ 171.5, 171.0, 169.55, 169.51, 169.1, 141.1, 141.0, 138.71, 138.69, 135.14, 135.09, 132.6, 132.5, 130.7, 130.6, 128.3, 128.19, 128.17, 127.2, 127.1, 126.64, 126.67, 123.6, 123.6, 95.1, 74.5, 52.0, 51.9, 46.94, 46.89, 37.4, 37.3, 34.4, 34.3, 31.6, 23.54, 23.51, 20.5, 20.4.
SFC analysis: **3.11b** (CHIRALPAK® AS-3, 20% 1:1 MeOH:^{i}PrOH with 0.2% formic acid in CO_2, 2.5 mL/min, 210 nm) indicated 86:16 d.r. for asymmetric induction arising from formation of the major relative diastereomer using **GP5**: t_R (major diastereomer) = 2.50 min., t_R (minor diastereomer) = 2.84 min, t_R (inseparable major + minor) = 1.92 min.
Note: The other two diastereomers represented by the peak at 1.92 min were inseparable, and the d.r. was acquired from the diastereomers at 2.50 and 2.84 min only. Suppression of the peak at 1.92 min. in the chromatogram for **SI4** indicates that these diastereomers correspond to both diastereomers of the cyclopropane with *R* glutarimide stereogenic centers.

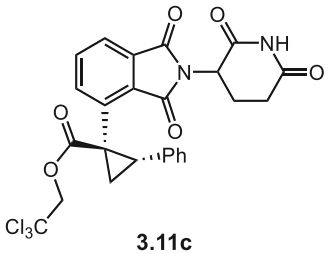

3.11c

2,2,2-trichloroethyl (1*R*,2*S*)-1-(2-(2,6-dioxopiperidin-3-yl)-1,3-dioxoisoindolin-4-yl)-2-phenylcyclopropane-1-carboxylate (11c).

Compound **3.11c** was prepared via **GP5** using styrene (57 µL, 5.0 equiv, 0.50 mmol), Rh_2(*S*-*tetra*-p-Br-PPTTL)$_4$ (3.7 mg, 1 mol%, 1.0 µmol), **3.6c** (47 mg, 1.0 equiv, 0.10 mmol), 1,1,1,3,3,3-hexafluoropropan-2-ol (0.10 mL, 10.0 equiv, 1.0 mmol), and 1.0 mL CH_2Cl_2 at room temperature with a 0.25 hour slow addition of diazo and 0.5 h additional stirring. Purification via flash column chromatography (SiO_2, gradient of 20% to 40% EtOAc in hexanes) afforded 2,2,2-trichloroethyl (1*R*,2*S*)-1-(2-(2,6-dioxopiperidin-3-yl)-1,3-dioxoisoindolin-4-yl)-2-phenylcyclopropane-1-carboxylate **(3.11c)** as an amorphous white solid (40 mg, 73 µmol, 73% yield).

HRMS (APCI) *m/z*: $[M+H]^+$ calcd for $C_{25}H_{20}O_6N_2{}^{35}Cl_3$ 549.0382; Found 549.0385
^1H NMR (400 MHz, $CDCl_3$, reported as a mixture of diastereomers): δ 8.00 (s, 1H), 7.73 – 7.61 (m, 1H), 7.61 – 7.37 (m, 2H), 7.08 – 6.90 (m, 3H), 6.88 – 6.71 (m, 2H), 4.82 (dd, *J* = 12.0, 5.7 Hz, 2H), 4.75 (d, *J* = 11.9 Hz, 1H), 4.64 and 4.62 (d, *J* = 11.9 Hz, 1H), 3.59 – 3.43 (m, 1H), 2.95 – 2.80 (m, 1H), 2.77 – 2.58 (m, 2H), 2.38 – 2.26 (m, 1H), 2.22 and 2.17 (t, *J* = 6.6 Hz, 1H), 2.03 – 1.86 (m, 1H).
$^{13}C\{^1H\}$ NMR (151 MHz, $CDCl_3$, reported as a mixture of diastereomers): δ 170.99, 170.97, 170.6, 170.5, 167.63, 167.57, 166.9, 166.8, 166.7, 133.93, 133.90, 132.02, 131.99, 131.7, 128.4, 128.2, 127.94, 127.86, 127.12, 127.09, 122.94, 122.88, 94.6, 94.5, 75.3, 75.1, 49.1, 49.0, 34.3, 34.2, 34.1, 31.5, 31.4, 22.8, 22.5.
SFC analysis: Using **GP5**, **3.11c** (CHIRALPAK® AD-3, 20% 1:1 MeOH:^{i}PrOH with 0.2% formic acid in CO_2, 2.5 mL/min, 210 nm) indicated 60:40 d.r. for asymmetric induction observed

from formation of the major relative diasteromer: t_R (major diastereomers) = 2.0 and 2.5 min., t_R (minor diastereomers) = 2.2 and 3.5 min.

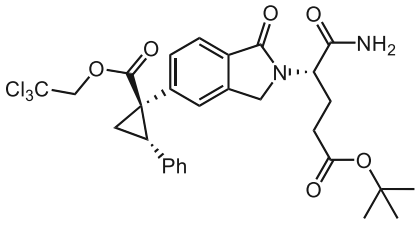

3.12a

2,2,2-trichloroethyl (1*R*,2*S*)-1-(2-((*S*)-1-amino-5-(*tert*-butoxy)-1,5-dioxopentan-2-yl)-1-oxoisoindolin-5-yl)-2-phenylcyclopropane-1-carboxylate (3.12a).

Compound **3.12a** was prepared via **GP6** using styrene (57 µL, 5.0 equiv, 0.50 mmol), Rh_2(*S*-*tetra*-p-Br-PPTTL)$_4$ (3.7 mg, 1 mol%, 1.0 µmol), **3.8a** (53 mg, 1.0 equiv, 0.10 mmol), 1,1,1,3,3,3-hexafluoropropan-2-ol (0.10 mL, 10.0 equiv, 1.0 mmol), and 1.0 mL CH_2Cl_2 at room temperature with a 0.25 hour slow addition of diazo and 0.5 h additional stirring. Purification via flash column chromatography (SiO_2, gradient of 40% to 100% EtOAc in hexanes) afforded 2,2,2-trichloroethyl (1*R*,2*S*)-1-(2-((*S*)-1-amino-5-(*tert*-butoxy)-1,5-dioxopentan-2-yl)-1-oxoisoindolin-5-yl)-2-phenylcyclopropane-1-carboxylate **(3.12a)** as an amorphous white solid (53 mg, 88 µmol, 88% yield).

HRMS (APCI) *m/z*: $[M+H]^+$ calcd for $C_{29}H_{32}O_6N_2{}^{35}Cl_3$, 609.1320; Found 609.1320.

^{1}H NMR (400 MHz, $CDCl_3$): δ 7.58 (d, *J* = 8.2 Hz, 1H), 7.20 – 7.14 (m, 2H), 7.11 – 7.03 (m, 3H), 6.81 (dd, *J* = 6.7, 2.9 Hz, 2H), 6.40 (s, 1H), 5.49 (s, 1H), 4.84 (d, *J* = 12.0 Hz) 4.83 (dd, *J* = 3.3, 2.8 Hz), 4.63 (d, *J* = 11.9 Hz, 1H), 4.32 (s, 2H), 3.29 (dd, *J* = 9.4, 7.5 Hz, 1H), 2.38 – 2.09 (m, 5H), 2.06 (dd, *J* = 7.4, 5.4 Hz, 1H), 1.40 (s, 9H).

^{13}C NMR (101 MHz, $CDCl_3$): δ 171.9, 171.7, 171.5, 169.1, 141.2, 138.5, 135.0, 132.4, 130.9, 128.3, 128.2, 127.2, 126.7, 123.2, 95.0, 81.0, 74.5, 54.0, 47.1, 37.3, 34.3, 32.0, 28.2, 24.2, 20.4.

SFC analysis: Using **GP6**, **3.12a** (Trefoil® CEL1, 10% 1:1 MeOH:^{i}PrOH with 0.2% formic acid in CO_2, 2.5 mL/min, 210 nm) indicated 91:9 d.r. for asymmetric induction observed from formation of the major relative diasteromer: t_R (major diastereomer) = 5.1 min., t_R (minor diastereomer) = 5.6 min.

Specific Rotation: $[\alpha]_D^{22}$ **-**40.5 (*c* 1.0, $CHCl_3$)

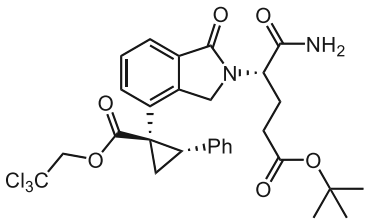

3.12b

2,2,2-trichloroethyl (1*R*,2*S*)-1-(2-((S)-1-amino-5-(*tert*-butoxy)-1,5-dioxopentan-2-yl)-1-oxoisoindolin-4-yl)-2-phenylcyclopropane-1-carboxylate (3.12b).

Compound **3.12b** was prepared via **GP6** using styrene (57 µL, 5.0 equiv, 0.50 mmol), Rh_2(*S*-*tetra*-p-Br-PPTTL)$_4$ (3.7 mg, 1 mol%, 1.0 µmol), **3.8b** (53 mg, 1.0 equiv, 0.10 mmol), 1,1,1,3,3,3-hexafluoropropan-2-ol (0.10 mL, 10.0 equiv, 1.0 mmol), and 1.0 mL CH_2Cl_2 at room temperature with a 0.25 hour slow addition of diazo and 0.5 h additional stirring. Purification via flash column chromatography (SiO_2, gradient of 40% to 100% EtOAc in hexanes) afforded 2,2,2-trichloroethyl (1*R*,2*S*)-1-(2-((*S*)-1-amino-5-(*tert*-butoxy)-1,5-dioxopentan-2-yl)-1-oxoisoindolin-4-yl)-2-phenylcyclopropane-1-carboxylate **(3.12b)** as an amorphous white solid (51 mg, 84 µmol, 84% yield).

HRMS (ESI) *m/z*: $[M+H]^+$ calcd for $C_{29}H_{32}O_6N_2{}^{35}Cl_3$, 609.1321; Found 609.1316.

^{1}H NMR (400 MHz, $CDCl_3$) δ 7.75 – 7.68 (m, 1H), 7.48 – 7.35 (m, 2H), 7.11 – 6.97 (m, 3H), 6.84 – 6.66 (m, 2H), 5.72 (s, 1H), 5.11 (s, 1H), 4.79 (d, *J* = 11.9 Hz, 1H), 4.74 (dd, *J* = 9.0, 6.1 Hz, 1H), 4.68 (d, *J* = 11.9 Hz, 1H), 4.37 (d, *J* = 17.1 Hz, 1H), 3.65 (d, *J* = 17.1 Hz, 1H), 3.27 (dd, *J* = 9.6, 7.4 Hz, 1H), 2.39 (dd, *J* = 9.5, 5.1 Hz, 1H), 2.35 – 2.21 (m, 2H), 2.19 – 2.08 (m, 1H), 2.01 – 1.91 (m, 1H, partially obscured by signal at 2.00), 2.00 (dd, *J* = 7.4, 5.3 Hz, 1H), 1.41 (s, 8H).

^{13}C{^{1}H} NMR (151 MHz, $CDCl_3$): δ 171.8, 171.2, 170.7, 169.0, 143.8, 135.23, 135.16, 131.9, 129.7, 128.5, 128.2, 127.6, 127.1, 123.7, 94.8, 80.9, 74.7, 54.1, 46.8, 35.1, 33.8, 32.1, 28.2, 24.0, 21.5.

SFC analysis: Using **GP6**, **3.12b** (Trefoil® CEL1, 10% 1:1 MeOH:^{i}PrOH with 0.2% formic acid in CO_2, 2.5 mL/min, 210 nm) indicated 93:7 d.r. for asymmetric induction observed from formation of the major relative diasteromer: t_R (major diastereomer) = 2.4 min., t_R (minor diastereomer) = 2.8 min.

Specific Rotation: $[\alpha]_D^{22}$ -76.5 (*c* 1, $CHCl_3$).

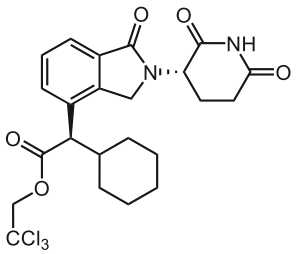

3.13

2,2,2-trichloroethyl (*R*)-2-cyclohexyl-2-(2-((*S*)-2,6-dioxopiperidin-3-yl)-1-oxoisoindolin-4-yl)acetate (3.13).

Compound **3.13** was produced following **GP 7**, using **3.10b** (15 mg, 1.0 equiv, 25 µmol) and benzenesulfonic acid (7.8 mg, 2.0 equiv, 49 µmol) in acetonitrile (0.12 mL) at 70 °C for 3.5 h. Purification via flash column chromatography (SiO_2, 65% ethyl acetate in hexanes) gave 2,2,2-trichloroethyl (*R*)-2-cyclohexyl-2-(2-((*S*)-2,6-dioxopiperidin-3-yl)-1-oxoisoindolin-4-yl)acetate **(3.13)** as an amorphous white solid (7.9 mg, 62% yield, 15 µmol).

HRMS (APCI) *m/z*: $[M+H]^+$ calcd for $C_{23}H_{26}O_5N_2{}^{35}Cl_3$ 515.0902; Found 515.0902

^{1}H NMR (400 MHz, $CDCl_3$): δ 8.05 (s, 1H), 7.82 (dd, *J* = 7.5, 1.0 Hz, 1H), 7.68 (dd, *J* = 7.7, 1.1 Hz, 1H), 7.51 (t, *J* = 7.6 Hz, 1H), 5.22 (dd, *J* = 13.3, 5.1 Hz, 1H), 4.72 (d, *J* = 11.9 Hz, 1H), 4.64 (d, *J* = 12.0 Hz, 1H), 4.59 (d, *J* = 16.0 Hz, 1H), 4.40 (d, *J* = 16.0 Hz, 1H), 3.44 (d, *J* = 11.1 Hz, 1H), 3.11 – 2.64 (m, 2H), 2.43 (qd, *J* = 13.1, 5.0 Hz, 1H), 2.30 – 2.18 (m, 2H), 2.00 – 1.90 (m, 1H), 1.85 – 1.74 (m, 1H), 1.71 – 1.59 (m, 2H), 1.47 – 1.32 (m, 2H), 1.22 – 1.05 (m, 3H), 0.82 – 0.66 (m, 1H).

^{13}C{^{1}H} NMR (101 MHz, $CDCl_3$): δ 171.1, 169.33, 169.27, 141.0, 132.1, 131.9, 131.6, 129.3, 123.7, 94.7, 74.3, 55.1, 52.0, 46.7, 39.7, 32.1, 31.7, 30.4, 26.2, 25.9, 23.6.

SFC analysis: **3.13** (CHIRALPAK® AD-3, 20% 1:1 MeOH:^{i}PrOH with 0.2% formic acid in CO_2, 2.5 mL/min, 210 nm) indicated 99:1 d.r. for retained asymmetric induction arising from formation of the major relative diastereomer and 99:1 d.r. for major relative configuration of the glutarimide stereogenic center: t_R (major diastereomer) = 2.9 min., t_R (minor diastereomers) = 2.1, 2.3, and 3.3 min.

Specific Rotation: $[\alpha]_D^{24}$ -37.9 (c 0.5, $CHCl_3$).

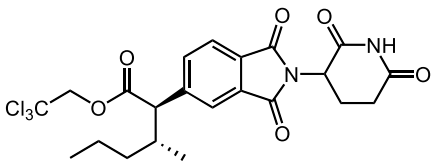

(2*R*,3*S*)-3.14

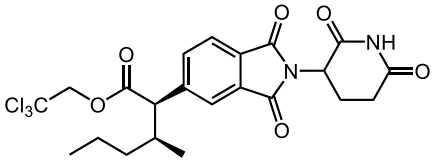

(2*R*,3*R*)-3.14

2,2,2-trichloroethyl (2*R*,3*S*)-2-(2-(2,6-dioxopiperidin-3-yl)-1,3-dioxoisoindolin-5-yl)-3-methylhexanoate ((2*R*,3*S*)-3.14).

2,2,2-trichloroethyl (2*R*,3*S*)-2-(2-(2,6-dioxopiperidin-3-yl)-1,3-dioxoisoindolin-5-yl)-3-methylhexanoate ((2*R*,3*R*)-3.14).

Compound **3.14** was produced via **GP1** using **3.6a** (47 mg, 1.0 equiv, 0.10 mmol), 1,1,1,3,3,3-hexafluoroisopropanol (0.11 mL, 10.0 equiv, 1.00 mmol), Rh_2(*S*-*tetra*-p-Br-PPTTL)$_4$ (20 mM in CH_2Cl_2, 50 µL, 1 mol%, 1.0 µmol), and pentane (1.0 mL). Purification via flash column

chromatography (SiO_2, 20% to 50% ethyl acetate in hexanes) produced a mixture of 2,2,2-trichloroethyl (2*R*,3*S*)-2-(2-(2,6-dioxopiperidin-3-yl)-1,3-dioxoisoindolin-5-yl)-3-methylhexanoate **((2*R*,3*S*)-3.14)** and 2,2,2-trichloroethyl (2*R*,3*S*)-2-(2-(2,6-dioxopiperidin-3-yl)-1,3-dioxoisoindolin-5-yl)-3-methylhexanoate **((2*R*,3*R*)-3.14)** as an amorphous white solid (42 mg, 82 µmol, 82% yield). **((2*R*,3*S*)-3.14)** was generated as the major diastereomer in 3.7:1 d.r.

HRMS (APCI) *m/z*: $[M+H]^+$ calcd for $C_{22}H_{24}O_6N_2{}^{35}Cl_3$ 517.0695; Found 517.0696
^{1}H NMR (600 MHz, $CDCl_3$, reported as a mixture of diastereomers): δ 8.07 (s, 1H), 7.94 (s, 1H), 7.852 and 7.848 (d, *J* = 7.8 Hz, 1H), 7.775, 7.772, and 7.770 (d, *J* = 7.8 Hz, 1H), 4.991 and 4.987 (dd, *J* = 12.7, 5.4 Hz, 1H), 4.80 and 4.79 (d, *J* = 11.9 Hz, 1H), 4.65 (d, *J* = 12.0 Hz, 1H), 3.61 and 3.60 (d, *J* = 10.5 Hz, 1H), 2.96 – 2.89 (m, 1H), 2.88 – 2.70 (m, 2H), 2.41 – 2.30 (m, 1H), 2.21 – 2.11 (m, 1H), 1.54-1.44 and 1.30 – 1.23 (m, 1H), 1.41 – 1.31 (m, 1H), 1.22 – 1.15 (m, 1H), 1.14 – 1.06 and 0.99 – 0.95 (m, 1H, partially occluded by signal at 1.09), 1.09 and 0.74 (d, *J* = 6.6 Hz, 3H), 0.92 and 0.74 (t, *J* = 6.8 Hz, 3H)
^{13}C{^{1}H} NMR (151 MHz, $CDCl_3$, reported as a mixture of diastereomers): δ 171.13, 171.06, 170.8, 167.99, 167.97, 167.1, 167.0, 145.04, 145.01, 135.3, 135.21, 135.24, 132.34, 132.32, 131.07, 131.05, 124.4, 124.3, 124.2, 124.1, 94.7, 74.4, 59.0, 49.5, 37.4, 36.7, 36.6, 35.8, 31.5, 22.8, 19.9, 19.6, 17.8, 16.8, 14.3, 14.2.
SFC analysis: Using **GP1**, **(2*R*,3*S*)-3.14 and (2*R*,3*R*)-3.14** (CHIRALCEL® OX-3, 15% 1:1 MeOH:^{i}PrOH with 0.2% formic acid in CO_2, 2.0 mL/min, 210 nm) indicated 96:4 d.r. for the asymmetric induction arising from formation of the major relative diastereomer: t_R (major diastereomers) = 9.3 and 11.4 min., t_R (minor diastereomers) = 14.2 and 16.6 min., and 95:5 d.r. for the asymmetric induction arising from formation of the minor relative diastereomer: t_R (major diastereomers) = 10.5 and 12.3 min., t_R (minor diastereomers) = 13.3 and 15.2 min.

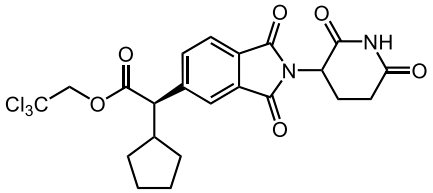

3.15

2,2,2-trichloroethyl (2*R*)-2-cyclopentyl-2-(2-(2,6-dioxopiperidin-3-yl)-1,3-dioxoisoindolin-5-yl)acetate (3.15).

Compound 3.**15** was produced via **GP1** using 3.**6a** (47 mg, 1.0 equiv, 0.10 mmol), 1,1,1,3,3,3-hexafluoroisopropanol (0.11 mL, 10.0 equiv, 1.00 mmol), Rh_2(*S*-*tetra*-p-Br-PPTTL)$_4$ (20 mM in CH_2Cl_2, 50 µL, 1 mol%, 1.0 µmol), and cyclopentane (1.0 mL). Purification via flash column chromatography (SiO_2, 20% to 50% ethyl acetate in hexanes) produced 2,2,2-trichloroethyl (2*R*)-2-cyclopentyl-2-(2-(2,6-dioxopiperidin-3-yl)-1,3-dioxoisoindolin-5-yl)acetate **(3.15)** as an amorphous white solid (50 mg, 50 µmol, 96% yield).

HRMS (APCI): *m/z* $[M+H]^+$ calcd for $C_{22}H_{22}O_6N_2{}^{35}Cl_3$ 515.0538, Found 515.0546
^{1}H NMR (400 MHz, $CDCl_3$, reported as a mixture of diastereomers): δ 8.05 (s, 1H), 7.96 – 7.94 (m, 1H), 7.85 (dd, *J* = 7.7, 0.7 Hz, 1H), 7.78 (dd, *J* = 7.8, 1.5 Hz, 1H), 4.99 (dd, *J* = 12.5, 5.3 Hz,

1H), 4.79 (d, J = 12.0 Hz, 1H), 4.66 (d, J = 12.0 Hz, 1H), 3.61 (d, J = 11.1 Hz, 1H), 3.03 – 2.72 (m, 3H), 2.72 – 2.59 (m, 1H), 2.23 – 2.08 (m, 1H), 2.06 – 1.95 (m, 1H), 1.76 – 1.58 (m, 3H), 1.56 – 1.42 (m, 2H), 1.41-1.31 (m, 1H) 1.08 – 0.93 (m, 1H).

^{13}C{^{1}H} NMR (151 MHz, $CDCl_3$, reported as a mixture of diastereomers): δ 171.04, 171.02, 168.1, 167.1, 167.0, 145.7, 134.8, 132.4, 131.0, 124.2, 124.0, 94.7, 74.4, 57.9, 49.5, 43.6, 43.6, 31.6, 31.5, 30.9, 25.2, 25.0, 22.7.

SFC analysis: Using **GP1**, **3.15** (CHIRALCEL® OX-3, 30% 1:1 MeOH:^{i}PrOH with 0.2% formic acid in CO_2, 2.5 mL/min, 230 nm) indicated >99:1 d.r. for the asymmetric induction observed at the newly formed stereogenic center: t_R (major diastereomers) = 2.6 and 3.0 min., t_R (minor diastereomers) = 3.3 and 3.6 min.

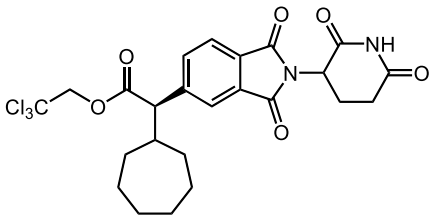

3.16

2,2,2-trichloroethyl (2*R*)-2-cycloheptyl-2-(2-(2,6-dioxopiperidin-3-yl)-1,3-dioxoisoindolin-5-yl)acetate (3.16).

Compound **3.16** was produced via **GP1** using **3.6a** (47 mg, 1.0 equiv, 0.10 mmol), 1,1,1,3,3,3-hexafluoroisopropanol (0.11 mL, 10.0 equiv, 1.00 mmol), Rh_2(*S*-*tetra*-p-Br-PPTTL)$_4$ (20 mM in CH_2Cl_2, 50 µL, 1 mol%, 1.0 µmol), and cycloheptane (1.0 mL). Purification via flash column chromatography (SiO_2, 20% to 50% ethyl acetate in hexanes) produced 2,2,2-trichloroethyl (2*R*)-2-cycloheptyl-2-(2-(2,6-dioxopiperidin-3-yl)-1,3-dioxoisoindolin-5-yl)acetate **(3.16)** as an amorphous white solid (52 mg, 96 µmol, 96% yield).

HRMS (APCI) *m/z*: $[M+H]^+$ calcd for $C_{24}H_{26}O_6N_2{}^{35}Cl_3$, 543.0851; Found 543.0857.

^{1}H NMR (400 MHz, $CDCl_3$, reported as a mixture of diastereomers): δ 8.07 (s, 1H), 7.94 (dd, J = 1.7, 0.6 Hz, 1H), 7.84 (dd, J = 7.7, 0.7 Hz, 1H), 7.77 (dd, J = 7.8, 1.5 Hz, 1H), 4.99 (dd, J = 12.3, 5.2 Hz, 1H), 4.77 (d, J = 12.0 Hz, 1H), 4.655 and 4.653 (d, J = 12.0 Hz, 1H), 3.65 (d, J = 10.8 Hz, 1H), 2.97 – 2.66 (m, 3H), 2.47 – 2.28 (m, 1H), 2.20 – 2.09 (m, 1H), 1.93 – 1.77 (m, 1H), 1.76 – 1.66 (m, 1H), 1.64 – 1.30 (m, 9H), 1.10 – 0.98 (m, 1H).

^{13}C{^{1}H} NMR (151 MHz, $CDCl_3$, reported as a mixture of diastereomers): δ 171.2, 170.8, 168.0, 167.1, 167.0, 145.3, 135.3, 132.3, 131.0, 124.4, 124.2, 94.7, 74.5, 59.1, 49.5, 42.6, 33.1, 31.6, 31.5, 28.3, 28.2, 26.31, 26.29, 26.2, 22.8.

SFC analysis: Using **GP1**, **3.16** (Trefoil® AMY1, 30% 1:1 MeOH:^{i}PrOH with 0.2% formic acid in CO_2, 2.5 mL/min, 230 nm) indicated 95:5 d.r. for the asymmetric induction observed at the newly formed stereogenic center: t_R (major diastereomers) = 2.9 and 7.9 min., t_R (minor diastereomers) = 2.4 and 5.3 min.

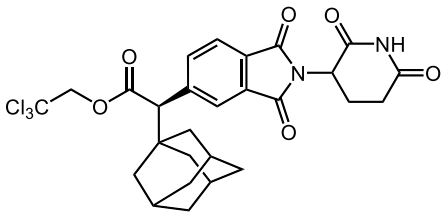

3.17

2,2,2-trichloroethyl (2*R*)-2-((3*R*,5*R*,7*R*)-adamantan-1-yl)-2-(2-(2,6-dioxopiperidin-3-yl)-1,3-dioxoisoindolin-5-yl)acetate (3.17).

Compound **3.17** was prepared via **GP3** using admantane (140 mg, 10.0 equiv, 1.0 mmol), Rh_2(*S*-*tetra*-p-Br-PPTTL)$_4$ (3.7 mg, 1 mol%, 1.0 µmol), **3.6a** (47 mg, 1.0 equiv, 0.10 mmol), 1,1,1,3,3,3-hexafluoropropan-2-ol (0.10 mL, 10.0 equiv, 1.0 mmol), and 1.0 mL CH_2Cl_2 at room temperature with a one hour slow addition of diazo and 0.5 h additional stirring. Excess adamantane was removed after reaction by sublimation via Kugelrohr (100 °C, <10 torr, 10 min). Purification via flash column chromatography (SiO_2, gradient of 20% to 50% EtOAc in hexanes) afforded 2,2,2-trichloroethyl (2*R*)-2-((3*R*,5*R*,7*R*)-adamantan-1-yl)-2-(2-(2,6-dioxopiperidin-3-yl)-1,3-dioxoisoindolin-5-yl)acetate **(3.17)** as an amorphous white solid (47 mg, 81 µmol, 81% yield).

HRMS (APCI) *m/z*: $[M+H]^+$ calcd for $C_{27}H_{28}O_6N_2{}^{35}Cl_3$ 581.1008; Found 581.1006

^{1}H NMR (600 MHz, $CDCl_3$, reported as a mixture of diastereomers): δ 8.05 – 7.93 (m, 2H), 7.84 (d, *J* = 7.7 Hz, 1H), 7.80 (dt, *J* = 7.8, 1.9 Hz, 1H), 5.00 (dd, *J* = 12.6, 5.4 Hz, 1H), 4.812 and 4.811 (d, *J* = 12.0 Hz, 1H), 4.665 and 4.663 (d, *J* = 12.0 Hz, 1H), 3.61 (s, 1H), 2.97 – 2.89 (m, 1H), 2.89 – 2.81 (m, 1H), 2.79 – 2.69 (m, 1H), 2.18 – 2.13 (m, 1H), 2.04 – 1.81 (m, 2H), 1.82 – 1.63 (m, 3H), 1.61 – 1.38 (m, 3H).

^{13}C{^{1}H} NMR (151 MHz, $CDCl_3$, reported as a mixture of diastereomers): δ 170.9, 170.0, 168.1, 167.3, 167.2, 141.9, 136.4, 131.6, 130.8, 125.6, 123.3, 94.7, 74.5, 63.2, 49.5, 40.0, 37.4, 36.6, 31.5, 28.6, 22.8.

SFC analysis: Using **GP3**, **3.17** (CHIRALCEL® OX-3, 30% 1:1 MeOH:^{i}PrOH with 0.2% formic acid in CO_2, 2.5 mL/min, 230 nm) indicated 98:2 d.r. for the asymmetric induction observed at the newly formed stereogenic center: t_R (major diastereomers) = 3.8 and 4.7 min., t_R (minor diastereomers) = 5.3 and 5.8 min.

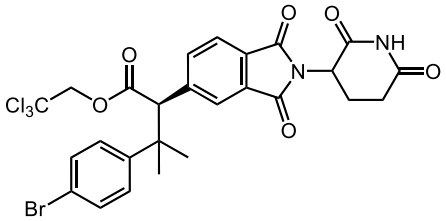

3.18

2,2,2-trichloroethyl (2*S*)-3-(4-bromophenyl)-2-(2-(2,6-dioxopiperidin-3-yl)-1,3-dioxoisoindolin-5-yl)-3-methylbutanoate (3.18).

Compound **3.18** was prepared via **GP3** using 1-bromo-4-isopropylbenzene (0.16 mL, 10.0 equiv, 1.0 mmol), Rh_2(*S*-*tetra*-p-Br-PPTTL)$_4$ (3.7 mg, 1 mol%, 1.0 µmol), **3.6a** (47 mg, 1.0 equiv, 0.10 mmol), 1,1,1,3,3,3-hexafluoropropan-2-ol (0.10 mL, 10.0 equiv, 1.0 mmol), and 1.0 mL CH_2Cl_2 at room temperature with a one hour slow addition of diazo and 0.5 h additional stirring. Excess 1-bromo-4-isopropylbenzene was removed from the reaction mixture via Kugelrohr distillation (100 °C, <10 torr, 10 min). Purification via flash column chromatography (SiO_2, gradient of 20% to 50% EtOAc in hexanes) followed by further purification (C18, 40-90% MeCN in H_2O, 0.1% v/v as buffer) afforded 2,2,2-trichloroethyl (2*S*)-3-(4-bromophenyl)-2-(2-(2,6-dioxopiperidin-3-yl)-1,3-dioxoisoindolin-5-yl)-3-methylbutanoate **(3.18)** as an amorphous white solid (23 mg, 35 µmol, 35% yield).

HRMS (APCI) *m/z*: $[M+H]^+$ calcd for $C_{26}H_{23}O_6N_2{}^{79}Br^{35}Cl_3$ 642.9800; Found 642.9805

^{1}H NMR (400 MHz, $CDCl_3$, reported as a mixture of diastereomers): δ 8.09 (s, 1H), 7.96 – 7.84 (m, 1H), 7.77 – 7.71 (m, 1H), 7.53 – 7.46 (m, 1H), 7.42 (d, *J* = 8.7 Hz, 2H), 7.19 (d, *J* = 8.6 Hz, 2H), 4.99 (dd, *J* = 12.3, 5.3 Hz, 1H), 4.62 (d, *J* = 12.0 Hz, 1H), 4.49 (d, *J* = 12.0 Hz, 1H), 4.15 (s, 1H), 2.96 – 2.88 (m, 1H), 2.87 – 2.63 (m, 2H), 2.20 – 2.11 (m, 1H), 1.55 (s, 3H), 1.38 (s, 3H).

^{13}C{^{1}H} NMR (151 MHz, $CDCl_3$, reported as a mixture of diastereomers): δ 170.8, 169.7, 168.0, 167.03, 167.02, 166.95, 144.7, 142.0, 136.44, 136.40, 131.7, 131.5, 131.1, 128.4, 125.31, 125.30, 123.4, 121.1, 94.4, 74.5, 62.3, 49.5, 41.8, 31.5, 26.40, 26.37, 25.2, 25.1, 22.7.

SFC analysis: Using **GP3**, **3.18** (CHIRALPAK® AD-3, 20% 1:1 MeOH:^{i}PrOH with 0.2% formic acid in CO_2, 2.5 mL/min, 210 nm) indicated 92:8 d.r. for the asymmetric induction observed at the newly formed stereogenic center: t_R (major diastereomers) = 2.4 and 2.7 min., t_R (minor diastereomers) = 4.4 and 15.0 min.

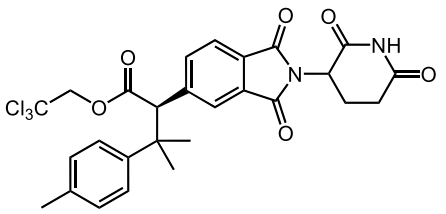

3.19

2,2,2-trichloroethyl (2*S*)-2-(2-(2,6-dioxopiperidin-3-yl)-1,3-dioxoisoindolin-5-yl)-3-methyl-3-(p-tolyl)butanoate (3.19).

Compound **3.19** was produced via **GP1** using **3.6a** (47 mg, 1.0 equiv, 0.10 mmol), 1,1,1,3,3,3-hexafluoroisopropanol (0.11 mL, 10.0 equiv, 1.00 mmol), Rh_2(*S-tetra*-p-Br-PPTTL)$_4$ (20 mM in CH_2Cl_2, 50 µL, 1 mol%, 1.0 µmol), and *p*-cymene (1.0 mL). Purification via flash column chromatography (SiO_2, 20% to 50% ethyl acetate in hexanes) produced afforded 2,2,2-trichloroethyl (2*S*)-2-(2-(2,6-dioxopiperidin-3-yl)-1,3-dioxoisoindolin-5-yl)-3-methyl-3-(p-tolyl)butanoate **(3.19)** as an amorphous white solid (58 mg, 99 µmol, 99% yield).

Compound **3.19** was prepared via **GP3** using *p*-cymene (0.16 mL, 10.0 equiv, 1.0 mmol), Rh_2(*S-tetra*-p-Br-PPTTL)$_4$ (3.7 mg, 1 mol%, 1.0 µmol), **3.6a** (47 mg, 1.0 equiv, 0.10 mmol), 1,1,1,3,3,3-hexafluoropropan-2-ol (0.10 mL, 10.0 equiv, 1.0 mmol), and 1.0 mL CH_2Cl_2 at room temperature with a one hour slow addition of diazo and 0.5 h additional stirring. Excess *p*-cymene was removed from the reaction mixture via Kugelrohr distillation (100 °C, <10 torr, 10 min). Purification via flash column chromatography (SiO_2, gradient of 20% to 50% EtOAc in hexanes) afforded 2,2,2-trichloroethyl (2*S*)-2-(2-(2,6-dioxopiperidin-3-yl)-1,3-dioxoisoindolin-5-yl)-3-methyl-3-(p-tolyl)butanoate **(3.19)** as an amorphous white solid (31 mg, 53 µmol, 53% yield).

NMR spectra contaminated with ca. 10% primary insertion product. Yields reported as a combined yield of diastereomers and regioisomers.
HRMS (APCI) *m/z*: $[M+H]^+$ calcd for $C_{27}H_{26}O_6N_2{}^{35}Cl_3$ 579.0851; Found 579.0850
^{1}H NMR (400 MHz, $CDCl_3$, reported as a mixture of diastereomers): δ 8.05 (s, 1H), 7.89 (dd, *J* = 5.1, 1.4 Hz, 1H), 7.71 (dt, *J* = 7.8, 1.0 Hz, 1H), 7.47 (ddd, *J* = 7.7, 6.0, 1.6 Hz, 1H), 7.17 (d, *J* = 8.4 Hz, 2H), 7.10 (d, *J* = 8.6 Hz, 2H), 4.98 (dd, *J* = 12.2, 5.3 Hz, 1H), 4.62 (d, *J* = 12.0 Hz, 1H), 4.52 (d, *J* = 12.0 Hz, 1H), 4.17 (s, 1H), 2.96 – 2.87 (m, 1H), 2.88 – 2.67 (m, 2H), 2.31 (s, 3H), 1.55 (s, 3H), 1.39 (s, 3H).

^{13}C{^{1}H} NMR (151 MHz, $CDCl_3$, reported as a mixture of diastereomers): δ 171.02, 171.00, 169.9, 168.1, 167.13, 167.12, 167.09, 142.52, 142.50, 136.6, 136.43, 136.40, 131.5, 130.8, 129.1, 128.9, 126.9, 126.4, 125.33, 125.31, 123.2, 94.55, 94.48, 74.4, 62.6, 49.52, 49.46, 41.8, 31.5, 26.0, 25.6, 22.7, 21.0.

SFC analysis: Using **GP1**, **3.19** (Trefoil® AMY1, 20% 1:1 MeOH:^{i}PrOH with 0.2% formic acid in CO_2, 2.5 mL/min, 210 nm) indicated 78:22 d.r. for the asymmetric induction observed for the formation of the major regioisomer: t_R (major diastereomers) = 4.2 and 5.2 min., t_R (minor diastereomers) = 8.6 and 21.1 min. Using **GP3**, **3.19** indicated 90:10 d.r.

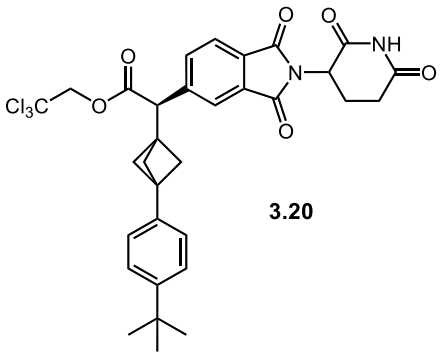

2,2,2-trichloroethyl (2*R*)-2-(3-(4-(*tert*-butyl)phenyl)bicyclo[1.1.1]pentan-1-yl)-2-(2-(2,6-dioxopiperidin-3-yl)-1,3-dioxoisoindolin-5-yl)acetate (3.20).

Compound **3.20** was prepared via **GP3** using 1-(4-(tert-butyl)phenyl)bicyclo[1.1.1]pentane (168 mg, 10.0 equiv, 1.0 mmol), Rh_2(*S*-*tetra*-p-Br-PPTTL)$_4$ (3.7 mg, 1 mol%, 1.0 µmol), **3.6a** (47 mg, 1.0 equiv, 0.10 mmol), 1,1,1,3,3,3-hexafluoropropan-2-ol (0.10 mL, 10.0 equiv, 1.0 mmol), and 1.0 mL CH_2Cl_2 at room temperature with a one hour slow addition of diazo and 0.5 h additional stirring. Purification via flash column chromatography (SiO_2, gradient of 20% to 50% EtOAc in hexanes) afforded 2,2,2-trichloroethyl (2*R*)-2-(3-(4-(*tert*-butyl)phenyl)bicyclo[1.1.1]pentan-1-yl)-2-(2-(2,6-dioxopiperidin-3-yl)-1,3-dioxoisoindolin-5-yl)acetate **(3.20)** as an amorphous white solid (40 mg, 64 µmol, 46% yield).

HRMS (APCI) *m/z*: $[M+H]^+$ calcd for $C_{32}H_{32}O_6N_2{}^{35}Cl_3$ 645.1321; Found 645.1323

^{1}H NMR (400 MHz, $CDCl_3$, reported as a mixture of diastereomers): δ 8.00 (s, 1H), 7.94 (s, 1H), 7.89 (d, *J* = 7.7 Hz, 1H), 7.77 (dt, *J* = 7.8, 1.6 Hz, 1H), 7.32 (d, *J* = 8.4 Hz, 1H), 7.10 (d, *J* = 8.3 Hz, 1H), 5.00 (dd, *J* = 12.2, 5.2 Hz, 1H), 4.87 (d, *J* = 12.0 Hz, 1H), 4.756 and 4.755 (dd, *J* = 12.0 Hz, 1H), 4.17 (s, 1H), 2.97 – 2.89 (m, 1H), 2.88 – 2.70 (m, 1H), 2.17 (ddd, *J* = 10.3, 5.1, 2.9 Hz, 1H), 2.08 – 1.99 (m, 6H), 1.29 (s, 9H).

^{13}C{^{1}H} NMR (151 MHz, $CDCl_3$, reported as a mixture of diastereomers): δ 170.9, 169.3, 168.0, 167.1, 167.0, 149.9, 143.4, 136.8, 135.02, 135.00, 132.3, 131.0, 125.8, 125.3, 124.2, 124.1, 94.6, 74.6, 53.6, 52.0, 49.5, 42.5, 39.5, 34.6, 31.53, 31.47, 22.8.

SFC analysis: Using **GP3**, **3.20** (CHIRALCEL® OX-3, 20% 1:1 MeOH:^{i}PrOH with 0.2% formic acid in CO_2, 2.5 mL/min, 210 nm) indicated 99:1 d.r. for the asymmetric induction observed at the newly formed stereogenic center: t_R (major diastereomers) = 10.6 and 11.8 min., t_R (minor diastereomers) = 10.3 and 14.0 min.

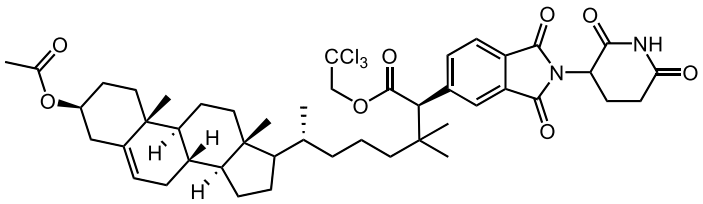

3.21

2,2,2-trichloroethyl (2*R*,7*R*)-7-((3*S*,8*S*,9*S*,10*R*,13*R*,14*S*)-3-acetoxy-10,13-dimethyl-2,3,4,7,8,9,10,11,12,13,14,15,16,17-tetradecahydro-1H-cyclopenta[*a*]phenanthren-17-yl)-2-(2-(2,6-dioxopiperidin-3-yl)-1,3-dioxoisoindolin-5-yl)-3,3-dimethyloctanoate (3.21).

Compound **3.21** was prepared via **GP3** using (3*S*,8*S*,9*S*,10*R*,13*R*,14*S*)-10,13-dimethyl-17-((*R*)-6-methylheptan-2-yl)-2,3,4,7,8,9,10,11,12,13,14,15,16,17-tetradecahydro-1H-cyclopenta[*a*]phenanthren-3-yl acetate (430 mg, 10.0 equiv, 1.0 mmol), Rh_2(*S-tetra*-p-Br-PPTTL)$_4$ (3.7 mg, 1 mol%, 1.0 μmol), **3.6a** (47 mg, 1.0 equiv, 0.10 mmol), 1,1,1,3,3,3-hexafluoropropan-2-ol (0.10 mL, 10.0 equiv, 1.0 mmol), and 1.0 mL CH_2Cl_2 at room temperature with a one hour slow addition of diazo and 0.5 h additional stirring. Purification via flash column chromatography (SiO_2, gradient of 20% to 50% EtOAc in hexanes) afforded **2,2,2-**trichloroethyl (2*R*,7*R*)-7-((3*S*,8*S*,9*S*,10*R*,13*R*,14*S*)-3-acetoxy-10,13-dimethyl-2,3,4,7,8,9,10,11,12,13,14,15,16,17-tetradecahydro-1H-cyclopenta[*a*]phenanthren-17-yl)-2-(2-(2,6-dioxopiperidin-3-yl)-1,3-dioxoisoindolin-5-yl)-3,3-dimethyloctanoate **(3.21)** as an amorphous white solid (28 mg, 32 μmol, 32% yield).

HRMS (APCI) *m/z*: $[M+Na]^+$ calcd for $C_{46}H_{59}O_8N_2{}^{35}Cl_3{}^{23}Na$ 895.3229; Found 895.3244

^{1}H NMR (600 MHz, $CDCl_3$, reported as a mixture of diastereomers): δ 8.04 (s, 1H), 8.00 (d, *J* = 4.8 Hz, 1H), 7.89 – 7.79 (m, 2H), 5.37 (d, *J* = 5.1 Hz, 1H), 4.99 (dd, *J* = 12.6, 5.4 Hz, 1H), 4.84 (d, *J* = 12.0 Hz, 1H), 4.66 – 4.52 (m, 2H), 3.84 (s, 1H), 2.99 – 2.89 (m, 1H), 2.89 – 2.64 (m, 2H), 2.38-2.29 (m, 2H), 2.21 – 2.12 (m, 1H), 2.03 (s, 3H), 2.02 – 1.92 (m, 2H), 1.89-1.82 (m, 1H), 1.81 – 1.75 (m, 1H), 1.61 – 1.34 (m, 10H), 1.34 – 1.27 (m, 1H), 1.26 – 1.10 (m, 6H), 1.09 (s, 3H), 1.07 – 1.03 (m, 1H), 1.01 (s, 3H), 1.00 – 0.96 (m, 2H), 0.95 (s, 3H), 0.92 (d, *J* = 6.5 Hz, 3H), 0.67 (s, 3H).

^{13}C{^{1}H} NMR (151 MHz, $CDCl_3$, reported as a mixture of diastereomers): δ 170.9, 170.7, 170.5, 168.1, 167.2, 167.1, 143.1, 139.8, 136.41, 136.38, 131.7, 130.9, 125.6, 125.5, 123.4, 122.7, 94.7, 74.4, 74.1, 60.6, 56.8, 56.2, 50.1, 49.5, 42.5, 41.4, 39.8, 38.3, 37.1, 36.73, 36.71, 35.9, 32.01, 31.98, 31.5, 28.4, 27.9, 24.85, 24.83, 24.43, 24.41, 24.39, 22.8, 21.6, 21.2, 20.4, 19.4, 18.9, 12.0.

SFC analysis: Using **GP3**, **3.20** (CHIRALCEL® OX-3, 35% 1:1 MeOH:^{i}PrOH with 0.2% formic acid in CO_2, 2.5 mL/min, 230 nm) indicated 99:1 d.r. for the asymmetric induction observed at the newly formed stereogenic center: t_R (major diastereomers) = 6.8 and 8.0 min., t_R (minor diastereomers) = 9.7 and 11.0 min.

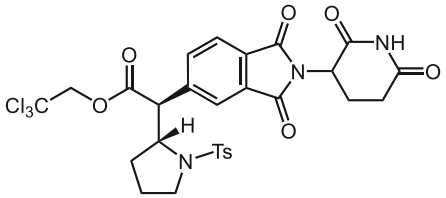

3.22

2,2,2-trichloroethyl (2*S*)-2-(2-(2,6-dioxopiperidin-3-yl)-1,3-dioxoisoindolin-5-yl)-2-((*R*)-1-tosylpyrrolidin-2-yl)acetate (3.22).

Compound **3.22** was prepared via **GP3** using 1-*N*-tosylpyrrolidine (0.23 g, 10.0 equiv, 1.0 mmol), Rh_2(*S-tetra*-p-Br-PPTTL)$_4$ (3.7 mg, 1 mol%, 1.0 µmol), **3.6a** (47 mg, 1.0 equiv, 0.10 mmol), 1,1,1,3,3,3-hexafluoropropan-2-ol (0.10 mL, 10.0 equiv, 1.0 mmol), and 1.0 mL CH_2Cl_2 at room temperature with a one hour slow addition of diazo and 0.5 h additional stirring. Purification via flash column chromatography (SiO_2, gradient of 10% to 65% EtOAc in hexanes) afforded 2,2,2-trichloroethyl (2*S*)-2-(2-(2,6-dioxopiperidin-3-yl)-1,3-dioxoisoindolin-5-yl)-2-((*R*)-1-tosylpyrrolidin-2-yl)acetate (**3.22**) as an amorphous white solid (36 mg, 53 µmol, 53% yield).

Compound **3.12** was prepared via **GP8** using 1-*N*-tosylpyrrolidine (0.23 g, 10.0 equiv, 1.0 mmol), Rh_2(*S-tetra*-p-Br-PPTTL)$_4$ (20 mM in CH_2Cl_2, 50 µL, 1 mol%, 1.0 µmol), **3.6a** (47 mg, 1.0 equiv, 0.10 mmol), and 1.0 mL CH_2Cl_2 at room temperature for 0.5 h. Purification via flash column chromatography (SiO_2, gradient of 10% to 65% EtOAc in hexanes) afforded 2,2,2-trichloroethyl (2*S*)-2-(2-(2,6-dioxopiperidin-3-yl)-1,3-dioxoisoindolin-5-yl)-2-((*R*)-1-tosylpyrrolidin-2-yl)acetate (**3.22**) as an amorphous white solid (57 mg, 85 µmol, 85% yield).

HRMS (APCI) *m/z*: $[M+H]^+$ calcd for $C_{29}H_{32}O_6N_2{}^{35}Cl_3$ 670.0579; Found 670.0579

^{1}H NMR (400 MHz, $CDCl_3$, reported as a mixture of diastereomers): δ 8.14 (s, 1H), 7.98 – 7.90 (m, 1H), 7.92 – 7.78 (m, 3H), 7.64 (d, *J* = 8.2 Hz, 2H), 7.30 (d, *J* = 8.0 Hz, 2H), 5.00 (dd, *J* = 12.2, 5.2 Hz, 1H), 4.83 – 4.79 (m, 2H), 4.37 (m, 1H), 4.27 (d, *J* = 6.8 Hz, 1H), 3.42 – 3.34 (m, 1H), 3.32 – 3.18 (m, 1H), 2.99 – 2.63 (m, 3H), 2.41 (s, 3H), 2.23 – 2.12 (m, 1H), 1.99 – 1.88 (m, 1H), 1.77 – 1.63 (m, 1H), 1.51 – 1.33 (m, 1H).

^{13}C{^{1}H} NMR (101 MHz, $CDCl_3$, reported as a mixture of diastereomers): δ 171.0, 169.35 and 169.33, 168.1, 167.04 and 166.99, 144.2, 144.1, 142.1, 136.0, 134.6, 134.5, 132.1, 131.4, 130.0, 127.7, 127.6, 125.0, 124.0, 94.6, 74.6, 62.94 and 62.92, 56.0, 49.5, 49.4, 31.5, 29.8, 24.2, 22.7, 21.7.

SFC analysis: **3.22** (Trefoil® AMY1, 30% 1:1 MeOH:^{i}PrOH with 0.2% formic acid in CO_2, 1.5 mL/min, 210 nm) indicated 97:3 d.r. for asymmetric induction arising from formation of the major relative diastereomer using **GP3**: t_R (major diastereomers) = 11.2 and 20.7 min., t_R (minor diastereomers) = 10.0 and 13.6 min. **GP8** gave **3.22** in 95:5 d.r.

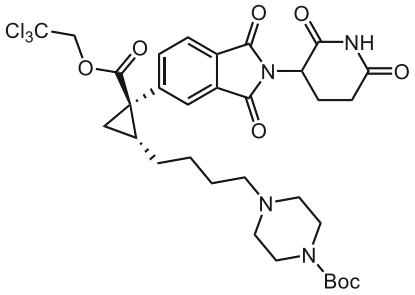

3.24

***tert*-butyl 4-(4-((1*R*,2*R*)-2-(2-(2,6-dioxopiperidin-3-yl)-1,3-dioxoisoindolin-5-yl)-2-((2,2,2-trichloroethoxy)carbonyl)cyclopropyl)butyl)piperazine-1-carboxylate (3.24).**

Compound **3.24** was prepared via **GP5** using **13** (30 mg, 1.1 equiv, 0.11 mmol), Rh_2(*S-tetra*-p-Br-PPTTL)$_4$ (3.7 mg, 1 mol%, 1.0 µmol), **3.6a** (47 mg, 1.0 equiv, 0.10 mmol), 1,1,1,3,3,3-hexafluoropropan-2-ol (0.20 mL, 20.0 equiv, 2.0 mmol), and 1.0 mL CH_2Cl_2 at room temperature with a 0.5 h slow addition of diazo and 0.25 h additional stirring. Purification via flash column chromatography (SiO_2, gradient of 50% to 100% EtOAc in hexanes) afforded tert-butyl 4-(4-((1*R*,2*R*)-2-(2-(2,6-dioxopiperidin-3-yl)-1,3-dioxoisoindolin-5-yl)-2-((2,2,2-trichloroethoxy)carbonyl)cyclopropyl)butyl)piperazine-1-carboxylate **(3.24)** as an amorphous white solid (35 mg, 49 µmol, 49% yield).

Compound **3.24** was prepared via **GP8** using **3.13** (30 mg, 1.1 equiv, 0.11 mmol), Rh_2(*S-tetra*-p-Br-PPTTL)$_4$ (3.7 mg, 1 mol%, 1.0 µmol), **3.6a** (47 mg, 1.0 equiv, 0.10 mmol), and 1.0 mL CH_2Cl_2 at room temperature with a 0.5 h slow addition of diazo and 0.25 h additional stirring. Purification via flash column chromatography (SiO_2, gradient of 50% to 100% EtOAc in hexanes) afforded tert-butyl 4-(4-((1*R*,2*R*)-2-(2-(2,6-dioxopiperidin-3-yl)-1,3-dioxoisoindolin-5-yl)-2-((2,2,2-trichloroethoxy)carbonyl)cyclopropyl)butyl)piperazine-1-carboxylate **(3.24)** as an amorphous white solid (22 mg, 30 µmol, 30% yield).

HRMS (ESI): *m/z* $[M+H]^+$ calcd for $C_{32}H_{40}O_8N_4{}^{35}Cl_3$ 713.1906; Found 713.1904.

^{1}H NMR (400 MHz, $CDCl_3$, reported as a mixture of diastereomers): δ 8.25 and 8.14 (s, 1H), 7.92 – 7.83 (m, 1H), 7.83 – 7.79 (m, 1H), 7.72 (dd, *J* = 7.7, 1.5 Hz, 1H), 4.990 and 4.987 (dd, *J* = 12.5, 5.3 Hz, 1H), 4.81 and 4.80 (d, *J* = 11.9 Hz, 1H), 4.58 and 4.57 (d, *J* = 11.9 Hz, 1H), 3.48 – 3.41 (m, 4H), 3.00 – 2.89 (m, 1H), 2.88 – 2.71 (m, 2H), 2.42 – 2.32 (m, 5H), 2.20 – 2.13 (m, 1H), 2.09 – 1.94 (m, 2H), 1.68 – 1.36 (m, 7H, overlapping with s at 1.44) 1.44 (s, 9H, overlapping with multiplet from 1.68-1.36), 1.32 (dd, *J* = 6.6, 4.3 Hz, 1H).

^{13}C{^{1}H} NMR (151 MHz, $CDCl_3$, reported as a mixture of diastereomers): δ 171.6, 170.92, 170.91, 168.2, 168.1, 167.2, 167.1, 154.8, 143.2, 137.9, 131.93, 131.92, 130.88, 130.86, 126.71, 126.68, 123.7, 123.6, 94.9, 74.5, 58.4, 53.0, 49.5, 33.9, 33.8, 31.6, 30.6, 30.5, 30.1, 28.6, 27.0, 22.8, 22.32, 22.27.

SFC analysis: **3.24** (CHIRALPAK® AD-3, 30% 1:1 MeOH:^{i}PrOH with 0.2% formic acid in CO_2, 1.5 mL/min, diode array) indicated 96:4 d.r. for asymmetric induction arising from formation of the major relative diastereomer using **GP5**: t_R (major diastereomer) = 4.5 min., t_R (minor diastereomer) = 2.1 min., t_R (inseparable major + minor) = 1.7 min. **GP8** gave **3.24** in 97:3 d.r.

Note: The other two diastereomers represented by the peak at 1.7 min were inseparable, and the d.r. was acquired from the diastereomers at 2.1 and 4.5 min. only.

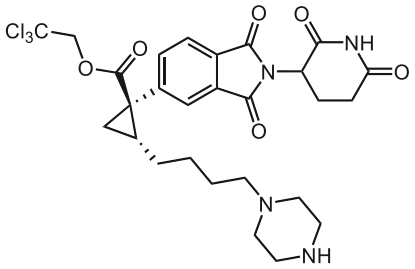

SI1

2,2,2-trichloroethyl (1*R*,2*R*)-1-(2-(2,6-dioxopiperidin-3-yl)-1,3-dioxoisoindolin-5-yl)-2-(4-(piperazin-1-yl)butyl)cyclopropane-1-carboxylate (SI1).

Compound **3.24** (27 mg, 38 µmol, 1.0 equiv) was added to a vial equipped with a PTFE magnetic stir bar under ambient conditions, and 0.5 mL CH_2Cl_2 were added. The vial was cooled to 0 °C in an ice bath, and 0.5 mL trifluoroacetic acid was added in one portion. The ice bath was removed and the reaction was allowed to come to room temperature, stirring for one hour. The reaction was concentrated in vacuuo and the residual trifluoroacetic acid was removed by concentration from toluene (3x). The obtained residue was dissolved in ethyl acetate (5 mL) and washed twice with a saturated aqueous solution of sodium bicarbonate (5 mL). The organic layer was dried over sodium sulfate, filtered, and concentrated under vacuum. The crude 2,2,2-trichloroethyl (1*R*,2*R*)-1-(2-(2,6-dioxopiperidin-3-yl)-1,3-dioxoisoindolin-5-yl)-2-(4-(piperazin-1-yl)butyl)cyclopropane-1-carboxylate **(SI1)** was carried forward to the next step without further purification.

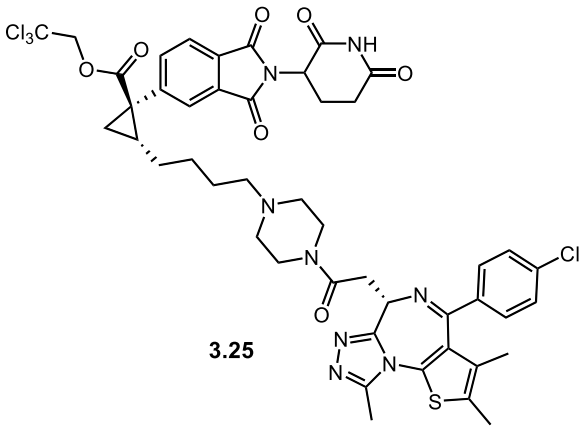

3.25

2,2,2-trichloroethyl (1*R*,2*R*)-2-(4-(4-(2-((*S*)-4-(4-chlorophenyl)-2,3,9-trimethyl-6H-thieno[3,2-f][1,2,4]triazolo[4,3-a][1,4]diazepin-6-yl)acetyl)piperazin-1-yl)butyl)-1-(2-(2,6-dioxopiperidin-3-yl)-1,3-dioxoisoindolin-5-yl)cyclopropane-1-carboxylate (3.25).

A flame-dried vial equipped with a PTFE magnetic stir bar and under inert atmosphere was charged with (*S*)-2-(4-(4-chlorophenyl)-2,3,9-trimethyl-6H-thieno[3,2-f][1,2,4]triazolo[4,3-a][1,4]diazepin-6-yl)acetic acid (9.0 mg, 22 µmol, 1.0 equiv) and HATU (17 mg, 45 µmol, 2.0

equiv). Dry DMF (0.5 mL) was charged by syringe along with DIPEA (12 µL, 67 µmol, 3.0 equiv). The reaction was stirred at room temperature for 0.5 hours, after which a solution of **SI1** (15 mg, 25 µmol, 1.1 equiv) in 0.5 mL dry DMF was charged by syringe. The reaction was allowed to stir for 4 hours at room temperature, after which it was partitioned between saturated aqueous sodium chloride solution (5 mL) and ethyl acetate (5 mL). The aqueous layer was extracted thrice with ethyl acetate (5 mL portions), after which the combined organic layers were washed with saturated aqueous sodium chloride solution (5 mL). The combined organic layers were dried over sodium sulfate, filtered, and concentrated in vacuuo. Flash column chromatography (SiO_2, 5% to 10% MeOH in CH_2Cl_2) afforded 2,2,2-trichloroethyl (1*R*,2*R*)-2-(4-(4-(2-((*S*)-4-(4-chlorophenyl)-2,3,9-trimethyl-6H-thieno[3,2-f][1,2,4]triazolo[4,3-a][1,4]diazepin-6-yl)acetyl)piperazin-1-yl)butyl)-1-(2-(2,6-dioxopiperidin-3-yl)-1,3-dioxoisoindolin-5-yl)cyclopropane-1-carboxylate **(3.25)** as a tan amorphous solid (16 mg, 22 µmol, 72% yield).

HRMS (ESI) *m/z*: $[M+H]^+$ calcd for $C_{46}H_{47}O_7N_8{}^{35}Cl_4{}^{32}S$ 995.2037; Found 995.2065

^{1}H NMR (800 MHz, DMSO-*d*6, sample at 80 °C, reported as a mixture of diastereomers): δ 10.87 (s, 1H), 7.90 (t, *J* = 7.6 Hz, 1H), 7.88 (d, *J* = 1.4 Hz, 1H), 7.86 (dt, *J* = 7.7, 1.3 Hz, 1H), 7.46 (d, *J* = 9.0 Hz, 2H), 7.44 (d, *J* = 8.6 Hz, 2H), 5.13 and 5.12 (dd, *J* = 12.6, 5.6 Hz, 1H), 4.90 (d, *J* = 12.3 Hz, 1H), 4.791 and 4.790 (d, *J* = 12.3 Hz, 1H), 4.59 (t, *J* = 6.7 Hz, 1H), 3.62 – 3.55 (m, 5H), 3.398 and 3.396 (dd, *J* = 16.1, 6.5 Hz, 1H), 2.88 (ddt, *J* = 17.0, 13.4, 5.3 Hz, 1H), 2.66 – 2.54 (m, 3 H), 2.60 (s, 3H, overlapping with m from 2.66-2.54), 2.53 – 2.50 (m, 1H, overlapping with solvent signal at 2.50), 2.42 (s, 3H), 2.41 – 2.15 (m, 5H), 2.13 – 2.09 (m, 1H), 2.05 – 1.99 (m, 1H), 1.87 (dd, *J* = 9.1, 4.8 Hz, 1H), 1.65 (s, 3H), 1.58 (dd, *J* = 7.1, 4.9 Hz, 1H), 1.46 – 1.38 (m, 5H).

^{13}C{^{1}H} NMR (201 MHz, DMSO-*d*6, sample at 80 °C, reported as a mixture of diastereomers): δ 171.9, 170.7, 169.1, 166.5, 166.4, 155.0, 149.2, 142.4, 137.3, 136.6, 134.9, 131.8, 130.9, 130.3, 129.9, 129.7, 129.55, 129.46, 128.0, 125.7, 122.5, 95.0, 73.6, 73.4, 57.1, 54.0, 48.9, 34.4, 33.1, 30.6, 30.1, 29.2, 29.0, 25.9, 21.70, 21.68, 21.0, 13.4, 12.23, 12.01, 10.74, 10.72.

Purity (HPLC): 97%

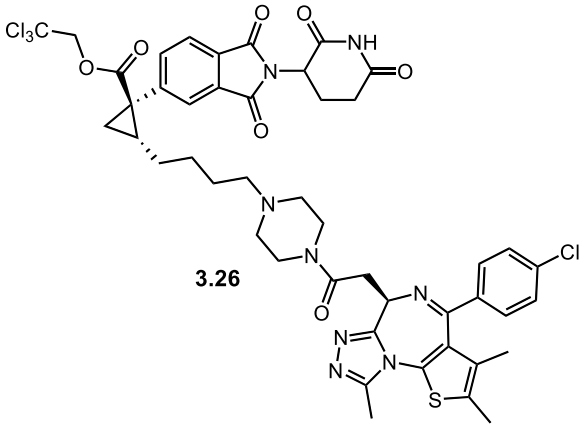

3.26

2,2,2-trichloroethyl (1*R*,2*R*)-2-(4-(4-(2-((*R*)-4-(4-chlorophenyl)-2,3,9-trimethyl-6H-thieno[3,2-f][1,2,4]triazolo[4,3-a][1,4]diazepin-6-yl)acetyl)piperazin-1-yl)butyl)-1-(2-(2,6-dioxopiperidin-3-yl)-1,3-dioxoisoindolin-5-yl)cyclopropane-1-carboxylate (3.26).

A flame-dried vial equipped with a PTFE magnetic stir bar and under inert atmosphere was charged with (*R*)-2-(4-(4-chlorophenyl)-2,3,9-trimethyl-6H-thieno[3,2-f][1,2,4]triazolo[4,3-a][1,4]diazepin-6-yl)acetic acid (12 mg, 30 µmol, 1.0 equiv) and HATU (23 mg, 60 µmol, 2.0 equiv). Dry DMF (0.5 mL) was charged by syringe along with DIPEA (16 µL, 90 µmol, 3.0 equiv). The reaction was stirred at room temperature for 0.5 hours, after which a solution of **SI1** (20 mg, 33 µmol, 1.1 equiv) in 0.5 mL dry DMF was charged by syringe. The reaction was allowed to stir for 4 hours at room temperature, after which it was partitioned between saturated aqueous sodium chloride solution (5 mL) and ethyl acetate (5 mL). The aqueous layer was extracted thrice with ethyl acetate (5 mL portions), after which the combined organic layers were washed with saturated aqueous sodium chloride solution (5 mL). The combined organic layers were dried over sodium sulfate, filtered, and concentrated in vacuuo. Flash column chromatography (SiO_2, 5% to 10% MeOH in CH_2Cl_2) afforded 2,2,2-trichloroethyl (1*R*,2*R*)-2-(4-(4-(2-((*R*)-4-(4-chlorophenyl)-2,3,9-trimethyl-6H-thieno[3,2-f][1,2,4]triazolo[4,3-a][1,4]diazepin-6-yl)acetyl)piperazin-1-yl)butyl)-1-(2-(2,6-dioxopiperidin-3-yl)-1,3-dioxoisoindolin-5-yl)cyclopropane-1-carboxylate **(3.26)** as a tan amorphous solid (14 mg, 30 µmol, 47% yield).

HRMS (ESI) *m/z*: $[M+H]^+$ calcd for $C_{46}H_{47}O_7N_8{}^{35}Cl_4{}^{32}S$ 995.2037; Found 995.2049
^{1}H NMR (800 MHz, DMSO-*d*6, sample at 80 °C, reported as a mixture of diastereomers): δ 10.86 (s, 1H), 7.90 (d, *J* = 7.7 Hz, 2H), 7.88 (d, *J* = 1.5 Hz, 2H), 7.86 (dt, *J* = 7.7, 1.4 Hz, 2H), 7.46 (d, *J* = 8.8 Hz, 3H), 7.44 (d, *J* = 8.7 Hz, 4H), 5.13 and 5.12 (dd, *J* = 12.6, 5.5 Hz, 1H), 4.90 (d, *J* = 12.3 Hz, 1H), 4.792 and 4.790 (d, *J* = 12.2 Hz, 1H), 4.59 (t, *J* = 6.7 Hz, 1H), 3.68-3.43 (m, 4H, overlapped with dd at 3.57), 3.57 (dd, *J* = 16.0, 6.8 Hz, 1H), 3.40 and 3.39 (dd, *J* = 16.1, 6.5 Hz, 1H), 2.88 (ddt, *J* = 17.0, 13.4, 5.3 Hz, 1H), 2.65 – 2.55 (m, 3H, overlapped with s at 2.60), 2.60 (s, 3H, overlapped with m from 2.65-2.55), 2.53 – 2.49 (m, 1H, partially overlapped with solvent signal), 2.42 (s, 3H), 2.41 – 2.16 (m, 5H), 2.14 – 2.09 (m, 1H), 2.06 – 2.00 (m, 1H), 1.87 (dd, *J* = 9.1, 4.8 Hz, 1H), 1.66 (s, 3H), 1.58 (dd, *J* = 7.1, 4.9 Hz, 1H), 1.44 – 1.34 (m, 5H).
^{13}C{^{1}H} NMR (201 MHz, DMSO-*d*6, sample at 80 °C, reported as a mixture of diastereomers): δ 171.9, 170.7, 169.1, 167.8, 166.5, 166.4, 162.4, 155.0, 149.2, 142.4, 137.3, 136.6, 134.9, 131.8,

130.9, 130.3, 129.9, 129.7, 129.54, 129.46, 128.0, 125.8, 122.5, 95.0, 73.4, 57.1, 54.0, 48.9, 34.4, 33.1, 30.6, 30.1, 29.2, 29.04, 28.96, 25.9, 25.4, 21.70, 21.68, 21.0, 13.4, 12.2, 10.7.
Purity (HPLC): 95%

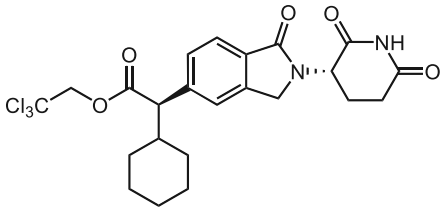

SI2

2,2,2-trichloroethyl (*R*)-2-cyclohexyl-2-(2-((*S*)-2,6-dioxopiperidin-3-yl)-1-oxoisoindolin-5-yl)acetate (SI2).

Compound **SI2** was produced following **GP 7**, using using **3.10a** (21 mg, 1.0 equiv, 34 µmol) and benzenesulfonic acid (11 mg, 2.0 equiv, 68 µmol) in acetonitrile (0.17 mL) at 70 °C for 3.5 h. Purification via flash column chromatography (SiO_2, 70% ethyl acetate in hexanes) gave 2,2,2-trichloroethyl (*R*)-2-cyclohexyl-2-(2-((*S*)-2,6-dioxopiperidin-3-yl)-1-oxoisoindolin-5-yl)acetate **(SI2)** as an amorphous white solid (13 mg, 73% yield, 34 µmol).

HRMS (APCI) *m/z*: $[M+H]^+$ calcd for $C_{23}H_{26}O_5N_2{}^{35}Cl_3$ 515.0902; Found 515.0902
^{1}H NMR (600 MHz, $CDCl_3$): δ 7.98 (s, 1H), 7.84 (d, *J* = 7.9 Hz, 1H), 7.53 (s, 1H), 7.47 (d, *J* = 7.9 Hz, 1H), 5.23 (dd, *J* = 13.4, 5.1 Hz, 1H), 4.80 (d, *J* = 12.0 Hz, 1H), 4.62 (d, *J* = 12.0 Hz, 1H), 4.50 (d, *J* = 15.9 Hz, 1H), 4.33 (d, *J* = 15.9 Hz, 1H), 3.51 (d, *J* = 10.6 Hz, 1H), 2.98 – 2.89 (m, 1H), 2.84 (ddd, *J* = 18.1, 13.4, 5.4 Hz, 1H), 2.36 (qd, *J* = 13.2, 4.6 Hz, 1H), 2.25 – 2.19 (m, 1H), 2.17 – 2.08 (m, 1H), 1.93 – 1.86 (m, 1H), 1.81 – 1.75 (m, 1H), 1.73 – 1.61 (m, 2H), 1.37 – 1.28 (m, 2H), 1.20 – 1.09 (m, 3H), 0.85 – 0.75 (m, 1H).
^{13}C{^{1}H} NMR (101 MHz, $CDCl_3$): δ 171.6, 171.1, 169.5, 169.1, 141.0, 138.7, 135.1, 132.5, 130.6, 128.3, 128.2, 127.2, 126.7, 123.6, 95.1, 74.5, 51.9, 46.9, 37.3, 34.4, 31.6, 23.5, 20.4.
SFC analysis: **SI2** (CHIRALCEL® OZ-3, 20% 1:1 MeOH:^{i}PrOH with 0.2% formic acid in CO_2, 2.5 mL/min, 210 nm) indicated 99:1 d.r. for retained asymmetric induction arising from formation of the major relative diastereomer and 99:1 d.r. for major relative configuration of the glutarimide stereogenic center: t_R (major diastereomer) = 6.7 min., t_R (minor diastereomers) = 7.2, 15.0, and 15.8min.
Specific Rotation: $[\alpha]_D^{24}$ -7.4 (*c* 1.0, $CHCl_3$)

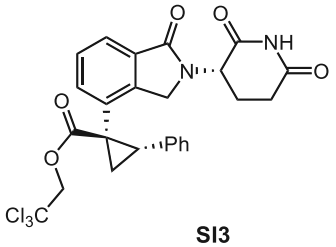

SI3

2,2,2-trichloroethyl (1*R*,2*S*)-1-(2-((*S*)-2,6-dioxopiperidin-3-yl)-1-oxoisoindolin-4-yl)-2-phenylcyclopropane-1-carboxylate (SI3).

Compound **SI3** was produced following **GP 7**, using using **3.12b** (15 mg, 1.0 equiv, 25 μmol) and benzenesulfonic acid (7.8 mg, 2.0 equiv, 50 μmol) in acetonitrile (0.12 mL) at 70 °C for 3.5 h. Purification via flash column chromatography (SiO_2, 70% ethyl acetate in hexanes) gave 2,2,2-trichloroethyl (1*R*,2*S*)-1-(2-((*S*)-2,6-dioxopiperidin-3-yl)-1-oxoisoindolin-4-yl)-2-phenylcyclopropane-1-carboxylate **(SI3)** as an amorphous white solid (7.5 mg, 57% yield, 25 μmol).

HRMS (APCI) *m/z*: $[M+H]^+$ calcd for $C_{25}H_{22}O_5N_2{}^{35}Cl_3$ 535.0589; Found 535.0591
^{1}H NMR (400 MHz, $CDCl_3$): δ 7.91 (s, 1H), 7.80 – 7.71 (m, 1H), 7.48 – 7.34 (m, 2H), 7.18 – 7.02 (m, 3H), 6.79 – 6.66 (m, 2H), 5.02 (dd, *J* = 13.2, 5.1 Hz, 1H), 4.87 (d, *J* = 11.9 Hz, 1H), 4.57 (d, *J* = 12.0 Hz, 1H), 4.29 (d, *J* = 16.0 Hz, 1H), 3.70 (d, *J* = 16.0 Hz, 1H), 3.25 (dd, *J* = 9.6, 7.4 Hz, 1H), 2.93 – 2.82 (m, 1H), 2.81 – 2.69 (m, 1H), 2.38 (dd, *J* = 9.6, 5.1 Hz, 1H), 2.23 (qd, *J* = 13.1, 4.8 Hz, 1H), 2.13 – 2.06 (m, 1H), 2.02 (dd, *J* = 7.5, 5.2 Hz, 1H).
^{13}C{^{1}H} NMR (101 MHz, $CDCl_3$): δ 171.1, 170.9, 169.0, 168.7, 143.7, 135.3, 134.7, 131.7, 129.5, 128.5, 128.3, 127.6, 127.4, 124.0, 94.9, 74.6, 51.8, 46.7, 35.1, 34.2, 31.6, 23.5, 21.4.
SFC analysis: **SI3** (CHIRALCEL® OZ-3, 20% 1:1 MeOH:^{i}PrOH with 0.2% formic acid in CO_2, 2.5 mL/min, 210 nm) indicated 93:7 d.r. for retained asymmetric induction arising from formation of the major relative diastereomer and 99:1 d.r. for major relative configuration of the glutarimide stereogenic center: t_R (major diastereomer) = 6.30 min., t_R (minor diastereomers) = 7.00, 12.94, and 20.28 min.
Specific Rotation: $[\alpha]_D^{24}$ -11.6 (*c* 0.5, $CHCl_3$)

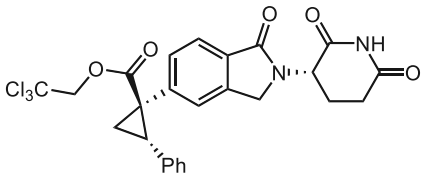

SI4

2,2,2-trichloroethyl (1*R*,2*S*)-1-(2-((*S*)-2,6-dioxopiperidin-3-yl)-1-oxoisoindolin-5-yl)-2-phenylcyclopropane-1-carboxylate (SI4).

Compound **SI4** was produced following **GP 7**, using using **3.12a** (15 mg, 1.0 equiv, 25 μmol) and benzenesulfonic acid (7.8 mg, 2.0 equiv, 50 μmol) in acetonitrile (0.12 mL) at 70 °C for 3.5 h. Purification via flash column chromatography (SiO_2, 65% ethyl acetate in hexanes) gave 2,2,2-trichloroethyl (1*R*,2*S*)-1-(2-((*S*)-2,6-dioxopiperidin-3-yl)-1-oxoisoindolin-5-yl)-2-

phenylcyclopropane-1-carboxylate **(SI4)** as an amorphous white solid (7.9 mg, 62% yield, 25 μmol).

HRMS (APCI): *m/z* $[M+H]^+$ calcd for $C_{25}H_{22}O_5N_2{}^{35}Cl_3$ 535.0589; Found 535.0592
^{1}H NMR (400 MHz, $CDCl_3$): δ 8.01 (s, 1H), 7.66 (d, *J* = 7.9 Hz, 1H), 7.24 (d, *J* = 8.1 Hz, 1H), 7.15 (s, 1H), 7.11 – 7.06 (m, 3H), 6.83 – 6.79 (m, 2H), 5.16 (dd, *J* = 13.3, 5.2 Hz, 1H), 4.86 (d, *J* = 11.9 Hz, 1H), 4.64 (d, *J* = 11.9 Hz, 1H), 4.29 (d, *J* = 15.9 Hz, 1H), 4.21 (d, *J* = 16.0 Hz, 1H), 3.29 (dd, *J* = 9.4, 7.5 Hz, 1H), 2.94 – 2.87 (m, 1H), 2.80 (m, 1H), 2.36 (dd, *J* = 9.4, 5.2 Hz, 1H), 2.29 (qd, *J* = 13.0, 4.9 Hz, 1H), 2.21 – 2.14 (m, 1H), 2.06 (dd, *J* = 7.5, 5.3 Hz, 1H).
^{13}C{^{1}H} NMR (101 MHz, $CDCl_3$): δ 171.6, 171.1, 169.5, 169.1, 141.0, 138.7, 135.1, 132.5, 130.6, 128.3, 128.2, 127.2, 126.7, 123.6, 95.1, 74.5, 51.9, 46.9, 37.3, 34.4, 31.6, 23.5, 20.4.
SFC analysis: **SI4** (CHIRALPAK® AS-3, 20% 1:1 MeOH:^{i}PrOH with 0.2% formic acid in CO_2, 2.5 mL/min, 210 nm) indicated 91:9 d.r. for retained asymmetric induction arising from formation of the major relative diastereomer and 97:3 d.r. for major relative configuration of the glutarimide stereogenic center: t_R (major diastereomer) = 2.50 min., t_R (minor diastereomers) = 1.92 and 2.84 min.
Specific Rotation: $[\alpha]_D^{24}$ 2.3 (*c* 0.5, $CHCl_3$).

Section 3: Computation Details

The data in this section were generated by Duc Ly and checked by Djamaladdin Musaev.

All calculations were performed using Gaussian-16 suite of programs.[9] Images of 3D structures were rendered using VMD[10] and Vesta.[11] Geometry and vibrational frequencies of the presented $Rh_2(OAc)_4$-carbene complexes were calculated at the B3LYP-D3(BJ)[12] level of theory in conjunction with Lanl2dz[13] basis set for rhodium and 6-31G(d,p)[14] basis set for other atoms. Geometry and vibrational frequencies of the Rh_2(*S-tetra*-BrPhTPPTTL)$_4$ systems with approximately 400 atoms and their carbene complexes were calculated by using the two-layer ONIOM[15] approach via partitioning of the complex Rh_2(*S-tetra*-BrPhTPPTTL)$_4$ into the two layers. (**Figure S3-2**) The highlighted catalyst structure and Rh-coordinated carbene fragment were treated at the B3LYP level of theory in conjunction with Lanl2dz basis set for rhodium and 6-31G(d,p) basis set for other atoms. The real system with all atoms from the catalyst and upcoming carbene fragment was calculated by using the molecular mechanics UFF[16] approach. The resulting approach is called the ONIOM(B3LYP:UFF) approach. The solvent effect (the CH_2Cl_2 was chosen as a solvent) was incorporated in all presented calculations by using the IFF-PCM method.[17] Frequency analyses and Gibbs free energy and zero-point energy corrections were calculated at a temperature and pressure corresponding to standard reaction conditions (i.e. at the 298.15K and 1 atm, respectively).

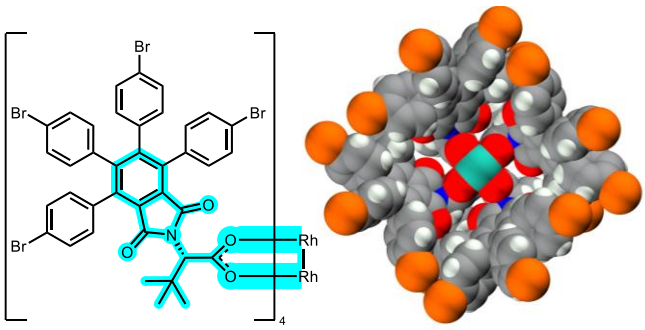

Figure S3-2. ONIOM Partitioning and the solid-state Structure of studied catalyst. The blue-highlighted atoms were modeled with QM layer (B3LYP), the rest was modeled with MM layer (UFF).

Analysis of the metal-carbene complex with $Rh_2(OAc)_4$

As the aryl fragment of the carbene moiety is unsymmetrical, there are four stereoisomers that will be formed upon the formation of the carbene complex due to the hinder rotation of the ester group and the aryl groups. As the studied catalyst is achiral and the stereocenter on the diazo is very far away from the ester group, it is expected that the diastereomer isomers resulted from the rotation of the carbene-ester bond will have comparable energy. In contrast, the rotation around the carbene-aryl bond would result in a significant energy difference as the configuration **II** (**SI-2**) is thermodynamically more stable than **I** (**SI-1**) by 2.6 kcal/mol.

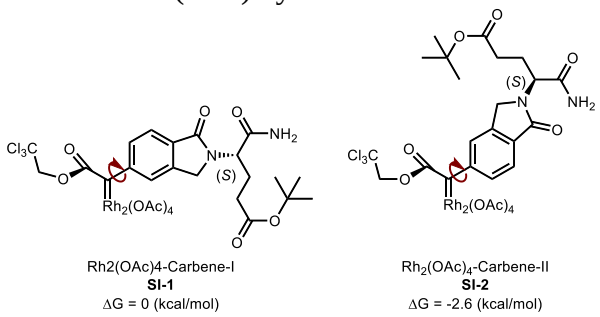

Figure S3-3. Study of $Rh_2(OAc)_4$-carbene complexes with isomers resulted from the rotation around the carbene-aryl bond.

1. Validation for ONIOM approach

The ONIOM approach can divide the study system into a QM level layer and an MM level layer. Increasing the size of the MM layer will help save computational cost but also imposed the loss of information especially weal interaction. Therefore, a comparison between structures obtaining from two layering of the ONIOM approach (**A** and **A-SI-1)** and the optimized structure from fully QM level (**A-SI-2**). The structure of model metal-carbene is displaced in **Error! Reference source not found.-4** and its optimized structure is displaced in **Figure S3-5**. The significant difference between the two ONIOM layering methods and the full QM level is the rhodium-carbene length. As the ONIOM low level layer become bigger, the rhodium-carbene bond length becomes slightly longer by 0.01 Å and 0.04 Å, respectively. However, the optimized structures from ONIOM approach showed a good agreement with the optimized structure obtained from QM level with Root-Mean-Squares Deviation (RMSD) was only 0.65 Å and 0.94 Å. (**Figure S3-5**) This

comparison showed that the ONIOM approach showed a fairly good correlation with the full QM level. As a result, the first layering approach to structure **A** was selected for the rest of this study.

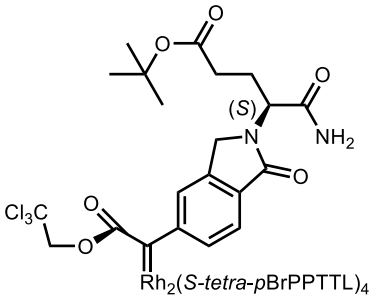

Figure S3-4 Structure of metal-carbene model study for Rh_2(S-tetra-pBrPPTTL)$_4$

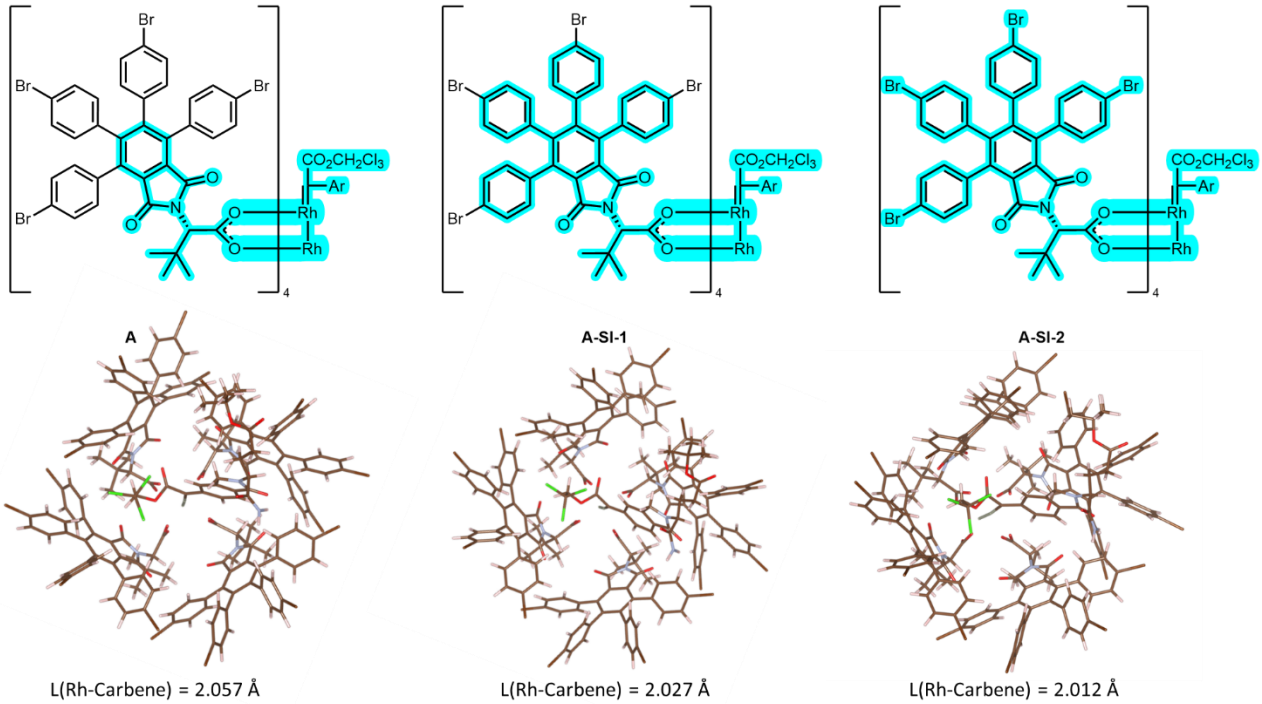

Figure S3-5. Optimized structure of metal-carbene complex. A. structure was optimized at ONIOM(B3LYP:UFF) with highlighted structure included in QM level while the rest in MM level. B. structure was optimized at ONIOM(B3LYP:UFF) with highlighted structure included in QM level while the rest in MM level. C. Structure was optimized at B3LYP-D3(BJ)/6-31G(d,p) (C,H,N,O,Br,Cl) – Lan2ldz (Rh). The reported bond length is Rhodium-carbene length

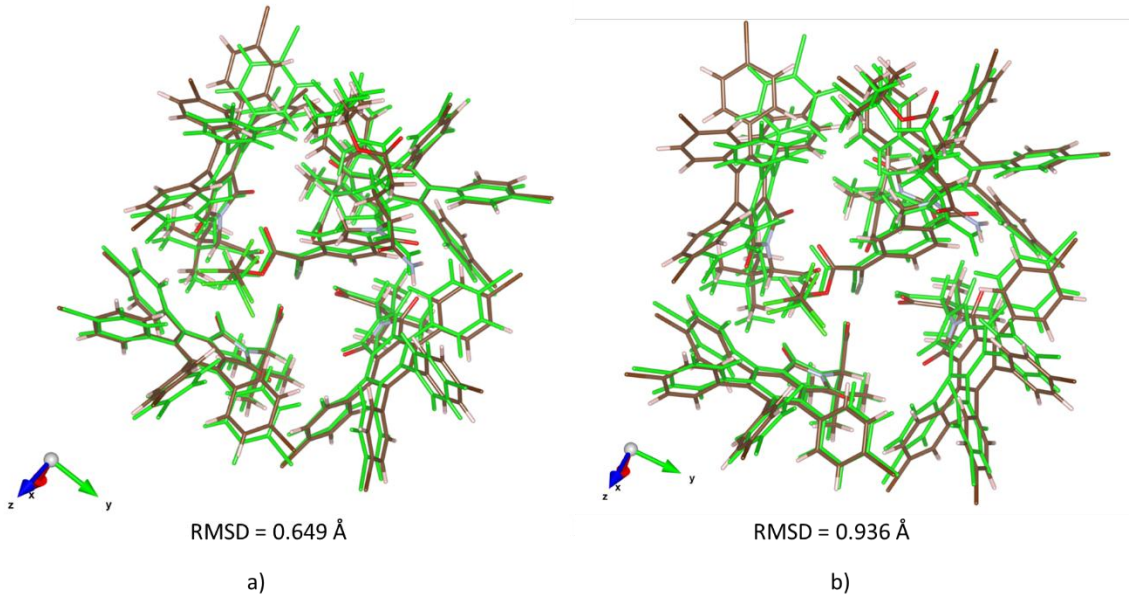

Figure S3-6 Comparison between structures obtained from ONIOM approach and normal QM approach. a) an overlay between structure A (colorful) and A-SI-2 (green). b) an overlay between structure A-SI-1 (colorful) and A-SI-2 (green). Layering structures were generated by Vesta program. Root-Mean-Squares Deviation (RMSD) was calculated by Pymol using align function.

Analysis of the metal-carbene complexes with Rh_2(*S-tetra*-Br-TPPTTL)$_4$ and Rh_2(*R-tetra*-Br-TPPTTL)$_4$

Based on experimental results and previous computation models, the open face of the Rh_2(*S-tetra*-Br-TPPTTL)$_4$ is *Re* – face and the open face of the Rh_2(*R-tetra*-Br-TPPTTL)$_4$ is *Si* – face. Previously, we showed that the attack of the substrate in C-H insertion favored the approach from the trichloroethyl (TCE) side over the carbonyl side (**Figure S3-7**).[18] Because of the above reasoning and cost of calculation, we only consider the carbene diastereomer resulted from Rh_2(*S-tetra*-Br-TPPTTL)$_4$ with the TCE group located on the *Re* – face and the one resulted from Rh_2(*R-tetra*-Br-TPPTTL)$_4$ with the TCE group located on the *Si* – face. The calculated relative free energy of the metal-carbene complex showed that a carbene in a configuration **II** is more stable than configuration **I**, which is in good agreement with a model study with $Rh_2(OAc)_4$. (**Figure S3-8**) However, the energy difference between 2 configurations is now much more significant at 9.6 and 7.1 kcal/mol. This difference can be attributed to the effect of the bowl-shaped structure of the catalyst as the structure of the catalyst is significantly distorted in configuration **I** compared to configuration **II**. Additionally, the carbene complex resulted from Rh_2(*S-tetra*-Br-TPPTTL)$_4$ is more energetically favored than the one from Rh_2(*R-tetra*-Br-TPPTTL)$_4$. This could explain why the yield of the reaction with the *R* enantiomer of the catalyst is lower than the *S* enantiomer.

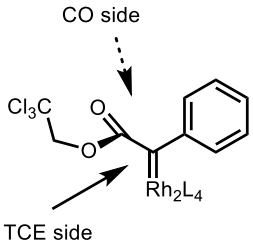

Figure S3-7 Illustration of the side of approach during C-H insertion reaction

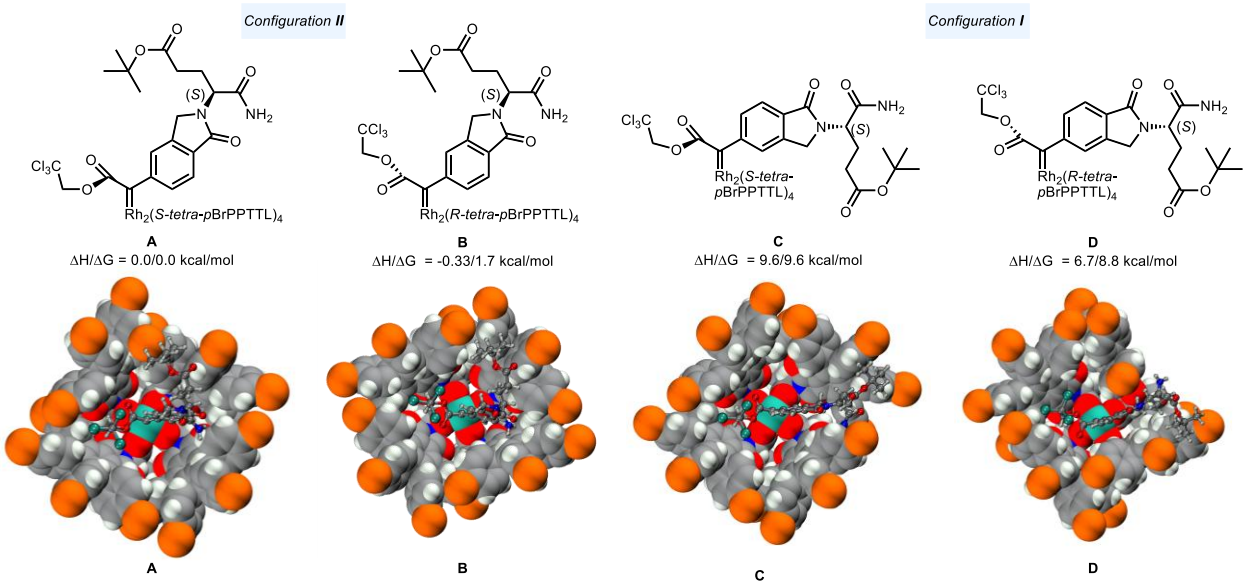

Figure S3-8. Structure of metal-carbene complex from Rh_2(S-tetra-BrTPPTTL)$_4$ and Rh_2(R-tetra-BrTPPTTL)$_4$ with I and II configuration. The reported relative enthalpies and free energy are in kcal/mol unit and relative to structure A.

Tables of energies

Table S3-1. zero-point correction (ZPE), thermal correction to enthalpy (TCH), thermal correction to Gibbs free energy (TCG), energies (E), enthalpies (H), and Gibbs free energies (G) (in Hartree) of the structures calculated at the B3LYP-D3(BJ) +CPCM(CH2Cl2) level of theory

Structure	ZPE	TCH	TCG	E	H	G	Imaginary Frequency
SI-1	0.633920	0.691141	0.529830	-3888.905165	-3888.214024	-3888.375335	-
SI-2	0.633718	0.690998	0.529273	-3888.908780	-3888.217782	-3888.379507	-

Table S3-2 zero-point correction (ZPE), thermal correction to enthalpy (TCH), thermal correction to Gibbs free energy (TCG), energies (E), enthalpies (H), and Gibbs free energies (G) (in Hartree) of the structures calculated at the ONIOM[B3LYP:UFF]+CPCM(CH_2Cl_2) level of theory followed Figure S3-1

Structure	ZPE	TCH	TCG	E	H	G	Imaginary Frequency
A	2.710880	2.913795	2.430058	-6564.904862	-6561.991066	-6562.474804	-
B	2.711298	2.913860	2.433357	-6564.905450	-6561.991590	-6562.472093	-
C	2.711768	2.914275	2.430523	-6564.890041	-6561.975766	-6562.459518	-
D	2.712272	2.914810	2.434298	-6564.895144	-6561.90334	-6562.460846	-

.

Cartesian coordinates for calculated structure

Structure SI-1

Rh	6.44401000	12.42180000	-7.03264900
Rh	8.55091000	12.50559000	-5.77183300
O	7.63247900	13.89605300	-4.54137300
O	9.11967000	14.04434900	-7.02630400
O	9.29875900	11.13646300	-7.13402300
O	7.79839300	10.94897900	-4.62877300
O	5.68279800	13.81226100	-5.69917800
O	7.17658100	13.96625400	-8.19772000
O	7.34614400	11.03746800	-8.28494200
O	5.84787700	10.87588100	-5.78485200
C	6.42595800	14.25013400	-4.77268400
C	8.32384400	14.44133200	-7.94429700
C	8.54594600	10.69795700	-8.07270300
C	6.63587900	10.47632200	-4.87921100
C	10.23313900	12.55340600	-4.66258800
C	9.17733300	9.68858300	-8.99972800
H	10.01179500	10.15798700	-9.52865500
H	8.44741300	9.31862300	-9.71897800
H	9.58264500	8.85894200	-8.41446900
C	5.86286600	15.29619700	-3.84156300
H	6.42323800	16.22719700	-3.96927000
H	5.99056600	14.97143500	-2.80579400
H	4.80846800	15.47171200	-4.05277400
C	8.80599600	15.60401700	-8.77670100
H	8.69226000	16.52415500	-8.19433500
H	8.21933200	15.68724700	-9.69151100
H	9.86568700	15.48453200	-9.00970800
C	6.17959400	9.35027100	-3.98411000
H	5.95662500	9.75374700	-2.99144400
H	6.98232200	8.61797800	-3.87221100
H	5.28600700	8.87659800	-4.38979200
C	11.06195900	11.46785500	-4.26904700
C	12.19635200	11.68598100	-3.42358300
C	10.74540400	10.14474800	-4.69489000
C	12.99697200	10.63503300	-3.01110400

H	12.43093100	12.69431500	-3.10249300
C	11.54951400	9.10759400	-4.26825900
H	9.89018600	9.98288000	-5.33378000
C	12.65075900	9.35283500	-3.44047400
H	13.86001800	10.79011800	-2.37353300
C	11.45813000	7.63176500	-4.55174400
C	13.33453300	8.06299500	-3.16353800
N	12.56764500	7.09706800	-3.76096300
H	11.59226700	7.40417600	-5.61650700
H	10.50056200	7.20773700	-4.23284300
O	14.38903400	7.87372800	-2.55381600
C	12.99296200	5.69995500	-3.79626300
C	13.95049000	5.52678400	-5.00053800
C	11.80391800	4.74736300	-3.86163900
H	13.56030800	5.54115700	-2.87407200
N	15.19571200	6.00694300	-4.77337000
O	13.58463100	5.02226200	-6.05889200
C	12.24007700	3.28605900	-3.70257900
H	11.29456900	4.86025100	-4.82019200
H	11.09897500	5.01611900	-3.06815000
H	15.83896300	6.06119100	-5.55048200
H	15.38124700	6.55455600	-3.94003100
C	11.08540300	2.30280200	-3.71737900
H	12.78496900	3.12882800	-2.76852500
H	12.90720300	3.02020900	-4.53033400
O	10.98793300	1.36338500	-2.94987400
O	10.21891900	2.60292000	-4.69692100
C	9.00533800	1.79782200	-4.94366300
C	9.40106100	0.37308700	-5.33245300
C	8.35848200	2.52503100	-6.12106500
C	8.09932800	1.83962800	-3.71269900
H	8.50778100	-0.17975100	-5.63816400
H	9.86816700	-0.14712300	-4.49646900
H	10.09738200	0.39073500	-6.17609300
H	7.43313900	2.01857900	-6.40866400
H	8.12023700	3.55784400	-5.85136800
H	9.03157900	2.53649000	-6.98281500
H	7.89386100	2.87640100	-3.42962800
H	8.55752100	1.32467400	-2.86858000
H	7.14716700	1.35474000	-3.94778300
C	10.55072900	13.90424700	-4.16466400
O	11.17484400	14.73161700	-4.79452200
O	9.98889300	14.10524800	-2.94569200
C	9.95929500	15.43875300	-2.45135100
C	10.81334100	15.54413500	-1.18435400
H	10.34441700	16.13354100	-3.19824400
H	8.92480300	15.67559500	-2.19969600
Cl	12.53544900	15.18200300	-1.55493600
Cl	10.66781700	17.22892200	-0.57656300
Cl	10.22543800	14.39677500	0.06618700

Structure SI-2

Rh	6.31900300	13.05991200	-6.97477400
Rh	8.41675200	12.71143400	-5.74531000
O	7.71143500	14.08338100	-4.36323200
O	9.20008000	14.27415700	-6.84685000
O	8.96149900	11.39927400	-7.25064700
O	7.44879600	11.16966600	-4.75575700
O	5.76926400	14.40119400	-5.49192400
O	7.26466100	14.59802600	-7.98684900
O	7.01310500	11.69756700	-8.37386900

O	5.50751800	11.49484800	-5.88414900
C	6.56817800	14.62911800	-4.53636000
C	8.46917000	14.87478800	-7.70607200
C	8.15244400	11.16957300	-8.21589200
C	6.23045000	10.89554900	-5.03497100
C	10.09264900	12.41572400	-4.66700800
C	8.62843800	10.17687500	-9.24731600
H	9.54123200	10.55361800	-9.71733000
H	7.86320300	10.01348400	-10.00540300
H	8.87606100	9.23260700	-8.75504300
C	6.15987700	15.63468300	-3.48779600
H	6.89094900	16.44774100	-3.46446600
H	6.16600000	15.15647800	-2.50455400
H	5.16891000	16.03389500	-3.70146700
C	9.11251800	16.03593900	-8.42348000
H	9.13660100	16.89698000	-7.74767200
H	8.54093400	16.29850900	-9.31361400
H	10.14236500	15.78947500	-8.68850100
C	5.61791900	9.76025000	-4.25253300
H	5.47591100	10.07921800	-3.21528900
H	6.29875300	8.90608300	-4.24696200
H	4.65590700	9.47617100	-4.67818100
C	10.80052500	11.20777200	-4.42361200
C	10.31804500	9.97394800	-4.95863400
C	11.97950700	11.21446500	-3.61676100
C	10.97612300	8.78125800	-4.69907200
H	9.42296200	9.99041800	-5.56199700
C	12.62778100	10.02275700	-3.37897800
H	12.35370200	12.14348100	-3.20203700
C	12.12806800	8.82830300	-3.91572600
H	10.61463100	7.83675900	-5.09007400
C	13.86811400	9.73050400	-2.57765700
C	13.00207200	7.70987500	-3.47492700
N	14.02625900	8.28824200	-2.77305000
H	13.74073500	9.96946000	-1.51486100
H	14.73897600	10.28063500	-2.94728700
O	12.84581500	6.50097300	-3.66092700
C	15.03561400	7.48192700	-2.09117000
C	14.47279900	7.09058900	-0.70278800
C	16.37036700	8.21270100	-1.99029700
H	15.14186600	6.57337000	-2.69173100
N	13.55121600	6.10107500	-0.75357300
O	14.82683900	7.65526900	0.32949400
C	17.47854000	7.29765400	-1.45562900
H	16.27042600	9.07146800	-1.32439100
H	16.63945100	8.58367200	-2.98457600
H	13.03344200	5.88045800	0.08543800
H	13.19439700	5.78766500	-1.64966700
C	18.83544600	7.97090900	-1.37926400
H	17.59557800	6.40489300	-2.07478200
H	17.21656100	6.97223800	-0.44253400
O	19.87452500	7.43863000	-1.72483100
O	18.72512900	9.20402900	-0.86381100
C	19.89576400	10.08616300	-0.67753200
C	20.86909500	9.45027200	0.31515300
C	19.26835900	11.35042300	-0.09330800
C	20.54375600	10.37509100	-2.03182100
H	21.66711600	10.16244900	0.54531300
H	21.31372400	8.54407500	-0.09571800
H	20.35191900	9.20344700	1.24707400

H	20.04382600	12.09788200	0.09466700
H	18.53817900	11.77393600	-0.78870400
H	18.76281600	11.12821900	0.85057000
H	19.79934700	10.76770900	-2.73097100
H	20.98972700	9.47540900	-2.45536400
H	21.32503200	11.13028100	-1.90472500
C	10.56455700	13.64691500	-4.00404100
O	11.25346400	14.49198300	-4.53505500
O	10.06514400	13.71984300	-2.74383100
C	10.21354700	14.95160500	-2.04682200
C	11.14278000	14.76071400	-0.84329300
H	10.63137300	15.71679600	-2.70180800
H	9.22798100	15.24787100	-1.68561200
Cl	12.79862000	14.31276900	-1.38736800
Cl	11.20361500	16.32179100	0.04325500
Cl	10.51250500	13.47299700	0.23859800

Structure A

Rh	0	-0.39893618	0.06648936	0.00000000 H
Rh	0	1.85221582	-0.06469364	-1.00789600 H
Br	0	2.43003582	-7.93353664	4.44283300 L
Br	0	-1.02574818	-7.40566664	10.85677700 L
Br	0	-1.77997218	5.86830436	9.38045400 L
Br	0	-3.44282618	-0.51664964	13.50629800 L
O	0	2.60074482	0.53922036	0.82655100 H
O	0	0.55046782	0.50968236	1.79236400 H
O	0	0.86986382	2.36349036	5.28219000 H
O	0	2.04447482	-1.70759164	3.55351600 H
N	0	1.73761382	0.49086136	4.23502800 H
C	0	1.81312382	0.69096436	1.80159900 H
C	0	2.36313782	1.22729636	3.13591800 H
H	0	1.92160282	2.22904036	3.21399700 H
C	0	3.91018382	1.41989336	3.29107300 H
C	0	4.36827082	2.51933536	2.30719100 H
H	0	3.80414982	3.44647236	2.45940800 H
H	0	4.24437982	2.21020636	1.26839500 H
H	0	5.42725682	2.74129036	2.47536200 H
C	0	4.18329882	1.92766336	4.72389700 H
H	0	3.96110082	1.16627536	5.47760400 H
H	0	3.58829382	2.81641636	4.95238800 H
H	0	5.24078382	2.19169436	4.82246700 H
C	0	4.71644482	0.12849836	3.05723100 H
H	0	4.57530482	-0.25329964	2.04447100 H
H	0	4.43364382	-0.65775564	3.76227800 H
H	0	5.78250982	0.33668036	3.20031000 H
C	0	1.02017982	1.15824336	5.23618100 H
C	0	1.63778682	-0.89799264	4.36840700 H
C	0	0.92638282	-1.13635964	5.67174700 H
C	0	0.52476782	0.10436436	6.16989600 H
C	0	-0.17012118	0.23448536	7.36569100 H
C	0	-0.43657818	-0.94713064	8.10058900 H
C	0	-0.01877118	-2.21271964	7.60909100 H
C	0	0.65864782	-2.31627864	6.36214200 H
C	0	1.07637682	-3.62612964	5.80238800 L H 35
C	0	2.43907282	-3.92080764	5.63733000 L
H	0	3.19156882	-3.17544564	5.86376400 L
C	0	2.83785682	-5.19252564	5.21562300 L
H	0	3.89111882	-5.41548164	5.10492900 L
C	0	1.88026682	-6.17910964	4.96018700 L
C	0	0.52042982	-5.88472364	5.09960400 L
H	0	-0.22378518	-6.64396764	4.89789100 L

C	0	0.11820682	-4.61283064	5.51636800	L
H	0	-0.93712418	-4.40378364	5.63795200	L
C	0	-0.26225918	-3.44433564	8.41254700	L H 34
C	0	-1.57222318	-3.85936264	8.70306700	L
H	0	-2.41783618	-3.27462564	8.36989200	L
C	0	-1.79702818	-5.03221764	9.42820900	L
H	0	-2.81096818	-5.34498164	9.64185900	L
C	0	-0.71594818	-5.79853664	9.87369000	L
C	0	0.59183782	-5.38572664	9.60019200	L
H	0	1.43175582	-5.97375364	9.94686600	L
C	0	0.81931582	-4.21209564	8.87602000	L
H	0	1.83703882	-3.90244764	8.67312100	L
C	0	-1.15586818	-0.84508264	9.39733100	L H 33
C	0	-2.49657118	-0.42967564	9.42951100	L
H	0	-3.01630218	-0.18718064	8.51099400	L
C	0	-3.17307218	-0.33225664	10.64842500	L
H	0	-4.20696518	-0.01249864	10.66430800	L
C	0	-2.51616318	-0.64871064	11.84206100	L
C	0	-1.17990318	-1.06145164	11.81589700	L
H	0	-0.66770118	-1.30585564	12.73749300	L
C	0	-0.50008918	-1.15801864	10.59853900	L
H	0	0.53598782	-1.47340564	10.59010800	L
C	0	-0.56096018	1.58037836	7.85136800	L H 32
C	0	-1.51235118	2.33771436	7.14943000	L
H	0	-1.96528418	1.94690236	6.24741800	L
C	0	-1.87634118	3.60783936	7.60572200	L
H	0	-2.60645518	4.18781336	7.05575800	L
C	0	-1.29258418	4.12936736	8.76455400	L
C	0	-0.34519718	3.37886536	9.46836400	L
H	0	0.11037182	3.78030836	10.36429100	L
C	0	0.02029382	2.10845236	9.01453900	L
H	0	0.75959982	1.53893636	9.56414700	L
Br	0	-1.27224518	-5.49218664	-7.83898200	L
Br	0	-7.98391118	-8.78309964	-5.76247100	L
Br	0	-4.63546618	-6.85566064	6.97143800	L
Br	0	-9.93043318	-9.01478564	1.61188800	L
O	0	1.94968182	-2.04117064	-0.37268800	H
O	0	-0.17515818	-1.94747564	0.40622200	H
O	0	-1.12940718	-4.89875764	2.46789900	H
O	0	-0.23072118	-4.23944764	-1.95834300	H
N	0	-0.27917718	-4.64036764	0.32717300	H
C	0	0.93346482	-2.53897464	0.18288600	H
C	0	0.96304382	-3.97911164	0.72941900	H
H	0	0.84427082	-3.84853464	1.81193500	H
C	0	2.24996982	-4.84647364	0.53626100	H
C	0	3.38440382	-4.20308764	1.36303100	H
H	0	3.09804182	-4.09001464	2.41376200	H
H	0	3.65010982	-3.21668364	0.97747500	H
H	0	4.27530182	-4.83821364	1.32155300	H
C	0	1.95178982	-6.24448864	1.11880500	H
H	0	1.24862382	-6.80295764	0.49388600	H
H	0	1.52386482	-6.17359964	2.12276600	H
H	0	2.87701682	-6.82545364	1.18225300	H
C	0	2.69917682	-5.00399864	-0.92879700	H
H	0	2.94569182	-4.04001164	-1.37714900	H
H	0	1.92928682	-5.47925164	-1.54105000	H
H	0	3.59282282	-5.63724064	-0.96214900	H
C	0	-1.24779818	-5.02857664	1.26226800	H
C	0	-0.77703818	-4.71584464	-0.97843000	H
C	0	-2.09299118	-5.42409264	-0.88078900	H

C	0	-2.39206218	-5.58081064	0.47344100	H
C	0	-3.59188618	-6.13827964	0.90307200	H
C	0	-4.51319218	-6.54083964	-0.09395500	H
C	0	-4.19052018	-6.42451564	-1.46964700	H
C	0	-2.95769418	-5.85965064	-1.88166600	H
C	0	-2.55767118	-5.77129564	-3.30969400	L H 108
C	0	-1.38971318	-6.41156964	-3.75663000	L
H	0	-0.77355118	-6.97241164	-3.06450900	L
C	0	-1.01068718	-6.33023664	-5.09971200	L
H	0	-0.10372718	-6.81830664	-5.43222900	L
C	0	-1.80039918	-5.61981164	-6.00892500	L
C	0	-2.97185018	-4.99332464	-5.57394000	L
H	0	-3.58774318	-4.44354564	-6.27389500	L
C	0	-3.34466718	-5.06085364	-4.22959400	L
H	0	-4.24296718	-4.55392764	-3.90577800	L
C	0	-5.10852918	-6.99285664	-2.48718500	L H 107
C	0	-6.20322918	-6.24804464	-2.94824400	L
H	0	-6.38237118	-5.25206564	-2.56562100	L
C	0	-7.05424318	-6.77890364	-3.92127700	L
H	0	-7.89142118	-6.19437164	-4.27989900	L
C	0	-6.81976318	-8.05906564	-4.43360500	L
C	0	-5.72956618	-8.80639764	-3.97461800	L
H	0	-5.54330318	-9.79647264	-4.37018200	L
C	0	-4.87410918	-8.27471864	-3.00511400	L
H	0	-4.02989618	-8.85809064	-2.65861700	L
C	0	-5.81062618	-7.13614864	0.30914500	L H 106
C	0	-6.98233318	-6.36562464	0.26703800	L
H	0	-6.94591018	-5.33248464	-0.05577700	L
C	0	-8.20366918	-6.92422264	0.65293900	L
H	0	-9.10341218	-6.32348564	0.61913600	L
C	0	-8.26070718	-8.25360164	1.08451400	L
C	0	-7.09338618	-9.02378364	1.13205600	L
H	0	-7.13318618	-10.05199664	1.46762600	L
C	0	-5.87029218	-8.46714664	0.74653600	L
H	0	-4.97136218	-9.06991964	0.78722000	L
C	0	-3.85452118	-6.31822964	2.35213000	L H 105
C	0	-4.92515518	-5.65373864	2.97022500	L
H	0	-5.56378718	-4.99278564	2.39813200	L
C	0	-5.16771618	-5.82908564	4.33552700	L
H	0	-5.99363418	-5.30995564	4.80439200	L
C	0	-4.33186218	-6.65284564	5.09692300	L
C	0	-3.26374018	-7.31719264	4.48688500	L
H	0	-2.61461718	-7.95579964	5.07196600	L
C	0	-3.02915718	-7.15717564	3.11852100	L
H	0	-2.20085618	-7.68059664	2.65672600	L
Br	0	-0.92670518	7.74422236	-5.92705800	L
Br	0	-8.68832918	7.83856036	-6.85345500	L
Br	0	-9.33174018	-4.35306364	-2.10610800	L
Br	0	-12.73451018	1.56653936	-4.77804200	L
O	0	0.92354282	-0.66175164	-2.78561500	H
O	0	-1.12919918	-0.34287064	-1.88438200	H
O	0	-3.80240818	-1.96574864	-3.78599400	H
O	0	-1.32249718	1.82856336	-4.33641900	H
N	0	-2.27239318	-0.28862264	-4.27067600	H
C	0	-0.33636118	-0.65146764	-2.83595200	H
C	0	-1.07635418	-1.11735564	-4.10538400	H
H	0	-1.48904318	-2.09271464	-3.81626400	H
C	0	-0.25599418	-1.36698864	-5.41654800	H
C	0	0.63300282	-2.60951264	-5.18692300	H
H	0	0.03826582	-3.47360964	-4.87267800	H

H	0	1.38900682	-2.42325264	-4.42184100	H
H	0	1.14451782	-2.87357564	-6.11822300	H
C	0	-1.25663318	-1.68540864	-6.54776200	H
H	0	-1.84172618	-0.80647164	-6.83346800	H
H	0	-1.95633118	-2.47411364	-6.25789200	H
H	0	-0.71266618	-2.02685464	-7.43389700	H
C	0	0.62362782	-0.17917964	-5.85276000	H
H	0	1.35893282	0.07520336	-5.08698800	H
H	0	0.02813182	0.71126736	-6.06439500	H
H	0	1.16277582	-0.45098864	-6.76708000	H
C	0	-3.55922218	-0.80429264	-4.05174900	H
C	0	-2.30236718	1.10561536	-4.38815800	H
C	0	-3.75186518	1.47790636	-4.52738100	H
C	0	-4.50263918	0.33940736	-4.22924700	H
C	0	-5.89092118	0.36159236	-4.18067800	H
C	0	-6.53800218	1.56783236	-4.54878400	H
C	0	-5.77985618	2.71590936	-4.90354300	H
C	0	-4.35913618	2.68968936	-4.85207400	H
C	0	-3.53406718	3.89882036	-5.11117300	L H 181
C	0	-2.55396718	3.89093736	-6.11752300	L
H	0	-2.39085218	3.00348836	-6.71662300	L
C	0	-1.77921118	5.02998836	-6.35614100	L
H	0	-1.01896218	5.01036536	-7.12621800	L
C	0	-1.98914618	6.19097636	-5.60552900	L
C	0	-2.97698118	6.21325336	-4.61720700	L
H	0	-3.14310818	7.10997636	-4.03456500	L
C	0	-3.74176818	5.07099336	-4.36541100	L
H	0	-4.49035718	5.09696536	-3.58444300	L
C	0	-6.47275718	3.95045236	-5.36545900	L H 180
C	0	-7.34356618	4.64265236	-4.50869000	L
H	0	-7.51665418	4.28665236	-3.50325400	L
C	0	-7.99898518	5.79480536	-4.94986000	L
H	0	-8.67056418	6.31886336	-4.28215300	L
C	0	-7.78631118	6.26810236	-6.24840700	L
C	0	-6.91567818	5.58759636	-7.10543700	L
H	0	-6.74845618	5.95036236	-8.11133600	L
C	0	-6.26222718	4.43222036	-6.66778900	L
H	0	-5.59717718	3.90904836	-7.34382000	L
C	0	-8.02405118	1.60359736	-4.59897600	L H 179
C	0	-8.77725918	1.48437736	-3.41986900	L
H	0	-8.28233018	1.39003536	-2.46163200	L
C	0	-10.17336718	1.47383936	-3.47728600	L
H	0	-10.74834818	1.37028536	-2.56940000	L
C	0	-10.82684518	1.59014236	-4.70716900	L
C	0	-10.08227118	1.71710536	-5.88400300	L
H	0	-10.58429518	1.80510036	-6.83877900	L
C	0	-8.68558318	1.72047236	-5.83203200	L
H	0	-8.11876418	1.80357336	-6.75115100	L
C	0	-6.64233918	-0.82914964	-3.71302500	L H 178
C	0	-6.55409318	-1.22894364	-2.36961700	L
H	0	-5.89682018	-0.70609364	-1.68600900	L
C	0	-7.34126918	-2.28324464	-1.89595800	L
H	0	-7.27968318	-2.57412164	-0.85507100	L
C	0	-8.21916018	-2.94560264	-2.76090200	L
C	0	-8.29246918	-2.56726964	-4.10537200	L
H	0	-8.96827618	-3.07944464	-4.77792900	L
C	0	-7.50701118	-1.51331764	-4.58161800	L
H	0	-7.58730318	-1.21598064	-5.61987200	L
Br	0	3.86994982	5.30766836	6.79502600	L
Br	0	-1.96959318	9.80336436	8.71669500	L

Br	0	-6.47935818	8.94561936	-3.71086700	L
Br	0	-7.37735718	11.42918336	3.63794100	L
O	0	1.63612882	1.92391836	-1.55851800	H
O	0	-0.34057118	2.09780536	-0.47111300	H
O	0	-2.06145318	5.43180036	-1.78988300	H
O	0	1.19740982	4.26379736	1.20215000	H
N	0	-0.19271218	4.79156936	-0.58092800	H
C	0	0.61583382	2.56010736	-1.17961000	H
C	0	0.40384082	4.00666936	-1.66264600	H
H	0	-0.41137818	3.91702936	-2.39306600	H
C	0	1.57421782	4.73240836	-2.41077000	H
C	0	1.82792182	4.00611036	-3.75055900	H
H	0	0.91138882	3.95061736	-4.34919500	H
H	0	2.19984582	2.99224836	-3.59787000	H
H	0	2.57171282	4.56162736	-4.33117700	H
C	0	1.11325082	6.17023936	-2.73849400	H
H	0	0.98872782	6.77663536	-1.83637500	H
H	0	0.16533282	6.17359436	-3.28541000	H
H	0	1.86643182	6.65964436	-3.36373900	H
C	0	2.87310982	4.79732536	-1.58599000	H
H	0	3.24880382	3.79893236	-1.35311800	H
H	0	2.72794982	5.33622036	-0.64584900	H
H	0	3.64162982	5.32723736	-2.15926700	H
C	0	-1.40796318	5.46008036	-0.76309700	H
C	0	0.24370282	4.87132936	0.74956900	H
C	0	-0.70723218	5.81246336	1.44128100	H
C	0	-1.70303818	6.15152136	0.52260700	H
C	0	-2.73187118	7.03082636	0.82933400	H
C	0	-2.76845418	7.56238036	2.13789000	H
C	0	-1.76477218	7.22173336	3.08209000	H
C	0	-0.70188018	6.34224036	2.73243700	H
C	0	0.40029582	6.02246236	3.67834400	L H 254
C	0	1.72968082	6.33101936	3.34419900	L
H	0	1.96582782	6.76468436	2.38021300	L
C	0	2.75946282	6.10331836	4.26209000	L
H	0	3.78024782	6.34334636	3.99417800	L
C	0	2.46846682	5.58776136	5.52874400	L
C	0	1.14840682	5.28261236	5.87059800	L
H	0	0.92005582	4.88318236	6.84997000	L
C	0	0.12029682	5.48118236	4.94476700	L
H	0	-0.89550718	5.22835436	5.22025300	L
C	0	-1.80555418	7.82854536	4.43918300	L H 253
C	0	-2.83603318	7.49525136	5.33293400	L
H	0	-3.60002818	6.78318336	5.04607400	L
C	0	-2.88316518	8.08088736	6.60086800	L
H	0	-3.68260318	7.82094336	7.28258600	L
C	0	-1.90006218	8.99809636	6.98669200	L
C	0	-0.86775518	9.32860936	6.10284500	L
H	0	-0.10530318	10.03796136	6.39758600	L
C	0	-0.82051318	8.74847436	4.83229700	L
H	0	-0.02188818	9.01862336	4.15242300	L
C	0	-3.87007518	8.49085936	2.50399100	L H 252
C	0	-5.19232218	8.02303836	2.56739800	L
H	0	-5.41560918	6.98345736	2.36044500	L
C	0	-6.23116618	8.89530736	2.90330100	L
H	0	-7.24757918	8.52614636	2.95089100	L
C	0	-5.95683618	10.23921436	3.17757900	L
C	0	-4.64154618	10.71123536	3.11263200	L
H	0	-4.42563718	11.75103636	3.32151100	L
C	0	-3.60081218	9.84174136	2.77416300	L

H	0	-2.58733018	10.21945536	2.71862100	L
C	0	-3.65178718	7.49141936	-0.23539500	L H 251
C	0	-4.69377618	6.66793436	-0.68524600	L
H	0	-4.84882218	5.69402336	-0.23998200	L
C	0	-5.53600518	7.10337436	-1.71391400	L
H	0	-6.33273918	6.46388736	-2.06739700	L
C	0	-5.34281718	8.36102936	-2.29398700	L
C	0	-4.31143018	9.18857636	-1.83999500	L
H	0	-4.15883718	10.16281236	-2.28604100	L
C	0	-3.46862718	8.75665036	-0.81276300	L
H	0	-2.66761018	9.40187636	-0.47315400	L
C	0	-2.32647618	0.00878736	0.71560900	H
C	0	-3.45845818	0.80075536	0.35603100	H
C	0	-2.61275618	-1.18061664	1.55970300	H
C	0	-3.31821018	1.91255936	-0.53182200	H
C	0	-4.74715718	0.51452436	0.90753100	H
O	0	-2.98211218	-2.23417164	1.08449500	H
O	0	-2.38429018	-0.94981164	2.87496400	H
C	0	-4.39229118	2.73770836	-0.83160000	H
H	0	-2.34408918	2.11348136	-0.95252500	H
C	0	-5.80732418	1.33555636	0.59331000	H
H	0	-4.88888718	-0.33381664	1.56589400	H
C	0	-2.53140918	-2.04043164	3.79020100	H
C	0	-5.62509518	2.43739036	-0.25275700	H
H	0	-4.27421318	3.59148036	-1.48919900	H
C	0	-7.24841418	1.26315136	1.02538600	H
C	0	-3.79905918	-1.87919064	4.64624800	H
H	0	-2.56296218	-2.99591864	3.26462500	H
H	0	-1.66979418	-2.00699564	4.45775400	H
C	0	-6.92118618	3.15804236	-0.36827100	H
N	0	-7.83377618	2.40887436	0.32671000	H
H	0	-7.36226118	1.35991036	2.11205800	H
H	0	-7.71839518	0.32253836	0.71895700	H
Cl	0	-5.29458118	-2.06661164	3.65791900	H
Cl	0	-3.76189718	-3.17202564	5.89211900	H
Cl	0	-3.83071718	-0.27309164	5.45209000	H
O	0	-7.15728518	4.22359636	-0.93823800	H
C	0	-9.24096918	2.80625736	0.40301900	H
C	0	-9.44861018	3.76655236	1.60372300	H
C	0	-10.16059818	1.58686436	0.44546400	H
H	0	-9.42382518	3.37904936	-0.51310800	H
N	0	-8.90140818	4.99045236	1.41645500	H
O	0	-10.05192118	3.42678236	2.61876500	H
C	0	-11.63579318	1.94730336	0.21070800	H
H	0	-10.05795518	1.07466036	1.40507900	H
H	0	-9.82615418	0.89100636	-0.32880100	H
H	0	-8.90419618	5.65013836	2.18146500	H
H	0	-8.34081418	5.18294836	0.59328900	H
C	0	-12.48883918	0.79316736	-0.29582000	H
H	0	-11.74249418	2.74487136	-0.53162000	H
H	0	-12.08303818	2.32553836	1.13669300	H
O	0	-13.48239918	0.95299836	-0.98118100	H
O	0	-11.99770018	-0.38938764	0.10423500	H
C	0	-12.51894618	-1.68220464	-0.39503500	H
C	0	-13.98750918	-1.85785164	-0.00003000	H
C	0	-11.63475718	-2.69577864	0.33426600	H
C	0	-12.30177118	-1.75062764	-1.91006900	H
H	0	-14.30999918	-2.87276764	-0.25317700	H
H	0	-14.62627118	-1.14428264	-0.51996800	H
H	0	-14.10967718	-1.72284164	1.07914900	H

H	0	-11.89093818	-3.71152764	0.01996100	H
H	0	-10.57906518	-2.51728564	0.11065600	H
H	0	-11.77514318	-2.62302764	1.41665000	H
H	0	-11.24887418	-1.57429064	-2.15259000	H
H	0	-12.91247218	-1.01125664	-2.43040700	H
H	0	-12.57298118	-2.74579864	-2.27527400	H

Structure B

Rh	0	-2.27393623	0.41223404	0.00000000	H
Rh	0	0.09611277	0.28628704	0.68644900	H
Br	0	-0.99085923	-7.62470996	-4.90914100	L
Br	0	-5.68014623	-6.44779296	-10.65385400	L
Br	0	-3.64206523	6.57371804	-9.66849400	L
Br	0	-7.44567423	0.64511904	-12.84089600	L
O	0	0.58432577	0.83633504	-1.25363500	H
O	0	-1.58369823	0.89970504	-1.90676600	H
O	0	-1.51618923	2.79897704	-5.48533600	H
O	0	-0.64886623	-1.39622396	-3.86857400	H
N	0	-0.78931423	0.83033204	-4.51160600	H
C	0	-0.32827523	1.01023504	-2.10758600	H
C	0	0.05952977	1.49167204	-3.51896800	H
H	0	-0.28652823	2.53323804	-3.54302800	H
C	0	1.57991477	1.53276104	-3.90389900	H
C	0	2.28235377	2.59374604	-3.02746400	H
H	0	1.79328577	3.57032104	-3.12184900	H
H	0	2.28586577	2.31233004	-1.97385600	H
H	0	3.32033977	2.70950504	-3.35632600	H
C	0	1.69455277	1.99418804	-5.37414300	H
H	0	1.29134677	1.25189004	-6.06966600	H
H	0	1.17004977	2.93913804	-5.54242300	H
H	0	2.74948877	2.14146104	-5.62554900	H
C	0	2.27978877	0.16861604	-3.75608000	H
H	0	2.25414777	-0.18501796	-2.72380600	H
H	0	1.81677577	-0.59217096	-4.39057900	H
H	0	3.32791577	0.26327304	-4.06045700	H
C	0	-1.51948223	1.58386504	-5.43759300	H
C	0	-1.06791823	-0.53794196	-4.62495600	H
C	0	-1.97028323	-0.67891596	-5.82448600	H
C	0	-2.25379923	0.60725804	-6.29049200	H
C	0	-3.05637923	0.84002304	-7.39943300	H
C	0	-3.62046123	-0.28472896	-8.04617600	H
C	0	-3.32944923	-1.59681796	-7.58845200	H
C	0	-2.48239323	-1.80892596	-6.46389500	H
C	0	-2.12079023	-3.17536196	-6.00012500	L H 35
C	0	-0.77494123	-3.57734196	-5.96514100	L
H	0	0.01232077	-2.87970196	-6.22312500	L
C	0	-0.43939923	-4.89143196	-5.62467500	L
H	0	0.60039177	-5.19077596	-5.59967300	L
C	0	-1.44486223	-5.82096496	-5.34091600	L
C	0	-2.78570123	-5.42969496	-5.37579500	L
H	0	-3.56595723	-6.14552196	-5.15386400	L
C	0	-3.12256623	-4.10859496	-5.68176800	L
H	0	-4.16510623	-3.81825696	-5.69268100	L
C	0	-3.89152023	-2.76520896	-8.31763400	L H 34
C	0	-5.27506523	-3.00261996	-8.31321400	L
H	0	-5.93995623	-2.34339696	-7.76964600	L
C	0	-5.80283023	-4.09189196	-9.01085500	L
H	0	-6.86977323	-4.26772196	-9.00520700	L
C	0	-4.95418123	-4.95649496	-9.70845100	L
C	0	-3.57443323	-4.72829496	-9.71221000	L
H	0	-2.91403023	-5.39494596	-10.25145900	L

C	0	-3.04353923	-3.63498896	-9.02215600	L
H	0	-1.97440523	-3.46277796	-9.03814900	L
C	0	-4.53565723	-0.06760896	-9.20043300	L H 33
C	0	-5.74193023	0.62883204	-9.01932500	L
H	0	-6.01601323	1.00288704	-8.04073500	L
C	0	-6.59738323	0.84736004	-10.10184100	L
H	0	-7.52040123	1.39032204	-9.95549500	L
C	0	-6.26292323	0.36213704	-11.36936100	L
C	0	-5.06206023	-0.32939696	-11.55768600	L
H	0	-4.79668923	-0.70157696	-12.53870500	L
C	0	-4.19657723	-0.53721396	-10.47993800	L
H	0	-3.26266623	-1.06092696	-10.64143300	L
C	0	-3.20421623	2.21400304	-7.93640600	L H 32
C	0	-3.90820123	3.19015504	-7.21577700	L
H	0	-4.34861723	2.94676804	-6.25819400	L
C	0	-4.03812523	4.48424704	-7.72917600	L
H	0	-4.57888423	5.23345304	-7.16807400	L
C	0	-3.46870623	4.80863204	-8.96492000	L
C	0	-2.77127823	3.83723704	-9.68896900	L
H	0	-2.33032723	4.08380004	-10.64616200	L
C	0	-2.63926323	2.54391104	-9.17798500	L
H	0	-2.09311223	1.80049204	-9.74568400	L
Br	0	-2.84065423	-5.14927496	7.84827000	L
Br	0	-8.92623123	-9.56291196	5.95551800	L
Br	0	-7.15211123	-6.51282896	-6.73233300	L
Br	0	-11.36854723	-9.64868196	-1.23005000	L
O	0	0.08385677	-1.69115296	0.07293700	H
O	0	-2.11342423	-1.60250796	-0.47681200	H
O	0	-3.07137623	-4.74005896	-2.52185700	H
O	0	-1.97315923	-3.93263796	1.84005700	H
N	0	-2.15080023	-4.32910196	-0.43949400	H
C	0	-0.98413923	-2.18953296	-0.37680600	H
C	0	-0.97667323	-3.61871696	-0.94772900	H
H	0	-1.20706923	-3.47151796	-2.01024400	H
C	0	0.34974177	-4.44850096	-0.90094700	H
C	0	1.40092177	-3.73521396	-1.77969400	H
H	0	1.02579577	-3.57853496	-2.79715100	H
H	0	1.68264777	-2.76577296	-1.36574300	H
H	0	2.30170677	-4.35413696	-1.84651200	H
C	0	0.06204777	-5.82724296	-1.53417300	H
H	0	-0.62274423	-6.42371496	-0.92398200	H
H	0	-0.37391023	-5.72286196	-2.53186300	H
H	0	0.99631777	-6.38920796	-1.62936800	H
C	0	0.90411277	-4.65651896	0.52085100	H
H	0	1.14339377	-3.70530396	0.99948000	H
H	0	0.19590277	-5.19215896	1.15829000	H
H	0	1.82086777	-5.25401096	0.46632600	H
C	0	-3.12951023	-4.82217196	-1.31089100	H
C	0	-2.54661823	-4.44863396	0.89683700	H
C	0	-3.80111023	-5.27973196	0.88199700	H
C	0	-4.18377823	-5.43759696	-0.45214700	H
C	0	-5.34680623	-6.10447096	-0.81809300	H
C	0	-6.12008423	-6.68212696	0.21936700	H
C	0	-5.71010623	-6.57005096	1.57514000	H
C	0	-4.54421923	-5.83439796	1.92305000	H
C	0	-4.12328523	-5.64322996	3.33559900	L H 108
C	0	-2.85485523	-6.06870596	3.76350000	L
H	0	-2.16611123	-6.52713296	3.06452200	L
C	0	-2.47266423	-5.91352896	5.09931300	L
H	0	-1.49096023	-6.23923496	5.41798600	L

C	0	-3.35947023	-5.34958396	6.02175600	L
C	0	-4.62808223	-4.93535296	5.60611700	L
H	0	-5.31787223	-4.49843596	6.31677700	L
C	0	-5.00608823	-5.07270096	4.26751400	L
H	0	-5.98571123	-4.73369396	3.95593600	L
C	0	-6.47860223	-7.27053596	2.64051500	L H 107
C	0	-7.80589023	-6.90702196	2.92024000	L
H	0	-8.27919623	-6.10216696	2.37488800	L
C	0	-8.53104623	-7.58901396	3.90030500	L
H	0	-9.55640623	-7.30725696	4.10186100	L
C	0	-7.93304723	-8.62955996	4.61817500	L
C	0	-6.60778523	-8.98869496	4.35327200	L
H	0	-6.14121923	-9.79357296	4.90634100	L
C	0	-5.88304423	-8.31466096	3.36656000	L
H	0	-4.86140223	-8.61012096	3.16162900	L
C	0	-7.37709623	-7.39655096	-0.12689100	L H 106
C	0	-8.47038123	-6.68547996	-0.64643200	L
H	0	-8.40560323	-5.61501696	-0.79464900	L
C	0	-9.65283723	-7.35435096	-0.97329900	L
H	0	-10.49127823	-6.79811996	-1.37212200	L
C	0	-9.75134323	-8.73673096	-0.78435700	L
C	0	-8.66401523	-9.45085196	-0.27006700	L
H	0	-8.73563623	-10.52091796	-0.12434900	L
C	0	-7.47925823	-8.78481896	0.05582000	L
H	0	-6.64143323	-9.34820896	0.44766400	L
C	0	-5.73462123	-6.20093796	-2.24778200	L H 105
C	0	-6.04108123	-5.04012696	-2.97597300	L
H	0	-5.95957423	-4.06650496	-2.51064400	L
C	0	-6.45897323	-5.13249796	-4.30662700	L
H	0	-6.69965823	-4.23263696	-4.85836200	L
C	0	-6.56652123	-6.38401496	-4.92104900	L
C	0	-6.24673823	-7.54287396	-4.20644600	L
H	0	-6.32459323	-8.51290296	-4.68009600	L
C	0	-5.83119123	-7.45321796	-2.87501300	L
H	0	-5.59025223	-8.35817796	-2.33117500	L
Br	0	-3.47229323	8.34164604	4.73936700	L
Br	0	-10.42675723	7.50539504	7.46782300	L
Br	0	-9.04057323	-5.66796296	6.91590600	L
Br	0	-13.41947923	0.56579204	8.39799100	L
O	0	-0.56562323	-0.26047396	2.57872400	H
O	0	-2.73434623	-0.12832196	1.93987200	H
O	0	-4.84819023	-2.02242496	4.70470400	H
O	0	-2.89970023	2.07724704	4.15533300	H
N	0	-3.53258223	-0.12805996	4.50778400	H
C	0	-1.80725723	-0.35012396	2.78559000	H
C	0	-2.31546923	-0.85585396	4.14648500	H
H	0	-2.68056623	-1.86771596	3.92618700	H
C	0	-1.29143423	-1.01004696	5.32303200	H
C	0	-0.28918923	-2.12785796	4.95908700	H
H	0	-0.80928723	-3.06638096	4.73471200	H
H	0	0.32155577	-1.85856496	4.09634900	H
H	0	0.37702277	-2.31231896	5.80827400	H
C	0	-2.06883223	-1.46667796	6.57744500	H
H	0	-2.73617923	-0.68514696	6.95283400	H
H	0	-2.66944323	-2.35827796	6.37444200	H
H	0	-1.36123723	-1.70880796	7.37647300	H
C	0	-0.53926723	0.29399804	5.64770800	H
H	0	0.05131577	0.63709804	4.79596900	H
H	0	-1.22647823	1.09514804	5.93291100	H
H	0	0.14074477	0.12195204	6.48924900	H

C	0	-4.71793223	-0.81486196	4.78406700	H
C	0	-3.73312123	1.25961204	4.50229100	H
C	0	-5.14086123	1.47553104	4.99759400	H
C	0	-5.72129623	0.21654404	5.16652800	H
C	0	-7.00199523	0.04439204	5.67251600	H
C	0	-7.73204523	1.20591204	6.01149500	H
C	0	-7.16335923	2.49272004	5.82365200	H
C	0	-5.84445623	2.64031904	5.30804400	H
C	0	-5.22841023	3.97845104	5.10782400	L H 181
C	0	-4.04960423	4.32731304	5.78758900	L
H	0	-3.55310023	3.60864804	6.42788700	L
C	0	-3.51989423	5.61572204	5.66493800	L
H	0	-2.61002823	5.87450604	6.19087400	L
C	0	-4.17538623	6.57210804	4.88276500	L
C	0	-5.35101823	6.23357204	4.20755800	L
H	0	-5.85982823	6.97046304	3.60060900	L
C	0	-5.86641723	4.93863304	4.30381900	L
H	0	-6.77422023	4.68966804	3.76903800	L
C	0	-7.94290723	3.69927704	6.21374400	L H 180
C	0	-9.13463223	4.02044404	5.54362800	L
H	0	-9.48843323	3.40119904	4.72857100	L
C	0	-9.87438323	5.14319004	5.92386600	L
H	0	-10.79533523	5.37916804	5.40674300	L
C	0	-9.42246123	5.96204704	6.96326900	L
C	0	-8.23418223	5.65030304	7.63158900	L
H	0	-7.88222023	6.28013904	8.43832700	L
C	0	-7.49862323	4.52059704	7.26279300	L
H	0	-6.58527023	4.28334904	7.79426500	L
C	0	-9.09621323	1.05736604	6.58411100	L H 179
C	0	-10.13630623	0.53221204	5.80095900	L
H	0	-9.95410323	0.24094904	4.77368900	L
C	0	-11.41743423	0.38673704	6.34020600	L
H	0	-12.21413623	-0.01760496	5.72928900	L
C	0	-11.66805823	0.76378504	7.66366800	L
C	0	-10.63458123	1.28465304	8.44929800	L
H	0	-10.82389023	1.57536604	9.47452000	L
C	0	-9.35179723	1.42909304	7.91356500	L
H	0	-8.55724223	1.82658904	8.53295000	L
C	0	-7.50565123	-1.31821796	5.96141500	L H 178
C	0	-7.89363623	-2.17111096	4.91755000	L
H	0	-7.83836223	-1.83489096	3.89045500	L
C	0	-8.35118523	-3.46231996	5.20038600	L
H	0	-8.64428923	-4.11919196	4.39210600	L
C	0	-8.42375223	-3.90538396	6.52540700	L
C	0	-8.04276523	-3.05564796	7.56824700	L
H	0	-8.09771423	-3.39485896	8.59456600	L
C	0	-7.58590623	-1.76556996	7.28856100	L
H	0	-7.28813423	-1.11706996	8.10344500	L
Br	0	2.29365877	5.80998904	-6.57040000	L
Br	0	-3.80065923	10.39331304	-8.55470400	L
Br	0	-9.66905223	6.94737704	2.80446900	L
Br	0	-10.00189823	10.29722604	-4.12390100	L
O	0	-0.03821423	2.27532604	1.27237800	H
O	0	-2.17738623	2.41082004	0.53962100	H
O	0	-3.91333123	5.49353704	1.70541600	H
O	0	-0.50175223	4.69036004	-1.22217300	H
N	0	-1.94327623	5.10821604	0.54903100	H
C	0	-1.12542423	2.88461004	1.08990300	H
C	0	-1.31284623	4.32124804	1.61083200	H
H	0	-2.11111023	4.21899004	2.35648100	H

C	0	-0.12815623	5.03206904	2.34080500	H
C	0	0.18457377	4.24207104	3.63086100	H
H	0	-0.70806823	4.13694204	4.25763200	H
H	0	0.56703377	3.24405704	3.40986400	H
H	0	0.94142877	4.77740404	4.21341900	H
C	0	-0.61335723	6.43938804	2.74992100	H
H	0	-0.80110423	7.07593504	1.88015300	H
H	0	-1.53485323	6.38539004	3.33745900	H
H	0	0.15000877	6.92850104	3.36296000	H
C	0	1.14548177	5.16655404	1.48564400	H
H	0	1.52659577	4.18995004	1.18143500	H
H	0	0.96912477	5.76035004	0.58538500	H
H	0	1.92138077	5.67078904	2.07226800	H
C	0	-3.25229123	5.58974104	0.69033600	H
C	0	-1.49863123	5.22832904	-0.77309000	H
C	0	-2.52466423	6.06941904	-1.48051800	H
C	0	-3.61386723	6.20594604	-0.61934000	H
C	0	-4.78934123	6.83466204	-1.00645600	H
C	0	-4.82489723	7.41982104	-2.29410300	H
C	0	-3.69645623	7.34114204	-3.15457400	H
C	0	-2.53434923	6.62193504	-2.76088100	H
C	0	-1.37606123	6.42672404	-3.67150800	L H 254
C	0	-0.08872823	6.83335404	-3.28329600	L
H	0	0.07182977	7.29520704	-2.31687800	L
C	0	0.99855477	6.64667904	-4.14194000	L
H	0	1.98817677	6.95387504	-3.82943500	L
C	0	0.80699177	6.06951404	-5.40104600	L
C	0	-0.47418523	5.68054404	-5.80233100	L
H	0	-0.62784123	5.23636704	-6.77755800	L
C	0	-1.56022923	5.84962604	-4.93904300	L
H	0	-2.54336523	5.52458904	-5.25543400	L
C	0	-3.70921223	8.05491004	-4.46078800	L H 253
C	0	-4.63355623	7.70347504	-5.45747500	L
H	0	-5.33476623	6.89732004	-5.29182400	L
C	0	-4.66168523	8.39829804	-6.66902200	L
H	0	-5.38579823	8.12644304	-7.42600800	L
C	0	-3.75796023	9.43998304	-6.90082300	L
C	0	-2.82598423	9.78700304	-5.91769900	L
H	0	-2.12509323	10.59294304	-6.09268600	L
C	0	-2.80236623	9.09996004	-4.70084800	L
H	0	-2.08462723	9.38666504	-3.94209700	L
C	0	-6.06326323	8.11158604	-2.73656800	L H 252
C	0	-7.23508223	7.37514004	-2.97303900	L
H	0	-7.24149523	6.29950704	-2.84357900	L
C	0	-8.40245823	8.02560804	-3.38090100	L
H	0	-9.30274823	7.45238504	-3.55639400	L
C	0	-8.40639023	9.41251204	-3.56084800	L
C	0	-7.24148423	10.15072404	-3.32699100	L
H	0	-7.24105123	11.22442104	-3.46327900	L
C	0	-6.07365923	9.50414304	-2.91282800	L
H	0	-5.17890823	10.08568004	-2.72789600	L
C	0	-5.94989423	6.86323904	-0.08578500	L H 251
C	0	-6.61887823	5.67212904	0.23851700	L
H	0	-6.28720823	4.72755204	-0.17616900	L
C	0	-7.72197823	5.69790304	1.09626000	L
H	0	-8.23102723	4.77547304	1.34453700	L
C	0	-8.16427123	6.91190604	1.63215900	L
C	0	-7.50185223	8.10110004	1.31029200	L
H	0	-7.84066123	9.04189804	1.72435700	L
C	0	-6.39733023	8.07833504	0.45435900	L

H	0	-5.89001423	9.00437804	0.21347400 L
C	0	-4.24799323	0.54591204	-0.50599200 H
C	0	-4.83369323	1.32961604	-1.54976500 H
C	0	-5.18446323	-0.17638696	0.39202300 H
C	0	-4.14616923	2.46606404	-2.07618800 H
C	0	-6.10273123	0.96507604	-2.09539800 H
O	0	-5.52421923	0.32083204	1.44435100 H
O	0	-5.57774423	-1.39452096	-0.06043600 H
C	0	-4.71483423	3.24789504	-3.07322600 H
H	0	-3.18572823	2.72463704	-1.65386300 H
C	0	-6.60876223	1.69820204	-3.14765900 H
H	0	-6.62636723	0.09157004	-1.72671400 H
C	0	-6.39010923	-2.20111796	0.80283500 H
C	0	-5.93834923	2.83937704	-3.60478000 H
H	0	-4.21654423	4.13412504	-3.45069500 H
C	0	-7.84629523	1.47436104	-3.97712300 H
C	0	-7.88368123	-2.14048696	0.42381400 H
H	0	-6.05042523	-3.22808396	0.66936400 H
H	0	-6.27230823	-1.89291296	1.84252400 H
C	0	-6.73594223	3.44152204	-4.70841500 H
N	0	-7.76599223	2.56882404	-4.94683400 H
H	0	-8.76723423	1.53546304	-3.38380500 H
H	0	-7.82771423	0.49779704	-4.47155000 H
Cl	0	-8.11897423	-2.52798096	-1.31811600 H
Cl	0	-8.72903323	-3.37437396	1.42427100 H
Cl	0	-8.59753423	-0.52461096	0.75813400 H
O	0	-6.54336223	4.50338004	-5.30262400 H
C	0	-8.69985323	2.77621004	-6.05583200 H
C	0	-9.89201923	3.64341104	-5.57588300 H
C	0	-9.13459323	1.44988104	-6.68333000 H
H	0	-8.13840423	3.36452204	-6.79038500 H
N	0	-9.56276023	4.93964504	-5.36652100 H
O	0	-11.01782223	3.18132304	-5.40500800 H
C	0	-9.90349923	1.65081104	-7.99377100 H
H	0	-9.75644123	0.88971204	-5.98037300 H
H	0	-8.23675723	0.85539204	-6.87199900 H
H	0	-10.25545223	5.55872404	-4.97050100 H
H	0	-8.59640623	5.24099104	-5.43107200 H
C	0	-10.08433123	0.41091304	-8.85878500 H
H	0	-9.41286723	2.39346604	-8.63314900 H
H	0	-10.90335823	2.04723904	-7.78617400 H
O	0	-10.48084423	0.47248704	-10.00887600 H
O	0	-9.76213223	-0.71407696	-8.20398100 H
C	0	-9.81354323	-2.05025496	-8.84344200 H
C	0	-11.24588223	-2.36775096	-9.28136300 H
C	0	-9.37509323	-2.97922396	-7.70907700 H
C	0	-8.82088223	-2.09607596	-10.00831300 H
H	0	-11.29567023	-3.40496896	-9.62715700 H
H	0	-11.56775423	-1.71179996	-10.09018100 H
H	0	-11.93499023	-2.25766596	-8.43834900 H
H	0	-9.34680423	-4.01360296	-8.06327900 H
H	0	-8.37922323	-2.70924496	-7.34744800 H
H	0	-10.07374423	-2.92108296	-6.86948100 H
H	0	-7.81773323	-1.82670396	-9.66537800 H
H	0	-9.11673423	-1.41435196	-10.80602200 H
H	0	-8.77990323	-3.11162396	-10.41355700 H

Structure C

Rh	0	0.75797874	0.23936170	0.00000000 H
Rh	0	3.00840674	0.35525470	-1.00785500 H
Br	0	4.34449374	-7.70164230	3.88086700 L

Br	0	1.37251274	-7.70626330	10.78525800 L
Br	0	0.19018174	5.51870770	10.20170300 L
Br	0	-1.29211926	-1.21443330	13.85186800 L
O	0	3.73356274	0.90137470	0.83605700 H
O	0	1.69805674	0.70117870	1.81064200 H
O	0	2.14257774	2.35422670	5.49359800 H
O	0	3.34845074	-1.54037530	3.41329300 H
N	0	2.97527074	0.59315870	4.24690400 H
C	0	2.95002974	0.94973470	1.82347200 H
C	0	3.51047574	1.42957170	3.17412100 H
H	0	3.02341674	2.39978470	3.33371800 H
C	0	5.05534674	1.69015270	3.28696000 H
C	0	5.41701374	2.88955070	2.38337000 H
H	0	4.81519874	3.76961470	2.63498000 H
H	0	5.26315674	2.66189670	1.32778500 H
H	0	6.47019174	3.15174270	2.52841600 H
C	0	5.36844674	2.08906170	4.74618700 H
H	0	5.24553474	1.24852270	5.43597600 H
H	0	4.72563574	2.90424970	5.08720800 H
H	0	6.40858274	2.42179270	4.81642900 H
C	0	5.91834274	0.46736970	2.91981700 H
H	0	5.77154674	0.16780170	1.88111500 H
H	0	5.69556274	-0.39106330	3.55924700 H
H	0	6.97553774	0.71913270	3.05893300 H
C	0	2.34052174	1.16301670	5.35685900 H
C	0	2.97171374	-0.80350330	4.30793700 H
C	0	2.40617674	-1.15376030	5.65816200 H
C	0	1.99858274	0.03406570	6.26988200 H
C	0	1.44196474	0.06225770	7.54245100 H
C	0	1.29708174	-1.17422830	8.21837300 H
C	0	1.72556374	-2.38538930	7.61207700 H
C	0	2.28748074	-2.38193830	6.30569900 H
C	0	2.76001974	-3.62623630	5.64778900 L H 35
C	0	4.11645574	-3.77581730	5.31559700 L
H	0	4.81674674	-2.96962130	5.49681300 L
C	0	4.58112274	-4.97775430	4.77457000 L
H	0	5.62964874	-5.08622930	4.52920000 L
C	0	3.69822974	-6.04231130	4.57100400 L
C	0	2.34483374	-5.89676930	4.88954100 L
H	0	1.66025174	-6.71829030	4.73081800 L
C	0	1.87392374	-4.69251630	5.42109800 L
H	0	0.82359874	-4.59559230	5.66889500 L
C	0	1.63739474	-3.66512030	8.36882900 L H 34
C	0	0.38927974	-4.18375030	8.75054900 L
H	0	-0.52255726	-3.66150930	8.49451500 L
C	0	0.31377574	-5.37626530	9.47456200 L
H	0	-0.65184826	-5.76139530	9.77467100 L
C	0	1.48102974	-6.06887830	9.80938300 L
C	0	2.72723974	-5.56018230	9.43073100 L
H	0	3.63372074	-6.09094230	9.69148900 L
C	0	2.80701974	-4.36028330	8.71862700 L
H	0	3.77881474	-3.97058230	8.44176900 L
C	0	0.67997274	-1.18635830	9.57054600 L H 33
C	0	-0.66997326	-0.83532830	9.72962200 L
H	0	-1.26881926	-0.56113930	8.86954500 L
C	0	-1.25318226	-0.84388930	10.99956400 L
H	0	-2.29510326	-0.57395730	11.11342600 L
C	0	-0.49285526	-1.20159630	12.11784800 L
C	0	0.85357174	-1.54885830	11.96530100 L
H	0	1.44574674	-1.82412730	12.82841800 L

C	0	1.44021374	-1.53948930	10.69679300 L
H	0	2.48513374	-1.80369930	10.59073400 L
C	0	1.12407974	1.36202070	8.18511700 L H 32
C	0	0.12148574	2.19301070	7.65980800 L
H	0	-0.43479826	1.89092670	6.78277500 L
C	0	-0.15419826	3.42741370	8.25587800 L
H	0	-0.92257326	4.06612870	7.83915400 L
C	0	0.56493974	3.83627670	9.38363400 L
C	0	1.56143374	3.01114970	9.91370600 L
H	0	2.12147474	3.32520470	10.78501600 L
C	0	1.84216974	1.77947770	9.31680200 L
H	0	2.62479874	1.15503570	9.72981900 L
Br	0	-1.81212626	-5.00824930	-7.65550400 L
Br	0	-7.69971926	-8.31502930	-4.42475000 L
Br	0	-2.05589926	-7.28353330	7.40695700 L
Br	0	-7.88287526	-9.46717330	3.04883300 L
O	0	3.20979574	-1.67039530	-0.49697300 H
O	0	1.10808874	-1.74922930	0.34326400 H
O	0	0.59201874	-4.75262230	2.51133000 H
O	0	0.72229074	-3.90524730	-1.97447900 H
N	0	1.06649474	-4.39205230	0.26946800 H
C	0	2.23648374	-2.26311430	0.04544300 H
C	0	2.35368574	-3.73025230	0.50205000 H
H	0	2.39922274	-3.65128030	1.59617600 H
C	0	3.60443174	-4.56710630	0.07752400 H
C	0	4.84146274	-3.97159430	0.78544700 H
H	0	4.70592374	-3.95369330	1.87264600 H
H	0	5.04459074	-2.95305530	0.44961300 H
H	0	5.72104974	-4.58639930	0.56845200 H
C	0	3.39851774	-6.00687330	0.59462000 H
H	0	2.60955674	-6.52803730	0.04468300 H
H	0	3.12974074	-6.01304630	1.65522000 H
H	0	4.32376274	-6.57905230	0.47507800 H
C	0	3.84055674	-4.60658230	-1.44349200 H
H	0	4.01628374	-3.60661230	-1.84543700 H
H	0	2.99015574	-5.04287130	-1.97281700 H
H	0	4.72233374	-5.22088230	-1.65689000 H
C	0	0.27454574	-4.83237330	1.33849400 H
C	0	0.34601774	-4.41322930	-0.93284800 H
C	0	-0.94184726	-5.12797630	-0.63794900 H
C	0	-0.98265526	-5.36506330	0.73769900 H
C	0	-2.06348326	-5.98413330	1.35223200 H
C	0	-3.14412926	-6.37347430	0.52853200 H
C	0	-3.10484626	-6.15077630	-0.87028500 H
C	0	-1.98795126	-5.51506330	-1.47665900 H
C	0	-1.90200726	-5.31746830	-2.94814600 L H 108
C	0	-0.84477426	-5.88779530	-3.67676300 L
H	0	-0.05884526	-6.43176830	-3.16738400 L
C	0	-0.81096426	-5.78300230	-5.07063300 L
H	0	0.00770374	-6.22627130	-5.62258000 L
C	0	-1.84233026	-5.12717030	-5.74994000 L
C	0	-2.89680226	-4.55638630	-5.03265300 L
H	0	-3.69542426	-4.04536630	-5.55471500 L
C	0	-2.91869426	-4.63376430	-3.63748900 L
H	0	-3.73602126	-4.17360030	-3.09669100 L
C	0	-4.20874926	-6.66872230	-1.71964700 L H 107
C	0	-5.46086326	-6.03445530	-1.72095300 L
H	0	-5.63023826	-5.15626630	-1.11071900 L
C	0	-6.49605026	-6.52574130	-2.52067600 L
H	0	-7.45931426	-6.03240530	-2.51404400 L

C	0	-6.28528426	-7.64717930	-3.32968300	L
C	0	-5.03709326	-8.27861130	-3.33683000	L
H	0	-4.86946626	-9.14566730	-3.96254300	L
C	0	-4.00145126	-7.79270730	-2.53370300	L
H	0	-3.03921426	-8.28979330	-2.54448400	L
C	0	-4.28219326	-7.11137730	1.12935400	L H 106
C	0	-5.41997926	-6.42092630	1.57234500	L
H	0	-5.47699326	-5.34352630	1.47838100	L
C	0	-6.48760126	-7.12089430	2.14117200	L
H	0	-7.36251526	-6.58200930	2.48106400	L
C	0	-6.42370226	-8.51242430	2.27094000	L
C	0	-5.28962726	-9.20386030	1.83120500	L
H	0	-5.23599726	-10.28029330	1.93044200	L
C	0	-4.22056826	-8.50594130	1.26200300	L
H	0	-3.34606126	-9.04876430	0.92480200	L
C	0	-2.03899426	-6.26630230	2.80644100	L H 105
C	0	-2.93144126	-5.61477230	3.67058700	L
H	0	-3.62282826	-4.87533630	3.28757100	L
C	0	-2.93814826	-5.92038130	5.03410300	L
H	0	-3.63889026	-5.42306130	5.69197800	L
C	0	-2.04336926	-6.86547330	5.54532900	L
C	0	-1.14523526	-7.51077030	4.68988200	L
H	0	-0.45370526	-8.24562530	5.08132000	L
C	0	-1.14245326	-7.21395730	3.32404400	L
H	0	-0.44944626	-7.72704330	2.66851700	L
Br	0	1.55519174	7.78567170	-6.10761100	L
Br	0	-5.17459326	8.05146870	-9.95142200	L
Br	0	-7.62511726	-4.34211230	-5.34785400	L
Br	0	-10.33993826	2.32760670	-8.61253200	L
O	0	2.18583374	-0.22769430	-2.80897300	H
O	0	0.09702474	-0.21786430	-1.93620500	H
O	0	-2.41733326	-1.63458930	-4.63942600	H
O	0	0.34274074	2.01160270	-4.58894200	H
N	0	-0.73373626	-0.04445430	-4.63454200	H
C	0	0.94065374	-0.40161230	-2.87998500	H
C	0	0.32546874	-0.94913630	-4.18219600	H
H	0	-0.21957226	-1.84324530	-3.85854100	H
C	0	1.28921874	-1.41286030	-5.32969600	H
C	0	2.15477374	-2.57573730	-4.79861400	H
H	0	1.53396174	-3.38623030	-4.40443600	H
H	0	2.82903274	-2.24785330	-4.00560600	H
H	0	2.76086774	-2.97929830	-5.61642300	H
C	0	0.41799174	-1.96067130	-6.48151900	H
H	0	-0.16666026	-1.17263830	-6.96596700	H
H	0	-0.27405826	-2.72945430	-6.12777200	H
H	0	1.06142474	-2.40853130	-7.24501100	H
C	0	2.19432274	-0.29611030	-5.88459300	H
H	0	2.84204274	0.11759770	-5.11053400	H
H	0	1.61470474	0.52137170	-6.32122000	H
H	0	2.82608174	-0.71114930	-6.67773100	H
C	0	-2.03569826	-0.50496330	-4.87095600	H
C	0	-0.62126426	1.32789770	-4.88261400	H
C	0	-1.91695926	1.73687670	-5.52605300	H
C	0	-2.78493226	0.64821870	-5.45532800	H
C	0	-4.09168226	0.71338670	-5.92068500	H
C	0	-4.50586426	1.91240770	-6.55414000	H
C	0	-3.60718526	3.00894570	-6.68225000	H
C	0	-2.30053126	2.93368870	-6.12341200	H
C	0	-1.37359026	4.09177570	-6.11986800	L H 181
C	0	-0.14731326	4.02428070	-6.80002500	L

H	0	0.13376974	3.12461470	-7.33363700	L
C	0	0.71920574	5.12134270	-6.79727800	L
H	0	1.66447774	5.06010670	-7.32072800	L
C	0	0.36671074	6.29179470	-6.11716900	L
C	0	-0.85572626	6.36566670	-5.44190300	L
H	0	-1.13291426	7.26882770	-4.91362000	L
C	0	-1.72335226	5.27074770	-5.44374800	L
H	0	-2.66575426	5.33940270	-4.91848100	L
C	0	-3.99390126	4.21925270	-7.46392800	L H 180
C	0	-5.09459426	5.00527570	-7.08308800	L
H	0	-5.68851126	4.73875470	-6.22306900	L
C	0	-5.44396026	6.13879070	-7.82113400	L
H	0	-6.29565126	6.73440570	-7.51848400	L
C	0	-4.69705626	6.50022070	-8.94587900	L
C	0	-3.60293126	5.72215970	-9.33584300	L
H	0	-3.02424826	5.99578370	-10.20860300	L
C	0	-3.25417026	4.58522470	-8.60154000	L
H	0	-2.40982326	3.98703270	-8.92117000	L
C	0	-5.90121626	2.01349170	-7.05526300	L H 179
C	0	-6.97347026	1.99311570	-6.14919000	L
H	0	-6.78876426	1.90687370	-5.08563400	L
C	0	-8.28773026	2.08679270	-6.61226900	L
H	0	-9.10658026	2.06799270	-5.90602100	L
C	0	-8.54158626	2.20187270	-7.98260400	L
C	0	-7.47753626	2.21996070	-8.89084300	L
H	0	-7.66990026	2.30640070	-9.95238800	L
C	0	-6.16094626	2.12245370	-8.43058000	L
H	0	-5.34499126	2.13069070	-9.14262600	L
C	0	-4.97304626	-0.47129530	-5.78640500	L H 178
C	0	-5.35324726	-0.92710430	-4.51367400	L
H	0	-5.02898426	-0.39978530	-3.62450300	L
C	0	-6.14071426	-2.07482030	-4.38449600	L
H	0	-6.41939526	-2.42731330	-3.39971000	L
C	0	-6.56030426	-2.76817230	-5.52446600	L
C	0	-6.19402426	-2.31126030	-6.79478100	L
H	0	-6.51521926	-2.84655830	-7.67890800	L
C	0	-5.40204626	-1.16716130	-6.92688900	L
H	0	-5.11082026	-0.83182930	-7.91468100	L
Br	0	5.69150974	5.53365470	6.48549400	L
Br	0	-0.12073826	9.41677770	9.54201800	L
Br	0	-6.92879726	8.96416770	-1.17622200	L
Br	0	-6.32177626	10.72907370	5.57476100	L
O	0	2.58919474	2.37342670	-1.42136200	H
O	0	0.57929474	2.26532070	-0.38540200	H
O	0	-1.49622426	5.54402370	-1.08317400	H
O	0	2.19116974	4.39932070	1.37476400	H
N	0	0.56293174	4.97077870	-0.17668900	H
C	0	1.50147974	2.87308770	-1.02403900	H
C	0	1.13033974	4.33416870	-1.37177900	H
H	0	0.27138074	4.23077670	-2.04539300	H
C	0	2.17461174	5.22131870	-2.12984600	H
C	0	2.44472174	4.58388670	-3.51043900	H
H	0	1.51283374	4.36013170	-4.03890100	H
H	0	3.00782674	3.65421270	-3.41874700	H
H	0	3.02519674	5.27874270	-4.12616300	H
C	0	1.53870874	6.61035770	-2.35705100	H
H	0	1.38093874	7.14666370	-1.41648900	H
H	0	0.57552074	6.53589770	-2.87139400	H
H	0	2.20590874	7.21954070	-2.97418200	H
C	0	3.50260474	5.39975270	-1.37020300	H

H	0	3.98331074	4.43914870	-1.17622100	H
H	0	3.36200874	5.91290870	-0.41535800	H
H	0	4.18327374	6.00806570	-1.97588000	H
C	0	-0.71496826	5.53666670	-0.14309800	H
C	0	1.15872374	4.98069970	1.09594200	H
C	0	0.25613674	5.79387170	1.97418700	H
C	0	-0.89093526	6.09524770	1.23221300	H
C	0	-1.93440426	6.83552470	1.77311900	H
C	0	-1.80201126	7.27805570	3.11005000	H
C	0	-0.63205326	6.99634770	3.85628000	H
C	0	0.42740774	6.24240870	3.28395700	H
C	0	1.69790074	5.99462970	4.01559500	L H 254
C	0	2.91690874	6.45258070	3.48802600	L
H	0	2.94646874	6.94512370	2.52384700	L
C	0	4.10138574	6.30272370	4.21508900	L
H	0	5.03473474	6.66051670	3.80010300	L
C	0	4.07703874	5.71039870	5.48123000	L
C	0	2.86861374	5.25187070	6.01347900	L
H	0	2.84484974	4.79014870	6.99247300	L
C	0	1.68557474	5.38288770	5.28062700	L
H	0	0.75802974	5.01967670	5.70473800	L
C	0	-0.49169326	7.55617670	5.22676100	L H 253
C	0	-1.31248226	7.09482970	6.26828700	L
H	0	-2.03781726	6.31122270	6.08731700	L
C	0	-1.20160326	7.64704370	7.54705500	L
H	0	-1.84362826	7.29112870	8.34230000	L
C	0	-0.26534826	8.65597370	7.79660700	L
C	0	0.56131274	9.11231170	6.76487600	L
H	0	1.28644674	9.89329770	6.95364800	L
C	0	0.44759074	8.56745170	5.48301300	L
H	0	1.08408274	8.93688670	4.68838300	L
C	0	-2.88368826	8.10419370	3.70508200	L H 252
C	0	-4.08302126	7.50526670	4.11868900	L
H	0	-4.22472526	6.43662170	4.01494900	L
C	0	-5.10224726	8.28501670	4.67228700	L
H	0	-6.02504826	7.81623170	4.98865500	L
C	0	-4.92844926	9.66548670	4.81768700	L
C	0	-3.73317426	10.26620270	4.40824200	L
H	0	-3.59479626	11.33390870	4.51899800	L
C	0	-2.71311726	9.48897770	3.85240300	L
H	0	-1.79256026	9.96313970	3.53487500	L
C	0	-3.08178726	7.26026170	0.94244500	L H 251
C	0	-4.26734226	6.51122270	0.93290500	L
H	0	-4.31882626	5.56152670	1.45101900	L
C	0	-5.40718626	7.01415170	0.29668400	L
H	0	-6.32849026	6.44892470	0.31798300	L
C	0	-5.36356526	8.25797670	-0.34252600	L
C	0	-4.17439826	8.99334570	-0.35795100	L
H	0	-4.13637626	9.95638170	-0.85029300	L
C	0	-3.03695826	8.49804570	0.28469200	L
H	0	-2.13209126	9.09314570	0.30120200	L
C	0	-1.11166826	0.11711170	0.80754500	H
C	0	-2.22755226	0.92485670	0.44130900	H
C	0	-1.32940926	-0.97342030	1.78456400	H
C	0	-3.34787926	1.09099070	1.31897000	H
C	0	-2.21593326	1.59731870	-0.81380200	H
O	0	-1.66636826	-2.07421830	1.39819000	H
O	0	-1.07205126	-0.63813030	3.07043900	H
C	0	-4.39581826	1.93614270	0.99055000	H
H	0	-3.35581526	0.57492070	2.27224700	H

C	0	-3.29645426	2.38713470	-1.14619700 H
H	0	-1.39124426	1.44480770	-1.49409100 H
C	0	-1.11283726	-1.68147730	4.05245700 H
C	0	-4.35090826	2.57263170	-0.25253300 H
H	0	-5.23305526	2.09191570	1.66224700 H
C	0	-3.57495126	3.15366770	-2.40244500 H
C	0	-2.35492826	-1.55473030	4.94998500 H
H	0	-1.10630926	-2.66329930	3.57681200 H
H	0	-0.22923826	-1.55957130	4.67880600 H
C	0	-5.35668126	3.48968170	-0.86685200 H
N	0	-4.83932026	3.83912770	-2.09894900 H
H	0	-3.70162026	2.48687970	-3.26426200 H
H	0	-2.77580326	3.86472070	-2.63830400 H
Cl	0	-3.86702726	-1.86410130	4.02435000 H
Cl	0	-2.18870726	-2.78325430	6.25237400 H
Cl	0	-2.44899426	0.08274970	5.68659700 H
O	0	-6.41992026	3.83782970	-0.36647000 H
C	0	-5.49058126	4.58240970	-3.18066900 H
C	0	-5.01138226	6.04427670	-3.34906300 H
C	0	-7.02984426	4.45420670	-3.29015600 H
H	0	-5.10601426	4.09622070	-4.08434500 H
N	0	-3.93735926	6.44285370	-2.63496500 H
O	0	-5.56805726	6.76540670	-4.17649000 H
C	0	-7.88710026	5.46696370	-2.51511200 H
H	0	-7.30522226	3.43225970	-3.01375900 H
H	0	-7.26373126	4.57378970	-4.34850200 H
H	0	-3.57932926	7.36843670	-2.82212300 H
H	0	-3.45128726	5.88407970	-1.94821600 H
C	0	-9.35195026	5.42545270	-2.91287400 H
H	0	-7.53208326	6.47421170	-2.75303500 H
H	0	-7.81813626	5.30527370	-1.44159800 H
O	0	-10.27486826	5.35649470	-2.12074800 H
O	0	-9.48198926	5.51148470	-4.24972500 H
C	0	-10.79269726	5.54760270	-4.93105600 H
C	0	-11.56085726	4.25073570	-4.66116500 H
C	0	-10.39346226	5.65085670	-6.40497800 H
C	0	-11.57193526	6.78968070	-4.48874400 H
H	0	-12.47316326	4.23605470	-5.26558100 H
H	0	-11.83563626	4.16691070	-3.60938200 H
H	0	-10.95686926	3.38238270	-4.93924200 H
H	0	-11.28563526	5.65906670	-7.03750500 H
H	0	-9.82792126	6.56885970	-6.58933500 H
H	0	-9.77050026	4.80023270	-6.69440500 H
H	0	-10.97098926	7.69103370	-4.64419600 H
H	0	-11.85035626	6.72704070	-3.43629500 H
H	0	-12.48307326	6.88077970	-5.08833300 H

Structure D

Rh	0	-1.15691492	-0.18617021	0.00000000 H
Rh	0	1.17783408	-0.03636821	0.79760900 H
Br	0	2.16678308	-7.89540721	-4.76350300 L
Br	0	-1.56075392	-7.67144521	-11.07926600 L
Br	0	-3.47681592	5.30241579	-9.86863500 L
Br	0	-4.48187092	-1.00187721	-13.70247800 L
O	0	1.69211608	0.65668579	-1.07271900 H
O	0	-0.40795992	0.39227379	-1.87799000 H
O	0	-0.33481592	2.21443279	-5.52449500 H
O	0	1.01769308	-1.78442321	-3.73237100 H
N	0	0.59584708	0.39005479	-4.42838200 H
C	0	0.83090108	0.67079779	-1.99612900 H
C	0	1.29050808	1.14848479	-3.38941200 H

H	0	0.87294908	2.15873179	-3.48462800	H
C	0	2.83953208	1.28611779	-3.64419100	H
C	0	3.39990508	2.41155579	-2.74442500	H
H	0	2.77041508	3.30576579	-2.76143200	H
H	0	3.47693308	2.08806879	-1.70625300	H
H	0	4.39880008	2.69436879	-3.09254500	H
C	0	3.04310008	1.68940479	-5.12226700	H
H	0	2.79714908	0.87007879	-5.80439300	H
H	0	2.43318108	2.55080479	-5.40389400	H
H	0	4.09302808	1.94903679	-5.28743000	H
C	0	3.63608608	-0.00873821	-3.38718000	H
H	0	3.51710208	-0.35591221	-2.35960700	H
H	0	3.33735108	-0.81549221	-4.06023000	H
H	0	4.69986008	0.19010779	-3.55904900	H
C	0	-0.13758592	1.01581079	-5.44844200	H
C	0	0.57875608	-1.00269321	-4.55795600	H
C	0	-0.09262092	-1.28769021	-5.86926300	H
C	0	-0.56942692	-0.07565521	-6.37408400	H
C	0	-1.25643492	-0.00375121	-7.57815500	H
C	0	-1.44617092	-1.20591121	-8.30188600	H
C	0	-0.93766992	-2.43520421	-7.80915500	H
C	0	-0.25583292	-2.48501721	-6.56255700	H
C	0	0.31025408	-3.74846021	-6.02628200	L H 35
C	0	1.69878308	-3.88323521	-5.86429800	L
H	0	2.35776508	-3.04883121	-6.07105100	L
C	0	2.24652208	-5.10769621	-5.47147200	L
H	0	3.31878908	-5.20580821	-5.36206900	L
C	0	1.41354508	-6.20714621	-5.24354900	L
C	0	0.02880608	-6.07322121	-5.37953900	L
H	0	-0.61730092	-6.92056421	-5.19741700	L
C	0	-0.52337092	-4.84874821	-5.76602800	L
H	0	-1.59647492	-4.76428821	-5.88382800	L
C	0	-1.09019892	-3.67932321	-8.61327600	L H 34
C	0	-2.36513492	-4.20992321	-8.86891400	L
H	0	-3.25031892	-3.71004821	-8.50038000	L
C	0	-2.50302992	-5.39131821	-9.60200100	L
H	0	-3.48992392	-5.79342621	-9.79106300	L
C	0	-1.36996992	-6.05180921	-10.08648600	L
C	0	-0.09754892	-5.52466121	-9.84391000	L
H	0	0.78199108	-6.03110021	-10.21986100	L
C	0	0.04315508	-4.34139121	-9.11345200	L
H	0	1.03373908	-3.94206421	-8.93407400	L
C	0	-2.17227192	-1.15988321	-9.59704700	L H 33
C	0	-3.54900092	-0.88750321	-9.62324900	L
H	0	-4.09067192	-0.71782621	-8.70064200	L
C	0	-4.23234092	-0.84019421	-10.84133900	L
H	0	-5.29403092	-0.63021421	-10.85328800	L
C	0	-3.54613392	-1.06549821	-12.03930600	L
C	0	-2.17403892	-1.33740421	-12.01814300	L
H	0	-1.63944992	-1.51158321	-12.94296600	L
C	0	-1.48750692	-1.38326421	-10.80153200	L
H	0	-0.42435192	-1.58990321	-10.79607400	L
C	0	-1.74175592	1.29979579	-8.08459300	L H 32
C	0	-2.88219792	1.88914879	-7.52223200	L
H	0	-3.38562992	1.41995479	-6.68829900	L
C	0	-3.39845492	3.06999279	-8.05942500	L
H	0	-4.30090192	3.49368379	-7.64532700	L
C	0	-2.76308792	3.68733379	-9.14069400	L
C	0	-1.61189292	3.11444079	-9.69221600	L
H	0	-1.11749392	3.58706079	-10.53098400	L

C	0	-1.10585092	1.91907679	-9.17136500	L
H	0	-0.22728592	1.47067079	-9.61867200	L
Br	0	-1.01026892	-6.33796821	7.59356500	L
Br	0	-7.61163192	-9.83642621	5.64188100	L
Br	0	-4.98731492	-7.22275221	-7.09233100	L
Br	0	-9.70416692	-10.14605721	-1.64060600	L
O	0	1.45483208	-1.97527221	0.09518100	H
O	0	-0.72753492	-2.15037421	-0.47941000	H
O	0	-1.42522492	-5.08644421	-2.66594900	H
O	0	-0.40336092	-4.52762521	1.74890200	H
N	0	-0.51386192	-4.82164021	-0.55008700	H
C	0	0.46222108	-2.59637221	-0.37578100	H
C	0	0.63095608	-4.00971721	-0.96759300	H
H	0	0.45942608	-3.85836521	-2.04061100	H
C	0	2.01524108	-4.73000121	-0.84571100	H
C	0	3.03342508	-3.95660721	-1.71179300	H
H	0	2.68991108	-3.86835121	-2.74761100	H
H	0	3.20441808	-2.95031421	-1.32461400	H
H	0	3.99030908	-4.48881521	-1.71682100	H
C	0	1.85022608	-6.14606821	-1.43687200	H
H	0	1.24699508	-6.78959321	-0.78988800	H
H	0	1.36848208	-6.11167221	-2.41796300	H
H	0	2.83145808	-6.61602021	-1.55502200	H
C	0	2.54737008	-4.85025221	0.59499000	H
H	0	2.69794908	-3.86887621	1.04869500	H
H	0	1.86860408	-5.42089721	1.23253200	H
H	0	3.51115708	-5.37141021	0.57751700	H
C	0	-1.47625792	-5.27450421	-1.46353500	H
C	0	-0.94050692	-5.01296521	0.76799200	H
C	0	-2.17804492	-5.85174621	0.68928500	H
C	0	-2.52162692	-5.97678421	-0.65730900	H
C	0	-3.67894892	-6.63310621	-1.06277200	H
C	0	-4.51321792	-7.16282621	-0.04918200	H
C	0	-4.14504092	-7.06975321	1.31660300	H
C	0	-2.95065792	-6.41234221	1.70350400	H
C	0	-2.48226792	-6.37333921	3.11269100	L H 108
C	0	-1.24198292	-6.93623721	3.45738400	L
H	0	-0.61607492	-7.38919821	2.69824100	L
C	0	-0.80621192	-6.92377121	4.78533700	L
H	0	0.15324508	-7.35515621	5.03971100	L
C	0	-1.60894992	-6.35901221	5.78082200	L
C	0	-2.84744892	-5.80316921	5.44613200	L
H	0	-3.47080892	-5.36102421	6.21262600	L
C	0	-3.27889992	-5.80204321	4.11750600	L
H	0	-4.23167292	-5.35287421	3.87276500	L
C	0	-4.98041192	-7.73606321	2.34579100	L H 107
C	0	-6.12174992	-7.09678921	2.85083400	L
H	0	-6.39380592	-6.11108021	2.49718500	L
C	0	-6.90147592	-7.72002721	3.82848500	L
H	0	-7.77752492	-7.21744821	4.21762000	L
C	0	-6.54609692	-8.98623121	4.30503300	L
C	0	-5.40747492	-9.62722621	3.80417400	L
H	0	-5.12799992	-10.60603321	4.17192200	L
C	0	-4.62489592	-9.00399421	2.82754800	L
H	0	-3.74375092	-9.50585921	2.44706600	L
C	0	-5.75639192	-7.87789821	-0.42835900	L H 106
C	0	-6.99910692	-7.23520921	-0.32531000	L
H	0	-7.05787892	-6.21206921	0.02465900	L
C	0	-8.16945992	-7.90944321	-0.68346600	L
H	0	-9.12478392	-7.40749521	-0.60048300	L

C	0	-8.10423992	-9.22662421	-1.15021200 L
C	0	-6.86587092	-9.86878721	-1.25979100 L
H	0	-6.81112392	-10.88707121	-1.62244800 L
C	0	-5.69384092	-9.19680221	-0.90060700 L
H	0	-4.73943792	-9.70131921	-0.98814000 L
C	0	-3.99476292	-6.77337321	-2.50506800 L H 105
C	0	-5.14749792	-6.17886321	-3.04079800 L
H	0	-5.80662692	-5.59620621	-2.40999700 L
C	0	-5.44949692	-6.32613521	-4.39731900 L
H	0	-6.33914092	-5.86138221	-4.80225700 L
C	0	-4.59538792	-7.05499721	-5.23112200 L
C	0	-3.44759792	-7.65270521	-4.70247900 L
H	0	-2.78816392	-8.22328821	-5.34341300 L
C	0	-3.14799792	-7.51538721	-3.34401700 L
H	0	-2.25760892	-7.98602821	-2.94530400 L
Br	0	-1.07894492	6.74059579	6.88809400 L
Br	0	-8.75867992	6.77169979	7.91867800 L
Br	0	-9.30114992	-5.12327121	2.14523900 L
Br	0	-12.86812292	0.41197279	5.26303000 L
O	0	0.56083708	-0.82646621	2.61116600 H
O	0	-1.60480192	-0.76108021	1.95029000 H
O	0	-3.86450992	-2.72233821	3.94976100 H
O	0	-1.51410992	1.09826579	4.83444300 H
N	0	-2.37692292	-1.03089021	4.50661600 H
C	0	-0.67144692	-1.03006321	2.78131000 H
C	0	-1.16905192	-1.72663121	4.06512800 H
H	0	-1.55256892	-2.68797421	3.70120600 H
C	0	-0.14541492	-2.07689521	5.20011700 H
C	0	0.76172908	-3.21167121	4.67601100 H
H	0	0.17580408	-4.07841221	4.35539200 H
H	0	1.36263108	-2.88074721	3.82611800 H
H	0	1.44219508	-3.53489021	5.47066500 H
C	0	-0.95157192	-2.60947821	6.40373800 H
H	0	-1.51906692	-1.81469421	6.89652700 H
H	0	-1.65848992	-3.38723221	6.10312800 H
H	0	-0.26863392	-3.04021521	7.14252700 H
C	0	0.73362608	-0.90463821	5.67924400 H
H	0	1.34182908	-0.50299521	4.86709400 H
H	0	0.13668008	-0.09073921	6.09387200 H
H	0	1.40697108	-1.26732021	6.46414500 H
C	0	-3.65381192	-1.58728421	4.33130100 H
C	0	-2.45570292	0.32524579	4.83221300 H
C	0	-3.90041192	0.60543779	5.09907000 H
C	0	-4.62824092	-0.51815321	4.70686500 H
C	0	-6.01841092	-0.52786121	4.69918800 H
C	0	-6.67860692	0.62581979	5.19310300 H
C	0	-5.93542992	1.74309679	5.65459900 H
C	0	-4.52119192	1.75686479	5.56934800 H
C	0	-3.71385792	2.95624579	5.90508500 L H 181
C	0	-2.75913292	2.90529379	6.93308000 L
H	0	-2.61419992	1.99412879	7.50042600 L
C	0	-1.98130192	4.02946279	7.22693900 L
H	0	-1.24032692	3.97859379	8.01414800 L
C	0	-2.15740092	5.21330279	6.50285700 L
C	0	-3.11572992	5.27382279	5.48677700 L
H	0	-3.25532292	6.18742979	4.92364300 L
C	0	-3.88731892	4.14909479	5.18458100 L
H	0	-4.61162092	4.20478679	4.38365700 L
C	0	-6.63638192	2.92687879	6.21030700 L H 180
C	0	-7.38497392	3.75410479	5.36498100 L

H	0	-7.45194592	3.51894679	4.31264600	L
C	0	-8.01687692	4.89278779	5.87174200	L
H	0	-8.58688192	5.53200779	5.21051800	L
C	0	-7.90389192	5.20954879	7.22919100	L
C	0	-7.15692092	4.38584079	8.07860100	L
H	0	-7.06397392	4.62908579	9.12909600	L
C	0	-6.52141092	3.24841779	7.57106200	L
H	0	-5.93880392	2.62060879	8.23391500	L
C	0	-8.16303592	0.65811479	5.21301000	L H 179
C	0	-8.88474492	0.72844679	4.01077000	L
H	0	-8.36386092	0.80612379	3.06452200	L
C	0	-10.28144792	0.67458879	4.02651900	L
H	0	-10.83078892	0.71675279	3.09490400	L
C	0	-10.96379192	0.54650579	5.24142900	L
C	0	-10.24919292	0.50422779	6.44312300	L
H	0	-10.77407192	0.41250579	7.38514600	L
C	0	-8.85309492	0.56241379	6.43070100	L
H	0	-8.30827492	0.50593579	7.36502300	L
C	0	-6.75261192	-1.67749921	4.11373700	L H 178
C	0	-6.60371592	-1.97950221	2.75055300	L
H	0	-5.92454792	-1.40270021	2.13655100	L
C	0	-7.34550192	-3.01272021	2.17133200	L
H	0	-7.23210292	-3.22916621	1.11665200	L
C	0	-8.24338292	-3.75079421	2.94933000	L
C	0	-8.38020992	-3.46955321	4.31304000	L
H	0	-9.07061892	-4.04154221	4.91930700	L
C	0	-7.63703892	-2.43766721	4.89513800	L
H	0	-7.75952292	-2.22267321	5.94933500	L
Br	0	5.92059808	6.21932579	-4.28247900	L
Br	0	0.89086408	8.37104679	-9.71322000	L
Br	0	-9.02261892	4.23876879	-2.61258100	L
Br	0	-6.66569892	7.90266679	-8.27368400	L
O	0	0.74541208	1.92125879	1.41854800	H
O	0	-1.32345192	1.81766479	0.50351000	H
O	0	-3.22616092	4.67839279	0.25025500	H
O	0	1.21794708	4.42738879	-0.83604100	H
N	0	-0.91197092	4.56809979	0.09637700	H
C	0	-0.36504392	2.42153879	1.09712000	H
C	0	-0.71475192	3.89995179	1.39496300	H
H	0	-1.73398792	3.84594479	1.78943300	H
C	0	0.09836008	4.68727279	2.46957800	H
C	0	-0.01577792	3.89799279	3.79156400	H
H	0	-1.05493292	3.66659879	4.04348700	H
H	0	0.52859508	2.95287379	3.74302500	H
H	0	0.40424908	4.49060679	4.61066100	H
C	0	-0.59075692	6.05708579	2.64951100	H
H	0	-0.51470992	6.66981179	1.74586800	H
H	0	-1.65262392	5.94495579	2.89369600	H
H	0	-0.11417192	6.60654479	3.46740800	H
C	0	1.58763608	4.91066979	2.14737500	H
H	0	2.10145108	3.96528479	1.96548700	H
H	0	1.72759308	5.54857879	1.27289600	H
H	0	2.06273508	5.40302679	3.00341000	H
C	0	-2.20420592	4.81284079	-0.39888000	H
C	0	0.04971708	4.75726479	-0.91014600	H
C	0	-0.67608692	5.35800079	-2.07618400	H
C	0	-2.04250892	5.27296379	-1.80977200	H
C	0	-2.99962492	5.60122579	-2.76414300	H
C	0	-2.53624792	6.10718379	-4.00655700	H
C	0	-1.14572692	6.23812279	-4.25992900	H

C	0	-0.19044292	5.83820579	-3.28985500	H
C	0	1.27369708	5.92732279	-3.52827900	L H 254
C	0	2.08601308	6.68396779	-2.66749800	L
H	0	1.65207508	7.20750379	-1.82441700	L
C	0	3.46322208	6.76927479	-2.89144100	L
H	0	4.08157108	7.34891779	-2.21833100	L
C	0	4.03849008	6.11008279	-3.98222600	L
C	0	3.23458308	5.36716879	-4.85128100	L
H	0	3.67596808	4.85541679	-5.69661900	L
C	0	1.85915408	5.27080179	-4.62317500	L
H	0	1.25205508	4.67731879	-5.29386600	L
C	0	-0.67913292	6.76208879	-5.57061400	L H 253
C	0	-0.87464592	6.01164679	-6.74149300	L
H	0	-1.37517492	5.05219479	-6.69929900	L
C	0	-0.40500892	6.48928279	-7.96779600	L
H	0	-0.54677992	5.90047779	-8.86402400	L
C	0	0.25322008	7.72111879	-8.03509900	L
C	0	0.44742008	8.47410979	-6.87237700	L
H	0	0.95883508	9.42676979	-6.92012700	L
C	0	-0.01441592	7.99614879	-5.64279900	L
H	0	0.14549908	8.58414579	-4.74742800	L
C	0	-3.52004392	6.53375379	-5.03901800	L H 252
C	0	-4.36629192	5.59335279	-5.64716700	L
H	0	-4.30096892	4.54628279	-5.37913900	L
C	0	-5.30535392	6.00292379	-6.59807900	L
H	0	-5.96098892	5.27339779	-7.05528000	L
C	0	-5.39398492	7.34991979	-6.96139700	L
C	0	-4.55062992	8.29110679	-6.36303800	L
H	0	-4.61825392	9.33548879	-6.63886000	L
C	0	-3.62084192	7.88694879	-5.40109900	L
H	0	-2.98207692	8.62702579	-4.93510900	L
C	0	-4.43140892	5.29523279	-2.52863000	L H 251
C	0	-4.85032192	3.95637179	-2.45854600	L
H	0	-4.12314492	3.15327779	-2.46521700	L
C	0	-6.21261592	3.64558079	-2.45302500	L
H	0	-6.52616792	2.60990779	-2.44150300	L
C	0	-7.16479292	4.66804179	-2.50554600	L
C	0	-6.75330892	6.00469479	-2.52448800	L
H	0	-7.48741792	6.79874279	-2.56561300	L
C	0	-5.39126192	6.31943979	-2.53284500	L
H	0	-5.08453492	7.35633979	-2.59263700	L
C	0	-3.13642392	-0.47497121	-0.57337300	H
C	0	-4.36538892	0.15315079	-0.19397000	H
C	0	-3.29724392	-1.68048121	-1.43194300	H
C	0	-5.62259992	-0.44583721	-0.54990400	H
C	0	-4.36947492	1.41929679	0.46849100	H
O	0	-3.48939092	-2.79653721	-0.99809100	H
O	0	-3.18481192	-1.35406021	-2.74309700	H
C	0	-6.82611092	0.18631279	-0.30091100	H
H	0	-5.63162492	-1.42218021	-1.01632000	H
C	0	-5.58376692	2.05443579	0.68205200	H
H	0	-3.42638292	1.88177879	0.73063600	H
C	0	-3.25945592	-2.39345621	-3.72195700	H
C	0	-6.78115592	1.44659079	0.29679900	H
H	0	-7.77355792	-0.26132421	-0.58059200	H
C	0	-5.89008192	3.41918279	1.23829100	H
C	0	-4.56358092	-2.28693321	-4.53103600	H
H	0	-2.42577492	-2.24333821	-4.40827100	H
H	0	-3.19015892	-3.37934221	-3.26018100	H
C	0	-7.90998492	2.39269279	0.52545000	H

N	0	-7.35423292	3.51543879	1.09305900 H
H	0	-5.37890992	4.20222679	0.67151900 H
H	0	-5.60020692	3.52628679	2.28624000 H
Cl	0	-4.77977892	-0.62819221	-5.18789500 H
Cl	0	-4.44015592	-3.45353021	-5.89259800 H
Cl	0	-5.99796092	-2.70446121	-3.52514600 H
O	0	-9.08657292	2.21720579	0.21570100 H
C	0	-8.09694692	4.78264679	1.18573600 H
C	0	-7.19169392	5.88536979	1.76715100 H
C	0	-9.37607992	4.65490379	2.04195800 H
H	0	-8.40182292	5.06365679	0.17045400 H
N	0	-7.09709392	7.00599179	1.01226100 H
O	0	-6.62774692	5.75614679	2.84962200 H
C	0	-10.18139792	5.96331179	2.09818800 H
H	0	-9.10469992	4.35647479	3.05176100 H
H	0	-9.98350392	3.85808579	1.61011800 H
H	0	-6.58278192	7.79449579	1.37924000 H
H	0	-7.60002792	7.12646279	0.14756000 H
C	0	-11.47535392	5.83681979	2.88570500 H
H	0	-10.45181492	6.31364779	1.09833500 H
H	0	-9.58987192	6.75423879	2.57602400 H
O	0	-12.54988292	6.24925579	2.48814500 H
O	0	-11.25731292	5.23624879	4.06554800 H
C	0	-12.35130292	4.92922379	5.01411900 H
C	0	-12.97866292	6.22970479	5.52201400 H
C	0	-11.61747392	4.20166279	6.14227800 H
C	0	-13.36980392	4.00695379	4.33842800 H
H	0	-13.69818292	6.00089579	6.31452200 H
H	0	-13.49641692	6.75811279	4.72091300 H
H	0	-12.20842992	6.88439479	5.94142200 H
H	0	-12.33391992	3.83242679	6.88115800 H
H	0	-11.05355292	3.35341079	5.74733200 H
H	0	-10.91830992	4.87324079	6.64622100 H
H	0	-12.86098092	3.14767579	3.89144500 H
H	0	-13.92294192	4.52967579	3.55804700 H
H	0	-14.07894292	3.63607579	5.08466600 H

Structure A-SI-1

ONIOM total E = -10262.097654 Hartree
ZPE = 2.604137 Hartree
TCH = 2.816067 Hartree
TCG = 2.302779 Hartree
H = -10259.281587 Hartree
G = -10259.794875 Hartree
No Imaginary frequency

Rh	0	14.88064600	10.34251700	20.96964100 H
Rh	0	17.12325600	10.19437600	19.96527300 H
Br	0	18.20396200	2.33354700	25.41544100 L H 41
Br	0	14.53449800	2.78683000	32.05078500 L H 51
Br	0	14.32492700	16.13021700	30.73105300 L H 71
Br	0	12.64486000	9.68903600	34.92528900 L H 61
O	0	17.88913600	10.68203900	21.81433900 H
O	0	15.84508500	10.66259900	22.79043300 H
O	0	16.33786400	12.53067600	26.35261400 H
O	0	17.38417100	8.43384700	24.58664100 H
N	0	17.10116400	10.64003900	25.25170800 H
C	0	17.11087400	10.82891200	22.79682900 H
C	0	17.69847300	11.35540200	24.12191300 H
H	0	17.28339100	12.36791000	24.20737100 H
C	0	19.25963500	11.51036000	24.22066000 H
C	0	19.71144100	12.60531900	23.22787400 H

H	0	19.17661100	13.54520400	23.39951600	H
H	0	19.54769000	12.30446400	22.19292600	H
H	0	20.78169400	12.79693100	23.36416200	H
C	0	19.60450800	12.00147900	25.64425300	H
H	0	19.38147500	11.24633700	26.40508100	H
H	0	19.06208200	12.91655600	25.89859400	H
H	0	20.67686900	12.21532500	25.70216400	H
C	0	20.02833100	10.20270800	23.94821300	H
H	0	19.83374000	9.82510100	22.94360800	H
H	0	19.76488300	9.41717300	24.66119300	H
H	0	21.10384200	10.39235500	24.04247100	H
C	0	16.47316300	11.32432100	26.30513400	H
C	0	17.02948800	9.25093000	25.41521200	H
C	0	16.42484000	9.03148000	26.77427100	H
C	0	16.05495000	10.27805900	27.28901900	H
C	0	15.47476400	10.42400300	28.54866300	H
C	0	15.25102700	9.23263900	29.29251100	H
C	0	15.62384100	7.96619900	28.77269500	H
C	0	16.23883600	7.85022800	27.49323900	H
C	0	16.69762700	6.53102000	26.95896900	H
C	0	18.06991900	6.26680100	26.83821600	H
H	0	18.78866800	7.03558600	27.10734700	H
C	0	18.51714100	5.02666900	26.38563100	H
H	0	19.58452500	4.84042500	26.30785300	H
C	0	17.59529700	4.03702300	26.03373600	H
C	0	16.22790500	4.30023900	26.12994200	H
H	0	15.49443700	3.55537600	25.83935500	H
C	0	15.78174100	5.53698300	26.59530300	H
H	0	14.71607200	5.72609500	26.66968400	H
C	0	15.36617300	6.72594500	29.57565100	H
C	0	14.05394900	6.32280900	29.86274300	H
H	0	13.22300800	6.92673100	29.51374200	H
C	0	13.80792200	5.16030900	30.59266200	H
H	0	12.78176400	4.86867400	30.79839500	H
C	0	14.87175300	4.38343900	31.05510500	H
C	0	16.18278100	4.77945100	30.78309600	H
H	0	17.02234500	4.18796900	31.13720100	H
C	0	16.42688900	5.93884600	30.04694400	H
H	0	17.44897500	6.23225800	29.82939900	H
C	0	14.62496700	9.33239500	30.65050900	H
C	0	13.30613300	9.78737200	30.79249300	H
H	0	12.73775500	10.06027400	29.90860000	H
C	0	12.71928500	9.88815000	32.05384300	H
H	0	11.69415800	10.23788900	32.13721000	H
C	0	13.44627000	9.54536400	33.19560000	H
C	0	14.76240700	9.09686200	33.06622700	H
H	0	15.34198300	8.82733700	33.94464800	H
C	0	15.34472400	8.98808300	31.80364900	H
H	0	16.36539100	8.63012700	31.70961500	H
C	0	15.16309700	11.78017800	29.09673100	H
C	0	14.21143500	12.60370300	28.48032000	H
H	0	13.68462400	12.24476100	27.60198800	H
C	0	13.95382500	13.88302400	28.97078900	H
H	0	13.21415100	14.50545800	28.47517100	H
C	0	14.65441500	14.36403100	30.07930500	H
C	0	15.60464200	13.55157700	30.70087100	H
H	0	16.15905100	13.91118100	31.56306900	H
C	0	15.85295400	12.26763800	30.21552100	H
H	0	16.59318400	11.64087400	30.70282100	H
Br	0	13.26825600	4.43154200	13.19614100	L H 114

Br	0	7.42680900	0.39408500	15.77006300	L H 124
Br	0	11.39487100	2.92165900	28.30459300	L H 144
Br	0	6.06329700	-0.05691700	23.34224400	L H 134
O	0	17.15387200	8.19548000	20.49817000	H
O	0	15.03282800	8.30238600	21.27940100	H
O	0	14.24798600	5.30678500	23.51594000	H
O	0	14.83994600	5.85450800	19.01172500	H
N	0	14.93603400	5.57835000	21.31664900	H
C	0	16.13713800	7.70160300	21.05433400	H
C	0	16.18981400	6.27083600	21.62251500	H
H	0	16.13738300	6.42608500	22.70786600	H
C	0	17.48130800	5.41795500	21.36488800	H
C	0	18.65793800	6.08692400	22.11086600	H
H	0	18.43987400	6.20889600	23.17679900	H
H	0	18.88886000	7.06910900	21.69624200	H
H	0	19.55048300	5.45815300	22.01788700	H
C	0	17.25547500	4.02288400	21.98695300	H
H	0	16.48608800	3.45660400	21.45234700	H
H	0	16.96221600	4.09528000	23.03897000	H
H	0	18.18435100	3.44533200	21.93428800	H
C	0	17.83913100	5.24974300	19.87545200	H
H	0	18.01857200	6.21371200	19.39718400	H
H	0	17.05081200	4.73871200	19.31852800	H
H	0	18.75310800	4.64993900	19.79362900	H
C	0	14.07416100	5.12288800	22.32430100	H
C	0	14.37636600	5.40185900	20.03944300	H
C	0	13.13740600	4.58255700	20.24967600	H
C	0	12.96189800	4.40762100	21.62483800	H
C	0	11.90479800	3.66732000	22.15247100	H
C	0	10.99402400	3.09635700	21.22244100	H
C	0	11.18976700	3.24753300	19.82528000	H
C	0	12.28121700	4.00337800	19.31558800	H
C	0	12.53216900	4.11859700	17.84519900	H
C	0	13.08780100	3.04177500	17.14114600	H
H	0	13.34448200	2.12927800	17.67165200	H
C	0	13.31274600	3.13375700	15.76739500	H
H	0	13.75204300	2.29054400	15.24161800	H
C	0	12.96872600	4.29927300	15.07948400	H
C	0	12.40946500	5.37300400	15.77500500	H
H	0	12.12002600	6.28540700	15.26489400	H
C	0	12.20395800	5.28883300	17.15188200	H
H	0	11.78198500	6.13948000	17.67593500	H
C	0	10.26619500	2.56690700	18.86034000	H
C	0	9.45974700	3.30844300	17.98472600	H
H	0	9.49403300	4.39306400	18.00921400	H
C	0	8.62038100	2.66585800	17.07455100	H
H	0	8.01171100	3.26220300	16.40116400	H
C	0	8.57423200	1.27168900	17.02222200	H
C	0	9.37479700	0.52326500	17.88727100	H
H	0	9.35452200	-0.56253500	17.85760600	H
C	0	10.21204300	1.16671100	18.79806200	H
H	0	10.83169400	0.57862100	19.46800900	H
C	0	9.81118300	2.32856800	21.73019700	H
C	0	8.51030900	2.80664200	21.51530400	H
H	0	8.36754300	3.73227400	20.96603600	H
C	0	7.40365000	2.10547800	21.99350200	H
H	0	6.40648500	2.49841100	21.81557100	H
C	0	7.57931000	0.90850700	22.69076900	H
C	0	8.86955600	0.42155900	22.90919500	H
H	0	9.02371900	-0.50816600	23.44958400	H

C	0	9.97523700	1.12846000	22.43665400	H
H	0	10.97550000	0.74767100	22.61822500	H
C	0	11.75952600	3.47746500	23.62889800	H
C	0	10.69322600	4.05109500	24.33305300	H
H	0	9.95291200	4.63786500	23.79849900	H
C	0	10.58010000	3.88026000	25.71350700	H
H	0	9.75037800	4.34330300	26.23947400	H
C	0	11.52857900	3.12772500	26.40862000	H
C	0	12.58697100	2.53874800	25.71262100	H
H	0	13.32804900	1.94291800	26.23831000	H
C	0	12.70262100	2.71688500	24.33470600	H
H	0	13.53328600	2.26688900	23.79881100	H
Br	0	14.33341300	18.35988400	15.42224700	L H 187
Br	0	6.76447200	18.41795500	13.98663400	L H 197
Br	0	6.08256200	5.62474300	17.31552900	L H 217
Br	0	2.76909800	11.82733700	14.36010600	L H 207
O	0	16.20700200	9.72985800	18.16444200	H
O	0	14.14718000	10.06210200	19.04264000	H
O	0	11.54565600	8.40795900	16.61645400	H
O	0	13.97598300	12.29063800	16.67478300	H
N	0	13.06714600	10.15774900	16.56200600	H
C	0	14.94962900	9.76789300	18.09332500	H
C	0	14.25918200	9.33461100	16.78421800	H
H	0	13.84337400	8.34842700	17.02796300	H
C	0	15.15899200	9.12549700	15.51356700	H
C	0	16.06773900	7.89948400	15.76050800	H
H	0	15.47941800	7.01027000	16.01241600	H
H	0	16.77603100	8.08040800	16.56953200	H
H	0	16.63550200	7.67833600	14.85001000	H
C	0	14.23811900	8.79592200	14.31877500	H
H	0	13.59784100	9.64080500	14.04611000	H
H	0	13.59799700	7.93382600	14.52880400	H
H	0	14.85106400	8.55222100	13.44496100	H
C	0	16.02191900	10.35036300	15.15245800	H
H	0	16.70118700	10.61331300	15.96461900	H
H	0	15.41225100	11.22767700	14.92466800	H
H	0	16.62229300	10.11670500	14.26570300	H
C	0	11.78262900	9.59714600	16.51635700	H
C	0	13.02180600	11.55947300	16.49088000	H
C	0	11.59189500	11.90672800	16.18331500	H
C	0	10.83868800	10.73302700	16.28907100	H
C	0	9.45517100	10.70935000	16.11706700	H
C	0	8.83667800	11.93618200	15.74440000	H
C	0	9.59982200	13.12614700	15.62307700	H
C	0	11.00430200	13.13239800	15.86404500	H
C	0	11.80911100	14.38664500	15.76187100	H
C	0	12.82998500	14.50234700	14.80729500	H
H	0	13.04124500	13.66891200	14.14388100	H
C	0	13.57103900	15.67808300	14.70072300	H
H	0	14.35296300	15.74856500	13.94985600	H
C	0	13.30966500	16.75113100	15.55746100	H
C	0	12.30270300	16.64145200	16.51789400	H
H	0	12.09614400	17.45507400	17.20574700	H
C	0	11.55308200	15.46989000	16.61297000	H
H	0	10.76538900	15.39975000	17.35575500	H
C	0	8.91784600	14.40342700	15.23317100	H
C	0	7.98101400	15.00470600	16.08583800	H
H	0	7.76251000	14.55455700	17.04879200	H
C	0	7.34534600	16.18948800	15.71422500	H
H	0	6.62344900	16.63838000	16.39093000	H

C	0	7.63460800	16.79134000	14.48814200	H
C	0	8.56889400	16.20137500	13.63440700	H
H	0	8.80864400	16.65793100	12.67823200	H
C	0	9.20702500	15.01835200	14.00647200	H
H	0	9.93968300	14.56940200	13.34249400	H
C	0	7.37007600	11.94924600	15.43038700	H
C	0	6.41112200	11.65390700	16.40992600	H
H	0	6.73972900	11.43275100	17.42086700	H
C	0	5.05156700	11.61952300	16.09694800	H
H	0	4.32144500	11.36414900	16.85975000	H
C	0	4.63031300	11.88431600	14.79201000	H
C	0	5.57380400	12.18249800	13.80707400	H
H	0	5.26135800	12.38869900	12.78718000	H
C	0	6.93176100	12.21343600	14.12420800	H
H	0	7.66004300	12.44420500	13.35310700	H
C	0	8.67293300	9.45886700	16.36251300	H
C	0	8.66618300	8.89923800	17.64927500	H
H	0	9.26220200	9.35913500	18.43233000	H
C	0	7.90690800	7.76433800	17.93036500	H
H	0	7.91546800	7.35180600	18.93581000	H
C	0	7.14861100	7.16248000	16.92314800	H
C	0	7.16743500	7.69737200	15.63336900	H
H	0	6.58982500	7.23643300	14.83737300	H
C	0	7.92125800	8.83811000	15.35615200	H
H	0	7.91666100	9.25653200	14.35503700	H
Br	0	20.23088900	15.69336400	27.27820400	L H 260
Br	0	14.53906200	20.18073500	29.96431800	L H 270
Br	0	8.43912100	18.86801000	18.10471800	L H 290
Br	0	8.72674900	22.02156200	25.40073100	L H 280
O	0	16.97776800	12.20543300	19.50061100	H
O	0	15.01170400	12.39936100	20.60308900	H
O	0	13.28915000	15.70497400	19.52778000	H
O	0	16.85489600	14.63313700	22.18636500	H
N	0	15.28568000	15.11899900	20.54560700	H
C	0	15.97394200	12.85527400	19.89306100	H
C	0	15.78626400	14.31250400	19.42986500	H
H	0	14.92621700	14.25722000	18.74943500	H
C	0	16.94043500	14.98793000	18.61009300	H
C	0	17.08038200	14.24453500	17.26233600	H
H	0	16.12899600	14.21796800	16.72053500	H
H	0	17.42204100	13.21839100	17.40231000	H
H	0	17.81144000	14.76641900	16.63495500	H
C	0	16.51474000	16.44094400	18.30444200	H
H	0	16.46512400	17.05287700	19.21081600	H
H	0	15.53852400	16.47953400	17.81082200	H
H	0	17.24975800	16.90264300	17.63696300	H
C	0	18.29602300	15.00374500	19.34197200	H
H	0	18.63904100	13.99309100	19.56864700	H
H	0	18.24849600	15.56161700	20.28022800	H
H	0	19.04420100	15.48541300	18.70185200	H
C	0	14.04742800	15.77472000	20.47718300	H
C	0	15.86521900	15.23587100	21.81971800	H
C	0	14.99982500	16.20694200	22.57158800	H
C	0	13.89407000	16.50861100	21.77056700	H
C	0	12.90074100	17.40040700	22.17334500	H
C	0	13.04222000	17.97551900	23.46447300	H
C	0	14.15379000	17.65717500	24.28712100	H
C	0	15.17323400	16.77191200	23.83523200	H
C	0	16.38637900	16.48554900	24.66011900	H
C	0	17.64100700	16.95440000	24.24255000	H

H	0	17.72441800	17.50198500	23.30796100	H
C	0	18.77674800	16.72726300	25.01781500	H
H	0	19.73810400	17.10230400	24.67813100	H
C	0	18.67379200	16.01804900	26.21786800	H
C	0	17.43180000	15.53466800	26.63245600	H
H	0	17.33291200	14.95895900	27.54677000	H
C	0	16.29494600	15.77019000	25.85949700	H
H	0	15.33816400	15.37993800	26.18859300	H
C	0	14.25612400	18.26235900	25.65486900	H
C	0	13.31265900	17.94648300	26.64324500	H
H	0	12.50525200	17.25928000	26.40964900	H
C	0	13.39591600	18.51059800	27.91594200	H
H	0	12.65043500	18.25179300	28.66272400	H
C	0	14.42546100	19.40290500	28.22170200	H
C	0	15.37162600	19.72330900	27.24622600	H
H	0	16.17997000	20.41424700	27.46810600	H
C	0	15.28884000	19.15517100	25.97512100	H
H	0	16.03388500	19.40221200	25.22547400	H
C	0	12.00674000	18.94952400	23.93922500	H
C	0	10.68627200	18.53479700	24.16408600	H
H	0	10.41781300	17.49609600	23.99668400	H
C	0	9.71843000	19.43962700	24.60013900	H
H	0	8.70376100	19.09216000	24.77352000	H
C	0	10.05322100	20.77904500	24.80805100	H
C	0	11.36320900	21.20523800	24.57958900	H
H	0	11.63974300	22.24430500	24.73440300	H
C	0	12.33134100	20.29703000	24.15213800	H
H	0	13.34979800	20.63367300	23.98492600	H
C	0	11.78599900	17.77081900	21.24733000	H
C	0	10.80679100	16.83570100	20.89006100	H
H	0	10.83998000	15.83902400	21.31984100	H
C	0	9.80813300	17.16041700	19.97223800	H
H	0	9.07785300	16.40521900	19.69786300	H
C	0	9.77917100	18.43328800	19.39636200	H
C	0	10.74240400	19.37892000	19.75525400	H
H	0	10.73028000	20.37319700	19.31750000	H
C	0	11.73715700	19.05011500	20.67693800	H
H	0	12.48847400	19.78593700	20.94706500	H
C	0	12.97457800	10.26872300	21.65591200	H
C	0	11.83070400	11.01295100	21.20236600	H
C	0	12.68854900	9.09944700	22.52962300	H
C	0	12.01554100	12.20370200	20.44140500	H
C	0	10.50375900	10.58633000	21.51221800	H
O	0	12.26516700	8.04776800	22.10033000	H
O	0	12.98565200	9.35473600	23.82767700	H
C	0	10.93502900	12.97218200	20.02202500	H
H	0	13.02569900	12.51708800	20.21546400	H
C	0	9.43833200	11.34163200	21.06635000	H
H	0	10.34444800	9.67041400	22.06939700	H
C	0	12.87258200	8.27823600	24.75724300	H
C	0	9.65475300	12.52012700	20.33754700	H
H	0	11.09188100	13.89012600	19.46559100	H
C	0	7.95453600	11.11766500	21.22838700	H
C	0	11.68168900	8.49592000	25.70494700	H
H	0	12.76127200	7.32071700	24.24536300	H
H	0	13.78498400	8.27626000	25.35592200	H
C	0	8.33481800	13.12923600	20.02772800	H
N	0	7.38842400	12.24756500	20.48845300	H
H	0	7.63548800	11.14008100	22.27887300	H
H	0	7.63230900	10.16237000	20.79807500	H

Cl	0	10.11332200	8.42478300	24.81544200	H
Cl	0	11.72358800	7.17641400	26.92406800	H
Cl	0	11.80135200	10.08723300	26.53630300	H
O	0	8.09186600	14.21522900	19.49366800	H
C	0	5.95933200	12.56314700	20.42726900	H
C	0	5.57730100	13.37898800	21.68984400	H
C	0	5.09951300	11.30949100	20.26374800	H
H	0	5.84720500	13.20734600	19.54894100	H
N	0	5.95840500	14.68253200	21.62662100	H
O	0	5.00583800	12.87263000	22.64645700	H
C	0	3.62771200	11.65953300	19.96760200	H
H	0	5.14019300	10.70439000	21.17287500	H
H	0	5.51379300	10.71727900	19.43956600	H
H	0	5.85480900	15.24643800	22.45779200	H
H	0	6.56378100	15.00098200	20.87856200	H
C	0	2.86647400	10.45235200	19.45089100	H
H	0	3.55676900	12.42975100	19.19488900	H
H	0	3.15769700	12.03071300	20.88278700	H
O	0	2.45666100	10.35060000	18.30975300	H
O	0	2.74774200	9.51899100	20.41071300	H
C	0	2.10833200	8.21049000	20.15355600	H
C	0	0.63792100	8.41629300	19.77673900	H
C	0	2.23222400	7.50860900	21.50765100	H
C	0	2.88780000	7.45523300	19.07205900	H
H	0	0.14002600	7.44381600	19.70573600	H
H	0	0.54451500	8.92872300	18.81897600	H
H	0	0.12653900	9.00325200	20.54601100	H
H	0	1.78451300	6.51170600	21.45583400	H
H	0	3.28260800	7.40225100	21.79404200	H
H	0	1.71978000	8.07949700	22.28710400	H
H	0	3.94533400	7.38211700	19.34521900	H
H	0	2.80716800	7.95276400	18.10536200	H
H	0	2.49127500	6.43903200	18.97900500	H

Structure A-SI-2 (Frequency calculation was limited due to the physical limitation of our facility)

E = -51396.217145 Hartree

Rh	15.09725200	10.03737200	20.90350600
Rh	17.31015400	9.97665200	19.82163600
Br	17.23291500	2.07032200	25.55601600
Br	14.11498100	3.00626400	31.85702400
Br	14.62035400	16.26513100	30.41712200
Br	12.42185100	10.16452800	34.53223900
O	18.06578600	10.63761600	21.62788500
O	16.05071800	10.51565600	22.65898600
O	16.56749500	12.52352500	26.11334000
O	17.33453100	8.35804600	24.38498400
N	17.22586800	10.57698300	25.05730600
C	17.30413100	10.74012900	22.62945800
C	17.87932600	11.26208200	23.94715500
H	17.50078000	12.29000600	24.01410400
C	19.42988700	11.34635800	24.08848200
C	19.95230000	12.42122500	23.11420900
H	19.46009100	13.38319000	23.29670500
H	19.78392900	12.13950800	22.07475600
H	21.02713300	12.56064600	23.26720400
C	19.75716000	11.81033900	25.52127800
H	19.46653400	11.06372800	26.26621300
H	19.25749400	12.75130200	25.76535600
H	20.83603000	11.96692100	25.61315600
C	20.11892700	9.99713800	23.82726800
H	19.91871700	9.63644300	22.81717100

H	19.78326600	9.23476600	24.53485100
H	21.20134500	10.11190400	23.94600000
C	16.61926400	11.30999700	26.08478600
C	17.02753400	9.19989700	25.21013200
C	16.36596000	9.03386600	26.55091200
C	16.09851400	10.31180000	27.05392300
C	15.49161500	10.52396400	28.28466200
C	15.15571500	9.37210500	29.03883200
C	15.43453000	8.07594900	28.55074300
C	16.04057100	7.88594700	27.27361600
C	16.31729900	6.51482400	26.76577500
C	17.62582000	6.12226500	26.45419100
H	18.43468100	6.84106500	26.52027700
C	17.90807900	4.80710500	26.09119400
H	18.92361300	4.50368500	25.86745100
C	16.86279800	3.88622000	26.02800700
C	15.55027800	4.25875800	26.29835400
H	14.74502700	3.54153300	26.21859000
C	15.28558800	5.57217500	26.67052700
H	14.26633200	5.85581100	26.90246700
C	15.11569000	6.88339800	29.39086000
C	13.80881900	6.62997300	29.82750700
H	13.01836300	7.33199600	29.59721300
C	13.50367100	5.48378000	30.55708700
H	12.48559500	5.28845300	30.87102400
C	14.52649800	4.59255200	30.87167800
C	15.84265500	4.83440200	30.48298200
H	16.63100200	4.13941600	30.74610800
C	16.12749700	5.97873400	29.74228000
H	17.14718500	6.16130500	29.42258000
C	14.50388800	9.55353200	30.36649700
C	13.23993900	10.15167400	30.44752000
H	12.73791000	10.47142700	29.54086500
C	12.61376100	10.33232800	31.67889200
H	11.63282200	10.78863600	31.73649200
C	13.26985700	9.91673100	32.83571200
C	14.53017800	9.32430600	32.78393200
H	15.02750500	9.00957900	33.69353000
C	15.13948100	9.14278600	31.54439900
H	16.11712100	8.67589600	31.49350600
C	15.25918200	11.89957600	28.80632800
C	14.38685100	12.78072100	28.15663700
H	13.88094700	12.47158900	27.25006600
C	14.17147900	14.06599300	28.64712000
H	13.48705400	14.74210200	28.14830000
C	14.86527200	14.48017500	29.78281600
C	15.74595500	13.62724800	30.44512700
H	16.28057800	13.96426100	31.32509200
C	15.92932400	12.33505500	29.95643900
H	16.60730900	11.66260800	30.47049000
Br	14.94602200	3.52779200	13.47026100
Br	7.27679600	3.12475600	15.10547800
Br	10.78170100	4.20969400	28.00639800
Br	5.07317600	3.54628700	22.39556600
O	17.53033000	8.05869800	20.55013800
O	15.40102500	8.04503900	21.32439000
O	14.54829500	5.43082600	23.54604300
O	15.67504200	5.65119400	19.13170000
N	15.51184900	5.39791000	21.43689100
C	16.56084000	7.53317000	21.15662000

C	16.70161000	6.15733700	21.81612400
H	16.55785200	6.36083300	22.88300500
C	18.04564700	5.38950800	21.69075400
C	19.11818100	6.19314800	22.45295900
H	18.82183300	6.35777900	23.49286500
H	19.28871700	7.16709700	21.99041700
H	20.06249800	5.63944400	22.44826900
C	17.85314500	4.03465400	22.39422400
H	17.14868800	3.39789400	21.85154900
H	17.47532700	4.16670400	23.40989300
H	18.80957300	3.50657300	22.45567500
C	18.50746500	5.14481800	20.24562300
H	18.65005200	6.08379500	19.70903300
H	17.78825800	4.54041900	19.69005600
H	19.46172200	4.60714200	20.26467400
C	14.46340700	5.20146900	22.35453800
C	15.05222900	5.29369000	20.11498700
C	13.65730300	4.78498100	20.20519400
C	13.29281900	4.74583300	21.55066300
C	11.99340800	4.45150900	21.95118200
C	11.03912700	4.26045600	20.92154500
C	11.41499400	4.28455300	19.55727400
C	12.76092700	4.50863400	19.17824200
C	13.25979600	4.31967300	17.78635700
C	14.06497600	3.20079100	17.53018900
H	14.29868800	2.51404400	18.33736100
C	14.56820500	2.95311300	16.25452900
H	15.18977700	2.08607600	16.06542600
C	14.25775400	3.84112300	15.22766000
C	13.46207500	4.96051400	15.45576600
H	13.23361200	5.64148100	14.64543600
C	12.97033200	5.19997300	16.73852400
H	12.38360800	6.09065100	16.91604400
C	10.39786900	4.01238300	18.50140500
C	9.97505900	5.03114700	17.63899800
H	10.34594200	6.04221100	17.76097700
C	9.06216200	4.76672700	16.62058100
H	8.74687100	5.55752500	15.95354600
C	8.55224000	3.47930100	16.48626000
C	8.94073200	2.45072300	17.34194200
H	8.53124500	1.45420400	17.22690400
C	9.86821200	2.72536300	18.34575300
H	10.18334800	1.93074300	19.01386600
C	9.60759700	4.05525700	21.27849900
C	8.66768100	5.02747700	20.91747600
H	8.99841300	5.90215400	20.37032800
C	7.32511000	4.88674400	21.25515500
H	6.59879800	5.63868100	20.97591300
C	6.92297400	3.74976900	21.95148300
C	7.83557300	2.76456200	22.32345500
H	7.50576100	1.88583400	22.86471300
C	9.17968800	2.92767400	21.98874600
H	9.89905200	2.17065500	22.28208300
C	11.64767900	4.37178000	23.39334000
C	10.68999500	5.22014100	23.96339500
H	10.17475300	5.94468400	23.34430100
C	10.40739100	5.15970300	25.32649700
H	9.68046100	5.83090200	25.76550700
C	11.09403500	4.24253800	26.11945700
C	12.03115900	3.36892300	25.57348400

H	12.53956700	2.64720600	26.20175500
C	12.30658200	3.44397800	24.21016500
H	13.04702600	2.77906800	23.77857100
Br	13.96226200	18.21085800	15.75402100
Br	6.71175800	18.03308800	14.35970200
Br	5.79225900	5.60040200	17.98489400
Br	2.64200000	11.39833500	15.70900400
O	16.31155100	9.35307600	18.08051900
O	14.29526800	9.62052700	19.07301400
O	11.51752100	8.11152700	17.00296900
O	13.97512100	11.96220700	16.98833500
N	13.04525200	9.84747200	16.78036200
C	15.05241700	9.37920200	18.07715500
C	14.25582600	9.02634200	16.81457500
H	13.87747700	8.01695900	17.01344200
C	15.01917700	8.95542300	15.45771400
C	15.97714000	7.74788300	15.51522900
H	15.43975900	6.82468500	15.75309900
H	16.75563400	7.89621600	16.26463300
H	16.45559700	7.61422600	14.54015200
C	13.97978700	8.71175800	14.34697100
H	13.33913600	9.58502600	14.19533000
H	13.33463700	7.85904300	14.57842300
H	14.49134100	8.50261800	13.40313400
C	15.81420700	10.23128900	15.13131700
H	16.53881600	10.45846100	15.91501800
H	15.16064700	11.09685100	15.00941800
H	16.35686300	10.08335600	14.19187800
C	11.75999900	9.29928800	16.87780700
C	13.00364400	11.25154700	16.80319200
C	11.56175700	11.61842400	16.61156400
C	10.81455500	10.44337600	16.76352900
C	9.42692200	10.43421500	16.71857700
C	8.78592000	11.65968500	16.40060400
C	9.53429300	12.83596600	16.18373200
C	10.95206900	12.84368100	16.33878400
C	11.71343900	14.11274100	16.21082500
C	12.81614600	14.22291300	15.35307800
H	13.14470900	13.36465800	14.77849400
C	13.48883000	15.43488700	15.21200400
H	14.33706500	15.51906300	14.54342900
C	13.04769200	16.54048200	15.93926100
C	11.96088300	16.45750900	16.80358000
H	11.64188100	17.31514500	17.38156200
C	11.30122800	15.24080300	16.93206800
H	10.46344200	15.16803100	17.61336500
C	8.83154500	14.07596100	15.74312600
C	7.81576900	14.64921200	16.51882500
H	7.54765500	14.20268700	17.46702000
C	7.17630700	15.81423000	16.10566600
H	6.40772100	16.26549000	16.72047300
C	7.55538600	16.40471800	14.90279800
C	8.54815700	15.84652000	14.10105300
H	8.82831300	16.31418300	13.16477600
C	9.18192300	14.68168900	14.52892500
H	9.96522600	14.24774600	13.91692300
C	7.30171600	11.66025000	16.24369000
C	6.47267500	11.37300300	17.33490800
H	6.91637800	11.18382900	18.30458300
C	5.09007500	11.30481700	17.18409900

H	4.44651000	11.07889800	18.02318300
C	4.53636700	11.52232700	15.92445800
C	5.33657500	11.81987200	14.82350700
H	4.89170700	11.98742600	13.84997900
C	6.71829500	11.88960000	14.99185700
H	7.34841500	12.11763900	14.13915400
C	8.61749000	9.21608100	16.99464500
C	8.52496200	8.72994500	18.30385000
H	9.11660000	9.18823700	19.08915400
C	7.66170100	7.68052500	18.61329300
H	7.57257600	7.33204900	19.63310900
C	6.91283000	7.09375900	17.59470100
C	6.99862200	7.55250100	16.28101800
H	6.41542900	7.08222000	15.49839500
C	7.84846200	8.61726800	15.98957400
H	7.90152400	8.99464300	14.97443200
Br	19.69520400	15.37813600	27.37518800
Br	13.70269400	19.72631400	29.65865700
Br	8.42381700	18.68637100	17.78246500
Br	7.94964600	20.89846600	25.07528200
O	16.99257000	11.92289500	19.21393000
O	15.10280200	12.04896800	20.45153000
O	13.10630700	15.14543500	19.28965100
O	16.67083600	14.19829700	21.97523300
N	15.12532900	14.69336000	20.31969300
C	15.98376200	12.52827400	19.66059500
C	15.67793200	13.94911100	19.19515700
H	14.82489700	13.82339600	18.51626700
C	16.76884200	14.72242200	18.39850000
C	16.95699200	14.02490800	17.03634900
H	16.00734000	13.96893000	16.49411000
H	17.34516300	13.01252700	17.15391800
H	17.66202400	14.59859600	16.42644300
C	16.23623400	16.14424500	18.13870600
H	16.15046900	16.71990000	19.06493700
H	15.25490000	16.12183900	17.65838900
H	16.92321700	16.67826900	17.47574400
C	18.10829700	14.81033300	19.14699200
H	18.52123500	13.81885900	19.34121400
H	17.99898000	15.32777000	20.10310800
H	18.82670100	15.37131800	18.54011400
C	13.84502000	15.25060800	20.25087200
C	15.65782500	14.77032900	21.61472500
C	14.71295300	15.64708000	22.38707400
C	13.61725400	15.91893900	21.55781600
C	12.56819200	16.74233900	21.94363800
C	12.62247000	17.26896300	23.25697100
C	13.71767000	16.99350900	24.10616100
C	14.80540000	16.18268200	23.67307200
C	15.98547000	15.95618500	24.54907800
C	17.27997400	16.23619600	24.08799100
H	17.42779400	16.59430100	23.07577700
C	18.38502500	16.06991600	24.91965900
H	19.38320100	16.28769000	24.55906100
C	18.18469800	15.62469300	26.22603000
C	16.91305100	15.34198700	26.71150500
H	16.77060600	14.97111600	27.71791400
C	15.82238700	15.50471600	25.86434700
H	14.83467400	15.26333000	26.23321300
C	13.73879000	17.61709200	25.46145000

C	12.75815900	17.29697400	26.40942100
H	11.99203500	16.56880600	26.16539000
C	12.74660000	17.90925200	27.66086000
H	11.98956800	17.65473000	28.39234700
C	13.72367900	18.85801700	27.95546400
C	14.71595600	19.18855200	27.03566400
H	15.47113300	19.92512300	27.28246000
C	14.71955500	18.56005000	25.79221700
H	15.48989200	18.80963300	25.07055200
C	11.50826100	18.14915800	23.71137700
C	10.20519700	17.64084700	23.78917000
H	10.01687500	16.60347400	23.53397700
C	9.14495700	18.44790400	24.19649100
H	8.14035700	18.04713600	24.26136500
C	9.39765600	19.77945300	24.51884100
C	10.68262600	20.31368900	24.44342100
H	10.86133200	21.35267800	24.69317400
C	11.73265500	19.49180500	24.04060900
H	12.73561700	19.89972000	23.98328700
C	11.52286200	17.18112100	20.97478500
C	10.52167300	16.32612200	20.50406200
H	10.47190400	15.30098500	20.85277900
C	9.58210000	16.77324000	19.57523800
H	8.82114200	16.09583900	19.21165500
C	9.66282100	18.08381400	19.10909100
C	10.64680700	18.95858200	19.56537300
H	10.69751500	19.97471000	19.19290700
C	11.56948400	18.49974500	20.50289500
H	12.34109900	19.17138100	20.86405800
C	13.20975500	9.92016300	21.59163200
C	12.06405000	10.61774000	21.10587000
C	12.97133900	8.78322500	22.50949200
C	12.22805900	11.72192900	20.21633000
C	10.75260100	10.26815400	21.55193400
O	12.50222200	7.72421900	22.14445100
O	13.38741000	9.06983300	23.76090100
C	11.15051700	12.50074300	19.82402000
H	13.22014000	11.96525500	19.87373400
C	9.68766400	11.04044000	21.14301800
H	10.60528300	9.41618600	22.20251900
C	13.15519200	8.10305900	24.78346100
C	9.89286200	12.14339400	20.30039500
H	11.29193600	13.36513900	19.18745100
C	8.22471300	10.93772300	21.48285400
C	12.09445300	8.64477600	25.74757000
H	12.83137800	7.14963700	24.36536200
H	14.09102300	7.97307400	25.32483100
C	8.59287600	12.81839700	20.08835100
N	7.65554700	12.05503800	20.72371000
H	8.03890200	11.06251600	22.55594800
H	7.78730800	9.98449400	21.17079200
Cl	10.49854900	8.78348400	24.92201700
Cl	11.96309100	7.50305000	27.11679200
Cl	12.56478400	10.26432800	26.36673200
O	8.37272000	13.87842300	19.49301900
C	6.26361700	12.48383300	20.83229800
C	6.12680600	13.40811400	22.06628200
C	5.32522600	11.28629500	20.88636000
H	6.06790800	13.07561400	19.93280400
N	6.66529000	14.63572100	21.88621100

O	5.59530100	13.02911800	23.10630700
C	3.85331000	11.69827400	20.75487400
H	5.46807300	10.74055300	21.82082300
H	5.59568800	10.60529800	20.07513400
H	6.71431500	15.26884200	22.67159700
H	7.17531100	14.85706700	21.03966500
C	2.96374300	10.57876400	20.24559900
H	3.72644000	12.53180200	20.05792700
H	3.47419000	12.03867900	21.72405300
O	1.98733400	10.76756600	19.54303100
O	3.41503300	9.38579700	20.65275600
C	2.87760000	8.11508400	20.11758500
C	1.41459300	7.95199400	20.52632200
C	3.75972600	7.07522600	20.80564500
C	3.07290100	8.09362800	18.60092000
H	1.06908900	6.95463900	20.23815900
H	0.78637100	8.69829700	20.04063700
H	1.31090300	8.04921800	21.61106600
H	3.48926900	6.06959100	20.47575300
H	4.81013000	7.24535100	20.55685500
H	3.64336600	7.12894500	21.89158200
H	4.11919100	8.28944100	18.35034800
H	2.44439200	8.83658100	18.10918100
H	2.81748200	7.10313400	18.21568700

Section 4: Spectroscopic Data

^{1}H NMR Spectra

^{1}H NMR (500 MHz) Spectrum for Compound 3.4.

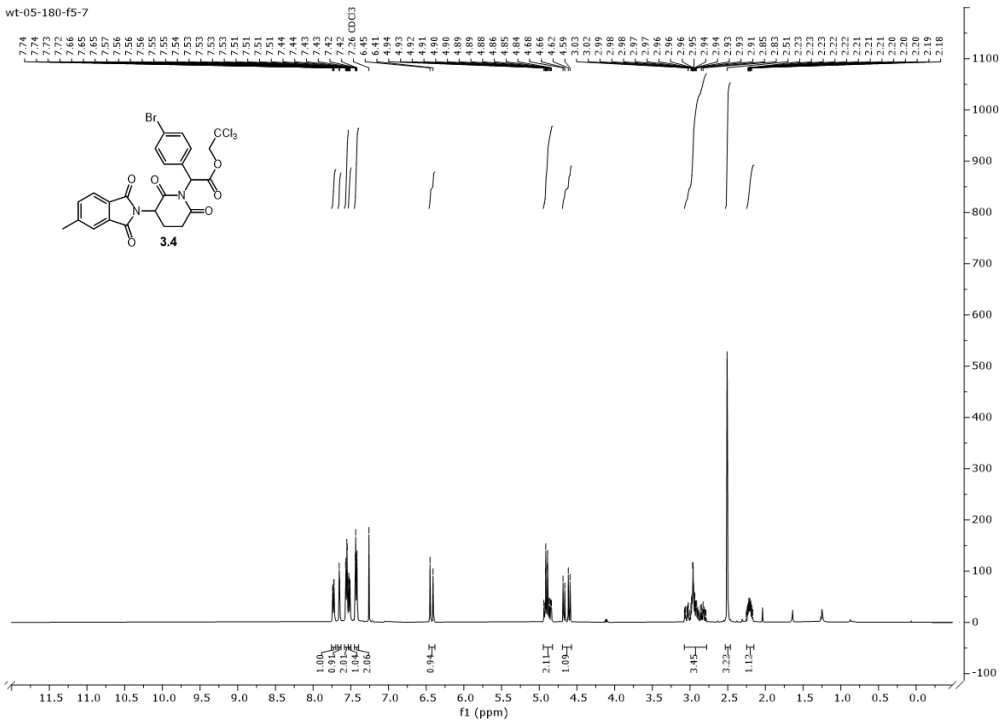

^{1}H NMR (400 MHz) Spectrum for Compound 3.6a.

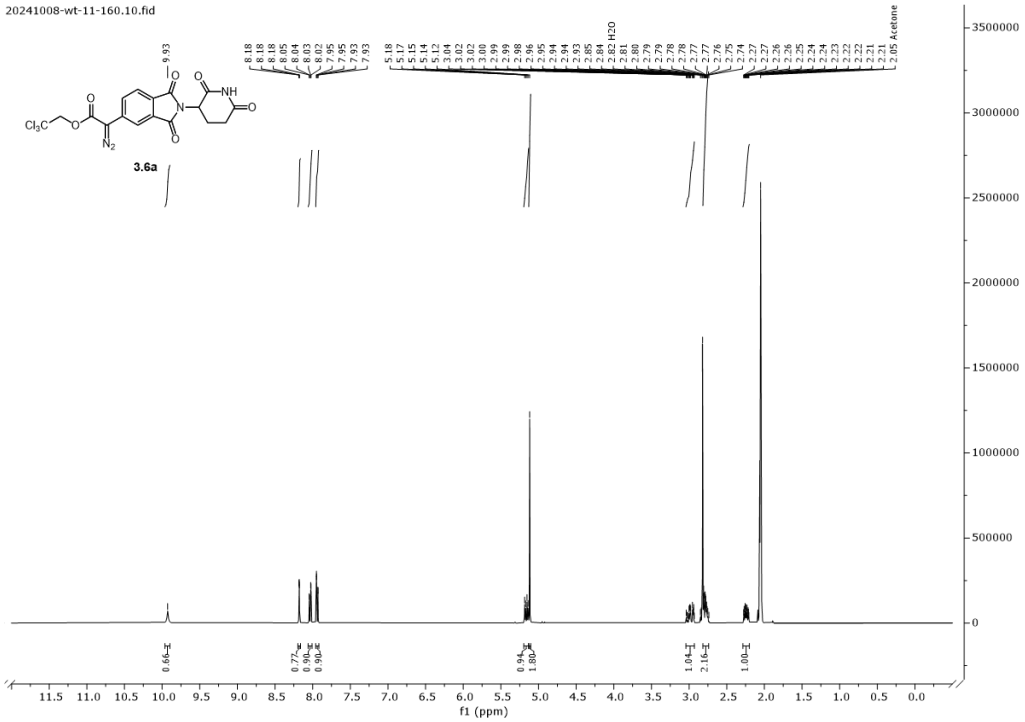

^{1}H NMR (600 MHz) Spectrum for Compound 3.6b.

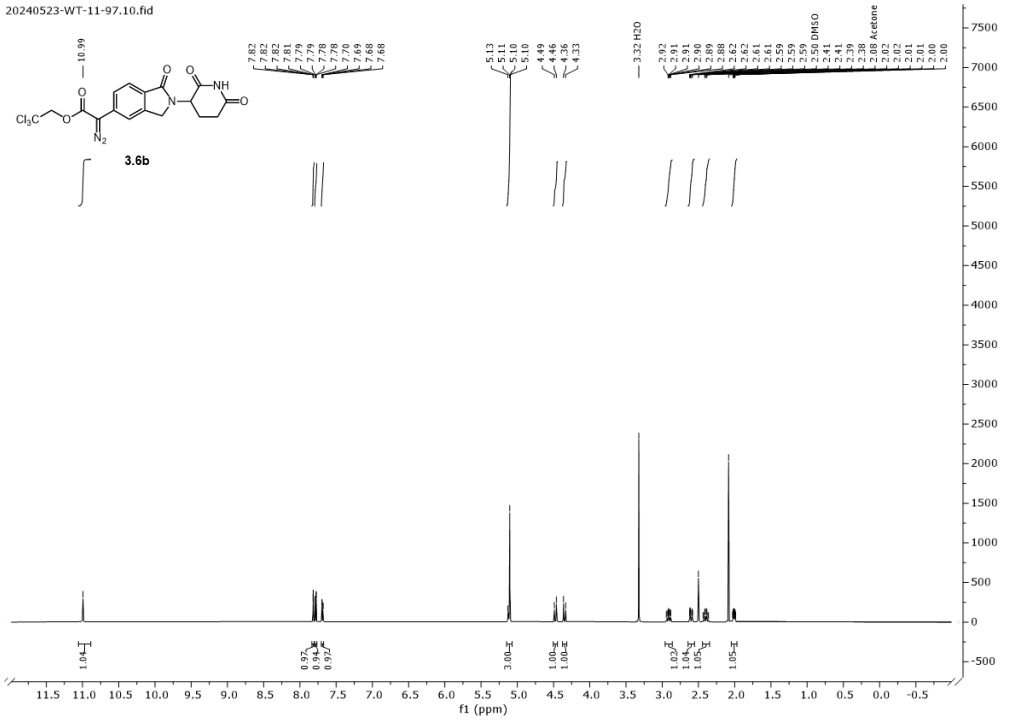

^{1}H NMR (400 MHz) Spectrum for Compound 3.6c.

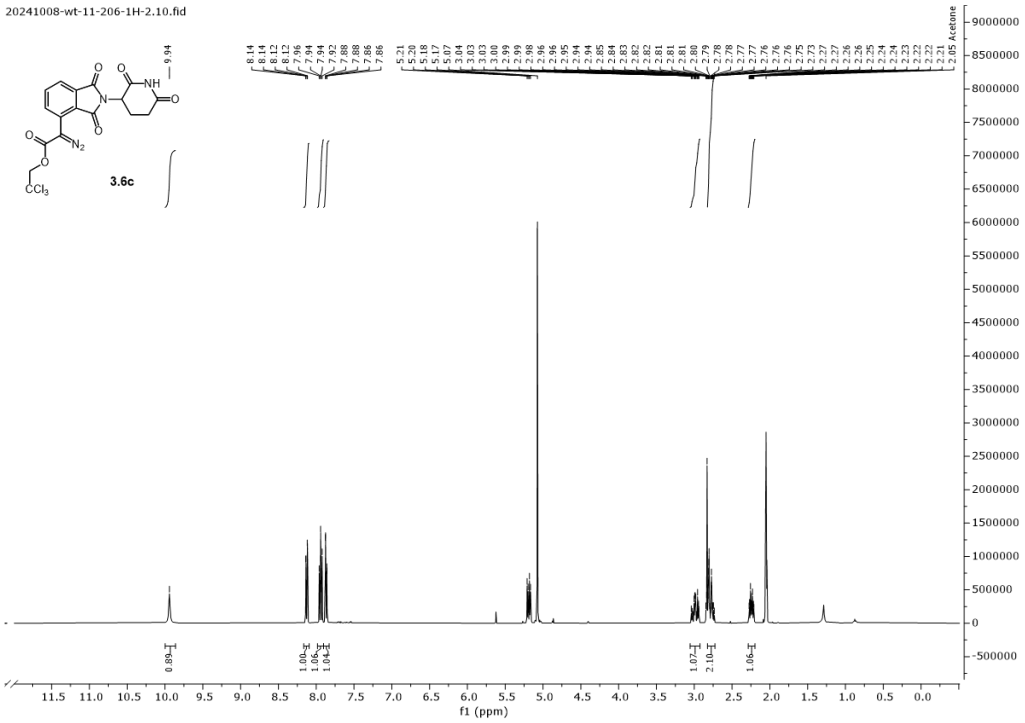

^{1}H NMR (400 MHz) Spectrum for Compound 3.8a.

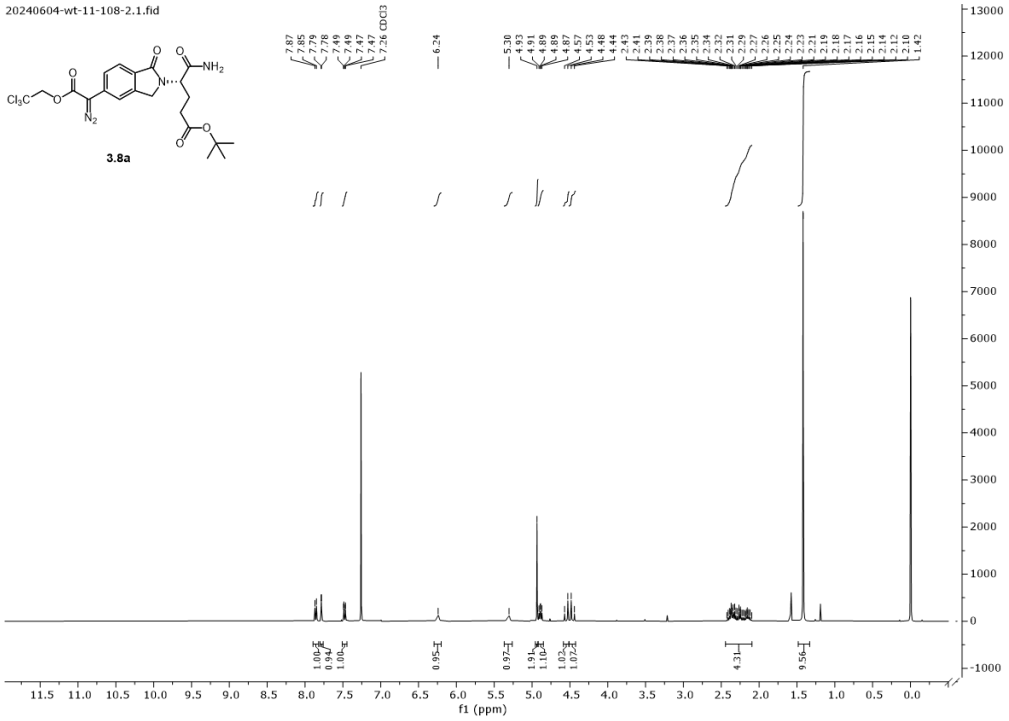

^{1}H NMR (400 MHz) Spectrum for Compound 3.8b.

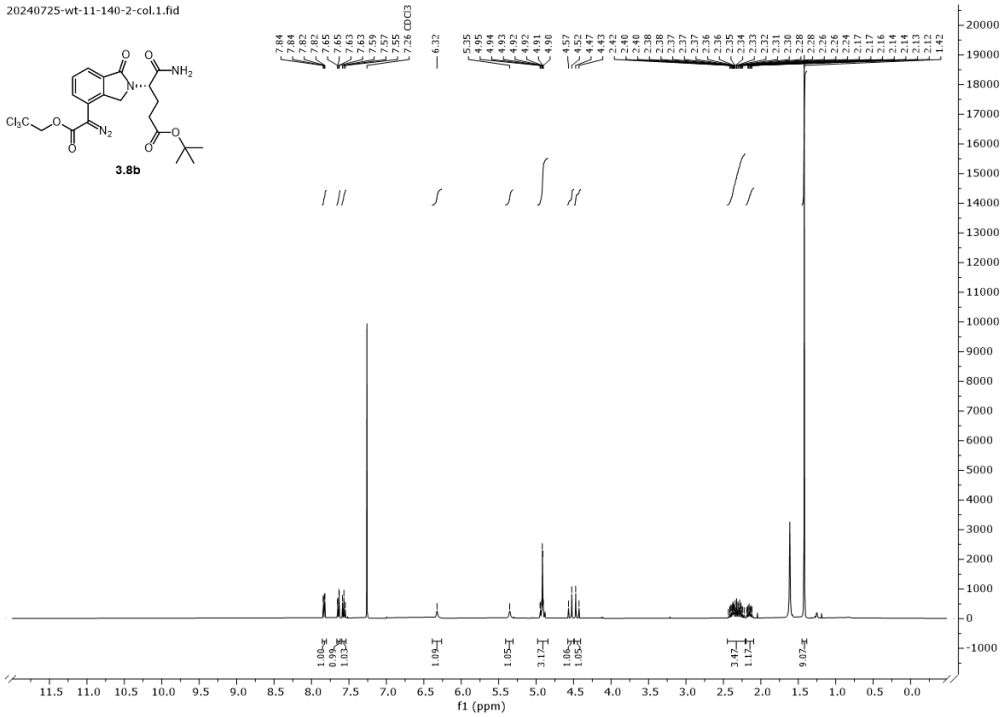

^{1}H NMR (400 MHz) Spectrum for Compound 3.9a.

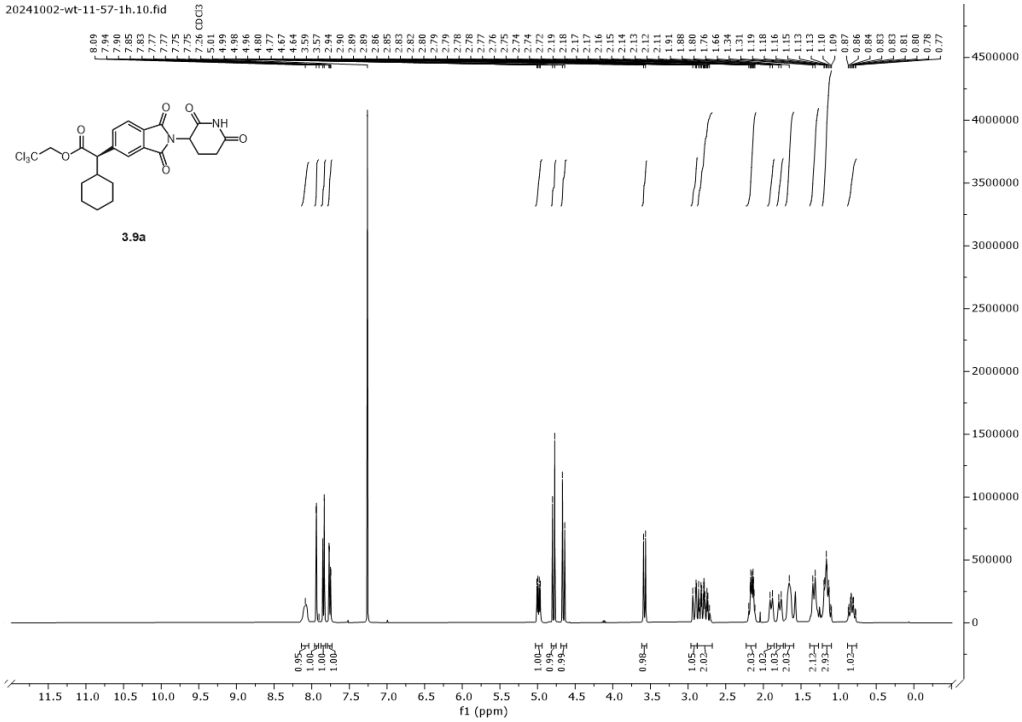

^{1}H NMR (400 MHz) Spectrum for Compound 3.9b.

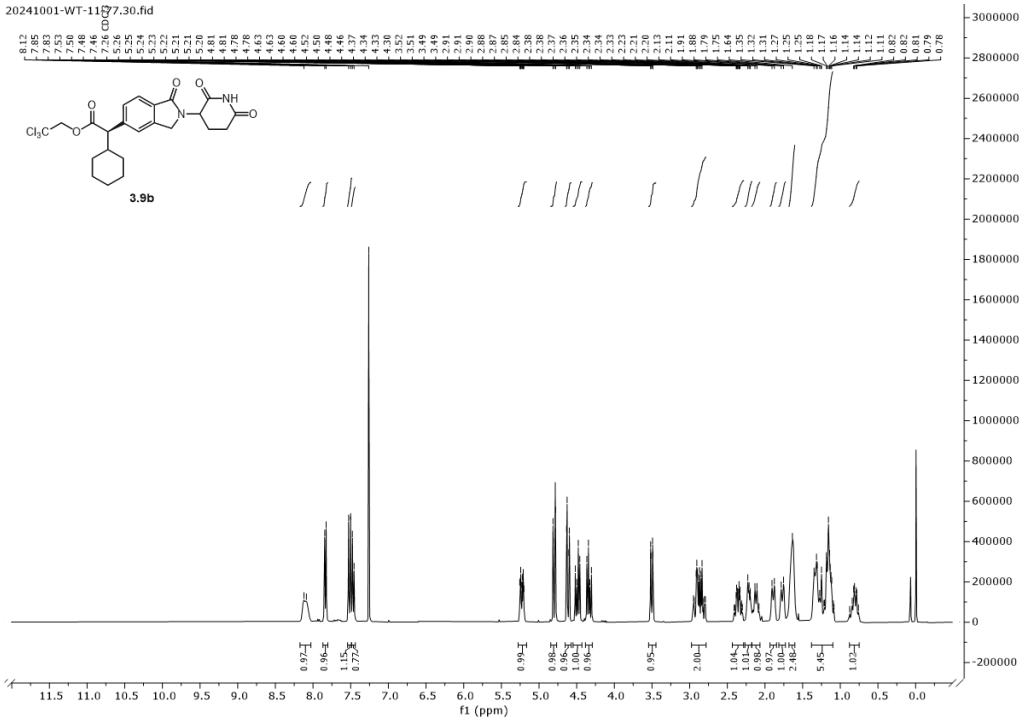

^{1}H NMR (600 MHz) Spectrum for Compound 3.9c.

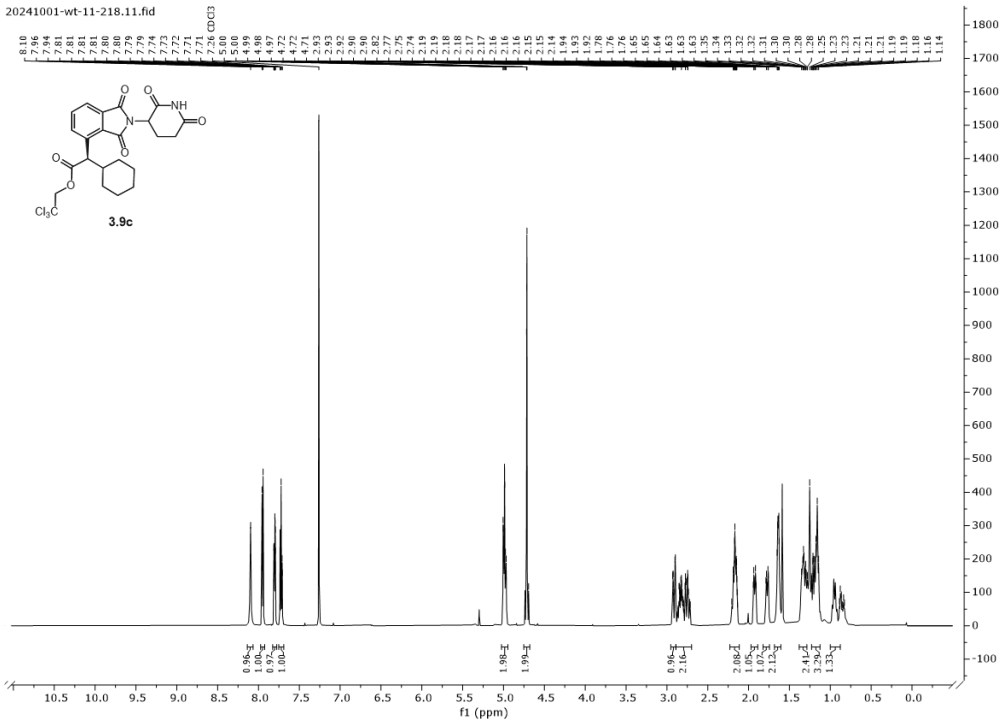

^{1}H NMR (600 MHz) Spectrum for Compound (*S*,*R*)-3.10a.

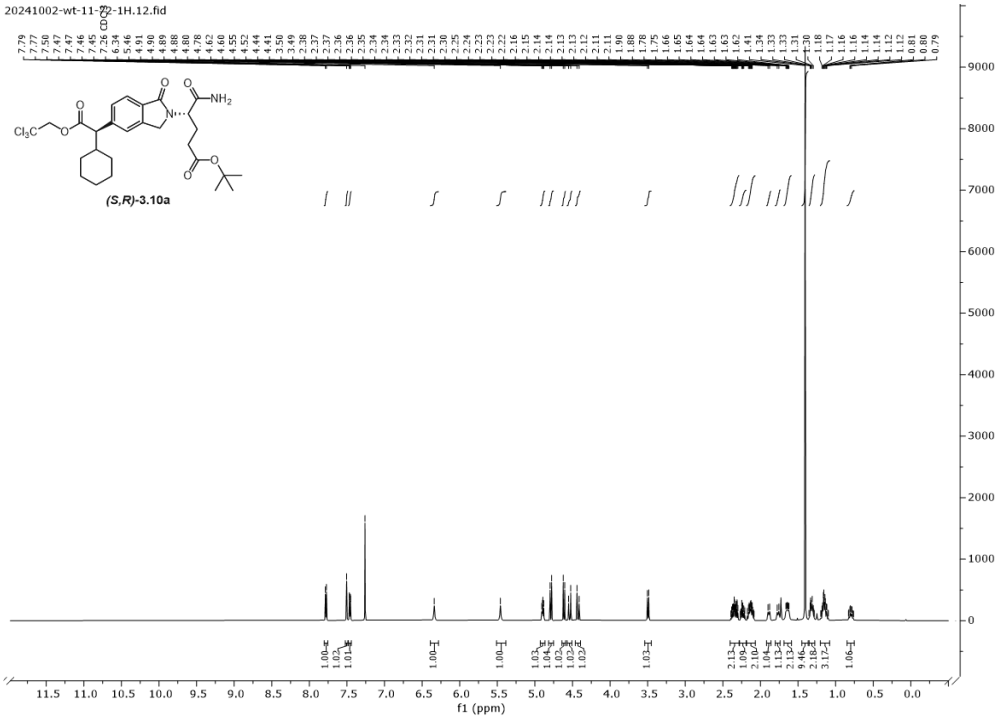

^{1}H NMR (400 MHz) Spectrum for Compound (*S*,*S*)-3.10a.

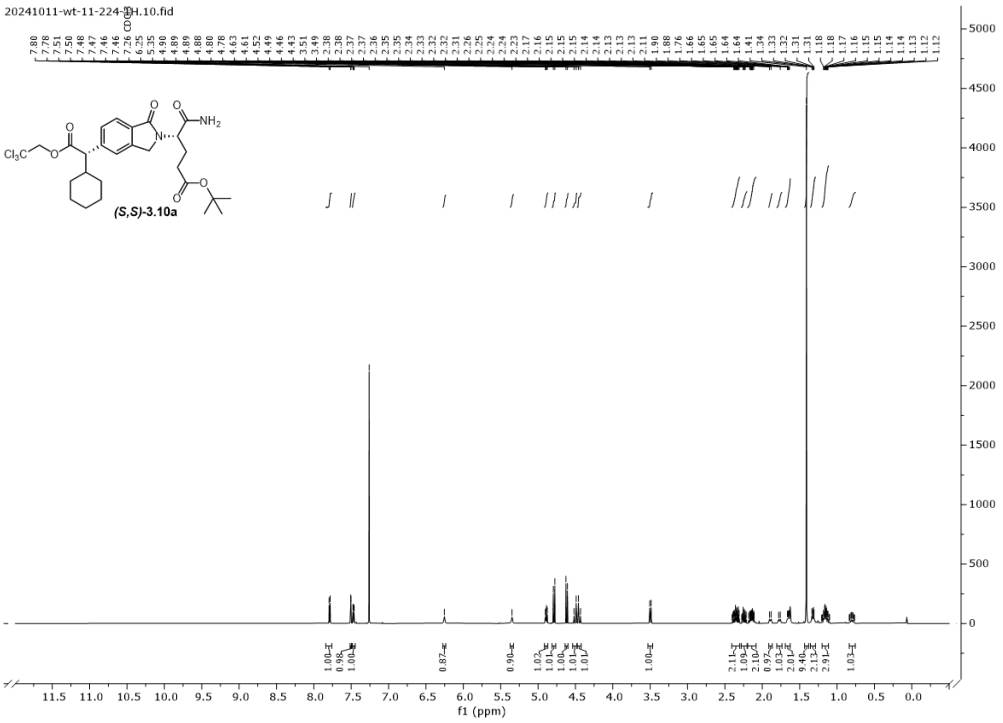

^{1}H NMR (400 MHz) Spectrum for Compound 3.10b.

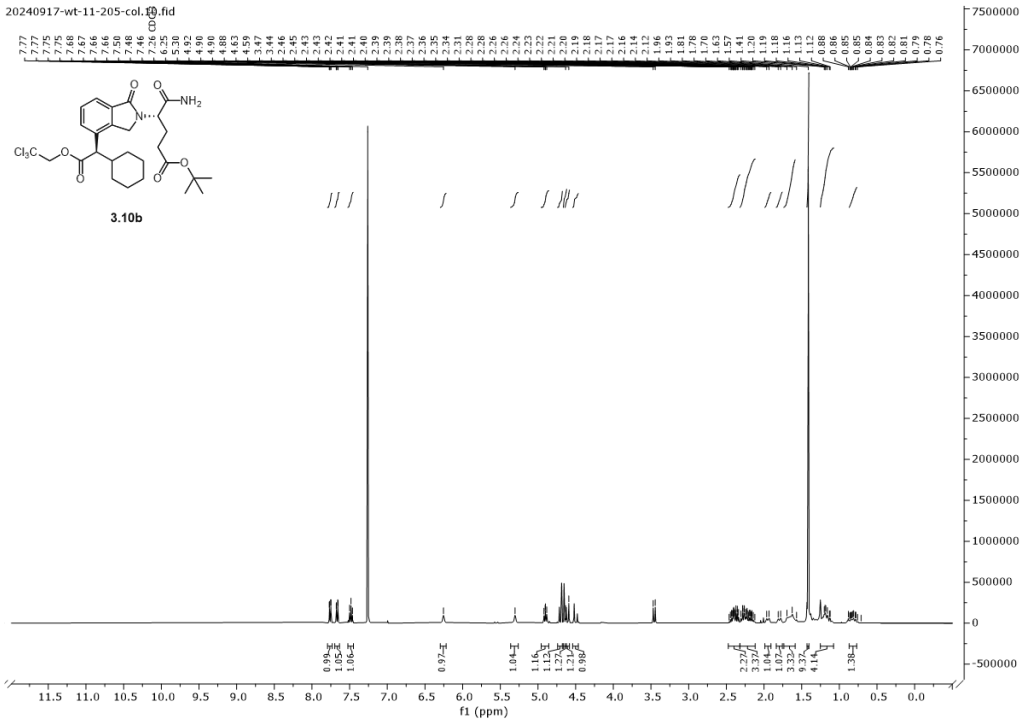

^{1}H NMR (400 MHz) Spectrum for Compound 3.11a.

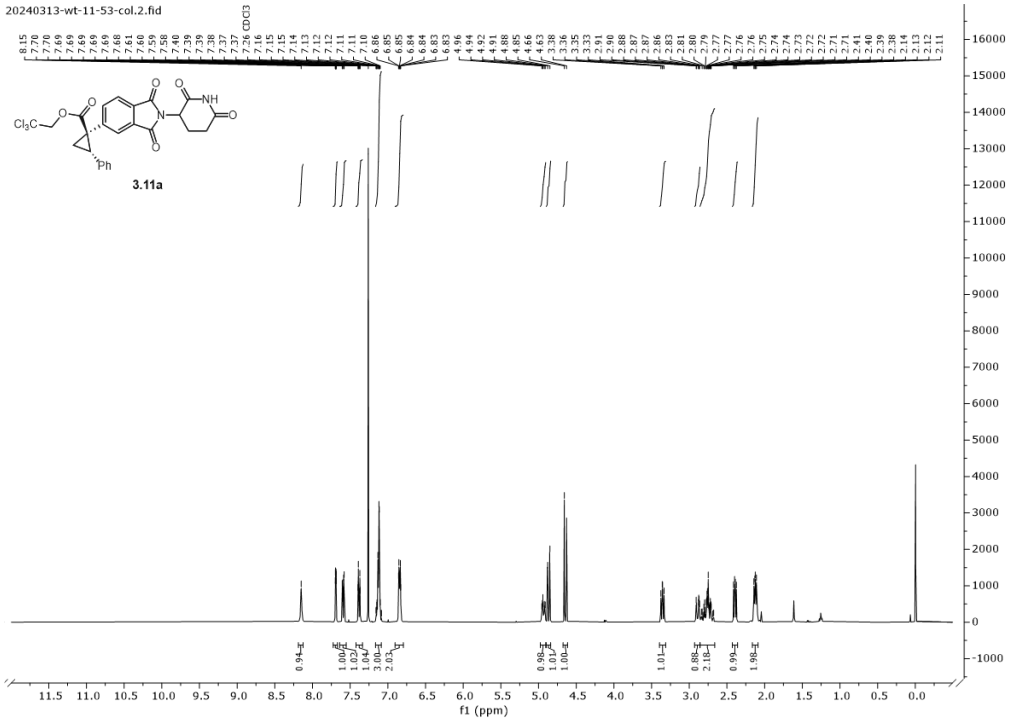

^{1}H NMR (600 MHz) Spectrum for Compound 3.11b.

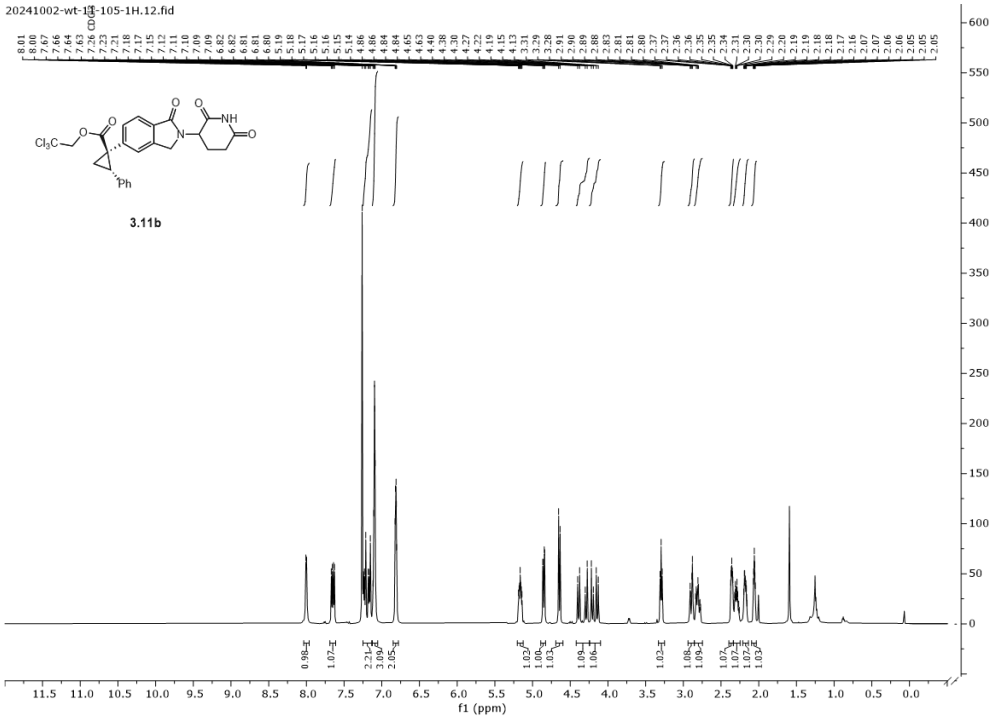

^{1}H NMR (400 MHz) Spectrum for Compound 3.11c.

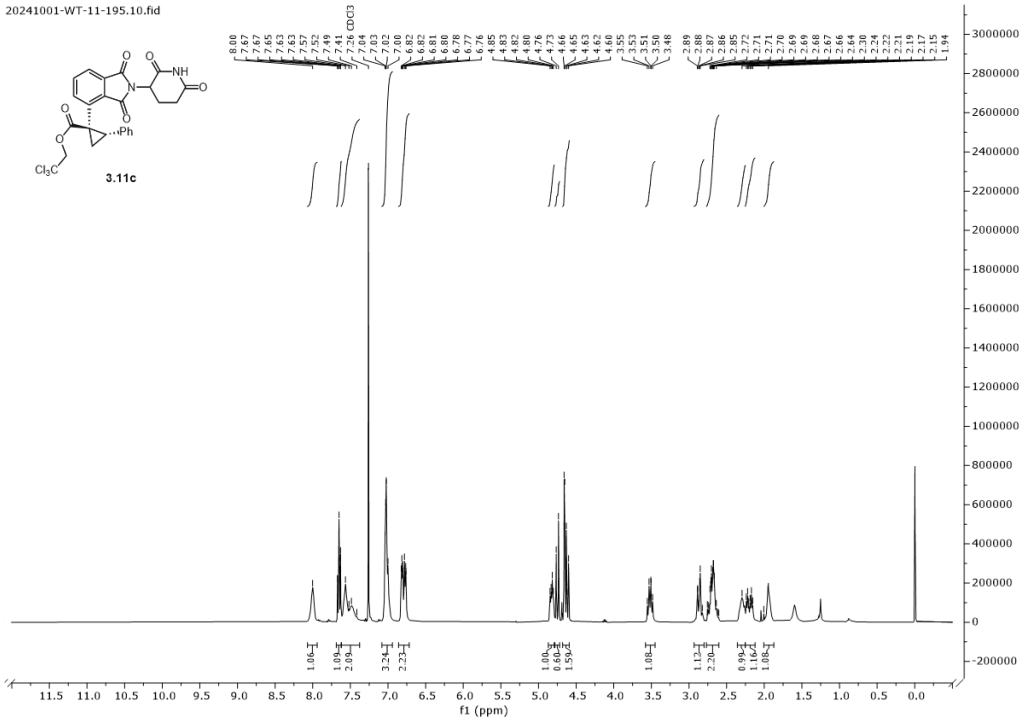

^{1}H NMR (400 MHz) Spectrum for Compound 3.12a.

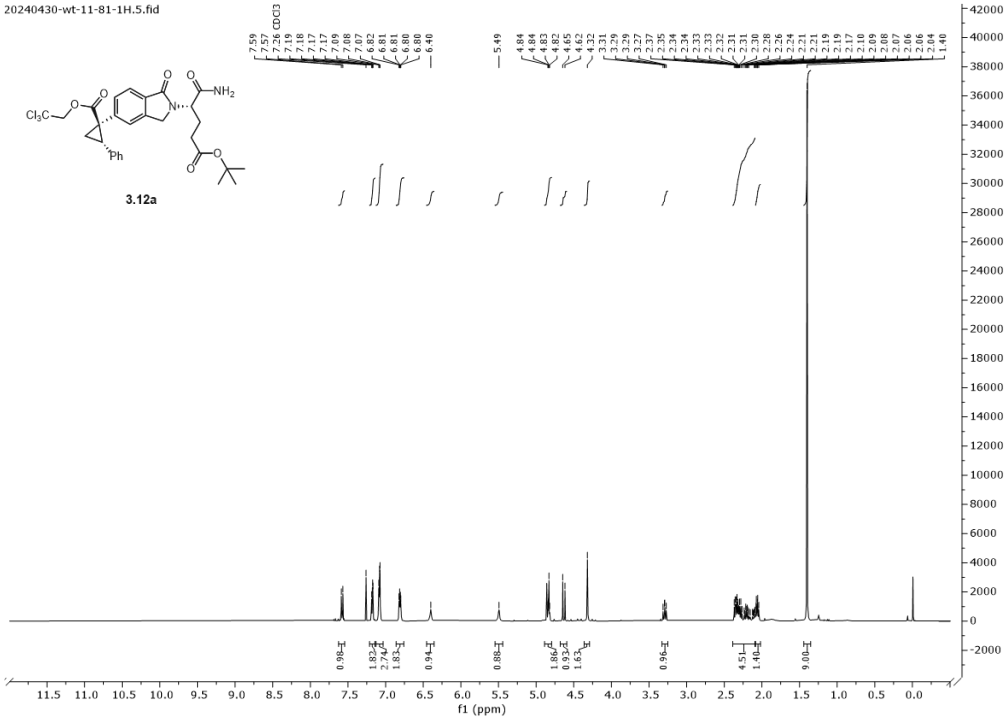

^{1}H NMR (400 MHz) Spectrum for Compound 3.12b.

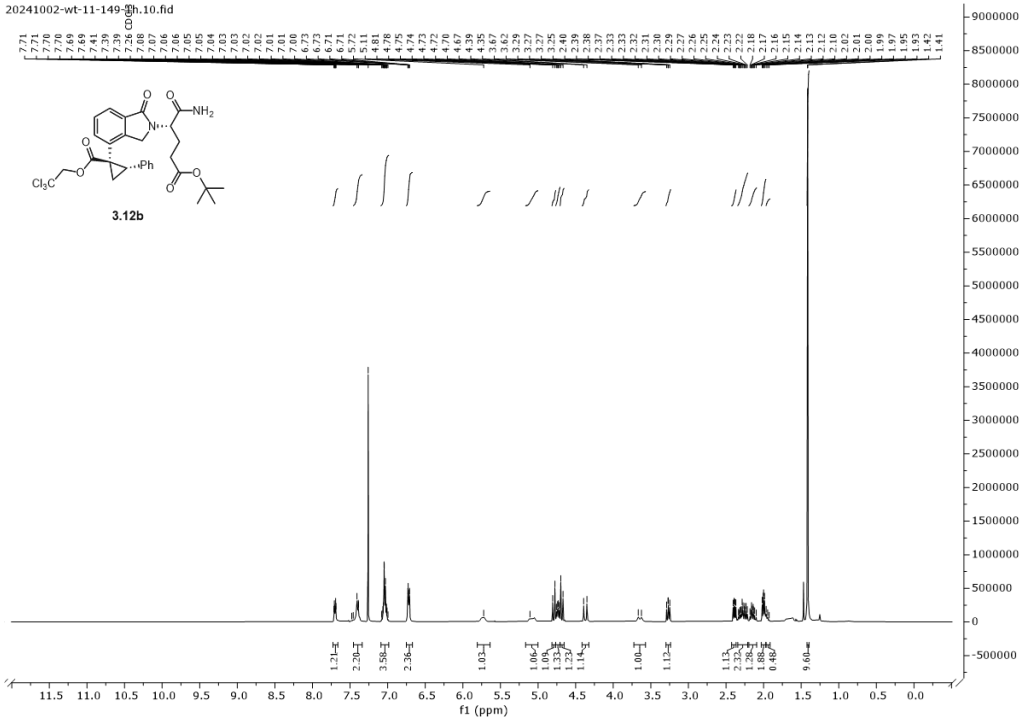

^{1}H NMR (400 MHz) Spectrum for Compound 3.13.

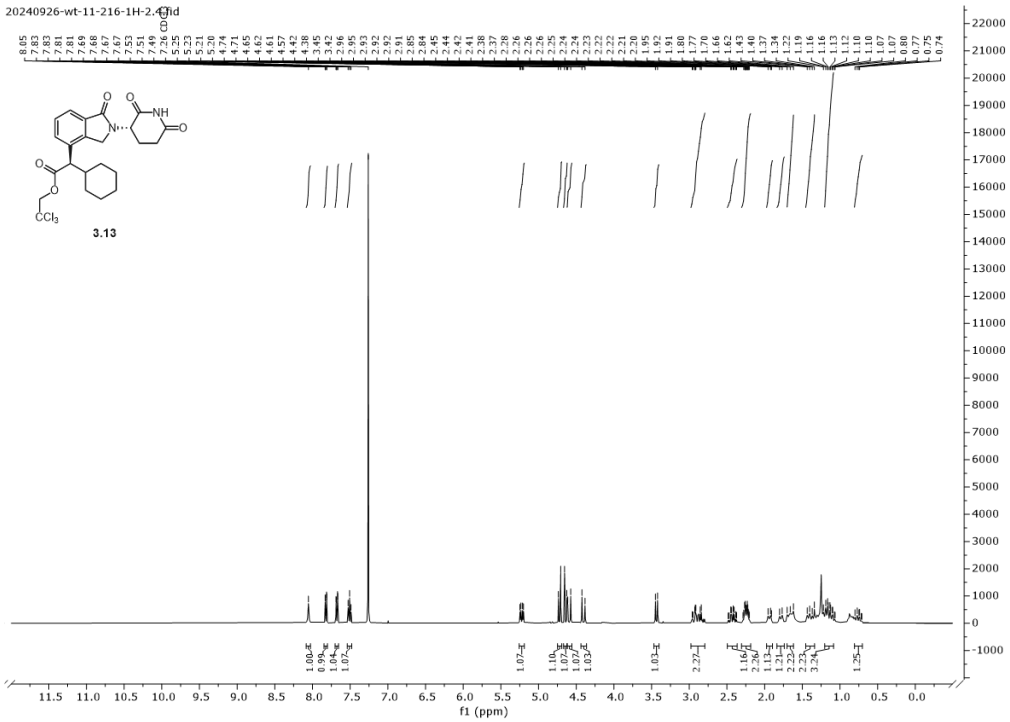

^{1}H NMR (600 MHz) Spectrum for Compound 3.14.

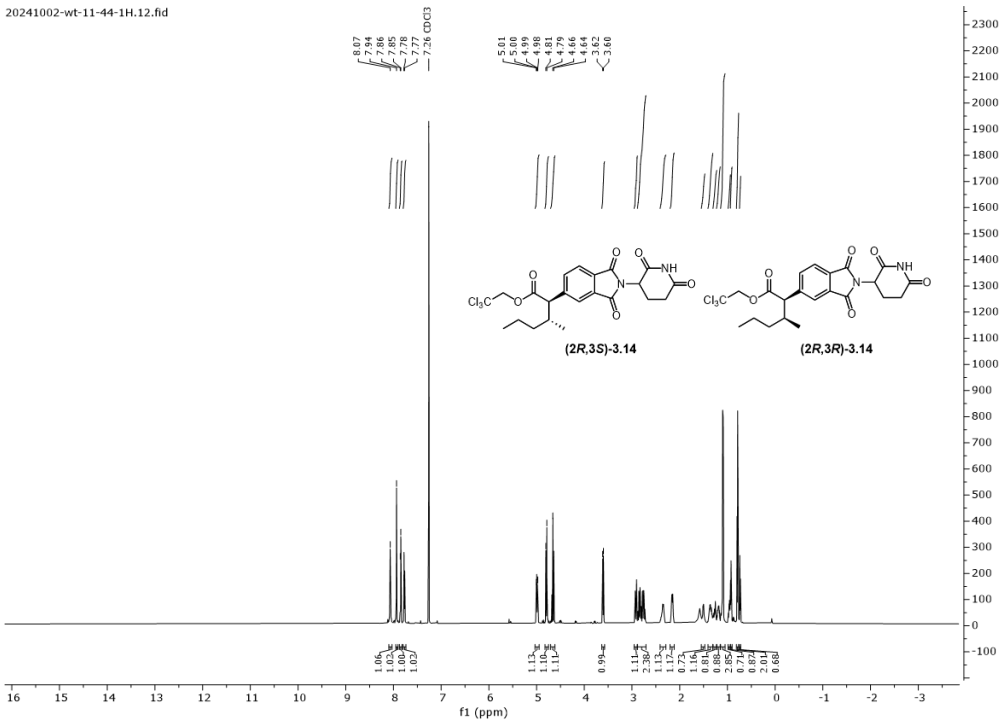

^{1}H NMR (400 MHz) Spectrum for Compound 3.15.

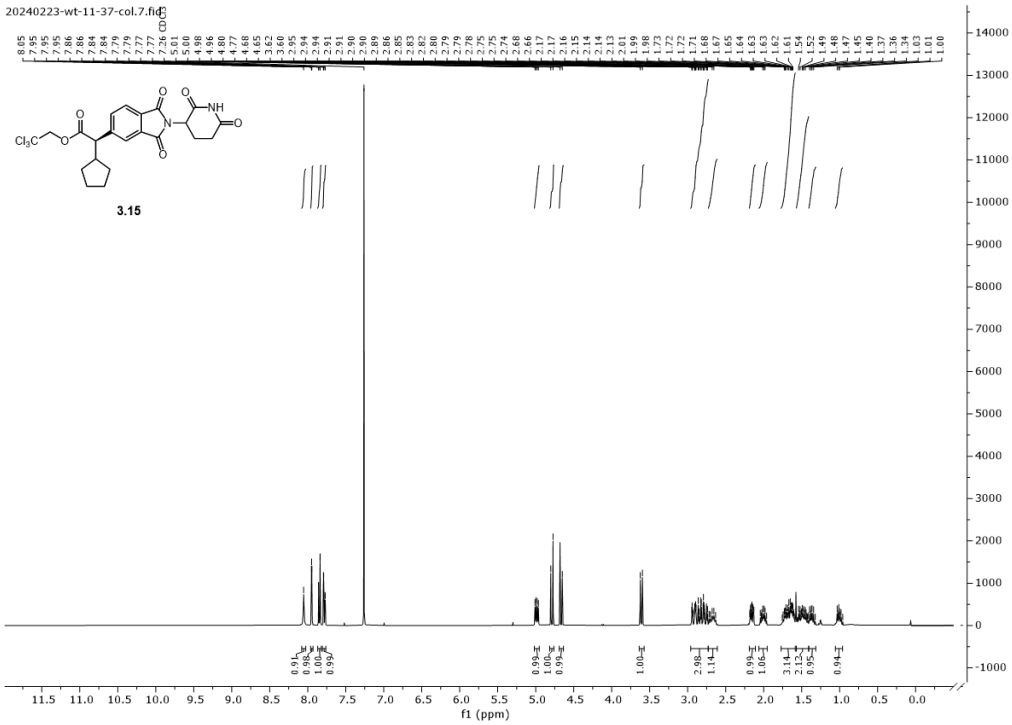

^{1}H NMR (400 MHz) Spectrum for Compound 3.16.

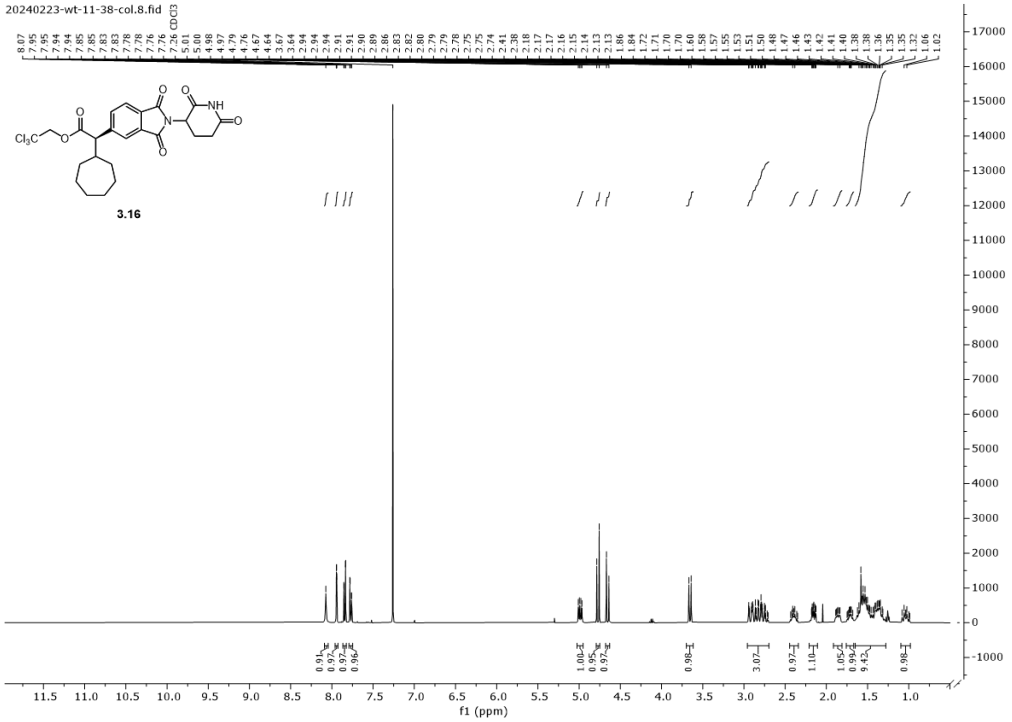

^{1}H NMR (600 MHz) Spectrum for Compound 3.17.

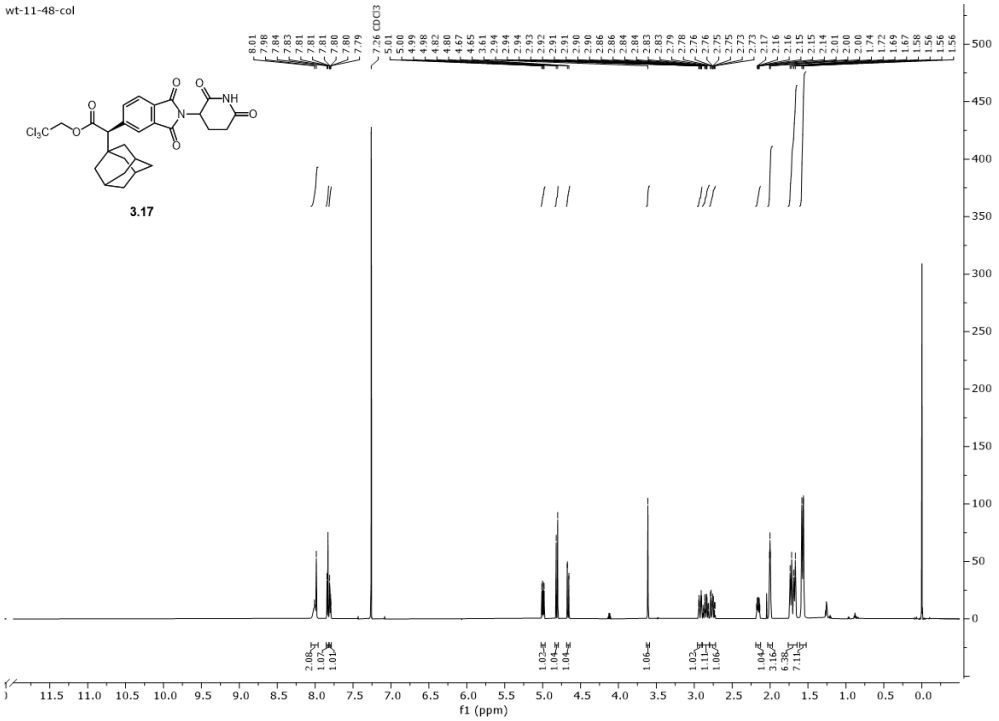

^{1}H NMR (400 MHz) Spectrum for Compound 3.18.

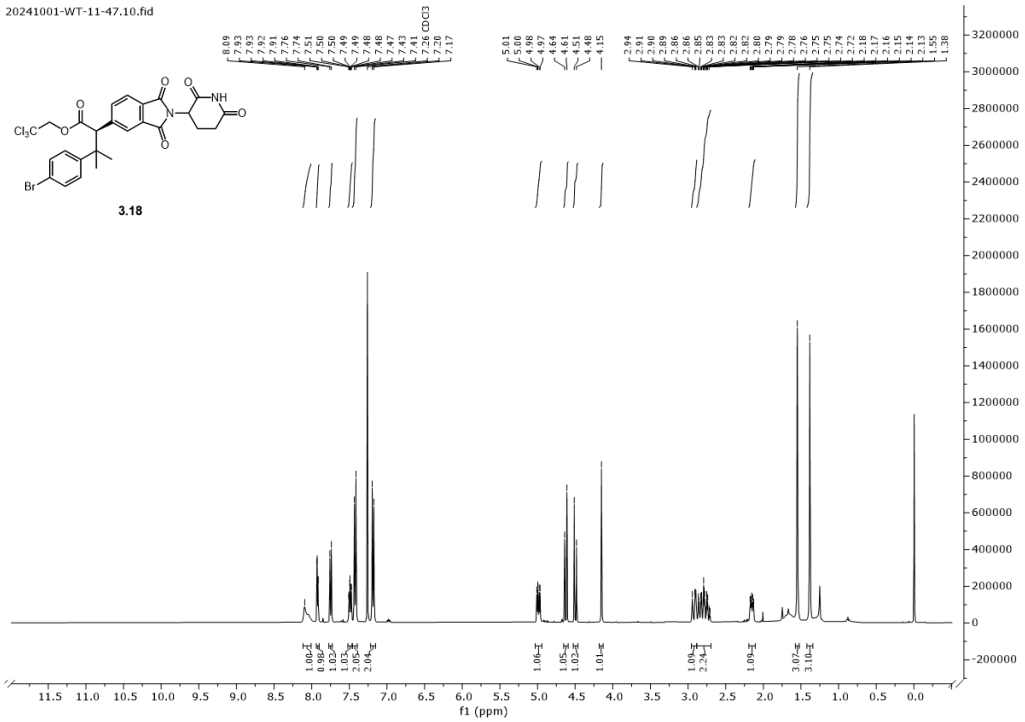

^{1}H NMR (400 MHz) Spectrum for Compound 3.19.

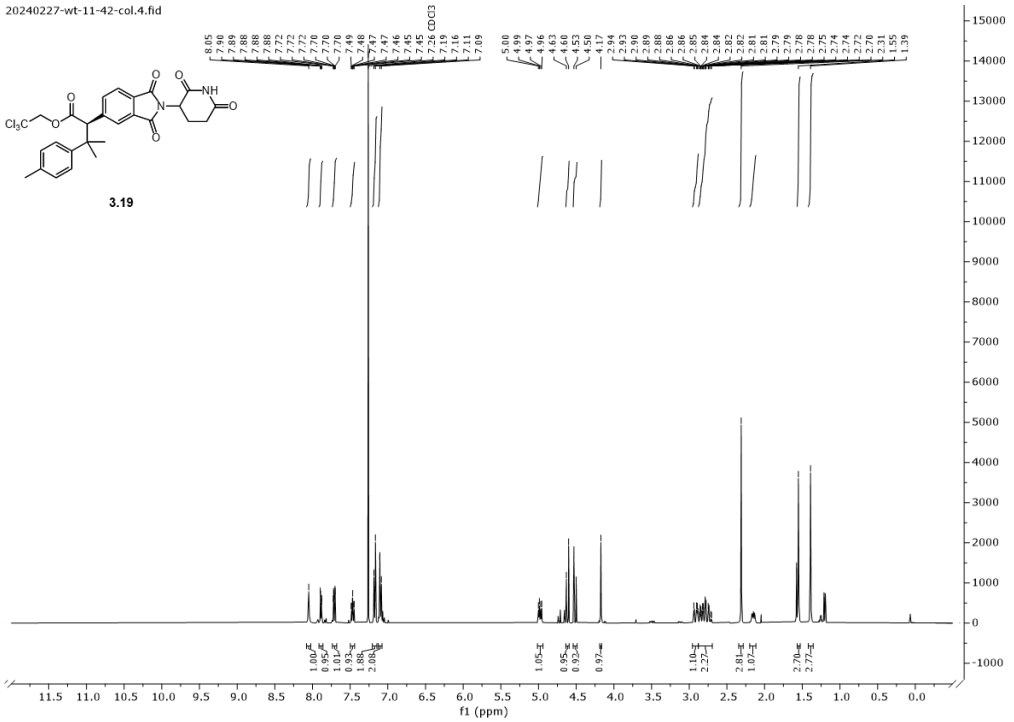

^{1}H NMR (400 MHz) Spectrum for Compound 3.20.

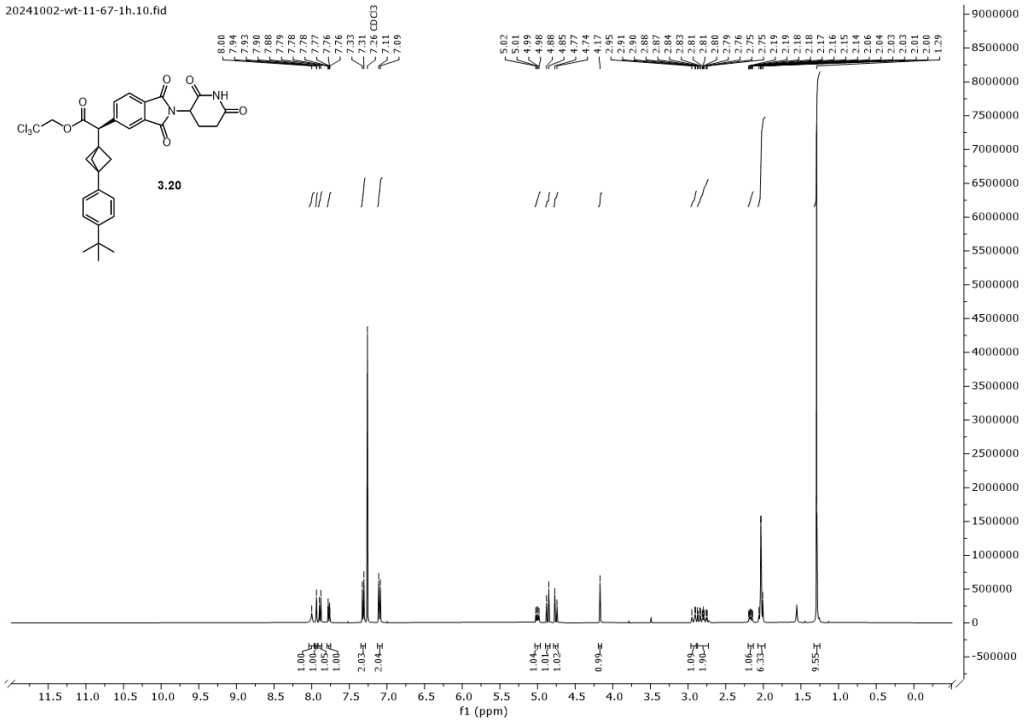

^{1}H NMR (600 MHz) Spectrum for Compound 3.21.

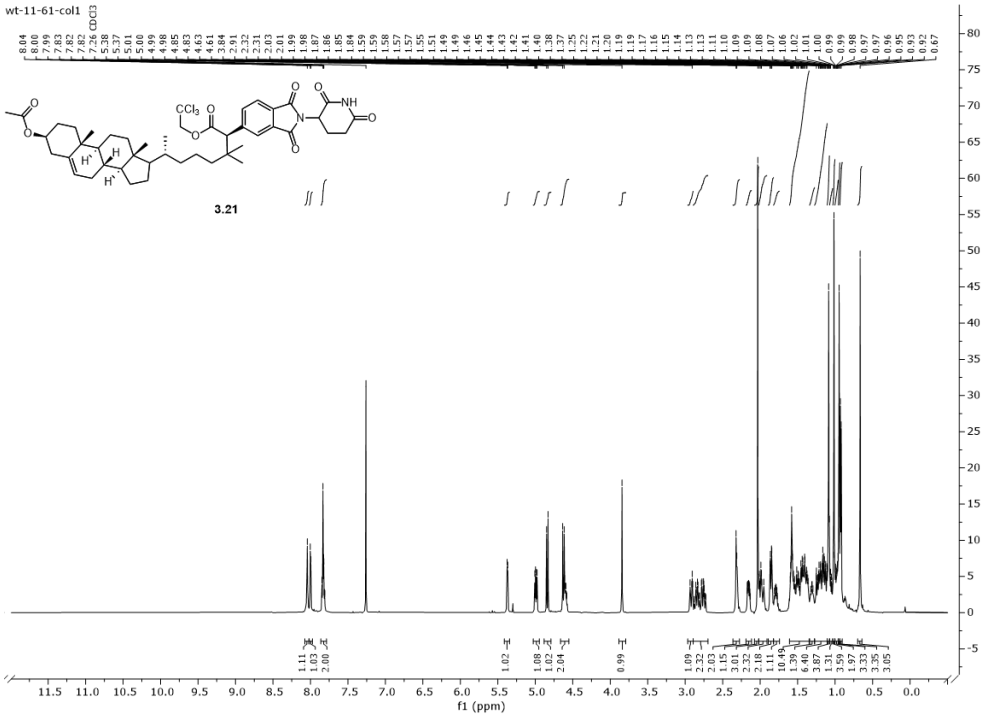

^{1}H NMR (400 MHz) Spectrum for Compound 3.22.

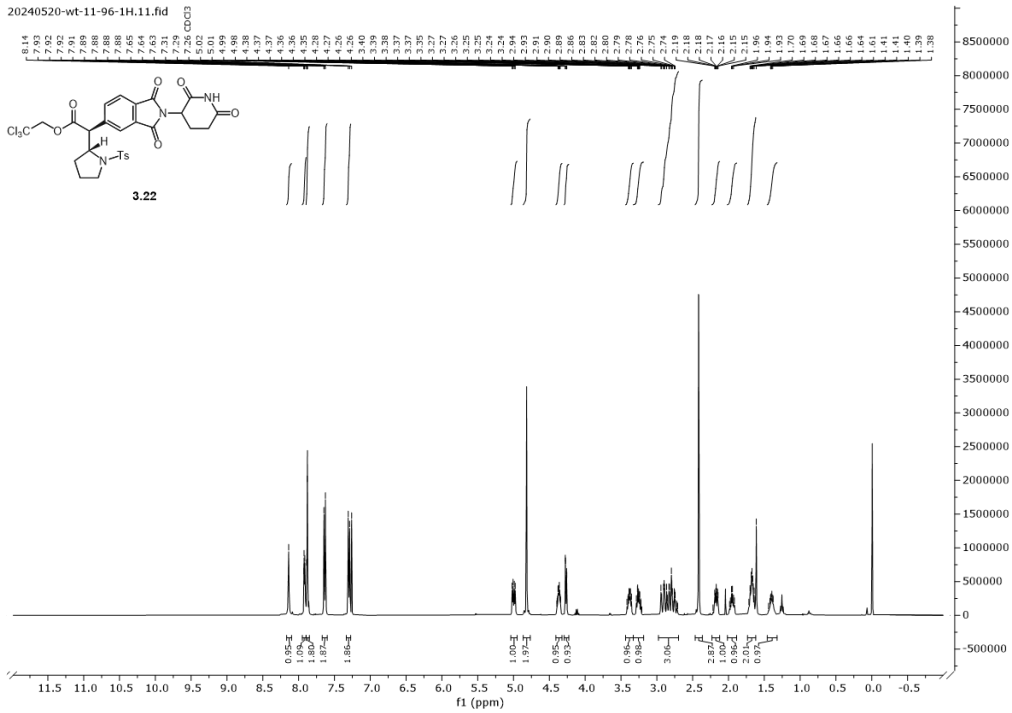

^{1}H NMR (400 MHz) Spectrum for Compound 3.23.

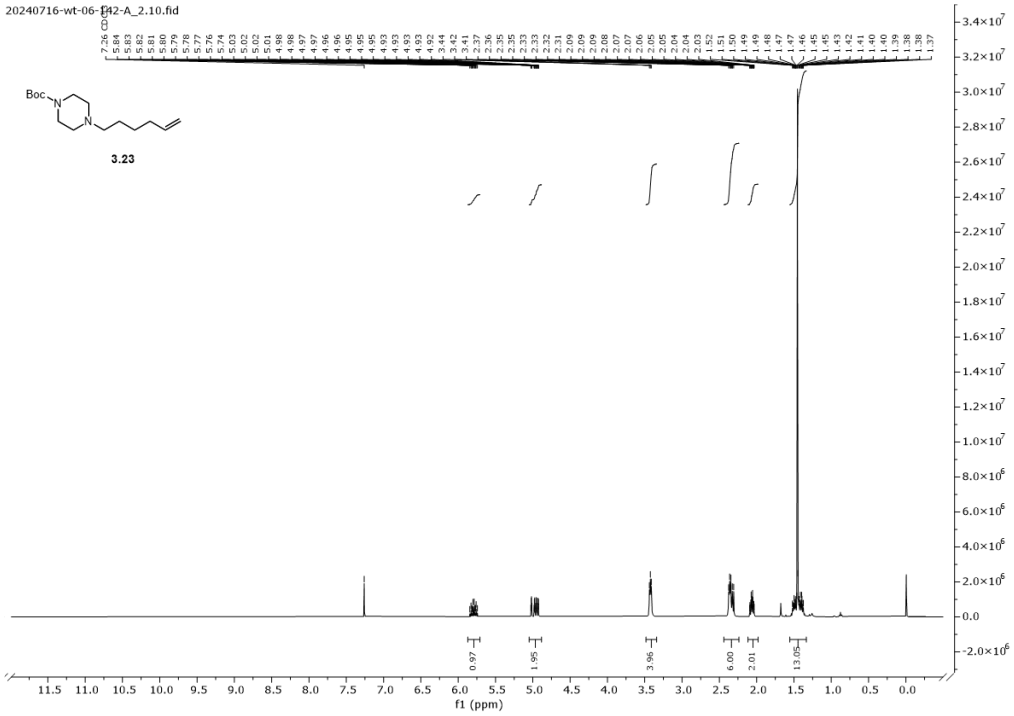

^{1}H NMR (400 MHz) Spectrum for Compound 3.24.

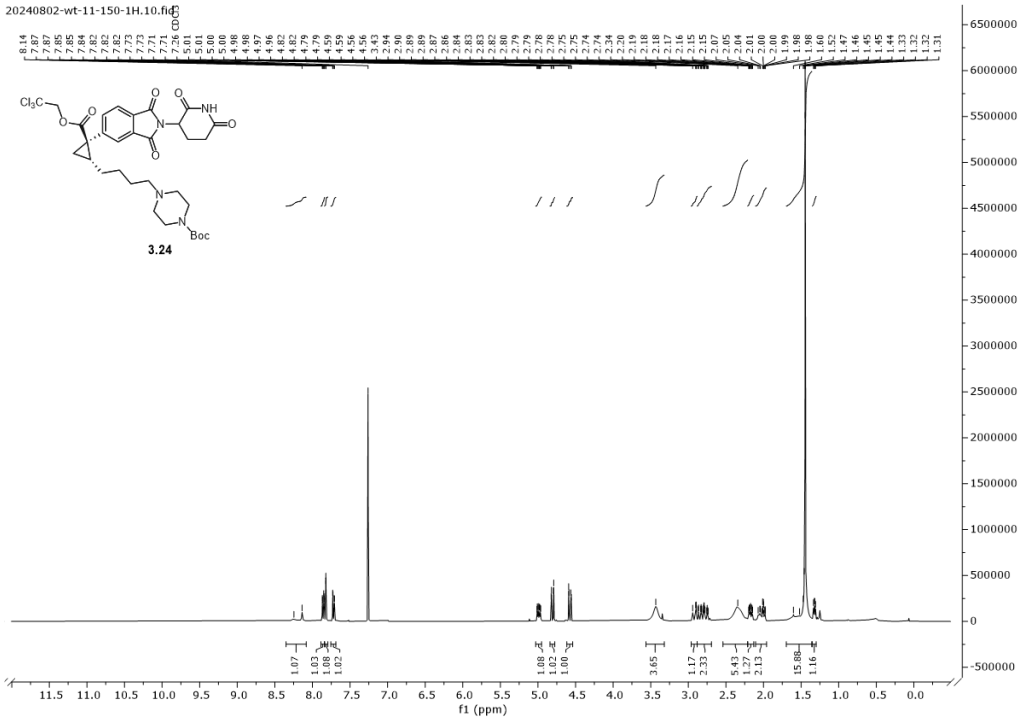

^{1}H NMR (800 MHz) Spectrum for Compound 3.25 at 23 °C.

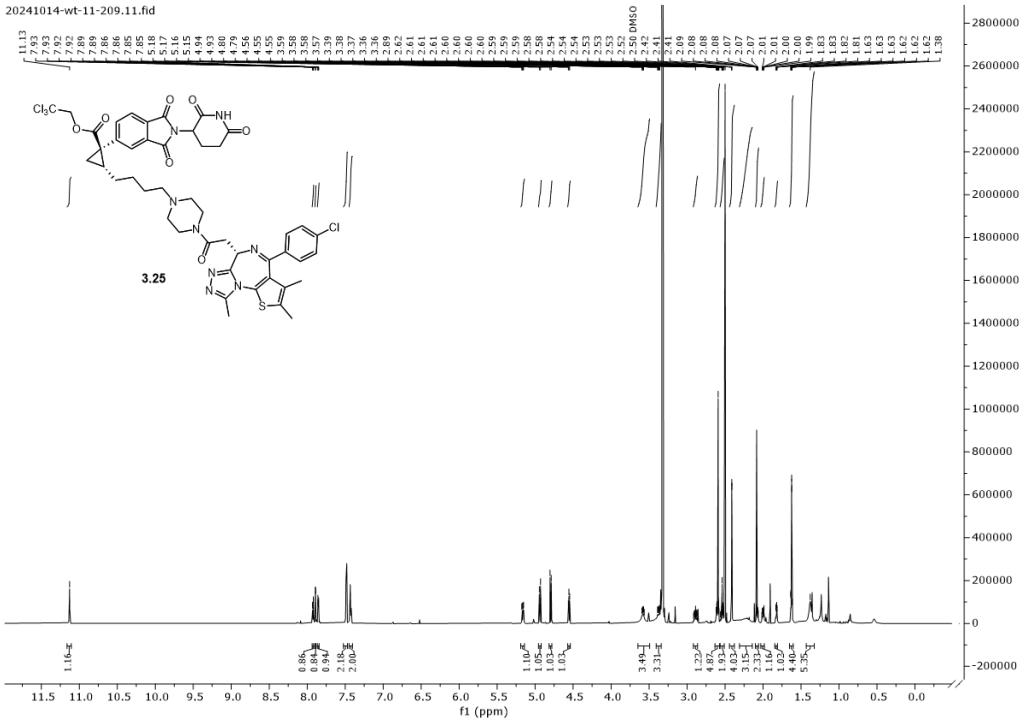

^{1}H NMR (800 MHz) Spectrum for Compound 3.25 at 80 °C.

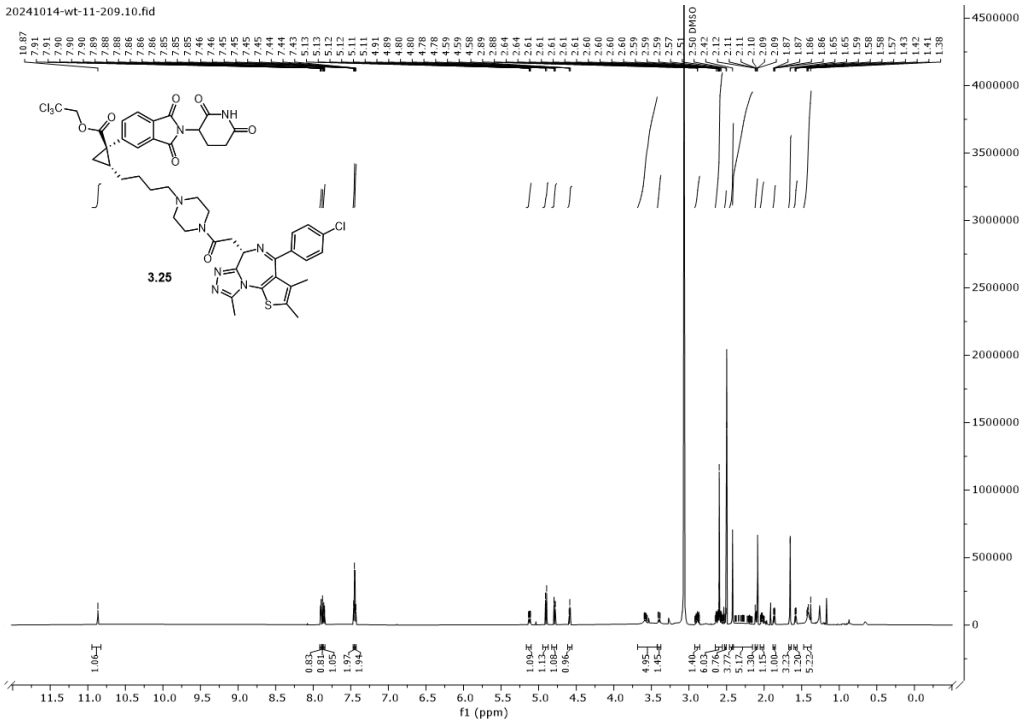

^{1}H NMR (800 MHz) Spectrum for Compound 3.26 at 23 °C.

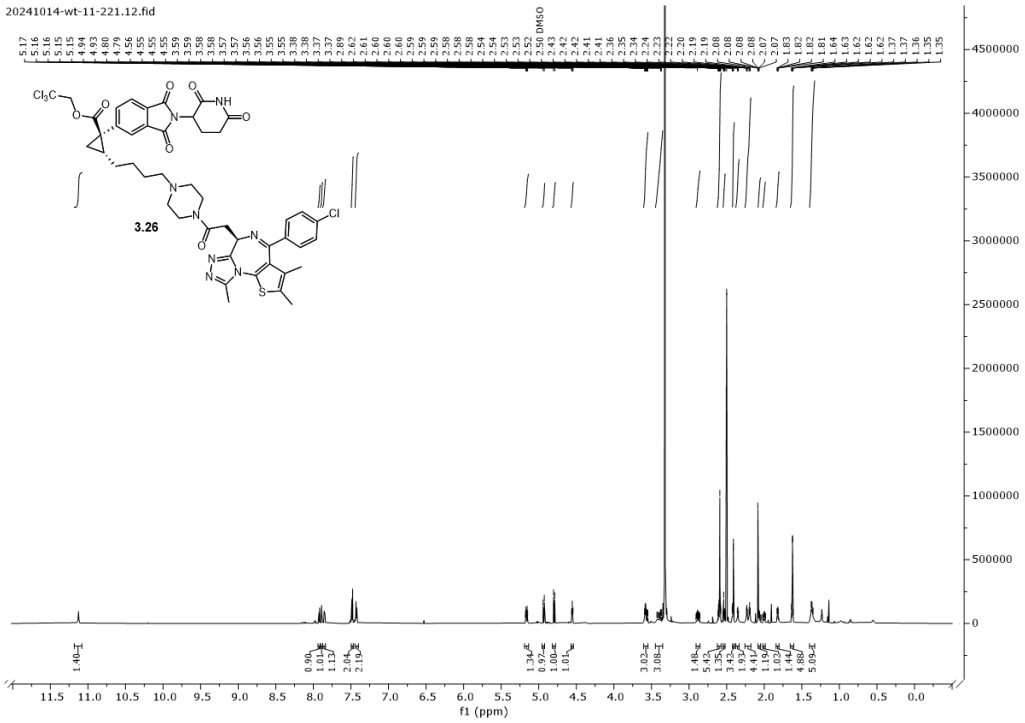

^{1}H NMR (800 MHz) Spectrum for Compound 3.26 at 80 °C.

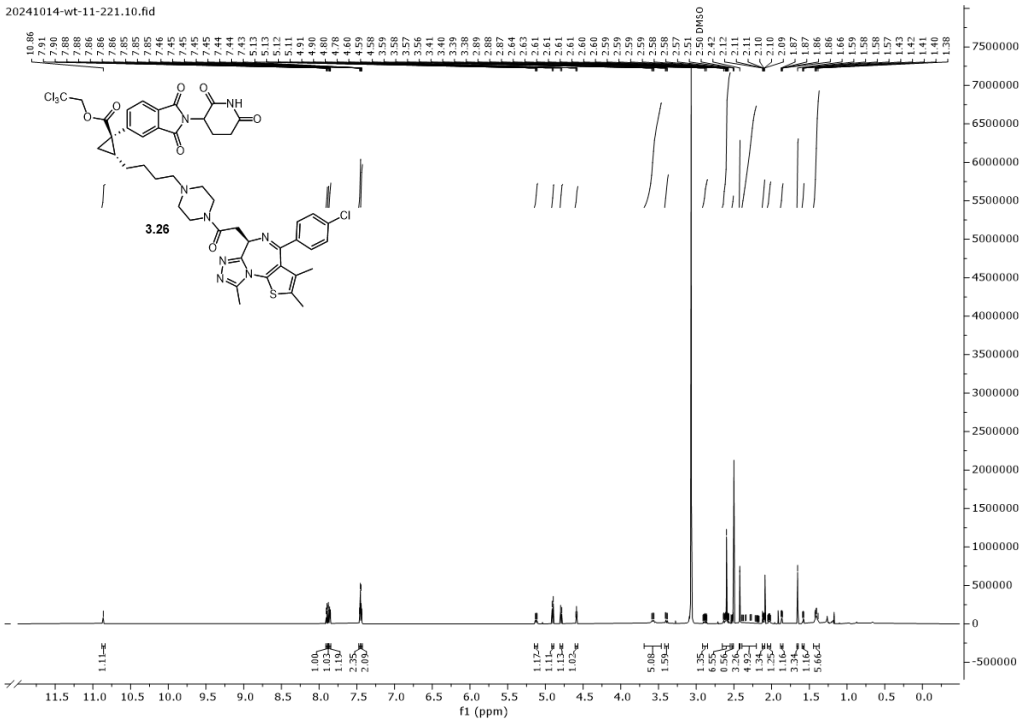

^{1}H NMR (600 MHz) Spectrum for Compound SI2.

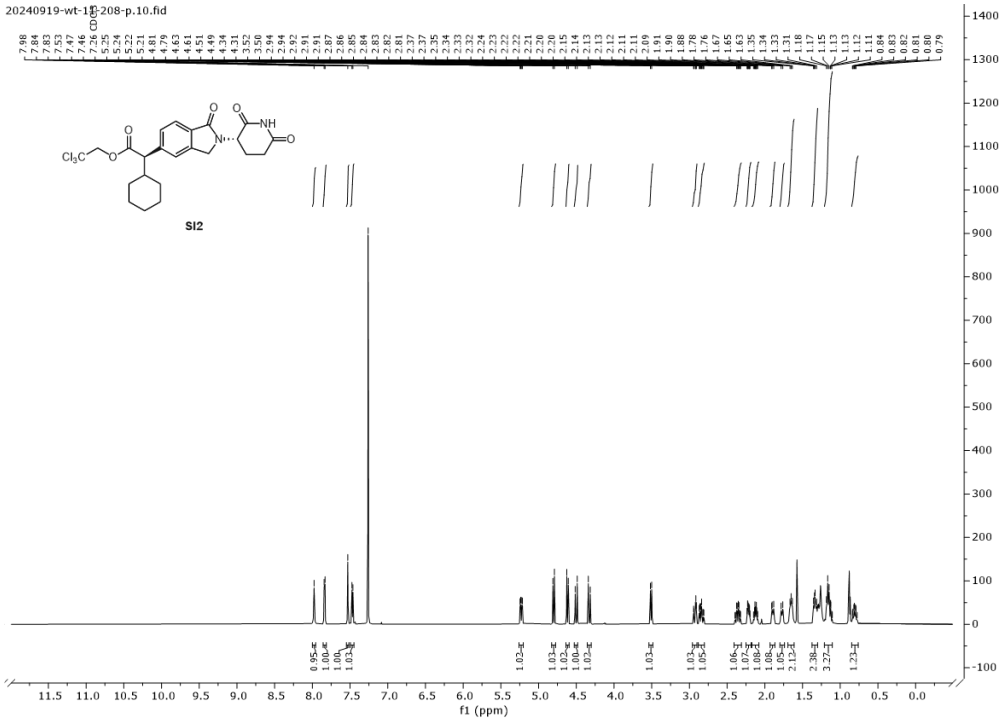

^{1}H NMR (400 MHz) Spectrum for Compound SI3.

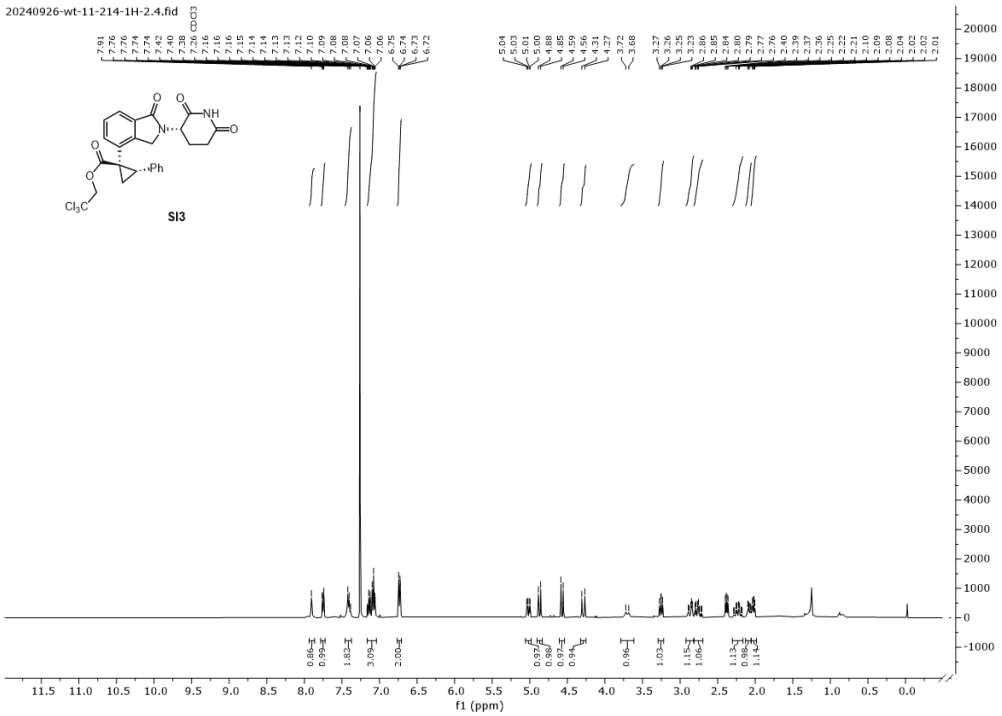

^{1}H NMR (400 MHz) Spectrum for Compound SI4.

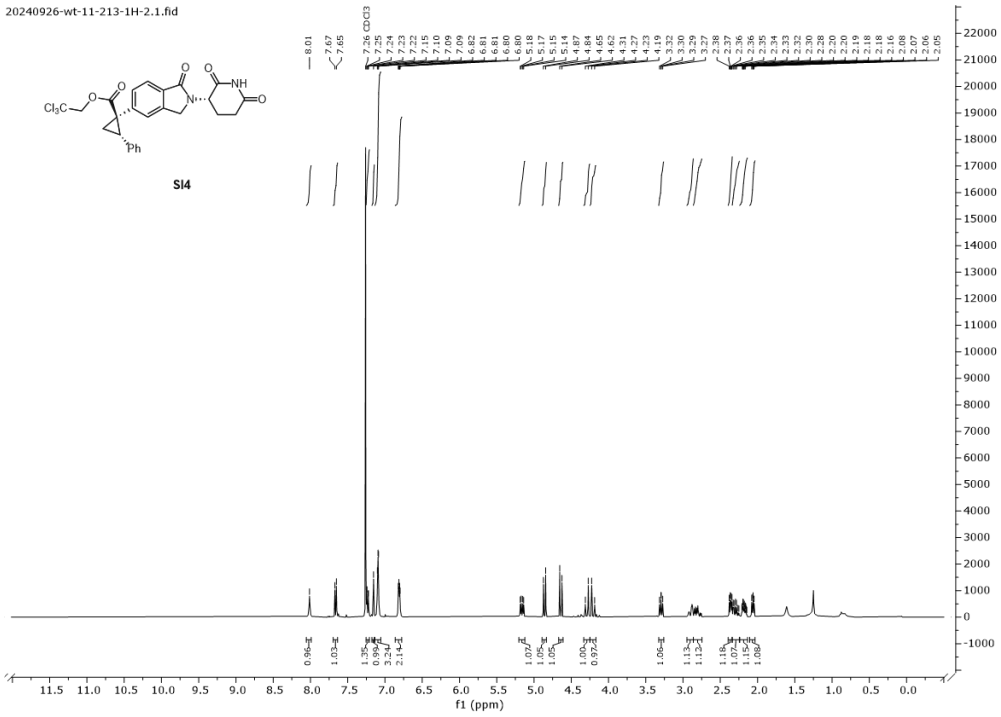

^{13}C NMR Spectra
^{13}C{^{1}H} (151 MHz) Spectrum for Compound 3.4.

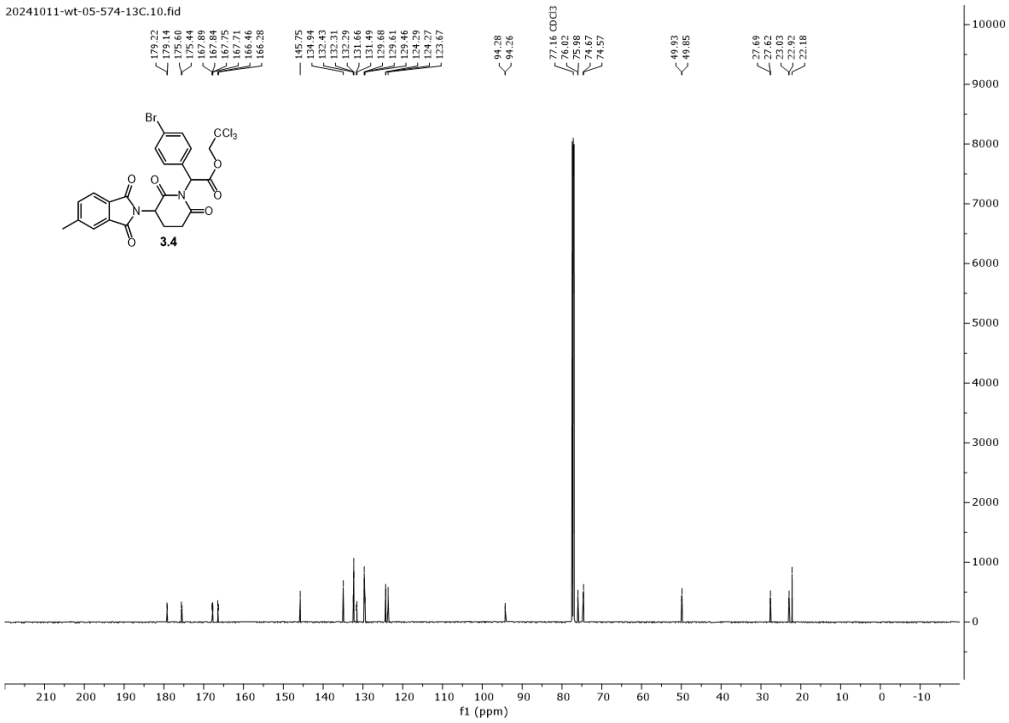

$^{13}C\{^{1}H\}$ (151 MHz) Spectrum for Compound 3.6a.

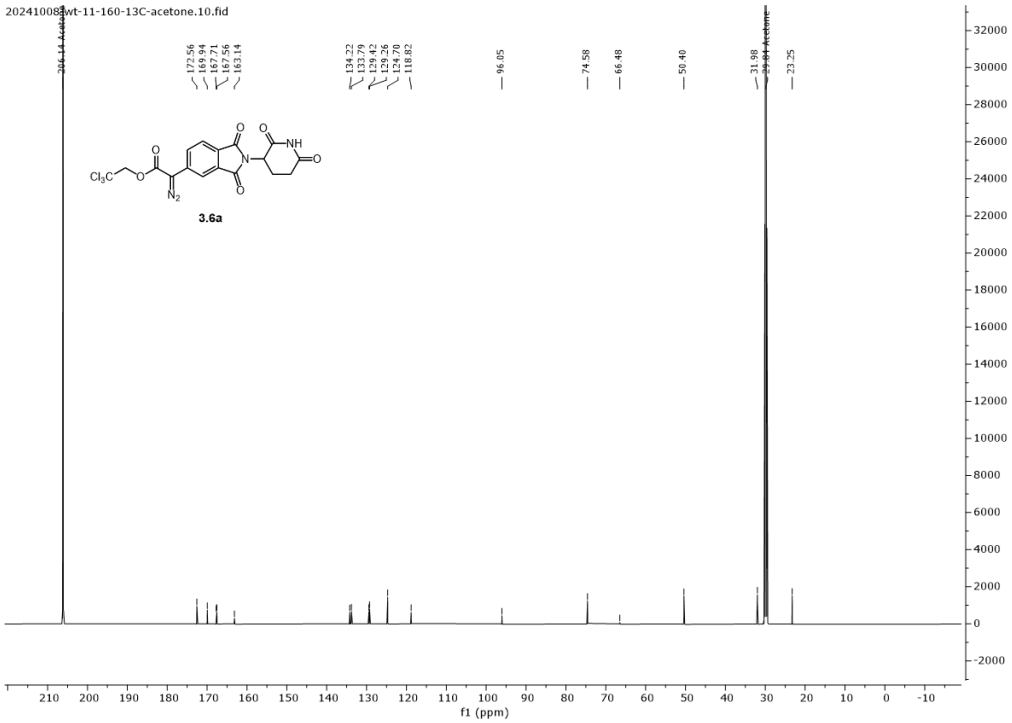

$^{13}C\{^{1}H\}$ (151 MHz). Spectrum for Compound 3.6b

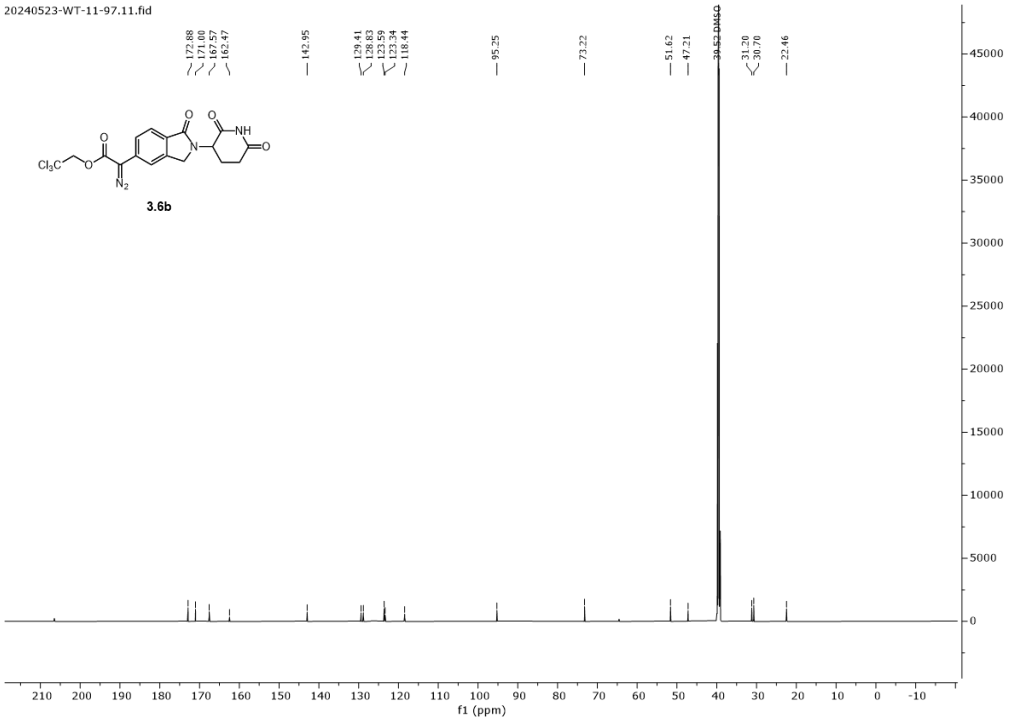

$^{13}C\{^{1}H\}$ (151 MHz) Spectrum for Compound 3.6c.

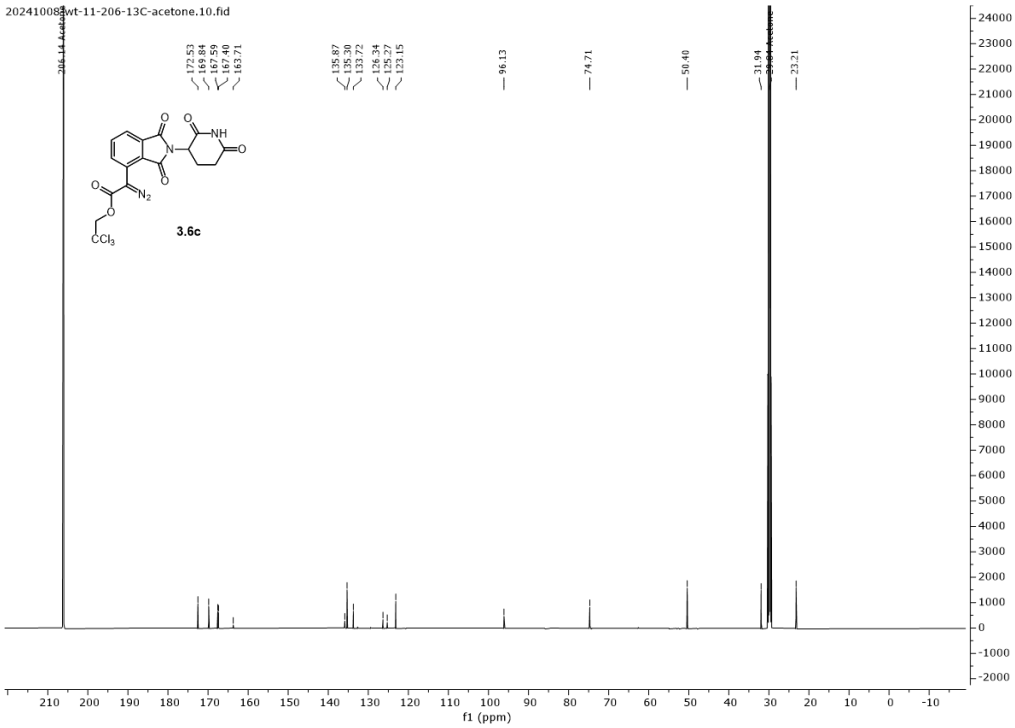

$^{13}C\{^{1}H\}$ (101 MHz) Spectrum for Compound 3.8a.

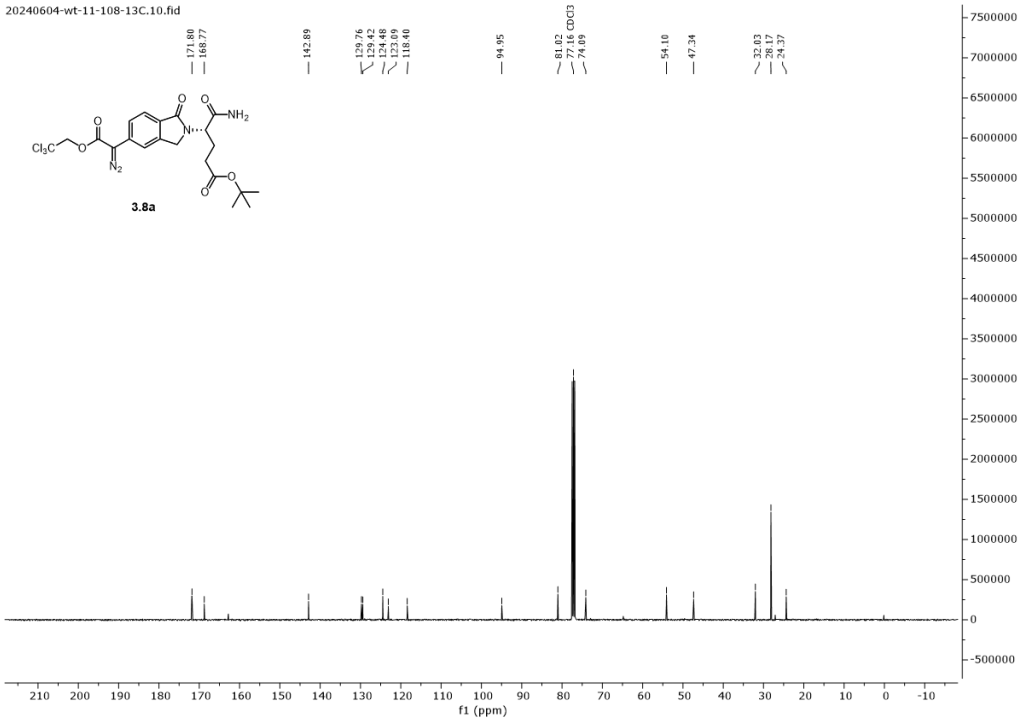

$^{13}C\{^{1}H\}$ (151 MHz) Spectrum for Compound 3.8b.

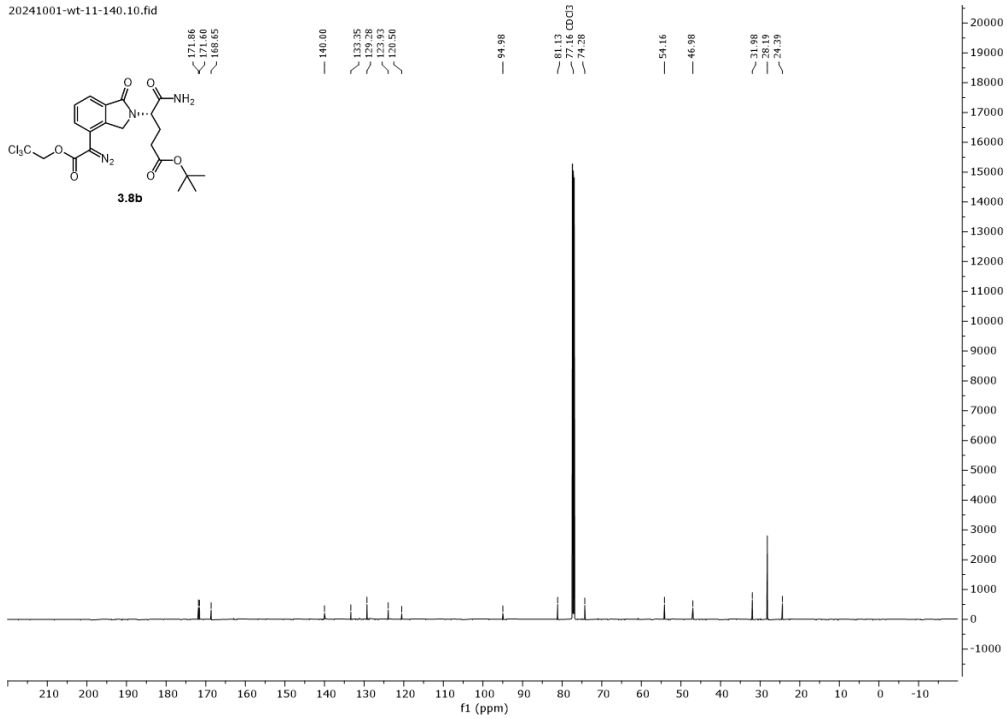

$^{13}C\{^{1}H\}$ (151 MHz) Spectrum for Compound 3.9a.

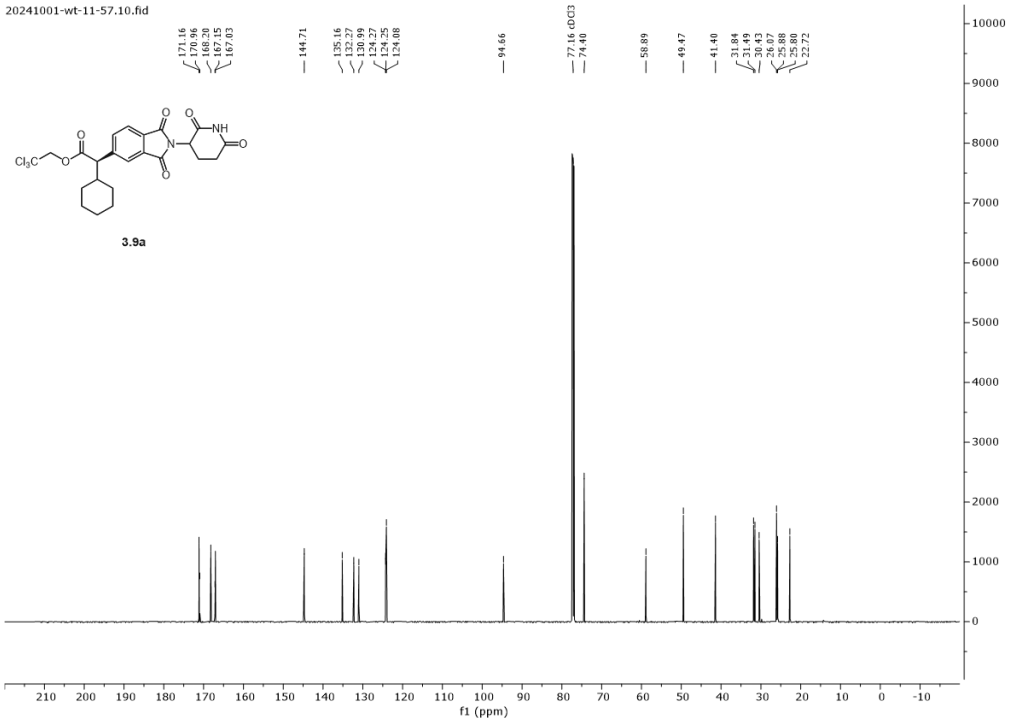

$^{13}C\{^{1}H\}$ (151 MHz) Spectrum for Compound 3.9b.

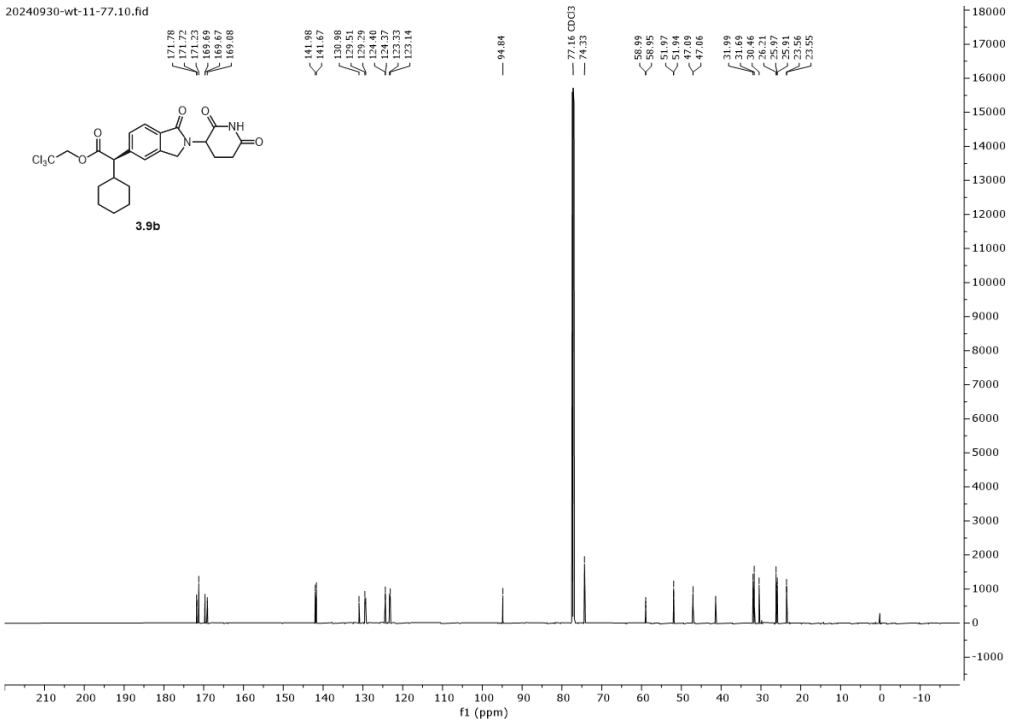

$^{13}C\{^{1}H\}$ (151 MHz) Spectrum for Compound 3.9c.

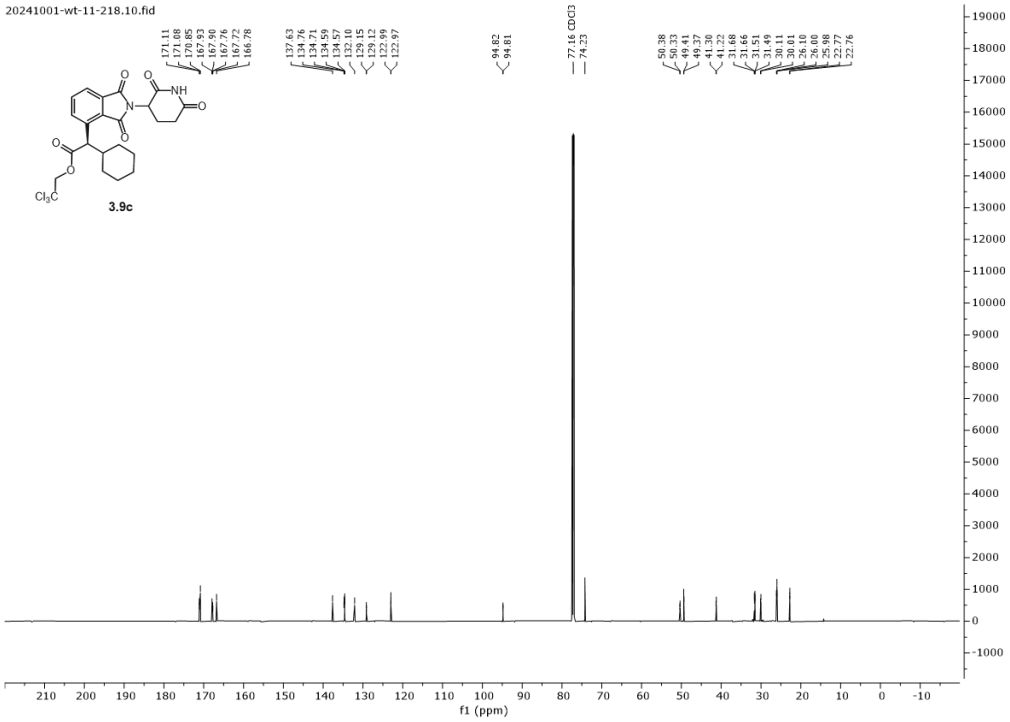

$^{13}C\{^{1}H\}$ (151 MHz) Spectrum for Compound (*S*,*R*)- 3.10a.

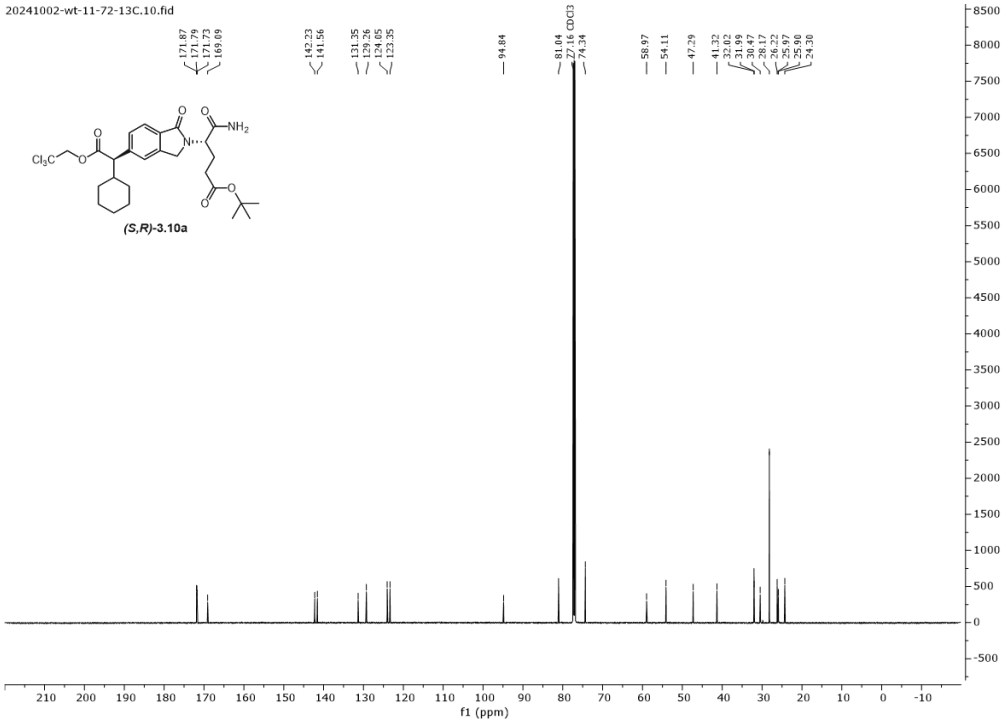

$^{13}C\{^{1}H\}$ (151 MHz) Spectrum for Compound (*S*,*S*)- 3.10a.

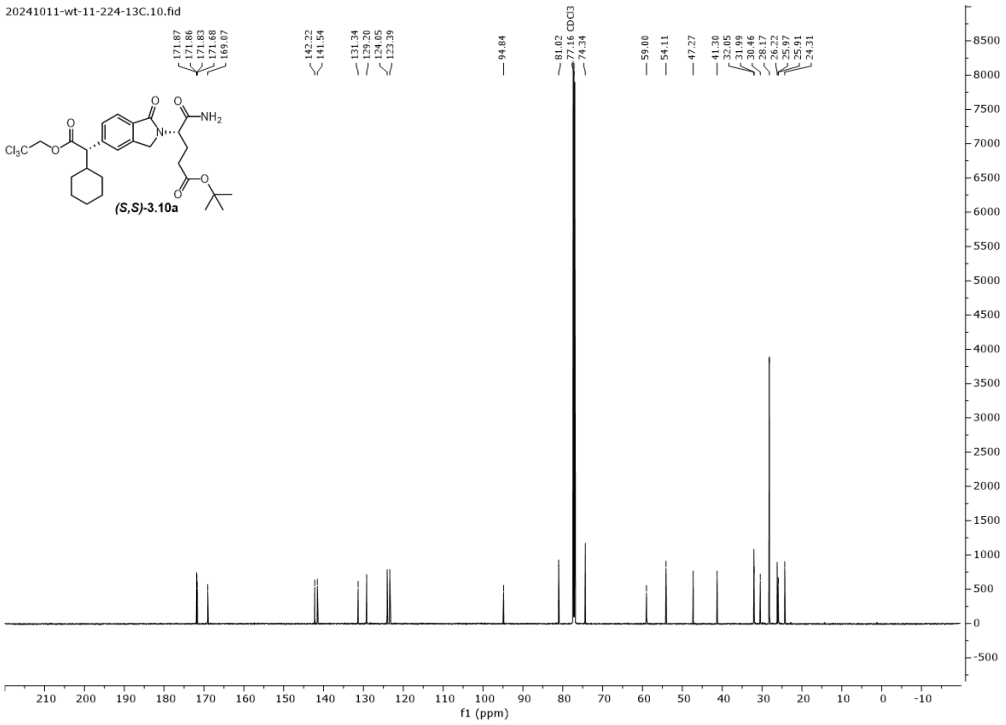

$^{13}C\{^{1}H\}$ (151 MHz) Spectrum for Compound 3.10b.

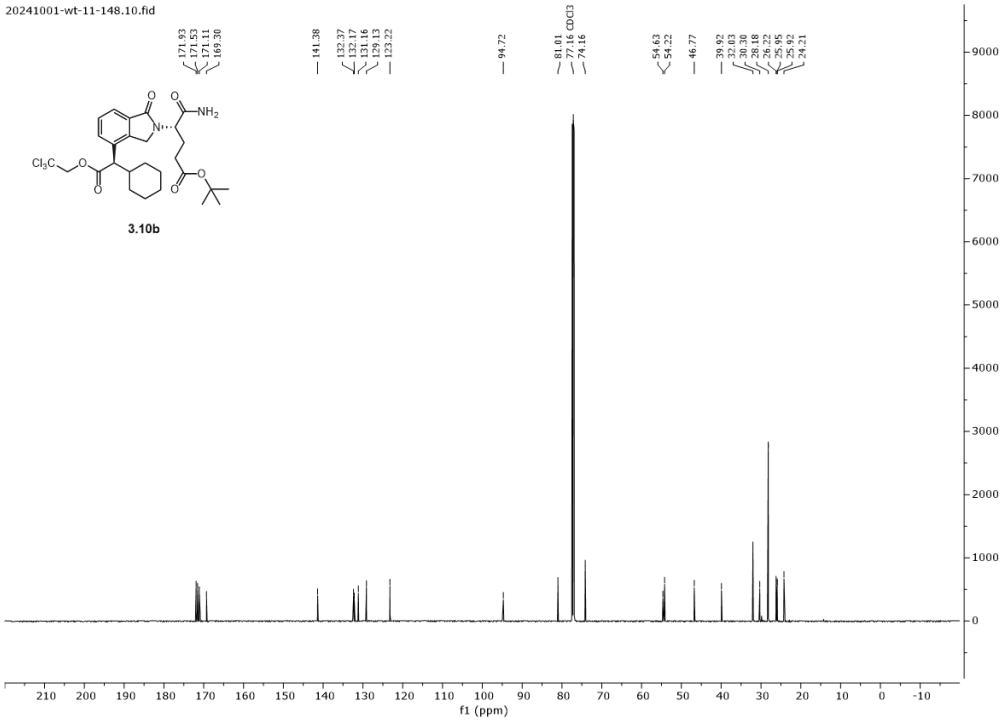

$^{13}C\{^{1}H\}$ (151 MHz) Spectrum for Compound 3.11a.

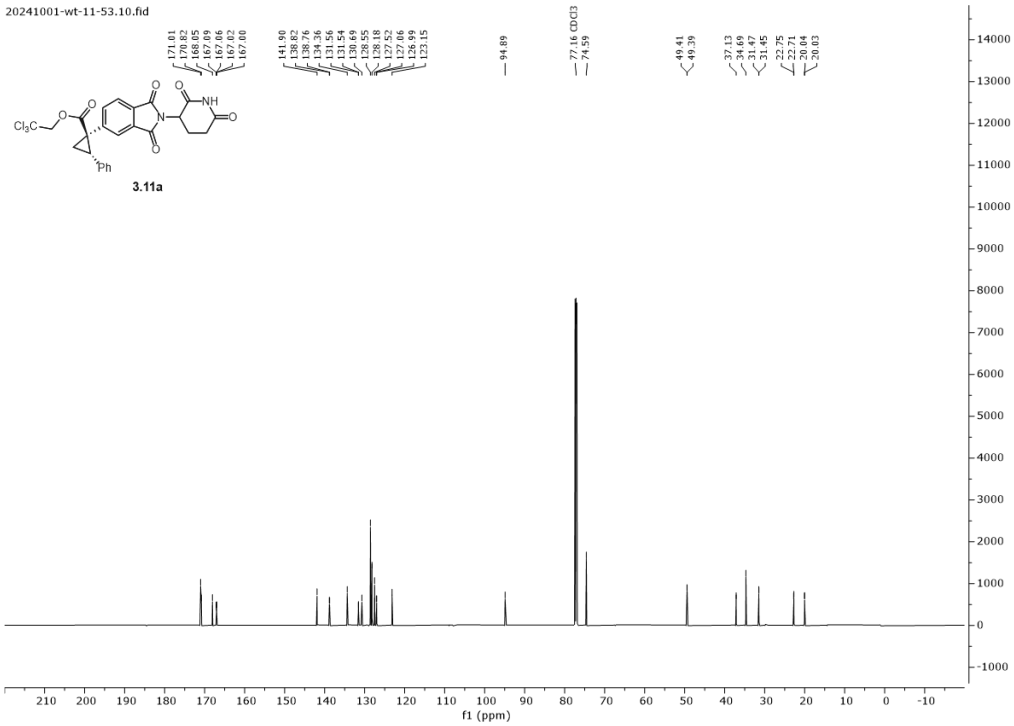

$^{13}C\{^1H\}$ (151 MHz) Spectrum for Compound 3.11b.

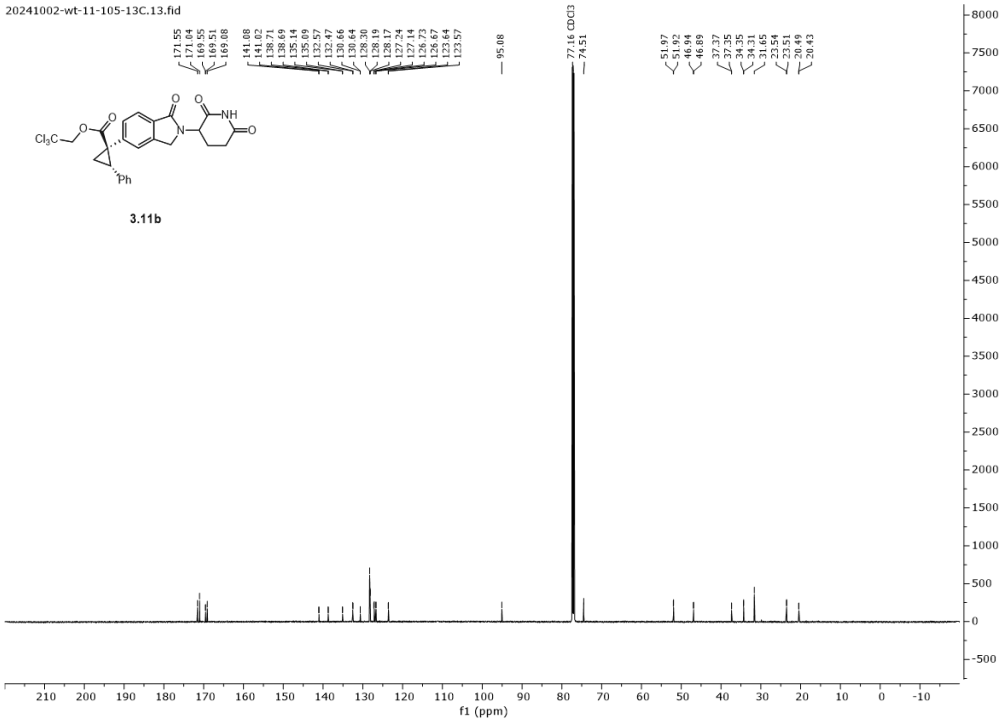

$^{13}C\{^1H\}$ (151 MHz) Spectrum for Compound 3.11c.

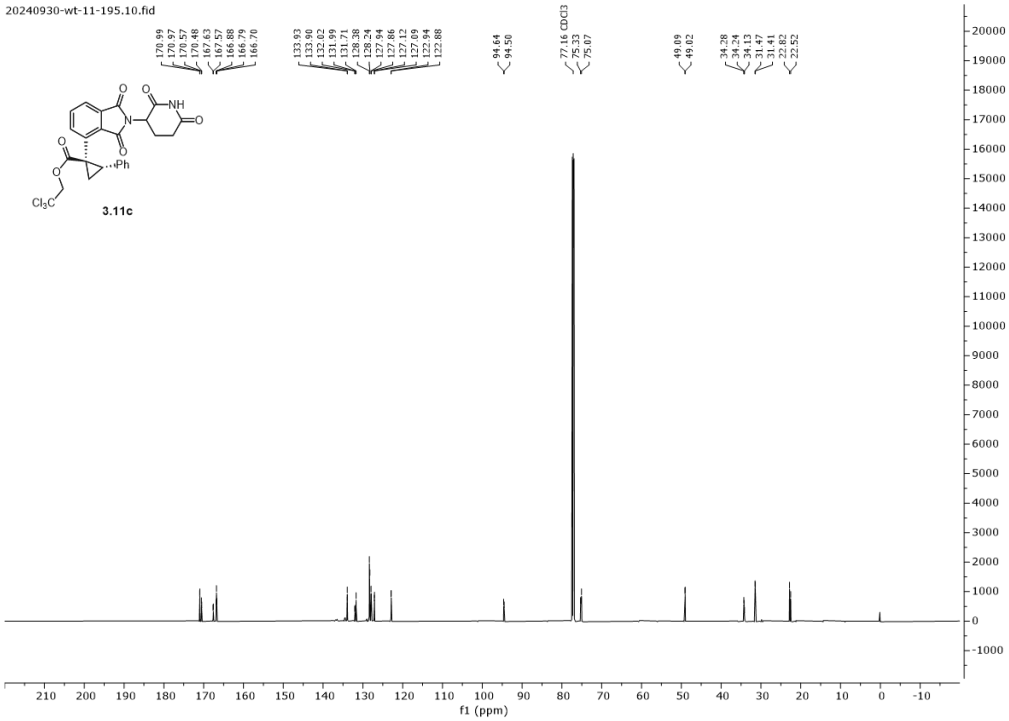

$^{13}C\{^1H\}$ (101 MHz) Spectrum for Compound 3.12a.

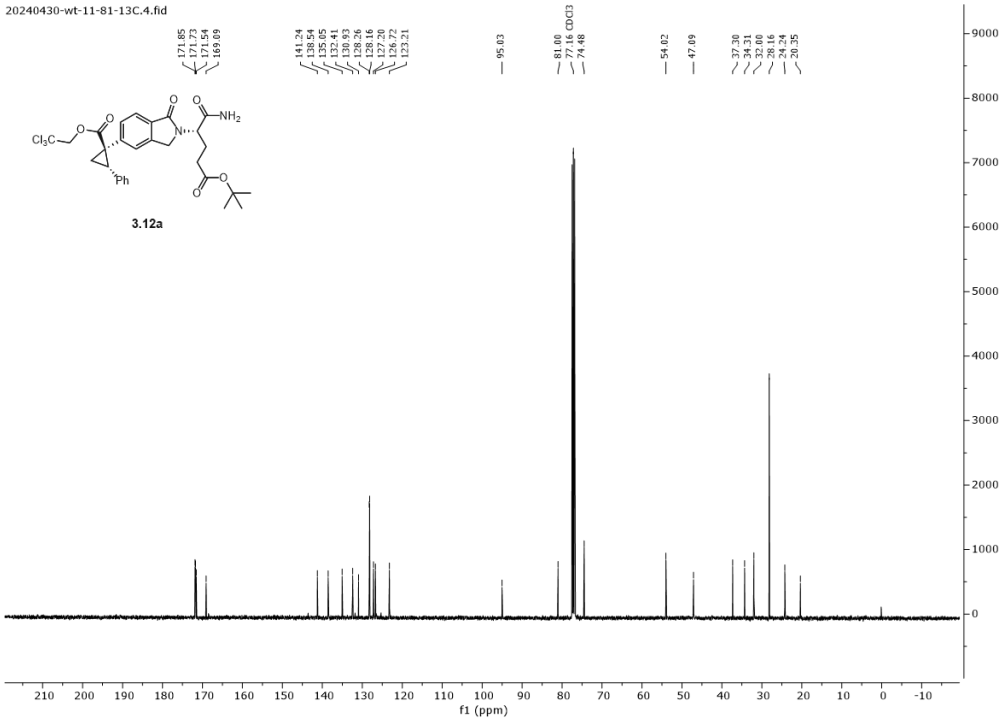

$^{13}C\{^1H\}$ (151 MHz) Spectrum for Compound 3.12b.

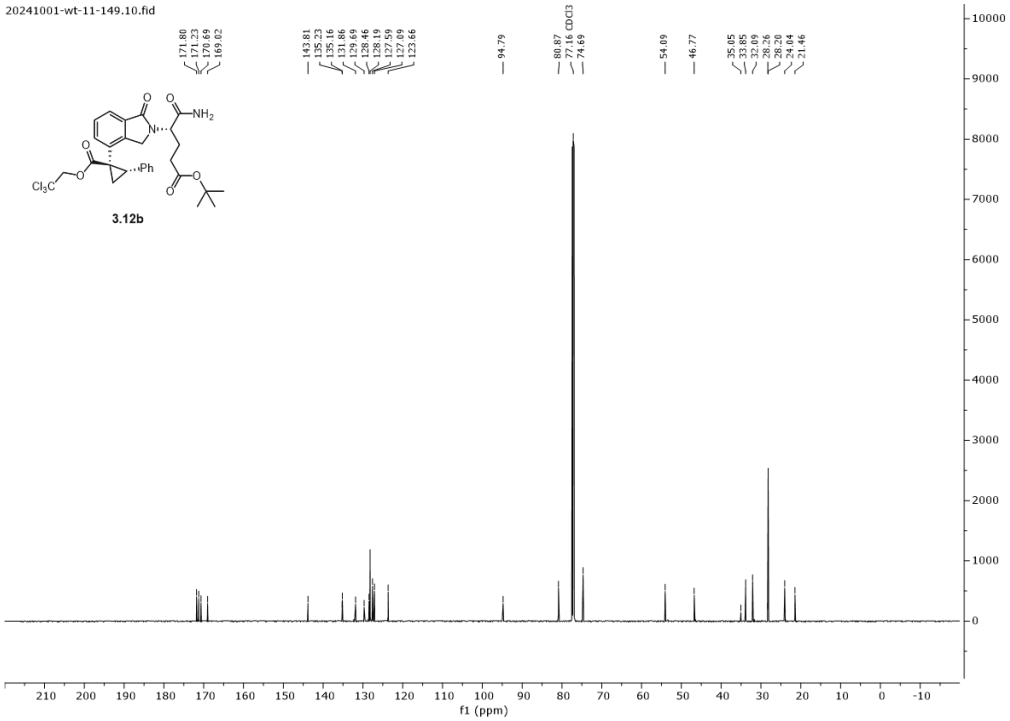

$^{13}C\{^{1}H\}$ (101 MHz) Spectrum for Compound 3.13.

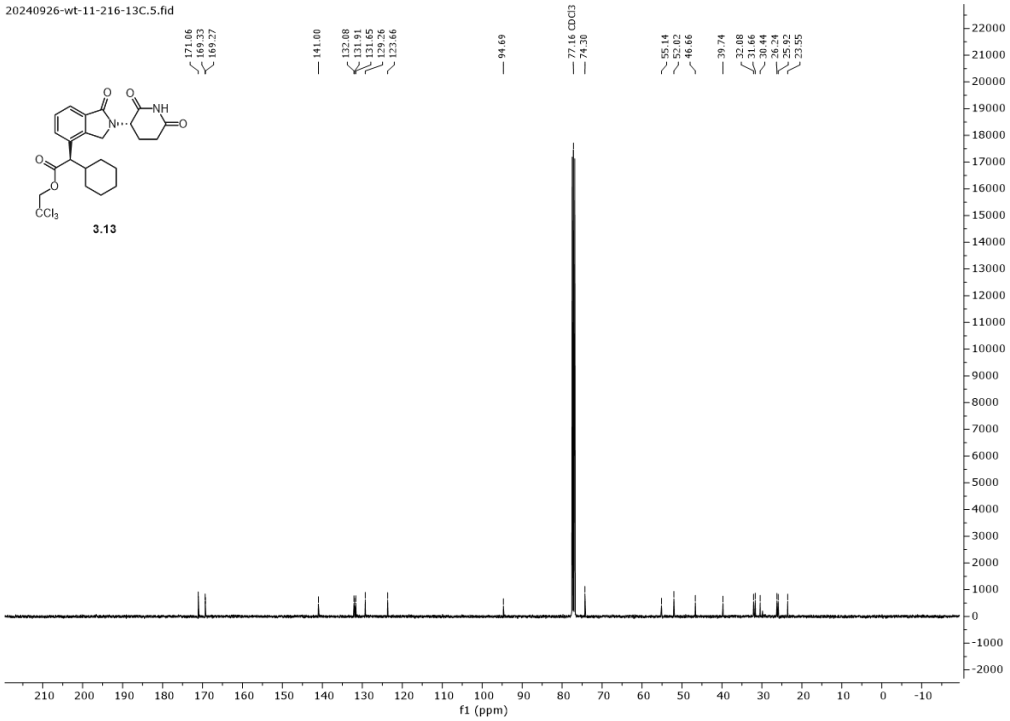

$^{13}C\{^{1}H\}$ (151 MHz) Spectrum for Compound 3.14.

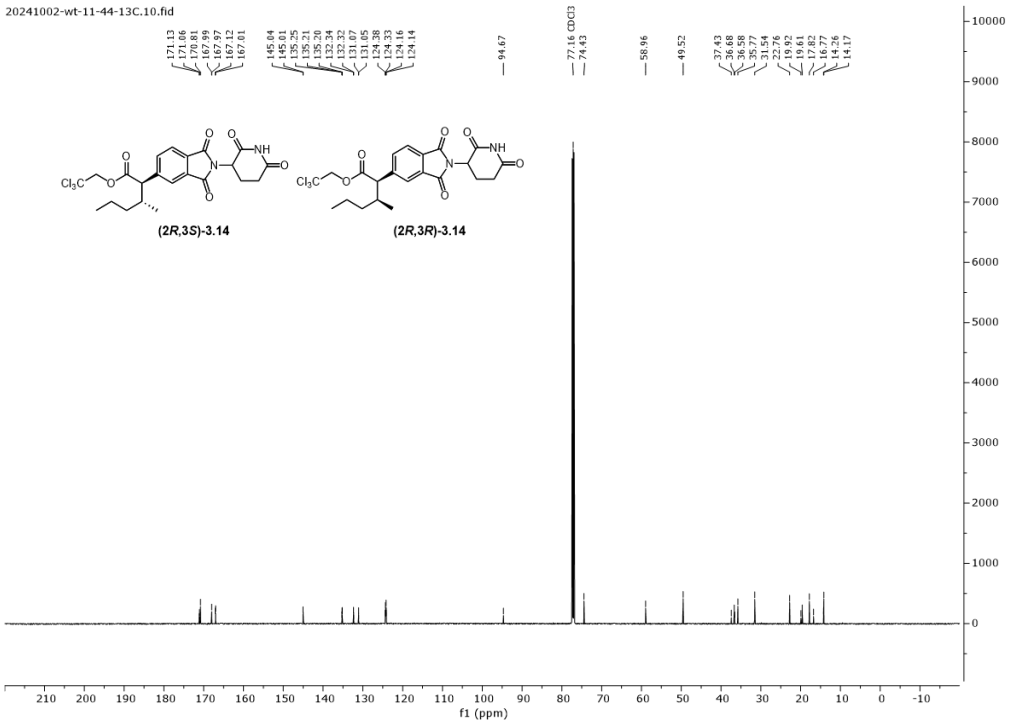

$^{13}C\{^{1}H\}$ (151 MHz) Spectrum for Compound 3.15.

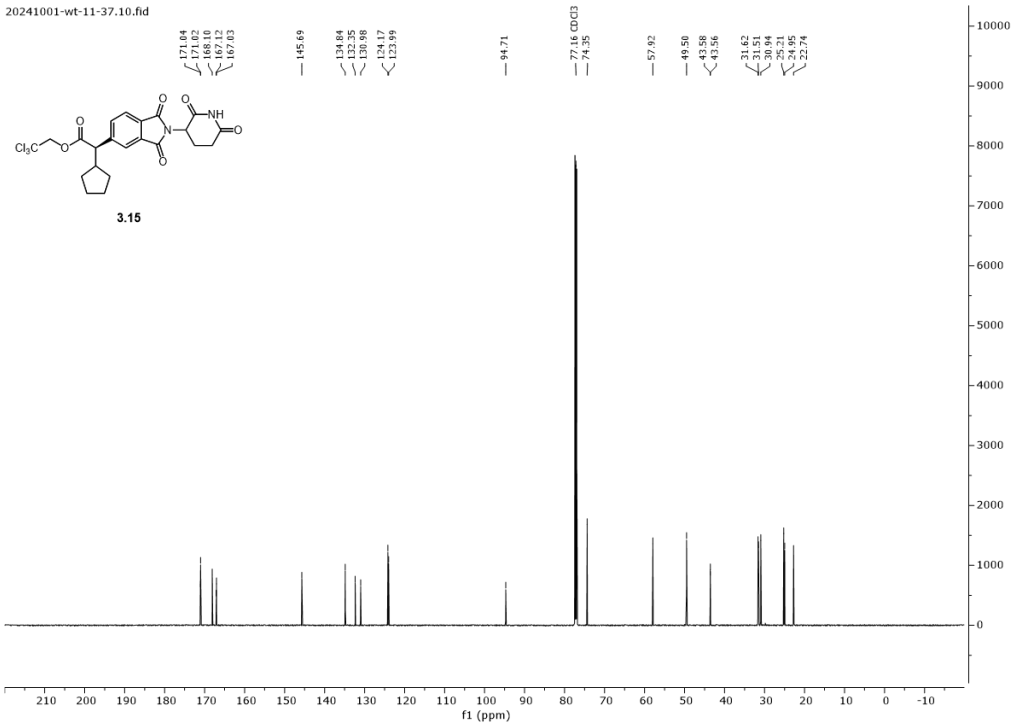

$^{13}C\{^{1}H\}$ (151 MHz) Spectrum for Compound 3.16.

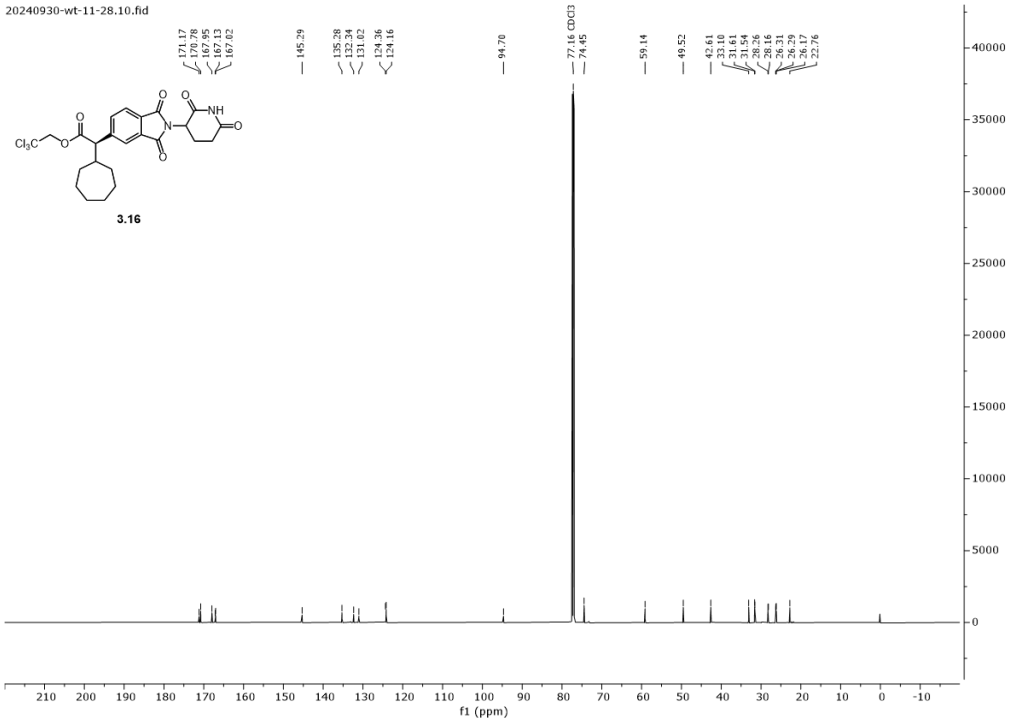

$^{13}C\{^{1}H\}$ (151 MHz) Spectrum for Compound 3.17.

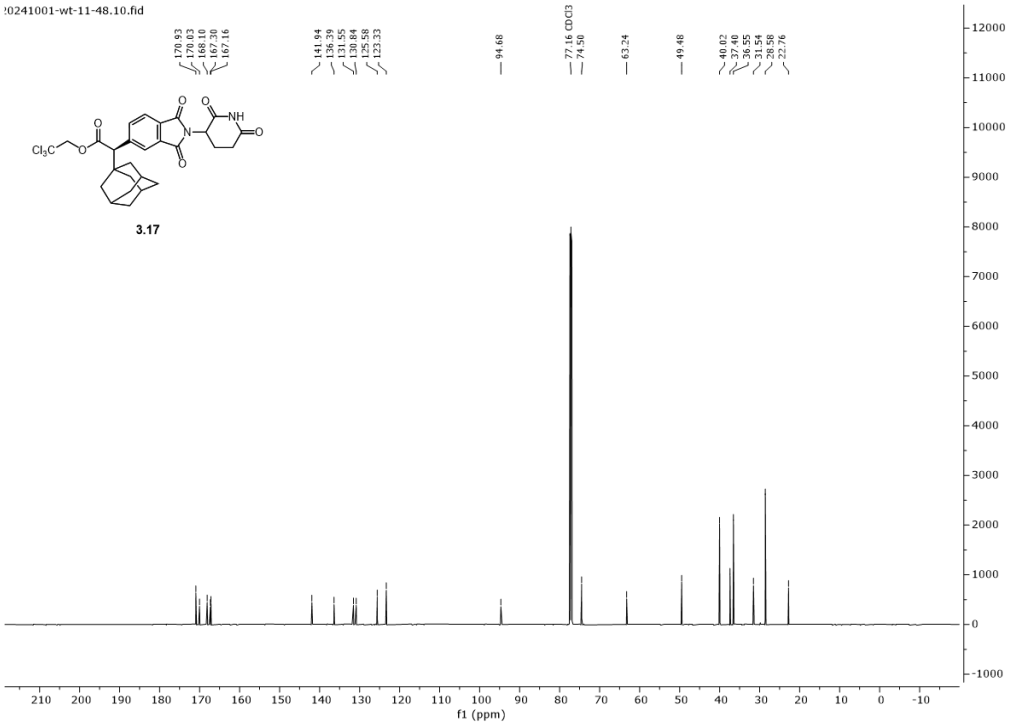

$^{13}C\{^{1}H\}$ (151 MHz) Spectrum for Compound 3.18.

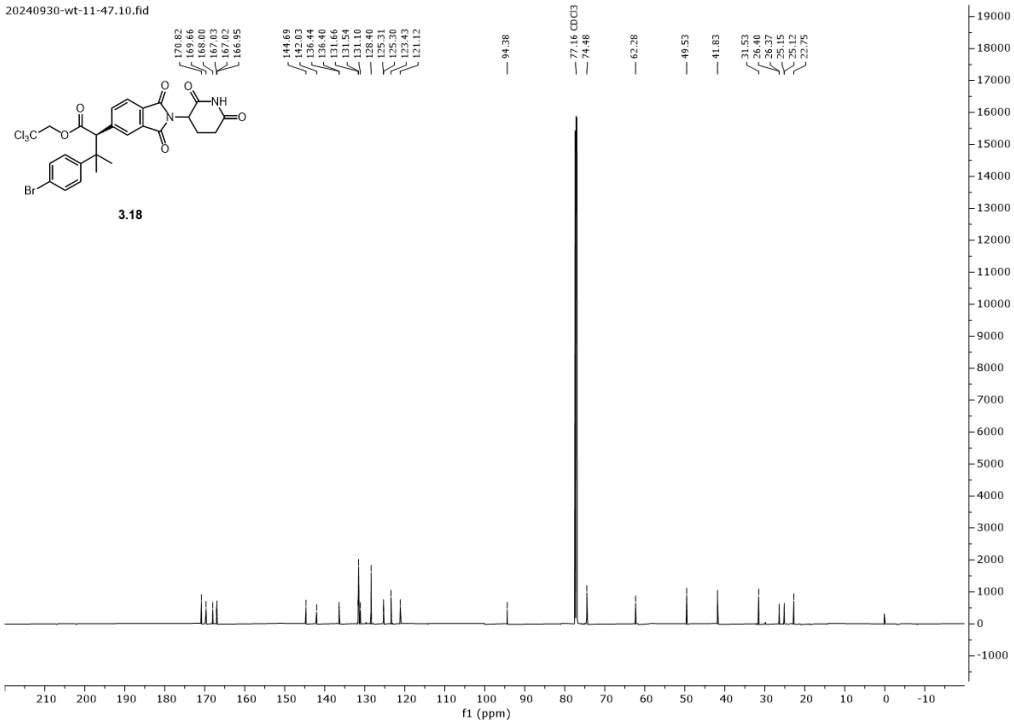

$^{13}C\{^{1}H\}$ (151 MHz) Spectrum for Compound 3.19.

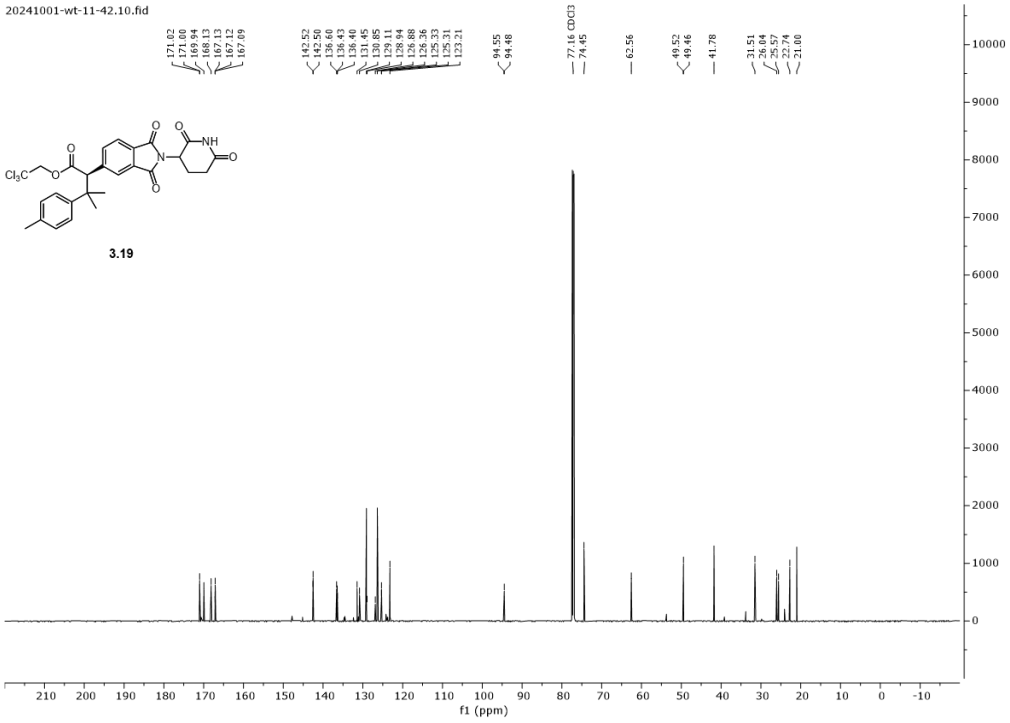

$^{13}C\{^{1}H\}$ (151 MHz) Spectrum for Compound 3.20.

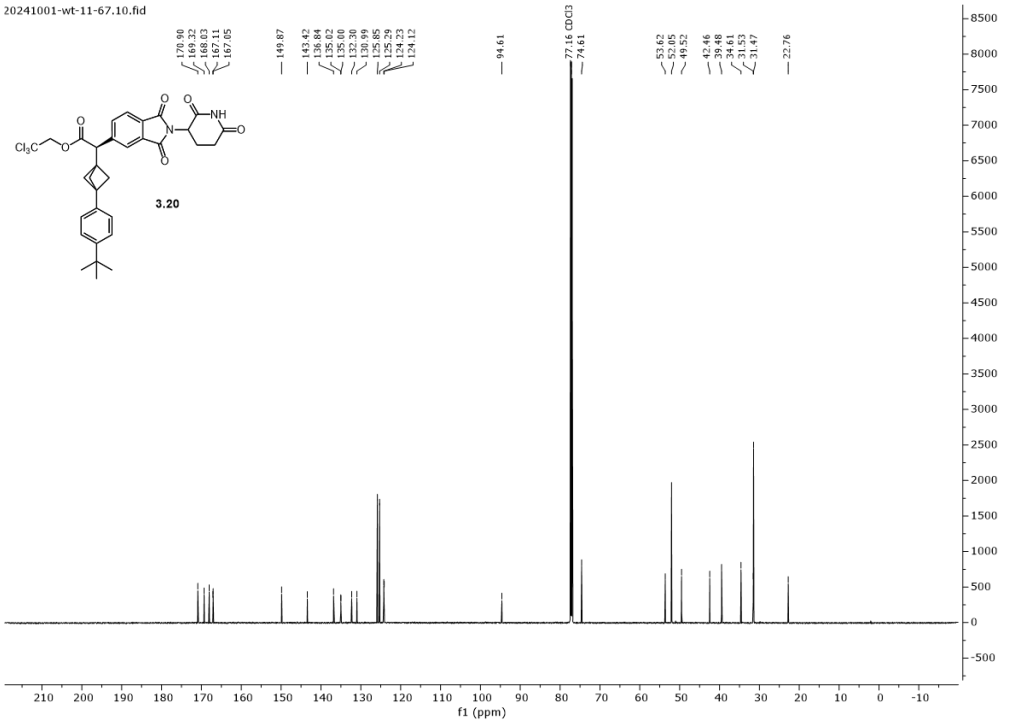

$^{13}C\{^{1}H\}$ (151 MHz) Spectrum for Compound 3.21.

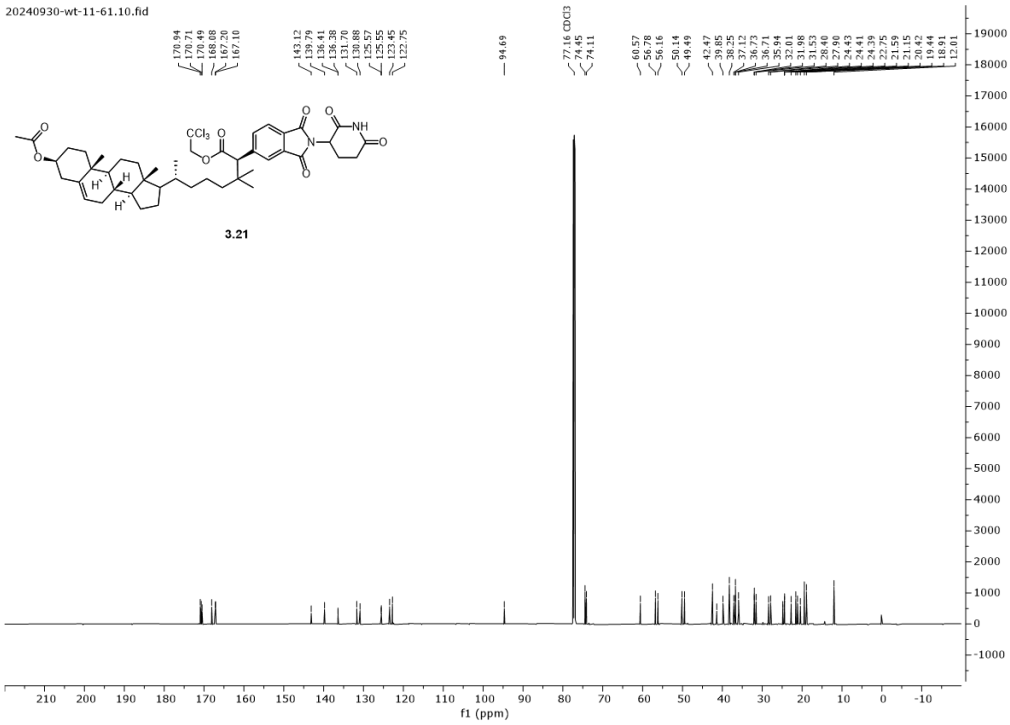

$^{13}C\{^{1}H\}$ (101 MHz) Spectrum for Compound 3.22.

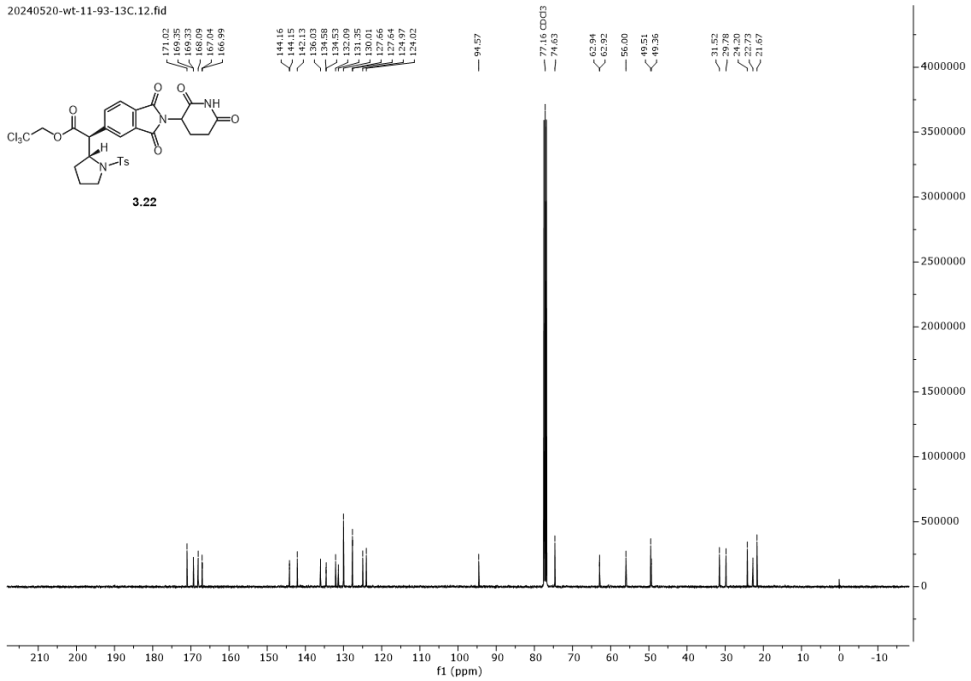

$^{13}C\{^{1}H\}$ (151 MHz) Spectrum for Compound 3.23.

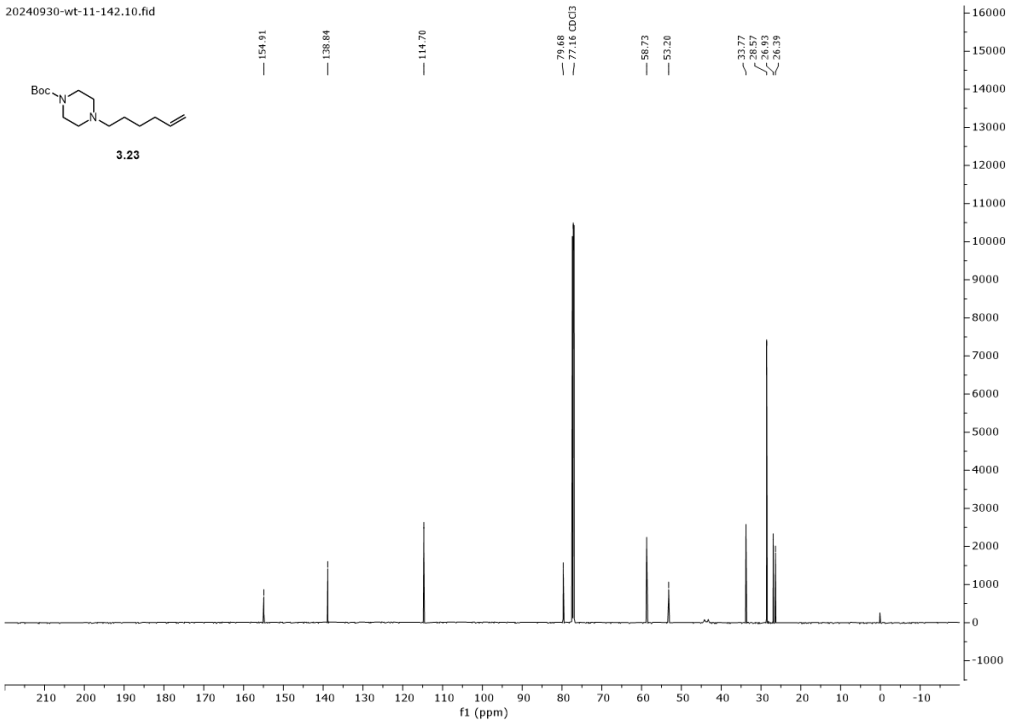

$^{13}C\{^{1}H\}$ (151 MHz) Spectrum for Compound 3.24.

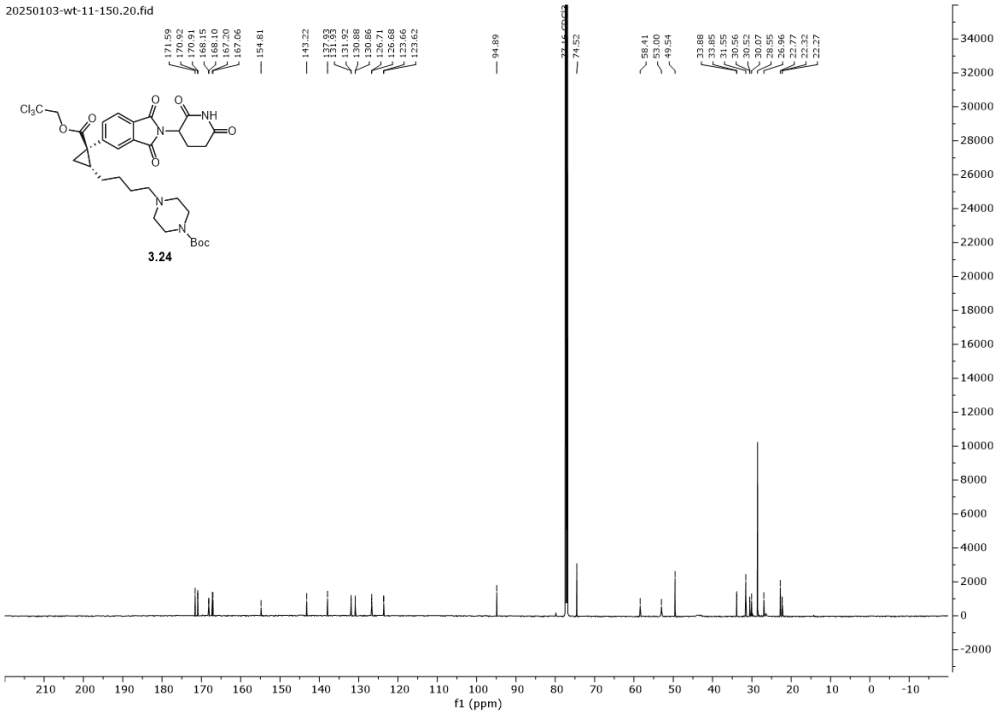

$^{13}C\{^{1}H\}$ (201 MHz) Spectrum for Compound 3.25 at 80 °C.

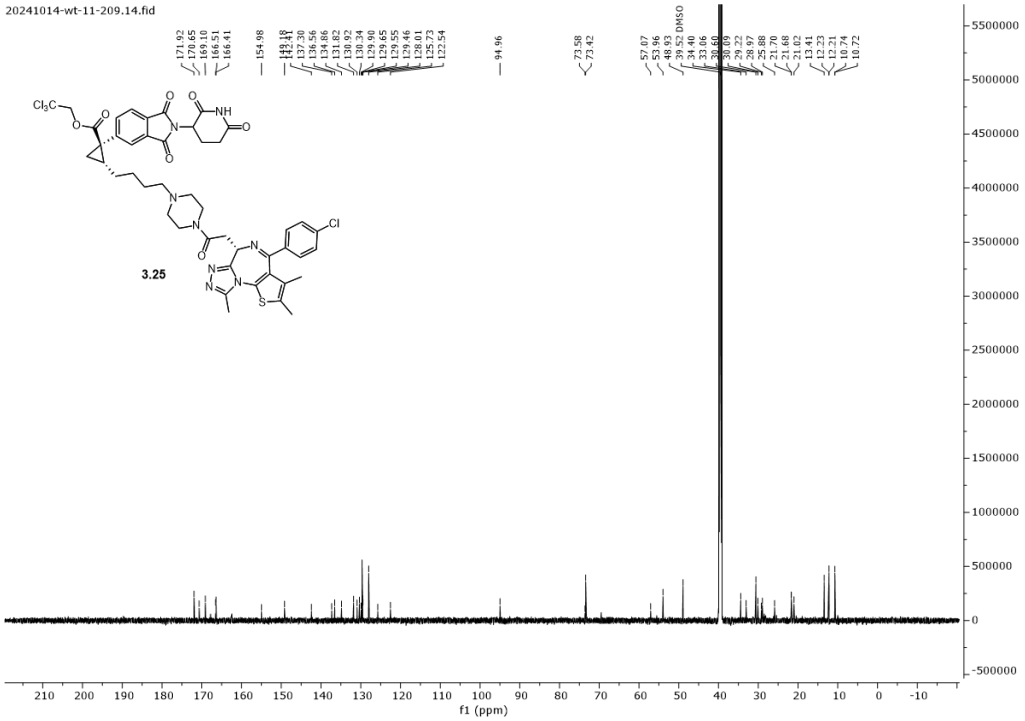

$^{13}C\{^{1}H\}$ (201 MHz) Spectrum for Compound 3.26 at 80 °C.

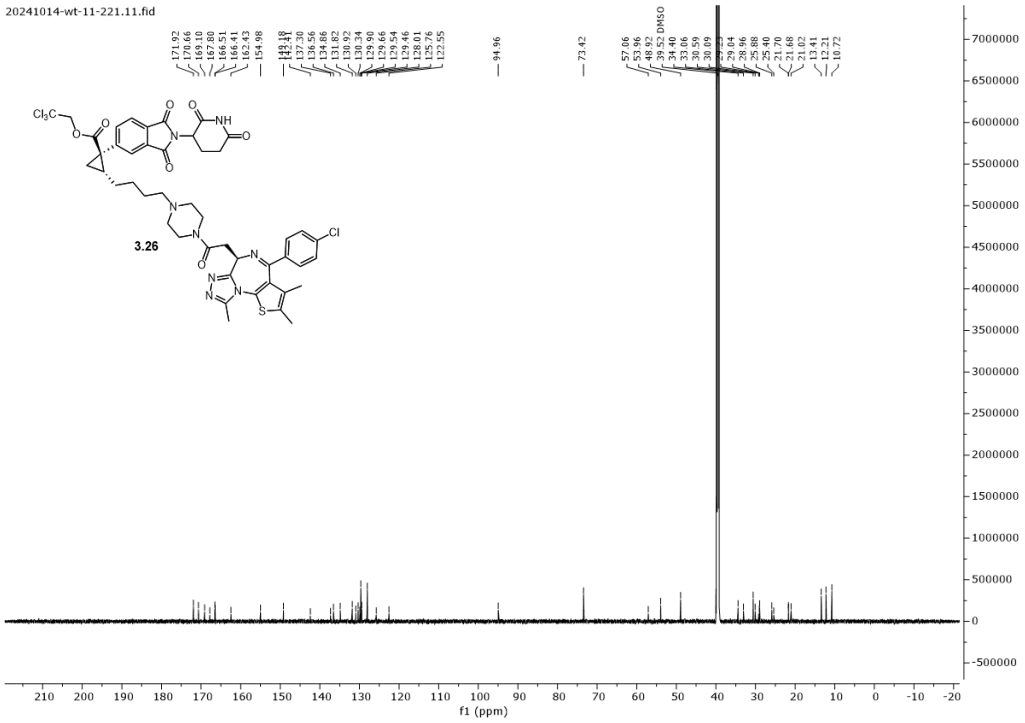

$^{13}C\{^{1}H\}$ (101 MHz) Spectrum for Compound SI2.

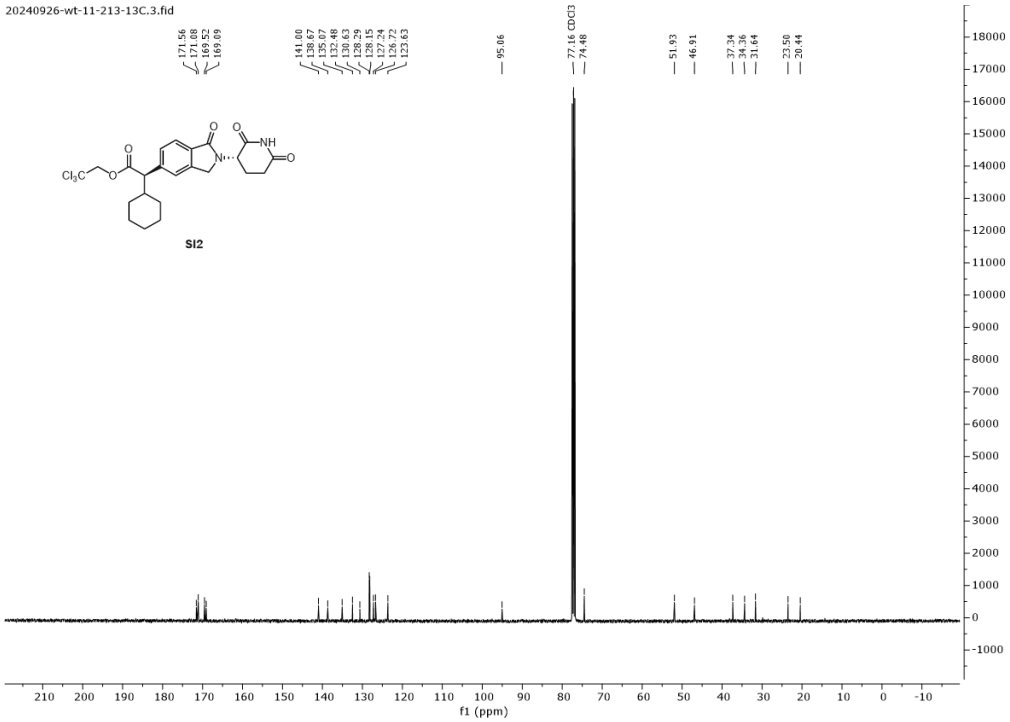

$^{13}C\{^{1}H\}$ (101 MHz) Spectrum for Compound SI3.

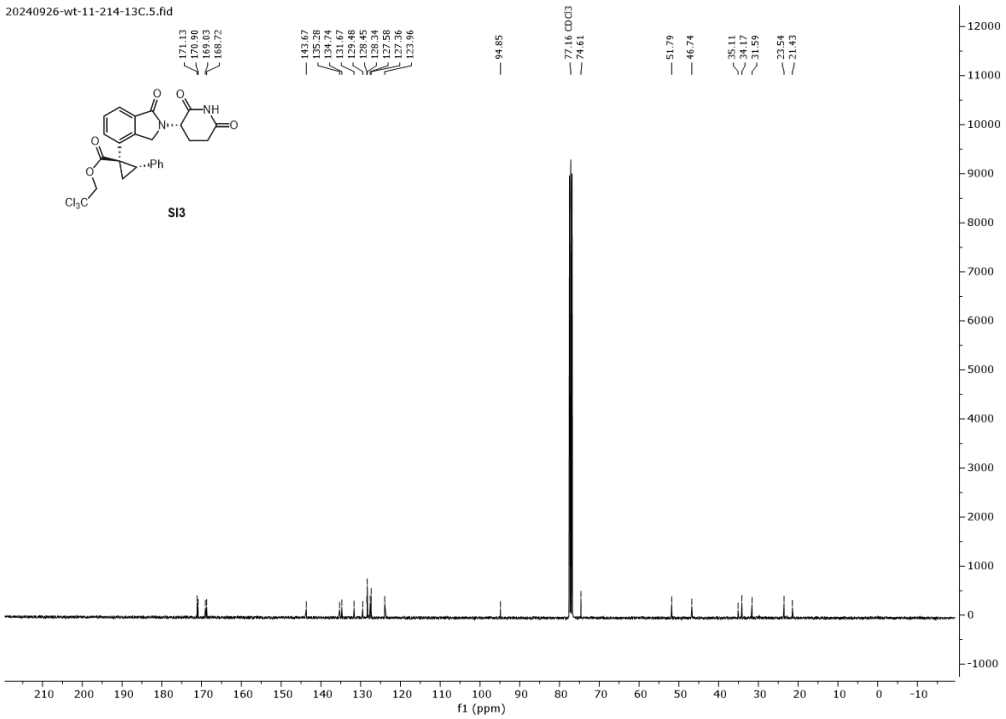

$^{13}C\{^{1}H\}$ (101 MHz) Spectrum for Compound SI4.

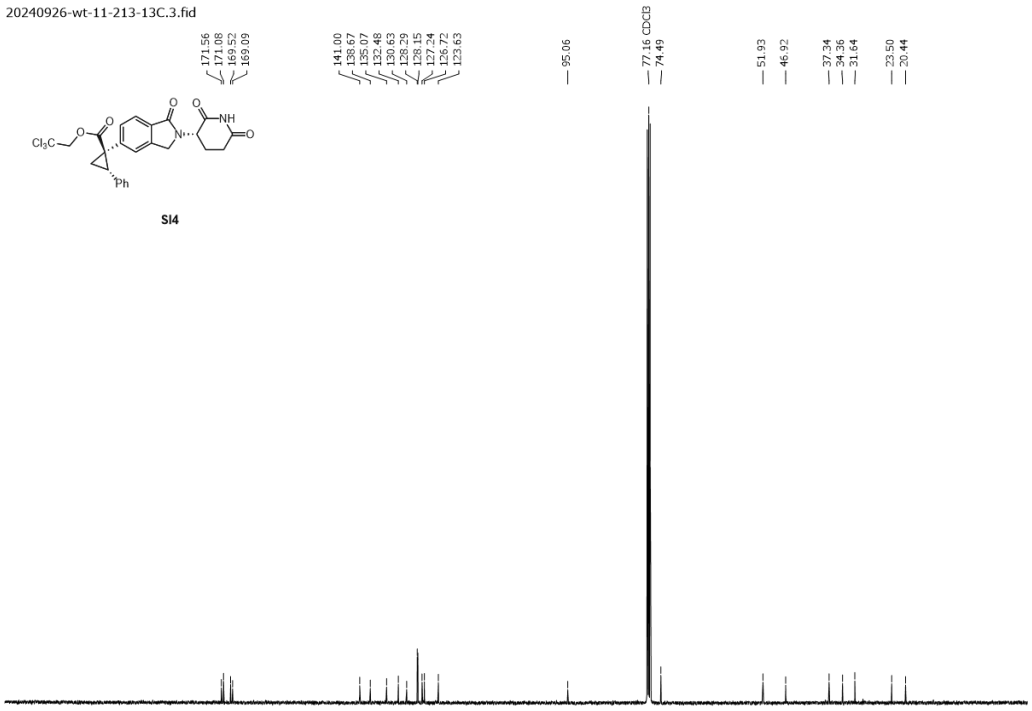

Supplementary NMR Spectra

^{1}H NMR spectrum for 3.10b showing support for d.r. determination

3.10b *epimerized with DBU showing appearance of diastereomeric peaks*

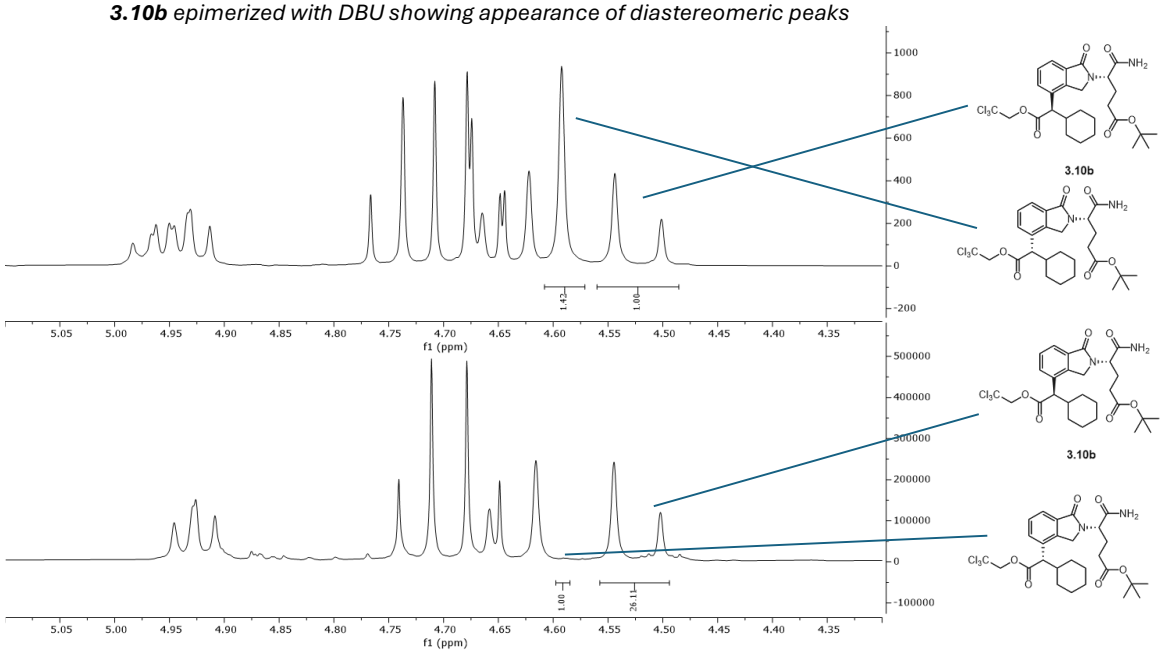

Reaction of ***3.8b*** *with S catalyst showing absence of diastereomeric peaks in* ***3.10b***

^{1}H NMR spectrum for (S,R)-3.10a and (S,S)-3.10a showing support for d.r. determination

*Reaction of **3.8a** with R/S catalyst showing appearance of diastereomeric peaks for **(S,S)-3.10a***

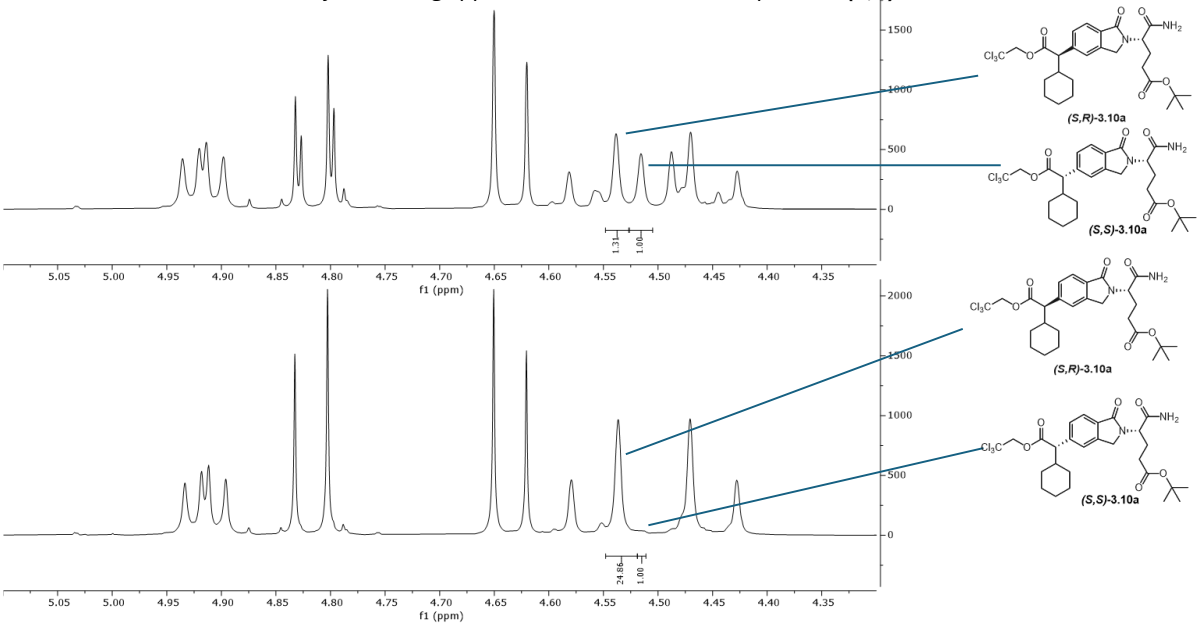

*Reaction of **3.8a** with S catalyst showing disappearance of diastereomeric peaks for **(S,S)-3.10a***

^{1}H NMR spectrum for 3.12b showing support for d.r. determination

*Reaction of **3.8a** with R/S catalyst showing appearance of diastereomeric peaks for **(S,S)-3.10a***

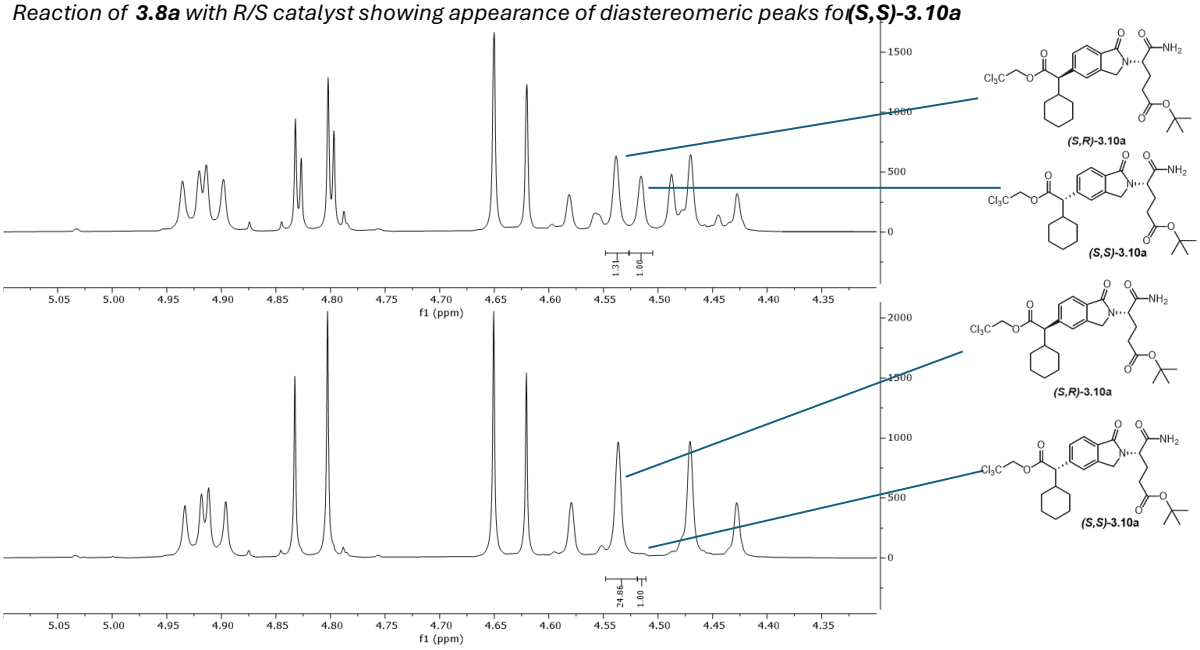

*Reaction of **3.8a** with S catalyst showing disappearance of diastereomeric peaks for **(S,S)-3.10a***

^{1}H NMR spectrum for 3.14 showing support for r.r. determination

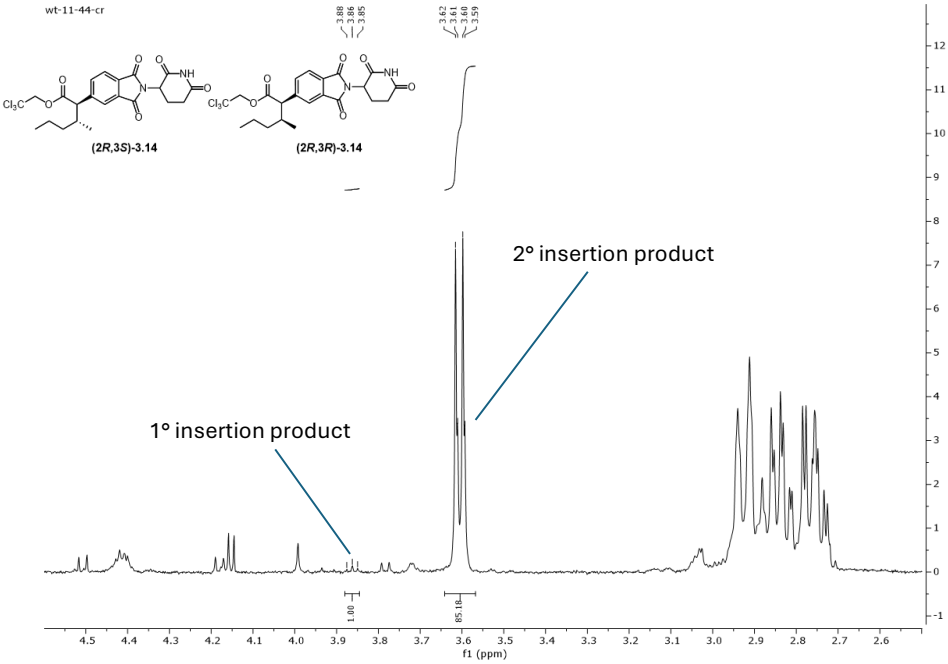

^{1}H NMR spectrum for 3.14 showing support for d.r. (relative configuration of the two new stereocenters) determination

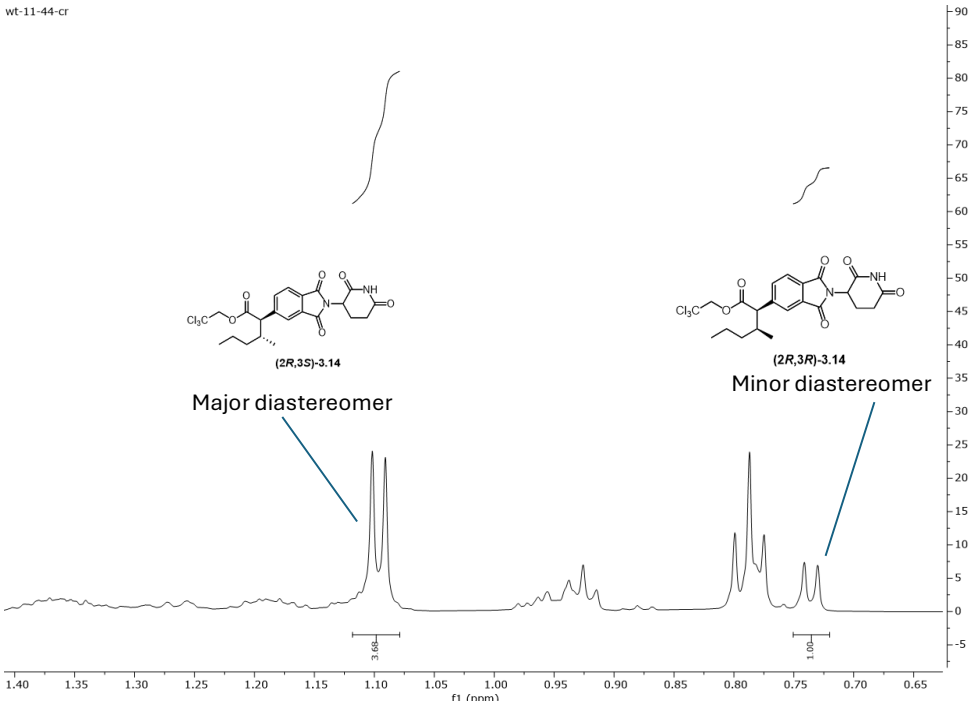

^{1}H NMR spectrum for 3.19 showing support for r.r. determination, Method A.

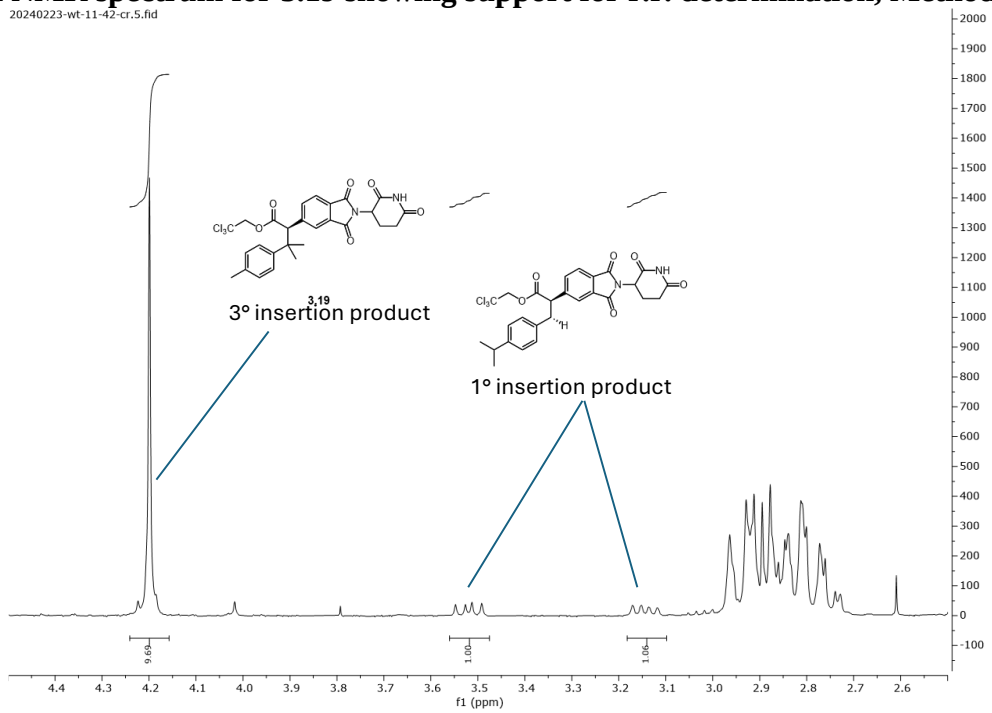

^{1}H NMR spectrum for 3.19 showing support for r.r. determination, Method B.

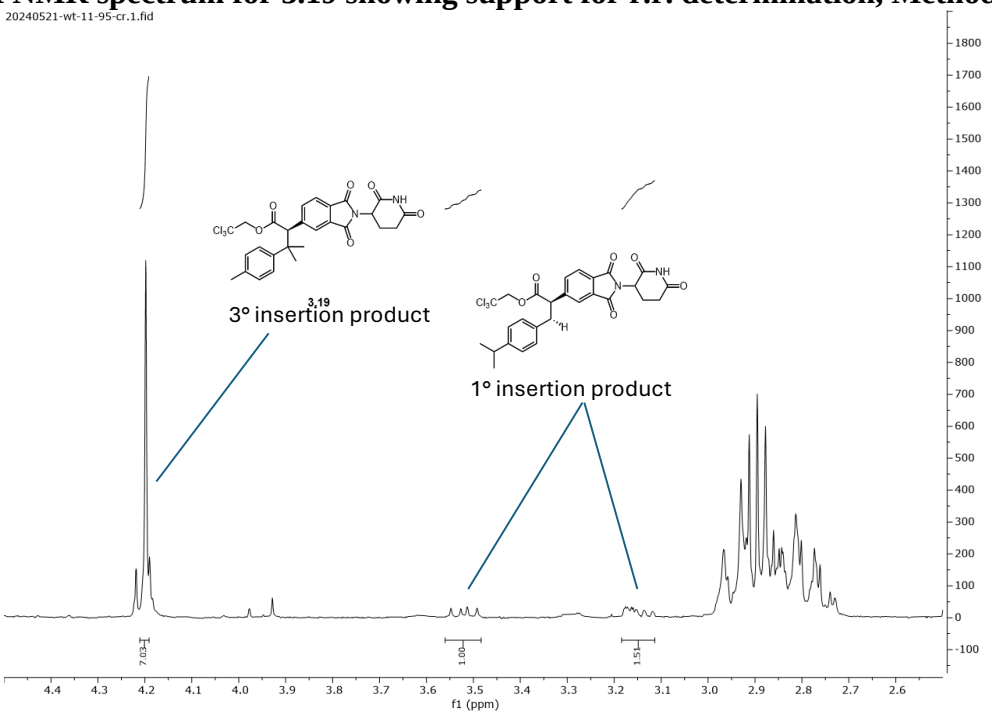

Section 5: Chromatographic Data

Chiral SFC Chromatograms

Racemic Chromatogram for Compound 3.9a

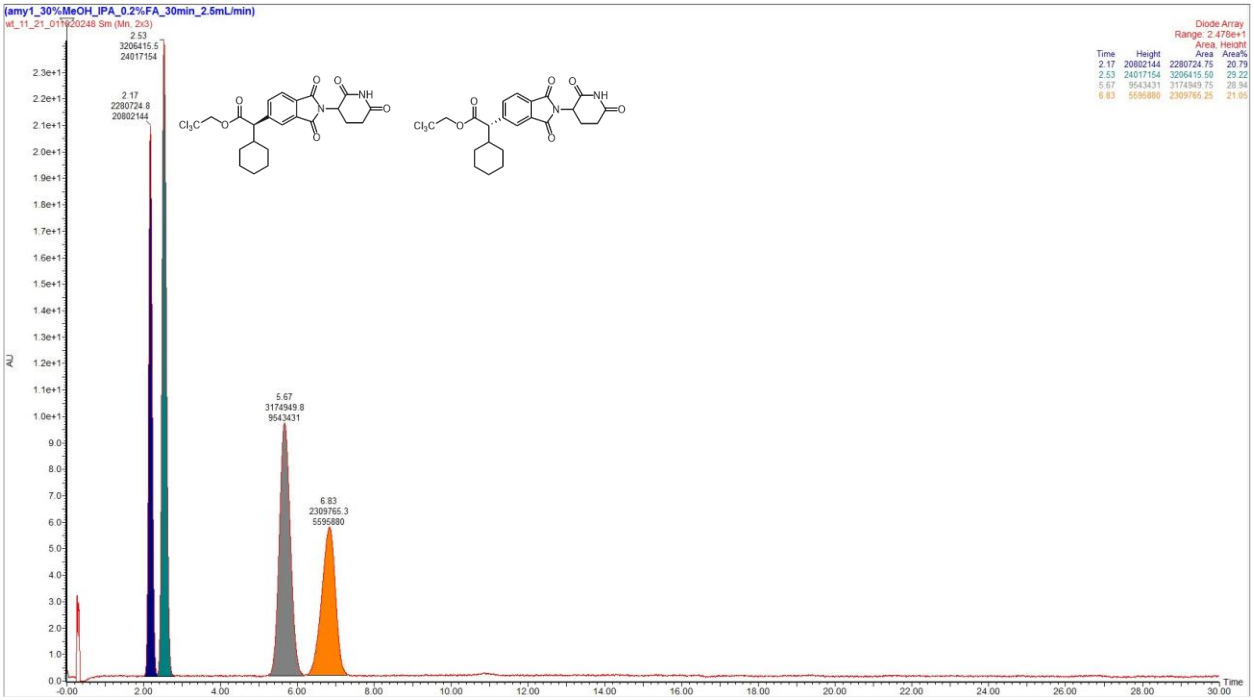

Chromatogram for Compound 3.9a Using GP1

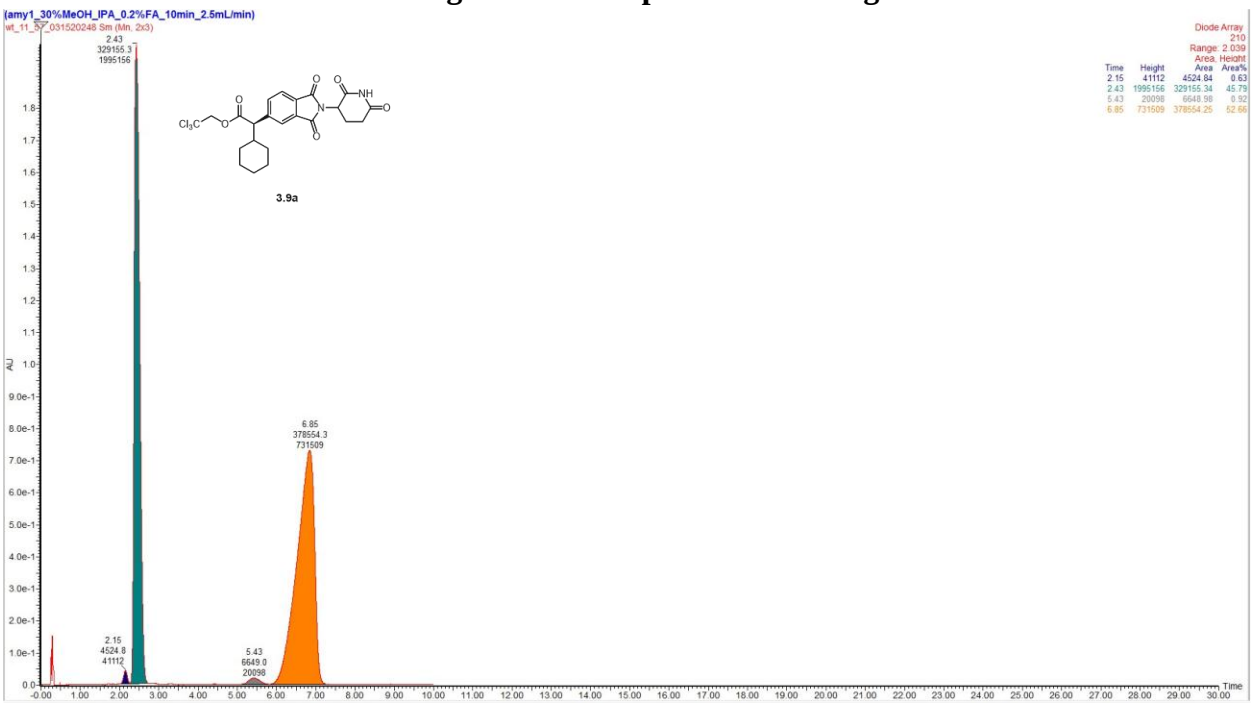

Chromatogram for Compound 3.9a Using GP2

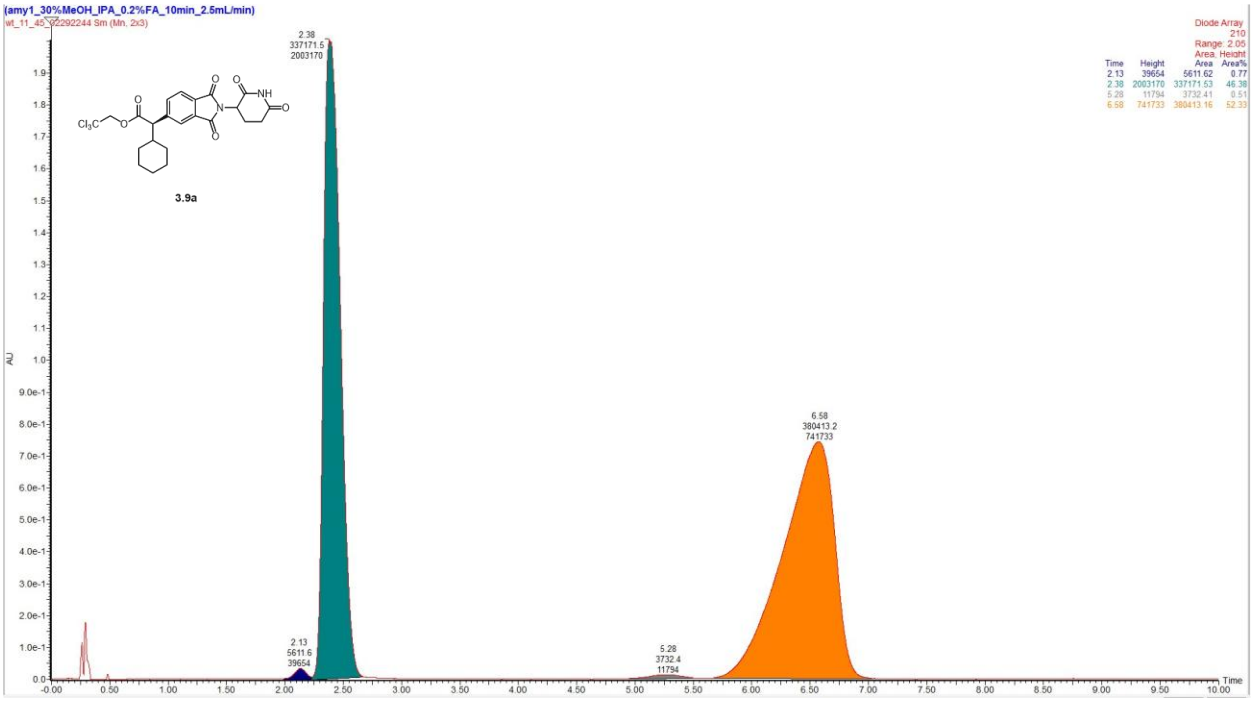

Chromatogram for Compound 3.9a Using GP3

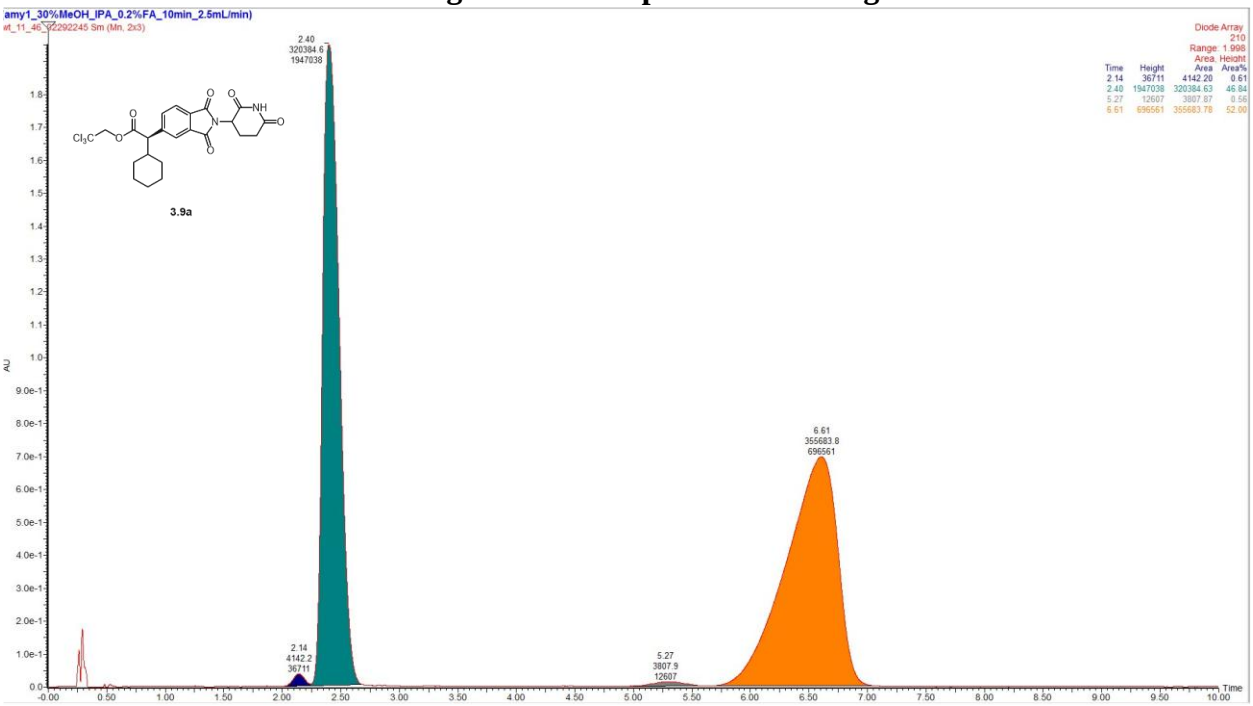

Racemic Chromatogram for Compound 3.9b

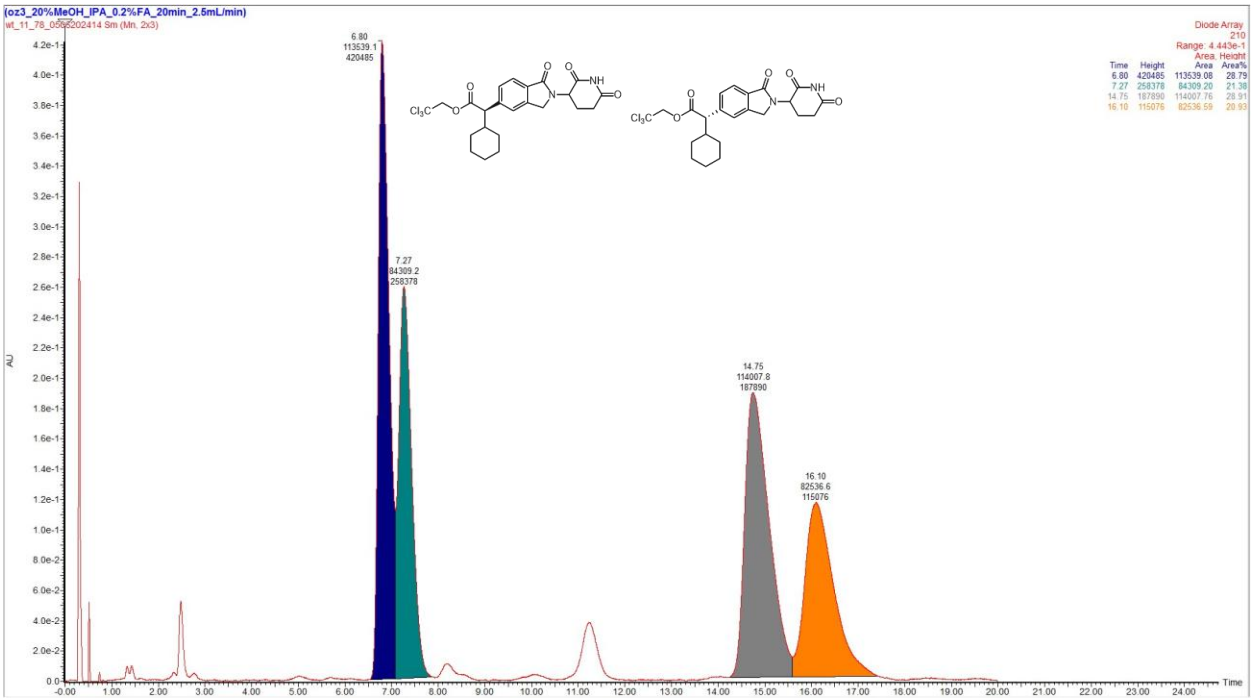

Chromatogram for Compound 3.9b Using GP1

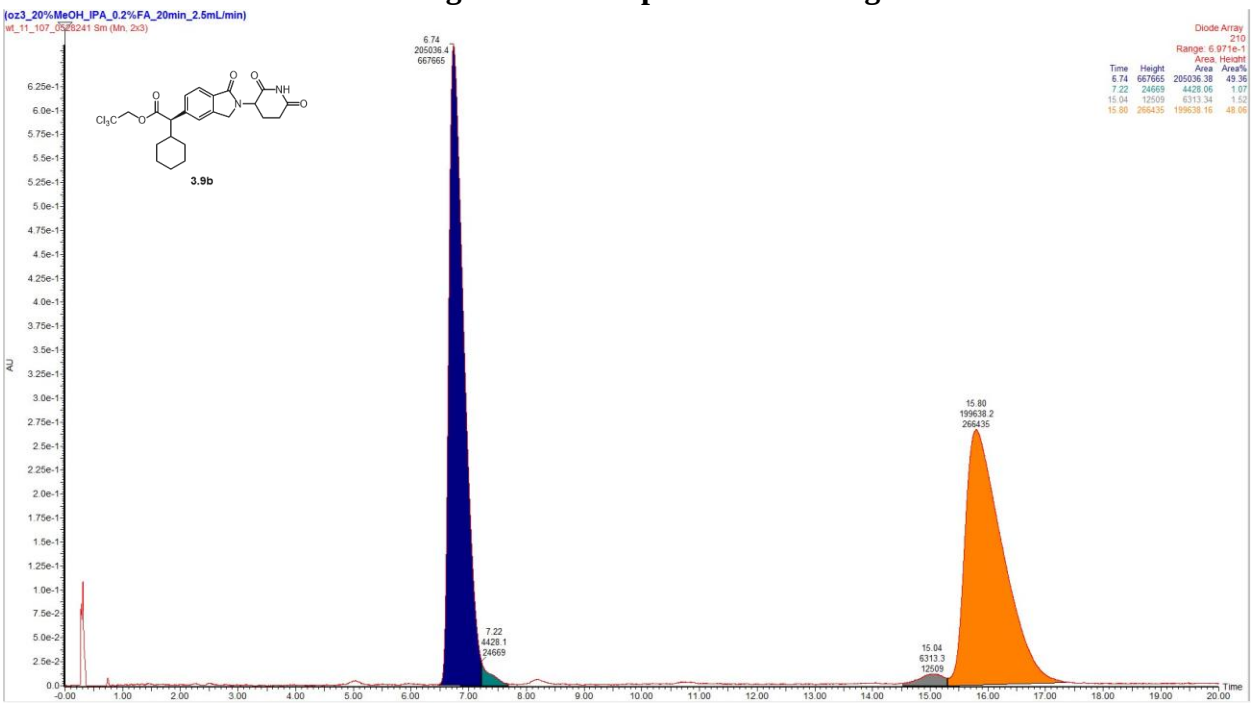

Chromatogram for Compound 3.9b Using GP3

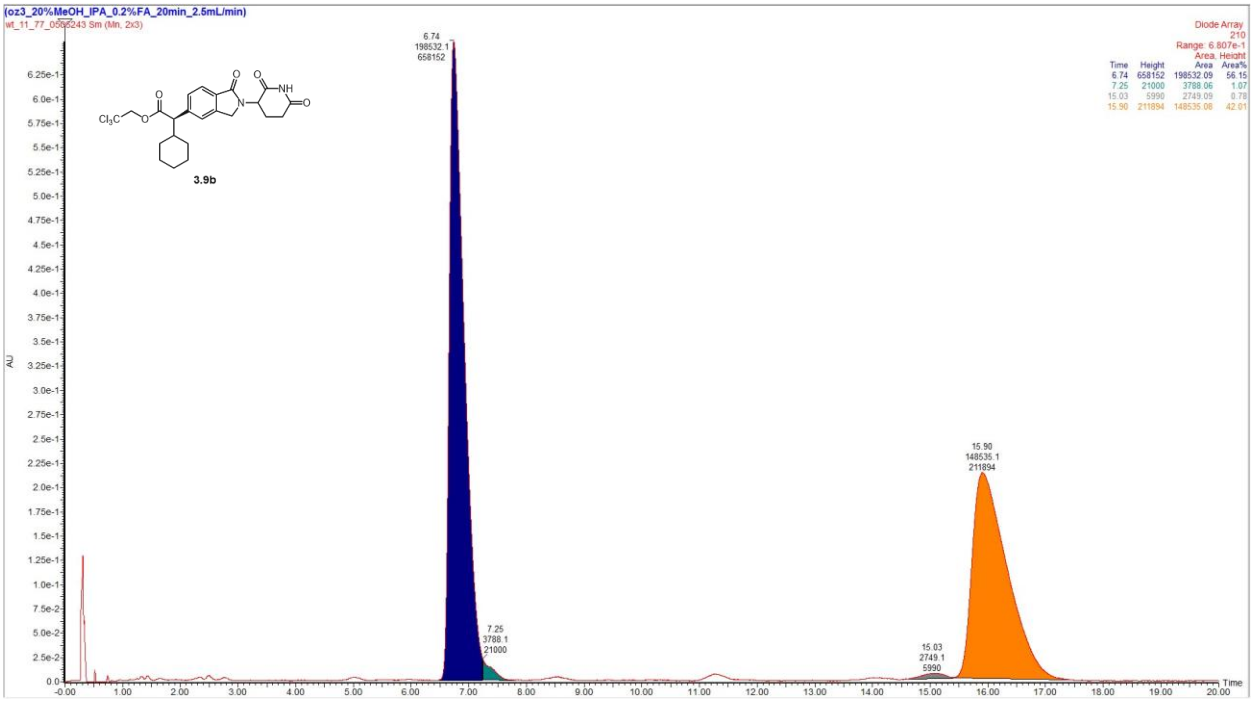

Racemic Chromatogram for Compound 3.9c

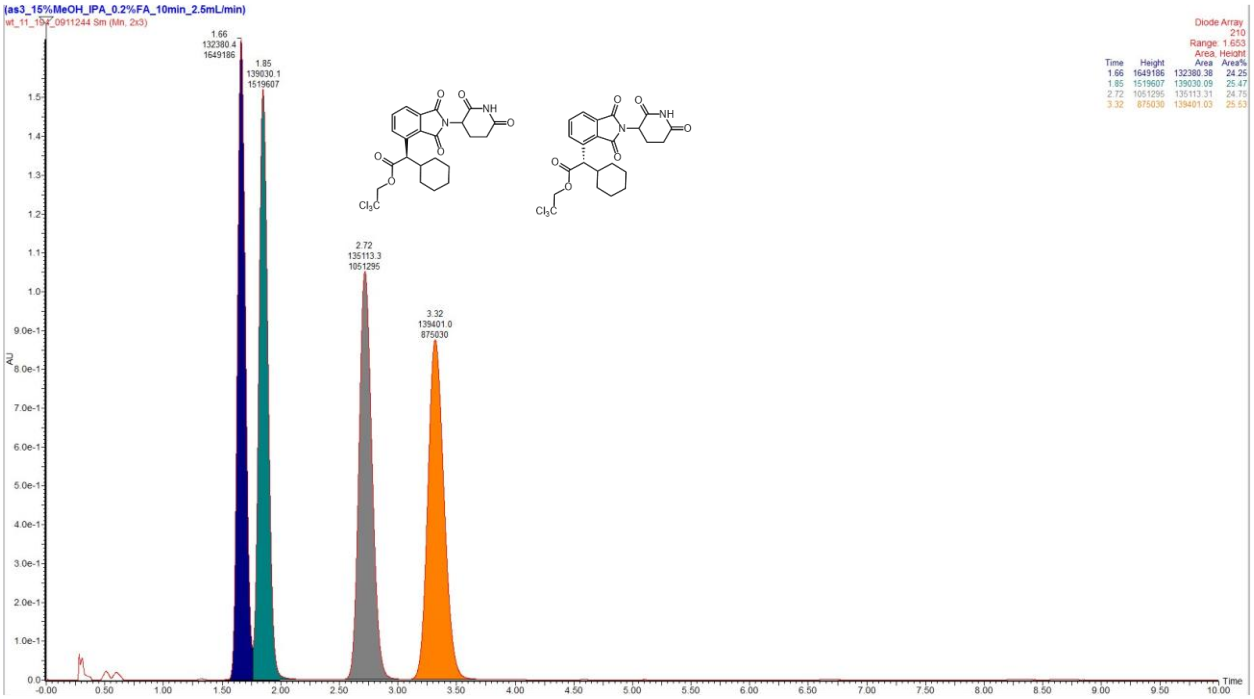

Chromatogram for Compound 3.9c Using GP1

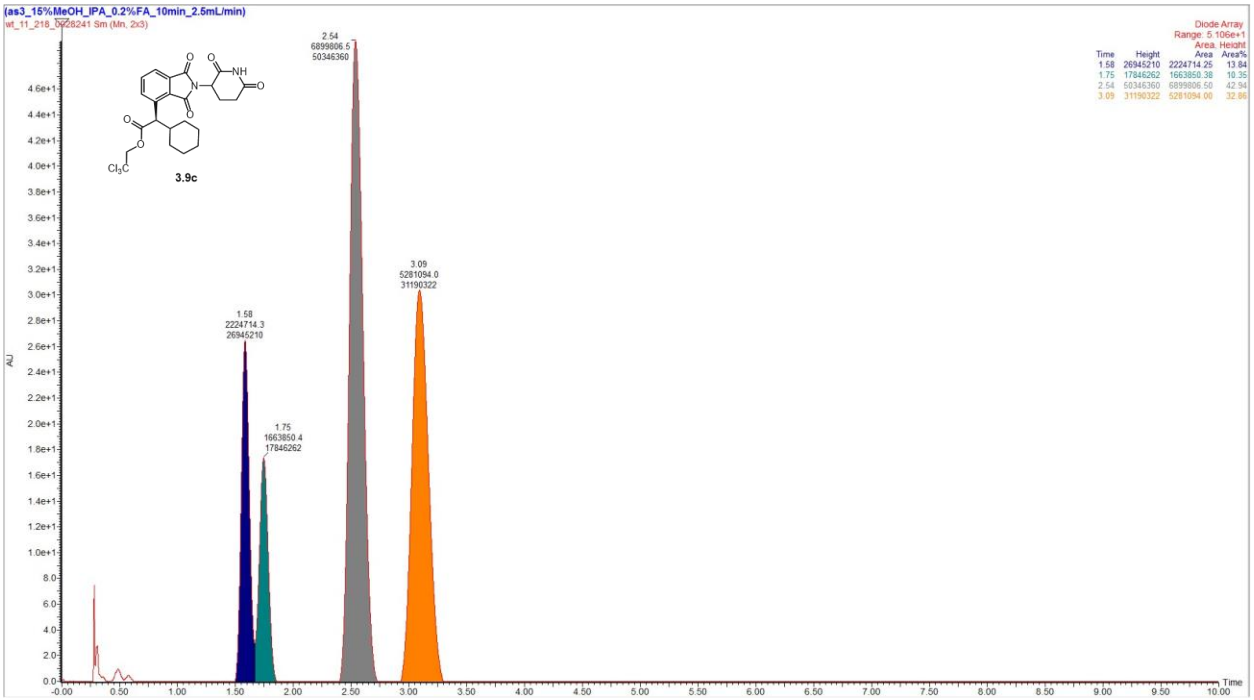

Chromatogram for Compound 3.9c Using GP3

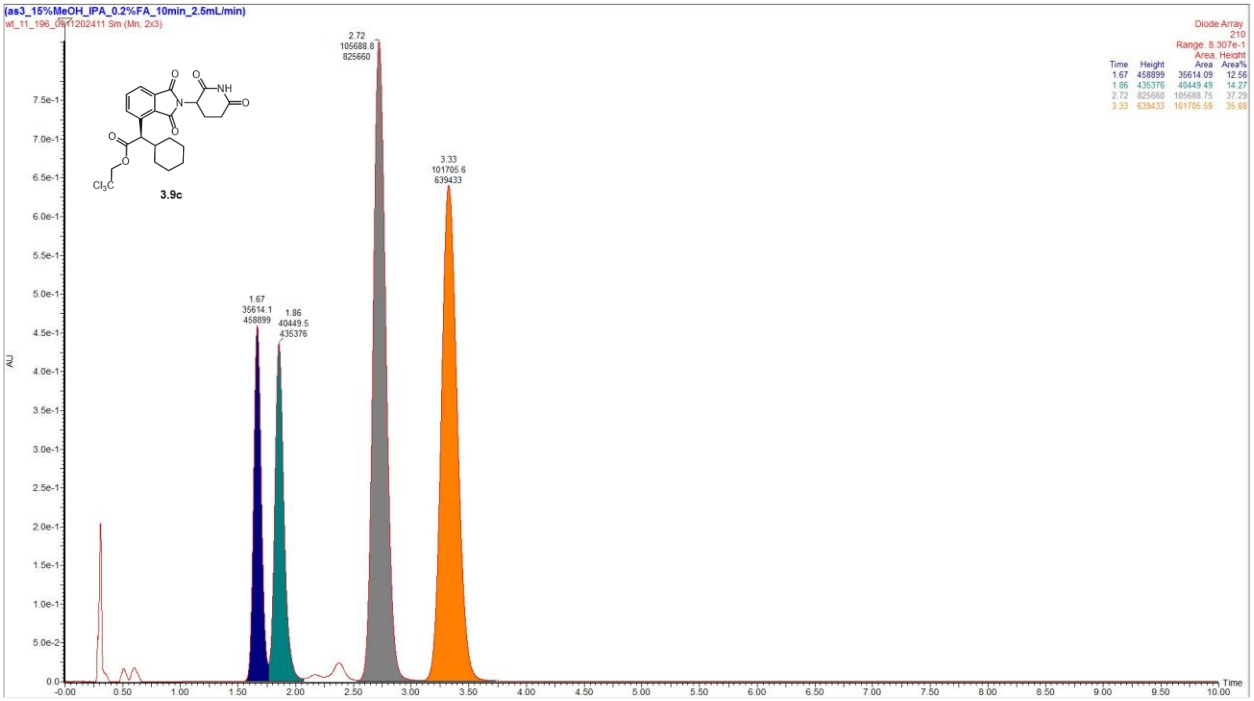

Racemic Chromatogram for Compound 3.10a

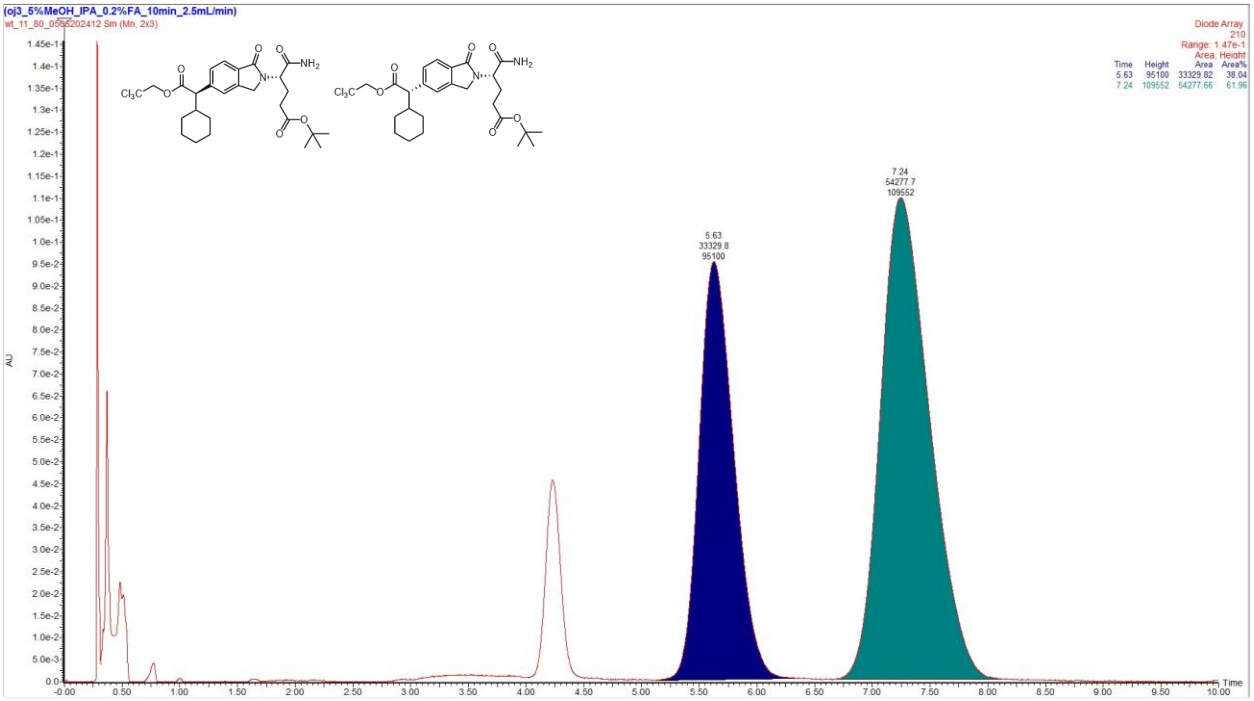

Chromatogram for Compound (S,R)-3.10a Using GP1

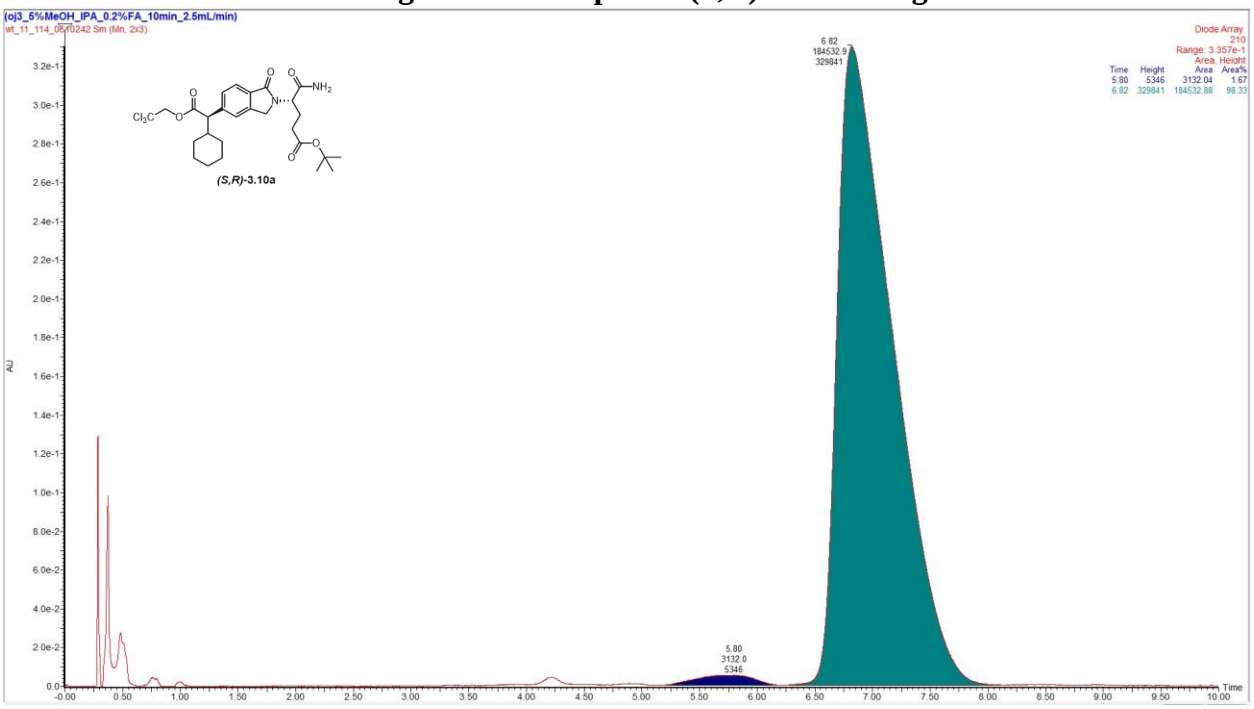

Chromatogram for Compound (S,R)-3.10a Using GP4

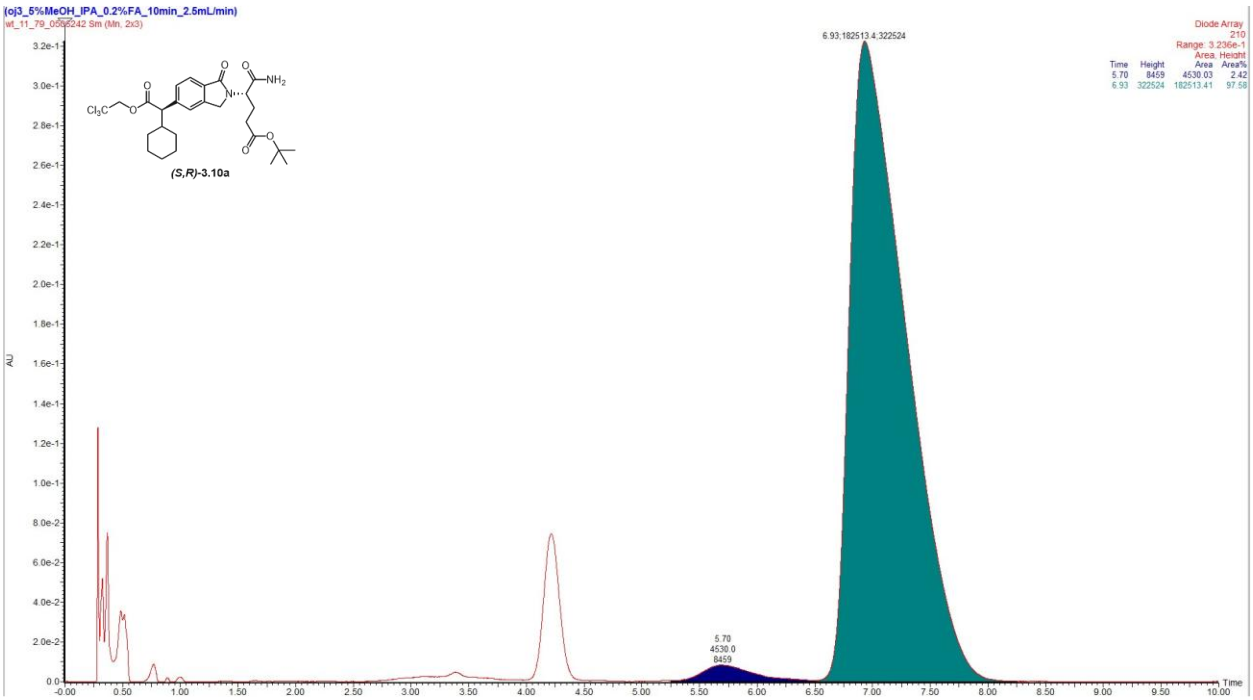

Chromatogram for Compound (S,S)-3.10a Using GP4

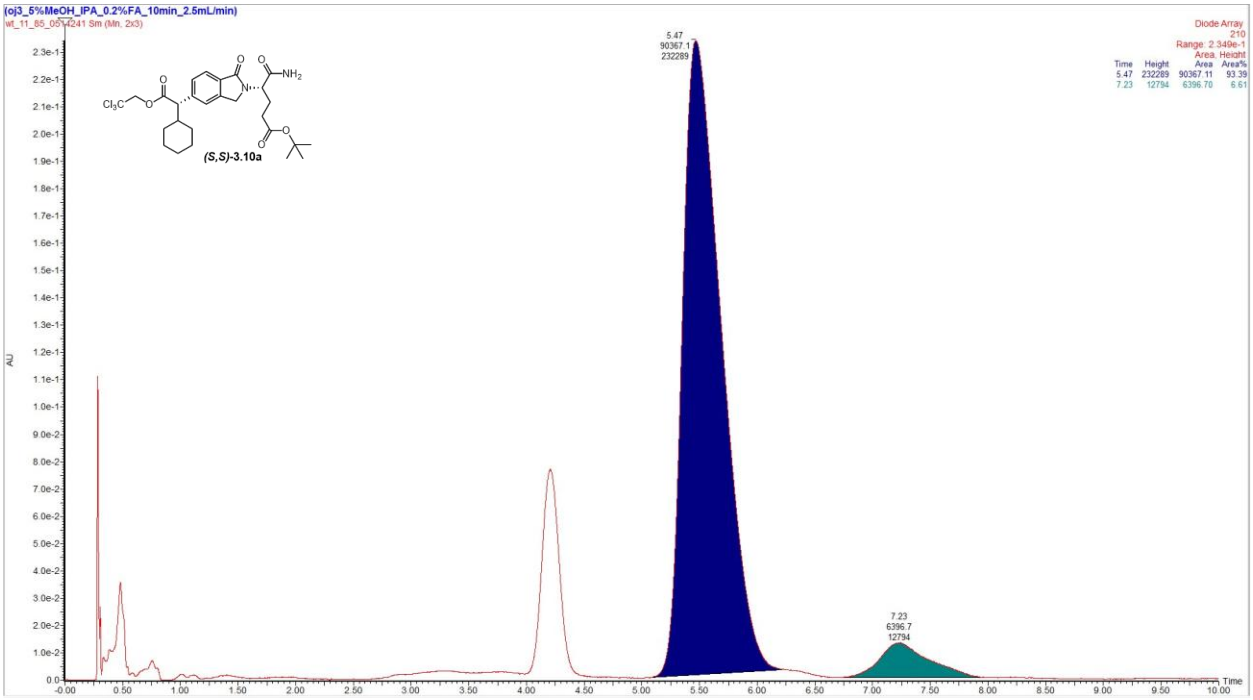

Racemic Chromatogram for Compound 3.10b

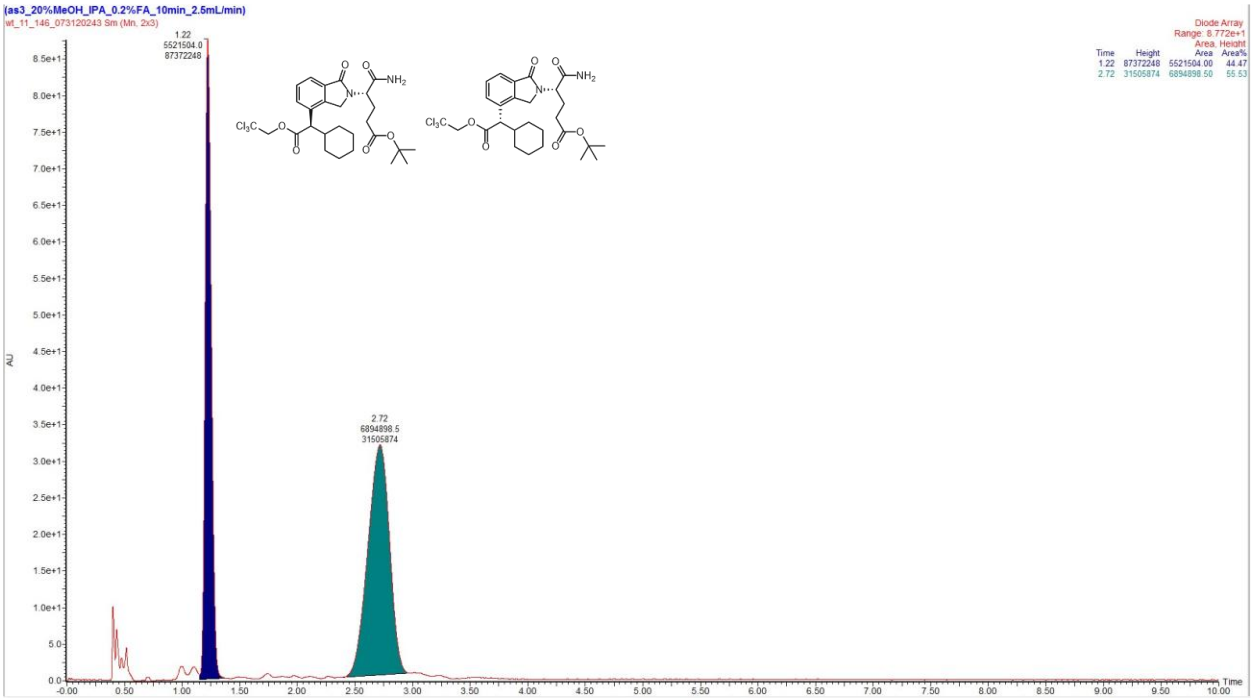

Chromatogram for Compound 3.10b Using GP1

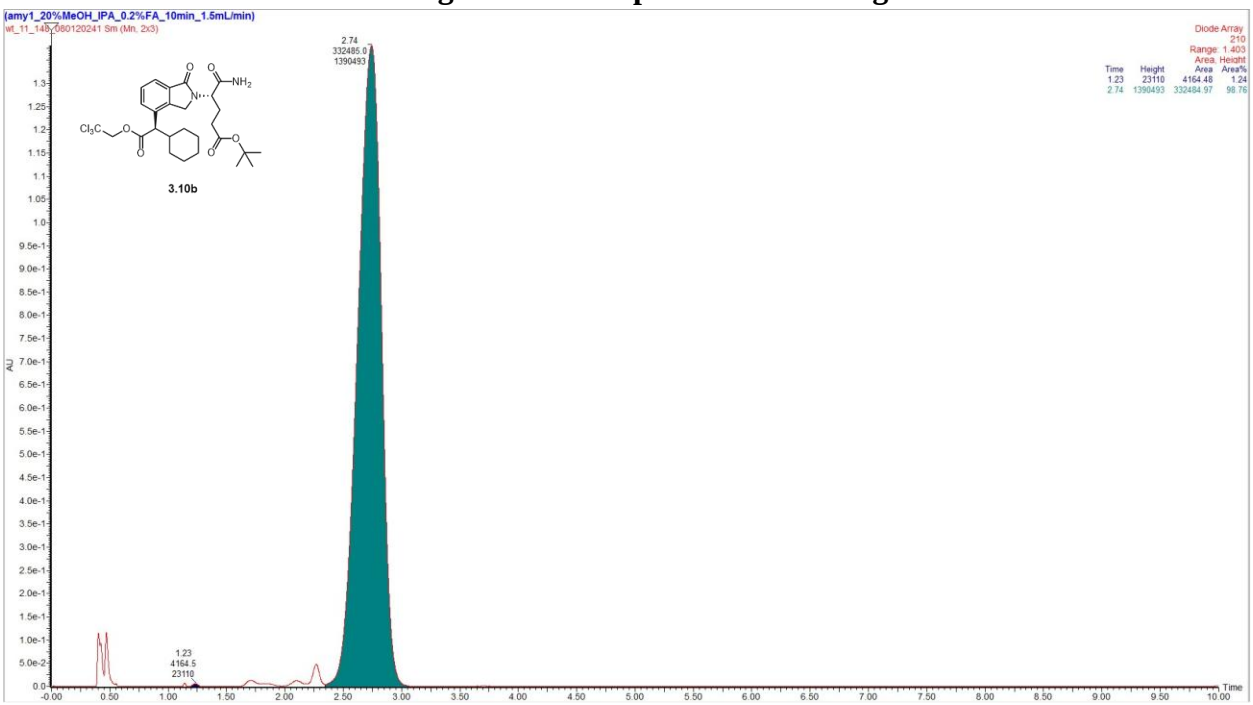

Chromatogram for Compound 3.10b Using GP4

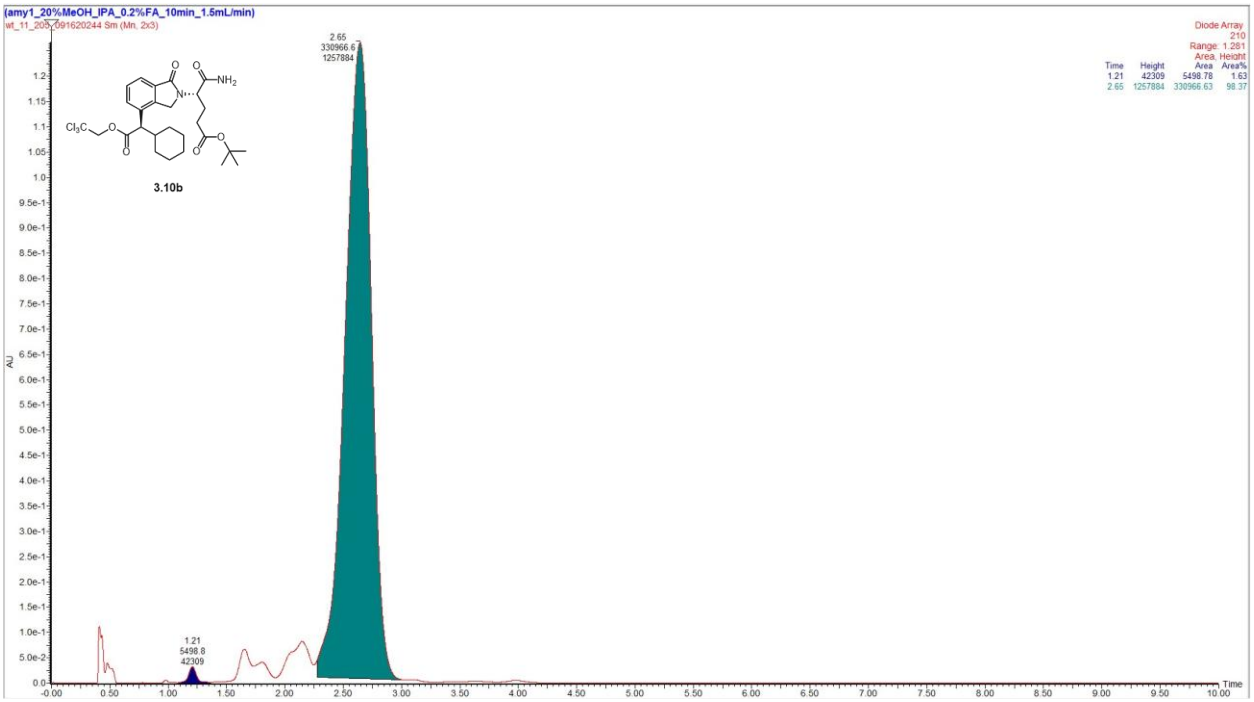

Racemic Chromatogram for Compound 3.11a

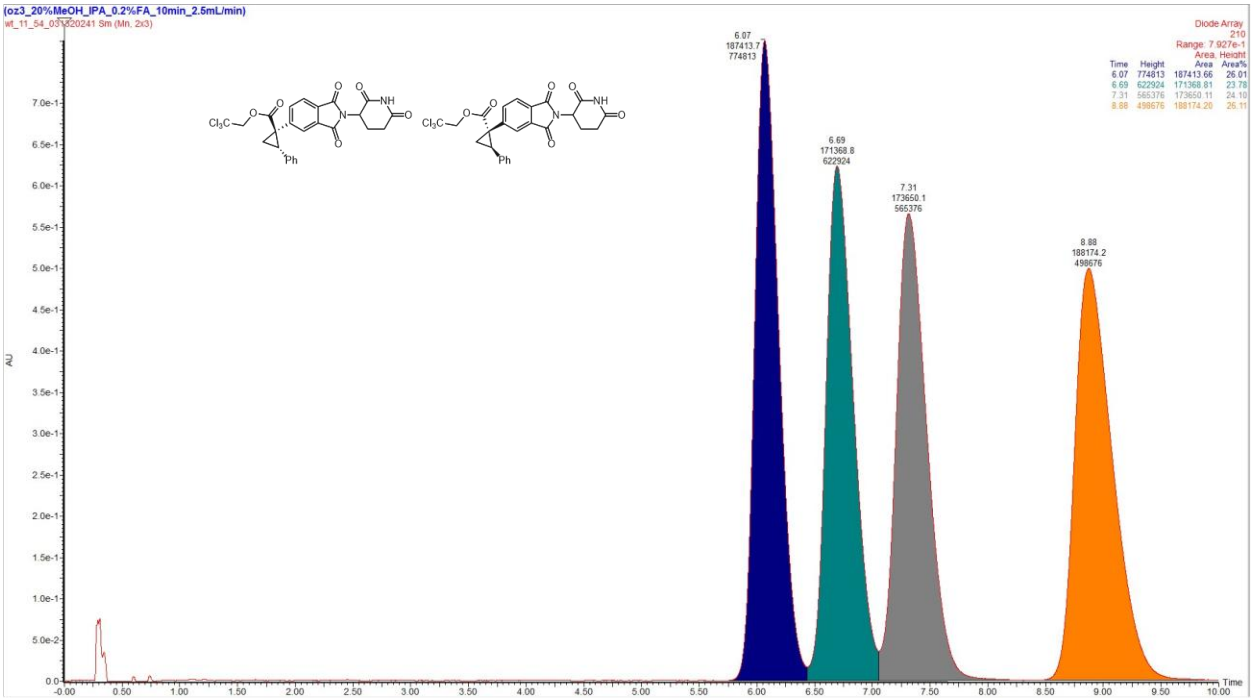

Chromatogram for Compound 3.11a Using GP5

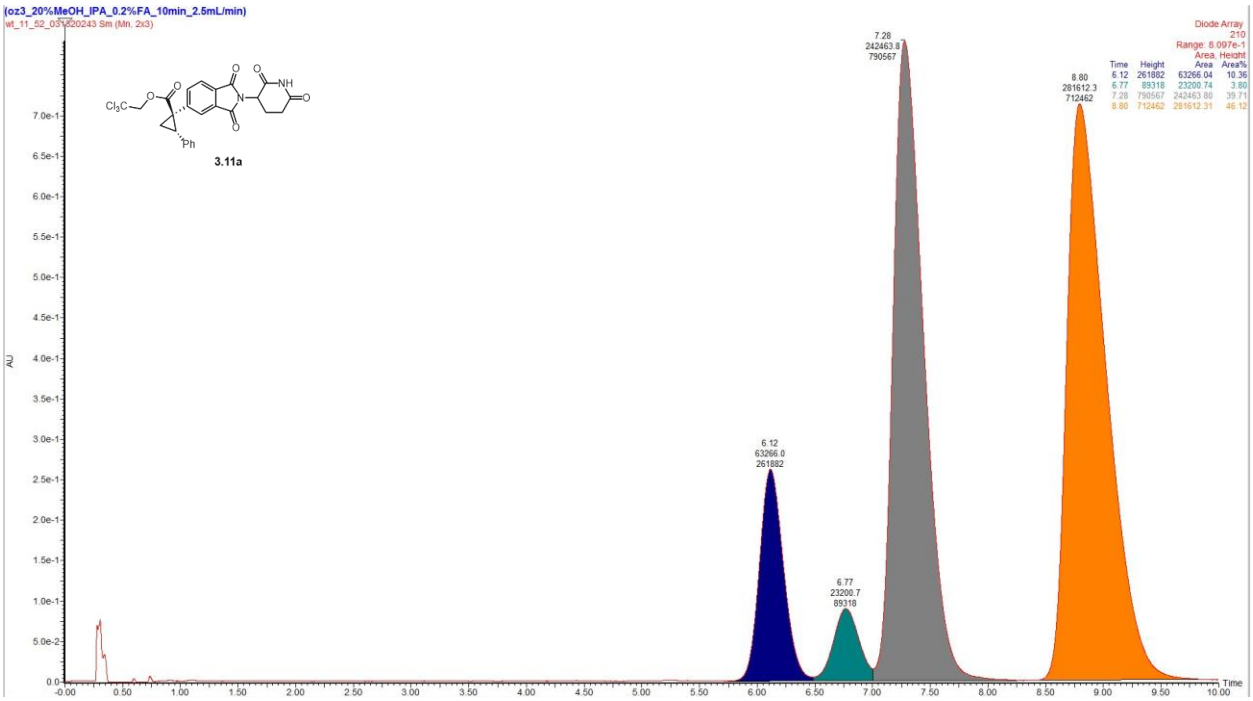

Racemic Chromatogram for Compound 3.11b

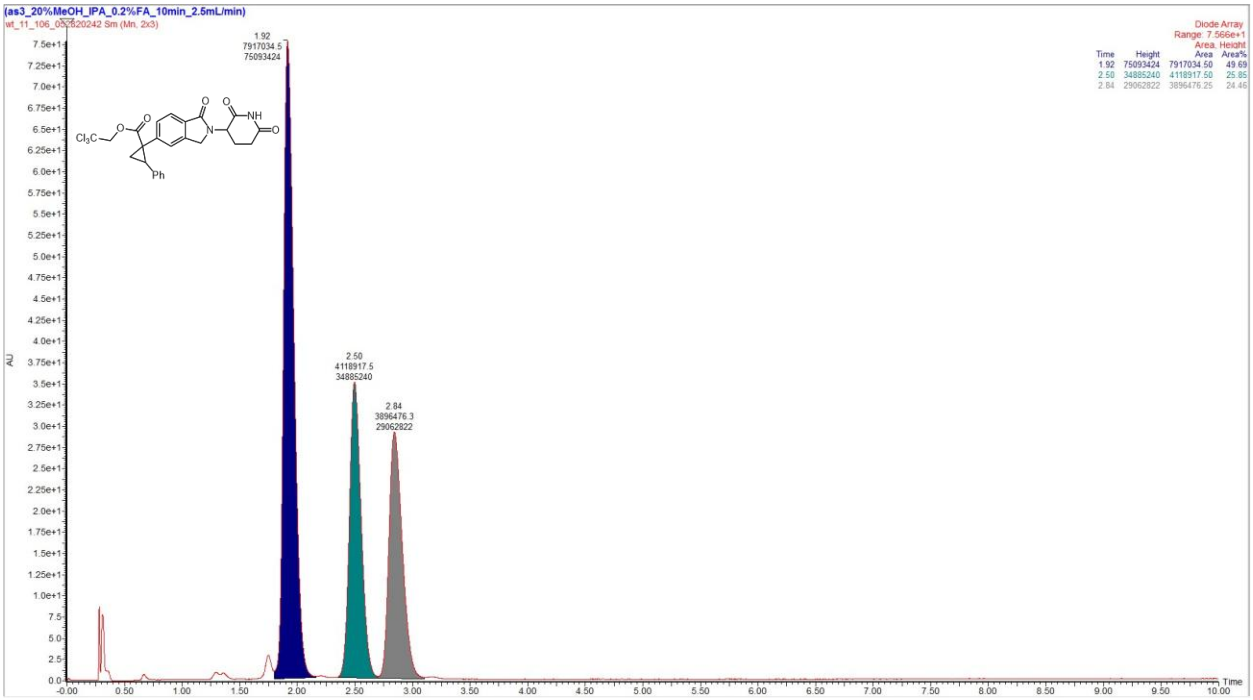

Chromatogram for Compound 3.11b Using GP5

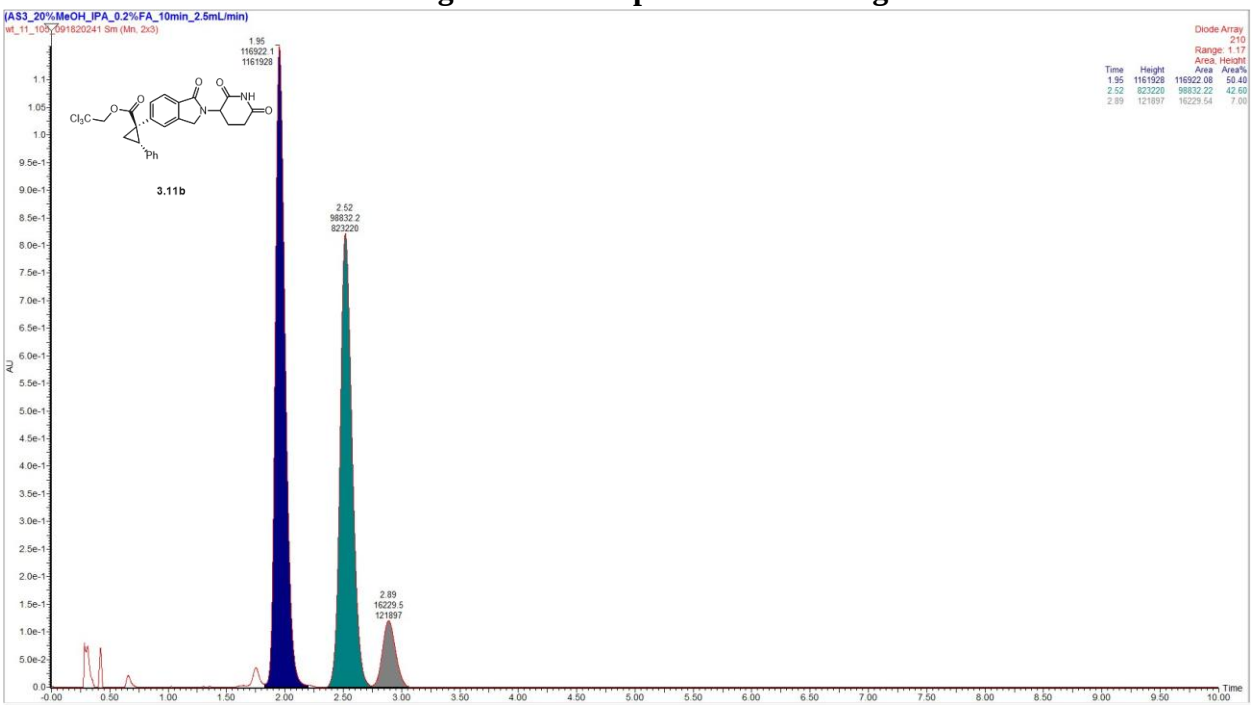

Racemic Chromatogram for Compound 3.11c

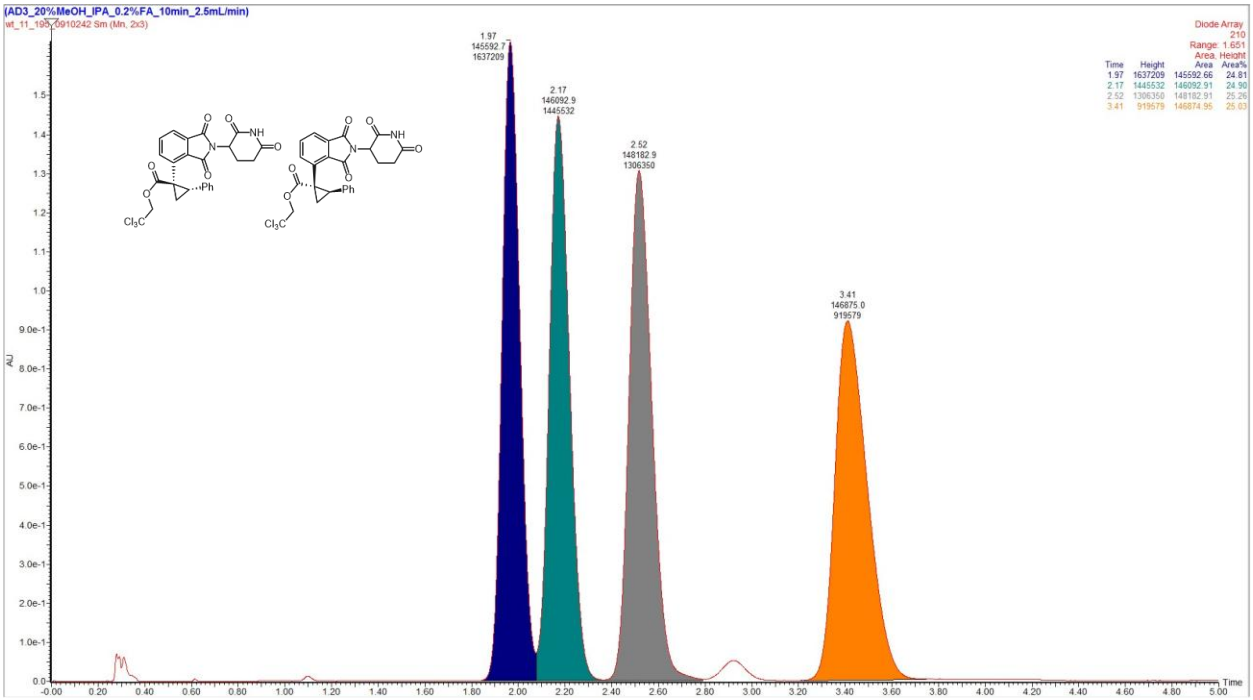

Chromatogram for Compound 3.11c Using GP5

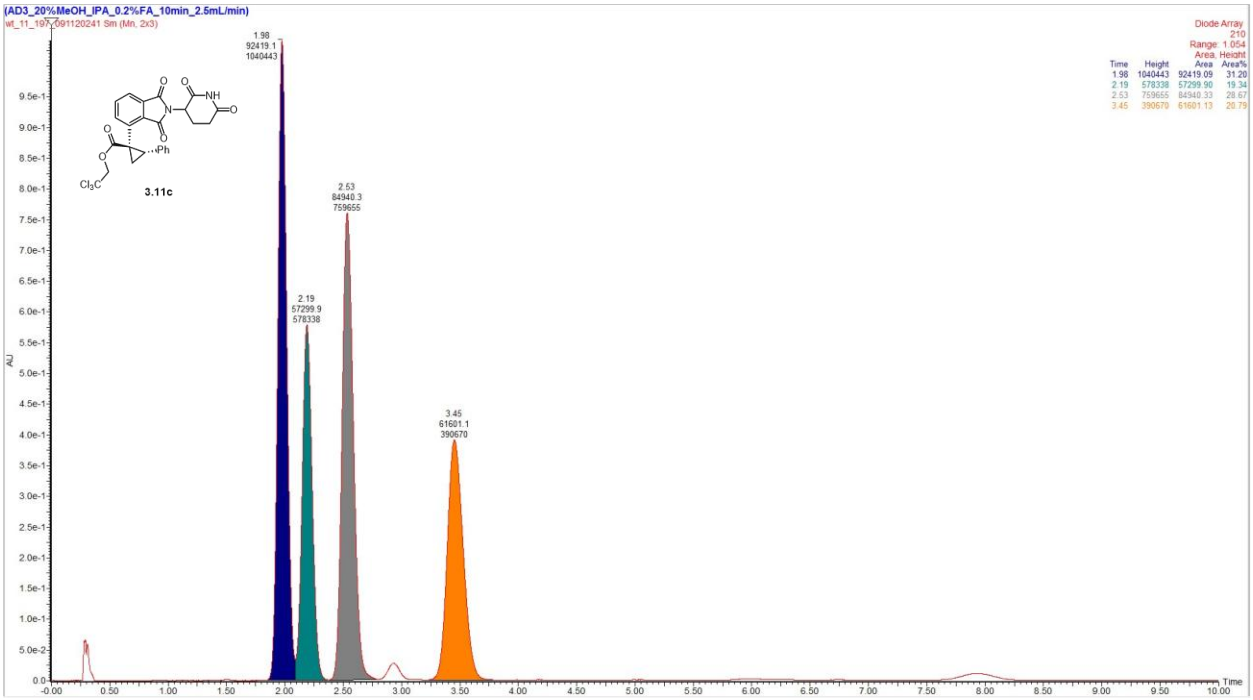

Racemic Chromatogram for Compound 3.12a

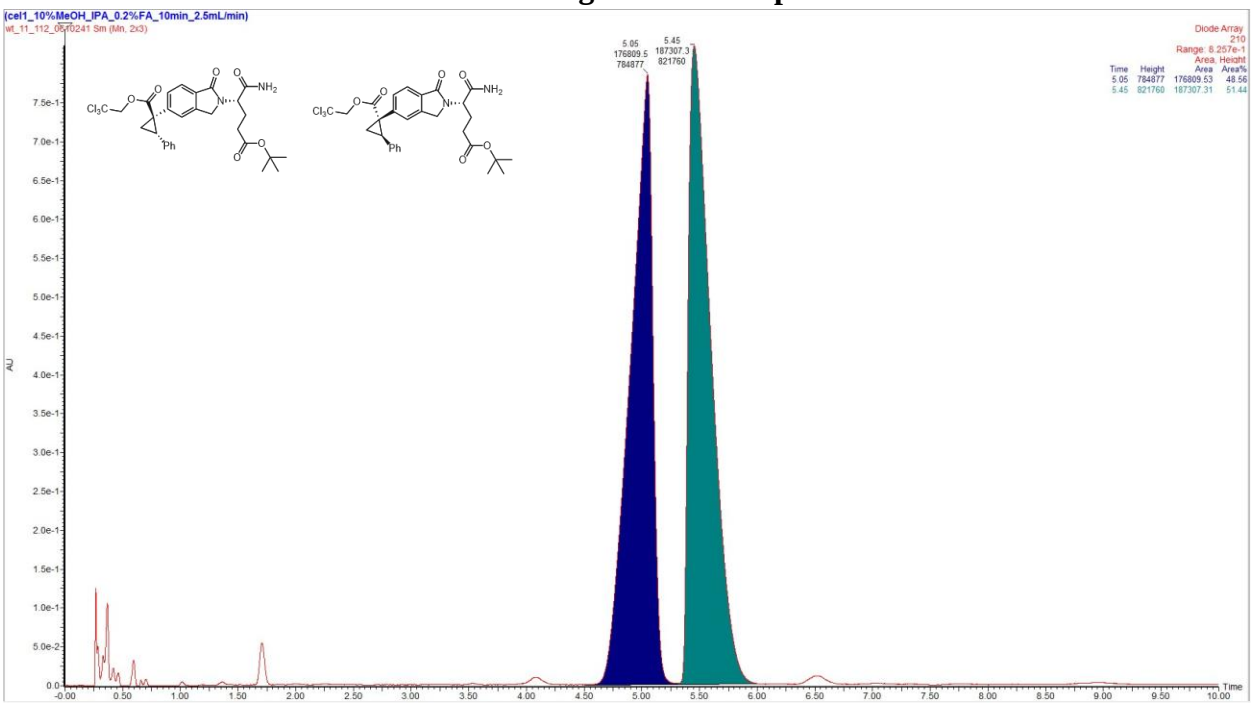

Chromatogram for Compound 3.12a Using GP6

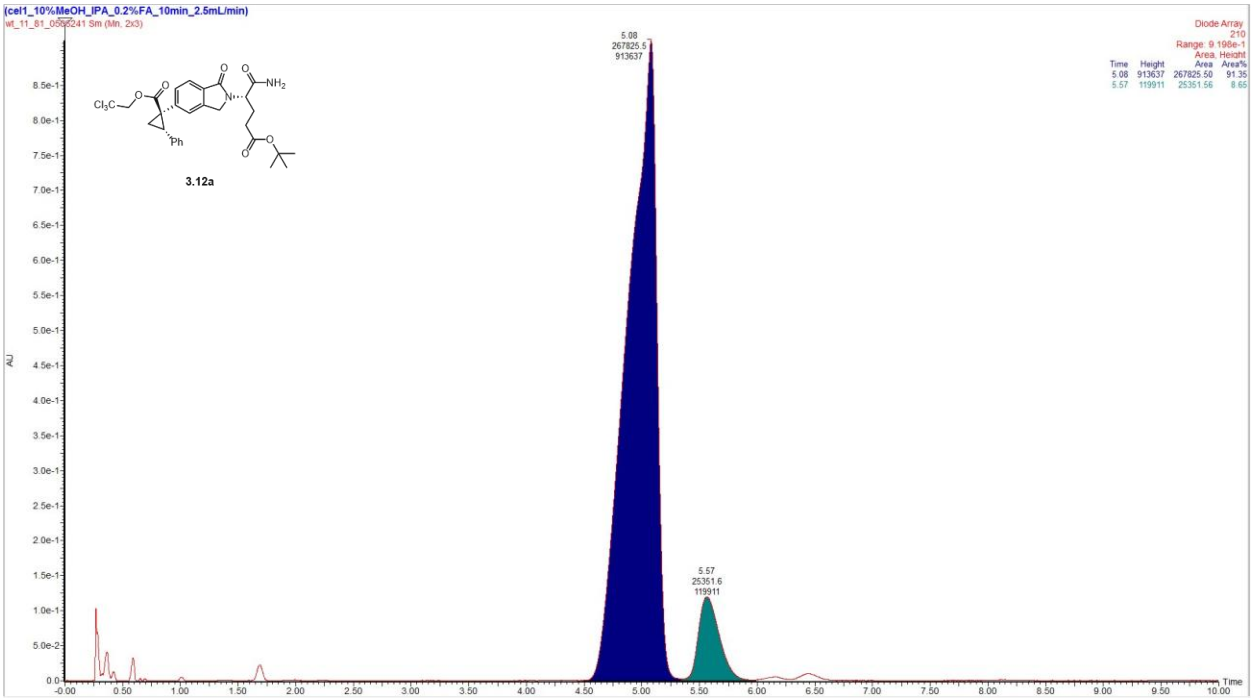

Racemic Chromatogram for Compound 3.12b

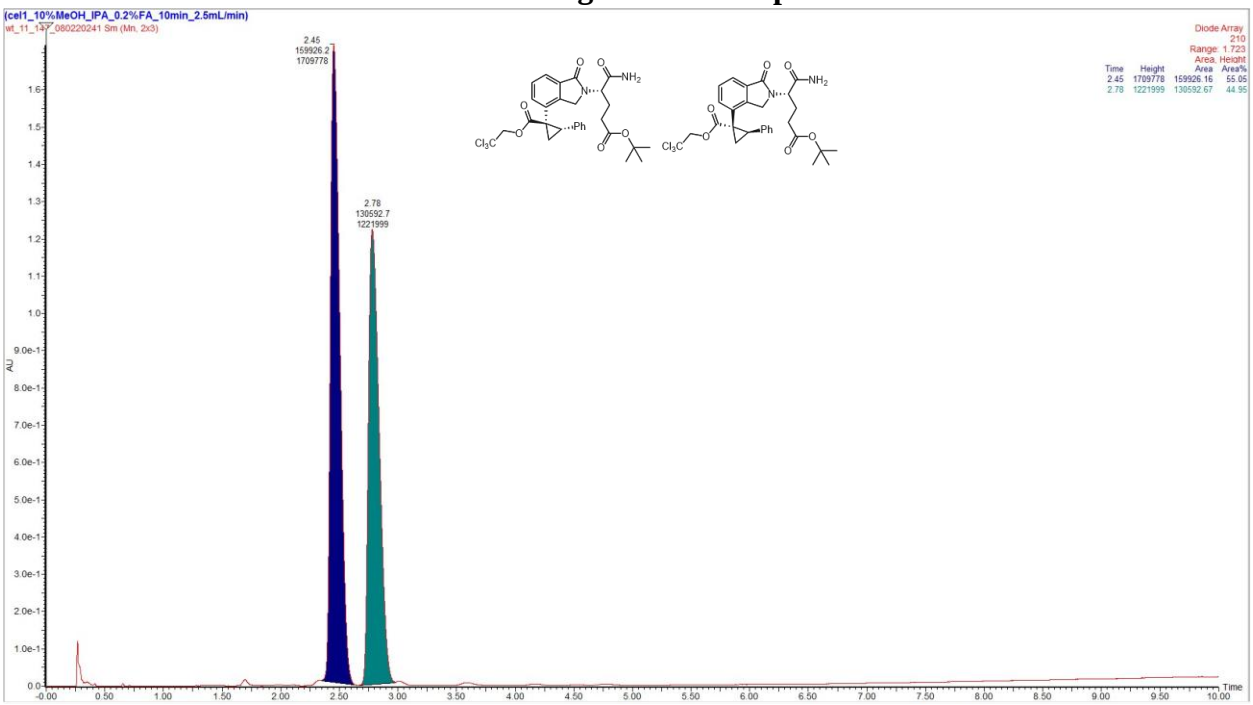

Chromatogram for Compound 3.12b Using GP6

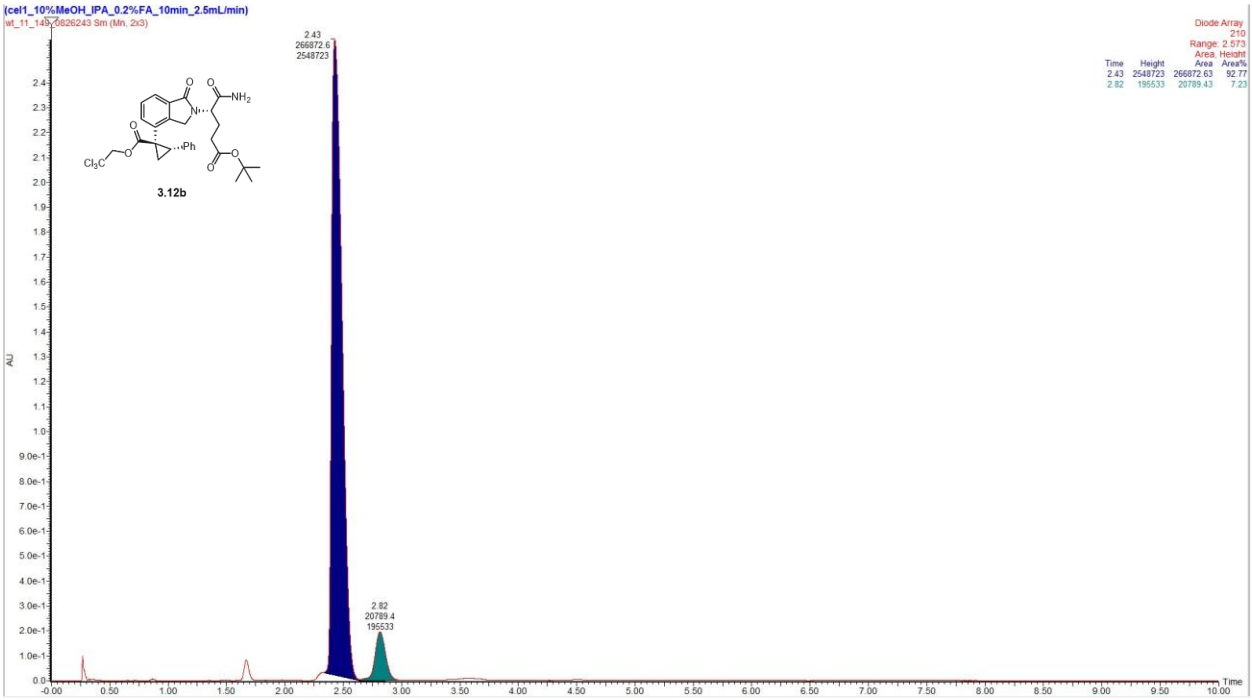

Racemic Chromatogram for Compound 3.13

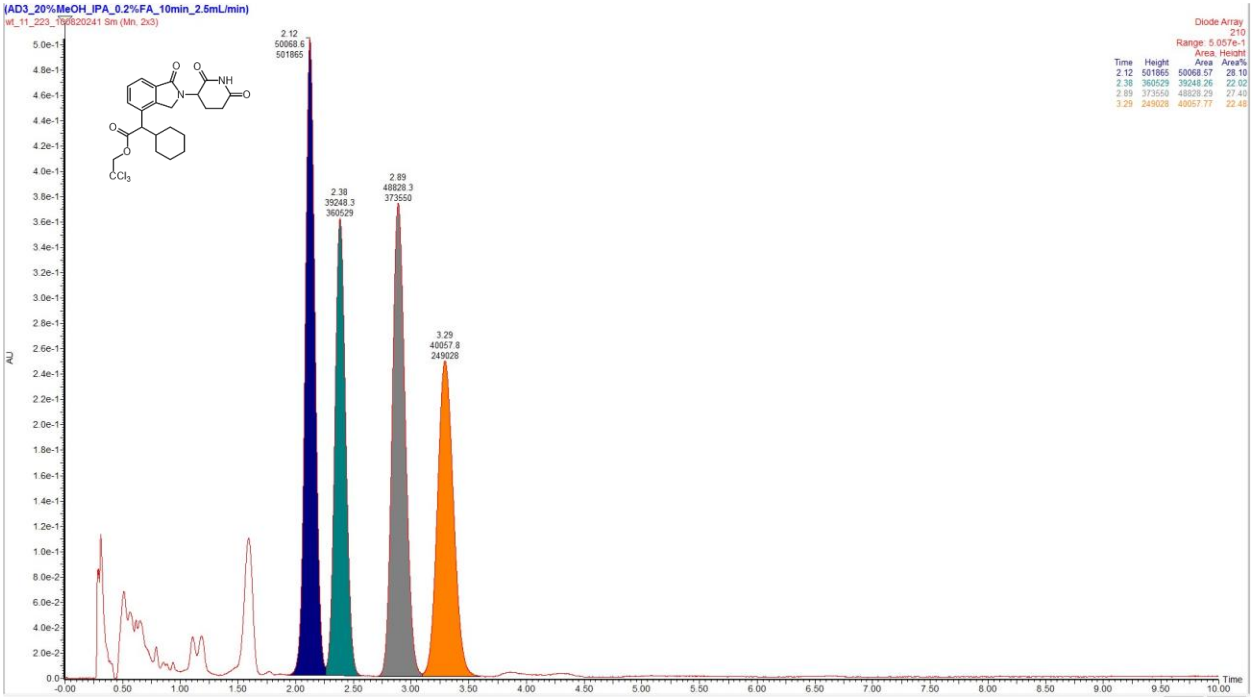

Chromatogram for Compound 3.13

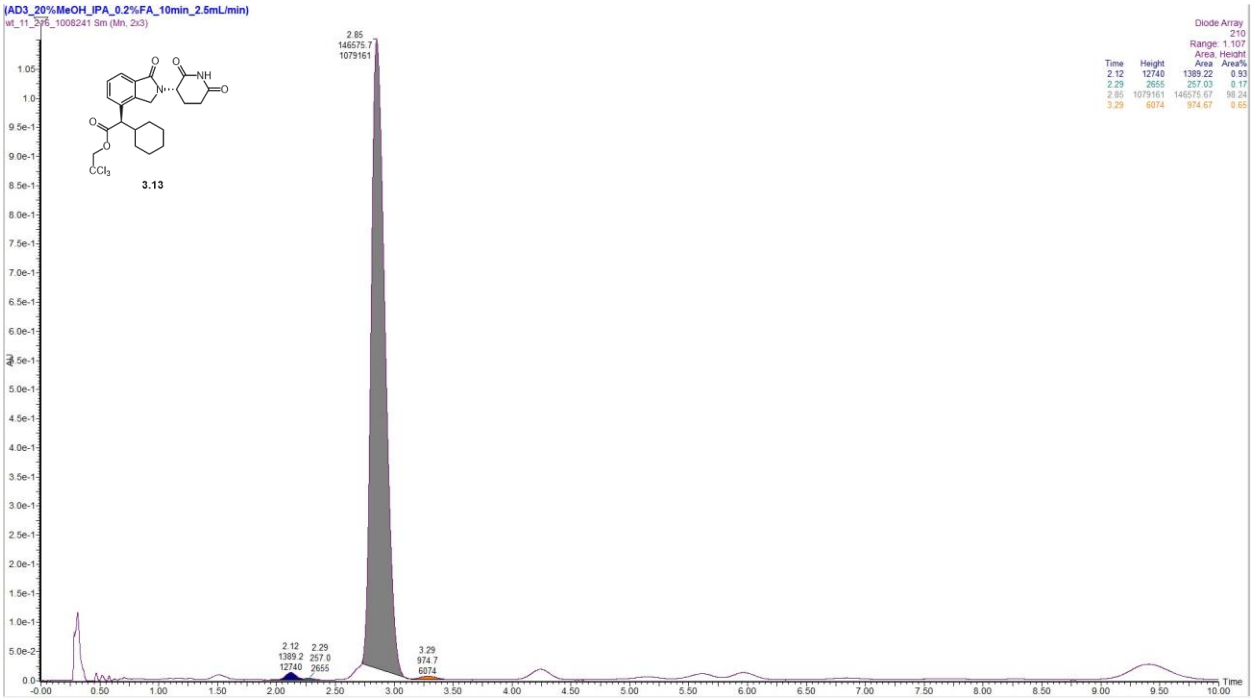

Racemic Chromatogram for Compound 3.14 and Chromatogram for Compound 3.14 Using GP1, Major Relative Diastereomer (2R,3S)- 3.14

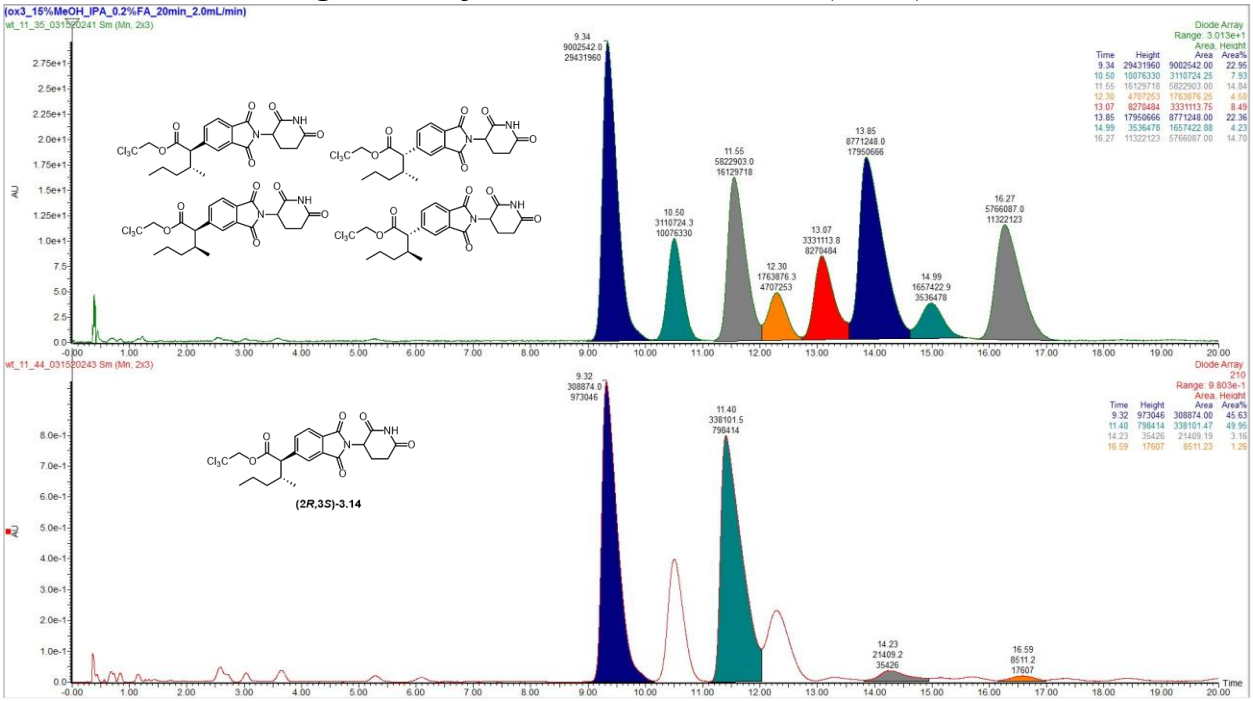

Racemic Chromatogram for Compound 3.14 and Chromatogram for Compound 3.14 Using GP1, Minor Relative Diastereomer (2R,3R)- 3.14

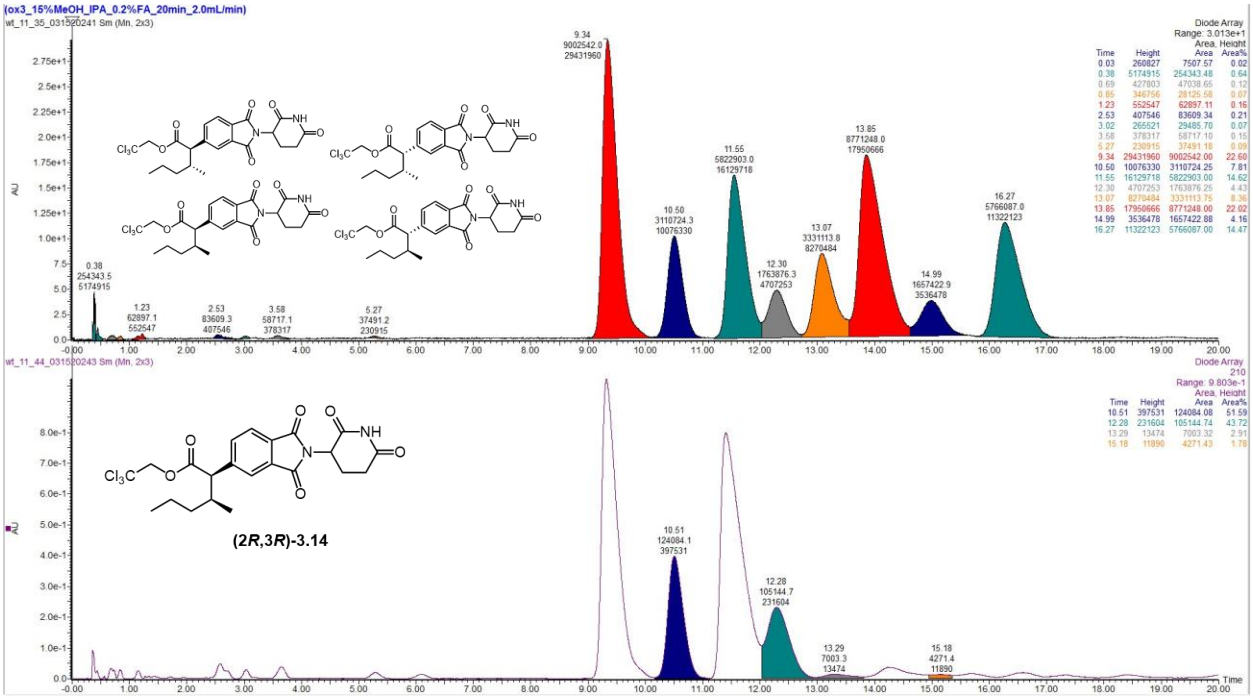

Racemic Chromatogram for Compound 3.15

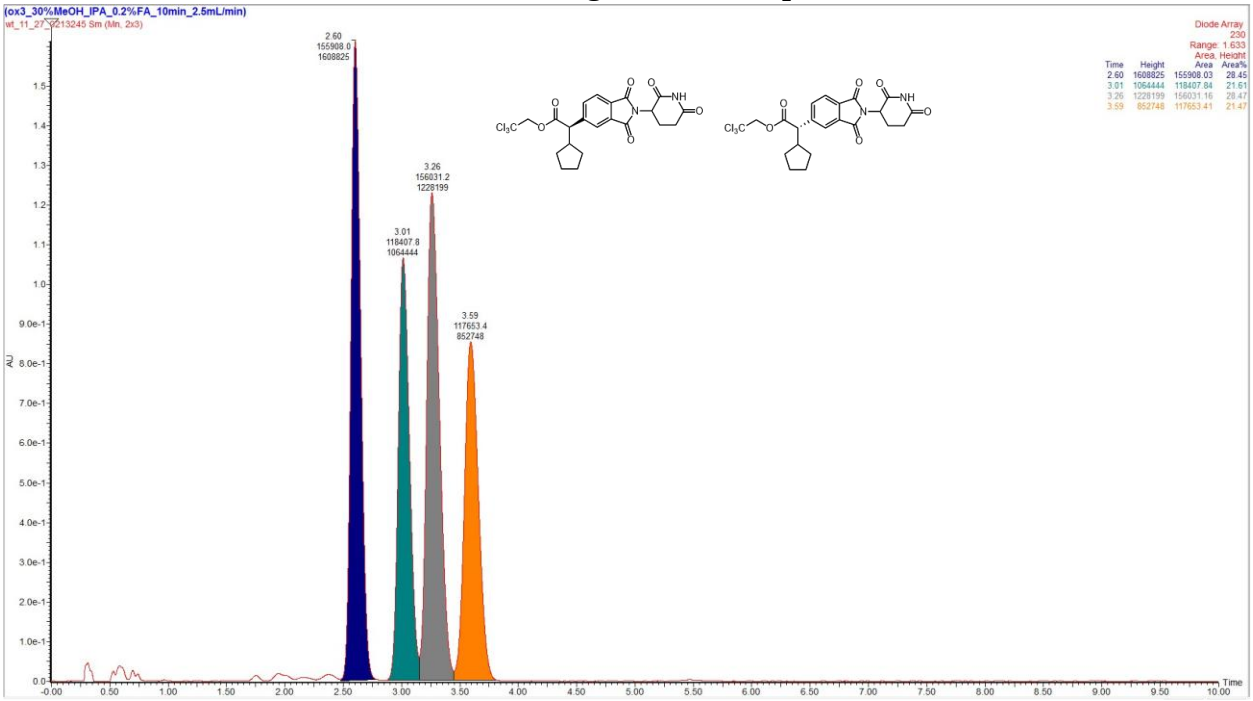

Chromatogram for Compound 3.15 Using GP1

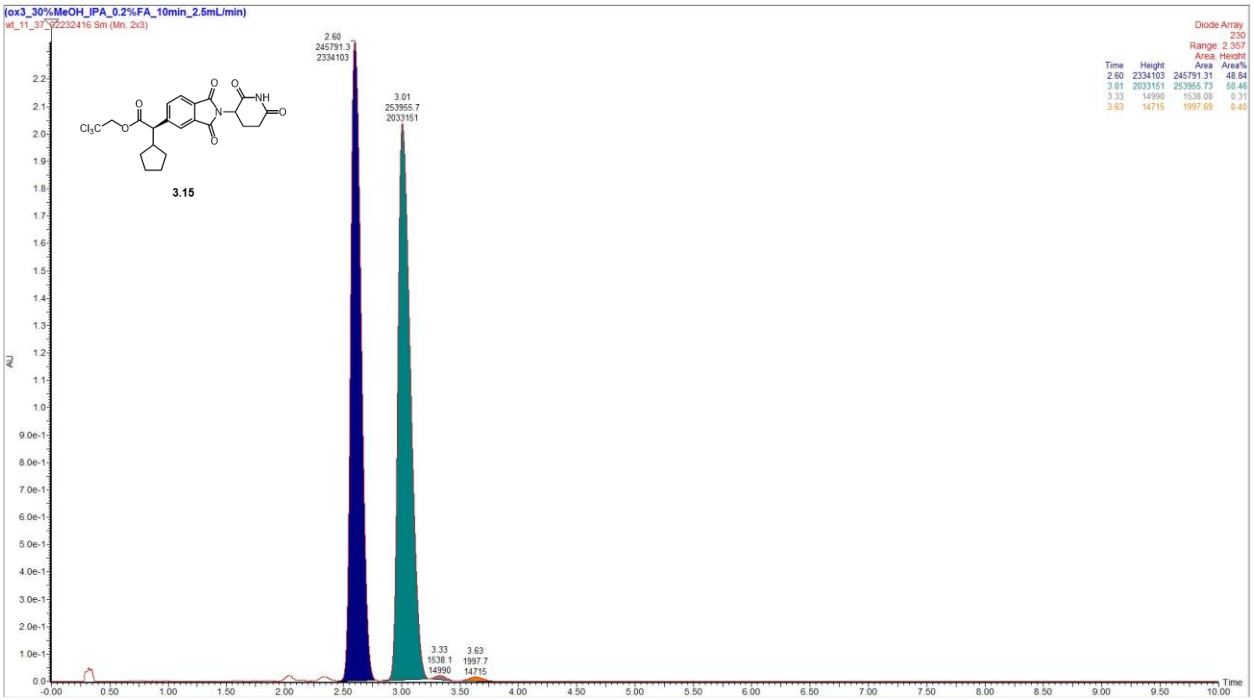

Racemic Chromatogram for Compound 3.16

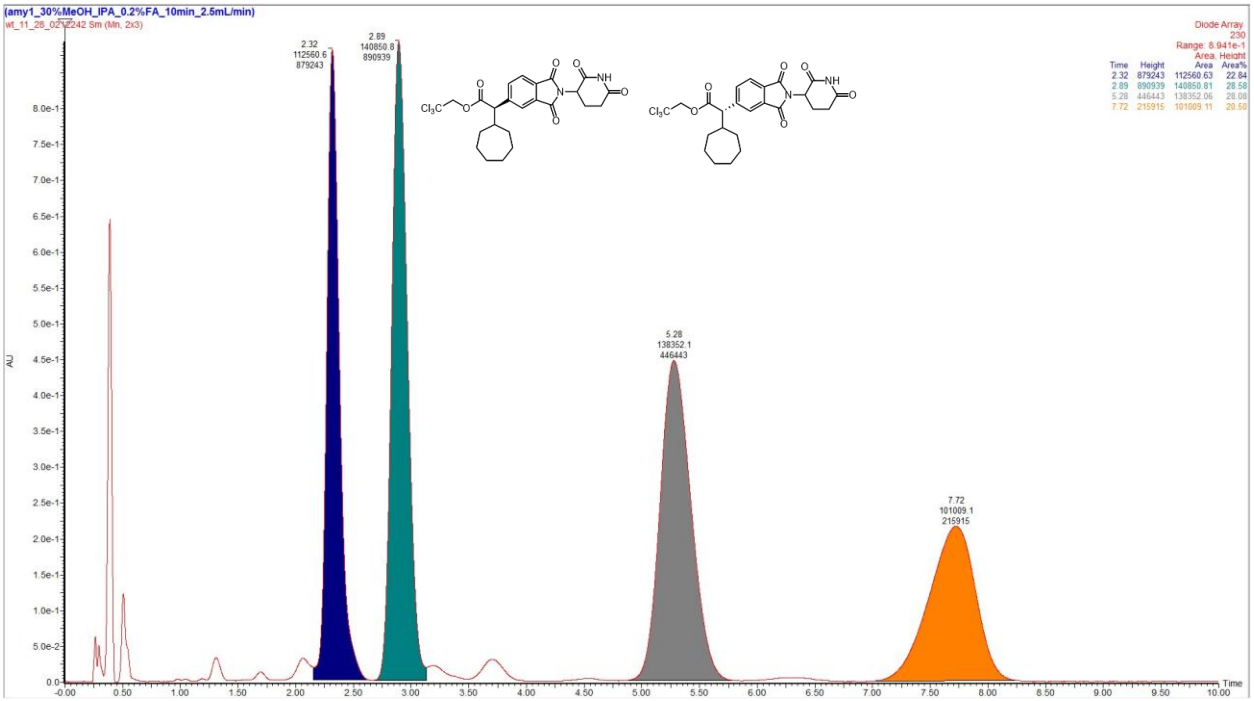

Chromatogram for Compound 3.16 Using GP1

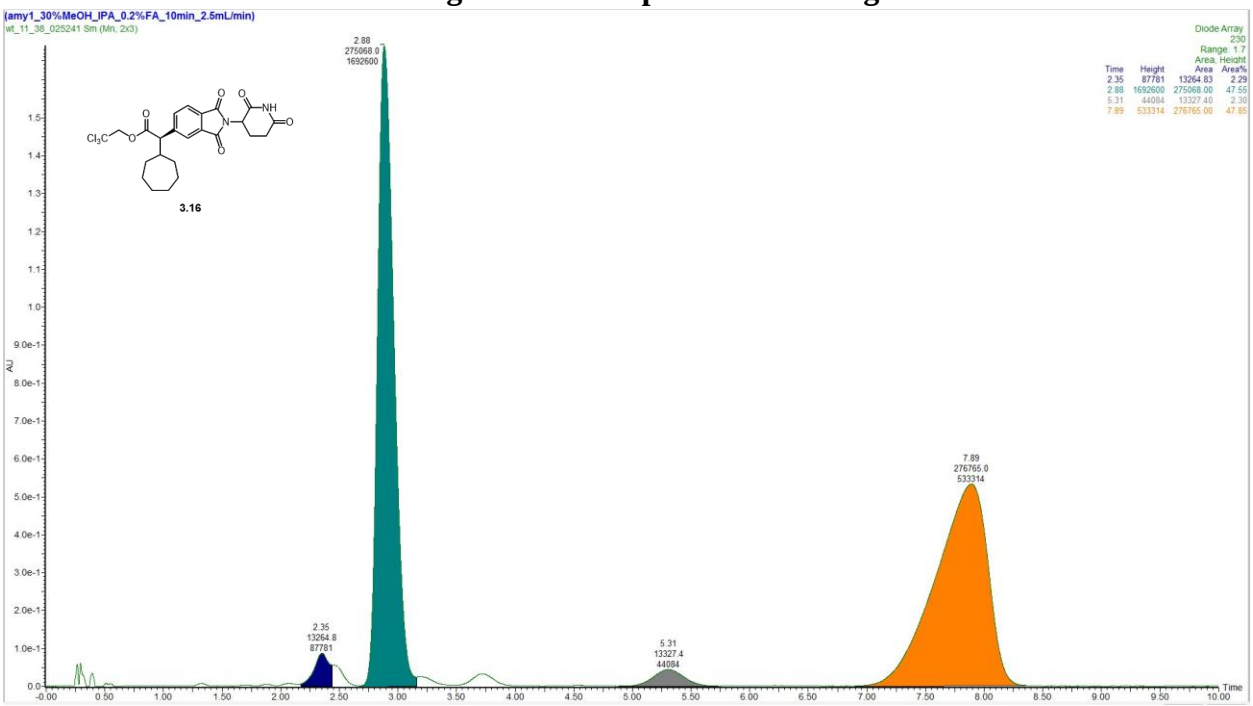

Racemic Chromatogram for Compound 3.17

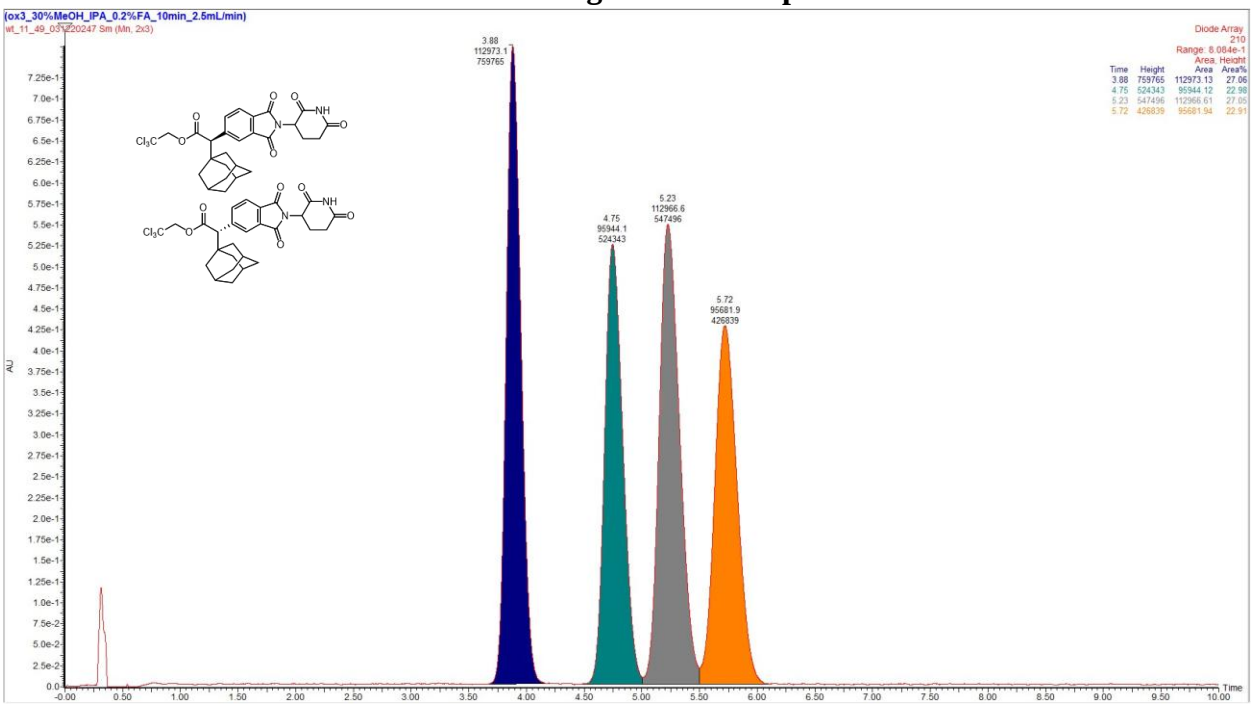

Chromatogram for Compound 3.17 Using GP3

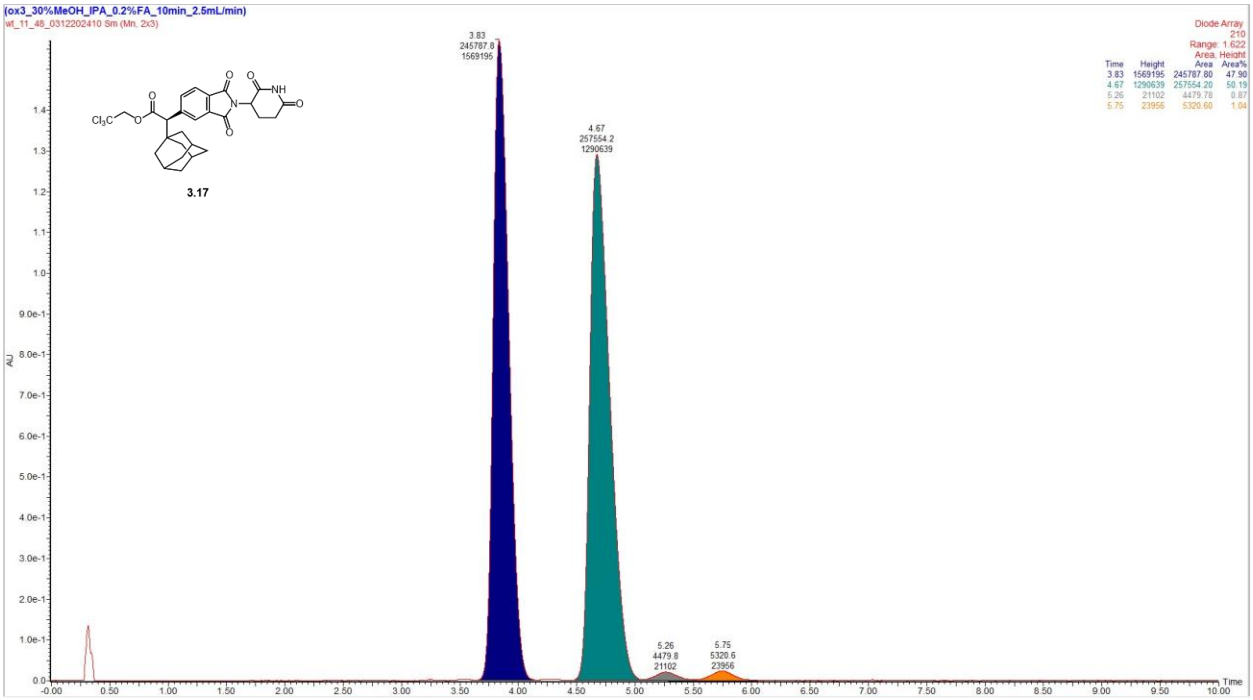

Racemic Chromatogram for Compound 3.18

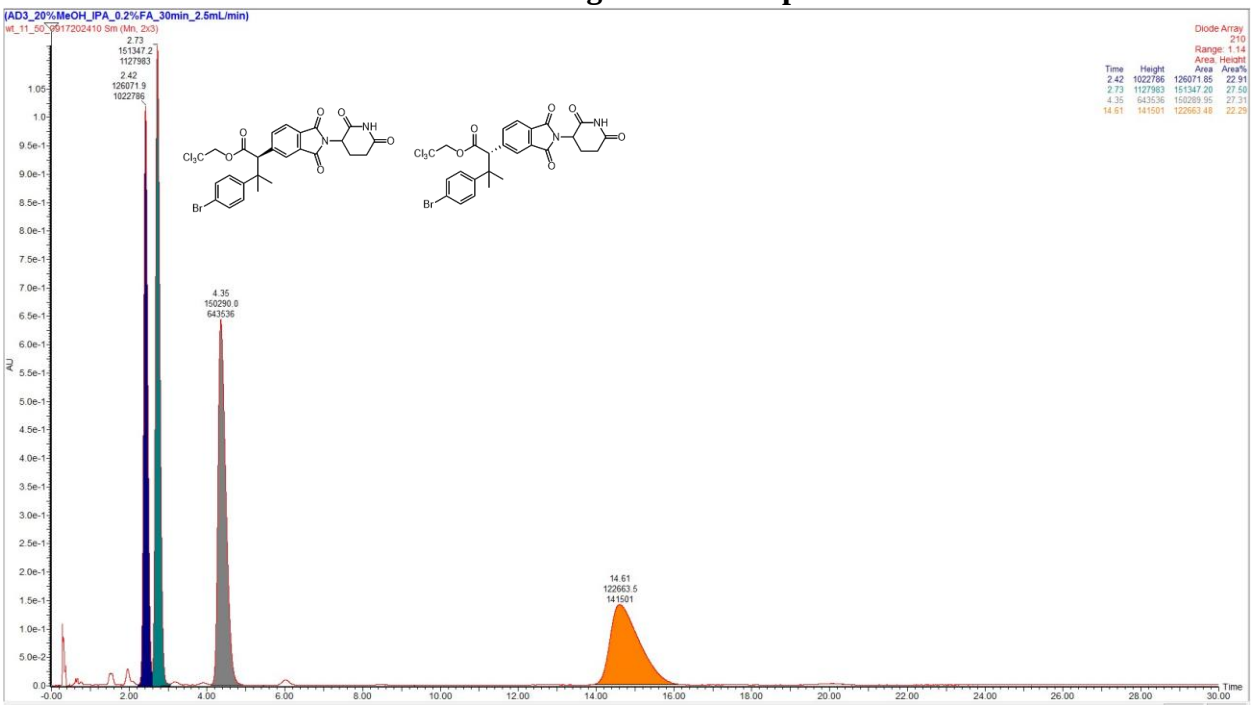

Chromatogram for Compound 3.18 Using GP3

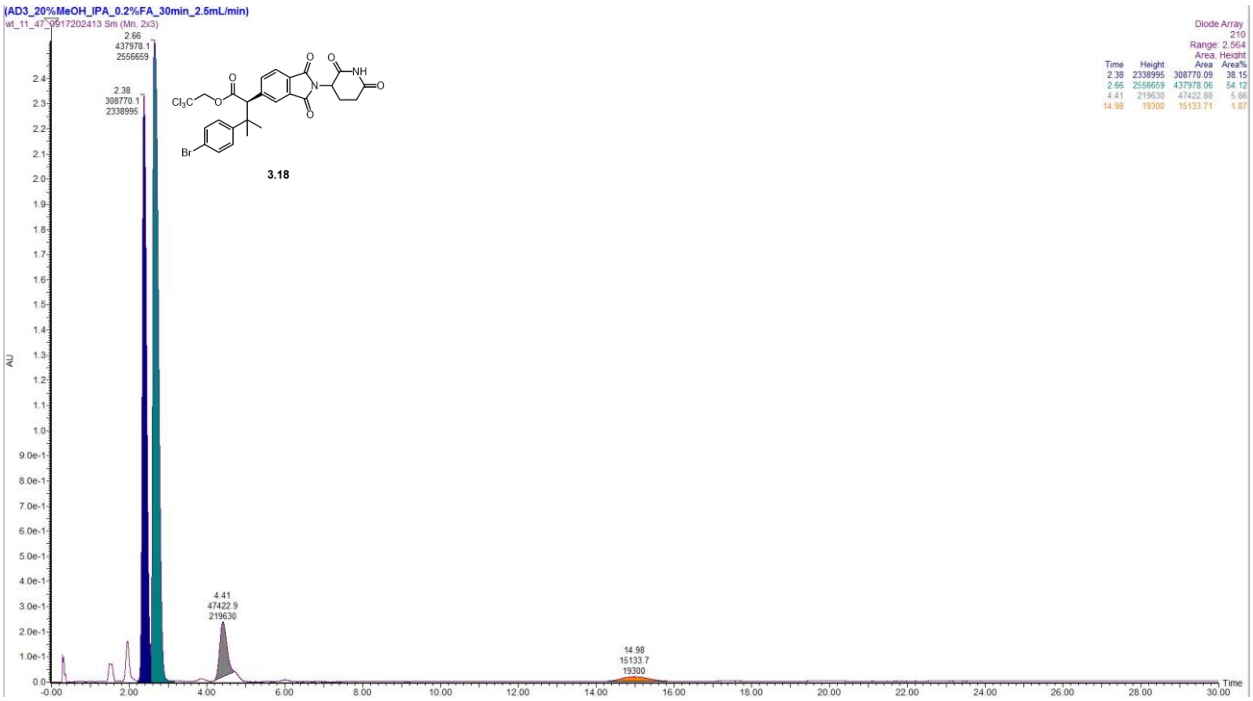

Racemic Chromatogram for Compound 3.19

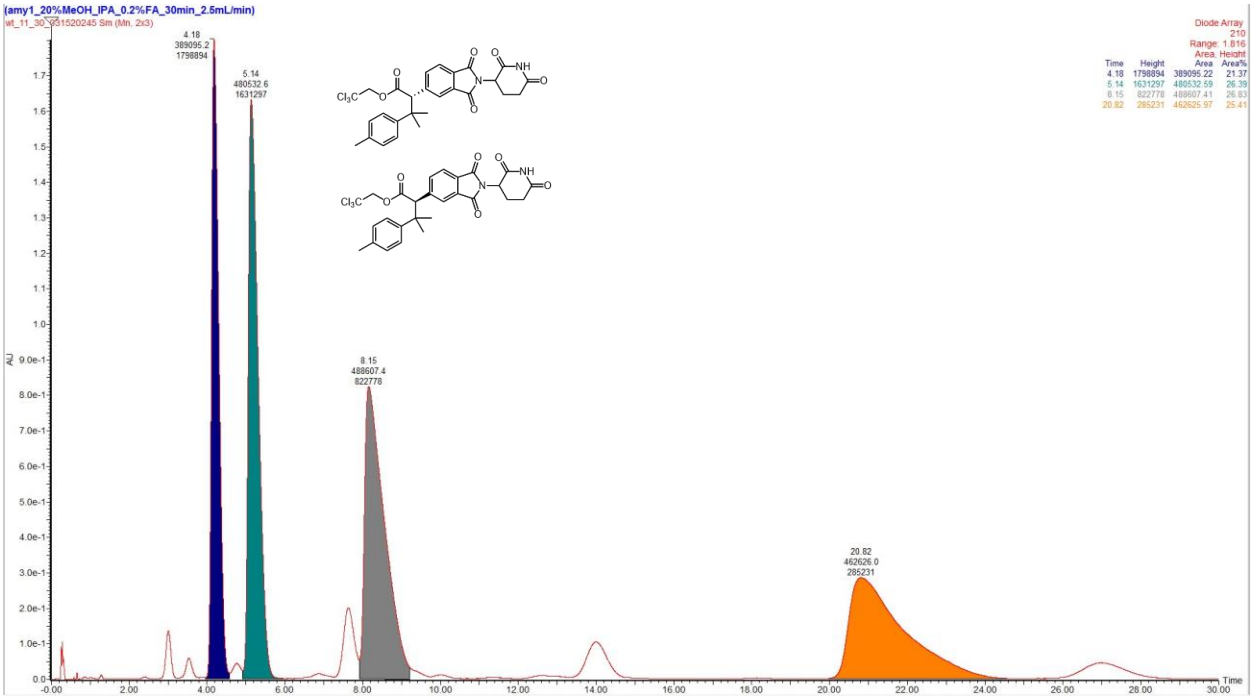

Chromatogram for Compound 3.19 Using GP1

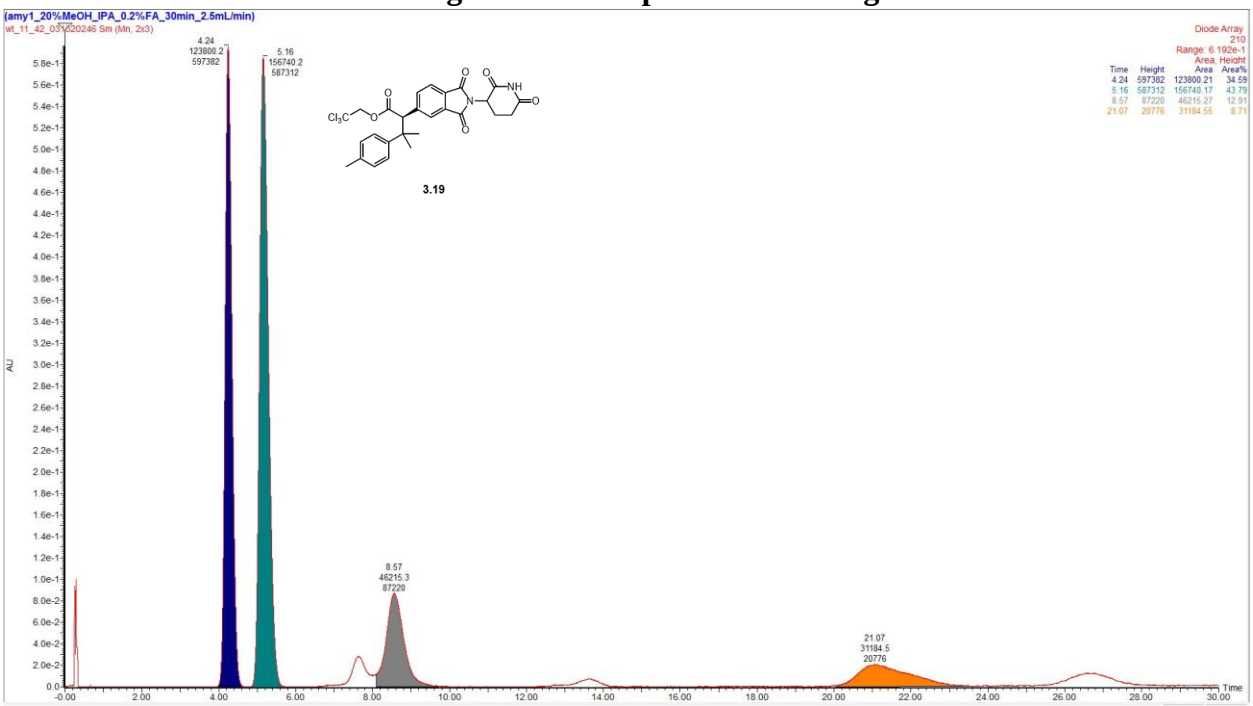

Chromatogram for Compound 3.19 Using GP3

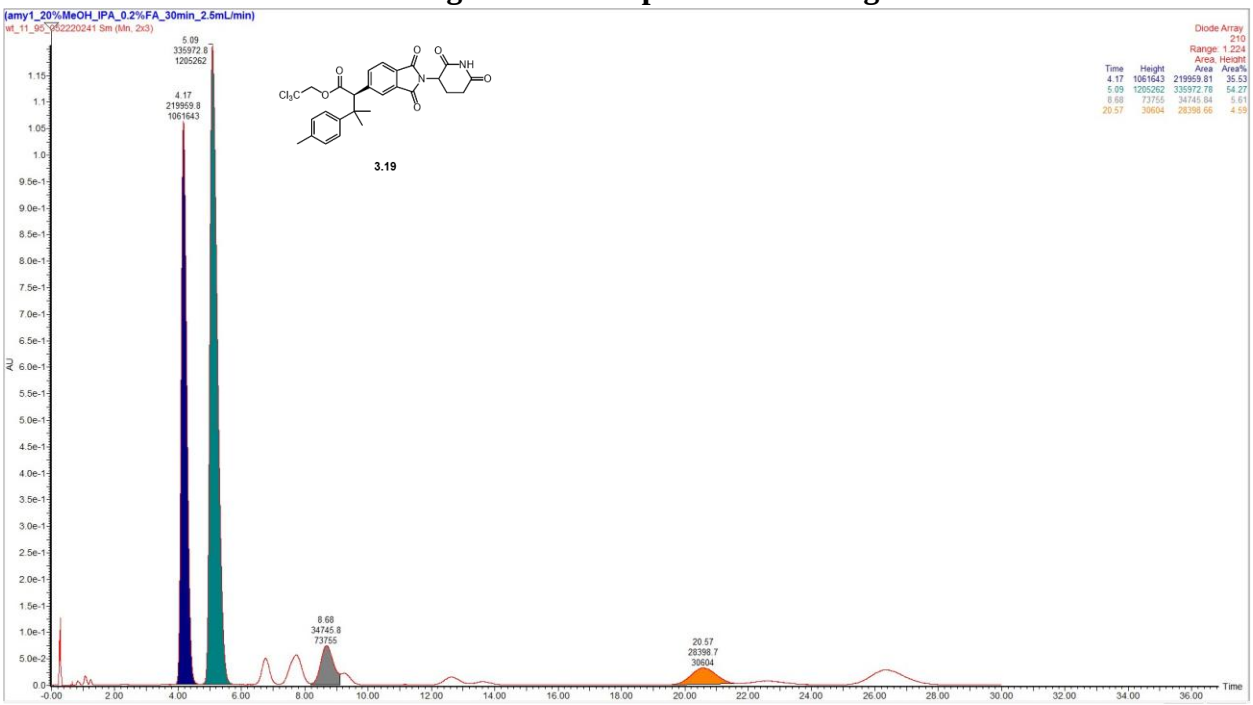

Racemic Chromatogram for Compound 3.20

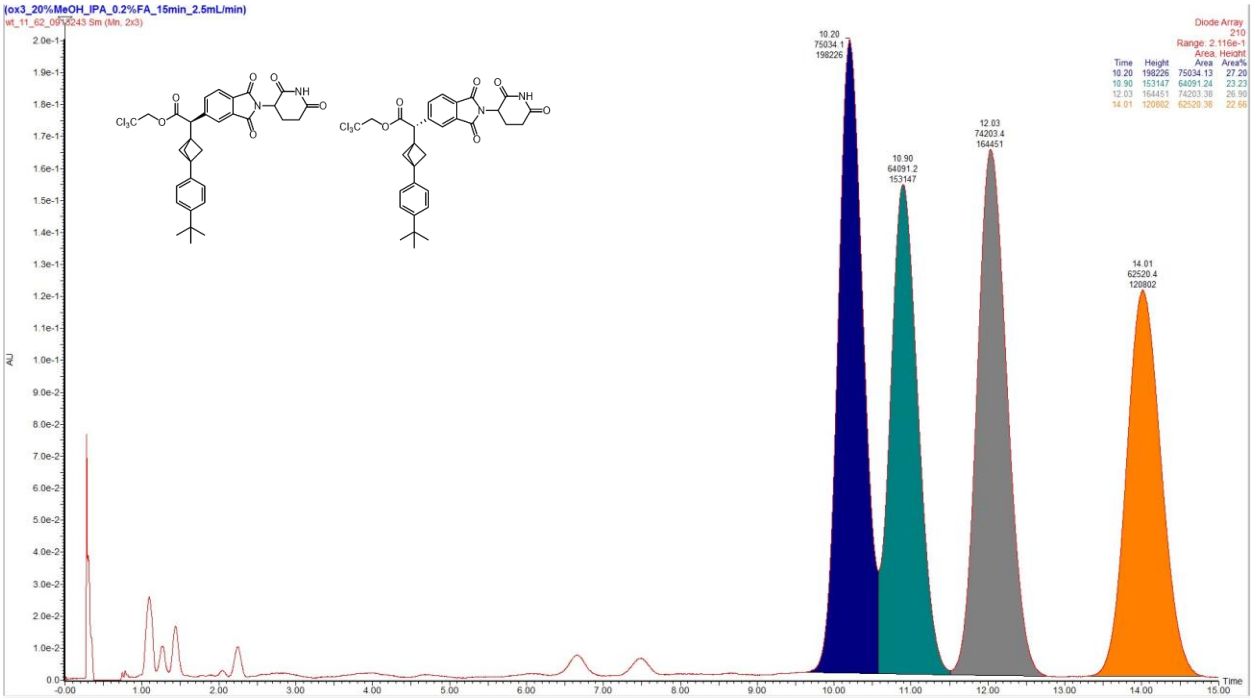

Chromatogram for Compound 3.20 Using GP3

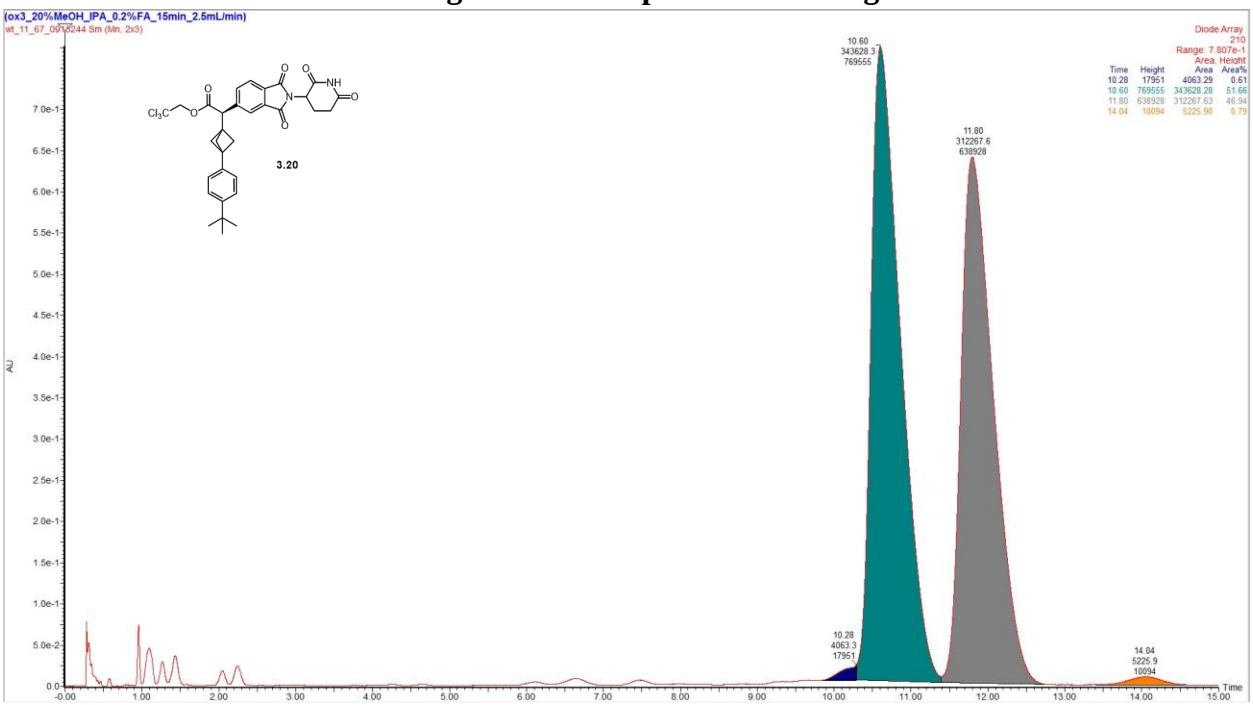

Racemic Chromatogram for Compound 3.21

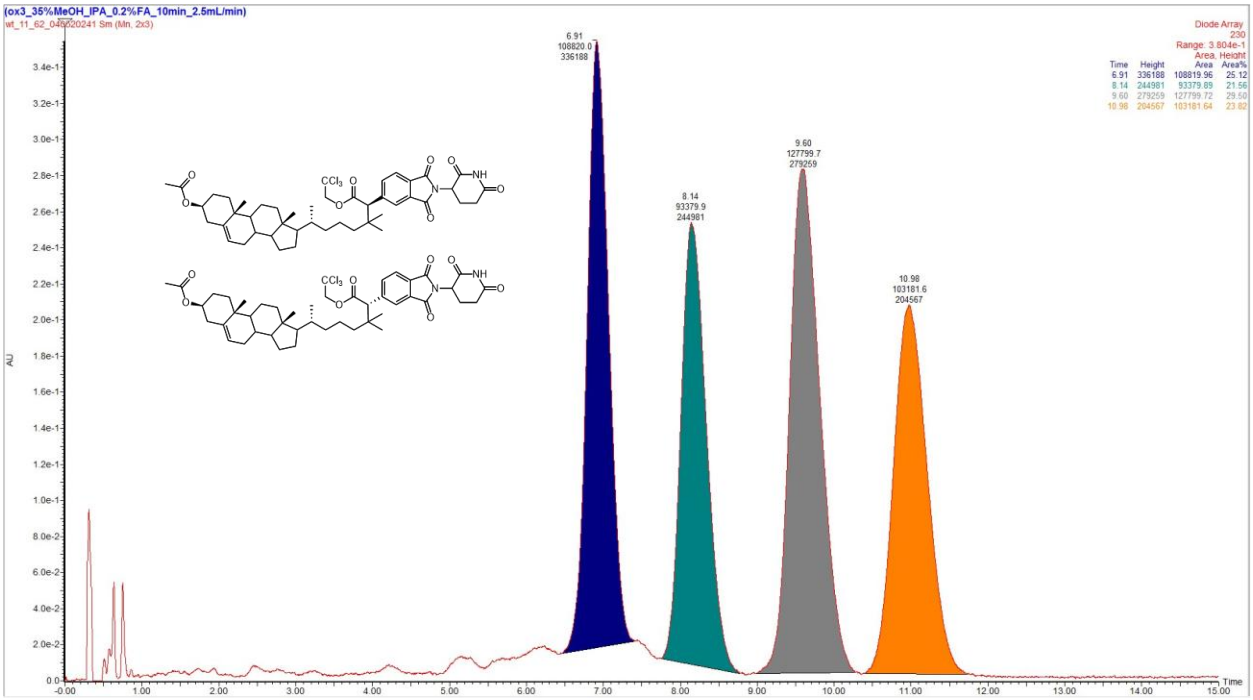

Chromatogram for Compound 3.21 Using GP3

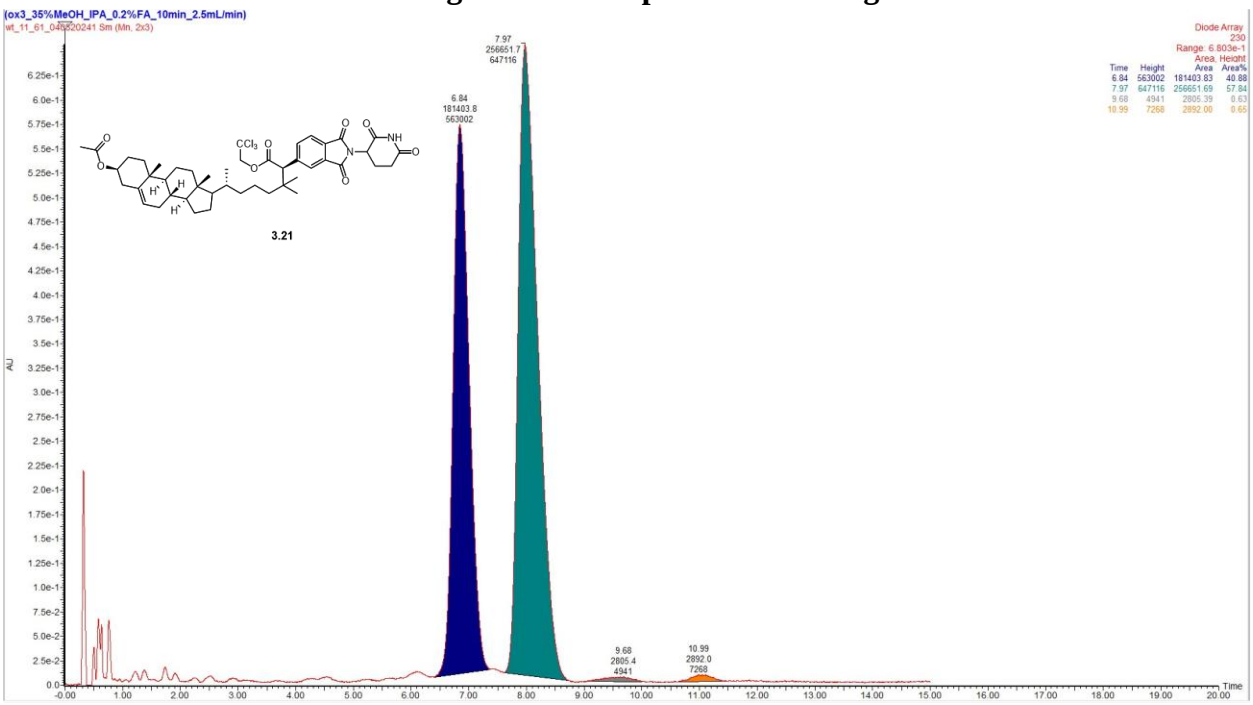

Racemic Chromatogram for Compound 3.22

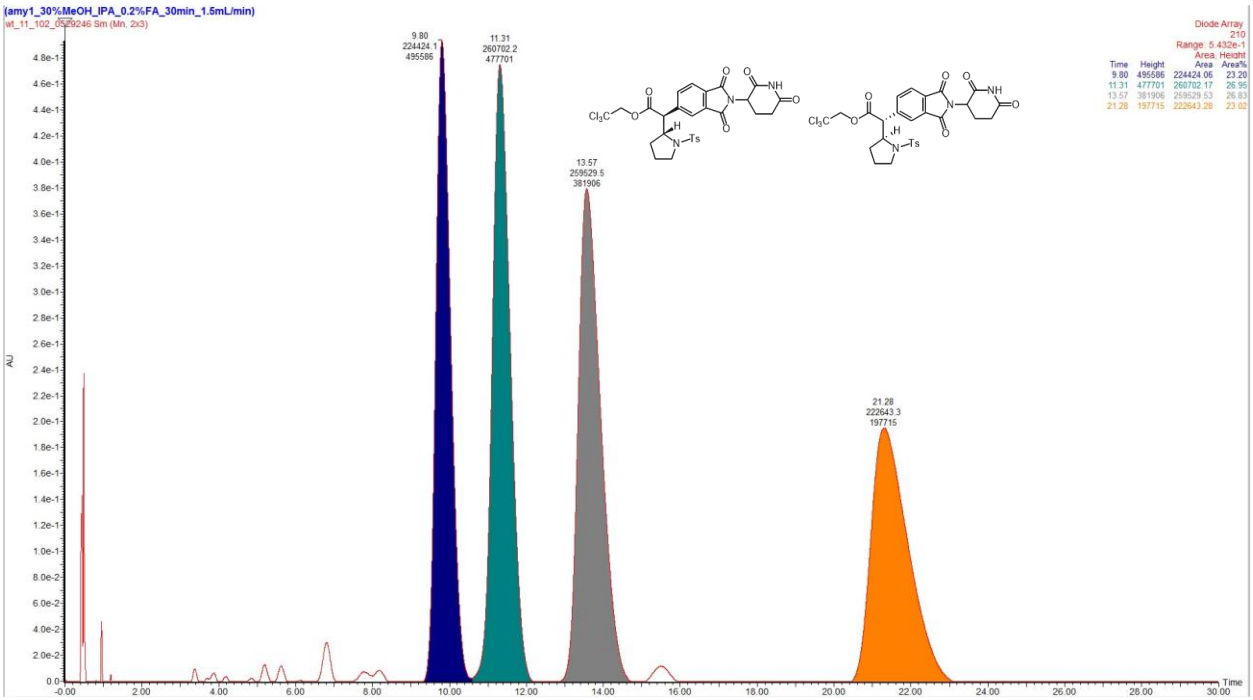

Chromatogram for Compound 3.22 Using GP3

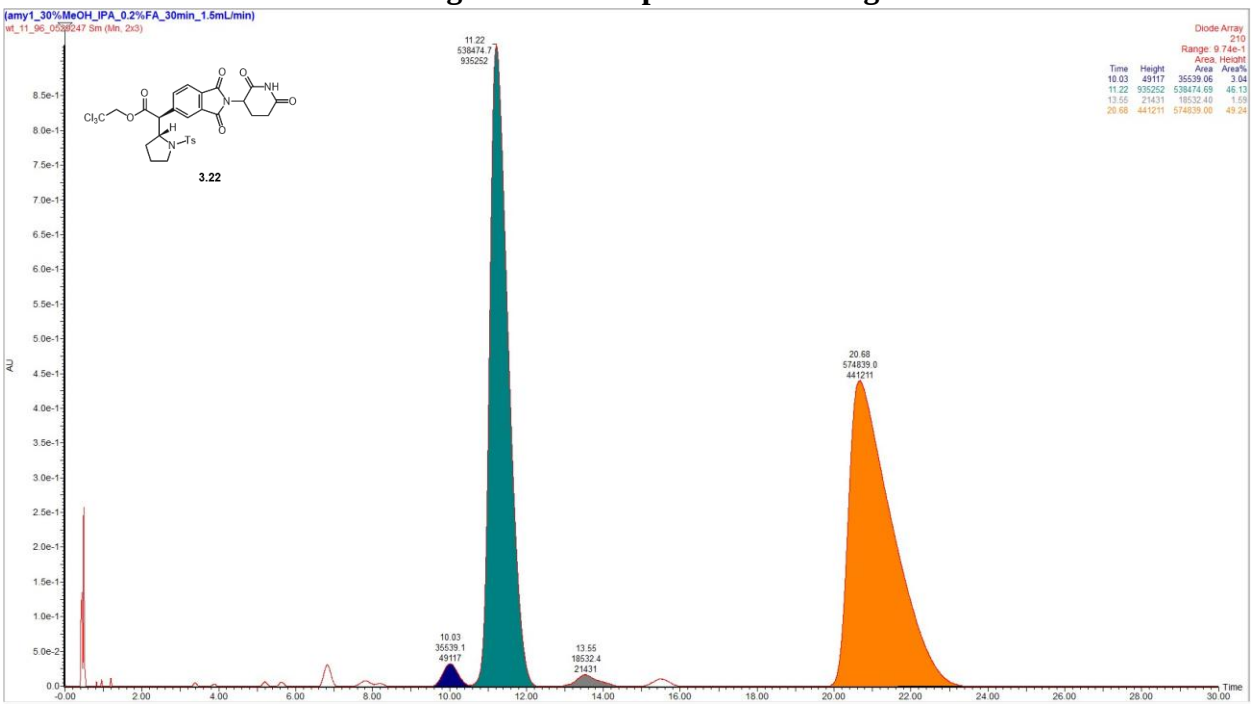

Chromatogram for Compound 3.22 Using GP8

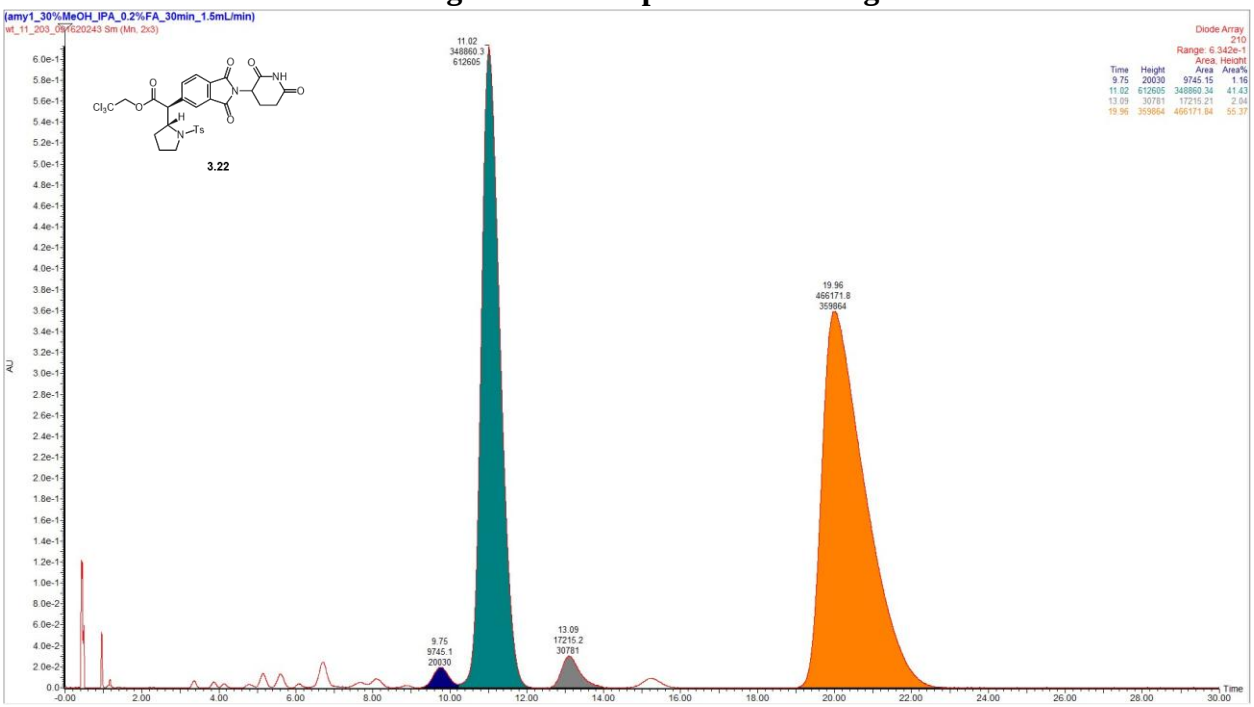

Racemic Chromatogram for Compound 3.24

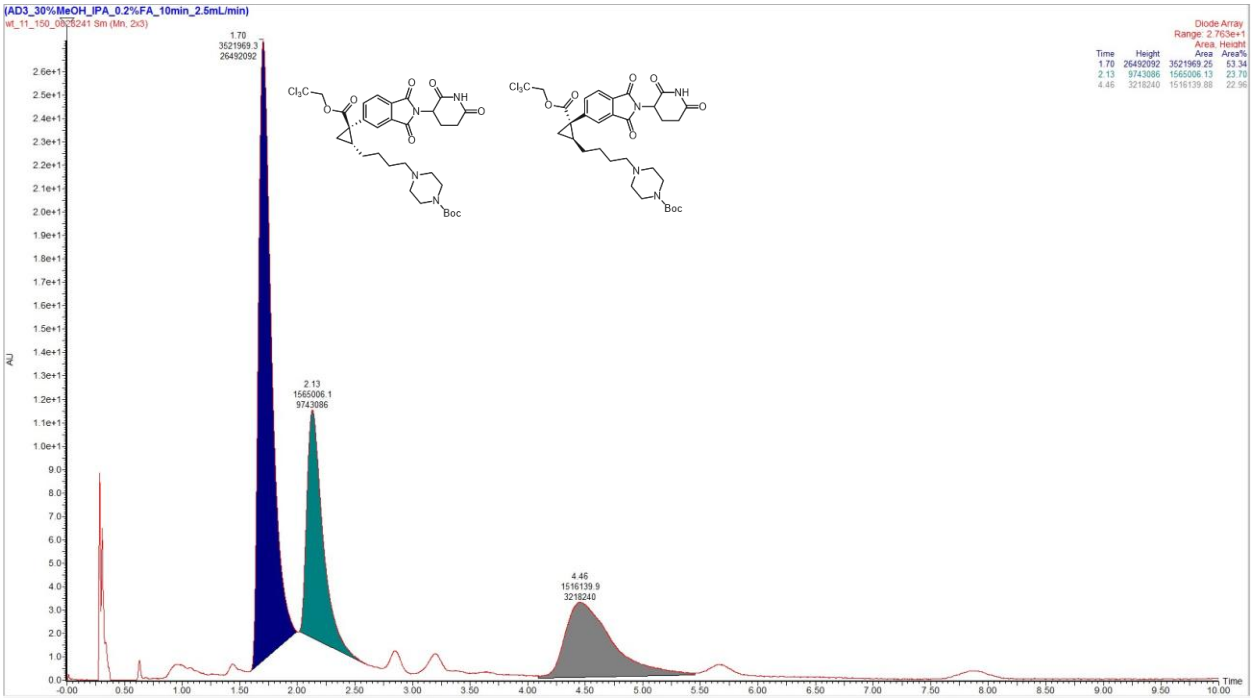

Chromatogram for Compound 3.24 Using GP5

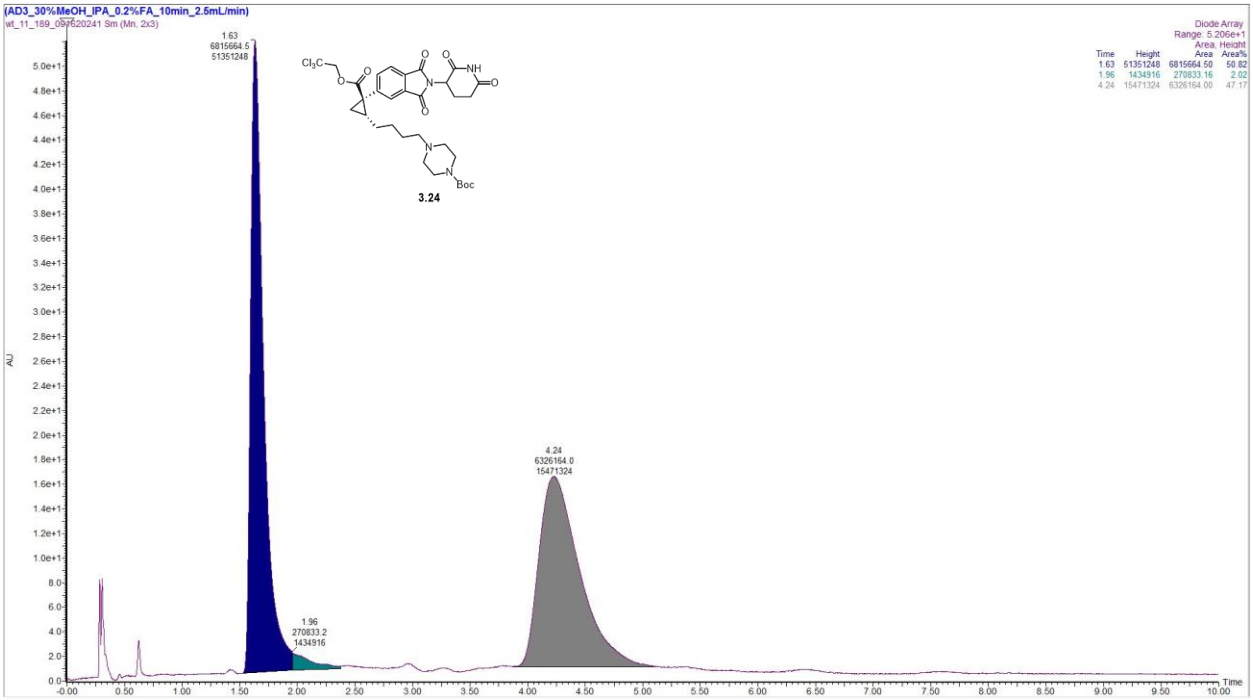

Chromatogram for Compound 3.24 Using GP8

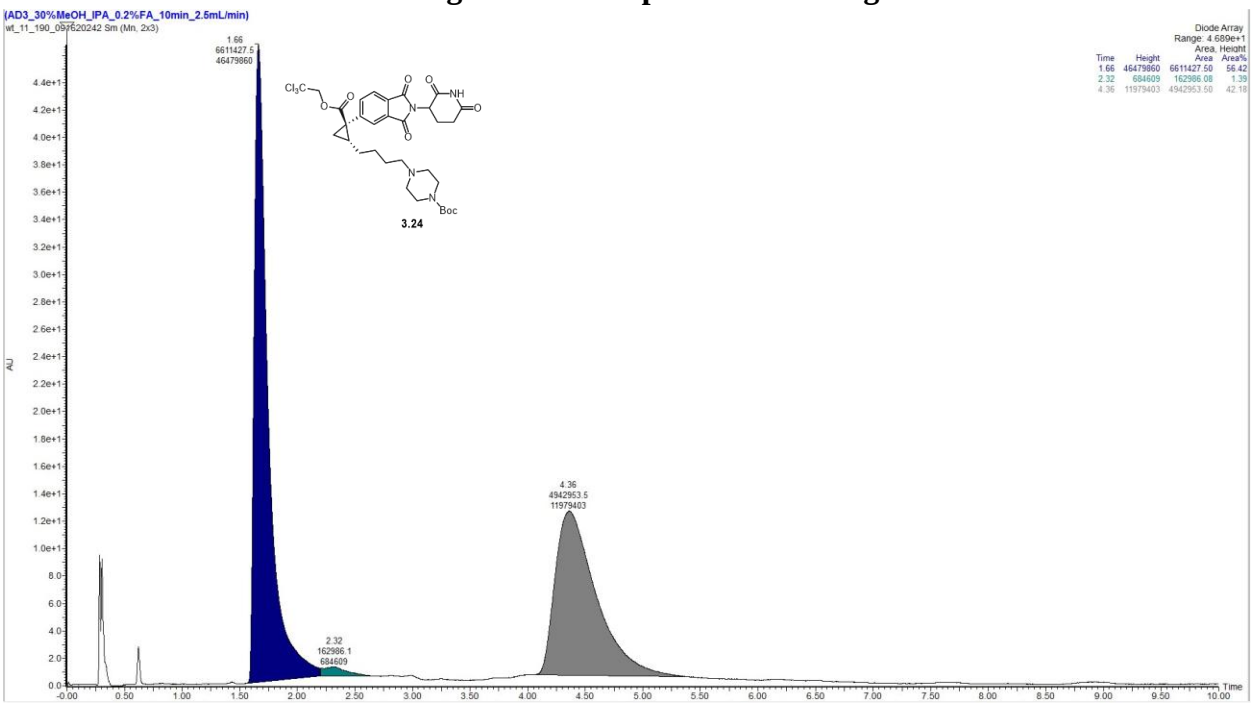

Chromatogram for Compound SI2 Using GP7

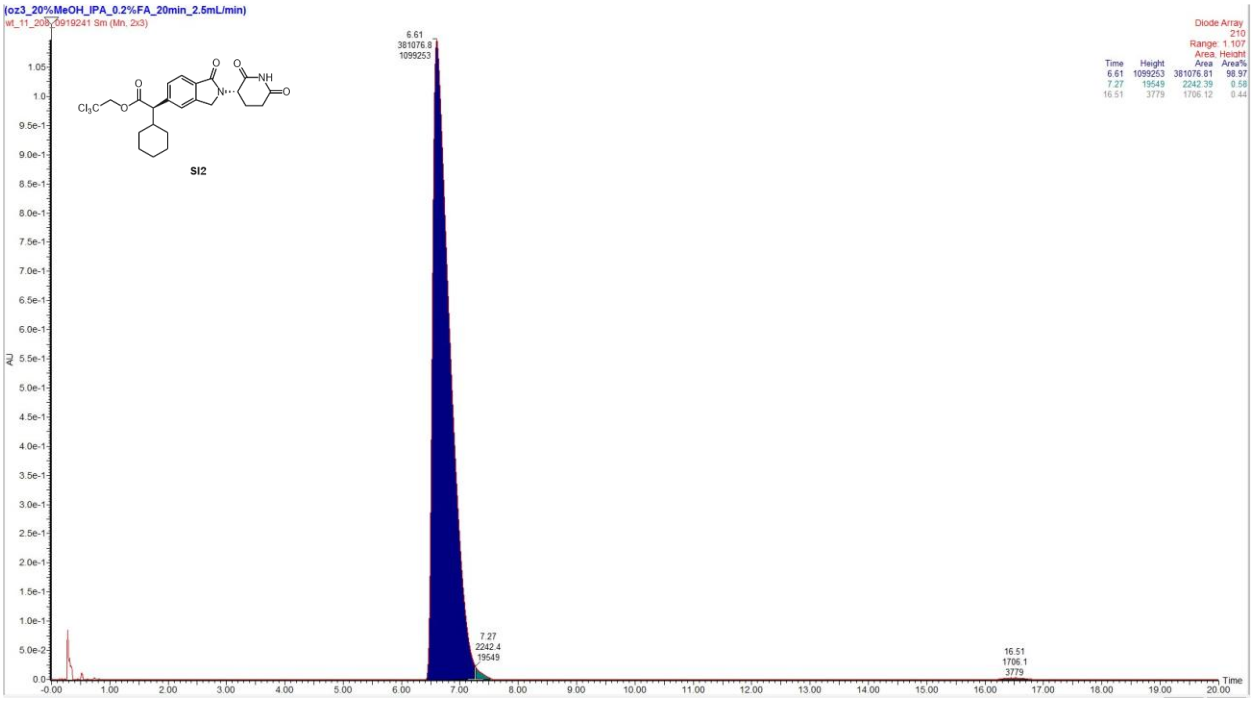

Racemic Chromatogram for Compound SI3

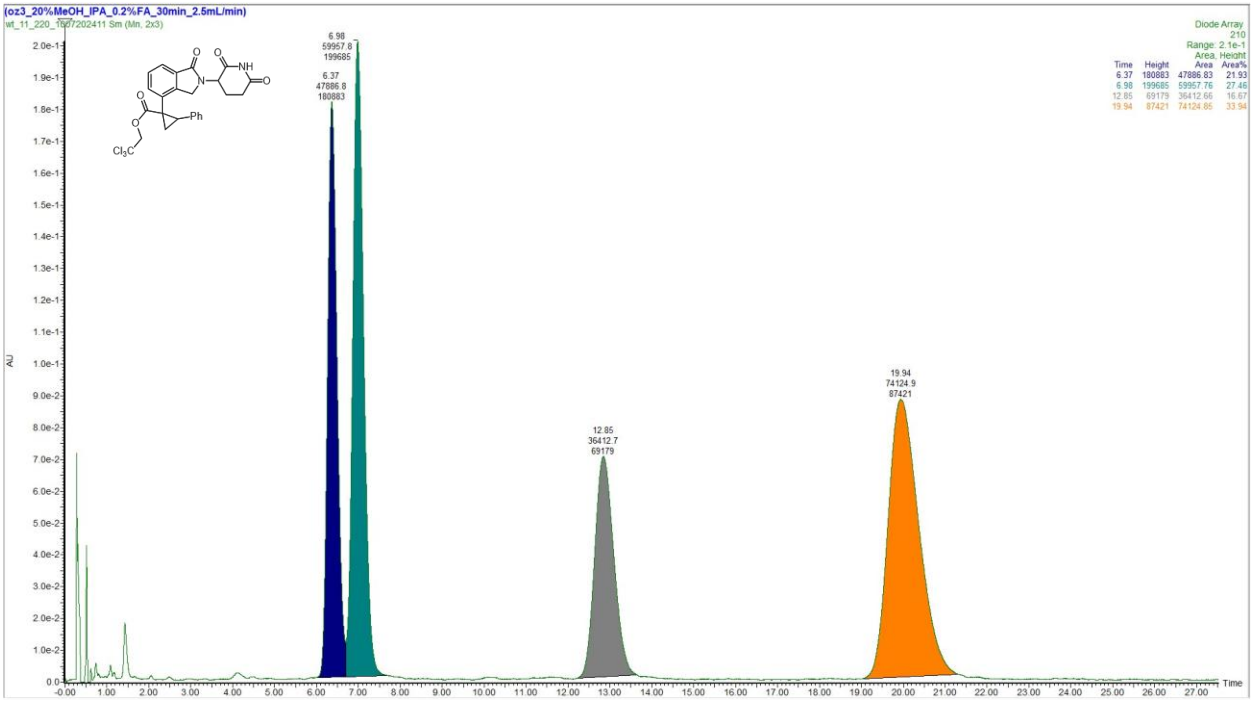

Chromatogram for Compound SI3 Using GP7

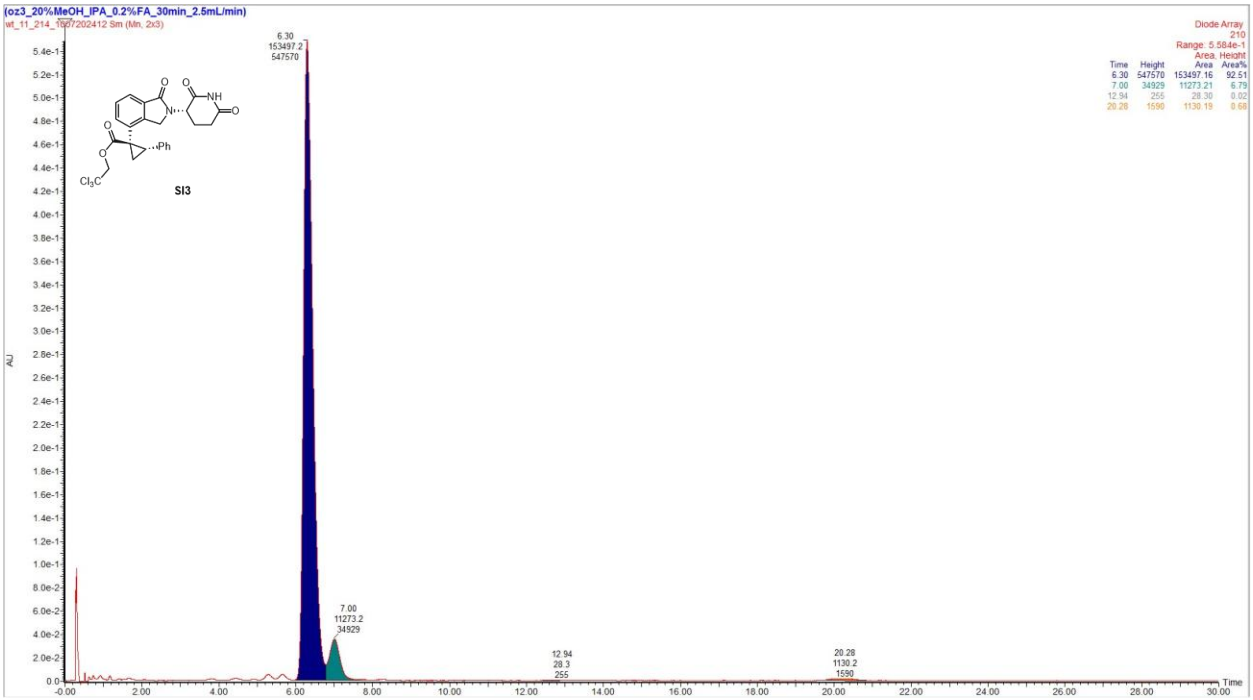

Chromatogram for Compound SI4 Using GP7

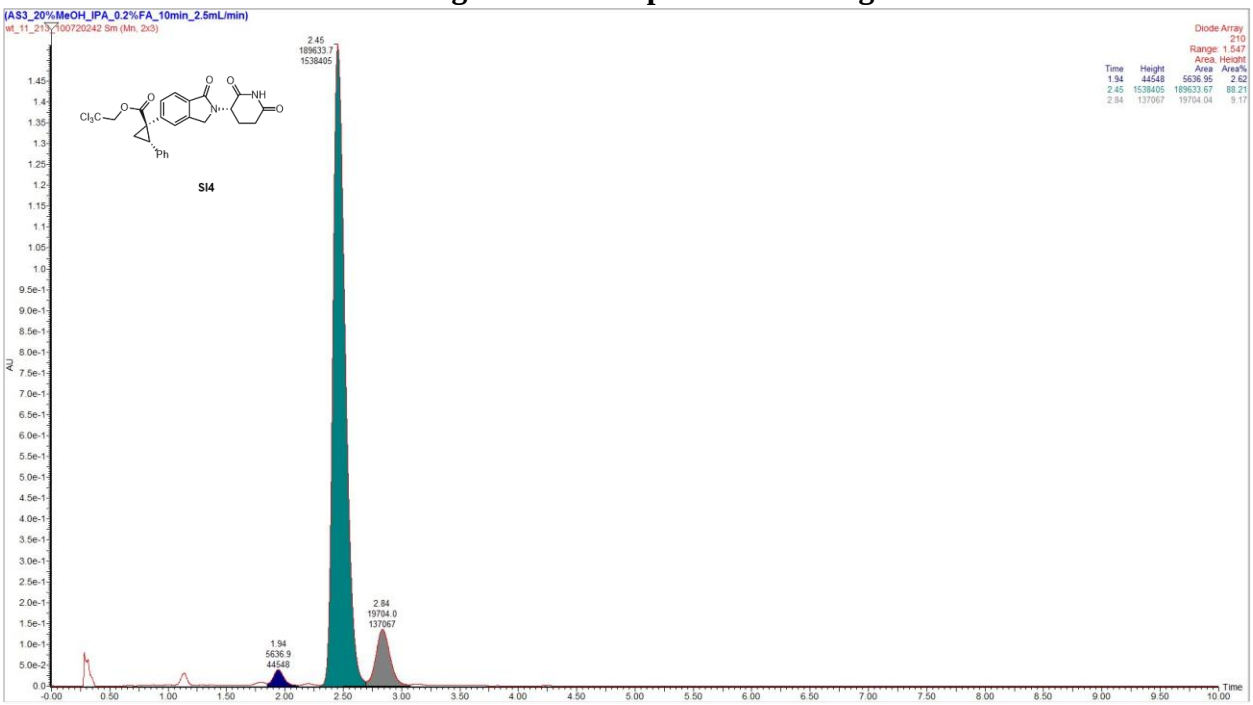

Section 6: Assay Protocols

The A549-BRD4-HiBiT cell line, created via CRISPR/Cas9, is used for detecting intracellular BRD4 protein degradation through a chemiluminescent signal. This cell line is based on the human A549 cell line (CCL-185) which co-expresses chimeric BRD4 (the target) and HiBiT (detection tag) designed by Promaga. Routine passaging and assays are performed using RPMI 1640 medium with 10% heat-inactivated fetal bovine serum and 1X penicillin/streptomycin. Test compound detection is carried out on a 1536-well tissue culture plate (Corning #3727), with cells seeded in 3.5 µL of core-RPMI 1640 at a density of 0.20 million/mL. Pre-titrated test compounds in DMSO are dispensed onto the assay plate using the ECHO liquid handling system (Labcyte), which employs acoustic energy. The assay is incubated for 24 hours at 37°C with 5% CO2, followed by 30 minutes of plate cooling at room temperature. The detection reagent mix (Cat# N3050, Nano-Glo® HiBiT Lytic Detection System from Promega) is then added at 3.5 µL per well in a predefined proportion. Luminescence is measured using an EnVision reader (PerkinElmer) 60 minutes after the addition of the detection reagent mix. Raw data are collected and processed using Dotmatics (a data analysis tool) to determine the test compound's potency values, including EC_{50} and Y_{min}.

Section 7: Results of the High-Throughput Screen for the Diazo Cross-Coupling

The data in this section were generated by Jake Ganley.

Title: Davies Collab - Diazo Alpha Arylation - Ligand/Solvent/Additive/Base/Precatalyst Screen, rt
Date: 11/1/22

Notes and conclusions:

Conclusions: No promising hits found w/ < 3% RAP desired product formed in all cases
1) Largely intact Ar-Br SM; no protodehalogenation observed
2) Pd(PPh3)4 with Et3N as base largely preserved diazo coupling component, whereas significant consumption was observed with DBU as base or any other catalyst combination
3) No obvious trends with respect to halide scavenger or solvent
4) No decomposed diazo product observed, indicating that this is not the reason for low RAP
5)
Next Steps: Potentially re-run plate at elevated temperature for longer reaction time to look for formation/decomposition of product

Notebook					JMG-A3BF6-078			(See key below!)													UV (254 _ nm, PDA on, UHPLCMS)			
					Ar-Br	Diazo Ester		Precatalyst			Ligand	Base		Halide Scavenger		Solvent				Time	C-X pdt.	Ar-Br	Diazo	Pdt.:
UPLC	library	in library	row	column	Name	Name	equiv	Name	µmol	mol %	Name	Name	equiv	Name	equiv	Solvent1	µL	M		h	RAP	RAP	RAP	Ar-Br
149	BMSP	201912	A	1	indolinone	Diazo Ester	1.3	Pd(PPh3)4	0.5	5.0%		DBU	1.5	KTFA	1.5	EtOAc	100	0.10		6.0	1.69%	73.34%	24.97%	2:98
150	BMSP	201912	A	2	indolinone	Diazo Ester	1.3	Pd(PPh3)4	0.5	5.0%		DBU	1.5	KTFA	1.5	MeCN	100	0.10		6.0	0.54%	94.50%	4.96%	1:99
151	BMSP	201912	A	3	indolinone	Diazo Ester	1.3	Pd(PPh3)4	0.5	5.0%		DBU	1.5	KTFA	1.5	DMF	100	0.10		6.0	1.17%	97.15%	1.68%	1:99
152	BMSP	201912	A	4	indolinone	Diazo Ester	1.3	Pd(PPh3)4	0.5	5.0%		DBU	1.5	NaTFA	1.5	EtOAc	100	0.10		6.0	1.26%	59.37%	39.38%	2:98
153	BMSP	201912	A	5	indolinone	Diazo Ester	1.3	Pd(PPh3)4	0.5	5.0%		DBU	1.5	NaTFA	1.5	MeCN	100	0.10		6.0	0.82%	81.13%	18.05%	1:99
154	BMSP	201912	A	6	indolinone	Diazo Ester	1.3	Pd(PPh3)4	0.5	5.0%		DBU	1.5	NaTFA	1.5	DMF	100	0.10		6.0	0.42%	96.25%	3.33%	0:100
155	BMSP	201912	A	7	indolinone	Diazo Ester	1.3	Pd(PPh3)4	0.5	5.0%		DBU	1.5	KOTf	1.5	EtOAc	100	0.10		6.0		62.39%	37.61%	
156	BMSP	201912	A	8	indolinone	Diazo Ester	1.3	Pd(PPh3)4	0.5	5.0%		DBU	1.5	KOTf	1.5	MeCN	100	0.10		6.0	0.15%	81.17%	18.68%	0:100
157	BMSP	201912	A	9	indolinone	Diazo Ester	1.3	Pd(PPh3)4	0.5	5.0%		DBU	1.5	KOTf	1.5	DMF	100	0.10		6.0	0.41%	96.09%	3.50%	0:100
158	BMSP	201912	A	10	indolinone	Diazo Ester	1.3	Pd(PPh3)4	0.5	5.0%		DBU	1.5	NaOTf	1.5	EtOAc	100	0.10		6.0	0.92%	57.46%	41.62%	2:98
159	BMSP	201912	A	11	indolinone	Diazo Ester	1.3	Pd(PPh3)4	0.5	5.0%		DBU	1.5	NaOTf	1.5	MeCN	100	0.10		6.0	0.78%	75.77%	23.45%	1:99
160	BMSP	201912	A	12	indolinone	Diazo Ester	1.3	Pd(PPh3)4	0.5	5.0%		DBU	1.5	NaOTf	1.5	DMF	100	0.10		6.0	0.59%	93.80%	5.62%	1:99
161	BMSP	201912	B	1	indolinone	Diazo Ester	1.3	Pd(PPh3)4	0.5	5.0%		TEA	1.5	KTFA	1.5	EtOAc	100	0.10		6.0	1.47%	42.27%	56.26%	3:97
162	BMSP	201912	B	2	indolinone	Diazo Ester	1.3	Pd(PPh3)4	0.5	5.0%		TEA	1.5	KTFA	1.5	MeCN	100	0.10		6.0	1.39%	72.27%	26.34%	2:98
163	BMSP	201912	B	3	indolinone	Diazo Ester	1.3	Pd(PPh3)4	0.5	5.0%		TEA	1.5	KTFA	1.5	DMF	100	0.10		6.0	0.27%	45.10%	54.63%	1:99
164	BMSP	201912	B	4	indolinone	Diazo Ester	1.3	Pd(PPh3)4	0.5	5.0%		TEA	1.5	NaTFA	1.5	EtOAc	100	0.10		6.0	0.18%	45.10%	54.71%	0:100
165	BMSP	201912	B	5	indolinone	Diazo Ester	1.3	Pd(PPh3)4	0.5	5.0%		TEA	1.5	NaTFA	1.5	MeCN	100	0.10		6.0	0.29%	78.79%	20.92%	0:100
166	BMSP	201912	B	6	indolinone	Diazo Ester	1.3	Pd(PPh3)4	0.5	5.0%		TEA	1.5	NaTFA	1.5	DMF	100	0.10		6.0	0.27%	45.07%	54.66%	1:99
167	BMSP	201912	B	7	indolinone	Diazo Ester	1.3	Pd(PPh3)4	0.5	5.0%		TEA	1.5	KOTf	1.5	EtOAc	100	0.10		6.0	0.25%	43.15%	56.60%	1:99
168	BMSP	201912	B	8	indolinone	Diazo Ester	1.3	Pd(PPh3)4	0.5	5.0%		TEA	1.5	KOTf	1.5	MeCN	100	0.10		6.0	1.31%	71.43%	27.25%	2:98
169	BMSP	201912	B	9	indolinone	Diazo Ester	1.3	Pd(PPh3)4	0.5	5.0%		TEA	1.5	KOTf	1.5	DMF	100	0.10		6.0	1.17%	44.53%	54.30%	3:97
170	BMSP	201912	B	10	indolinone	Diazo Ester	1.3	Pd(PPh3)4	0.5	5.0%		TEA	1.5	NaOTf	1.5	EtOAc	100	0.10		6.0	0.22%	44.98%	54.80%	0:100
171	BMSP	201912	B	11	indolinone	Diazo Ester	1.3	Pd(PPh3)4	0.5	5.0%		TEA	1.5	NaOTf	1.5	MeCN	100	0.10		6.0	0.30%	78.39%	21.31%	0:100
172	BMSP	201912	B	12	indolinone	Diazo Ester	1.3	Pd(PPh3)4	0.5	5.0%		TEA	1.5	NaOTf	1.5	DMF	100	0.10		6.0	0.28%	44.59%	55.13%	1:99
173	BMSP	201912	C	1	indolinone	Diazo Ester	1.3	Pd(PPh3)4	0.5	5.0%	PPh3	DBU	1.5	KTFA	1.5	EtOAc	100	0.10		6.0	1.07%	60.54%	38.39%	2:98
174	BMSP	201912	C	2	indolinone	Diazo Ester	1.3	Pd(PPh3)4	0.5	5.0%	PPh3	DBU	1.5	KTFA	1.5	MeCN	100	0.10		6.0	0.70%	78.03%	21.27%	1:99
175	BMSP	201912	C	3	indolinone	Diazo Ester	1.3	Pd(PPh3)4	0.5	5.0%	PPh3	DBU	1.5	KTFA	1.5	DMF	100	0.10		6.0	0.51%	93.84%	5.65%	1:99
176	BMSP	201912	C	4	indolinone	Diazo Ester	1.3	Pd(PPh3)4	0.5	5.0%	PPh3	DBU	1.5	NaTFA	1.5	EtOAc	100	0.10		6.0	1.04%	54.01%	44.95%	2:98
177	BMSP	201912	C	5	indolinone	Diazo Ester	1.3	Pd(PPh3)4	0.5	5.0%	PPh3	DBU	1.5	NaTFA	1.5	MeCN	100	0.10		6.0	0.70%	75.36%	23.94%	1:99
178	BMSP	201912	C	6	indolinone	Diazo Ester	1.3	Pd(PPh3)4	0.5	5.0%	PPh3	DBU	1.5	NaTFA	1.5	DMF	100	0.10		6.0	0.46%	93.49%	6.05%	0:100
179	BMSP	201912	C	7	indolinone	Diazo Ester	1.3	Pd(PPh3)4	0.5	5.0%	PPh3	DBU	1.5	KOTf	1.5	EtOAc	100	0.10		6.0		59.24%	40.76%	
180	BMSP	201912	C	8	indolinone	Diazo Ester	1.3	Pd(PPh3)4	0.5	5.0%	PPh3	DBU	1.5	KOTf	1.5	MeCN	100	0.10		6.0	0.71%	75.40%	23.89%	1:99
181	BMSP	201912	C	9	indolinone	Diazo Ester	1.3	Pd(PPh3)4	0.5	5.0%	PPh3	DBU	1.5	KOTf	1.5	DMF	100	0.10		6.0	0.51%	92.86%	6.64%	1:99
182	BMSP	201912	C	10	indolinone	Diazo Ester	1.3	Pd(PPh3)4	0.5	5.0%	PPh3	DBU	1.5	NaOTf	1.5	EtOAc	100	0.10		6.0	1.51%	85.33%	13.16%	2:98
183	BMSP	201912	C	11	indolinone	Diazo Ester	1.3	Pd(PPh3)4	0.5	5.0%	PPh3	DBU	1.5	NaOTf	1.5	MeCN	100	0.10		6.0	0.55%	79.32%	20.13%	1:99
184	BMSP	201912	C	12	indolinone	Diazo Ester	1.3	Pd(PPh3)4	0.5	5.0%	PPh3	DBU	1.5	NaOTf	1.5	DMF	100	0.10		6.0	0.44%	92.31%	7.25%	0:100
185	BMSP	201912	D	1	indolinone	Diazo Ester	1.3	Pd(PPh3)4	0.5	5.0%	PPh3	TEA	1.5	KTFA	1.5	EtOAc	100	0.10		6.0	0.26%	42.47%	57.28%	1:99
186	BMSP	201912	D	2	indolinone	Diazo Ester	1.3	Pd(PPh3)4	0.5	5.0%	PPh3	TEA	1.5	KTFA	1.5	MeCN	100	0.10		6.0		43.34%	56.66%	
187	BMSP	201912	D	3	indolinone	Diazo Ester	1.3	Pd(PPh3)4	0.5	5.0%	PPh3	TEA	1.5	KTFA	1.5	DMF	100	0.10		6.0	1.27%	44.93%	53.80%	3:97

188	BMSP	201912	D	4	indolinone Diazo Ester	1.3	Pd(PPh3)4	0.5	5.0%	PPh3	TEA	1.5	NaTFA	1.5	EtOAc	100	0.10	6.0	0.24%	42.37%	57.40%	1:99
189	BMSP	201912	D	5	indolinone Diazo Ester	1.3	Pd(PPh3)4	0.5	5.0%	PPh3	TEA	1.5	NaTFA	1.5	MeCN	100	0.10	6.0		43.38%	56.62%	
190	BMSP	201912	D	6	indolinone Diazo Ester	1.3	Pd(PPh3)4	0.5	5.0%	PPh3	TEA	1.5	NaTFA	1.5	DMF	100	0.10	6.0	0.31%	44.15%	55.54%	1:99
191	BMSP	201912	D	7	indolinone Diazo Ester	1.3	Pd(PPh3)4	0.5	5.0%	PPh3	TEA	1.5	KOTf	1.5	EtOAc	100	0.10	6.0	0.28%	43.01%	56.71%	1:99
192	BMSP	201912	D	8	indolinone Diazo Ester	1.3	Pd(PPh3)4	0.5	5.0%	PPh3	TEA	1.5	KOTf	1.5	MeCN	100	0.10	6.0		43.40%	56.60%	
193	BMSP	201912	D	9	indolinone Diazo Ester	1.3	Pd(PPh3)4	0.5	5.0%	PPh3	TEA	1.5	KOTf	1.5	DMF	100	0.10	6.0	1.09%	43.59%	55.32%	2:98
194	BMSP	201912	D	10	indolinone Diazo Ester	1.3	Pd(PPh3)4	0.5	5.0%	PPh3	TEA	1.5	NaOTf	1.5	EtOAc	100	0.10	6.0	0.27%	43.03%	56.70%	1:99
195	BMSP	201912	D	11	indolinone Diazo Ester	1.3	Pd(PPh3)4	0.5	5.0%	PPh3	TEA	1.5	NaOTf	1.5	MeCN	100	0.10	6.0		43.28%	56.72%	
196	BMSP	201912	D	12	indolinone Diazo Ester	1.3	Pd(PPh3)4	0.5	5.0%	PPh3	TEA	1.5	NaOTf	1.5	DMF	100	0.10	6.0	0.34%	42.79%	56.87%	1:99
197	BMSP	201912	E	1	indolinone Diazo Ester	1.3	Pd(OAc)2	0.5	5.0%	PPh3	TEA	1.5	KTFA	1.5	EtOAc	100	0.10	6.0		71.92%	28.08%	
198	BMSP	201912	E	2	indolinone Diazo Ester	1.3	Pd(OAc)2	0.5	5.0%	P(fur)3	TEA	1.5	KTFA	1.5	EtOAc	100	0.10	6.0	0.22%	63.28%	36.50%	0:100
199	BMSP	201912	E	3	indolinone Diazo Ester	1.3	Pd(OAc)2	0.5	5.0%	P(p-F-Ph)3	TEA	1.5	KTFA	1.5	EtOAc	100	0.10	6.0	0.28%	69.47%	30.24%	0:100
200	BMSP	201912	E	4	indolinone Diazo Ester	1.3	Pd(OAc)2	0.5	5.0%	A-taPhos	TEA	1.5	KTFA	1.5	EtOAc	100	0.10	6.0		68.71%	31.29%	
201	BMSP	201912	E	5	indolinone Diazo Ester	1.3	Pd(OAc)2	0.5	5.0%	Xantphos	TEA	1.5	KTFA	1.5	EtOAc	100	0.10	6.0	0.19%	53.02%	46.79%	0:100
202	BMSP	201912	E	6	indolinone Diazo Ester	1.3	Pd(OAc)2	0.5	5.0%	tB-Xantphos	TEA	1.5	KTFA	1.5	EtOAc	100	0.10	6.0	0.37%	68.32%	31.31%	1:99
203	BMSP	201912	E	7	indolinone Diazo Ester	1.3	Pd(OAc)2	0.5	5.0%	X-Phos	TEA	1.5	KTFA	1.5	EtOAc	100	0.10	6.0	0.27%	52.59%	47.14%	1:99
204	BMSP	201912	E	8	indolinone Diazo Ester	1.3	Pd(OAc)2	0.5	5.0%	tB-XPhos	TEA	1.5	KTFA	1.5	EtOAc	100	0.10	6.0	0.37%	66.30%	33.33%	1:99
205	BMSP	201912	E	9	indolinone Diazo Ester	1.3	Pd(OAc)2	0.5	5.0%	DPPF	TEA	1.5	KTFA	1.5	EtOAc	100	0.10	6.0	0.94%	52.36%	46.70%	2:98
206	BMSP	201912	E	10	indolinone Diazo Ester	1.3	Pd(OAc)2	0.5	5.0%	DtBPF	TEA	1.5	KTFA	1.5	EtOAc	100	0.10	6.0	1.90%	65.76%	32.34%	3:97
207	BMSP	201912	E	11	indolinone Diazo Ester	1.3	Pd(OAc)2	0.5	5.0%	CX-A	TEA	1.5	KTFA	1.5	EtOAc	100	0.10	6.0	0.29%	69.98%	29.73%	0:100
208	BMSP	201912	E	12	indolinone Diazo Ester	1.3	Pd(OAc)2	0.5	5.0%	PCy3 HBF4	TEA	1.5	KTFA	1.5	EtOAc	100	0.10	6.0	0.17%	60.11%	39.72%	0:100
209	BMSP	201912	F	1	indolinone Diazo Ester	1.3	Pd(OAc)2	0.5	5.0%	PPh3	TEA	1.5	KTFA	1.5	DMF	100	0.10	6.0	0.56%	85.22%	14.22%	1:99
210	BMSP	201912	F	2	indolinone Diazo Ester	1.3	Pd(OAc)2	0.5	5.0%	P(fur)3	TEA	1.5	KTFA	1.5	DMF	100	0.10	6.0	0.23%	53.39%	46.38%	0:100
211	BMSP	201912	F	3	indolinone Diazo Ester	1.3	Pd(OAc)2	0.5	5.0%	P(p-F-Ph)3	TEA	1.5	KTFA	1.5	DMF	100	0.10	6.0	0.51%	80.95%	18.54%	1:99
212	BMSP	201912	F	4	indolinone Diazo Ester	1.3	Pd(OAc)2	0.5	5.0%	A-taPhos	TEA	1.5	KTFA	1.5	DMF	100	0.10	6.0		60.00%	40.00%	
213	BMSP	201912	F	5	indolinone Diazo Ester	1.3	Pd(OAc)2	0.5	5.0%	Xantphos	TEA	1.5	KTFA	1.5	DMF	100	0.10	6.0	0.15%	51.13%	48.72%	0:100
214	BMSP	201912	F	6	indolinone Diazo Ester	1.3	Pd(OAc)2	0.5	5.0%	tB-Xantphos	TEA	1.5	KTFA	1.5	DMF	100	0.10	6.0	0.24%	63.13%	36.63%	0:100
215	BMSP	201912	F	7	indolinone Diazo Ester	1.3	Pd(OAc)2	0.5	5.0%	X-Phos	TEA	1.5	KTFA	1.5	DMF	100	0.10	6.0		49.57%	50.43%	
216	BMSP	201912	F	8	indolinone Diazo Ester	1.3	Pd(OAc)2	0.5	5.0%	tB-XPhos	TEA	1.5	KTFA	1.5	DMF	100	0.10	6.0	0.12%	60.53%	39.34%	0:100
217	BMSP	201912	F	9	indolinone Diazo Ester	1.3	Pd(OAc)2	0.5	5.0%	DPPF	TEA	1.5	KTFA	1.5	DMF	100	0.10	6.0	1.23%	47.84%	50.92%	3:97
218	BMSP	201912	F	10	indolinone Diazo Ester	1.3	Pd(OAc)2	0.5	5.0%	DtBPF	TEA	1.5	KTFA	1.5	DMF	100	0.10	6.0	1.00%	66.92%	32.08%	1:99
219	BMSP	201912	F	11	indolinone Diazo Ester	1.3	Pd(OAc)2	0.5	5.0%	CX-A	TEA	1.5	KTFA	1.5	DMF	100	0.10	6.0	0.18%	70.46%	29.36%	0:100
220	BMSP	201912	F	12	indolinone Diazo Ester	1.3	Pd(OAc)2	0.5	5.0%	PCy3 HBF4	TEA	1.5	KTFA	1.5	DMF	100	0.10	6.0	0.12%	59.27%	40.61%	0:100
221	BMSP	201912	G	1	indolinone Diazo Ester	1.3	Pd(dba)2	0.5	5.0%	PPh3	TEA	1.5	KTFA	1.5	EtOAc	100	0.10	6.0	0.14%	60.86%	39.00%	0:100
222	BMSP	201912	G	2	indolinone Diazo Ester	1.3	Pd(dba)2	0.5	5.0%	P(fur)3	TEA	1.5	KTFA	1.5	EtOAc	100	0.10	6.0	0.19%	62.63%	37.18%	0:100
223	BMSP	201912	G	3	indolinone Diazo Ester	1.3	Pd(dba)2	0.5	5.0%	P(p-F-Ph)3	TEA	1.5	KTFA	1.5	EtOAc	100	0.10	6.0	0.23%	59.30%	40.46%	0:100
224	BMSP	201912	G	4	indolinone Diazo Ester	1.3	Pd(dba)2	0.5	5.0%	A-taPhos	TEA	1.5	KTFA	1.5	EtOAc	100	0.10	6.0		69.69%	30.31%	
225	BMSP	201912	G	5	indolinone Diazo Ester	1.3	Pd(dba)2	0.5	5.0%	Xantphos	TEA	1.5	KTFA	1.5	EtOAc	100	0.10	6.0	0.17%	41.33%	58.51%	0:100
226	BMSP	201912	G	6	indolinone Diazo Ester	1.3	Pd(dba)2	0.5	5.0%	tB-Xantphos	TEA	1.5	KTFA	1.5	EtOAc	100	0.10	6.0	0.53%	57.04%	42.43%	1:99
227	BMSP	201912	G	7	indolinone Diazo Ester	1.3	Pd(dba)2	0.5	5.0%	X-Phos	TEA	1.5	KTFA	1.5	EtOAc	100	0.10	6.0	0.12%	47.57%	52.31%	0:100
228	BMSP	201912	G	8	indolinone Diazo Ester	1.3	Pd(dba)2	0.5	5.0%	tB-XPhos	TEA	1.5	KTFA	1.5	EtOAc	100	0.10	6.0	0.51%	56.32%	43.17%	1:99
229	BMSP	201912	G	9	indolinone Diazo Ester	1.3	Pd(dba)2	0.5	5.0%	DPPF	TEA	1.5	KTFA	1.5	EtOAc	100	0.10	6.0	0.24%	41.32%	58.44%	1:99
230	BMSP	201912	G	10	indolinone Diazo Ester	1.3	Pd(dba)2	0.5	5.0%	DtBPF	TEA	1.5	KTFA	1.5	EtOAc	100	0.10	6.0	0.13%	46.65%	53.22%	0:100
231	BMSP	201912	G	11	indolinone Diazo Ester	1.3	Pd(dba)2	0.5	5.0%	CX-A	TEA	1.5	KTFA	1.5	EtOAc	100	0.10	6.0	0.14%	57.85%	42.01%	0:100
232	BMSP	201912	G	12	indolinone Diazo Ester	1.3	Pd(dba)2	0.5	5.0%	PCy3 HBF4	TEA	1.5	KTFA	1.5	EtOAc	100	0.10	6.0	0.17%	60.37%	39.46%	0:100
233	BMSP	201912	H	1	indolinone Diazo Ester	1.3	Pd(dba)2	0.5	5.0%	PPh3	TEA	1.5	KTFA	1.5	DMF	100	0.10	6.0	0.31%	77.33%	22.36%	0:100
234	BMSP	201912	H	2	indolinone Diazo Ester	1.3	Pd(dba)2	0.5	5.0%	P(fur)3	TEA	1.5	KTFA	1.5	DMF	100	0.10	6.0	0.31%	56.26%	43.43%	1:99
235	BMSP	201912	H	3	indolinone Diazo Ester	1.3	Pd(dba)2	0.5	5.0%	P(p-F-Ph)3	TEA	1.5	KTFA	1.5	DMF	100	0.10	6.0	0.73%	75.39%	23.88%	1:99
236	BMSP	201912	H	4	indolinone Diazo Ester	1.3	Pd(dba)2	0.5	5.0%	A-taPhos	TEA	1.5	KTFA	1.5	DMF	100	0.10	6.0		61.39%	38.61%	
237	BMSP	201912	H	5	indolinone Diazo Ester	1.3	Pd(dba)2	0.5	5.0%	Xantphos	TEA	1.5	KTFA	1.5	DMF	100	0.10	6.0		42.78%	57.22%	
238	BMSP	201912	H	6	indolinone Diazo Ester	1.3	Pd(dba)2	0.5	5.0%	tB-Xantphos	TEA	1.5	KTFA	1.5	DMF	100	0.10	6.0	0.18%	59.88%	39.94%	0:100
239	BMSP	201912	H	7	indolinone Diazo Ester	1.3	Pd(dba)2	0.5	5.0%	X-Phos	TEA	1.5	KTFA	1.5	DMF	100	0.10	6.0	0.49%	49.68%	49.84%	1:99
240	BMSP	201912	H	8	indolinone Diazo Ester	1.3	Pd(dba)2	0.5	5.0%	tB-XPhos	TEA	1.5	KTFA	1.5	DMF	100	0.10	6.0	0.27%	58.17%	41.57%	0:100
241	BMSP	201912	H	9	indolinone Diazo Ester	1.3	Pd(dba)2	0.5	5.0%	DPPF	TEA	1.5	KTFA	1.5	DMF	100	0.10	6.0	0.27%	44.61%	55.13%	1:99
242	BMSP	201912	H	10	indolinone Diazo Ester	1.3	Pd(dba)2	0.5	5.0%	DtBPF	TEA	1.5	KTFA	1.5	DMF	100	0.10	6.0	0.23%	50.92%	48.85%	0:100
243	BMSP	201912	H	11	indolinone Diazo Ester	1.3	Pd(dba)2	0.5	5.0%	CX-A	TEA	1.5	KTFA	1.5	DMF	100	0.10	6.0	0.31%	69.47%	30.22%	0:100
244	BMSP	201912	H	12	indolinone Diazo Ester	1.3	Pd(dba)2	0.5	5.0%	PCy3 HBF4	TEA	1.5	KTFA	1.5	DMF	100	0.10	6.0	0.18%	65.19%	34.62%	0:100

Section 8: References

(1) Garlets, Z. J.; Sanders, J. N.; Malik, H.; Gampe, C.; Houk, K. N.; Davies, H. M. L., Enantioselective C–H functionalization of bicyclo[1.1.1]pentanes. *Nat. Catal.* **2020,** *3*, 351-357.

(2) Tortoreto, C.; Rackl, D.; Davies, H. M. L., Metal-Free C–H Functionalization of Alkanes by Aryldiazoacetates. *Org. Lett.* **2017,** *19*, 770-773.

(3) Fu, L.; Mighion, J. D.; Voight, E. A.; Davies, H. M. L., Synthesis of 2,2,2,-Trichloroethyl Aryl- and Vinyldiazoacetates by Palladium-Catalyzed Cross-Coupling. *Chem. Eur. J.* **2017,** *23*, 3272-3275.

(4) Qin, C.; Davies, H. M. L., Role of Sterically Demanding Chiral Dirhodium Catalysts in Site-Selective C–H Functionalization of Activated Primary C–H Bonds. *J. Am. Chem. Soc.* **2014,** *136*, 9792-9796.

(5) Garlets, Z. J.; Boni, Y. T.; Sharland, J. C.; Kirby, R. P.; Fu, J.; Bacsa, J.; Davies, H. M. L., Design, Synthesis, and Evaluation of Extended C4–Symmetric Dirhodium Tetracarboxylate Catalysts. *ACS Catal.* **2022,** *12*, 10841-10848.

(6) Fu, J.; Ren, Z.; Bacsa, J.; Musaev, D. G.; Davies, H. M. L., Desymmetrization of cyclohexanes by site- and stereoselective C–H functionalization. *Nature* **2018,** *564*, 395-399.

(7) Green, S. P.; Wheelhouse, K. M.; Payne, A. D.; Hallett, J. P.; Miller, P. W.; Bull, J. A., Thermal Stability and Explosive Hazard Assessment of Diazo Compounds and Diazo Transfer Reagents. *Org. Process Res. Dev.* **2020,** *24*, 67-84.

(8) Zacuto, M. J.; Traverse, J. F.; Geherty, M. E.; Bostwick, K. F.; Jordan, C.; Zhang, C., Chirality Control in the Kilogram-Scale Manufacture of Single-Enantiomer CELMoDs: Synthesis of Iberdomide·BSA, Part 2. *Org. Process Res. Dev.* **2024,** *28*, 57-66.

(9) Frisch, M. J.; Trucks, G. W.; Schlegel, H. B.; Scuseria, G. E.; Robb, M. A.; Cheeseman, J. R.; Scalmani, G.; Barone, V.; Petersson, G. A.; Nakatsuji, H.; Li, X.; Caricato, M.; Marenich, A. V.; Bloino, J.; Janesko, B. G.; Gomperts, R.; Mennucci, B.; Hratchian, H. P.; Ortiz, J. V.; Izmaylov, A. F.; Sonnenberg, J. L.; Williams; Ding, F.; Lipparini, F.; Egidi, F.; Goings, J.; Peng, B.; Petrone, A.; Henderson, T.; Ranasinghe, D.; Zakrzewski, V. G.; Gao, J.; Rega, N.; Zheng, G.; Liang, W.; Hada, M.; Ehara, M.; Toyota, K.; Fukuda, R.; Hasegawa, J.; Ishida, M.; Nakajima, T.; Honda, Y.; Kitao, O.; Nakai, H.; Vreven, T.; Throssell, K.; Montgomery Jr., J. A.; Peralta, J. E.; Ogliaro, F.; Bearpark, M. J.; Heyd, J. J.;

Brothers, E. N.; Kudin, K. N.; Staroverov, V. N.; Keith, T. A.; Kobayashi, R.; Normand, J.; Raghavachari, K.; Rendell, A. P.; Burant, J. C.; Iyengar, S. S.; Tomasi, J.; Cossi, M.; Millam, J. M.; Klene, M.; Adamo, C.; Cammi, R.; Ochterski, J. W.; Martin, R. L.; Morokuma, K.; Farkas, O.; Foresman, J. B.; Fox, D. J., Gaussian 16 Rev. C.01. **2016**.

(10) Humphrey, W.; Dalke, A.; Schulten, K., VMD: Visual molecular dynamics. *J. Mol. Graph.* **1996,** *14*, 33-38.

(11) Momma, K.; Izumi, F., VESTA: a three-dimensional visualization system for electronic and structural analysis. *J. Appl. Crystallogr.* **2008,** *41*, 653-658.

(12) (a) Lee, C.; Yang, W.; Parr, R. G., Development of the Colle-Salvetti correlation-energy formula into a functional of the electron density. *Phys. Rev. B* **1988,** *37*, 785-789; (b) Becke, A. D., Density-functional thermochemistry. III. The role of exact exchange. *J. Chem. Phys.* **1993,** *98*, 5648-5652; (c) Becke, A. D., A new mixing of Hartree–Fock and local density-functional theories. *J. Chem. Phys.* **1993,** *98*, 1372-1377; (d) Grimme, S.; Antony, J.; Ehrlich, S.; Krieg, H., A consistent and accurate ab initio parametrization of density functional dispersion correction (DFT-D) for the 94 elements H-Pu. *J. Chem. Phys.* **2010,** *132*, 154104; (e) Grimme, S.; Hansen, A.; Brandenburg, J. G.; Bannwarth, C., Dispersion-Corrected Mean-Field Electronic Structure Methods. *Chem. Rev.* **2016,** *116*, 5105-5154; (f) Johnson, E. R.; Becke, A. D., A post-Hartree-Fock model of intermolecular interactions: Inclusion of higher-order corrections. *J. Chem. Phys.* **2006,** *124*, 174104.

(13) (a) Hay, P. J.; Wadt, W. R., Ab initio effective core potentials for molecular calculations. Potentials for K to Au including the outermost core orbitals. *J. Chem. Phys.* **1985,** *82*, 299-310; (b) Roy, L. E.; Hay, P. J.; Martin, R. L., Revised Basis Sets for the LANL Effective Core Potentials. *J. Chem. Theory Comput.* **2008,** *4*, 1029-1031.

(14) (a) Hariharan, P. C.; Pople, J. A., The influence of polarization functions on molecular orbital hydrogenation energies. *Theor. Chim. Acta* **1973,** *28*, 213-222; (b) Hehre, W. J.; Ditchfield, R.; Pople, J. A., Self—Consistent Molecular Orbital Methods. XII. Further Extensions of Gaussian—Type Basis Sets for Use in Molecular Orbital Studies of Organic Molecules. *J. Chem. Phys.* **1972,** *56*, 2257-2261.

(15) (a) Vreven, T.; Byun, K. S.; Komáromi, I.; Dapprich, S.; Montgomery, J. A., Jr.; Morokuma, K.; Frisch, M. J., Combining Quantum Mechanics Methods with Molecular

Mechanics Methods in ONIOM. *J. Chem. Theory Comput.* **2006,** *2*, 815-826; (b) Dapprich, S.; Komáromi, I.; Byun, K. S.; Morokuma, K.; Frisch, M. J., A new ONIOM implementation in Gaussian98. Part I. The calculation of energies, gradients, vibrational frequencies and electric field derivatives1Dedicated to Professor Keiji Morokuma in celebration of his 65th birthday.1. *J. Mol. Struct. THEOCHEM* **1999,** *461-462*, 1-21.

(16) Rappe, A. K.; Casewit, C. J.; Colwell, K. S.; Goddard, W. A., III; Skiff, W. M., UFF, a full periodic table force field for molecular mechanics and molecular dynamics simulations. *J. Am. Chem. Soc.* **1992,** *114*, 10024-10035.

(17) (a) Cossi, M.; Rega, N.; Scalmani, G.; Barone, V., Energies, structures, and electronic properties of molecules in solution with the C-PCM solvation model. *J. Comput. Chem.* **2003,** *24*, 669-681; (b) Barone, V.; Cossi, M., Quantum Calculation of Molecular Energies and Energy Gradients in Solution by a Conductor Solvent Model. *J. Phys. Chem. A* **1998,** *102*, 1995-2001.

(18) Ren, Z.; Musaev, D. G.; Davies, H. M. L., Key Selectivity Controlling Elements in Rhodium-Catalyzed C–H Functionalization with Donor/Acceptor Carbenes. *ACS Catal.* **2022,** *12*, 13446-13456.